Chapter 15: Accident Analyses

Table of Contents

Chapter 15: Accident Analyses

Table of Contents (continued)

Chapter 15: Accident Analyses

Table of Contents (continued)

Chapter 15: Accident Analyses

Table of Contents (continued)

Chapter 15: Accident Analyses

Table of Contents (continued)

Chapter 15: Accident Analyses

Table of Contents (continued)

Chapter 15: Accident Analyses

List of Tables

Chapter 15: Accident Analyses

List of Tables (continued)

Chapter 15: Accident Analyses

List of Tables (continued)

Chapter 15: Accident Analyses

List of Figures

Chapter 15: Accident Analyses

List of Figures (continued)

Chapter 15: Accident Analyses

List of Figures (continued)

Chapter 15: Accident Analyses

List of Figures (continued)

Chapter 15: Accident Analyses

List of Figures (continued)

Chapter 15: Accident Analyses

List of Figures (continued)

Chapter 15: Accident Analyses

List of Figures (continued)

Chapter 15: Accident Analyses

List of Figures (continued)

Chapter 15: Accident Analyses

List of Figures (continued)

Chapter 15: Accident Analyses

List of Figures (continued)

Chapter 15: Accident Analyses

List of Figures (continued)

Chapter 15: Accident Analyses

List of Figures (continued)

Chapter 15: Accident Analyses

List of Figures (continued)

Chapter 15
ACCIDENT ANALYSES

Since 1970 Westinghouse has been using the American Nuclear Society (ANS) classification of plant conditions, which divides plant conditions into four categories in accordance with anticipated frequency of occurrence and potential radiological consequences to the public. The four categories are:

Condition I: Normal Operation and Operational Transients

Condition II: Faults of Moderate Frequency

Condition III: Infrequent Faults

Condition IV: Limiting Faults

The basic principle applied in relating design requirements to each of the conditions is that the most frequent occurrences must yield little or no radiological risk to the public, and extreme situations having the potential for the greatest risk to the public shall be those least likely to occur. Where applicable, reactor trip system and engineered safety features functioning is assumed, to the extent allowed by considerations such as the single-failure criterion, in fulfilling this principle.

The basic philosophy behind the Atomic Energy Commission (AEC) classification as given in the guide, *Standard Format and Content of Safety Analysis Reports for Nuclear Power Plants*, U.S. Atomic Energy Commission, February 1972, is to group accidents solely in accordance with their radiological consequences, independent of their likelihood of occurrence. In general, the ANS and AEC classifications have a common foundation.

It has been felt that the philosophy behind AEC Classes 1, 2, and 3 to a great extent resembles the one behind ANS Conditions II, III and IV, respectively. Example-by-example comparison has demonstrated that, by and large, this is the case. However, identity cannot be claimed, e.g., accidental depressurization of the reactor coolant system by means of safety valve lifting is an ANS Condition II event but could not be classified as an AEC Class I event since it leads to a breach of a primary coolant barrier against fission product release.

In evaluating radiological consequences associated with a spectrum of accident conditions, numerous assumptions must be postulated. In many instances these assumptions are a product of extremely conservative judgements. This is because many physical phenomena are presently not understood well enough to make accurate predictions. Therefore, the set of assumptions postulated would predominantly determine the accident classification.

Vepco has elected to continue to use the ANS classification of plant conditions as a basis for structuring the accident analyses chapter because of the correctness of the philosophy of balancing consequence with the likelihood of the accident conditions.

This chapter addresses itself to the accident conditions listed on pages 15-3 and 15-4 of the AEC SAR Guide dated February 1972 (Revision 0), as they apply to the North Anna Units 1 and 2.

Certain items in the February 1972 guide warrant comments, as follows.

Item 12—On-line refueling and fuel followers are not used in North Anna Units 1 and 2. The xenon poisoning, fuel burnup, and reactivity feedback effects are taken into account in the design and analyses describing development of fault conditions postulated in this chapter, as well as in the analyses presented in Chapter 4.

Item 13—A reactor coolant flow controller is not a feature of the North Anna Units 1 and 2. Treatment of the performance of the reactivity controller in a number of accident conditions is offered in this chapter.

Item 14—No feature in the North Anna design shifts action of instrumentation from one of prevention to one of actuating safeguards.

Item 15—The reactor coolant system components whose failure could cause a Condition III or Condition IV loss-of-coolant accident (LOCA) are Safety Class I components, which means that they are designed to withstand consequences of the design-basis earthquake. In addition, the maximum credible accident is defined as a rupture of the largest pipe in the reactor coolant system in conjunction with an earthquake that may result in the loss of offsite power.

Item 26—No instrument lines from the reactor coolant system boundary penetrate the containment. (For the definition of the reactor coolant system boundary, refer to ANS 18.2, Nuclear Safety Criteria for the Design of Stationary PWR Plants, Section 5.)

In addition to the analysis presented in this chapter, in response to Revision 0 of *Standard Format and Content of Safety Analysis Reports for Nuclear Plants*, additional hypothetical events were added to Section 15 by Revision 1, dated October 1972.

Certain of the added events in the October 1972 guide warrant comments, as follows.

Event 27—Overpressurization of the residual heat removal system is not considered to be credible (References 1 & 2).

Event 30—The loss of service water is not a credible accident because the service water system is designed to withstand a single failure. The ultimate heat sink consists of two separate cooling water sources: (1) the Service Water Reservoir, which is the primary source, and (2) the North Anna Reservoir, which is a backup source. Either cooling water source can provide the necessary cooling for safe shutdown and cooldown. For DBA conditions the Service Water Reservoir, with its associated four service water pumps and seismic qualification, has the capability to satisfy the cooling requirements of both units for at least 30 days without makeup.

Adequate redundancy exists for the service water system, as aligned to the Service Water Reservoir, since a single failure can be tolerated without loss of the design function. The two sources are connected to the main supply and discharge headers by completely separate runs of buried or concrete-encased pipe These supply and discharge headers from each source to the main headers are redundant. The main supply and discharge headers supplying the components are redundant, and buried or encased in concrete below the service building. Isolation valves are provided to isolate branch headers to individual components.

Event 31—The four 125V dc systems are shown on Reference Drawing 1. The loss of one (redundant) dc system does not reduce the safety systems below the minimum engineered safety features for which the station was designed.

The heat transfer correlations used for the sequential phases of LOCAs were provided by the LOCTA-IV program, described in Section 15.3.

All accident analyses were originally performed assuming the use of Zircaloy fuel rod cladding. The impact of the use of ZIRLO as an alternate cladding material was evaluated by Westinghouse (Reference 3). The properties of these two Zirconium-based alloys are essentially identical except for the temperature at which the alpha to beta phase change occurs, and its related effect on the thermophysical properties (particularly the specific heat over the phase transformation temperature range). Therefore, the use of ZIRLO does not affect the analyses of non-LOCA accidents for which the clad temperature remains below the ZIRLO phase change temperature (1380°F). This includes all Condition I and Condition II events. The only non-LOCA accident analyses in which the clad temperatures are predicted to reach 1380°F or greater are the locked rotor analysis (Section 15.4.4) and the rupture of a control rod mechanism housing (Section 15.4.6). The assessment from Reference 3 confirmed that the conclusions in the North Anna UFSAR for these two affected non-LOCA accidents remain valid. The impact of the use of the ZIRLO alloy on the small break LOCA (Section 15.3.1) and the large break LOCA (Section 15.4.1) analyses was also assessed (References 4 & 5).

For the implementation of the Framatome Advanced Mark-BW fuel product at North Anna, all accident analyses were reviewed for potential impact upon the NSSS predictions. The Advanced Mark-BW fuel assembly has a slightly larger pressure drop than NAIF fuel, due to the use of mid-span mixing grids. The increase in pressure drop has a small impact on RCS flow reduction transients such as the loss of reactor coolant flow and the reactor coolant pump locked rotor/sheared shaft. In addition to the larger pressure drop, the Advanced Mark-BW has slightly different fuel thermal properties for safety analysis design inputs than the Westinghouse NAIF. These changes and the incorporation of M5 cladding properties impact the rod heatup calculations for the control rod ejection transient. Therefore, these accident events were reanalyzed: complete loss of reactor coolant flow (Section 15.3.4), the reactor coolant pump locked rotor/sheared shaft (Section 15.4.4), and the control rod ejection (Section 15.4.6). The accident analysis NSSS simulations were conducted by assuming full cores of each fuel type modeled (Westinghouse

standard, Westinghouse NAIF, or Framatome ANP Advanced Mark-BW). Results from the full core analyses bound the effects of the mixed core configuration with respect to core pressure drop. The implementation of the Framatome Advanced Mark-BW also has an impact on the calculated DNBR results for the Chapter 15 accident analyses. The DNB analyses for the loss of flow and locked rotor are discussed with the results of their NSSS reanalyses in Sections 15.3.4 and 15.4.4, respectively. The DNBR analyses were conducted using the analytical tools and thermal design limit (TDL) specified in Chapter 4.5.

15 REFERENCES

1. Letter from W. L. Stewart (Virginia Power) to USNRC, *Virginia Electric and Power Company, North Anna Power Station Units 1 and 2, Proposed Technical Specification Change, Residual Heat Removal System,* Serial No. 90-183, April 27, 1990.

2. Letter from L. B. Engle (USNRC) to W. L. Stewart (Virginia Power), *North Anna Units 1 and 2–Issuance of Amendments Re: Removal of Automatic Isolation Requirement (TAC Nos. M76956 and M76957),* September 22, 1993 (Virginia Power Serial No. 93-636).

3. Davidson, S. L. and Ryan, T. L. (Eds.), *VANTAGE+ Fuel Assembly Reference Core Report*, WCAP-12610-P-A (Proprietary), April 1995.

4. Letter from W. L. Stewart (Virginia Power) to USNRC, *North Anna Power Station Units 1 and 2–Proposed Technical Specifications Changes–Implementation of ZIRLO Cladding,* Serial No. 93-614, October 4, 1993.

5. Letter from L. B. Engle (USNRC) to W. L. Stewart (Virginia Power), *North Anna Units 1 and 2–Issuance of Amendments Re: Use of ZIRLO Material for Fuel Cladding (TAC Nos. M88072 and M88073),* May 26, 1994 (Virginia Power Serial No. 94-344).

15 REFERENCE DRAWINGS

The list of Station Drawings below is provided for information only. The referenced drawings are not part of the UFSAR. This is not intended to be a complete listing of all Station Drawings referenced from this section of the UFSAR. The contents of Station Drawings are controlled by station procedure.

	Drawing Number	Description
1.	11715-FE-1E	One Line Diagram: 125V DC

15.1 CONDITION I - NORMAL OPERATION AND OPERATIONAL TRANSIENTS

Condition I occurrences are those that are expected frequently or regularly in the course of power operation, refueling, maintenance, or maneuvering of the plant. As such, no Condition I occurrence causes any plant parameter to reach the value requiring either automatic or manual protective action. Inasmuch as Condition I occurrences are frequent or regular, they must be considered from the point of view of their effect on the consequences of fault conditions (Conditions II, III, and IV). In this regard, analysis of each fault condition described is generally based on a conservative set of initial conditions corresponding to the most adverse set of conditions that can occur during Condition I operation.

A typical list of Condition I events follows:

1. Steady-state and shutdown operations.
   a. Power operation (approximately 15 to 100% of full power).
   b. Start-up (or standby) (critical, 0 to 15% of full power).
   c. Hot shutdown (subcritical, residual heat removal system isolated).
   d. Cold shutdown (subcritical, residual heat removal system in operation).
   e. Refueling.
2. Operation with permissible deviations.

   Various deviations that may occur during continued operation as permitted by the plant Technical Specifications must be considered in conjunction with other operational modes. These include:

   a. Operation with components or systems out of service (such as power operation with a power-operated relief valve or spray line out of service).
   b. Leakage from fuel with cladding defects.
   c. Activity in the reactor coolant.
      1) Fission products.
      2) Corrosion products.
      3) Tritium.
   d. Operation with steam generator leaks, which is restricted by the maximum I-131 activity in the secondary side of the steam generator, as specified in the Technical Specifications.

3. Operational transients.

   a. Plant heatup and cooldown (reactor coolant system heatup of 60°F/hr and cooldown of 100°F/hr; pressurizer heatup of 100°F/hr and cooldown of 200°F/hr).

   b. Step load changes (up to ±10%).

   c. Ramp load changes (up to 5%/minute).

   d. Load rejection up to and including design load rejection transient (up to 50% step).

15.1.1 Optimization of Control Systems

A setpoint study was performed in order to simulate performance of the reactor control and protection systems. Emphasis was placed on the development of a control system that automatically maintains prescribed conditions in the plant even under the most conservative set of reactivity parameters with respect to both system stability and transient performance.

For each mode of plant operation, a group of optimum controller setpoints was determined. In areas where the resultant setpoints were different, compromises based on the optimum overall performance were made and verified. A consistent set of control system parameters was derived satisfying plant operational requirements throughout the core life and for power levels between 15 and 100%. The study comprised an analysis of the following control systems: rod cluster assembly control, steam dump, steam generator level, pressurizer pressure, and pressurizer level.

15.1.2 Initial Power Conditions Assumed in Accident Analyses

15.1.2.1 Power Rating

Table 15.1-1 lists the principal power rating values that are assumed in analyses performed in this section. Two ratings are given:

1. The guaranteed nuclear steam supply system thermal power output. This is the current nominal power output of the nuclear steam supply system (References 14 & 15). This power output includes the thermal power generated by the reactor coolant pumps.

2. The engineered safety features design rating. The engineered safety features are designed for a thermal power higher than the guaranteed value in order not to preclude realization of future potential power capability. The Reference 14 license amendment took advantage of this capability. This higher thermal power value is designated as the engineered safety features design rating. This power output includes the thermal power generated by the reactor coolant pumps.[1]

1. The thermal power attributed to the reactor coolant pumps includes the total net heat addition to the reactor coolant system, due to sources other than the reactor core, as determined by a reactor coolant system heat balance.

Reference 14 submitted a license amendment to increase the maximum core Rated Thermal Power to 2893 MWt (2905 MWt NSSS). The NRC approved this request in Reference 15. Safety analyses dependent on heat removal capacity of the plant and engineered safety systems have assumed a core power rating that conservatively bounds 2893 MWt (2905 MWt NSSS).

Where initial power operating conditions are assumed in accident analyses, the "guaranteed nuclear steam supply system thermal power output" plus allowance for errors in steady-state power determination is assumed. Where demonstration of adequacy of the containment and engineered safety features is concerned, the "engineered safety features design rating" plus allowance for error is assumed. The thermal power values used for each transient analyzed are given in Table 15.1-2.

15.1.2.2 **Initial Conditions**

For those transients which are DNB limited, nominal values of initial conditions are assumed. The allowances on power, temperature and pressure are determined on a statistical basis and are included in the DNBR limit, as described in VEP-NE-2-A (Reference 13). This is the Virginia Power Statistical DNBR Evaluation Methodology. The Framatome Statistical Core Design (SCD) Methodology is employed for the statistical analysis of Advanced Mark-BW fuel (Reference 21).

For transients which are not DNB limited or for which Statistical DNBR Evaluation Methodology is not employed, initial conditions are obtained by adding maximum steady-state errors to rated values.

The following steady-state errors are used for all accident analyses unless stated otherwise:

1. Core power — +2 percent allowance for calorimetric error.
2. Average RCS temperature — +4°F controller deadband and measurement error allowance.
3. Pressurizer pressure — ±30 psi—steady-state fluctuations and measurement error allowance.
4. Reactor Flow — Minimum Measured Flow -2%

The present design value for the average reactor coolant system temperature is 586.8°F.

The ranges of permissible initial reactor operating conditions of core flow rate, system temperature, and system pressure are stated in the Technical Specifications for North Anna Power Station.

The North Anna Units 1 and 2 Technical Specifications minimum allowable Reactor Coolant System (RCS) total flow rate is 295,000 gpm. The RCS total flow rate is the basis for the minimum measured flow (MMF) which is used to analyze those events for which the Virginia Power Statistical Evaluation Methodology (Reference 13) is the governing DNB methodology.

Other DNBR-related transients and events that are limited by considerations such as heat sink or pressurization criteria are currently analyzed assuming a lower-bounding design flow. The MMF is 295,000 gpm and the lower-bounding design flow is 289,100 gpm.

These flow rates represent increases in the flow rates assumed for the Chapter 15 transients in most cases. An increased RCS flow creates a benefit for transients that have a DNBR acceptance criterion. For other transients that are limited by considerations such as heat sink or pressurization criteria, lower flow is limiting (i.e., increased RCS flow is a benefit) or the event is insensitive to RCS flow rate. Therefore, Chapter 15 transients analyzed at these or lower assumed RCS flow rates are bounding with respect to expected actual plant behavior.

Initial values for core power, average reactor coolant system temperature, and pressurizer pressure are selected to minimize the initial departure from nucleate boiling ratio (DNBR) unless otherwise stated in the sections describing specific accidents.

15.1.2.3 **Power Distribution**

The transient response of the reactor system is dependent on the initial power distribution. The nuclear design of the reactor core minimizes adverse power distribution through the placement of control rods and operating instructions. The power distribution may be characterized by the radial peaking factor $F_{\Delta H}$ and the total peaking factor F_Q. The peaking factor limits are given in the Core Operating Limits Report (COLR).

For transients that may be DNB-limited, the radial peaking factor is important. The radial peaking factor increases with decreasing power level due to rod insertion. This increase in $F_{\Delta H}$ is included in the core limits illustrated in Figure 15.1-1. All transients that may be DNB-limited are assumed to begin with a $F_{\Delta H}$ consistent with the initial power level defined in the Technical Specifications.

North Anna Technical Specifications require periodic testing of all control and shutdown RCCAs in the core during power operation to ensure that the rods are able to fall into the core upon receipt of a reactor trip signal. Control rod urgent failure alarms may be received during the test. An urgent failure condition during rod operability testing may result in an immobile group or bank up to 18 steps below the insertion limits. In addition, there is a potential that an immobile group or bank may result from power maneuvers (e.g., during turbine valve freedom testing) where the insertion limits are fully met but the affected rods cannot move. The North Anna Technical Specifications were amended (References 19 & 20) to allow continued operation with (1) one or more RCCA banks immovable and (2) a maximum of one bank inserted up to 18 steps below the insertion limit for a period of up to 72 hours.

References 19 and 20 require analytical checks on the radial power distribution as part of the reload safety evaluation process established in Reference 12. The radial peaking factor ($F_{\Delta h}$) will be checked for the allowed conditions for each reload core by modeling the testing of each

control and shutdown bank using the NRC methods in Reference 12. Based on the results of these calculations, verification is made that the DNBR criterion for ANS Condition II transients initiated from the test condition is met. Since the probability of a more severe (Condition III or IV) event during the 72-hour repair period is negligible, additional evaluation of these events is not required.

The axial power shape used in the DNB calculation is the 1.55 chopped cosine, as discussed in Section 4.4.3.2.2.

For transients that may be overpower-limited, the total peaking factor F_Q is important. The value of F_Q may increase with decreasing power level so that full-power hot-spot heat flux is not exceeded, i.e., $F_Q \times$ Power = design hot-spot heat flux. All transients that may be overpower-limited are assumed to begin with a value of F_Q consistent with the initial power level as defined in the Technical Specifications.

The value of peak kW/ft can be directly related to fuel temperature, as illustrated on Figure 4.4-1. For transients that are slow with respect to the fuel rod thermal time constant, the fuel temperatures are illustrated on Figure 4.4-1. For transients that are fast with respect to the fuel rod thermal time constant, e.g., rod ejection, a detailed heat transfer calculation is made.

15.1.3 Trip Points and Time Delays to Trip Assumed in Accident Analyses

A reactor trip signal acts to open two trip breakers, connected in series, feeding power to the control rod drive mechanisms. The loss of power to the mechanism coils causes the mechanisms to release the rod cluster control assemblies, which then fall by gravity into the core. There are various instrumentation delays associated with each trip function, including delays in signal actuation, in opening the trip breakers, and in the release of the rods by the mechanisms. The total delay to trip is defined as the time delay from the time that trip conditions are reached to the time the rods are free and begin to fall. Limiting trip setpoints assumed in accident analyses and the time delay assumed for each trip function are given in Table 15.1-3.

The difference between the limiting trip point assumed for the analysis and the nominal trip point represents an allowance for instrumentation channel error and setpoint error. Periodic instrument testing and calibration demonstrate that actual instrument errors and time delays are equal to or less than the values assumed in the safety analysis.

In lieu of actual measurement, time delays may be verified for selected components provided that the components and methodology for verification have been previously reviewed and approved by the NRC.

15.1.4 Instrumentation Drift and Calorimetric Errors - Power Range Neutron Flux

The instrumentation drift and calorimetric errors used in establishing the maximum overpower setpoint are presented in Table 15.1-4.

The calorimetric error is the error assumed in the determination of core thermal power as obtained from secondary plant measurements. The total ion chamber current (sum of the top and bottom sections) is calibrated (set equal) to this measured power on a periodic basis. The secondary power is obtained from measurement of feedwater or steam flow, feedwater inlet temperature to the steam generators, and steam pressure. High-accuracy instrumentation is provided for these measurements, with accuracy tolerances much tighter than those that would be required to control feedwater flow.

15.1.5 Rod Cluster Control Assembly Insertion Characteristic

The negative reactivity insertion following a reactor trip is a function of the acceleration of the rod cluster control assemblies and the variation in rod worth as a function of rod position. With respect to accident analyses, the critical parameter is the time of insertion up to the dashpot entry, approximately 85% of the rod cluster travel. For accident analyses, the insertion time to dashpot entry is conservatively taken as 2.7 seconds. The rod cluster control assembly position versus time assumed in accident analyses is shown in Table 15.1-8.

Table 15.1-7 shows the fraction of total negative reactivity insertion versus normalized rod insertion for a core where the axial distribution is skewed to the lower region of the core. An axial distribution that is skewed to the lower region of the core can arise from operation within relaxed power distribution control axial offset bands. This curve is used as input to all point kinetics core models used in transient analyses.

There is conservatism in the use of this curve in that it is based on the bottom-skewed distribution. For cases other than bottom-skewed power distributions, significant negative reactivity would have been inserted sooner due to the more favorable axial distribution existing prior to trip.

The time from rod cluster control assembly release versus rod position is presented in Table 15.1-8. The information presented in Tables 15.1-7 and 15.1-8 may be combined to determine control rod worth versus time. A total negative reactivity insertion following trip of 4% delta k is assumed in the transient analyses except where specifically noted otherwise. This assumption is conservative with respect to the calculated trip reactivity worth available.

The normalized rod cluster control assembly negative reactivity insertion versus time curve for an axial power distribution skewed to the bottom is used in transient analyses. Where special analyses require use of three-dimensional or axial one-dimensional core models, the negative reactivity insertion resulting from reactor trip is calculated directly by the reactor kinetic code and is not separable from other reactivity feedback effects. In this case, the rod cluster control assembly position versus time of Table 15.1-8 is used as code input.

15.1.6 Reactivity Coefficients

The transient response of the reactor system is dependent on reactivity feedback effects, in particular the moderator temperature coefficient and the Doppler coefficient. These reactivity coefficients and their values are discussed in detail in Chapter 4.

In the analysis of certain events, conservatism requires the use of large reactivity coefficient values, whereas in the analysis of other events, conservatism requires the use of small reactivity coefficient values. Some analyses, such as loss of reactor coolant from cracks or ruptures in the reactor coolant system, do not depend on reactivity feedback effects. The values used are given in Table 15.1-2. The justification for use of conservatively large versus small reactivity coefficient values is treated on an event-by-event basis. To facilitate comparison, individual sections in which justification for the use of large or small reactivity coefficient values is to be found are referenced below:

1. Condition II Events	Section
a. Uncontrolled rod cluster control assembly bank withdrawal from a subcritical condition.	15.2.1
b. Uncontrolled rod cluster control assembly bank withdrawal at power.	15.2.2
c. Rod cluster control assembly misalignment.	15.2.3
d. Uncontrolled boron dilution.	15.2.4
e. Partial loss of forced reactor coolant flow.	15.2.5
f. Start-up of an inactive reactor coolant loop.	15.2.6
g. Loss of external electrical load and/or turbine trip.	15.2.7
h. Loss of normal feedwater.	15.2.8
i. Loss of all offsite power to the station.	15.2.9
j. Excessive heat removal due to feedwater system malfunctions.	15.2.10
k. Excessive load increase.	15.2.11
l. Accidental depressurization of the reactor coolant system.	15.2.12
m. Accidental depressurization of main steam system.	15.2.13

n. Spurious operation of the safety injection system at power. 15.2.14

2. Condition III Events

a. Complete loss of forced reactor coolant flow. 15.3.4

b. Single rod cluster control assembly withdrawal at full power. 15.3.7

3. Condition IV Events

a. Rupture of a steam pipe. 15.4.2.1

b. Rupture of a main feedwater pipe. 15.4.2.2

c. Single reactor coolant pump locked rotor. 15.4.4

d. Rupture of a control rod drive mechanism housing (rod cluster control assembly ejection). 15.4.6

15.1.7 Fission Product Inventories

15.1.7.1 Activities in the Core

The calculation of the core iodine fission product inventory is consistent with the inventories given in TID-14844 (Reference 1). The fission product inventories for other isotopes that are potential health hazards are calculated using the data from APED 5398 (Reference 2). These inventories for 15 x 15 and 17 x 17 fuel assemblies are given in Tables 11.1-1 and 15.1-5, respectively. The isotopes included in these tables are the significant isotopes for inhalation doses (iodines) and direct doses due to immersion (noble gases). The source term used in design basis accident analysis is based on the alternative source term as described in Section 15.4.

The isotopic yields used in the calculations are from the data of APED-5398, using the isotopic yield data for thermal fissioning of U-235 as the sole fissioning source. The change in fission product inventory resulting from the fissioning of other fissionable atoms has been reviewed. The results of this review indicated that inclusion of all fission source data would result in small (less than 10%) change in the isotopic inventories.

15.1.7.2 Activities in the Fuel Pellet Cladding Gap

The computed gap activities as shown for both the 15 x 15 (Table 11.1-1) and 17 x 17 (Table 15.1-5) fuel assemblies are based on buildup in the fuel from the fission process, and diffusion to the gap at rates dependent on the operating temperature. A comparison of the gap activities for these two fuel assemblies shows that the gap activities for the 17 x 17 fuel assembly are only about one-half of those for the 15 x 15 fuel assembly. This is a result of the lower operating temperatures, and therefore the slower diffusion rate, in the 17 x 17 fuel. For this

reason, the offsite dose calculations in Chapter 11 have not been recalculated for the 17 x 17 fuel assembly, since the results would only have been less.

The temperature distribution used in the calculation of the gap activity for the 15 x 15 fuel assembly is described in Section 11.1 and shown in Table 11.1-2. The temperature dependence for the 17 x 17 fuel assembly is accounted for by determining the core fuel fraction operating within each of nine temperature regions (Table 15.1-6), each with the release rate to the gap dependent on the mean fuel temperature within that region. Since the temperature distribution changes during core life, the highest expected values are used. The temperature dependence of the diffusion coefficient, D', for Xe and Kr in UO_2, follows the Arrhenius law:

$$D'(T) = D'(1673)^{-\frac{E}{R}\left(\frac{1}{T}-\frac{1}{1673}\right)}$$

where:

D'(T) = diffusion coefficient at temperature T, sec^{-1}

E = activation energy, 82 kcal/mole

D'(1673) = diffusion coefficient at 1673 K = 1×10^{-11} sec^{-1}

T = temperature, K

R = gas constant, 1.99×10^{-3} kcal/mole/K

The above expression is valid for temperatures above 1100°C. Below 1100°C fission gas release occurs mainly by two temperature-independent mechanisms, recoil and knockout, and is predicted using D' at 1100°C. The value used for D' (1673 K), based on data at burnups greater than 10^{19} fissions/cm^3, accounts for possible fission gas release by other mechanisms, as well as pellet cracking during irradiation.

The diffusion coefficient for iodine isotopes was conservatively assumed to be the same as for Xe and Kr. Toner and Scott (Reference 3) observed that iodine diffuses in UO_2 at about the same rate as Xe and Kr, and has about the same activation energy. Data reported by Belle (Reference 4) indicate that the iodine diffuses at slightly slower rates than Xe and Kr.

With the diffusion coefficient determined for the fuel temperature region of interest, the fraction of radioactive fission gas that crosses the fuel boundary into the fuel rod gap is found from:

$$f = 3\sqrt{\frac{D'}{\lambda}}\left[\operatorname{Coth}\sqrt{\frac{\lambda}{D'}} - \frac{D'}{\lambda}\right]$$

where:

f = fraction of a given radioactive fission gas in fuel rod gap

λ = fission gas decay constant, sec^{-1}

D' = diffusion coefficient, sec^{-1}

The above expression is the steady-state solution of the diffusion equation in spherical geometry as given by Booth (Reference 5).

Table 15.1-5 lists the total core activities as well as activities present in the gap of the 17 x 17 fuel assembly for each pertinent isotope obtained using the above equations and the fuel temperature distribution given in Table 15.1-6.

The activities (for the 15 x 15 fuel assembly) in the reactor coolant as well as in the volume control tank, pressurizer, and waste gas decay tanks are given in Chapter 11, including the data on which the computation of these activities is based.

15.1.8 Residual Decay Heat

Residual heat in a subcritical core consists of:

1. Fission product decay energy.
2. Decay of neutron capture products.
3. Residual fissions due to the effect of delayed neutrons.

These constituents are discussed separately in the following paragraphs.

15.1.8.1 Fission Product Decay

Non-LOCA calculations performed with the RETRAN code (Section 15.1.9.2) are based on either a 23-group fit to the 1979 ANS Standard (Reference 18) with a two-sigma uncertainty or an 11-group fit to the Draft 1973 ANS Standard (Reference 17) increased by 20%. LOCA analyses are performed with the Draft 1973 ANS Standard (Reference 17) increased by 20% for conservatism (Section 15.3.1.4).

15.1.8.2 Decay of U-238 Capture Products

Betas and gammas from the decay of U-239 (23.5-minute half-life) and Np-239 (2.35-day half-life) contribute significantly to the heat generation after shutdown. The cross sections for production of these isotopes and their decay schemes are relatively well known. Calculations using RETRAN incorporate the actinide contribution to decay heat (contributions due to U-239 and Pu-239) and are based upon the ANSI/ANS 1979 Standard (Reference 18). The decay heat contributions from these isotopes are presented in Reference 18.

15.1.8.3 **Residual Fissions**

The time dependence of residual fission power after shutdown depends on core properties throughout a transient under consideration. Core average conditions are more conservative for the calculation of reactivity and power level than actual local conditions as they would exist in hot areas of the core. Thus, unless otherwise stated in the text, static power shapes have been assumed in the analyses, and these are factored by the time behavior of core average fission power calculated by a point-model kinetics calculation with six delayed neutron groups.

For the purpose of illustration only, a one-delayed neutron group calculation, with a constant shutdown reactivity of -4% delta k, is shown in Figure 15.1-2.

15.1.8.4 **Distribution of Decay Heat Following a LOCA**

During a LOCA, the core is rapidly shut down by void formation or rod cluster control assembly insertion, or both, and a large fraction of the heat generation to be considered comes from fission product decay gamma rays. This heat is not distributed in the same manner as steady-state fission power. Local peaking effects that are important for the neutron-dependent part of the heat generation do not apply to the gamma-ray contribution. The steady-state factor of 0.974 that represents the fraction of heat generated within the clad and pellet drops to 0.95 for the hot rod in a LOCA.

For example, consider the transient resulting from the postulated double-ended break of the largest reactor coolant system pipe; 0.5 second after the rupture, about 30% of the heat generated in the fuel rods is from gamma-ray absorption. The gamma power shape is less peaked than the steady-state fission power shape, reducing the energy deposited in the hot rod at the expense of adjacent colder rods. A conservative estimate of this effect is a reduction of 10% of the gamma-ray contribution, or 3% of the total. Since the water density is considerably reduced at this time, an average of 98% of the available heat is deposited in the fuel rods, the remaining 2% being absorbed by water, thimbles, sleeves, and grids. The net effect is a factor of 0.95, rather than 0.974, to be applied to the heat production in the hot rod.

15.1.9 Computer Codes Used

Summaries of some of the principal computer codes used in transient analyses are given below. Other codes—in particular, very specialized codes in which the modeling has been developed to simulate one given accident (such as the SATAN-VI Code used in the analysis of the reactor coolant system pipe rupture [Section 15.4]) and which consequently have a direct bearing on the analysis of the accident itself—are summarized in their respective accident analyses sections. The codes used in the analysis of each transient are listed in Table 15.1-2.

15.1.9.1 **FACTRAN**

FACTRAN (Reference 6) calculates the transient temperature distribution in a cross section of a metal-clad UO_2 fuel rod and the transient heat flux at the surface of the clad using as input the nuclear power and the time-dependent coolant parameters (pressure, flow, temperature, density). The code uses a fuel model that exhibits the following features simultaneously:

1. A sufficiently large number of radial space increments to handle fast transients such as rod-ejection accidents.
2. Material properties that are functions of temperature and a sophisticated fuel-to-clad gap heat transfer calculation.
3. The necessary calculations to handle post-DNB transients: film-boiling heat transfer correlations, Zirconium-water reaction, and partial melting of the materials.

The gap heat transfer coefficient is calculated according to an elastic pellet model (refer to Figure 15.1-3). The thermal expansion of the pellet is calculated as the sum of the radial (one-dimensional) expansions of the rings. Each ring is assumed to expand freely. The cladding diameter is calculated based on thermal expansion and internal and external pressures.

If the outside radius of the expanded pellet is smaller than the inside radius of the expanded clad, there is no fuel-clad contact and the gap conductance is calculated on the basis of the thermal conductivity of the gas contained in the gap. If the pellet outside radius so calculated is larger than the clad inside radius (negative gap), the pellet and the clad are pictured as exerting upon each other a pressure sufficiently important to reduce the gap to zero by elastic deformation of both. This contact pressure determines the gap heat transfer coefficient.

15.1.9.2 **RETRAN**

The RETRAN (Reference 8) code is used to determine the detailed transient behavior of multi-loop pressurized-water reactor systems caused by prescribed initial perturbations in process parameters. The code is useful in predicting plant behavior when different conditions are present in the reactor coolant loops. The physical, thermal, and hydraulic characteristics of a multi-loop plant are currently modeled with one loop for each RCS loop. Some transients were analyzed with lumped RCS loops (one- or two-loop models). In the model with two “equivalent” loops, the perturbation occurs in one loop and the other equivalent loop represents, in lumped form, the remaining loops in the plant.

The code simulates the coolant flow through the reactor vessel, hot leg, cold leg, and steam generator, plus the pressurizer surge line. Neutron point kinetics, fuel-clad heat transfer, and various control system characteristics are modeled. Simulation of the reactor trip system, engineered safety features (safety injection), and primary and secondary pressure control systems is provided.

Extensive description and qualification of Virginia Power's RETRAN models is provided in Reference 8.

15.1.9.3 **LOFTRAN**

The LOFTRAN (Reference 9) program is used for studies of transient response of a pressurized-water reactor system to specified perturbations in process parameters. LOFTRAN simulates a multi-loop system by a lumped-parameter single-loop model containing reactor vessel, hot- and cold-leg piping, steam generator (tube and shell sides), and pressurizer. The pressurizer heaters, spray, and relief and safety valves are also considered in the program. Point-model neutron kinetics, and reactivity effects of the moderator, fuel, boron, and rods are included. The secondary side of the steam generator uses a homogeneous, saturated mixture for the thermal transients, and a water-level correlation for indication and control. The reactor protection system is simulated to include reactor trips on neutron flux, overpower and over-temperature reactor coolant delta T, high and low pressure, low flow, and high pressurizer level. Control systems are also simulated, including rod control, steam dump, feedwater control, and pressurizer pressure control. The safety injection system, including the accumulators, is also modeled.

LOFTRAN is a versatile program that is suited to both accident evaluation and control studies, as well as parameter sizing.

LOFTRAN also has the capability of calculating the transient value of DNBR based on the input from the core limits illustrated on Figure 15.1-1. The core limits represent the minimum value of DNBR as calculated for a typical or thimble cell.

15.1.9.4 **COBRA**

The COBRA-IIIC/MIT (Reference 10) computer code calculates the flow and enthalpy within interconnected flow channels by solving finite difference equations of continuity, energy and momentum. The mathematical model is applicable to both steady-state and transient conditions and the model considers both turbulent mixing and diversion crossflow. In formulating the model one-dimensional, two-phase, separated slip flow is assumed to exist during boiling.

The same equations are used for both steady state and transient computations. Initial conditions are obtained by performing a steady state calculation and then the transient calculation is performed. Time dependent forcing functions obtained from the system transient code (e.g., RETRAN) consisting of inlet temperature, inlet flow, system pressure and core average heat flux are used to establish boundary conditions at succeeding times.

Once the flow solution is obtained, additional correlations are used in calculating a DNBR distribution. COBRA-IIIC/MIT code allows user specification of the appropriate correlations, and has been qualified for both the W-3 (Reference 10) and WRB-1 (Reference 11) correlations.

15.1.9.5 **Core Neutronics Calculations for Accident Analysis**

Virginia Power's methodology for developing core neutronics input to the accident analysis is described in Reference 12. This methodology includes the development of global, or non accident specific parameters such as shutdown margins, trip reactivity shape, reactivity coefficients (doppler, moderator, boron), prompt and delayed neutron characteristics and local power peaking factors. Also, techniques for predicting peaking factors and reactivity coefficients for off-normal (accident) conditions have been developed and qualified.

15.1.9.6 **THINC**

The THINC code is described in Section 4.4.3.4.

15.1.9.7 **LYNXT**

The LYNXT code is described in Section 4.5.4.3.4.1.

15.1.9.8 **VIPRE-D**

The VIPRE-D code is described in Section 4.5.4.3.4.3.

15.1 REFERENCES

1. J. J. DiNunno et al., *Calculation of Distance Factors for Power and Test Reactor Sites*, TID-14844, March 1962.
2. M. E. Meek and B. F. Rider, *Summary of Fission Product Yields for U-235, U-238, Pu-239, and Pu-241 at Thermal Fission Spectrum and 14 Mev Neutron Energies*, APED-5398, March 1968.
3. D. F. Toner and J. S. Scott, *Fission-Product Release from UO_2*, Nuclear Safety 3, No. 2, pp. 15-20, December 1961.
4. J. Belle, *Uranium Dioxide Properties and Nuclear Applications*, Naval Reactors, Division of Reactor Development, United States Atomic Energy Commission, 1961.
5. A. H. Booth, *A Suggested Method for Calculating the Diffusion of Radioactive Rare Gas Fission Products from UO_2 Fuel Elements,* DCI-27, 1957.
6. C. Hunin, FACTRAN, *a Fortran IV Code for Thermal Transients in a UO_2 Fuel Rod*, WCAP-7908, June 1972.
7. J. M. Geets and R. Salvatori, *Long-Term Transient Analysis Program for PWRs* (BLKOUT Code), WCAP-7898, June 1972.
8. N. A. Smith, VEPCO, *Reactor System Transient Analysis Using the RETRAN Computer Code*, VEP-FRD-41, Rev. 0.1-A, June 2004.

9. T. W. T. Burnett, C. J. McIntyre, J. C. Buker, et. al, *LOFTRAN Code Description*, WCAP-7907-A, April 1984.

10. F. W. Sliz and K. L. Basehore, *Vepco Core Thermal-Hydraulic Analysis Using the COBRA IIIC/MIT Computer Code*, VEP-FRD-33A, October 1983.

11. R. C. Anderson and N. P. Wolfhope, *Qualification of the WRB-1 CHF Correlation in the Virginia Power COBRA Code*, VEP-NE-3-A, July 1990.

12. *Reload Nuclear Design Methodology*, VEP-FRD-42 Rev. 2.1-A, August 2003.

13. R. C. Anderson, *Statistical DNBR Evaluation Methodology*, VEP-NE-2-A, dated June 1987.

14. Letter from W. L. Stewart (Virginia Power) to Harold R. Denton (NRC), *Amendment to Operating Licenses NPF-4 and NPF-7, North Anna Power Station Unit Nos. 1 and 2, Proposed Technical Specification Changes (for Rated Thermal Power of 2893 MWt),* Serial No. 85-077, May 2, 1985.

15. Letter from L. B. Engle (NRC) to W. L. Stewart (Virginia Power), Serial No. 86-575, August 25, 1986 (Topic: 2893 MWt Rated Thermal Power Approval for North Anna Units 1 and 2).

16. Chelemer, H.; Bowman, L. H.; Sharp, D. R., *Improved Thermal Design Procedure*, WCAP-8567, July 1975.

17. *Decay Energy Release Rates Following Shutdown of Uranium Fueled Thermal Reactors,* Draft Standard ANS 5.1, American Nuclear Society, 1973.

18. Decay Heat Power in Light Water Reactors, ANSI/ANS-5.1-1979, American Nuclear Society, 1979.

19. Letter from W. L. Stewart (VEPCO) to the NRC, *Virginia Electric and Power Company, North Anna Power Station Units 1 and 2, Proposed Technical Specifications, Operation with a Control Rod Urgent Failure Condition,* Serial No. 93-125, March 18, 1993.

20. Letter from L. B. Engle (NRC) to W. L. Stewart (VEPCO), *North Anna Units 1 and 2—Issuance of Amendments Re: Control Rod Urgent Failure Condition (TAC Nos. M86040 and M86041),* March 1, 1994 (Virginia Power Serial #94-144).

21. BAW-10170P-A, *Statistical Core Design For Mixing Vane Cores,* December 1988.

Table 15.1-1
NUCLEAR STEAM SUPPLY SYSTEM POWER RATINGS

Guaranteed Nuclear Steam Supply System thermal power output (maximum calculated turbine rating)	2905 MWt
The Engineered Safety Features design rating	2910 MWt
Thermal Power generated by the reactor coolant pumps	12 MWt
Guaranteed Core Thermal Power	2893 MWt

Table 15.1-2
SUMMARY OF INITIAL CONDITIONS AND COMPUTER CODES USED

Reactivity Coefficients Assumed

Faults	Computer Codes Used	Moderator[a, b] Temperature (Δk/k-°F)	Moderator[a, b] Density (Δk/gm/cc)	Doppler Temperature (Dk/k-°F)	Initial NSSS Thermal Power Output Assumed (MWt)
Condition II					
Uncontrolled RCC assembly bank withdrawal from a subcritical condition	RETRAN	$+6 \times 10^{-5}$	---	-2.25×10^{-5} [c]	Hot Zero Power
Uncontrolled RCC assembly bank withdrawal at power	RETRAN/COBRA RETRAN/VIPRE-D	$+6 \times 10^{-5}/-59 \times 10^{-5}$	---	$-1.4 \times 10^{-5}/-2.9 \times 10^{-5}$	2905
RCC assembly misalignment	PDQ/COBRA PDQ/VIPRE-D RETRAN/LOFTRAN	---	0	NA	2905
Uncontrolled boron dilution	RETRAN	NA	NA	NA	Hot Zero Power and 2905
Partial loss of forced reactor coolant flow [d]	LOFTRAN, FACTRAN, THINC	$+6 \times 10^{-5}$	---	NA	2905
Start-up of an inactive reactor coolant loop [e]					
Loss of external electrical load and/or turbine trip	RETRAN/COBRA RETRAN/VIPRE-D	$+6 \times 10^{-5}/-59 \times 10^{-5}$	---	-1.4×10^{-5}	2905
Loss of normal feedwater	RETRAN	$+6 \times 10^{-5}/-59 \times 10^{-5}$	NA	NA	2905

Table 15.1-2 (continued)
SUMMARY OF INITIAL CONDITIONS AND COMPUTER CODES USED

Faults	Computer Codes Used	Reactivity Coefficients Assumed: Moderator[a, b] Temperature (Δk/k-°F)	Reactivity Coefficients Assumed: Moderator[a, b] Density (Δk/gm/cc)	Reactivity Coefficients Assumed: Doppler Temperature (Dk/k-°F)	Initial NSSS Thermal Power Output Assumed (MWt)
Condition II (continued)					
Loss of offsite power to the plant auxiliaries (plant blackout)	RETRAN	---	NA	NA	2905
Excessive heat removal due to feedwater system malfunctions	RETRAN	-59×10^{-5}	---	-2.9×10^{-5}	2905
Excessive load increase	RETRAN	-59×10^{-5}	---	$-1.4 \times 10^{-5}/-2.9 \times 10^{-5}$	2905
Accidental depressurization of the reactor coolant system	RETRAN	$+6 \times 10^{-5}/-59 \times 10^{-5}$	---	$-1.4 \times 10^{-5}/-2.9 \times 10^{-5}$	2905
Accidental depressurization of the main steam system	RETRAN/COBRA RETRAN/VIPRE-D	---	Function of moderator temperature. See Section 15.2.13 (Figure 15.2-53).	(Figure 15.4-57)	Hot Zero Power
Inadvertent operation of ECCS during power operation	LOFTRAN	$+6 \times 10^{-5}$	0.43	NA	2910

Table 15.1-2 (continued)
SUMMARY OF INITIAL CONDITIONS AND COMPUTER CODES USED

Faults	Computer Codes Used	Reactivity Coefficients Assumed: Moderator[a, b] Temperature (Δk/k-°F)	Reactivity Coefficients Assumed: Moderator[a, b] Density (Δk/gm/cc)	Reactivity Coefficients Assumed: Doppler Temperature (Dk/k-°F)	Initial NSSS Thermal Power Output Assumed (MWt)
Condition III					
Loss of reactor coolant from small ruptured pipes or from cracks in large pipe that actuate emergency core cooling	NOTRUMP, LOCTA-IV				2905
Inadvertent loading of a fuel assembly into an improper position	LEOPARD, TURTLE	---	NA	NA	2785
Complete loss of forced reactor coolant flow	RETRAN/COBRA RETRAN/LYNXT RETRAN/VIPRE-D	$+6 \times 10^{-5}$	---	-1.4×10^{-5}	2905
Waste gas decay tank rupture	NA	---	NA	NA	2910
Single RCC assembly withdrawal at full power	PDQ/COBRA PDQ/VIPRE-D	$+6 \times 10^{-5}/-59 \times 10^{-5}$ [f]	NA	NA	2905

Table 15.1-2 (continued)
SUMMARY OF INITIAL CONDITIONS AND COMPUTER CODES USED

Faults	Computer Codes Used	Reactivity Coefficients Assumed: Moderator[a, b] Temperature (Δk/k-°F)	Reactivity Coefficients Assumed: Moderator[a, b] Density (Δk/gm/cc)	Reactivity Coefficients Assumed: Doppler Temperature (Dk/k-°F)	Initial NSSS Thermal Power Output Assumed (MWt)
Condition IV					
Major rupture of pipes containing reactor coolant up to and including double-ended rupture of the largest pipe in the reactor coolant system (LOCA)	SATAN VI, COCO, BASH, LOCBART	Function of moderator density. See Section 15.4.1.		Function of fuel temperature. See Section 15.4.1.	2905
Major secondary system pipe rupture up to and including double-ended rupture (rupture of a steam pipe)	RETRAN/COBRA RETRAN/VIPRE-D	Function of moderator temperature. See Section 15.2.13 (Figure 15.2-53).		(Figure 15.4-57)	Hot Zero Power
Steam generator tube rupture	NA	NA	NA	NA	2910
Single reactor coolant pump locked rotor	RETRAN/COBRA RETRAN/LYNXT RETRAN/VIPRE-D	$+6 \times 10^{-5}$	---	-1.4×10^{-5}	2905
Fuel-handling accident	NA	NA	NA		2910

Table 15.1-2 (continued)
SUMMARY OF INITIAL CONDITIONS AND COMPUTER CODES USED

Reactivity Coefficients Assumed

Faults	Computer Codes Used	Moderator[a, b] Temperature (Δk/k-°F)	Moderator[a, b] Density (Δk/gm/cc)	Doppler Temperature (Dk/k-°F)	Initial NSSS Thermal Power Output Assumed (MWt)
Condition IV (continued)					
Rupture of a control rod mechanism housing (RCCA ejection)	RETRAN	$+6 \times 10^{-5}$ BOL, HZP 0.0 BOL, HFP -13×10^{-5} EOL	---	See note g	2905
Major Rupture of a Main Feedwater Pipe	RETRAN	NA[h]	NA[h]	NA[h]	2905

a. Only one is used in an analysis, i.e., either moderator temperature or moderator density coefficient.

b. This corresponds to a +6 pcm/°F at zero power (no load T_{avg}) and becomes less positive at higher temperatures.

c. Zero power reference value. Doppler coefficient is dependent on fuel temperature. See Section 4.3.2.3.

d. Bounded by complete loss of flow accident.

e. Not a credible event under current Technical Specification restrictions.

f. Same assumption as uncontrolled assembly withdrawal at power.

g. Integral power defects of -1000×10^{-5} Δk/k and -1100×10^{-5} Δk/k are assumed.

h. Results are not sensitive to these parameters.

i. +6 pcm/°F is assumed for minimum feedback while 0.43@k/gm-cm^3 is used for maximum feedback.

Table 15.1-3
TRIP POINTS AND TIME DELAYS TO TRIP ASSUMED IN ACCIDENT ANALYSES

Trip Function	Limiting Trip Point Assumed In Analyses	Time Delay (seconds)
Power range high neutron flux, high setting	118%	0.5
Power range high neutron flux, low setting	35%	0.5
Overtemperature ΔT [a, b]	$K_1 = 1.390$ $K_2 = 0.022/°F$ $K_3 = 0.001152/psi$	8.0 [c]
(Applicable to NAPS 2 through Cycle 16 and NAPS 1 through Cycle 17)	$f(\Delta q) = -0.0167(\Delta q + 47\%)$, for $\Delta q \leq -47\%$ 0.0, for $-47\% < \Delta q < 6\%$ $0.020(\Delta q - 6\%)$, for $\Delta q \geq 6\%$	
(Applicable to NAPS 2 starting with Cycle 17 and NAPS 1 starting with Cycle 18)	$f(\Delta q) = -0.0167(\Delta q + 38\%)$, for $\Delta q \leq -38\%$ 0.0, for $-38\% < \Delta q < 6\%$ $0.020(\Delta q - 6\%)$, for $\Delta q \geq 6\%$	
Overpower ΔT [b, d]	$K_4 = 1.152$ $K_5 = 0.02/°F$, for T_{avg} increasing 0.00, for T_{avg} decreasing $K_6 = 0.00164/°F$ $f(\Delta q) = 0.0$, for all Δq	8.0 [c, e]
High pressurizer pressure	2406 psia	1.0
Low pressurizer pressure	1845 psia	2.0
Low reactor coolant flow (from loop flow detectors)	87% loop flow	1.0
High pressurizer level	100% narrow range span	2.0
Low low steam generator level	0% narrow range span [f]	2.0

a. Setpoint equation for Overtemperature ΔT is described in Section 7.2.1.1.2 (Equation 7.2-1).
b. Δq is defined in Section 7.2.1.1.2.
c. Total time delay (including RTD scoop delay, RTD time response, and trip circuit channel electronics delay) from the time the temperature difference in the coolant loops exceeds the trip setpoint until the rods are free to fall.
d. Setpoint equation for Overpower ΔT is described in Section 7.2.1.1.2 (Equation 7.2-2).
e. Transient analysis modeling of this trip assumes a time delay of 8.0 seconds. However, the Overpower ΔT trip is not credited as primary protection for any accident analysis currently performed.
f. Feedwater malfunction accident analysis models reactor trip on steam generator mass instead of level.

Table 15.1-4
DETERMINATION OF MAXIMUM OVERPOWER TRIP POINT POWER RANGE NEUTRON FLUX CHANNEL BASED ON NOMINAL SETPOINT CONSIDERING INHERENT INSTRUMENTATION ERRORS

	Assumed Error for Power Determination
A. Nominal setpoint	109
B. Calorimetric error	
Feedwater temperature	
Feedwater pressure	
Feedwater flow	
Steam pressure	
Total calorimetric error assumed	2. [a]
C. Axial power distribution effects on total ion chamber current	5.
D. Instrument channel drift and setpoint reproducibility	2. [b]
Maximum overpower trip point assuming all individual errors are simultaneously in the most adverse direction (sum of A, B, C, and D)	118.%

a. Total calorimetric error is £ 2.0% of rated thermal power for either steamflow or feedflow based calorimetrics performed at or near full power. Station procedures account for potential instrument decalibration effects resulting from extended operation at reduced power, where calorimetric power determination is inherently less accurate.
b. This value is deterministic and was selected to be more conservative than the statistical treatment of this parameter's components.

Table 15.1-5
CORE AND GAP ACTIVITIES FOR 17 x 17 FUEL ASSEMBLY OPERATION AT 2900 MWt
FOR 650 DAYS TEMPERATURE DISTRIBUTION SPECIFIED IN TABLE 15.1-6

Isotope	Curies in Core ($\times 10^7$)	Percent of Core Activity in Gap	Curies in Gap ($\times 10^{5)}$
I-131	7.16	0.90	6.44
I-132	10.9	0.0987	1.07
I-133	16.0	0.296	4.76
I-134	18.8	0.0610	1.15
I-135	14.6	0.168	2.45
Xe-131m	0.0543	1.10	0.0596
Xe-133	16.5	0.730	12.1
Xe-133m	0.420	0.478	0.201
Xe-135	4.52	0.197	0.892
Xe-135m	4.44	0.0332	0.148
Xe-138	14.6	0.0346	0.505
Kr-83m	1.33	0.0903	0.120
Kr-85	0.0813	17.6	1.43
Kr-85m	3.21	0.136	0.436
Kr-87	6.17	0.0733	0.452
Kr-88	8.79	0.108	0.952
Kr-89	11.4	0.0151	0.171

Table 15.1-6
CORE TEMPERATURE DISTRIBUTION 17 x 17 FUEL ASSEMBLY

Percent of Core Fuel Within Given Temperature Range	Power MWt	Fuel Temperature Range, °F
Near 0.0	.29412	Over 3400
0.2	7.15686	3400 - 3200
0.8	24.0196	3200 - 3000
1.6	46.37255	3000 - 2800
2.5	73.1373	2800 - 2600
3.6	104.902	2600 - 2400
4.7	137.255	2400 - 2200
5.6	162.06	2200 - 2000
80.9	2344.8	Under 2000

Table 15.1-7
NORMALIZED TRIP REACTIVITY WORTH VS ROD INSERTION

Normalized Insertion	Fraction of Total Reactivity Worth
0.00	0.00000
0.04	0.0008
0.06	0.0012
0.09	0.0020
0.13	0.0039
0.17	0.0075
0.21	0.0133
0.26	0.0160
0.30	0.0188
0.35	0.0230
0.40	0.0275
0.45	0.0338
0.51	0.0425
0.56	0.0525
0.62	0.0650
0.67	0.0825
0.73	0.113
0.79	0.191
0.85	0.350
0.95	0.675
1.0	1.0

Table 15.1-8
NORMALIZED ROD POSITION (NORMALIZED TO DASHPOT) VS NORMALIZED TIME FROM ROD RELEASE

Time From Release (Sec)	Rod Position
0	0
0.1	0.0162
0.15	0.0383
0.2	0.0596
0.25	0.0945
0.3	0.1285
0.35	0.1685
0.4	0.2085
0.45	0.2553
0.5	0.3021
0.55	0.3506
0.6	0.3983
0.65	0.4528
0.7	0.5072
0.75	0.5609
0.8	0.6153
0.85	0.6732
0.9	0.7314
0.95	0.7915
1.0	0.8511
1.05	0.8809
1.1	0.9106
1.15	0.9302
1.2	0.9532
1.25	0.9860
1.3	0.9787
1.35	0.9915
1.4	1.0000

Figure 15.1-1
ILLUSTRATION OF OVERTEMPERATURE
AND OVERPOWER DELTA-T PROTECTION

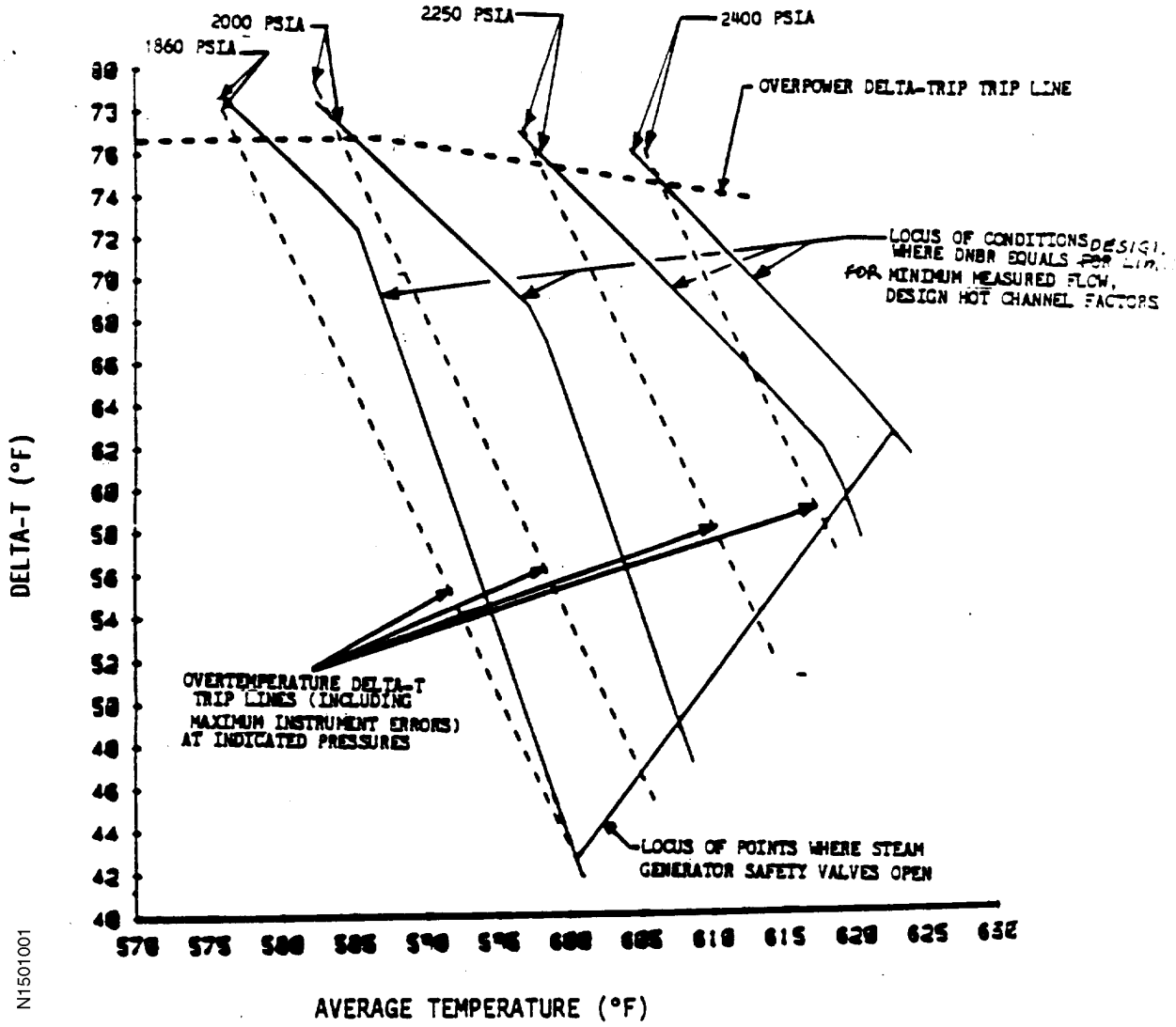

Figure 15.1-2
RESIDUAL DECAY HEAT

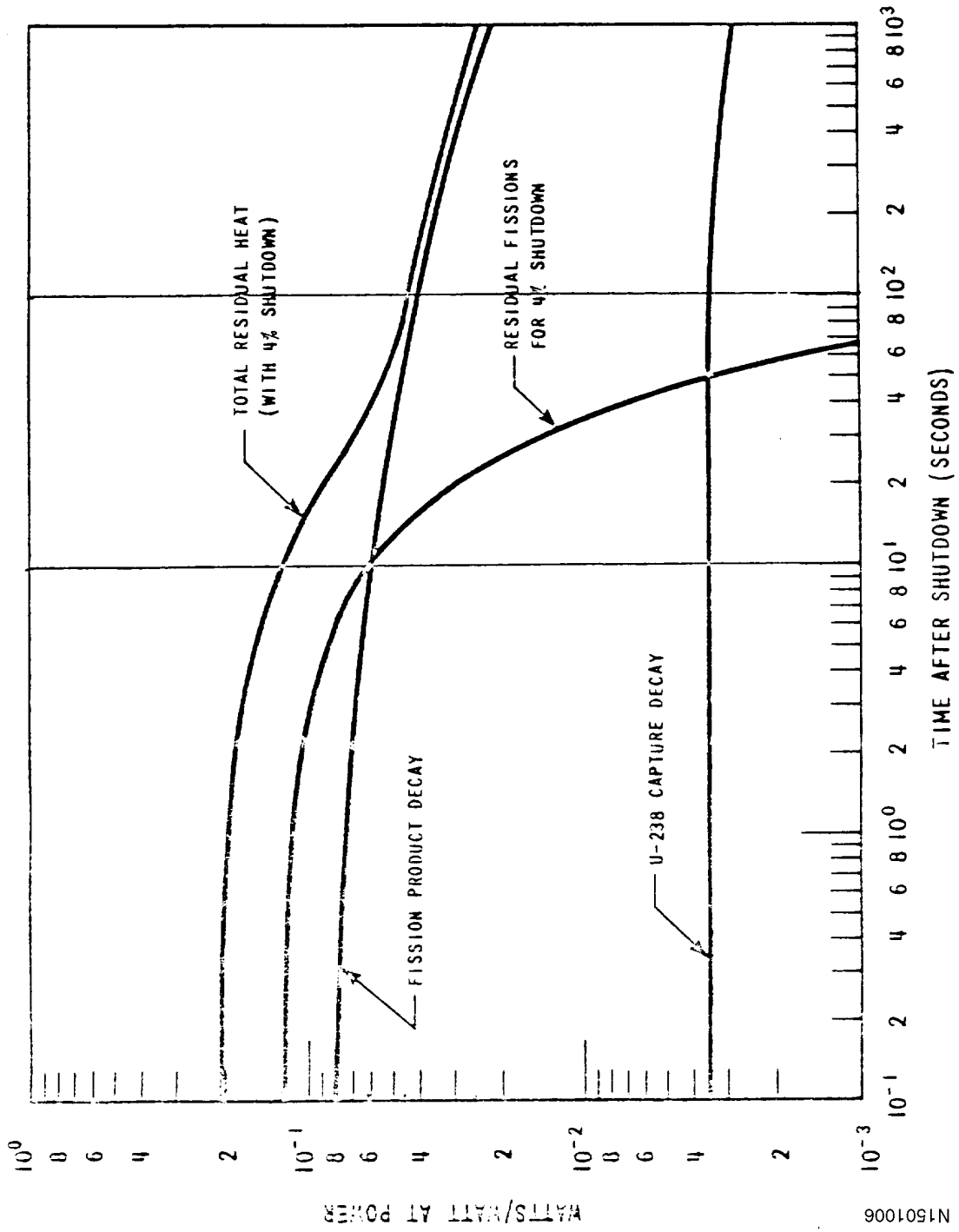

Figure 15.1-3
FUEL ROD CROSS SECTION

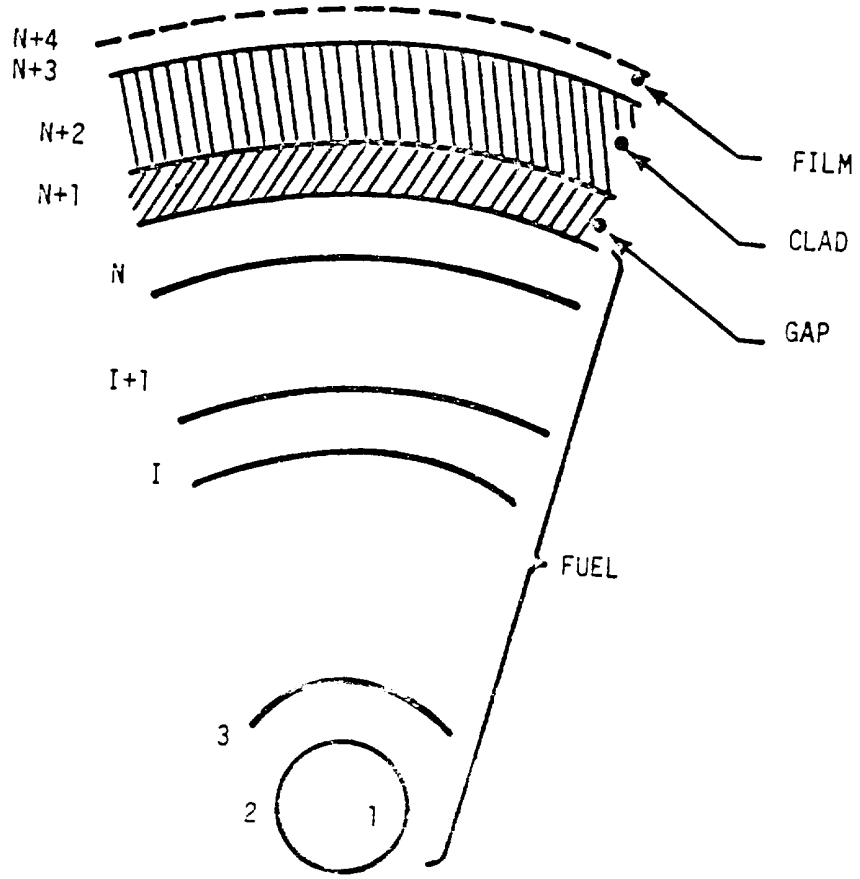

N1501007

Refer to FACTRAN description in WCAP-7908 for discussion.

15.2 CONDITION II - FAULTS OF MODERATE FREQUENCY

These faults result, at worst, in the reactor shutdown, with the plant capable of returning to operation. By definition, these faults (or events) do not propagate to cause a more serious fault, i.e., a Condition III or IV fault. In addition, Condition II events are not expected to result in fuel rod failures or reactor coolant system overpressurization. For the purposes of this report, the following faults have been grouped into this category:

1. Uncontrolled rod cluster control assembly bank withdrawal from a subcritical condition (Section 15.2.1).
2. Uncontrolled rod cluster control assembly bank withdrawal at power (Section 15.2.2).
3. Rod cluster control assembly misalignment (Section 15.2.3).
4. Uncontrolled boron dilution (Section 15.2.4).
5. Partial loss of forced reactor coolant flow (Section 15.2.5).
6. Start-up of an inactive reactor coolant loop (Section 15.2.6).
7. Loss of external electrical load and/or turbine trip (Section 15.2.7).
8. Loss of normal feedwater (Section 15.2.8).
9. Loss of offsite power to the station auxiliaries (station blackout) (Section 15.2.9).
10. Excessive heat removal due to feedwater system malfunctions (Section 15.2.10).
11. Excessive load increase (Section 15.2.11).
12. Accidental depressurization of the reactor coolant system (Section 15.2.12).
13. Accidental depressurization of the main steam system (Section 15.2.13).
14. Spurious operation of safety injection system at power (Section 15.2.14).

Reference 1 provides an evaluation of the design philosophy and the extent of protection system diversity. The Westinghouse design approach permits not only redundancy of control, providing its own desirable increment to overall plant safety, but also provides a protection system which continuously monitors numerous system variables by different means, i.e., protection system diversity. Although the protection system design basis requires only that random single failure not negate the protection system, a considerable depth of protection is achieved by the Westinghouse design approach.

An evaluation of the reliability of the reactor protection system actuation following initiation of Condition II events was performed for the relay protection logic in Reference 1 and for the solid-state protection system design in Reference 21. Standard reliability engineering techniques were used to assess likelihood of the trip failure due to random component failures. Common-mode failures were also qualitatively investigated. It was concluded from the evaluation

that the likelihood of no-trip following initiation of Condition II events is extremely small (on the order of 10^{-7} per demand).

Hence, because of the high reliability of the protection system, no special provision taken in the original design to cope with the consequences of Condition II events without trip. Subsequent to the original design, the NRC promulgated regulations to reduce the likelihood of an anticipated transient without scram (ATWS) in 10 CFR 50.62, *Requirements for Reduction of Risk from Anticipated Transients without Scram (ATWS) Events for Light-Water-Cooled Nuclear Power Plants.* Reference 22 provides the conceptual design for the ATWS Mitigation System (AMSAC) for Westinghouse plants. The AMSAC system is fully described in Section 7.7.1.14.

The time sequence of events during each Condition II fault is shown in Table 15.2-1.

15.2.1 Uncontrolled Rod Cluster Control Assembly Bank Withdrawal From A Subcritical Condition

15.2.1.1 Identification of Causes and Accident Description

A rod cluster control assembly withdrawal accident is defined as an uncontrolled addition of reactivity to the reactor core caused by withdrawal of the rod cluster control assemblies, thereby producing a power excursion. Potential causes for the event include malfunctions of the reactor control and control rod drive systems and operator error.

This event could occur with the reactor subcritical, as in one of the shutdown modes, at hot zero power or at power. A brief discussion of the protection afforded by the reactor protection system in each of these modes follows.

A. Protection at Cold Shutdown—When the reactor is at cold shutdown (Mode 5), the unit is at least 1% Δk/k subcritical. In addition, the shutdown margin requirement of 1.77% Δ k/k must be satisfied for this mode. Thus if the reactor is only 1% subcritical, at least another 0.77% Δk/k must be associated with withdrawn rods. During cold shutdown the reactor may or may not be at full flow conditions. At least one residual heat removal or one reactor coolant pump must be in operation. Protection against uncontrolled rod withdrawal in this mode is provided by the high source range count rate trip. A minimum of two source range channels must be operable whenever the reactor trip breakers are closed and the rod drive system is capable of withdrawal. Trip occurs on one of two channels exceeding a preselected setpoint. The action of the source range trip prevents any significant power generation in the core in the event of an uncontrolled rod withdrawal event.

B. Protection at Hot Standby and Hot Shutdown (Modes 3 and 4)—As in Mode 5, the source range trips are required to be operable whenever the trip breakers are closed and the rods are capable of being withdrawn. The requirements for shutdown margin and subcriticality remain the same as in Mode 5. Temperatures may be higher (up to the HZP temperature of 547°F in Mode 3), but the RCS flow requirements are increased in Mode 3 (above 350°F):

at least one reactor coolant pump must be in operation. As in Mode 5, operation of the source range trip serves to prevent any significant power generation in the event of an uncontrolled control rod withdrawal.

C. Protection during Start-up and Power Operation (Modes 1 and 2)—In these modes all three reactor coolant pumps must be in operation in accordance with Technical Specifications, thereby providing full core flow. The P-6 permissive setpoint (1 of 2 intermediate range current exceeding a preset value) allows the source range trips to be blocked in order for power escalation to continue. Protection against overpower for Modes 1 and 2 is provided by:

(1) Intermediate range high neutron flux reactor trip. This trip is actuated by 1 of 2 Intermediate Range (IR) channels exceeding a pre-selected setpoint. No credit is taken for the IR trip in the accident analysis. The IR trip can be blocked above the P-10 permissive setpoint (2 of 4 power range channels exceeding 10% of rated thermal power).

(2) Power range high neutron flux reactor trip. Reactor trip occurs when two out of the four power range channels exceed a preset power level. There are two trip setpoints associated with the power range channels. Below 10% of rated thermal power (the P-10 interlock setpoint) the power range trip setpoint is 25% of rated thermal power (nominal; the Technical Specification allowable value is 26%). Above 10% power this setpoint can be blocked. The high flux setpoint then increases to 109% power (nominal; the allowable is 110%). The response of the core to rod withdrawal events occurring at above 10% power, where the power range low setpoint is blocked, is discussed in Section 15.2.2, Uncontrolled Rod Cluster Control Assembly Bank Withdrawal at Power.

(3) Intermediate and power range rod stops. The rod stops serve to discontinue rod withdrawal on either 1 of 2 high IR flux signals or on 1 of 4 high power range flux signals, thereby eliminating the need to actuate the corresponding high flux level trips.

The reactor is normally brought to power from a subcritical condition by means of rod cluster control assembly withdrawal. Boration or dilution may be performed to ensure criticality at a desired control rod position. During the shutdown modes, all sources of primary grade water are locked, sealed or otherwise secured in the closed position except during planned boron dilution or makeup activities, thereby precluding an uncontrolled addition of reactivity to the core. During the approach to criticality (all RCS loops in operation), the maximum rate of reactivity resulting from boron dilution is less than assumed in this analysis (see also Section 15.2.4, Uncontrolled Boron Dilution).

The rod cluster control assembly drive mechanisms are wired into preselected bank configurations which are not altered during reactor life. These circuits prevent the assemblies from being withdrawn in other than their respective banks. Power supplied to the banks is

controlled so that no more than two banks can be withdrawn at the same time. The rod cluster control assembly drive mechanisms are of the magnetic latch type, and coil actuation is sequenced to provide variable speed travel. The maximum reactivity insertion rate analyzed is greater than that resulting from the simultaneous withdrawal of the combination of the two control banks having the maximum combined worth at maximum speed.

The neutron flux response to a continuous reactivity insertion is characterized by an exponential increase. Once the amount of reactivity inserted corresponds to the delayed neutron fraction of the core, the power increase is very rapid, and is terminated by the reactivity feedback effect of the negative Doppler coefficient. This self-limitation of the power burst is of primary importance since it limits the power to a tolerable level during the delay time for protective action.

15.2.1.2 **Analysis of Effects and Consequences**

15.2.1.2.1 Method of Analysis

Previous analyses of this transient are discussed in the original FSAR. The original FSAR evaluation assumed a moderator temperature coefficient of zero pcm/°F and a reactivity insertion rate of 75 pcm/sec. An earlier re-analysis utilized the RETRAN transient analysis code and considered operation of a single reactor coolant pump and a positive moderator temperature coefficient of +6.0 pcm/°F. A subsequent re-analysis utilized the Westinghouse TWINKLE and FACTRAN codes, and operation of two reactor coolant pumps was assumed. The most recent analysis of this event is presented below.

The transient is analyzed by the RETRAN digital computer code. This code includes the simulation of prompt and delayed neutrons (using the six-group model), the thermal kinetics of the fuel and moderator and the balance of the NSSS primary and secondary coolant system. Thermal feedback is modeled via temperature dependent temperature coefficients of reactivity. A detailed core thermal/hydraulics analysis, performed with the COBRA IIIC/MIT code, demonstrates that cladding integrity is maintained throughout the transient. The analysis conservatively accounts for achievable power distribution at low power.

1. Since the magnitude of the power peak reached during the initial part of the transient for any given rate of reactivity insertion is strongly dependent on the Doppler coefficient, conservative values (low absolute values) as a function of temperature are used.
2. Contribution of the moderator reactivity coefficient is negligible during the initial part of the transient because the heat transfer time between the fuel and moderator is much longer than the neutron flux response time. However, after the initial neutron flux peak, the succeeding rate of power change is affected by the moderator reactivity coefficient. The conservative value of +6.0E-5 $\Delta k/k/°F$ is used in the analysis to yield the maximum peak heat flux.
3. The reactor is assumed to be at hot zero power. This assumption is more conservative than that of a lower initial system temperature. The higher initial system temperature yields a larger fuel-water heat transfer coefficient, larger specific heats, and a less negative (smaller

absolute value) Doppler coefficient, all of which tends to reduce the Doppler feedback effect, thereby increasing the neutron flux peak. The initial effective multiplication factor is assumed to be 1.0, since this results in maximum neutron flux peaking.

4. Reactor trip is assumed to be initiated by power range high neutron flux (low setting). The most adverse combination of instrument and setpoint errors, as well as delays for trip signal actuation and rod cluster control assembly release, is taken into account. A 10% increase is assumed for the power range flux trip setpoint, raising it from the nominal value of 25% to 35%. Previous results, however, have shown that the initial rise in the neutron flux is so rapid that the effect of errors in the trip setpoint on the actual time at which the rods are released is negligible. In addition, the reactor trip insertion characteristic is based on the assumption that the highest-worth rod cluster control assembly is stuck in its fully withdrawn position. See Section 15.1.5 for rod cluster control assembly insertion characteristics.

5. The maximum positive reactivity insertion rate assumed (1.0E-3 Δk/k/sec) is greater than that for the simultaneous withdrawal of the combination of the two control banks having the greatest combined worth at maximum speed (45 in/min). Control rod drive mechanism design is discussed in Section 4.2.3.

6. The initial power level was assumed to be below the power level expected for any shutdown condition. The combination of highest reactivity insertion rate and lowest initial power produces the highest peak heat flux.

7. Since the magnitude of the heat flux increases with increasing effective beta, a high value of the effective delayed neutron fraction (BOL) is assumed.

8. The reactor coolant flow rate is assumed to correspond to 3 pumps in service, since the Technical Specifications require 3 reactor coolant pumps in operation above Permissive P-6 in Modes 1 and 2. (Reactor protection at power levels below Permissive P-6 is provided by the source range reactor trip.)

15.2.1.2.2 Results

The neutron flux overshoots the full-power nominal value, but this occurs for only a very short time. Hence, the energy release and the fuel temperature increases are relatively small. The beneficial effect of the inherent thermal lag in the fuel is evidenced by a peak heat flux less than the full-power nominal value. There is a large margin to DNB during the transient, since the rod surface heat flux remains below the design value, and there is a high degree of subcooling at all times in the core. The neutron power versus time, clad and fuel temperature versus time, and the cold leg pressure versus time are presented in Figure 15.2-1, Figure 15.2-2, and Figure 15.2-3, respectively. A verification of the peak RCS pressure for the event was performed assuming a +3% shift in the pressurizer safety lift setpoint (+3% tolerance). The maximum RCS and main steam pressures remain below 110% of the RCS and main steam design pressures as shown in Figures 15.2-4 and 15.2-5.

15.2.1.3 Conclusions

In the event of a rod cluster control assembly withdrawal accident from the subcritical condition, the core and the reactor coolant system are not adversely affected, since the combination of thermal power and the coolant temperature results in a DNBR above the limit value. For the case with three reactor coolant pumps operating, the detailed core thermal/hydraulics analysis demonstrates considerable margin to the DNBR limit.

15.2.2 Uncontrolled Rod Cluster Control Assembly Bank Withdrawal at Power

15.2.2.1 Identification of Causes and Accident Description

The Uncontrolled Rod Cluster Control Assembly (RCCA) Bank Withdrawal at Power (RWAP) event is characterized by a reactivity increase resulting from the withdrawal of one or more RCCA Banks from the core during power operation. The initiating event is a postulated single failure in a control system such as the rod control system or faulty action by a reactor operator. The energy removal capabilities of the secondary system tend to lag behind the core power increase resulting from the rod bank withdrawal. This energy mismatch causes the Reactor Coolant System (RCS) pressure and temperature to increase. Unless terminated by manual or automatic action, the possibility exists that the core heat flux could exceed the ability of the RCS fluid to conduct the heat from the fuel, potentially leading to a Departure from Nucleate Boiling (DNB) and subsequent cladding failure. The RCS temperature and pressure transients can be limited by the operation of RCS and main steam (MS) pressure relief valves; however, the power excursion generally continues until terminated by the addition of negative reactivity from the RCCA bank insertion due to a reactor trip signal. The Reactor Coolant Pumps (RCPs) remain operational throughout the event so that, in the absence of DNB, sufficient RCS flow exists to accommodate the transfer of energy from the fuel to the reactor coolant.

As stated above, maintaining the fuel cladding integrity is the primary safety concern for the RWAP event. However, maintaining the RCS as a fission product barrier is also of importance. Specifically, the heating of the RCS fluid during a RWAP event causes the fluid density to increase, resulting in a volumetric expansion of the fluid. Operation of the pressurizer sprays and power operated relief valves (PORVs) can mitigate the effects of the subsequent pressure increase, but do not counteract the volumetric expansion. Should the expansion of the RCS fluid continue uncontested, the potential exists for discharge of liquid through the PORVs or pressurizer safety valves (PSVs). For the rod bank withdrawal at power event, the reactor protection system terminates the heatup of the reactor coolant system before any liquid relief occurs.

Provided the integrity of the fission product barriers is not compromised, sensible and decay heat can be removed by steaming to the condenser through the steam bypass system, to the atmosphere through the MS PORV or the main steam safety valves (MSSVs), or any combination of the three methods. Feedwater remains available to the steam generators (SGs) from either the main feedwater (MFW) system or the auxiliary feedwater (AFW) system to replenish the secondary coolant. Shortly after reactor trip, the energy removal capability of the SGs will exceed

the RCS sensible and decay heat levels, and the reactor operators/automatic control systems will function to maintain the plant at the new equilibrium condition.

The automatic features of the reactor protection system that prevent core damage in the event of an RWAP incident include the following:

1. Power range neutron flux instrumentation actuates a reactor trip if two out of four channels exceed an overpower setpoint.
2. Reactor trip is actuated if any two out of three delta T channels exceed an overtemperature delta T setpoint. This setpoint is automatically varied with axial power imbalance, coolant temperature, and pressure to protect against DNB.
3. Reactor trip is actuated if any two out of three delta T channels exceed an overpower delta T setpoint. This setpoint is automatically varied with axial power imbalance and coolant temperature to ensure that the allowable heat generation rate (kW/ft) is not exceeded.
4. A high pressurizer pressure reactor trip actuated from any two out of three pressure channels is set at a fixed point. This set pressure is less than the set pressure for the pressurizer safety valves.
5. A high pressurizer water level reactor trip actuated from any two out of three level channels is set at a fixed point.
6. In addition to the above-listed reactor trips, there are the following rod cluster control assembly withdrawal blocks:
   a. High-neutron-flux (one out of four).
   b. Overpower delta T (two out of three).
   c. Overtemperature delta T (two out of three).

The manner in which the combination of overpower and overtemperature delta T trips provides protection over the full range of reactor coolant system conditions is described in Chapter 7 and illustrated in Figure 15.1-1. Figure 15.1-1 illustrates reactor coolant loop average temperature and delta T for the design-power distribution and flow as a function of primary coolant pressure. The boundaries of operation defined by the overpower delta T trip and the overtemperature delta T trip are represented as “protection lines” on this diagram. The protection lines are drawn to include all adverse instrumentation and setpoint errors so that under nominal conditions trip would occur well within the area bounded by these lines. This diagram is useful in that the limit imposed by any given DNBR can be represented as a line. The DNB lines represent the locus of conditions for which the DNBR equals the limit value. All points below and to the left of a DNB line for a given pressure have a DNBR greater than the limit value. The diagram shows that DNB is prevented for all cases if the area enclosed with the maximum protection lines is not traversed by the applicable DNBR line at any point.

The area of operation (power, pressure, and temperature) for which core limits are not violated for the design-power distribution and flow rate is bounded by the combination of reactor trips: high-neutron-flux (fixed setpoint), high-pressure (fixed setpoint), low-pressure (anticipatory rate dependent setpoint), overpower and overtemperature delta T (variable setpoints).

The analysis presented below shows that no fuel damage occurs by demonstrating that the DNBR limit is met for the rod bank withdrawal event. Also shown is that the RCS system pressure relieving devices have sufficient capacities to ensure the safety of the unit without relying on the mitigating capabilities of the pressurizer pressure control systems. The RCS pressure does not exceed 110% of the system design pressure. The main steam system (MSS) pressure relief devices are shown to maintain the secondary system pressure below 110% of the system design pressure.

15.2.2.2 **Analysis of Effects and Consequences**

15.2.2.2.1 Method of Analysis

The RWAP transient is analyzed with the RETRAN (Reference 9) and COBRA (Reference 10) codes. The RETRAN system code simulates the neutron kinetics, RCS, pressurizer, pressurizer relief and safety valves, pressurizer spray, steam generator, and steam generator safety valves. The code computes pertinent plant variables, including temperatures, pressures, and power level. The COBRA code is used to calculate the DNBR for the transient using the WRB-1 DNB correlation.

For the DNBR evaluation cases, the initial power level, pressurizer pressure, and RCS average temperature are assumed to be at values consistent with the nominal hot full power (2893 MWt) value. The effects of normal control system variations and measurement uncertainties associated with these parameters are treated statistically and incorporated into the design DNBR limit as described in Chapter 4 in accordance with Virginia Power's Statistical DNBR Methodology (Reference 17).

For cases where reactor coolant system pressures are of primary interest, the initial reactor power, pressurizer pressure and average reactor coolant temperature are assumed to be at values consistent with steady state operation, including allowances for calorimetric and other instrument errors. In addition, these cases are performed with the pressurizer pressure relieving devices (pressurizer spray and PORVs) disabled and a bounding tolerance of +3% applied to the pressurizer safety valve lift setpoint.

For cases where the secondary system pressures are of primary interest, the analysis assumptions from the RCS peak pressure analysis are applied with some exceptions. Pressurizer spray and PORVs are enabled to delay the time to automatic reactor trip conditions to allow an increase in the RCS stored energy prior to reactor trip actuation. This results in an increase in energy deposited into the steam generator secondary side, causing a greater pressurization.

To obtain conservative results, the following assumptions are made:

1. Cases have been analyzed at nominal conditions and at a reduced average reactor coolant temperature of 10°F below the nominal full power value. The reduced temperature analyses have been performed to support reduced temperature operation for the purpose of retarding steam generator tube degradation rates.

   For the reduced temperature study those cases which showed the potential for filling the pressurizer and produced the lowest DNBRs (full power, minimum reactivity feedback with slow reactivity insertion rates) were analyzed at the reduced temperature.

2. Reactivity coefficients—two cases are analyzed:

   a. Minimum reactivity feedback. A positive moderator coefficient which bounds the Technical Specifications limit is assumed. A least negative Doppler temperature coefficient is used in the analysis.

   b. Maximum reactivity feedback. A conservatively large negative moderator temperature coefficient and a large (in absolute magnitude) negative Doppler temperature coefficient are assumed.

3. The reactor trip on high neutron flux is assumed to be actuated at a conservative value of 118% of nominal full power. The high pressurizer water level and overtemperature delta T trips include all adverse instrumentation and setpoint errors, while the delays for the trip signal actuation are assumed at their maximum value. No credit is taken for the overpower delta T reactor trip.

4. The rod cluster control assembly trip insertion characteristic is based on the assumption that the highest-worth assembly is stuck in its fully withdrawn position.

5. A spectrum of reactivity insertion rates was analyzed. The maximum positive reactivity insertion rate analyzed is greater than the rate of two sequential control banks moving at maximum speed with normal overlap.

6. Analyses were performed with 15% steam generator tube plugging (SGTP). Analysis results were shown to be conservative for the RCS overpressure criteria. The SGTP assumption had a negligible impact on the cases performed for the other acceptance criteria.

The effect of rod cluster control assembly movement on the axial core power distribution is accounted for by causing a decrease in the overtemperature delta T trip setpoint proportional to a decrease in margin to DNB, if the axial offset is outside that associated with the overtemperature delta T f(delta I) function.

15.2.2.2.2 Results

Figures 15.2-6 and 15.2-7 show the response of neutron flux, pressure, average coolant temperature, and DNBR to a rapid rod cluster control assembly bank withdrawal incident starting from full power. Reactor trip on high neutron flux occurs shortly after start of the accident. Since

this is rapid with respect to the thermal time constants of the plant, small changes in T_{avg} and pressure result, and a large margin to DNB is maintained.

Table 15.2-1 presents the time sequence of events for the Uncontrolled RCCA Bank Withdrawal transient.

The response of neutron flux, average coolant temperature, pressure, and DNBR for a slow rod assembly withdrawal from full power is shown in Figures 15.2-8 and 15.2-9. Reactor trip on overtemperature delta T occurs after a longer period, and rise in temperature and pressure is consequently larger than for rapid rod cluster control assembly withdrawal.

Figure 15.2-10 shows the minimum DNBR as a function of reactivity insertion rate from initial full-power operation for minimum and maximum reactivity feedback effects. It can be seen that two reactor trip channels provide protection over the whole range of reactivity insertion rates. These are the high-neutron-flux and overtemperature delta T trip channels. The minimum DNBR was determined as a function of reactivity insertion rate using the COBRA (Reference 10) code. The limiting case for DNB margin is a reactivity insertion rate of 1.2 pcm/sec at nominal reactor coolant temperature. The minimum DNBR is never less than the limit value. These results demonstrate that the core and reactor coolant system are not adversely affected by the rod bank withdrawal at power event since the high neutron flux and overtemperature delta T trips prevent the core minimum DNB ratio from falling below the limit value.

Figure 15.2-11 demonstrates the effect of initial RCS average temperature on minimum DNBR as a function of reactivity insertion rate. The minimum feedback, full power cases are presented. The figure demonstrates that the protection system provides DNB protection for the range of operating temperatures considered.

Figures 15.2-12 and 15.2-13 show the minimum DNBR as a function of reactivity insertion rate for rod cluster control assembly withdrawal incidents starting at 60% and 10% power, respectively. The results are similar to the 100% power case, except that as the initial power is decreased, the overtemperature delta T trip is effective for a greater range of reactivity insertion rates. The minimum DNBR is always greater than the limit value.

RWAP accident analyses performed to determine the maximum RCS pressure were initiated at power levels of 10%, 60%, and 100% of full power for a spectrum of reactivity insertion rates. The conditions that provide the maximum RCS pressure are 10% power, minimum reactivity feedback and high reactivity insertion rates. For the limiting analysis, reactor trip is initiated by high pressurizer pressure. Peak cold leg pressures obtained for bounding reactivity insertion rates were shown to be below the overpressure limit of 2750 psia (110% of the RCS design pressure of 2500 psia).

RWAP accident analyses performed to determine the maximum MSS pressure were initiated at 10%, 60%, and 100% of full power for a spectrum of reactivity insertion rates. The conditions that provide the maximum MSS pressure are those which allow a gradual but large rise

in the RCS average temperature, with an eventual reactor trip on overtemperature delta T. The maximum MSS pressure is fairly constant over a range of insertion rates, but the limiting case was at 10% power with maximum reactivity feedback and a bounding reactivity insertion rate. The limiting MSS pressure was considerably less than the secondary system overpressure limit of 1210 psia (110% of the MSS design pressure of 1100 psia).

15.2.2.3 Uncontrolled Rod Withdrawal Transient for Two-Loop Operation With and Without the Loop Stop Valves Closed

The preceding analyses were for normal three-loop operation. In addition, an analysis of an uncontrolled rod withdrawal transient for two-loop operation with loop stop valves open and closed was performed with the following initial conditions using the LOFTRAN (Reference 4) code and the W-3 correlation.

1. Initial Power Levels

   a. 65% and 10% of nominal three-loop power for two-loop operation with loop stop valves closed.

   b. 60% and 10% of nominal three-loop power for two-loop operation with loop stop valves open.

   A 2% calorimetric error allowance was added to initial power levels. The initial $F_{\Delta H}$ (see Section 15.1.2.3) was assumed to be equal to 1.55 [1 + .2(1-P)], where P is the fraction of nominal power.

2. Initial Core Flow Rate

   a. 71.3% of nominal three-loop volumetric flow for two-loop operation with loop stop valves closed.

   b. 62.4% of nominal three-loop volumetric flow for two-loop operation with loop stop valves open.

3. Initial Core Inlet Temperature

   Temperatures were calculated for each initial power level based on the average temperature program, where T_{avg} is 580.3°F at 100% power and 547°F at zero power.

   An allowance of +4°F is added for deadband and measurement error, plus an additional 2.5°F allowance for a total of 6.5°F on the initial value of T_{avg}. Section 15.1.2.2 provides additional explanation of the temperature error allowance.

The DNBRs as a function of reactivity insertion rate are shown in Figures 15.2-14 through 15.2-17. In all cases, the minimum DNBR remains above 1.30. The minimum DNBR for this incident is less limiting for two-loop operation than for three-loop operation.

15.2.2.4 Conclusions

The high-neutron-flux and overtemperature delta T trip channels provide adequate protection over the entire range of possible reactivity insertion rates, i.e., the minimum value of DNBR is always larger than the limit value. Pressure at the most limiting RCS location is less than the overpressure limit of 2750 psia (110% of RCS design pressure). Pressure at the most limiting MSS location is less than 1210 psia (110% of MSS design pressure). Pressurizer overfill is prevented by the reactor trip system.

15.2.3 Rod Cluster Control Assembly Misalignment (System Malfunction or Operator Error)

15.2.3.1 Identification of Causes and Accident Description

Rod cluster control assembly (RCCA) misoperation accidents include:

1. One or more dropped RCCAs within the same group;
2. A dropped RCCA bank;
3. Statically misaligned RCCA.

Each RCCA has a position indicator channel which displays the position of the assembly. The displays of assembly positions are grouped for the operator's convenience. Fully inserted assemblies are further indicated by a rod at bottom signal, which actuates a local alarm and a control room annunciator. Group demand position is also indicated.

Full length RCCAs are always moved in preselected banks, and the banks are always moved in the same preselected sequence. Each bank of RCCAs is divided into two groups. The rods comprising a group operate in parallel through multiplexing thyristors. The two groups in a bank move sequentially such that the first group is always within one step of the second group in the bank. A definite schedule of actuation (or deactuation of the stationary gripper, movable gripper, and lift coils of a mechanism) is required to withdraw the RCCA attached to the mechanism. Since the stationary gripper, movable gripper, and lift coils associated with the four RCCAs of a rod group are driven in parallel, any single failure which would cause rod withdrawal would affect a minimum of one group. Mechanical failures are in the direction of insertion, or immobility.

A dropped RCCA or RCCA bank is detected by:

1. Sudden drop in the core power level as seen by the Nuclear Instrumentation System,
2. Asymmetric power distribution as seen on out-of-core neutron detectors or core exit thermocouples,
3. Rod at bottom signal,
4. Rod deviation alarm, or
5. Rod position indication.

Misaligned RCCAs are detected by:

1. Asymmetric power distribution as seen on out-of-core neutron detectors or core exit thermocouples,
2. Rod deviation alarm, or
3. Rod position indicators.

The resolution of the rod position indicator channel is ±5 percent of span (±7.2 inches). Deviation of any RCCA from its group by twice this distance (10% of span, or 14.4 inches) will not cause power distributions worse than the design limits. The deviation alarm alerts the operator to rod deviation with respect to the group position in excess of 5% of span.

If one or more rod position indicator channels should be out of service, detailed operating instructions shall be followed to assure the alignment of the non-indicated RCCAs. The operator is also required to take action as required by the Technical Specifications.

15.2.3.2 **Analysis of Effects and Consequences**

Method of Analysis

a. One or more dropped RCCAs from the same group.

   For evaluation of the dropped RCCA event, the transient system response is calculated using either the LOFTRAN (Reference 4) or RETRAN (Reference 9) code. These codes simulate the neutron kinetics, Reactor Coolant System, pressurizer, pressurizer relief and safety valves, pressurizer spray, steam generator, and steam generator safety valves. These codes compute pertinent plant variables including temperatures, pressures, and power level.

   Statepoints are calculated and nuclear models are used to obtain a hot channel factor consistent with the primary system conditions and reactor power. By incorporating the primary conditions from the transient and the hot channel factor from the nuclear analysis, the DNB design basis is shown to be met using the COBRA (Reference 10) code. The transient response, nuclear peaking factor analysis, and DNB design basis confirmation are performed in accordance with the methodology described in Reference 11.

b. Statically Misaligned RCCA

   Steady state power distributions are analyzed using the computer codes as described in Table 4.1-2. The peaking factors are then used as input to the COBRA (Reference 10) code to calculate the DNBR.

Results

a. One or more Dropped RCCAs

Single or multiple dropped RCCAs within the same group result in a negative reactivity insertion which may be detected by the power range negative neutron flux rate trip circuitry. If detected, the reactor is tripped within approximately 2.5 seconds following the drop of the RCCAs. The core is not adversely affected during this period, since power is decreasing rapidly. Following reactor trip, normal shutdown procedures are followed. The operator may manually retrieve the RCCA by following approved operating procedures.

For those dropped RCCAs which do not result in a reactor trip, power may be reestablished either by reactivity feedback or control bank withdrawal. Following a dropped rod event in manual rod control, the plant will establish a new equilibrium condition. The equilibrium process without control system interaction is monotonic, thus removing power overshoot as a concern, and establishing the automatic rod control mode of operation as the limiting case.

For a dropped RCCA event in the automatic control mode, the Rod Control System detects the drop in power and initiates control bank withdrawal. Power overshoot may occur due to this action by the automatic rod controller after which the control system will insert the control bank to restore nominal power. Figure 15.2-18 shows a typical transient response to a dropped RCCA (or RCCAs) in automatic control. Uncertainties in the initial condition are included in the DNB evaluation as described in Reference 17. In all cases, the minimum DNBR remains above the limit value.

b. Dropped RCCA Bank

A dropped RCCA bank typically results in a reactivity insertion greater than 500 pcm which will be detected by the power range negative neutron flux rate trip circuitry. The reactor is tripped within approximately 2.5 seconds following the drop of a RCCA Bank. The core is not adversely affected during this period, since power is decreasing rapidly. Following reactor trip, normal shutdown procedures are followed to further cool down the plant.

c. Statically Misaligned RCCA

The most severe misalignment situations with respect to DNBR at significant power levels arise from cases in which one RCCA is fully inserted, or where bank D is fully inserted with one RCCA fully withdrawn. Multiple independent alarms, including a bank insertion limit alarm, alert the operator well before the postulated conditions are approached. The bank can be inserted to its insertion limit with any one assembly fully withdrawn without the DNBR falling below the limit value.

The insertion limits in the Technical Specifications may vary from time to time depending on a number of limiting criteria. It is preferable, therefore, to analyze the misaligned RCCA case at full power for a position of the control bank as deeply inserted as the criteria on minimum DNBR and power peaking factor will allow. The full power insertion limits on control bank D must then be chosen to be above that position and will usually be dictated by other criteria. Detailed results will vary from cycle to cycle depending on fuel arrangements.

For this RCCA misalignment, with bank D inserted to its full power insertion limit and one RCCA fully withdrawn, DNBR does not fall below the limit value. This case is analyzed assuming the initial reactor power, pressure, and RCS temperatures are at their nominal values including uncertainties but with the increased radial peaking factor associated with the misaligned RCCA.

DNB calculations have not been performed specifically for RCCAs missing from other banks; however, power shape calculations have been done as required for the RCCA ejection analysis. Inspection of the power shapes shows that the DNB and peak kw/ft situation is less severe than the bank D case discussed above assuming insertion limits on the other banks equivalent to a bank D full-in insertion limit.

For RCCA misalignments with one RCCA fully inserted, the DNBR does not fall below the limit value. The case is analyzed assuming the initial reactor power pressure, and RCS temperatures are at their nominal values, including uncertainties but with the increased radial peaking factor associated with the misaligned RCCA.

DNB does not occur for the RCCA misalignment incident and thus the ability of the primary coolant to remove heat from the fuel rod is not reduced. The peak fuel temperature corresponds to a linear heat generation rate based on the radial peaking factor penalty associated with the misaligned RCCA and the design axial power distribution. The resulting linear heat generation is well below that which would cause fuel melting.

Following the identification of a RCCA group misalignment condition by the operator, the operator is required to take action as required by the plant Technical Specifications and operating instructions.

15.2.3.3 **Conclusions**

For cases of dropped RCCAs or dropped banks, for which the reactor is tripped by the power range negative neutron flux rate trip, there is no reduction in the margin to core thermal limits, and consequently the DNB design basis is met. It is shown for all cases which do not result in reactor trip that the DNBR remains greater than the limit value and, therefore, the DNB design basis is met.

For all cases of any RCCA fully inserted, or bank D inserted to its rod insertion limits with any single RCCA in that bank fully withdrawn (static misalignment), the DNBR remains greater than the limit value.

15.2.4 Uncontrolled Boron Dilution

15.2.4.1 Identification of Causes and Accident Description

Reactivity can be added to the core by feeding primary-grade water into the reactor coolant system via the reactor makeup portion of the chemical and volume control system. Boron dilution is a manual operation under strict administrative controls with procedures calling for a limit on the rate and duration of dilution. A boric acid blend system is provided to permit the operator to match the boron concentration of reactor coolant makeup water during normal charging to that in the reactor coolant system. The chemical and volume control system is designed to limit, even under various postulated failure modes, the potential rate of dilution to a value which, after indication through alarms and instrumentation, provides the operator sufficient time to correct the situation in a safe and orderly manner.

The opening of the primary water makeup control valve creates a dilution flow path to the reactor coolant system. Inadvertent dilution from this source can be readily terminated by closing the control valve. For makeup water to be added to the reactor coolant system at pressure, at least one charging pump must be running in addition to a primary grade water makeup pump.

The rate of addition of unborated makeup water to the reactor coolant system when it is not at pressure is limited by the capacity of the two primary grade water transfer pumps. The maximum addition rate is 245 gpm with both pumps running. Normally, only one charging pump is operating. The boric acid from the boric acid storage tank is blended with primary grade water in the blender; the composition is determined by the preset flow rates of boric acid and primary-grade water on the control board.

Two separate operations are required to dilute: (1) The operator must switch from the automatic makeup mode to the dilute mode. (2) The start position must be selected. Omitting either step prevents dilution.

Information on the status of the reactor coolant makeup is continuously available to the operator. Lights are provided on the control board to indicate the operating condition of the pumps in the chemical and volume control system. Alarms are actuated to warn the operator if boric acid or demineralized water flow rates deviate from preset values as a result of system malfunction.

15.2.4.2 Analysis of Effects and Consequences

15.2.4.2.1 Method of Analysis

Boron dilution events are considered for all operating modes, including refueling, cold shutdown, hot shutdown, hot standby, startup, and power operation (automatic and manual control modes). The case of an inadvertent dilution during a planned dilution or makeup activities is not considered here, since evaluation of such dilutions is not required by the Standard Review Plan. Boron dilution during startup of an inactive loop is discussed in Section 15.2.6.

15.2.4.2.2 Boron Dilution During Modes Other Than Power Operation

The effects of postulated boron dilution incidents have been analyzed in accordance with the conservative assumptions stated in Section 15.4.6 of the NRC Standard Review Plan. To ensure that the acceptance criteria given in Regulatory Position 15.4.6 are met during refueling, cold shutdown, hot shutdown, hot standby, and startup, the following actions shall be taken.

The following description is applicable to isolation of primary grade makeup water to the reactor coolant system for Unit 1 or Unit 2 (Unit 2 valve numbers are noted in parentheses). During refueling, cold shutdown, hot shutdown, and hot standby; manual valve 1-CH-217 (2-CH-140), the primary makeup water control valve, shall be locked in the closed position except during planned dilution or makeup activities. This ensures that the source of primary grade water is completely isolated from the reactor coolant system. Alternatively, manual valves 1-CH-220 (2-CH-160), 1-CH-241 (2-CH-156), and flow control valves FCV-1114B and FCV-1113B (FCV-2114B and FCV-2113B) may be locked shut if for any reason it is desired that 1-CH-217 (2-CH-140) be maintained open. This alternative combination of valve lockouts has the same effect as locking out valve 1-CH-217 (2-CH-140).

To protect against the potential effects of a boron dilution incident during an approach to critical, the shutdown rod banks shall be withdrawn from the core while the unit is at start-up conditions. Should an unplanned boron dilution incident occur at start-up conditions (either because of equipment failure or operator error), the high flux at shutdown alarm will alert the operator of this condition and the shutdown rod banks can be inserted into the core immediately. This will give the operator sufficient time to isolate the sources of primary grade water from the reactor coolant system before shutdown margin is lost.

The boron dilution analysis applicable to startup conditions (reactor critical with control rods above the rod insertion limits) demonstrates that Technical Specification shutdown margin requirements are adequate to ensure that 15 minutes are available for corrective operator action between positive indication of a boron dilution in progress and complete loss of shutdown margin. The analysis assumes that the transient is initiated from a zero power critical condition, and that positive indication of a dilution in progress is not generated until sufficient reactivity has been added to the core to create a prompt critical condition. For boron dilution events initiated from power levels greater than zero percent power, the boron dilution event analysis applicable to at-power conditions demonstrates the adequacy of shutdown margin requirements to provide sufficient time for corrective operator action in response to an inadvertent boron dilution event.

By the proper implementation of the above procedures, the probability of a boron dilution incident occurring is greatly reduced, and should it occur, a well-defined corrective action exists for the reactor operator to maintain shutdown margin while he terminates the flow of the primary grade water into the reactor coolant system.

15.2.4.2.3 Boron Dilution at Power

With the unit at power and the reactor coolant system at pressure, the dilution rate is limited by the capacity of the charging pump. The boron dilution analysis applicable to at-power conditions demonstrates that at least 15 minutes are available for corrective operator response between positive indication of a dilution in progress (by alarm or reactor trip) and complete loss of shutdown margin (Reference 16). A conservative dilution flow rate of 165 gpm was assumed. Credit is taken for the proper functioning of the overtemperature ΔT and power range high flux reactor trips, and the rod insertion limit alarm.

The time sequence of events for the boron dilution at power event is presented in Table 15.2-1.

15.2.4.3 **Conclusions**

Because of the procedures involved in the dilution process, and the administrative blocking of the primary grade water flow path, an erroneous dilution is not considered credible. Nevertheless, numerous alarms and indications are available to alert the operator to any unintentional dilution of boron in the reactor coolant. For credible boron dilution events, such as the case of boron dilution at power, the maximum reactivity addition rate is slow enough to allow the operator to determine the cause of the addition and to take corrective action before the excessive shutdown margin is lost.

15.2.5 Partial Loss of Forced Reactor Coolant Flow

15.2.5.1 **Identification of Causes and Accident Description**

A partial-loss-of-coolant-flow accident can result from a mechanical or electrical failure in a reactor coolant pump, from a fault in the power supply to the pump, or from inadvertent closure of a loop isolation valve. If the reactor is at power at the time of the accident, the immediate effect of loss of coolant flow is a rapid increase in the coolant temperature. This increase could result in DNB with subsequent fuel damage if the reactor is not tripped promptly.

The inadvertent closure of a reactor cooling loop isolation valve is unlikely, since the motor starters for these valves are locked out during normal operations. The starters would be made operational only in the process of isolating or unisolating a loop, which would then proceed according to specified operating instructions. The motors starters in the other loops would continue to be locked out during this procedure.

The necessary protection against a partial-loss-of-coolant-flow accident is provided by the low primary-coolant-flow reactor trip, which is actuated by two out of three low-flow signals in any reactor coolant loop. Above the power level associated with Permissive 8, low flow in any loop will actuate a reactor trip. Between the power level associated with Permissive 7 and the power level corresponding to Permissive 8, low flow in any two loops will actuate a reactor trip. A reactor trip signal from the pump breaker position is provided as an anticipatory signal, which serves as a backup to the low-flow signal. It functions essentially identically to the low-flow trip,

so that above Permissive 8 a breaker-open signal from any pump will actuate a reactor trip, and between Permissive 7 and Permissive 8 a breaker-open signal from any two pumps will actuate a reactor trip.

If a loop isolation valve were inadvertently closed, either with partial-loop or three-loop operation, the reactor would be tripped by a low-flow reactor trip signal in the affected loop. The resulting flow coastdown transient would be less severe than that resulting from a loss of power to a reactor coolant pump.

Normal power for the pumps is supplied through buses connected to the generator. Each pump is on a separate bus. When a generator trip occurs, the pumps are automatically transferred to a bus supplied from external power lines, and the pumps will continue to supply coolant flow to the core. Following any turbine trip where there are no electrical faults that require tripping the generator from the network, the generator remains connected to the network for approximately 30 seconds. The reactor coolant pumps remain connected to the generator, thus ensuring full flow for approximately 30 seconds after the reactor trip before any transfer is made.

15.2.5.2 **Analysis of Effects and Consequences**

15.2.5.2.1 Method of Analysis

The analysis of the complete loss of reactor coolant flow (UFSAR Section 15.3.4) has been performed using the identical reactor protection instrumentation and setpoints as would be used for the partial loss of flow (namely, low flow reactor trip). Also, the acceptance criteria associated with the partial loss of flow accident (Condition II) have been conservatively applied to the complete loss of flow (Condition III). Therefore, the partial loss of flow accident is bounded by the analysis of the complete loss of flow, and no specific partial loss of flow analyses are performed.

15.2.5.3 **Conclusions**

The analysis shows that for the more limiting complete loss of reactor coolant flow accident the DNBR will not decrease below the limit value at any time during the transient. Thus, there will be no cladding damage and no release of fission products to the reactor coolant system for the less limiting partial loss of flow accident.

15.2.6 Start-Up of An Inactive Reactor Coolant Loop

15.2.6.1 **Identification of Causes and Accident Description**

The Startup of an Inactive Loop (SUIL) event is defined as an uncontrolled reduction in coolant temperature or boron concentration in the region of the core resulting from either (a) the startup of an RCP on an idle loop (i.e., the Loop Stop Valves Open case), or (b) recirculation through a loop stop valve bypass line on an isolated loop (i.e., Loop Stop Valve Closed case), when a reduced coolant temperature or boron concentration exists in the idle (or isolated) loop. When no coolant temperature or boron concentration differential exists between the idle or

isolated loop and the active portion of the RCS, the startup of an inactive loop does not result in reactivity insertion, erosion of shutdown margin (SDM), power excursion, or reduction in margin to a Departure from Nucleate Boiling (DNB) condition.

The accident analyses demonstrate that fuel integrity limits are not challenged by a reactivity insertion event resulting from the startup of an inactive loop. For both the Loop Stop Valves Open and Loop Stop Valves Closed cases, no specific transient analysis is required to demonstrate that fuel integrity limits are not challenged by a reactivity insertion event resulting from the startup of an inactive loop. Instead, a high level of confidence that fuel integrity limits are not challenged is demonstrated through consideration of the Technical Specification requirements for isolated loop boron concentration, isolated loop temperature, and loop stop valve operation. Technical Specifications and associated procedures ensure that the preconditions necessary for significant reactivity insertion during a SUIL accident (i.e., significantly reduced temperature or boron concentration during loop startup) cannot be achieved under credible circumstances. Administrative controls on loop stop valve operations are described in Section 15.2.6.2.

Because startup of an inactive loop is a deliberate action under operator control governed by Technical Specifications, the sequence of operator errors required for a SUIL event to occur is considered non-credible. However, an analysis of the SUIL Loop Stop Valves Closed case is considered herein in which the loop stop valve bypass line recirculation activity required by Technical Specifications is performed assuming a conservatively large and non-credible boron concentration differential between the isolated loop and the active portion of the RCS. This analysis is described in Section 15.2.6.3. An analysis of the reactivity effects of inadvertent loop startup with reduced temperature in the isolated loop is also presented in Section 15.2.6.3.

15.2.6.2 **Controls on Loop Stop Valve Operation**

Two methods are available to the operations staff for restoring an idle loop to service: backfilling a drained loop and slow mixing of an undrained loop. If the idle loop is completely drained, it may be restored to service by partially opening the loop stop valves and allowing flow from the active portion of the RCS to the loop simultaneous with makeup from the chemical and volume control system. Administrative controls on fluid level in the active portion of the RCS limit the potential for loss of suction at the inlet to the residual heat removal pumps. Source range count rate is carefully monitored during the evolution to ensure that the makeup is at the proper boron concentration.

If the isolated loop is filled, the isolated section of the loop may be cooler than the temperature of the active loops. Administrative procedures require the temperature of the isolated loop to be brought to within 20°F of the active loops, and the boron concentration of the isolated loop to be verified prior to opening the loop stop valves and returning the loop to service.

Administrative controls are provided to ensure that an accidental start-up of an isolated loop that has a lower temperature or lower boron concentration than the core and active loops will be a

relatively slow event. The controls ensure that flow from the isolated loop to the remainder of the reactor coolant system takes place through the relief line bypassing the cold-leg stop valve for at least 90 minutes before the cold-leg stop valve can be opened. The flow through the bypass line is low (less than 330 gpm) so that any temperature or boron concentration differences between the isolated loop and the remainder of the system are brought to equilibrium at a relatively slow rate.

For an undrained isolated loop, procedures are provided to:

1. Prevent opening of a hot-leg loop stop valve unless the cold-leg stop valve in the same loop is fully closed.
2. Prevent starting a reactor coolant pump unless:
   a. The cold-leg loop stop valve in the same loop is fully closed and the bypass valve open, or
   b. Both the hot-leg loop stop valve and cold-leg loop stop valve are fully open.
3. Prevent opening of a cold-leg stop valve unless:
   a. For a period of at least 90 minutes:
      1) The hot-leg loop stop valve in the same loop has been open.
      2) The bypass valve in the loop has been open.
      3) Flow has existed through the relief line.
   b. The cold-leg temperature is within 20°F of the highest cold-leg temperature in the other loops.
   c. The reactor is subcritical by at least 1.77% $\Delta k/k$.

Verification of loop stop valve position and relief line flow is provided by instrumentation that includes the following redundancies:

1. Two independent limit switches to indicate that a valve is fully open.
2. Two independent limit switches to indicate that a valve is fully closed.
3. Two differential pressure switches in each line that bypasses a cold-leg loop stop valve to determine that flow exists in the line. Flow through the line indicates:
   a. The valves in the line are open.
   b. The pump in the isolated loop is running.

The indications meet the IEEE 279 criteria and, therefore, cannot be negated by a single failure.

15.2.6.3 **Analysis of Effects and Consequences**

15.2.6.3.1 Method of Analysis

The start-up of an inactive reactor coolant loop with the loop stop valves initially closed has been analyzed with both a “dilution front” and a “perfect mixing” model, and a set of conservative analysis assumptions. The “dilution front” model is appropriate for conditions in which the ratio of the flow rate in the active portion of the Reactor Coolant System to the dilution flow rate is not sufficiently high to permit a “perfect mixing” assumption. The model assumes that, because of the relative flow rates, the inventory transferred from the isolated loop causes a diluted slug of water to pass through the reactor core. With each loop transit, the boron concentration of the slug of water “steps down” to a value calculated as a weighted average based on the dilution flow rate and boron concentration and the RHR flow rate and the boron concentration of coolant in the active portion of the RCS. The “perfect mixing” model assumes that the inventory transferred from the isolated loop during each time step is instantaneously distributed throughout the active portion of the reactor coolant system. Likewise, the model assumes that inventory transferred from the active portion of the reactor coolant system during each time step is instantaneously distributed throughout the isolated loop.

The analysis assumes that three RCS loops are isolated and RHR is in operation when the isolated loop recirculation procedure is initiated. The analysis considers RHR flow rates as low as the design minimum flow rate of 2000 gpm. The volume of the active portion of the reactor coolant system is assumed to be 3345 ft^3, consistent with the aforementioned loop configuration. The analysis assumes an initial RCS boron concentration of 1800 ppm. This boron concentration conservatively bounds the predicted boron concentration required to meet the Core Operating Limits Report (COLR) minimum shutdown margin requirement of 1.77% $\Delta k/k$ at Cold Zero Power (CZP), Beginning of Cycle (BOC), All Rods In (ARI), No Xenon (Xe) conditions. The isolated loop boron concentration was assumed to be 1300 ppm, 500 ppm less than the 1800 ppm concentration assumed to exist initially in the active portion of the RCS. The concentration difference is conservative, given that the Technical Specifications governing restoration of isolated and drained loops to service ensure that the boron concentration in the isolated loop will be greater than or equal to the boron concentration corresponding to the mode-dependent shutdown margin requirement (e.g., 1800 ppm). The design maximum loop stop valve bypass line flow rate of 330 gpm was assumed to be transferred to the reduced RCS volume. The analysis assumes a differential boron worth that conservatively bounds values expected to occur over core life.

The erosion of shutdown margin due to the introduction of coolant with reduced temperature but with adequate boron concentration has also been analyzed. The analysis assumed introduction of 32°F water into a core operating at 200°F at end-of-cycle with no mixing between the cold loop and the other loops. This scenario is non-credible, but it conservatively bounds the conditions allowed under Technical Specifications (i.e., the cold-leg loop stop valve may not be

opened unless the cold-leg temperature is within 20°F of the highest cold-leg temperature in the other loops).

15.2.6.3.2 Results

Even with the assumption that Technical Specifications and plant procedures are violated to the extent that an attempt is made to open the loop stop valves with 1300 ppm in the inactive loop while the remaining portion of the system is at 1800 ppm, the dilution of the boron in the core is slow. In the "perfect mixing" model analysis, the calculated initial reactivity insertion rate during the transient was approximately 1.4 pcm/sec, well within the range of reactivity insertion rates considered in the Rod Withdrawal from Subcritical accident analysis. The time required for shutdown margin to be lost and the reactor to become critical was determined to be approximately 50.5 minutes. In the "dilution front" model analysis, the calculated average reactivity insertion rate during the transient was approximately 2.3 pcm/second. The time required for shutdown margin to be lost and the reactor to become critical was determined to be greater than 17.0 minutes. These results indicate that there is ample time for the operator to recognize a high count rate signal, and to terminate the dilution by turning off the pump in the inactive loop or by borating to counteract the dilution.

The reactivity addition at end of life due to an attempt to open stop valves when the inactive loop temperature is less than the core temperature is smaller than the reactivity addition considered in the above beginning-of-life case. The temperature-reduction analysis demonstrated that the net reactivity addition was less than one half of the minimum shutdown margin required by Technical Specifications.

15.2.6.4 **Conclusions**

The current SUIL design and licensing bases credit Technical Specification controls to preclude the possibility of a significant inadvertent reactivity addition during or following loop stop valve operations. Because startup of an inactive loop is a deliberate action under operator control governed by Technical Specifications, the sequence of operator errors required for a SUIL event to occur is considered non-credible. The administrative procedures governed by Technical Specifications ensure that the isolated loop's temperature and boron concentration are brought to equilibrium with the remainder of the system at a slow rate. However, an analysis of the reactivity effects of the loop stop valve bypass line recirculation activity required by Technical Specifications has been performed assuming a conservatively large and non-credible boron concentration differential between the isolated loop and the active portion of the RCS. The analysis demonstrates that the reactivity addition rate is slow enough to allow the operator to take corrective action before shutdown margin is lost.

In addition, an analysis has been performed to evaluate the reactivity effects of loop stop valve operation with reduced coolant temperature in the isolated loop. Neither the inadvertent opening of a loop stop valve nor the loop stop valve bypass line recirculation activity required by

Technical Specifications presents any concerns relative to loss of shutdown margin under conditions of reduced isolated loop temperature.

15.2.7 Loss of External Electrical Load and/or Turbine Trip

15.2.7.1 Identification of Causes and Accident Description

Major load loss on the plant can result from loss of external electrical load or from a turbine trip. For either case, offsite power is available for the continued operation of plant components such as the reactor coolant pumps. The case of loss of all ac power is analyzed in Section 15.2.9.

For a turbine trip, the reactor would be tripped directly (unless below approximately 30% power) from a signal derived from the turbine autostop oil pressure and turbine stop valves. The automatic steam dump system would accommodate the excess steam generation. Reactor coolant temperatures and pressure do not significantly increase if the steam dump system and pressurizer pressure control system are functioning properly. If the turbine condenser was not available, the excess steam generation would be dumped to atmosphere. Additionally, main feedwater flow would be lost if the turbine condenser was not available. For this situation, feedwater flow would be maintained by the auxiliary feedwater system.

For a loss of external electrical load without subsequent turbine trip, no direct reactor trip signal would be generated. The plant is designed to accept a 50% step loss of load without actuating a reactor trip. The automatic steam bypass system with 40% steam dump capacity to the condenser is able to accommodate this load rejection by reducing the transient imposed upon the reactor coolant system. The reactor power is reduced to the new equilibrium power level at a rate consistent with the capability of the rod control system. The pressurizer relief valves may be actuated, but the pressurizer safety valves and the steam generator safety valves do not lift for the 50% load rejection with steam dump.

Should the steam dump valves fail to open, or should their capacity be exceeded following a large loss of load, the steam generator safety valves may lift and the reactor may be tripped by the high pressurizer pressure signal, the high pressurizer water level signal, or the overtemperature delta T signal. The steam generator shell-side pressure and reactor coolant temperatures will increase rapidly. The pressurizer safety valves and steam generator safety valves are, however, sized to protect the reactor coolant system and steam generator against overpressure for all load losses without assuming the operation of the steam dump system, pressurizer spray, pressurizer power-operated relief valves, automatic rod cluster control assembly control, or direct reactor trip resulting from turbine trip.

The steam generator safety valve capacity is sized to remove the steam flow at the engineered safeguards design rating (approximately 105% of steam flow at rated power) from the steam generator without exceeding 110% of the steam system design pressure. The pressurizer safety valve capacity is based on a complete loss of heat sink with the plant initially operating at the maximum calculated turbine load along with operation of the steam generator safety valves.

The pressurizer safety valves are then able to maintain the reactor coolant system pressure within 110% of the reactor coolant system design pressure without direct or immediate reactor trip action. Consequently, this incident is not sensitive to initial pressurizer level, and the programmed level versus power is assumed.

A more complete discussion of overpressure protection can be found in Reference 8.

15.2.7.2 **Analysis of Effects and Consequences**

15.2.7.2.1 Method of Analysis

The total-loss-of-load transient is analyzed with the computer program RETRAN (Reference 9) for both DNBR and non-DNBR cases. The program simulates the neutron kinetics, reactor coolant system, pressurizer, pressurizer relief and safety valves, pressurizer spray, steam generator, and steam generator safety valves. The program computes pertinent plant variables including temperatures, pressures, flow, and power level.

For DNBR analysis, the COBRA (Reference 10) code is then used to calculate the minimum DNBR during the transient based upon the heat flux, flow, temperature, and pressure from RETRAN. The WRB-1 critical heat flux correlation is used.

The following assumptions are made in the DNBR cases:

1. The behavior of the unit is evaluated for a complete loss of steam load from 100% of full power without a direct reactor trip to demonstrate core protection margins. A statistical treatment of key DNBR analysis parameter uncertainties is employed. Therefore, normal initial RCS conditions are assumed, and allowances for calibration and instrument errors are incorporated into the limit DNBR value as described in Chapter 4.
2. A positive moderator temperature coefficient conservative for BOC conditions and a least negative Doppler temperature coefficient are assumed.
3. Credit is taken for the effect of pressurizer spray and power operated relief valves in reducing or limiting the coolant pressure.
4. Main Feedwater flow is isolated at the time of the turbine trip.

The following assumptions are made in the non-DNBR cases:

1. The behavior of the unit is evaluated for a complete loss of steam load from full power without a direct reactor trip to demonstrate the adequacy of the pressure-relieving devices. A deterministic treatment of uncertainties in initial RCS operating conditions (e.g., pressure, temperature, flow, and core power) is used in the analysis.
2. A zero moderator temperature coefficient and a most negative Doppler temperature coefficient are assumed.

3. The reactor is assumed to be in manual control, which is conservative from the standpoint of maximum pressure attained.
4. No credit is taken for the effect of pressurizer spray and power operated relief valves in reducing or limiting the coolant pressure.
5. The pressurizer safety valve tolerance is assumed +2%/-3% with no valve outside ±3%. (Only the results of the overpressure transients are sensitive to the safety valve tolerance. The DNBR results are not sensitive to this parameter.)
6. Main Feedwater flow is isolated at the time of the reactor trip.

The following assumptions are made in both the DNBR case and non-DNBR case:

1. No credit is taken for the operation of the steam dump system, steam generator power operated relief valves, or direct reactor trip on turbine trip. The reactor is tripped on high pressurizer pressure. The steam generator pressure rises to the safety valve setpoint, where steam release through safety valves limits secondary steam pressure at the setpoint value.
2. No credit is taken for auxiliary feedwater flow since a stabilized plant condition will be reached before auxiliary feedwater initiation is normally assumed to occur. The auxiliary feedwater flow would remove core decay heat following plant stabilization.

15.2.7.2.2 Results

The transient responses for a total loss of load from 100% full power case for DNBR analysis are shown in Figures 15.2-19 through 15.2-23. The minimum DNBR achieved during the transient is well above the limit value.

The transient responses for a total loss of load from 102% full power case for non-DNBR conditions (i.e., for RCS and main steam overpressurization concerns) are shown in Figures 15.2-25 through 15.2-30.

Table 15.2-1 presents the sequence of events for the Loss of External Electrical Load Transient.

Section 15.2.8 presents additional results of analysis for a complete loss of heat sink including loss of main feedwater. This report shows the overpressure protection that is afforded by the pressurizer and steam generator safety valves.

The analysis results show that the peak RCS pressure is below the acceptance criterion of 2750 psia and the main steam peak pressure is below the acceptance criterion of 1210 psia. Thus, the results of the loss of load transient analysis support the conclusion that this event poses no hazard to the integrity of the reactor coolant system or the main steam system.

15.2.7.3 Conclusions

Results of the analyses, including those in Section 15.2.8, show that a total loss of external electrical load without a direct or immediate reactor trip presents no hazard to the integrity of the reactor coolant system or the main steam system. Pressure-relieving devices incorporated in the two systems are adequate to keep the maximum pressures within the design limits.

The integrity of the core is maintained by operation of the reactor protection system, i.e., the DNBR will be maintained above the limit value. Thus there will be no cladding damage and no release of fission products to the reactor coolant system.

15.2.8 Loss of Normal Feedwater

15.2.8.1 Identification of Causes and Accident Description

A loss of normal feedwater (from pump failures, valve malfunctions, or loss of offsite ac power) results in a reduction in the capability of the secondary system to remove the heat generated in the reactor core. If the reactor were not tripped during this accident, core damage would possibly occur from a sudden loss of heat sink. If an alternative supply of feedwater were not supplied to the plant, residual heat following reactor trip would heat the primary system water to the point where water relief from the pressurizer occurs. Significant loss of water from the reactor coolant system could conceivably lead to core damage. Since the plant is tripped well before the steam generator heat transfer capability is reduced, the primary system variables never approach a DNB condition.

The following provide the necessary protection against a loss of normal feedwater:

1. Reactor trip on low-low water level in any steam generator or on water level below the AMSAC (ATWS Mitigating Systems Actuating Circuitry) setpoint in two steam generators after a time delay; providing C-20 permissive is satisfied.
2. Reactor trip on low feedwater flow signal in any steam generator. (This signal is actually a steam flow - feedwater flow mismatch in coincidence with low SG water level.)
3. Two motor-driven auxiliary feedwater pumps (capable of delivering at least 300 gpm each) that are started on:
   a. Low-low level in any steam generator.
   b. Trip of all main feedwater pumps.
   c. Any safety injection signal.
   d. Loss of offsite power.
   e. Manual actuation.
   f. AMSAC actuation.

4. One turbine-driven auxiliary feedwater pump which is started on the same signals as the motor-driven pumps.

The motor-driven auxiliary feedwater pumps are supplied by offsite power; the turbine-driven pump uses steam from the secondary system. Both types of pump are designed to start within 1 minute. The turbine-driven pump exhausts to the atmosphere. The auxiliary pumps take suction from a condensate water storage tank for delivery to the steam generators.

A reanalysis of the loss of normal feedwater event was performed to address the concern over the modeling of pressurizer heaters and sprays for events susceptible to pressurizer overfill. This analysis was performed with and without assumptions of ac power availability. A sensitivity study was also performed with and without pressurizer heaters and sprays along with other assumptions described in the following section.

The analysis acceptance criteria require that, following a loss of normal feedwater, the auxiliary feedwater system is capable of removing the stored and residual heat, thus preventing either overpressurization of the reactor coolant system or loss of water from the reactor core.

15.2.8.2 **Analysis of Effects and Consequences**

15.2.8.2.1 Method of Analysis

A detailed analysis using the RETRAN (Reference 9) code was performed to obtain the plant transient following a loss of normal feedwater. The simulation describes the plant thermal kinetics, reactor coolant system, pressurizer, steam generators, and feedwater system. The digital program computes pertinent variables, including the steam generator level, pressurizer water level, and reactor coolant average temperature.

Assumptions are:

1. Reactor trip occurs at the steam generator narrow range low-level tap in the steam generator.
2. The plant is operating at 102% of the rated thermal power level.
3. A conservative core residual heat generation based upon long-term operation at the initial power level preceding the trip.
4. The analysis was performed with and without ac power to the station auxiliaries.
5. Two motor-driven auxiliary feedwater pumps are available 1 minute after reactor trip actuation. The assumed flow rate for the pumps is 300 gpm each.
6. Auxiliary feedwater is delivered to two steam generators.
7. Secondary system steam relief is achieved through the self-actuated safety valves. Note that steam relief would be via the PORVs or condenser dump valves for most cases of loss of normal feedwater. However, for conservatism these valves are assumed unavailable.

8. The initial reactor coolant average temperature is 4°F higher than the nominal value, since this results in a greater expansion of reactor coolant system water during the transient and, thus, in a higher water level in the pressurizer.
9. An error of +6% in the full-power programmed-pressurizer level is assumed. It should be noted with regard to this incident that even if the pressurizer does fill, the low surge rate would not cause an excessive pressure rise.
10. Pressurizer heaters and sprays are assumed operational during the transient. In addition, a sensitivity study was performed with and without heaters and sprays available.
11. The pressurizer PORVs are assumed operational. In addition, a sensitivity study was performed with and without PORVs available.
12. Initial pressurizer pressure is 30 psi above its nominal value.
13. Up to 15 percent steam generator tube plugging is assumed.

15.2.8.2.2 Results

Following the reactor and turbine trip from full load, the water level in the steam generators will fall due to the reduction of steam generator void fraction and because steam flow through the safety valves continues to dissipate the stored and generated heat. One minute following the initiation of the low-low level trip, the auxiliary feedwater pumps are automatically started, reducing the rate of water level decrease.

A reanalysis of the loss of normal feedwater including pressurizer heaters and sprays operability demonstrated that the auxiliary feedwater system will remove the stored and residual heat, thus preventing overpressurization and relief of RCS liquid inventory through the pressurizer PORVs or safety valves. The analysis also confirmed that all the acceptance criteria for the loss of normal feedwater event are met.

For the case with ac power available, representative plots are presented in Figures 15.2-31 through 15.2-34 for a case with PORVs and sprays disabled and pressurizer heaters enabled. A time sequence of events for this case is given in Table 15.2-1.

15.2.8.3 **Conclusions**

Results of the analysis show that a loss of normal feedwater does not adversely affect the core, the reactor coolant system, or the main steam system, since the auxiliary feedwater capacity is such that the reactor coolant water is not relieved from the pressurizer relief or safety valves.

15.2.9 Loss of Offsite Power to the Station Auxiliaries

15.2.9.1 **Identification of Causes and Accident Description**

In the event of a complete loss of offsite power and a turbine trip, there will be a loss of power to the plant auxiliaries, i.e., the reactor coolant pumps, condensate pumps, etc.

A reanalysis of the loss of normal feedwater event was performed to address the concern over the modeling of pressurizer heaters and sprays for events susceptible to pressurizer overfill. This analysis was performed without ac power to the station auxiliaries. A sensitivity study was also performed with and without pressurizer heaters and sprays along with other assumptions for the loss of normal feedwater event.

The events following a loss of ac power with turbine and reactor trip are described in the sequence listed below:

1. Plant vital instruments are supplied by emergency power sources.
2. As the steam system pressure rises following the trip, the steam system power-operated relief valves are automatically opened to the atmosphere. Steam dump to the condenser is assumed not to be available. If the power-operated relief valves are not available, the steam generator self-actuated safety valves may lift to dissipate the sensible heat of the fuel and coolant plus the residual heat produced in the reactor.
3. As the no-load temperature is approached, the steam system power relief valves (or the self-actuated safety valves, if the power-operated relief valves are not available) are used to dissipate the residual heat and to maintain the plant at the hot shutdown condition.
4. The emergency diesel generators, started on loss of voltage on the plant emergency buses, begin to supply plant vital loads.

The auxiliary feedwater system is started automatically, as discussed in the loss-of-normal-feedwater analysis. Two motor driven pumps are available with each pump assumed to deliver 300 gpm. The motor driven pumps are powered from separate emergency busses. The pumps take suction directly from a condensate storage tank for delivery to the steam generators.

On loss of power to the reactor coolant pumps, coolant flow necessary for core cooling and the removal of residual heat is maintained by natural circulation in the reactor coolant loops.

15.2.9.2 **Analysis of Effects and Consequences**

15.2.9.2.1 Method of Analysis

A detailed analysis using the RETRAN (Reference 9) code is done to obtain the plant transient following a station blackout. The simulation describes the reactor kinetics, the reactor coolant system including natural circulation, pressurizer, steam generators, and feedwater system. The digital program computes pertinent variables, including the steam generator level, pressurizer water level, and reactor coolant average temperature.

The first few seconds of the transient will closely resemble a simulation of the complete loss-of-flow incident (see Section 15.3.4), i.e., core damage due to rapidly increasing core temperatures is prevented by promptly tripping the reactor. After the reactor trip, stored and residual heat must be removed to prevent damage to either the reactor coolant system or the core.

The assumptions used in the analyses are similar to the loss of normal feedwater flow incident, except that power is assumed to be lost to the reactor coolant pumps at the time of reactor trip and a conservative total auxiliary feedwater flow of 340 gpm has been used.

15.2.9.2.2 Results

The RETRAN results show that natural circulation flow available is sufficient to provide adequate core decay heat removal following a reactor trip and RCP coastdown.

The reanalysis of the loss of normal feedwater including pressurizer heaters and sprays operability demonstrated that the auxiliary feedwater system will remove the stored and residual heat, thus preventing overpressurization and relief of RCS liquid inventory through the pressurizer PORVs or safety valves. The analysis also confirmed that all the acceptance criteria for the loss of normal feedwater event without ac power are met.

For the case without ac power available, representative plots are presented in Figures 15.2-35 through 15.2-38 for the case with PORVs and sprays enabled and heaters disabled. A time sequence of events for this case is given in Table 15.2-1.

15.2.9.3 **Conclusions**

Analysis of the natural circulation capability of the RCS has demonstrated that sufficient heat removal capability exists following reactor coolant pump coastdown to prevent fuel or clad damage. The DNBR is maintained above the limit value. The Reactor Coolant System is not overpressurized and no water relief will occur through the pressurizer relief or safety valves. Thus there will be no cladding damage and no release of fission products to the Reactor Coolant System.

15.2.10 Excessive Heat Removal Due to Feedwater System Malfunctions

15.2.10.1 Identification of Causes and Accident Description

Reductions in feedwater temperature or additions of excessive feedwater can result in increases of core power above full power. Such transients are attenuated by the thermal capacity of the secondary plant and of the reactor coolant system. The overpower-overtemperature protection (neutron overpower, overtemperature, and overpower delta T trips) prevents any power increase that could lead to a DNBR less than the limit value.

Feedwater temperature reduction and subsequent primary system load increase can be initiated by any of the following events: inadvertent opening of a high-pressure feedwater heater bypass valve which diverts flow around a first-point feedwater heater, inadvertent opening of a low-pressure feedwater heater bypass valve which diverts flow around the second-, third-, and fourth-point feedwater heaters, or isolation of extraction steam to the first-point feedwater heaters. Inadvertent bypass valve opening or extraction steam isolation results in a sudden reduction in feedwater inlet temperature to the steam generators. The increased subcooling creates a greater

load demand on the reactor coolant system. The feedwater heater bypass valves can only be opened manually.

Another example of excessive heat removal would be a full opening of a feedwater control valve due to a feedwater control system malfunction or an operator error. At power this excess flow causes a greater load demand on the reactor coolant system due to increased subcooling in the steam generator. With the plant at no-load conditions the addition of cold feedwater may cause a decrease in reactor coolant system temperature and thus a reactivity insertion due to the effects of the negative moderator coefficient of reactivity. Continuous addition of excessive feedwater is prevented by the steam generator high-high-level trip which closes all feedwater control and isolation valves and trips the main feedwater pumps.

Design features have been provided to prevent the continuous addition of excessive feedwater to a steam generator. An alarm is actuated whenever the measured level in any steam generator differs by a fixed amount from the level setpoint. In addition, the following interlocks are provided:

1. An interlock is provided to close all main feedwater control valves by venting the valve actuators following a plant trip when the reactor coolant system temperature in two out of three loops falls below approximately 554°F. This interlock is redundant down to two venting solenoids per feedwater control valve, which vent the valve actuator.
2. An interlock is provided to close the main and bypass feedwater control valves, the motor-operated feedwater isolation valves (fast acting MOVs), the feedwater pump discharge MOVs and trip the main feedwater pumps on two out of three high-high water level signals in any steam generator or a safety injection actuation. This interlock is redundant down to the feedwater pump breakers and to two venting solenoids per feedwater control valve actuator. Tripping an operating main feedwater pump will also cause the associated feedwater pump discharge MOV to automatically close. Feedwater flow is stopped if either the feedwater control valves (main and bypass) close, the bypass feedwater control valves and the motor-operated feedwater isolation valves close or the feedwater pump discharge MOVs close. Each of these acts as a backup to the others.

The steam generator high-high-level trip prevents the continuous addition of feedwater by causing a turbine trip which is immediately followed by reactor trip when operating above the power level specified in Technical Specifications. However, in the analyses presented here no credit is taken for a turbine trip followed by reactor trip on high-high steam generator level signal.

15.2.10.2 Method of Analysis

The feedwater temperature reduction event is dispositioned by determining a conservative feedwater temperature reduction for the initiating events described in Section 15.2.10.1. The resulting feedwater temperature reduction is shown to be less than the temperature reduction required to achieve a primary system load increase of 10% of full power. The feedwater

temperature reduction event is thus shown to be bounded by the excessive load increase event presented in Section 15.2.11.

Excessive feedwater flow due to a feedwater control system malfunction or operator error, which allows a feedwater control valve to open fully, is analyzed with the transient analysis code RETRAN (Reference 9). DNBR analysis is performed with the thermal-hydraulic code COBRA (Reference 10). The RETRAN code simulates a multi-loop system, neutron kinetics, the pressurizer, pressurizer relief and safety valves, pressurizer spray, steam generator, and steam generator safety valves. The code computes pertinent plant variables, including temperatures, pressures, and power level.

Multiple loop malfunction transients are more severe than single loop transients. Four cases were analyzed as described below—one at hot zero power and three at full power.

1. Accidental opening of feedwater control valves in all three loops with the reactor just critical at zero load conditions, assuming a conservatively large moderator coefficient characteristic of end-of-core-life conditions.
2. Accidental opening of feedwater control valves in all three loops with the reactor in automatic control at full power analyzed at three flow levels.

The analysis is performed with the following assumptions:

1. The maximum capacity of the feedwater pumps at North Anna is 137% of nominal full power flow. Thus, three cases are evaluated at HFP, assuming step increases of feedwater flow from 100% to 137, 150 and 200% of full load (2893 MWt) equally to all three steam generators. Ample DNB margin exists in all cases. The case chosen for presentation here is the 150% excess feedwater transient which provides an extra flow margin beyond the 137% actual capacity of the feedwater pumps. Step increases in flow to greater than 150% of nominal are not credible.
2. For the full power transient the initial water level in the steam generator that signals feedwater isolation is assumed to be conservatively low, thus delaying the isolation signal actuated by the high-high steam generator level setpoint.
3. For the feedwater control valve accident at zero load condition, a feedwater valve malfunction results in a step increase in flow to all steam generators from zero to 137% of nominal full load.
4. For the zero load condition, feedwater temperature is at a conservatively low value of 70°F.
5. No credit is taken for the heat capacity of the reactor coolant system thick metal and steam generator thick metal in attenuating the resulting plant cooldown.
6. No credit is taken for the heat capacity of the steam and water in the unaffected steam generators.

7. The feedwater flow resulting from a fully open control valve is terminated by the steam generator high-high-level signal, which closes all feedwater control valves and motor-operated isolation valves and trips the main feedwater pumps.
8. The reactor is tripped when the steam generator water level reaches the low-low-level setpoint following the feedwater isolation.

15.2.10.3 **Results**

15.2.10.3.1 Feedwater Temperature Reduction Event

Inadvertent opening of a feedwater heater manual bypass valve or isolation of extraction steam to the first-point feedwater heaters results in a heat load increase on the primary system of less than 10% of full power. The increased thermal load would result in a transient similar, but of reduced magnitude, to the excessive load increase presented in Section 15.2.11. The excessive load increase event evaluates the consequences of a 10% step load increase from full power.

15.2.10.3.2 Excess Feedwater Transient at HZP

The excess feedwater transient at zero power is analyzed without automatic reactor control, because at start-up and low power the reactor is under manual control. A sudden increase of cold feedwater flow from near zero to 137% of full load is assumed in all loops. The neutronic power spikes at about 10 seconds into the transient resulting in a reactor trip on the power range low level flux setpoint of 35% full power. The normalized core heat flux peaks at just under 17% full power, although instantaneous neutronic power is observed to peak much higher. The thermal hydraulic analysis shows that DNB ratio is about 10 or higher throughout the transient, indicating a substantial margin above the design limit of 1.17. Therefore, detailed results of the excess feedwater accident at zero load are not presented.

15.2.10.3.3 Excess Feedwater Transient at HFP

Figures 15.2-39 through 15.2-43 represent the behavior of the multiple loop 150% excess feedwater accident with reactor control. Core power increases because of the positive reactivity feedback from the primary cooldown caused by excess feedwater flow. The pressurizer pressure falls, and there is a small decrease in core average temperature. The mismatch between feedwater and steam flows causes the steam generator level to rise steadily, until the high-high level setpoint is reached, when all feedwater control and isolation valves close and feedwater pumps are tripped. Continuous addition of feedwater is thus prevented. With no incoming feedwater and steam still being generated, the steam generator water level decreases. When it reaches the low-low level setpoint, the reactor is tripped, followed by a turbine trip soon after. Assuming the reactor to be in manual control results in a slightly less severe transient.

The time sequence of events for the Excessive Heat Removal due to Feedwater Malfunction is presented in Table 15.2-1

Transients results, provided in Figures 15.2-39 through 15.2-43, show the behavior of nuclear power, pressurizer pressure, reactor coolant average temperature, reactor coolant loop ΔT, and steam generator mass in response to the increased thermal load on the reactor. The DNBR remains above the limit value.

15.2.10.4 Conclusions

Primary system load increase due to opening a feedwater heater bypass valve or isolation of extraction steam to the first-point feedwater heaters is bounded by that assumed for the excessive load increase event presented in Section 15.2.11. Additionally, it has been shown that the reactivity insertion at no-load following excessive feedwater addition is less than the maximum value considered in the analysis of a rod-withdrawal accident from a subcritical condition. Also, the DNBR encountered for excessive feedwater addition at power is well above the limit value.

15.2.11 Excessive Load Increase Incident

15.2.11.1 Identification of Causes and Accident Description

An excessive load increase incident is defined as a rapid increase in the steam flow that causes a power mismatch between the reactor core power and the steam generator load demand. The reactor control system is designed to accommodate a 10% step load increase or a 5% per minute ramp load increase in the range of 15 to 100% of full power. Any loading rate in excess of these values may cause a reactor trip actuated by the reactor protection system.

This accident could result from either an administrative violation, such as excessive loading by the operator, or an equipment malfunction in the steam dump control or turbine speed control.

During power operation, steam dump to the condenser is controlled by reactor coolant condition signals; i.e., high reactor coolant temperature indicates a need for steam dump. A single controller malfunction does not cause steam dump; an interlock is provided that blocks the opening of the valves unless a large turbine load decrease or a turbine trip has occurred.

Protection against an excessive load increase accident is provided by the following reactor protection system signals:

1. Overpower delta T.
2. Overtemperature delta T.
3. Power range high neutron flux.

15.2.11.2 Analysis of Effects and Consequences

15.2.11.2.1 Method of Analysis

This accident was originally analyzed using the LOFTRAN (Reference 4) code and the Improved Thermal Design Procedures. The code simulates the neutron kinetics, reactor coolant system, pressurizer, pressurizer relief and safety valves, pressurizer spray, steam generator, and

steam generator safety valves. The code computes pertinent plant variables, including temperatures, pressures, and power level.

Four cases are analyzed to demonstrate the plant behavior following a 10% step load increase from rated load. These cases are as follows:

1. Manually controlled reactor at beginning of life.
2. Manually controlled reactor at end of life.
3. Reactor in automatic control at beginning of life.
4. Reactor in automatic control at end of life.

At beginning of life, the core is assumed to have a zero moderator temperature coefficient of reactivity and therefore the least inherent transient capability. At end of life, the moderator temperature coefficient of reactivity has its highest absolute value. This results in the largest amount of reactivity feedback due to changes in coolant temperature.

A conservative limit on the turbine valve flow area is assumed, and all cases are studied without credit being taken for pressurizer heaters. Initial operating conditions are assumed at nominal values consistent with the steady-state full-power operation. Allowances for calibration and instrument errors are included in the limit DNBR as described in Chapter 4.

Two cases of the excessive load increase event were reanalyzed to demonstrate the plant behavior following a 10% step load increase from rated load. These cases are as follows (Reference 15):

1. Manually Controlled at end of life.
2. Reactor in Automatic Control at end of life.

At the end of life, the most negative isothermal temperature coefficient is used. This results in the largest amount of reactivity feedback due to changes in coolant temperature. This accident also was reanalyzed using the RETRAN (Reference 9) code and statistical DNB methodology. The program simulates the neutron kinetics, reactor coolant system, pressurizer, pressurizer relief and safety valves, pressurizer spray, steam generator, and steam generator safety valves. The program computes pertinent plant variables, including temperatures, pressures, and power level. The COBRA (Reference 10) code is then used to calculate the minimum DNBR during the transient based upon the heat flux, core flow, core inlet temperature, and pressurizer pressure from RETRAN (Reference 9). The WRB-1 CHF correlation is used.

15.2.11.2.2 Results

Figures 15.2-45 through 15.2-47 illustrate the transient with the reactor in the manual control mode. As expected, for the beginning-of-life case there is a slight power increase, and the average core temperature shows a large decrease. The DNBR remains essentially unchanged from its initial value. For the end-of-life, manually controlled case, there is a much larger increase in

reactor power due to the moderator feedback. A reduction in DNBR is experienced, but the DNBR remains above the limit value.

Figures 15.2-48 through 15.2-49 illustrate the transient assuming the reactor is in the automatic control mode. Both the beginning-of-life and the end-of-life cases show that the core power increases. Due to the large increase in core power, the coolant average temperature shows a slight increase for the beginning-of-life case and a small decrease for the end-of-life case. For both cases, the minimum DNBR remains above the limit value.

15.2.11.3 Conclusions

It has been demonstrated that for an excessive load increase the minimum DNBR during the transient will not be below the limit value.

15.2.12 Accidental Depressurization of the Reactor Coolant System

15.2.12.1 Identification of Causes and Accident Description

The most severe core conditions resulting from an accidental depressurization of the reactor coolant system are associated with an inadvertent opening of a pressurizer safety valve. Initially the event results in a rapidly decreasing reactor coolant system pressure until this pressure reaches a value corresponding to the hot-leg saturation pressure. At that time, the pressure decrease is slowed considerably. The pressure continues to decrease, however, throughout the transient. The effect of the pressure decrease would be to decrease the neutron flux via the moderator density feedback, but the reactor control system (if in the automatic mode) functions to maintain the power essentially constant throughout the initial stage of the transient. The average coolant temperature decreases slowly, but the pressurizer level increases until reactor trip.

The reactor will be tripped by the following reactor protection system signals:

1. Pressurizer low pressure.
2. Overtemperature delta T.

Long term effects of this type of event, i.e., after reactor trip, are addressed in the analysis of the small break Loss of Coolant Accident (Section 15.3.1).

15.2.12.2 Analysis of Effects and Consequences

15.2.12.2.1 Method of Analysis

This analysis is performed to ensure that the reactor protection system provides the required DNBR protection for the most severe reactor coolant system depressurization event. The accidental depressurization transient is analyzed with the detailed digital computer code RETRAN (Reference 9). The code simulates the neutron kinetics, reactor coolant system, pressurizer, pressurizer relief and safety valves, pressurizer spray, steam generator, and steam generator safety valves. The RETRAN computer code calculates pressurizer pressure, core inlet

temperature, core inlet flow and power transient. The COBRA code with WRB-1 CHF correlation (Reference 10) is used to calculate the minimum DNBR during the transient.

In calculating the DNBR, the following conservative assumptions are made:

1. Initial core power, reactor coolant average temperature and reactor coolant pressure are assumed at their nominal values. Uncertainties in initial conditions are included in the DNBR limit as described in Chapter 4.
2. Four cases, assuming different combinations of BOC and EOC conditions and manual and automatic rod control, were analyzed. The limiting case relative to minimum DNBR is presented here. A most negative Doppler Temperature Coefficient along with a most negative Moderator Temperature Coefficient is used in this case.
3. In the DNBR analysis, the nuclear enthalpy rise factor, Fdh, is assumed to remain constant at its time zero value.

15.2.12.2.2 Results

Figure 15.2-50 illustrates the nuclear power transient following the accident. Reactor trip on overtemperature delta T occurs at approximately 40 seconds into the transient as shown in Figure 15.2-50. The pressure decay transient following the accident can be seen in Figure 15.2-51. The resulting DNBR never goes below the limit value, as shown in Figure 15.2-52. The time sequence of events is given in Table 15.2-1

15.2.12.3 **Conclusions**

The pressurizer low pressure and the overtemperature delta T reactor protection system signals provide adequate protection to mitigate the consequences of this accident; the minimum DNBR remains in excess of the limit value.

15.2.13 Accidental Depressurization of the Main Steam System

15.2.13.1 Identification of Causes and Accident Description

The most severe core conditions resulting from an accidental depressurization of the main steam system are associated with an inadvertent opening of a single steam dump, relief, or safety valve. The analyses performed assuming a rupture of a main steam pipe are given in Section 15.4.

The steam release as a consequence of this accident results in an initial increase in steam flow that decreases as the steam pressure falls. The energy removal from the reactor coolant system causes a reduction of coolant temperature and pressure. In the presence of a negative moderator temperature coefficient, the cooldown results in a reduction of core shutdown margin.

The current analysis is performed to demonstrate that the following criterion is satisfied: assuming a stuck rod cluster control assembly and a single failure in the engineered safety features, there will be no departure from nucleate boiling in the core for a steam release equivalent

to the spurious opening, with failure to close, of the largest of any single steam dump, relief, or safety valve.

The following systems provide the necessary protection against an accidental depressurization of the main steam system:

1. Safety injection system actuation from any of the following:
   a. Two out of three low-low pressurizer pressure signals.
   b. High differential pressure signals between steam lines.
2. The overpower reactor trips (neutron flux and delta T) and the reactor trip occurring in conjunction with receipt of the safety injection signal.
3. Redundant isolation of the main feedwater lines—Sustained high feedwater flow would cause additional cooldown. Therefore, in addition to the normal control action that will close the main feedwater valves following reactor trip, a safety injection signal will rapidly close all feedwater control valves, trip the main feedwater pumps, and close the feedwater pump discharge valves.

15.2.13.2 **Analysis of Effects and Consequences**

15.2.13.2.1 Method of Analysis

The following analyses of a secondary system steam release are performed for this section:

1. The core heat flux and reactor coolant system temperature and pressure resulting from the cooldown following an inadvertent opening of the largest capacity valve listed in section 15.2.13.1. The RETRAN code (Reference 9) was used for the analysis.
2. The thermal and hydraulic behavior of the core during this event. A detailed thermal and hydraulic digital-computer code, COBRA (Reference 10), was used to determine if departure from nucleate boiling occurs based on the system boundary conditions in 1 above.

The following conditions are assumed to exist at the time of a secondary-system-break accident:

1. End-of-life shutdown margin at no-load equilibrium xenon conditions, and with the most reactive rod cluster control assembly stuck in its fully withdrawn position. Operation of rod cluster control assembly banks during core burn-up is restricted so that addition of positive reactivity in a secondary-system-break accident will not lead to a more adverse condition than the case analyzed.
2. A negative moderator coefficient corresponding to the end-of-life rodded core with the most reactive rod cluster control assembly in the fully withdrawn position. The variation of the coefficient with temperature is included. The Doppler reactivity feedback corresponds to a most negative hot zero power Doppler temperature coefficient.

3. Minimum capability for injection of boric acid solution corresponding to the most restrictive single failure in the safety injection system. The most restrictive single failure corresponds to the flow delivered by one charging pump delivering its full contents to the cold-leg header. The safety injection lines downstream of the refueling water storage tank isolation valves, the BIT itself, and the safety injection lines downstream of the BIT have a 0% boron concentration. The boron enters the safety injection system after the charging pump suction switches over from the volume control tank to the refueling water storage tank upon safety injection actuation.

4. The case studied is an initial total steam flow of 262 lb/sec at 1020 psia from all steam generators, with offsite power available. This is the maximum capacity of any single steam dump or safety valve. Initial hot shutdown conditions at time zero are assumed, since this represents the bounding initial condition.

   Should the reactor be just critical or operating at power at the time of a steam release, the reactor will be tripped by the normal overpower protection when power level reaches the trip setpoint. Following a trip at power, the reactor coolant system contains more stored energy than at no-load, the average coolant temperature is higher than at no-load, and there is appreciable energy stored in the fuel.

   Thus, the additional stored energy is removed via the cooldown caused by the main steam depressurization before the no-load conditions of reactor coolant system temperature and shutdown margin assumed in the analyses are reached. After the additional stored energy has been removed, the cooldown and reactivity insertions proceed in the same manner as in the analysis, which assumes no-load condition at time zero. However, since the initial steam generator water inventory is greatest at no-load, the magnitude and duration of the reactor coolant system cooldown are less for main steam depressurization occurring at power.

5. In computing the steam flow, the Moody Curve for fL/D = 0 is used.

6. Perfect moisture separation in the steam generator is assumed.

7. In the original analysis of the steam line break incident, which is a depressurization transient, credit was taken for coincident low pressurizer pressure and level for safety injection actuation following a credible break (accidental depressurization of the main steam system). Since that analysis was performed, the low-level coincidence requirement has been removed from the plant protection circuitry. Thus, safety injection actuation can occur on the low pressurizer pressure signal.

15.2.13.2.2 Results

The results presented are a conservative indication of the events that would occur assuming a secondary system steam release, since it is postulated that all of the conditions described above occur simultaneously.

Figures 15.2-54 through 15.2-57 show the transients arising as the result of a steam release with an initial steam flow of 262 lb/sec at 1020 psia with steam release from one condenser dump valve. The assumed steam release bounds the capacity of any single steam dump, relief, or safety valve in the main steam system. In this case safety injection is initiated automatically by low pressurizer pressure. Operation of one centrifugal charging pump is considered. Boron solution at 2300 ppm enters the reactor coolant system, providing sufficient negative reactivity to limit the return-to-power to a level below 6% of the rated power. (Note: At the time of this analysis, the RWST contained boric acid at 2300 ppm and the SIAs contained boric acid at 2200 ppm. The boron concentration in the RWST and SIAs has since been increased to at least 2600 ppm in the RWST and 2500 ppm in the SIAs. The analysis conservatively assumes 2300 ppm in the RWST and 2200 ppm in the SIAs.) With the reactor coolant pumps still providing full flow, the minimum departure from nucleate boiling ratio is well above the limit for Condition II acceptance criteria. The reactivity transient for the case shown in Figure 15.2-57 is more severe than that of a faulted steam generator safety or relief valve, which is terminated by steam line differential pressure. The transient is quite conservative with respect to cooldown, since no credit is taken for the energy stored in the system metal other than that of the fuel elements. Since the transient occurs over a period of about 5 minutes, the neglected stored energy is likely to have a significant effect in slowing the cooldown.

15.2.13.3 **Failure of the Decay Heat Release Piping**

An analysis of a break (double-ended rupture of the 4-inch-diameter common header) in the decay heat release line has been performed. This break would result in a maximum break area of 0.0491 ft^2 for one 3-inch branch line and a break area of 0.0872 ft^2 shared for the other two 3-inch branch lines. The analysis referenced above, however, conservatively assumed a break in each 3-inch branch line with a break area of 0.0491 ft^2 for each branch line. The k_{eff} versus temperature at 1000 psi corresponding to the negative moderator temperature coefficient used is shown in Figure 15.2-53. In addition, no credit was taken for any piping friction losses either in the main steam lines or in the decay heat release lines. Other significant assumptions were as follows:

1. The shutdown margin, moderator coefficient, power peaking, stuck rod, and other pertinent items were the same as those used in Section 15.2.13.1 with the exception of the BIT boron concentration which was assumed to be 20,000 ppm. This transient with a BIT boron concentration of 12,950 ppm would have results similar to those for the accidental depressurization of the main steam system and would be bounded by the main steam line break analysis in Section 15.4.2.

2. Loss of offsite power.

The analysis was performed to determine (1) if the reactor remains subcritical following shutdown, (2) if adequate core cooling is available, and (3) the radiological consequences. Subcriticality for a small steam-line break is a Westinghouse criterion and is not necessarily required to demonstrate the safety of the reactor.

To determine whether the reactor remains subcritical following the break, the most limiting case of the reactor initially subcritical at hot zero power with no decay heat was assumed. This is more conservative than the full-power case since it results in minimum stored energy in the system, thereby resulting in most rapid cooldown and the greatest loss of shutdown margin. For this case, safety injection was initiated by coincident low pressurizer pressure and temperature signals. The rate of cooldown was accented by assuming that all three auxiliary feedwater pumps were operating.

The analysis of this limiting case showed that the reactor remains sub-critical. The sequence of events is shown in Table 15.2-1. Steam pressure, steam flow, reactor coolant system temperature, reactor coolant system pressure, and reactivity versus time are shown in Figure 15.2-58. Since the reactor does not return critical, there is no heat generation and therefore no problem with core cooling. The full-power case analyzed below substantiated that the zero-power case was more limiting. The sequence of events for this case is also shown in Table 15.2-1. Figure 15.2-59 shows steam pressure, steam flow, pressurizer water volume, reactor coolant system temperature, reactor coolant system pressure, and reactivity versus time.

To determine if core cooling is adequate, the decay heat release line break was assumed to occur with the reactor at full power. The effect of the break occurring at full power is to increase the steam demand from 102% of nominal (with an assumed 2% calorimetric error) to just under 110% of nominal. The initial part of this transient would be essentially the same as the excessive load increase event described in Section 15.2.11. The feedwater control system would act to increase feedwater flow to meet the additional steam demand and maintain steam generator level. The reactor will not trip on an overtemperature delta T signal since the plant has an adequate DNB margin to sustain this incident.

Should the feedwater system be unable to supply enough flow to meet the steam demand, the steam generator level would drop and the reactor would trip on low-low steam generator level. The transient was, therefore, analyzed starting with a reactor trip, with the reactor initially at 109.7% of nominal power and with the steam generator water level at the narrow range low-low level setpoint. At this time, main feed was assumed to be lost as a result of the loss of offsite power. One motor-driven auxiliary feedwater pump was assumed to start 1 minute after the incident. A conservative decay heat generation rate based on long-term generation of 102% of nominal power was used, since the time at 109.7% of nominal power is too short compared to the decay heat time constants to significantly alter the decay heat release rate. This transient is much like the loss-of-normal-feedwater accident presented in Section 15.2.8, except that in that analysis, both the initial power level and the decay heat fraction were based on 102% of the engineered safeguards design power or about 106.5% of the nominal power. The 3% higher initial power in the present analysis is more than offset by the 4.5% reduction in decay heat, since the decay heat contribution to the total energy release is about an order of magnitude higher than that due to residual fissions and stored energy over the time frame of interest. In addition, the unisolable break in the three branch lines causes continuous blowdown of all three steam

generators instead of forcing steam relief through the steam safety valves at a much higher pressure (and temperature), as in the analysis in Section 15.2.11.

The resulting sequence of events and variation of the principal parameters versus time are given in Table 15.2-1 and Figure 15.2-58, respectively.

Over the time period shown in the graphs, the consequences are less severe than in the main steam system depressurization shown in Section 15.2.13.2. Beyond the time shown, the steam generators continue to blow down and cool down the reactor coolant system at a slower and slower rate due to the reduction in the blowdown rate as steam pressure is reduced. The auxiliary feedwater flow becomes more than adequate to relieve the decay heat after about 3000 seconds. In this analysis, no credit was taken for the substantial increase in auxiliary feedwater flow as the steam pressure decreases.

The graphs of reactor coolant system pressure and pressurizer water volume versus time indicate that both reactor coolant system pressure and pressurizer water volume are increasing at 1500 seconds. These increases result from the injection of safety injection flow by the charging pumps. Past 1500 seconds, the reactor coolant system pressure will continue on up to the pressurizer safety valve setpoint plus 3% accumulation, and will remain at that point until the auxiliary feedwater flow is sufficient to relieve decay heat and lower the reactor coolant system temperature. While not necessary, the reactor operator could take action to shut off safety injection flow and arrest the pressure rise. In any event, a continuation of the above transient out to 4000 seconds resulted in a peak pressurizer water volume of only 1050 ft^3 compared to a total volume of 1400 ft^3; therefore, at no time during the transient are the safety valves required to relieve water. No credit has been taken for the pressurizer relief valves.

Since in either the zero- or full-power case the reactor does not return to critical, and since long-term core cooling is adequate, this steam break event cannot result in any core damage and release of additional fission products to the coolant. Thus, the radiological consequences of this accident would not exceed those calculated as a result of the main steam-line break analyzed in Section 15.4.2.1.3, using the same extreme assumptions. The resulting dose is therefore within the limits set forth in Regulatory Guide 1.183.

The steam lines to the auxiliary feedwater turbine also provide the potential for a slow unisolable blowdown of all three steam generators in the event of a rupture of the common header connecting these lines. This accident is bounded by the decay heat release line break accident.

The effects of piping system breaks outside the containment are addressed in Appendix 3C.

15.2.13.4 **Conclusions**

The analysis has shown that the criterion stated earlier in this section is satisfied. Since the reactor does not return to critical, the possibility of a DNBR less than 1.30 does not exist.

15.2.14 Spurious Operation of the Safety Injection System at Power

15.2.14.1 Identification of Causes and Accident Description

A spurious safety injection system operation at power could be caused by operator error or a false electrical actuating signal. A spurious signal in any of the following channels could cause this incident:

1. High containment pressure.
2. Low-low pressurizer pressure.
3. High steam-line differential pressure.
4. High steam-line flow and low-low average coolant temperature or low steam-line pressure.

Following the actuation signal, the suction of the coolant charging pumps is diverted from the volume control tank to the refueling water storage tank. The valves isolating the boron injection tank from the charging pumps and the valves isolating the boron injection tank from the injection header then automatically open. The charging pumps then force highly concentrated boric acid solution from the boron injection tank, through the header and injection line, and into the cold legs of each loop. The low head safety injection pumps also start automatically but provide no flow when the reactor coolant system is at normal pressure. The passive injection system also provides no flow at normal RCS pressure.

A safety injection signal normally results in a reactor trip followed by a turbine trip. However, it cannot be assumed that any single fault that actuates the safety injection system will also produce a reactor trip. Therefore, two different courses of events are considered:

Case A—Trip occurs at the same time spurious injection starts.

Case B—The reactor protection system produces a trip later in the transient.

Case A assumes reactor trip on the safety injection signal and is less limiting with respect to the acceptance criteria than Case B.

For Case B the reactor protection system does not produce an immediate trip and the reactor experiences a negative reactivity excursion, causing a decrease in reactor power. The power unbalance causes a drop in T_{avg} and consequent coolant shrinkage, and lowering of pressurizer pressure and level. Load will decrease due to the effect of reduced steam pressure on load if the electro-hydraulic governor fully opens the turbine throttle valve. If automatic rod control is used, these effects will be lessened until the rods have moved out of the core. The transient is eventually terminated by the reactor protection system low-pressure trip, or by manual trip.

The time to trip is affected by initial operating conditions, including core burn-up history that affects initial boron concentration, rate of change of boron concentration, Doppler, and moderator coefficients.

15.2.14.2 **Analysis of Effects and Consequences**

15.2.14.2.1 DNBR Analysis

The spurious operation of the safety injection system is analyzed by using the detailed digital computer program LOFTRAN (Reference 20). The code simulates the neutron kinetics, reactor coolant system, pressurizer, pressurizer relief and safety valves, pressurizer spray, steam generator, steam generator safety valves, and the effect of the safety injection system. The program computes pertinent plant variables, including temperatures, pressures, and power level.

Because of the power and temperature reduction during the transient, operating conditions do not approach the core limits. Analysis of several cases shows that the results are relatively independent of time to trip.

A typical transient is presented representing conditions at beginning of core life. Results at end of life are similar, except that moderator feedback effects result in a slower transient.

The assumptions are:

1. Initial operation conditions—The initial reactor power and reactor coolant system temperatures are assumed at their nominal values consistent with the steady-state full-power operation. Allowances for calibration and instrument errors are included in the limit DNBR as described in Chapter 4.
2. Moderator and Doppler coefficients of reactivity—The beginning-of-life positive moderator temperature coefficient was used. A low (absolute value) Doppler power coefficient was assumed.
3. Reactor control—The reactor was assumed to be in manual control.
4. Pressurizer heaters—Pressurizer heaters were assumed to be nonoperable in order to increase the rate of pressure drop.
5. Boron injection—At the start of the transient, two charging pumps inject 12,250 ppm borated water into the cold legs of each loop.
6. Turbine load—Turbine load was assumed constant until the electro-hydraulic governor drives the throttle valve wide open. Then the turbine load drops as steam pressure drops.
7. Reactor trip—Reactor trip was initiated conservatively by low pressure at 1775 psia.

The transient response is shown in Figures 15.2-60 and 15.2-61. Nuclear power starts decreasing immediately due to boron injection, but steam flow does not decrease until 43 seconds into the transient, when the turbine throttle valve goes wide open. The mismatch between load and nuclear power causes T_{avg}, pressurizer water level, and pressurizer pressure to drop. The low-pressure trip setpoint is reached at 59 seconds, and rods start moving into the core at 61 seconds.

After trip, pressures and temperatures slowly rise, since the turbine is tripped and the reactor is producing some power due to delayed neutron fissions and decay heat.

15.2.14.2.2 RCS Pressurization

An evaluation of potential RCS pressurization as a result of a spurious safety injection was performed. The evaluation showed that a single pressurizer safety valve provides adequate relief capacity assuming a spurious safety injection and concurrent post-trip heatup of the RCS. Three safety valves are provided. The heatup was assumed to progress from a no-load nominal average temperature and be driven by decay heat while assuming no secondary heat sink.

15.2.14.2.3 Event Propagation

The spurious safety injection was evaluated to assess its potential to propagate into a small break loss of reactor coolant event if one or more of the pressurizer safety or power operated relief valves (PORVs) were to fail open due to the spurious safety injection and if isolation were not possible.

Safety valve (Reference 18) and PORV (Reference 19) testing has revealed no instances of failure of the valves to reseat following water relief. Resulting leakage is within the capacity of the normal makeup system and is therefore not considered to be a small break loss of reactor coolant event. Therefore, the complete filling of the pressurizer and/or water relief via a safety valve as a result of a spurious safety injection does not constitute a failure to meet the event propagation acceptance criterion. Although primary credit for preventing the propagation of the event to a small break loss of reactor coolant event is the reseating of the PORVs and safety valves, it is noted that the PORVs (which open prior to the safety valves and, if open, preclude safety valve actuation for this event) are provided with block valves which the operator will close in the event of excessive PORV leakage.

The spurious safety injection event may result in multiple cycling of the PORV(s). Although the initial opening of a PORV will result in a significant thermal stress to the PORV piping, subsequent openings of a PORV during this event will not involve a large thermal stress. For these reasons, only the initial PORV cycle is counted against the design limit for this event.

In response to a spurious safety injection event, the operator will complete the actions in the emergency procedures as time and the specific accident scenario dictate. No specific analysis assumption is made for time to terminate safety injection following a spurious safety injection.

15.2.14.3 **Conclusions**

Results of the analysis show that spurious safety injection with or without immediate reactor trip presents no hazard to the integrity of the reactor coolant system.

DNBR is never less than the initial value. Thus there will be no cladding damage and no release of fission products to the reactor coolant system.

If the reactor does not trip immediately, the low-pressure reactor trip will be actuated. This trips the turbine and prevents excess cooldown, thereby expediting recovery from the incident.

A single pressurizer safety valve provides adequate relief capacity assuming a spurious safety injection and concurrent post-trip heatup of the RCS.

The complete filling of the pressurizer and/or water relief via a safety valve as a result of a spurious safety injection does not constitute a failure to meet the event propagation acceptance criterion.

15.2 REFERENCES

1. W. C. Gangloff, *An Evaluation of Anticipated Operational Transients in Westinghouse Pressurized Water Reactors*, WCAP-7486, May 1971.
2. D. B. Fairbrother and H. C. Hargrove, *WIT-6 Reactor Transient Analysis Computer Program Description*, WCAP-7980, November 1972.
3. C. Hunin, *FACTRAN, a Fortran N Code for Thermal Transients in UO_2 Fuel Rod*, WCAP-7908, June 1972.
4. S. T. Maher, *LOFTRAN Code Description*, WCAP-7878, Rev. 3, July 1981.
5. S. Altomare and R. F. Barry, *The TURTLE 24.0 Diffusion Depletion Code*, WCAP-7758, September 1971.
6. F. M. Bordelon, *Calculation of Flow Coastdown After Loss of Reactor Coolant Pump (PHOENIX Code)*, WCAP-7969, September 1972.
7. J. M. Geets, *MARVEL - a Digital Computer Code for Transient Analysis of a Multiloop PWR System*, WCAP-7909, June 1972.
8. M. A. Mongan, *Overpressure Protection for Westinghouse Pressurized Water Reactors*, WCAP-7769, Revision 1, June 1972.
9. N. A. Smith, *Vepco Reactor System Transient Analyses Using the RETRAN Computer Code*, VEP-FRD-41, Rev. 0.1-A, June 2004.
10. F. W. Sliz and K. L. Basehore, *Vepco Reactor Core Thermal-Hydraulic Analysis Using the COBRA III C/MIT Computer Code*, VEP-FRD-33-A, October 1983.
11. Haessker, R. L.; et al., *Methodology for the Analysis of the Dropped Rod Event*, WCAP-11394-P-A, January 1990.
12. Letter from W. L. Stewart (Vepco) to H. R. Denton (NRC), Serial No. 85-772A, *Virginia Electric Power Company, North Anna Power Station Units 1 and 2, Response to Request for Additional Information on Core Uprate*, February 6, 1986.

13. Letter from W. L. Stewart (Vepco) to H. R. Denton (NRC), Serial No. 666, *Amendment to Operating Licenses NPF-4 and NPF-7, North Anna Power Station Unit Nos. 1 and 2, Proposed Technical Specification Change*, February 7, 1985.

14. Letter from W. L. Stewart (Vepco) to H. R. Denton (NRC), Serial No. 85-077, *Amendment to Operating Licenses NPF-4 and NPF-7, North Anna Power Station Unit Nos. 1 and 2, Proposed Technical Specification Change*, May 2, 1985 (Core Uprate Request).

15. Letter from W. L. Stewart (Vepco) to H. R. Denton (NRC), Serial No. 87-377, *Virginia Electric and Power Company, North Anna Power Station Unit Nos. 1 and 2, Accident Reanalysis Information*, September 1987.

16. Letter from L. B. Engle (NRC) to W. R. Cartwright (VEPCO), *North Anna Units 1 and 2 - Issuance of Amendments Re: Steam Generator Tube Plugging*, dated January 17, 1989 (Virginia Power Serial Number 89-049).

17. R. C. Anderson, *Statistical DNBR Evaluation Methodology*, VEP-NE-2-A, June 1987.

18. EPRI NP-2770-LD, Volumes 3 and 4, *EPRI/CE PWR Safety Valve Test Reports for Dresser Safety Valve Models 31739A and 31709NA,* February and March 1983.

19. EPRI NP-2670-LD, Volume 6, *EPRI/Wyle Power-Operated Relief Valve Phase III Test Report,* October 1982.

20. T. W. T. Burnett et al., *LOFTRAN Code Description,* WCAP-7907-A, April 1984.

21. WCAP-7706, *An Evaluation of Solid State Logic Reactor Protection in Anticipated Operation Transients,* Westinghouse Nuclear Energy Services, July 1971.

22. WCAP-10858-P-A, Revision 1, *AMSAC Generic Design Package,* Westinghouse Nuclear Energy Services, July 1987.

Table 15.2-1
TIME SEQUENCE OF EVENTS FOR CONDITION II EVENTS

Accident	Event	Time (sec)
Uncontrolled RCCA withdrawal from a subcritical condition	Initiation of uncontrolled rod withdrawal: 1.0×10^{-3} $\Delta k/k$/sec reactivity insertion rate from 10^{-13} of nominal power	0.0
	Prompt criticality occurs	6.6
	Peak nuclear power occurs	7.6
	Minimum DNBR reached	10.15
	Peak pressurizer pressure occurs	13.9
	Peak cold leg pressure occurs	14.4
	Peak main steam pressure occurs	34
Uncontrolled RCCA bank withdrawal at power		
1. Case A	Initiation of uncontrolled RCCA withdrawal at a high reactivity insertion rate (75 pcm/sec)	0
	Power range high neutron flux high trip point reached	1.4
	Rods begin to fall into core	1.9
	Minimum DNBR occurs	2.95
2. Case B	Initiation of uncontrolled RCCA withdrawal at a slow reactivity insertion rate (1.2 pcm/sec)	0
	Overtemperature delta T reactor trip signal initiated	83.6
	Rods begin to drop into core	85.4
	Minimum DNBR occurs	86.1
Boron dilution at power event (BOC, HFP, pressure control)	Initiation of dilution	0
	Pressurizer PORV lift	108
	Reactor trip on overtemperature delta T	113
Loss of external electrical load		
1. With pressurizer control (BOC)	Loss of electrical load	0.1
	High pressurizer pressure trip point reached	7.99
	Rods begin to drop	8.99
	Initiation of steam release from steam generator safety valves	10.1
	Peak pressurizer pressure occurs	11.9

Table 15.2-1 (continued)
TIME SEQUENCE OF EVENTS FOR CONDITION II EVENTS

Accident	Event	Time (sec)
2. Without pressurizer control (BOC)	Loss of electrical load	0.1
	High pressurizer pressure reactor trip point reached	5.46
	Rods begin to drop	6.46
	Peak cold leg pressure occurs	8.82
	Initiation of steam release from steam generator safety valves	9.0
3. [Deleted]		
Excessive feedwater at full load	All feedwater control valves fail fully open	0.001
	Minimum DNBR occurs	90
	High-high SG level reached	92.6
	Main feedwater isolation begins	98.6
	Low-low SG level reached	167.2
	Rods begin to drop	169.2
	Turbine trip	171.2
Excessive load increase		
1. Manual reactor control (minimum feedback)	10% step load increase	0
	Equilibrium conditions reached (approximate times only)	175
2. Manual reactor control (maximum feedback)	10% step load increase	0
	Equilibrium conditions reached (approximate time only)	51.0
3. Automatic reactor control (minimum feedback)	10% step load increase	0
	Equilibrium conditions reached	280
4. Automatic reactor control (maximum feedback)	10% step load increase	0
	Equilibrium conditions reached (approximate time only)	61.0

Table 15.2-1 (continued)
TIME SEQUENCE OF EVENTS FOR CONDITION II EVENTS

Accident	Event	Time (sec)
Offsite power available, PORV disabled, pressurizer pressure limiting	Main feedwater flow stops	10.0
	Reactor trip, 2 seconds after reaching low-low SG level setpoint	32.7
	Turbine trip 0.5 seconds after reactor trip	33.2
	SG safety valve first opens	38.0
	AFW actuation, 60 seconds after low-low SG level	90.6
	Maximum pressurizer pressure reached	36.0
	Maximum pressurizer volume reached	36.0
	Minimum SG liquid mass	260.0
	End of transient	10,000.0
Offsite power not available, PORV enabled, pressurizer volume limiting	Main feedwater flow stops	10.0
	Reactor trip, 2 seconds after reaching low-low SG level setpoint	33.0
	Turbine trip 0.5 seconds after reactor trip	33.5
	SG safety valve first opens	39.0
	AFW actuation, 60 seconds after low-low SG level	90.9
	Maximum pressurizer pressure reached	36.0
	Maximum pressurizer volume reached	38.0
	Minimum SG liquid mass	255.0
	End of transient	10,000.0
Accidental depressurization of the reactor coolant system	Inadvertent opening of one RCS safety valve	0.0
	Overtemperature ΔT reactor trip setpoint reached	37.60
	Reactor trip	39.41
	Minimum DNBR occurs	40.0
Accidental depressurization of the main steam system	Inadvertent opening of one steam safety or relief valve	0
	Pressurizer empties	23
	2300 ppm boron reaches core (See note in Section 15.2.13.2.2)	345.2

Table 15.2-1 (continued)
TIME SEQUENCE OF EVENTS FOR CONDITION II EVENTS

Accident	Event	Time (sec)
Decay heat release line break		
Hot zero-power break	Break occurs	0.0
	Pressurizer empties	150
	Safety injection starts	172
	20,000 ppm reaches core	215
	Minimum shutdown margin reached	215
Hot full-power break	Low-low steam generator level trip	0.0
	Auxiliary feedwater starts	60
	Pressurizer empties	564
	Safety injection starts	566
	20,000 ppm reaches core	613
	Minimum shutdown margin reached	617
Inadvertent operation of ECCS during power operation	Charging pumps begin injecting borated water	0
	Low pressure trip point reached	59
	Rods begin to drop	61
Startup of an inactive reactor coolant loop	Initiation of flow through loop stop valve bypass line	0
	Loss of shutdown margin	984

Figure 15.2-1
UNCONTROLLED ROD WITHDRAWAL FROM A
SUBCRITICAL CONDITION
NEUTRON POWER VERSUS TIME

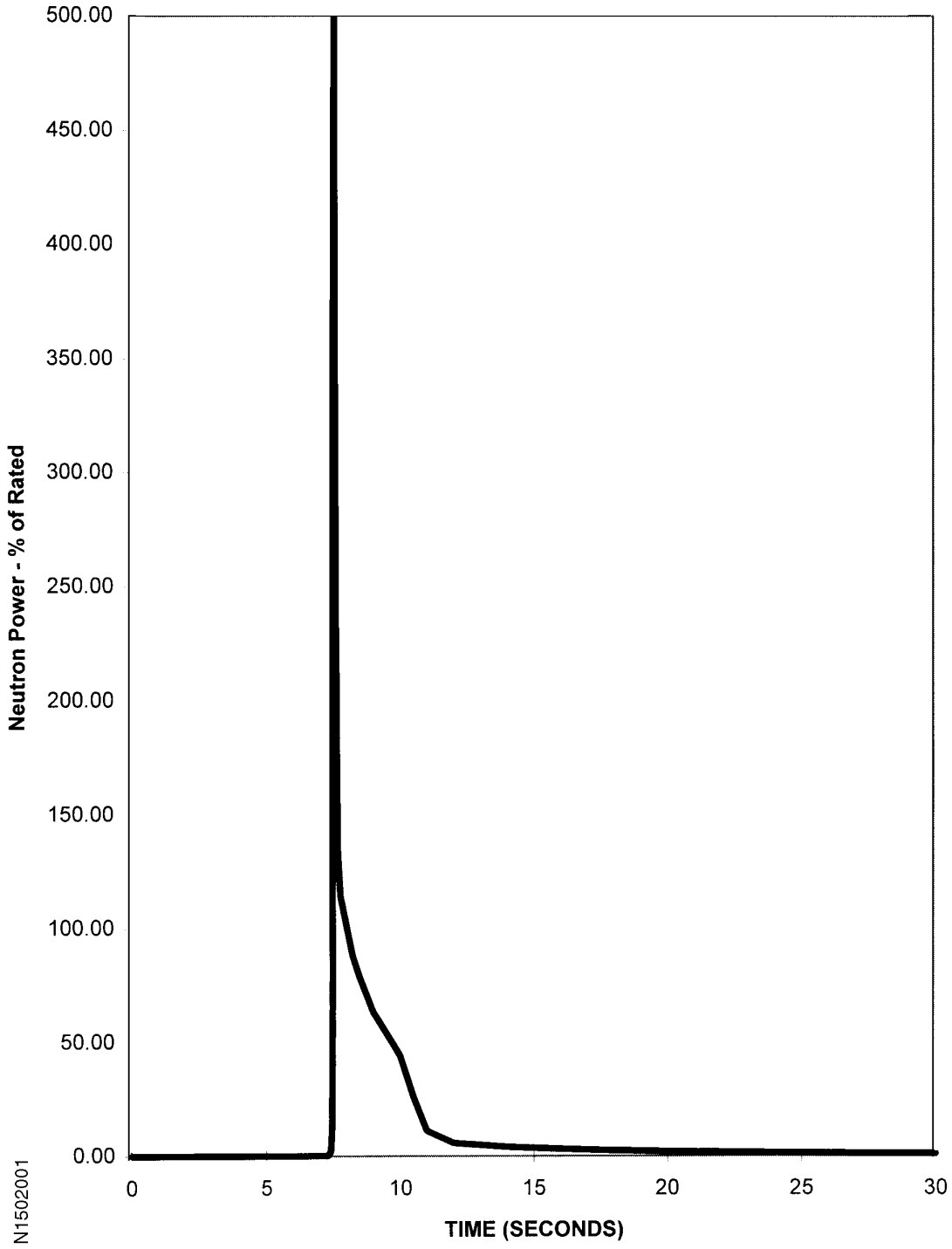

Figure 15.2-2
UNCONTROLLED ROD WITHDRAWAL FROM A
SUBCRITICAL CONDITION
CORE HEAT FLUX VERSUS TIME

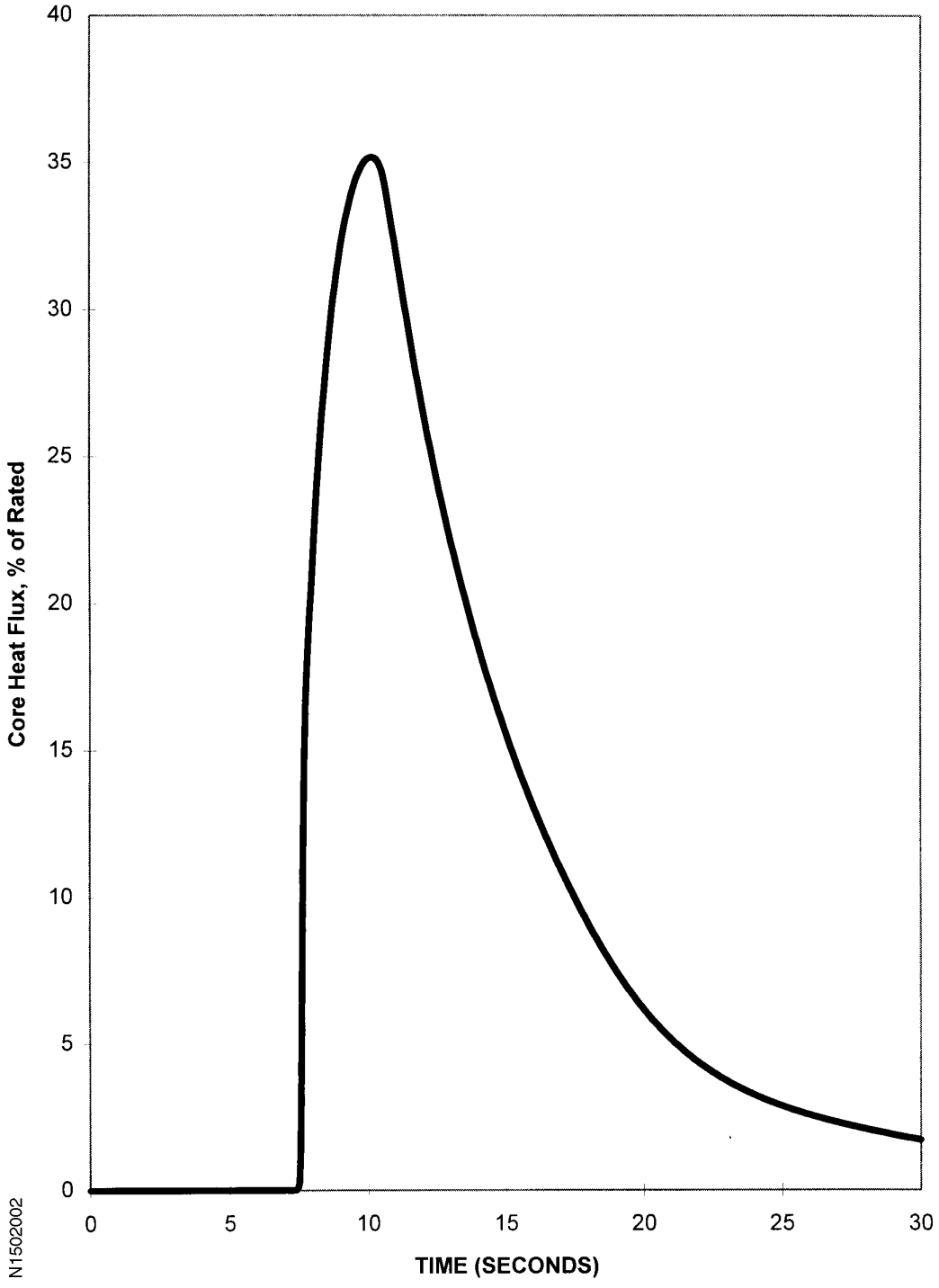

Figure 15.2-3
UNCONTROLLED ROD WITHDRAWAL FROM A
SUBCRITICAL CONDITION
CLAD AND FUEL TEMPERATURE VERSUS TIME

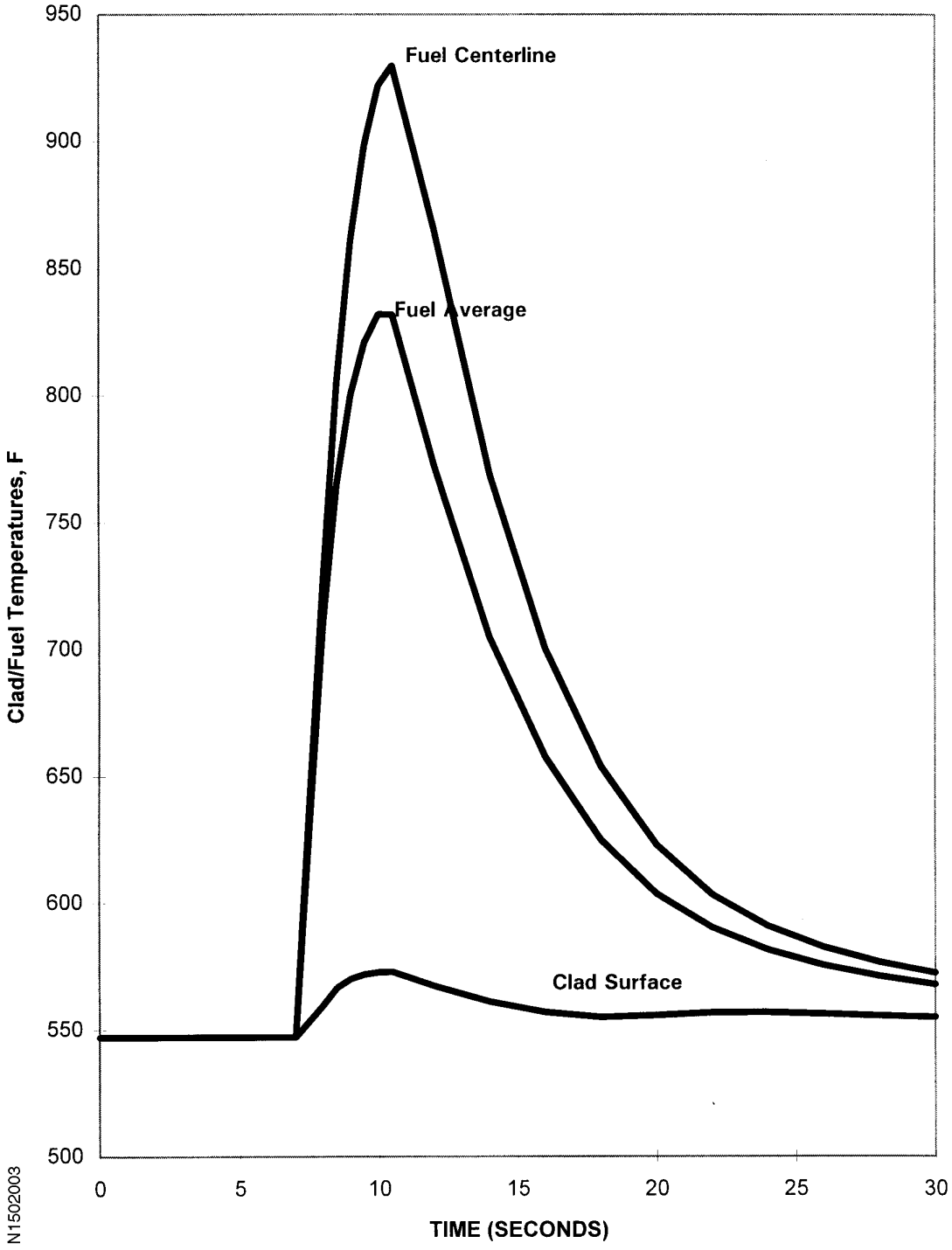

Figure 15.2-4
UNCONTROLLED ROD WITHDRAWAL FROM A
SUBCRITICAL CONDITION
COLD LEG PRESSURE VERSUS TIME

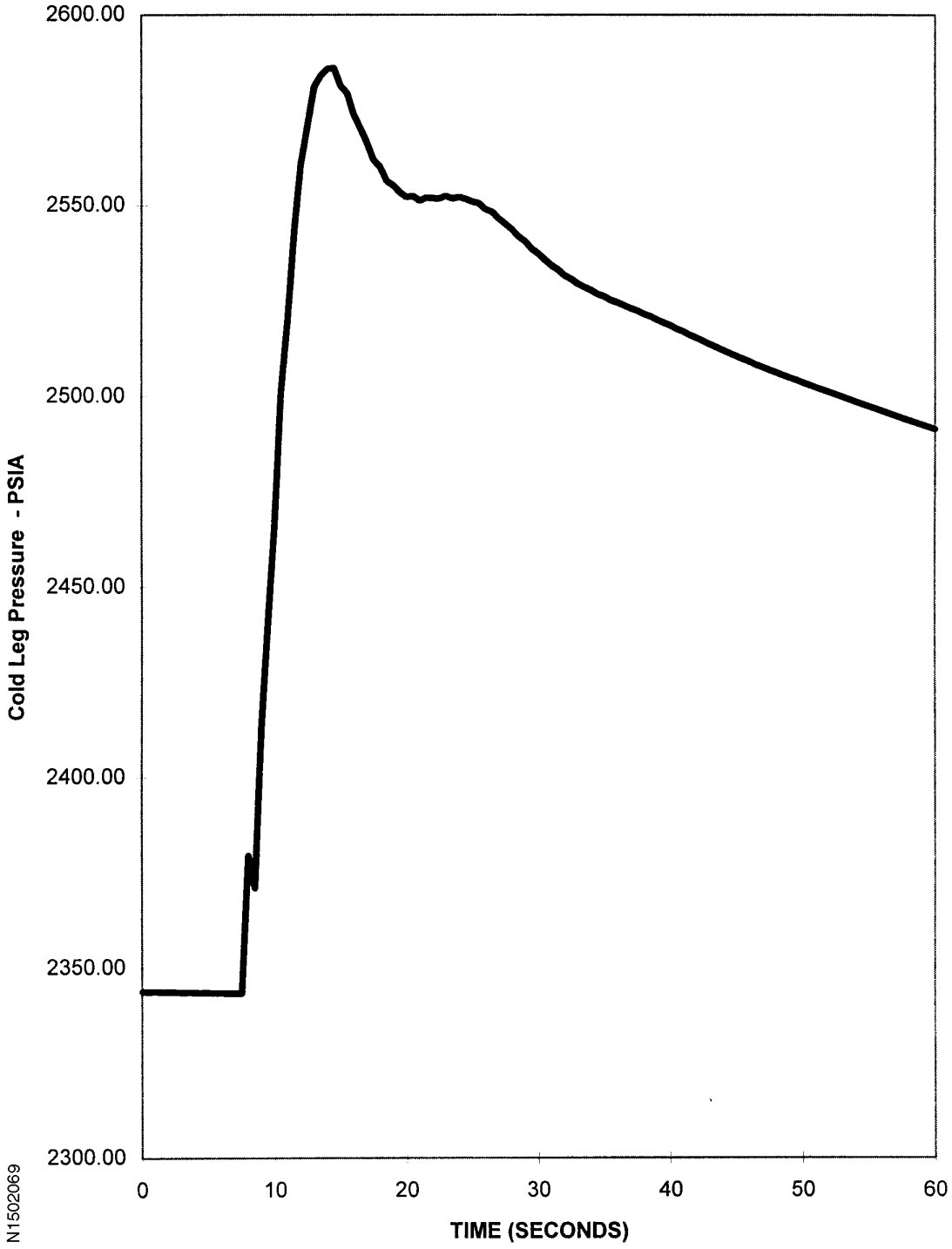

Figure 15.2-5
UNCONTROLLED ROD WITHDRAWAL FROM A
SUBCRITICAL CONDITION
STEAM PRESSURE VERSUS TIME

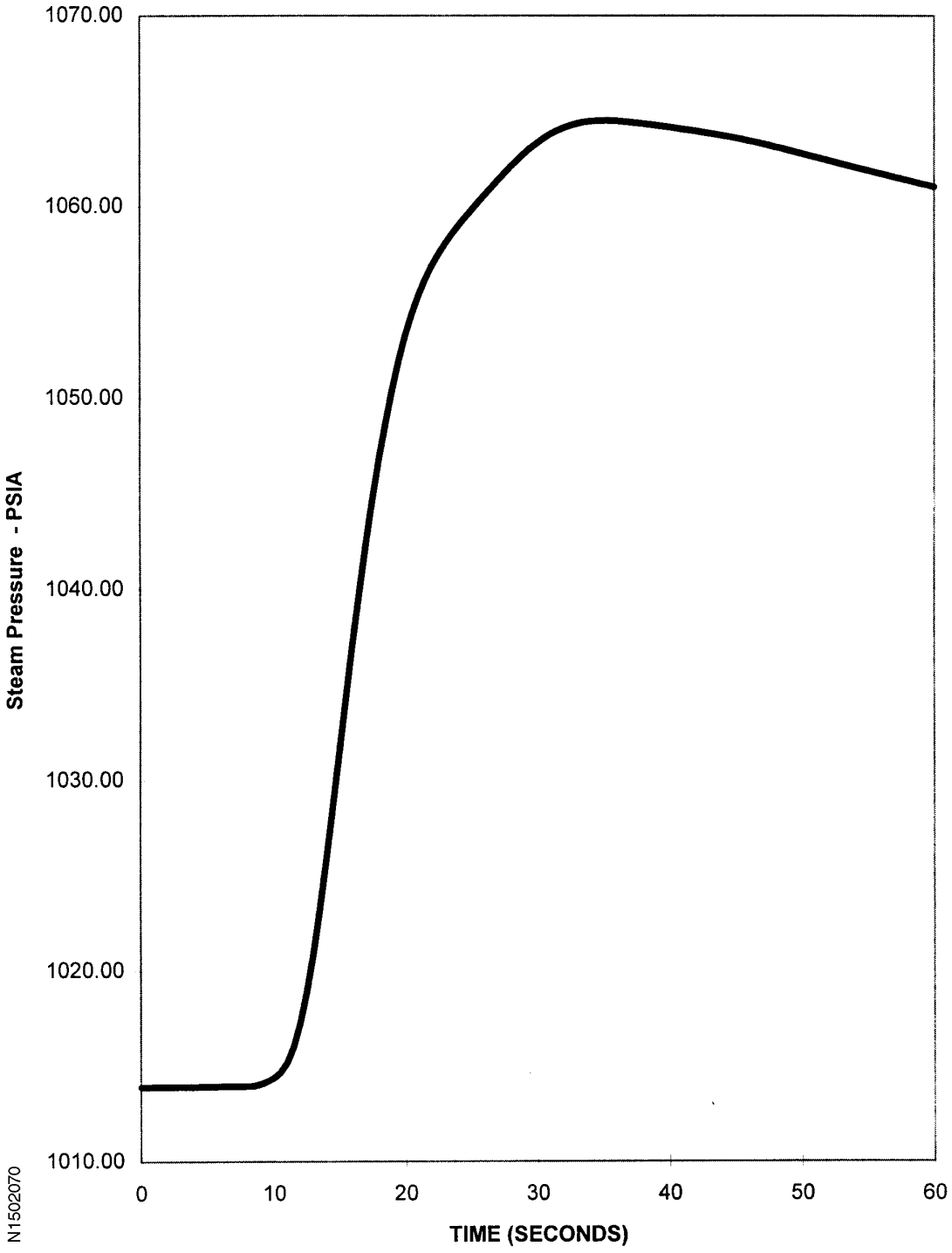

Figure 15.2-6
TRANSIENT RESPONSE FOR UNCONTROLLED ROD BANK
WITHDRAWAL FROM FULL POWER TERMINATED BY
HIGH NEUTRON FLUX TRIP
REACTIVITY INSERTION RATE = 75 PCM/SEC; MINIMUM FEEDBACK

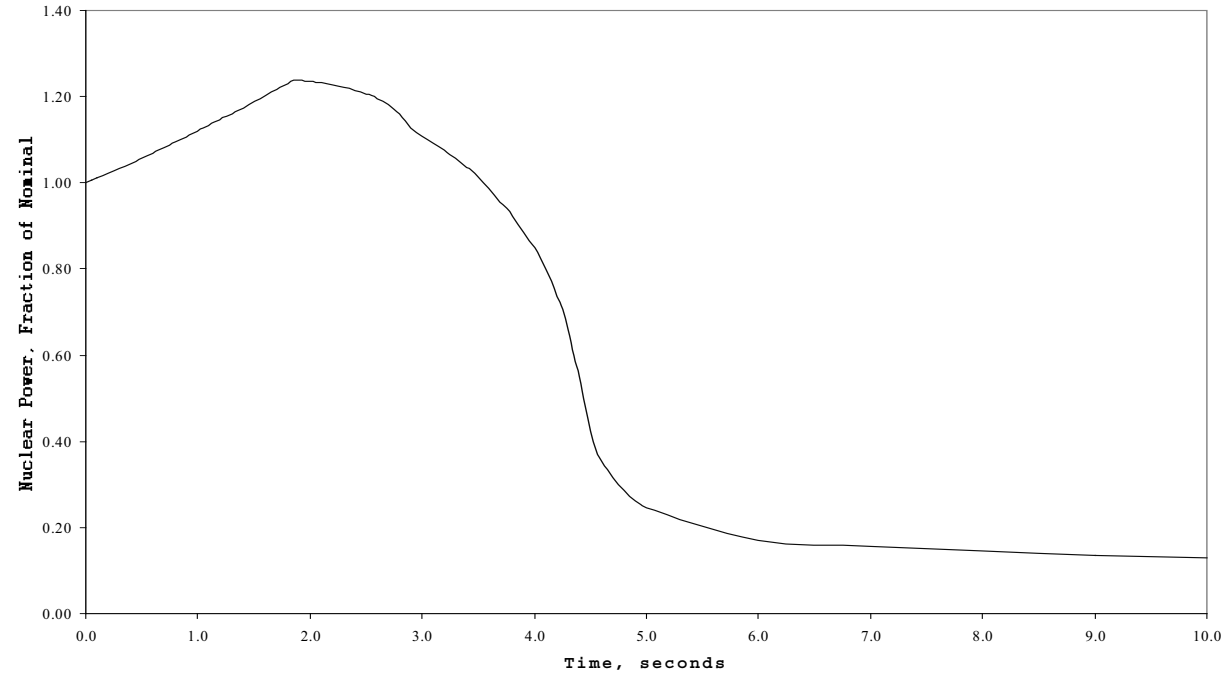

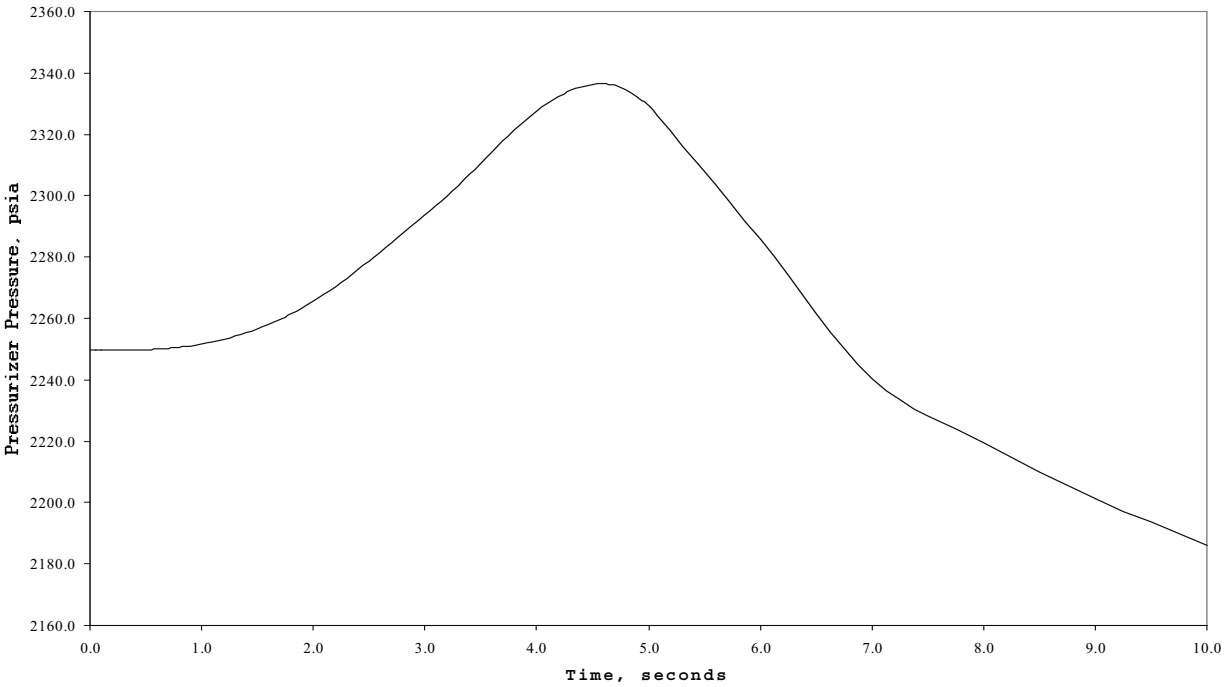

Figure 15.2-7
TRANSIENT RESPONSE FOR UNCONTROLLED ROD BANK
WITHDRAWAL FROM FULL POWER TERMINATED BY
HIGH NEUTRON FLUX TRIP
REACTIVITY INSERTION RATE = 75 PCM/SEC; MINIMUM FEEDBACK

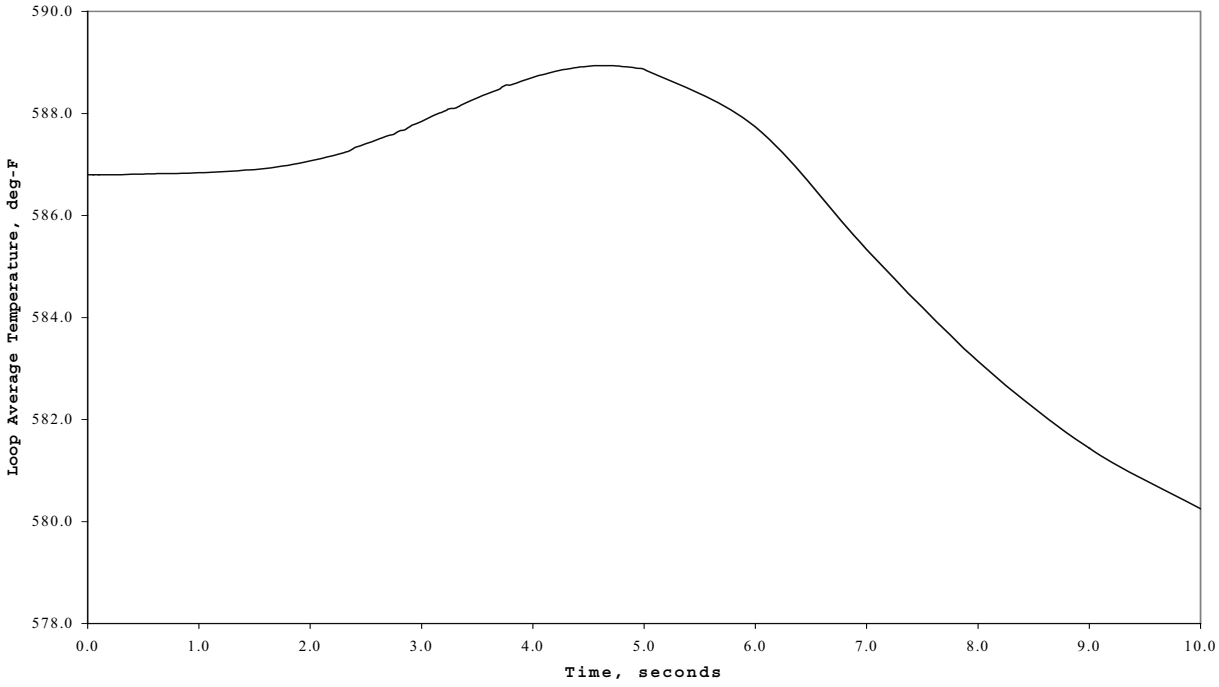

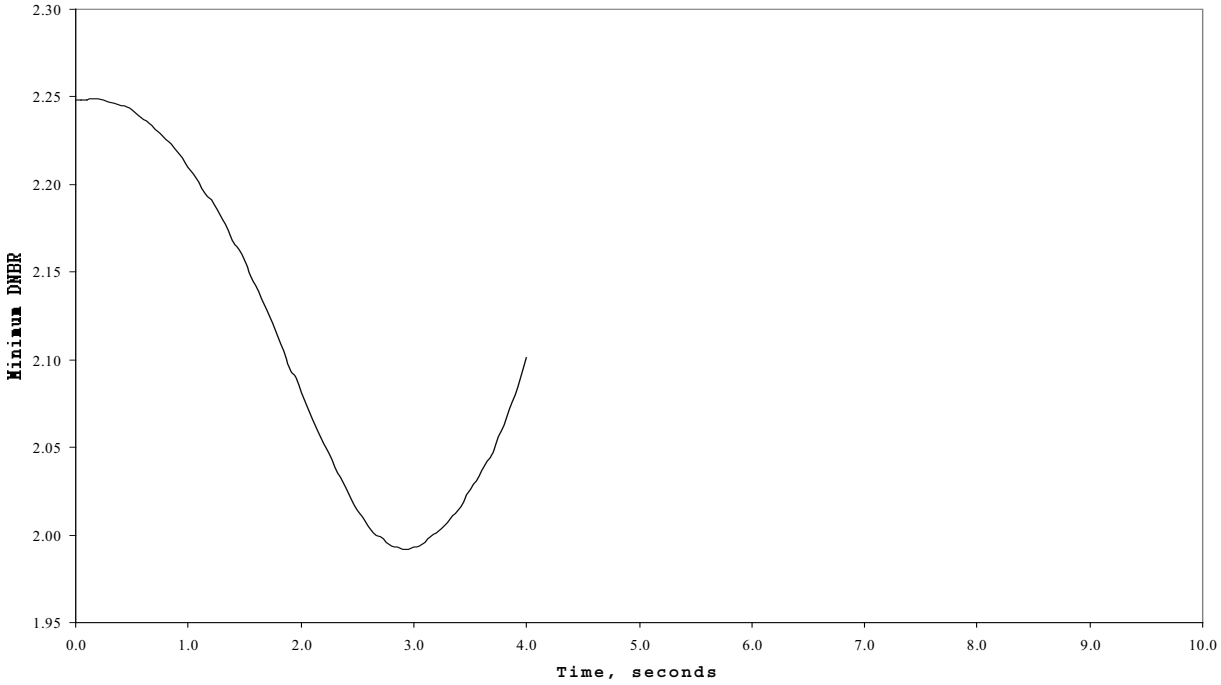

Figure 15.2-8
TRANSIENT RESPONSE FOR UNCONTROLLED ROD BANK
WITHDRAWAL FROM FULL POWER TERMINATED BY
OVERTEMPERATURE DELTA-T TRIP
REACTIVITY INSERTION RATE = 1.2 PCM/SEC; MINIMUM FEEDBACK

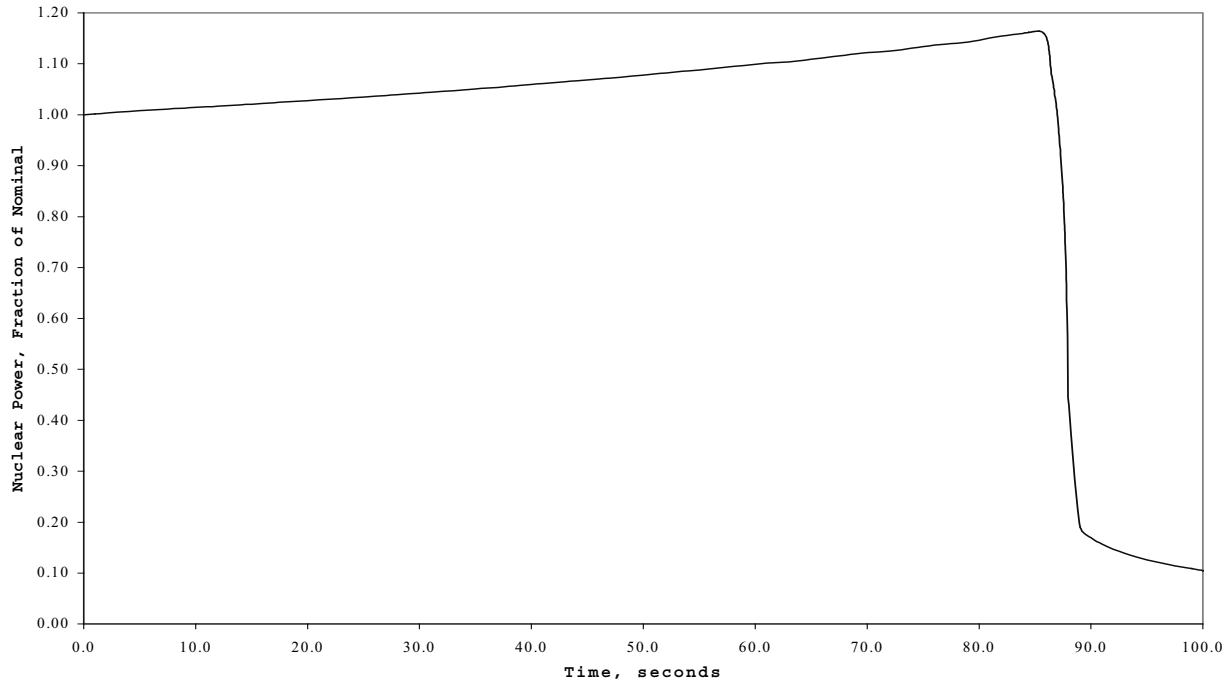

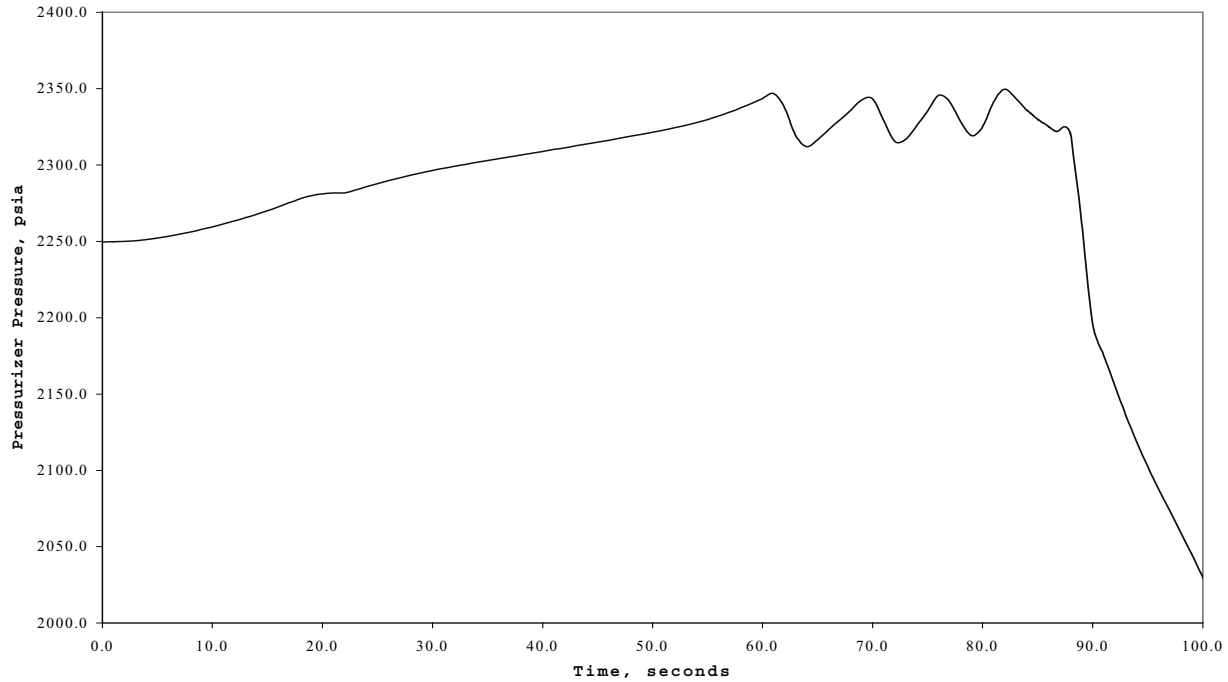

Figure 15.2-9
TRANSIENT RESPONSE FOR UNCONTROLLED ROD BANK
WITHDRAWAL FROM FULL POWER TERMINATED BY
OVERTEMPERATURE DELTA-T TRIP
REACTIVITY INSERTION RATE = 1.2 PCM/SEC; MINIMUM FEEDBACK

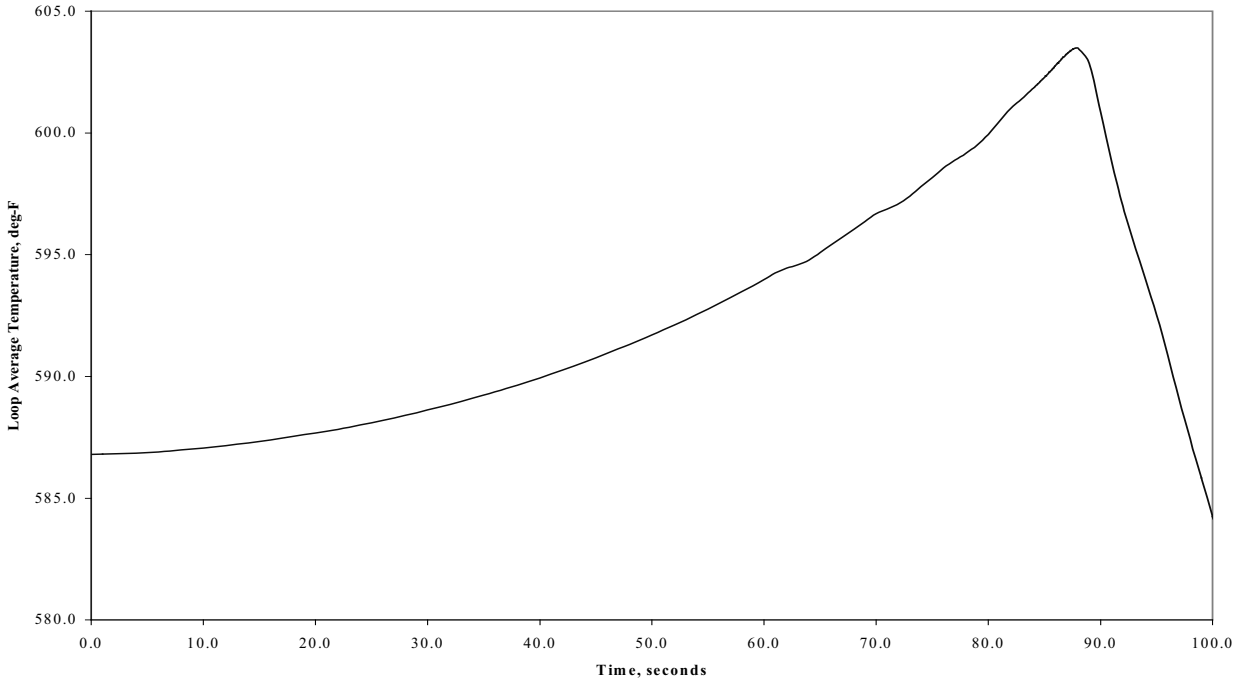

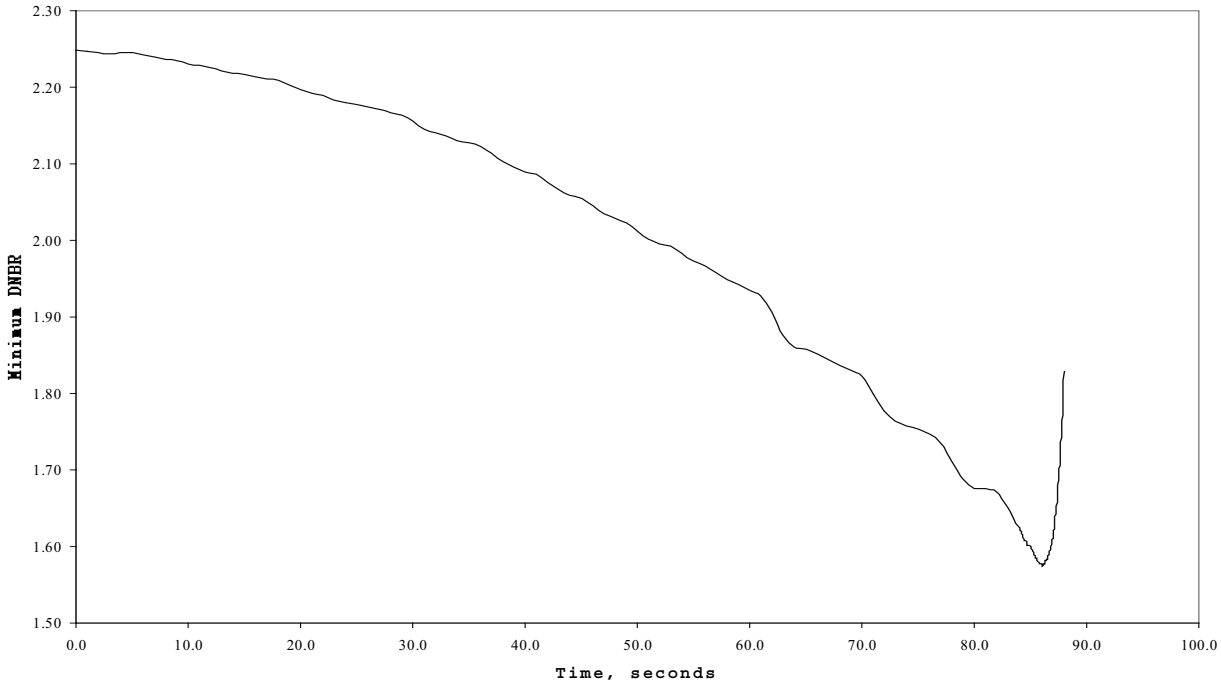

Figure 15.2-10
EFFECT OF REACTIVITY INSERTION RATE
ON MINIMUM DNBR FOR A ROD BANK WITHDRAWAL
ACCIDENT FROM 100% POWER

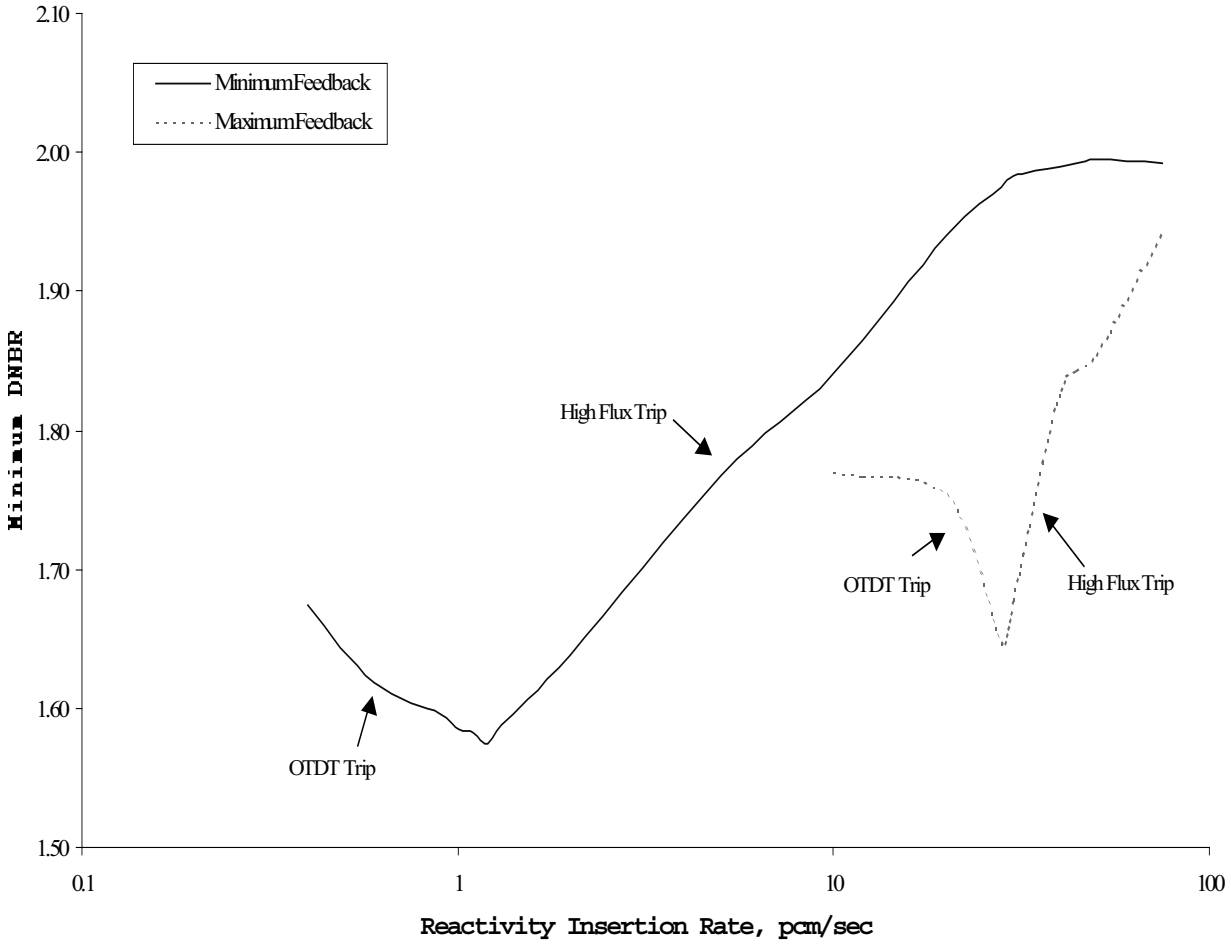

Figure 15.2-11
EFFECT OF REACTIVITY INSERTION RATE
ON MINIMUM DNBR FOR A ROD BANK WITHDRAWAL
ACCIDENT FROM 100% POWER; MINIMUM FEEDBACK

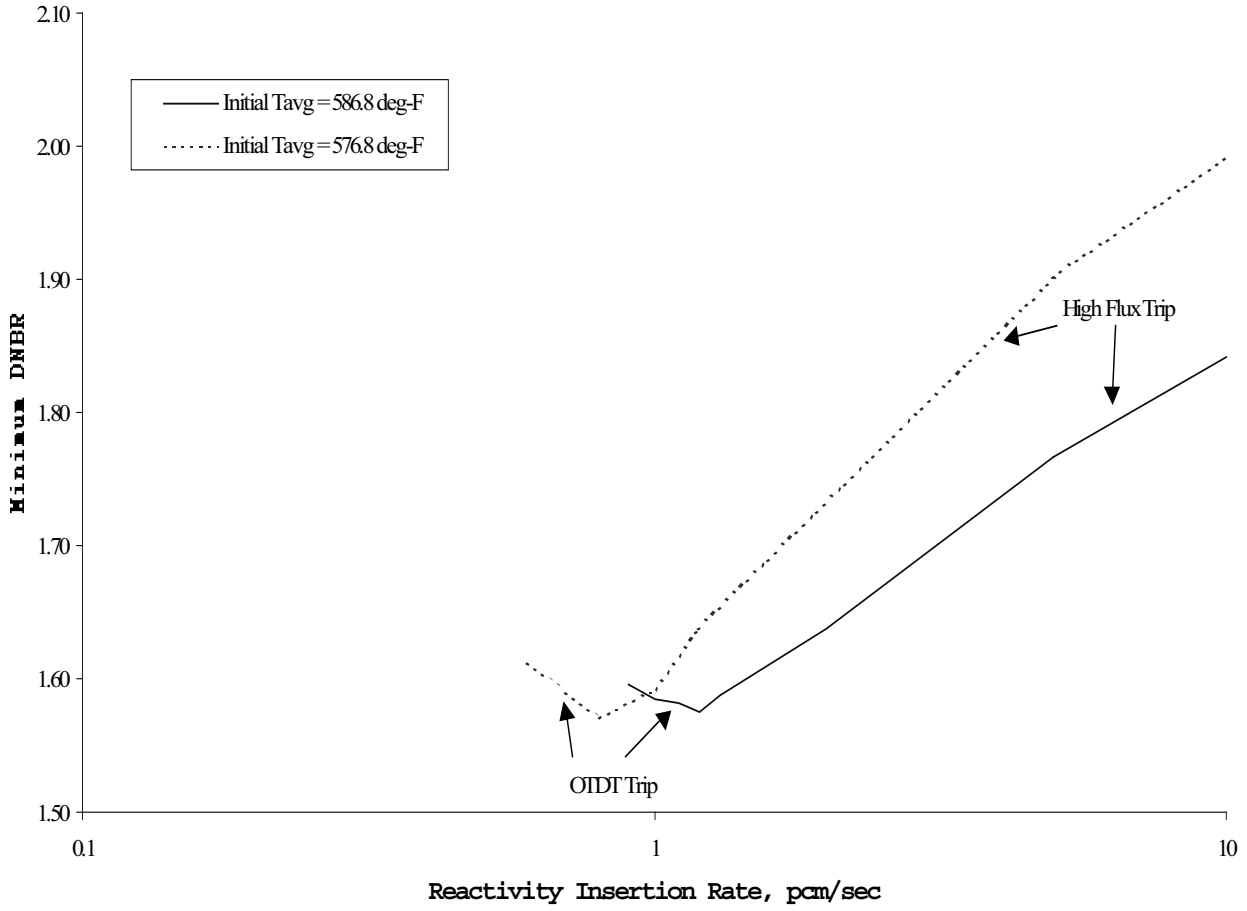

Figure 15.2-12
EFFECT OF REACTIVITY INSERTION RATE
ON MINIMUM DNBR FOR A ROD BANK WITHDRAWAL
ACCIDENT FROM 60% POWER

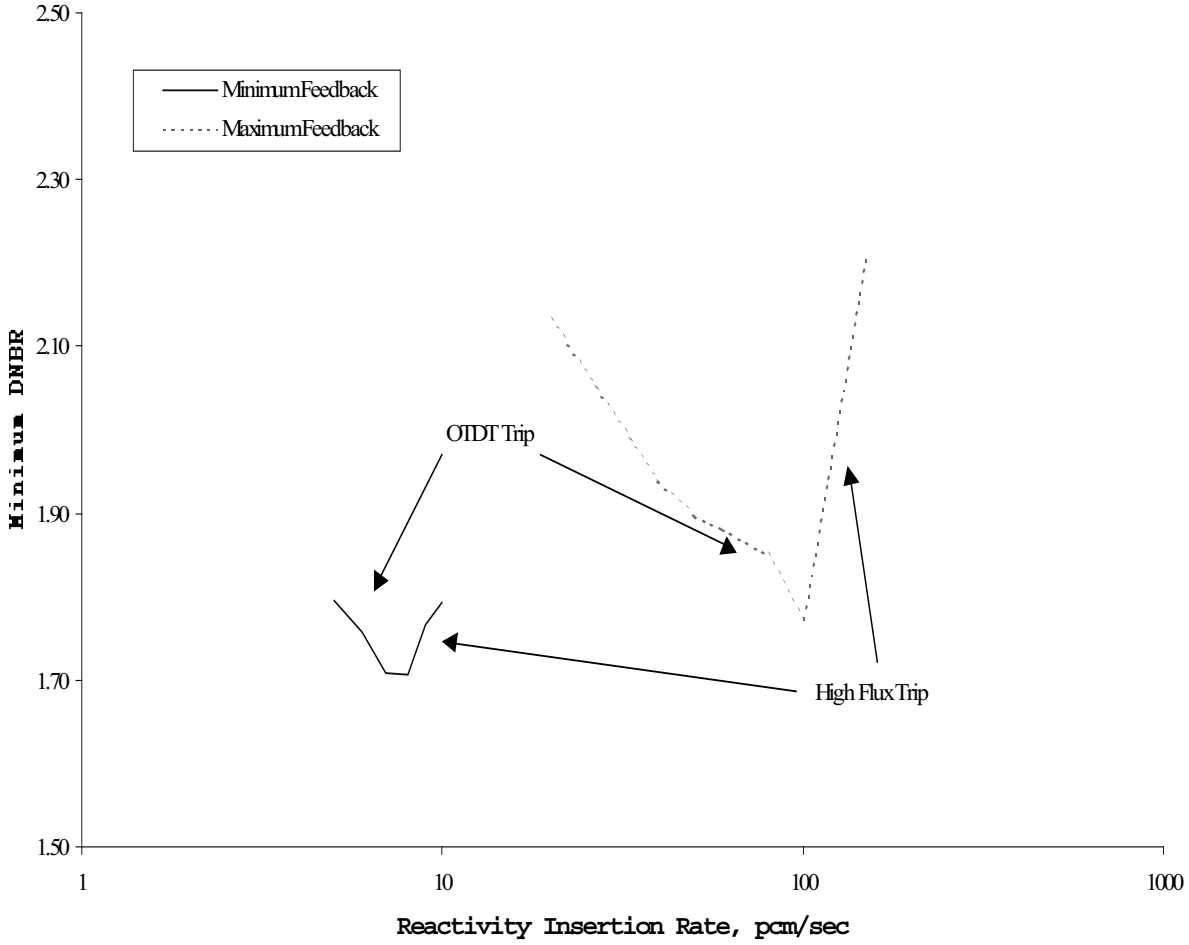

Figure 15.2-13
EFFECT OF REACTIVITY INSERTION RATE
ON MINIMUM DNBR FOR A ROD BANK WITHDRAWAL
ACCIDENT FROM 10% POWER

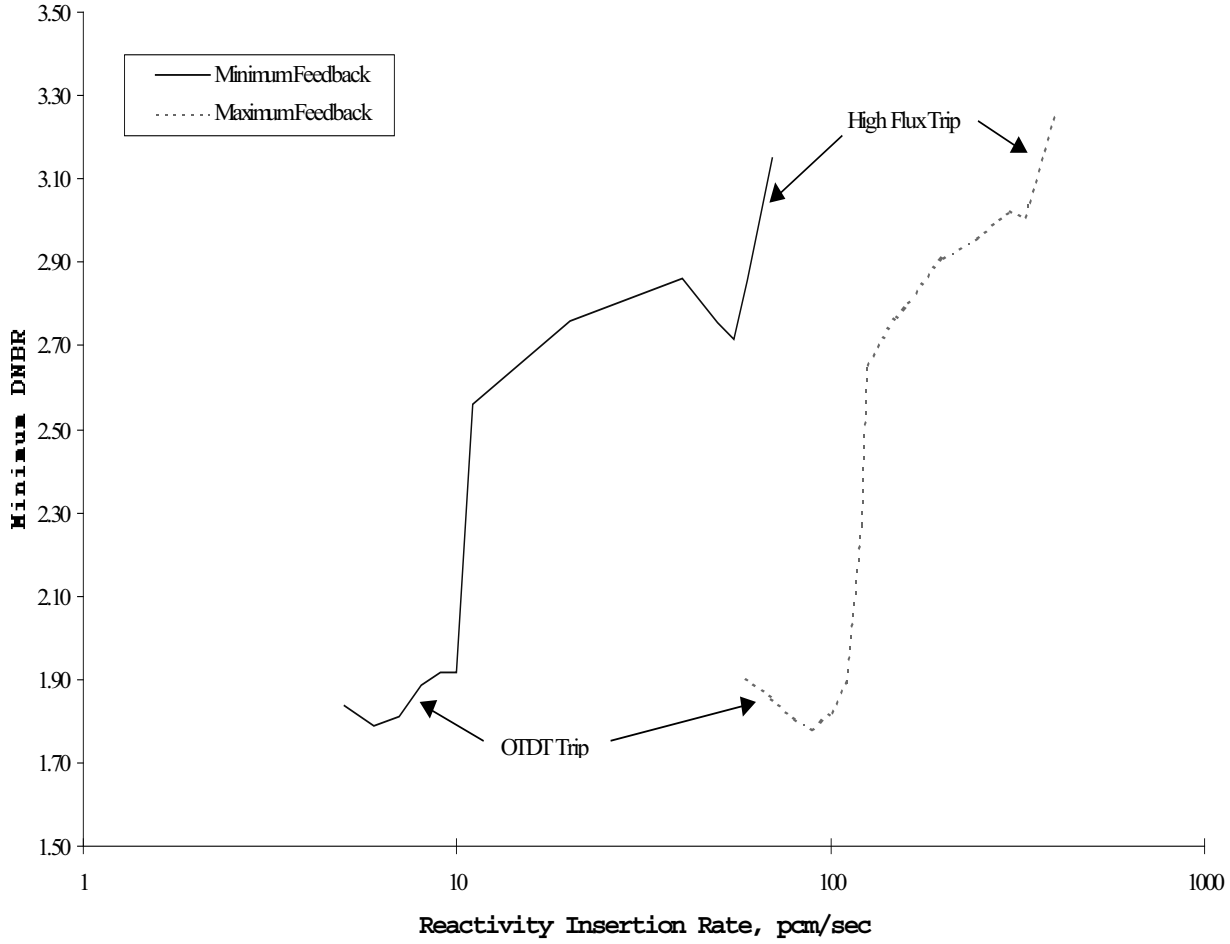

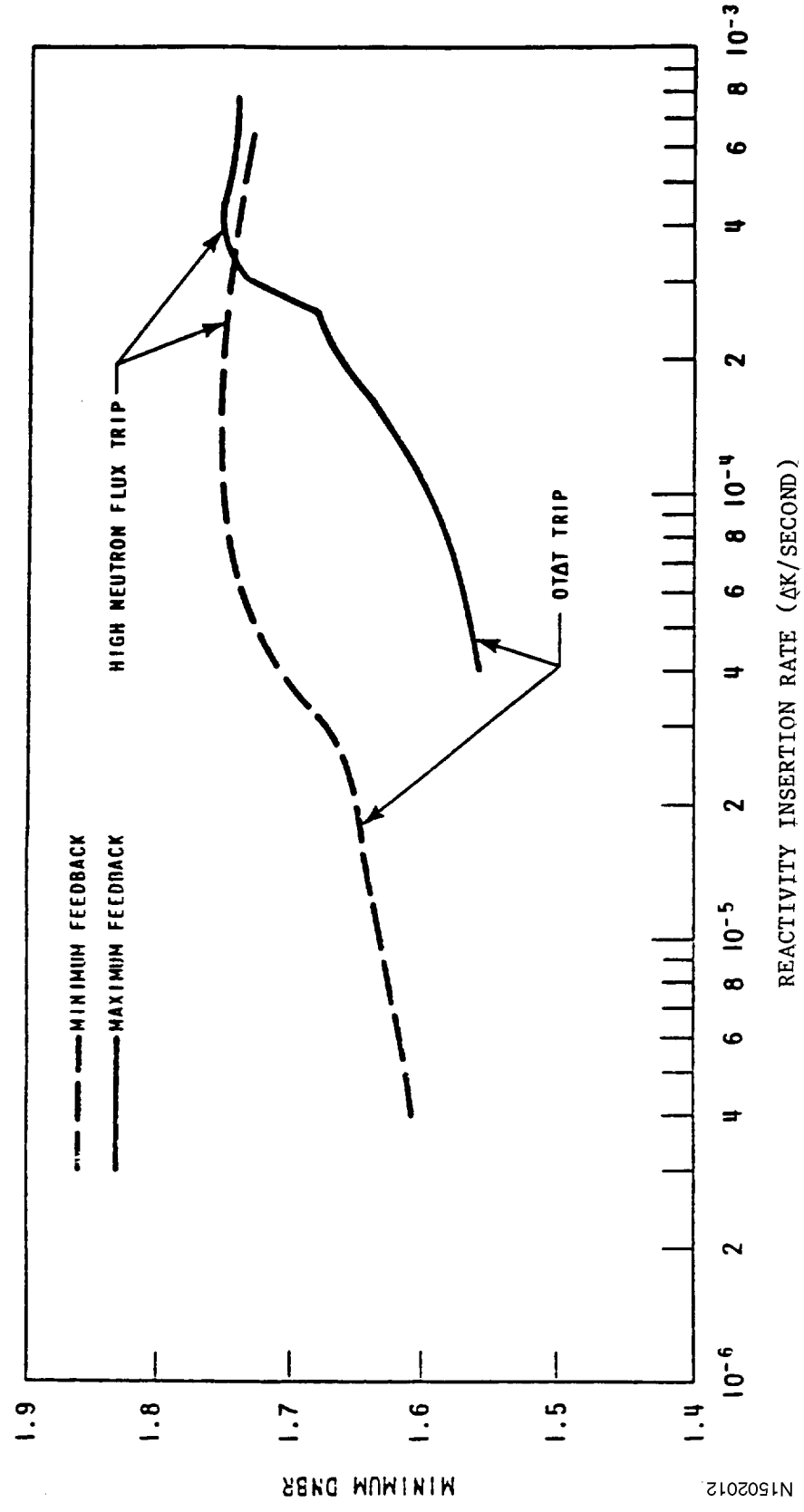

Figure 15.2-14
ROD WITHDRAWAL TRANSIENT AT 65% POWER,
TWO-LOOP OPERATION WITH LOOP STOP VALVES CLOSED

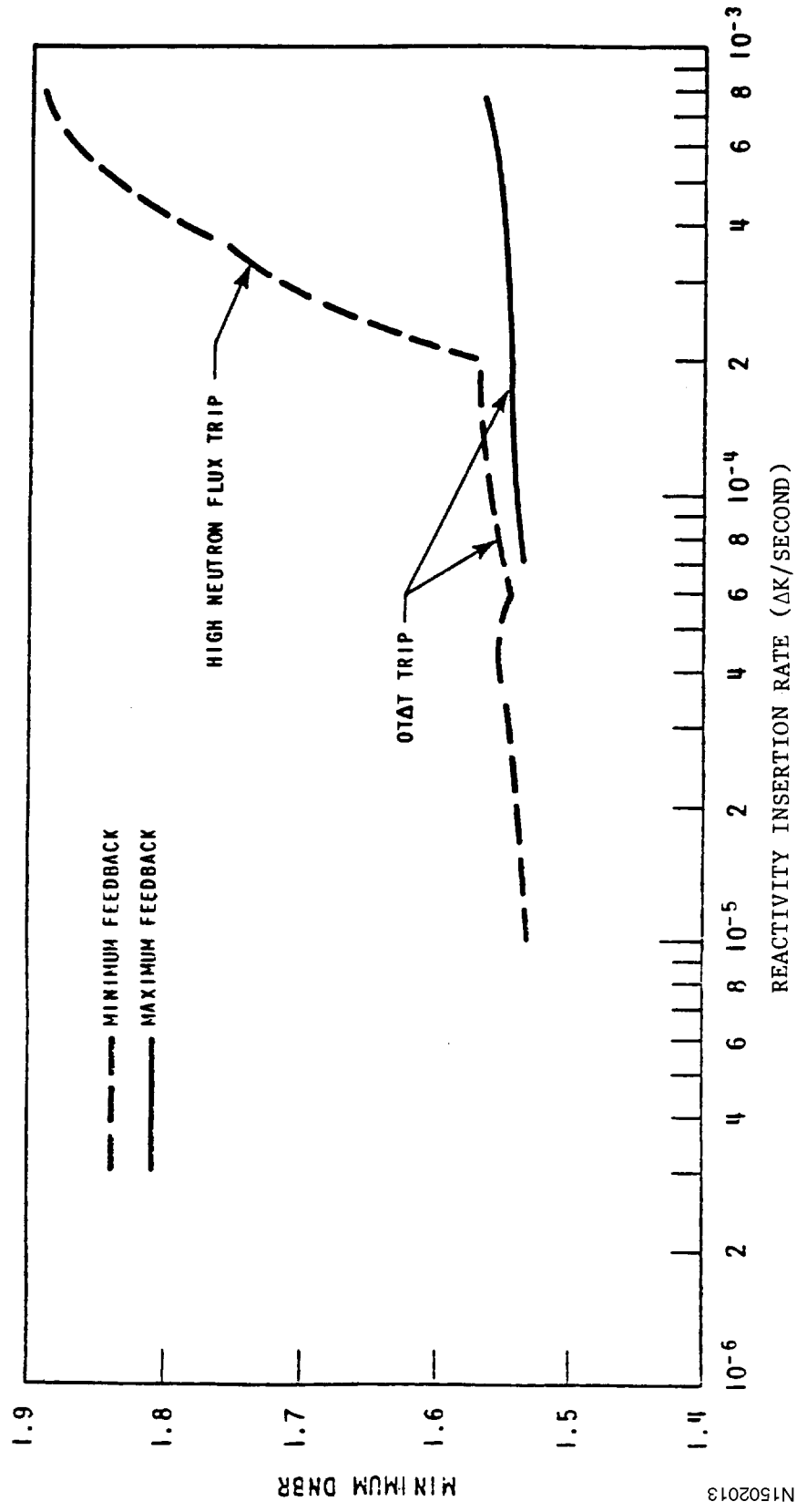

Figure 15.2-15
ROD WITHDRAWAL TRANSIENT AT 10% POWER,
TWO-LOOP OPERATION WITH LOOP STOP VALVES CLOSED

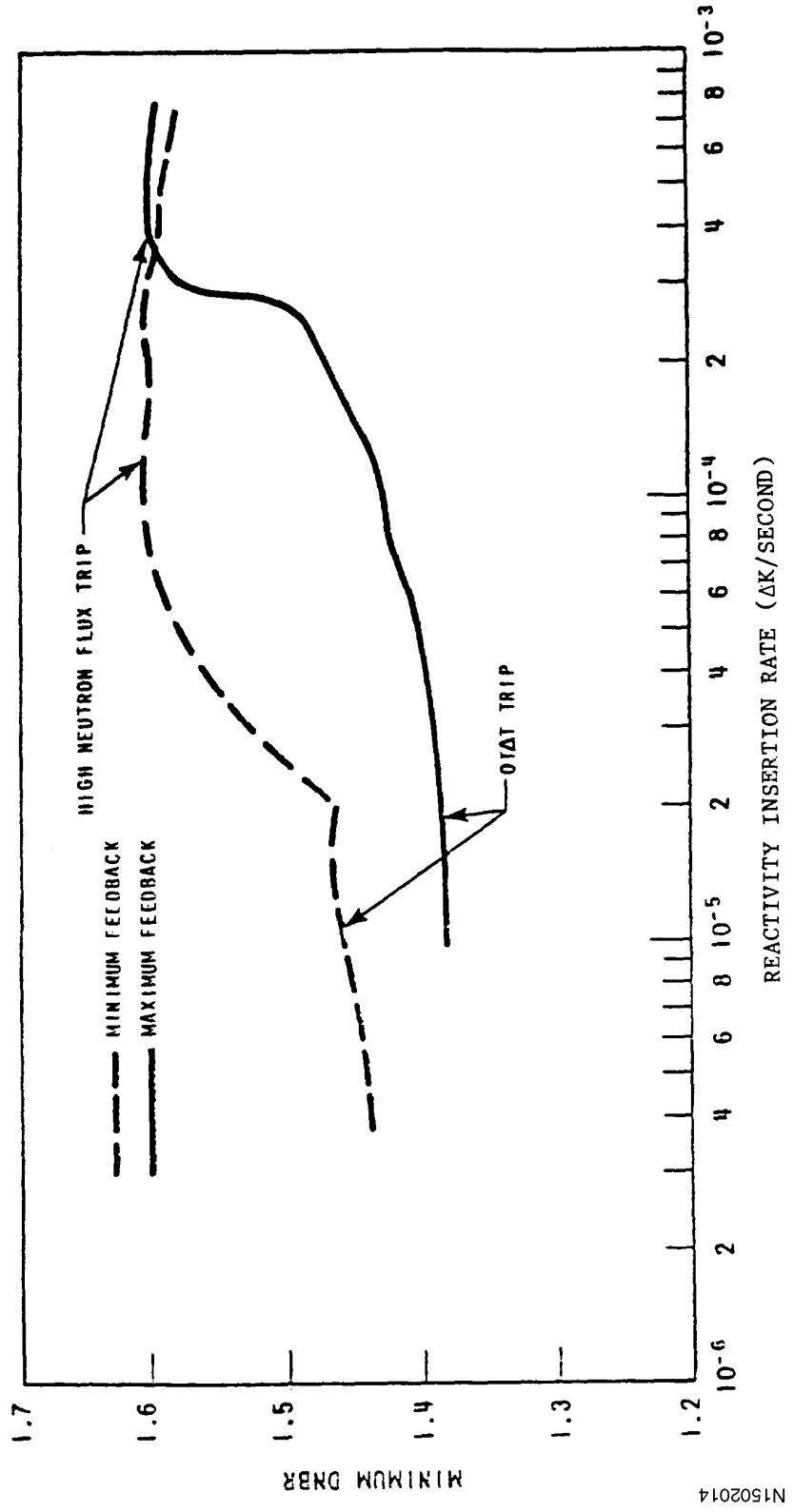

Figure 15.2-16
ROD WITHDRAWAL TRANSIENT AT 60% POWER,
TWO-LOOP OPERATION WITH LOOP STOP VALVES OPEN

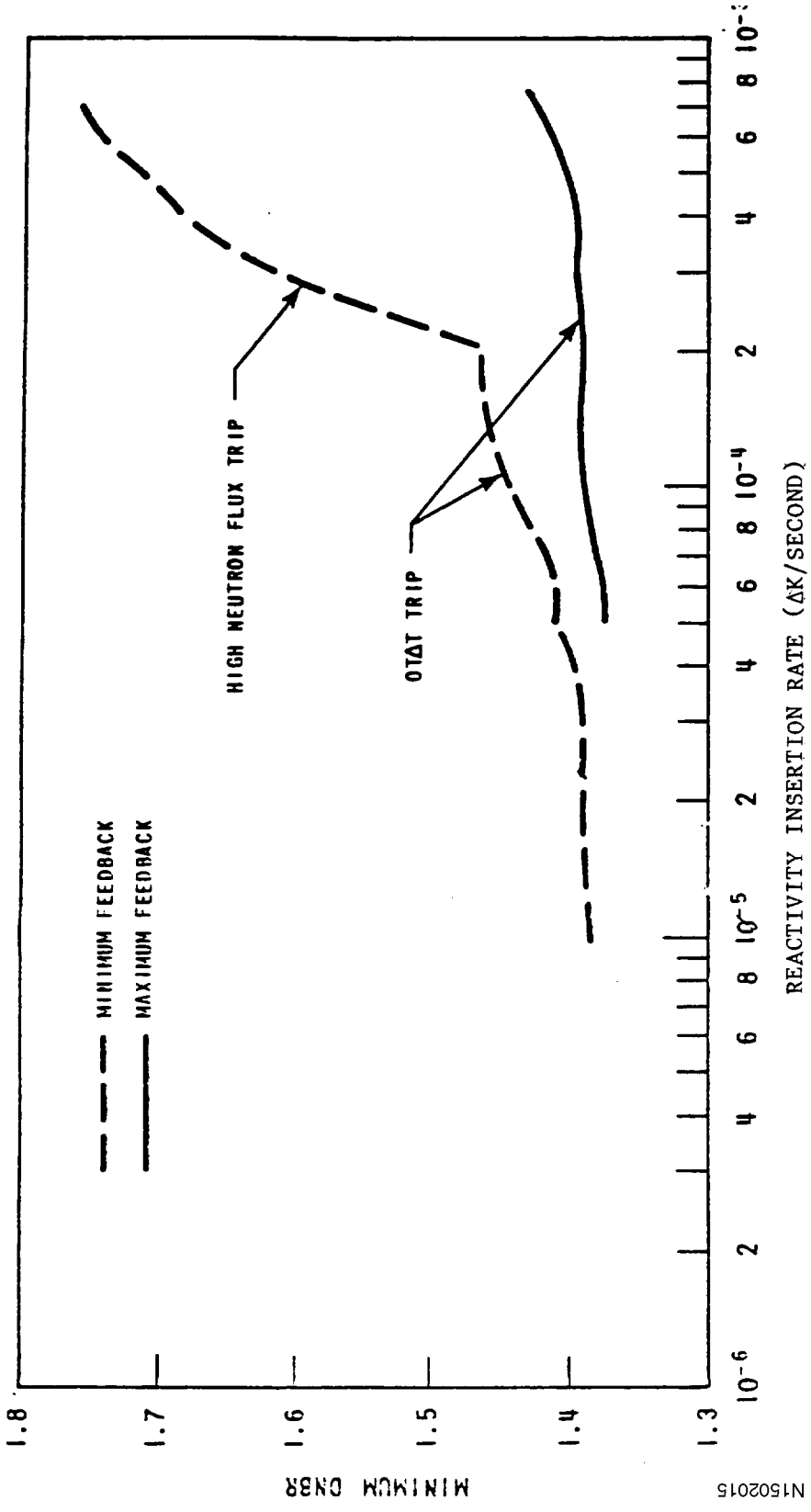

Figure 15.2-17
ROD WITHDRAWAL TRANSIENT AT 10% POWER,
TWO-LOOP OPERATION WITH LOOP STOP VALVES OPEN

Figure 15.2-18 (SHEET 1 OF 2)
TRANSIENT RESPONSE
TO A DROPPED ROD CLUSTER CONTROL ASSEMBLY

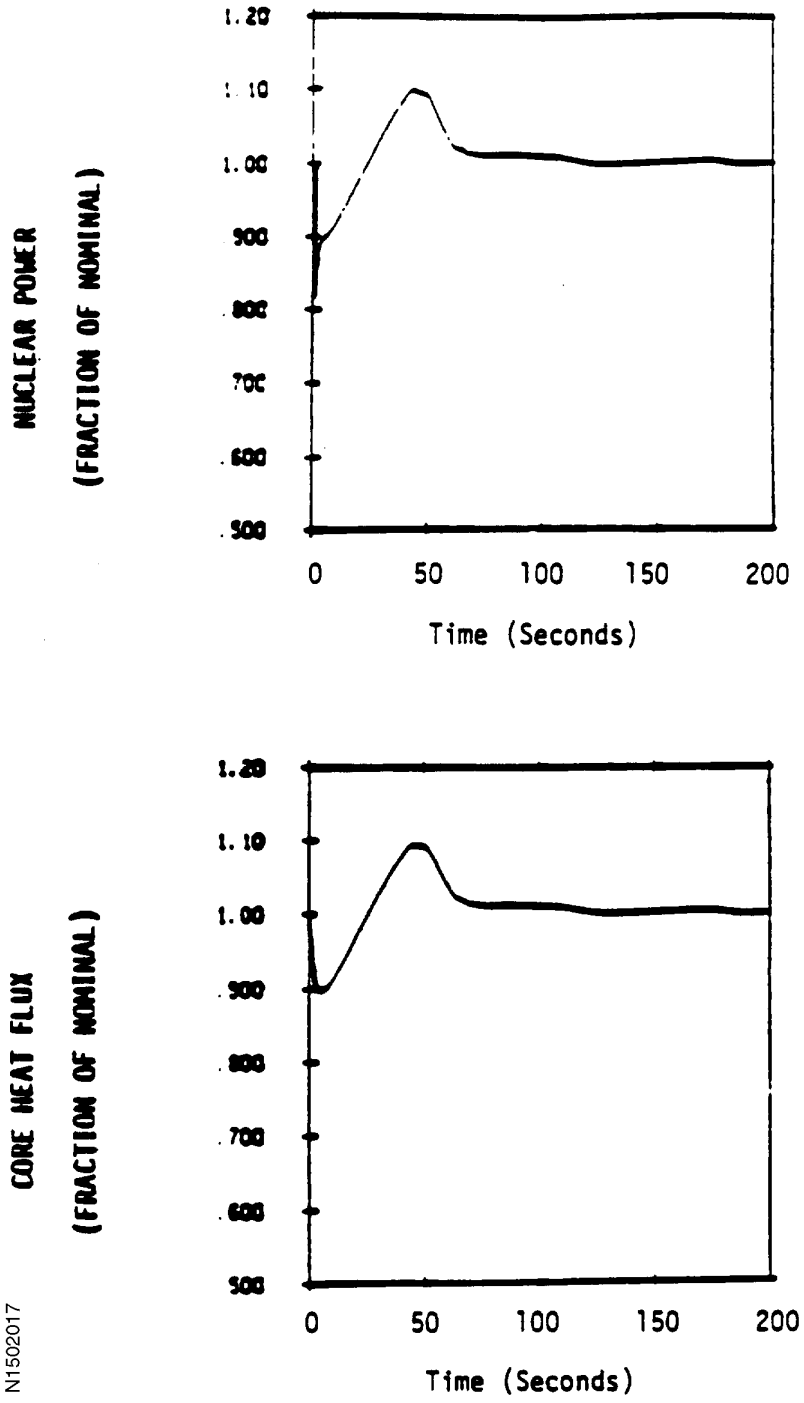

Figure 15.2-18 (SHEET 2 OF 2)
TRANSIENT RESPONSE
TO A DROPPED ROD CLUSTER CONTROL ASSEMBLY

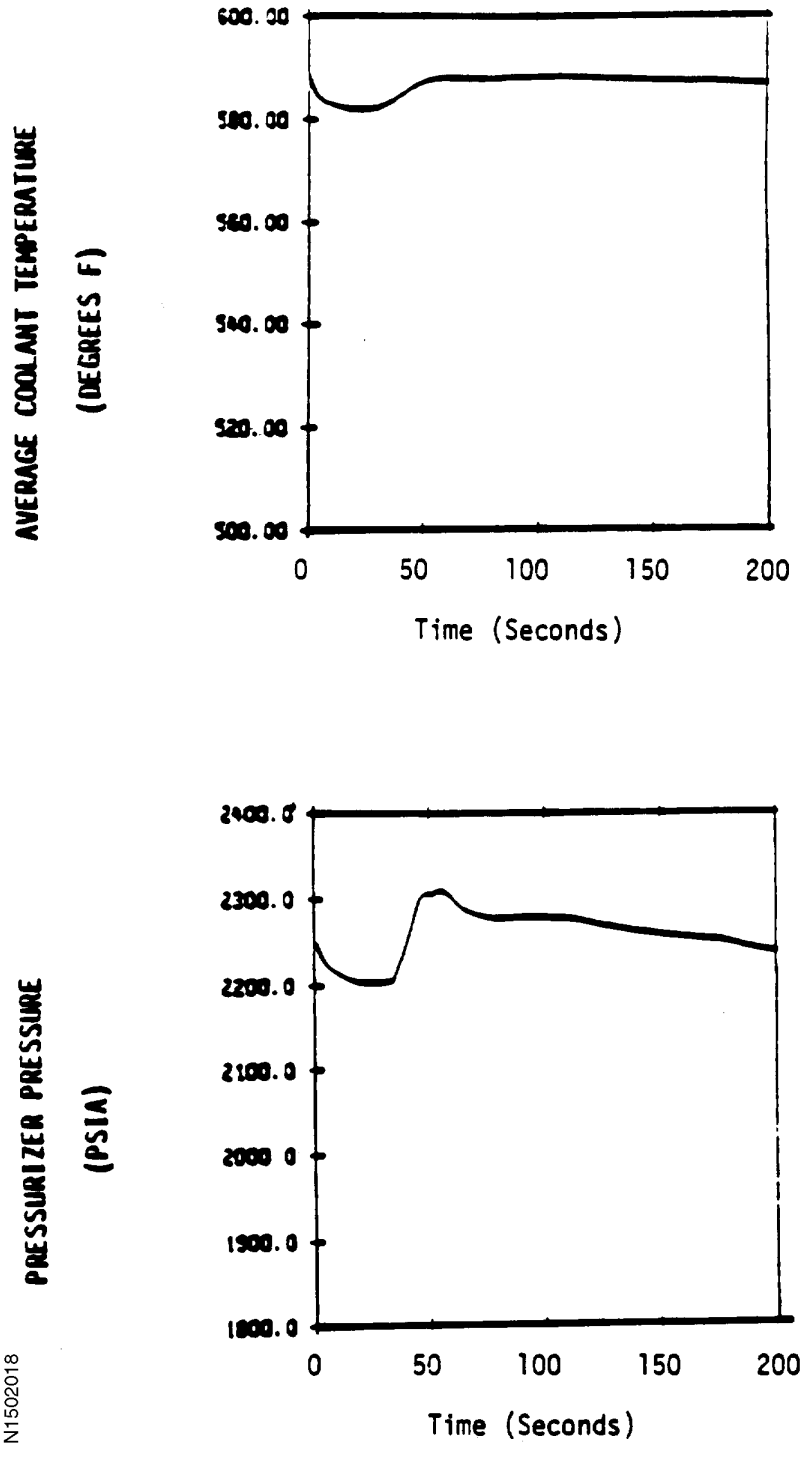

Figure 15.2-19
LOSS OF LOAD ACCIDENT, WITH PRESSURIZER SPRAY AND
POWER-OPERATED RELIEF VALVE, BEGINNING OF LIFE
(NUCLEAR POWER)

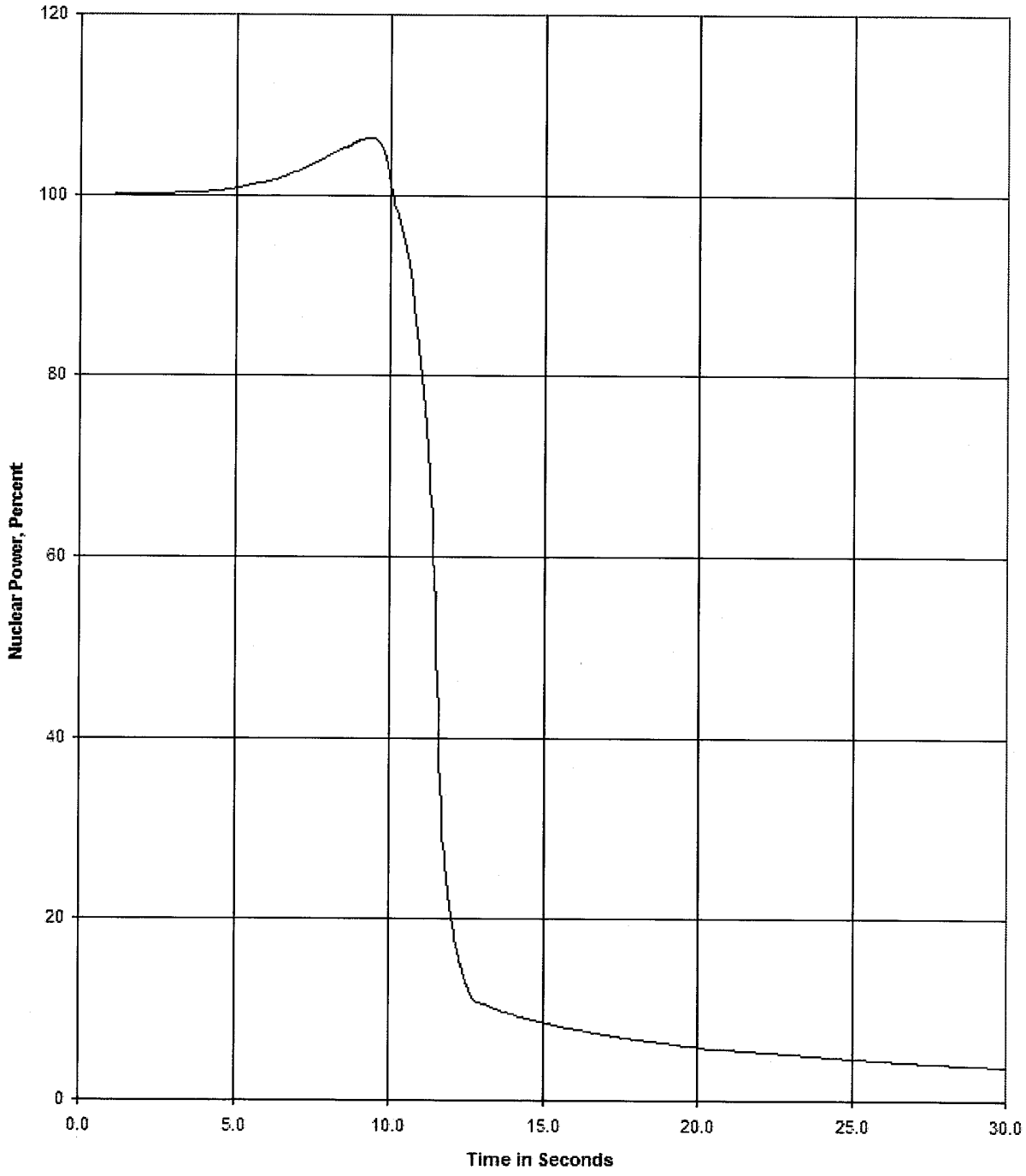

Figure 15.2-20
LOSS OF LOAD ACCIDENT, WITH PRESSURIZER SPRAY AND
POWER-OPERATED RELIEF VALVE, BEGINNING OF LIFE
(CORE INLET TEMPERATURE)

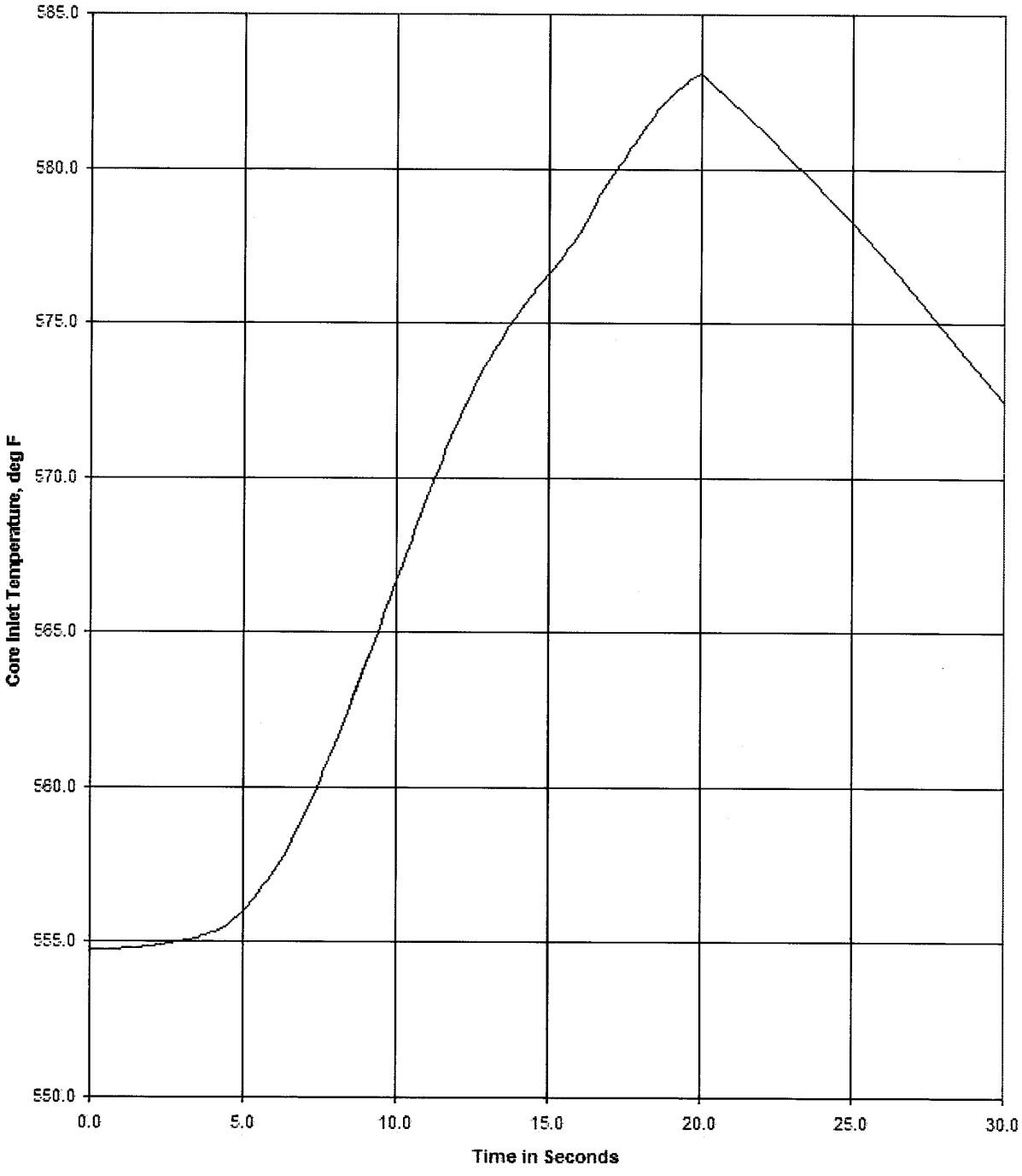

Figure 15.2-21
LOSS OF LOAD ACCIDENT, WITH PRESSURIZER SPRAY AND
POWER-OPERATED RELIEF VALVE, BEGINNING OF LIFE
(PRESSURIZER PRESSURE)

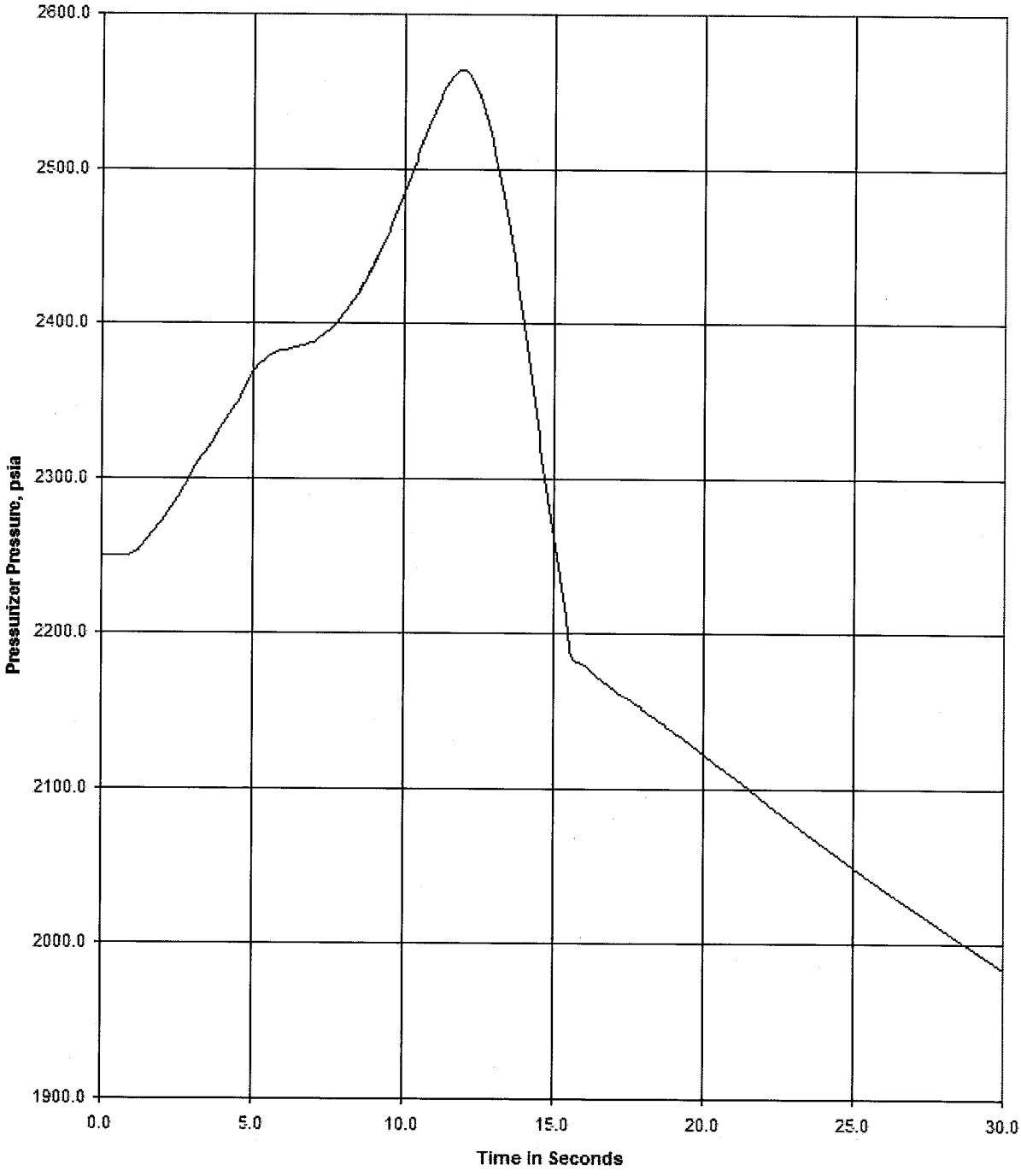

Figure 15.2-22
LOSS OF LOAD ACCIDENT, WITH PRESSURIZER SPRAY AND
POWER-OPERATED RELIEF VALVE, BEGINNING OF LIFE
(RCS AVG TEMPERATURE)

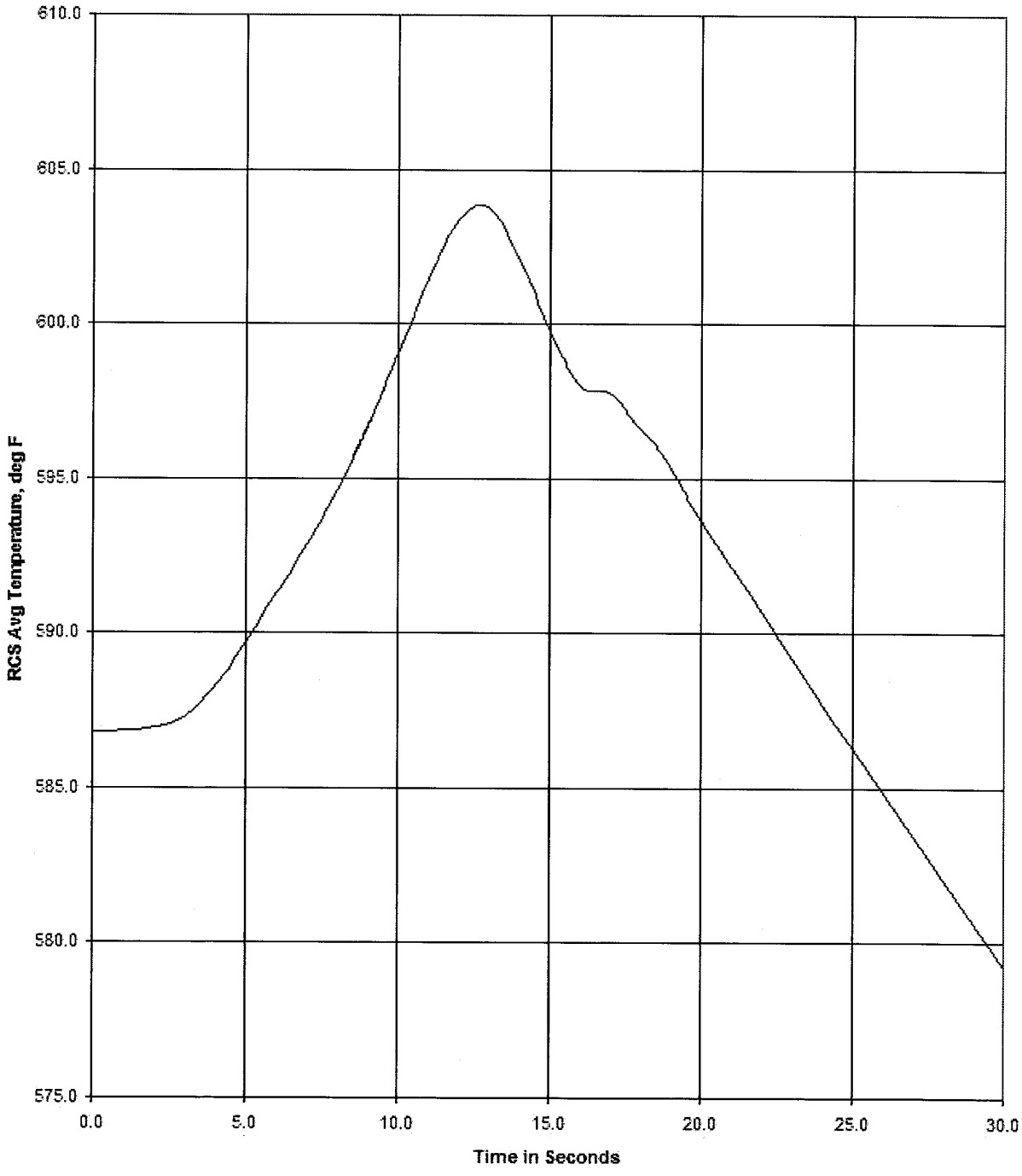

Figure 15.2-23
LOSS OF LOAD ACCIDENT, WITH PRESSURIZER SPRAY AND
POWER-OPERATED RELIEF VALVE, BEGINNING OF LIFE
(PRESSURIZER WATER VOLUME)

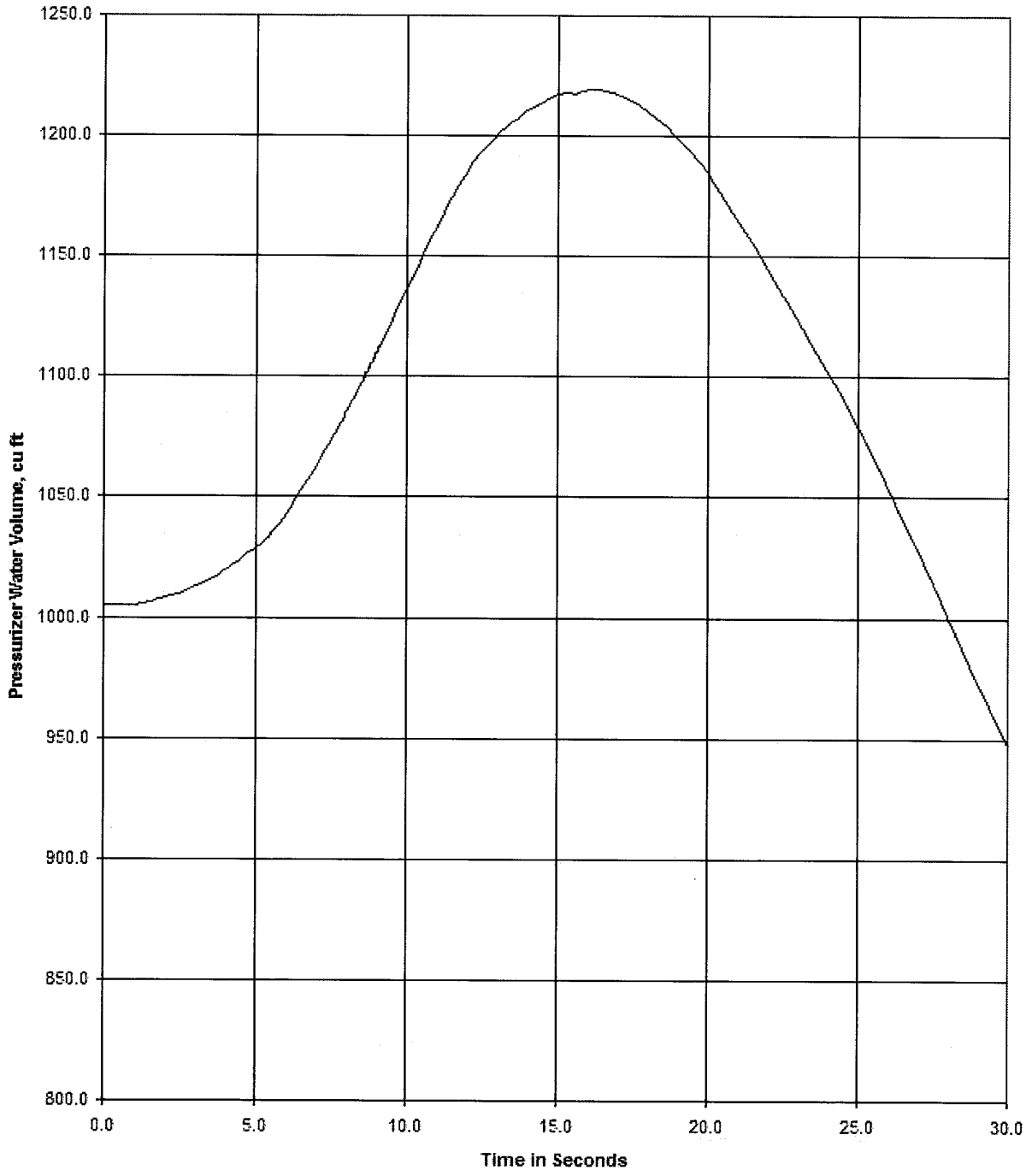

Figure 15.2-24
DELETED

Figure 15.2-25
LOSS OF LOAD ACCIDENT, WITHOUT PRESSURIZER SPRAY AND
POWER-OPERATED RELIEF VALVE, BEGINNING OF LIFE
(NUCLEAR POWER)

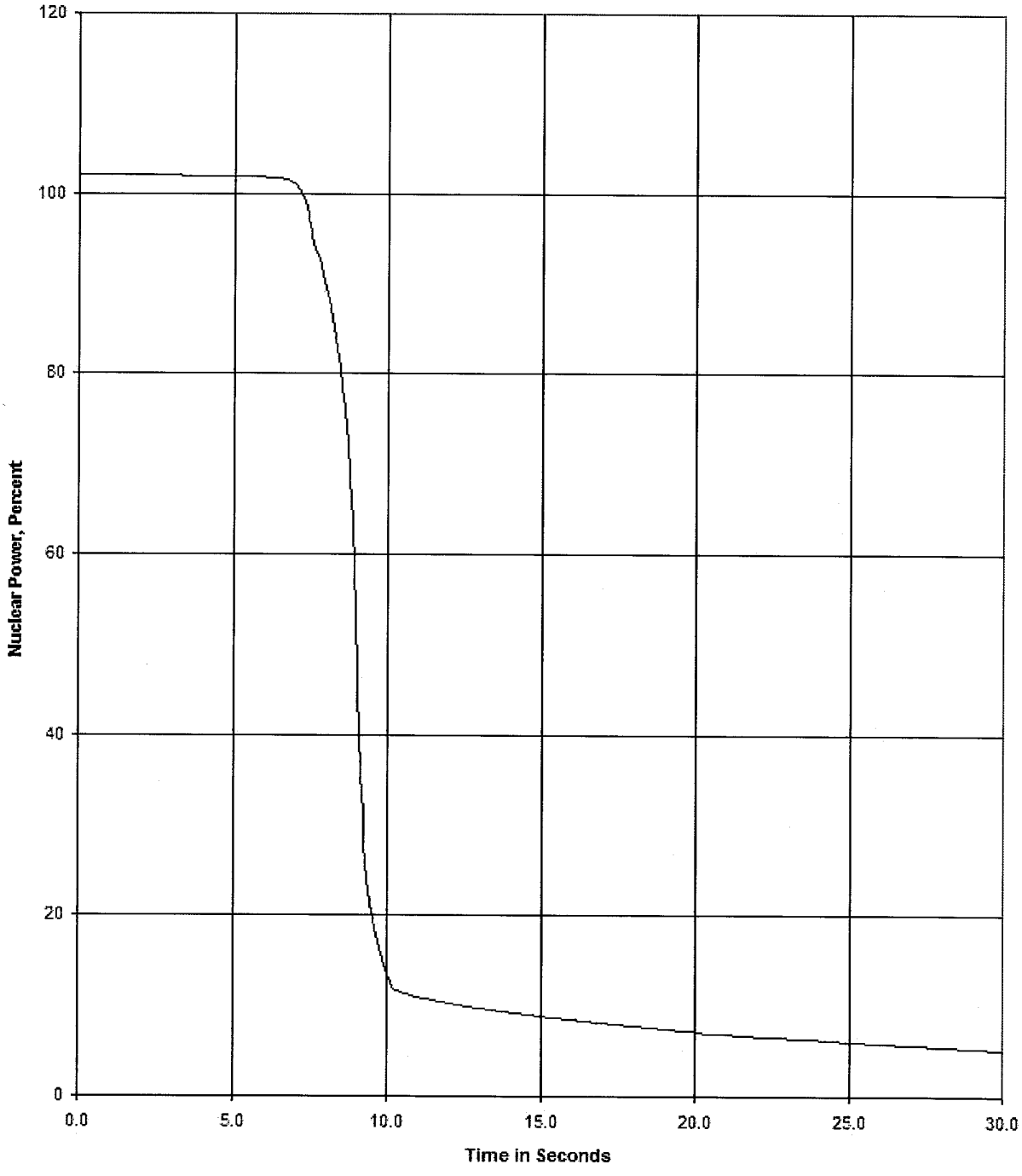

Figure 15.2-26
LOSS OF LOAD ACCIDENT, WITHOUT PRESSURIZER SPRAY AND
POWER-OPERATED RELIEF VALVE, BEGINNING OF LIFE
(CORE INLET TEMPERATURE)

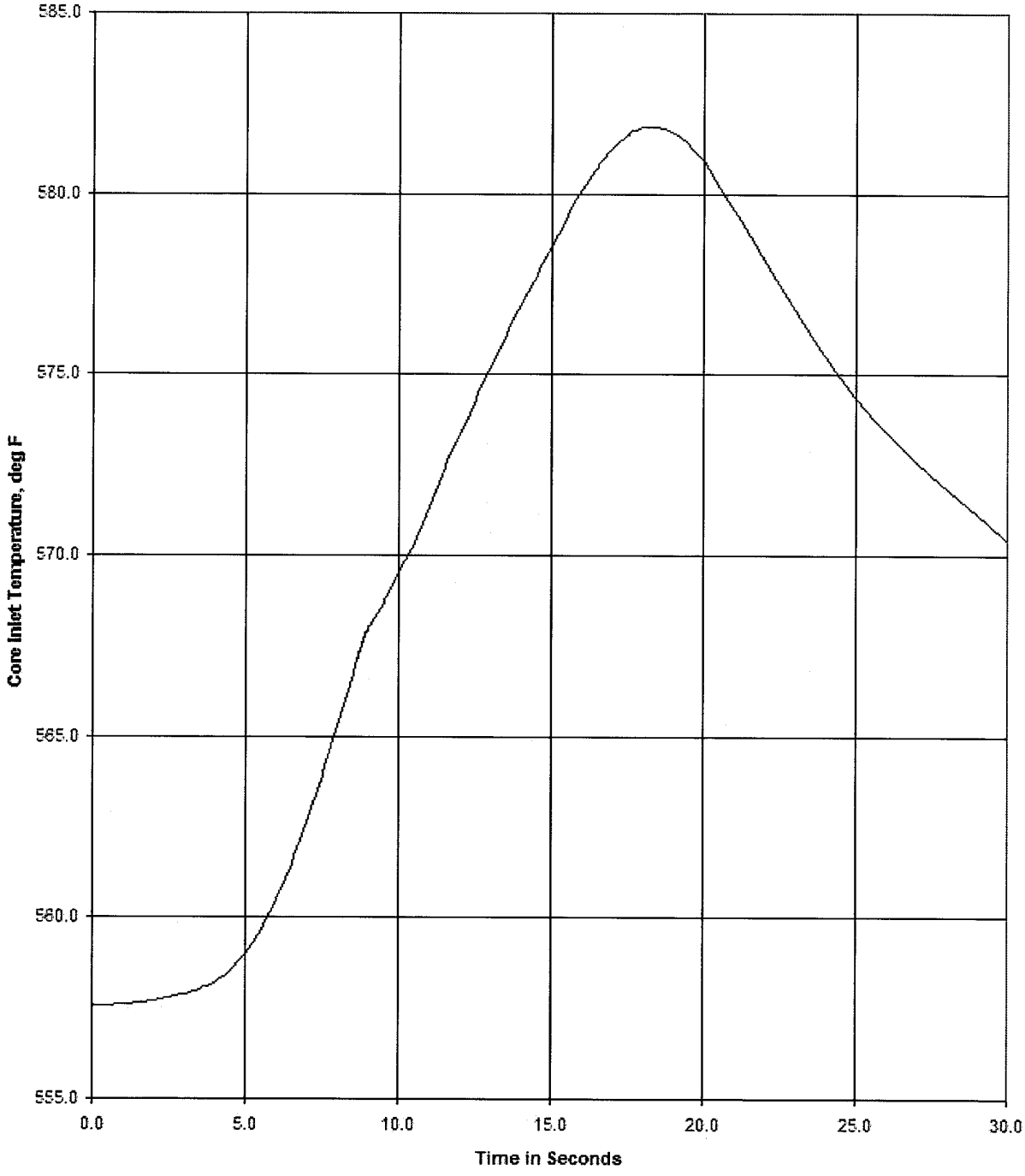

Figure 15.2-27
LOSS OF LOAD ACCIDENT, WITHOUT PRESSURIZER SPRAY AND
POWER-OPERATED RELIEF VALVE, BEGINNING OF LIFE
(SG PRESSURE)

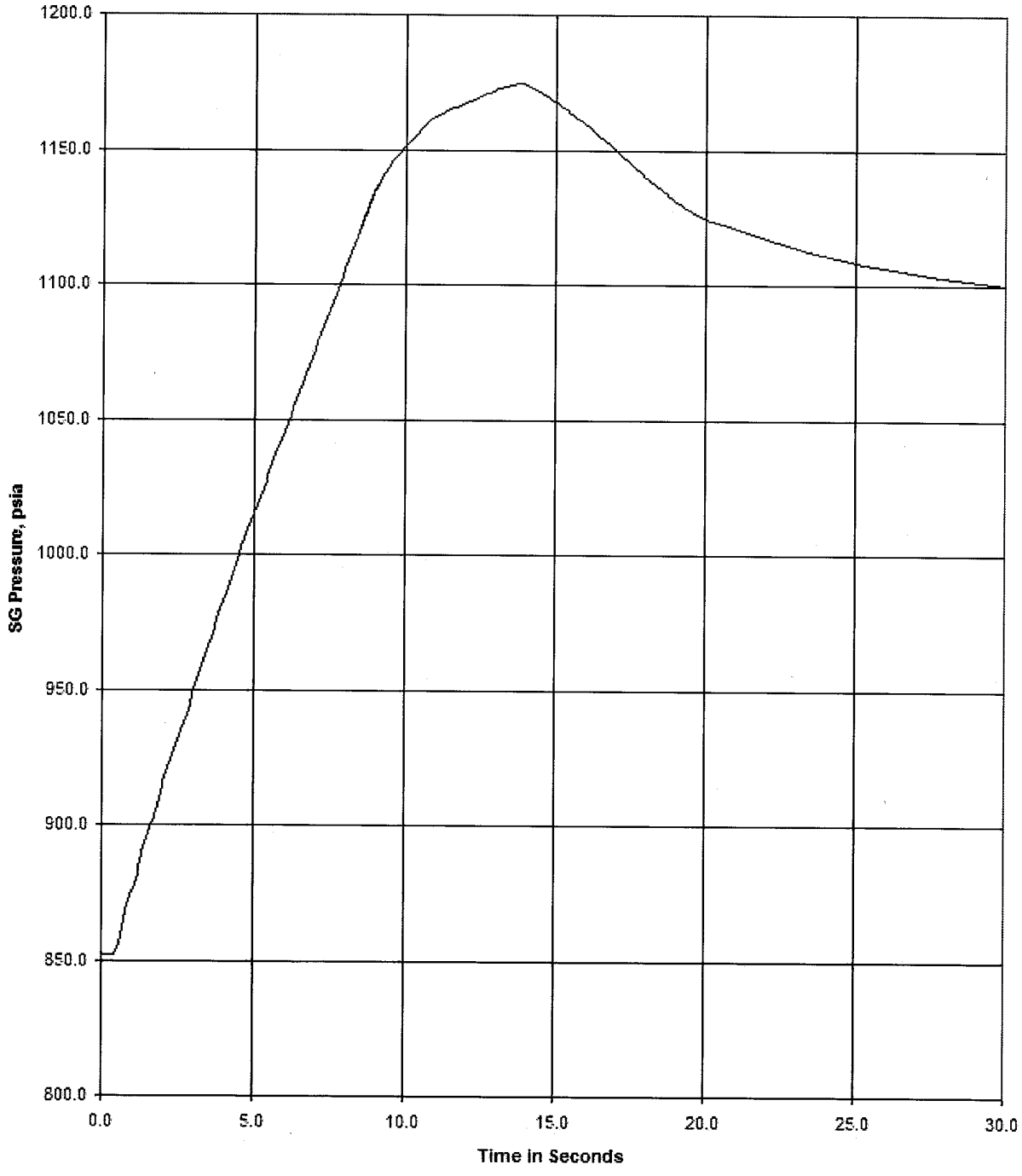

Figure 15.2-28
LOSS OF LOAD ACCIDENT, WITHOUT PRESSURIZER SPRAY AND
POWER-OPERATED RELIEF VALVE, BEGINNING OF LIFE
(RCS AVG TEMPERATURE)

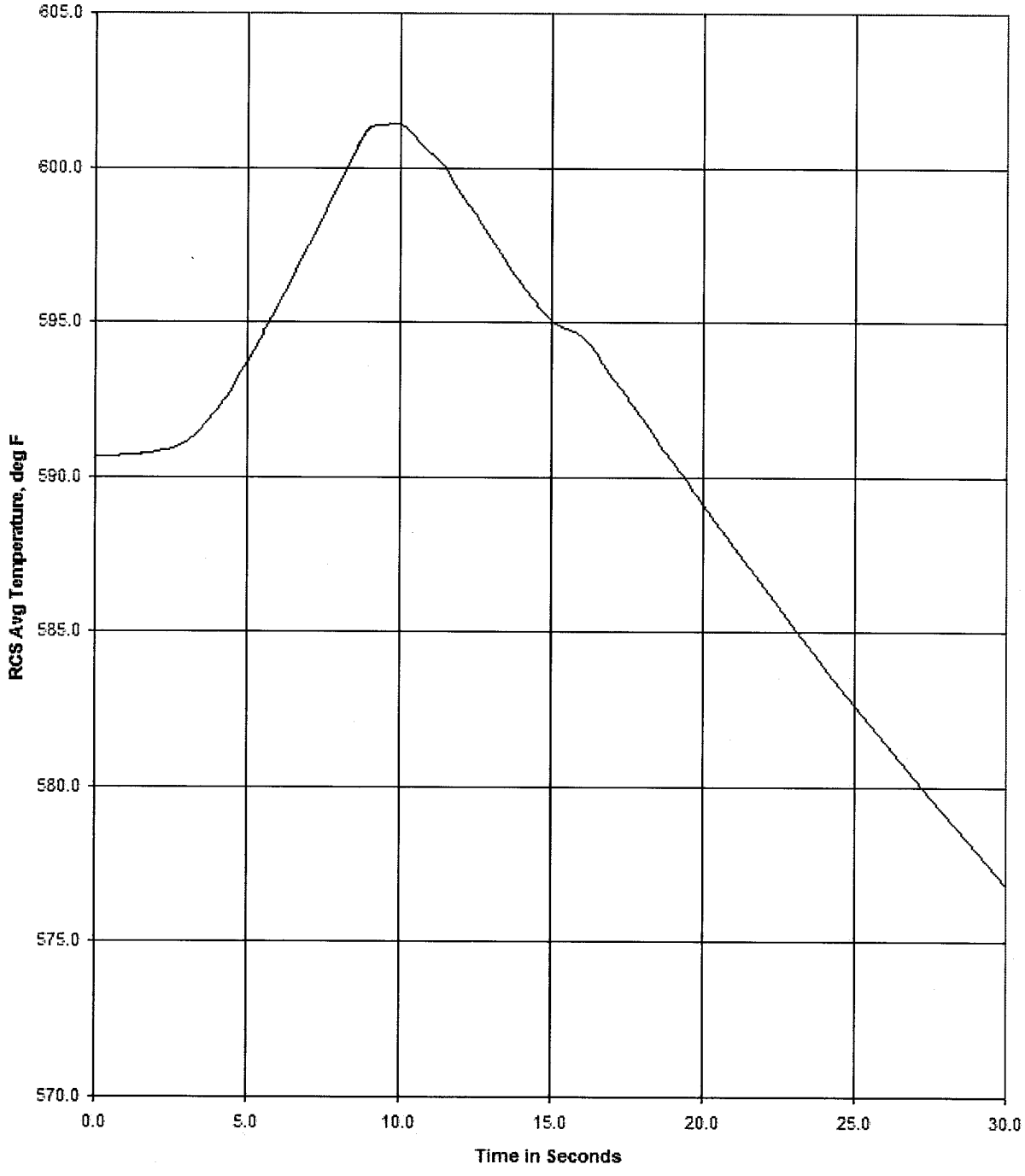

Figure 15.2-29
LOSS OF LOAD ACCIDENT, WITHOUT PRESSURIZER SPRAY AND
POWER-OPERATED RELIEF VALVE, BEGINNING OF LIFE
(PRESSURIZER WATER VOLUME)

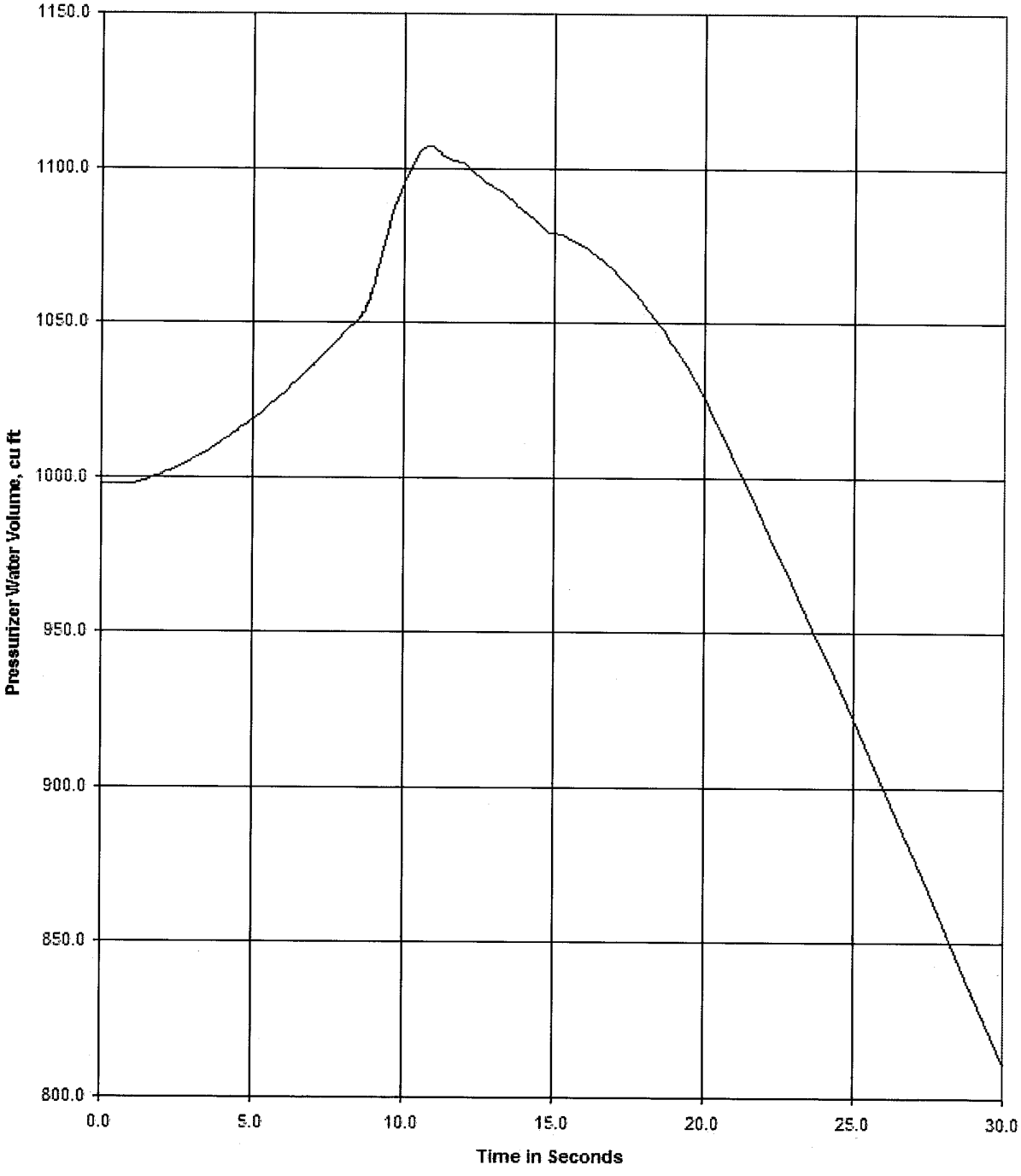

Figure 15.2-30
LOSS OF LOAD ACCIDENT, WITHOUT PRESSURIZER SPRAY AND
POWER-OPERATED RELIEF VALVE, BEGINNING OF LIFE
(COLD LEG PRESSURE)

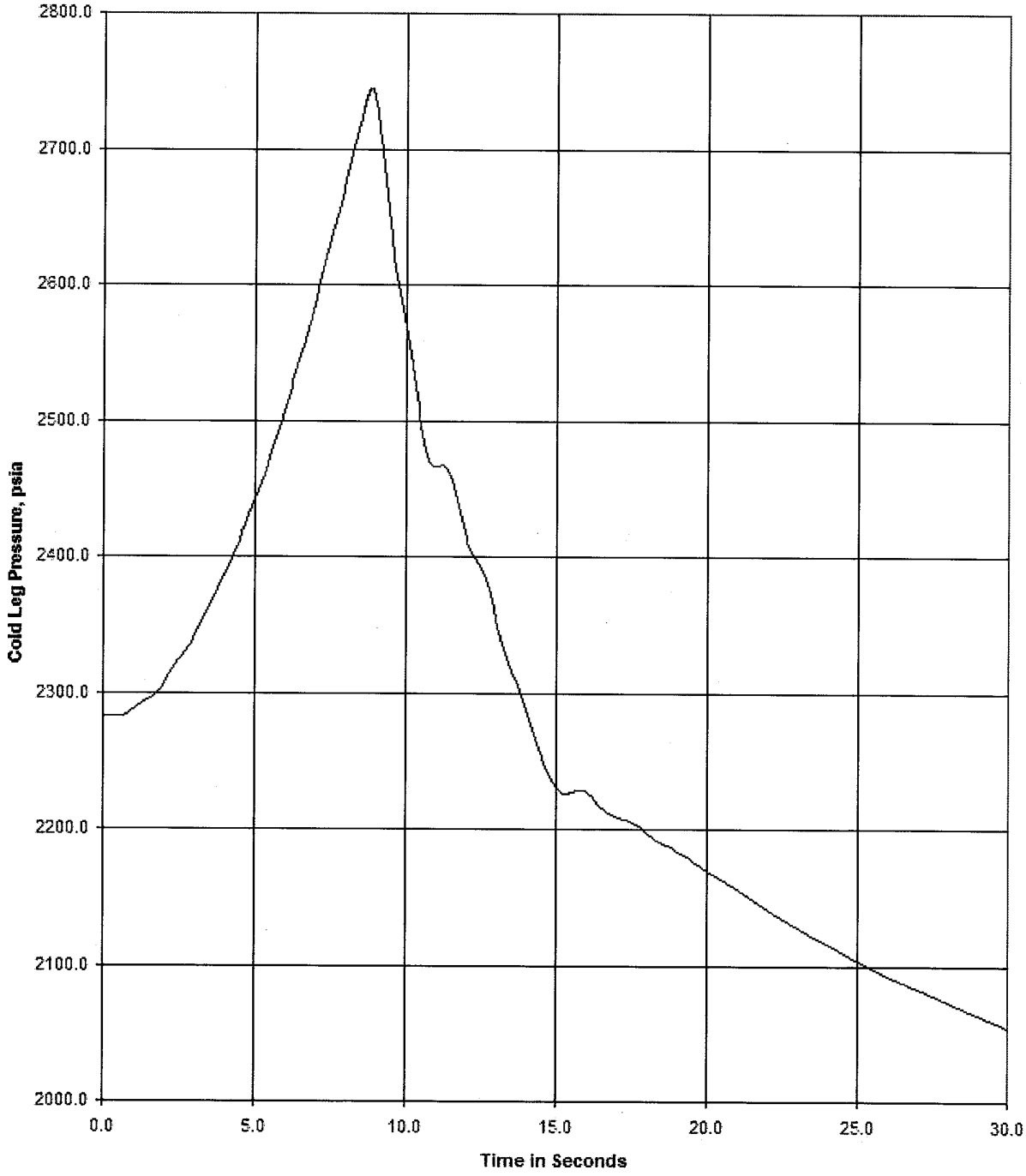

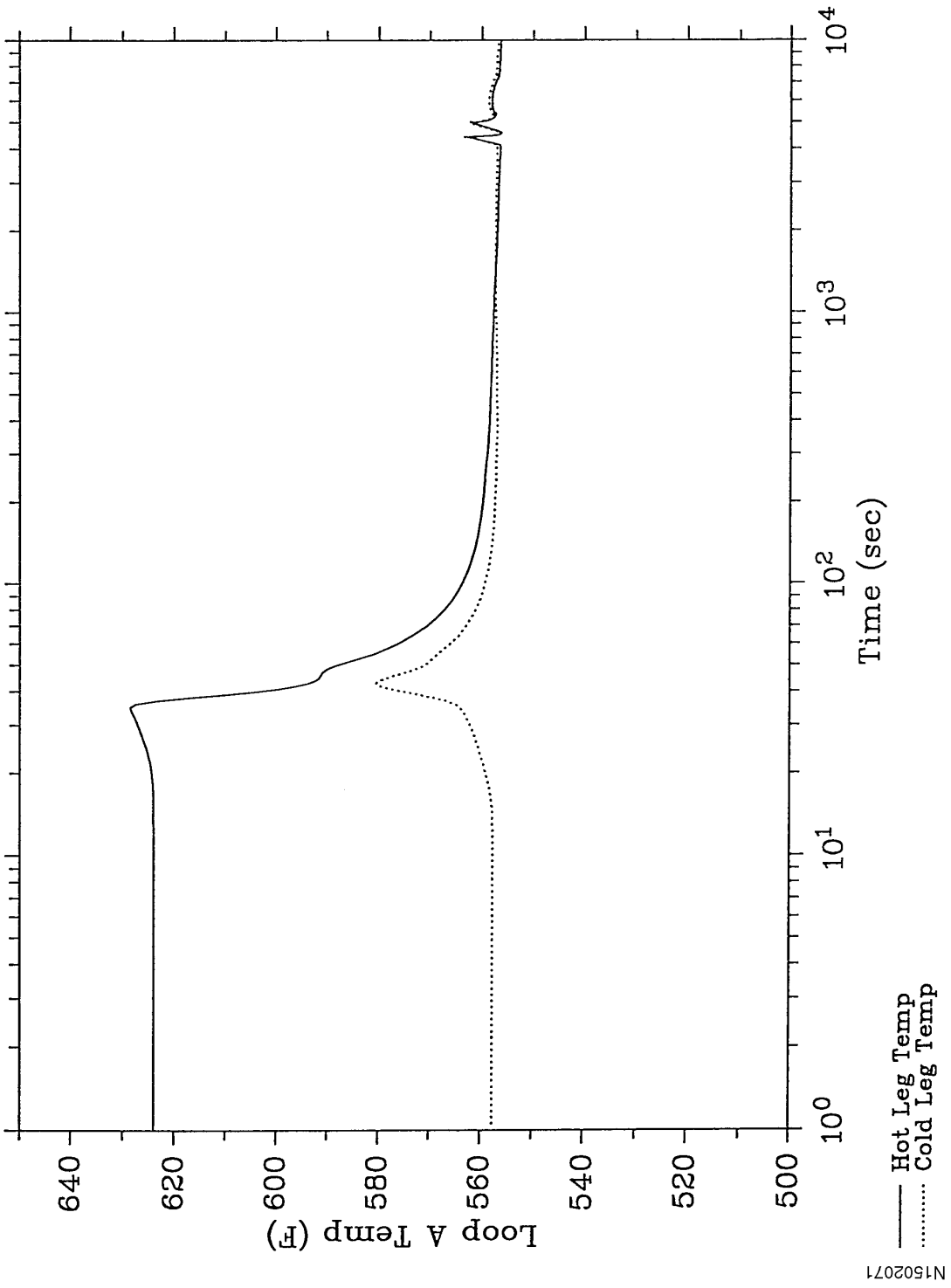

Figure 15.2-31
LOSS OF NORMAL FEEDWATER, PRIMARY TEMPERATURE OF LOOP NOT RECEIVING AFW
(WITH OFFSITE POWER AVAILABLE)

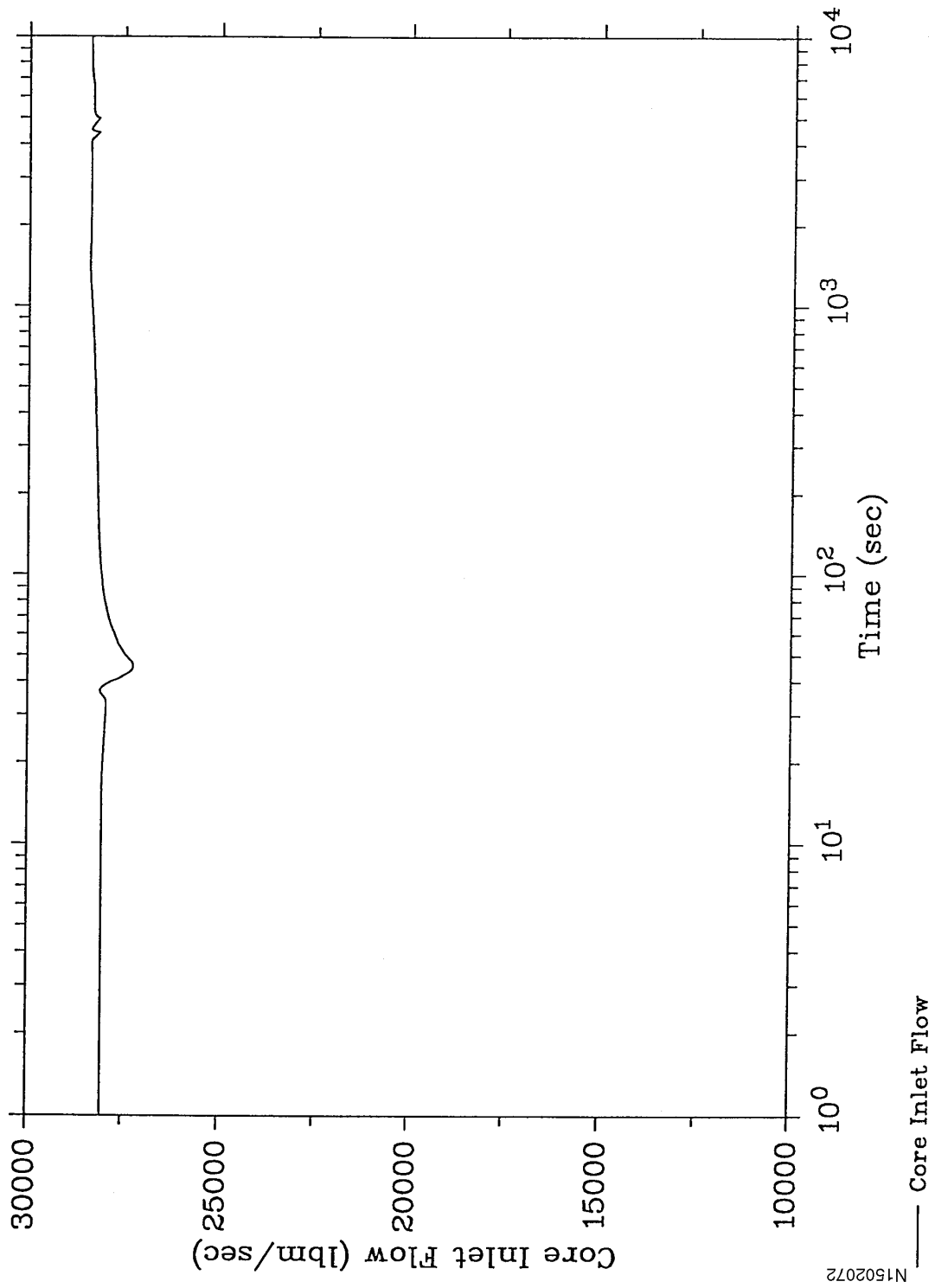

Figure 15.2-32
LOSS OF NORMAL FEEDWATER, VESSEL MASS FLOWRATE
(WITH OFFSITE POWER AVAILABLE)

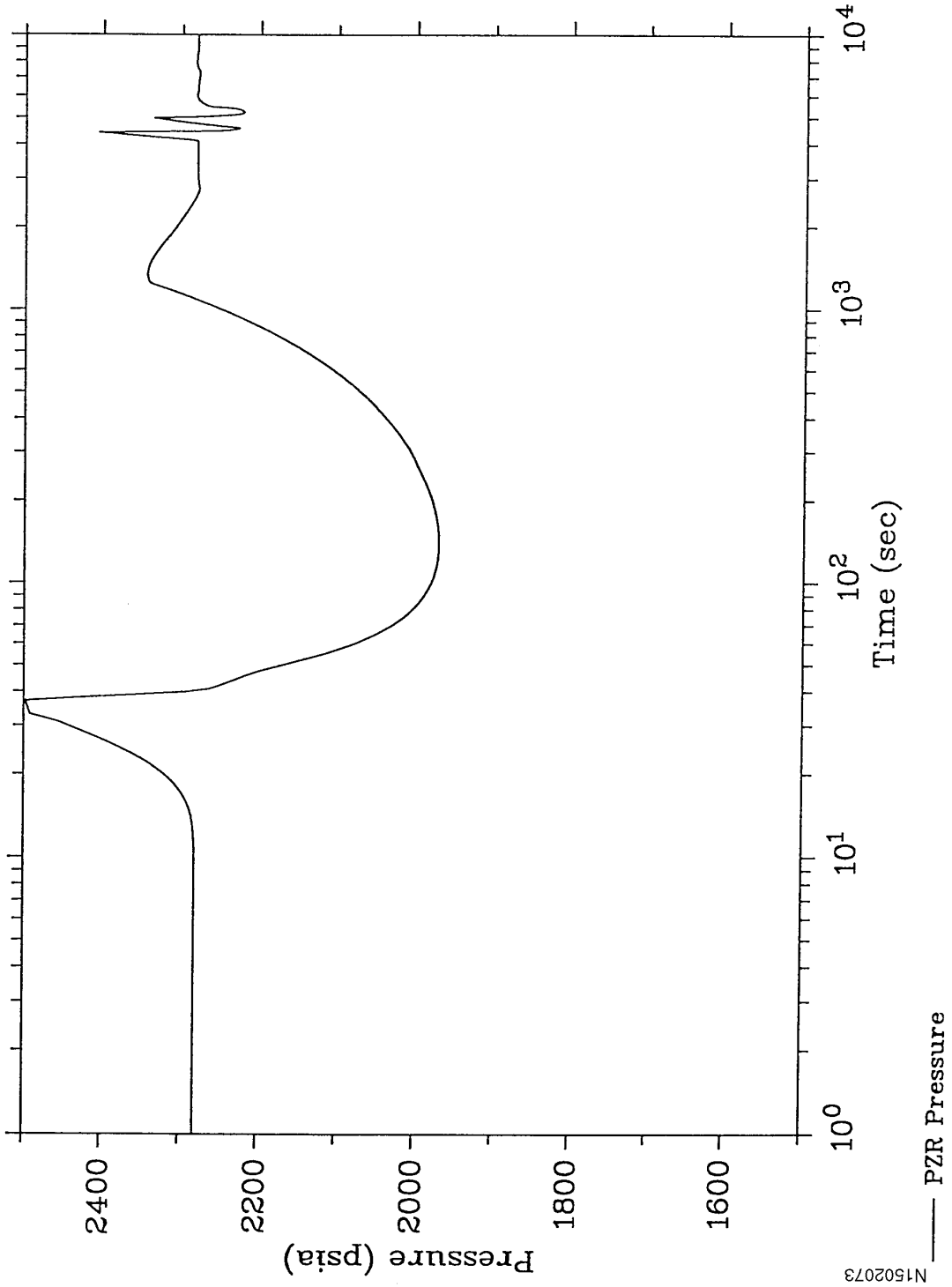

Figure 15.2-33
LOSS OF NORMAL FEEDWATER, PRESSURIZER PRESSURE
(WITH OFFSITE POWER AVAILABLE)

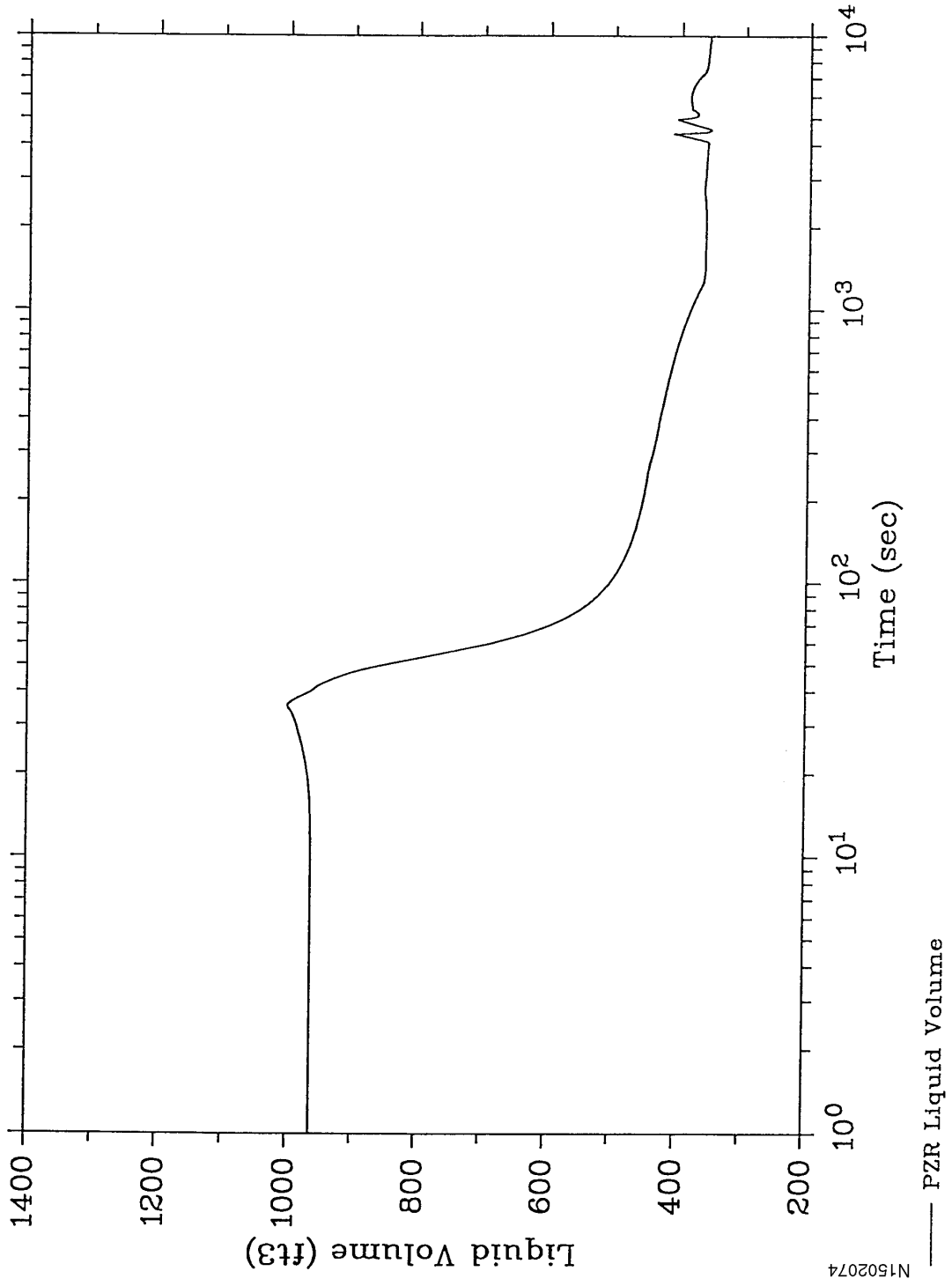

Figure 15.2-34
LOSS OF NORMAL FEEDWATER, PRESSURIZER WATER VOLUME
(WITH OFFSITE POWER AVAILABLE)

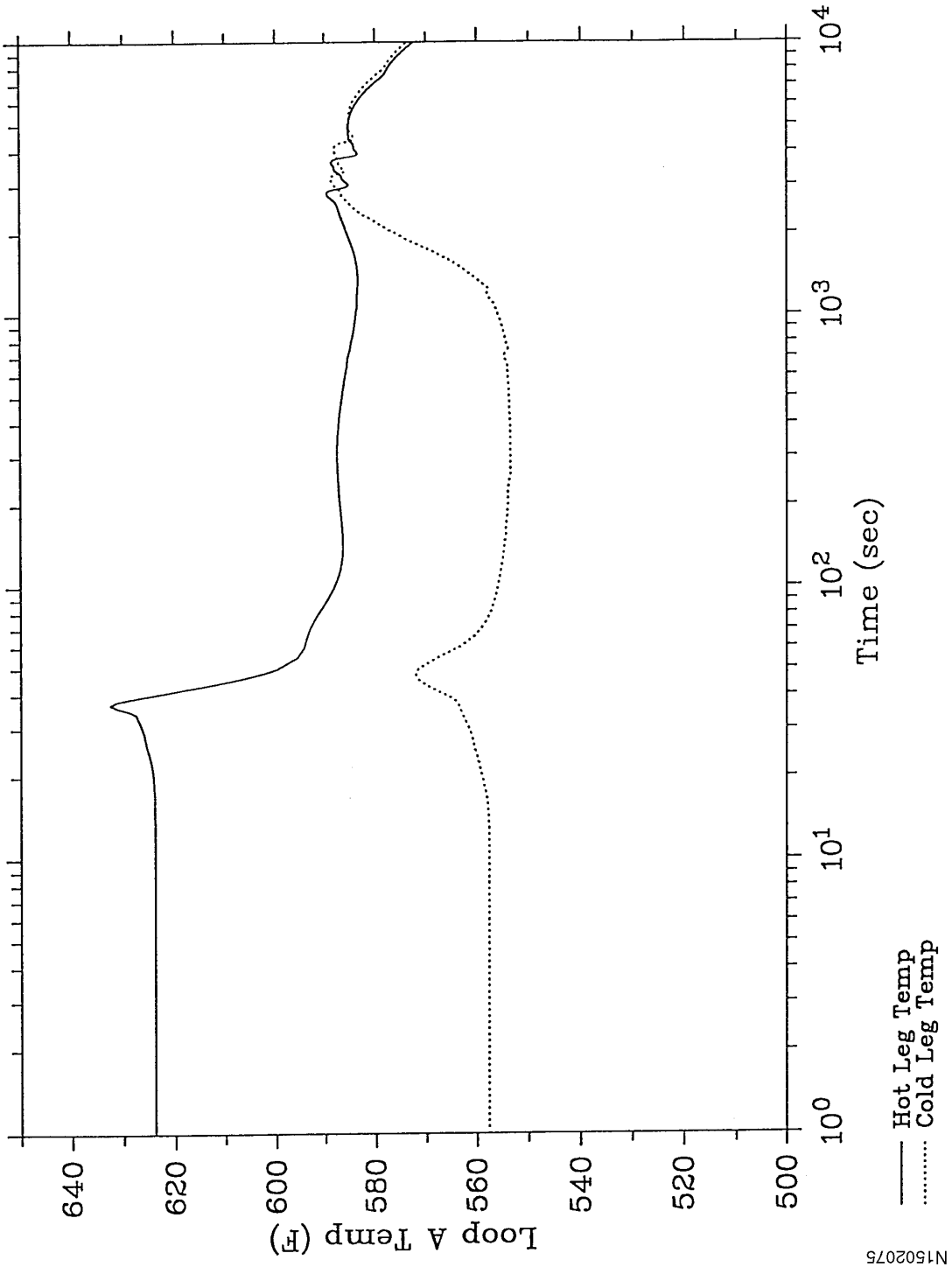

Figure 15.2-35
LOSS OF NORMAL FEEDWATER, PRIMARY TEMPERATURE OF LOOP NOT RECEIVING AFW
(WITHOUT OFFSITE POWER AVAILABLE)

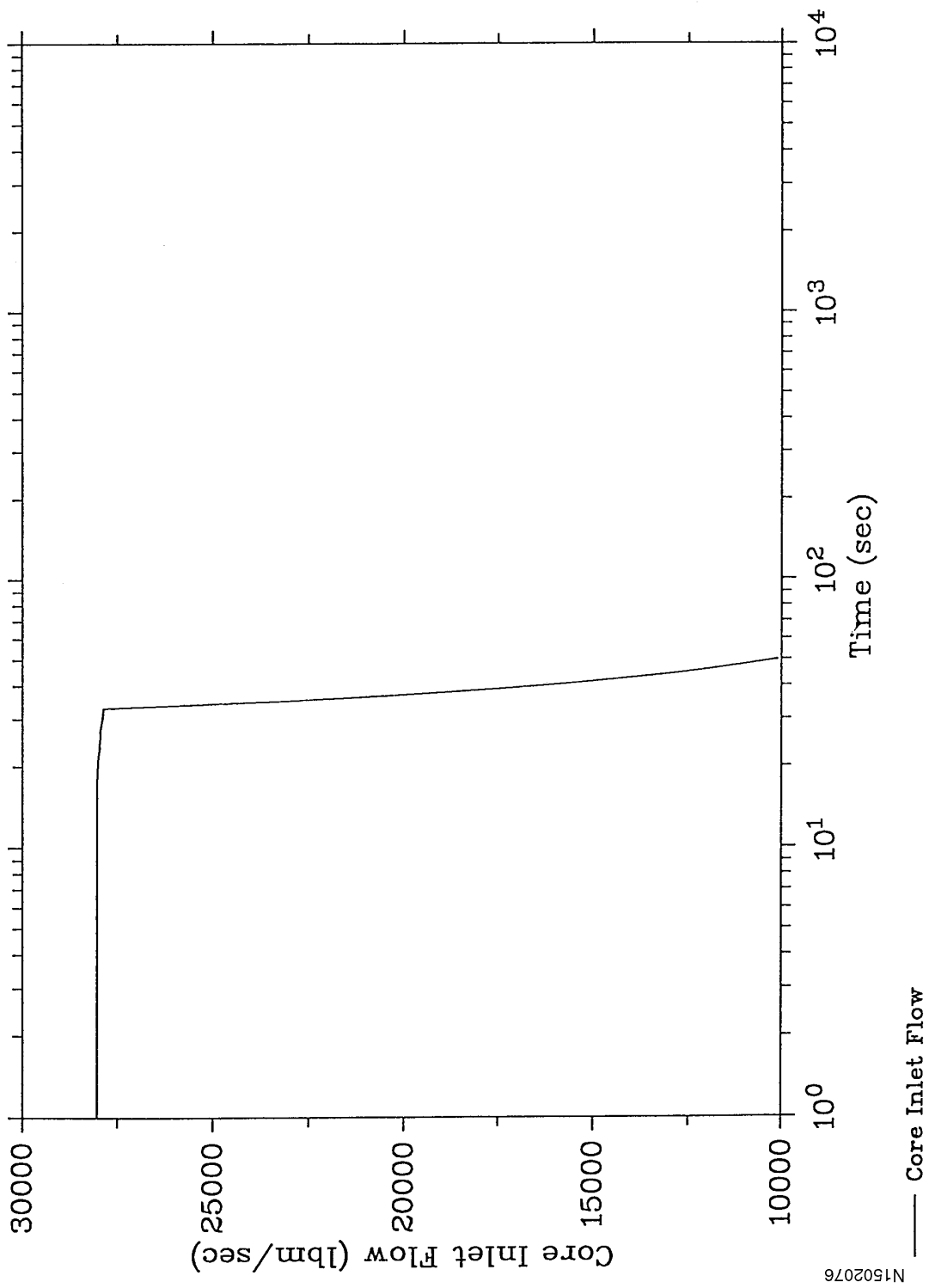

Figure 15.2-36
LOSS OF NORMAL FEEDWATER, VESSEL MASS FLOWRATE
(WITHOUT OFFSITE POWER AVAILABLE)

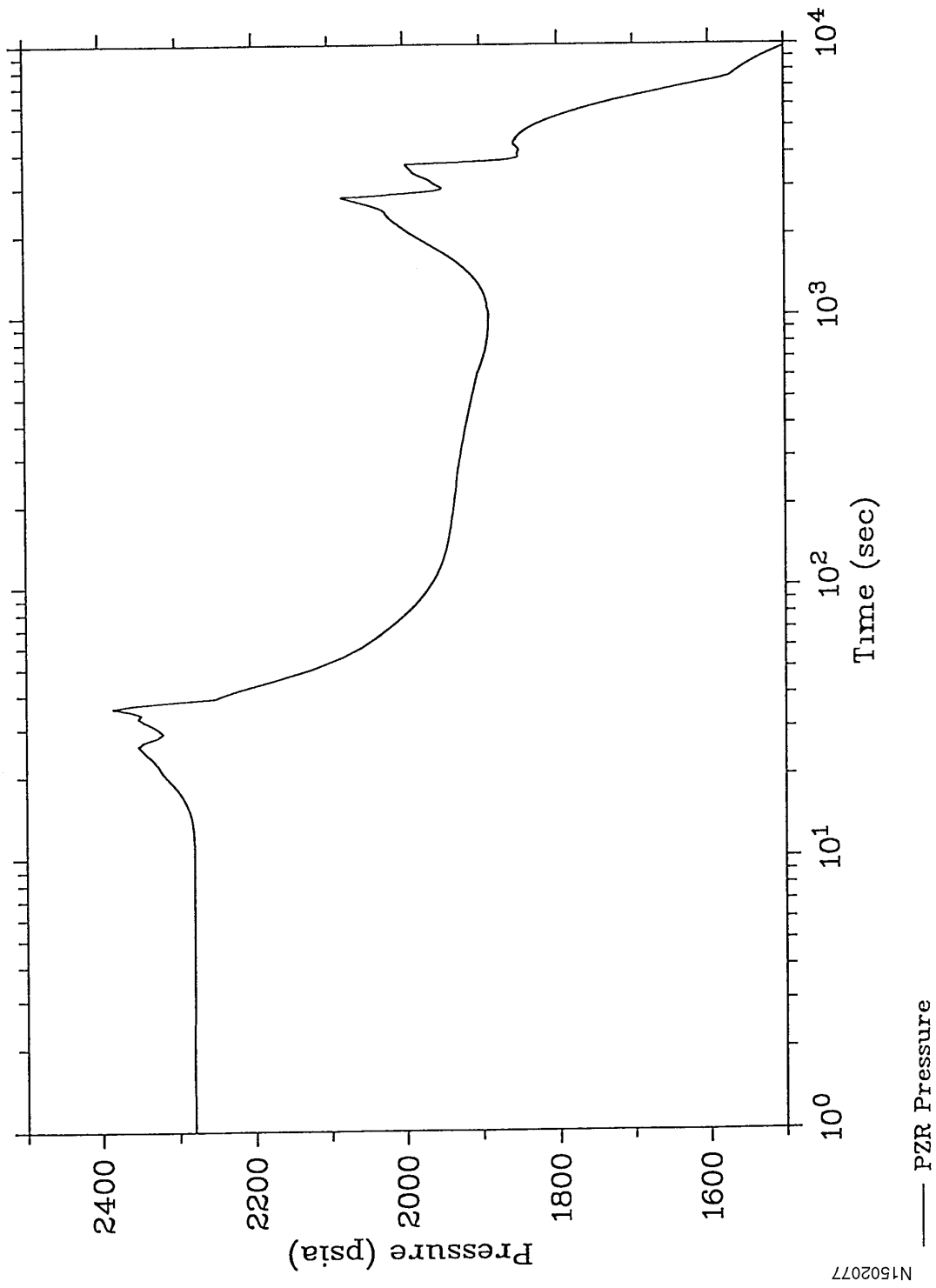

Figure 15.2-37
LOSS OF NORMAL FEEDWATER, PRESSURIZER PRESSURE
(WITHOUT OFFSITE POWER AVAILABLE)

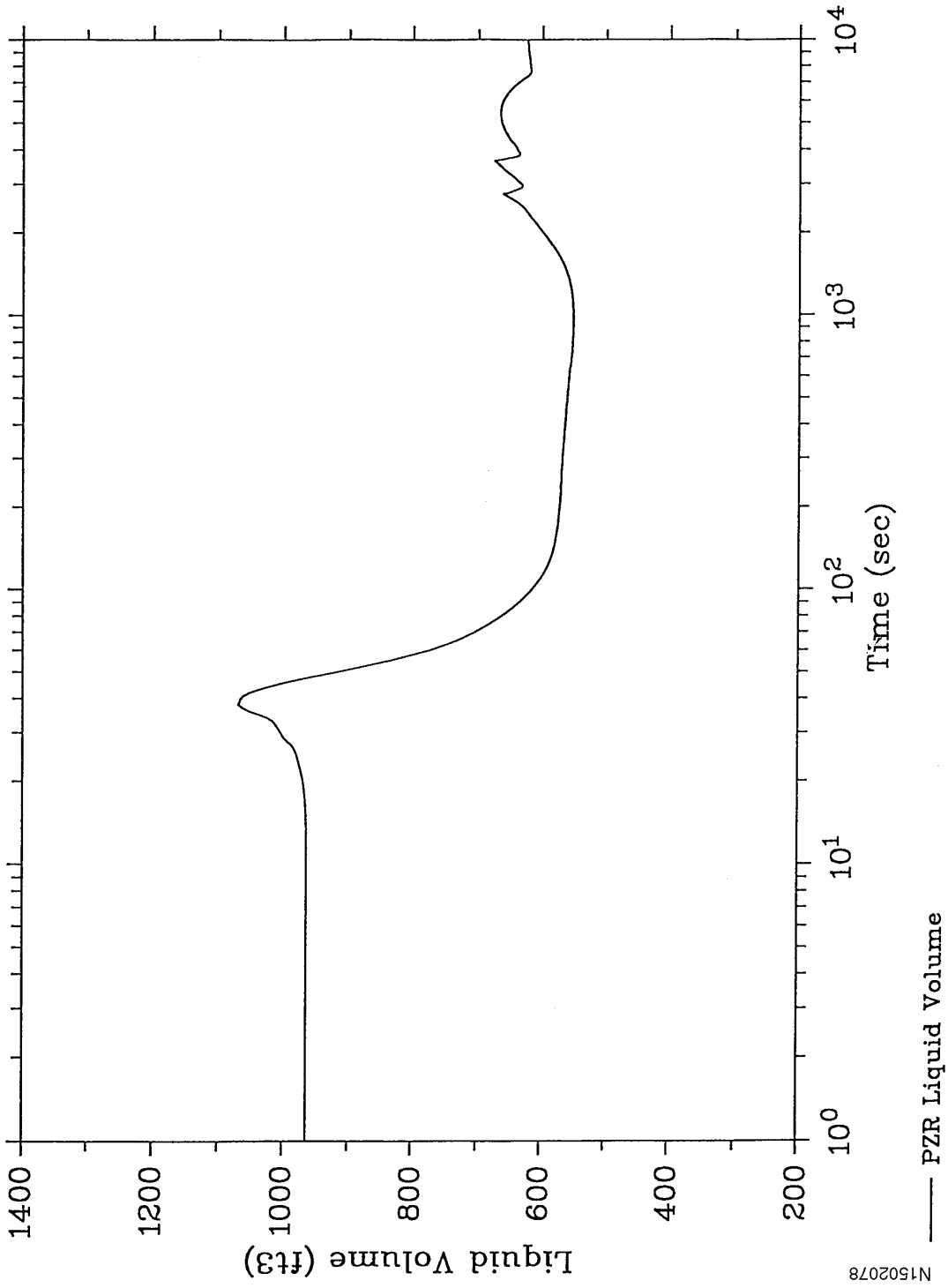

Figure 15.2-38
LOSS OF NORMAL FEEDWATER, PRESSURIZER WATER VOLUME
(WITHOUT OFFSITE POWER AVAILABLE)

Figure 15.2-39
MULTI-LOOP FW MALFUNCTION
150% FW FLOW HFP W/ROD CONTROL
NUCLEAR POWER, FRACTION OF NOMINAL

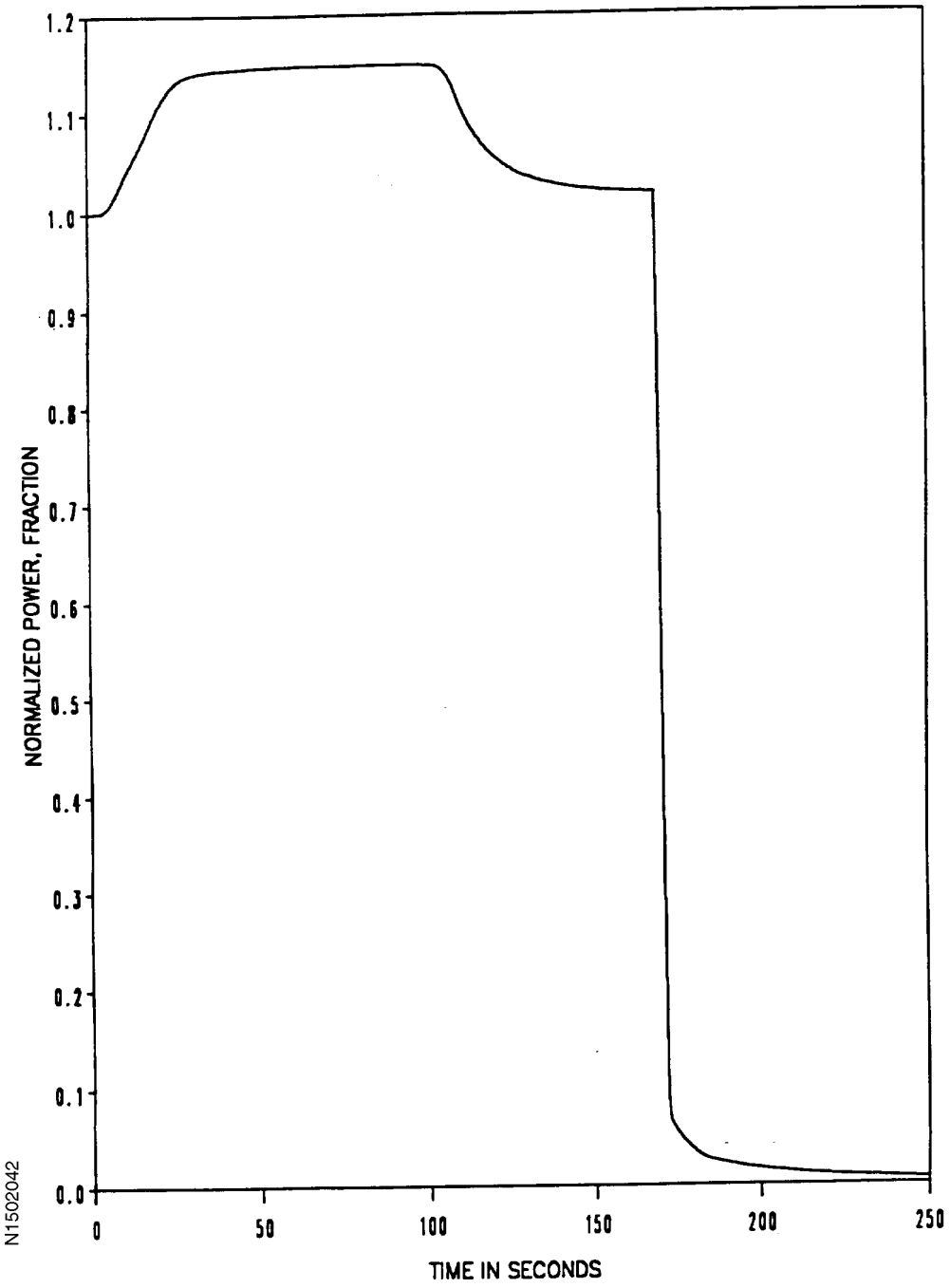

Figure 15.2-40
MULTI-LOOP FW MALFUNCTION
150% FW FLOW HFP W/ROD CONTROL
LOOP DELTA-T, DEG F

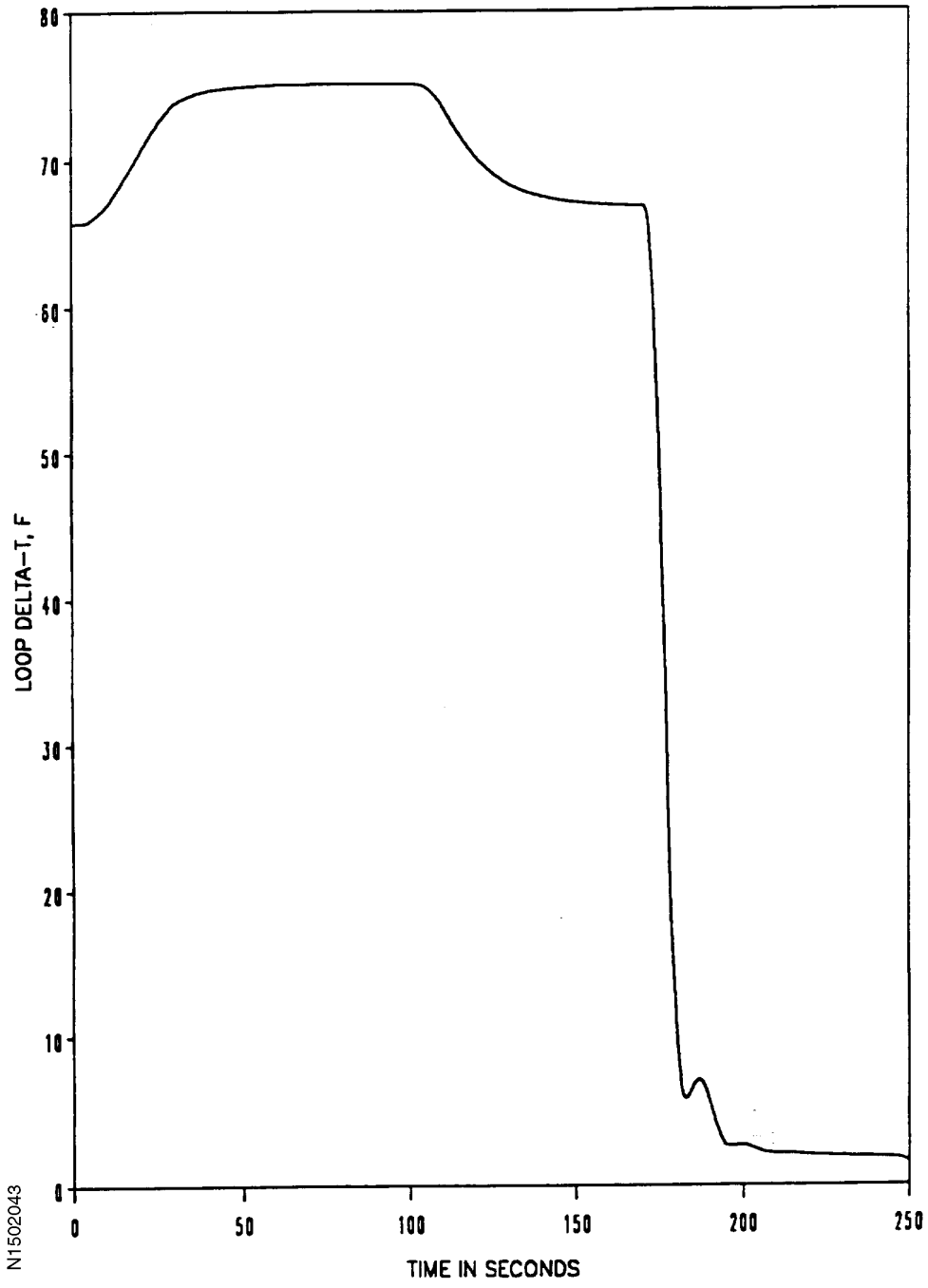

Figure 15.2-41
MULTI-LOOP FW MALFUNCTION
150% FW FLOW HFP W/ROD CONTROL
PRESSURIZER PRESSURE, PSIA

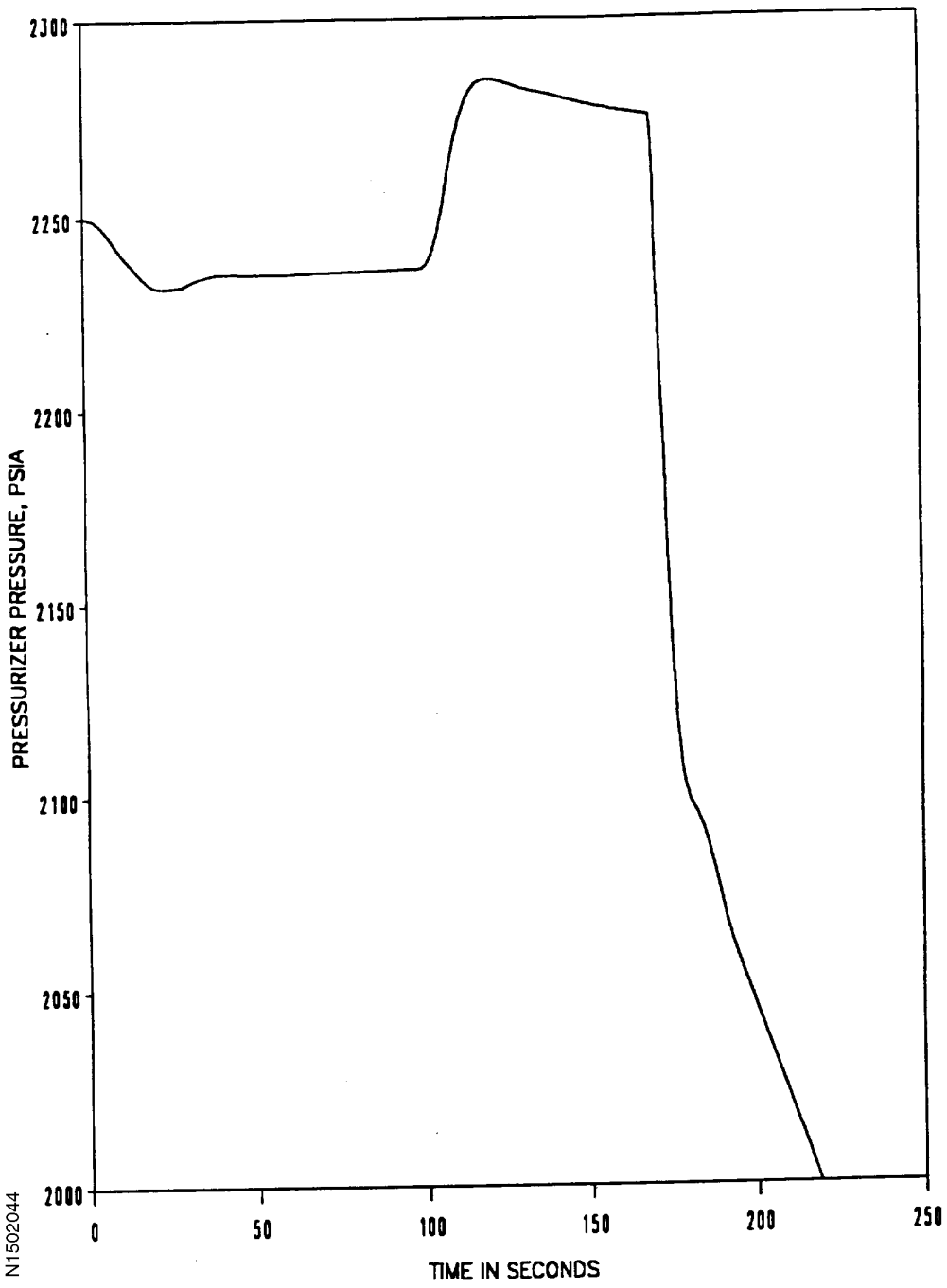

Figure 15.2-42
MULTI-LOOP FW MALFUNCTION
150% FW FLOW HFP W/ROD CONTROL
CORE AVERAGE TEMPERATURE, DEG F

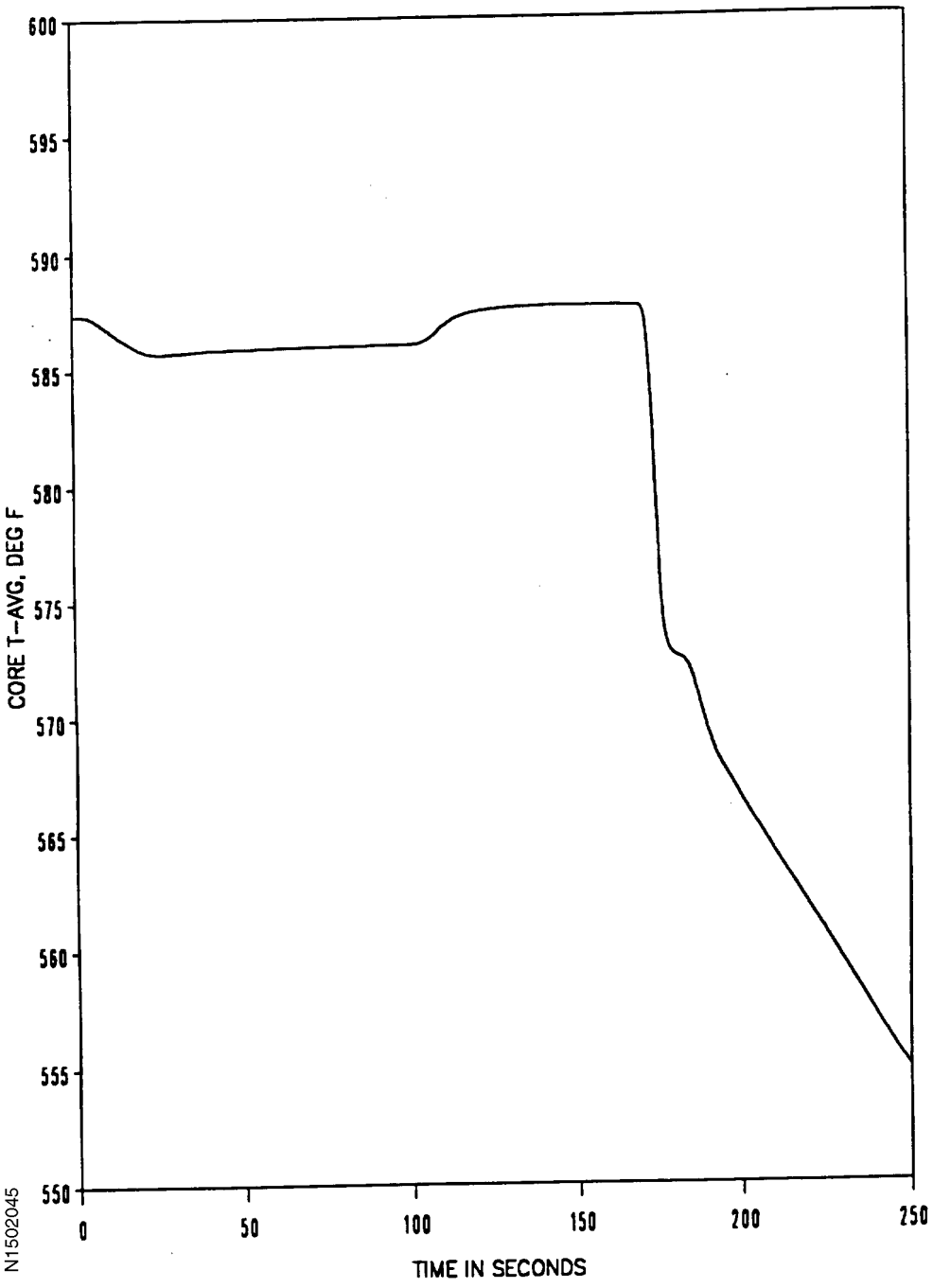

Figure 15.2-43
MULTI-LOOP FW MALFUNCTION
150% FW FLOW HFP W/ROD CONTROL
STEAM GENERATOR MASS, X1,000 LBM

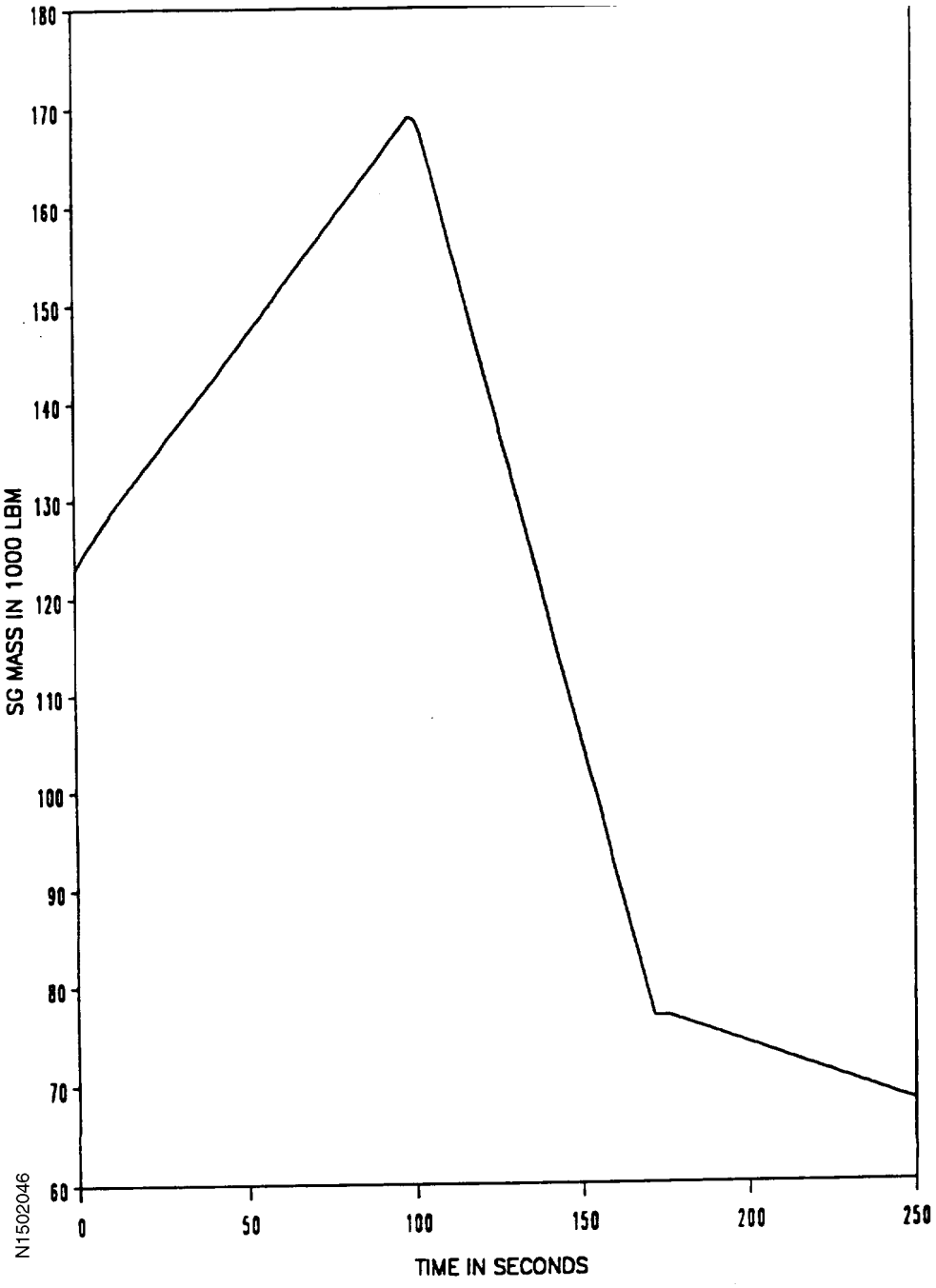

Figure 15.2-44
MULTI-LOOP FW MALFUNCTION
150% FW FLOW HFP W/ROD CONTROL
MINIMUM DNBR

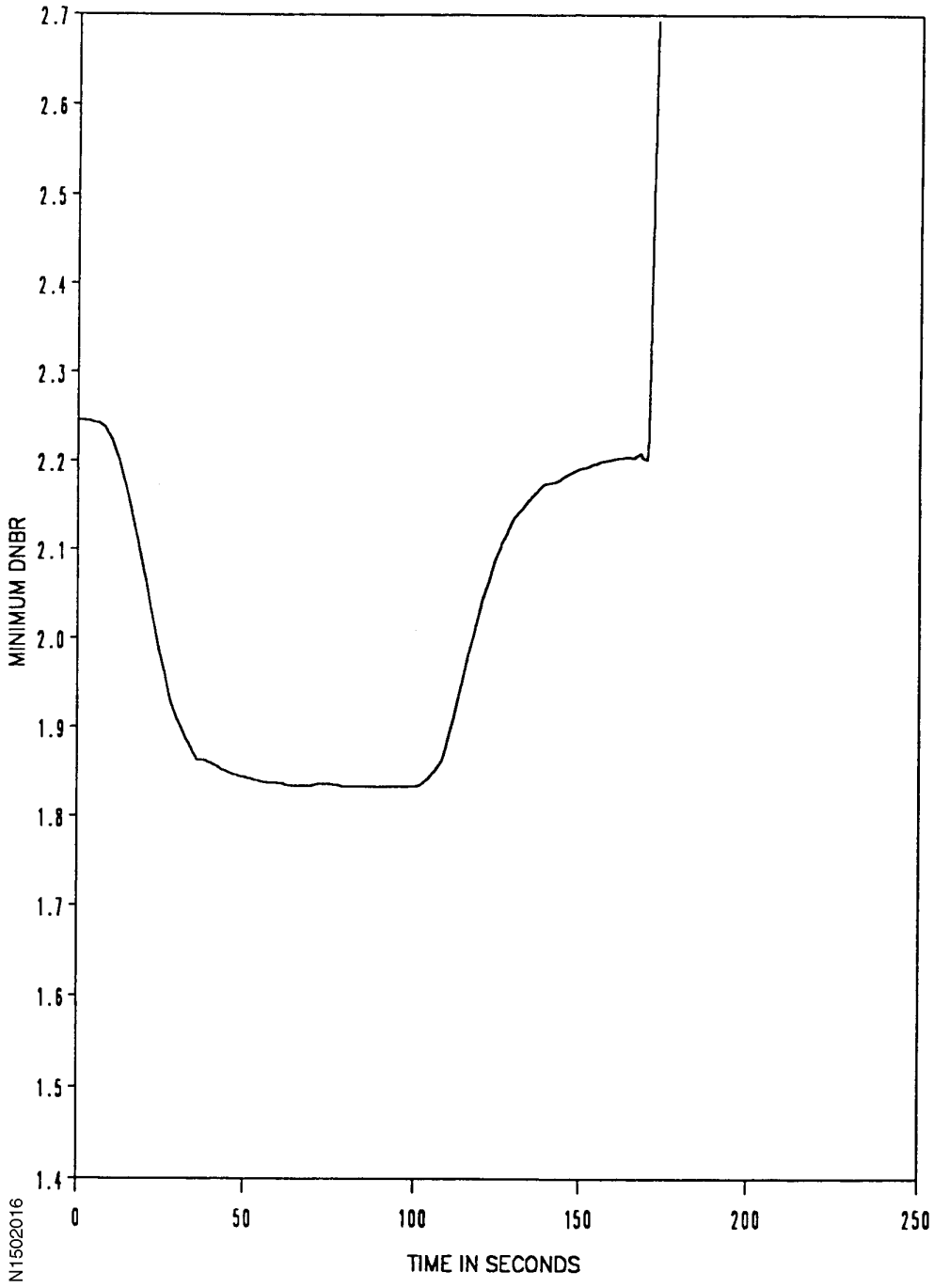

Figure 15.2-45
EXCESSIVE LOAD INCREASE WITH MANUAL ROD CONTROL
BEGINNING OF LIFE

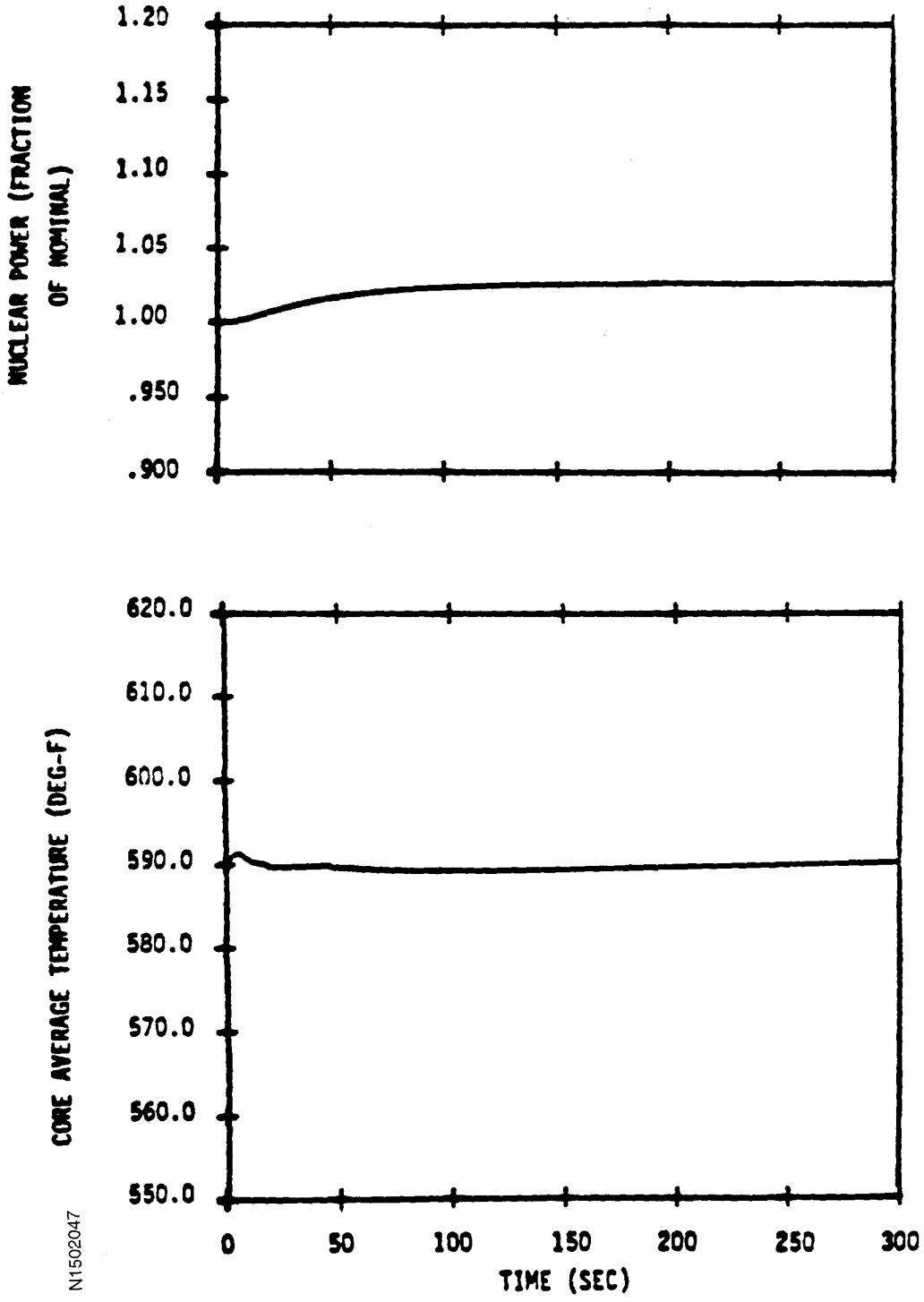

Figure 15.2-46
EXCESSIVE LOAD INCREASE WITH MANUAL ROD CONTROL
BEGINNING OF LIFE

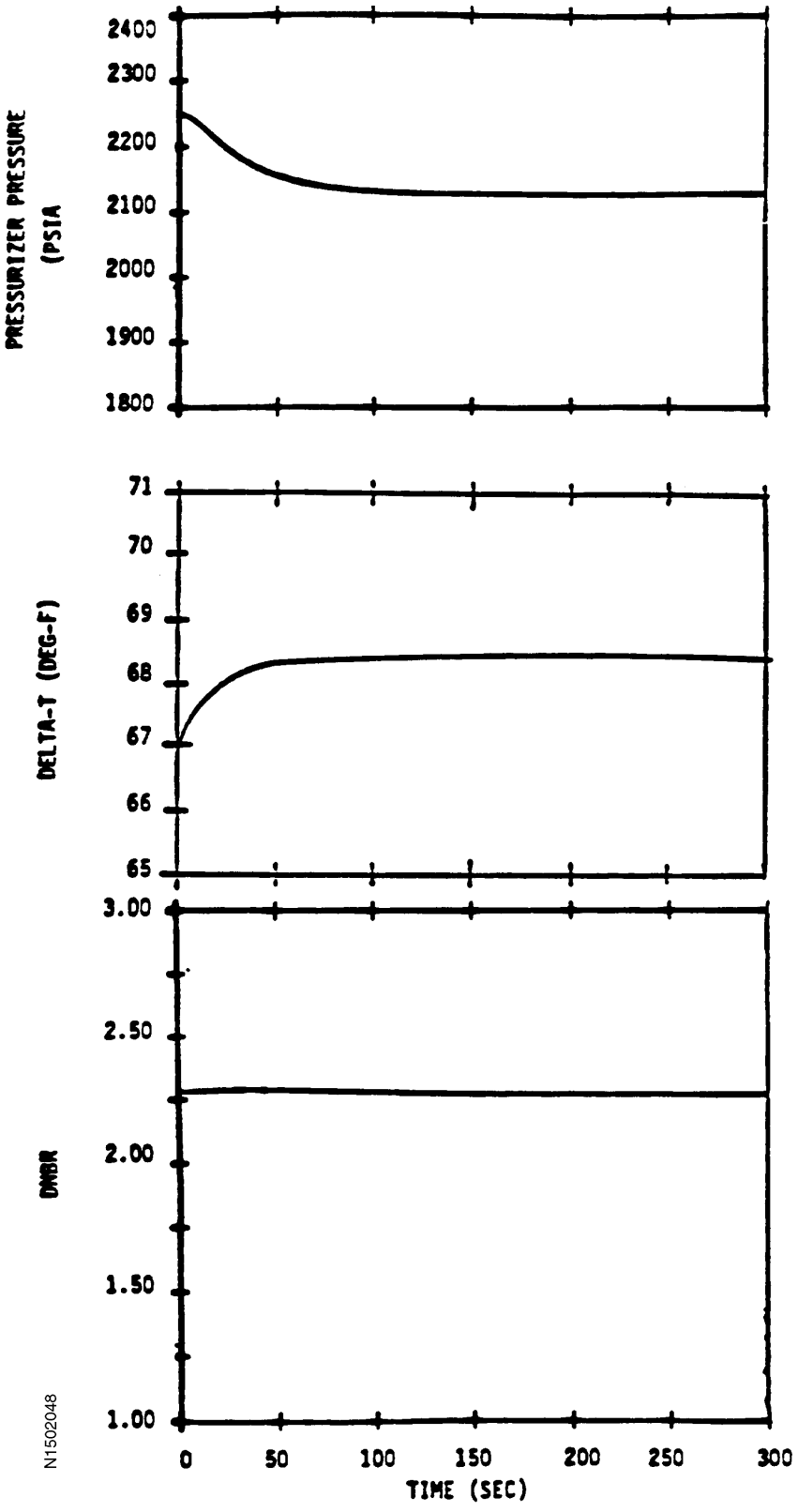

Figure 15.2-47 (SHEET 1 OF 2)
EXCESSIVE LOAD INCREASE WITH MANUAL ROD CONTROL
MAXIMUM FEEDBACK

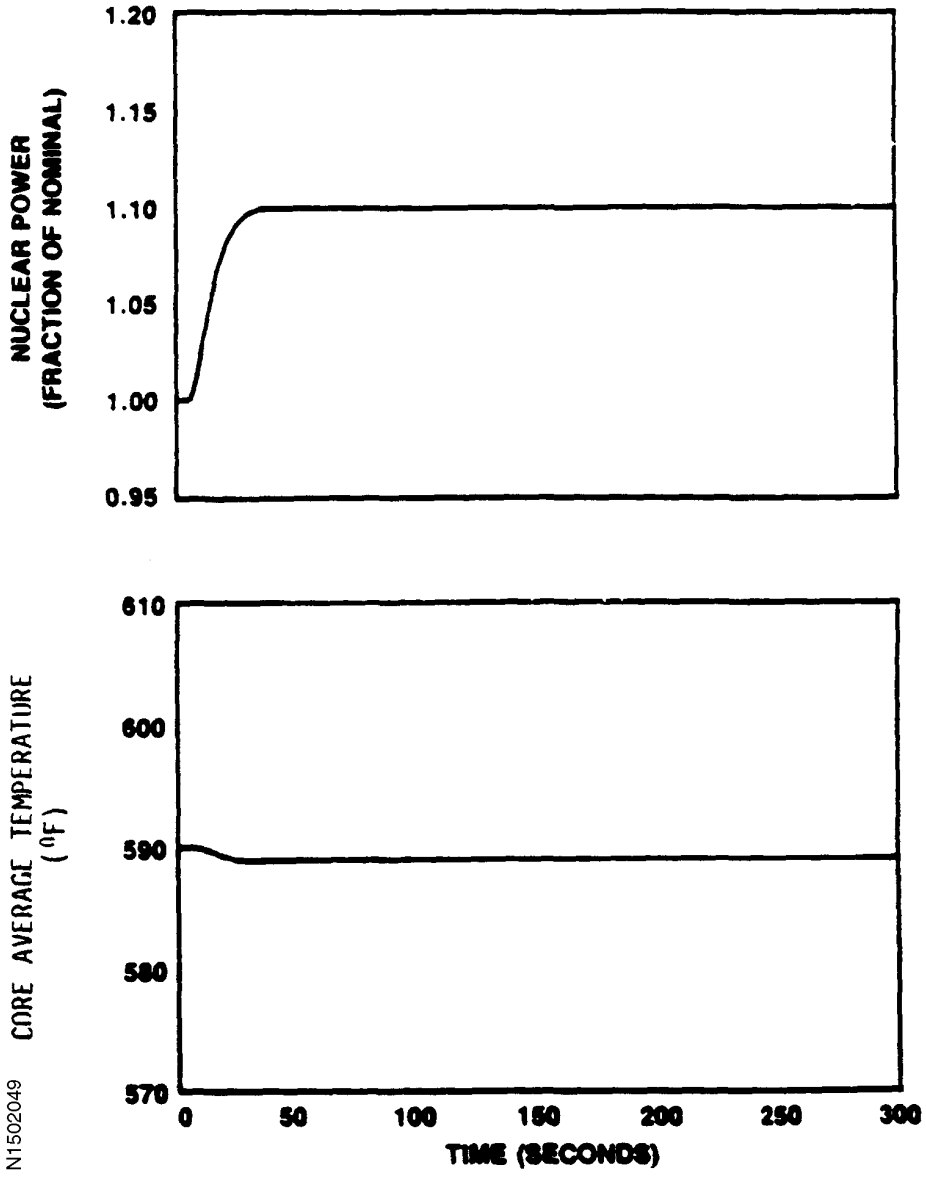

Figure 15.2-47 (SHEET 2 OF 2)
EXCESSIVE LOAD INCREASE WITH MANUAL ROD CONTROL
MAXIMUM FEEDBACK

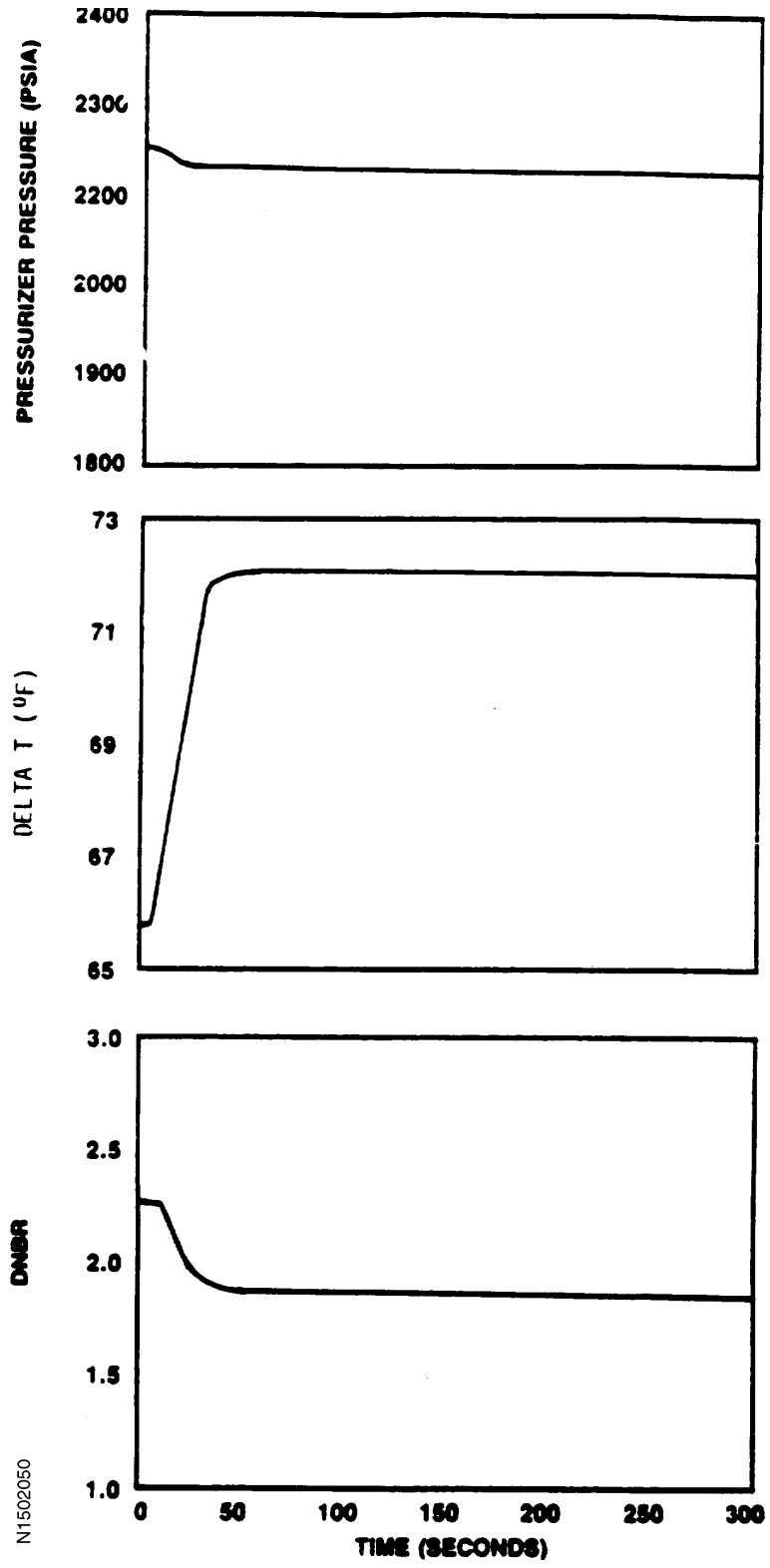

Figure 15.2-48 (SHEET 1 OF 2)
EXCESSIVE LOAD INCREASE WITH AUTOMATIC ROD CONTROL
BEGINNING OF LIFE

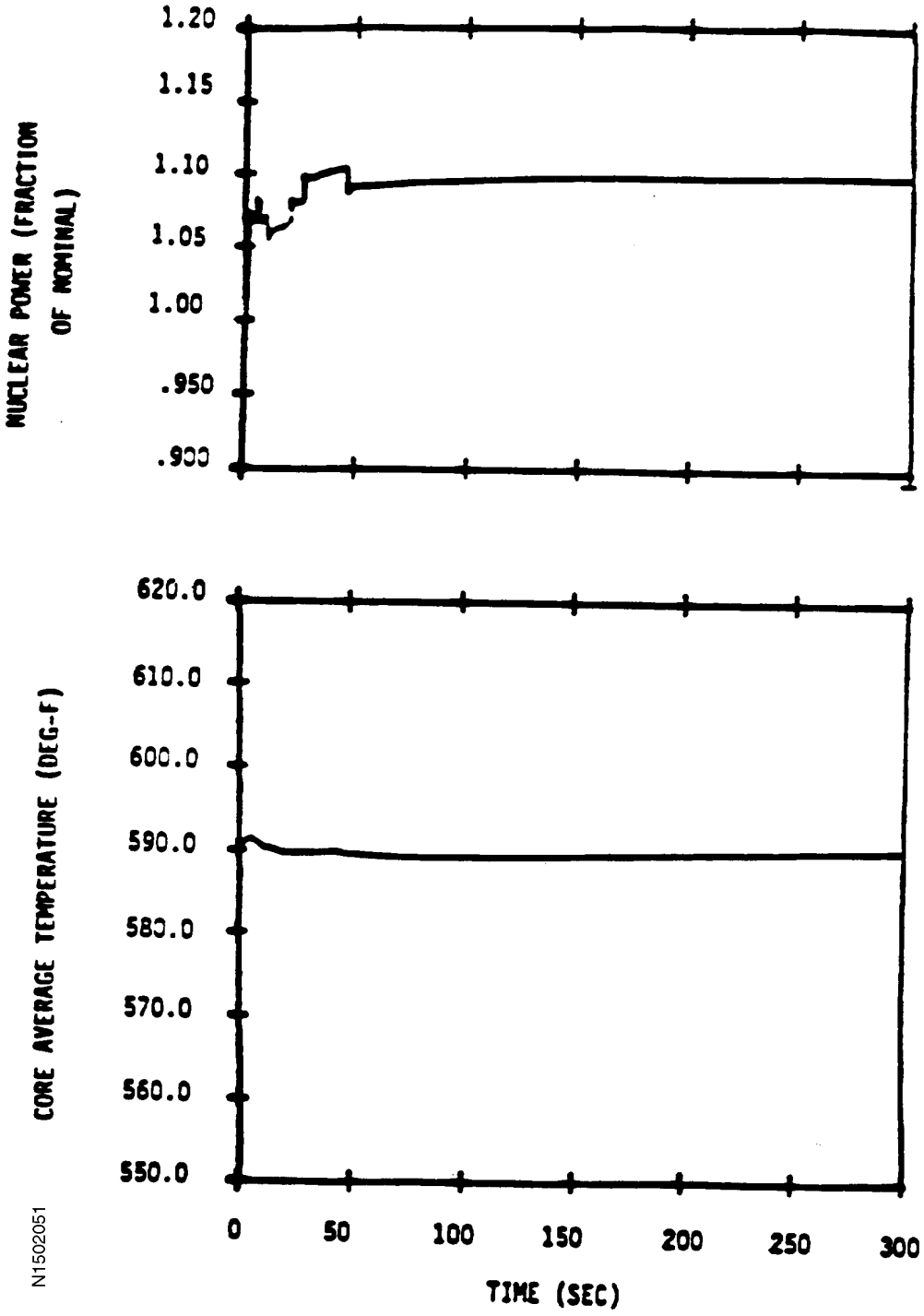

Figure 15.2-48 (SHEET 2 OF 2)
EXCESSIVE LOAD INCREASE WITH AUTOMATIC ROD CONTROL
BEGINNING OF LIFE

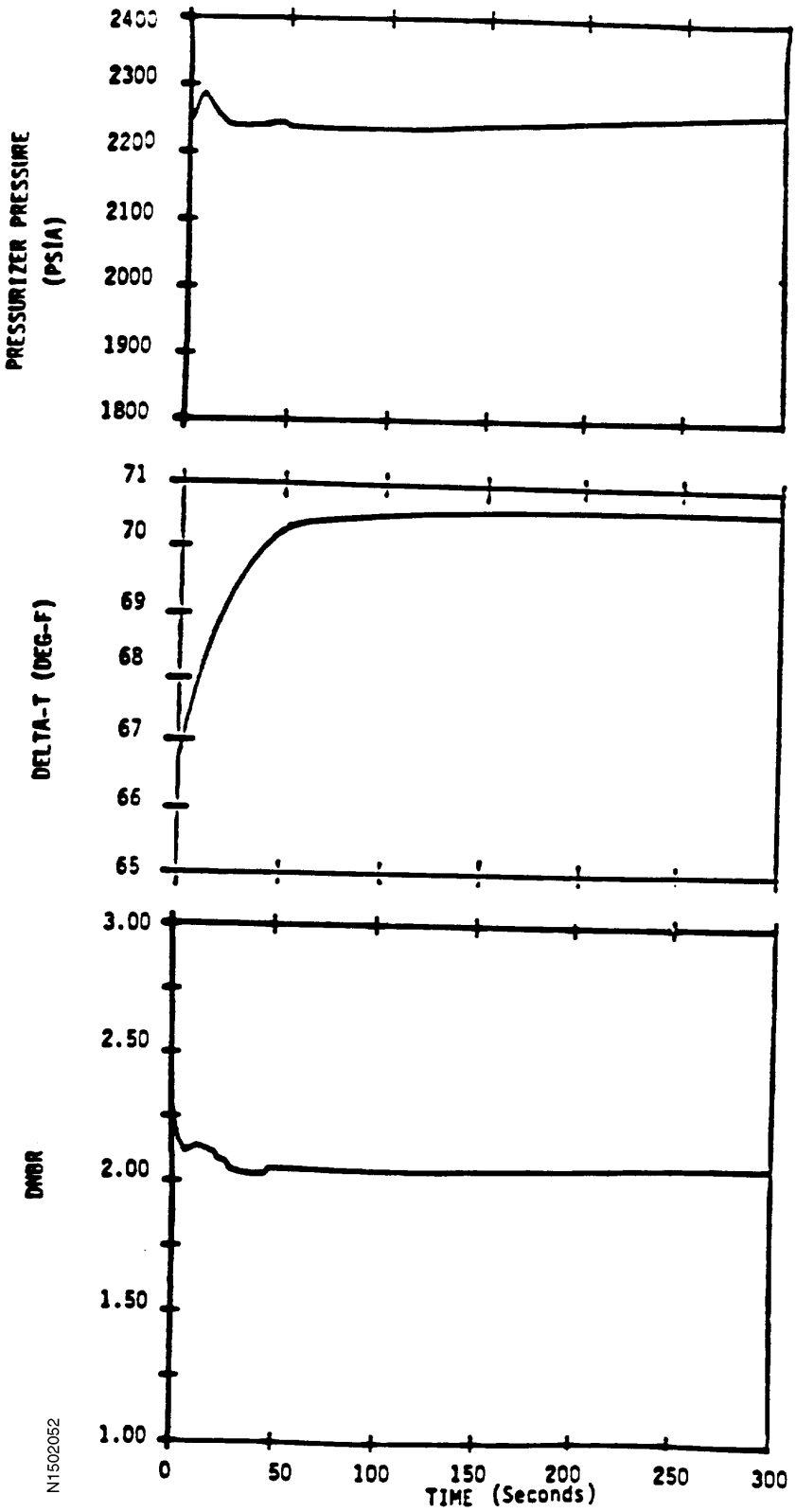

Figure 15.2-49 (SHEET 1 OF 2)
EXCESSIVE LOAD INCREASE WITH AUTOMATIC ROD CONTROL
MAXIMUM FEEDBACK

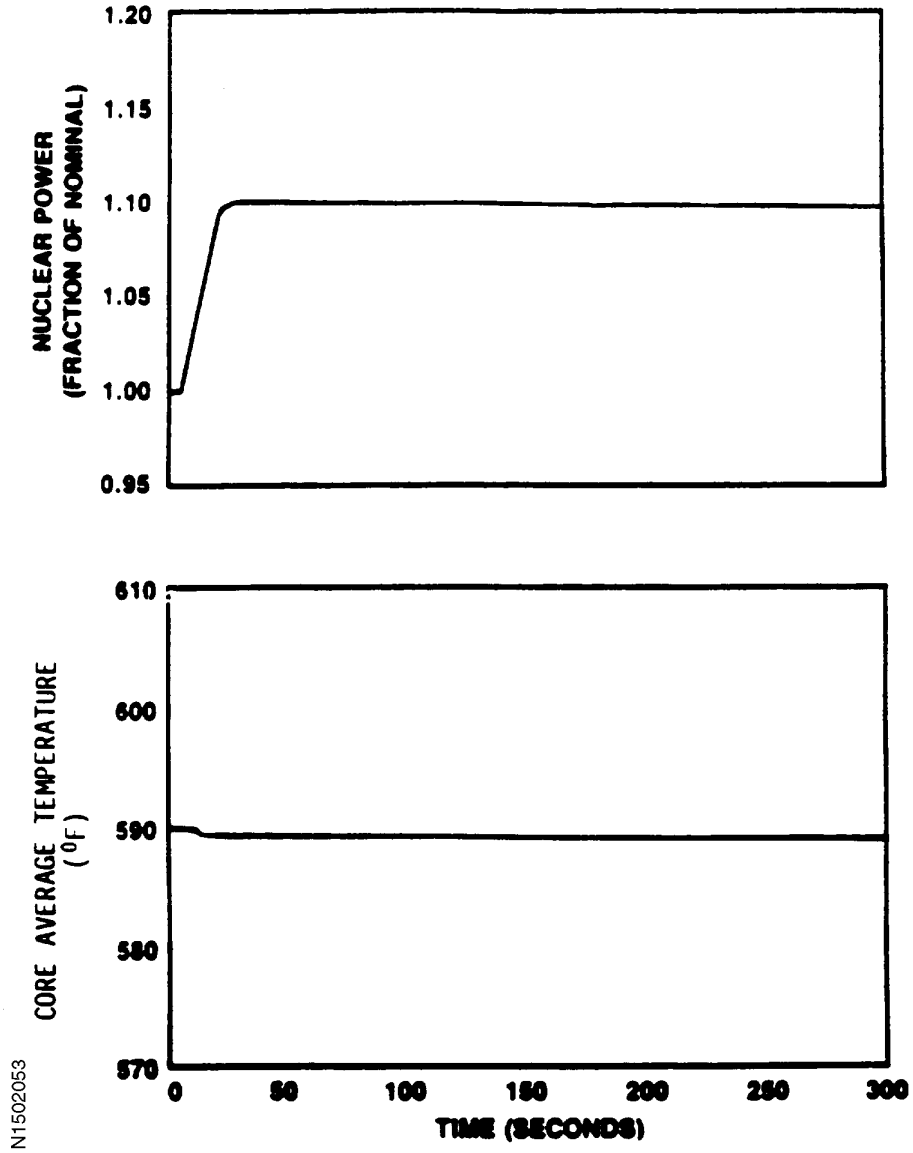

Figure 15.2-49 (SHEET 2 OF 2)
EXCESSIVE LOAD INCREASE WITH AUTOMATIC ROD CONTROL
MAXIMUM FEEDBACK

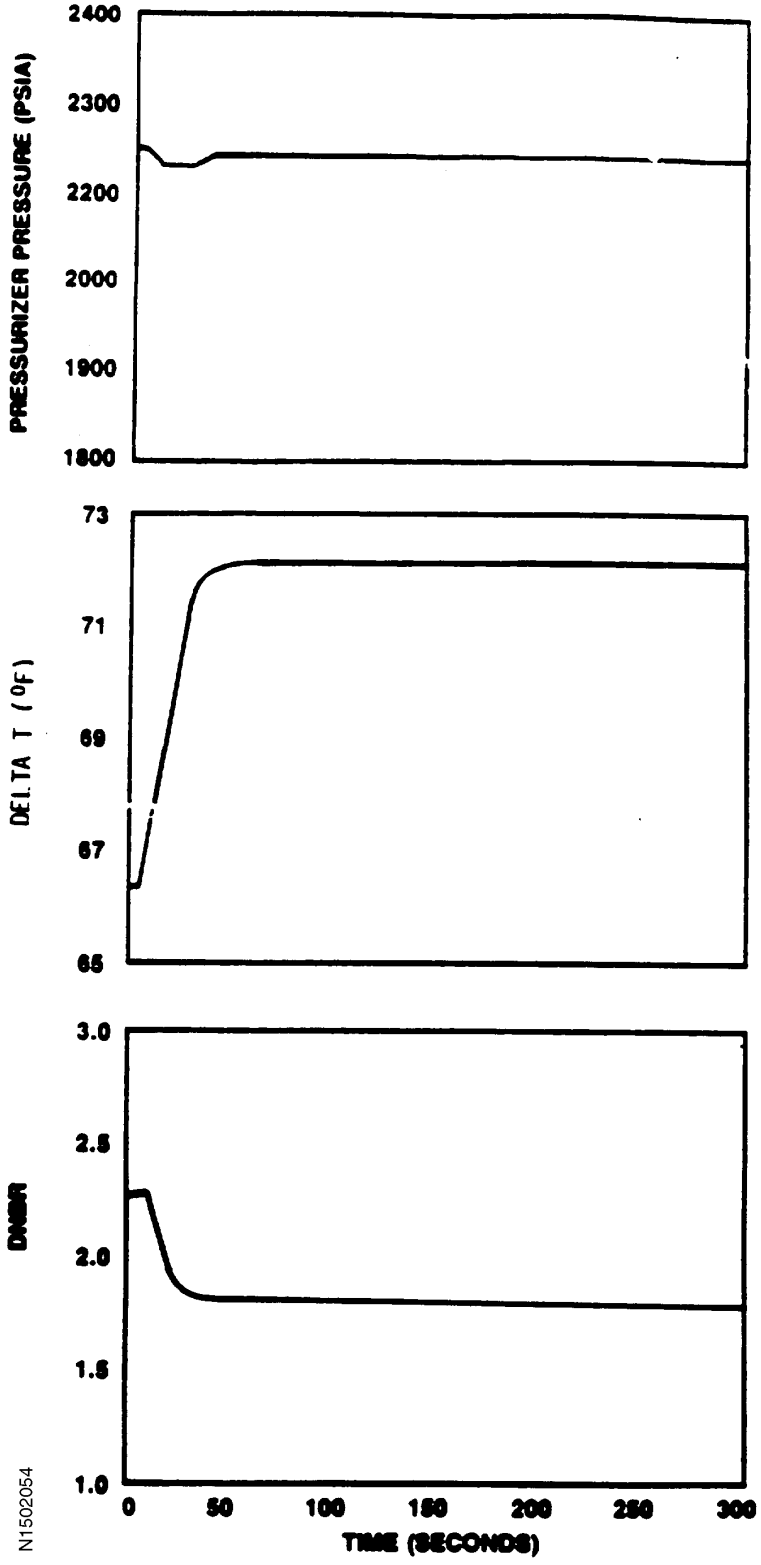

Figure 15.2-50
RCS DEPRESSURIZATION EOC MANUAL CONTROL
NUCLEAR POWER, PERCENT

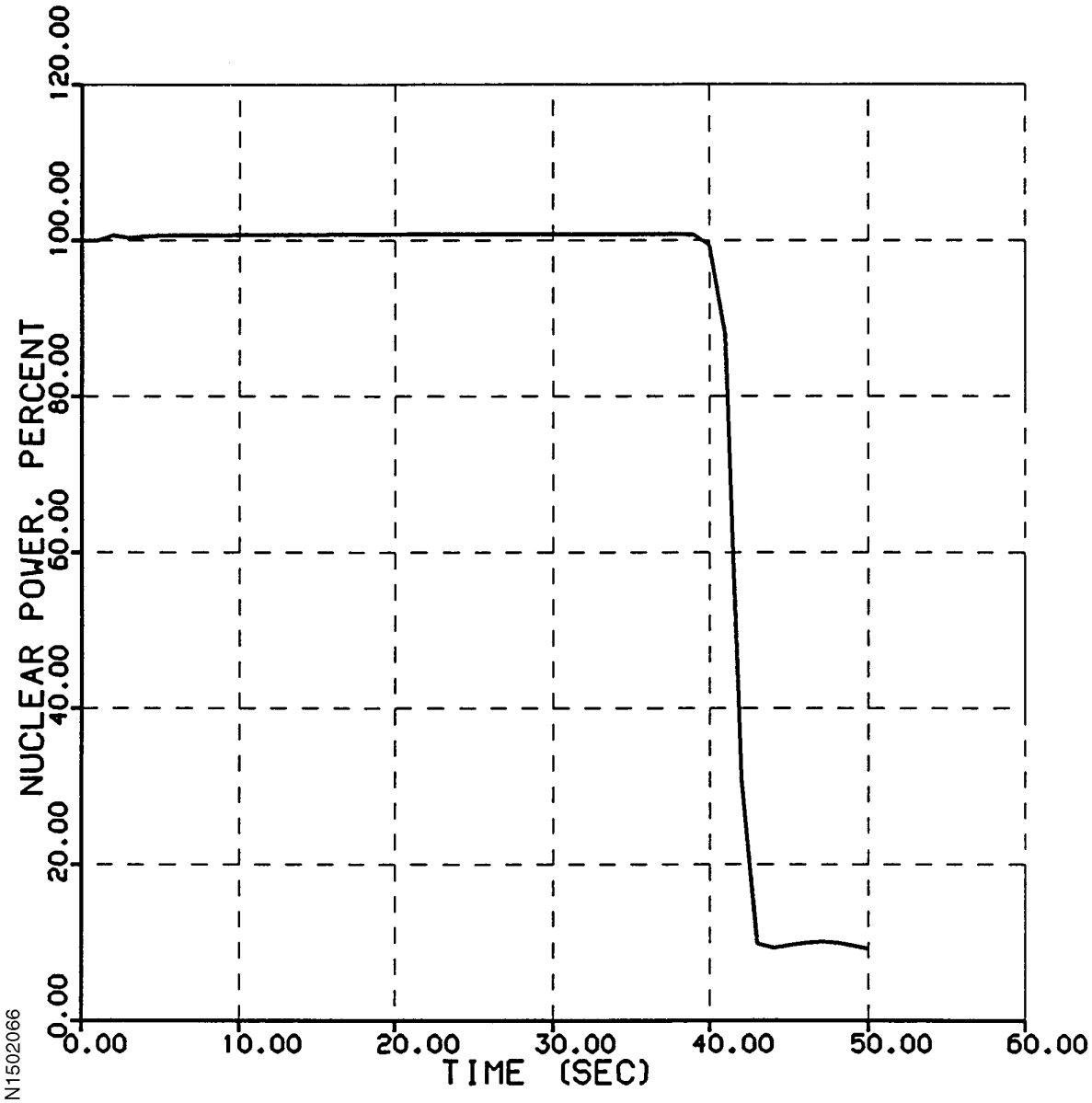

Figure 15.2-51
RCS DEPRESSURIZATION EOC MANUAL CONTROL
PRESSURIZER PRESSURE, PSIA

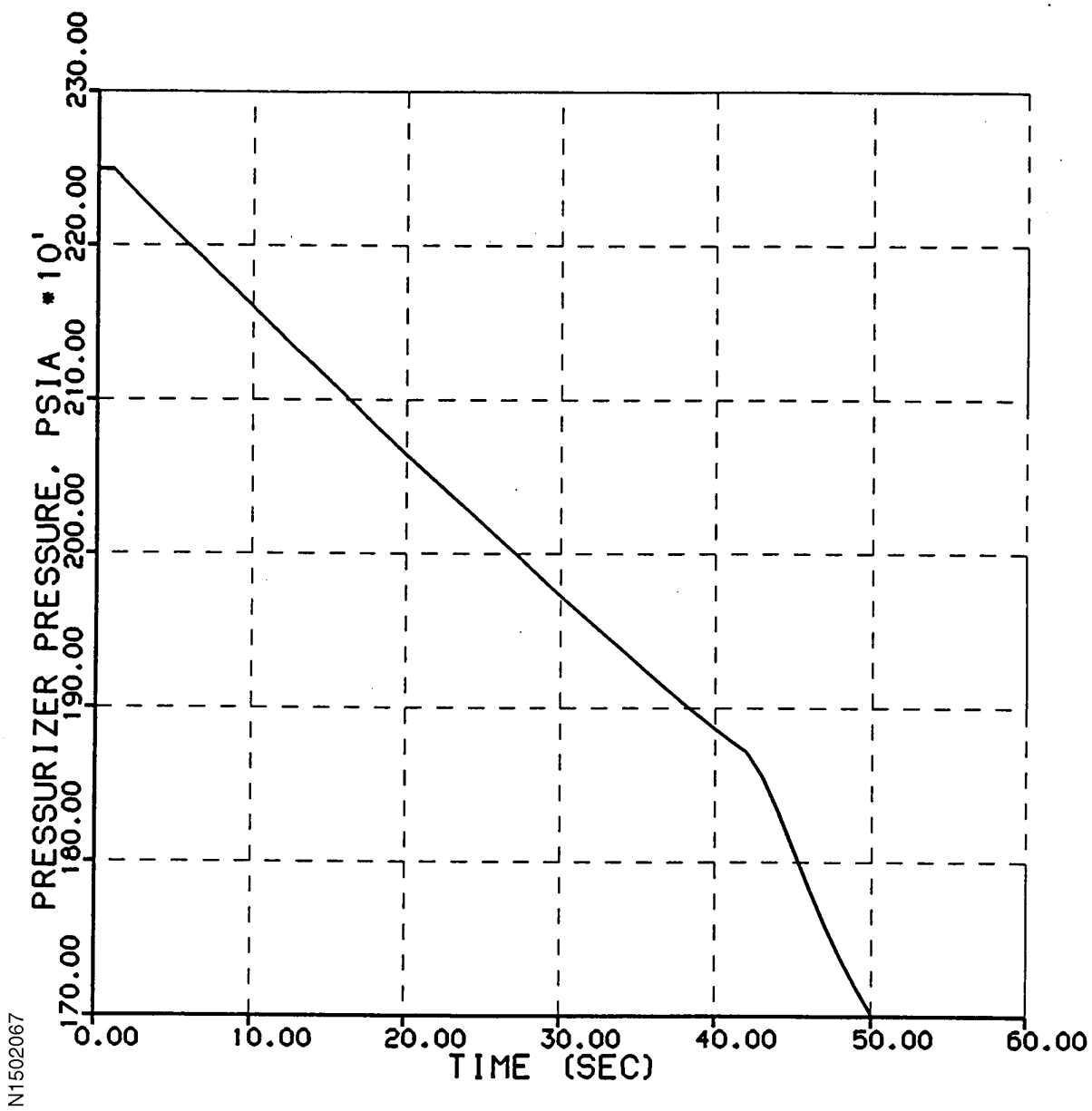

Figure 15.2-52
RCS DEPRESSURIZATION EOC MANUAL CONTROL
DNBR VS. TIME

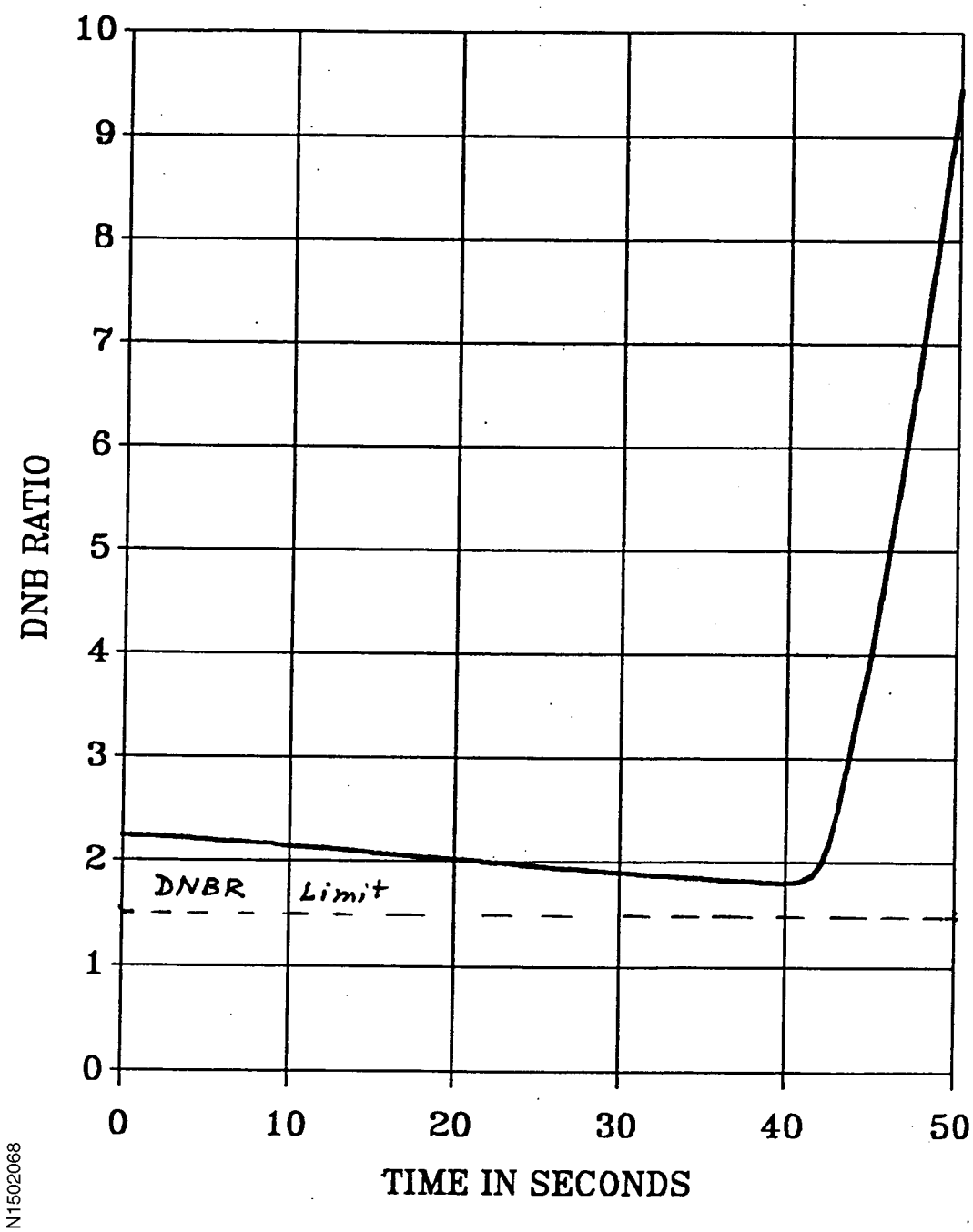

Figure 15.2-53
VARIATION OF k_{eff} WITH CORE TEMPERATURES

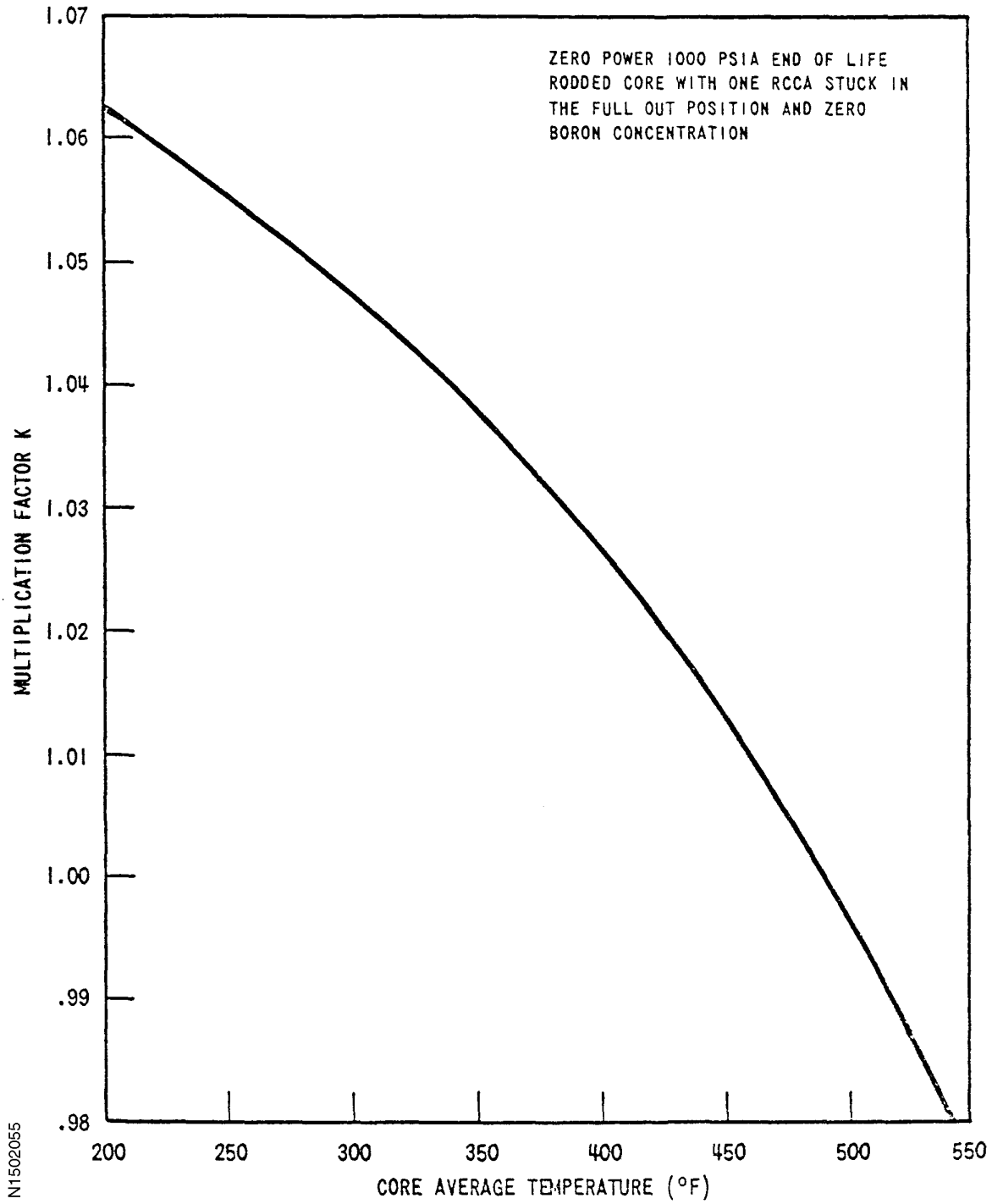

Figure 15.2-54
NAPS MAIN STEAM LINE BREAK ANALYSIS
CREDIBLE BREAK CASE
PRESSURIZER PRESSURE

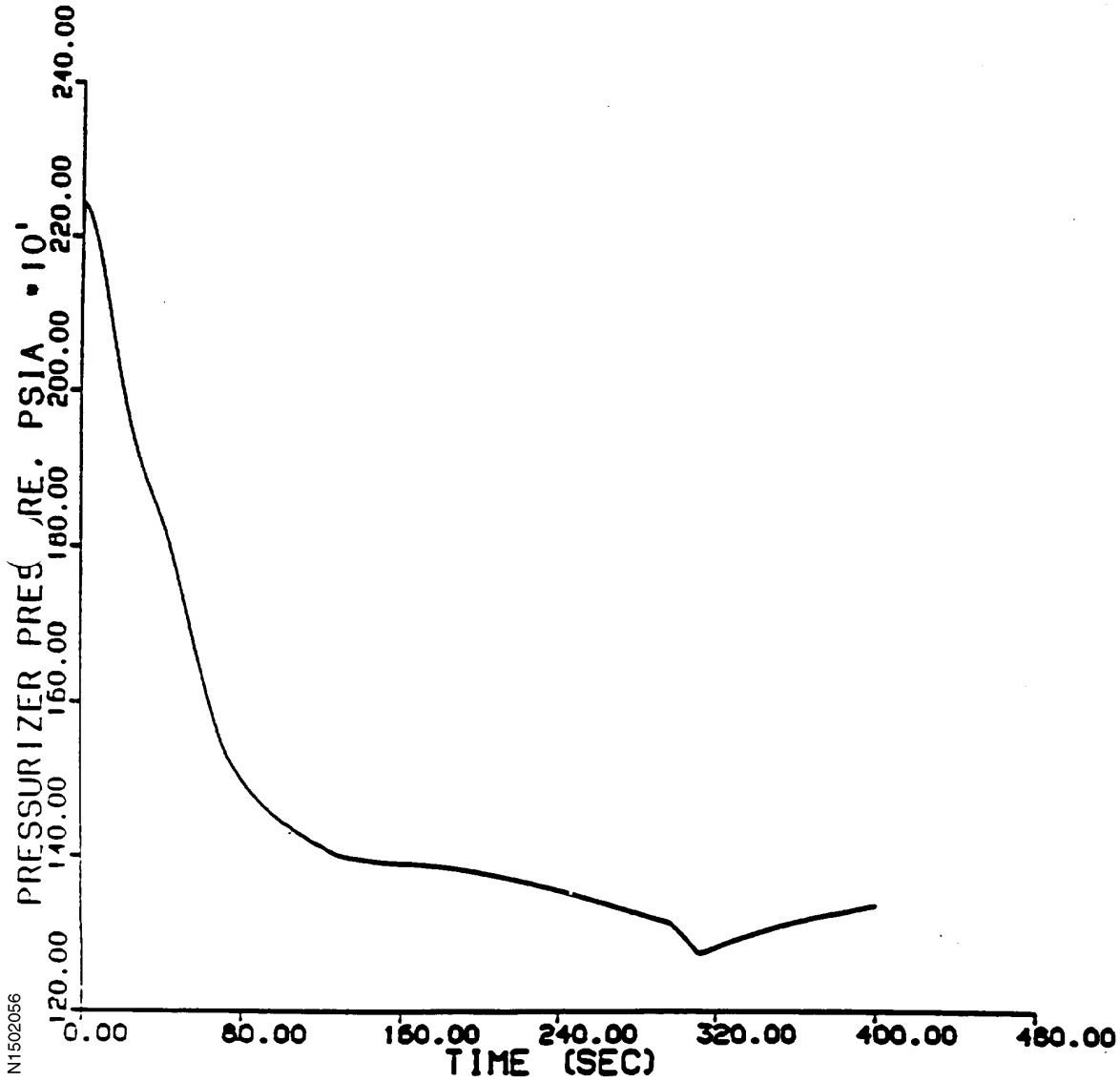

Figure 15.2-55
NAPS MAIN STEAM LINE BREAK ANALYSIS
CREDIBLE BREAK CASE
ACTUAL LOOP AVERAGE TEMPERATURES

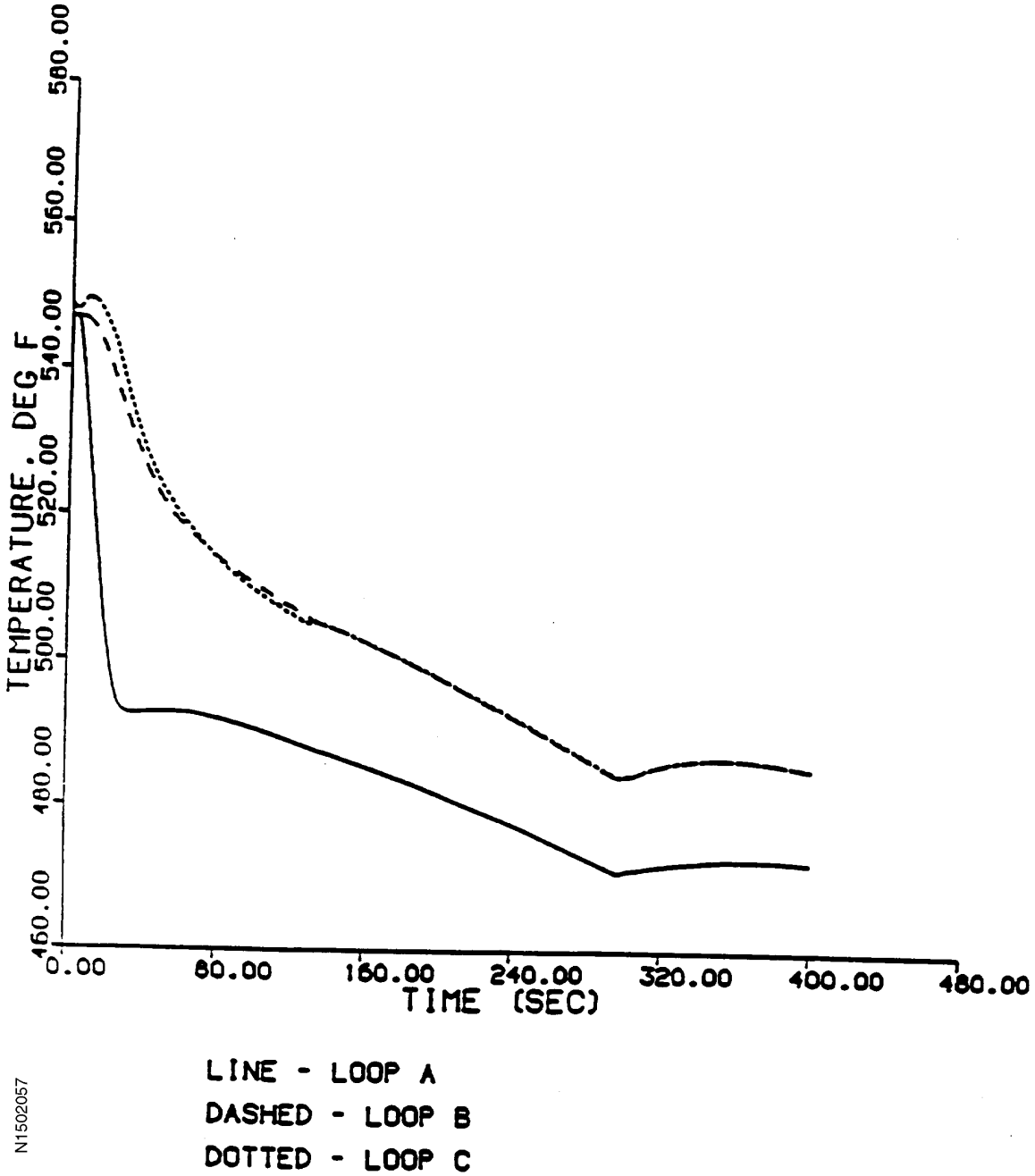

Figure 15.2-56
NAPS MAIN STEAM LINE BREAK ANALYSIS
CREDIBLE BREAK CASE
NORMALIZED CORE HEAT FLUX

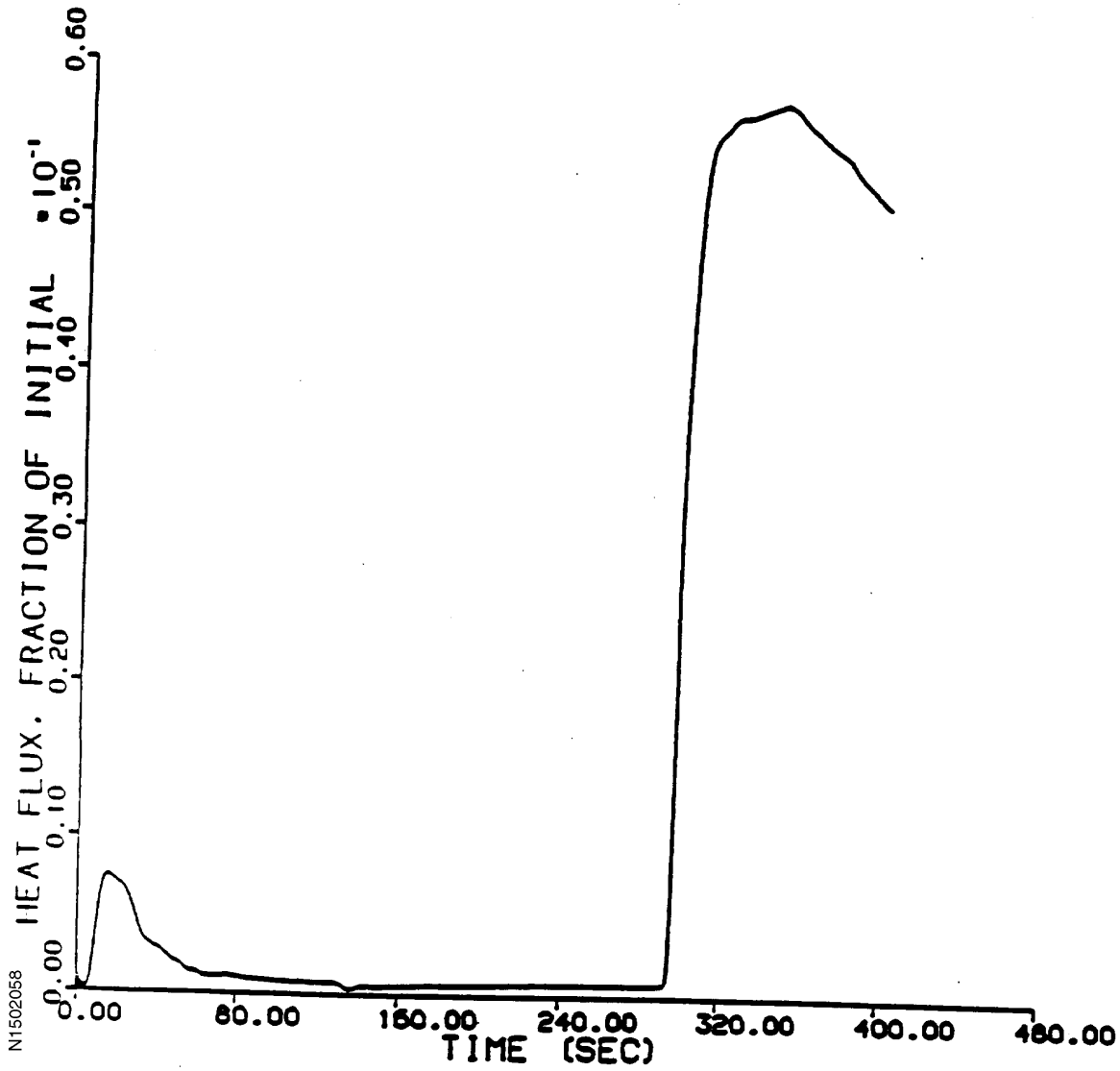

Figure 15.2-57
NAPS MAIN STEAM LINE BREAK ANALYSIS
CREDIBLE BREAK CASE
CORE REACTIVITY, %ΔK/K

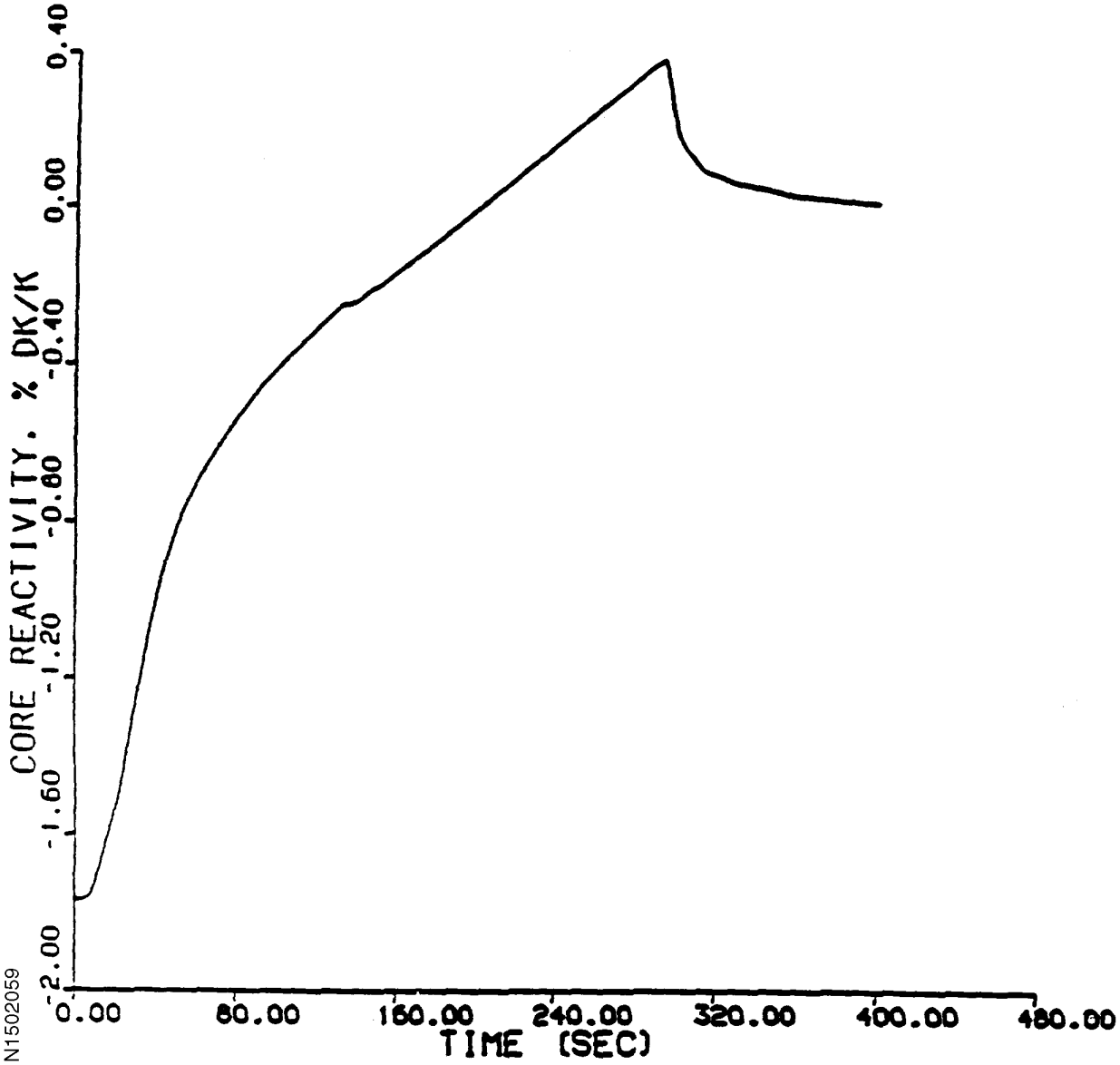

Figure 15.2-58 (SHEET 1 OF 2)
TRANSIENTS FOR A DECAY HEAT RELEASE LINE FAILURE
HOT ZERO POWER CASE

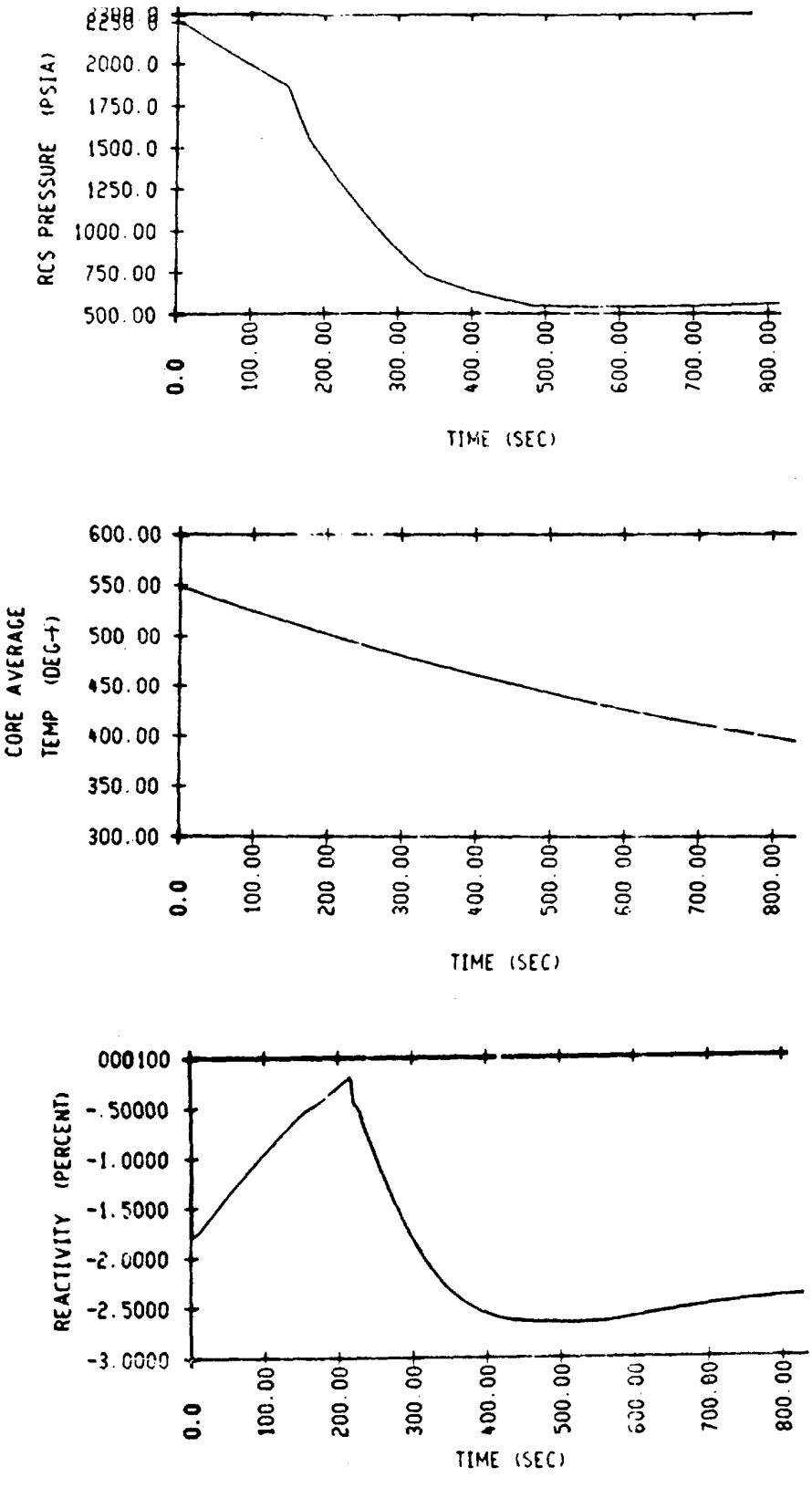

N1502060

Figure 15.2-58 (SHEET 2 OF 2)
TRANSIENTS FOR A DECAY HEAT RELEASE LINE FAILURE
HOT ZERO POWER CASE

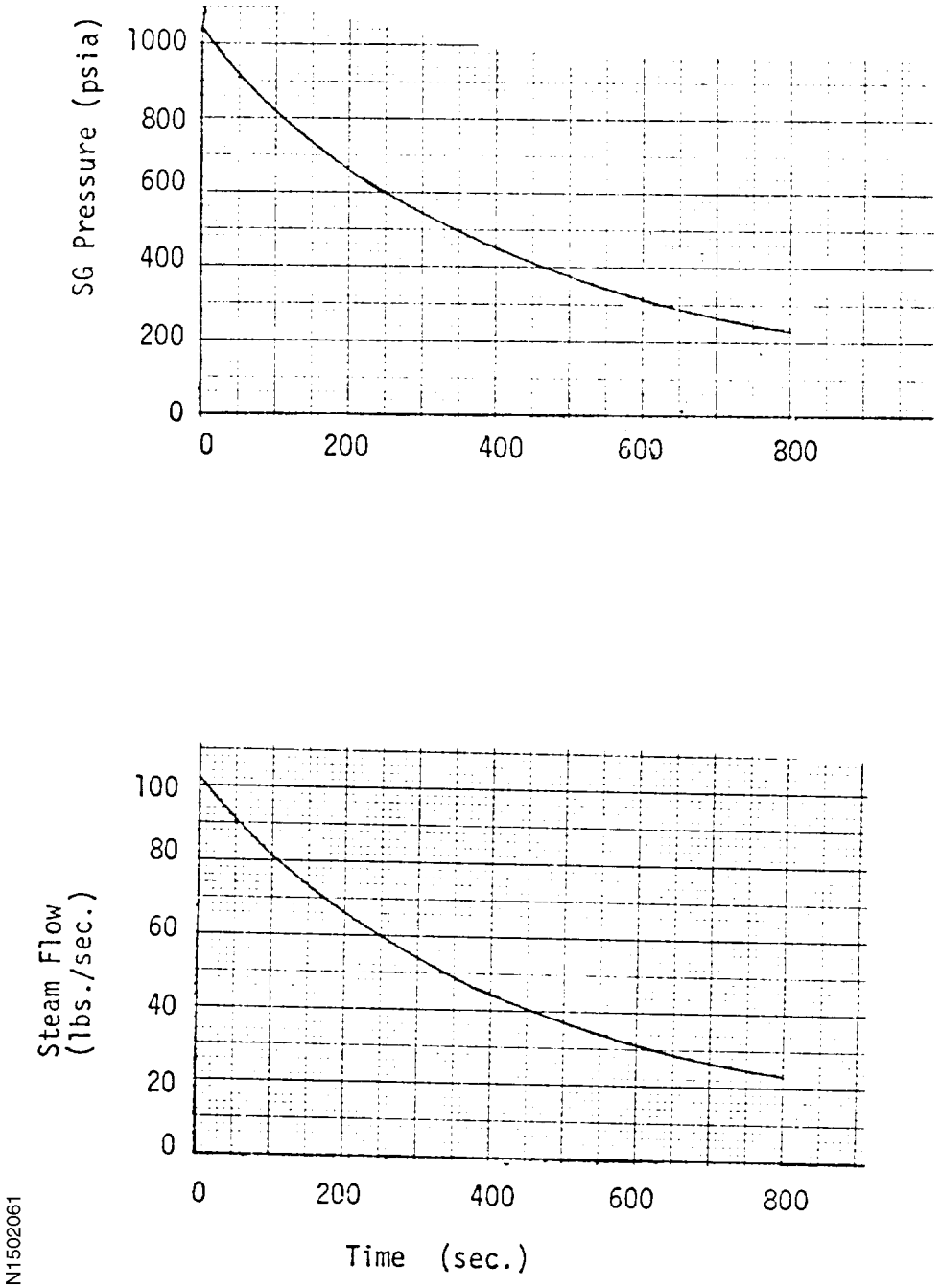

Figure 15.2-59 (SHEET 1 OF 2)
TRANSIENTS FOR A DECAY HEAT RELEASE LINE FAILURE
FULL POWER CASE

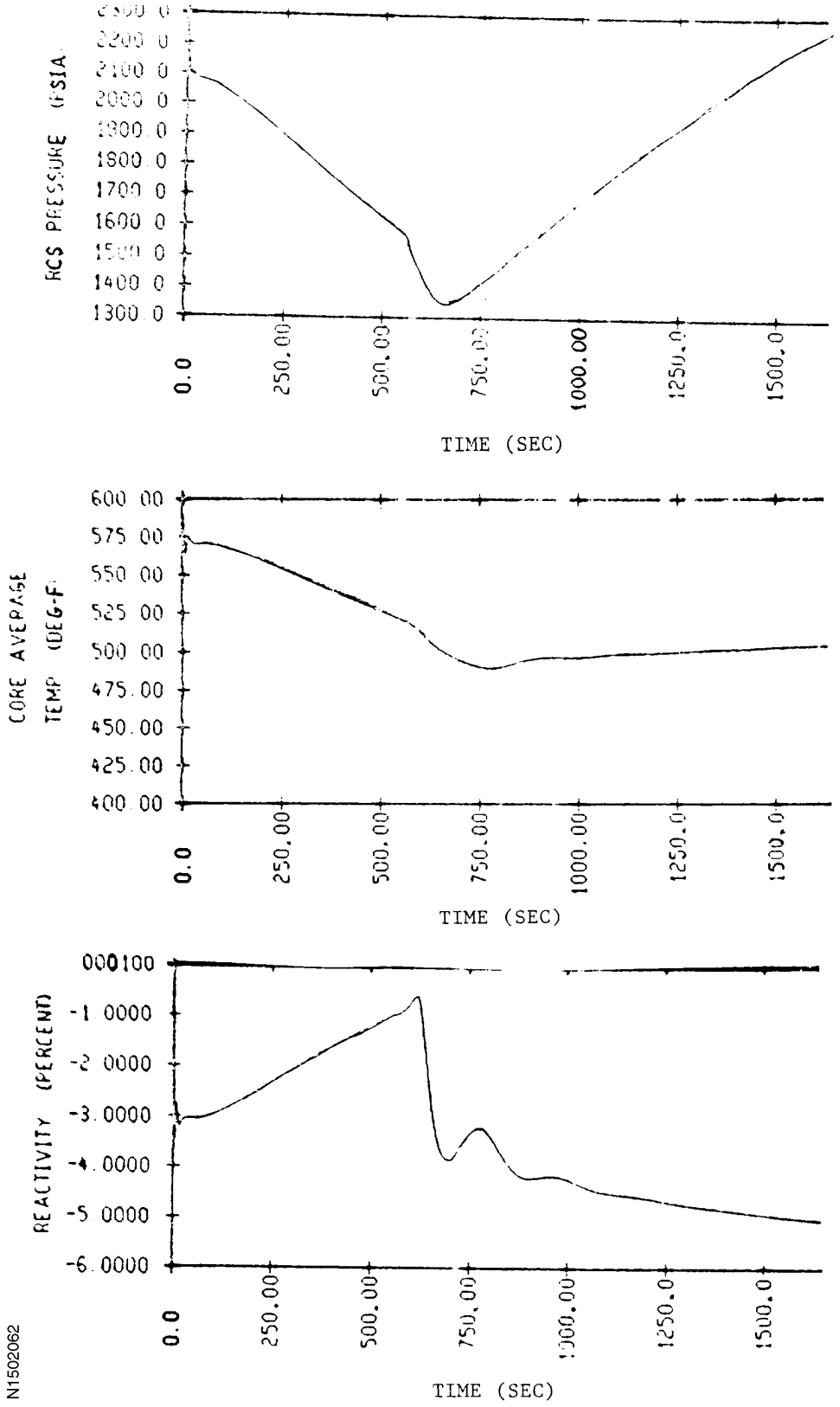

Figure 15.2-59 (SHEET 2 OF 2)
TRANSIENTS FOR A DECAY HEAT RELEASE LINE FAILURE
FULL POWER CASE

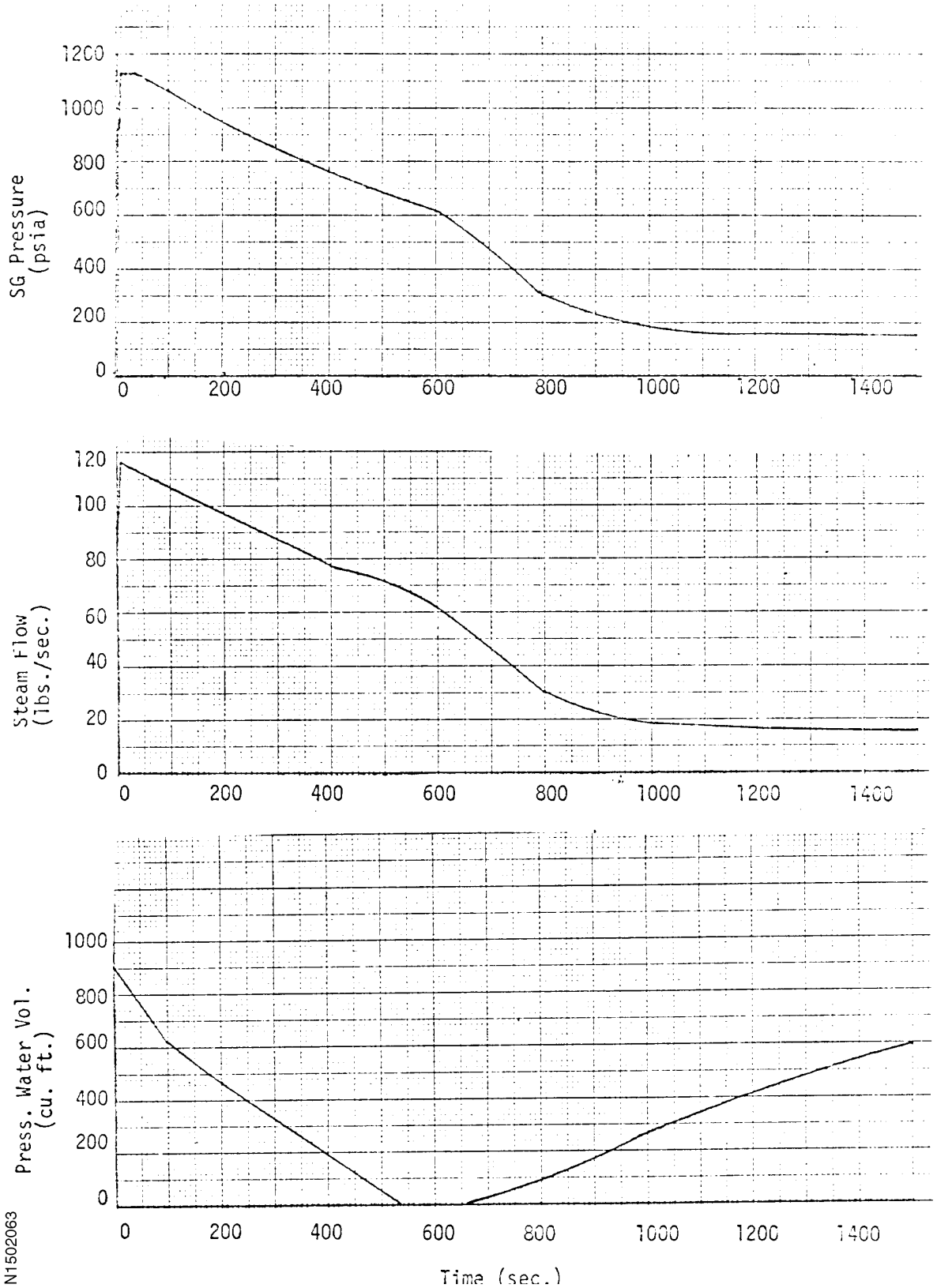

Figure 15.2-60
SPURIOUS ACTUATION OF SAFETY INJECTION SYSTEM AT POWER

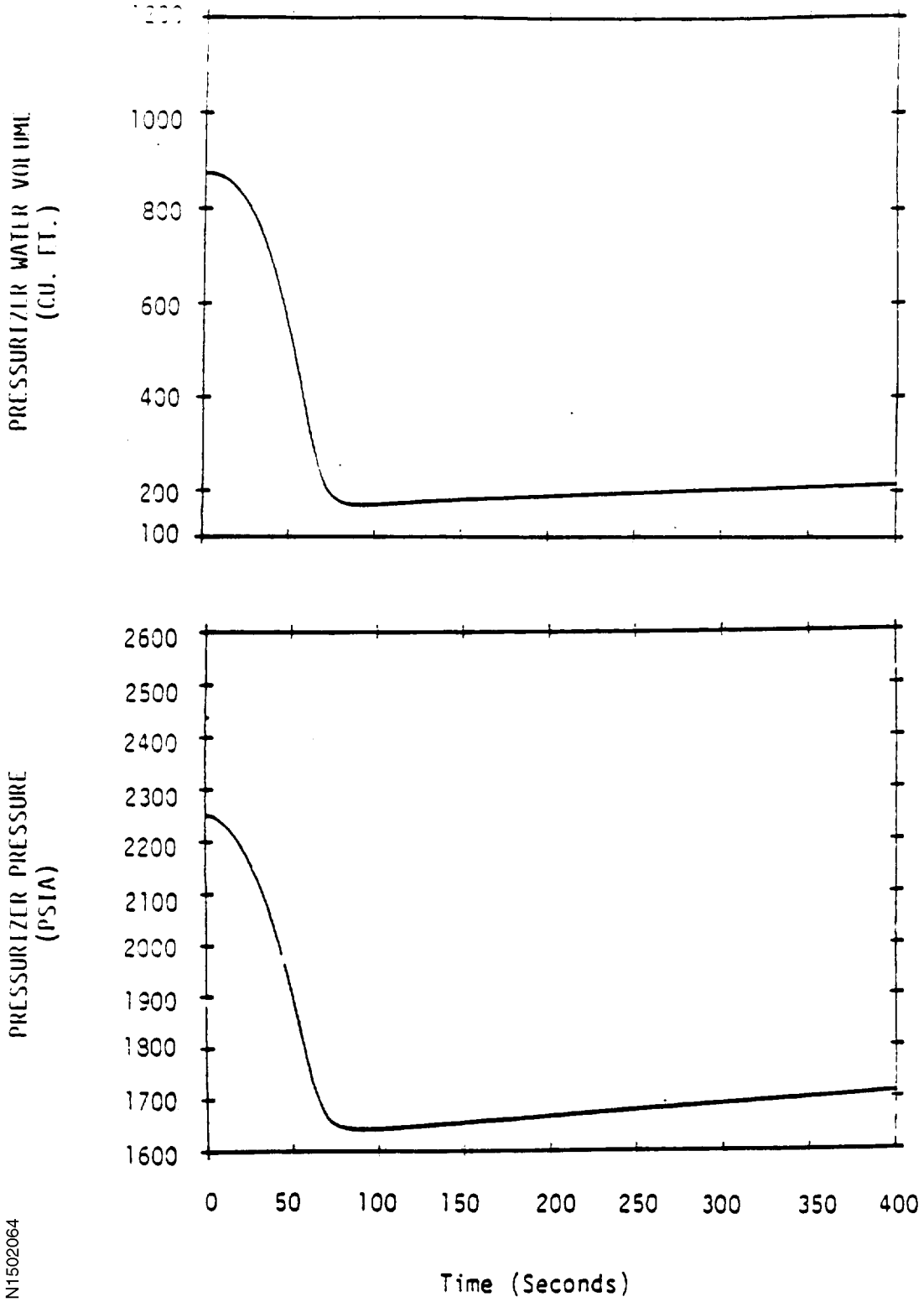

Figure 15.2-61
SPURIOUS ACTUATION OF SAFETY INJECTION SYSTEM AT POWER

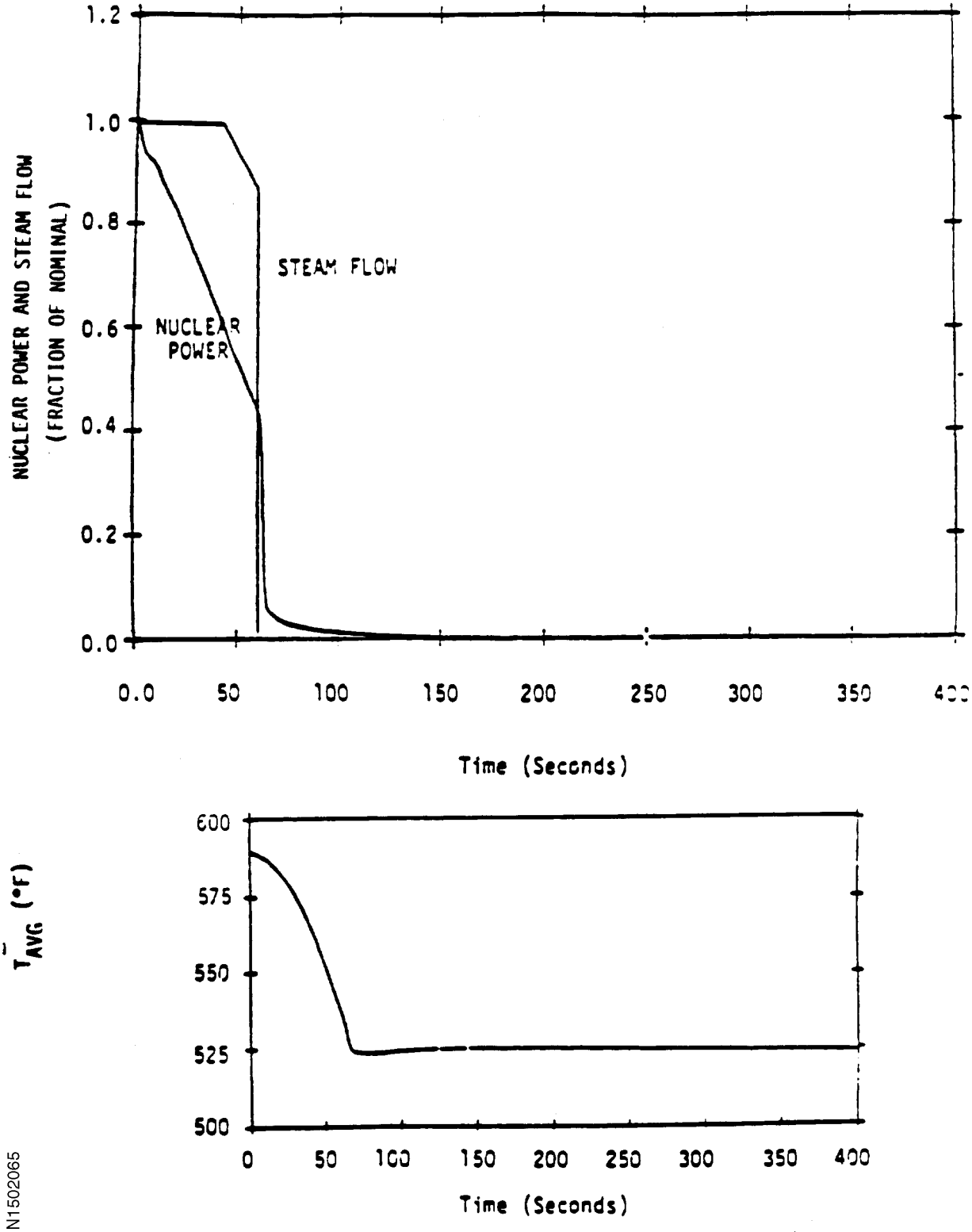

Intentionally Blank

15.3 CONDITION III - LOCA ACCIDENTS

15.3.1 Loss of Reactor Coolant From Small Ruptured Pipes or From Cracks in Large Pipes That Actuates the Emergency Core Cooling System (Small Break Loss of Coolant Accident)

The following sections present the results of the small break LOCA (SBLOCA) transient analyses for North Anna Units 1 and 2 fuel transition applications (Westinghouse NAIF to Framatome ANP Advanced Mark-BW). The Westinghouse and Framatome ANP (FANP) SBLOCA analyses are presented below. Section 15.3.1.1 through 15.3.1.7 presents results of the analysis for the Westinghouse NAIF fuel (Reference 25), which remain valid. The FANP Advanced Mark-BW SBLOCA analyses are presented in Sections 15.3.1.8 through 15.3.1.14.

15.3.1.1 Introduction

This discussion presents the results of a reanalysis of the small break LOCA transient for North Anna 1 and 2. The analysis was revised for North Anna Unit 1 operation with the upflow modification. Since prior Westinghouse and Virginia Power small break LOCA analyses have demonstrated that the upflow configuration bounds downflow, this analysis models only the Unit 1 upflow design.

The key analysis input changes required to provide acceptable results from the small break LOCA analysis are listed below. Each is described more fully in the following sections. Values of key input parameters assumed are given in Table 15.3-1.

- Assumption of 7% uniform steam generator tube plugging
- Peak Heat Flux Hot Channel Factor, F_Q, of 2.32 (changed from 2.20)[1]
- Peak value for Enthalpy Hot Channel Factor, $F\Delta h$, of 1.65 (changed from 1.55)[1]
- A minimum delivered HHSI flow rate calculated for LOCA analysis (at 0 psig backpressure)
- A full core of North Anna Improved Fuel (NAIF) with ZIRLO™ cladding and Performance+ features (bounds operation with 17 x 17 Standard and NAIF mixed cores)
- Upflow baffle/barrel design (changed from downflow baffle/barrel design)
- Safety injection in all loops (changed from safety injection occurring in intact loop only)
- COSI condensation model (changed from homogeneous equilibrium condensation model)

1. These values bound the limits in the current North Anna Units 1 and 2 COLRs.

15.3.1.2 General

A reanalysis of the Emergency Core Cooling System (ECCS) performance for the postulated small-break LOCA (SBLOCA) has been performed in compliance with Appendix K to 10 CFR 50. The results of this reanalysis are presented here, and are in compliance with 10 CFR 50.46, *Acceptance Criteria for Emergency Core Cooling Systems for Light Water Reactors*. This analysis was performed with the NRC-approved NOTRUMP code (Reference 22) of the Westinghouse LOCA-ECCS evaluation model (Reference 23). The thermal behavior of the fuel was analyzed using the LOCTA-IV code (Reference 24). The analytical techniques used are in full compliance with 10 CFR 50, Appendix K.

As required by Appendix K of 10 CFR 50, certain conservative assumptions were made for the LOCA-ECCS analysis. The assumptions pertain to the conditions of the reactor and associated safety system equipment at the time that the LOCA is assumed to occur, and include such items as the core peaking factor and the performance of the Emergency Core Cooling System. The details of the small break LOCA analysis are documented in Reference 25.

15.3.1.3 Identification of Causes and Accident Description

A LOCA can result from a rupture of the Reactor Coolant System (RCS) or of any line connected to that system up to the first isolation valve. Ruptures of a small cross section will cause expulsion of the coolant at a rate that can be accommodated by the charging pumps. These pumps maintain an operational water level in the pressurizer, permitting the operator to execute an orderly shutdown.

The maximum break size for which the normal makeup system can maintain the pressurizer level is obtained by comparing the calculated flow from the reactor coolant system through the postulated break against the charging pump makeup flow at normal RCS pressure, i.e., 2250 psia. A makeup flow rate from one centrifugal charging pump is typically adequate to sustain pressurizer level at 2250 psia for a break through a 3/8-inch diameter hole. This break results in a loss of approximately 21 lbm/sec.

For breaks in the range between 3/8-inch diameter and 1-ft^2 area, depressurization of the reactor coolant system causes fluid to flow to the reactor coolant system from the pressurizer, resulting in a pressure and fluid level decrease in the pressurizer. Reactor trip occurs when the pressurizer low-pressure trip setpoint is reached. The safety injection system (SIS) is actuated when the pressurizer low-low pressure setpoint is reached, activating the high head safety injection pumps. The SIS actuation and subsequent activation of the Emergency Core Cooling System, which occurs with the SIS signal, assumes the most limiting single failure. The consequences of the accident are limited in two ways:

1. Reactor trip and borated water injection complement void formation in causing rapid reduction of nuclear power to a residual level corresponding to the delayed fission and fission product decay.

2. Injection of borated water ensures sufficient flooding of the core to prevent excessive clad temperatures.

Before the break occurs, the unit is in an equilibrium condition, i.e., the heat generated in the core is being removed via the secondary system. During blowdown, heat from fission product decay, hot internals and the vessel continues to be transferred to the reactor coolant system. In the small break LOCA, the blowdown phase of the transient occurs over a long time period. There are three characteristic stages: a gradual blowdown in which the decrease in water level is checked by the inventory replenishment associated with safety injection; core recovery; and long-term recirculation. The heat transfer between the reactor coolant system and the secondary system may be in either direction, depending on the relative temperatures. For the case of continued heat addition to the secondary side, the secondary side pressure increases and the main steam safety valves may actuate to reduce the pressure. Makeup to the secondary side is automatically provided by the auxiliary feedwater system. Coincident with the safety injection signal, normal feedwater flow is stopped by closing the main feedwater control valves and tripping the main feedwater pumps. Emergency feedwater flow is initiated by starting the auxiliary feedwater pumps. The secondary side flow aids in the reduction of RCS pressure. When the reactor coolant system depressurizes to 600 psia, the accumulators begin to inject borated water into the reactor coolant loops. Reflecting the loss of offsite power assumption, the reactor coolant pumps are assumed to be tripped at the time of reactor trip, and the effects of pump coastdown are included in the blowdown analysis.

15.3.1.4 **Analysis Assumptions**

As required by Appendix K of 10 CFR 50, certain conservative assumptions were made for the Small Break LOCA-ECCS analysis. The assumptions pertain to the condition of the reactor and associated safety system equipment at the time that the LOCA is assumed to occur, and include such items as the core peaking factors, core decay heat and the performance of the Emergency Core Cooling System. Table 15.3-1 presents the values assumed for several key parameters in this analysis. Assumptions and initial operating conditions which reflect the requirements of Appendix K to 10 CFR 50 have been used in this analysis. These assumptions include:

- The break is located in the cold leg between the pump discharge and the vessel inlet.
- Safety injection occurs both in the intact loop and broken loop.
- The accumulator injection occurs both in the intact loop and broken loop.
- 120 percent of 1971 ANS decay heat is assumed following reactor trip.
- Initial power is 102% of the full core power, to account for the calorimetric uncertainty.
- The analysis assumes that 7% of the tubes in each steam generator are plugged.

- The safety injection system is assumed to be delivering to the reactor coolant system in 37 seconds from the generation of the SIS signal. The 37-second delay includes sufficient time to bound the time required for diesel start-up and loading of the safety injection pumps onto the emergency buses.

- The analysis included the auxiliary feedwater configuration which produces the limiting PCT results. The model accounted for the one-on-one design in which each auxiliary feedwater pump is aligned to feed a specific steam generator.

Several additional assumptions have been incorporated into the SBLOCA reanalysis described below to provide margin in key input parameters. These changes are discussed here.

In the previous NOTRUMP evaluation model, safety injection is delivered only in the intact loop, and the least resistance safety injection line is assumed to spill on the containment floor. This modeling was assumed to be conservative since the additional safety injection was considered to be a benefit. This assumption was based on older models which employed a homogenous equilibrium assumption for the mixing of different phases. Sensitivity studies with the previous evaluation model determined that safety injection in the broken loop, in conjunction with the existing condensation model, resulted in a PCT penalty. Reference 28 has documented this change to the NOTRUMP evaluation model. This modeling is used in this reanalysis.

To offset the penalties associated with the revised safety injection assumption, Westinghouse has incorporated a new condensation model in the NOTRUMP evaluation model. This model, referred to as the COSI model, is based on tests which modeled the configuration of the SI piping to the RCS cold leg. Use of this more realistic model for condensation of steam by pumped SI is demonstrated to provide a benefit larger than any penalty associated with injecting into the broken loop (Reference 28).

The analysis assumed a peak Heat Flux Hot Channel Factor, F_Q, value of 2.32 and a peak Nuclear Enthalpy Hot Channel Factor, $F\Delta h$, value of 1.65. As required by Technical Specification 5.6.5, the Core Operating Limits Report (COLR) documents the applicable limit values of key core-related parameters for each reload core. These values bound the limits in the current cycle specific COLRs. For future reload cycles, the COLR will specify the appropriate limits which account for all design considerations, particularly large and small break LOCA effects.

This analysis also employed a K(z) envelope, the hot channel factor normalized operating curve shown in Figure 15.3-2. K(z) is a multiplier on the allowable 3-dimensional peaking factor F_Q, and by nature cannot exceed 1.0. A new revised hot rod axial power shape (shown in Figure 15.3-3) was used in the LOCTA-IV code. This power shape has been chosen from a generic database of potential shapes achievable during power operation by assessing the characteristics which yield limiting small break LOCA results. The selected shape has been identified as the most limiting within the bounds of the proposed K(z) curve. Large Break LOCA assumptions will govern the allowable $F_Q \times K(z)$ limit at elevation, z.

The flow rates for the HHSI are provided by an engineering model of the HHSI subsystem that is based on the system configuration and measured data from the plant. This model includes allowances for imbalance between the separate injection lines, HHSI pump degradation, and instrument accuracy. The HHSI pump curves used in the model are based on the actual measured plant data for the installed HHSI pumps in each unit. For the calculated HHSI flows, it is assumed that the HHSI flow recirculation line is open above RCS pressures of 1000 psig and that it is closed below that RCS pressure. Other assumptions regarding HHSI system configuration, such as water levels and back pressure, are set to provide limiting conditions for the specified test condition. HHSI flow testing performed during refueling outages can be used to assess the condition of the HHSI pumps and maintain the required flow balance between the individual HHSI injection lines to meet small break LOCA requirements.

The analysis assumes a full core of North Anna Improved Fuel (NAIF) with ZIRLO™ (Reference 27), which is similar and compatible to Westinghouse Vantage 5 Hybrid (V5H) fuel. This modeling is applicable to full or mixed cores of either fuel product. The only mechanism available to cause a transition core to have a greater calculated small break LOCA PCT than a full core of either fuel product is the possibility of flow redistribution due to fuel assembly hydraulic resistance mismatch. The small break evaluation model assumes only one core channel. This assumption is acceptable, since the flowrate during a small break LOCA is low, providing enough time to maintain flow equilibrium and eliminate crossflow effects. As stated in Reference 26, mixed core hydraulic resistance mismatches are not a significant factor for small break analyses and it is not necessary to apply a LOCA analysis transition core penalty.

The inherent margin of the NOTRUMP ECCS evaluation model has been employed to accommodate these parameter changes and demonstrate adequate margin to the 2200°F PCT acceptance limit of 10 CFR 50.46.

15.3.1.5 **Analysis of Effects and Consequences**

15.3.1.5.1 Method of Analysis

A small break LOCA analysis was performed using the NOTRUMP computer code following the methodology and the model delineated in WCAP-10079-P-A (Reference 22) and WCAP-10054-P-A (Reference 23). The NOTRUMP computer code is used for loss of coolant accidents due to small breaks less than one square foot. The code calculates the transient depressurization of the RCS as well as describing the mass and enthalpy of flow through the break.

NOTRUMP is a general one-dimensional network code consisting of a number of advanced features. Among these features are the calculation of thermal non-equilibrium in all fluid volumes, flow regime-dependent drift flux calculations with counter-current flooding limitations, mixture level tracking logic in multiple-stacked fluid nodes and regime-dependent heat transfer correlations. The NOTRUMP small break LOCA emergency core cooling system (ECCS) evaluation model was developed to determine the RCS response to design basis small break

LOCAs and to address the NRC concerns expressed in NUREG-0611, *Generic Evaluation of Feedwater Transients and Small Break Loss-of-Coolant Accidents in Westinghouse-Designed Operating Plants.*

In NOTRUMP, the RCS is nodalized into volumes interconnected by flowpaths. The broken loop is modeled explicitly, with the intact loops lumped into a second loop. The transient behavior of the system is determined from the governing conservation equations of mass, energy and momentum applied throughout the system.

The use of NOTRUMP in the analysis involves, among other things, the representation of the reactor core as heated control volumes with an associated bubble rise model to permit a transient mixture height calculation. The multinode capability of the program enables as explicit and detailed spatial representation of various system components. In particular, it enables a proper calculation of the behavior of the loop seal during a loss-of-coolant accident.

The peak clad temperature in the core during a transient is calculated by utilizing the Westinghouse LOCTA-IV code (Reference 24) for a small break analysis. The transient thermal hydraulic NOTRUMP code writes data to a file for the LOCTA-IV code. The clad thermal analysis code uses the RCS pressure, core mixture level, normalized core power, and core exit mass flow rate from the thermal hydraulic code NOTRUMP as input.

The assumed SIS pumped injected flowrate, which is shown in Figure 15.3-1, is a function of reactor coolant system pressure. The injection flow used accounts for the effect of Low Head Safety Injection (LHSI) pump flow at RCS pressures less than the pump shutoff head. Also, minimum safeguards and emergency core cooling system capability and operability have been assumed in this analysis.

15.3.1.5.2 Results

For this analysis, cases were run assuming 2-inch, 3-inch, and 4-inch effective diameter cold leg breaks. Results for the 6-inch break are not reported but previous evaluations have demonstrated its peak clad temperature (PCT) to be less limiting than the 2, 3, and 4-inch breaks. The 6-inch break produces a more rapid depressurization and accumulator actuation, which results in primary core recovery sooner than for the smaller break cases. The PCT occurs during this initial, deep uncovery. Analyses of 6-inch break cases also typically exhibit a second, more shallow core uncovery, but fuel rod heatup is limited during this period by three factors: 1) greater accumulator and safety injection flows limit the uncovery to the top portion (approximately 2 feet) of the core, 2) the larger break size allows more energy removal from the core, and 3) the duration of the second uncovery is ultimately limited by significant additional flow from the low head safety injection pumps, which provide for full core recovery.

Results of key parameters for the cases analyzed are presented in Figures 15.3-4 through 15.3-27. Table 15.3-2 presents the time sequence of events, and Table 15.3-3 summarizes the peak clad temperature for each case analyzed. All cases presented assume the most limiting

feedwater lineup established in the sensitivity study discussed in Section 15.3.1.4. The 3-inch cold leg break was found to be the most limiting break size for a small break LOCA. The analysis resulted in a limiting peak clad temperature of 1704°F, a maximum local cladding oxidation level of 2.0%, and a total core metal-water reaction of less than 1.0%. The attached figures show the following:

- Pressurizer Pressure—Figures 15.3-4 through 15.3-6 show the calculated pressure for the different break sizes.
- Core Mixture Level—Figures 15.3-7 through 15.3-9 show that the core mixture level decreases, accompanied by the RCS depressurization, until the combined rate of the Safety Injection and the Accumulator Injection exceeds the break flow.
- Pumped SI Flow—Figures 15.3-10 through 15.3-12 show the pumped safety injection flow to the intact loop and Figures 15.3-13 through 15.3-15 to the broken loop.
- Core Exit Vapor Flow—Figures 15.3-16 through 15.3-18 show the core exit vapor flow.
- Hot Assembly Fluid Temperature—The fluid temperature in the hot assembly peaks at the same time as the clad temperature, with approximately the same magnitude, and is shown in Figures 15.3-19 through 15.3-21.
- Hot Assembly Heat Transfer Coefficient—Figures 15.3-22 through 15.3-24 show the heat transfer coefficient calculated by the code.
- Peak Clad Temperature—Figures 15.3-25 through 15.3-27 show the calculated hot-spot clad temperature transient. The peak clad temperature for the limiting 3-inch break size is 1704°F at the 11.75-foot core elevation.

15.3.1.6 **Post Analysis of Record Evaluations - Westinghouse Fuel**

In addition to the analyses presented in this section, evaluations and reanalyses may be performed as needed to address computer code errors, emergent issues or to support plant changes. The issues or changes are evaluated, and the impact on the PCT is determined. The resultant increase or decrease in PCT is applied to the analysis of record PCT. The PCTs, including all penalties and benefits, are presented in Table 15.3-4 for the small break LOCA. The resultant PCT is demonstrated to be less than the 10 CFR 50.46(b) requirement of 2200°F (Reference 36).

15.3.1.7 **Conclusions**

The fuel clad heatup summary in Table 15.3-3 presents results that are well within the acceptance criteria specified by 10 CFR 50.46. The calculated peak clad temperature for the limiting 3-inch break is less than the 2200°F limit. The maximum local metal water reaction is less than the embrittlement limit of 17%. The total zirconium-water reaction is well below the 1% limit. The results show that the clad temperature transient has peaked and sufficiently stabilized

while the core is still amenable to cooling. Consequently, it is concluded that the North Anna ECCS will be capable of mitigating the effects of a small break LOCA with a maximum FΔh of 1.65, at the rated thermal core power of 2893 MWt, for both 17 x 17 Standard and North Anna Improved Fuel products with ZIRLO^{TM} cladding and Performance+ features.

For the small break LOCA, the emergency core cooling system will thus meet the acceptance criteria as presented in 10 CFR 50.46, as follows:

1. The calculated peak fuel element clad temperature provides margin to the limit of 2200°F.
2. The amount of fuel element cladding that reacts chemically with water or steam does not exceed 1% of the total amount of Zircaloy in the reactor.
3. The clad temperature transient is terminated at a time when the core geometry is still amenable to cooling. The localized cladding oxidation limit of 17% is not exceeded.
4. The core remains amenable to cooling during and after the break.
5. The core temperature is reduced and decay heat is removed for an extended period of time, as required by the long-lived radioactivity remaining in the core.

15.3.1.8 **Framatome ANP SBLOCA Analysis**

SBLOCA analyses were performed to support operation with FANP Advanced Mark-BW fuel at the North Anna units (Reference 35). The work is discussed in the following sections. The SBLOCA calculations follow the NRC-approved methodology outlined in Volume II of the LOCA EM, Reference 30. The results of the small break studies demonstrate compliance with the regulatory criteria of 10 CFR 50.46.

Beginning with Cycle 17 for Unit 2 and Cycle 18 for Unit 1, the Advanced Mark-BW fuel product was introduced in mixed cores with the LOPAR and NAIF assemblies.

15.3.1.9 **Small Break LOCA Transient Description**

A SBLOCA transient is characterized as developing in distinct phases: (1) subcooled depressurization, (2) RCS loop saturation and flow coastdown, (3) loss of RCS loop circulation and reflux cooling, (4) loop seal clearing and core refill, and (5) long-term cooling provided by ECCS pumps and accumulators.

Following the break, the primary system rapidly depressurizes to the saturation pressure of the hot leg fluid. During the initial depressurization phase, a reactor trip is generated on low pressurizer pressure, and the turbine is tripped on the reactor trip. Loss-of-offsite power is assumed concurrent with the reactor trip, resulting in an RCP trip.

In the second phase, the reactor coolant pumps coast down. Natural circulation flow in the RCS loops provides continuous core heat removal via the steam generators.

The RCS loop draining phase that follows results in the interruption of natural circulation. During this period, heat transfer in the steam generator tubes is by reflux boiling. For smaller breaks, this cooling mode removes a significant portion of core decay heat from the reactor coolant system. The RCS pressure stabilizes at a quasi-equilibrium value somewhat above the steam generator secondary side pressure. The system reaches a quiescent state, characterized by a balance between core decay heat, break flow, and steam generator heat removal.

Loop seal clearing and core recovery occur in the next phase of a SBLOCA transient. RCS inventory continues to decrease. Steam venting from the core to the break is blocked by the presence of a liquid loop seal in the RCP suction piping. Steam buildup in the upper regions of the RCS suppresses liquid levels in the reactor core and in the steam generator side of the suction piping. During this buildup, the core mixture level descends into the active core region and a short temperature excursion ensues. Eventually, the level in the suction piping is suppressed below the spill under elevation and the loop seal clears. With the loop seals cleared, steam venting is established through the break, pressure at the core exit is reduced, and the hydrostatic heads in the various RCS components readjust, allowing the core mixture level to recover.

Following loop seal clearing, the ECCS flow may be insufficient to replenish the mass lost through core boiling. The duration and magnitude of this imbalance sets the core liquid inventory. During this period, the core may uncover and undergo a temperature excursion.

The final phase of a SBLOCA transient is characterized as the long-term cooling period. Steam continues to be relieved through the break and the RCS continues to depressurize, allowing ECCS flow to increase. Eventually, break flow energy removal plus ECCS-provided liquid inventory replacement will balance core decay heat. RCS inventory increases, the core is recovered, and any core temperature excursion is terminated.

15.3.1.10 **Framatome ANP SBLOCA Evaluation Model**

RELAP5 is used to predict the reactor coolant system thermal-hydraulic responses to small break LOCA. The code is NRC-approved for licensing applications and is documented and described in detail in Reference 31. The SBLOCA modeling configuration is discussed in the LOCA EM, Reference 30. The modeling used for the North Anna SBLOCA calculations is totally consistent with the approved EM as described in Reference 30. Noding diagrams are presented in Figures 15.3-45, 15.3-46, and 15.3-47. Figure 15.3-45 shows the loop noding for both North Anna units. Figure 15.3-46 shows the Unit 1 upflow barrel-baffle configuration. The barrel-baffle region coupling for the Unit 2 downflow model is shown in Figure 15.3-47.

The reactor core is divided into two regions: one region represents the hot fuel assembly (the hot fluid channel), and the second region represents the remainder of the core (the average fluid channel). The core is divided into twenty-nine axial segments. Crossflow junctions connect the hot fluid channel to the adjacent average fluid channel. This arrangement allows the computation of hot assembly cladding and vapor temperatures with proper coupling to the average, fluid channel coolant. Axial noding (above the mid-plane) resolves the mixture level to

within 0.3 feet. The average channel-to-hot channel crossflow is reduced by using a resistance factor ten times greater than the hot-to-average channel resistance in the upper core region. Initial fuel pin parameters are set based on TACO3 predictions (Reference 32). The TACO3 hot pin, volume-averaged, fuel temperature uncertainty, 11.5 percent, is conservatively applied to all fuel assemblies in the initialization of the core. The reactor vessel downcomer and upper plenum regions are represented in axial detail. This allows for a proper representation of the void distribution that affects the system hydrostatic balance.

The RCS is divided into two flow loops. One loop represents the broken loop and the other represents the two intact loops. The steam generator tubes are divided into two regions. One region represents the shortest half of the tubes and the other region represents the remainder of the tubes. This provides appropriate modeling accuracy to properly simulate tube-draining effects that can be sensitive to tube length. The reactor coolant pump suction nodalization is selected, per Reference 30, to produce an accurate hydrodynamic representation of loop seal clearing. Fine nodalization is used for the pump suction piping. This allows resolution of the void distributions and elevation heads that control the occurrence and timing of the loop seal clearing.

The SBLOCA EM is configured to promote the clearing of the loop seal in only one pipe, that representing the broken loop. The intent is to limit steam flow to the break, promote degradation of core conditions, and increase the potential for uncovering the core. The bias (to clear only the loop seal in a single loop) is enacted by artificially extending the bottom elevation of the intact loop pump suction piping at least one foot below that of the broken loop (Reference 30). This preferentially promotes the clearing of only the broken loop.

The intact loop reactor coolant pump discharge piping is modeled per the SBLOCA EM. Like the broken loop pump discharge piping, it is characterized by four nodes. This allows an accurate simulation of the hydrodynamic effects of ECCS injection.

The North Anna SBLOCA plant models are constructed within the guidelines of the EM, Reference 30, Volume II, based on plant-specific inputs. The small break models adhere to the requirements of 10 CFR 50, Appendix K. The models contain demonstrated conservatism regarding the ECCS mitigation of a postulated small break LOCA at the North Anna units.

15.3.1.11 Framatome ANP SBLOCA Inputs and Assumptions

The major plant operating parameters used in the North Anna SBLOCA analyses are listed in Table 15.3-5. The limiting single failure is the failure of a diesel generator, which results in the loss of one full train of ECC pumped injection. Tables 15.3-6 and 15.3-7 provide North Anna Unit 1 pumped LHSI (low-head safety injection) and HHSI (high-head safety injection) flows for pump discharge pipe breaks, respectively. Tables 15.3-8 and 15.3-9 provide the same information for a SI (safety injection) line break. The broken loop SI injection is assumed to spill to the containment for the SI line break. The HHSI flows in Tables 15.3-7 and 15.3-9 are also applicable to North Anna Unit 2. Tables 15.3-10 and 15.3-11 provide North Anna Unit 2 LHSI flows for RCS pipe breaks and the SI line break, respectively. The steam generator secondary system is

isolated on reactor trip and auxiliary feedwater is initiated on reactor trip with a 60-second delay. The steam generator level is maintained at 18 percent of the narrow range (39 feet above the top of the tubesheet). Loss of one AFW pump, consistent with the single failure assumption, is evaluated in addition to the no AFW failure scenario. For SBLOCA, pumped ECC injection is first delivered from the HHSI pumps. Initially, the HHSI system flow purges the water contained in the boron injection tank (BIT)—a tank containing approximately 900 gallons of high temperature, 146°F, water. Following BIT purge, the water temperatures of the SI injection during the initial injection and recirculation phases are 60°F and 150°F, respectively. The start of re-circulation is 70 minutes after SI initiation.

15.3.1.12 **Framatome ANP SBLOCA Analysis Break Spectrum**

A range of break sizes, along with unit differences, was accommodated in establishing the SBLOCA analysis case set. Cases were performed that addressed break spectrum, AFW availability, and mixed core configuration both for North Anna Unit 1 and Unit 2. Unit 1 has an upflow barrel-baffle configuration, while Unit 2 has a downflow configuration. The analyses accommodate the slightly different LHSI flows between units.

A spectrum of six cases was analyzed to predict core and system responses over a range of break sizes. Prior studies, for example the EM study (Volume II, Appendix A of Reference 30), indicate that break areas (in RCP discharge piping) ranging in diameter from 2- to 4-inches produce the greatest degree of core uncovering. For the North Anna units, break diameters of 2-, 2.5-, 3-, 4-, and 6-inches were analyzed. The breaks are located in the bottom of the RCP discharge piping. The spectrum also considered a 5.2-inch diameter break of a safety injection line (6" Schedule 160, ID = 5.187"). This break is in the top of the RCP discharge piping. Both high and low head safety injection lines tee into this safety injection pipe upstream of the break; hence, pumped injection into the RCS is significantly reduced for this break.

The limiting spectrum case was evaluated for AFW availability. The study accounts for the one-on-one lineup of AFW pumps to the three steam generators. The study evaluates the failure of one AFW pump. The limiting AFW configuration case was then used to investigate the mixed core configuration. The NAIF and Advanced Mark-BW fuel assemblies are thermal-hydraulically comparable, excepting a pressure drop difference of ~2.5 psi (based on rated flow) attributable to the three mid-span mixing grids (MSMG) located in the top half of the Advanced Mark-BW assembly. This fuel design difference was modeled by running a case with the MSMG resistance removed from the average core. This modeling approach maximizes the predicted flow diversion away from the one Advanced Mark-BW fuel assembly modeled in the hot channel.

All of the analyzed breaks, except for the SI line break, were simulated at the bottom of the RCS piping to minimize ECCS delivery to the reactor vessel. This break orientation selection is validated in Reference 33. The reference generically shows that breaks in the side or top of the pump discharge piping were non-limiting for T_{HOT} plants relative to bottom pipe breaks. In Reference 34, NRC concurred that top and side breaks were not limiting, noting “plant procedural

guidance instructs operators to begin a timely depressurization of the primary system prior to the onset of the extended core uncovery." The staff further concluded "that this issue is adequately addressed through plant procedural guidance, and a plant-specific break orientation analysis is not required." A review of the North Anna Emergency Operating Procedures (EOP) confirmed the existence of procedural guidance to depressurize the RCS. Hence, no top or side break analyses were required for the North Anna SBLOCA calculations.

15.3.1.12.1 North Anna Unit 1 Small Break LOCA Analysis Results

Table 15.3-12 presents a time sequence of events for the spectrum cases. The spectrum thermal responses for the hot fuel assembly are given in Table 15.3-13. SBLOCA parameters of interest are shown in Figures 15.3-50 through 15.3-91. A plot of RCS pressure, break flow, hot channel mixture level, hot spot cladding temperature, hot channel outlet vapor temperature, intact loop seal level, and broken loop seal level is provided for each spectrum case. Key elevations on the SBLOCA intact and broken loop seal level plots are: (1) the zero elevation is the centerline of the reactor vessel nozzle; (2) the top of the active core is - 4.8 feet; (3) the bottom of the active core is - 16.8 feet; (4) the top of the loop seal pipe is - 9.0 ft; and (5) the loop seal pipe bottom is - 11.6 ft. Key elevations on the core level plots are: (1) the zero elevation is the bottom of the active core; (2) the top of the active core is 12.00 feet; (3) the top of the loop seal pipe is 7.8 ft; and (4) the bottom of the loop seal pipe is 5.2 ft.

The results of the analyses demonstrate that the spectrum of breaks (including the SI line break) described in Section 15.3.1.12 is adequate to determine the limiting PCT. The SI injection is generally insufficient to makeup for the break flow, and the imbalance causes core uncovering. For the spectrum of breaks within the pump discharge piping, the worst case, PCT = 1348°F, occurs for the 3.0-inch break.

The limiting North Anna Unit 1 break is the safety injection (SI) line, between the nozzle in the RCS piping and the first check valve (PCT = 1380°F). The SI line accident evolves much like the 4.0-inch and 6.0-inch breaks. However, the assumed break in the SI line reduces ECCS flow to the intact loops and enhances the flow to the broken SI line. The downstream pressure for the broken SI line is the containment building pressure while the downstream pressure for the other SI lines is the reactor coolant system pressure. Because the SI systems incorporate a common header, flow is disproportionately directed away from the two intact loops to the broken line. This produced a much more severe core depression than the pump discharge pipe breaks.

Because the SI-line break is limiting, it serves as a base for the AFW availability study. Tables 15.3-14 and 15.3-15, and Figures 15.3-92 through 15.3-98 provide the results for this case. The relative large size of this break leads to a rapid decrease in RCS pressure below the steam generator secondary safety valve control pressure. Once the primary system pressure decreases below the secondary side pressure, the feed of coolant to the secondary side becomes relatively unimportant to the course of the accident. Therefore, the transient evolves along a nearly identical path to that of the full AFW case. The peak cladding temperature is 1395°F, which is essentially

the same as the 1380°F obtained for the full AFW case; this PCT difference of 15°F is well within the expected range of model resolution.

The results from the mixed core study are presented in Tables 15.3-16 and 15.3-17, and Figures 15.3-99 through 15.3-105. The SI-line break with a failed AFW pump served as the base case for the study. As discussed in Section 15.3.1.12 the mixed core was represented by removing the three MSMGs (located at 6.45 feet, 8.16 feet and 9.87 feet) from the fuel assemblies modeled in the average core. This was done to maximize flow diversion away from the Advanced Mark-BW fuel assembly modeled in the hot channel. Study results show that there is essentially no impact on PCT. The PCT is 1404°F, an increase of 9°F relative to the base case. This PCT difference is well within the resolution capability of the SBLOCA modeling.

In summary, the limiting PCT for North Anna Unit 1 is 1404°F. No substantive mixed core impact is noted. Both the local oxidation and the whole-core oxidation are substantially below the respective acceptance criteria of 17 percent and 1 percent.

15.3.1.12.2 North Anna Unit 2 Small Break LOCA Analysis Results

Table 15.3-18 presents a time sequence of events for the North Anna Unit 2 spectrum cases. The spectrum thermal response for the hot fuel assembly is given in Table 15.3-19. SBLOCA parameters of interest are shown in Figures 15.3-108 through 15.3-149.

Figure 15.3-106 provides an overlay of the North Anna Units 1 and 2 PCTs versus break size and configuration. The pipe break spectrums develop in a nearly identical manner between the two plants. The change in barrel-baffle configuration, from upflow to downflow, has some impact on the smaller break results (1100°F PCT for the Unit 1 2.0-inch break versus 1022°F for Unit 2). For the larger breaks in the main RCS piping, differences in results between units are within model accuracy.

The SI line break is 100°F cooler (1280°F) for Unit 2 than for Unit 1. The difference is due to a small variation in core inventories during core uncovering between 3000 and 4000 seconds. The reactor vessel flow dynamics, which the different core barrel-baffle configurations can affect, lead to an earlier core uncovering and a lower core mixture level for Unit 1 than for Unit 2 (see Figures 15.3-80 and 15.3-138). Thus, the Unit 1 cladding temperature is slightly higher when the LHSI ends the temperature excursion at around 3500 seconds. Following the occurrence of peak clad temperature, the mixture level for Unit 2 is consistently above the top of the core. Figure 15.3-107 shows that, for the RCS pressure near the time of PCT (~125 psia), the LHSI flow for Unit 1 is 10 to 20 percent lower than for Unit 2. This results in slightly earlier and longer cycles of core uncovering and recovery for Unit 1. Also apparent is that the combined LHSI and HHSI flow after 4000 seconds is able to assure a core mixture level above the active core region for Unit 2 but unable to provide a stable high mixture for Unit 1.

Thus, the most severe SBLOCA for North Anna Unit 2 is a 3.0-inch diameter break in the RCS piping at the pump discharge. This break was used for the AFW and mixed core studies with

much the same sensitivity results as occurred for Unit 1. For Unit 2, the PCT was 50°F lower when one AFW pump was disabled and the mixed core PCT was reduced by 25°F. Both these differences are within the expected range of model resolution. Data for these studies are provided in Tables 15.3-20 through 15.3-23, and plots of important variables are shown in Figures 15.3-150 through 15.3-163.

In summary, the limiting PCT for North Anna Unit 2 is 1370°F. Both the local oxidation and the whole-core oxidation are substantially below the respective acceptance criteria of 17 percent and 1 percent.

15.3.1.13 **Post Analysis of Record Evaluations - Framatome Fuel**

In addition to the analyses presented in this section, evaluations and reanalyses may be performed as needed to address computer code errors, emergent issues, or to support plant changes. The issues or changes are evaluated, and the impact on the PCT is determined. The resultant increase or decrease in PCT is applied to the analysis of record PCT. The PCTs, including all penalties and benefits, are presented in Table 15.3-24 for the small break LOCA. The resultant PCT is demonstrated to be less than the 10 CFR 50.46(b) requirement of 2200°F.

15.3.1.14 **Small Break LOCA Conclusions**

The SBLOCA calculations demonstrate compliance to the PCT and local metal-water reaction criteria of 10 CFR 50.46. The mixed core was evaluated with no significant impact noted on either co-resident fuel assemblies. The mixed core study modeled a mixed core configuration that directly included mixed core effects on the Advanced Mark-BW fuel. The PCT results for the mixed core cases confirm that mixed core effects are small. This reaffirms the existing evaluation in Section 15.3.1.4, which concludes that mixed core hydraulic mismatches are not a significant factor for small break analyses. In all cases, PCT and local metal-water are substantially below criterion limits of 2200°F and 17 percent, respectively. The analysis work also serves as the basis for demonstrating compliance with whole-core oxidation and coolable geometry criteria. The average hot channel oxidation is less than one percent. Thus, the whole-core oxidation criterion is met.

The fourth acceptance criterion of 10 CFR 50.46 requires coolable geometry compliance. The SBLOCA calculations discussed in this section assess core geometry alterations resulting from SBLOCA at the worst core location and demonstrate successful fuel pin cooling. As presented in Section 15.4, the large break LOCA plus seismic load combination may produce deformation in the fuel pin lattice for peripheral assemblies. The deformation does not alter the basic pin-coolant-channel-to-pin-coolant-channel arrangement for these assemblies. There is no significant consequence of the damage for the pool boiling and steam cooling environment of SBLOCA because of the low power level of the peripheral assemblies. Thus, the maximum cladding temperatures and local oxidation predicted by the LOCA calculation for SBLOCA are unchanged, and the fuel assemblies retain a coolable geometry, meeting the criteria of 10 CFR 50.46.

The fifth acceptance criterion of 10 CFR 50.46 requires assurance of long-term cooling. Successful initial operation of the ECCS is shown by demonstrating that the core is quenched and the cladding temperature is returned to near saturation temperature. Compliance to the long-term cooling criterion is demonstrated in the North Anna UFSAR for the systems and components specific to the units. Compliance to this criterion is independent of fuel design. The initial phase of core cooling results in low clad and fuel temperatures. A pumped injection system, re-circulation capable, is available and operated by the plants to provide extended coolant injection. Therefore, compliance with the long-term cooling criterion of 10 CFR 50.46 is assured.

Thus, for small break LOCA, the emergency core cooling system will meet the 10 CFR 50.46 acceptance criteria.

1. The calculated maximum fuel element clad temperature is substantially lower than the 2200°F limit.
2. The calculated total oxidation of the cladding nowhere exceeds the 17 percent limit.
3. The calculated total amount of hydrogen generation from the chemical reaction of the cladding with water or steam does not exceed the 1 percent limit.
4. The core remains amenable to cooling during and after the transient.
5. The core temperature is reduced and decay heat is removed for an extended time, as required by the long-lived radioactivity remaining in the core.

15.3.2 Minor Secondary System Pipe Breaks

15.3.2.1 Identification of Causes and Accident Description

Included in this grouping are ruptures of secondary system lines that would result in steam release rates equivalent to a 6-inch-diameter break or smaller.

15.3.2.2 Analysis of Effects and Consequences

Minor secondary system pipe breaks must be accommodated with the failure of only a small fraction of the fuel elements in the reactor. Since the results of the analyses presented in Section 15.4.2 for a major secondary system pipe rupture also meet this criterion, separate analysis for minor secondary system pipe breaks is not required.

The analysis of the more probable accidental opening of a secondary system steam dump, relief, or safety valve is presented in Section 15.2.13. These analyses are illustrative of a pipe break equivalent in size to a single valve opening.

15.3.2.3 Conclusions

The analyses presented in Section 15.4.2 demonstrate that the consequences of a minor secondary system pipe break are acceptable, since a DNBR of less than 1.30 does not occur even for a more critical major secondary system pipe break.

15.3.3 Inadvertent Loading of a Fuel Assembly Into an Improper Position

15.3.3.1 Identification of Causes and Accident Description

Fuel and core-loading errors, such as those that can arise from the inadvertent loading of one or more fuel assemblies into improper positions, loading a fuel rod during manufacture with one or more pellets of the wrong enrichment, or the loading of a full fuel assembly during manufacture with pellets of the wrong enrichment, will lead to increased heat fluxes if the error results in placing fuel in core positions calling for fuel of lesser enrichment. Also included among possible core-loading errors is the inadvertent loading of one or more fuel assemblies requiring burnable poison rods into a new core without burnable poison rods.

Any error in enrichment, beyond the normal manufacturing tolerances, can cause power shapes that are more peaked than those calculated with the correct enrichments. The incore system of movable flux detectors (Section 7.7.1.9) used to verify power shapes at the start of life is capable of revealing any assembly enrichment error or loading error that causes power shapes to be peaked in excess of the design value.

To reduce the probability of core-loading errors, each fuel assembly is marked with an identification number and loaded in accordance with a core-loading diagram. The core-loading operation is governed by a fuel shuffle plan, which is a step-by-step procedure that dictates the movement of new, irradiated, and spent-fuel assemblies between and within the fuel building and the reactor vessel. It provides for the positioning of the fuel assemblies into a final core-loading pattern that has been established for the operation of the reactor in the next cycle. An audit of the fuel shuffle plan is performed to ensure that all fuel assemblies will be placed in their proper locations. Also, a physical inventory is performed on the final core loading. The audit of the fuel shuffle plan and the physical inventory of the final core loading ensure that each fuel assembly is in the correct location.

Any power distortion due to a combination of misplaced fuel assemblies which would significantly raise peaking factors would be readily observable with incore flux monitors. In addition to the flux monitors, thermocouples are located at the outlet of about one third of the fuel assemblies in the core. There is a high probability that these thermocouples would also indicate any abnormally high coolant enthalpy rise. Incore flux measurements are taken during the start-up subsequent to every refueling operation.

15.3.3.2 Analysis of Effects and Consequences

15.3.3.2.1 Method of Analysis

Steady-state power distribution in the x-y plane of the core is calculated using the TURTLE (Reference 8) code based on a macroscopic cross section calculated by the LEOPARD (Reference 9) code. A discrete representation is used in which each individual fuel rod is described by a mesh interval. The power distributions in the x-y plane for a correctly loaded core are also given in Chapter 4, based on enrichments provided in that section.

For each core-loading error case analyzed, the percent deviations from detector readings for a normally loaded core are shown at all incore detector locations (see Figures 15.3-28 through 15.3-32).

15.3.3.2.2 Results

The following core-loading error cases have been analyzed:

Case A: Case in which a Region 1 assembly is interchanged with a Region 3 assembly. The particular case considered was the interchange of two adjacent assemblies near the periphery of the core (see Figure 15.3-28).

Case B: Case in which a Region 1 assembly is interchanged with a neighboring Region 2 fuel assembly. Two analyses have been performed for this case (see Figures 15.3-29 & 15.3-30).

In Case B-1, the interchange is assumed to take place with the burnable poison rods transferred and with the Region 2 assembly mistakenly loaded into Region 1.

In Case B-2, the interchange is assumed to take place closer to core center and with burnable poison rods located in the correct Region 2 position, but in a Region 1 assembly mistakenly loaded into the Region 2 position.

Case C: Enrichment error, a case in which a Region 2 fuel assembly is loaded in the core central position (see Figure 15.3-31).

Case D: Case in which a Region 2 fuel assembly instead of a Region 1 assembly is loaded near the core periphery (see Figure 15.3-32).

15.3.3.3 **Conclusions**

Fuel assembly enrichment errors would be prevented by administrative procedures implemented in fabrication.

In the event that a single pin or pellet has a higher enrichment than the nominal value, the consequences in terms of reduced DNBR and increased fuel and clad temperatures will be limited to the incorrectly loaded pin or pins.

Fuel assembly loading errors are prevented by administrative procedures implemented during core loading. Detailed power distribution measurements are made at various power levels during the power ascension following refueling. The power distributions are compared to predicted values at the various core conditions. Thus, in the unlikely event that a loading error occurs, the resulting power distribution effects will either be readily detected by the incore moveable detector system or will cause a sufficiently small perturbation to be acceptable within the uncertainties allowed between nominal and design power shapes.

15.3.4 Complete Loss of Forced Reactor Coolant Flow

15.3.4.1 Identification of Causes and Accident Description

A complete loss of forced reactor coolant flow may result from a simultaneous loss of electrical supplies to all reactor coolant pumps. If the reactor is at power at the time of the accident, the immediate effect of loss of coolant flow is a rapid increase in the coolant temperature. This increase could result in DNB with subsequent fuel damage if the reactor is not tripped promptly. The following reactor trips provide necessary protection against a loss-of-coolant-flow accident:

1. Undervoltage or underfrequency on reactor coolant pump power supply buses.
2. Loss of reactor coolant loop flow.
3. Pump circuit breaker opening.

The reactor trip on reactor coolant pump bus undervoltage is provided to protect against conditions that can cause a loss of voltage to all reactor coolant pumps, i.e., station blackout. This function is blocked below approximately the power level associated with Permissive 7.

The reactor trip on reactor coolant pump underfrequency is provided to open the reactor pump breakers and trip the reactor for an underfrequency condition resulting from frequency disturbances on the major power grid. The trip disengages the reactor coolant pumps from the power grid so that the pumps' kinetic energy is available for full coastdown.

The reactor trip on low primary-coolant-loop flow is provided to protect against loss-of-flow conditions that affect only one reactor coolant loop. It also serves as a backup to the undervoltage and underfrequency trips. This function is generated by two out of three low-flow signals per reactor coolant loop. Above the power level associated with Permissive 8, low flow in any loop will actuate a reactor trip. Between P-7 and P-8, low flow in any two loops will actuate a reactor trip. A reactor trip from pump breaker position is provided as an anticipatory signal that serves as a backup to the low-flow signals. Its function is essentially identical to the low-flow trip, so that, above Permissive 8, a breaker-open signal from any pump will actuate a reactor trip, and between Permissive 7 and Permissive 8, a breaker-open signal from any two pumps will actuate a reactor trip.

Normal power for the reactor coolant pumps is supplied through buses from a transformer connected to the generator. Each pump is on a separate bus. When generator trip occurs, the buses are automatically transferred to a transformer supplied from external power lines, and the pumps will continue to supply coolant flow to the core.

Following any turbine trip, where there are no electrical faults that require tripping the generator from the network, the generator remains connected to the network for approximately 30 seconds. The reactor coolant pumps remain connected to the generator, thus ensuring full flow for 30 seconds after the reactor trip before any transfer is made.

15.3.4.2 **Analysis of Effects and Consequences**

15.3.4.2.1 Method of Analysis

The complete loss of flow analysis considers the effects of a 1.7% power uprate by assuming a nominal initial core power level of 2893 × 1.017 MWt (2942 MWt). The transient analysis models the Westinghouse Standard and NAIF fuel products and the Framatome Advanced Mark-BW fuel product. The detailed core thermal/hydraulic analysis models the 17 x 17 Westinghouse Standard and NAIF fuel products using the *Virginia Power Statistical DNBR Evaluation Methodology* (Reference 29). The detailed core thermal/hydraulic analysis for the Framatome Advanced Mark-BW fuel product is performed using the Framatome ANP Statistical Core Design Methodology with the Framatome ANP LYNXT thermal-hydraulic computer code and associated models, or the Dominion Statistical DNBR Evaluation Methodology with the VIPRE-D thermal-hydraulic computer code and associated models, as discussed in Section 4.5.

The analysis discussed below encompasses both the Westinghouse and Framatome fuel products. Beginning with Cycle 17 for Unit 2 and Cycle 18 for Unit 1, the Advanced Mark-BW fuel product was introduced in mixed cores with LOPAR and NAIF assemblies.

The two limiting cases that were analyzed are as follows:

1. Loss of three out of three RCPs from a nominal power level of 100% (2942 MWt), due to an undervoltage condition.
2. Loss of three out of three RCPs from a nominal power level of 100% (2942 MWt), due to a frequency decay condition (-5 Hz per second).

Partial loss of flow from the loss of fewer than three reactor coolant pumps are protected by the same low flow reactor trip. Because of the identical protection setpoint, and correspondingly higher coolant flow rates throughout the transient, the partial loss of flow events are less limiting than the complete loss of flow events. Therefore, the partial loss of flow events are bounded by the complete loss of flow analyses and no specific partial loss of flow analyses are run.

The normal power supplies for the pumps are three buses supplied by the generator. Each bus supplies power to one pump. When a generator trip occurs, the pumps are automatically transferred to a bus supplied from external power lines, and the pumps continue to supply coolant flow to the core. The simultaneous loss of power to all reactor coolant pumps is a highly unlikely event. Following any turbine trip, where there are no electrical faults that require tripping the generator from the pump supply network, the generator remains connected to the network for approximately 30 seconds. The reactor coolant pumps remain connected to the generator, thus ensuring full flow for 30 seconds after the reactor trip before any transfer is made. Since each pump is on a separate bus, a single-bus fault would not result in the loss of more than one pump.

A full unit simulation is used in the analysis to compute the core average and hot-spot heat flux transient responses, including flow coastdown, temperature, reactivity, and control-rod assembly insertion effects.

These data are then used in a detailed thermal-hydraulic computation to compute the DNB margin. This computation solves the continuity, momentum, and energy equations of fluid flow, together with the WRB-1 DNB correlation discussed in Section 4.4.2. The assumptions made in the calculations are discussed below.

15.3.4.2.2 Initial Operating Conditions

The initial operating conditions which are assumed in the analysis are presented below. These conditions are consistent with the statistical treatment of key analysis parameters for the 17 x 17, NAIF, and Framatome Advanced Mark-BW Standard assemblies.

Nominal 100% power - 3 Loops Operating

Power	2942 MWt
Pressure	2249.7 psia
Inlet Temperature	554.2°F
Minimum Measured Flow	295,000 gpm

15.3.4.2.3 Reactivity Coefficients

A least negative Doppler Temperature Coefficient (-1.4 pcm/°F) and most positive Moderator Temperature Coefficient (+6 pcm/°F) were assumed since these result in higher heat flux at the time of minimum DNBR. A sensitivity to the effective delayed neutron was performed. A maximum delayed neutron fraction (0.0066) was used because it produced the most limiting DNBR.

15.3.4.2.4 Reactor Trip

Following the loss of flow induced by underfrequency or undervoltage, the reactor is assumed to trip on low flow in any loop. The low flow trip setting is 90% of full loop flow; the trip signal is assumed to be initiated at 87% of minimum measured flow, allowing 3% for instrumentation errors. The time from initiation of the low flow signal to the initiation of control rod assembly motion is assumed to be 1.0 second. It is also assumed that, upon reactor trip, the most reactive control rod assembly is stuck in its fully withdrawn position, resulting in a minimum insertion of negative reactivity. The assumed trip reactivity was ≈4000 pcm which is confirmed to be bounding for each reload cycle.

15.3.4.2.5 Flow Coastdown

Reactor coolant flow coastdown curves for the limiting undervoltage and underfrequency induced loss of flow accidents are shown in Figures 15.3-33 and 15.3-34, respectively.

The flow profile for the undervoltage transient includes an initial 5% flow penalty to account for the potential of a "back EMF" phenomenon prior to the trip of the RCP. The RCP will maintain flow at or above approximately 98% for undervoltage conditions less severe than the undervoltage trip setpoint. This is conservatively modeled by a prompt drop in flow from 100% to 95% minimum measured flow followed by a 5-second delay prior to the RCP trip on (undervoltage). The reactor is not assumed to trip until the low flow setpoint has been reached.

The flow profile for the underfrequency transient includes an 8.33% drop in pump speed to account for decreasing RCP motor frequency at a constant rate of 5 Hz/sec prior to the trip of the RCP. The RCP pump speed will ramp down at 8.33% per second for 1.88 seconds prior to RCP trip on underfrequency. The reactor is not assumed to trip until the low flow setpoint has been reached.

15.3.4.2.6 Results

Both the underfrequency and the undervoltage trip events were analyzed. The minimum DNBRs for the two accidents showed a significant margin to the design DNBR limit.

The transient responses of power, heat flux, inlet temperature, pressurizer pressure, and DNBR for NAPS Standard and NAIF fuel types are plotted in Figures 15.3-35 through 15.3-39 for the undervoltage case and 15.3-40 through 15.3-44 for the underfrequency case.

15.3.4.3 **Conclusions**

The analyses performed on the scenarios as described in Section 15.3.4.2.1 have demonstrated that for the complete loss of reactor coolant flow, the DNBR does not decrease below the limit value during the transient, and thus there is no clad damage or release of fission products to the reactor coolant system. Figures 15.3-33 through 15.3-44 represent the transient system performance for the uprated Westinghouse core. The transient system performance will be similar for the Framatome core.

15.3.5 Waste Gas Decay Tank Rupture

15.3.5.1 Identification of Causes and Accident Description

No cause is postulated for a waste gas decay tank rupture, as the waste gas decay tanks are designed and constructed to stringent quality control standards, are provided with pressure relief valves to prevent overpressurization, are missile-shielded by installation below grade, and have their gaseous contents controlled to prevent potentially explosive mixtures.

15.3.5.2 Analysis of Effects and Consequences

Although no specific cause for rupture has been defined, this analysis assumes that a waste gas decay tank rupture takes place at the instant when the tank has the greatest inventory of waste gases at maximum expected activity. The operation of the gaseous waste disposal system is described in Section 11.3.

The activities of the gases in the tank were generated by the ACTIVITY computer code. This code calculates the inventory of radionuclides in the radioactive systems of both units as a function of the units' power history and system flow rates. For the gaseous waste disposal system, the code also calculates the dose at the exclusion area boundary for a waste gas decay tank rupture.

The inventory of gases in the waste gas decay tank at the instant of rupture was based on the following conservative operating history:

1. One unit feed cycle is 4 weeks behind the other unit.
2. 365-day feed is stored in the waste gas decay tank, and in addition all noble gas and 0.1% of the iodine are stripped from the reactor coolant of one unit at the end of the feed cycle to the same waste gas decay tank, at which point the tank is assumed to rupture.
3. All the noble gas and 0.1% of the iodine from one reactor coolant volume were in the waste gas decay tank at the beginning of the 365-day feed cycle.
4. Letdown to the boron recovery system from two units in a base load cycle is 0.94 gpm.
5. Initial coolant gaseous activity at beginning of feed cycle equals zero.
6. Initial fuel activity at beginning of feed cycle is equal to that from one-third of a core 2 years old, one-third of a core 1 year old, and one-third of a core new.
7. All of the gases and 0.1% of the iodine in the letdown are removed at the gas stripper and sent to the waste gas decay tank.
8. One percent failed fuel.
9. 15 x 15 fuel assembly array. North Anna uses 17 x 17 fuel assemblies. The use of 15 x 15 assemblies in this analysis is conservative, as described in Section 11.1.1.

The entire gaseous content of the waste gas decay tank is assumed to be released in a ground-level release. The total activity released would be 73,000 Ci of Xe-133 equivalent and 0.084 Ci of I-131 equivalent.

With Pasquill F conditions and a 1 m/sec invariant wind speed, the χ/Q at the exclusion boundary is 4.0×10^{-4} sec/m^3. Since the tanks are located in the yard, no credit is taken for building wake effects. The whole-body dose at the exclusion boundary would be about 1.6 rem, and the thyroid dose about 0.017 rem. These doses are well below the guidelines of 10 CFR 100.

15.3.6 Volume Control Tank Rupture

15.3.6.1 Identification of Causes and Accident Description

Since the volume control tank is designed and constructed to stringent quality control standards, is provided with pressure relief valves to prevent overpressurization, and is located in a missile-protected enclosure, no cause is postulated for the volume control tank rupture.

15.3.6.2 Analysis of Effects and Consequences

Although no specific cause for rupture has been defined, for this analysis the volume control tank is assumed to rupture and release to the atmosphere all of the gases that have collected in the vapor space of the tank, and all of the gases in the liquid inventory of the tank and in the volume of liquid that continues to flow into the tank, until the tank is isolated. Isolation is assumed to take 25 minutes, and the flow rate of the entering liquid is assumed to be 160 gpm, a conservatively high letdown flow rate.

The activities of the gases in the vapor space are listed in Table 11.1-11. The activities of the gases and iodines in the liquid are based upon the reactor coolant equilibrium activities with 1% failed fuel, as listed in Table 11.1-6. For this analysis, activities in the liquid have been corrected for density. The analysis follows the guidance of NRC Branch Technical Position ETSB (Effluent Treatment System Branch) 11-5.

Using these sources, taking credit for building wake, a χ/Q of 3.1×10^{-4} sec/m^3, and assuming a "puff" ground release, the two-hour whole-body dose at the exclusion area boundary is below the 0.5 rem limit contained in Branch Technical Position 11-5. These doses are well below the guidelines in 10 CFR 100.

15.3.7 Single Rod Cluster Control Assembly Withdrawal at Full Power

15.3.7.1 Identification of Causes and Accident Description

No single electrical or mechanical failure in the rod control system could cause the accidental withdrawal of a single rod cluster control assembly from the inserted bank at full-power operation. The operator could deliberately withdraw a single rod cluster control assembly in the control bank. This feature is necessary to retrieve an assembly should one be accidentally dropped. In the extremely unlikely event of simultaneous electrical failures resulting in single rod cluster control assembly withdrawal, rod deviation and rod control urgent failure would both be displayed on the plant annunciator, and the rod position indicators would indicate the relative positions of the assemblies in the bank. The urgent failure alarm also inhibits automatic rod motion in the group in which it occurs. Withdrawal of a single rod cluster control assembly by operator action, whether deliberate or by a combination of errors, would result in activation of the same alarm and the same visual indications.

Each bank of rod cluster control assemblies in the system is divided into two groups of four mechanisms each. The rods comprising a group operate in parallel through multiplexing thyristors. The two groups in a bank move sequentially so that the first group is always within one step of the second group in the bank. A definite schedule of actuation and deactuation of the stationary gripper, movable gripper, and lift coils of a mechanism is required to withdraw the rod cluster control assembly attached to the mechanism. Since the stationary gripper, movable gripper, and lift coils associated with the four rod cluster control assemblies of a rod group are driven in parallel, any single failure that would cause rod withdrawal would affect a minimum of

one group, or four rod cluster control assemblies. Mechanical failures are in the direction of either insertion or immobility.

In the unlikely event of multiple failures that result in continuous withdrawal of a single rod cluster control assembly, it is not possible, in all cases, to provide assurance of automatic reactor trip so that core safety limits are not violated. Withdrawal of a single rod cluster control assembly results in both positive reactivity insertion tending to increase core power, and an increase in local power density in the core area "covered" by the rod cluster control assembly.

15.3.7.2 Analysis of Effects and Consequences

In terms of the overall system response, the transient response is similar to those presented in Section 15.2.2 for uncontrolled rod cluster control assembly bank withdrawal at power (RWAP). The supporting analyses for the RWAP event considered power levels of 10%, 60%, and 100% of full power for a spectrum of reactivity insertion rates and for minimum and maximum feedback cases. The analyses verified the adequacy of the design bases for DNB, RCS overpressurization, main steam system pressurization, and pressurizer overfill for the RWAP event. However, the single rod withdrawal event results in increased local power peaking in the area of the withdrawn rod cluster control assembly and produces lower minimum DNBRs than for the withdrawn bank cases.

The single rod withdrawal at power event is considered for both the manual and automatic control modes of operation:

1. If the reactor is in the manual control mode, continuous withdrawal of a single rod cluster control assembly results in both an increase in core power and coolant temperature, and an increase in the local hot-channel factor in the area of the failed rod cluster control assembly. Depending on initial bank insertion and location of the withdrawn rod cluster control assembly, automatic reactor trip may not occur sufficiently fast to prevent the minimum core DNBR from falling below the limit value. Evaluation of this case at the power and coolant conditions at which the overtemperature delta T trip would be expected to trip the plant shows that an upper limit for the number of rods with a DNBR less than the limit value is $< 5\%$.
2. If the reactor is in the automatic control mode, withdrawal of a single rod cluster control assembly will result in the immobility of the other rod cluster control assemblies in the controlling bank. The transient will then proceed as described above. For cases like the above, a trip will ultimately ensue, although not sufficiently fast in all cases to prevent a minimum DNBR in the core of less than the limit value.

15.3.7.3 Conclusions

For the case of one rod cluster control assembly fully withdrawn, with the reactor in the automatic or manual control mode and initially operating at full power with bank D at the

insertion limit, an upper bound of the number of fuel rods experiencing DNB is 5% of the total fuel rods in the core.

For every core reload, an evaluation of the core power distribution census (% of rods with a given $F_{\Delta H}$ or greater vs. $F_{\Delta H}$) for the limiting single rod withdrawal is performed. Using this power census, it can be shown that < 5% of the rods in the core will have $F_{\Delta H}$ greater than the design steady state limit value. Since the evaluation of rod withdrawal accidents in Section 15.2.2 demonstrates that the DNBR limit is met for the entire spectrum of reactivity insertion rates at the design $F_{\Delta H}$ limit, the power census check described above ensures that a single withdrawn rod will result in < 5% of the fuel rods in DNB as a result of a single rod withdrawal. The reload checks are done using the models and methods of Reference 21.

For both cases discussed, the indicators and alarms mentioned would alert the operator to the malfunction before departure from nucleate boiling could occur.

15.3.8 Breaks in Instrument Line or Lines From Reactor Coolant System That Penetrate Containment

There are no instrument lines penetrating the containment that contain reactor coolant.

15.3 REFERENCES

1. F. M. Bordelon et al., *Westinghouse Emergency Core Cooling System Evaluation Model-Summary*, WCAP-8339, June 1974.
2. V. J. Esposito, K. Kesavan, and B. A. Maul, *WFLASH-A FORTRAN IV Computer Program for Simulation of Transients in a Multi-Loop PWR*, WCAP-8261 Rev. 1, July 1974.
3. T. A. Porsching, J. H. Murphy, J. A. Redfield, and V. C. Davis, *FLASH-4: a Fully Implicit FORTRAN-IV Program for the Digital Simulation of Transients in a Reactor Plant*, WAPD-TM-84, Bettis Atomic Power Laboratory, March 1969.
4. F. M. Bordelon et al., *LOCTA-IV Program: Loss-of-Coolant Transient Analysis*, WCAP-8305, June 1974.
5. R. Salvatori, *Westinghouse ECCS-Plant Sensitivity Studies*, WCAP-8356, July 1974.
6. D. L. Paterline, S. Altomare, and C. Apollo, *Report on Small-Break Accidents for Westinghouse NSSS Systems*, WCAP 9600, October 1979.
7. Report submitted by Cordell Reed to D. F. Ross on August 15, 1979.
8. S. Altomare and R. F. Barry, *The TURTLE 24.0 Diffusion Depletion Code*, WCAP-7758, September 1971.
9. R. F. Barry, *LEOPARD - a Spectrum Dependent Non-Spatial Depletion Code for the IBM-7094*, WCAP 3269-26, September 1963.

10. S. T. Maher, *LOFTRAN Code Description*, WCAP 7878, Rev. 3, July 1981.

11. C. Hunin, *FACTRAN, a FACTRAN-IV Code for Thermal Transients in UO_2 Fuel Rods*, WCAP 7908, June 1972.

12. N. A. Smith, *Vepco Reactor System Transient Analyses Using the RETRAN Computer Code*, VEP-FRD-41, Rev. 0.1-A, June 2004.

13. F. W. Sliz and K. L. Basehore, *Vepco Reactor Core Thermal-Hydraulic Analysis Using the COBRA III C/MIT Computer Code*, VEP-FRD-33A, October 1983.

14. U.S. Nuclear Regulatory Commission Generic Letter No. 83-10c, *Resolution of TMI Action Item II.K.3.5, Automatic Trip of Reactor Coolant Pumps*, February 8, 1983.

15. Westinghouse Owners Group, *Evaluation of Alternate RCP Trip Criteria*, Letter from J. Sheppard, Chairman Westinghouse Owners Group to D. Eisenhut, USNRC. 0G-110, December 1, 1983.

16. Westinghouse Owners Group, *Justification of Manual RCP Trip for Small Break Events*, Letter from J. Sheppard, Chairman Westinghouse Owners Group to D. Eisenhut, USNRC. OG-117, March 9, 1984.

17. Letter from D. R. Beynon (Westinghouse) to W. R. Cartwright (Va. Power), *North Anna Units 1 and 2 - ECCS Flow Inconsistencies,* VRA-89-757, December 8, 1989.

18. *North Anna Units 1 and 2 (NA-1&2) - Approval of Continued Use of Negative Moderator Coefficient for NA-1 and Issuance of Amendment for NA-2*, Letter for L. B. Engle (USNRC) to W. R. Cartwright, Serial Number 89-498, dated June 30, 1989.

19. Letter from W. L. Stewart to NRC: *North Anna Power Station Units 1 and 2, Proposed Technical Specifications Change, North Anna Fuel Assembly Design Change*, NRC Letter Serial No. 89-795, dated January 15, 1990.

20. Letter from L. B. Engle to W. L. Stewart, North Anna Units 1 and 2 Technical Specifications Amendment Nos. 139 and 122, NRC Letter No. 90-564, dated September 6, 1990.

21. *Reload Nuclear Design Methodology*, VEP-FRD-42, Rev. 2.1-A, August 2003.

22. Meyer, P. E.: *NOTRUMP, A Nodal Transient Small Break And General Network Code*, WCAP-10079-P-A, August 1985.

23. Lee, N., et al.: *Westinghouse Small Break ECCS Evaluation Model Using The NOTRUMP Code*, WCAP-10054-P-A, August 1985.

24. Bordelon, F. M., et al.: *LOCTA-IV Program: Loss of Coolant Transient Analysis*, WCAP-8301, June, 1974.

25. *North Anna Power Station 10 CFR 50.59 Station Evaluation, Revised Large and Small Break LOCA Analyses, North Anna Power Station, Units 1 and 2*, 95-SE-OT-35, October 18, 1995.

26. Davidson, S. L., et al., *Vantage 5H Fuel Assembly*, WCAP-10444, Addendum 2, April 1988.

27. Davidson, S. L., et al., *Vantage+ Fuel Assembly Reference Core Report*, WCAP-12610, Addendum 1, 2, 3, and 4, June 1990.

28. Thomson, C. M., et al., *Addendum to the Westinghouse Small Break ECCS Evaluation Model Using the NOTRUMP Code: Safety Injection into the Broken Loop and COSI Condensation Model*, WCAP-10054, Addendum 2, August 1994.

29. R. C. Anderson, *Statistical DNBR Evaluation Methodology,* Topical Report VEP-NE-2-A, dated June 1987.

30. *RSG LOCA - BWNT Loss-of-Coolant Accident Evaluation Model for Recirculating Steam Generator Plants,* BAW-10168P-A, Revision 3, December 1996.

31. *RELAP5/MOD2-B&W - An Advanced Computer Program for Light Water Reactor LOCA and Non-LOCA Transient Analysis,* BAW-10164P-A, Revision 4, November 2002.

32. *TACO3 - Fuel Pin Thermal Analysis Code,* BAW-10162P-A, January 1990.

33. FTI Letter: J. J. Kelly, FTI, to Document Control Desk, NRC, *A Request to Rescind FTI's Commitment to Analyze Top and Side SBLOCAs for Thot Recirculating Steam Generator Plants - BAW-10168P-A, Revision 3, Volume II, December 1996,* FTI-98-3797, December 10, 1998.

34. NRC Letter: Stephen Dembek, NRC, to James F. Mallay, Framatome ANP, *Break Orientation Analysis For Small Break Loss Of Coolant Accident (TAC No. MA9313),* August 2, 2001.

35. Letter from L.N. Hartz (Va. Electric & Power Co.) to USNRC, *Virginia Electric and Power Company, North Anna Power Station Units 1 and 2, Small Break Loss of Coolant Accident (SBLOCA) Analysis Results for the Proposed Technical Specifications Changes and Exemption Request for Use of Framatome ANP Advanced Mark-BW Fuel,* Serial No. 03-245, May 27, 2003.

36. Letter from E.S. Grecheck (Dominion) to USNRC, *Virginia Electric and Power Company (Dominion), North Anna Power Station Units 1 and 2, Surry Power Station Units 1 and 2, 30 Day Report of Emergency Core Cooling System (ECCS) Model Changes Pursuant to the Requirements of 10 CFR 50.46,* Serial No. 07-0142, March 22, 2007.

Table 15.3-1
SIGNIFICANT INPUTS AND ASSUMPTIONS SMALL BREAK LOCA ACCIDENT

Parameter	Value
Core Power, 102% of	2893 MWt
Peak Heat Flux Hot Channel Factor	2.32 F_Q
Normalized Hot Channel Factor, K(z)	Figure 15.3-2
Peak Nuclear Enthalpy Hot Channel Factor	1.65 FΔh
Fuel Enrichment	5.0%
Fuel Pellets	Chamfered
Fuel Assembly Array	17 x 17 NAIF [a]
Accumulator Water Volume	1025 ft^3/accumulator
Accumulator Tank Volume	1450 ft^3/accumulator
Accumulator Gas Pressure	594 psia
Safety Injection Flow	Figure 15.3-1
Initial Loop Flow	9207.55 lbm/sec
Vessel Inlet Temperature,	550.80°F
Vessel Outlet Temperature	623.88°F
Reactor Coolant Pressure	2280 psia
Steam Pressure	834.0 psia
Steam Generator Tube Plugging (uniform)	7%
Low Pressurizer Pressure Setpoint	1845 psia
Low-Low Pressurizer Pressure Setpoint	1715 psia

a. This analysis was performed assuming the NAIF fuel product with ZIR-LO™. It is also applicable to 17 x 17 Standard Fuel.

Table 15.3-2
SMALL BREAK LOCA TIME SEQUENCE OF EVENTS

Event	Time After Start of LOCA (sec) For Each Break Size (Effective Diameter) 2-inch	3-inch	4-inch
Break Opens	0.0	0.0	0.0
Reactor Trip Signal	43.82	17.74	11.97
Safety Injection Signal	55.81	28.24	21.04
Broken Loop Seal Clearing	951.6	425.93	244.57
Top of Core is Uncovered	1359.03	412.46	308.78
Accumulator Injection Begins	N/A[a]	1177.63	244.57
Peak Clad Temperature Occurs	1719.5	1255.9	719.5
Top of Core is Covered	N/A[b]	2900.0	2141.43

a. RCS pressure never decreases enough to activate the accumulators.
b. Long-term RCS inventory recovery was established in the transient calculation prior to reaching this condition.

Table 15.3-3
SMALL BREAK LOCA RESULTS FUEL CLADDING DATA

	Break Size (Effective Diameter)		
Parameter	2-inch	3-inch	4-inch
Peak Clad Temperature	1043.2°F	1704.1°F	1606.7°F
Peak Clad Temperature Location	11.25 ft	11.75 ft	11.50 ft
Local Zr/H_20 Reaction, Maximum	0.0444%	2.008%	0.8214%
Local Zr/H_20 Reaction, Location	11.25 ft	11.75 ft	11.50 ft
Total Zr/H_20 Reaction	<1.0%	<1.0%	<1.0%
Hot Rod Burst Time [a]	N/A	N/A	N/A
Hot Rod Burst Location [a]	N/A	N/A	N/A

a. Burst was not calculated to occur.

Table 15.3-4
PEAK CLAD TEMPERATURE INCLUDING ALL PENALTIES AND BENEFITS
SMALL BREAK LOCA - WESTINGHOUSE FUEL

Unit 1	
PCT for Analysis of Record	1704°F
PCT Assessments Allocated to AOR	
A. NOTRUMP Specific Enthalpy Error	+20°F
B. SALIBRARY Double Precision Errors	-15°F
C. Fuel Rod Initialization Error	+10°F
D. Loop Seal Elevation Error	-44°F
E. NOTRUMP-Mixture Level Tracking Errors	+13°F
F. Removal of Part Length CRDMs	+1°F
G. NOTRUMP-Bubble Rise/Drift Flux Model Inconsistencies	+35°F
H. NOTRUMP-EM Refined Break Spectrum	+85°F
SBLOCA PCT for Comparison to 10 CFR 50.46 Requirements	1809°F
Unit 2	
PCT for Analysis of Record	1704°F
PCT Assessments Allocated to AOR	
A. NOTRUMP Specific Enthalpy Error	+20°F
B. SALIBRARY Double Precision Errors	-15°F
C. Fuel Rod Initialization Error	+10°F
D. Loop Seal Elevation Error	-44°F
E. Removal of Part-Length CRDM	+1°F
F. NOTRUMP-Mixture Level Tracking Errors	+13°F
G. NOTRUMP-Bubble Rise/Drift Flux Model Inconsistencies	+35°F
H. NOTRUMP-EM Refined Break Spectrum	+85°F
SBLOCA PCT for Comparison to 10 CFR 50.46 Requirements	1809°F

Table 15.3-5
NORTH ANNA UNITS 1 AND 2 SMALL BREAK LOCA
PLANT OPERATING PARAMETERS

Parameter	Value
Power Level, MWt	2951 (1.02% of 2893)
Total System Flow, gpm	289,100
Total Peaking, F_Q	2.32
Normalized Hot Channel Factor, K_Z	Figure 15.3-48
Axial Peaking Factor	1.4
Axial Power Shape	Figure 15.3-49
Average Core Temperature, °F	586.8
Fuel Assembly Array	17 x 17 Advanced Mark-BW w/M5™ clad
Accumulator Liquid Volume, ft^3	1025 [a]
Steam Generator Tube Plugging, % per SG	7
Reactor Trip, psia	1845
SIS Trip, psia	1715
ECCS Pumped Injection Delay Time, s	27 (after SIS)

a. This value includes the unusable accumulator tank volume (the volume below the accumulator outlet nozzle) and the accumulator line volume between the accumulator tank and the first check valve.

Table 15.3-6
NORTH ANNA UNIT 1 PUMPED LHSI INJECTION FOR RCS PIPE BREAK

RCS Pressure, psia	Intact Loop Flow, lbm/s	Broken Loop Flow, lbm/s
14.7	323.91	200.96
24.7	313.09	194.25
34.7	301.94	187.33
44.7	290.40	180.18
54.7	278.50	172.77
64.7	266.13	165.12
74.7	253.29	157.14
84.7	239.93	148.86
94.7	225.97	140.18
104.7	211.31	131.10
114.7	195.89	121.52
124.7	179.57	111.39
134.7	162.16	100.60
144.7	143.49	89.02
154.7	123.19	76.44
164.7	100.84	62.56
174.7	75.60	46.89
184.7	45.93	28.50
194.7	8.04	4.99
196.8	0.00	0.00

Table 15.3-7
NORTH ANNA UNIT 2 PUMPED LHSI INJECTION FOR RCS PIPE BREAK

RCS Pressure, psia	Intact Loop Flow, lbm/s	Broken Loop Flow, lbm/s
14.7	328.31	178.87
24.7	317.39	172.92
34.7	306.14	166.80
44.7	294.53	160.47
54.7	282.52	153.93
64.7	270.06	147.15
74.7	257.14	140.11
84.7	243.70	132.78
94.7	229.63	125.11
104.7	214.88	117.07
114.7	199.35	108.61
124.7	182.92	99.67
134.7	165.39	90.12
144.7	146.58	79.86
154.7	126.11	68.71
164.7	103.48	56.38
174.7	77.86	42.40
184.7	47.53	25.90
194.7	8.23	4.49
196.8	0.00	0.0

Table 15.3-8
NORTH ANNA UNITS 1 AND 2 PUMPED HHSI INJECTION FOR RCS PIPE BREAK

RCS Pressure, psia	Intact Loop Flow, lbm/s	Broken Loop Flow, lbm/s
14.7	44.89	24.46
64.7	44.42	24.21
114.7	43.94	23.94
264.7	44.17	24.07
514.7	41.73	22.75
764.7	39.16	21.36
1014.7	36.44	19.87
1264.7	31.46	17.16
1514.7	28	15.29
1764.7	24.74	13.51
2014.7	21.44	11.72
2114.7	20.82	11.39

Table 15.3-9
NORTH ANNA UNIT 1 PUMPED LHSI INJECTION FOR SI LINE BREAK [a]

RCS Pressure, psia	Intact Loop Flow, lbm/s	Broken Loop Flow, lbm/s
14.7	340.88	187.91
24.7	319.48	198.21
34.7	297.48	208.47
44.7	274.76	218.72
54.7	251.11	228.98
64.7	226.74	239.27
74.7	200.12	249.35
84.7	172.92	259.87
94.7	144.05	270.60
104.7	113.06	281.64
114.7	79.25	293.12
124.7	41.46	305.21
134.7	0.00	316.33

a. Note that the broken loop SI flow spills directly to the containment.

Table 15.3-10
NORTH ANNA UNIT 2 PUMPED LHSI INJECTION FOR SI LINE BREAK [a]

RCS Pressure, psia	Intact Loop Flow, lbm/s	Broken Loop Flow, lbm/s
14.7	341.67	164.57
24.7	320.60	174.67
34.7	298.99	184.67
44.7	276.76	194.58
54.7	253.00	204.15
64.7	229.03	213.99
74.7	204.05	223.88
84.7	177.86	233.82
94.7	150.20	243.90
104.7	120.70	254.16
114.7	88.80	264.71
124.7	53.62	275.68
134.7	9.48	287.23
136.8	0.00	287.23

a. Note that the broken loop SI flow spills directly to the containment

Table 15.3-11
NORTH ANNA UNITS 1 AND 2 PUMPED HHSI INJECTION FOR SI LINE BREAK [a]

RCS Pressure, psia	Intact Loop Flow, lbm/s	Broken Loop Flow, lbm/s
14.7	24.46	44.91
34.7	24.55	44.65
54.7	24.63	44.39
64.7	24.67	44.26
74.7	24.71	44.12
94.7	24.79	43.86
114.7	24.87	43.60
134.7	24.99	43.42
264.7	26.32	43.32
514.7	27.32	39.96
764.7	28.31	36.4
1014.7	29.33	32.6
1264.7	29.71	26.06
1514.7	30.82	21.22
1764.7	31.97	15.37

a. Note that the broken loop SI flow spills directly to the containment.

Table 15.3-12
NORTH ANNA UNIT 1 BREAK SPECTRUM TIME SEQUENCE OF EVENTS (SECONDS)

Event	2.0-inch	2.5-inch	3.0-inch	4.0-inch	5.2-inch [a]	6.0-inch
Break Initiation	0.0	0.0	0.0	0.0	0.0	0.0
Reactor Trip	44.40	30.12	22.43	15.04	11.64	10.68
MFW Isolation	44.40	30.12	22.43	15.05	11.64	10.68
MSIV Closure	44.91	30.62	22.93	15.55	12.15	11.19
SI Injection	77.11	61.56	53.38	45.14	39.97	37.04
Broken Loop Seal Clearing	940.0	615.0	585.0	315.0	205.0	155.0
Intact Loop Seal Clearing	NA	NA	NA	300.0	205.0	140.0
Core Uncovered	3365.0	1510.0	930.0	620.0	1715.0	NA
Accumulator Injection	NA	2140.0	1245.0	690.0	390.0	270.0
PCT Time	4708.0	2151.0	1277.0	702.0	3451.0	NA
Core Recovered	6525.0	5910.0	4305.0	3230.0	7190.0	NA

a. SI line break

Table 15.3-13
NORTH ANNA UNIT 1 BREAK SPECTRUM RESULTS

Parameter	2.0-inch	2.5-inch	3.0-inch	4.0-inch	5.2-inch [a]	6.0-inch
PCT, °F	1110.0	1223.0	1348.0	907.0	1380.0	702 [b]
PCT Location, ft	11.671	11.671	11.671	11.014	11.671	NA
Local Zr-H_2O Reaction, %	0.06	0.08	0.13	NA	0.25	NA
Whole-Core Zr-H_2O Reaction, %	< 0.01	< 0.01	< 0.02	NA	< 0.03	NA
Max Local Zr-H_2O Location, ft	11.671	11.671	11.671	NA	11.671	NA
Hot Rod Burst Location, ft	NA	NA	NA	NA	NA	NA
Hot Rod Burst Time, s	NA	NA	NA	NA	NA	NA

a. SI line break
b. Initial cladding temperature

Table 15.3-14
NORTH ANNA UNIT 1 AFW STUDY TIME SEQUENCE OF EVENTS (SECONDS)

Event	5.2-inch SI Line Break	5.2-inch SI Line Break
Intact Loop AFW	Yes	Yes
Broken Loop AFW	Yes	No
Break Initiation	0.0	0.0
Reactor Trip	11.64	11.64
MFW Isolation	11.64	11.64
MSIV Closure	12.15	12.15
SI Injection	39.97	39.97
Broken Loop Seal Clearing	205.0	205.0
Intact Loop Seal Clearing	205.0	180.0
Core Uncovered	1715.0	1800.0
Accumulator Injection	390.0	390.0
PCT Time	3451.0	3561.0
Core Recovered	7190.0	7510.0

Table 15.3-15
NORTH ANNA UNIT 1 AFW STUDY RESULTS

Parameter	5.2-inch SI Line Break	5.2-inch SI Line Break
Intact Loop AFW	Yes	Yes
Broken Loop AFW	Yes	No
PCT, °F	1380.0	1395.0
PCT Location, ft	11.671	11.671
Local Zr-H_2O Reaction, %	0.25	0.28
Whole-Core Zr-H_2O Reaction, %	< 0.03	< 0.03
Max Local Zr-H_2O Location, ft	11.671	11.671
Hot Rod Burst Location, ft	NA	NA
Hot Rod Burst Time, s	NA	NA

Table 15.3-16
NORTH ANNA UNIT 1 MIXED CORE STUDY TIME SEQUENCE OF EVENTS (SECONDS)

Event	FANP Core	Mixed Core
Break Initiation	0.0	0.0
Reactor Trip	11.64	11.58
MFW Isolation	11.64	11.58
MSIV Closure	12.15	12.09
SI Injection	39.97	39.91
Broken Loop Seal Clearing	205.0	205.0
Intact Loop Seal Clearing	180.0	180.0
Core Uncovered	1800.0	1825.0
Accumulator Injection	390.0	390.0
PCT Time	3561.0	3556.0
Core Recovered	7510.0	6985.0

Table 15.3-17
NORTH ANNA UNIT 1 MIXED CORE STUDY RESULTS

Cases	FANP Core	Mixed Core
PCT, °F	1395.0	1404.0
PCT Location, ft	11.671	11.671
Local Zr-H_2O Reaction, %	0.28	0.31
Whole-Core Zr-H_2O Reaction, %	< 0.03	< 0.03
Max Local Zr-H_2O Location, ft	11.671	11.671
Hot Rod Burst Location, ft	NA	NA
Hot Rod Burst Time, s	NA	NA

Table 15.3-18
NORTH ANNA UNIT 2 BREAK SPECTRUM TIME SEQUENCE OF EVENTS (SECONDS)

Event	2.0-inch	2.5-inch	3.0-inch	4.0-inch	5.2-inch [a]	6.0-inch
Break Initiation	0.0	0.0	0.0	0.0	0.0	0.0
Reactor Trip	44.31	30.06	22.38	14.99	11.63	10.67
MFW Isolation	44.31	30.06	22.38	14.99	11.63	10.67
MSIV Closure	44.82	30.56	22.88	15.5	12.14	11.18
SI Injection	77.05	61.50	53.32	45.08	39.90	37.0
Broken Loop Seal Clearing	935.0	615.0	600.0	300.0	205.0	155.0
Intact Loop Seal Clearing	NA	NA	NA	275.0	200.0	135.0
Core Uncovered	3515.0	1490.0	840.0	645.0	1805.0	NA
Accumulator Injection	NA	2015.0	1215.0	705.0	390.0	270.0
PCT Time	4649.0	2026.0	1248.0	3066.0	3548.0	NA
Core Recovered	7990.0	6235.0	4070.0	3320.0	3865.0	NA

a. SI line break

Table 15.3-19
NORTH ANNA UNIT 2 BREAK SPECTRUM RESULTS

Parameter	2.0-inch	2.5-inch	3.0-inch	4.0-inch	5.2-inch [a]	6.0-inch
PCT, °F	1022.0	1230.0	1370.0	913.0	1280.0	702 [b]
PCT Location, ft	11.671	11.671	11.671	11.014	11.671	NA
Local Zr-H_2O Reaction, %	0.01	0.08	0.16	NA	0.10	NA
Whole-Core Zr-H_2O Reaction, %	NA	< 0.01	< 0.02	NA	< 0.01	NA
Max Local Zr-H_2O Location, ft	11.671	11.671	11.671	NA	11.671	NA
Hot Rod Burst Location, ft	NA	NA	NA	NA	NA	NA
Hot Rod Burst Time, s	NA	NA	NA	NA	NA	NA

a. SI line break
b. Initial cladding temperature

Table 15.3-20
NORTH ANNA UNIT 2 AFW STUDY TIME SEQUENCE OF EVENTS (SECONDS)

Event	3-inch	3-inch
Intact Loop AFW	Yes	Yes
Broken Loop AFW	Yes	No
Break Initiation	0.0	0.0
Reactor Trip	22.38	22.38
MFW Isolation	22.38	22.38
MSIV Closure	22.88	22.88
SI Injection	53.32	53.32
Broken Loop Seal Clearing	600.0	470.0
Intact Loop Seal Clearing	NA	440.0 [a]
Core Uncovered	840.0	995.0
Accumulator Injection	1215.0	1325.0
PCT Time	1248.0	1334.0
Core Recovered	4070.0	6070.0

a. Resealed later

Table 15.3-21
NORTH ANNA UNIT 2 AFW STUDY RESULTS

Parameter	3-inch	3-inch
Intact Loop AFW	Yes	Yes
Broken Loop AFW	Yes	No
PCT, °F	1370.0	1324.0
PCT Location, ft	11.671	11.671
Local Zr-H_2O Reaction, %	0.16	0.13
Whole-Core Zr-H_2O Reaction, %	< 0.02	< 0.02
Max Local Zr-H_2O Location, ft	11.671	11.671
Hot Rod Burst Location, ft	NA	NA
Hot Rod Burst Time, s	NA	NA

Table 15.3-22
NORTH ANNA UNIT 2 MIXED CORE STUDY TIME SEQUENCE OF EVENTS (SECONDS)

Event	FANP Core	Mixed Core
Break Initiation	0.0	0.0
Reactor Trip	22.38	22.38
MFW Isolation	22.38	22.38
MSIV Closure	22.88	22.88
SI Injection	53.32	53.28
Broken Loop Seal Clearing	600.0	595.0
Intact Loop Seal Clearing	NA	NA
Core Uncovered	840.0	865.0
Accumulator Injection	1215.0	1230.0
PCT Time	1248.0	1242.0
Core Recovered	4070.0	4275.0

Table 15.3-23
NORTH ANNA UNIT 2 MIXED CORE STUDY RESULTS

Cases	FANP Core	Mixed Core
PCT, °F	1370.0	1345.0
PCT Location, ft	11.671	11.671
Local Zr-H_2O Reaction, %	0.16	0.14
Whole-Core Zr-H_2O Reaction, %	< 0.02	< 0.02
Max Local Zr-H_2O Location, ft	11.671	11.671
Hot Rod Burst Location, ft	NA	NA
Hot Rod Burst Time, s	NA	NA

Table 15.3-24

PEAK CLAD TEMPERATURE INCLUDING ALL PENALTIES AND BENEFITS - SMALL BREAK LOCA - ADVANCED MARK-BW FUEL

Unit 1	
PCT for Analysis of Record	1404°F
PCT Assessments Allocated to AOR	
A. Revised Test Flow Curve for HHSI	-24°F
B. RELAP5 Point Kinetics Programming Issue	-8°F
SBLOCA PCT for Comparison to 10 CFR 50.46 Requirements	1372°F
Unit 2	
PCT for Analysis of Record	1370°F
PCT Assessments Allocated to AOR	
A. RELAP5 Point Kinetics Programming Issue	-8°F
SBLOCA PCT for Comparison to 10 CFR 50.46 Requirements	1362°F

Figure 15.3-1
SAFETY INJECTION FLOW (LBM/SEC)

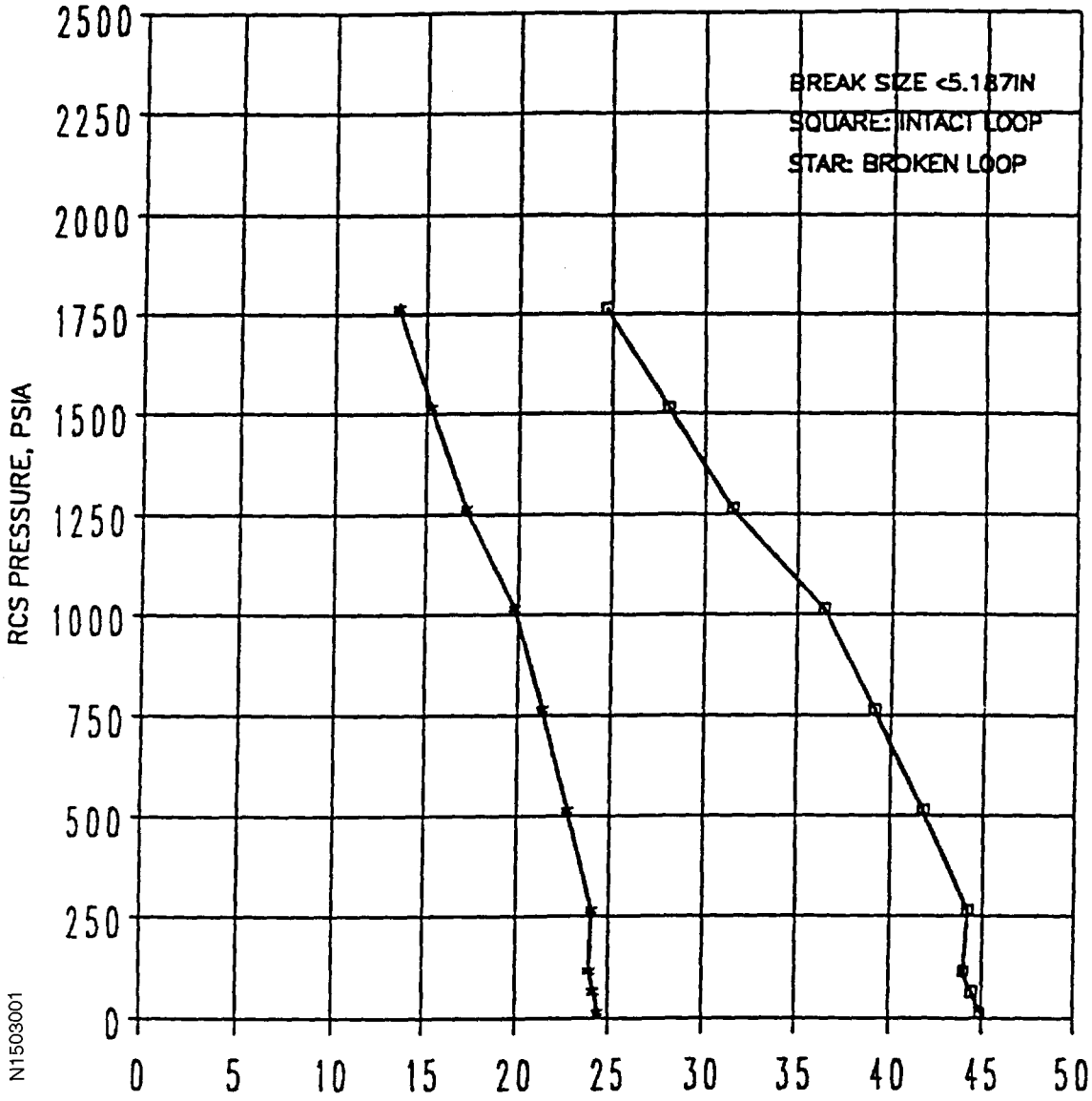

Figure 15.3-2
NORMALIZED HOT CHANNEL FACTOR

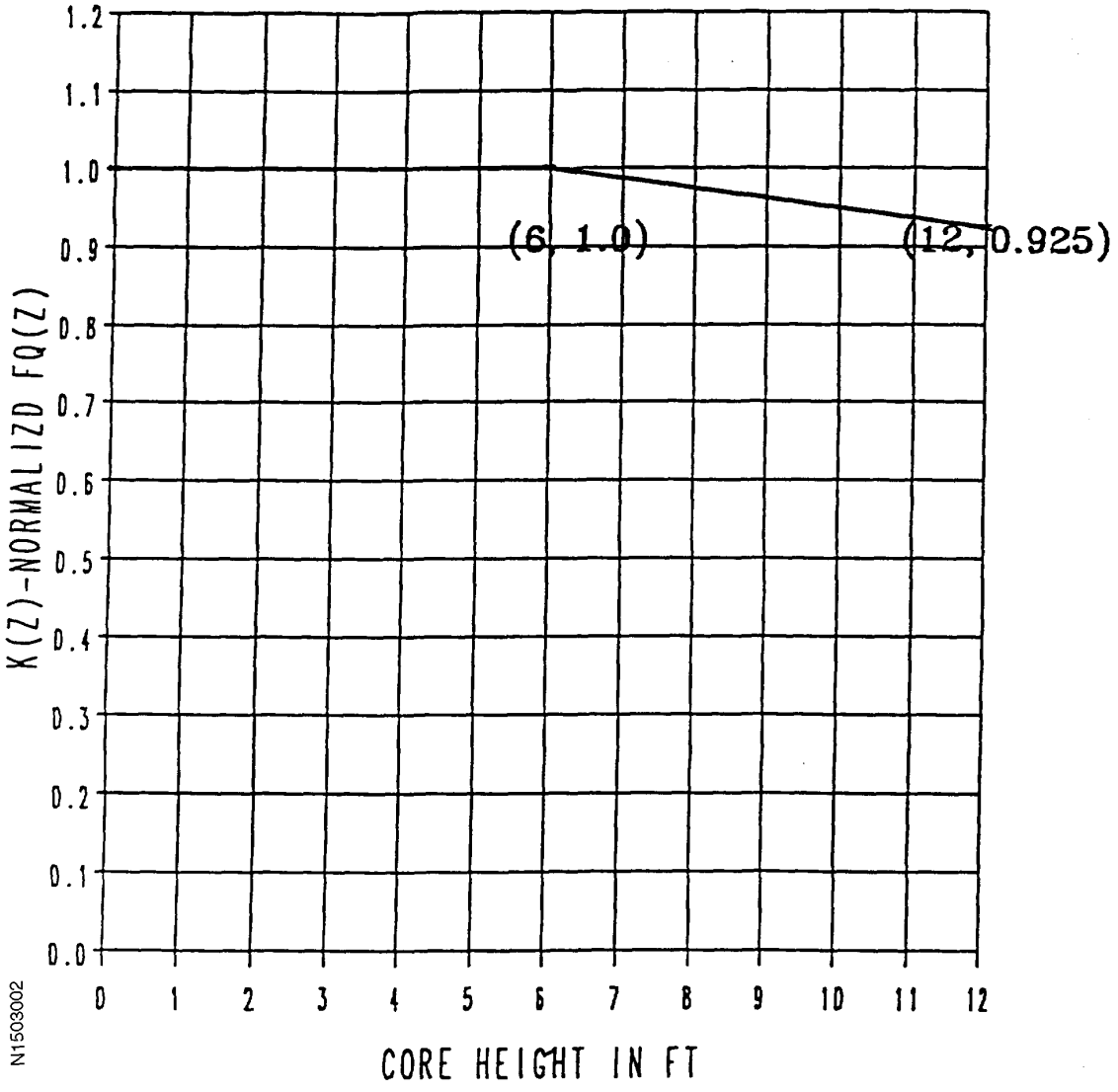

Figure 15.3-3
HOT ROD POWER SHAPE USED IN LOCTA-IV

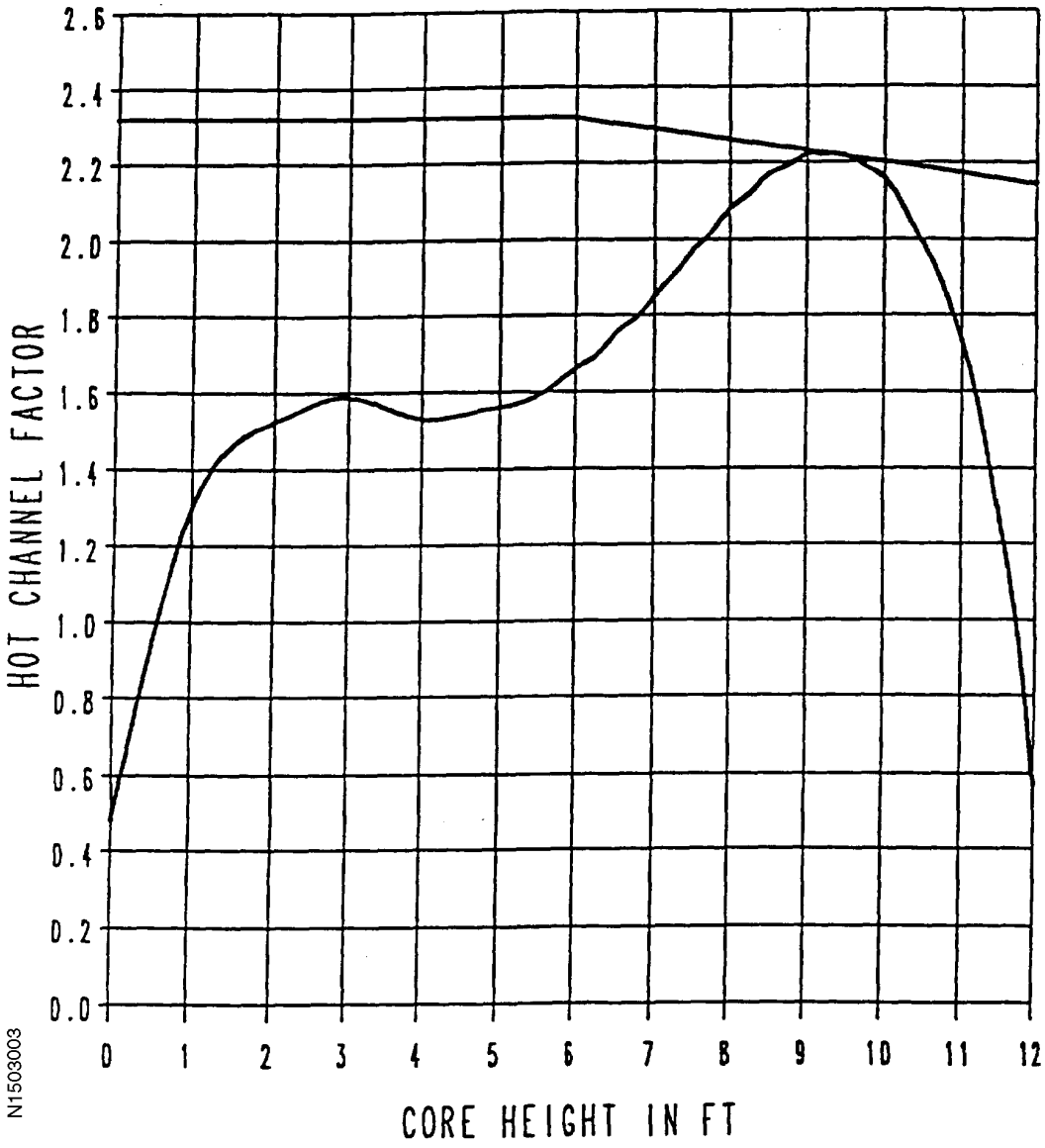

Figure 15.3-4
PRESSURIZER PRESSURE (PSIA), 2-INCH BREAK

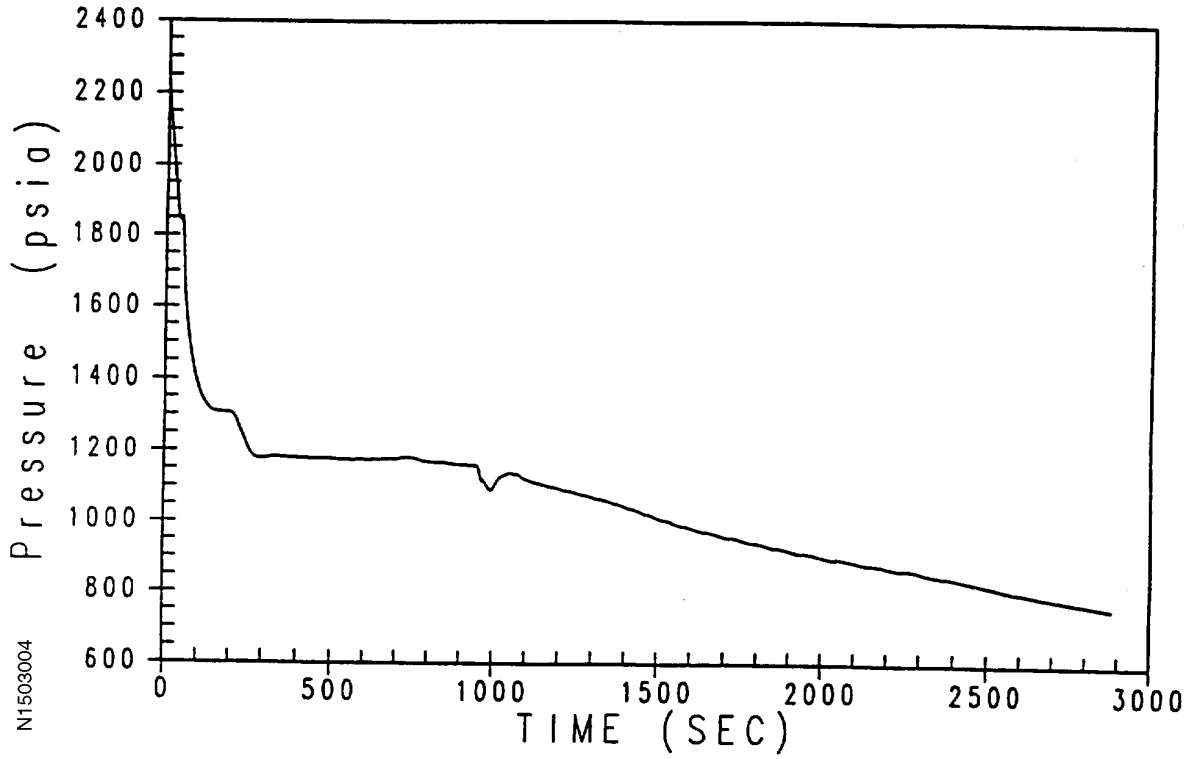

Figure 15.3-5
PRESSURIZER PRESSURE (PSIA), 3-INCH BREAK

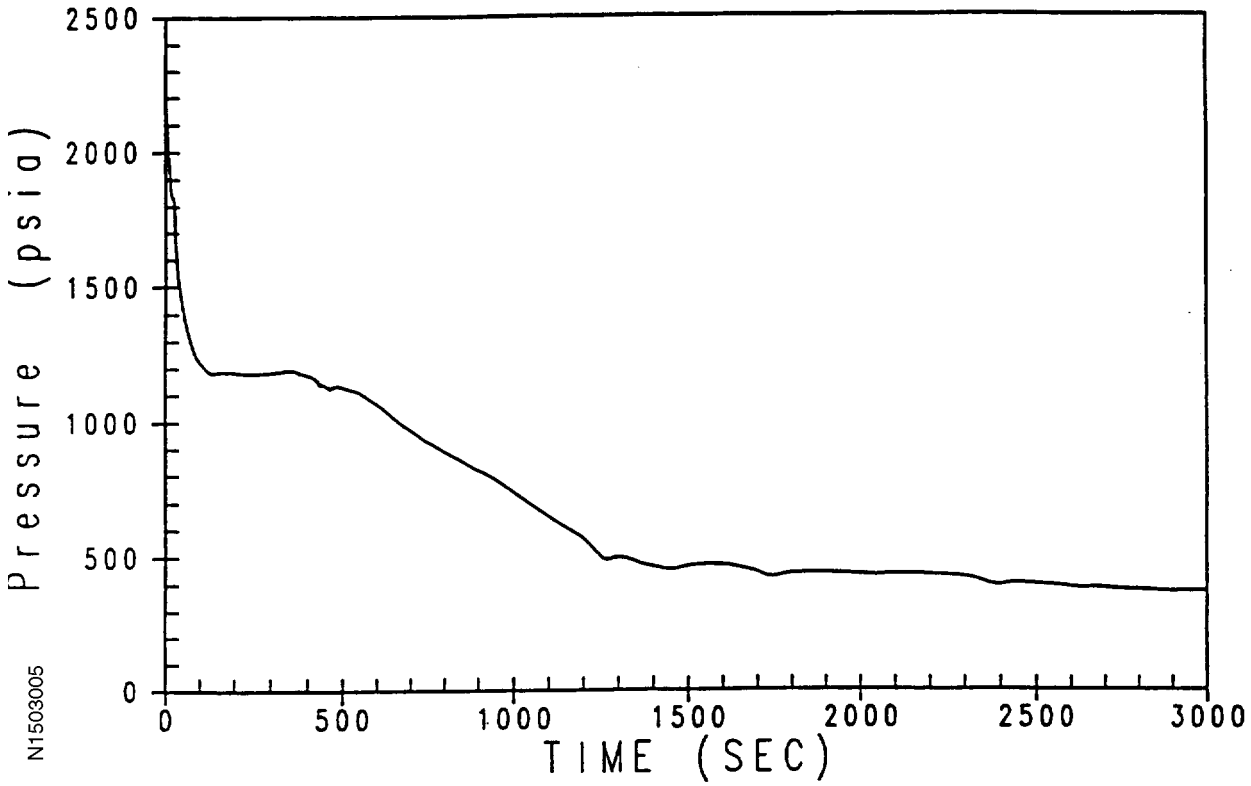

Figure 15.3-6
PRESSURIZER PRESSURE (PSIA), 4-INCH BREAK

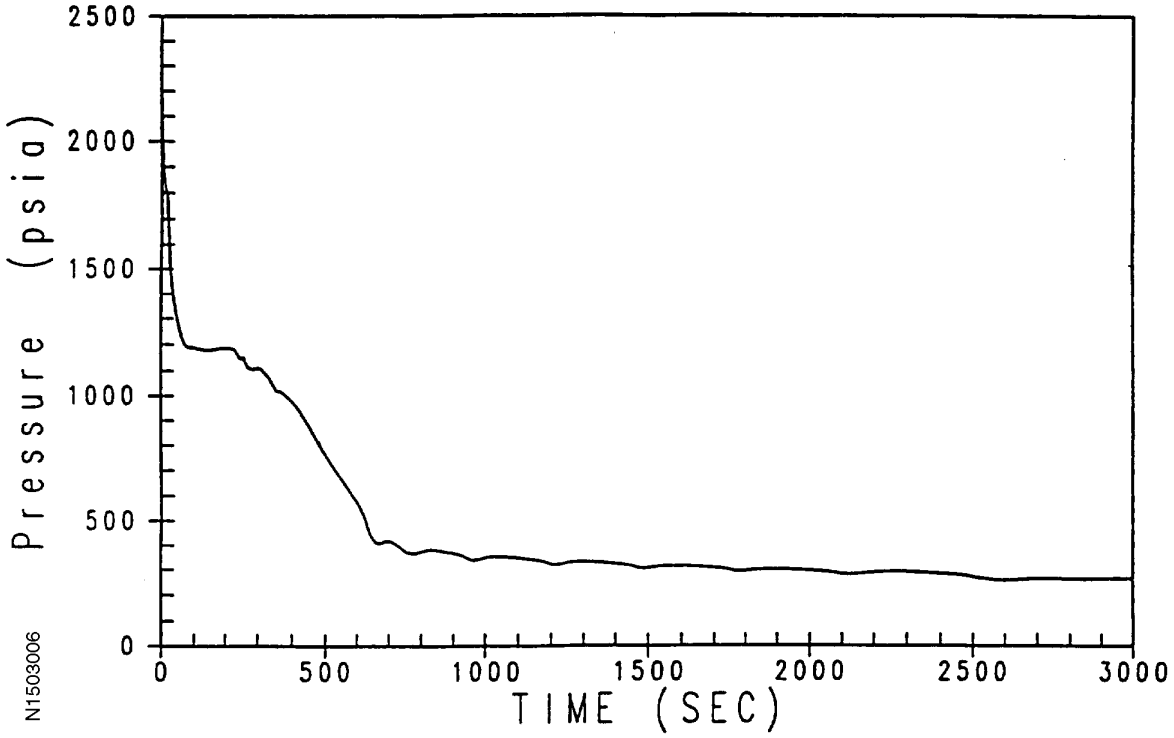

Figure 15.3-7
CORE MIXTURE LEVEL (FT), 2-INCH BREAK

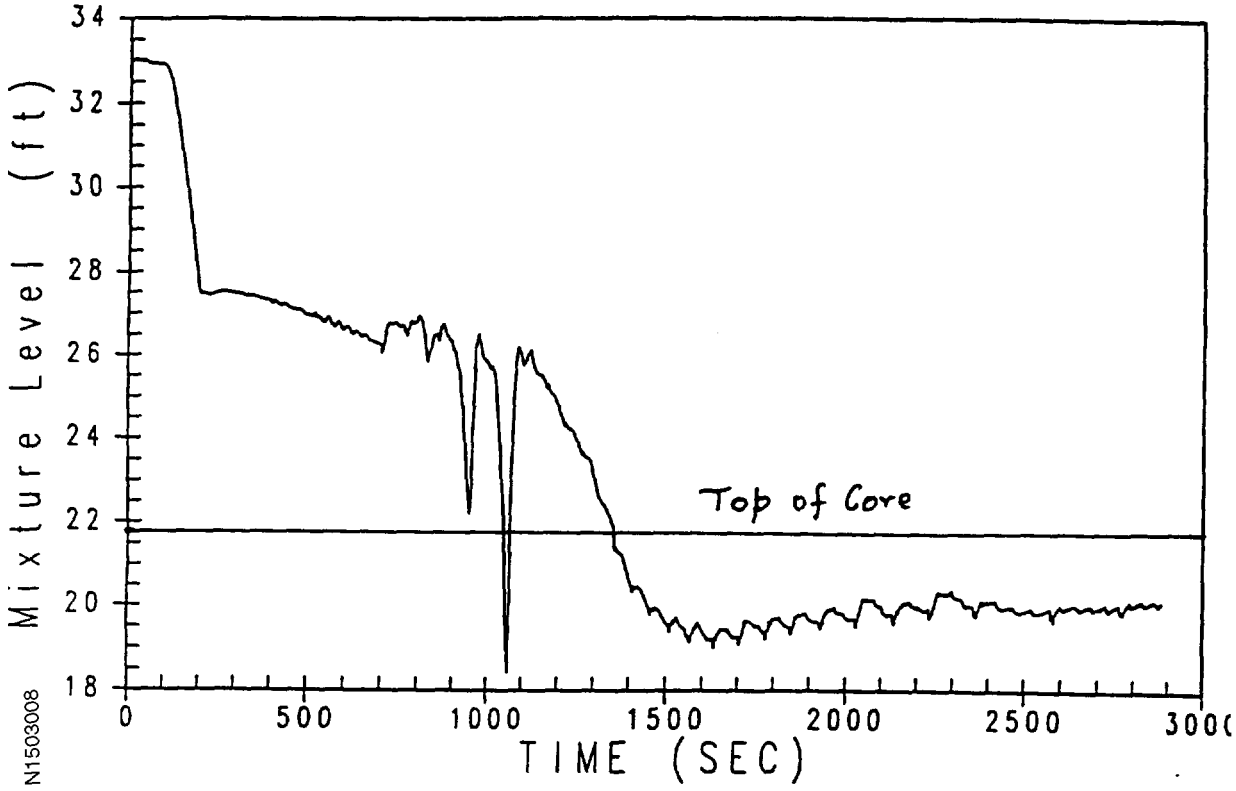

Figure 15.3-8
CORE MIXTURE LEVEL (FT), 3-INCH BREAK

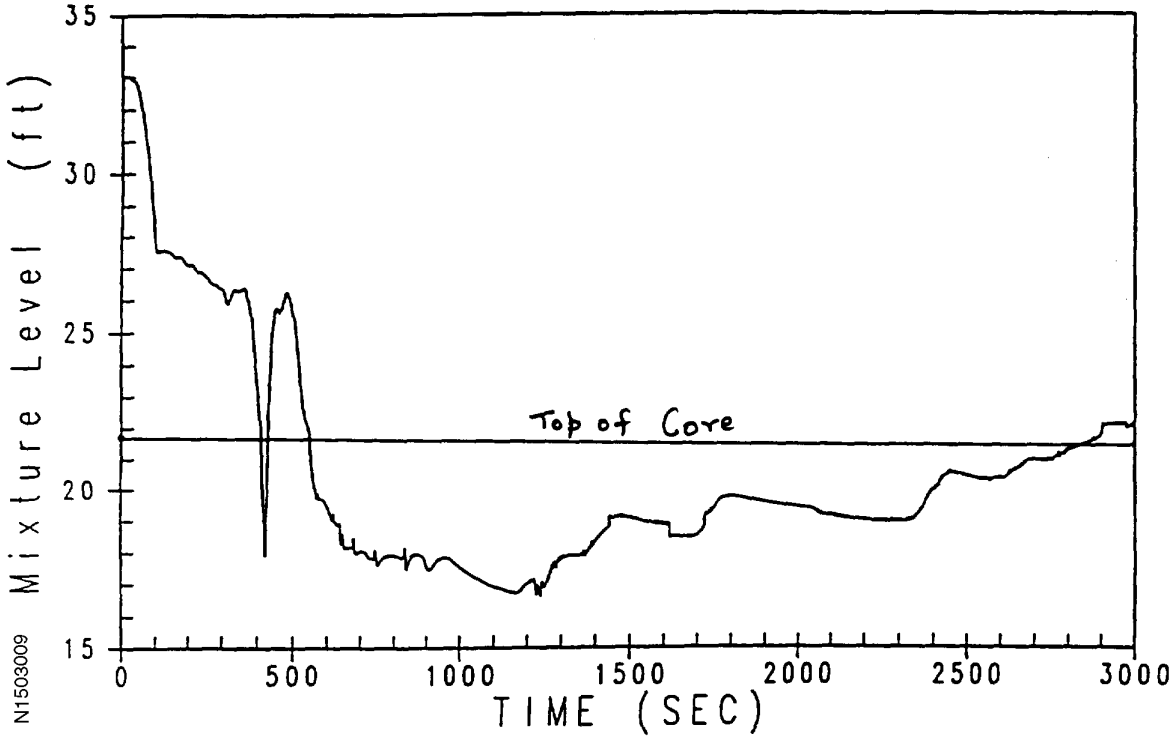

Figure 15.3-9
CORE MIXTURE LEVEL (FT), 4-INCH BREAK

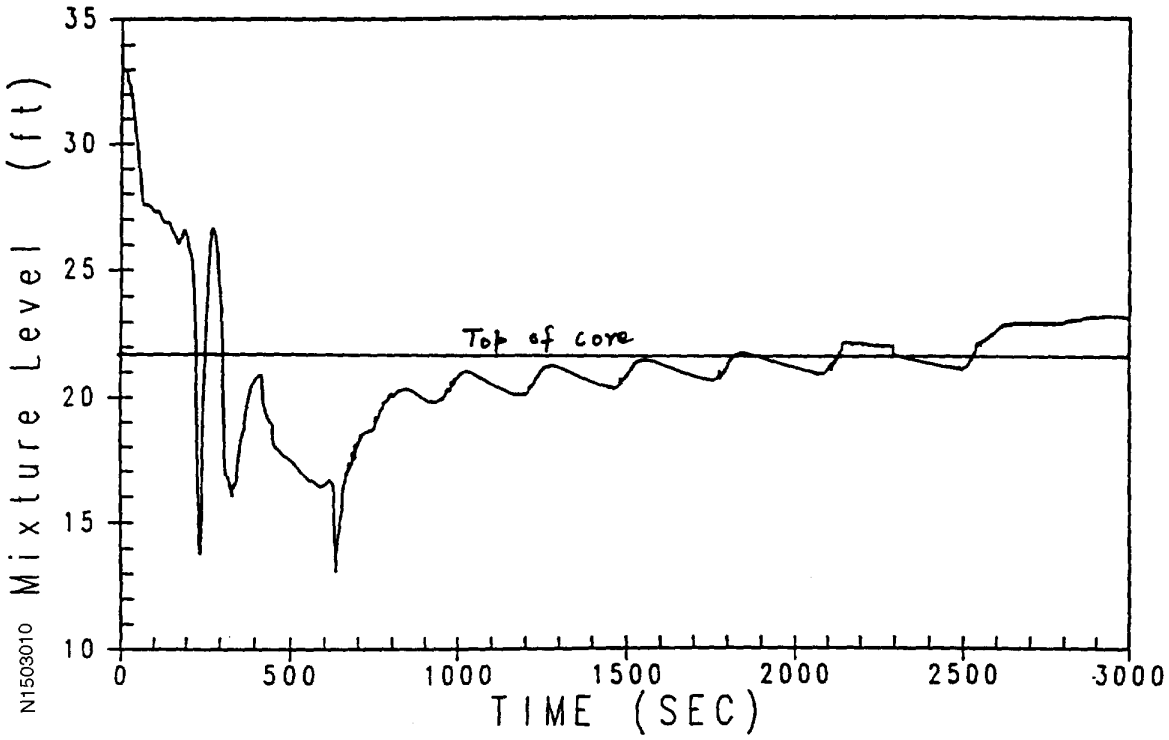

Figure 15.3-10
INTACT LOOP PUMPED SI FLOW (LBM/SEC), 2-INCH BREAK

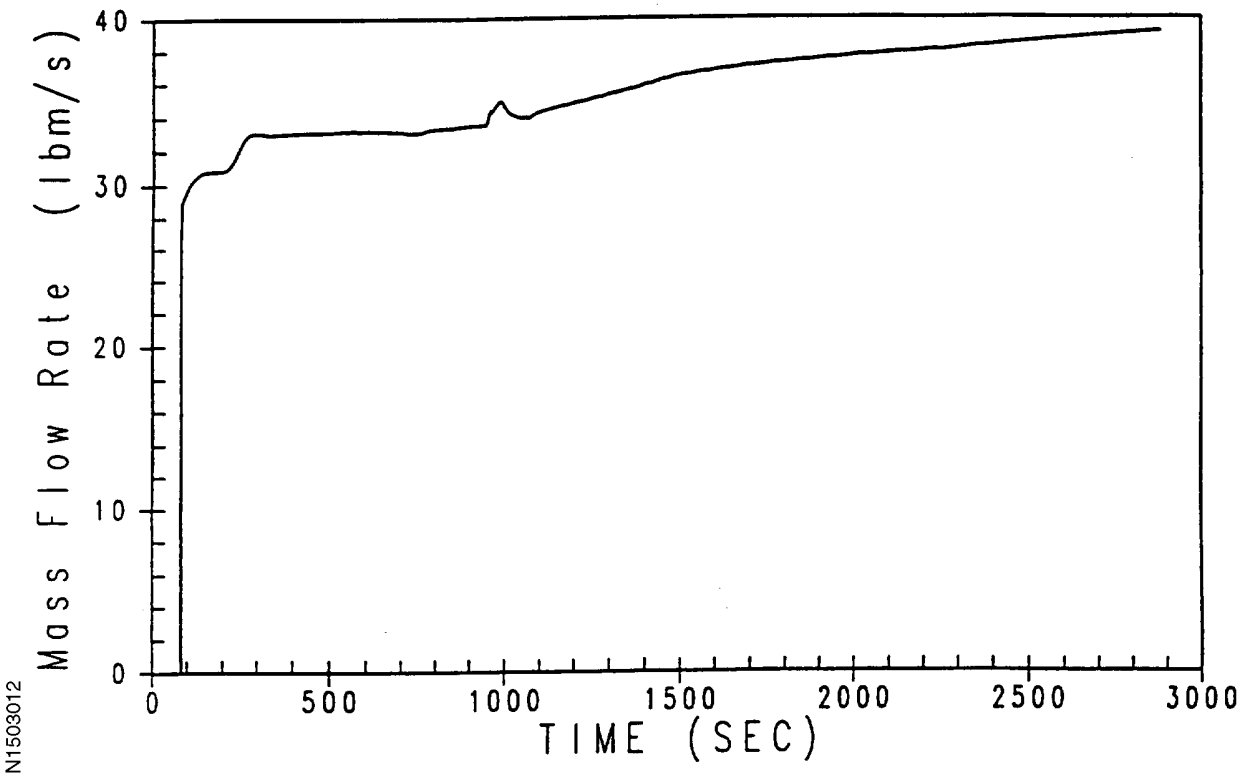

Figure 15.3-11
INTACT LOOP PUMPED SI FLOW (LBM/SEC), 3-INCH BREAK

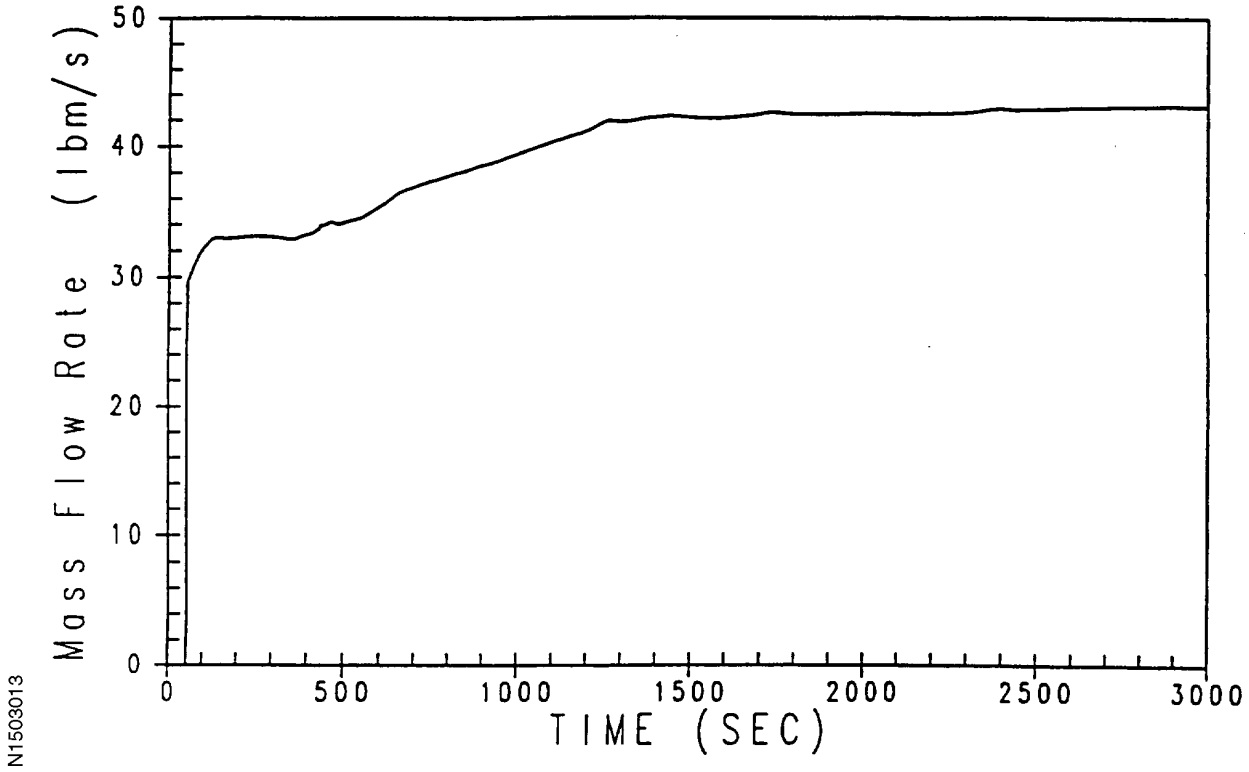

Figure 15.3-12
INTACT LOOP PUMPED SI FLOW (LBM/SEC), 4-INCH BREAK

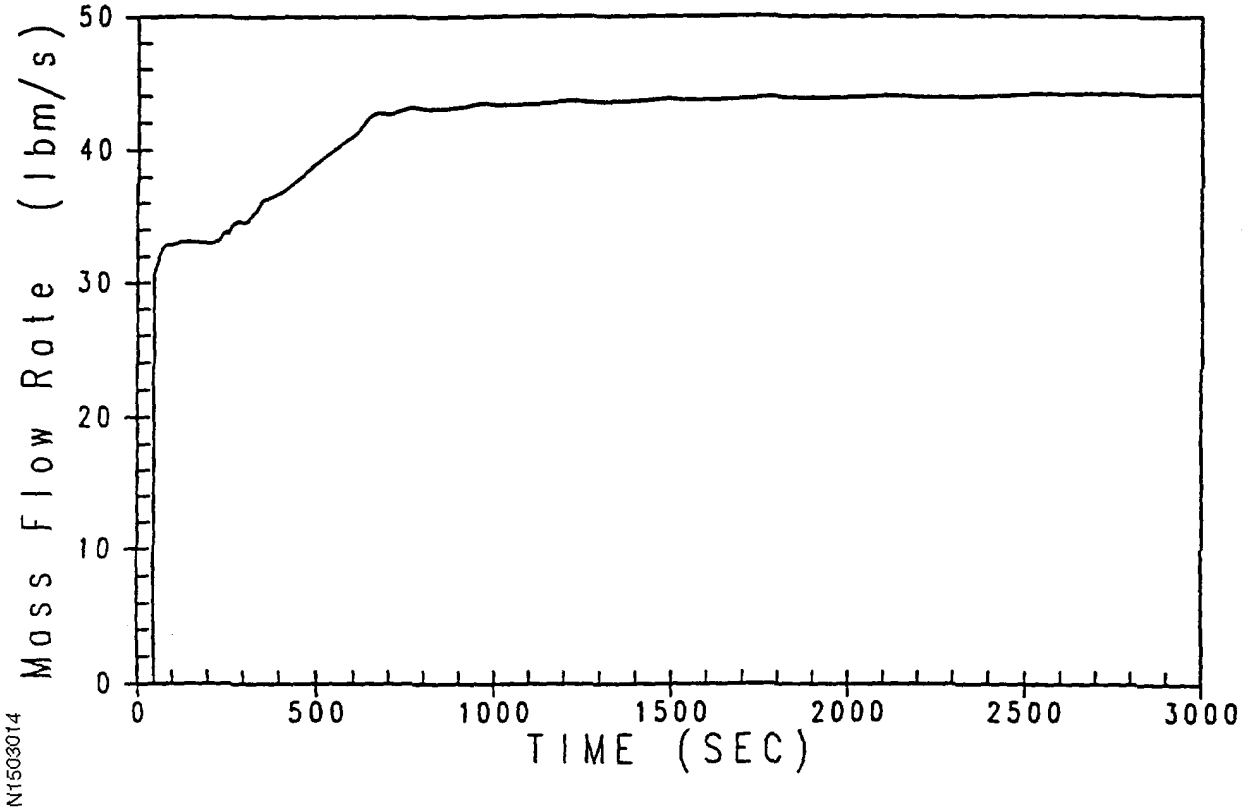

Figure 15.3-13
BROKEN LOOP PUMPED SI FLOW (LBM/SEC), 2-INCH BREAK

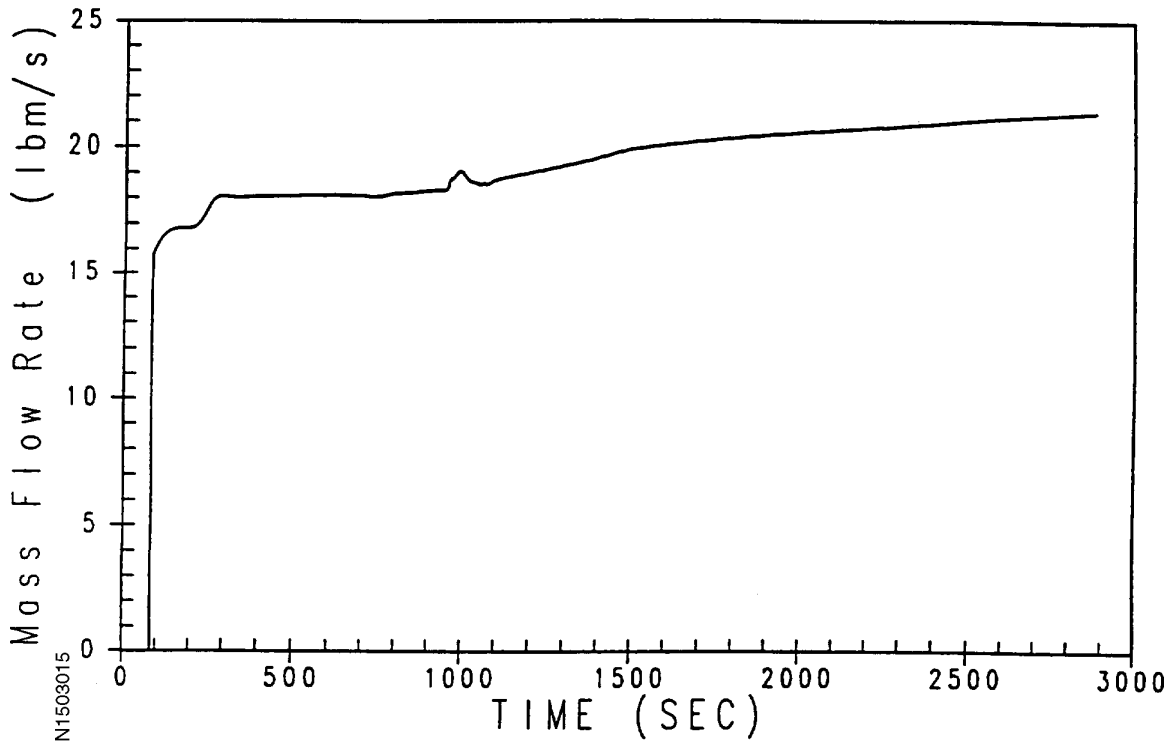

Figure 15.3-14
BROKEN LOOP PUMPED SI FLOW (LBM/SEC), 3-INCH BREAK

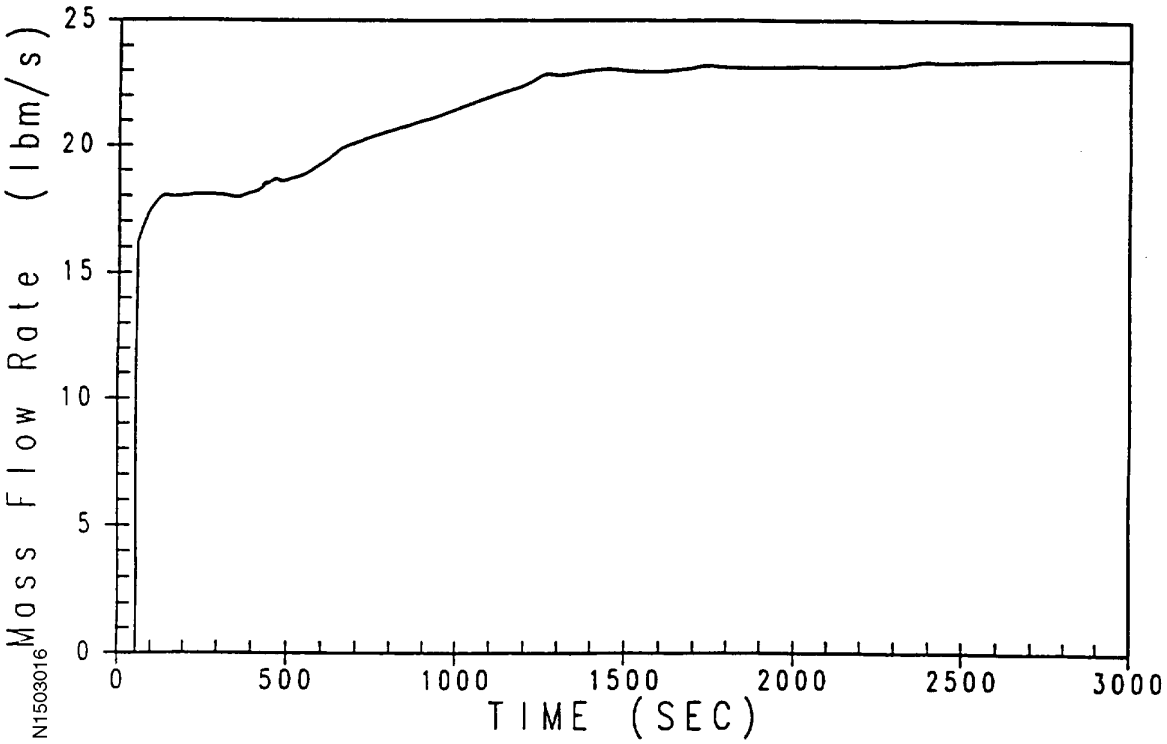

Figure 15.3-15
BROKEN LOOP PUMPED SI FLOW (LBM/SEC), 4-INCH BREAK

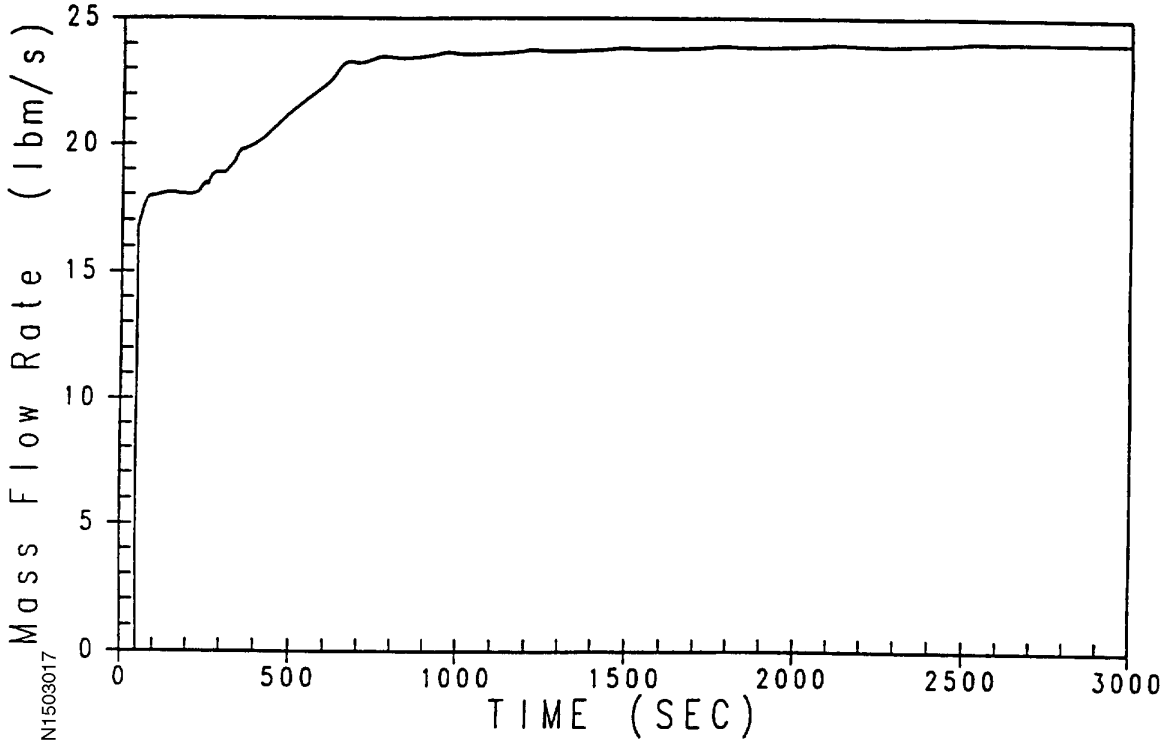

Figure 15.3-16
CORE EXIT VAPOR FLOW (LBM/SEC), 2-INCH BREAK

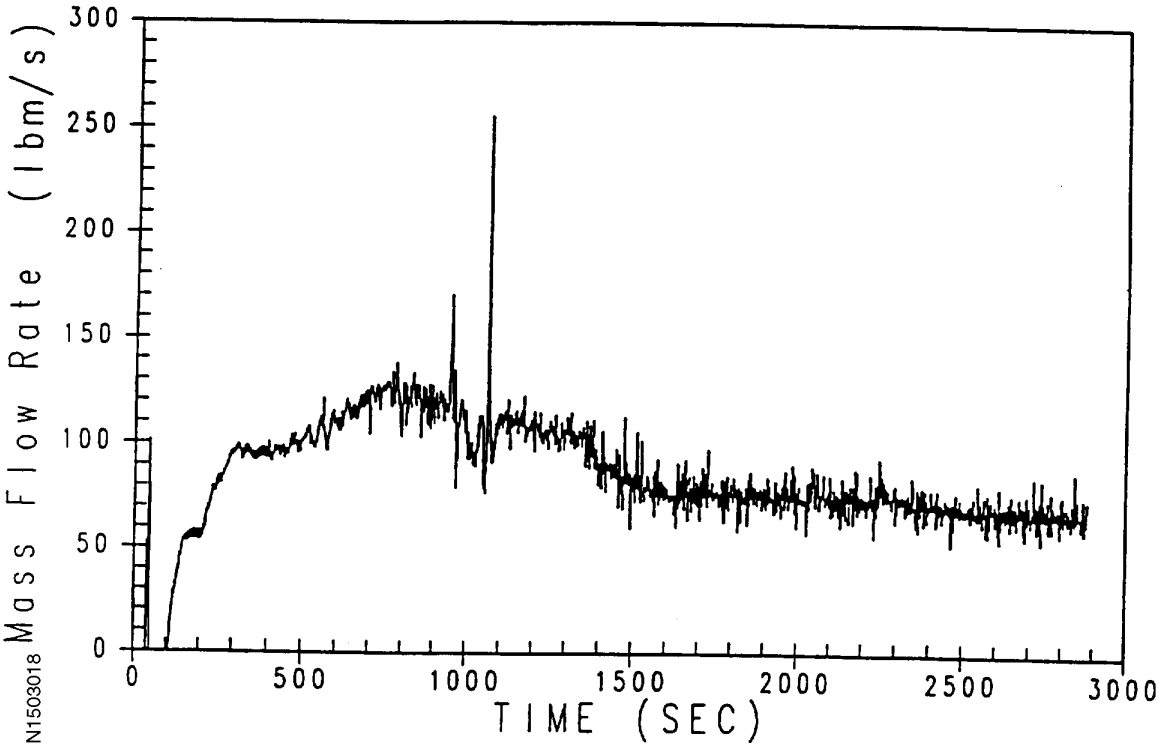

Figure 15.3-17
CORE EXIT VAPOR FLOW (LBM/SEC), 3-INCH BREAK

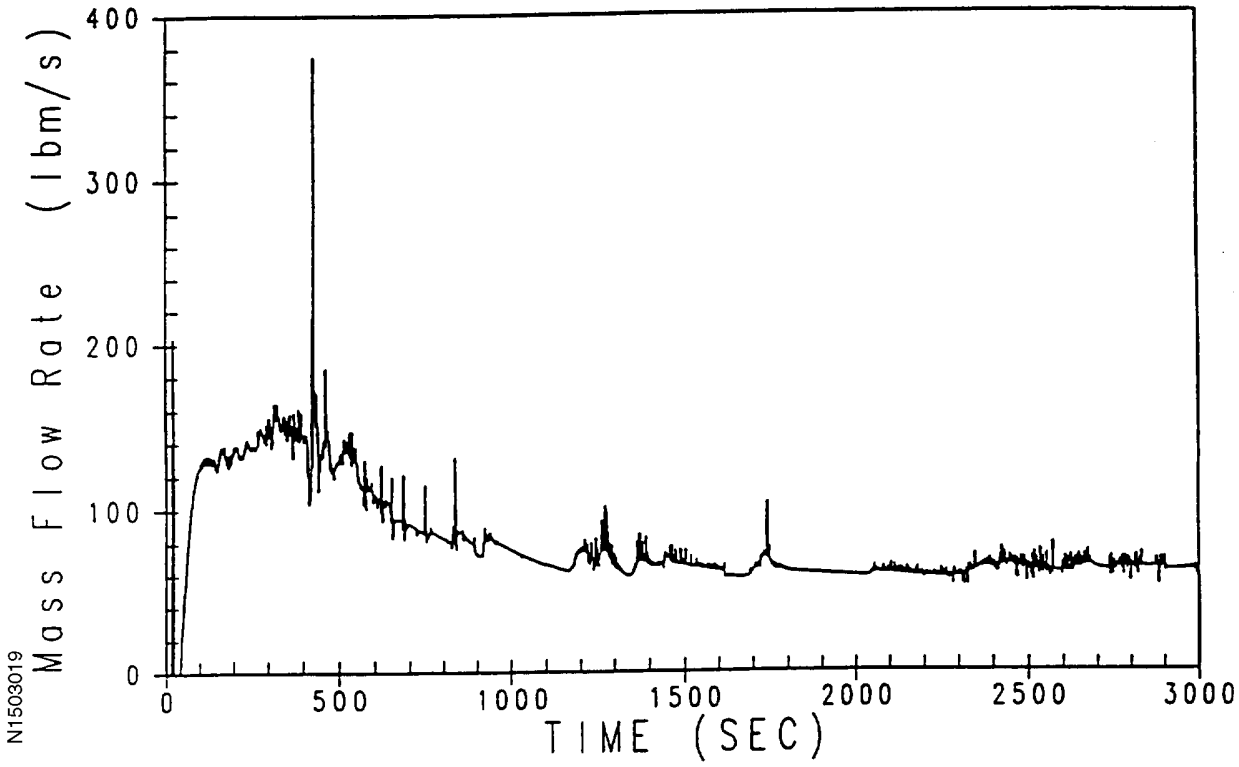

Figure 15.3-18
CORE EXIT VAPOR FLOW (LBM/SEC), 4-INCH BREAK

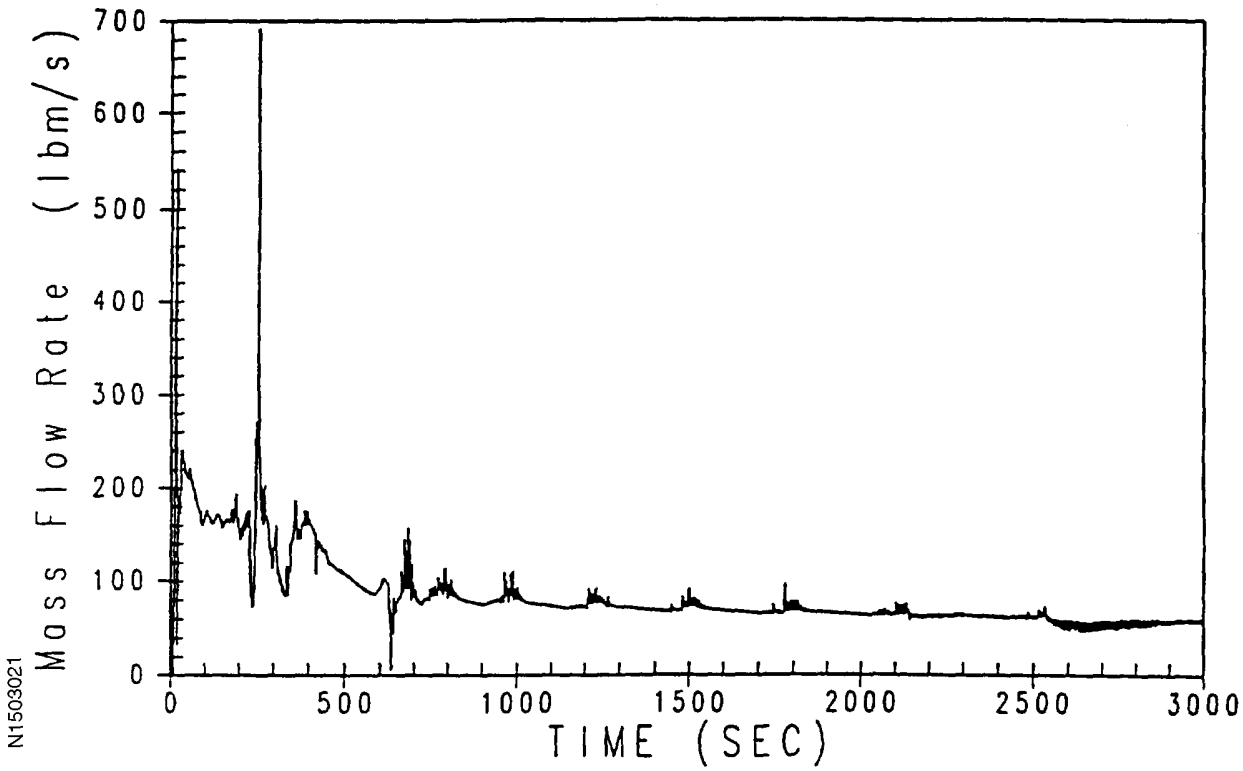

Figure 15.3-19
FLUID TEMPERATURE IN HOT ASSEMBLY (°F), 2-INCH BREAK

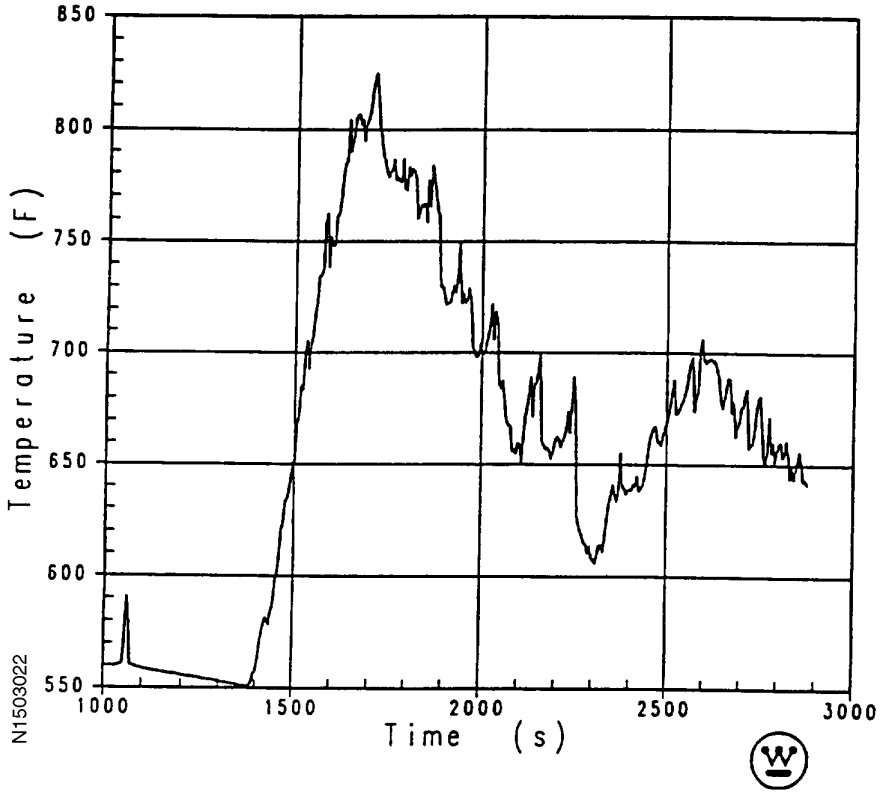

Figure 15.3-20
FLUID TEMPERATURE IN HOT ASSEMBLY (°F), 3-INCH BREAK

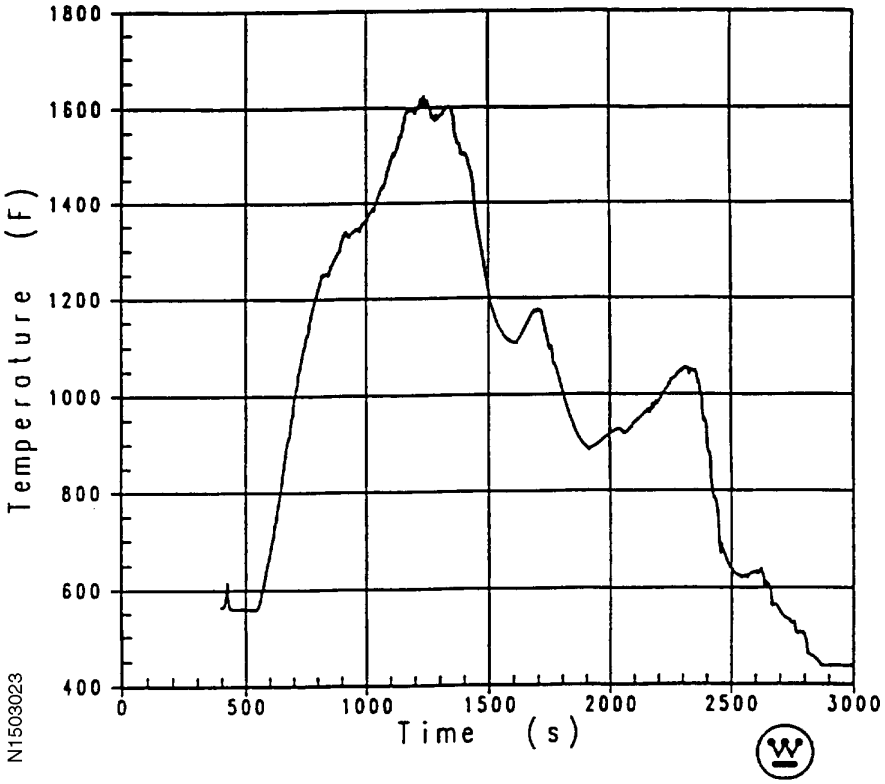

Figure 15.3-21
FLUID TEMPERATURE IN HOT ASSEMBLY (°F), 4-INCH BREAK

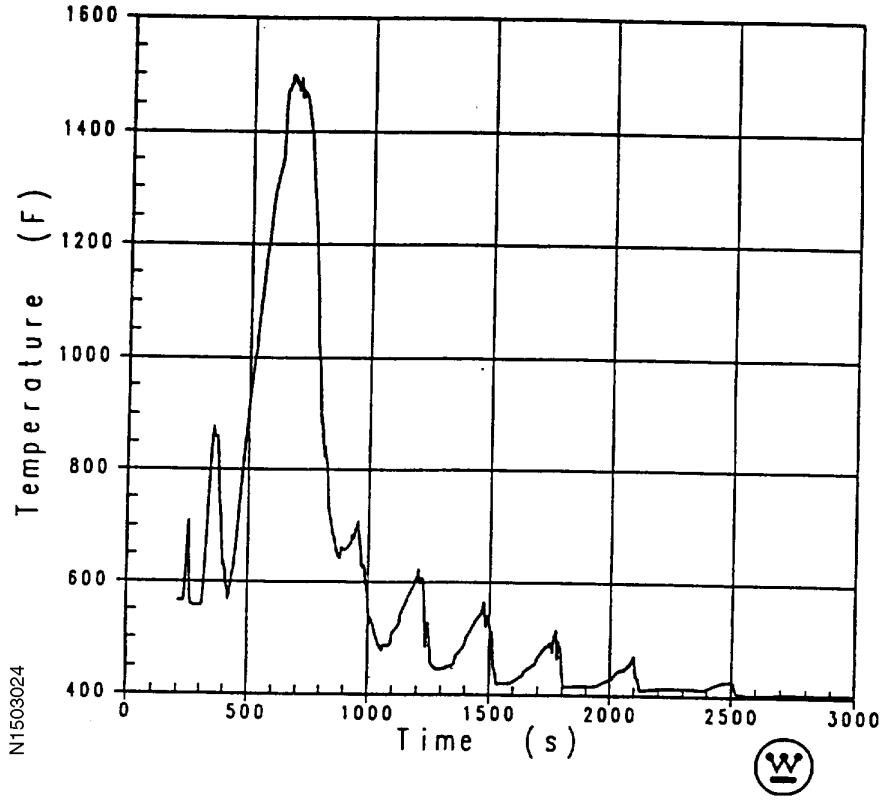

Figure 15.3-22
HEAT TRANSFER COEFFICIENT (BTU/HR-FT^2), 2-INCH BREAK

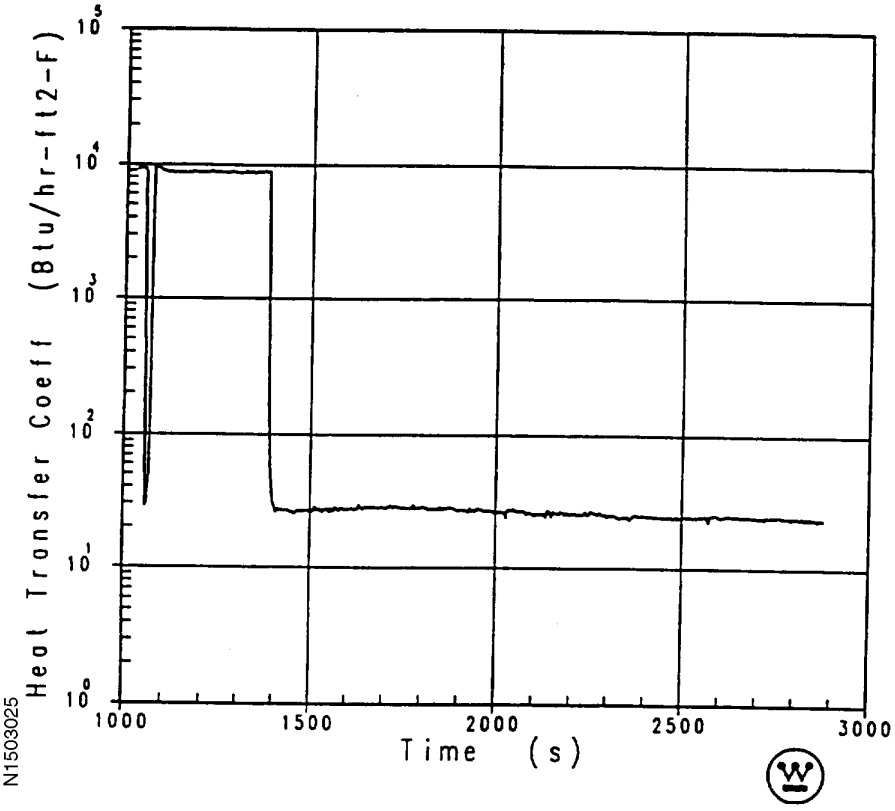

Figure 15.3-23
HEAT TRANSFER COEFFICIENT (BTU/HR-FT^2), 3-INCH BREAK

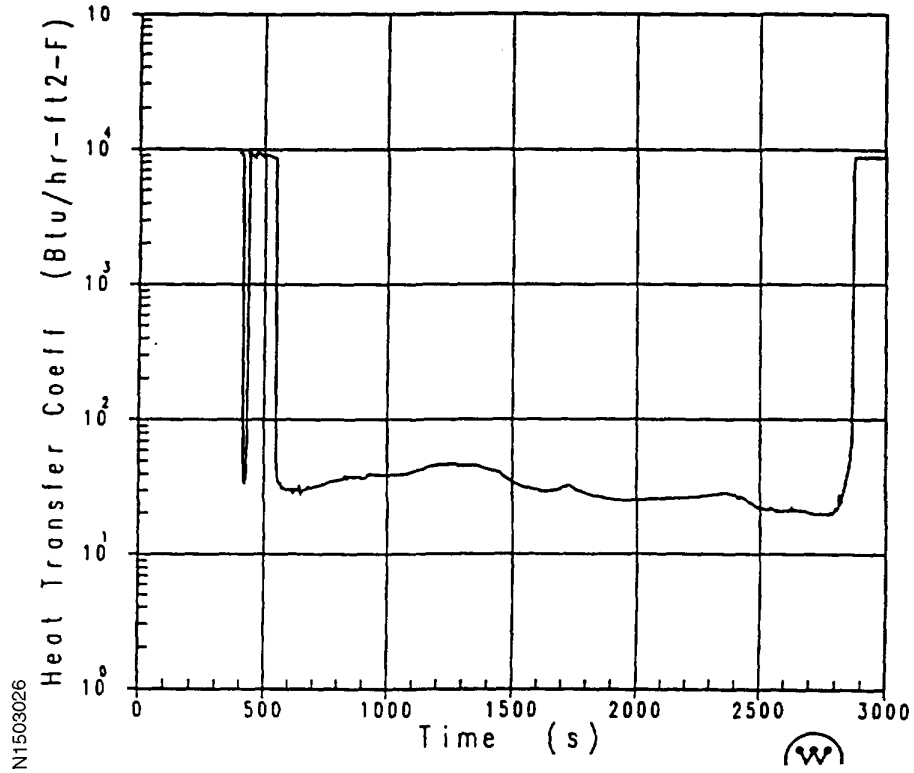

Figure 15.3-24
HEAT TRANSFER COEFFICIENT (BTU/HR-FT^2), 4-INCH BREAK

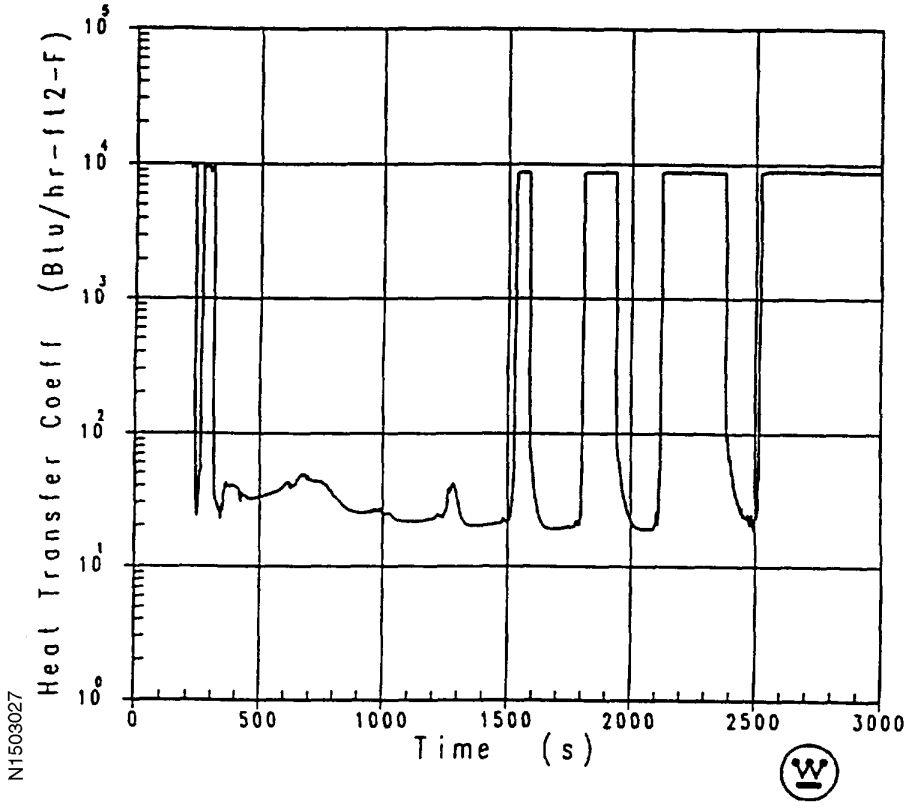

Figure 15.3-25
HOT ROD CLAD AVERAGE TEMPERATURE (°F), 2-INCH BREAK

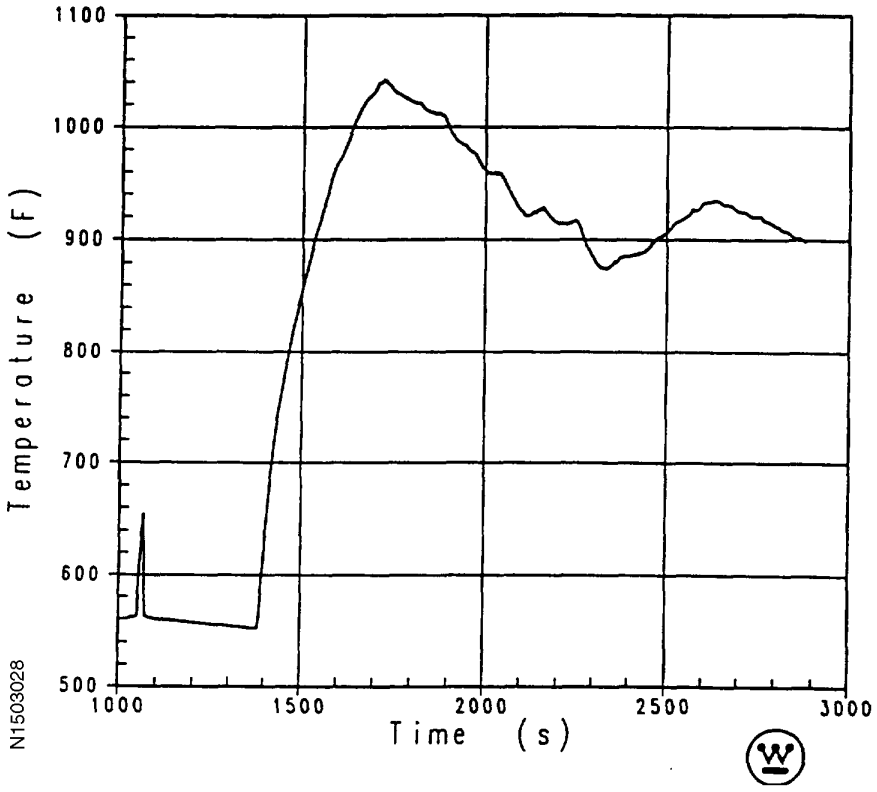

Figure 15.3-26
HOT ROD CLAD AVERAGE TEMPERATURE (°F), 3-INCH BREAK

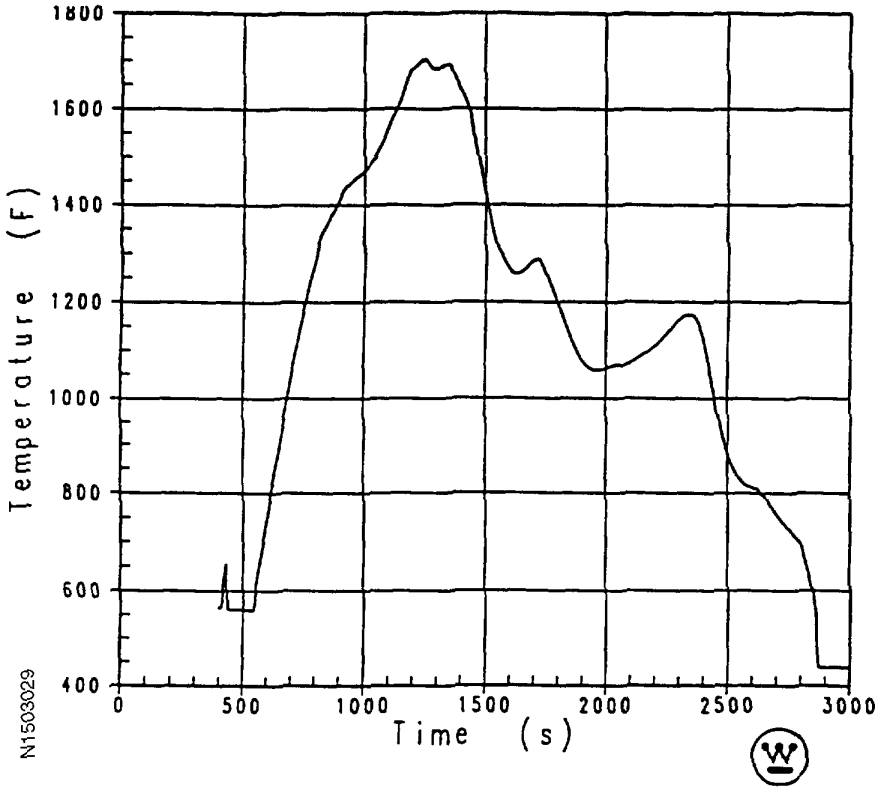

Figure 15.3-27
HOT ROD CLAD AVERAGE TEMPERATURE (°F), 4-INCH BREAK

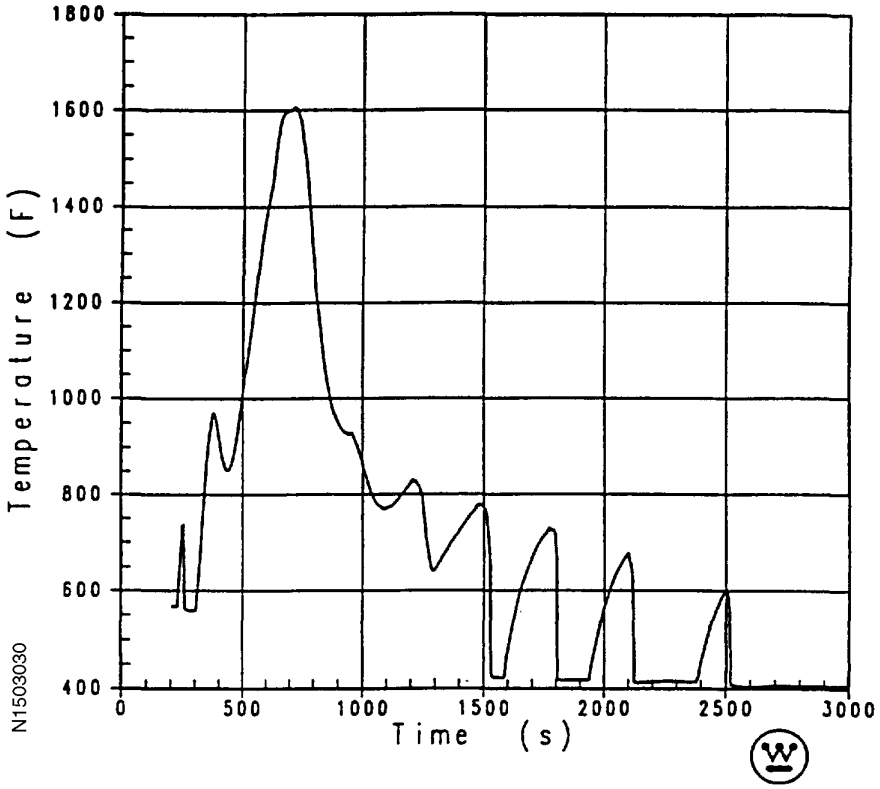

Figure 15.3-28
INTERCHANGE BETWEEN REGION 1 AND REGION 3 ASSEMBLY

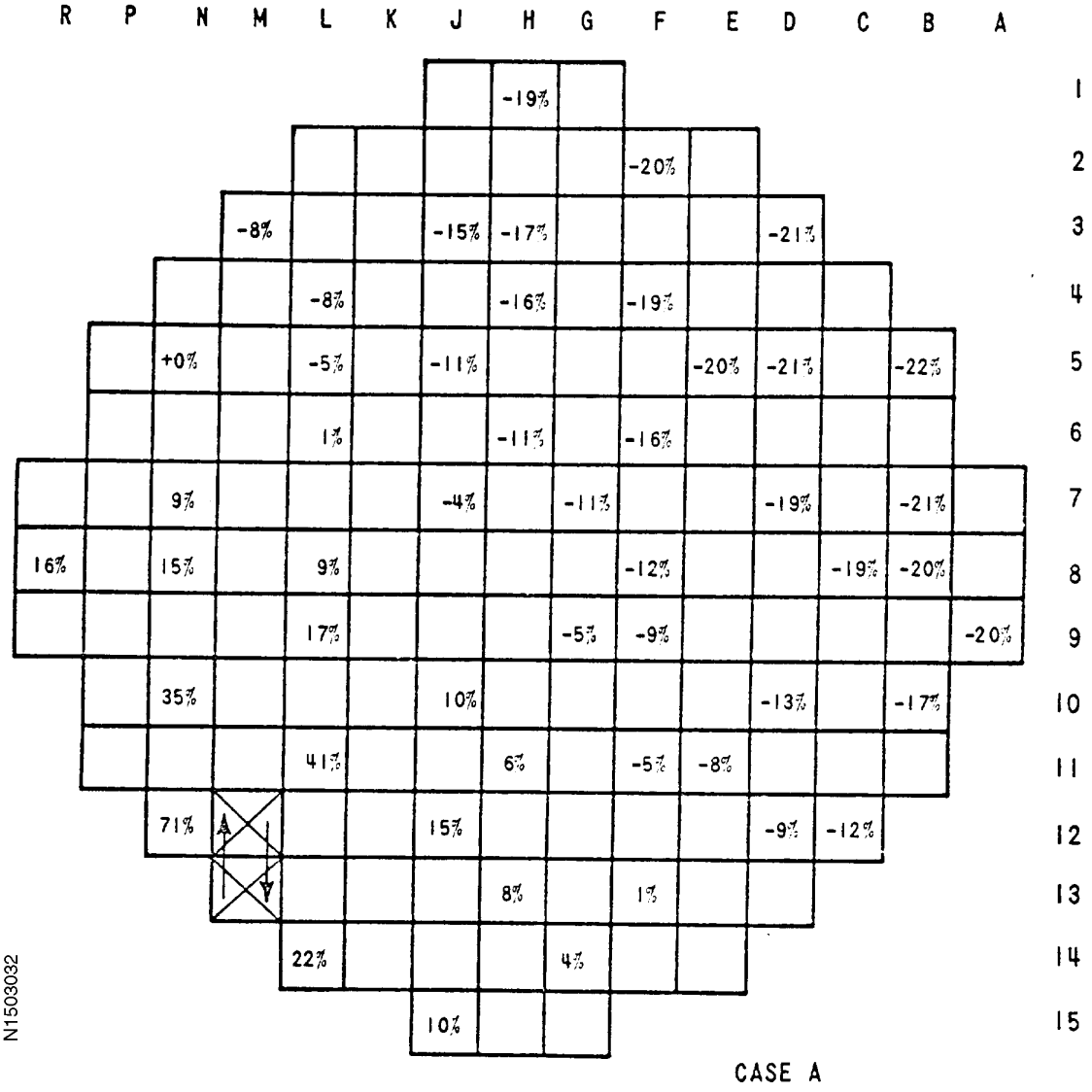

Figure 15.3-29
INTERCHANGE BETWEEN REGION 2 AND REGION 3 ASSEMBLY,
BURNABLE POISON RODS BEING RETAINED BY THE REGION 2 ASSEMBLY

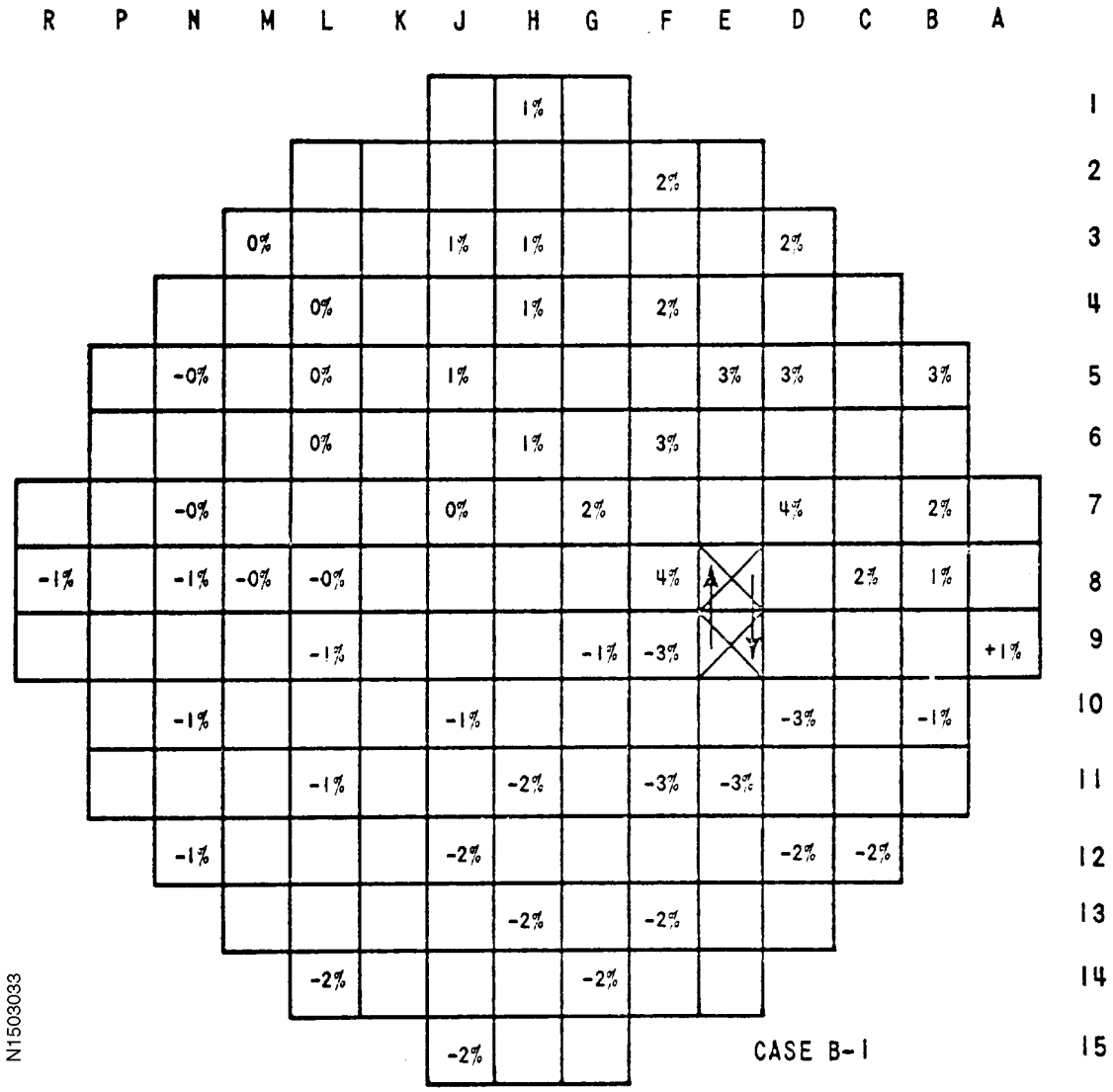

Figure 15.3-30
INTERCHANGE BETWEEN REGION 1 AND REGION 2 ASSEMBLY,
BURNABLE POISON RODS BEING TRANSFERRED TO THE REGION 1 ASSEMBLY

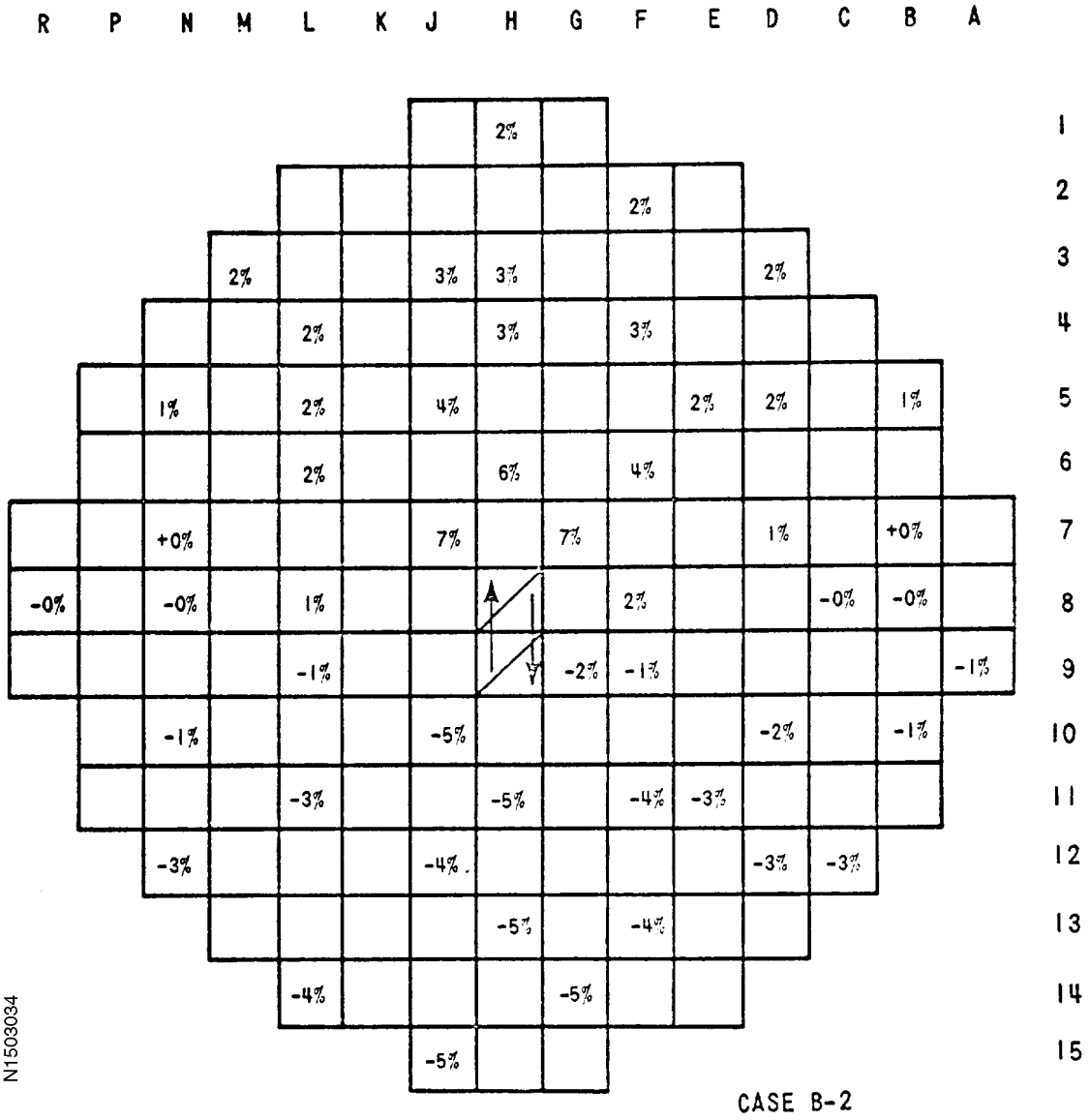

Figure 15.3-31
ENRICHMENT ERROR:
A REGION 2 ASSEMBLY LOADED INTO THE CORE CENTRAL POSITION

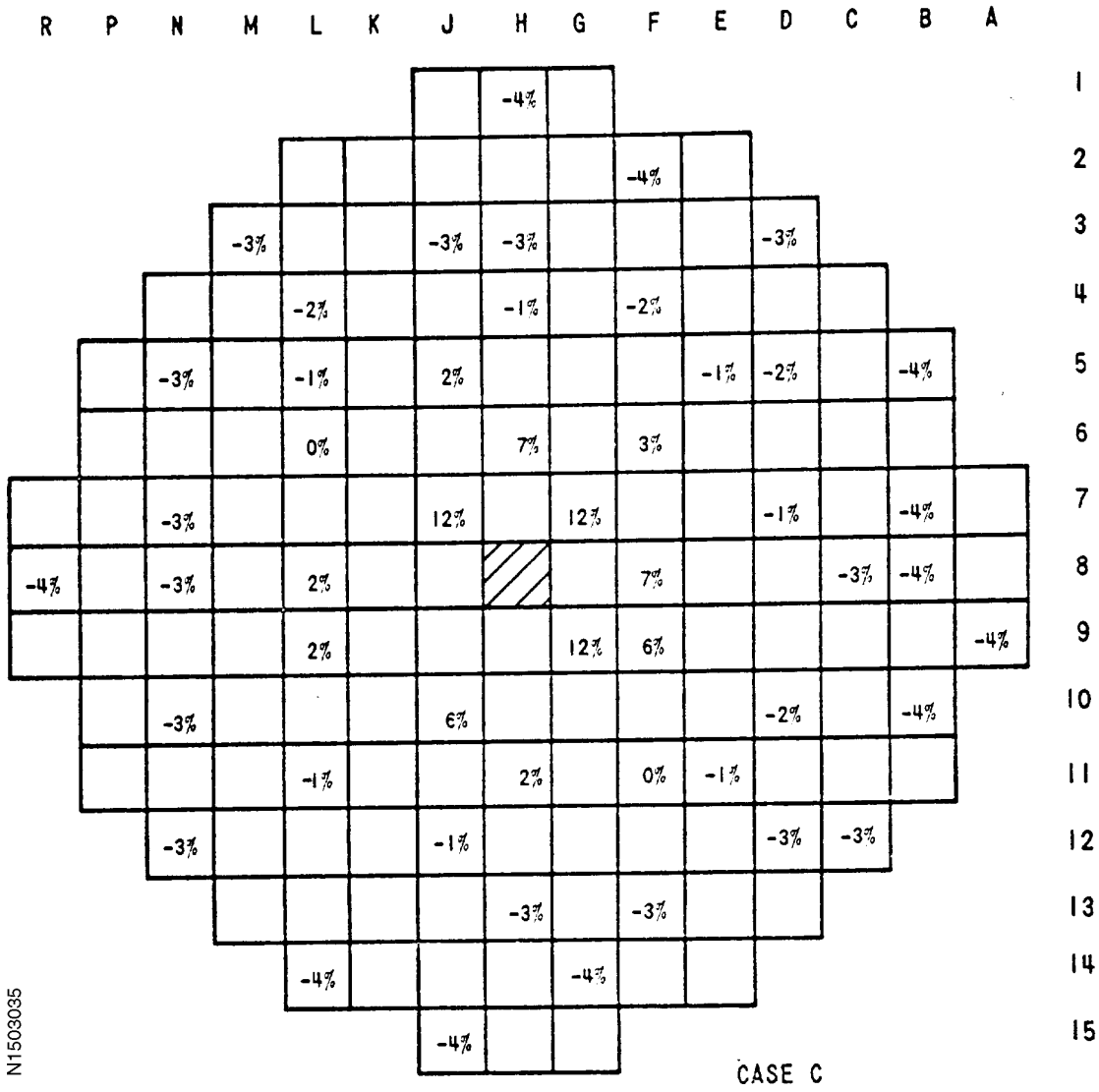

Figure 15.3-32
LOADING A REGION 2 ASSEMBLY
INTO A REGION 1 POSITION NEAR CORE PERIPHERY

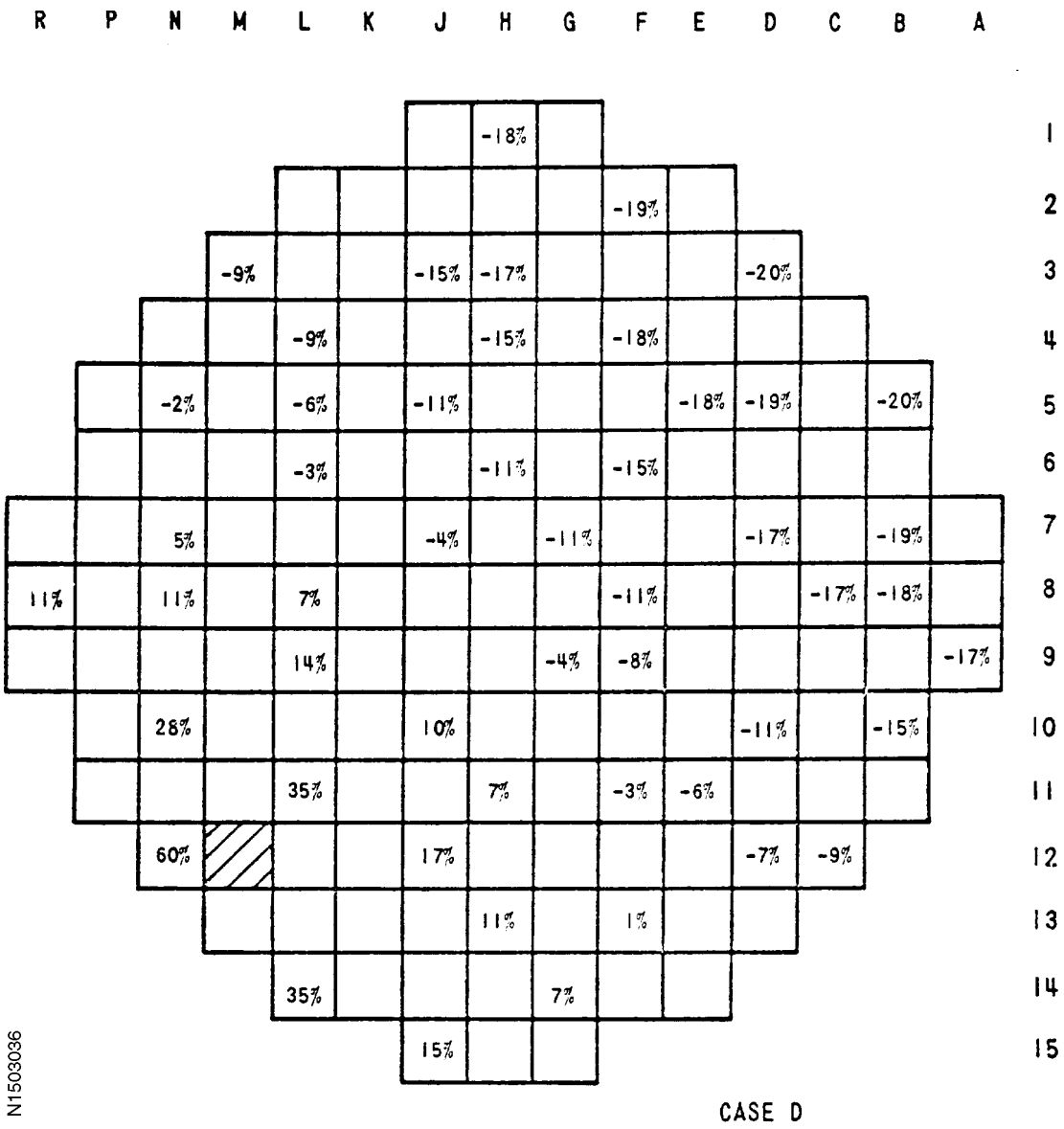

Figure 15.3-33
RCS MASS FLOW RATE VS. TIME
LOSS OF FLOW EVENT
UNDERVOLTAGE

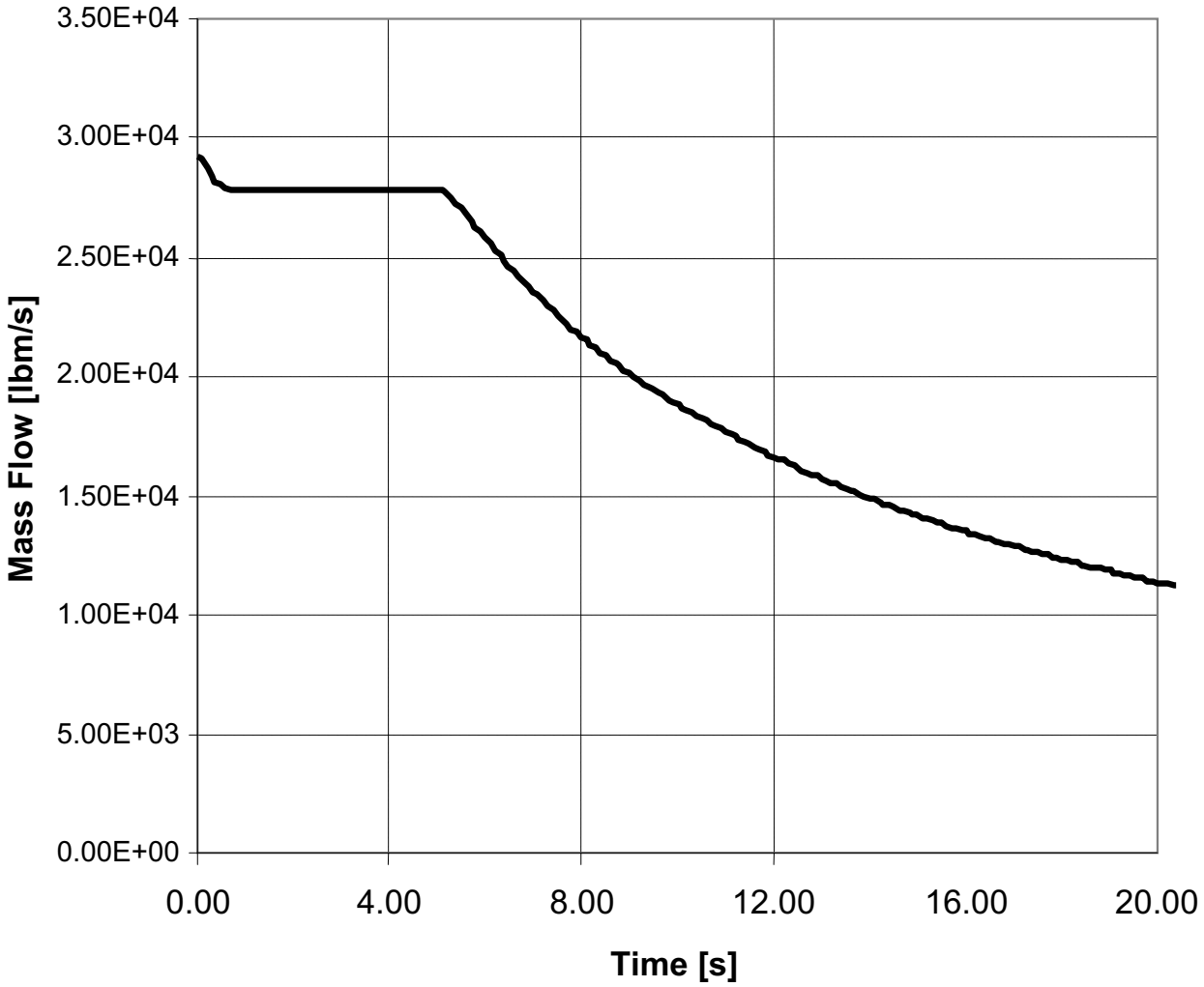

Figure 15.3-34
RCS MASS FLOW RATE VS. TIME
LOSS OF FLOW EVENT
UNDERFREQUENCY

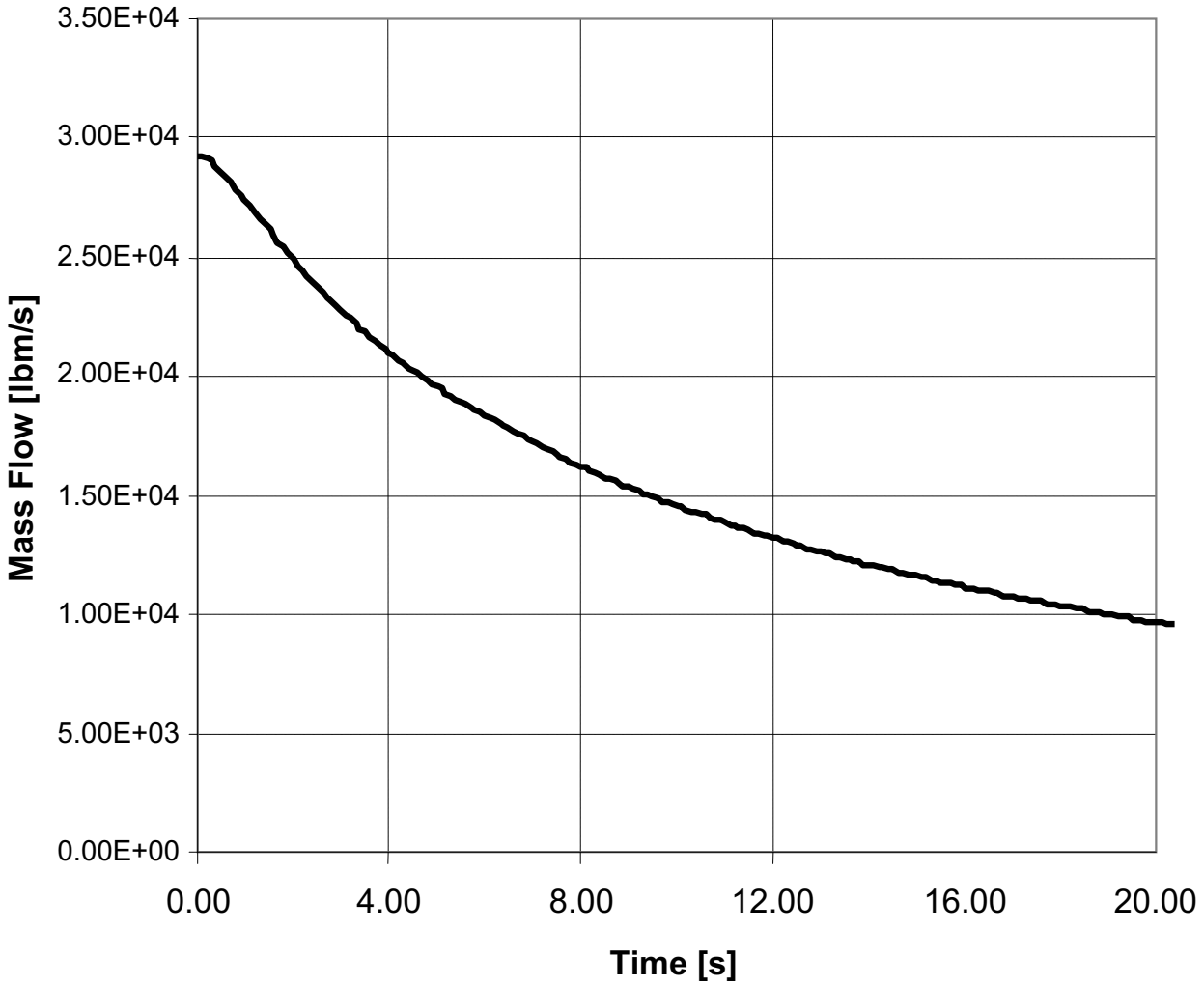

Figure 15.3-35
NUCLEAR POWER VS. TIME
LOSS OF FLOW EVENT
UNDERVOLTAGE

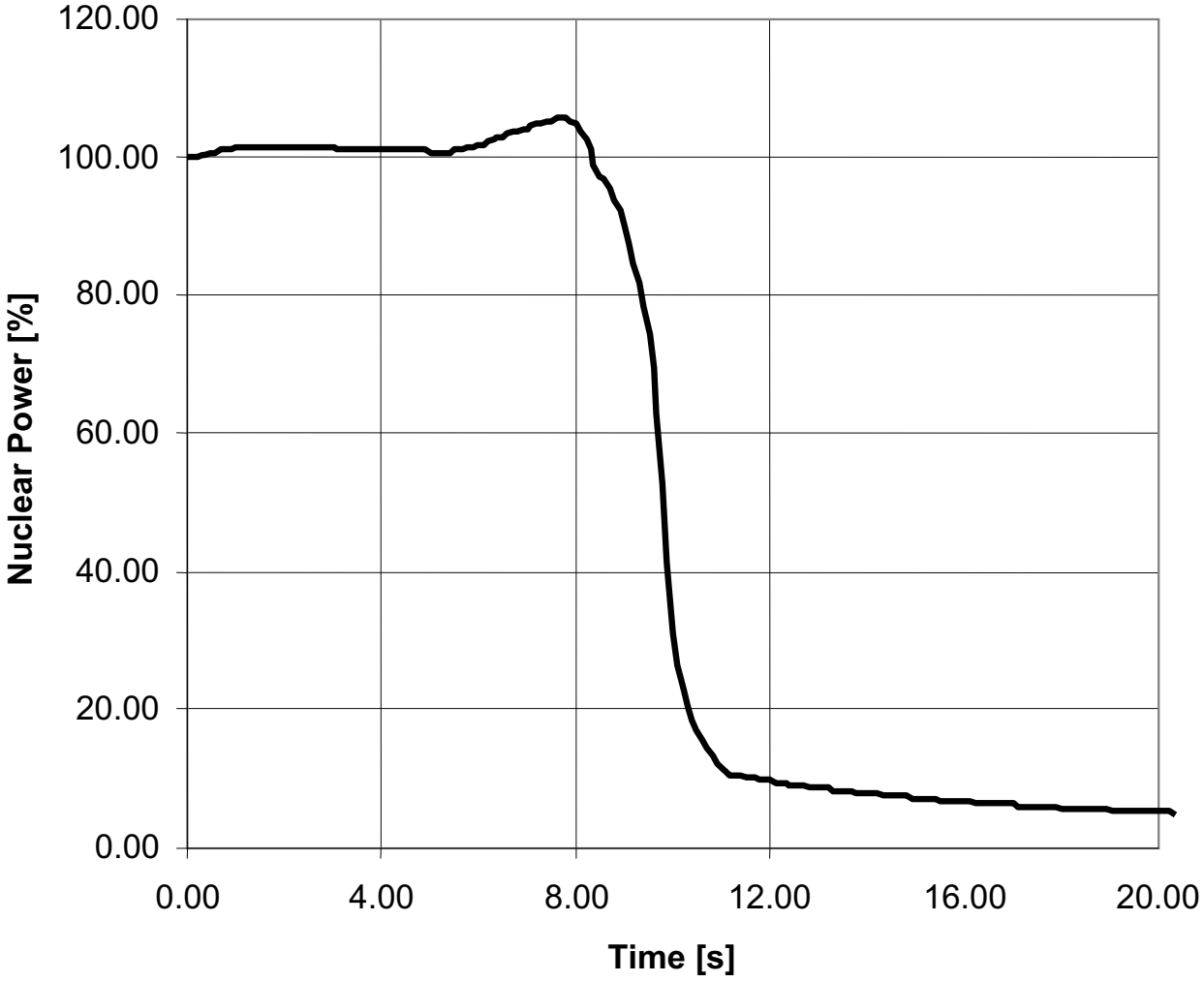

Figure 15.3-36
CORE AVERAGE HEAT FLUX VS. TIME
LOSS OF FLOW EVENT
UNDERVOLTAGE

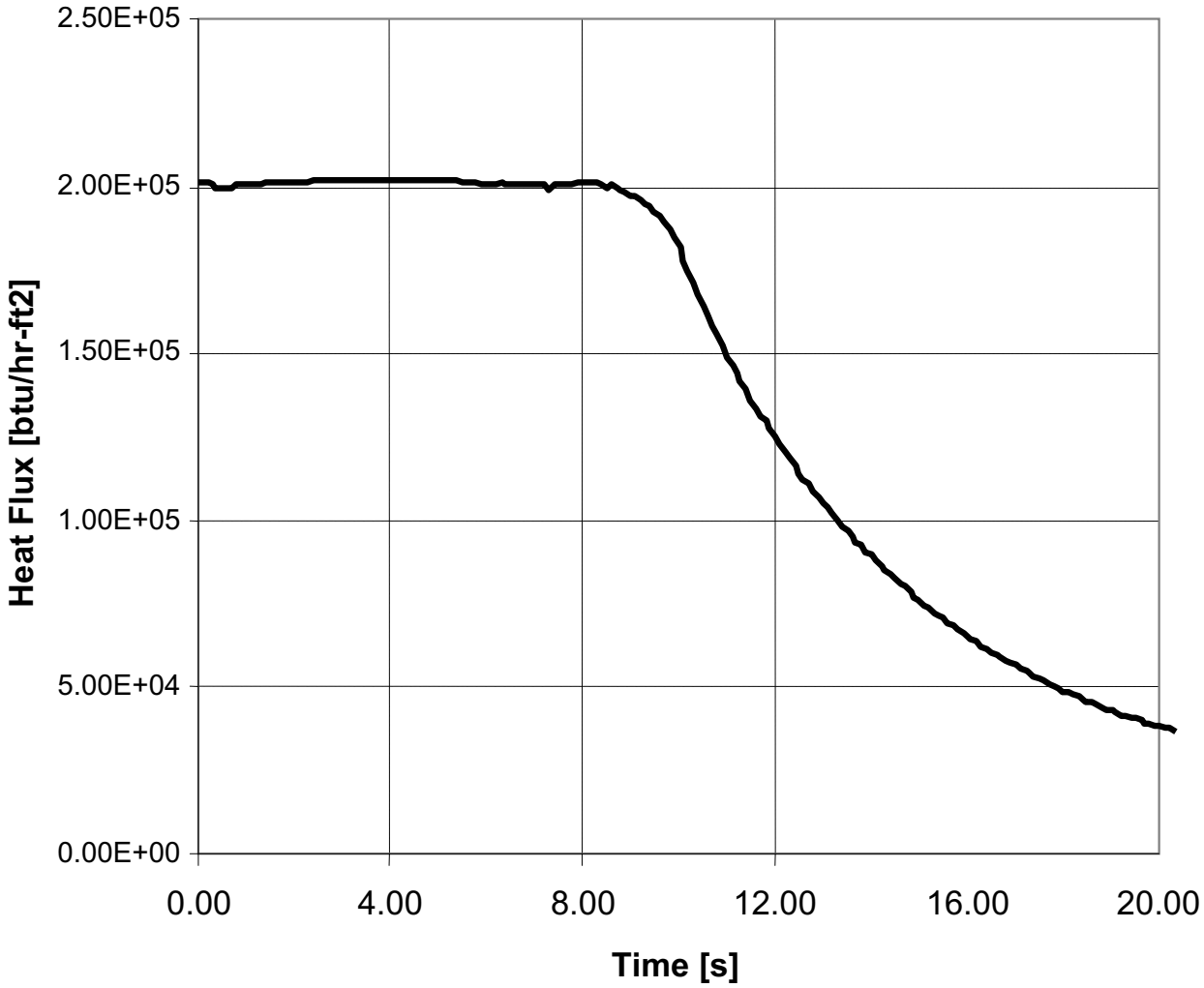

Figure 15.3-37
CORE INLET TEMPERATURE VS. TIME
LOSS OF FLOW EVENT
UNDERVOLTAGE

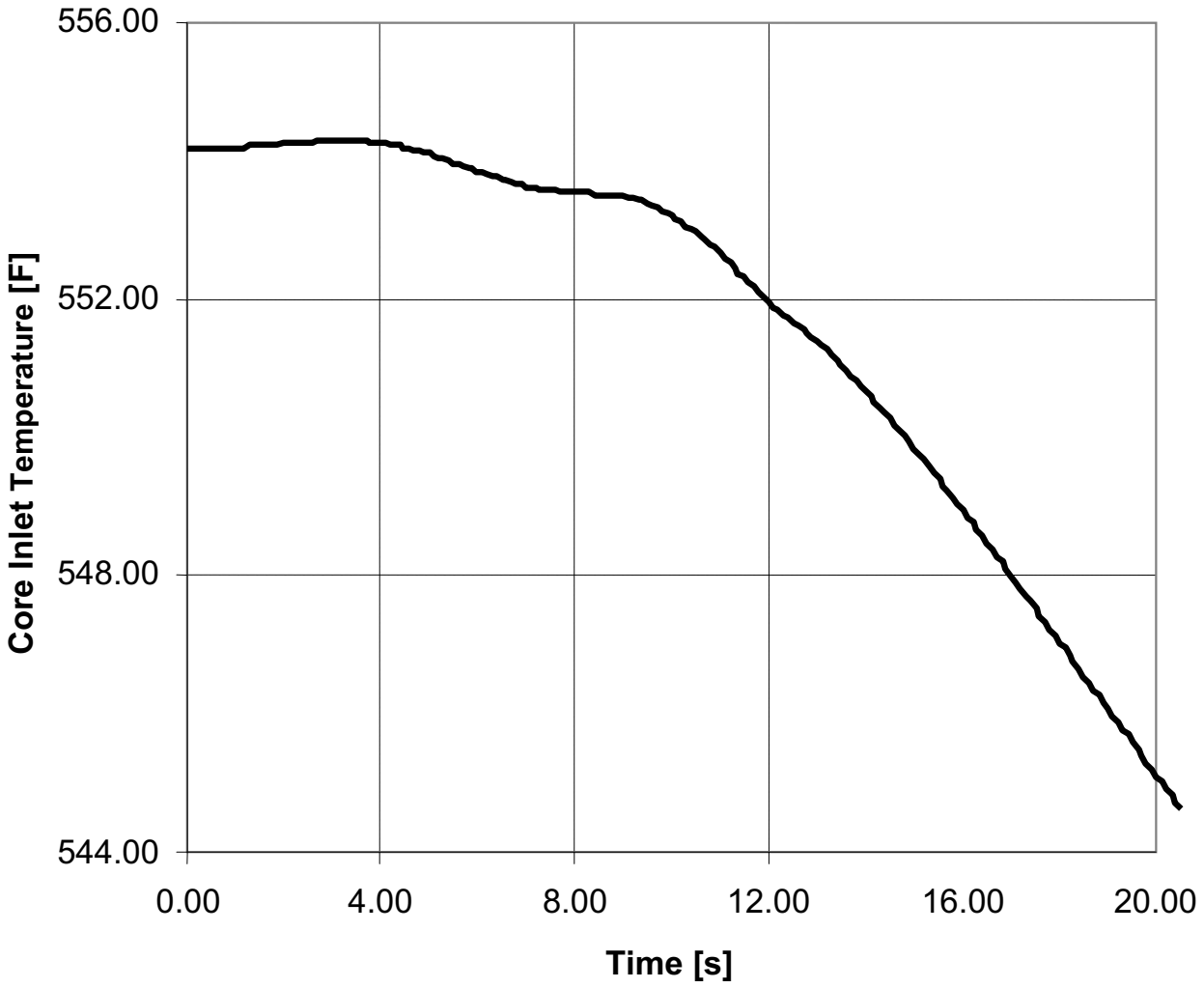

Figure 15.3-38
PRESSURIZER PRESSURE VS. TIME
LOSS OF FLOW EVENT
UNDERVOLTAGE

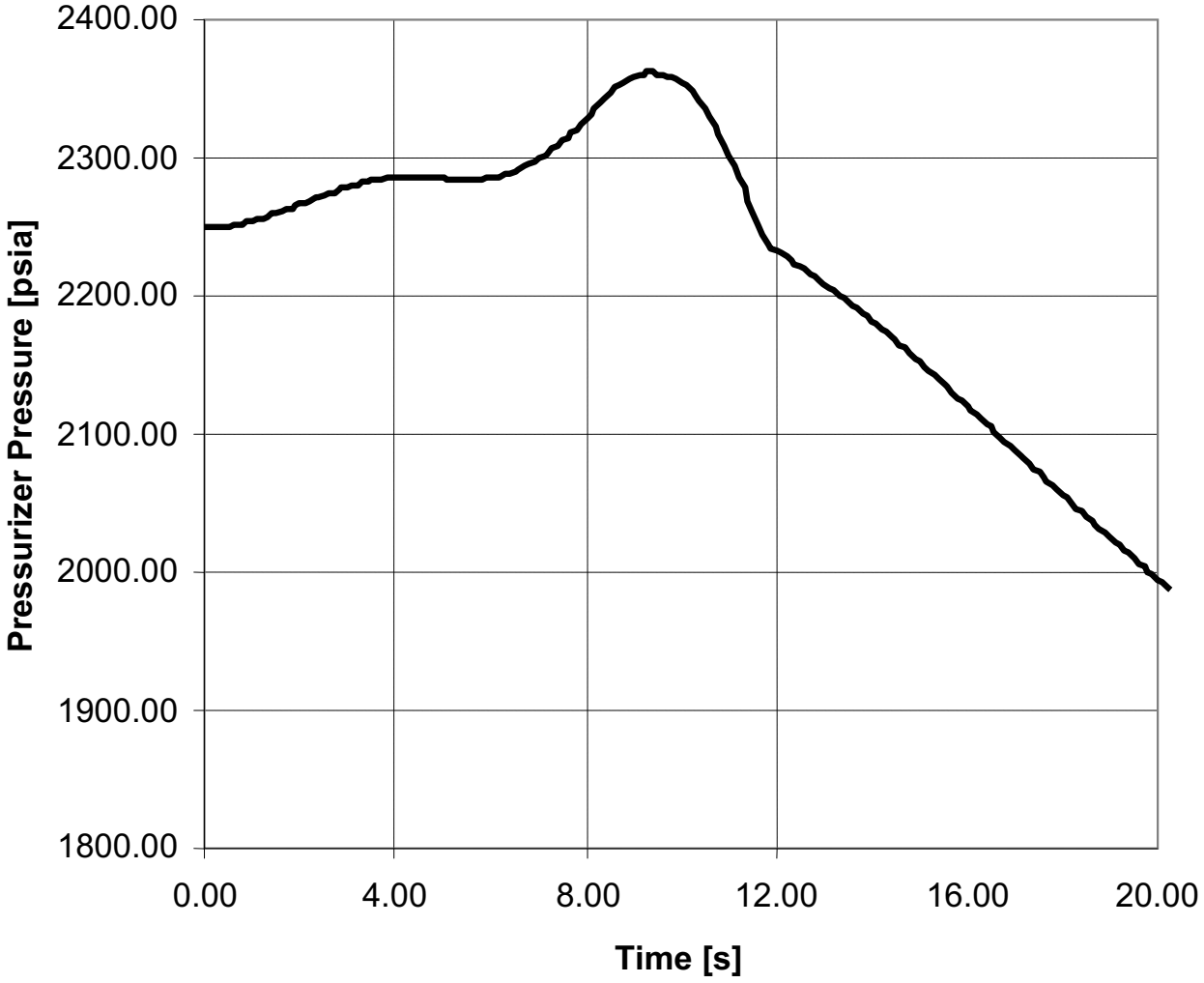

Figure 15.3-39
DNBR VS. TIME
LOSS OF FLOW EVENT
UNDERVOLTAGE

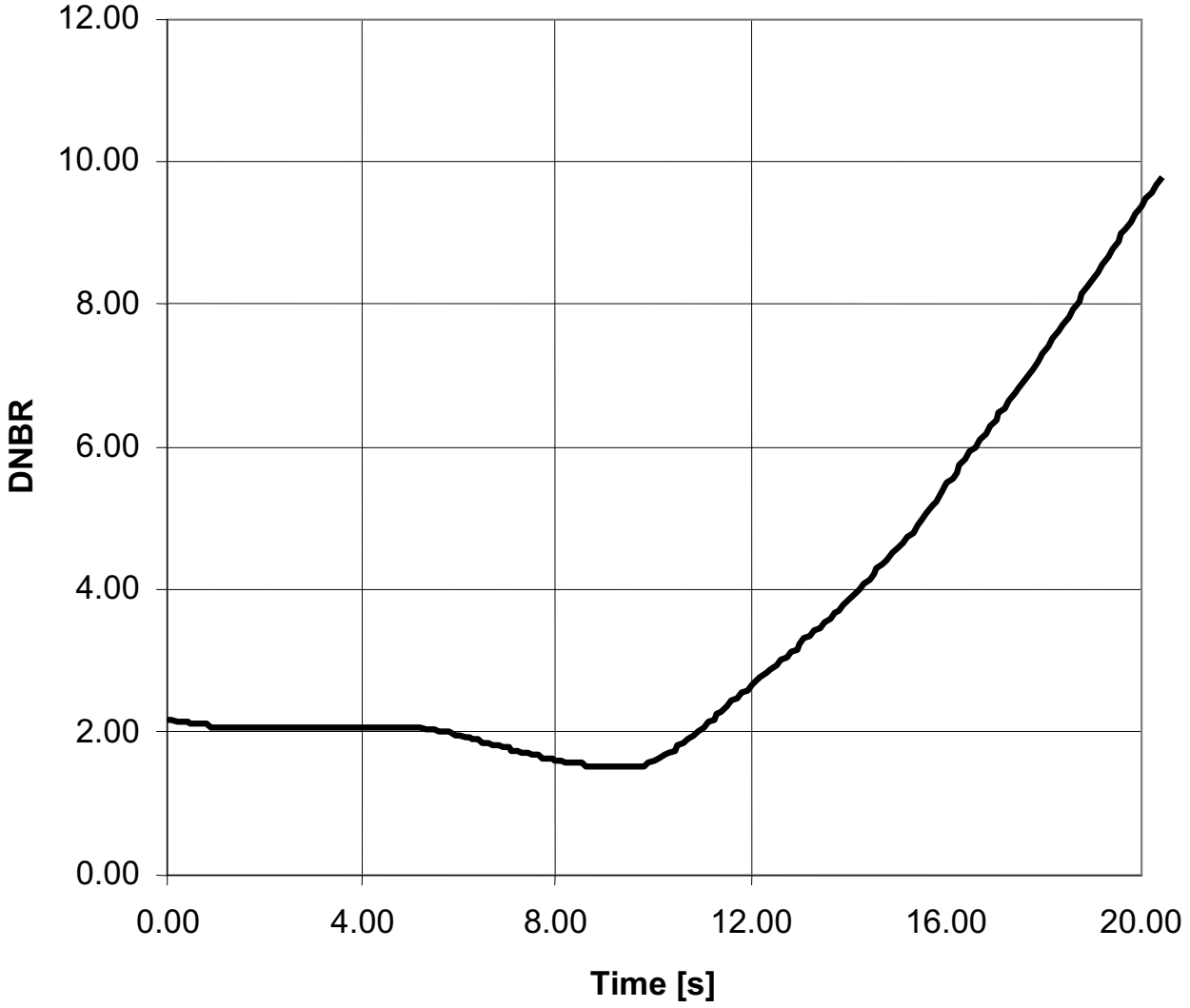

Figure 15.3-40
NUCLEAR POWER VS. TIME
LOSS OF FLOW EVENT
UNDERFREQUENCY

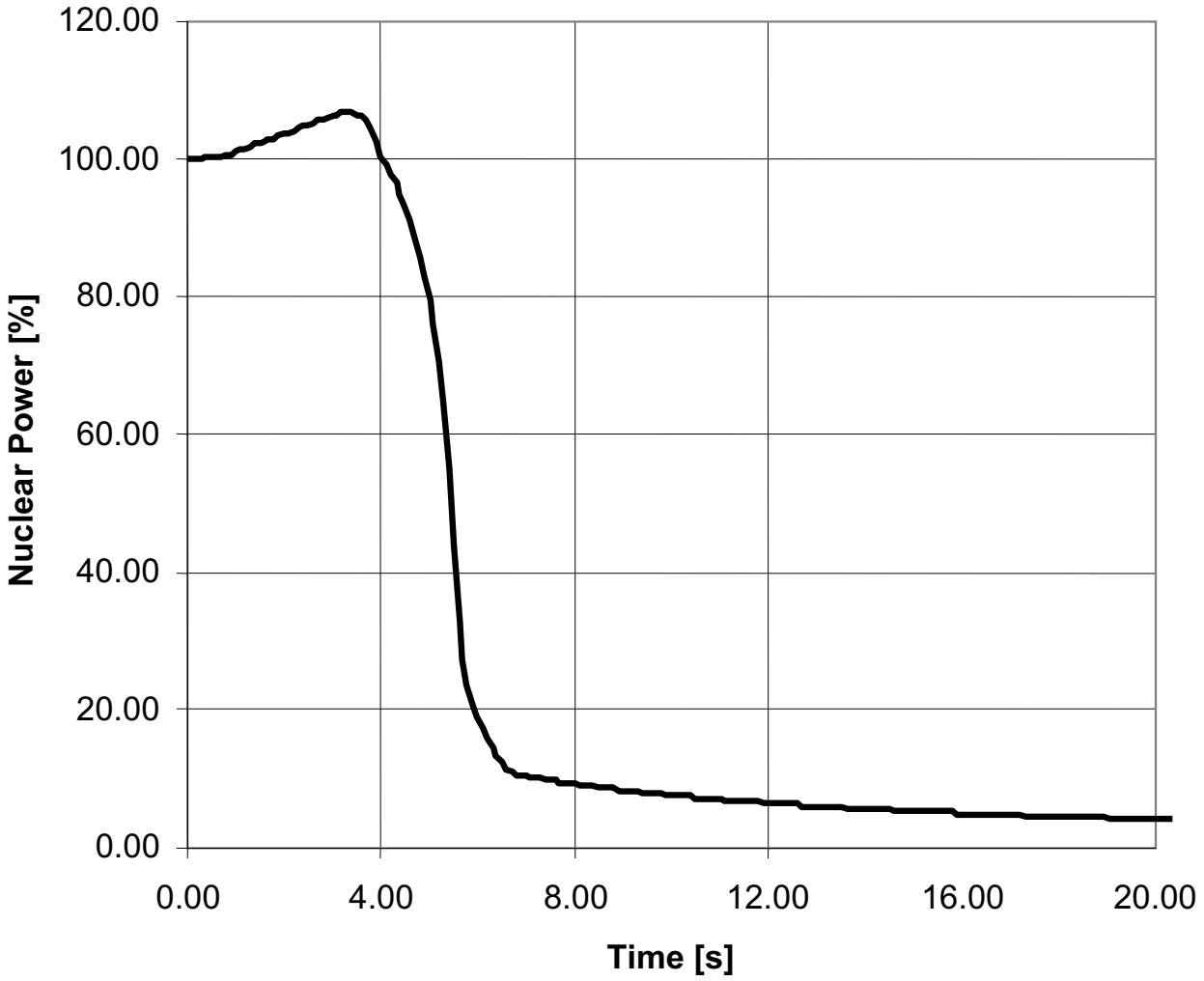

Figure 15.3-41
CORE AVERAGE HEAT FLUX VS. TIME
LOSS OF FLOW EVENT
UNDERFREQUENCY

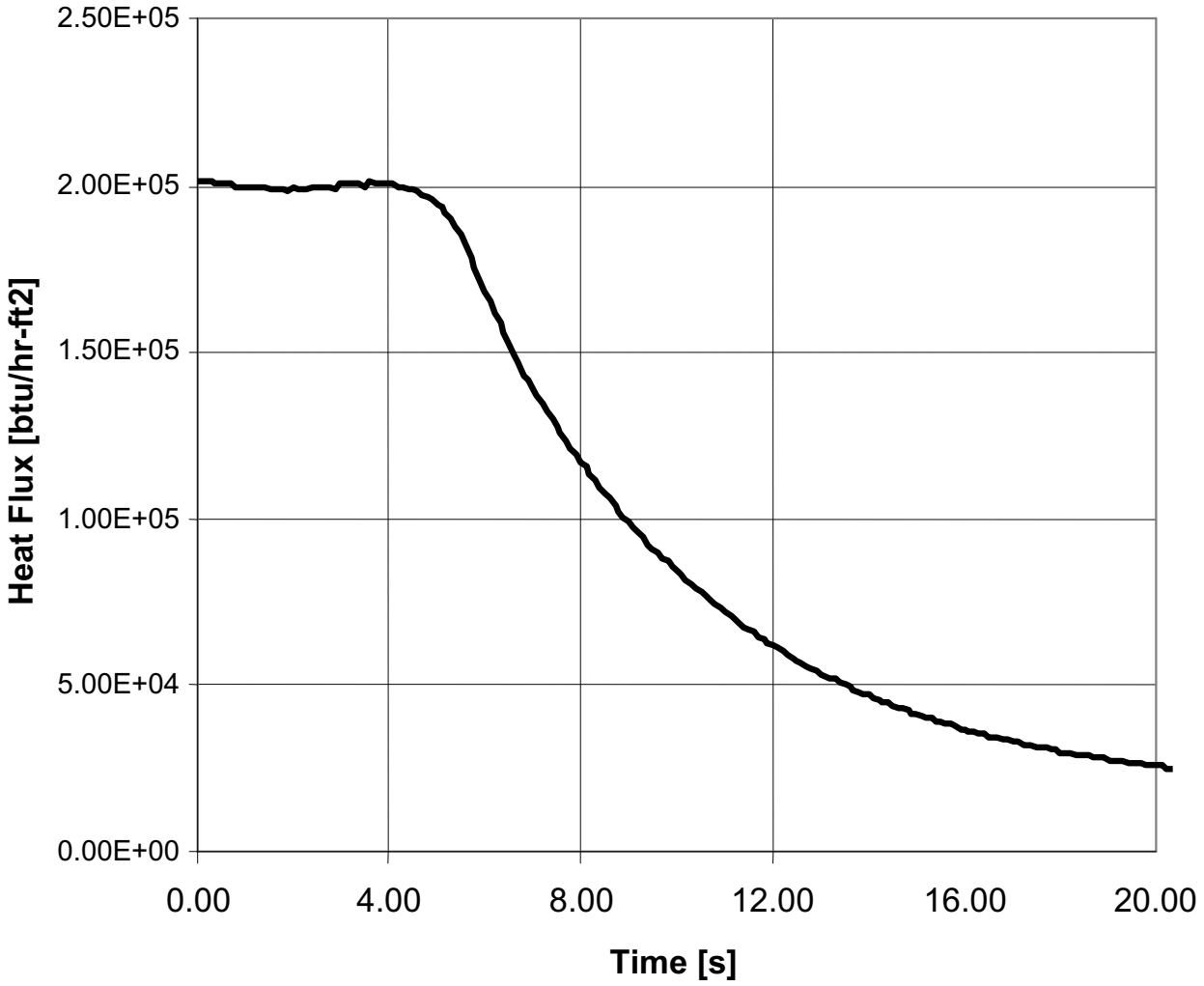

Figure 15.3-42
CORE INLET TEMPERATURE VS. TIME
LOSS OF FLOW EVENT
UNDERFREQUENCY

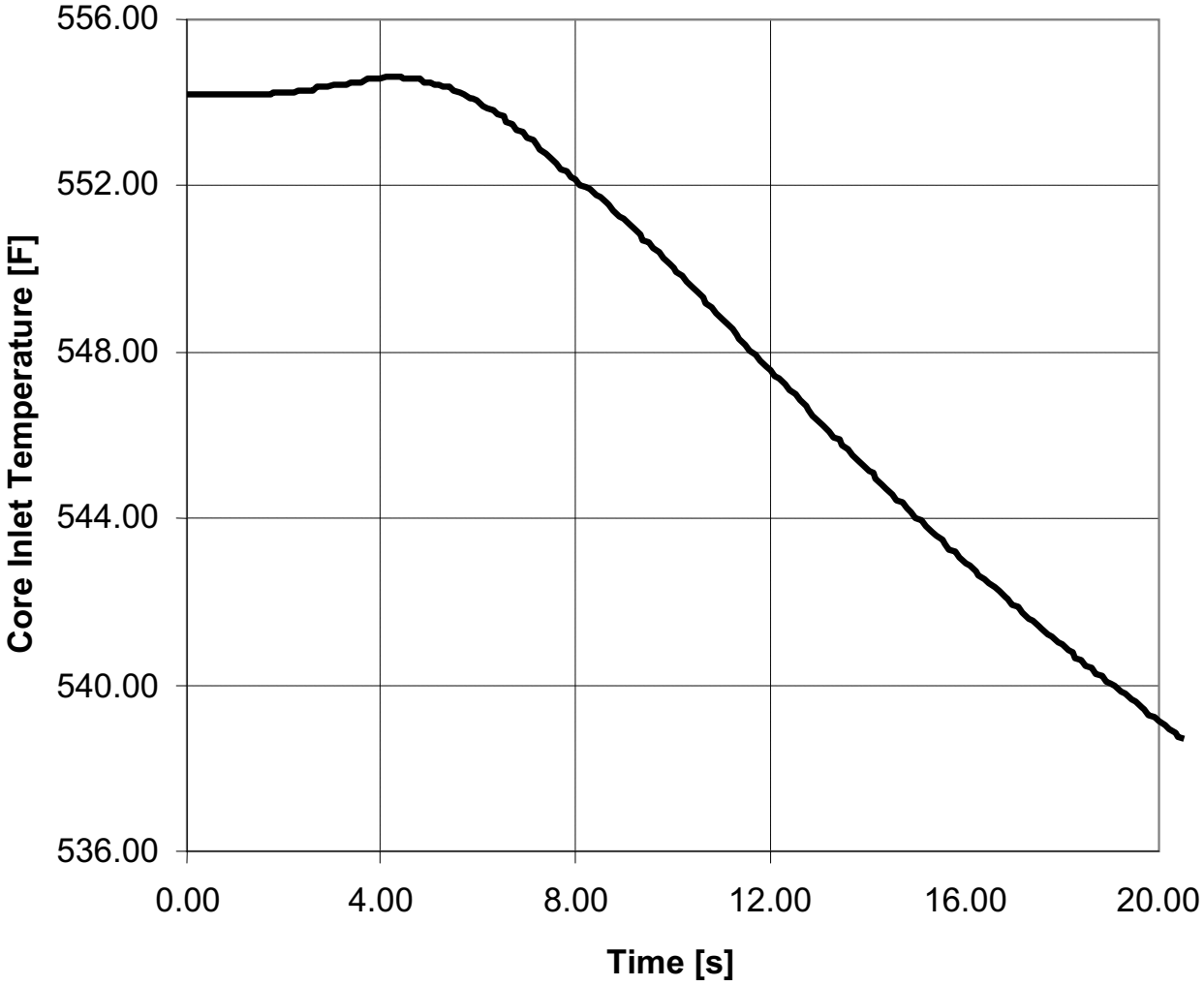

Figure 15.3-43
PRESSURIZER PRESSURE VS. TIME
LOSS OF FLOW EVENT
UNDERFREQUENCY

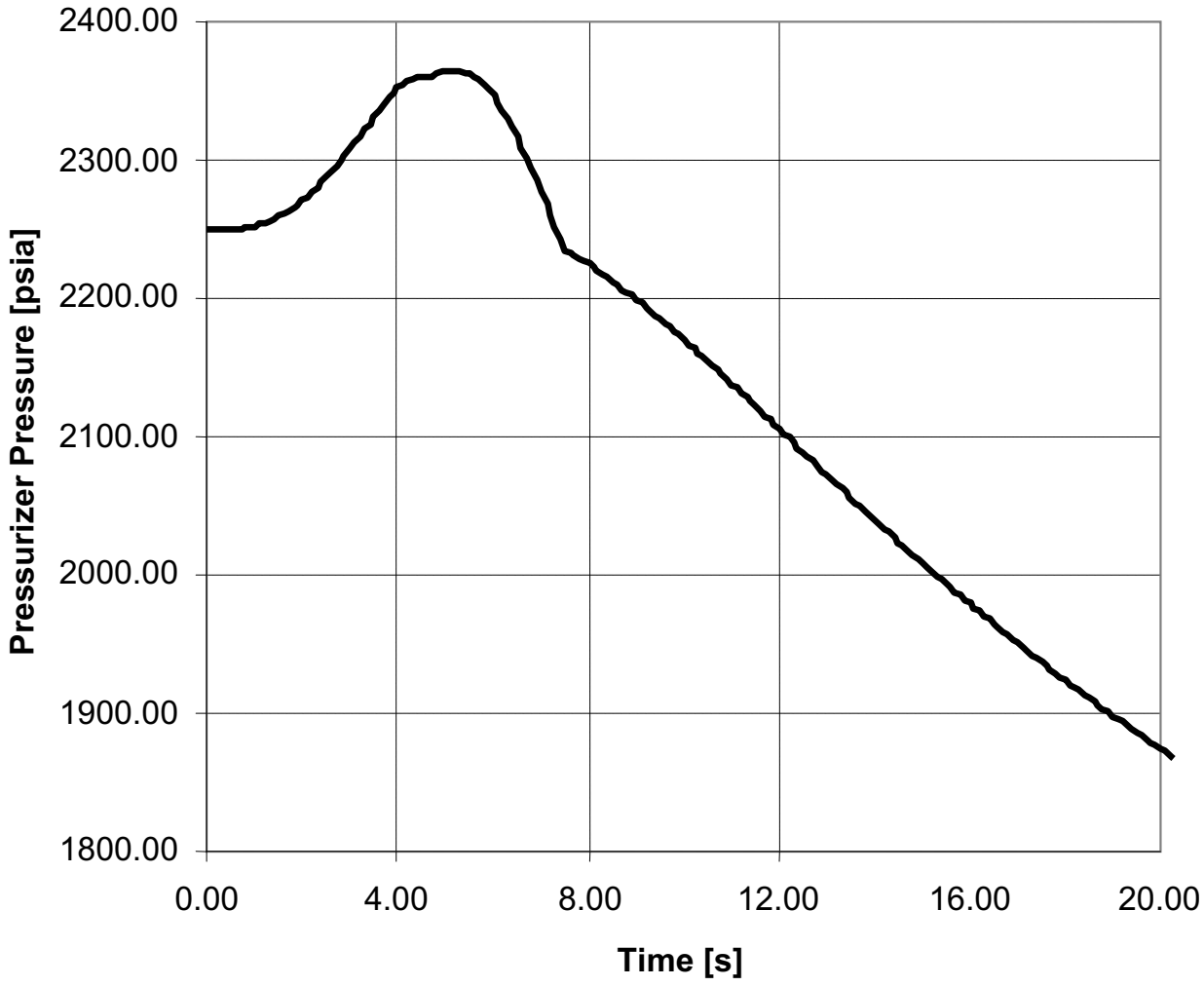

Figure 15.3-44
DNBR VS. TIME
LOSS OF FLOW EVENT
UNDERFREQUENCY

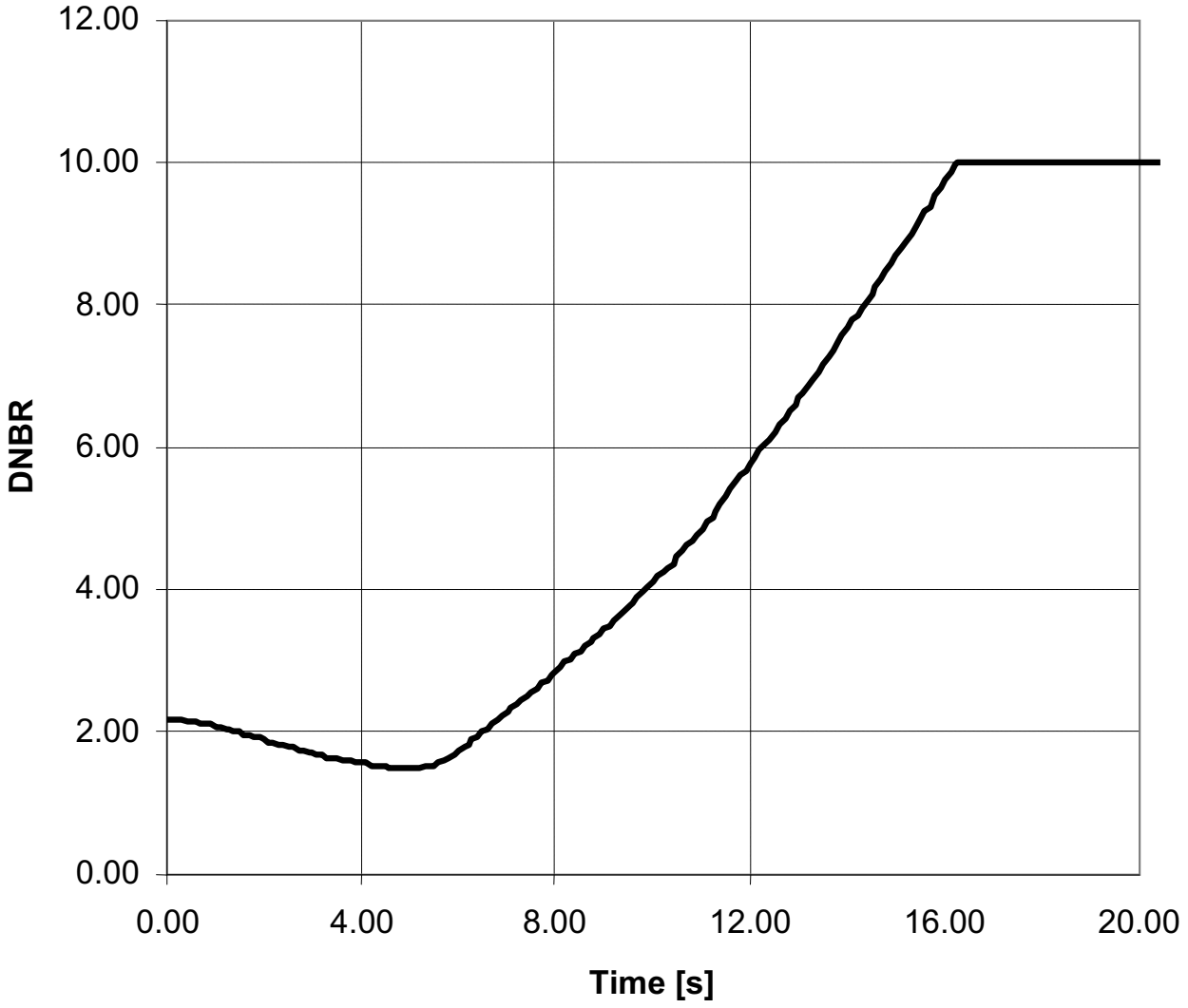

Figure 15.3-45
NORTH ANNA UNITS 1 AND 2 RELAP5 SBLOCA LOOP NODING DIAGRAM

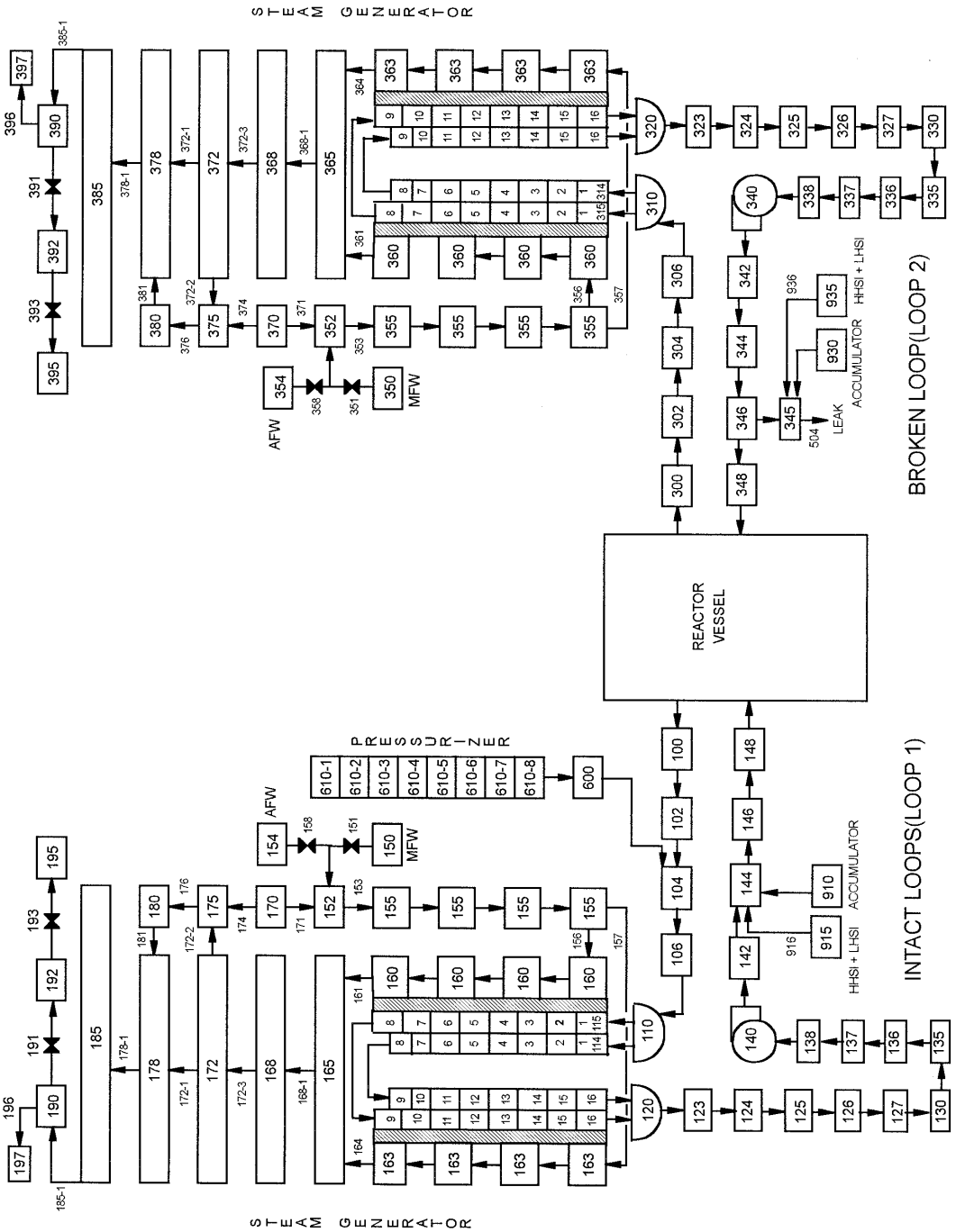

Figure 15.3-46
NORTH ANNA UNIT 1 RELAP5 CORE NODING DIAGRAM

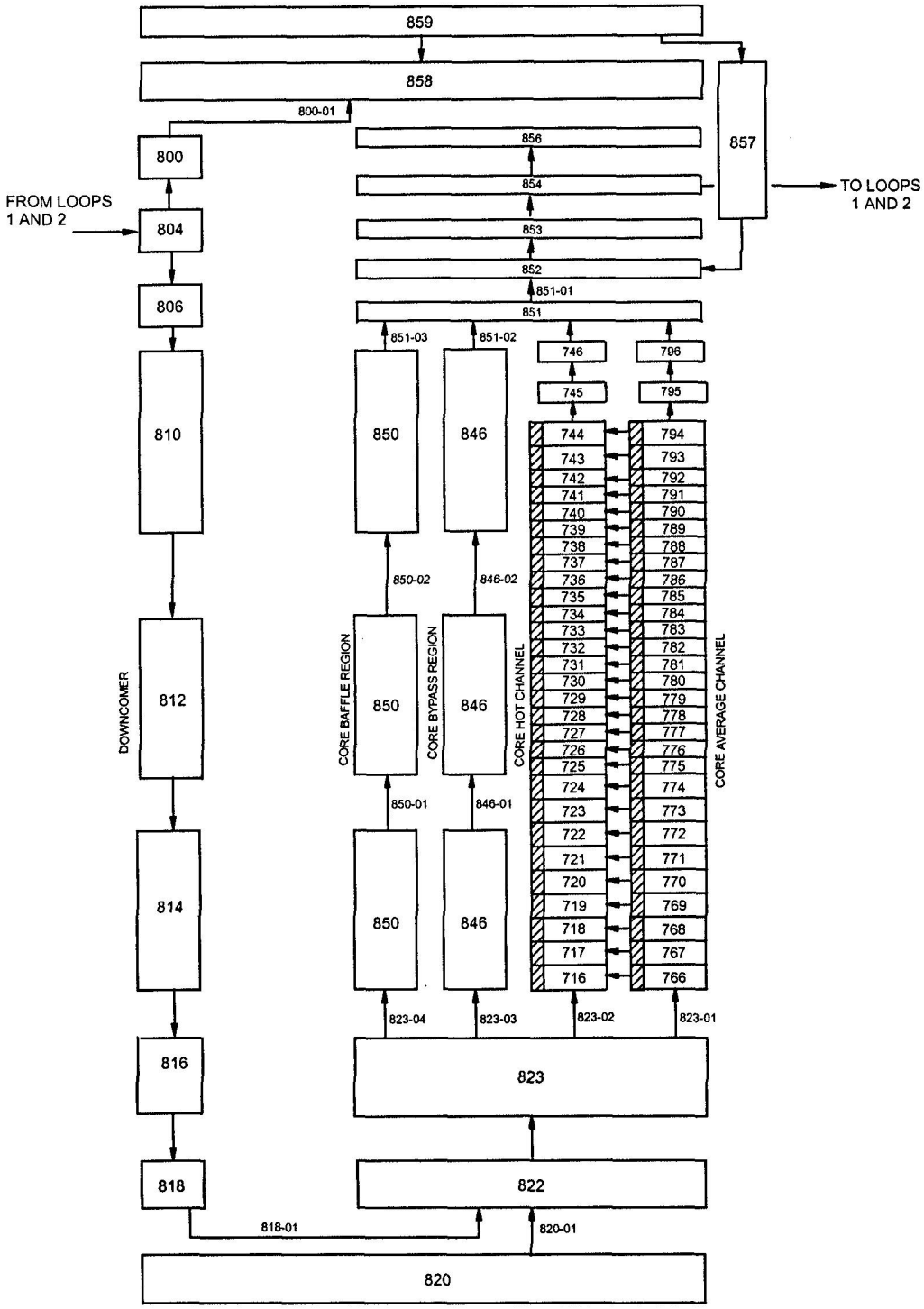

Figure 15.3-47
NORTH ANNA UNIT 2 RELAP5 CORE NODING DIAGRAM

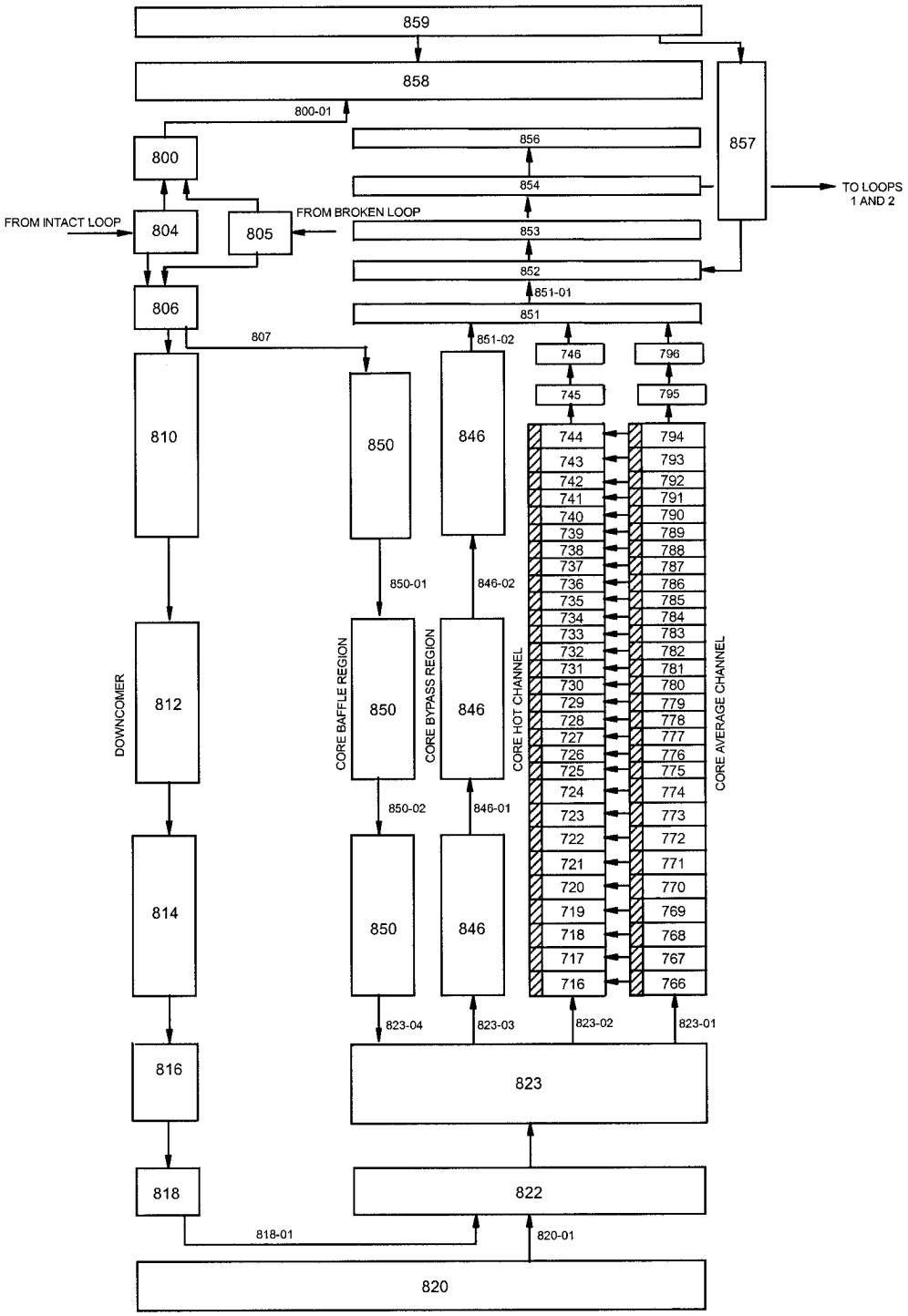

Figure 15.3-48
NORTH ANNA UNITS 1 AND 2 SMALL BREAK LOCA K_z CURVE

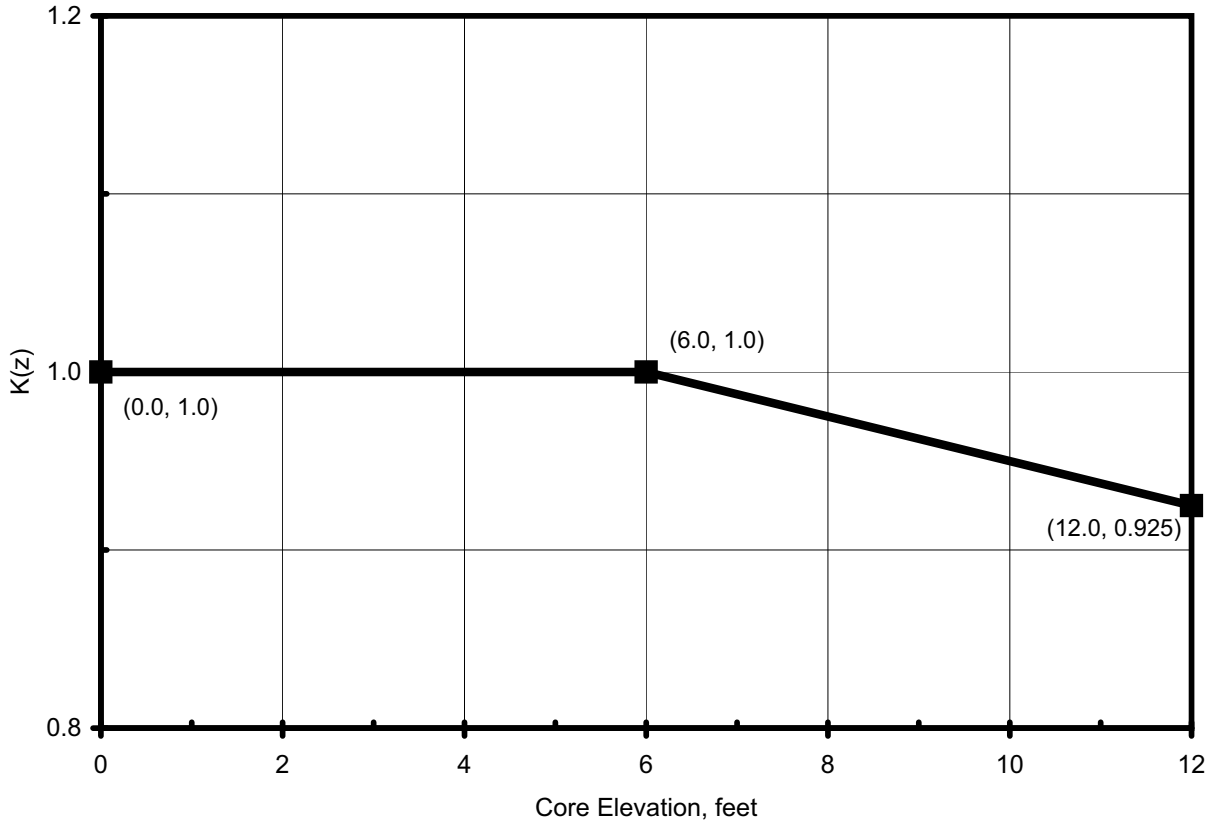

Figure 15.3-49
NORTH ANNA UNITS 1 AND 2 SMALL BREAK LOCA AXIAL POWER PROFILE

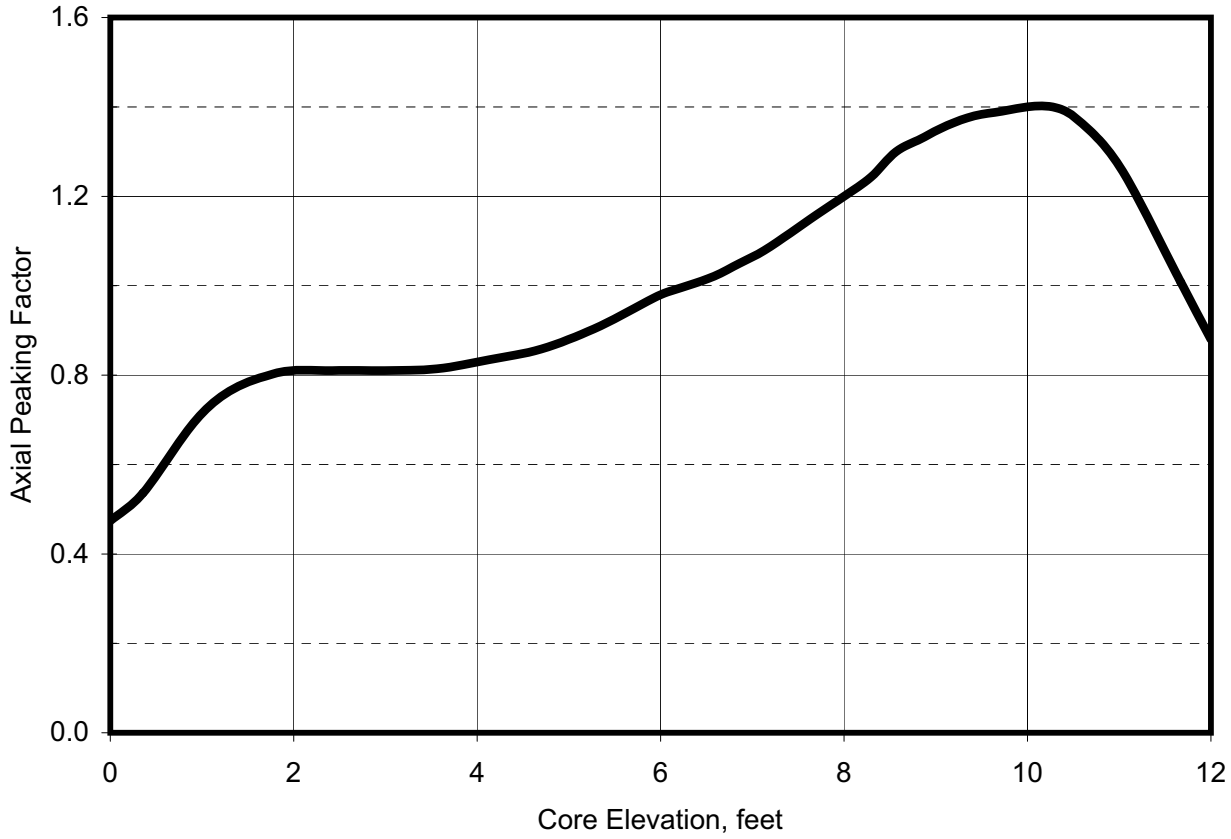

Figure 15.3-50
NORTH ANNA UNIT 1: RCS PRESSURE—2-INCH BREAK

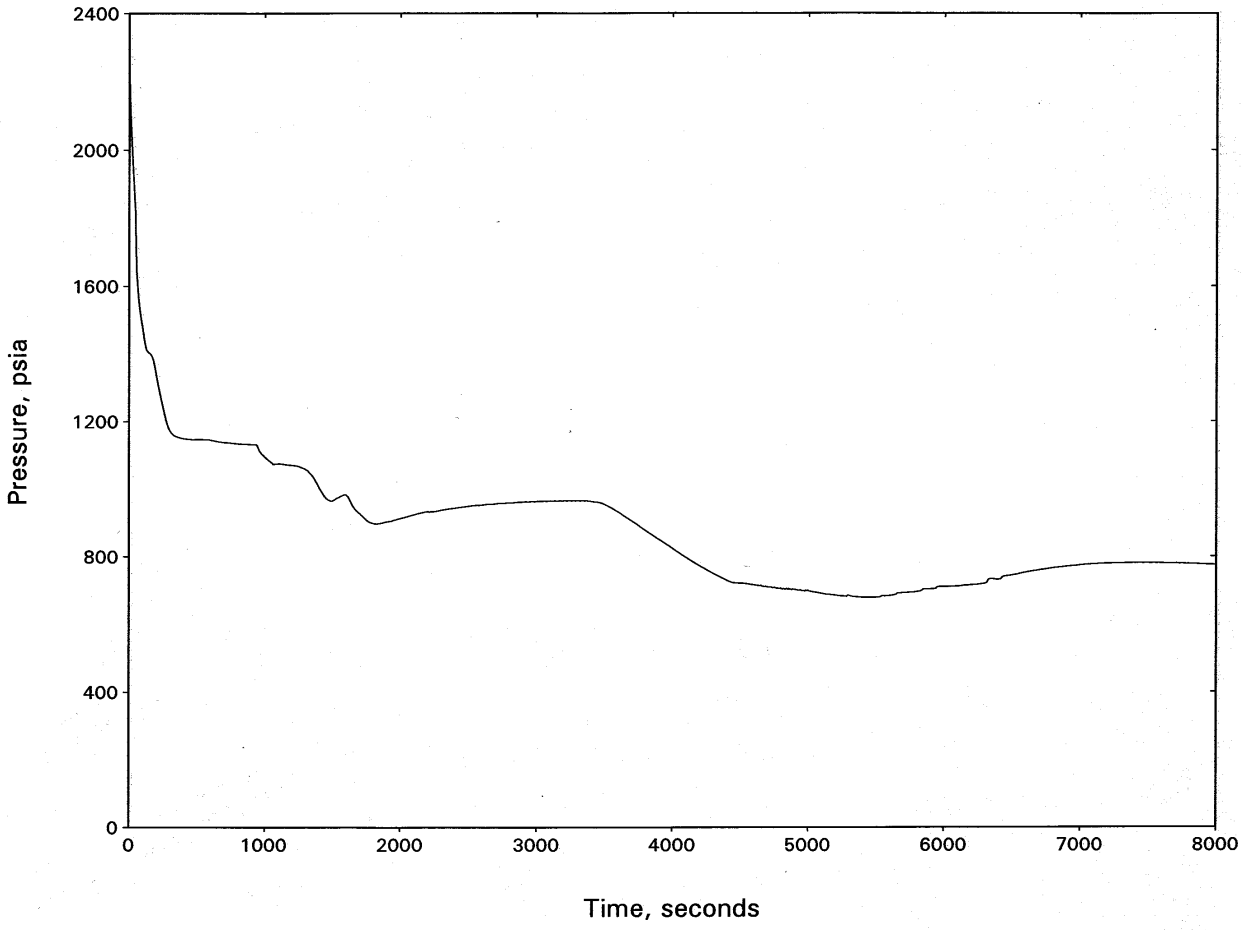

Figure 15.3-51
NORTH ANNA UNIT 1: BREAK FLOW—2-INCH BREAK

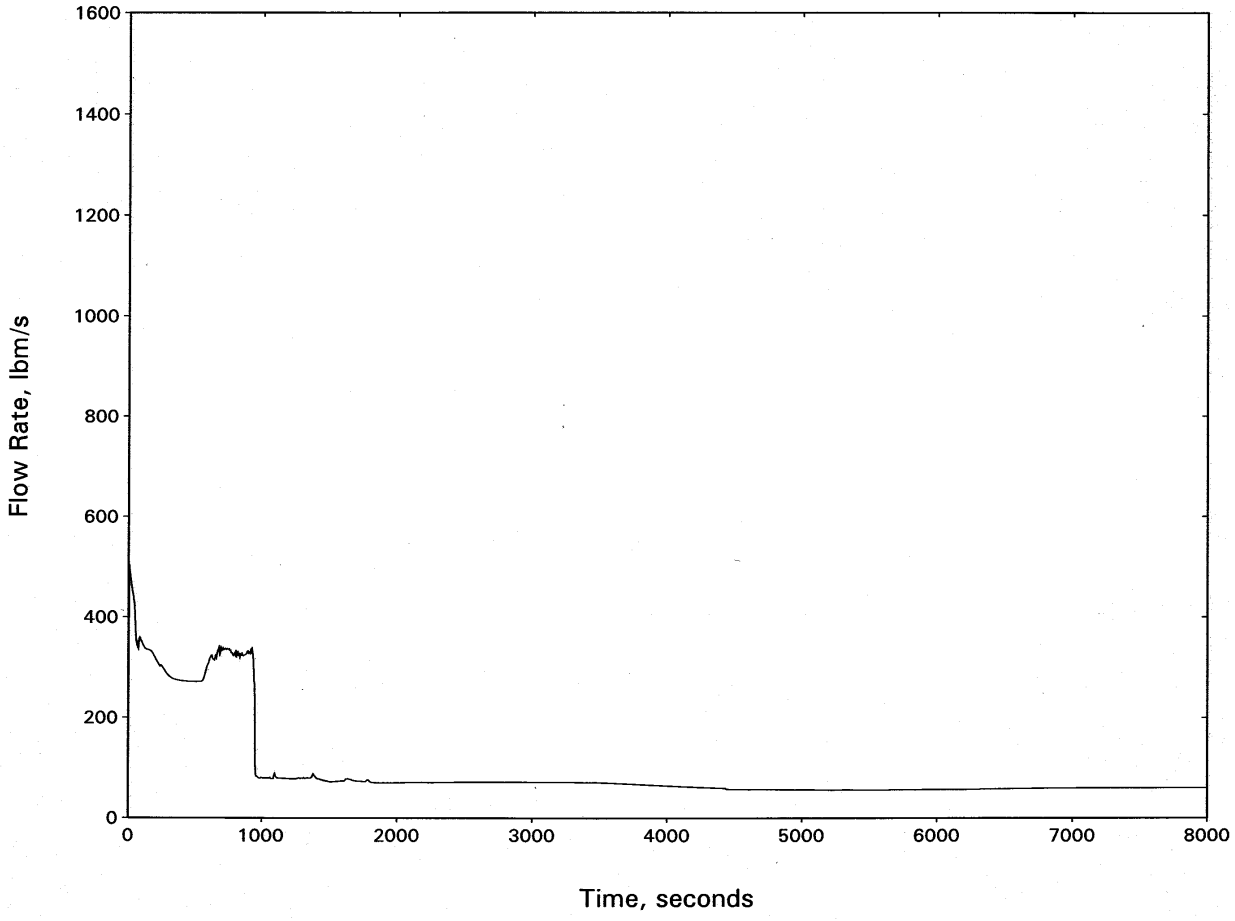

Figure 15.3-52
NORTH ANNA UNIT 1: HOT CHANNEL MIXTURE LEVEL—2-INCH BREAK

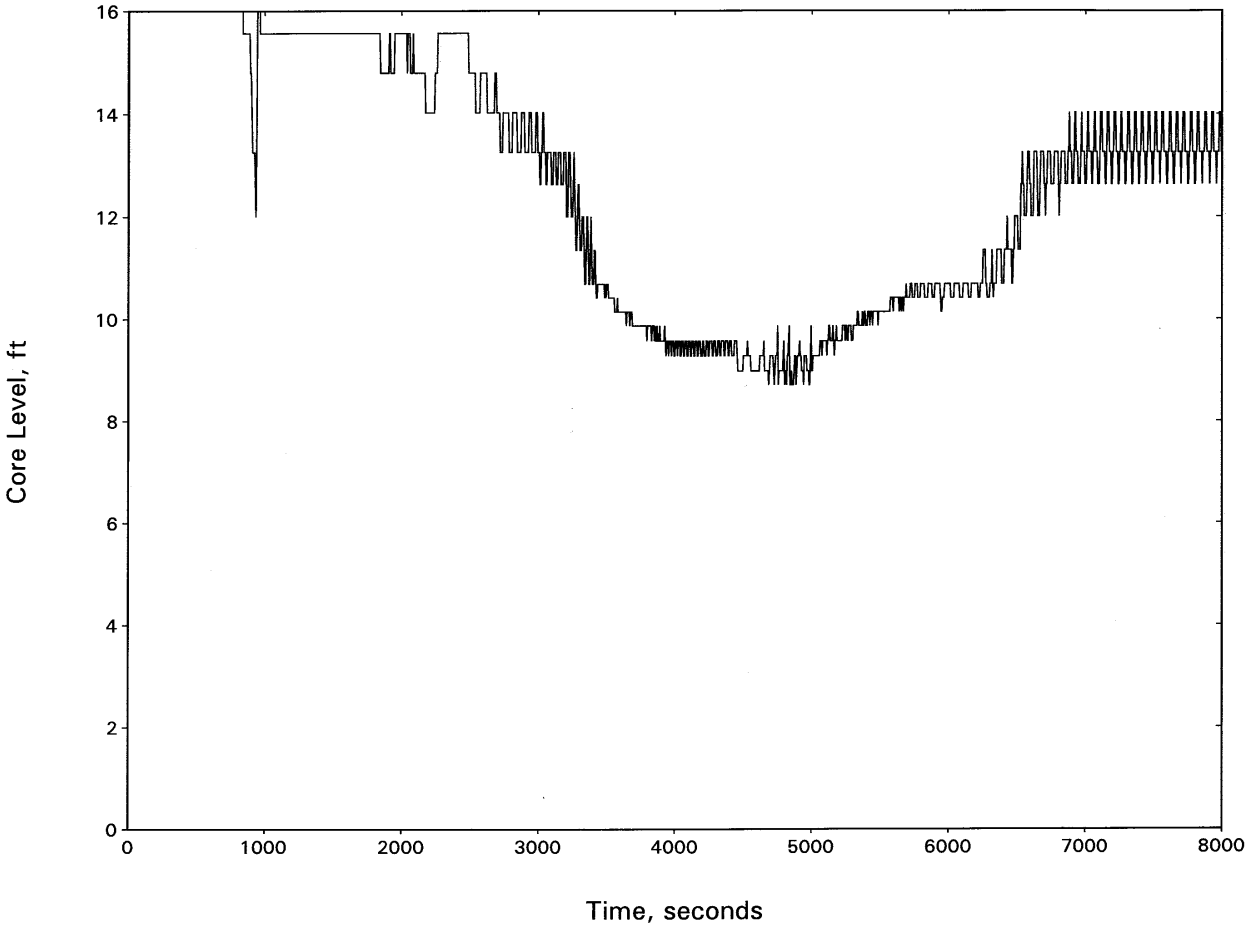

Figure 15.3-53
NORTH ANNA UNIT 1: HOT SPOT PCT—2-INCH BREAK

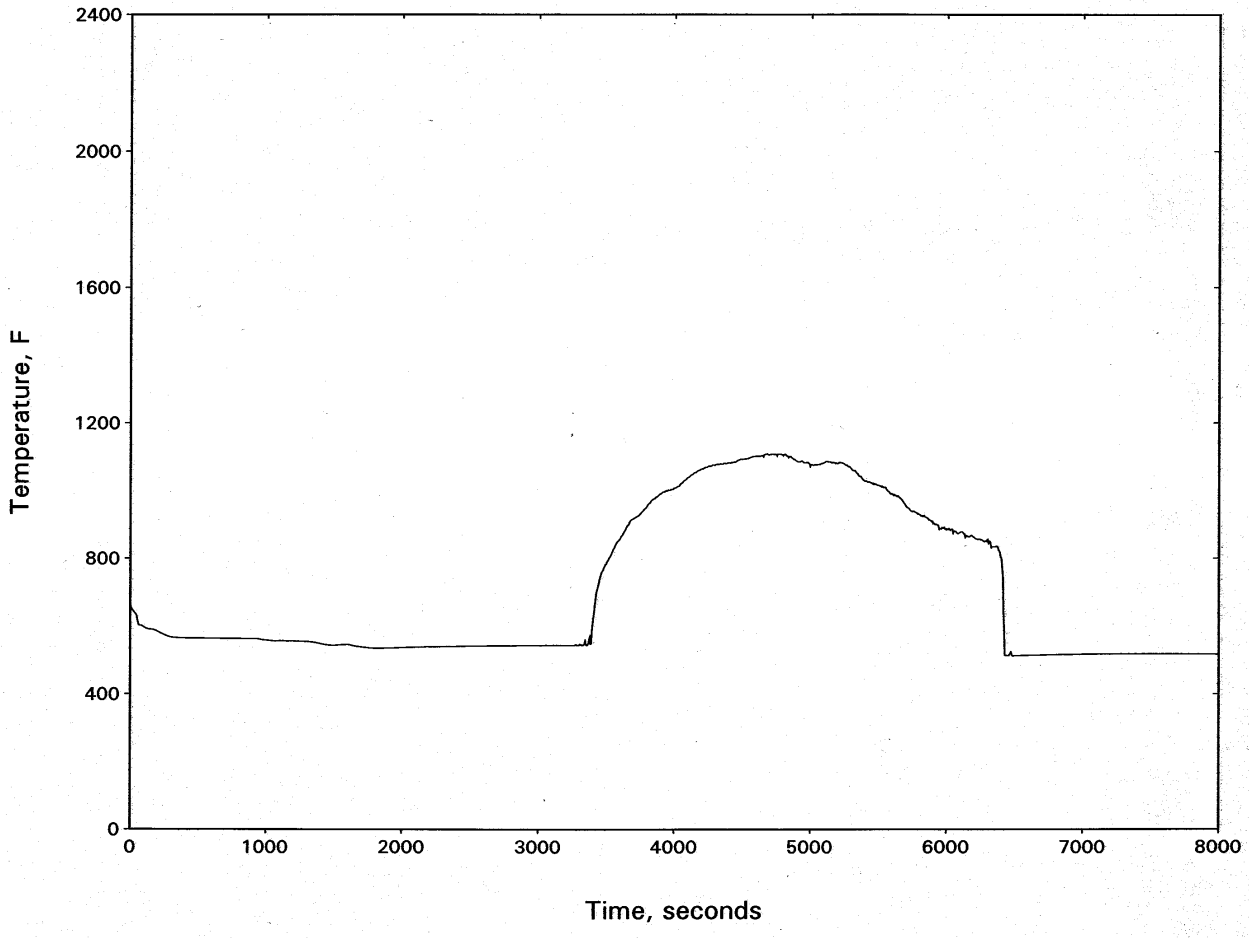

Figure 15.3-54
NORTH ANNA UNIT 1:
HOT CHANNEL OUTLET VAPOR TEMPERATURE—2-INCH BREAK

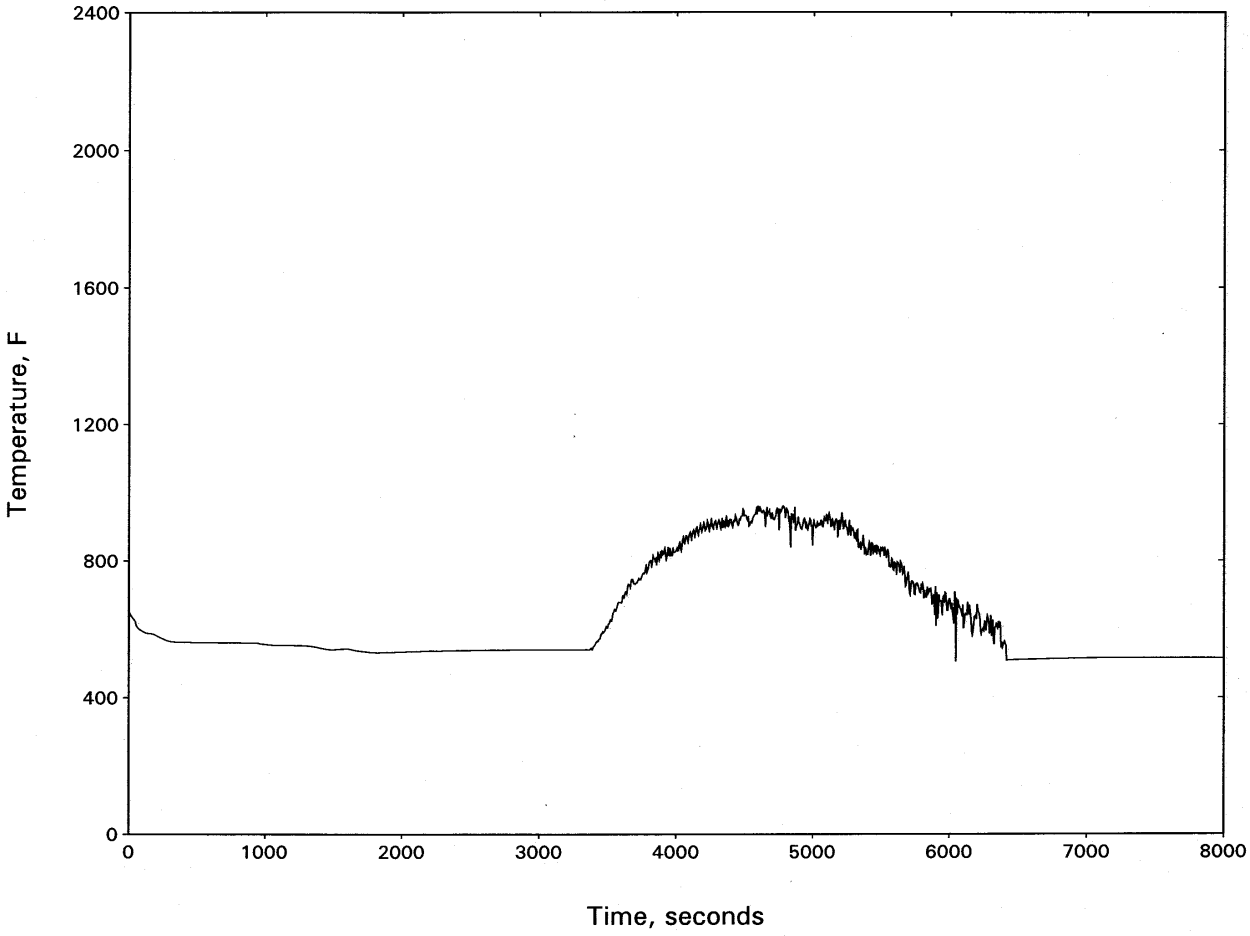

Figure 15.3-55
NORTH ANNA UNIT 1: INTACT LOOP SEAL LEVEL—2-INCH BREAK

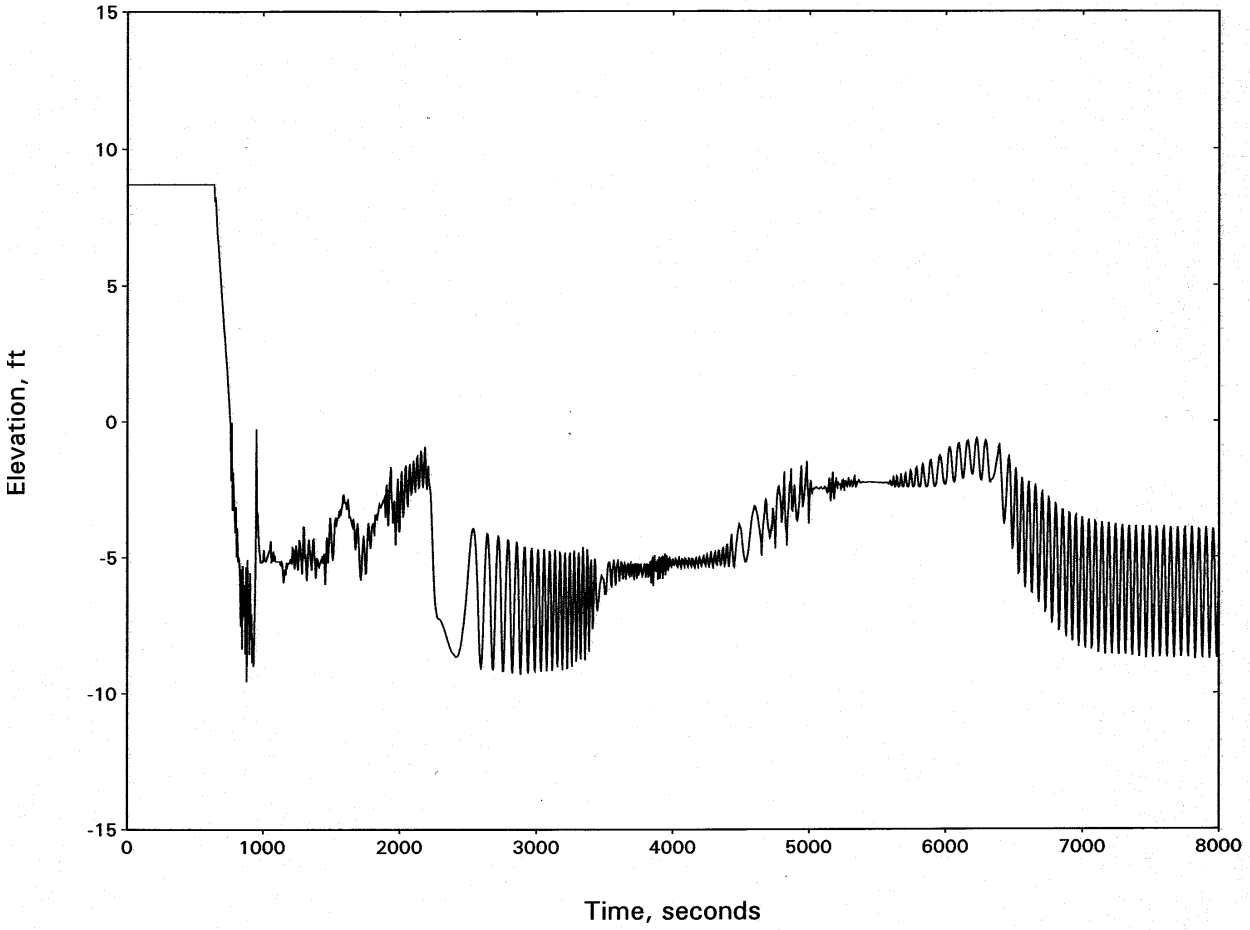

Figure 15.3-56
NORTH ANNA UNIT 1: BROKEN LOOP SEAL LEVEL—2-INCH BREAK

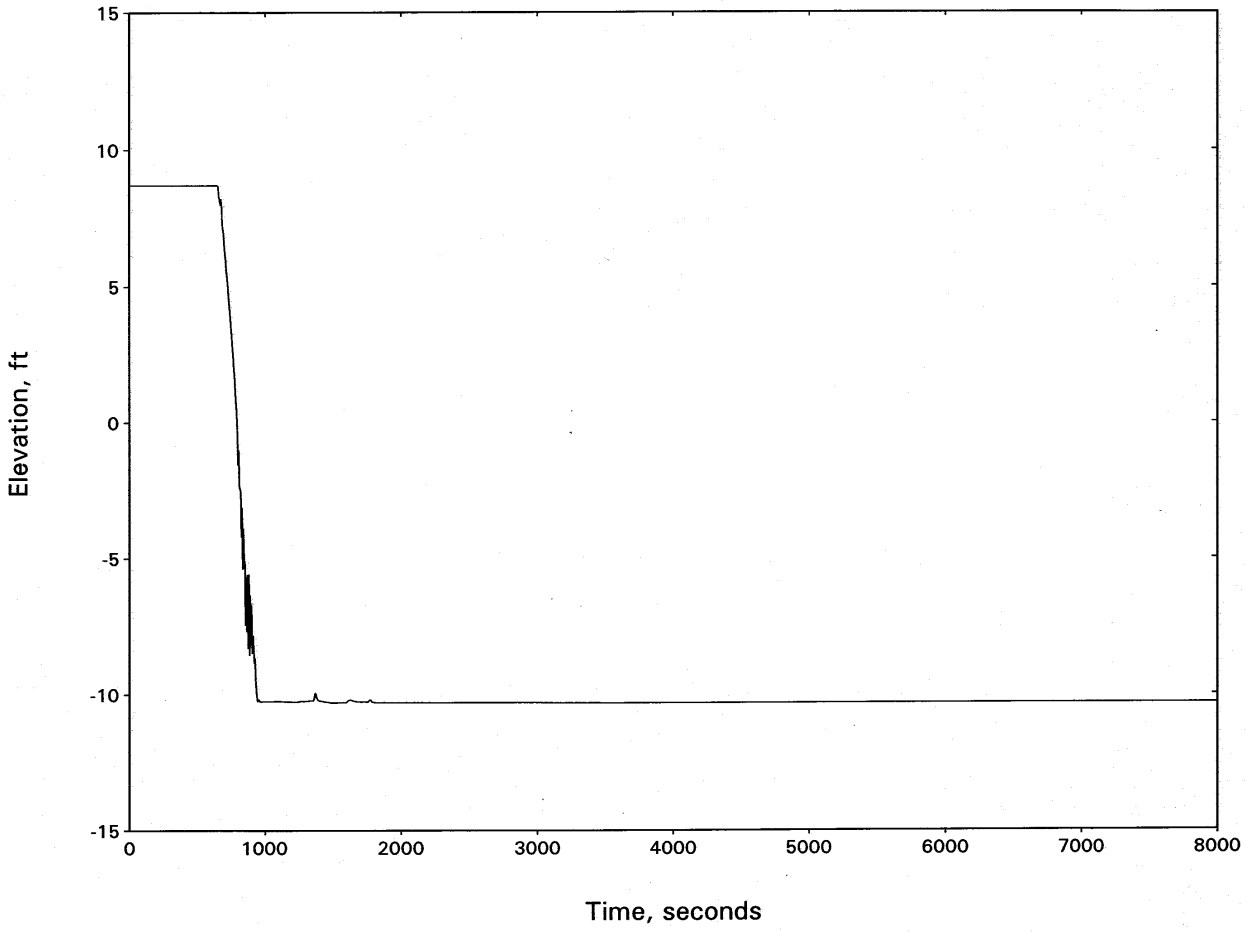

Figure 15.3-57
NORTH ANNA UNIT 1: RCS PRESSURE—2.5-INCH BREAK

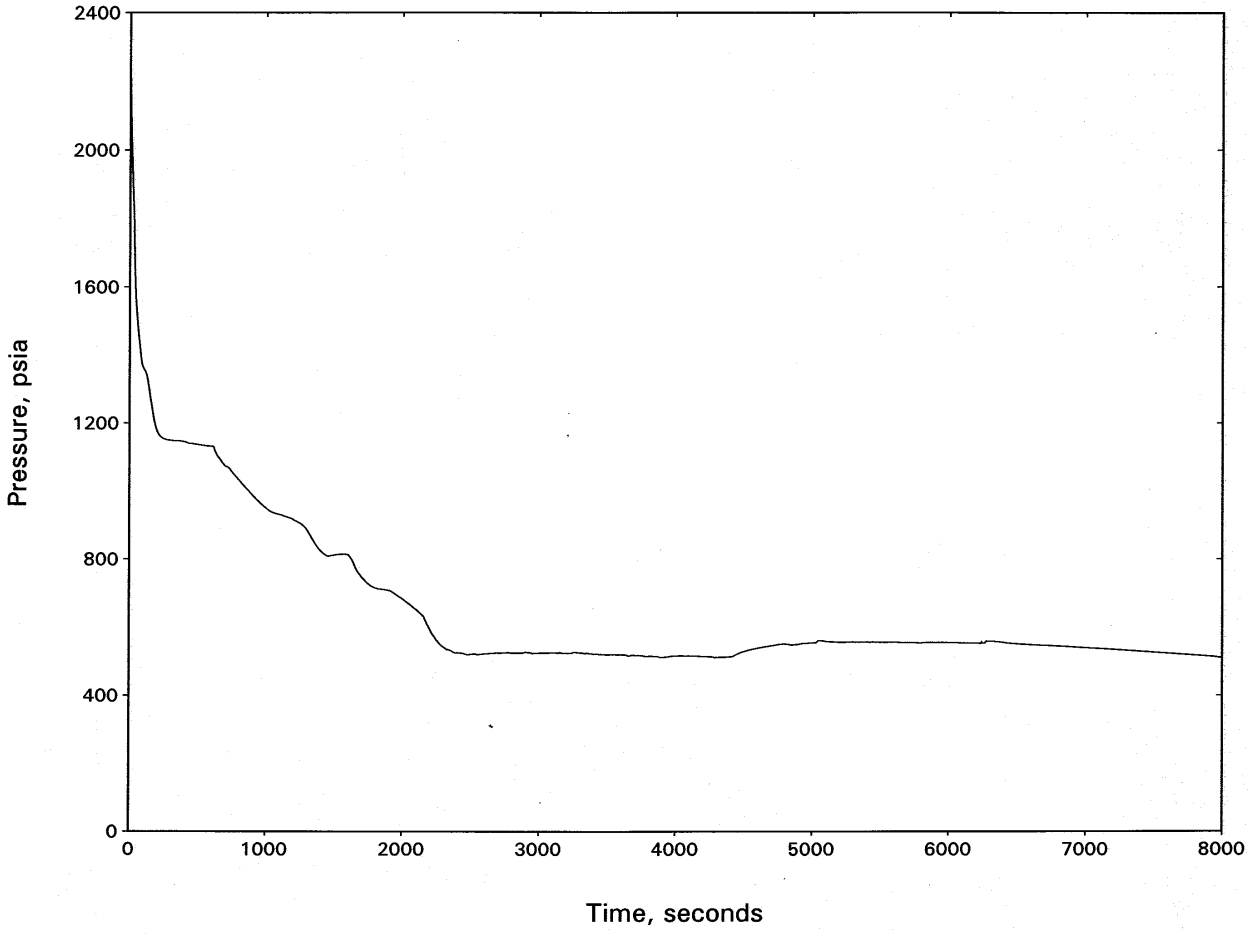

Figure 15.3-58
NORTH ANNA UNIT 1: BREAK FLOW—2.5-INCH BREAK

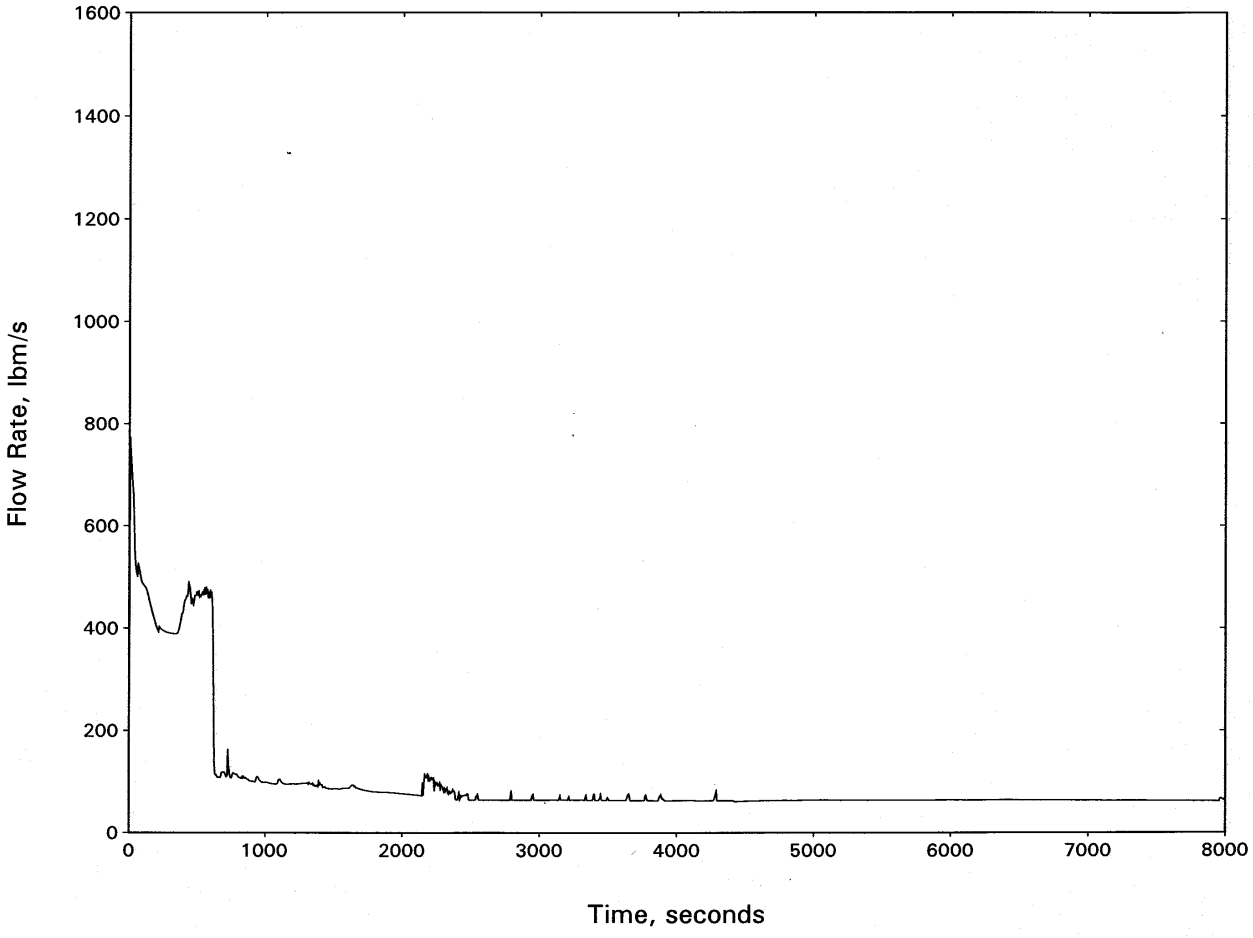

Figure 15.3-59
NORTH ANNA UNIT 1: HOT CHANNEL MIXTURE LEVEL—2.5-INCH BREAK

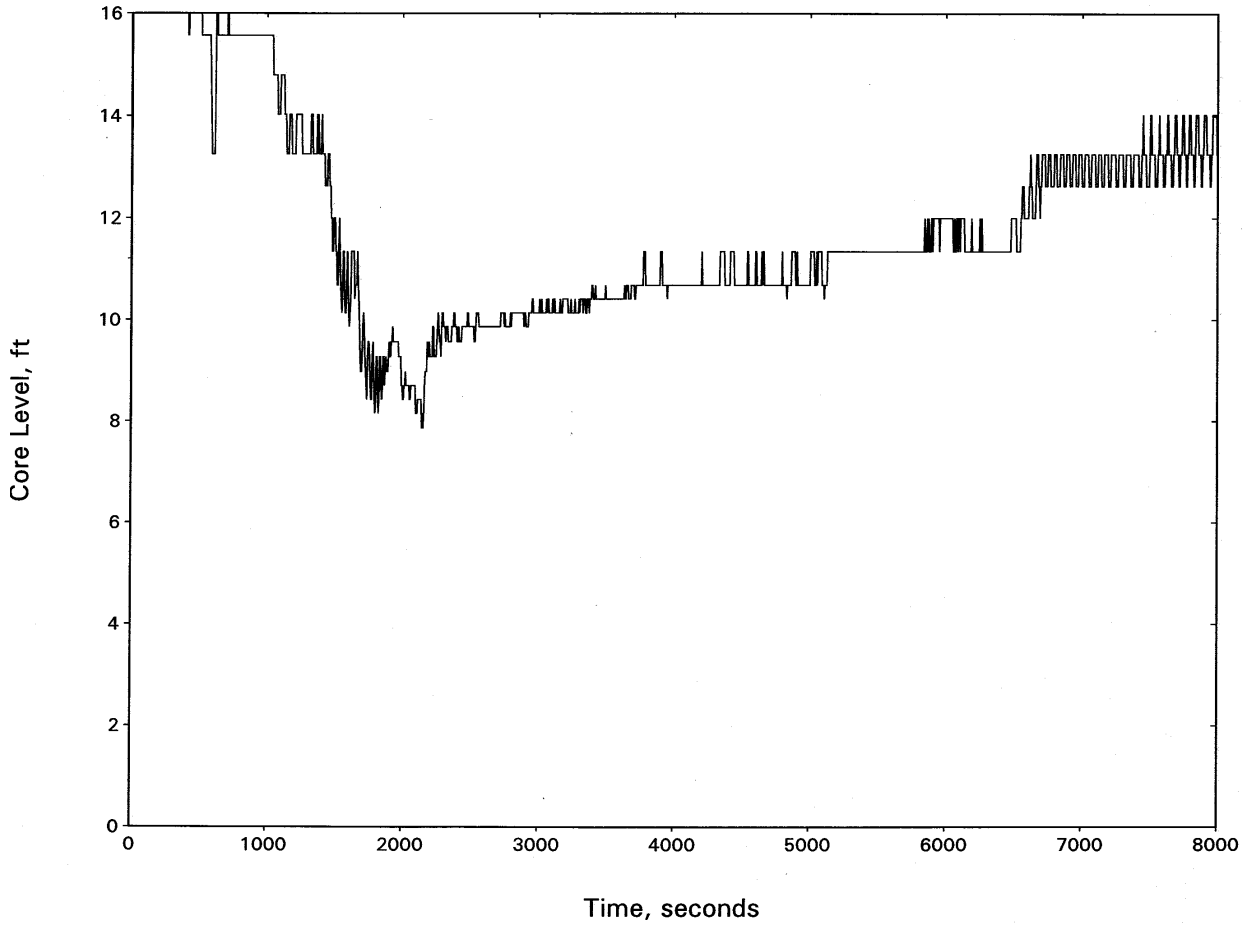

Figure 15.3-60
NORTH ANNA UNIT 1: HOT SPOT PCT—2.5-INCH BREAK

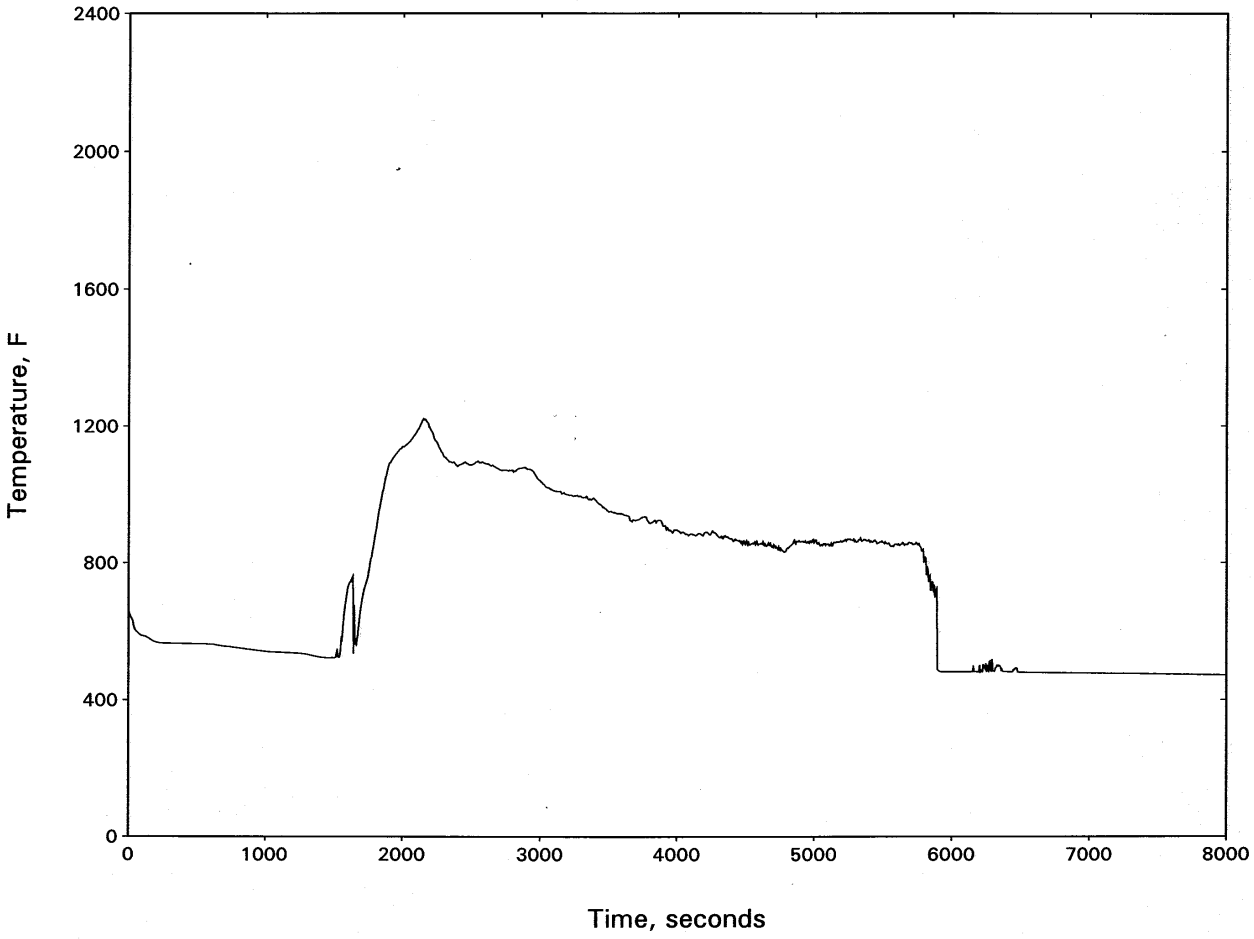

Figure 15.3-61
NORTH ANNA UNIT 1:
HOT CHANNEL OUTLET VAPOR TEMPERATURE—2.5-INCH BREAK

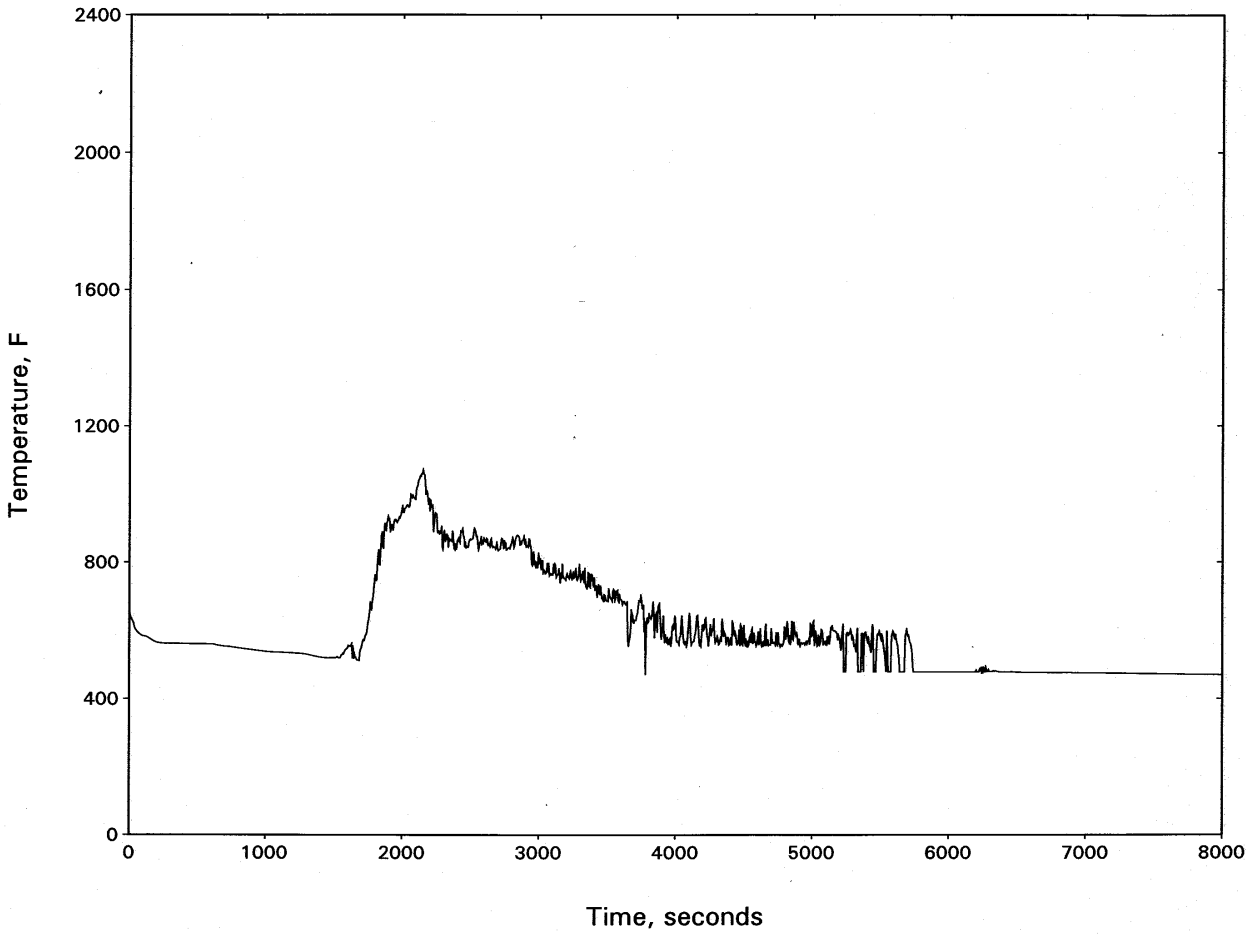

Figure 15.3-62
NORTH ANNA UNIT 1: INTACT LOOP SEAL LEVEL—2.5-INCH BREAK

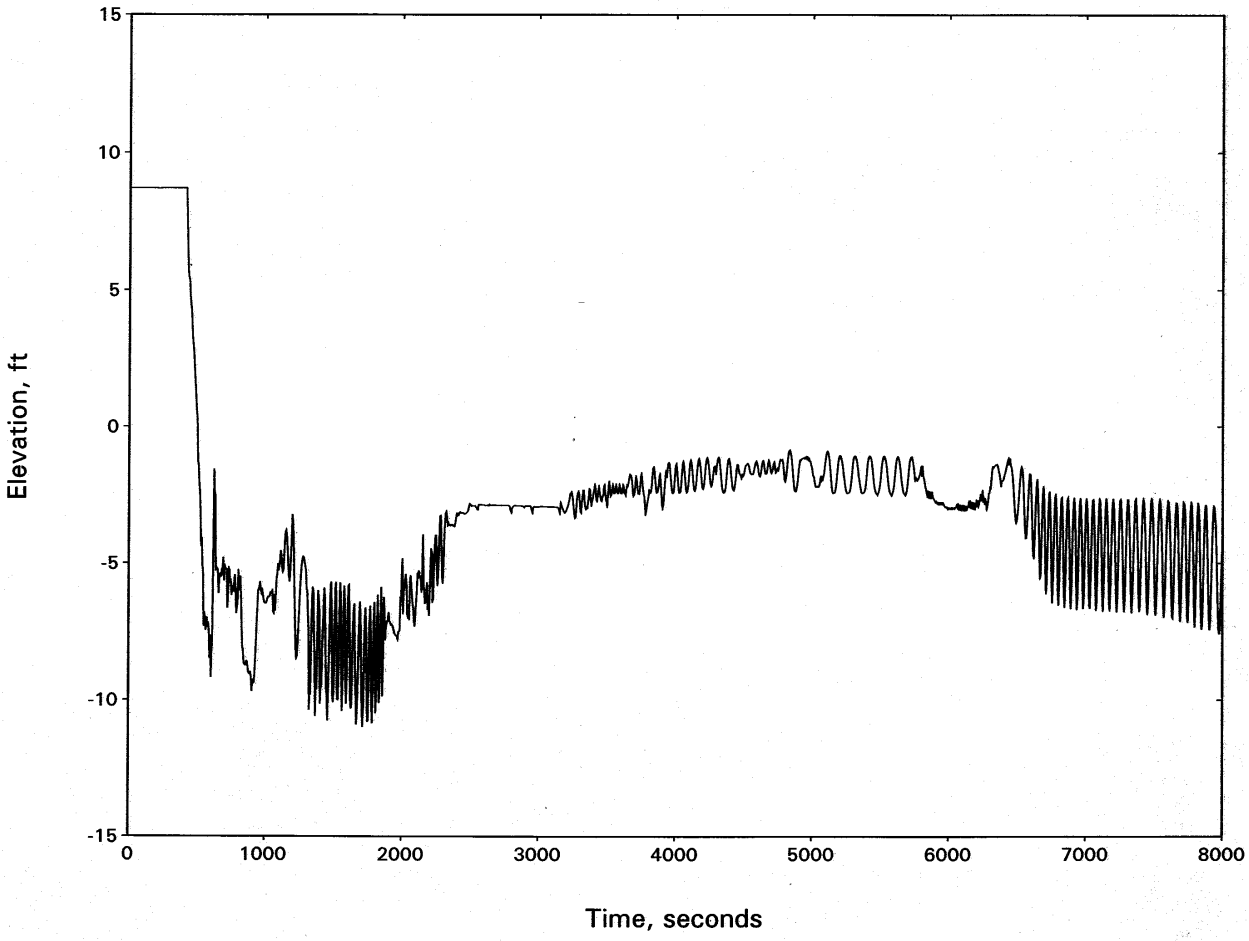

Figure 15.3-63
NORTH ANNA UNIT 1: BROKEN LOOP SEAL LEVEL—2.5-INCH BREAK

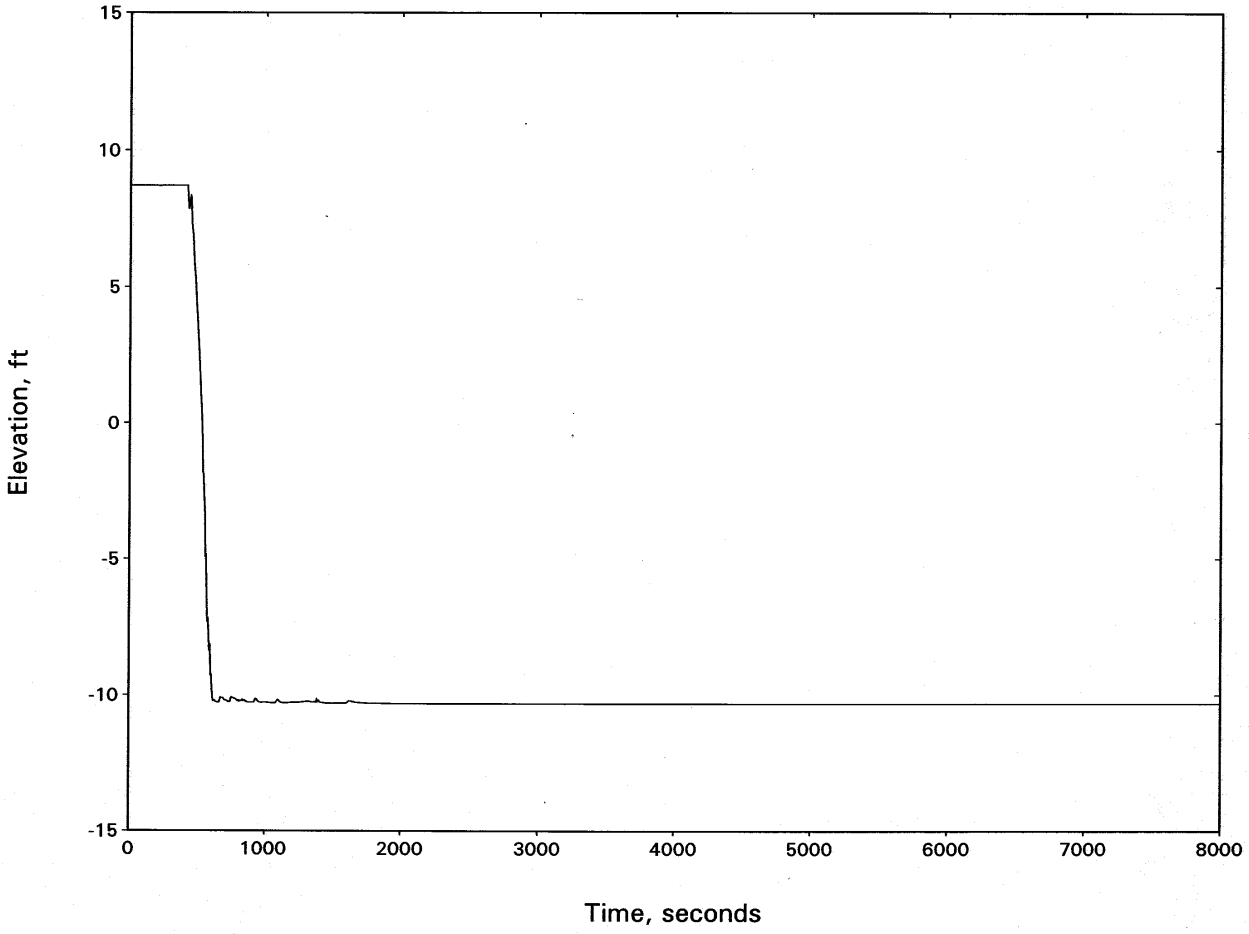

Figure 15.3-64
NORTH ANNA UNIT 1: RCS PRESSURE—3.0-INCH BREAK

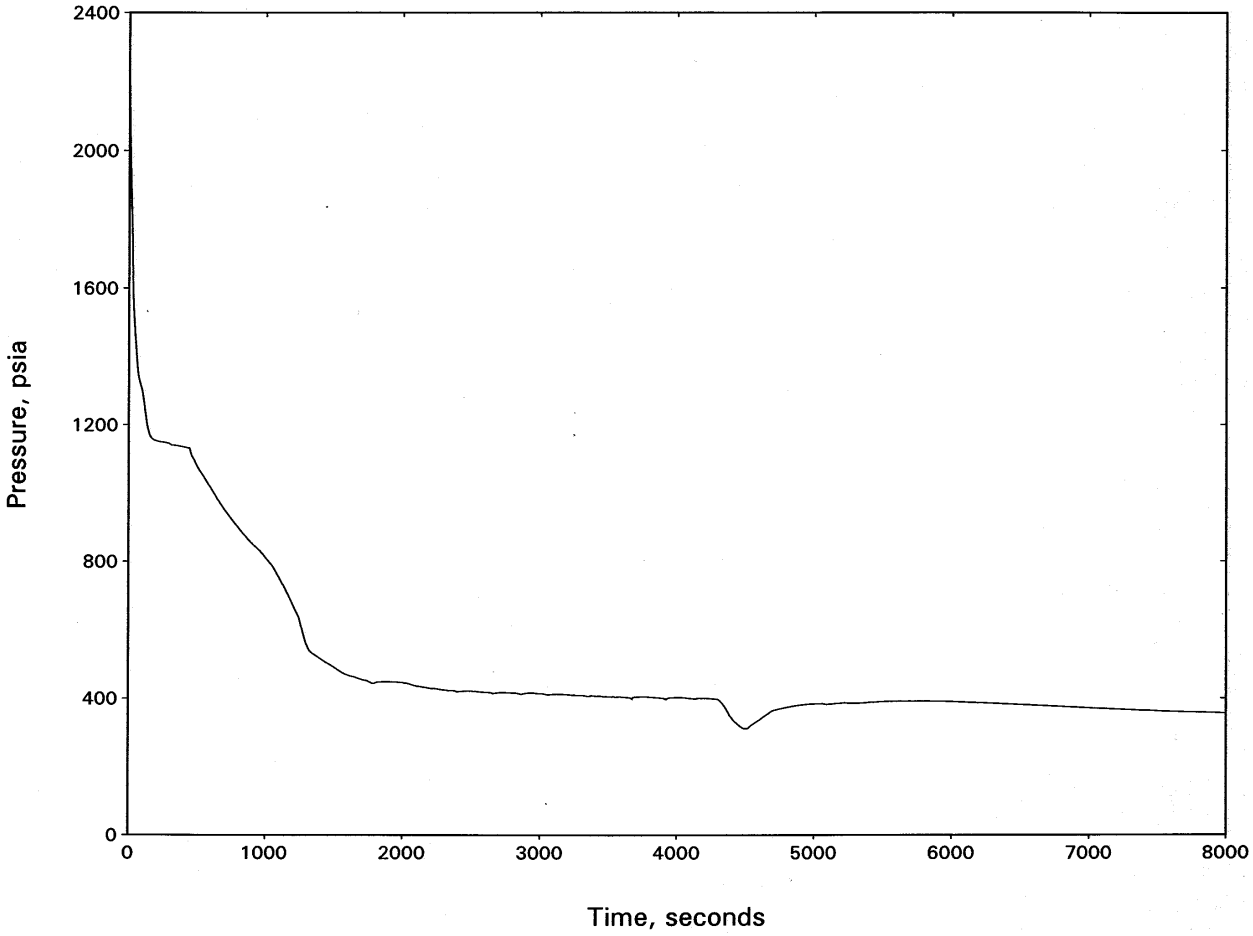

Figure 15.3-65
NORTH ANNA UNIT 1: BREAK FLOW—3.0-INCH BREAK

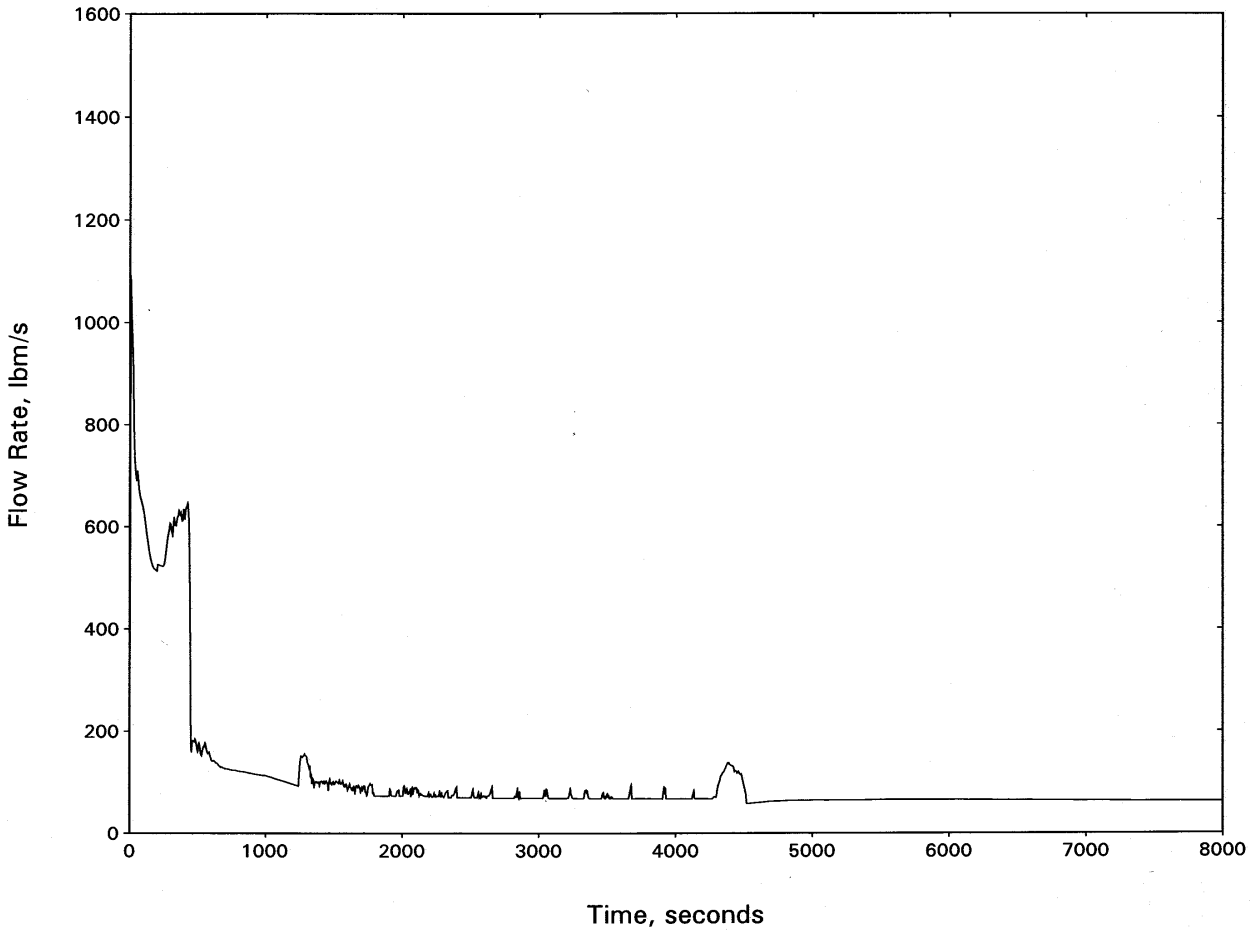

Figure 15.3-66
NORTH ANNA UNIT 1: HOT CHANNEL MIXTURE LEVEL—3.0-INCH BREAK

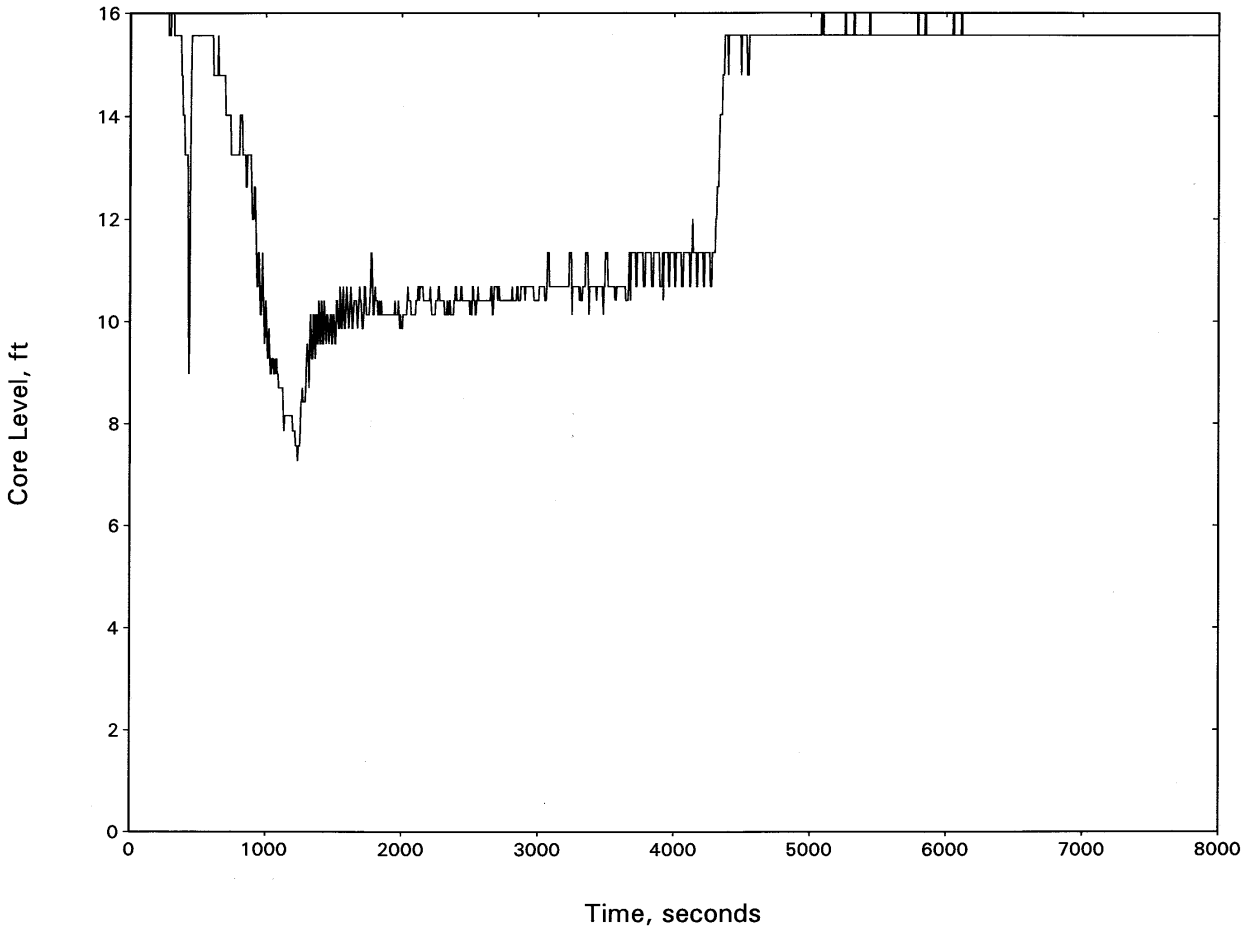

Figure 15.3-67
NORTH ANNA UNIT 1: HOT SPOT PCT—3.0-INCH BREAK

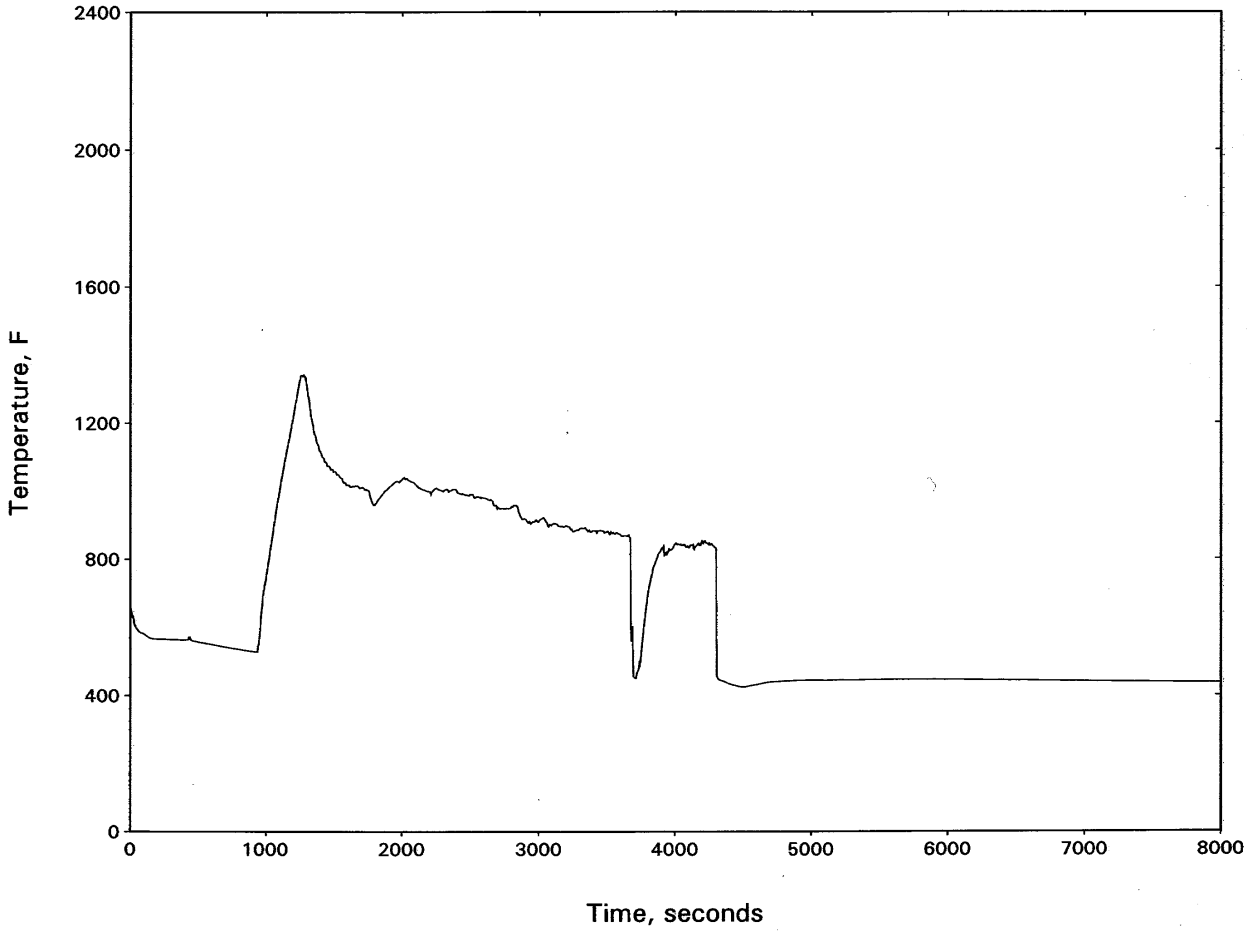

Figure 15.3-68
NORTH ANNA UNIT 1:
HOT CHANNEL OUTLET VAPOR TEMPERATURE—3.0-INCH BREAK

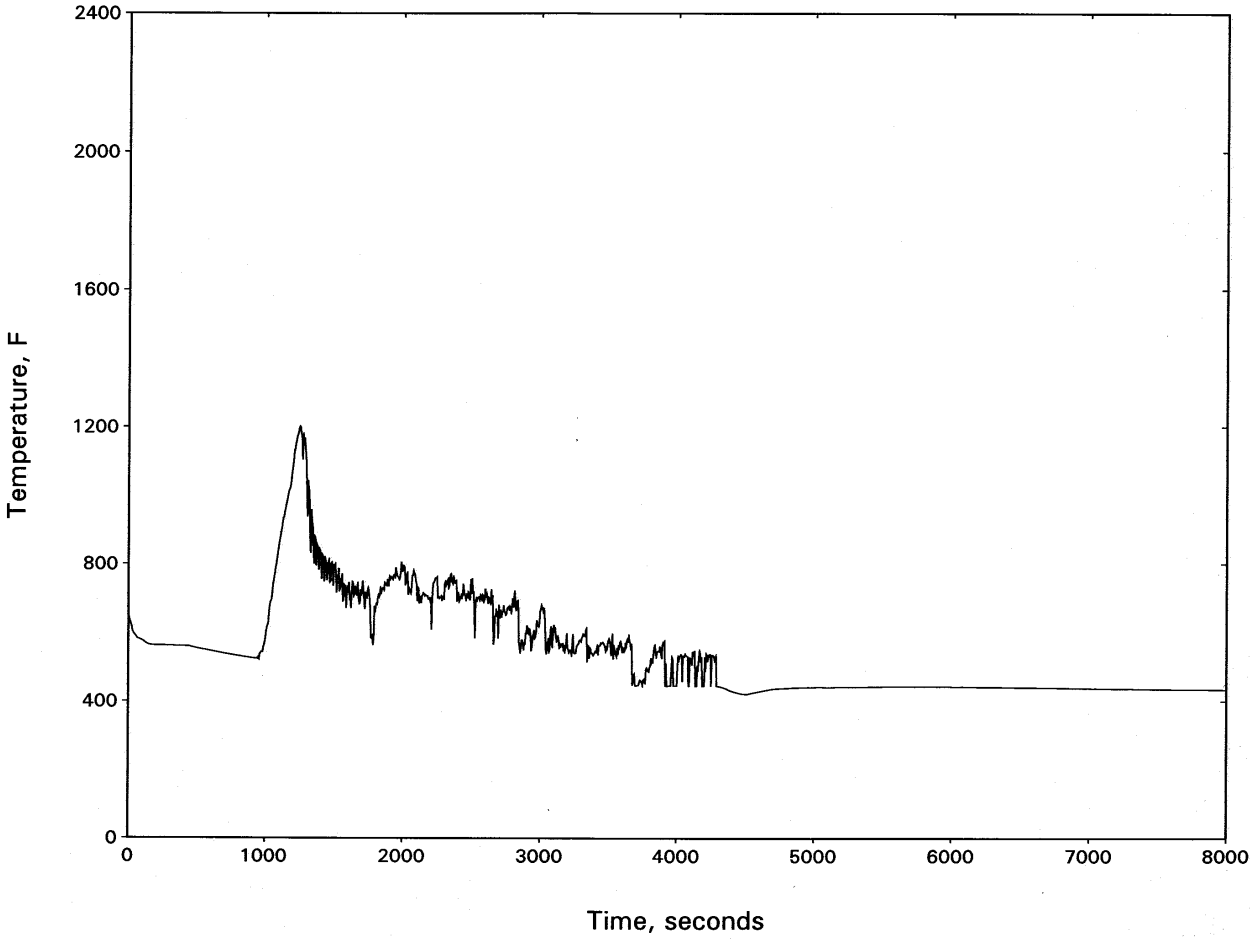

Figure 15.3-69
NORTH ANNA UNIT 1: INTACT LOOP SEAL LEVEL—3.0-INCH BREAK

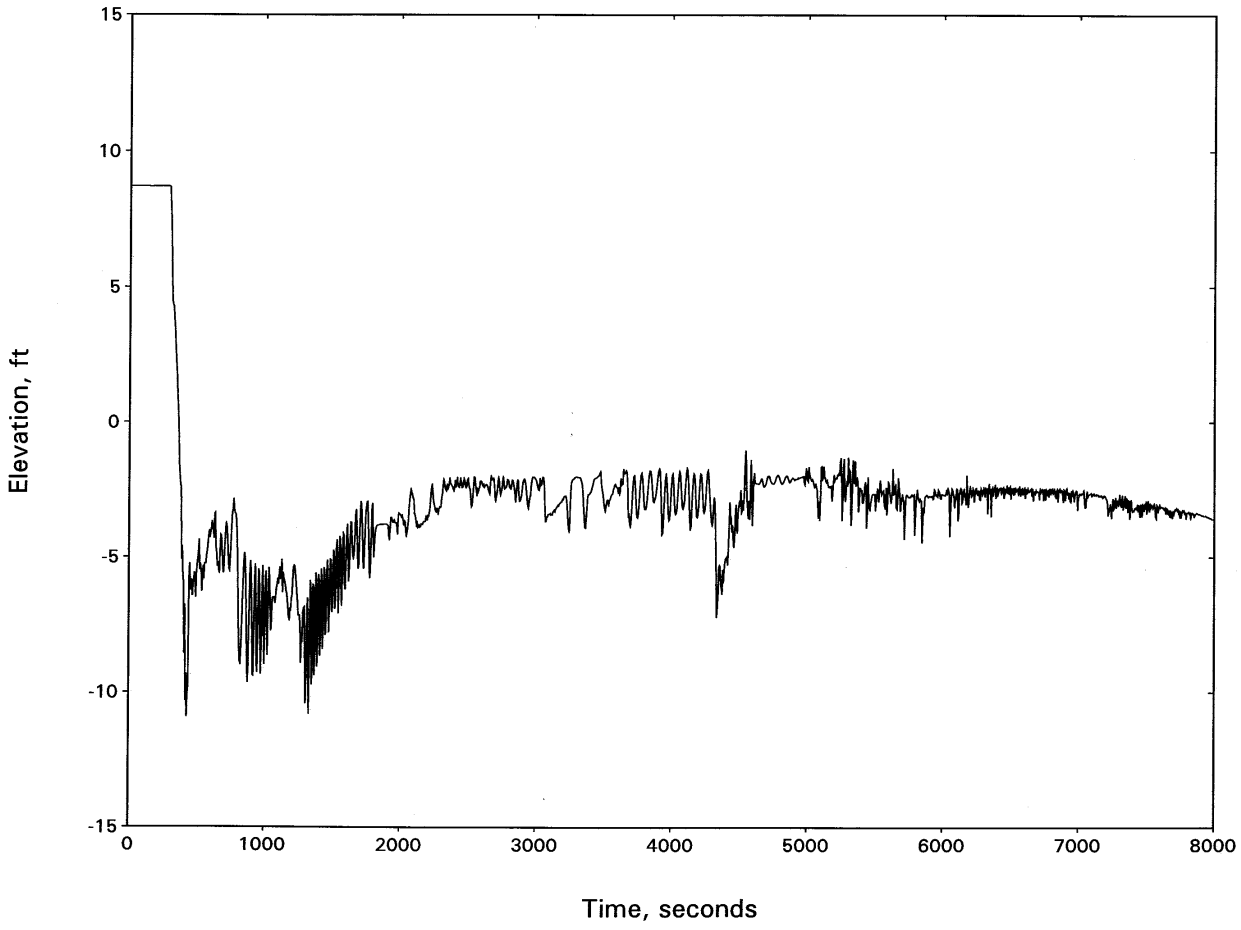

Figure 15.3-70
NORTH ANNA UNIT 1: BROKEN LOOP SEAL LEVEL—3.0-INCH BREAK

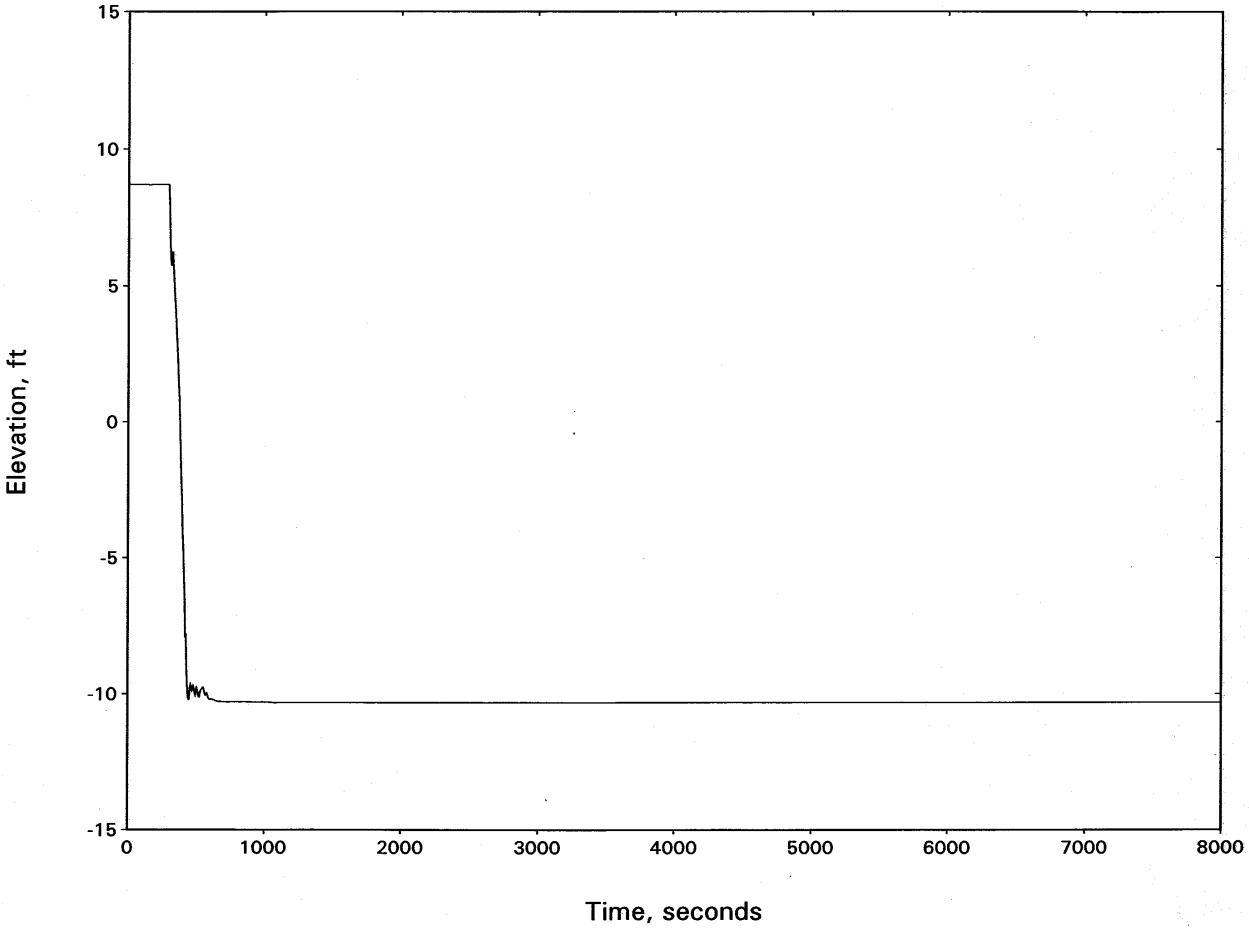

Figure 15.3-71
NORTH ANNA UNIT 1: RCS PRESSURE—4.0-INCH BREAK

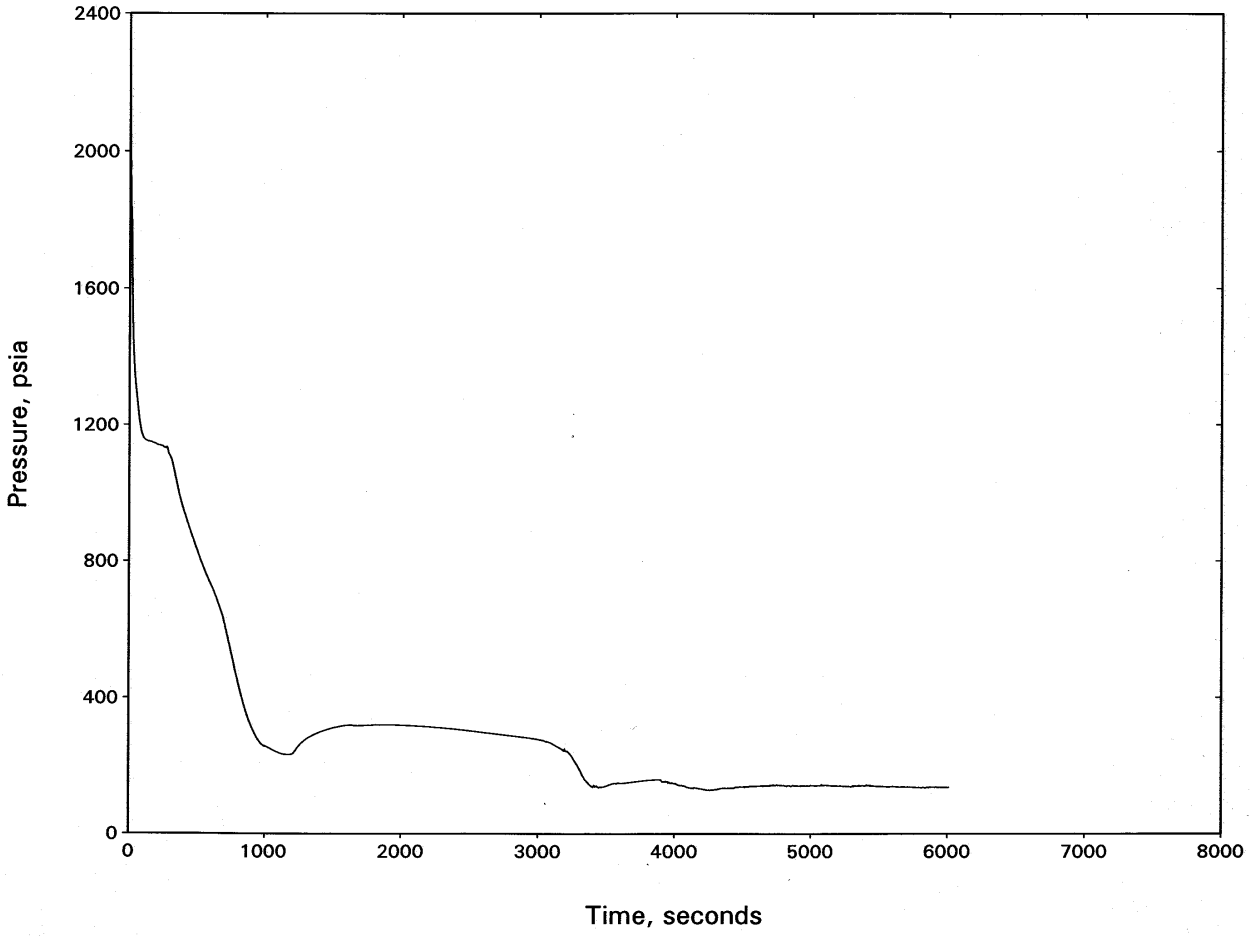

Figure 15.3-72
NORTH ANNA UNIT 1: BREAK FLOW—4.0-INCH BREAK

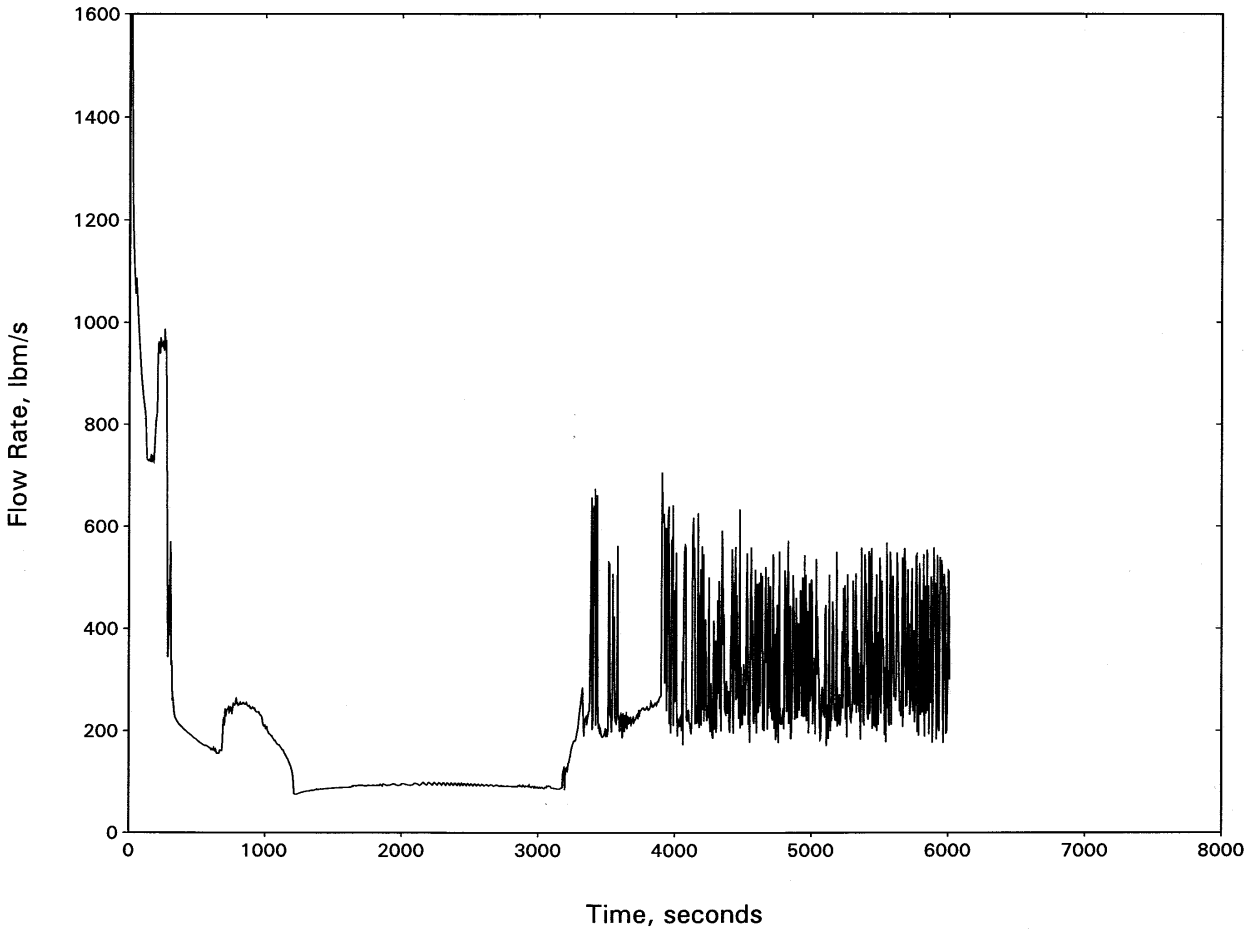

Figure 15.3-73
NORTH ANNA UNIT 1: HOT CHANNEL MIXTURE LEVEL—4.0-INCH BREAK

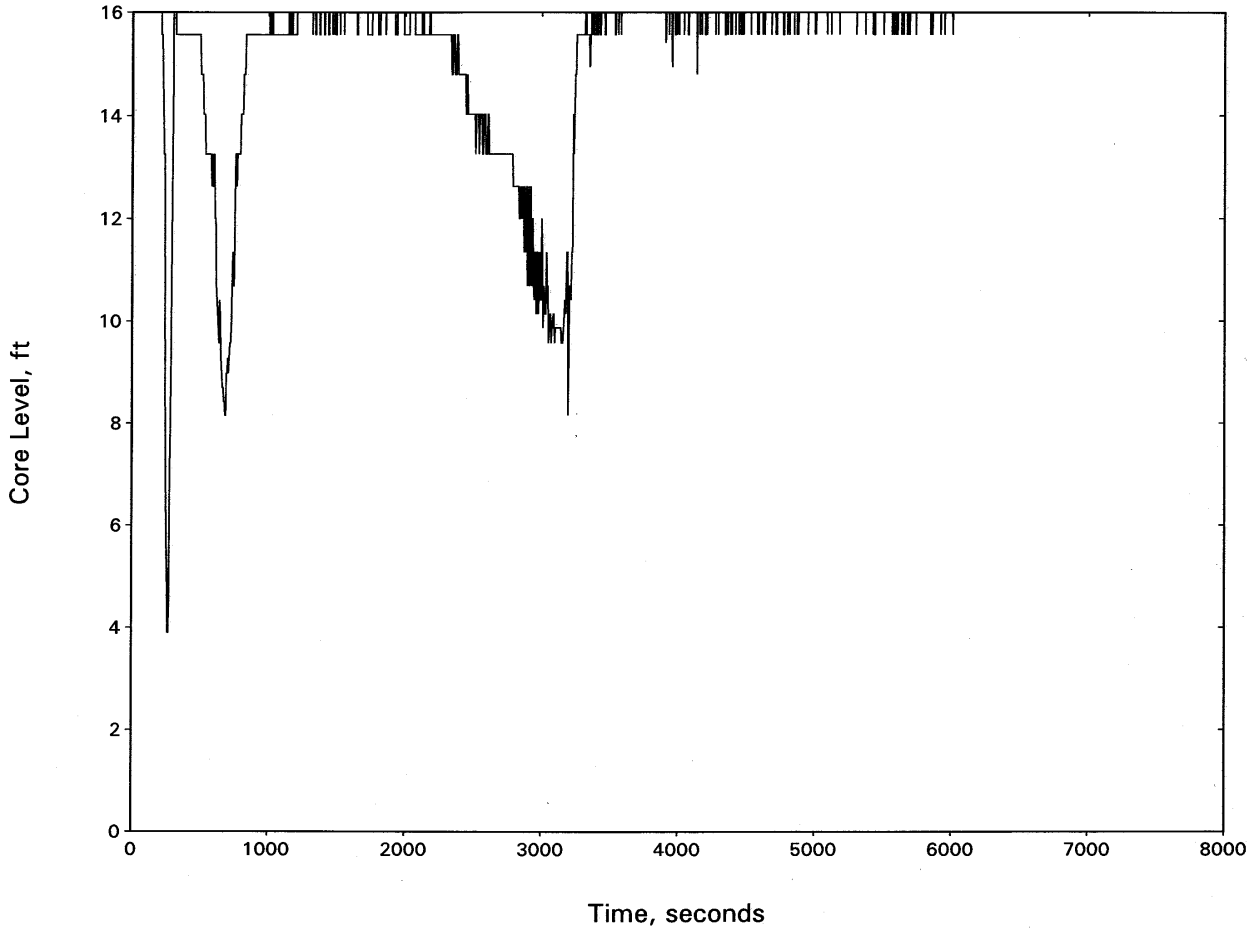

Figure 15.3-74
NORTH ANNA UNIT 1: HOT SPOT PCT—4.0-INCH BREAK

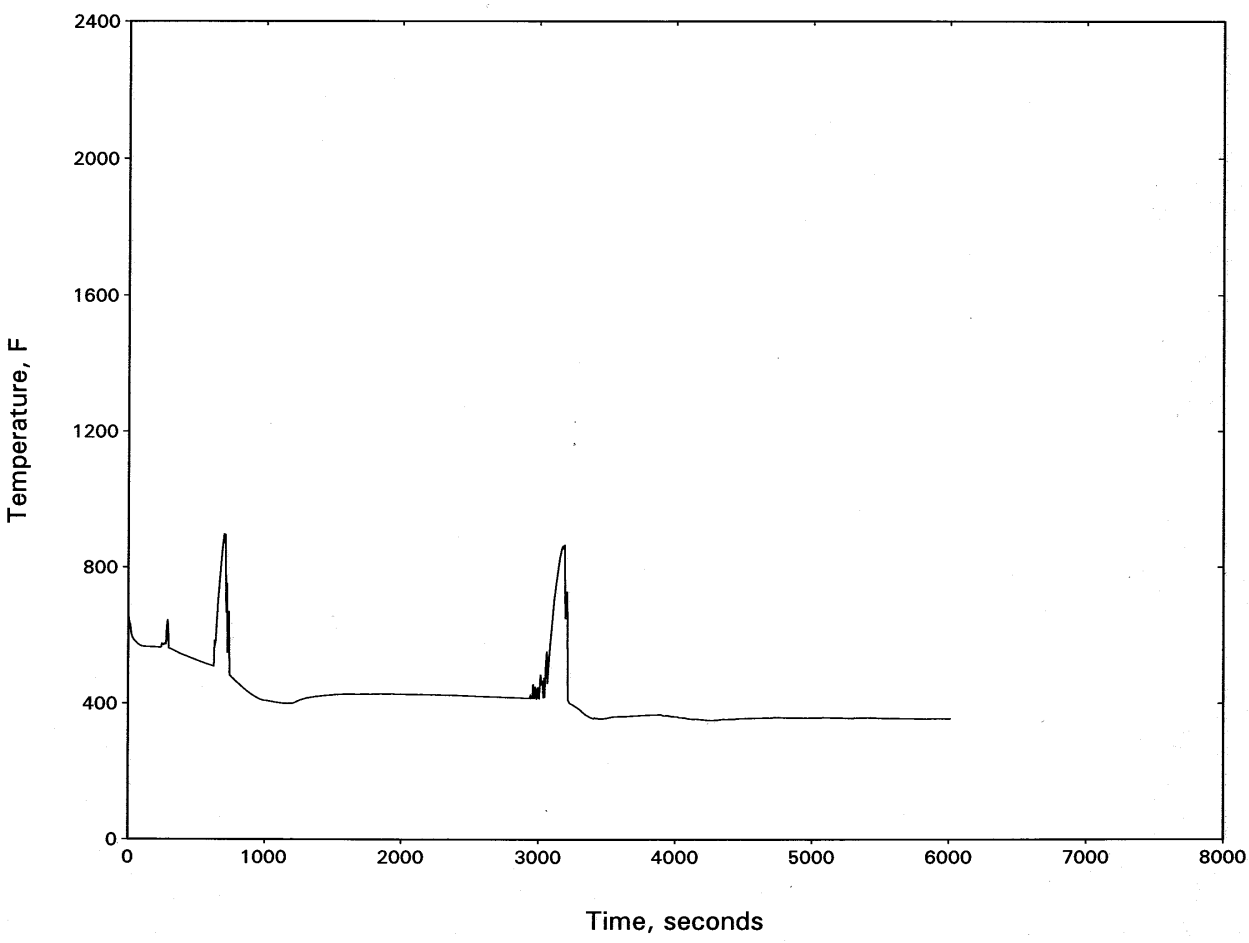

Figure 15.3-75
NORTH ANNA UNIT 1:
HOT CHANNEL OUTLET VAPOR TEMPERATURE—4.0-INCH BREAK

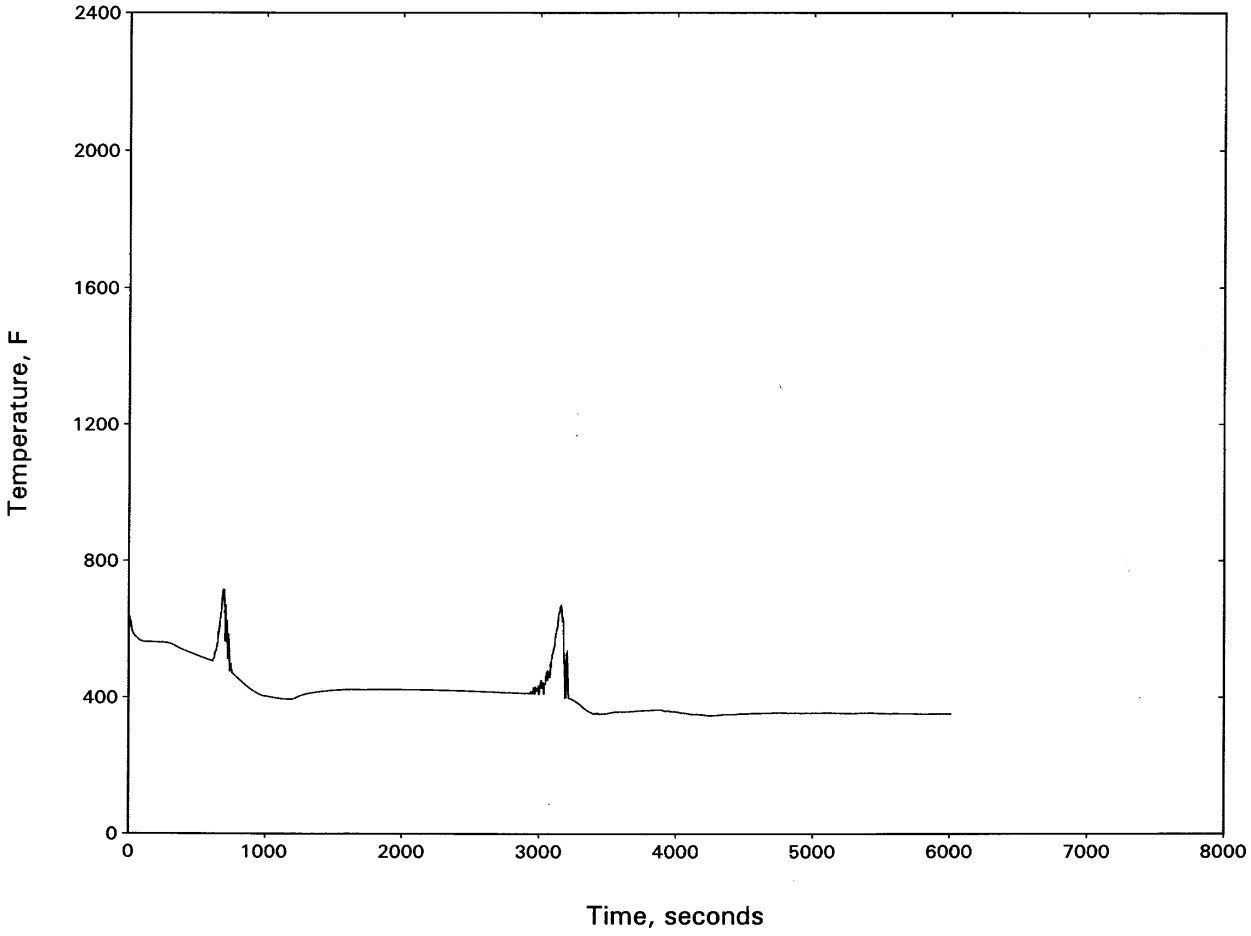

Figure 15.3-76
NORTH ANNA UNIT 1: INTACT LOOP SEAL LEVEL—4.0-INCH BREAK

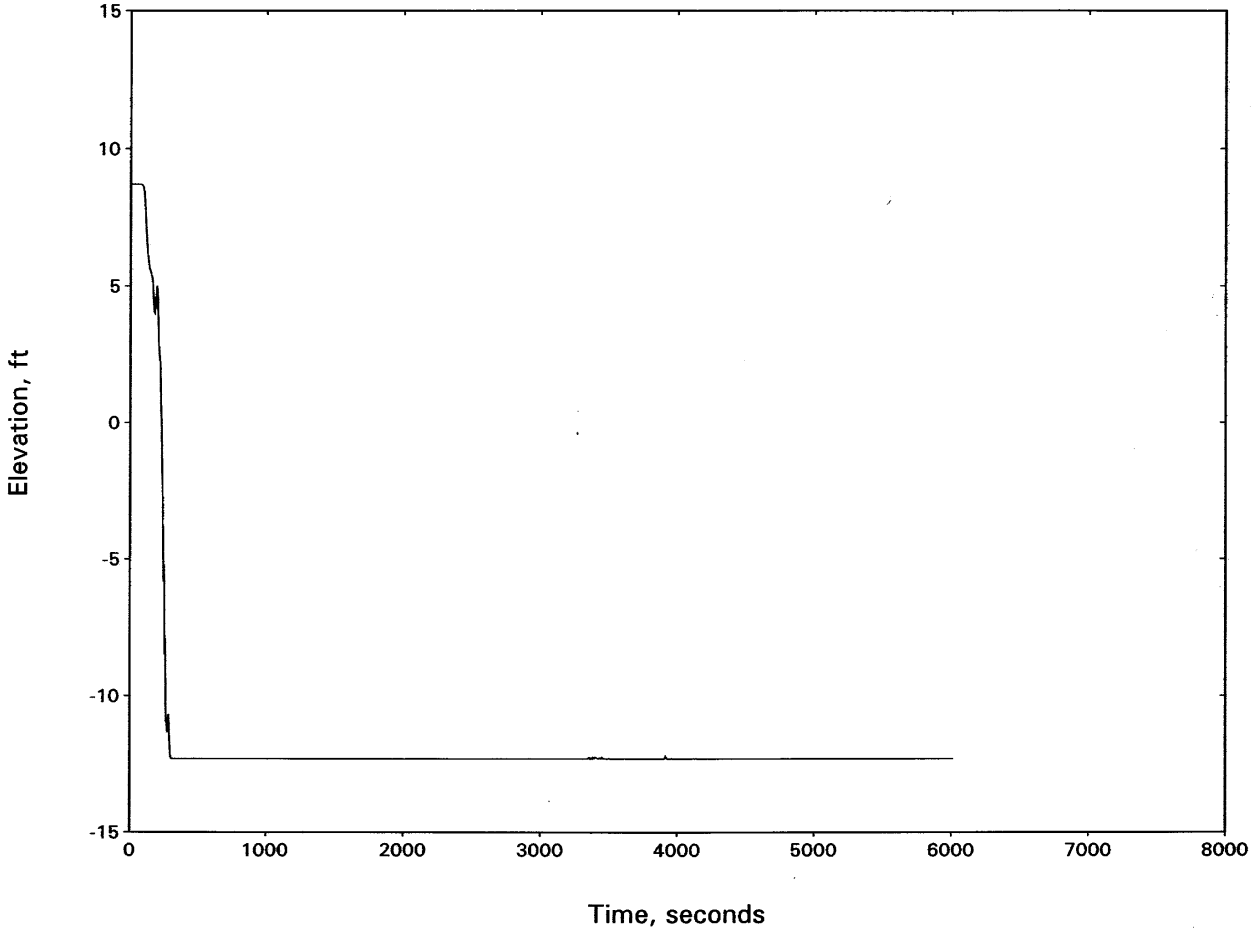

Figure 15.3-77
NORTH ANNA UNIT 1: BROKEN LOOP SEAL LEVEL—4.0-INCH BREAK

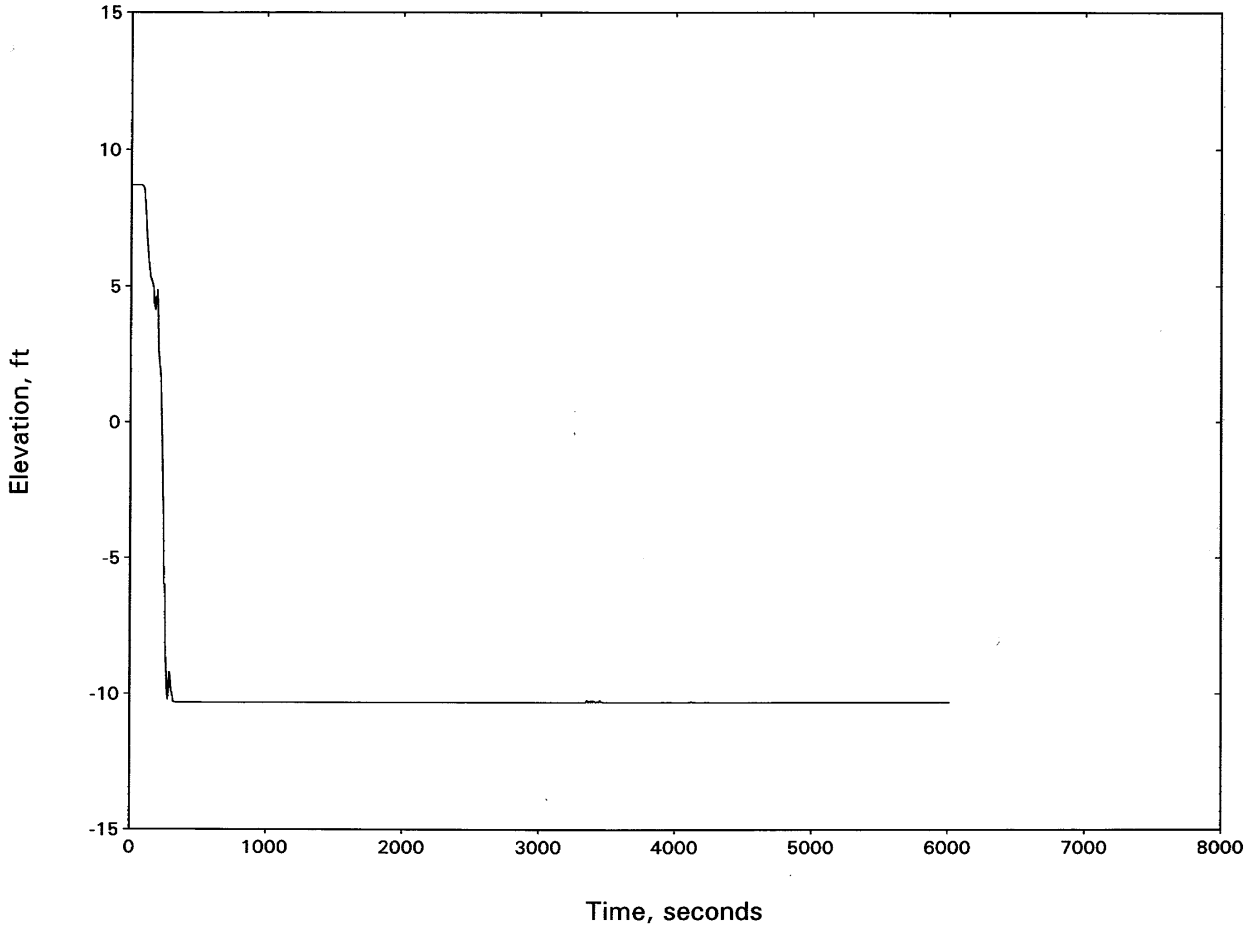

Figure 15.3-78
NORTH ANNA UNIT 1: RCS PRESSURE—5.2-INCH SI LINE BREAK

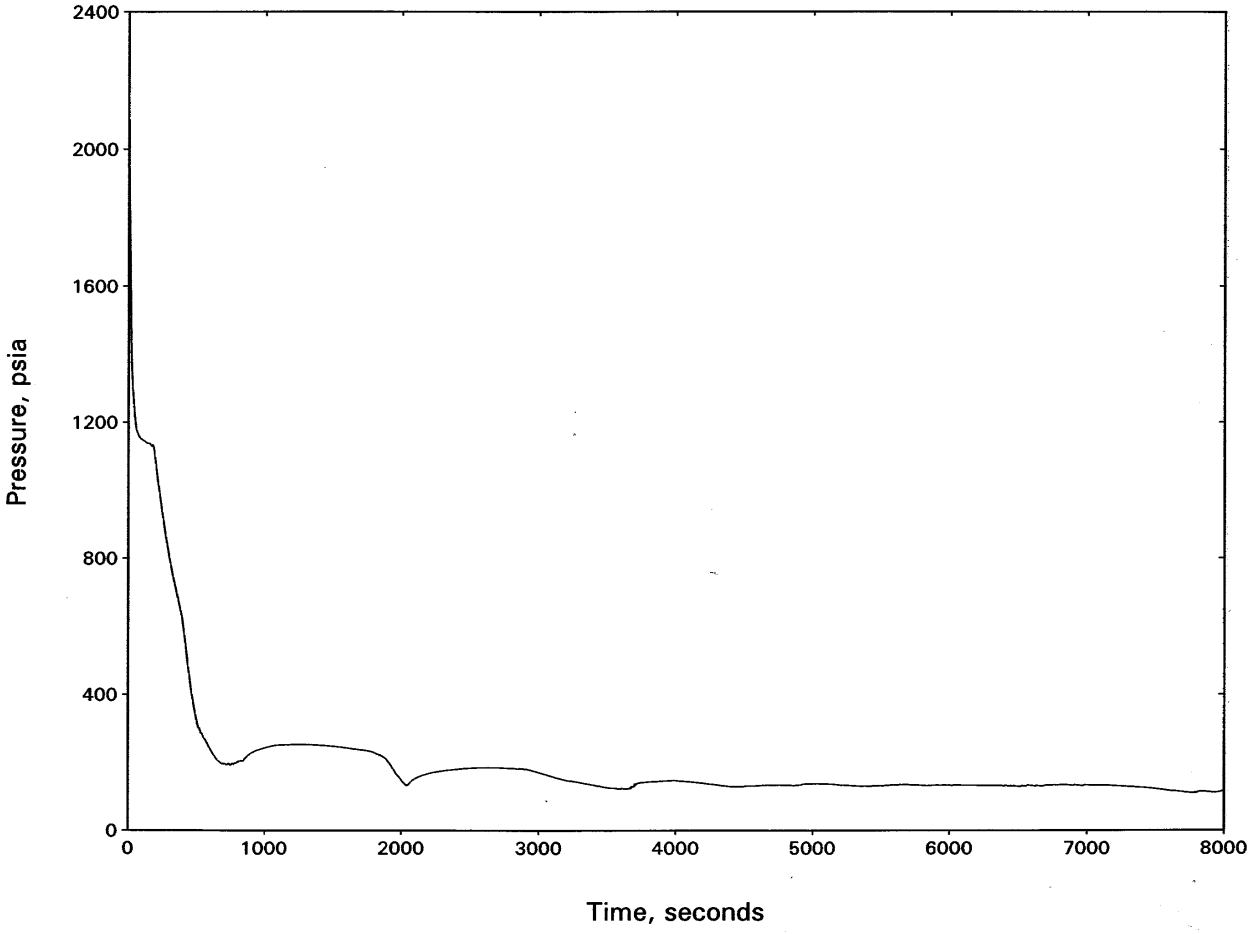

Figure 15.3-79
NORTH ANNA UNIT 1: BREAK FLOW—5.2-INCH SI LINE BREAK

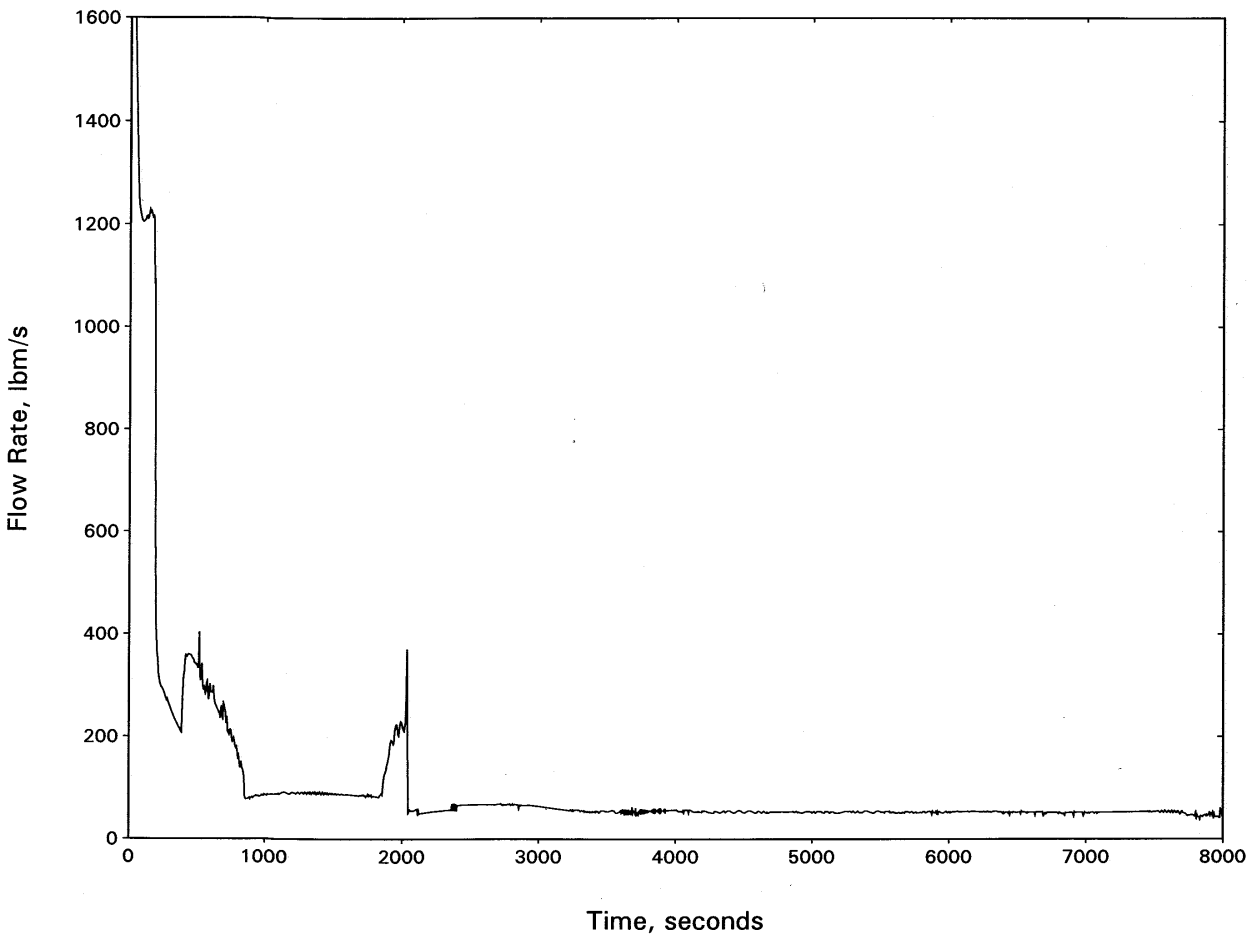

Figure 15.3-80
NORTH ANNA UNIT 1: HOT CHANNEL MIXTURE LEVEL—5.2-INCH SI LINE BREAK

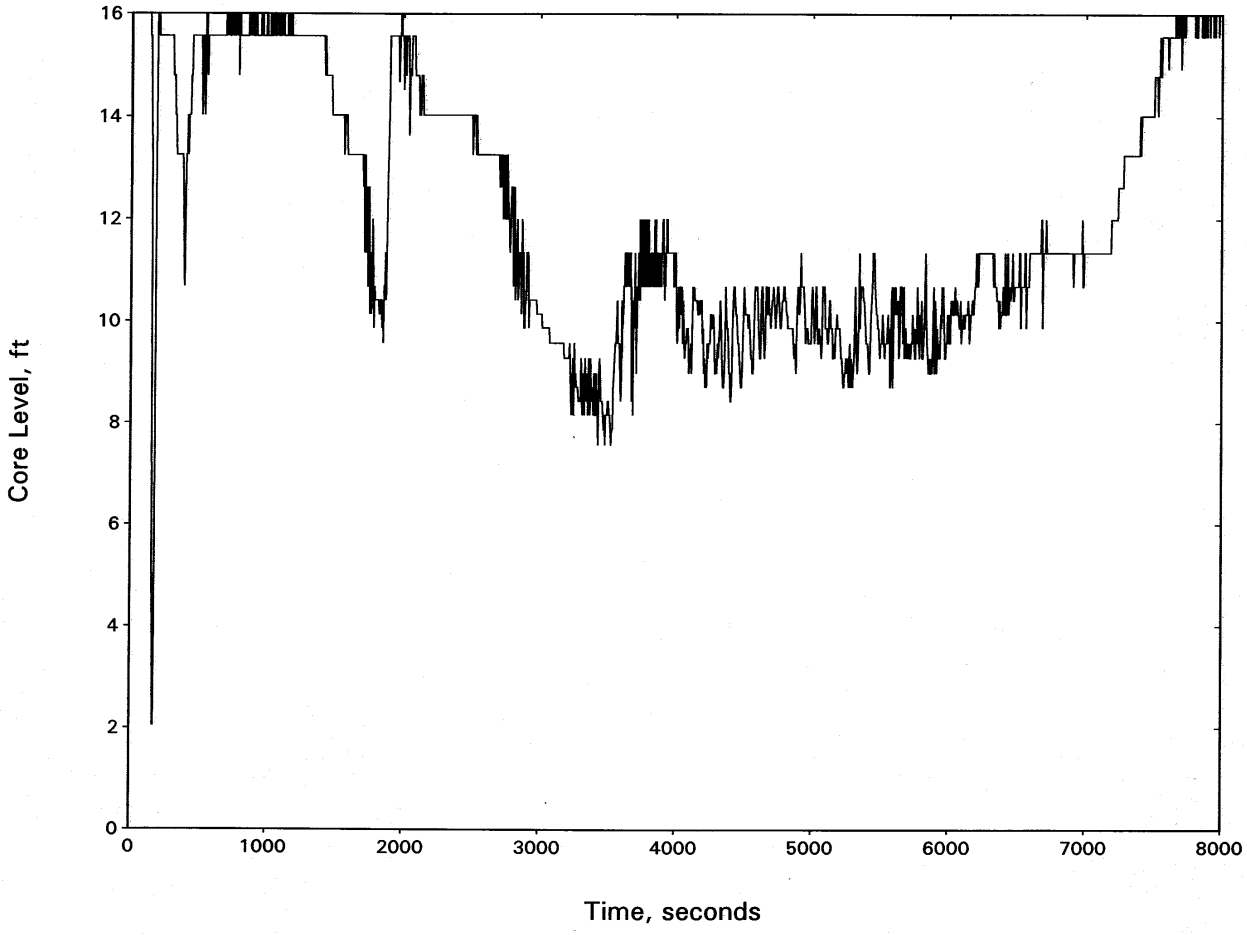

Figure 15.3-81
NORTH ANNA UNIT 1: HOT SPOT PCT—5.2-INCH SI LINE BREAK

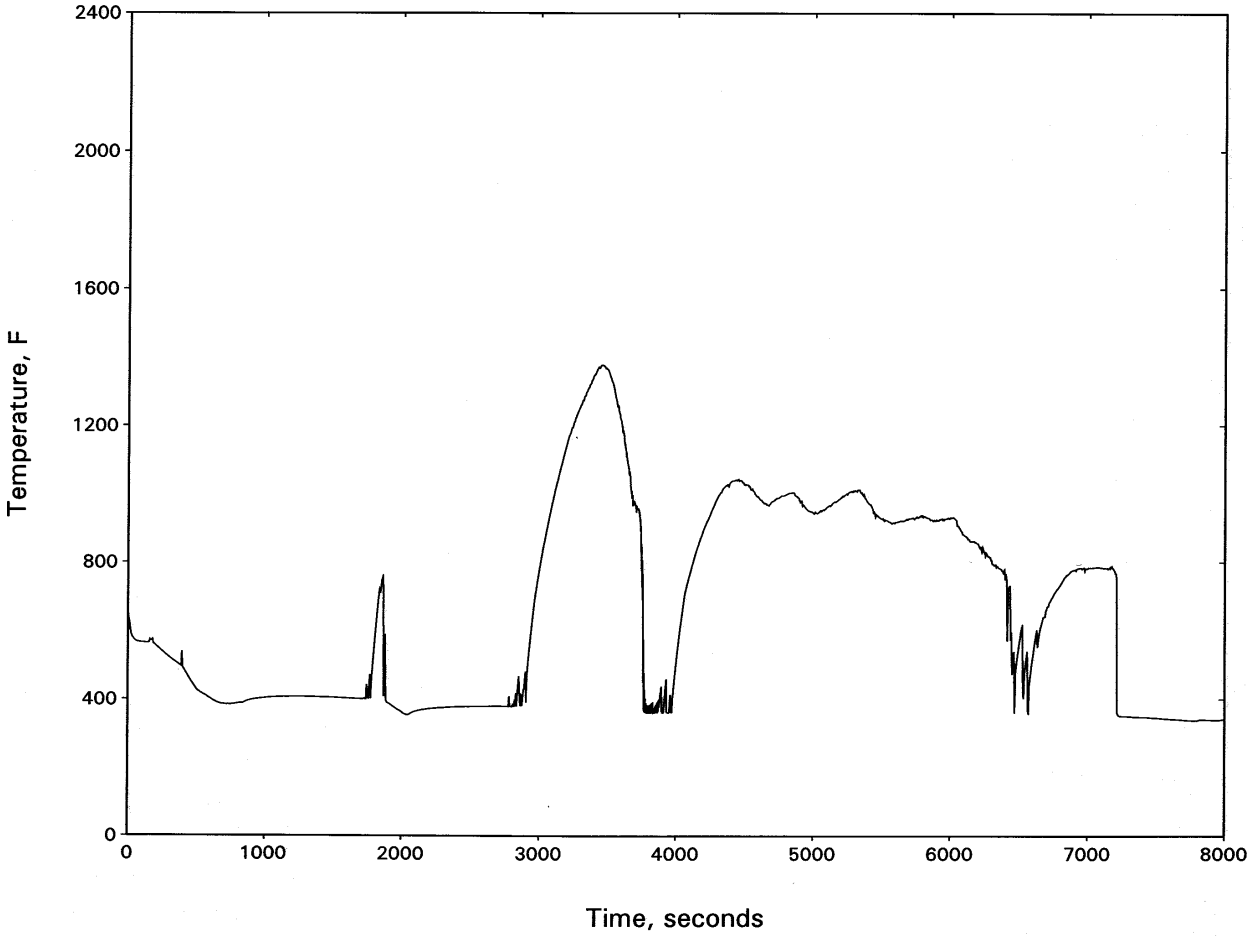

Figure 15.3-82
NORTH ANNA UNIT 1:
HOT CHANNEL OUTLET VAPOR TEMPERATURE—5.2-INCH SI LINE BREAK

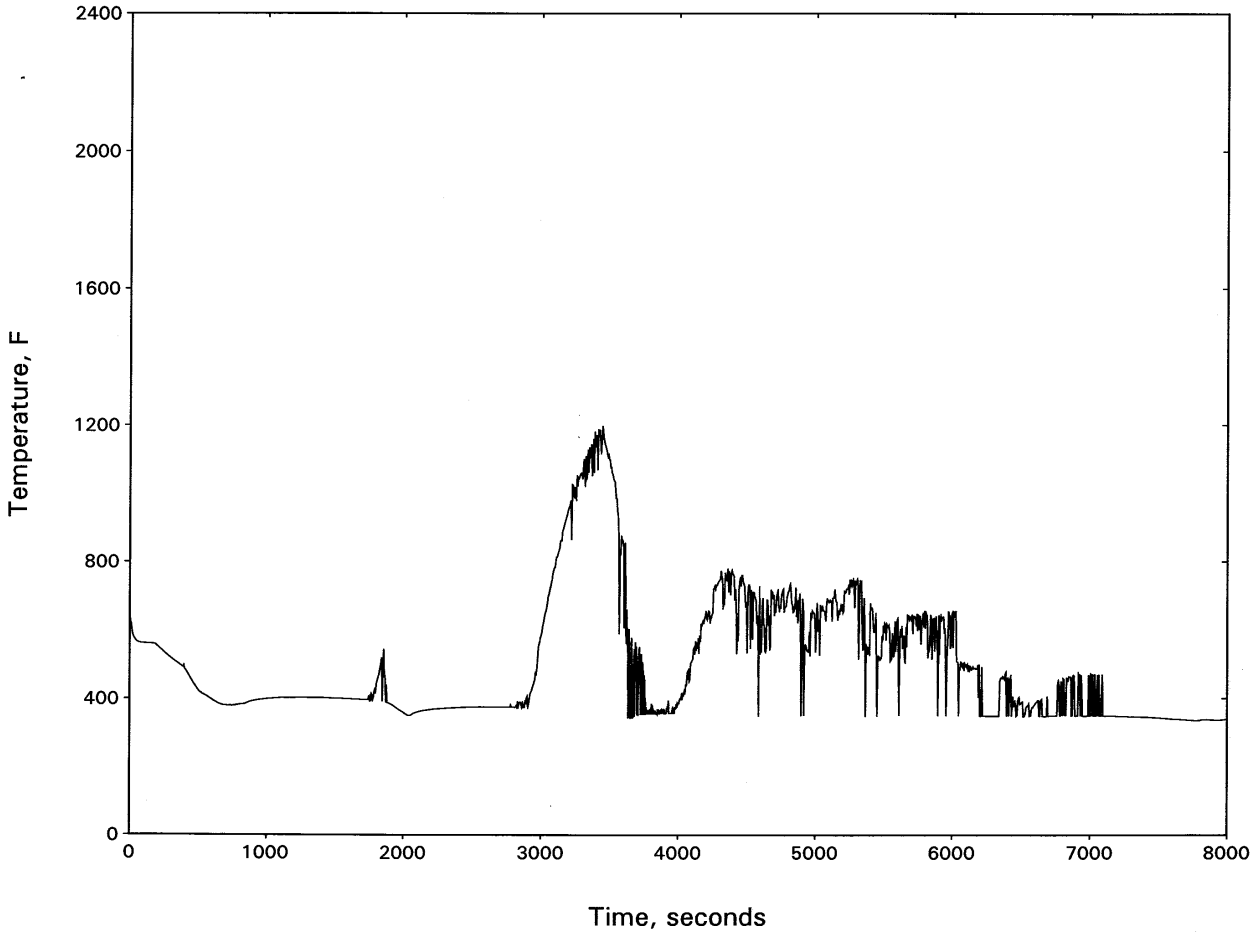

Figure 15.3-83
NORTH ANNA UNIT 1: INTACT LOOP SEAL LEVEL—5.2-INCH SI LINE BREAK

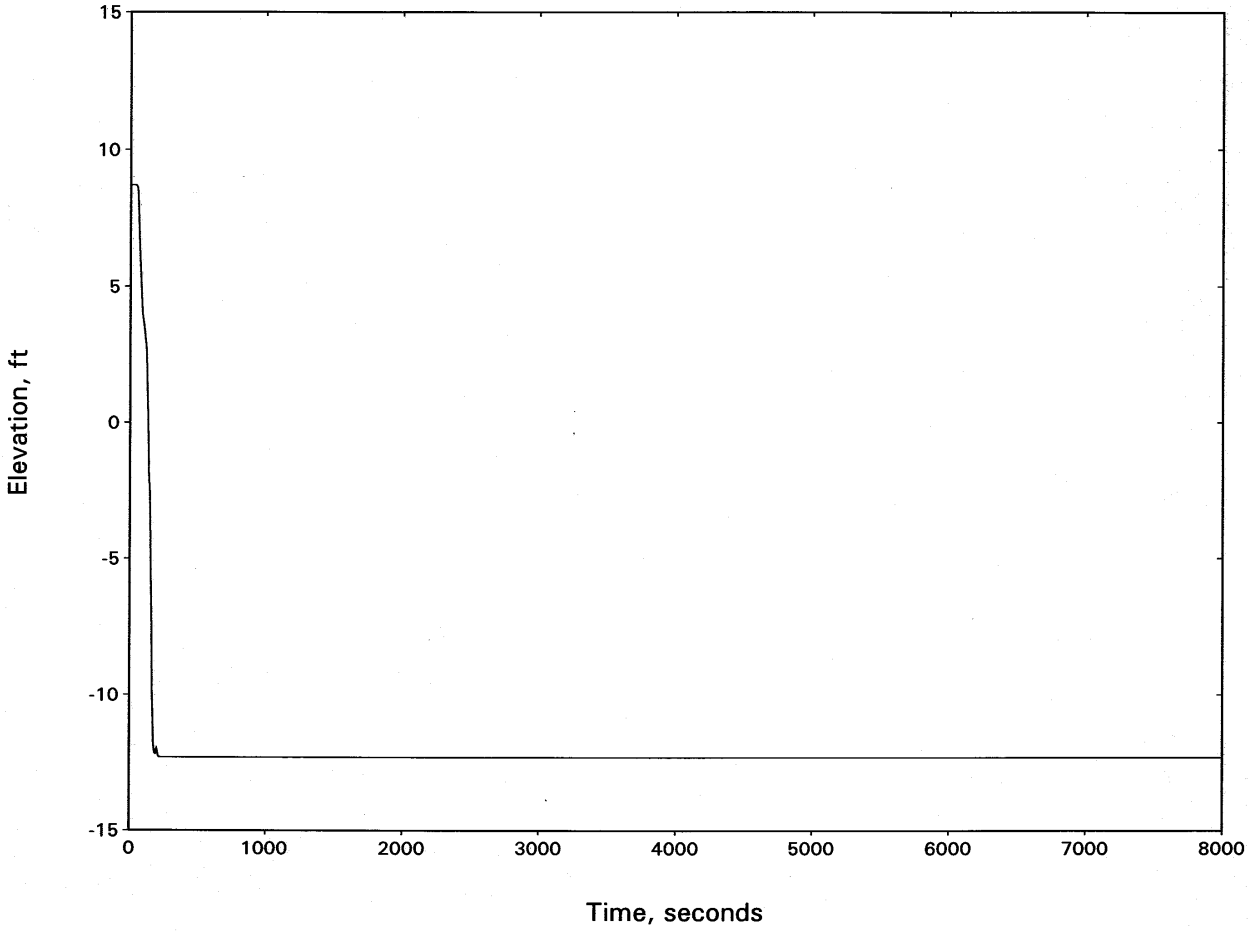

Figure 15.3-84
NORTH ANNA UNIT 1: BROKEN LOOP SEAL LEVEL—5.2-INCH SI LINE BREAK

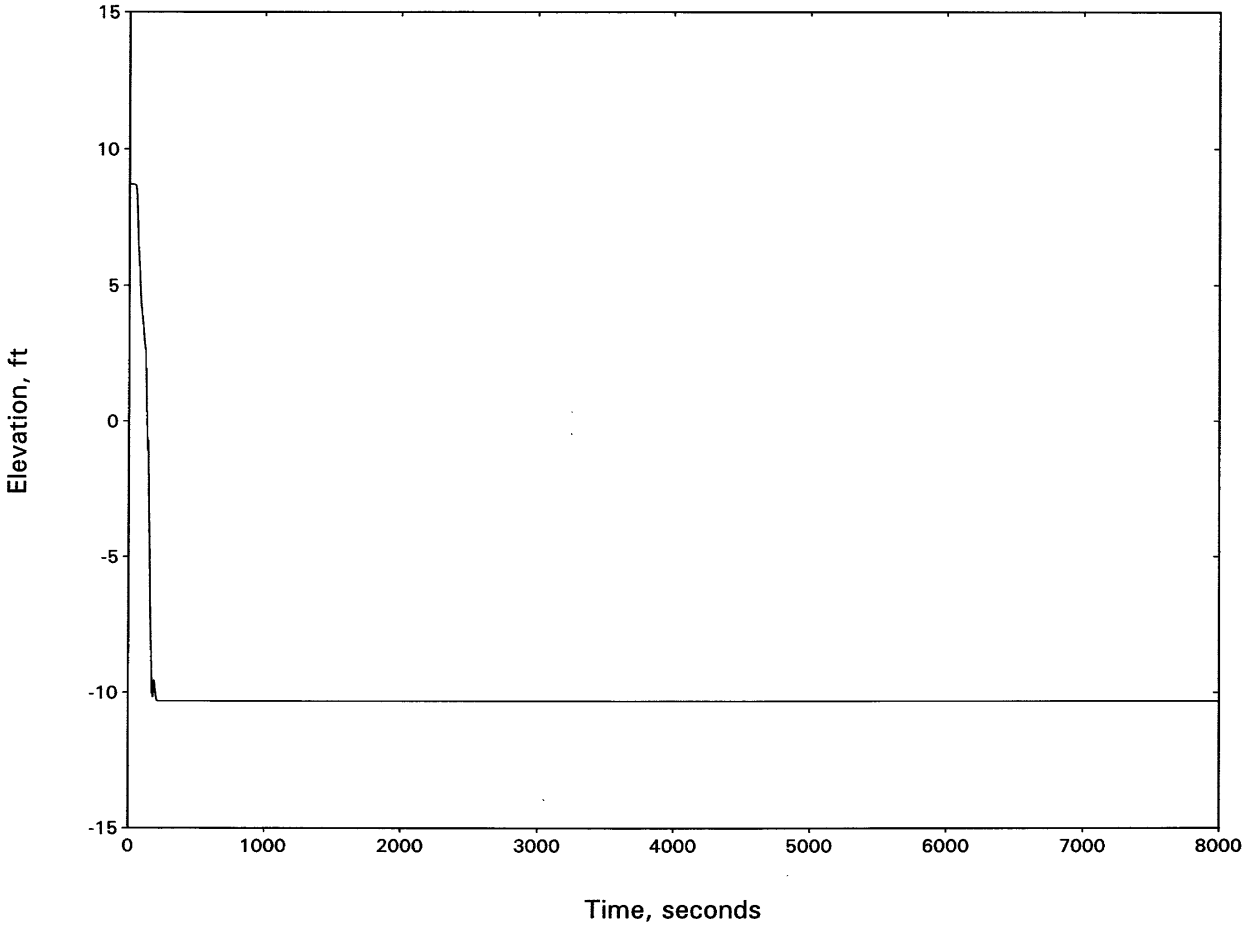

Figure 15.3-85
NORTH ANNA UNIT 1: RCS PRESSURE—6.0-INCH BREAK

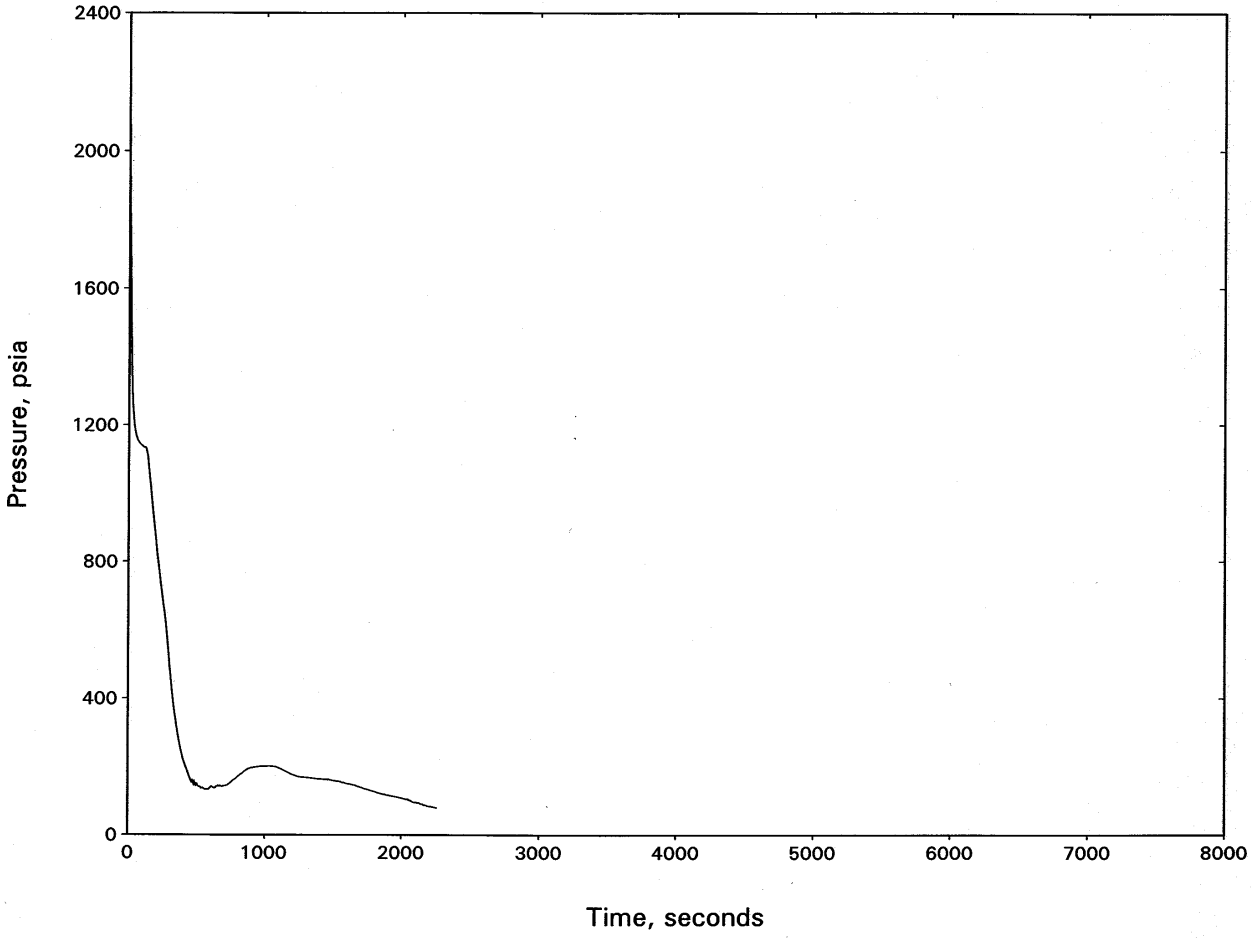

Figure 15.3-86
NORTH ANNA UNIT 1: BREAK FLOW—6.0-INCH BREAK

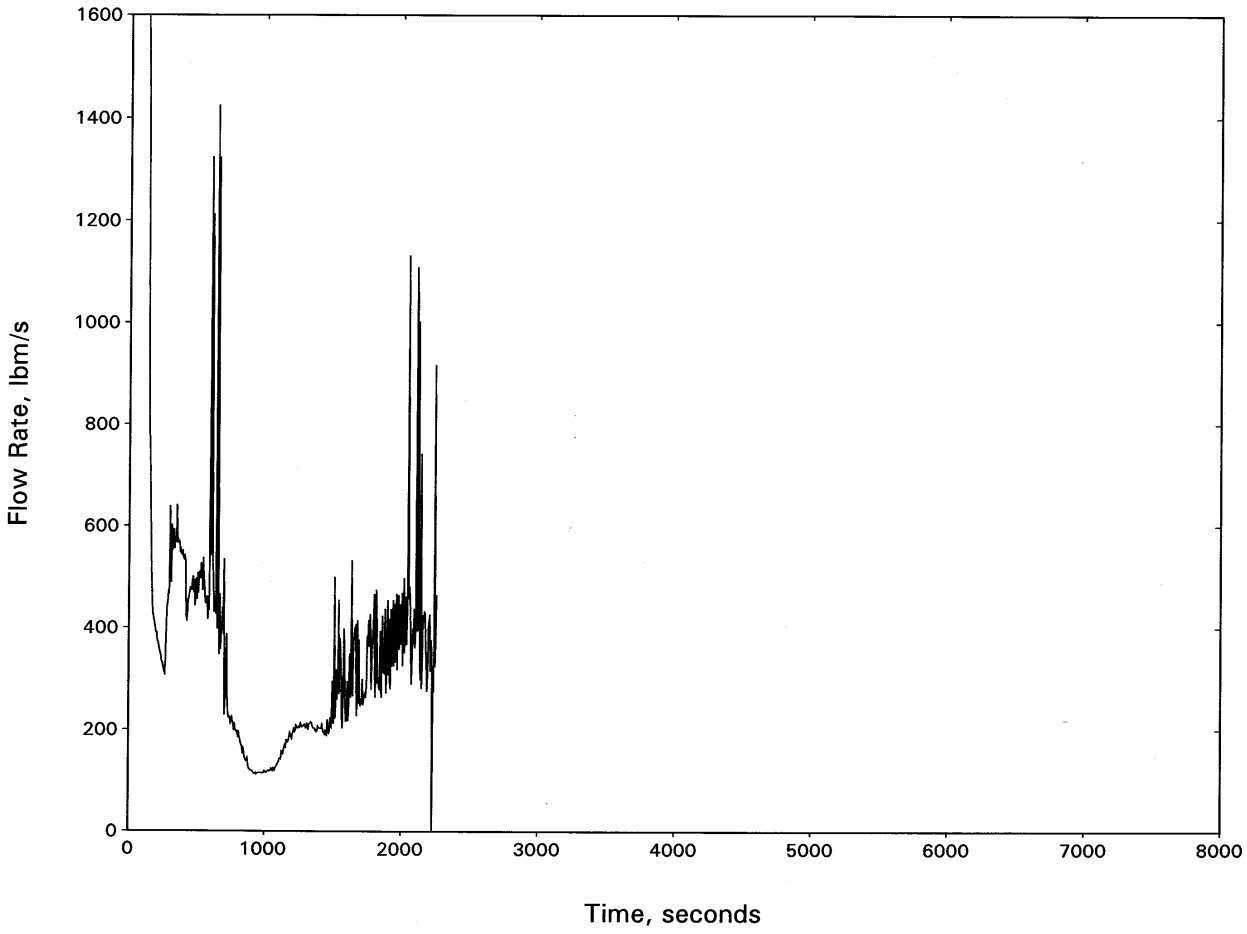

Figure 15.3-87
NORTH ANNA UNIT 1: HOT CHANNEL MIXTURE LEVEL—6.0-INCH BREAK

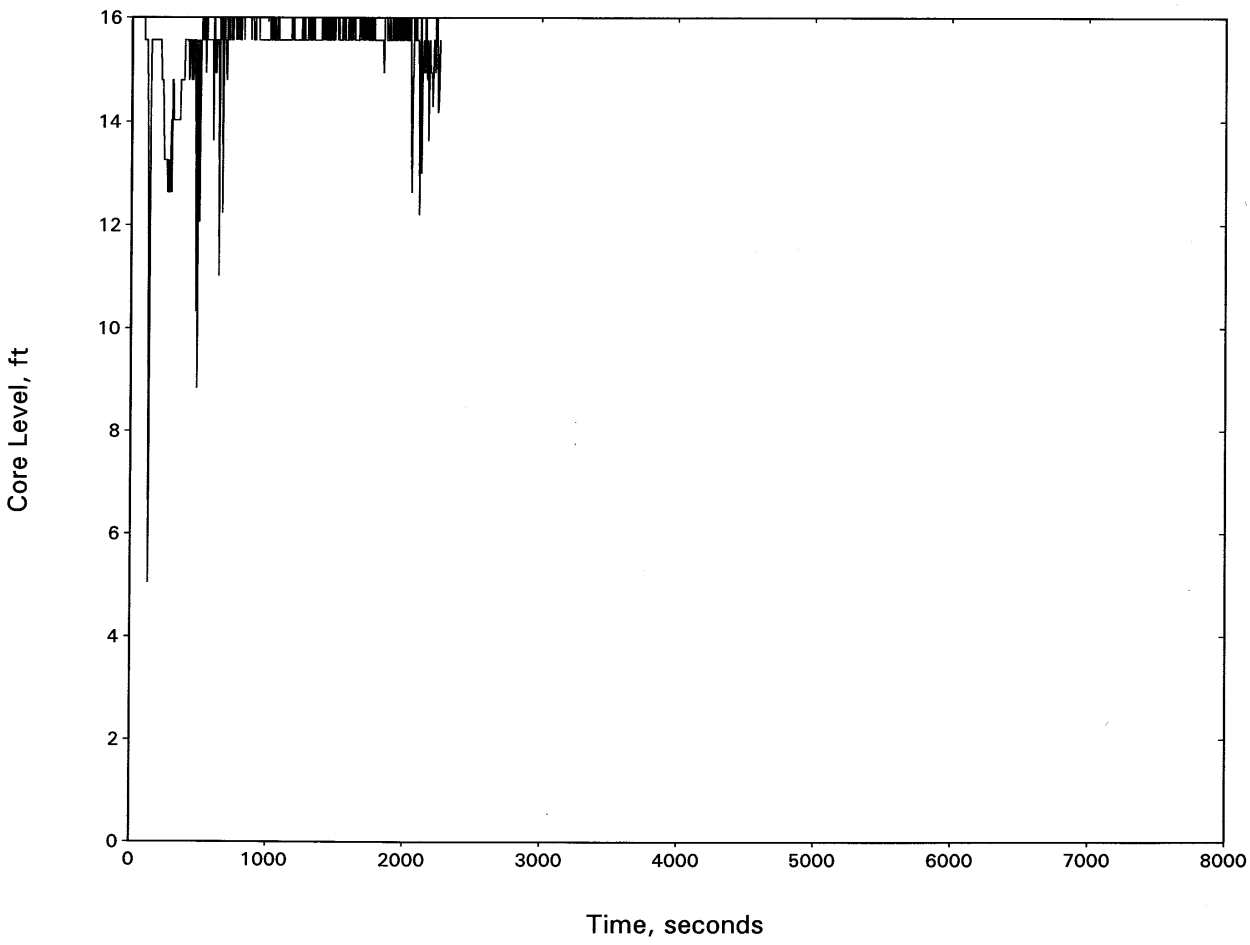

Figure 15.3-88
NORTH ANNA UNIT 1: HOT SPOT PCT—6.0-INCH BREAK

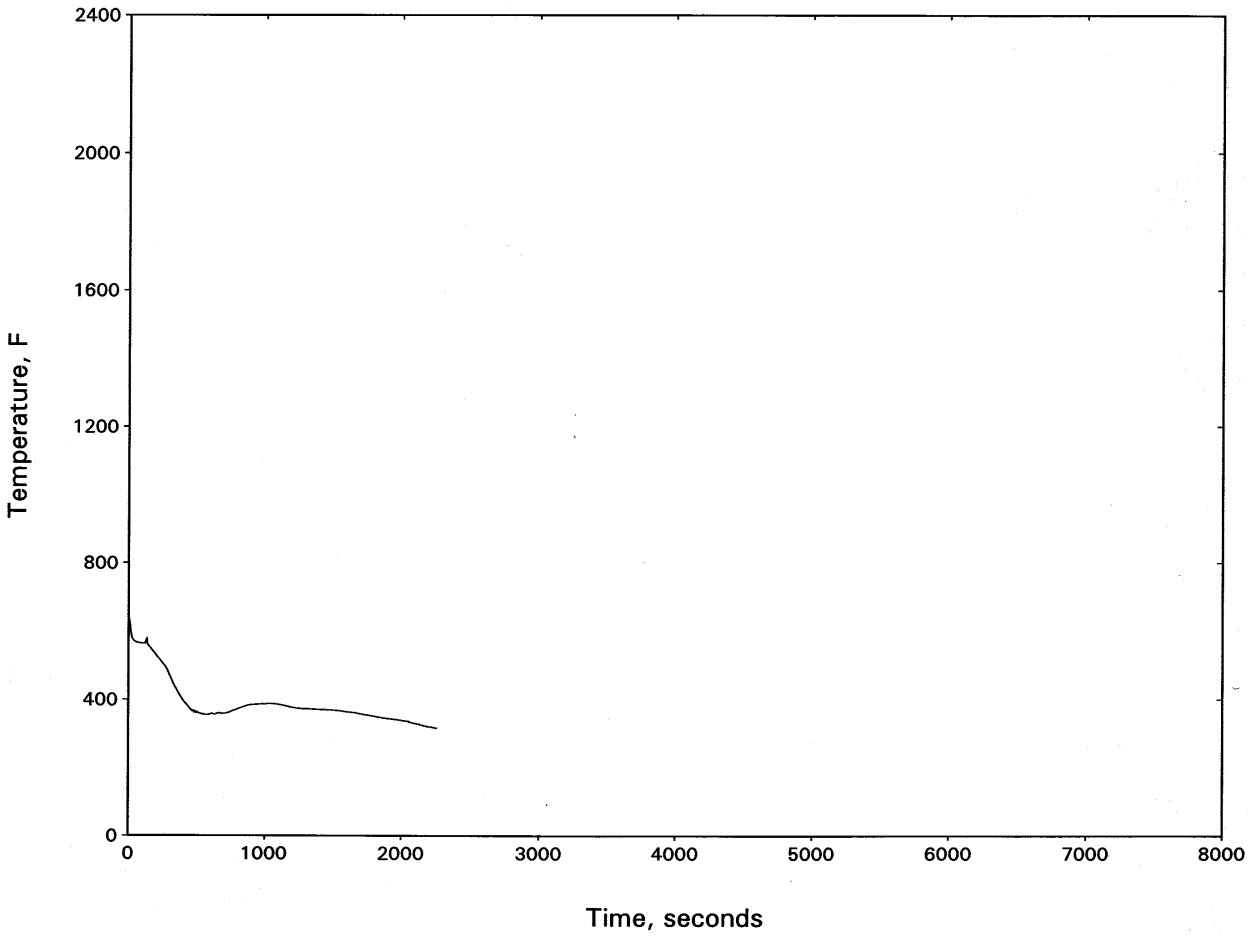

Figure 15.3-89
NORTH ANNA UNIT 1:
HOT CHANNEL OUTLET VAPOR TEMPERATURE—6.0-INCH BREAK

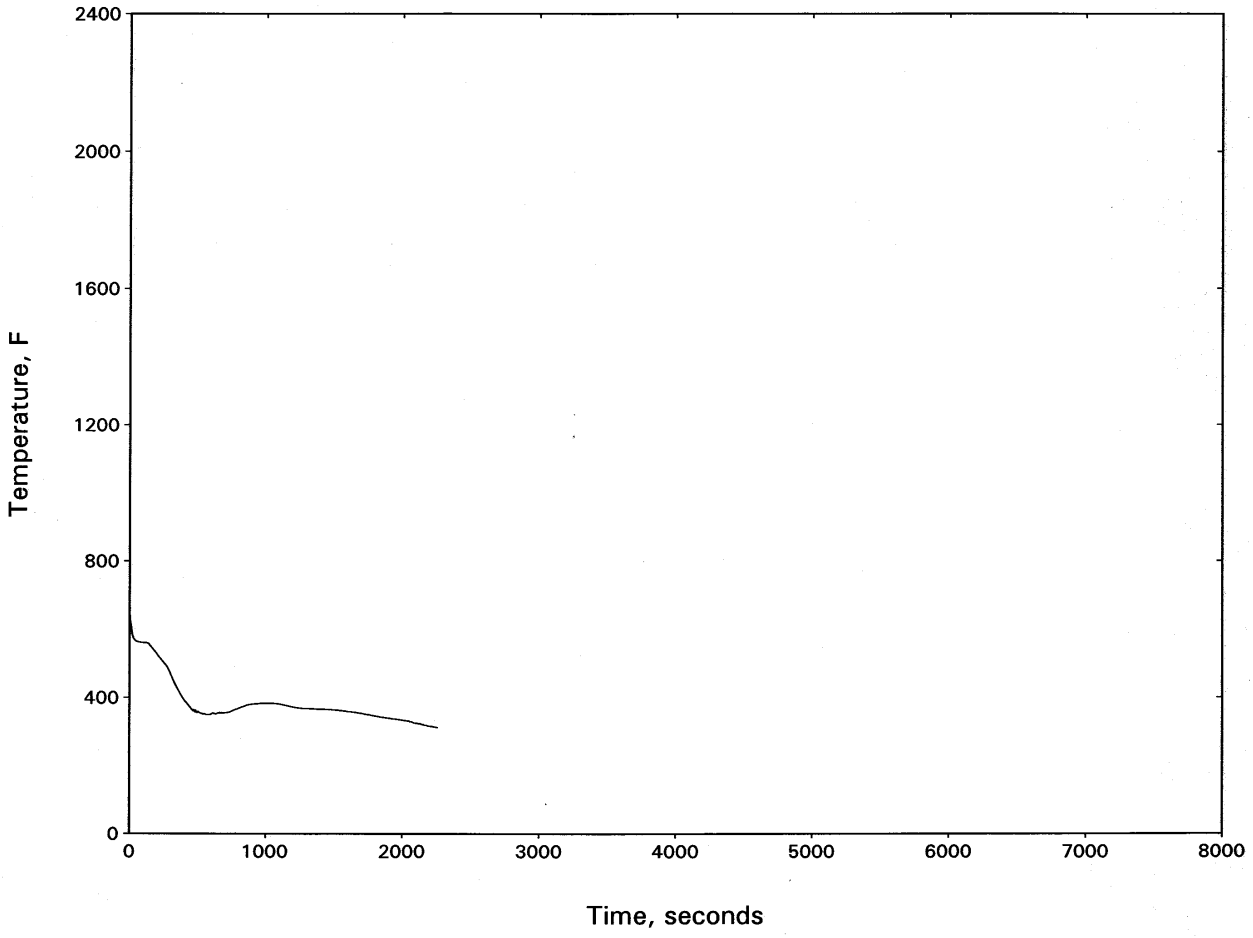

Figure 15.3-90
NORTH ANNA UNIT 1: INTACT LOOP SEAL LEVEL—6.0-INCH BREAK

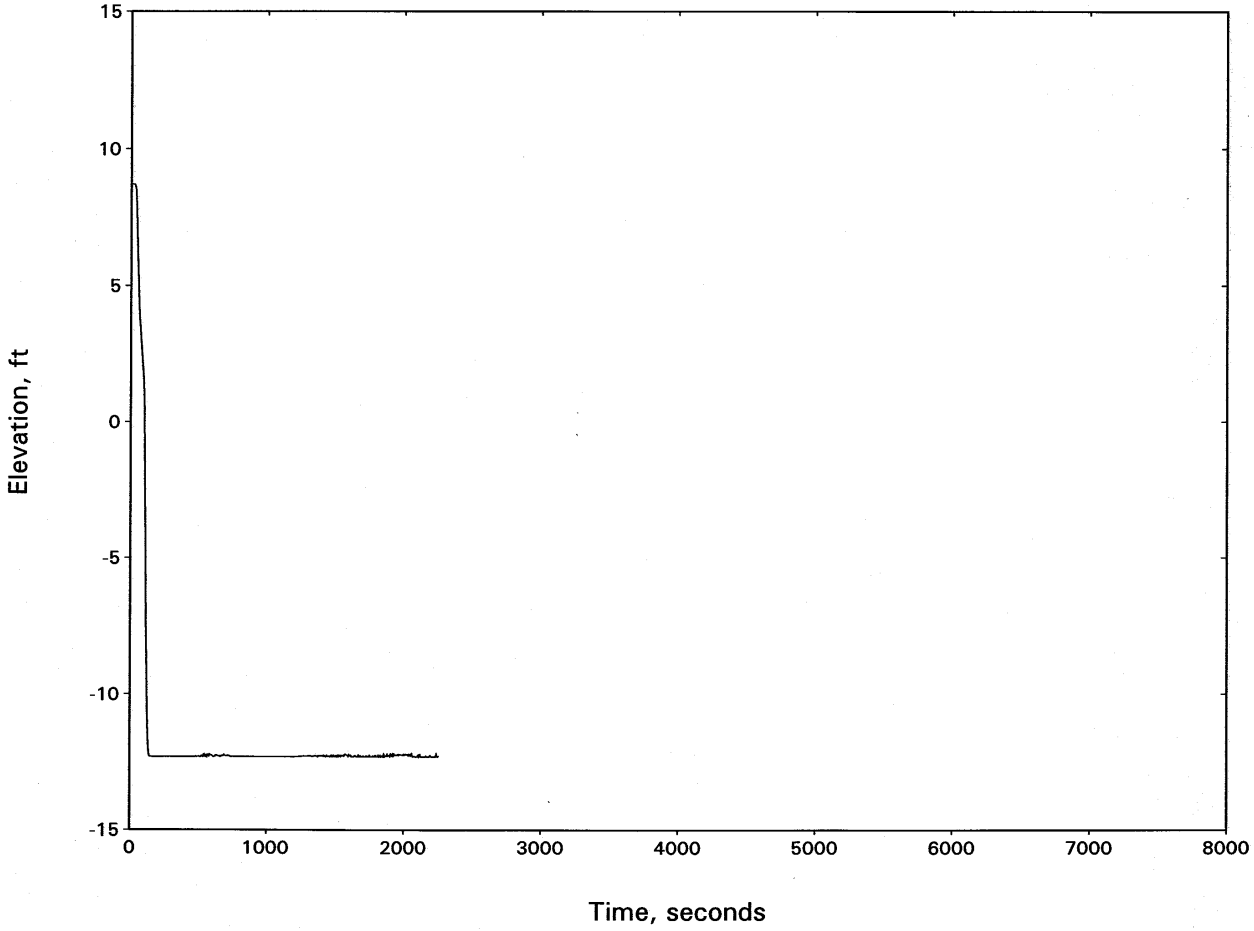

Figure 15.3-91
NORTH ANNA UNIT 1: BROKEN LOOP SEAL LEVEL—6.0-INCH BREAK

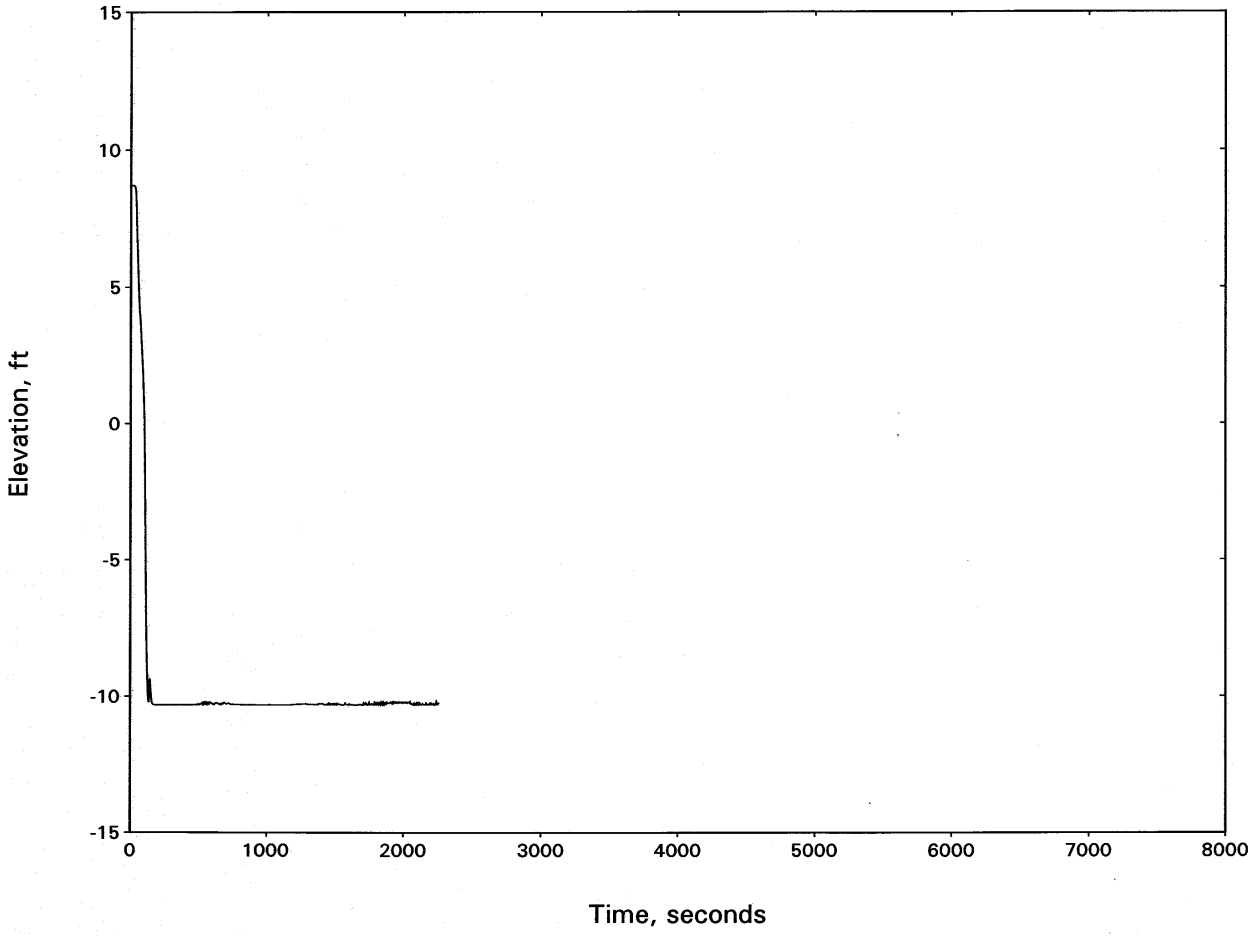

Figure 15.3-92
NORTH ANNA UNIT 1: RCS PRESSURE—5.2-INCH SI LINE BREAK W/AFW FAILURE

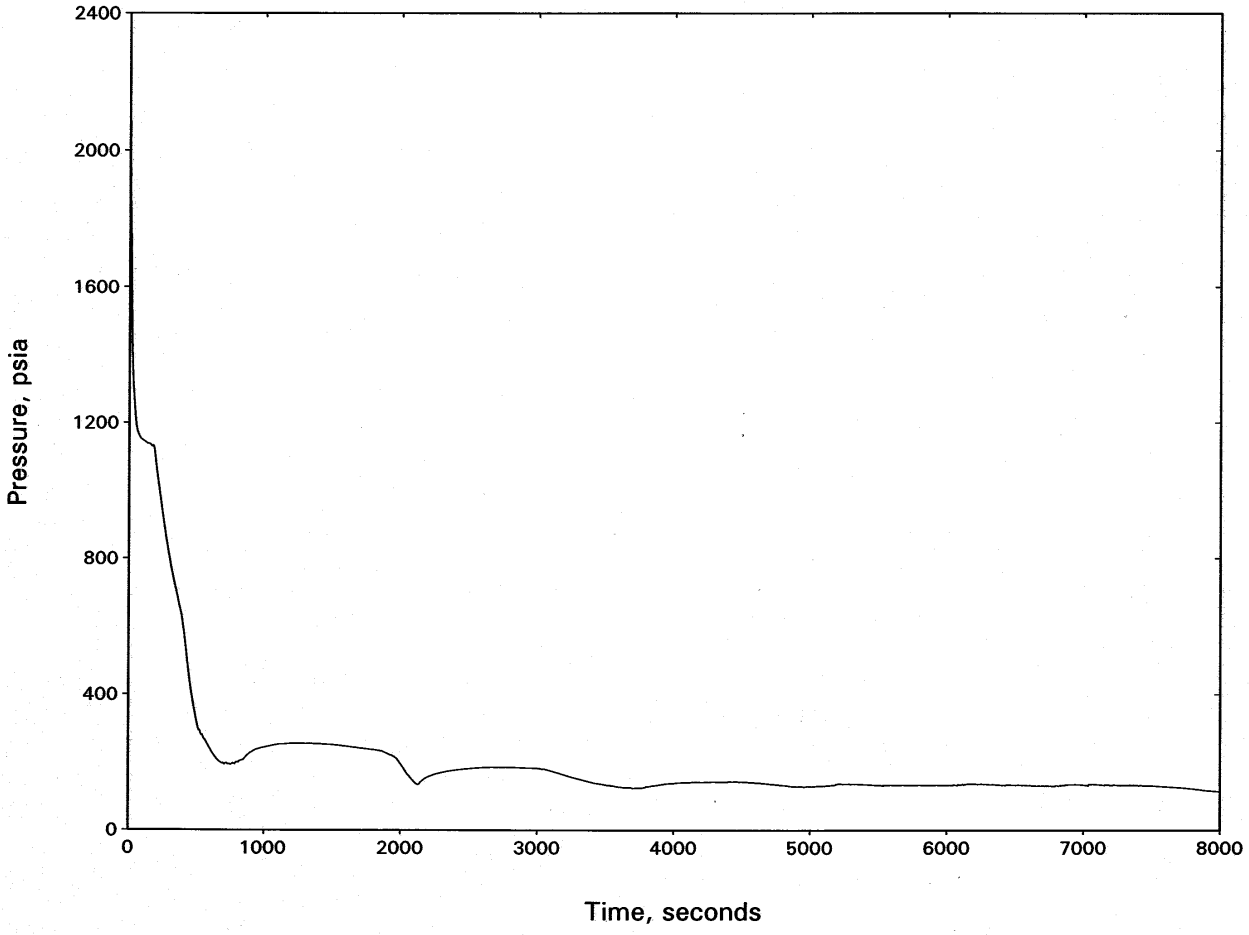

Figure 15.3-93
NORTH ANNA UNIT 1: BREAK FLOW—5.2-INCH SI LINE BREAK W/AFW FAILURE

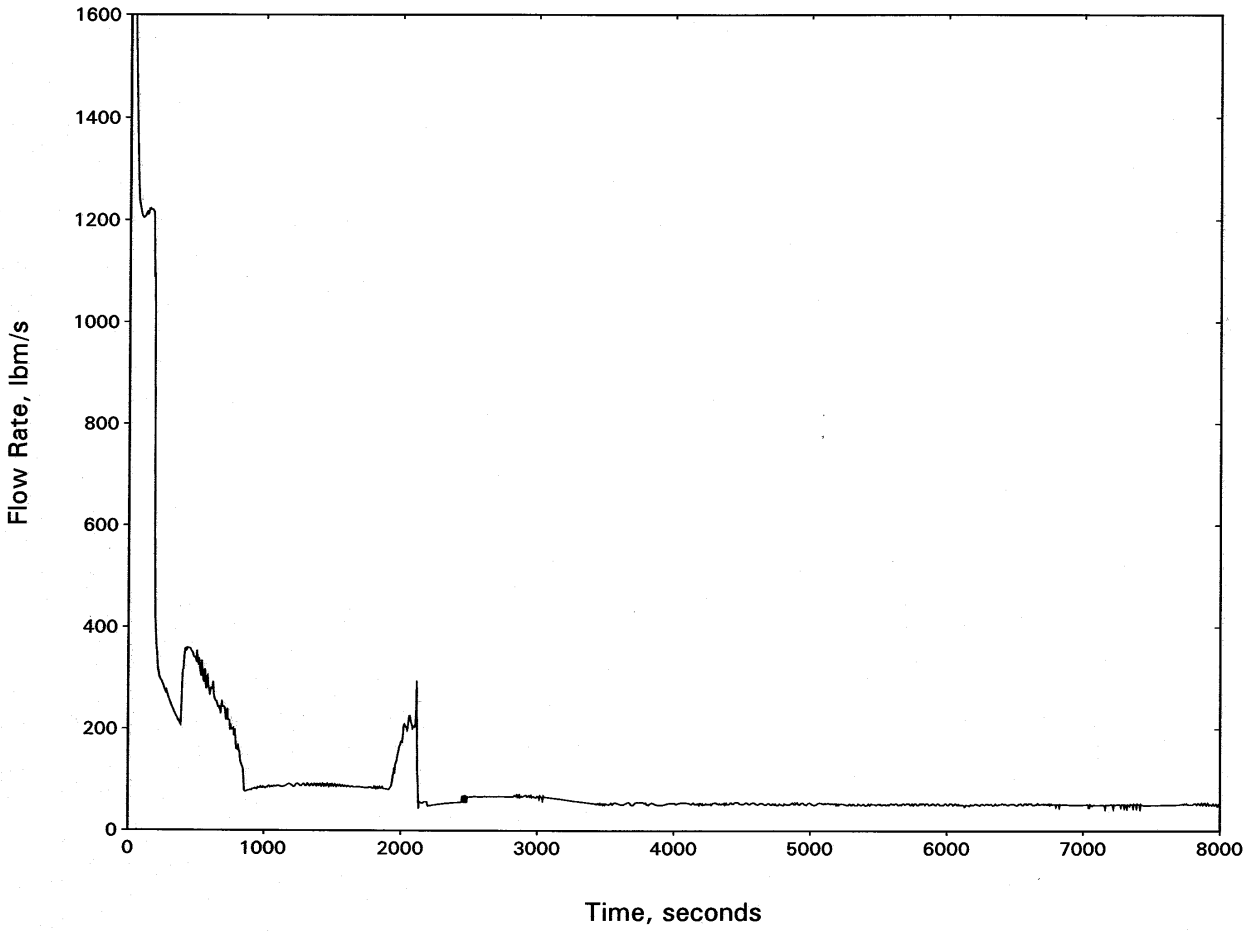

Figure 15.3-94
NORTH ANNA UNIT 1:
HOT CHANNEL MIXTURE LEVEL—5.2-INCH SI LINE BREAK W/AFW FAILURE

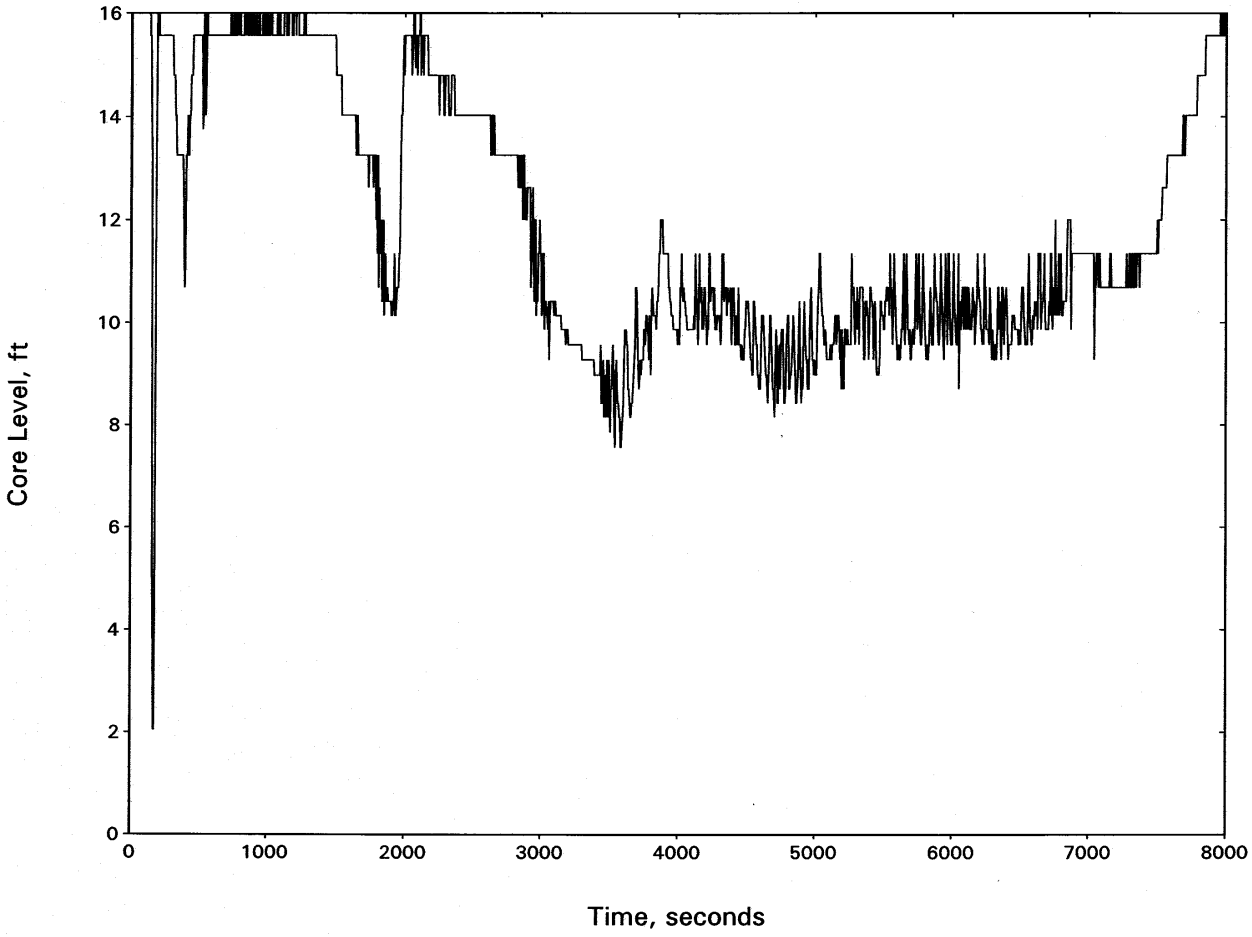

Figure 15.3-95
NORTH ANNA UNIT 1: HOT SPOT PCT—5.2-INCH SI LINE BREAK W/AFW FAILURE

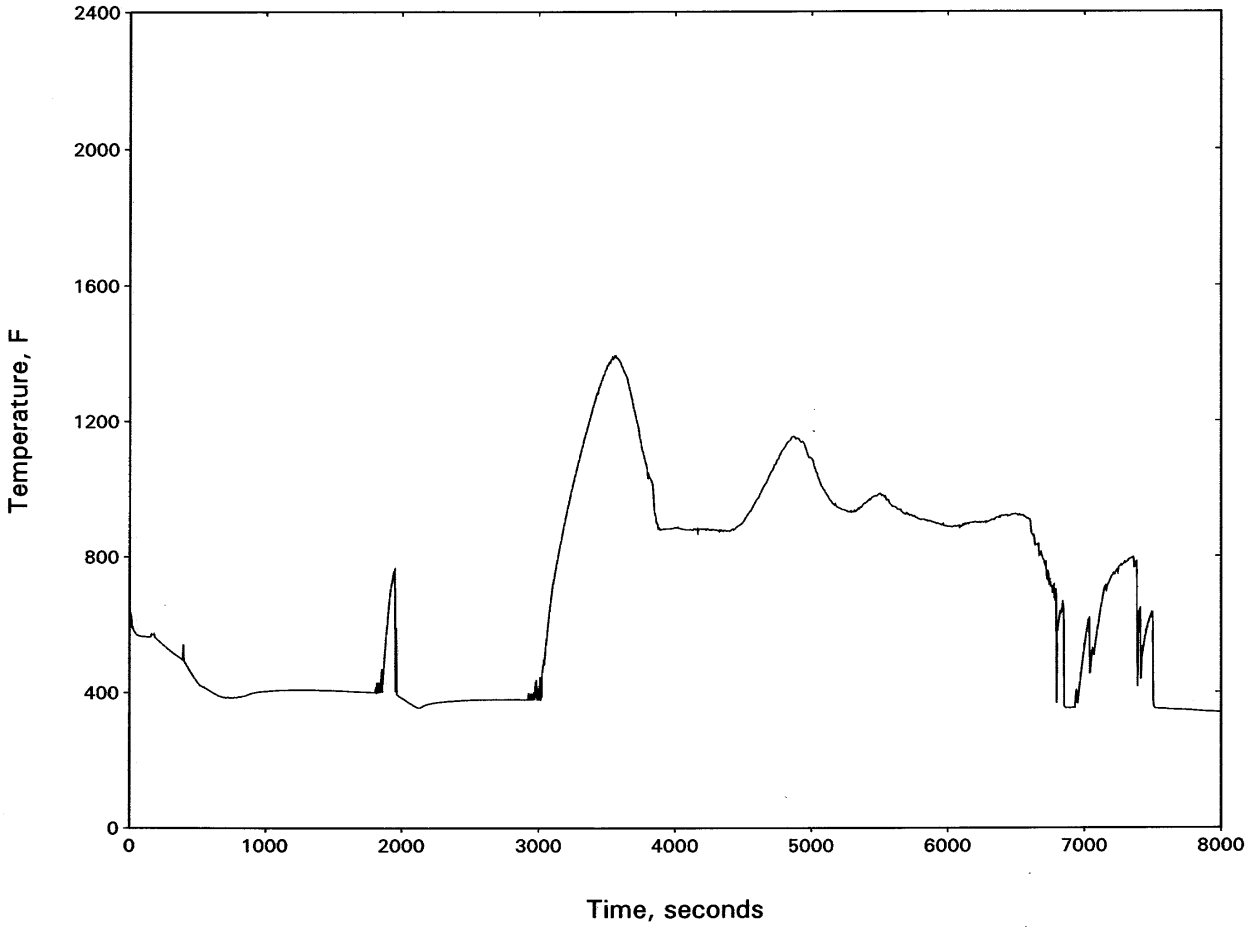

Figure 15.3-96
NORTH ANNA UNIT 1: HOT CHANNEL OUTLET VAPOR TEMPERATURE—5.2-INCH SI LINE BREAK W/AFW FAILURE

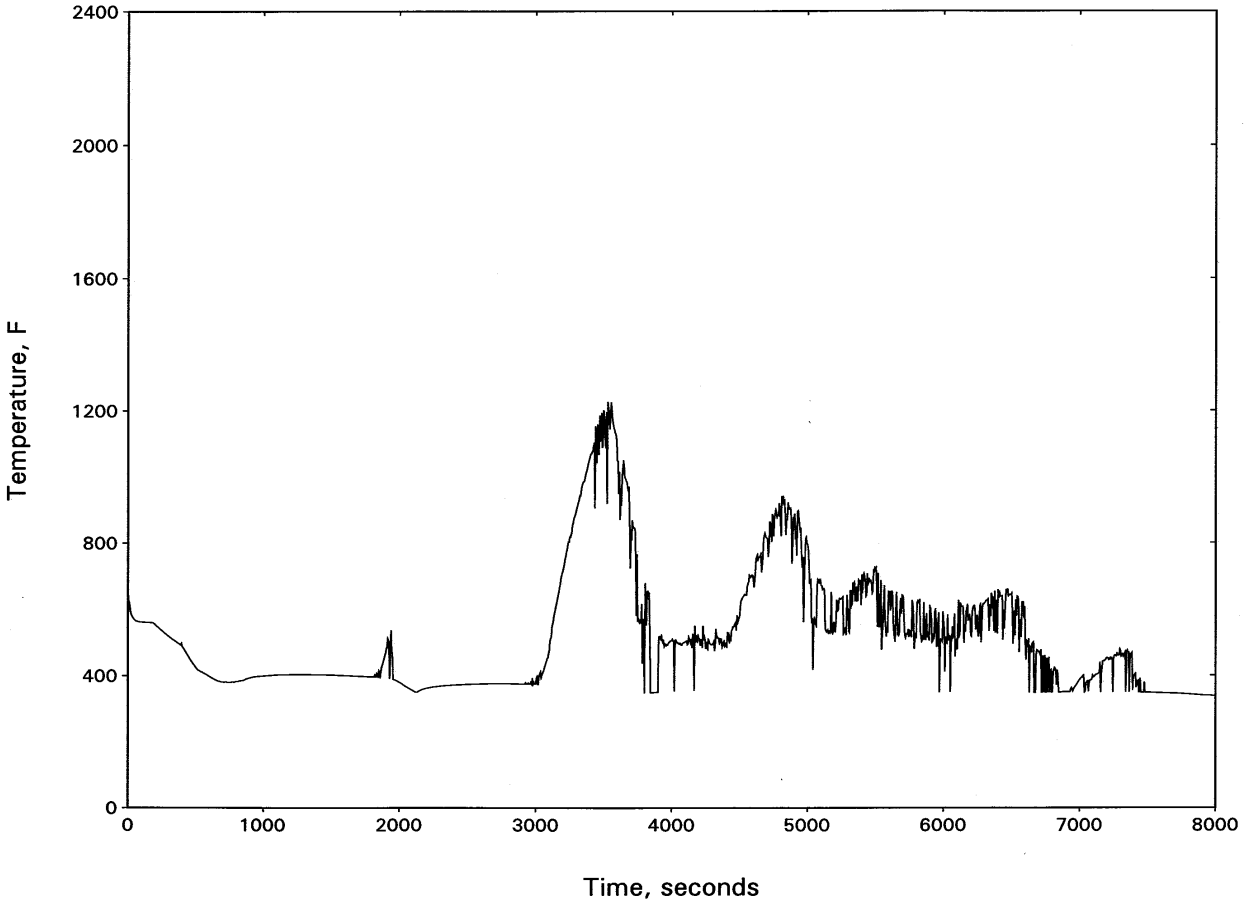

Figure 15.3-97
NORTH ANNA UNIT 1:
INTACT LOOP SEAL LEVEL—5.2-INCH SI LINE BREAK W/AFW FAILURE

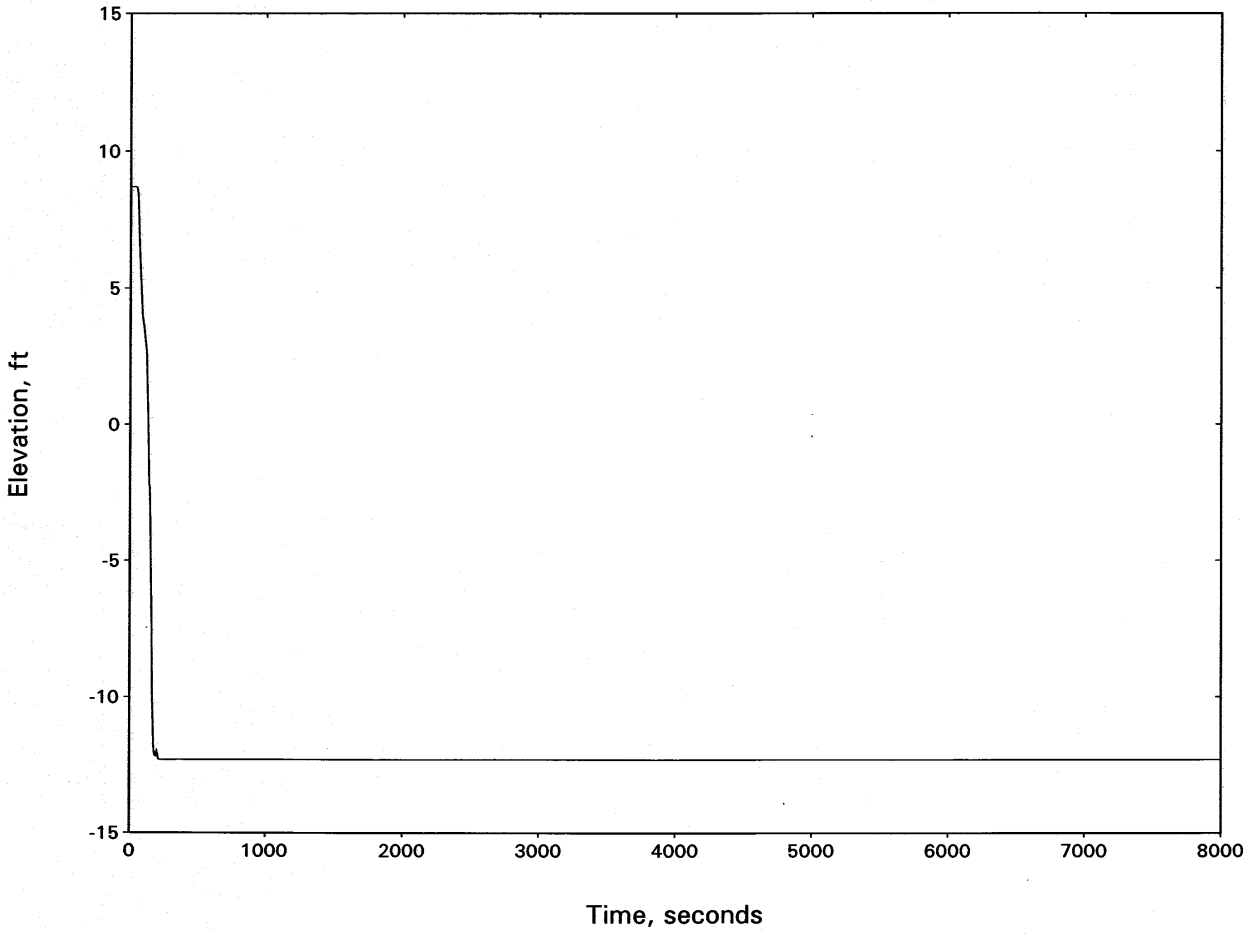

Figure 15.3-98
NORTH ANNA UNIT 1:
BROKEN LOOP SEAL LEVEL—5.2-INCH SI LINE BREAK W/AFW FAILURE

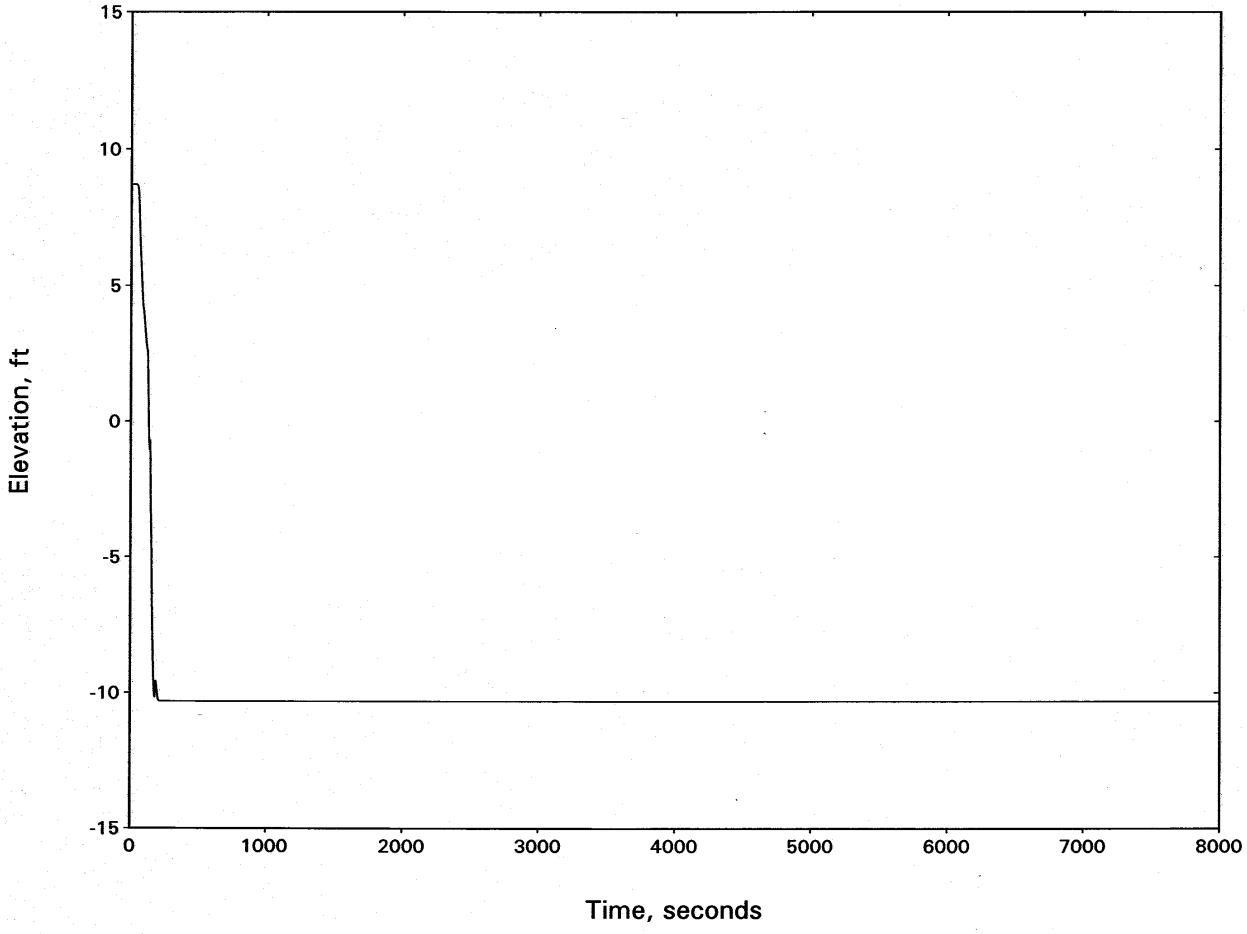

Figure 15.3-99
NORTH ANNA UNIT 1: RCS PRESSURE—5.2-INCH SI LINE BREAK MIXED CORE

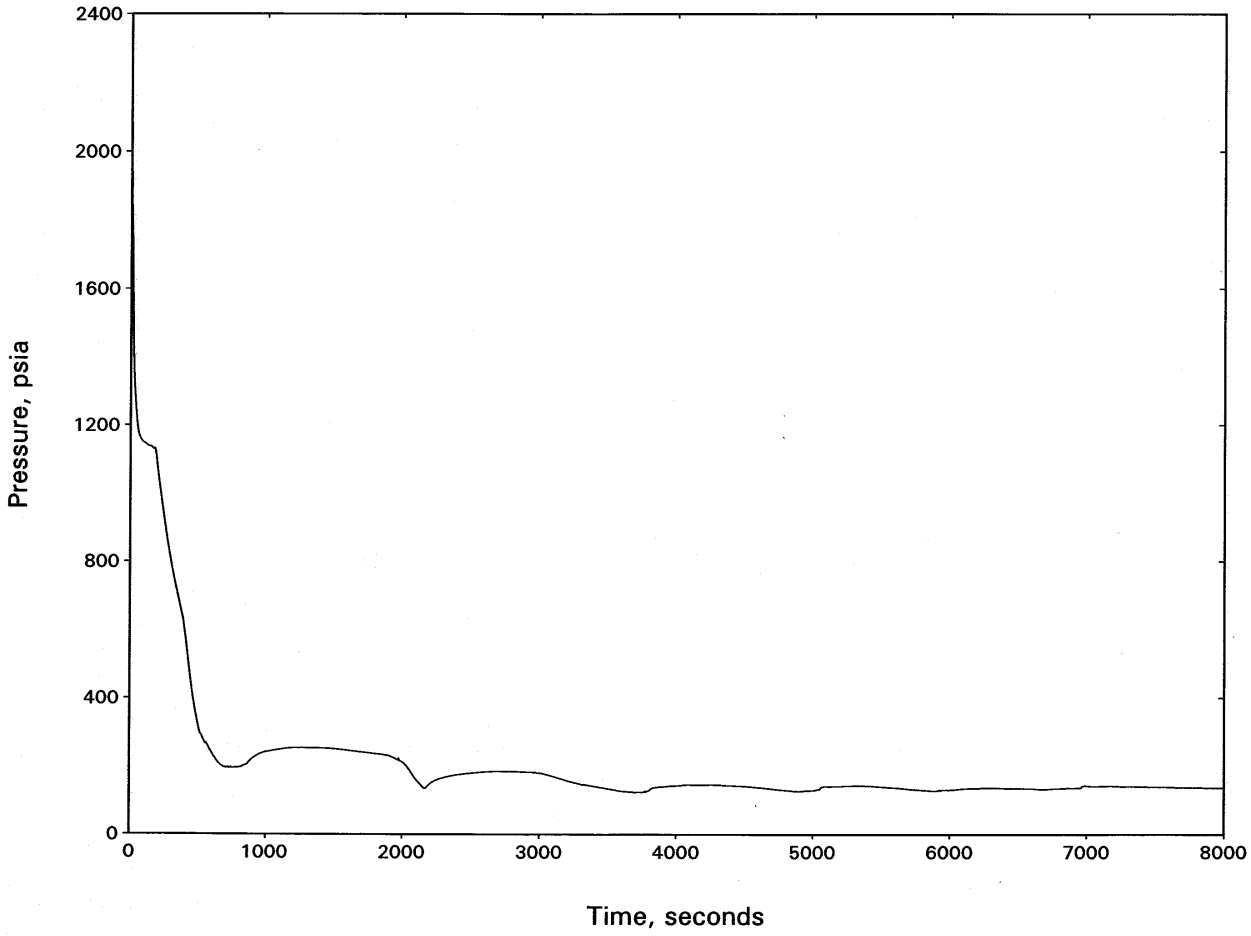

Figure 15.3-100
NORTH ANNA UNIT 1: BREAK FLOW—5.2-INCH SI LINE BREAK MIXED CORE

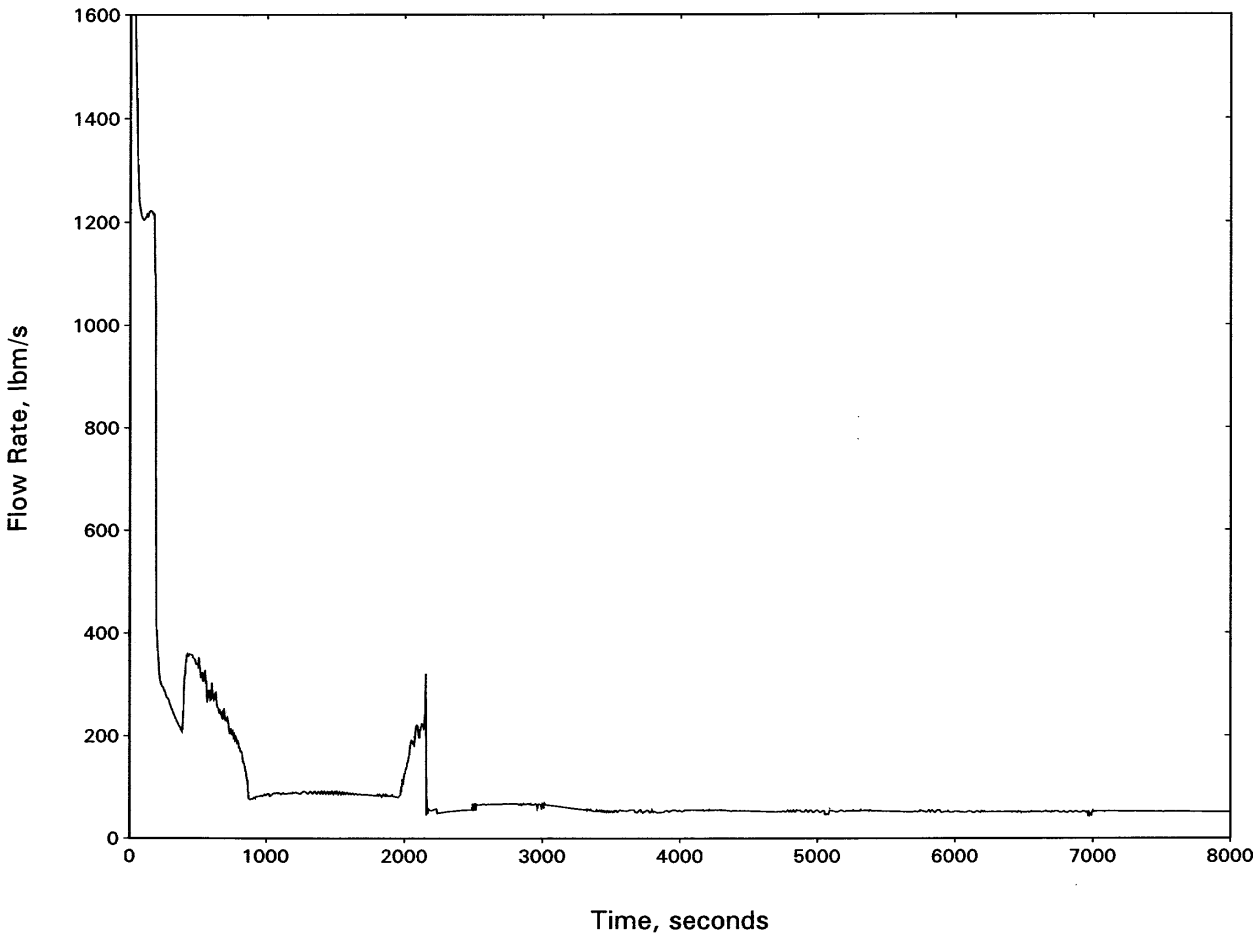

Figure 15.3-101
NORTH ANNA UNIT 1:
HOT CHANNEL MIXTURE LEVEL—5.2-INCH SI LINE BREAK MIXED CORE

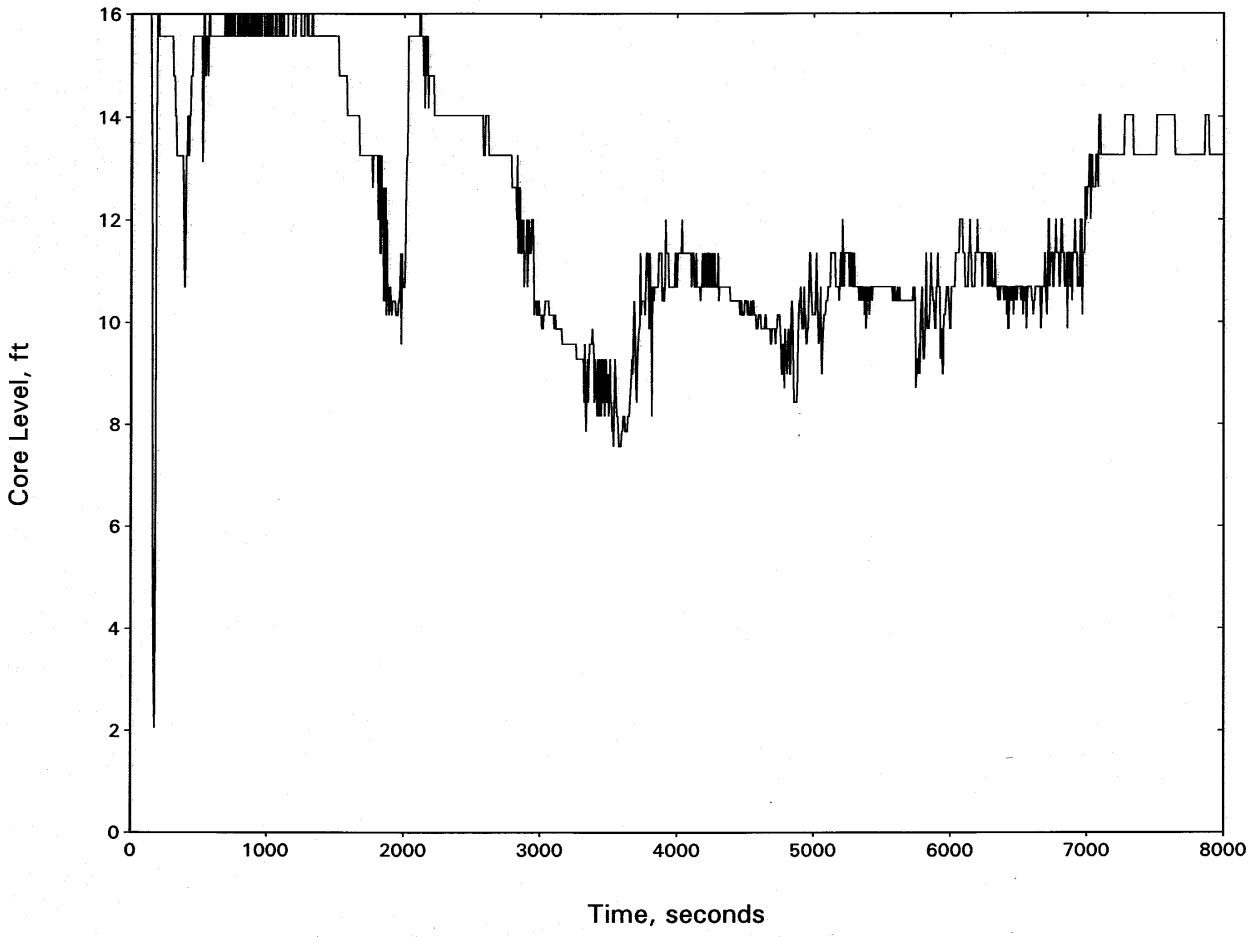

Figure 15.3-102
NORTH ANNA UNIT 1: HOT SPOT PCT—5.2-INCH SI LINE BREAK MIXED CORE

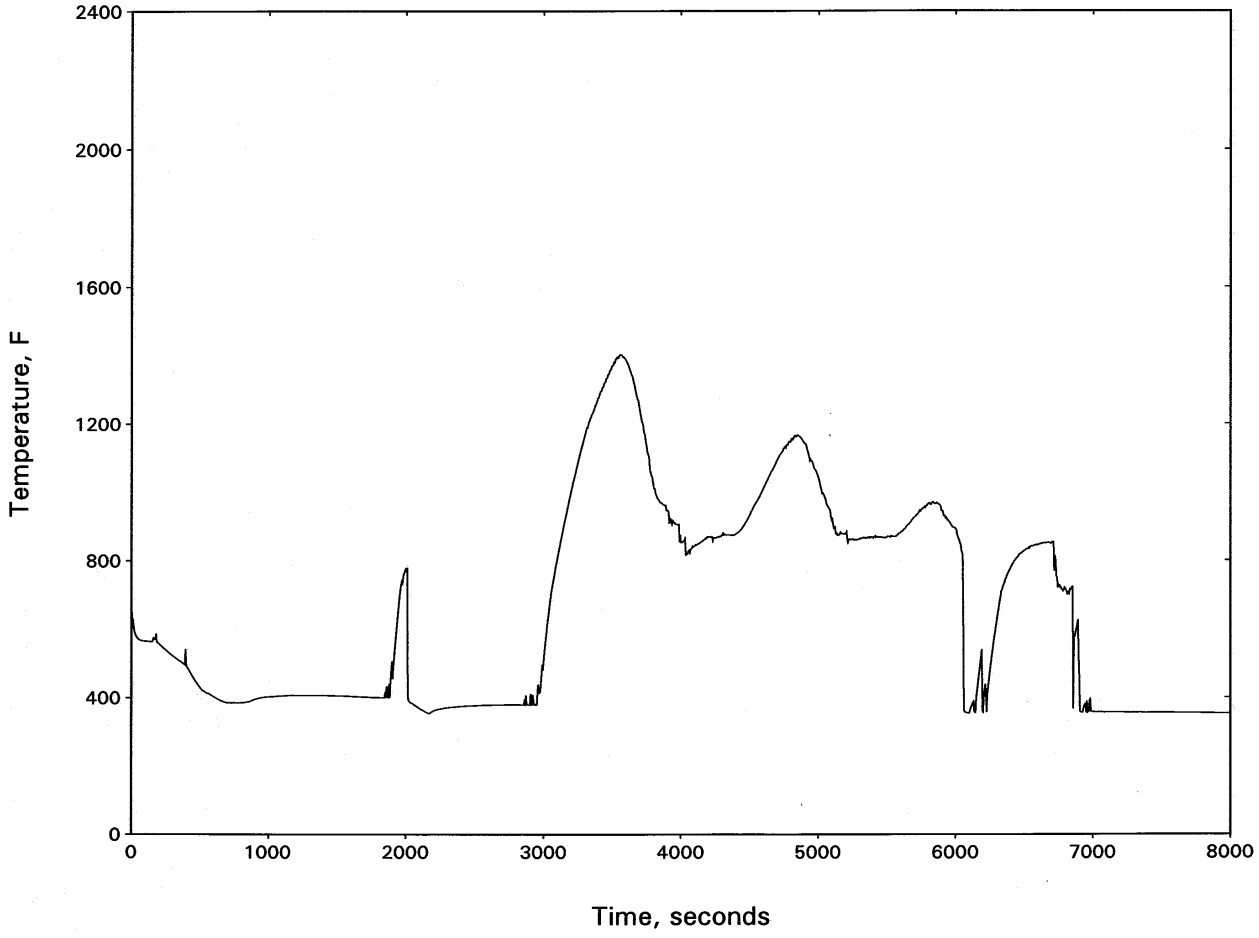

Figure 15.3-103
NORTH ANNA UNIT 1: HOT CHANNEL OUTLET VAPOR TEMPERATURE—5.2-INCH SI LINE BREAK MIXED CORE

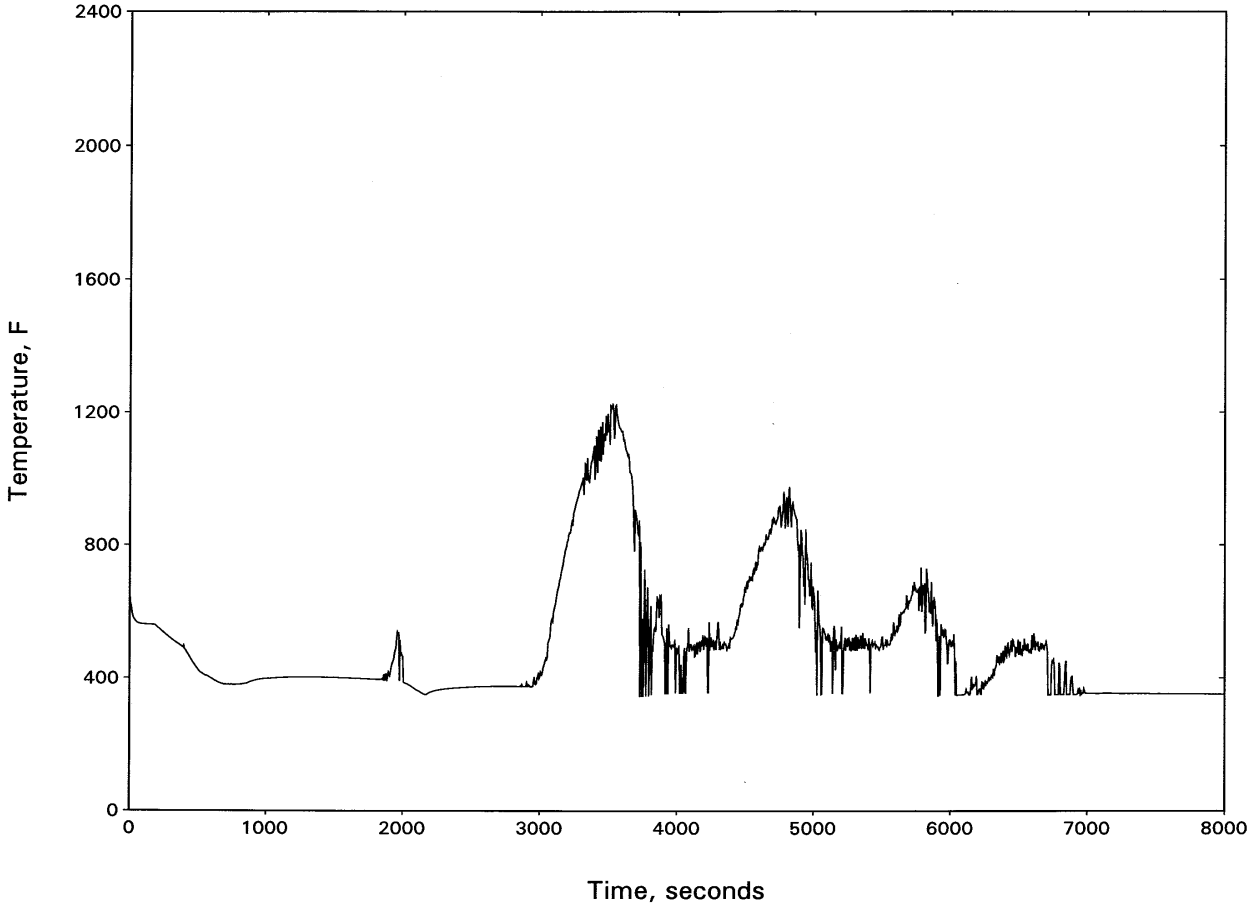

Figure 15.3-104
NORTH ANNA UNIT 1:
INTACT LOOP SEAL LEVEL—5.2-INCH SI LINE BREAK MIXED CORE

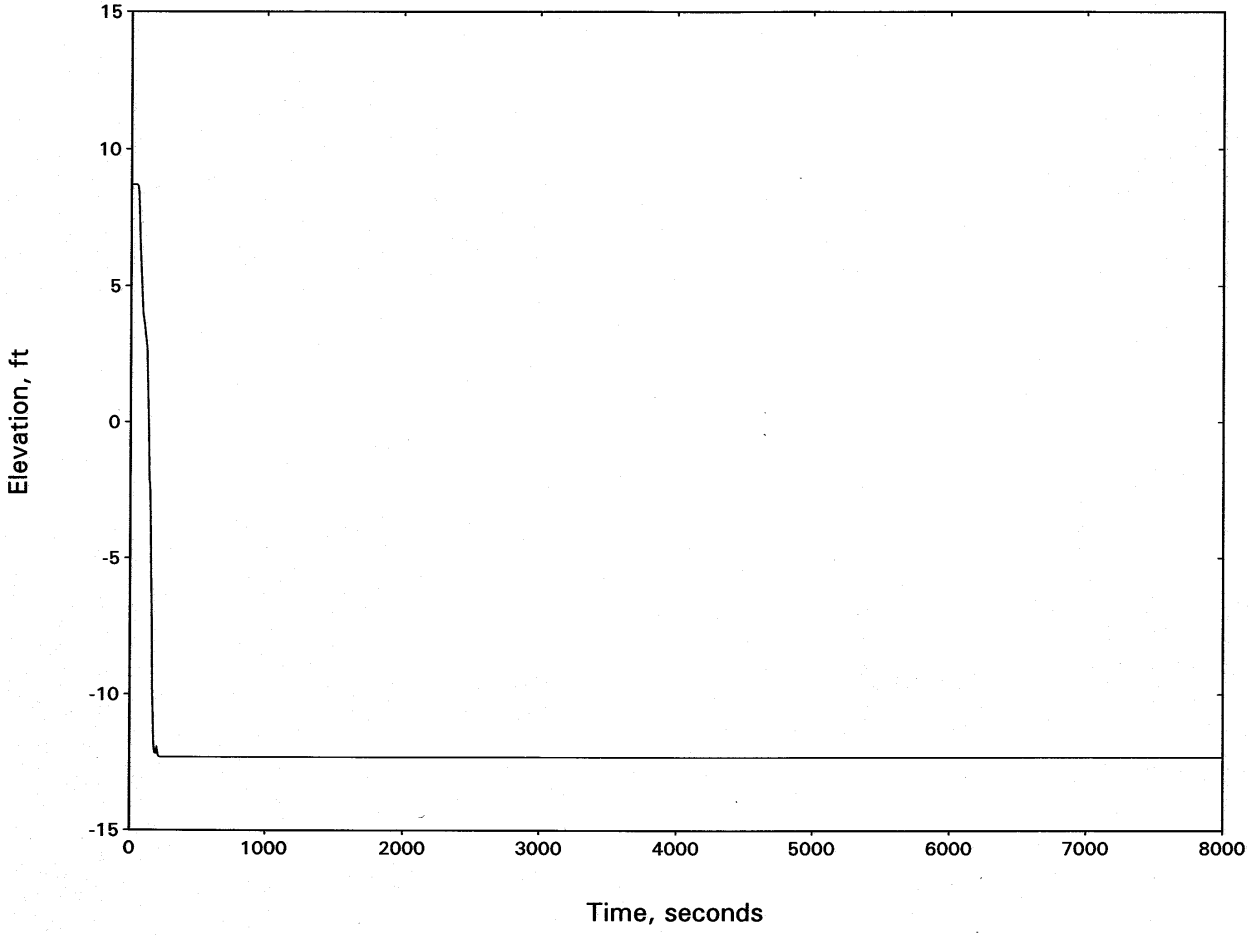

Figure 15.3-105
NORTH ANNA UNIT 1:
BROKEN LOOP SEAL LEVEL—5.2-INCH SI LINE BREAK MIXED CORE

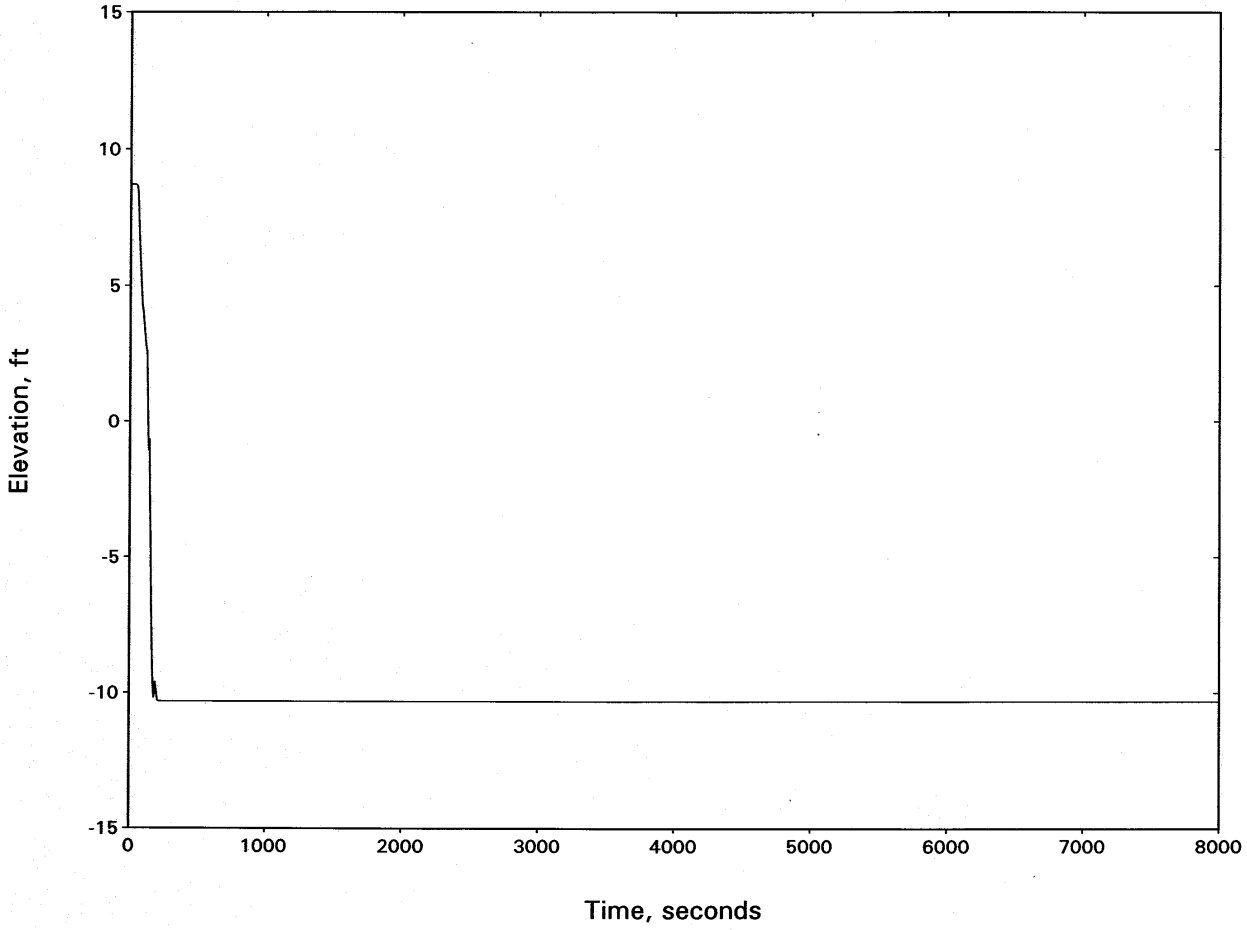

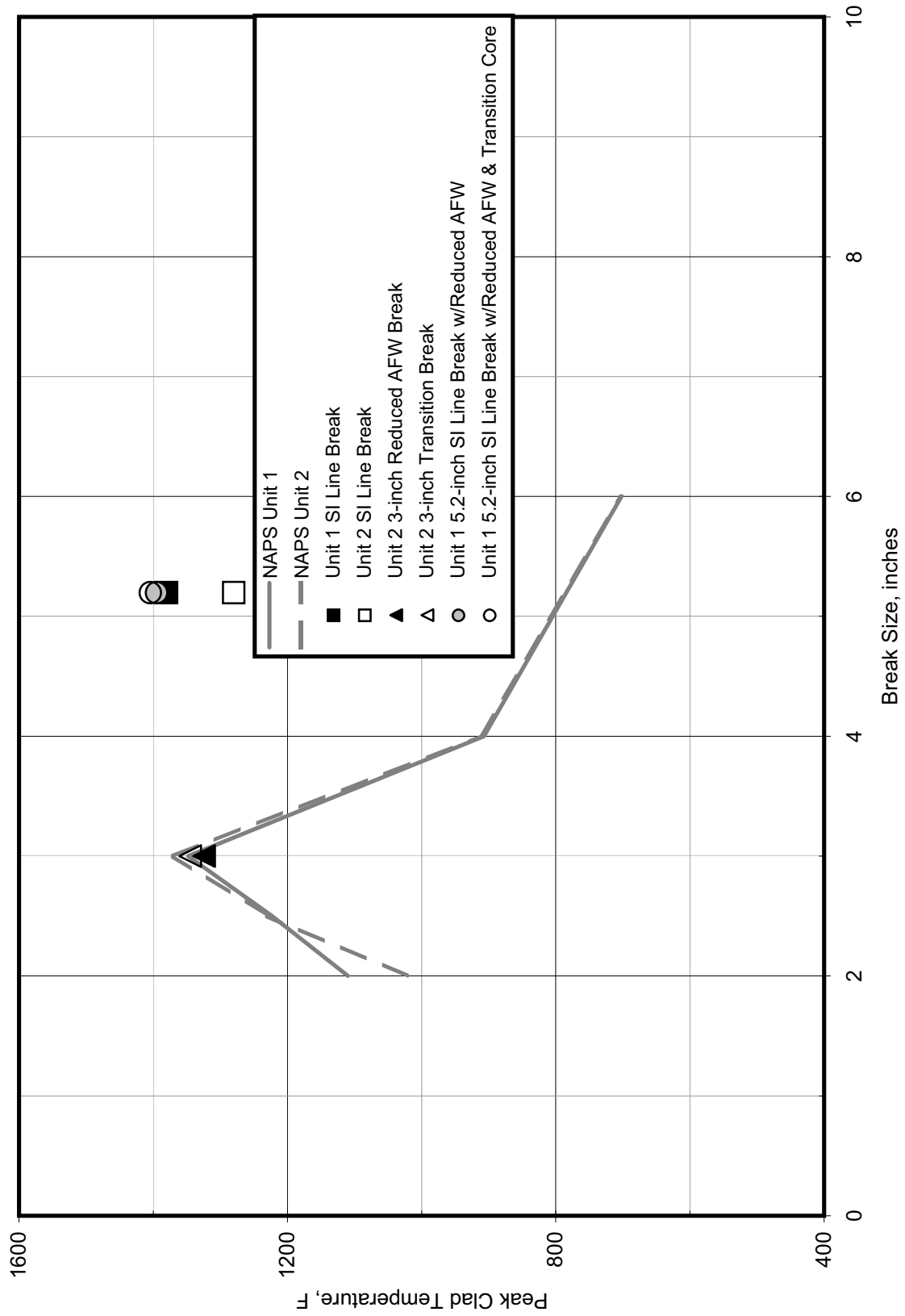

Figure 15.3-106
NORTH ANNA UNITS 1 AND 2 PCT VERSUS BREAK SIZE

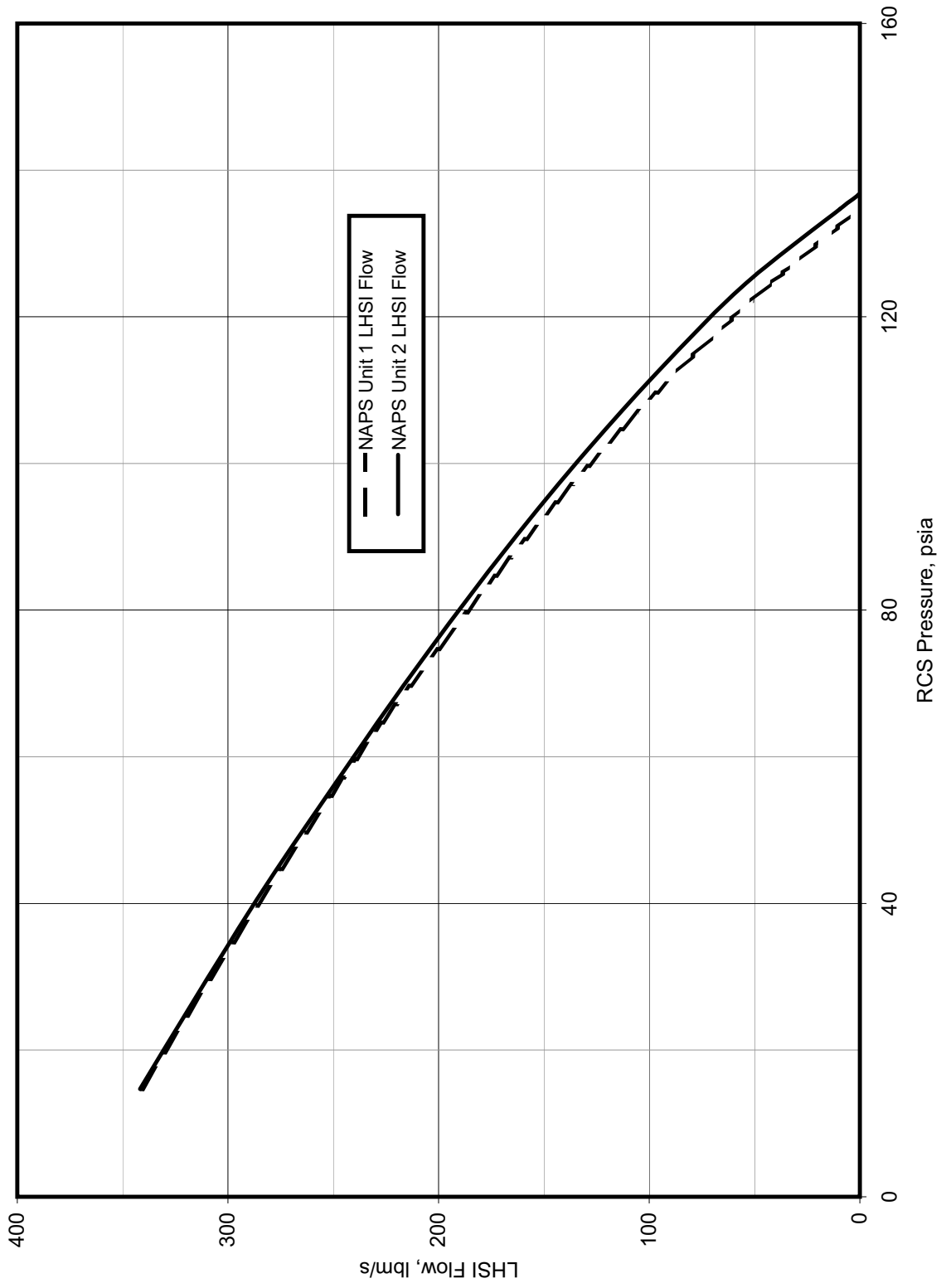

Figure 15.3-107
NORTH ANNA UNITS 1 AND 2 LHSI FLOW TO INTACT LOOP COMPARISON FOR SI LINE BREAK

Figure 15.3-108
NORTH ANNA UNIT 2: RCS PRESSURE—2-INCH BREAK

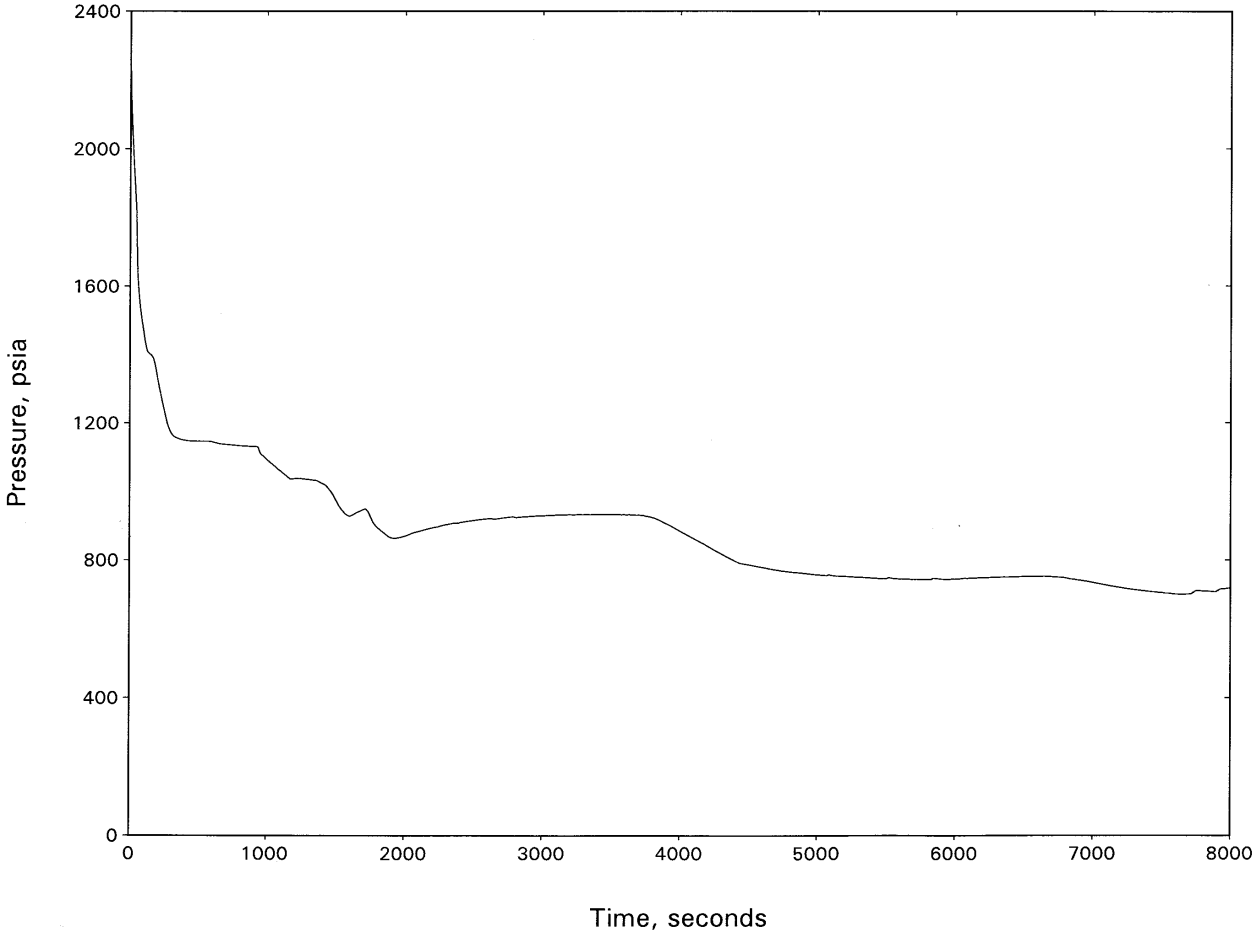

Figure 15.3-109
NORTH ANNA UNIT 2: BREAK FLOW—2-INCH BREAK

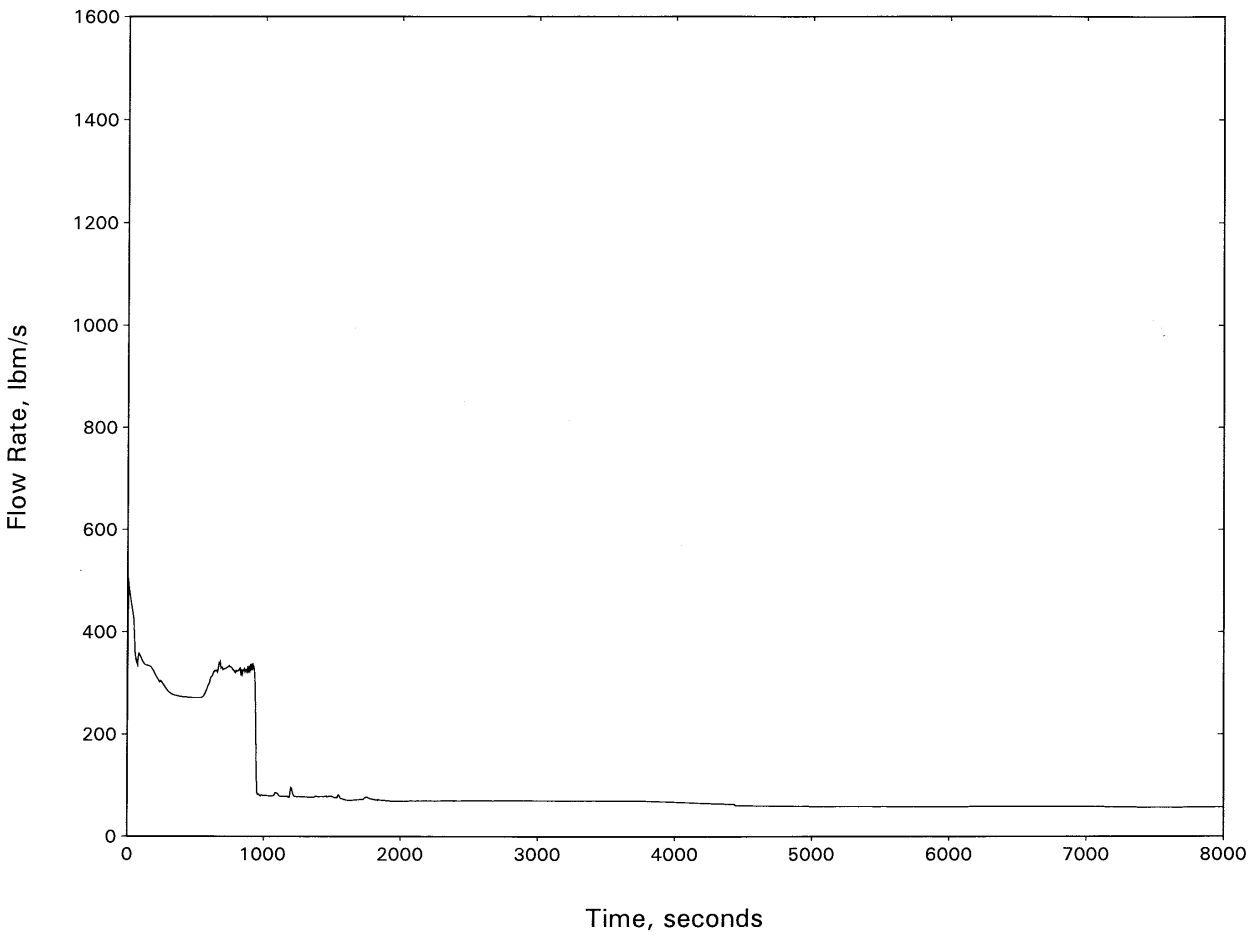

Figure 15.3-110
NORTH ANNA UNIT 2: HOT CHANNEL MIXTURE LEVEL—2-INCH BREAK

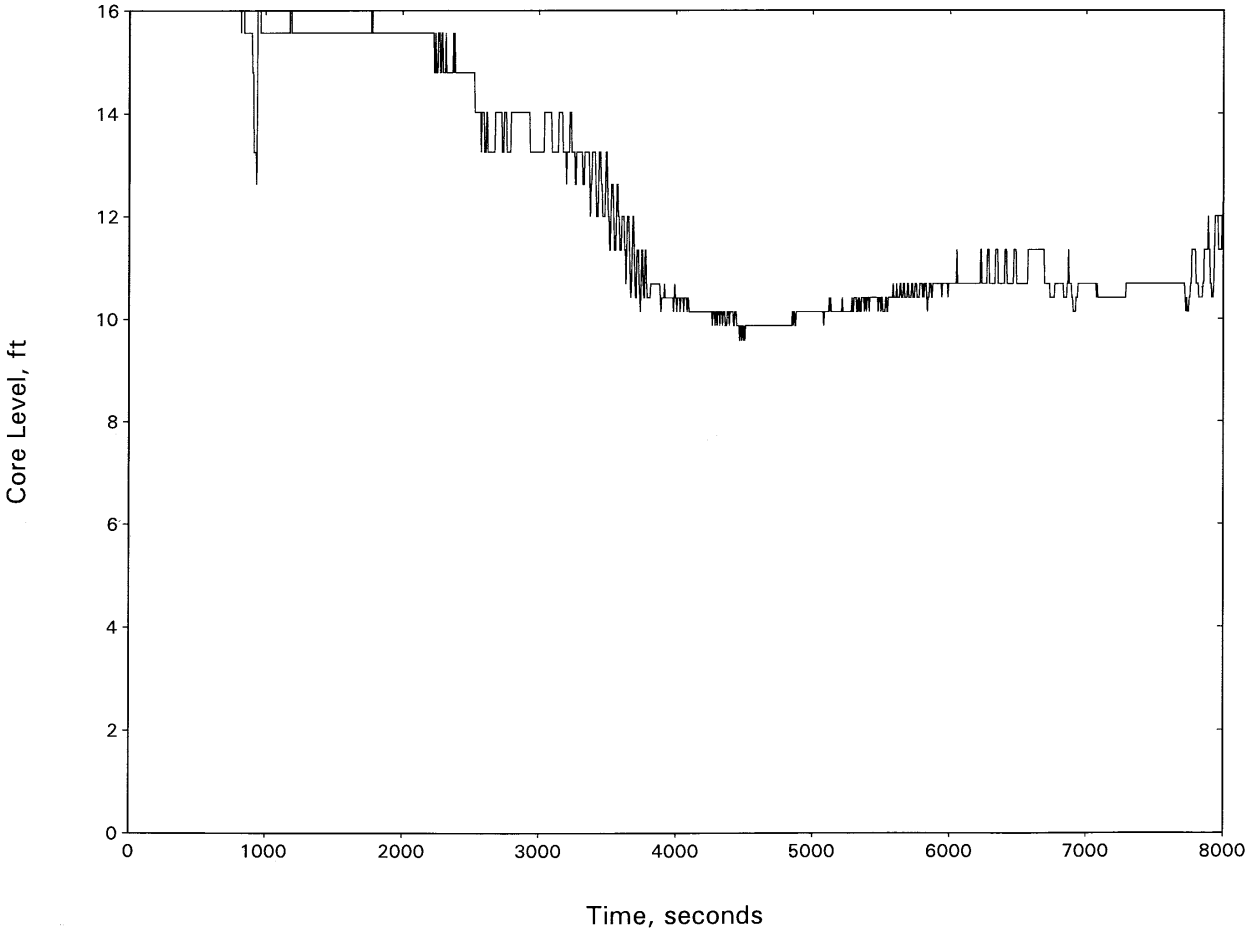

Figure 15.3-111
NORTH ANNA UNIT 2 HOT SPOT PCT—2-INCH BREAK

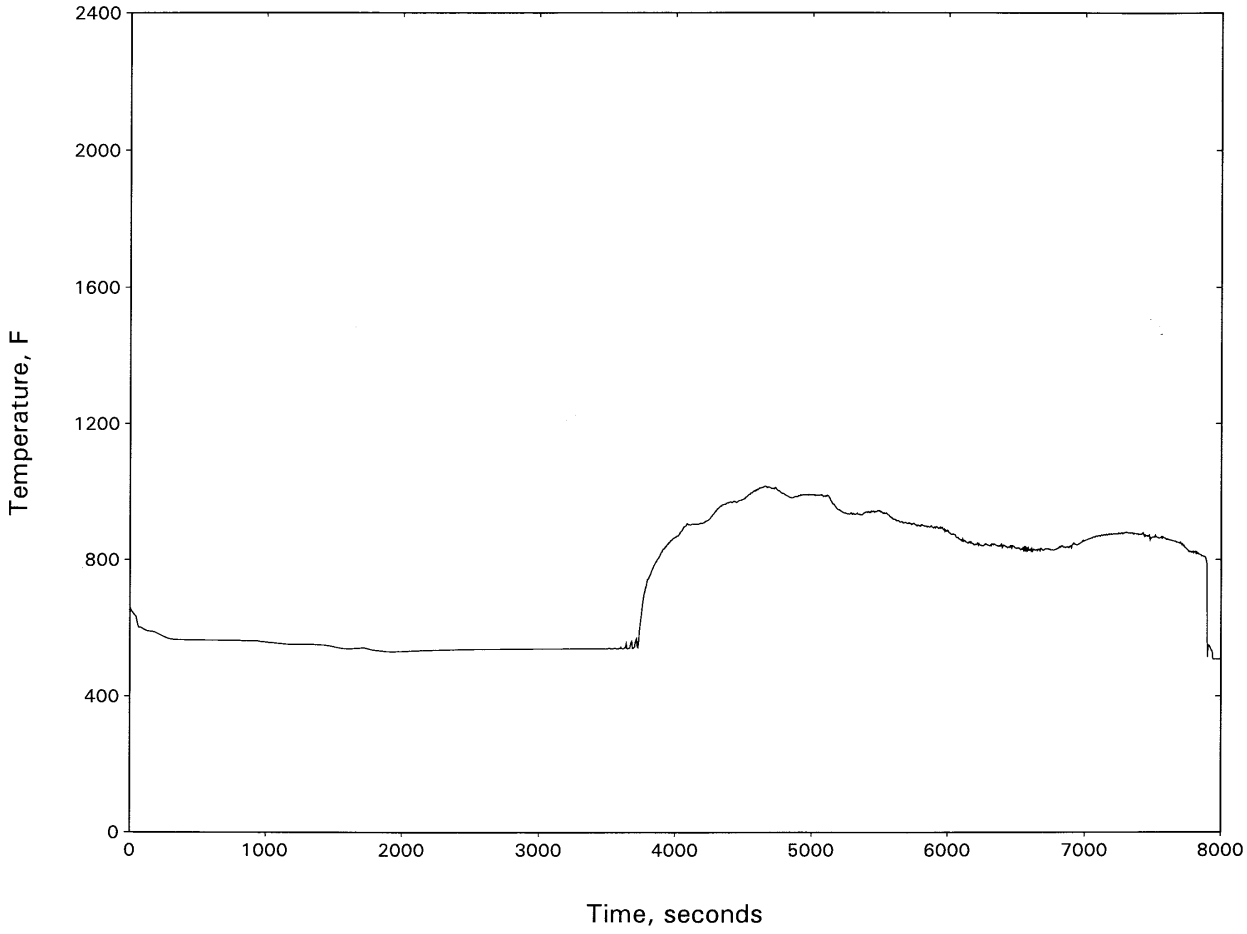

Figure 15.3-112
NORTH ANNA UNIT 2:
HOT CHANNEL OUTLET VAPOR TEMPERATURE—2-INCH BREAK

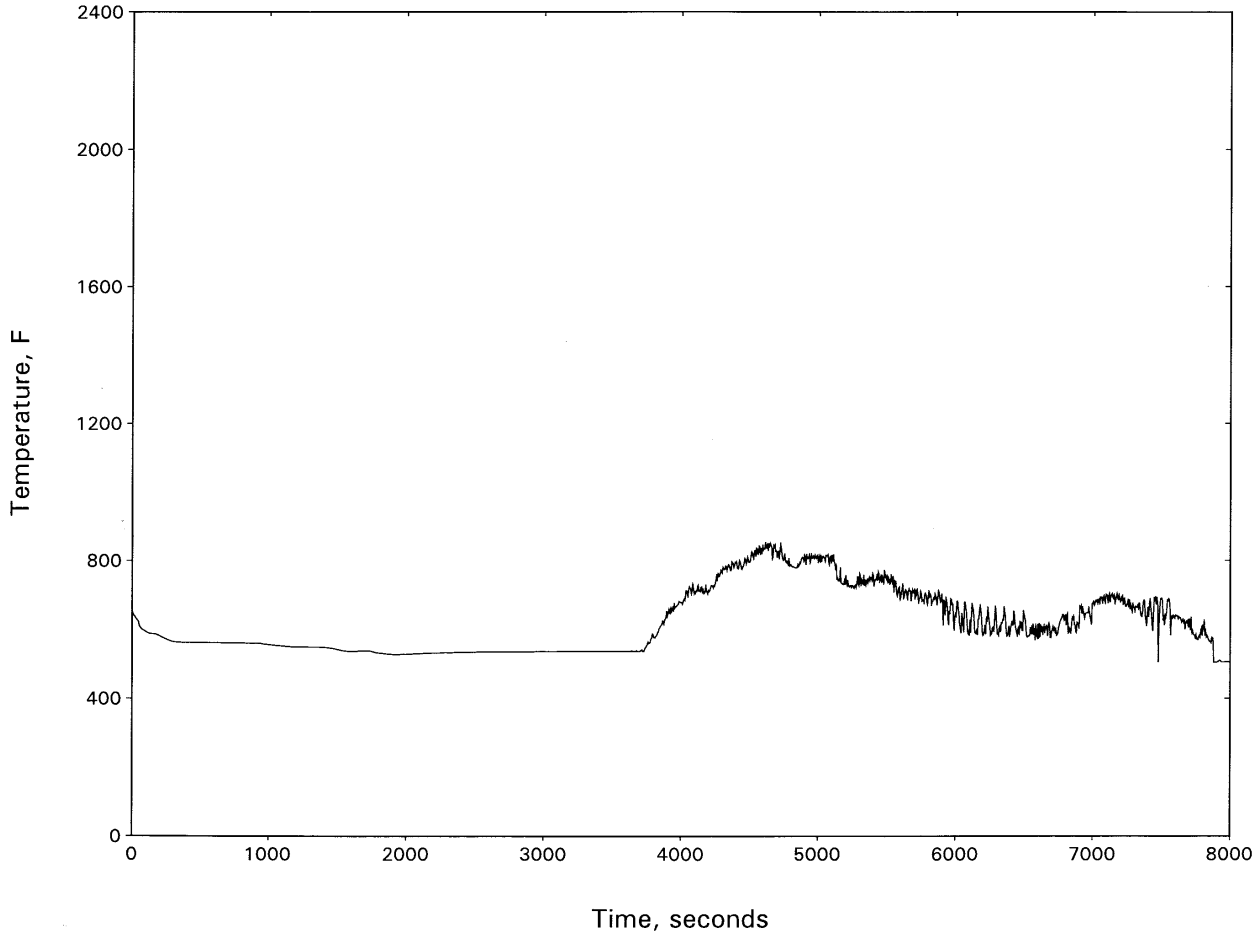

Figure 15.3-113
NORTH ANNA UNIT 2: INTACT LOOP SEAL LEVEL—2-INCH BREAK

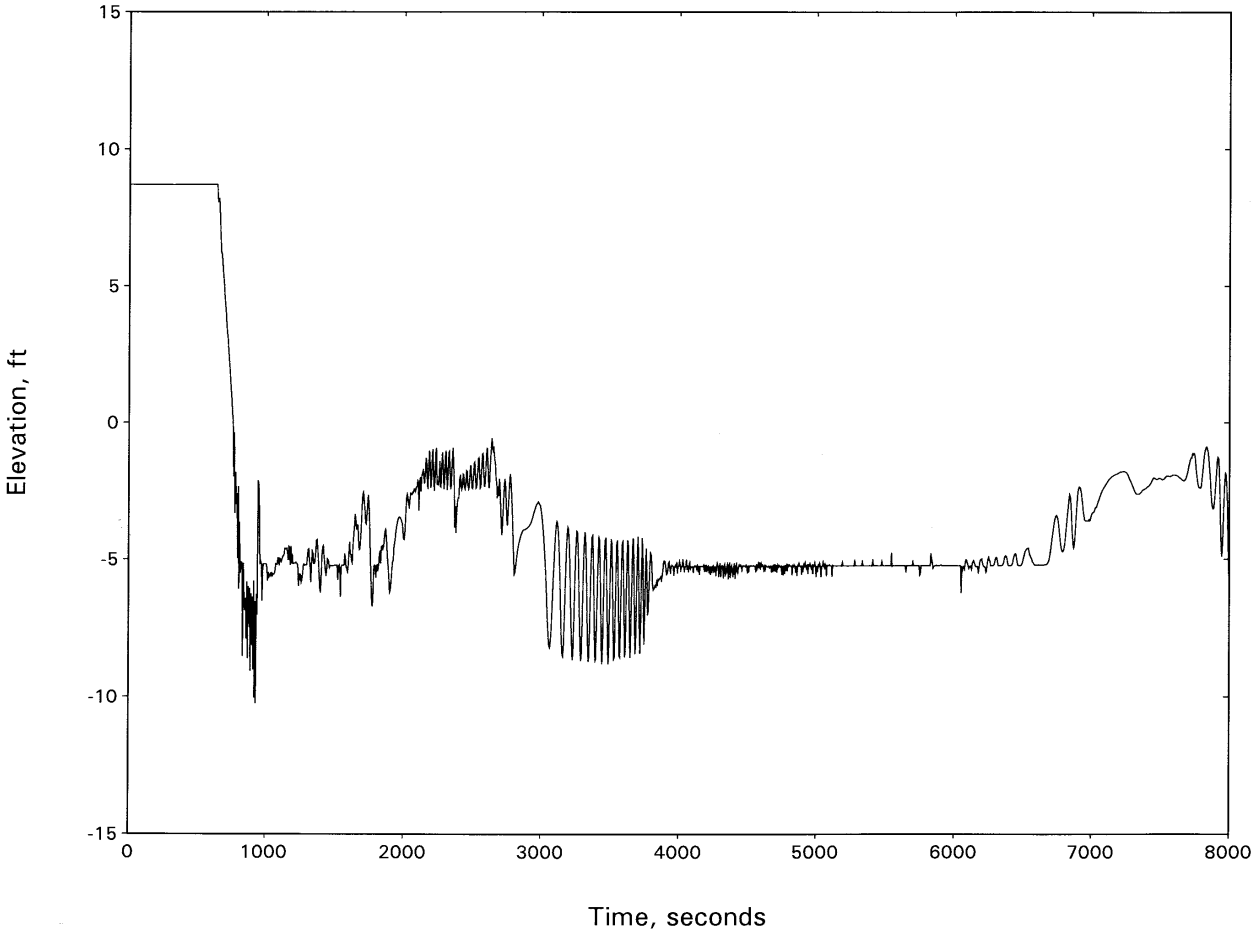

Figure 15.3-114
NORTH ANNA UNIT 2: BROKEN LOOP SEAL LEVEL—2-INCH BREAK

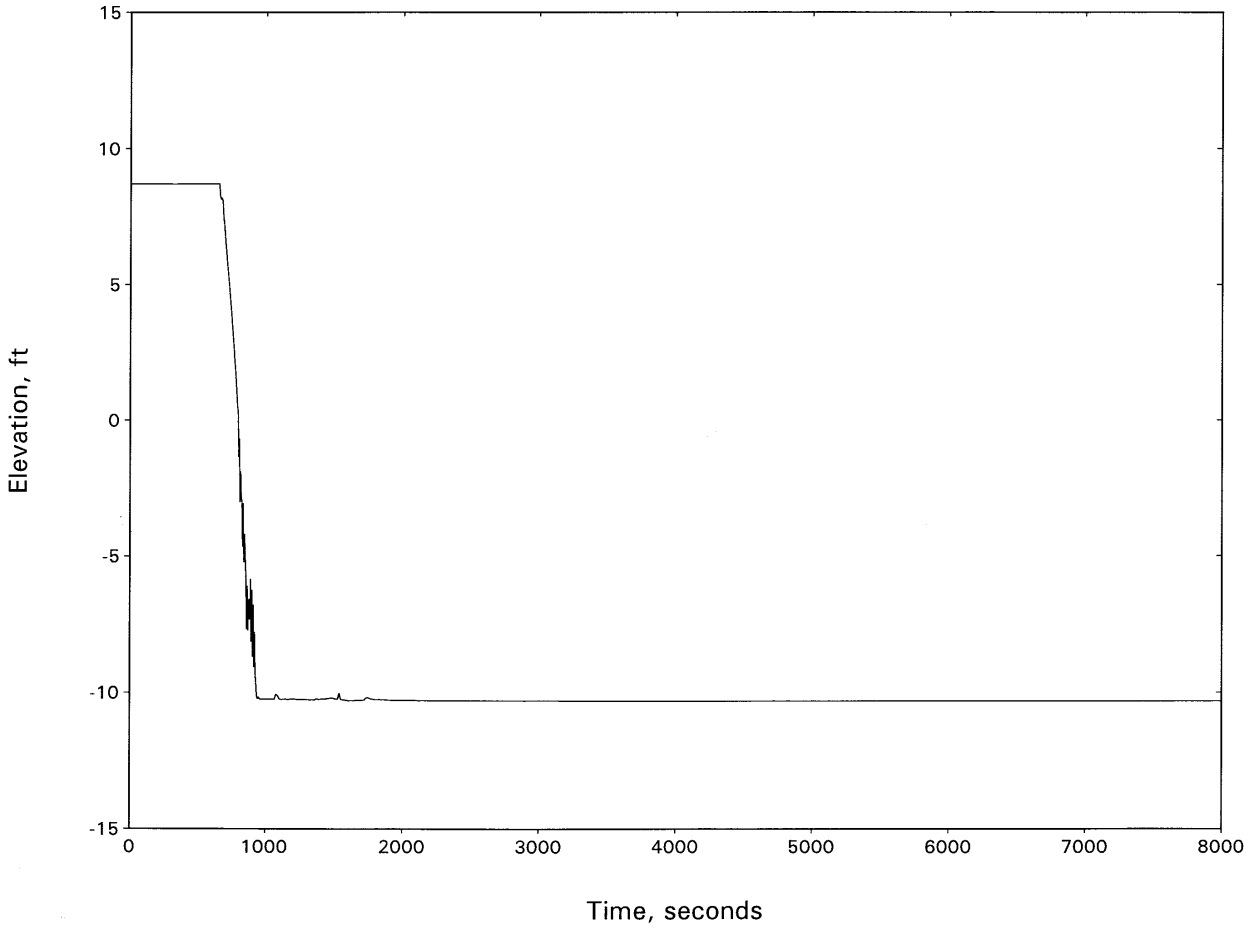

Figure 15.3-115
NORTH ANNA UNIT 2: RCS PRESSURE—2.5-INCH BREAK

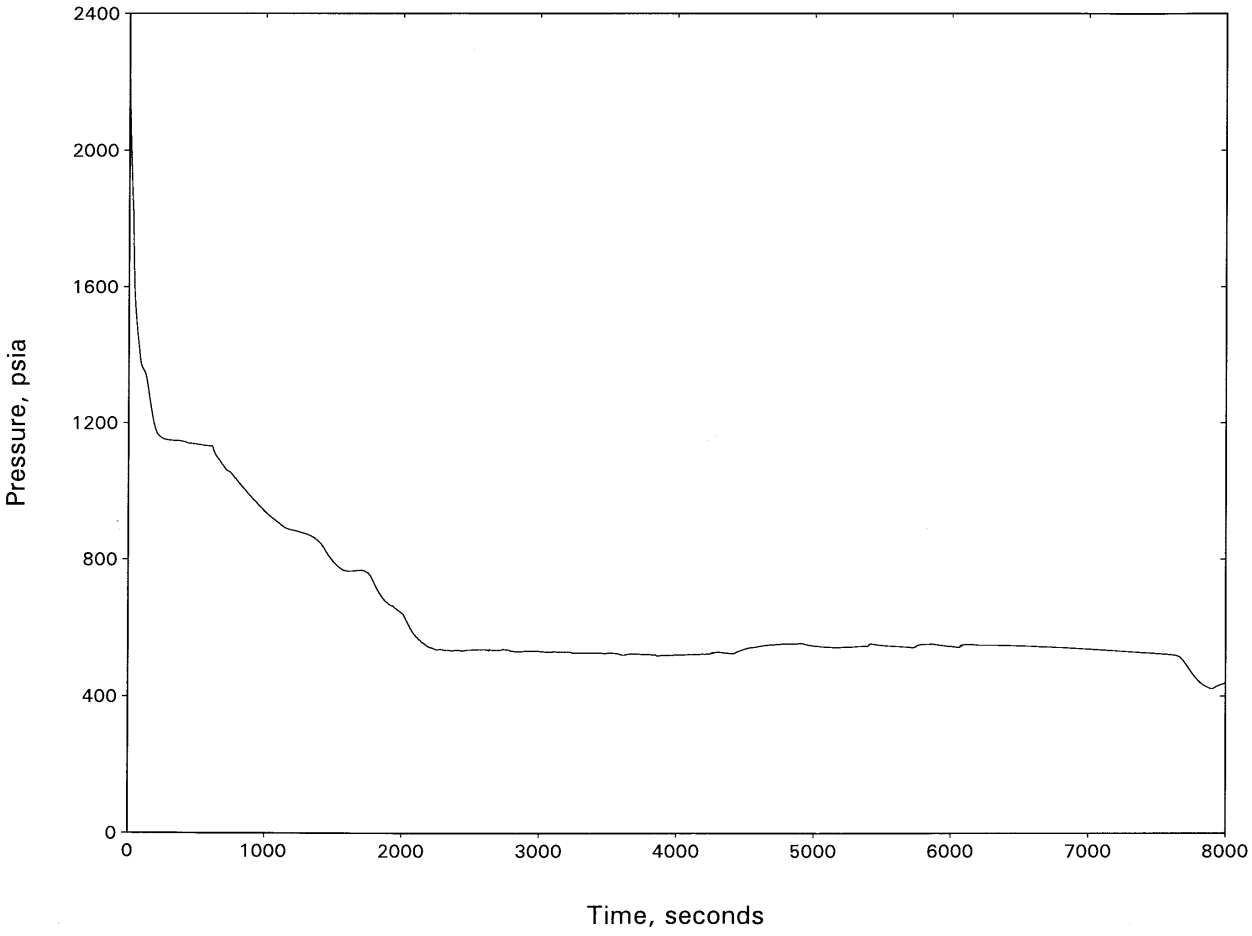

Figure 15.3-116
NORTH ANNA UNIT 2: BREAK FLOW—2.5-INCH BREAK

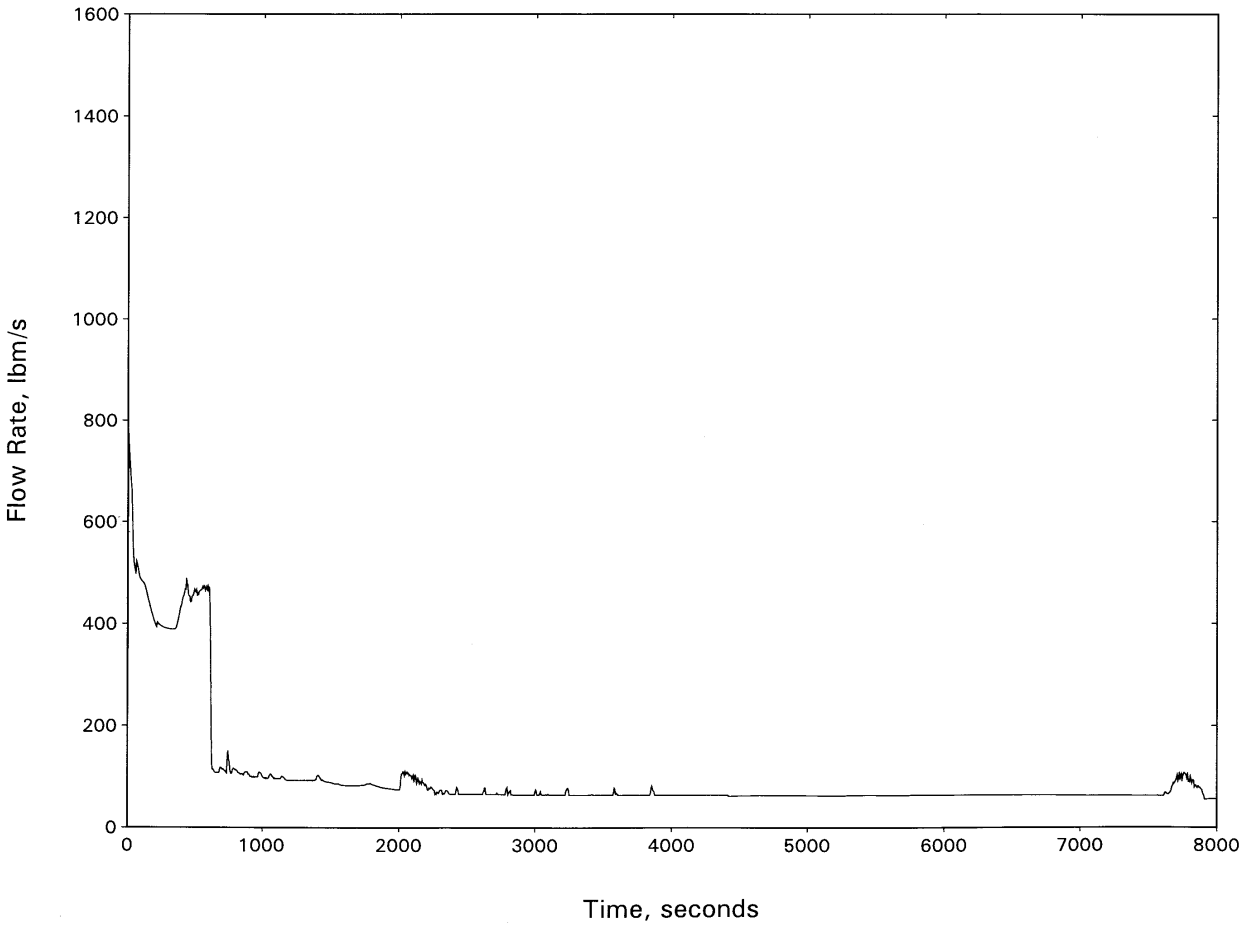

Figure 15.3-117
NORTH ANNA UNIT 2: HOT CHANNEL MIXTURE LEVEL—2.5-INCH BREAK

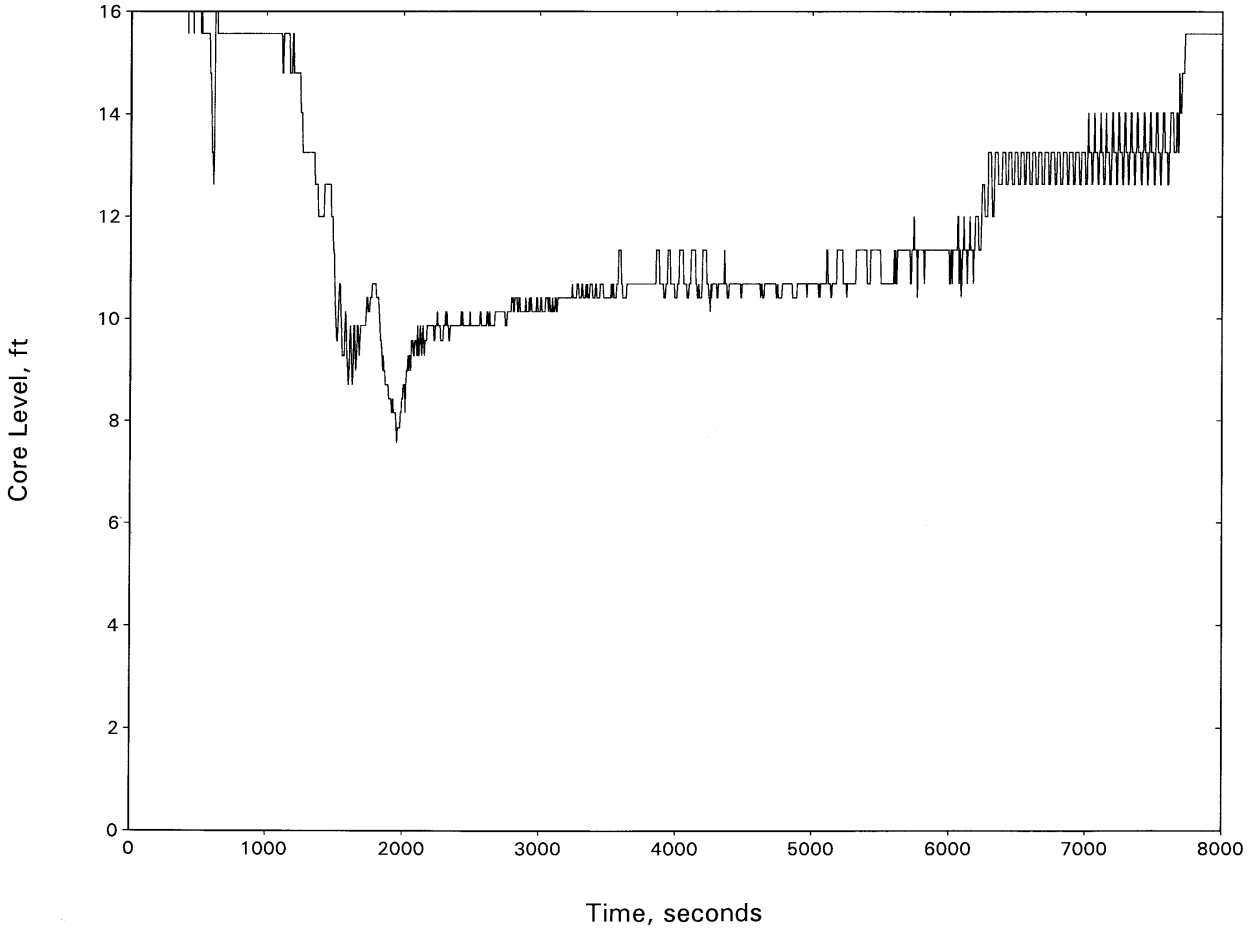

Figure 15.3-118
NORTH ANNA UNIT 2: HOT SPOT PCT—2.5-INCH BREAK

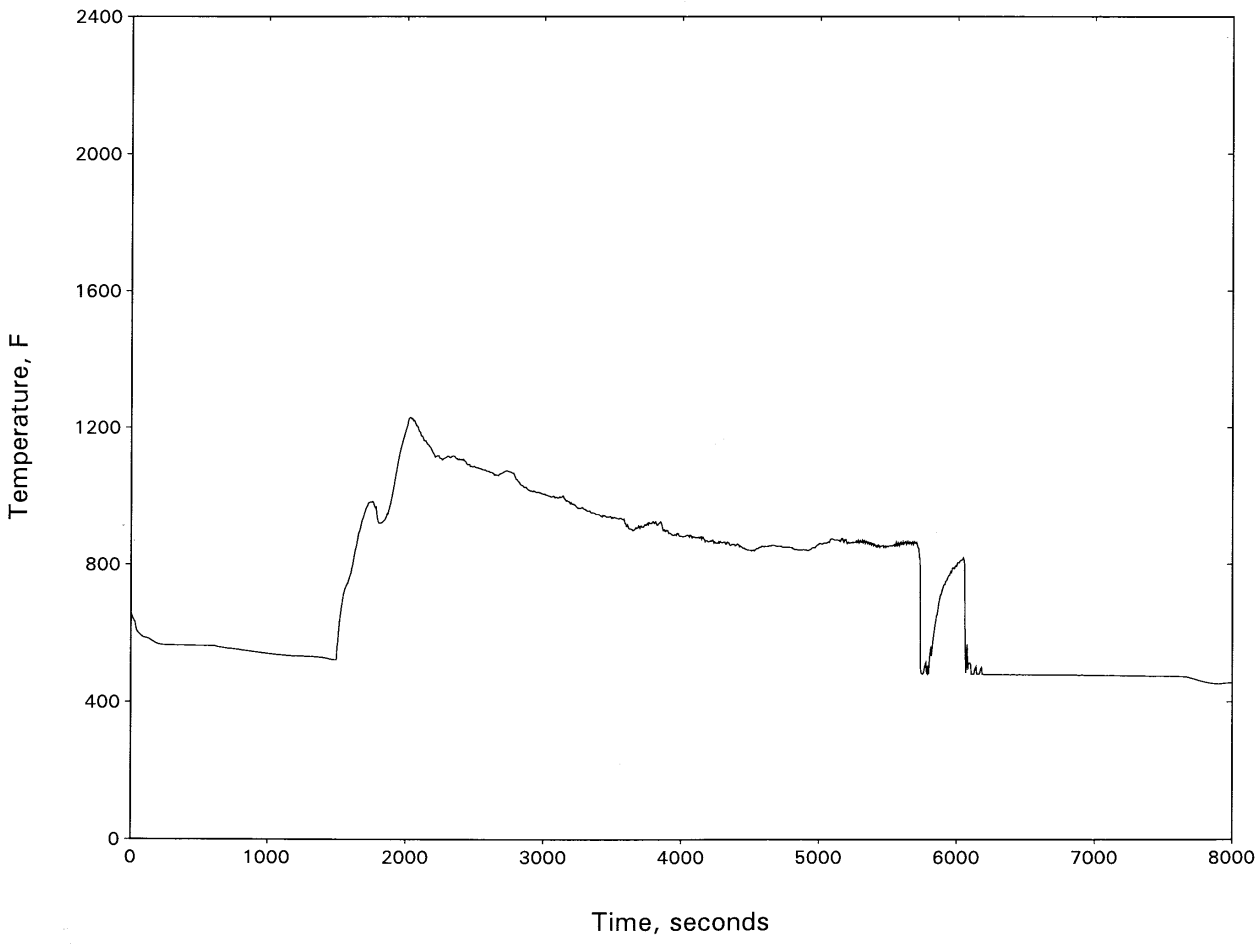

Figure 15.3-119
NORTH ANNA UNIT 2:
HOT CHANNEL OUTLET VAPOR TEMPERATURE—2.5-INCH BREAK

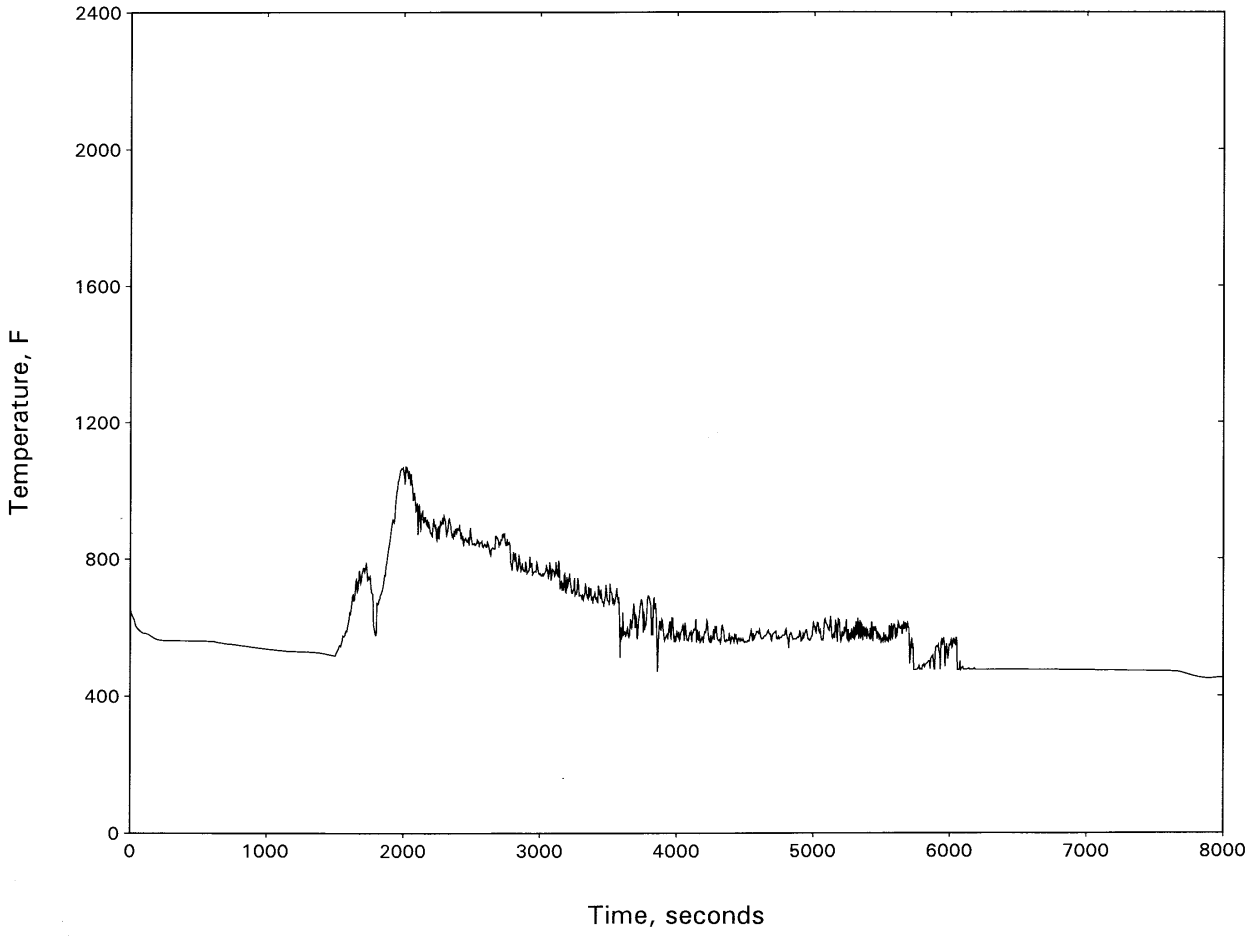

Figure 15.3-120
NORTH ANNA UNIT 2: INTACT LOOP SEAL LEVEL—2.5-INCH BREAK

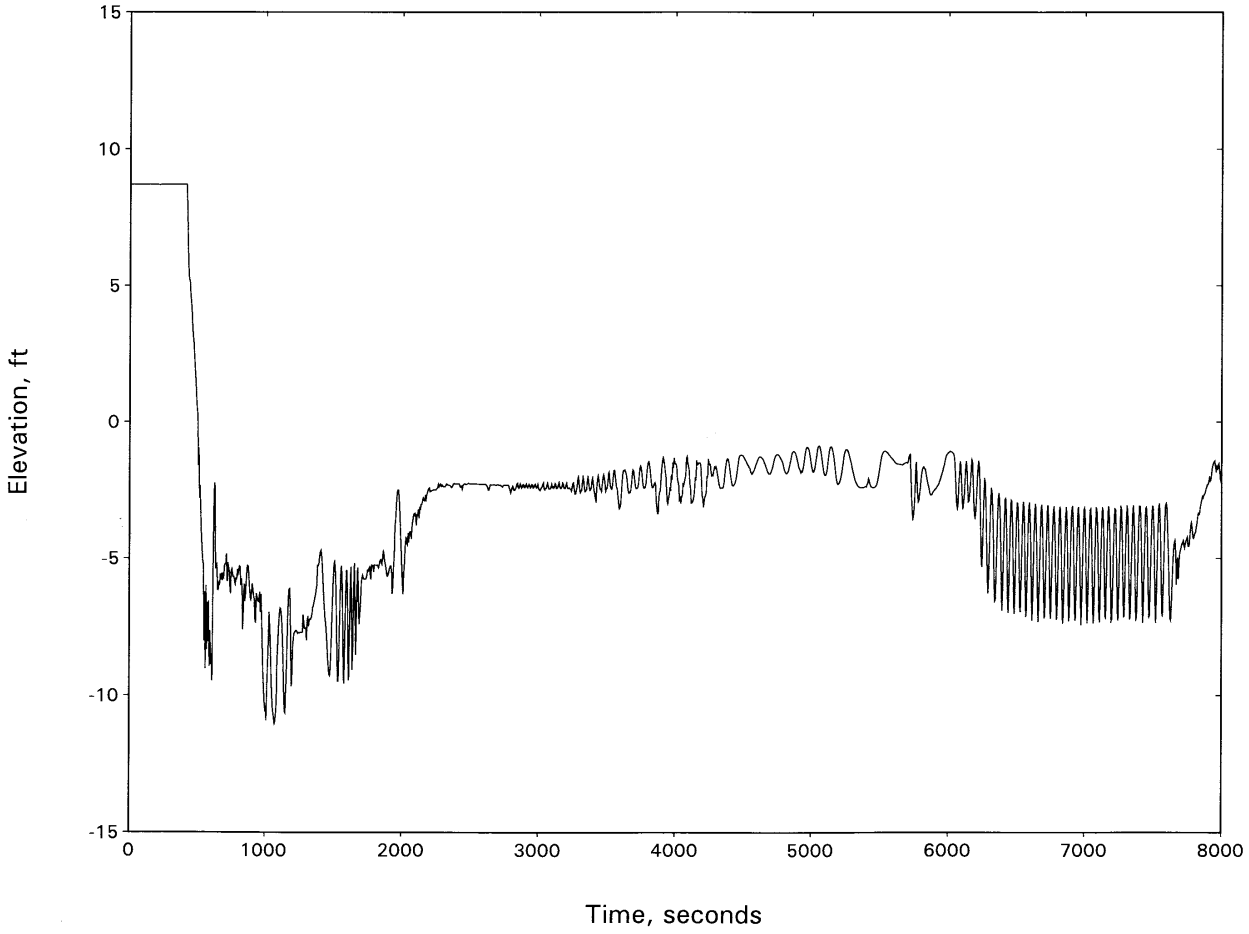

Figure 15.3-121
NORTH ANNA UNIT 2: BROKEN LOOP SEAL LEVEL—2.5-INCH BREAK

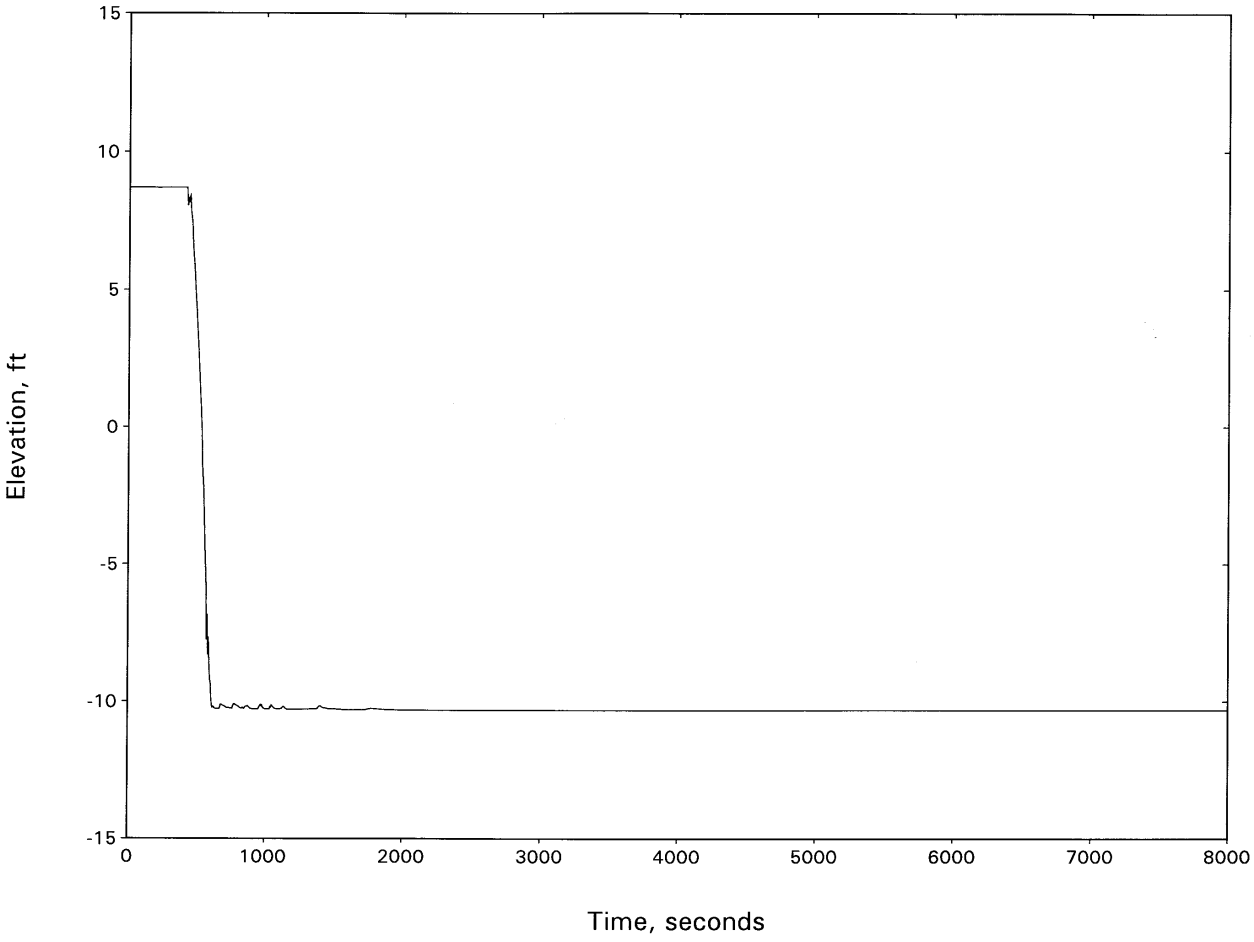

Figure 15.3-122
NORTH ANNA UNIT 2: RCS PRESSURE—3.0-INCH BREAK

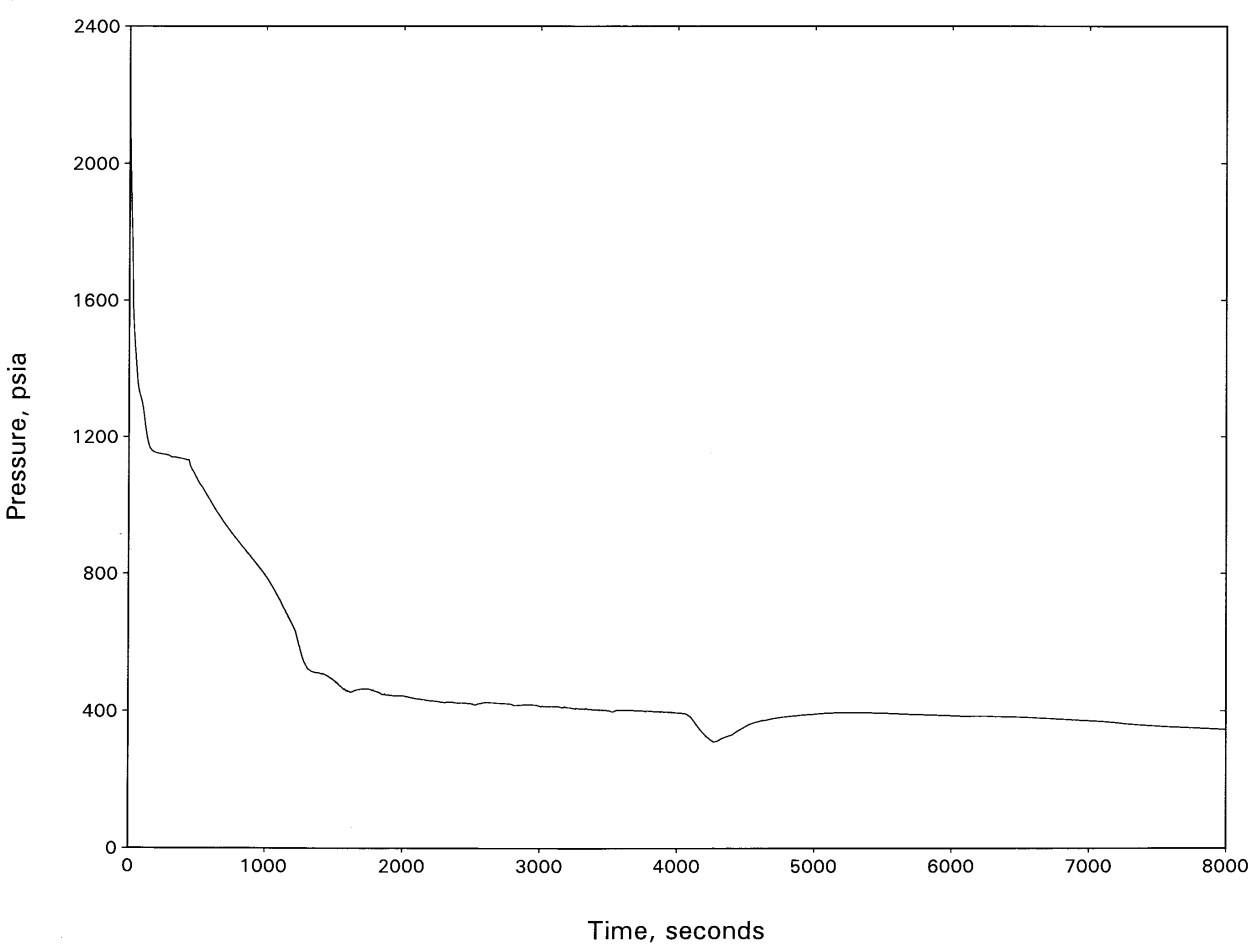

Figure 15.3-123
NORTH ANNA UNIT 2: BREAK FLOW—3.0-INCH BREAK

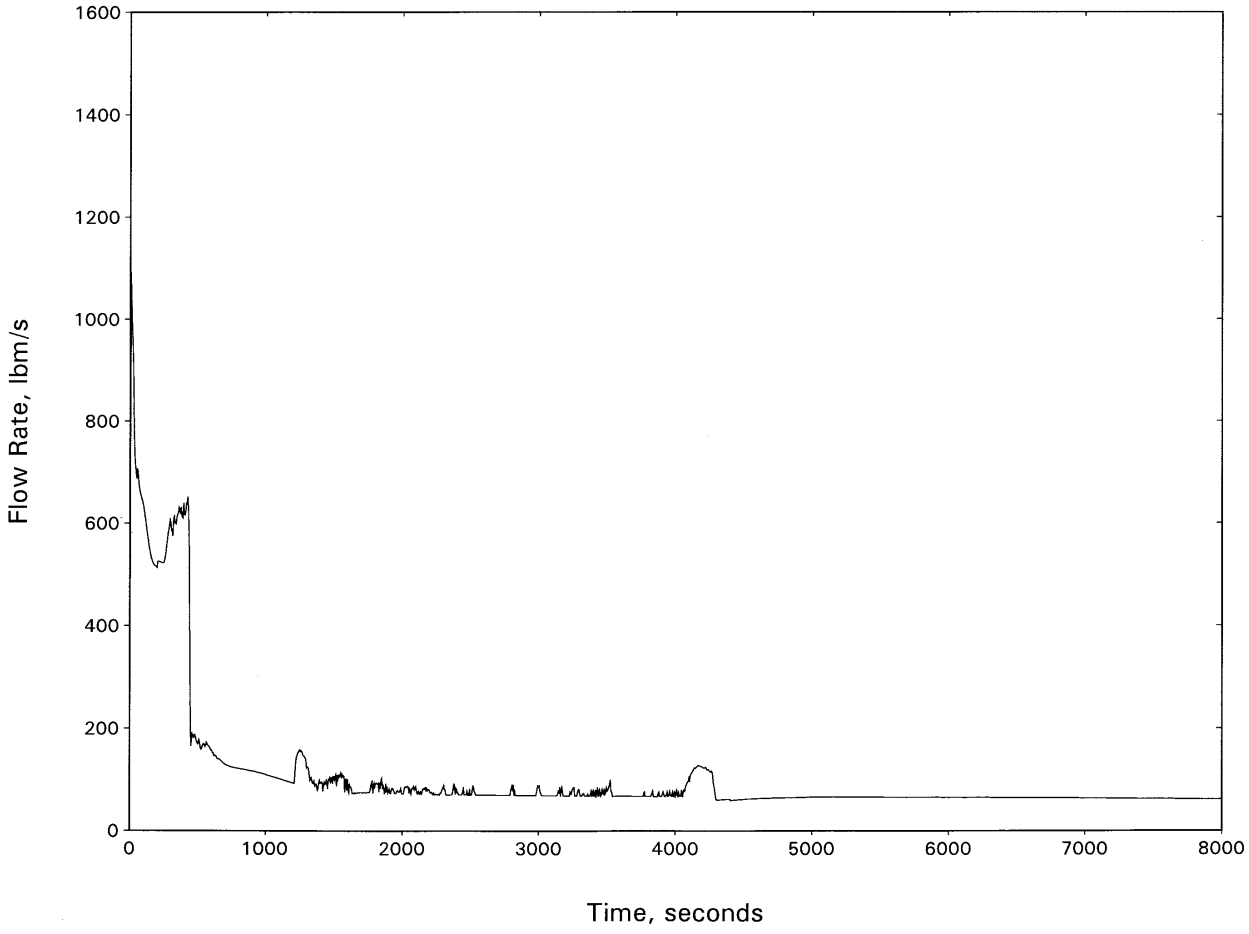

Figure 15.3-124
NORTH ANNA UNIT 2: HOT CHANNEL MIXTURE LEVEL—3.0-INCH BREAK

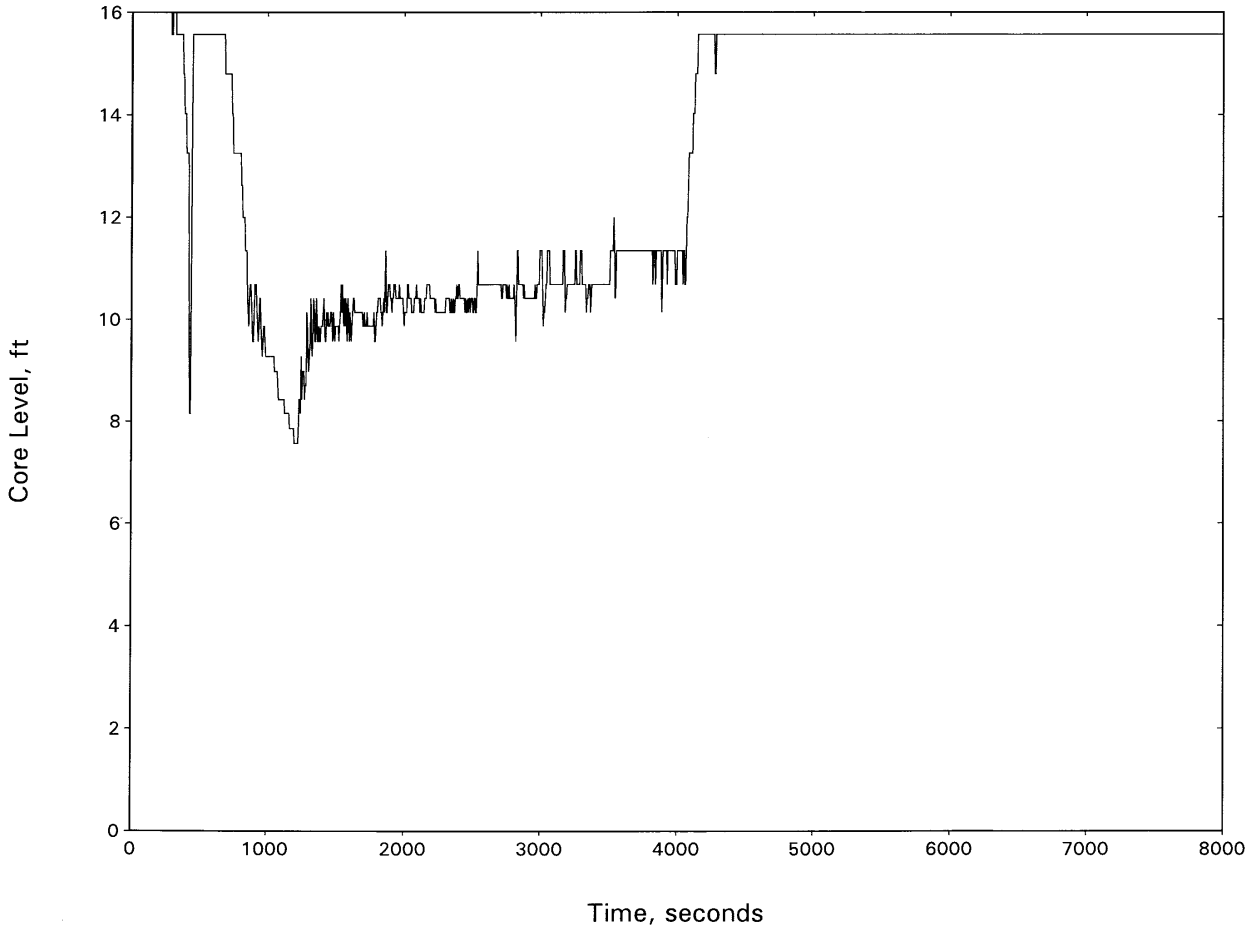

Figure 15.3-125
NORTH ANNA UNIT 2: HOT SPOT PCT—3.0-INCH BREAK

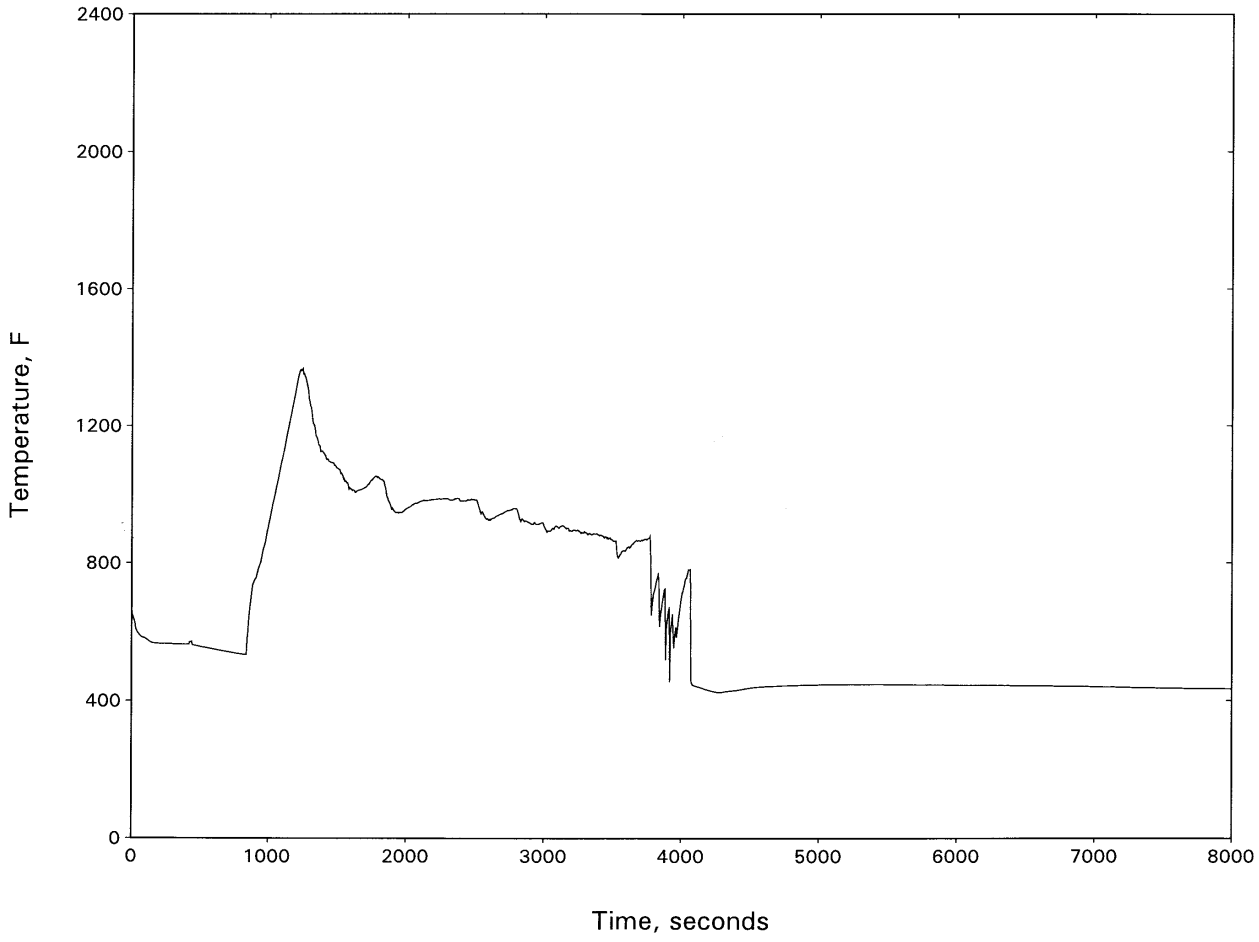

Figure 15.3-126
NORTH ANNA UNIT 2:
HOT CHANNEL OUTLET VAPOR TEMPERATURE—3.0-INCH BREAK

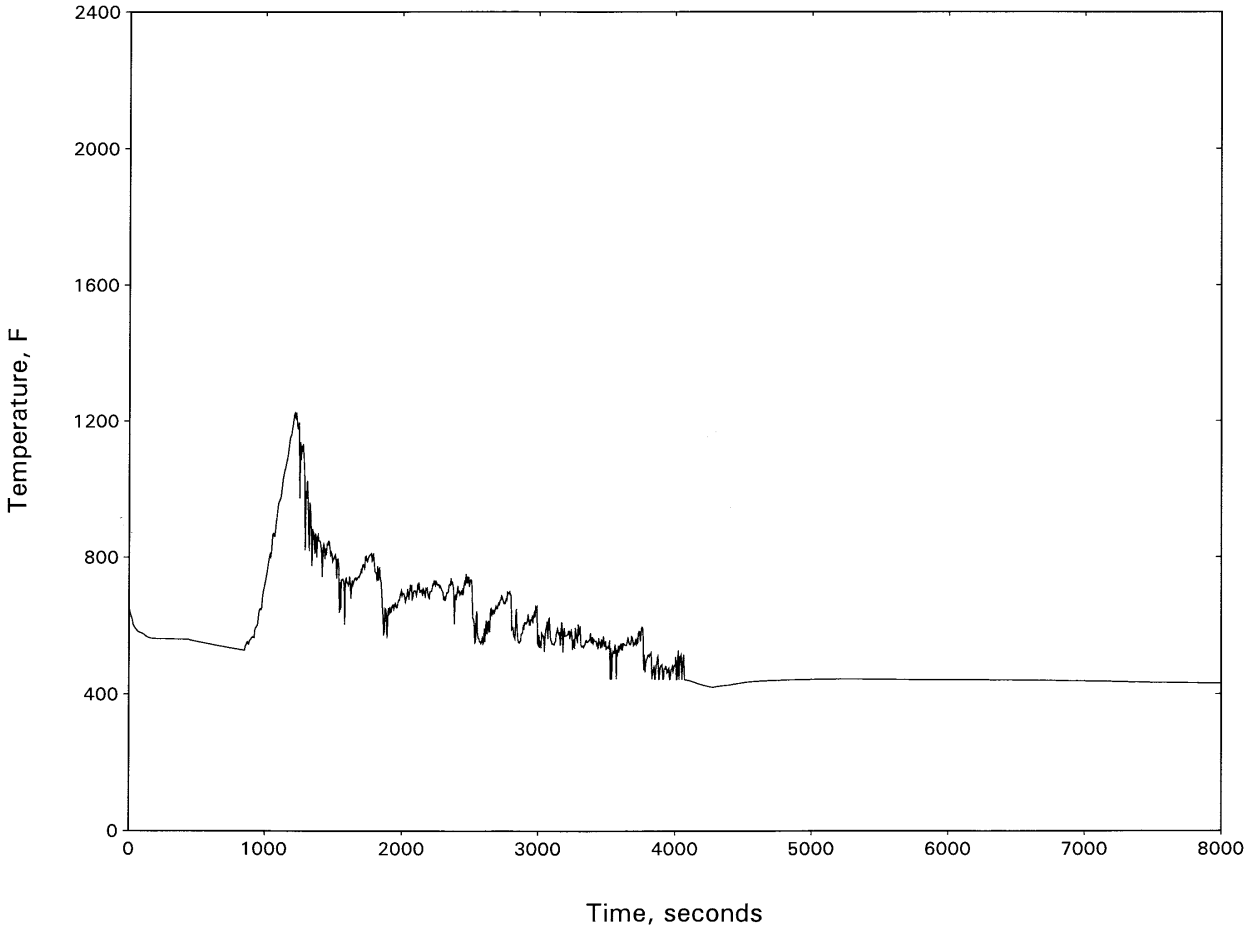

Figure 15.3-127
NORTH ANNA UNIT 2: INTACT LOOP SEAL LEVEL—3.0-INCH BREAK

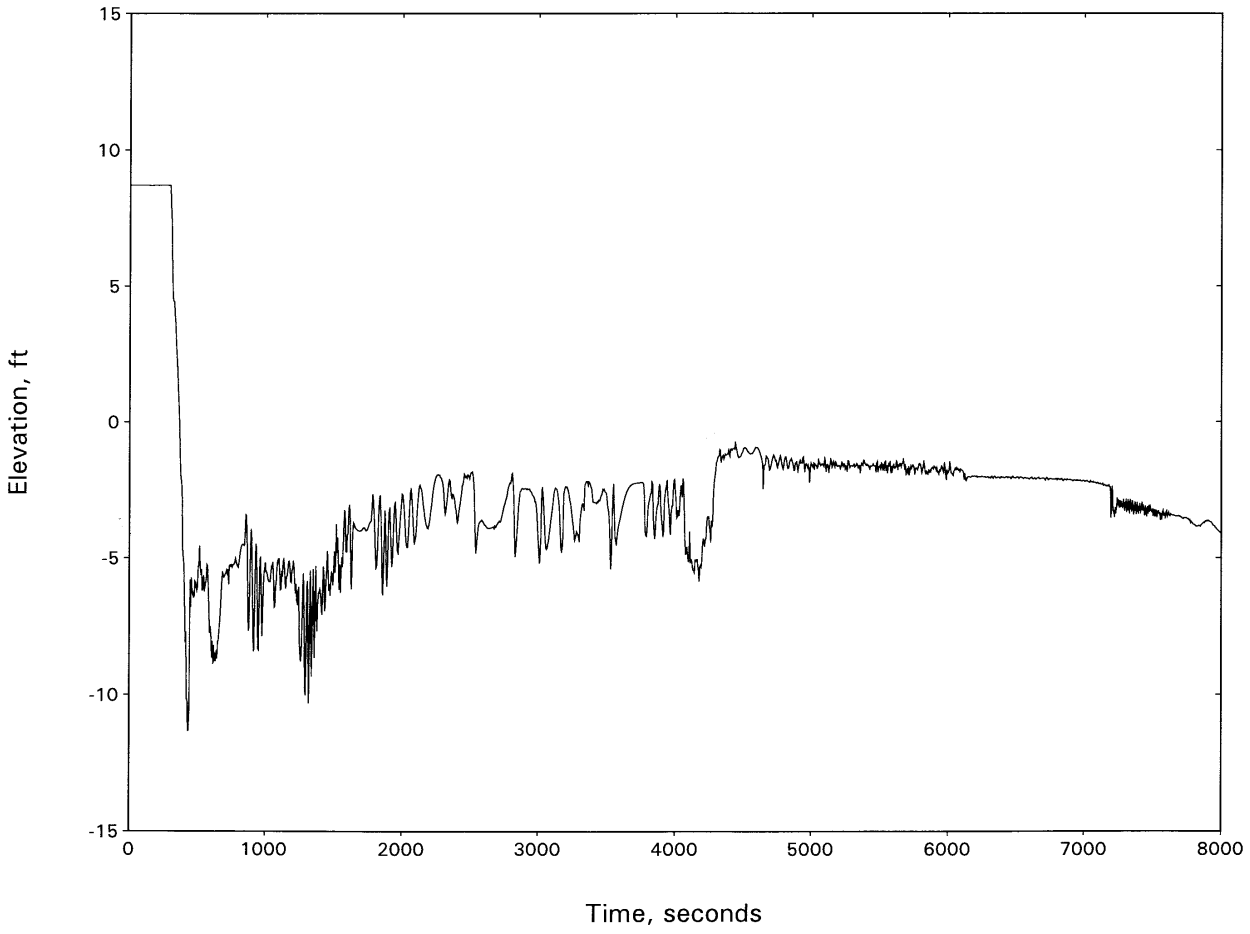

Figure 15.3-128
NORTH ANNA UNIT 2: BROKEN LOOP SEAL LEVEL—3.0-INCH BREAK

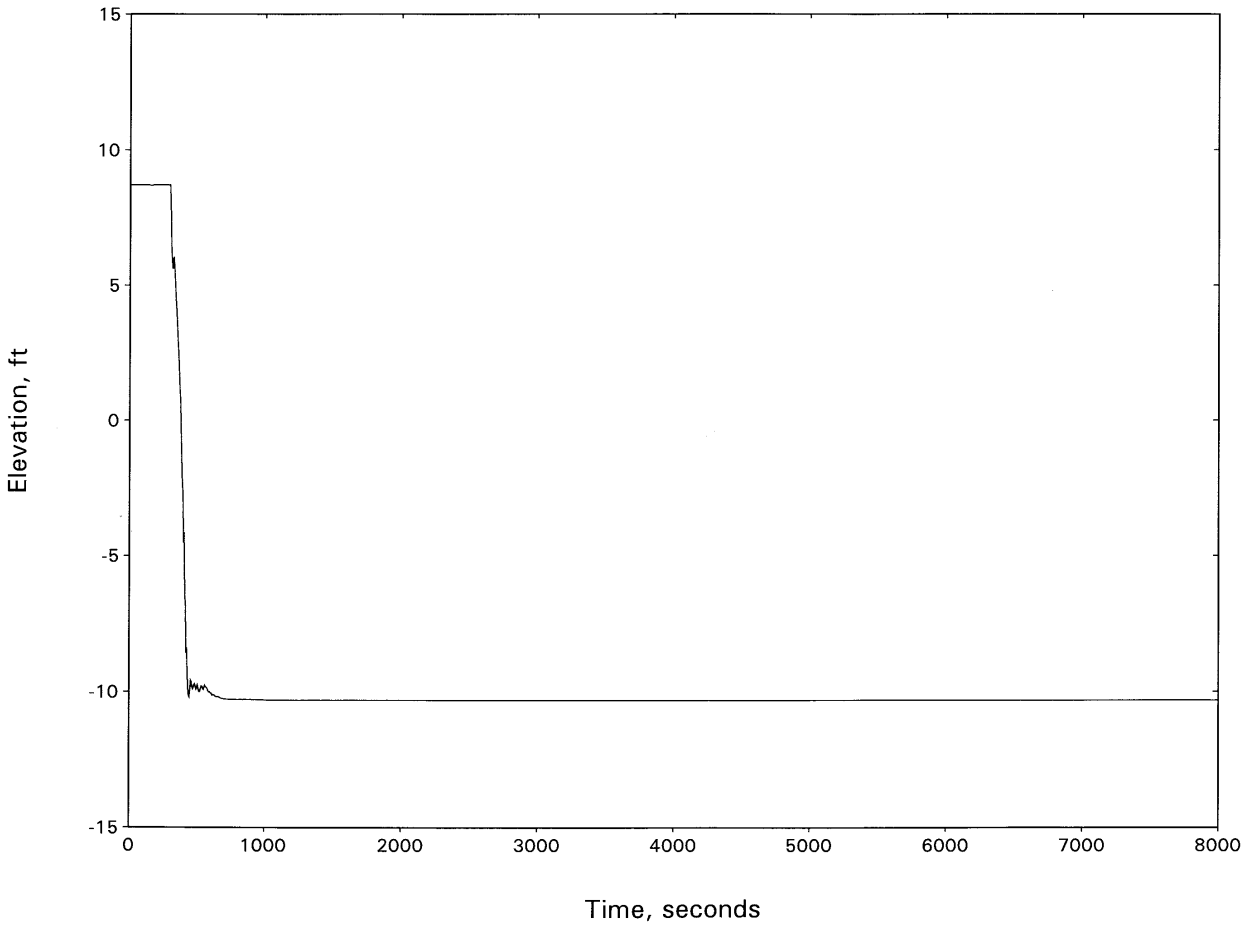

Figure 15.3-129
NORTH ANNA UNIT 2: RCS PRESSURE—4.0-INCH BREAK

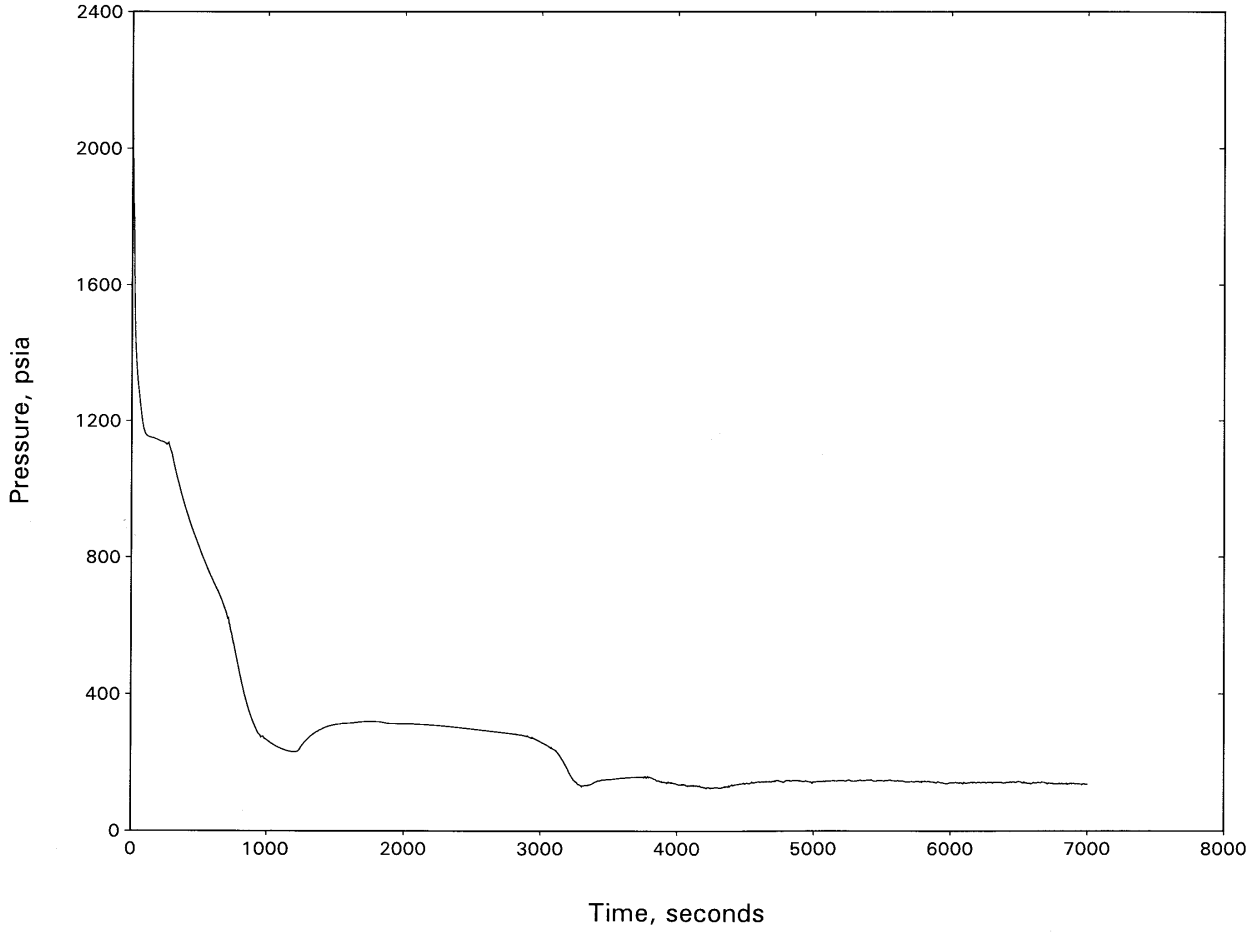

Figure 15.3-130
NORTH ANNA UNIT 2: BREAK FLOW—4.0-INCH BREAK

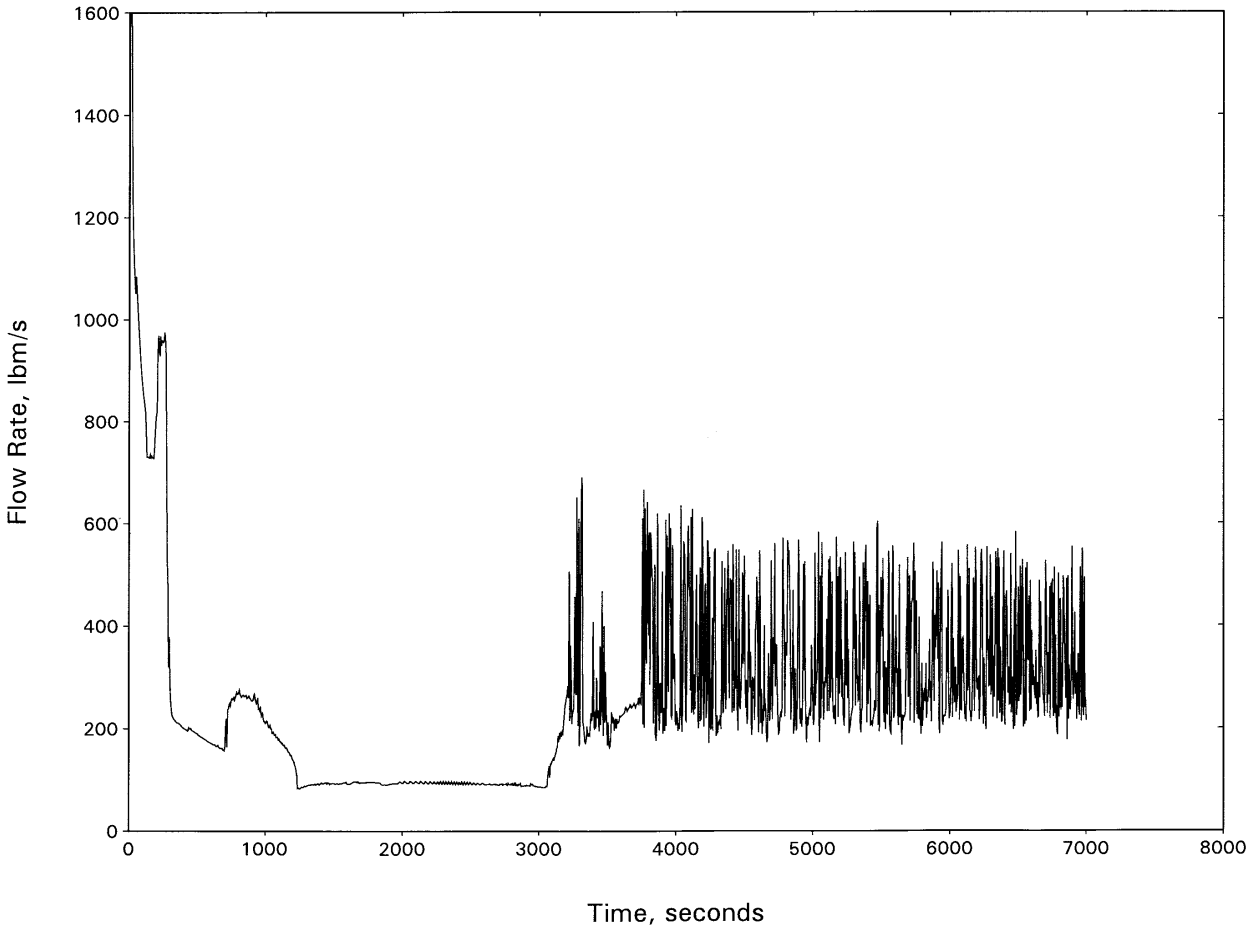

Figure 15.3-131
NORTH ANNA UNIT 2: HOT CHANNEL MIXTURE LEVEL—4.0-INCH BREAK

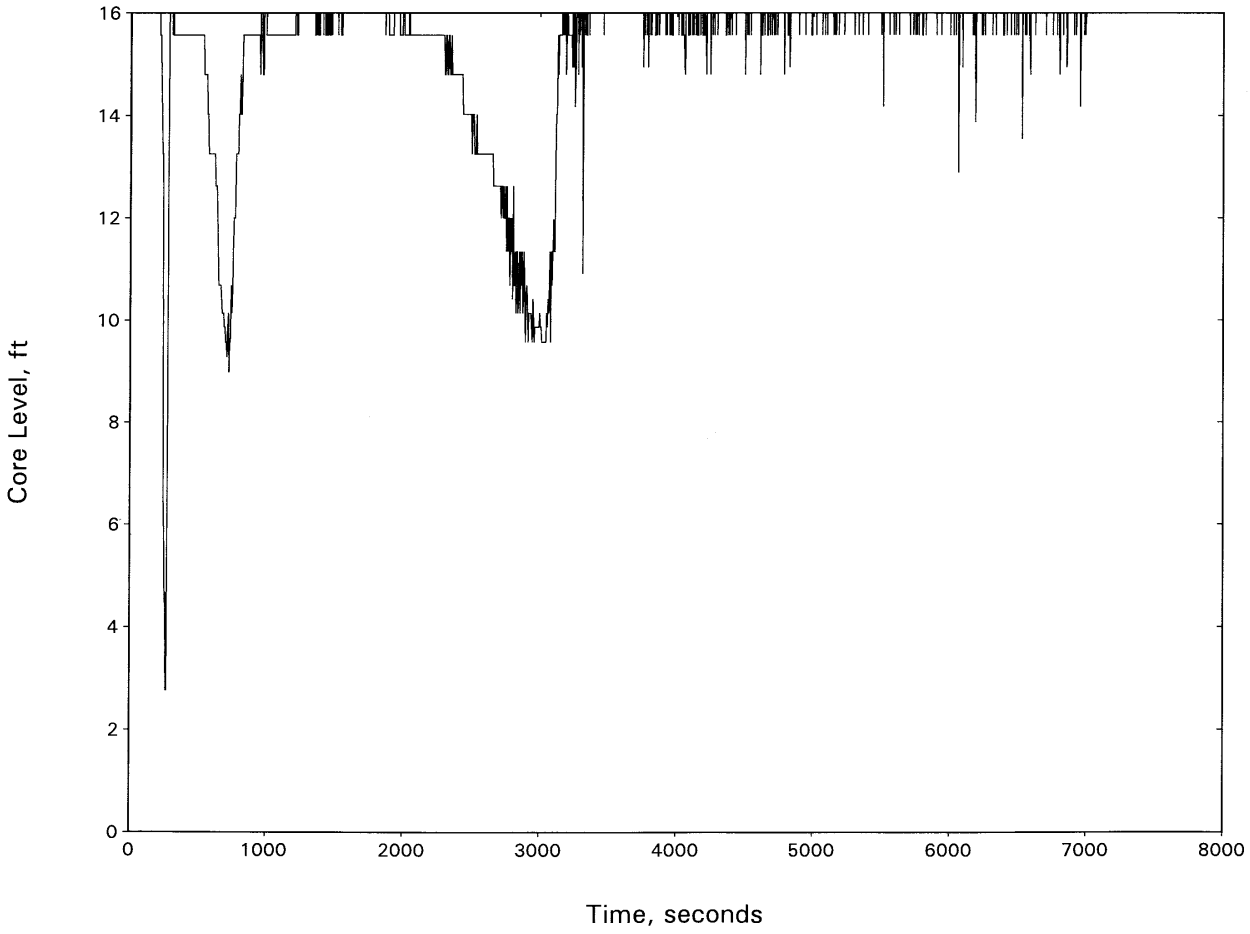

Figure 15.3-132
NORTH ANNA UNIT 2: HOT SPOT PCT—4.0-INCH BREAK

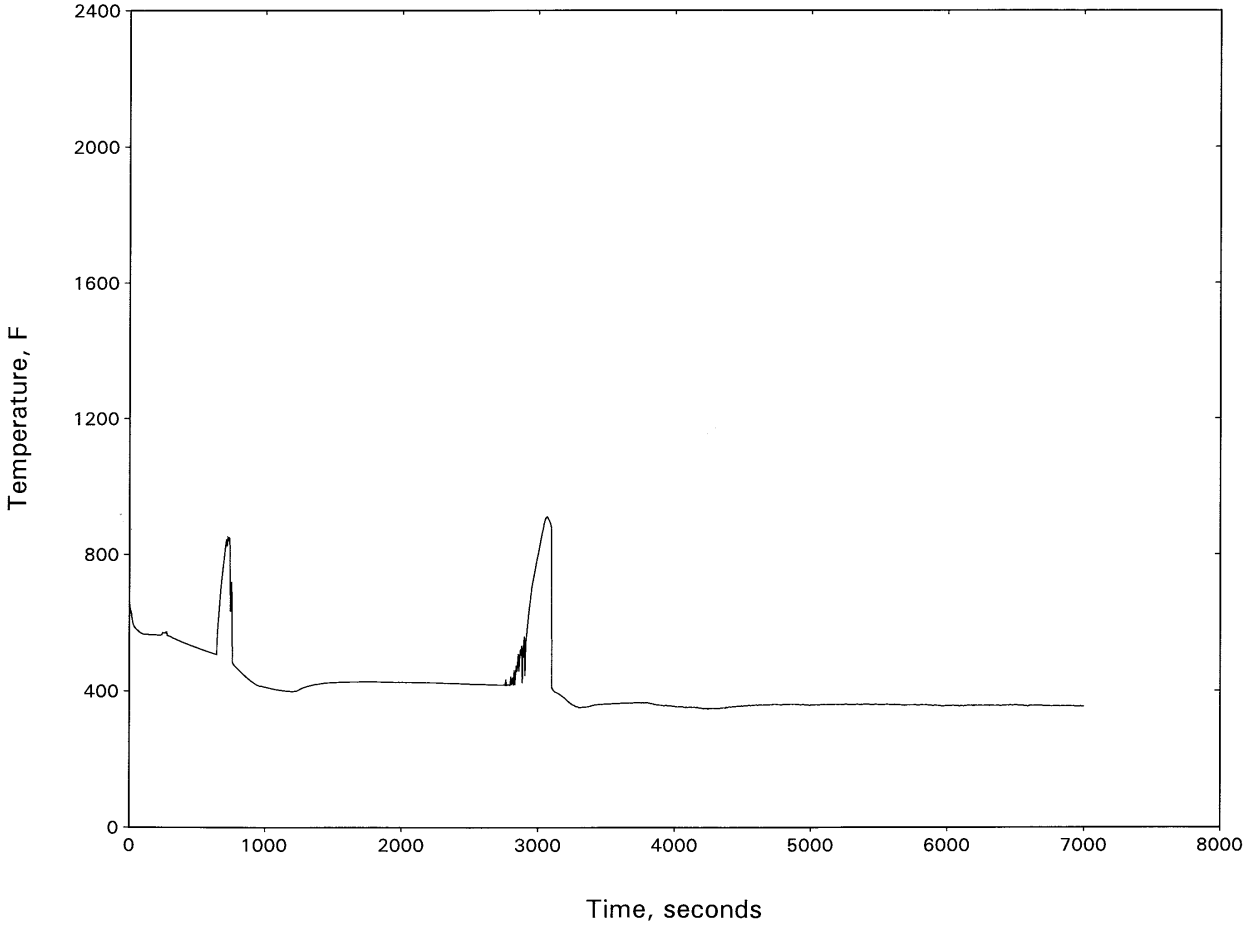

Figure 15.3-133
NORTH ANNA UNIT 2:
HOT CHANNEL OUTLET VAPOR TEMPERATURE—4.0-INCH BREAK

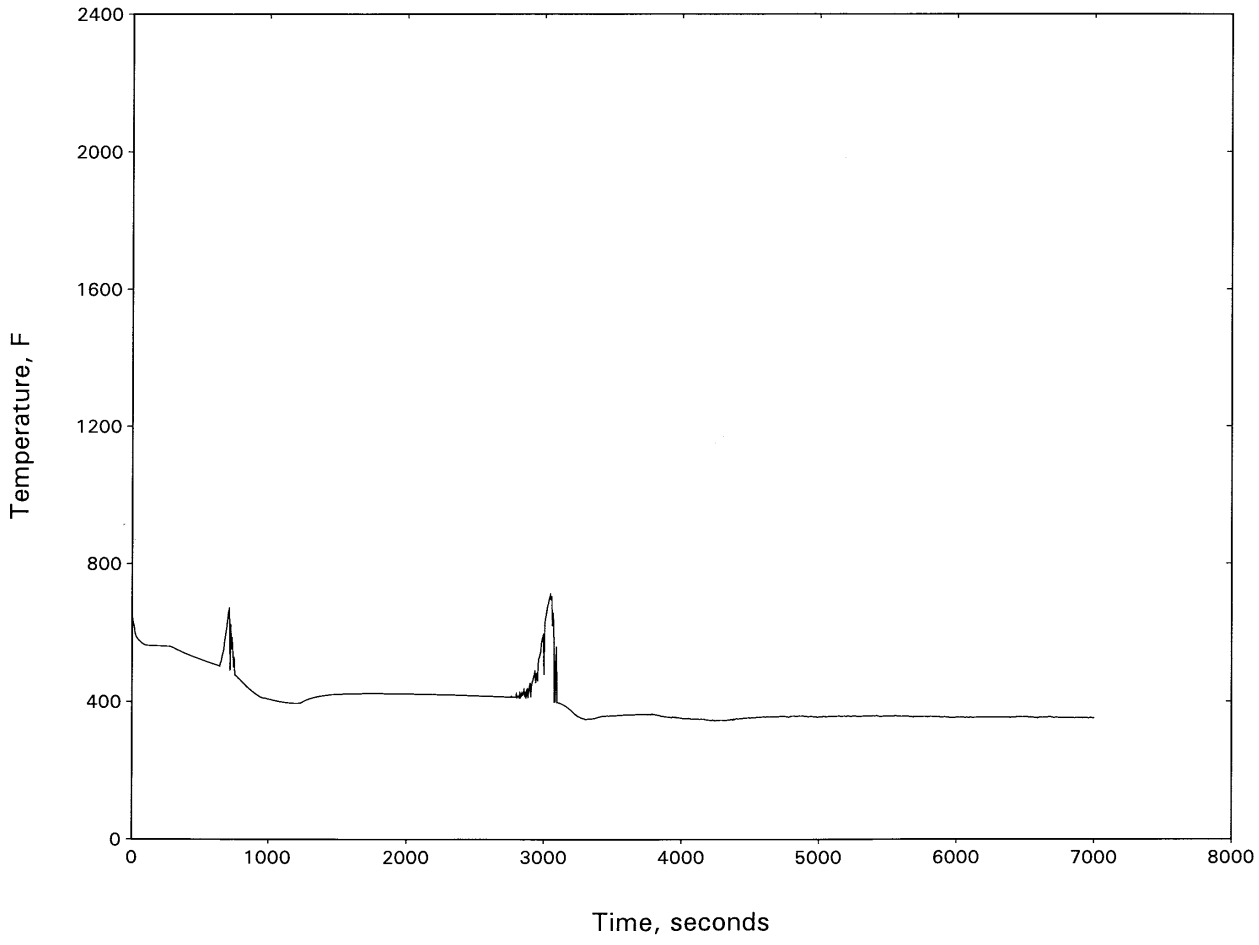

Figure 15.3-134
NORTH ANNA UNIT 2: INTACT LOOP SEAL LEVEL—4.0-INCH BREAK

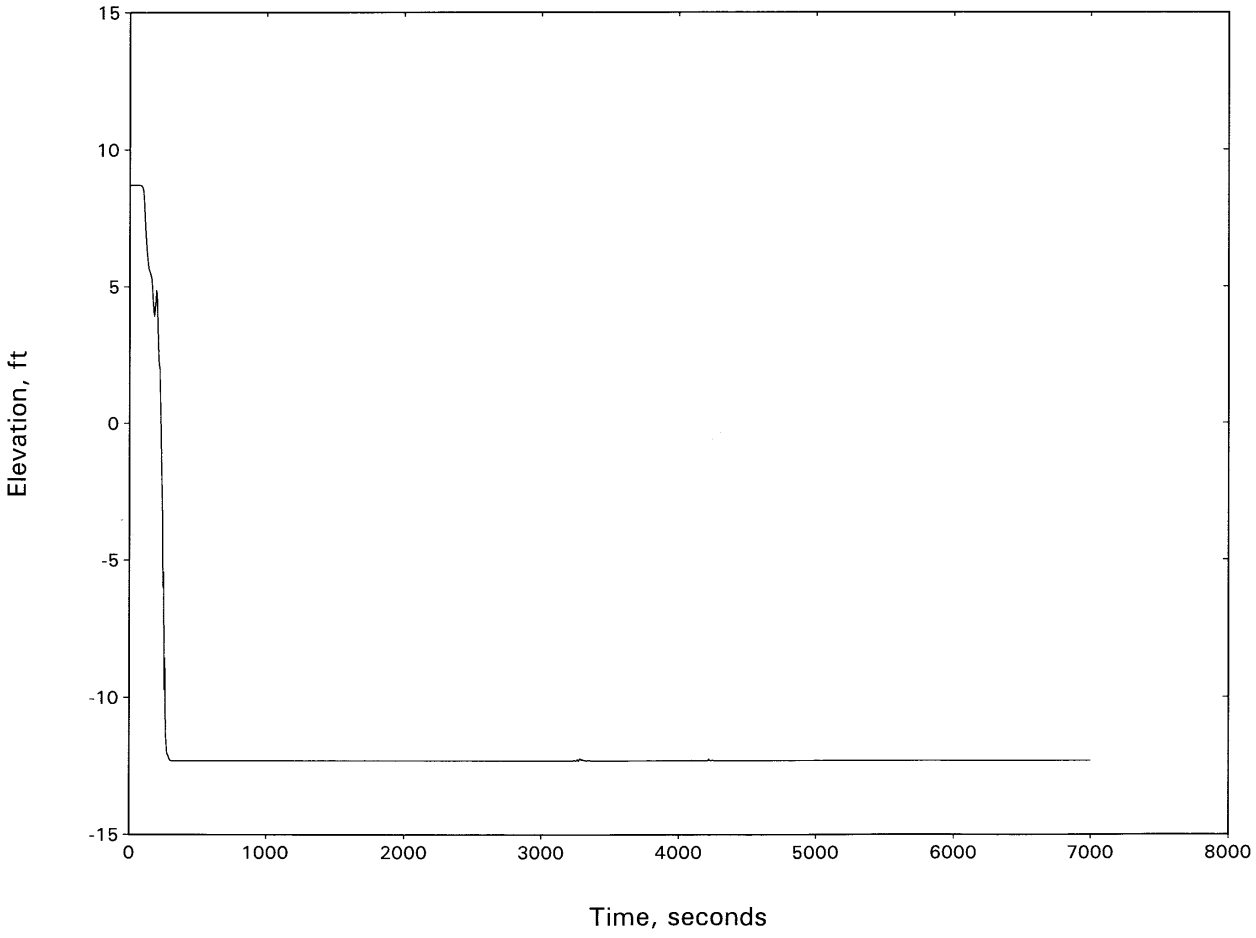

Figure 15.3-135
NORTH ANNA UNIT 2: BROKEN LOOP SEAL LEVEL—4.0-INCH BREAK

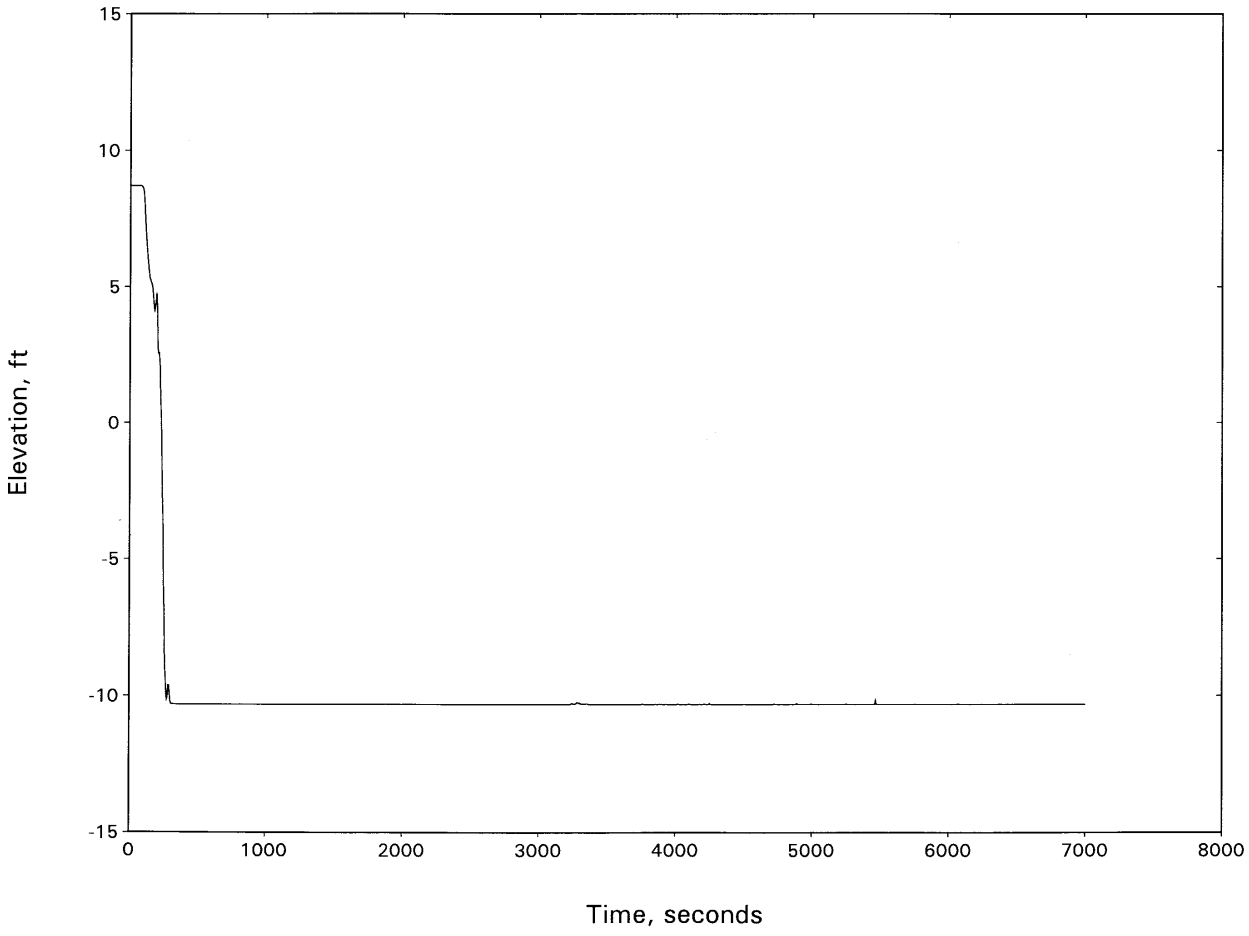

Figure 15.3-136
NORTH ANNA UNIT 2: RCS PRESSURE—5.2-INCH SI LINE BREAK

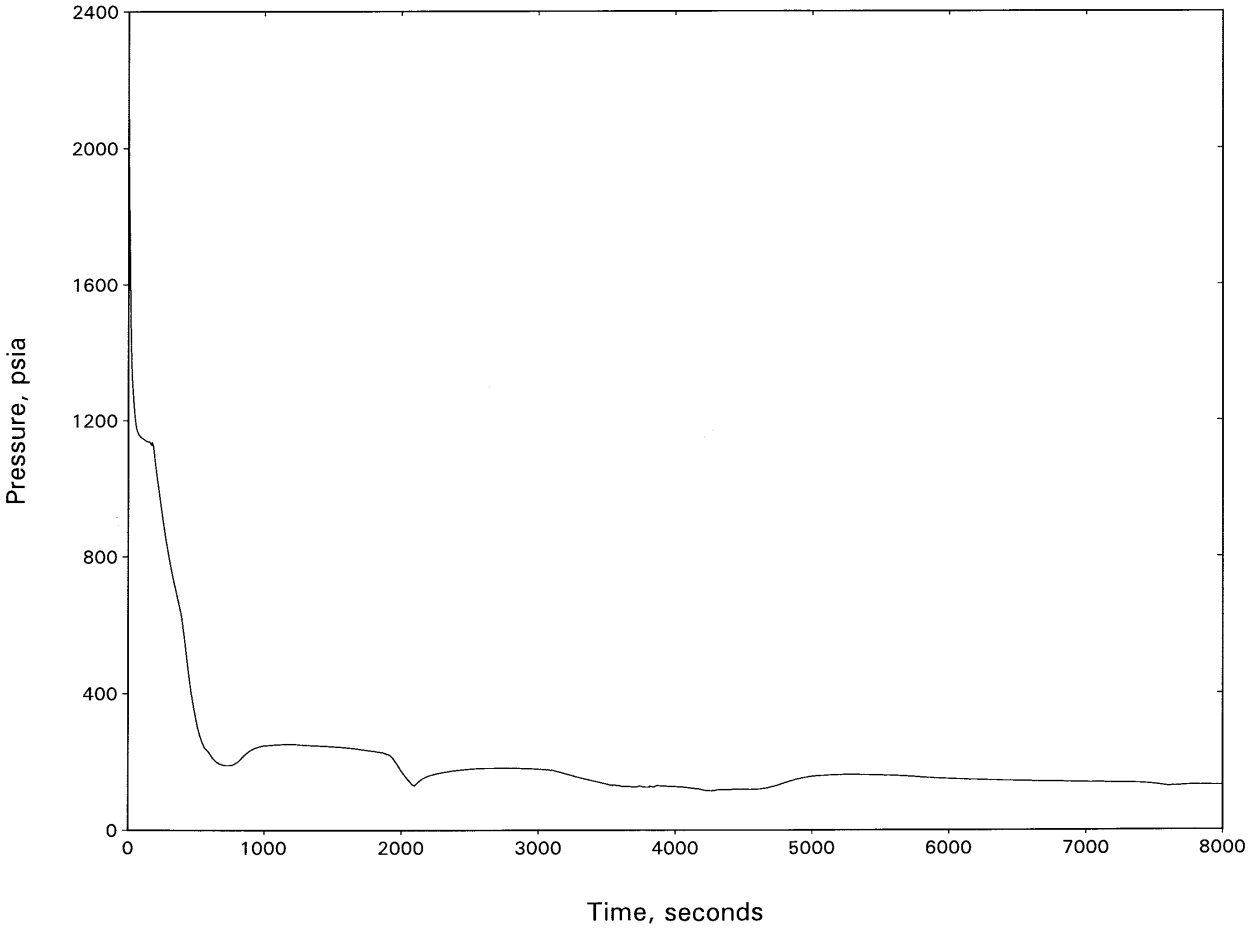

Figure 15.3-137
NORTH ANNA UNIT 2: BREAK FLOW—5.2-INCH SI LINE BREAK

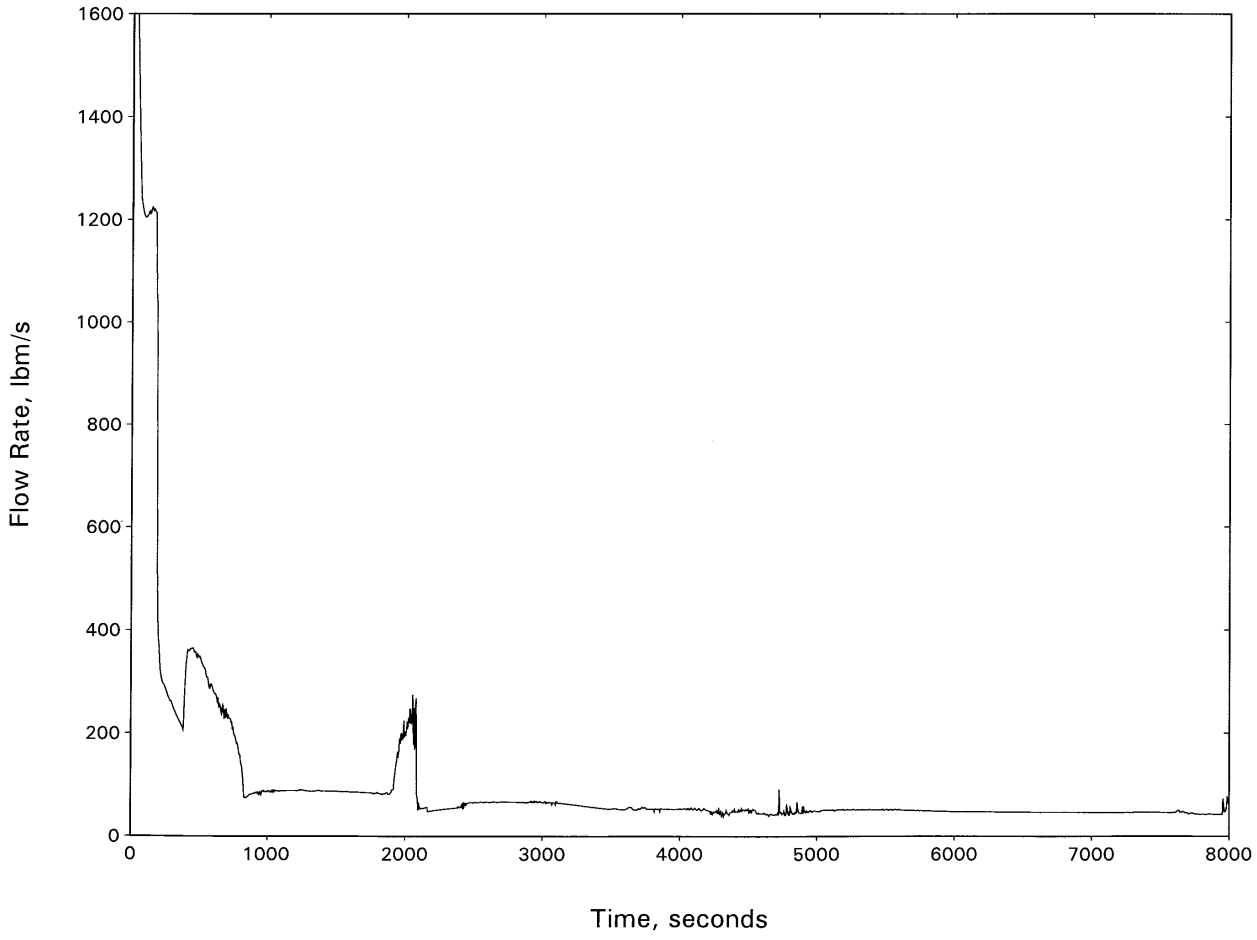

Figure 15.3-138
NORTH ANNA UNIT 2: HOT CHANNEL MIXTURE LEVEL—5.2-INCH SI LINE BREAK

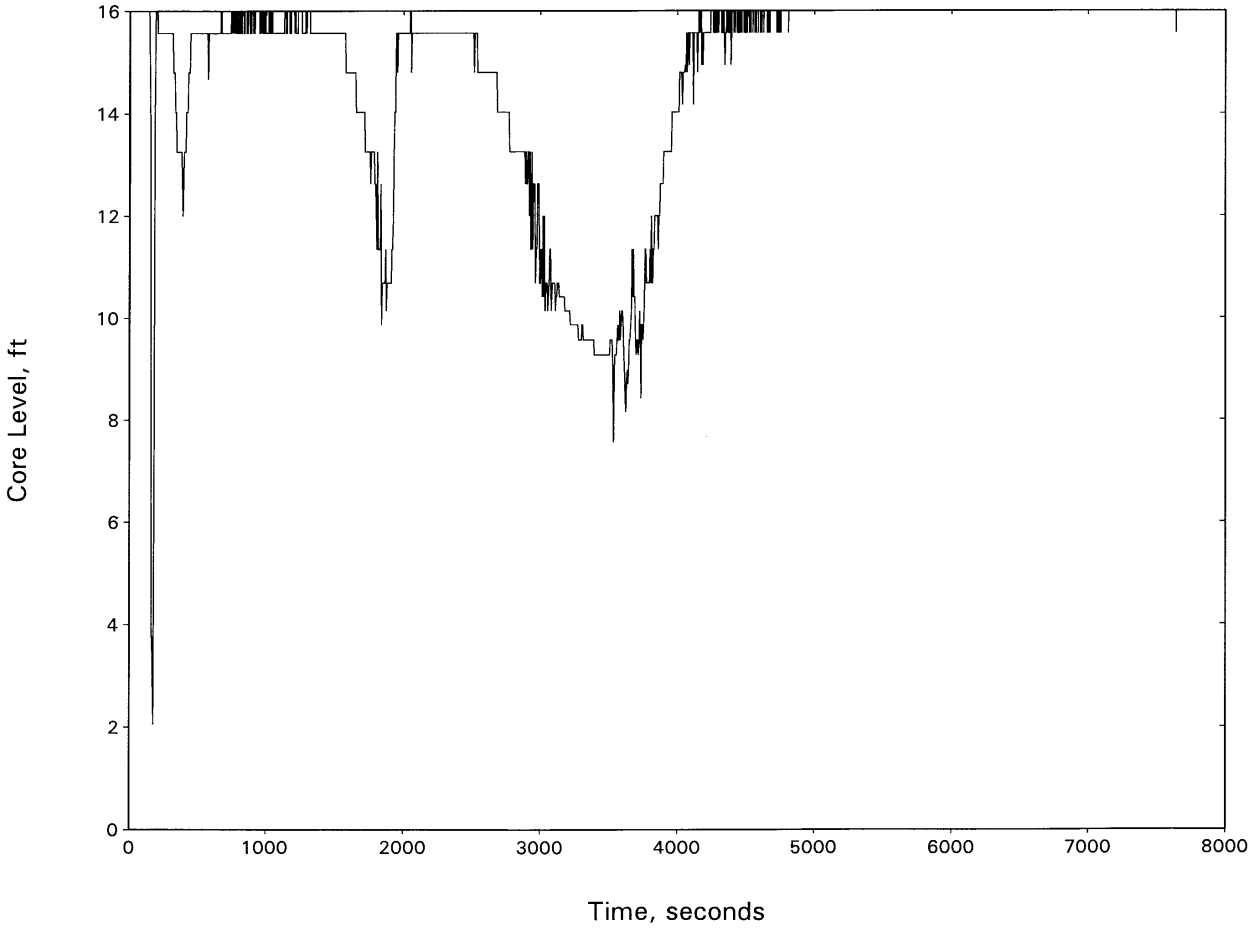

Figure 15.3-139
NORTH ANNA UNIT 2: HOT SPOT PCT—5.2-INCH SI LINE BREAK

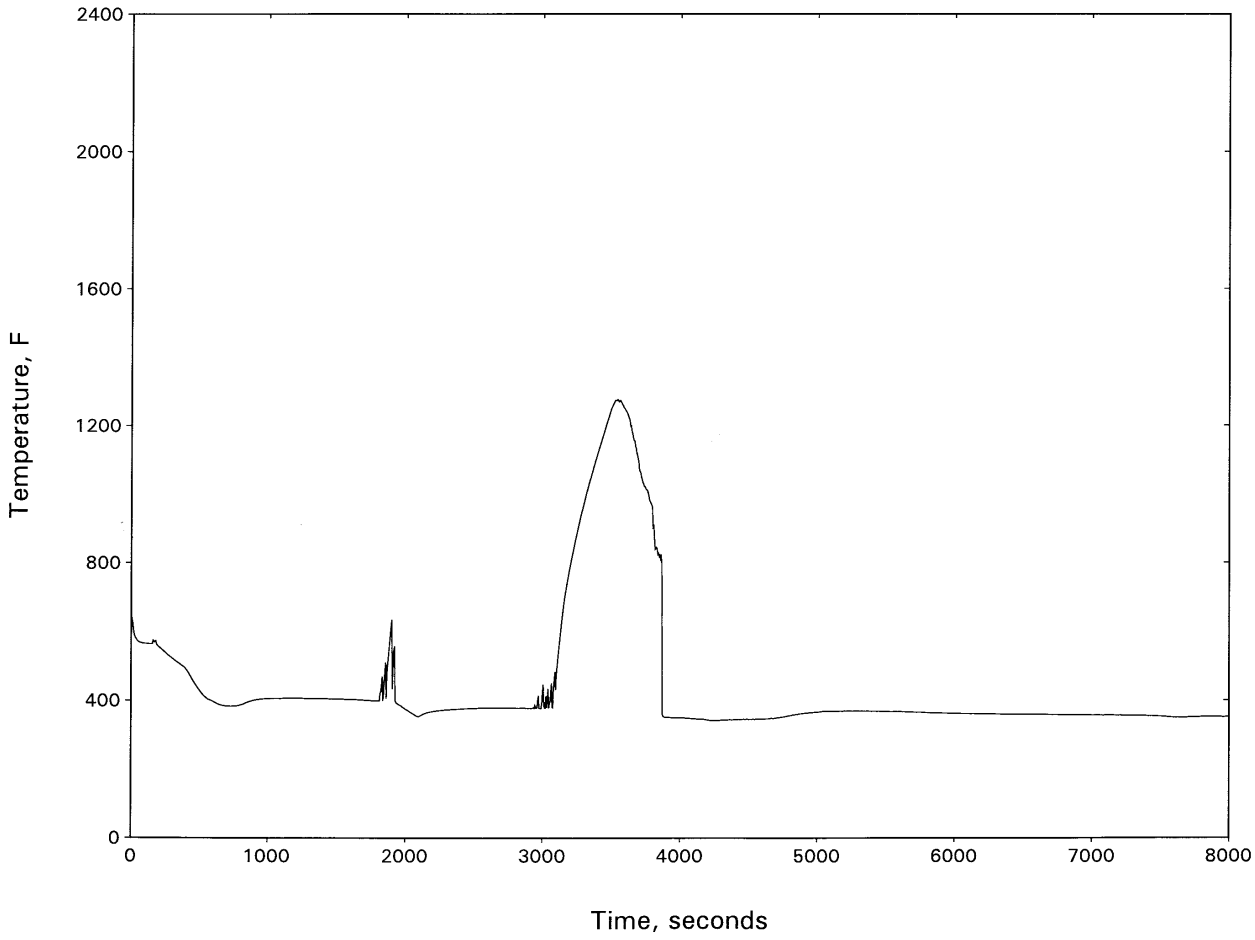

Figure 15.3-140
NORTH ANNA UNIT 2:
HOT CHANNEL OUTLET VAPOR TEMPERATURE—5.2-INCH SI LINE BREAK

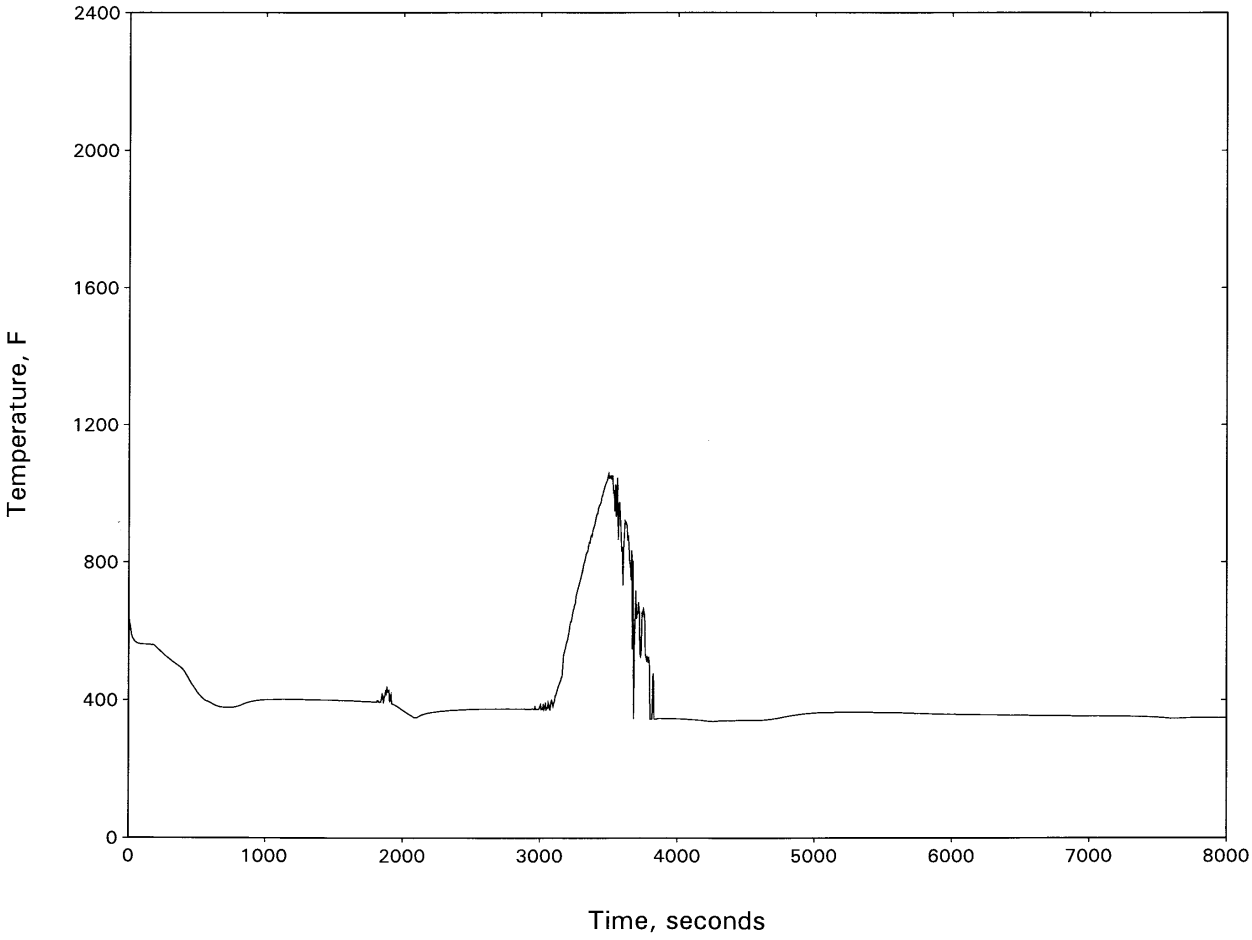

Figure 15.3-141
NORTH ANNA UNIT 2: INTACT LOOP SEAL LEVEL—5.2-INCH SI LINE BREAK

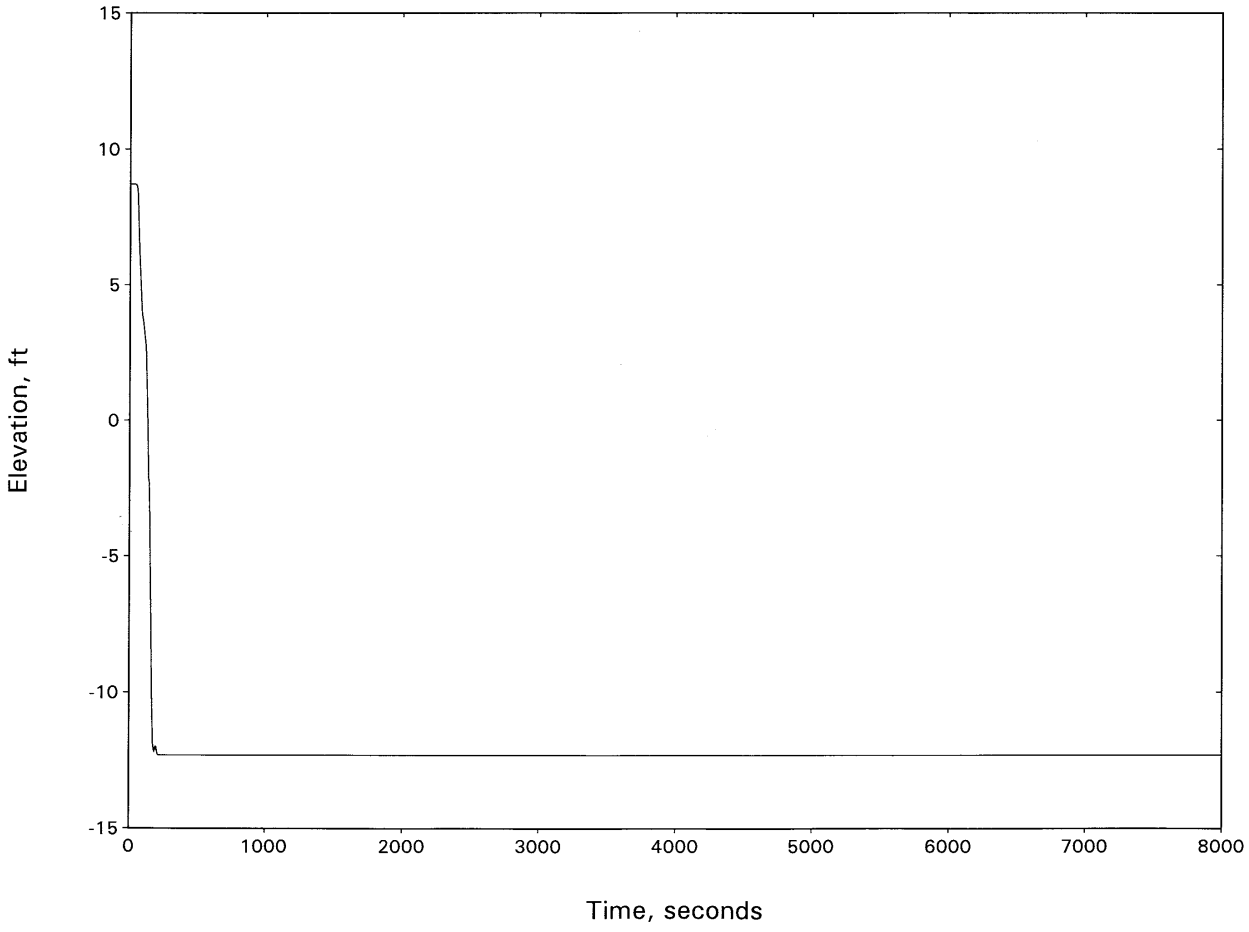

Figure 15.3-142
NORTH ANNA UNIT 2: BROKEN LOOP SEAL LEVEL—5.2-INCH SI LINE BREAK

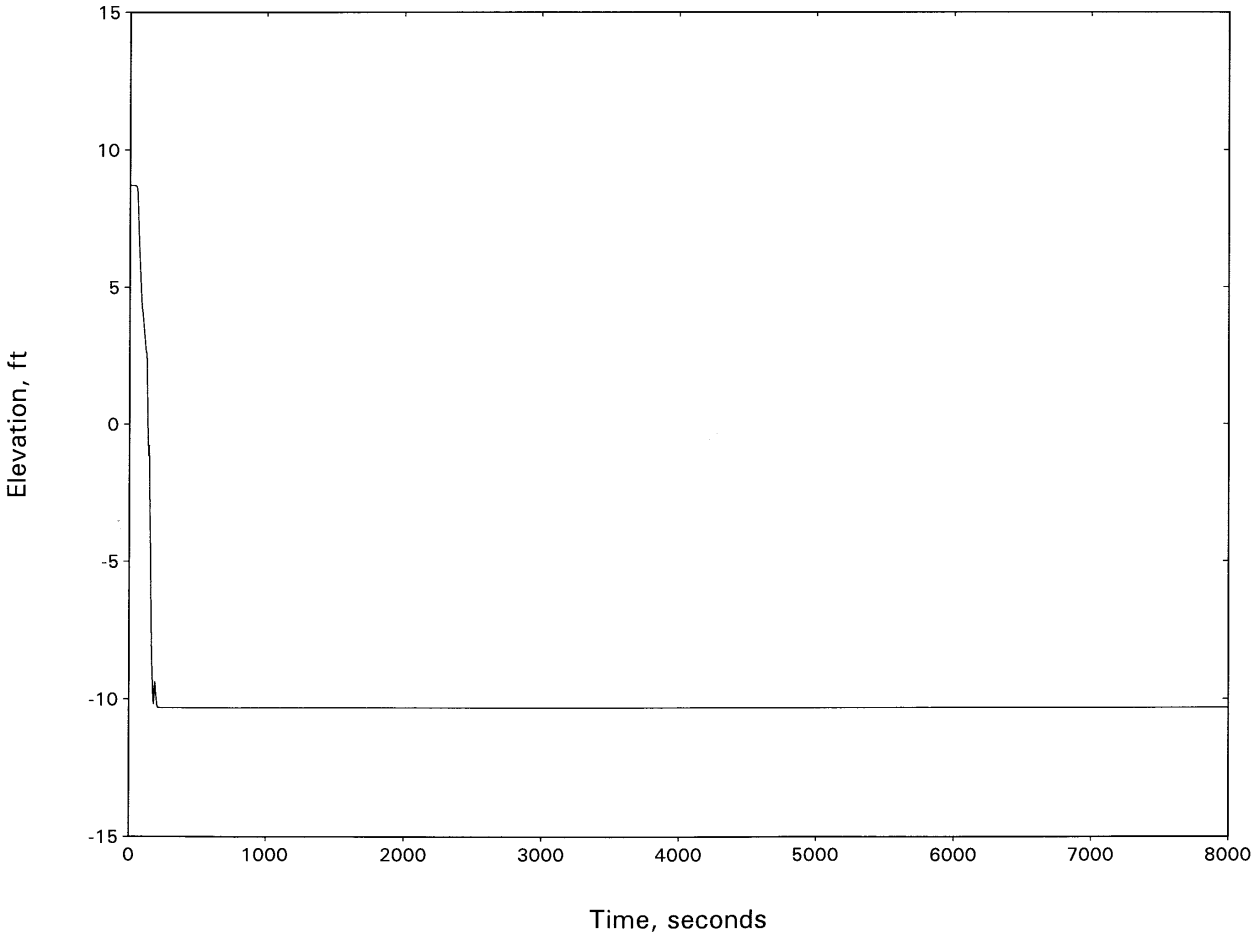

Figure 15.3-143
NORTH ANNA UNIT 2: RCS PRESSURE—6.0-INCH BREAK

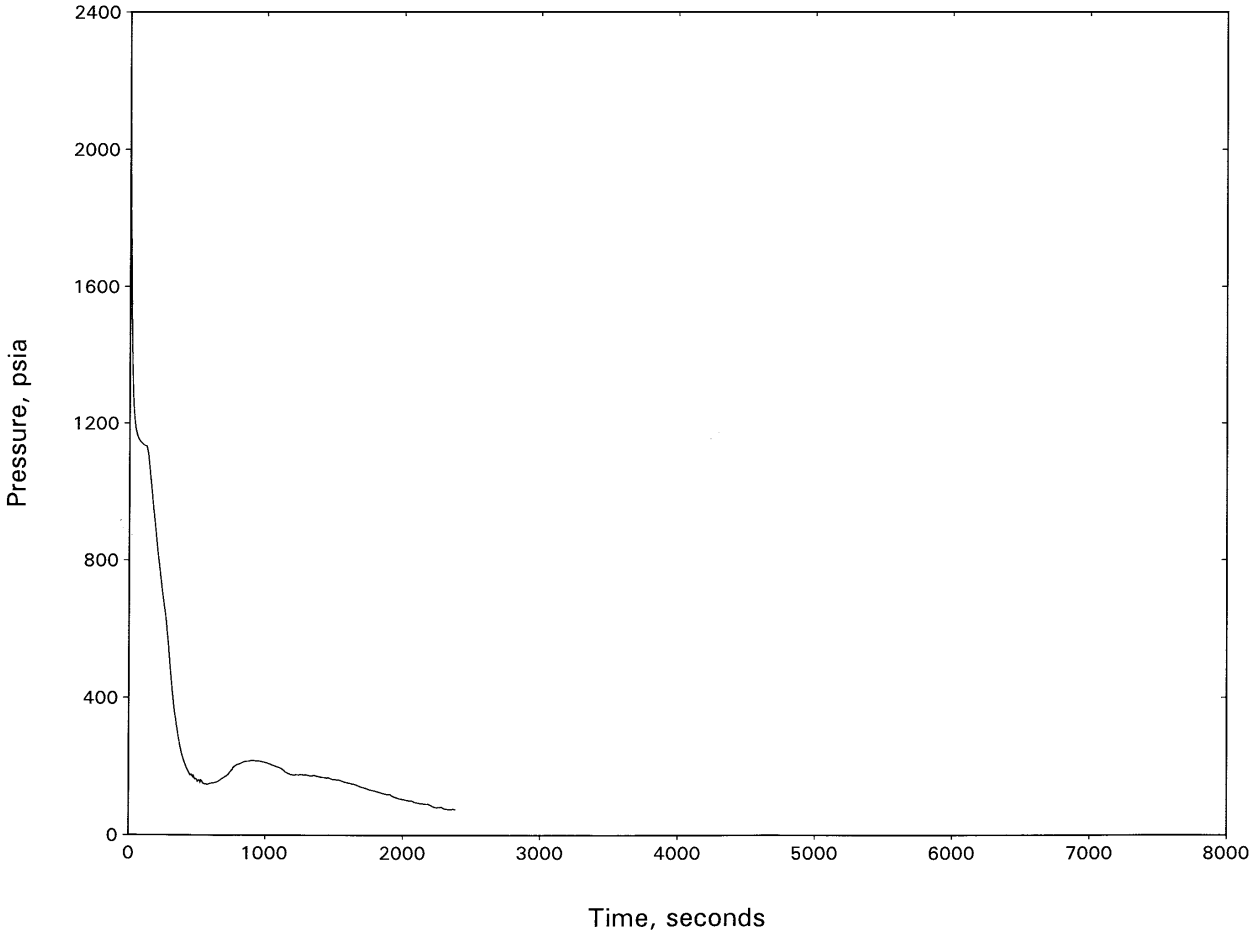

Figure 15.3-144
NORTH ANNA UNIT 2: BREAK FLOW—6.0-INCH BREAK

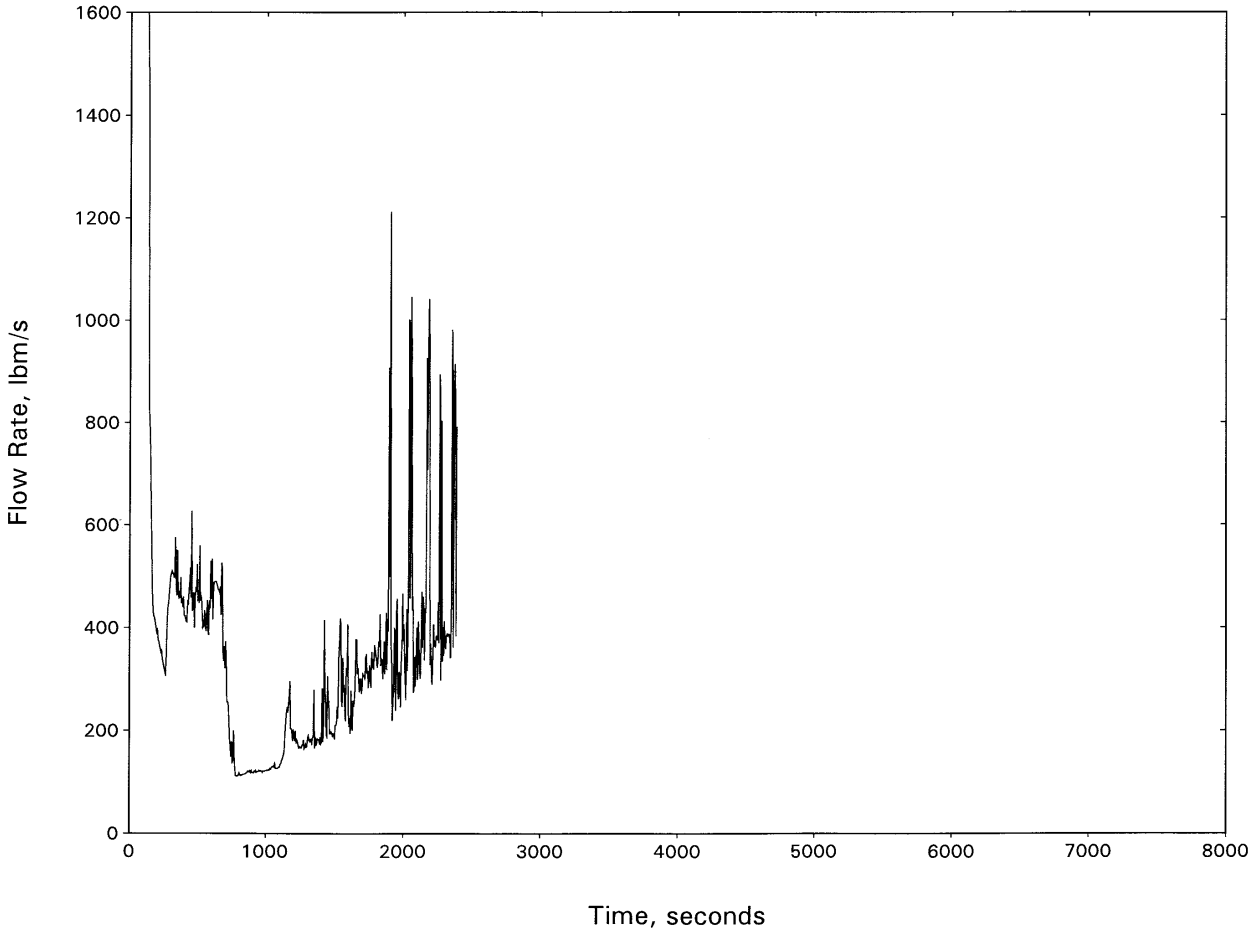

Figure 15.3-145
NORTH ANNA UNIT 2: HOT CHANNEL MIXTURE LEVEL—6.0-INCH BREAK

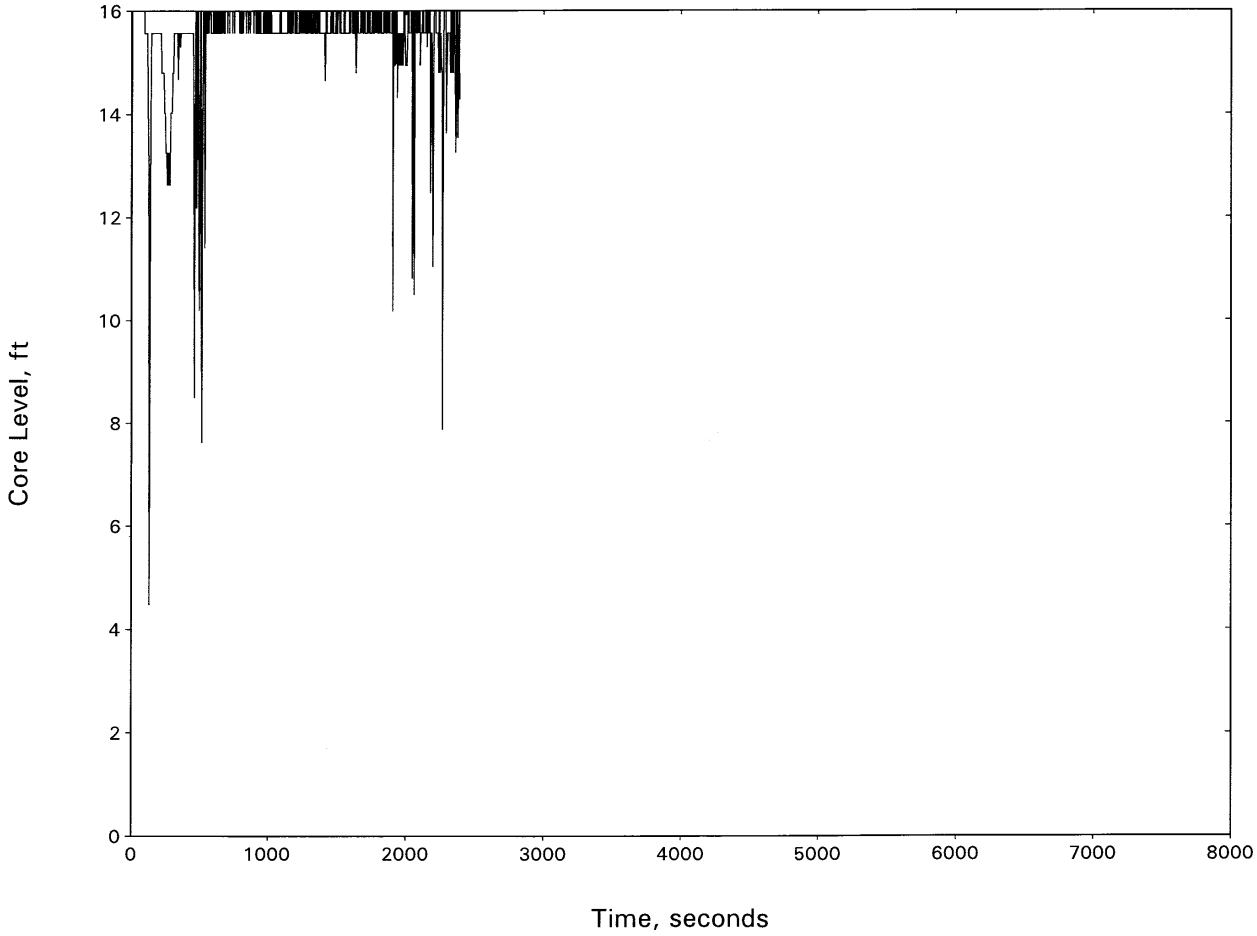

Figure 15.3-146
NORTH ANNA UNIT 2: HOT SPOT PCT—6.0-INCH BREAK

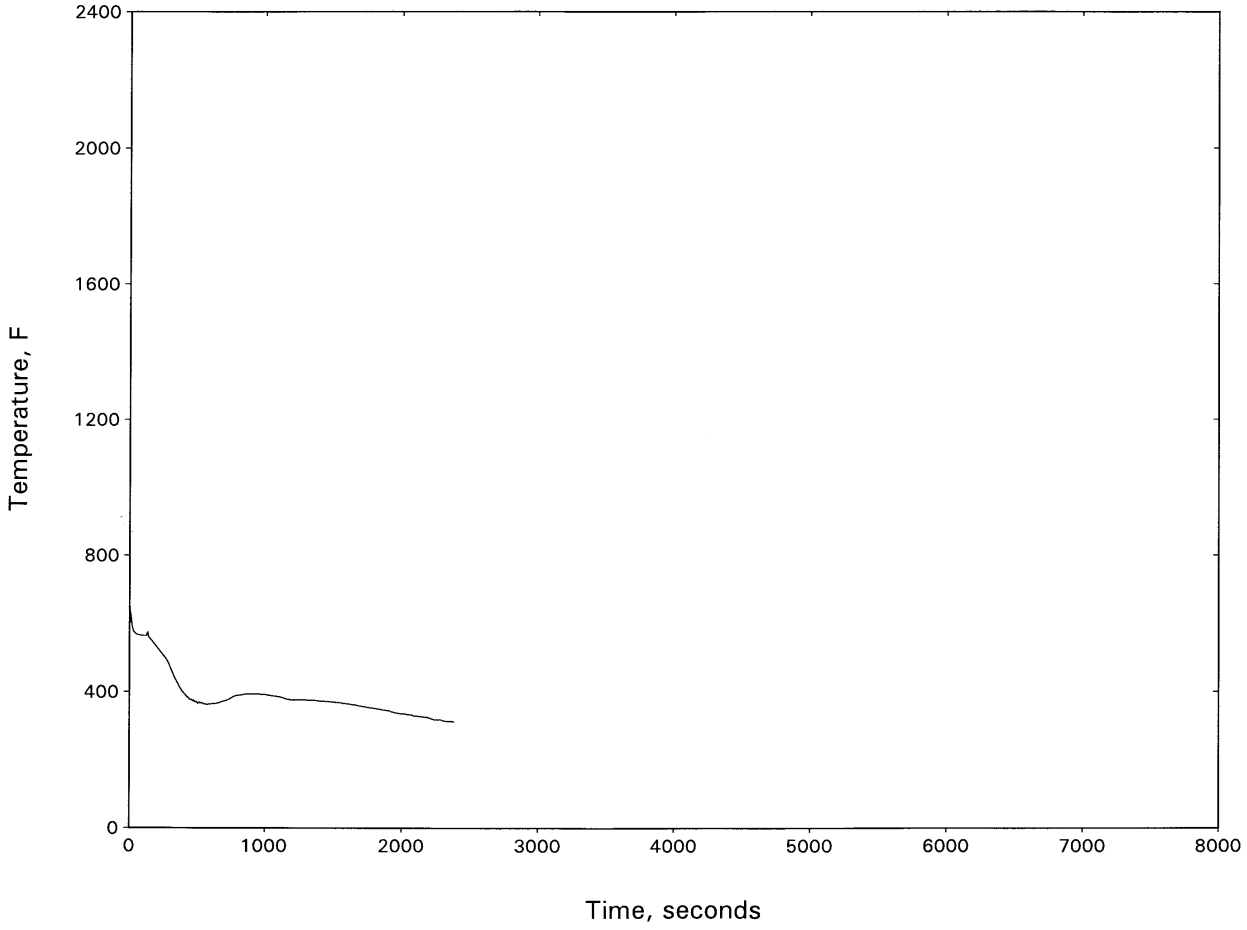

Figure 15.3-147
NORTH ANNA UNIT 2:
HOT CHANNEL OUTLET VAPOR TEMPERATURE—6.0-INCH BREAK

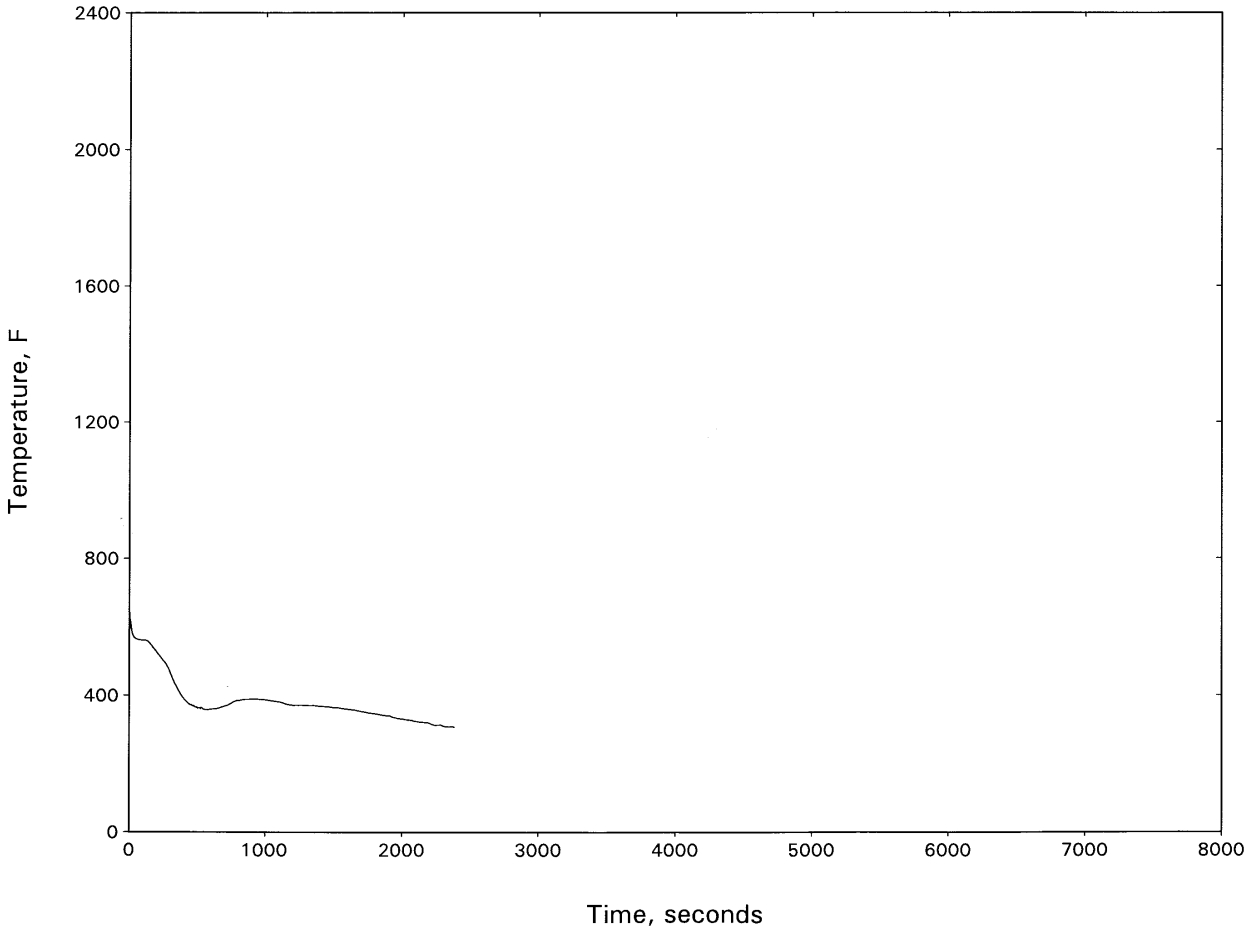

Figure 15.3-148
NORTH ANNA UNIT 2: INTACT LOOP SEAL LEVEL—6.0-INCH BREAK

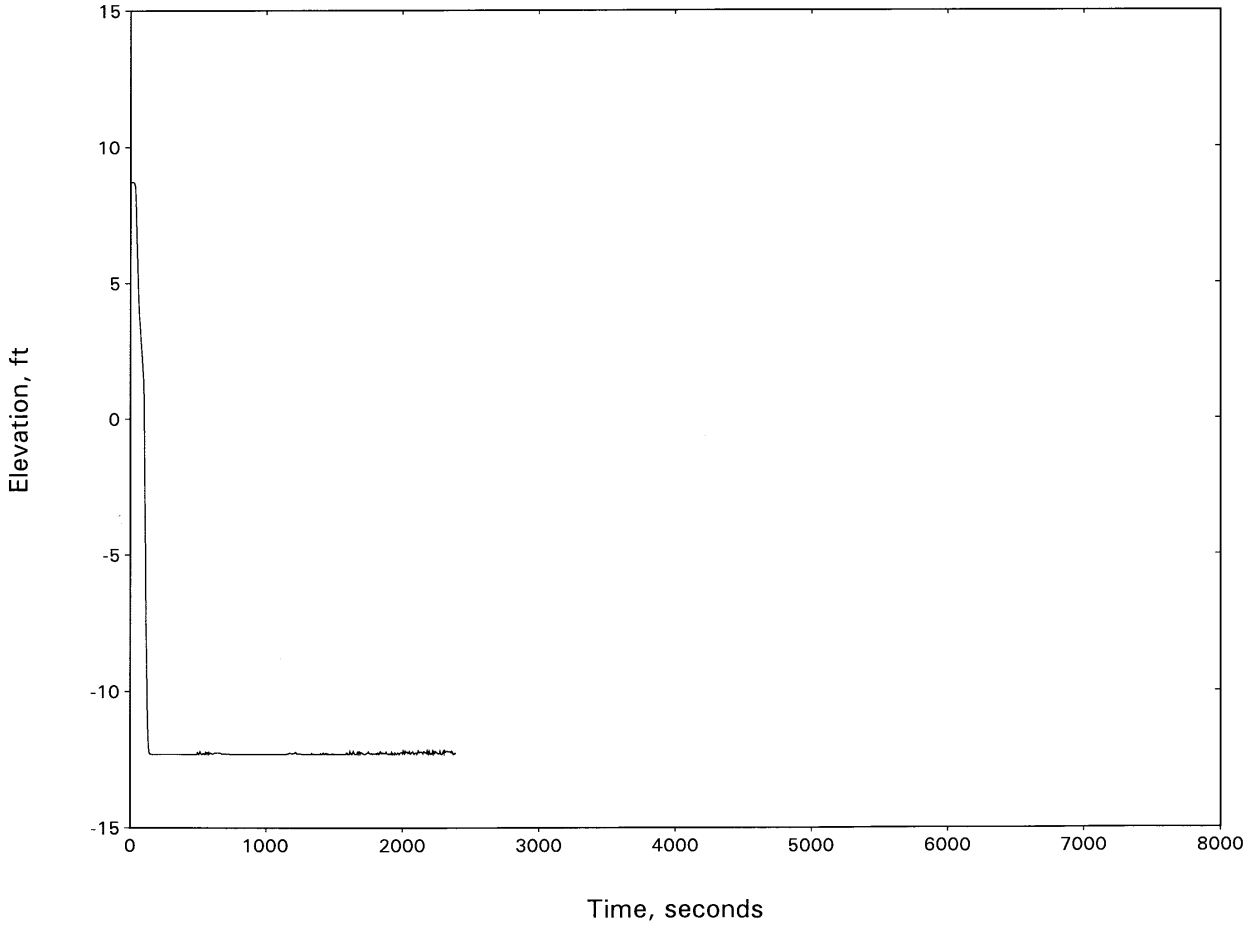

Figure 15.3-149
NORTH ANNA UNIT 2: BROKEN LOOP SEAL LEVEL—6.0-INCH BREAK

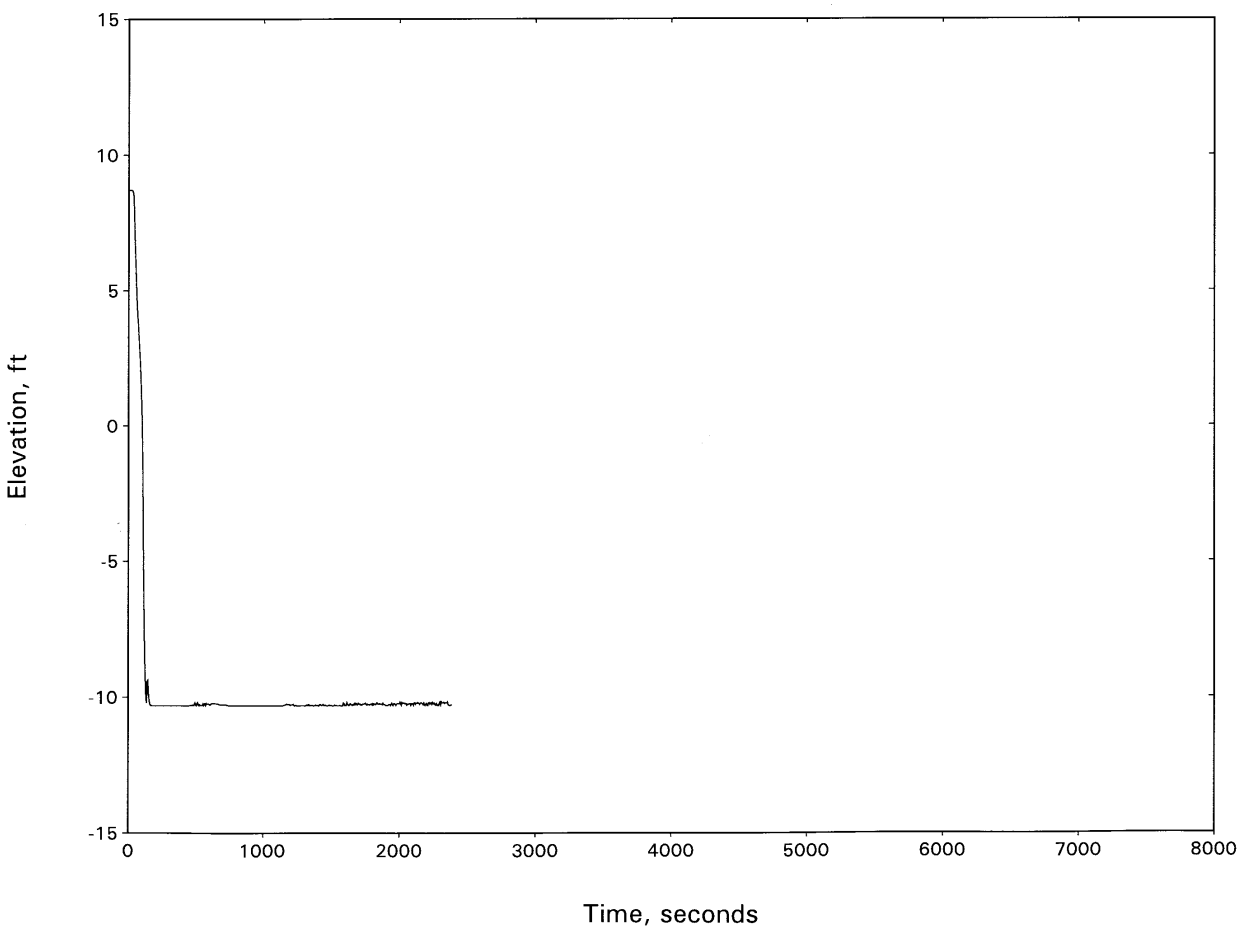

Figure 15.3-150
NORTH ANNA UNIT 2: RCS PRESSURE—3.0-INCH BREAK W/AFW FAILURE

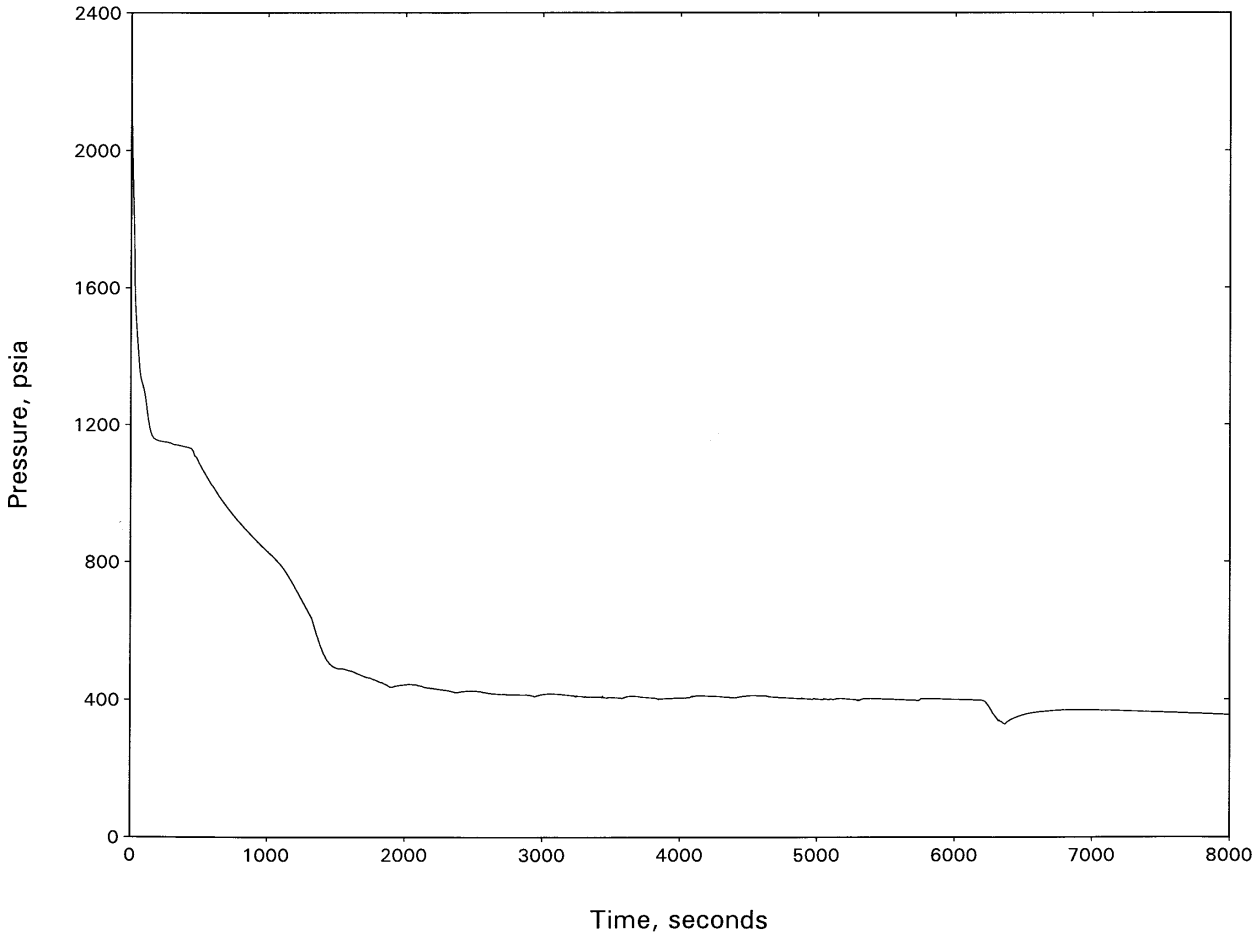

Figure 15.3-151
NORTH ANNA UNIT 2: BREAK FLOW—3.0-INCH BREAK W/AFW FAILURE

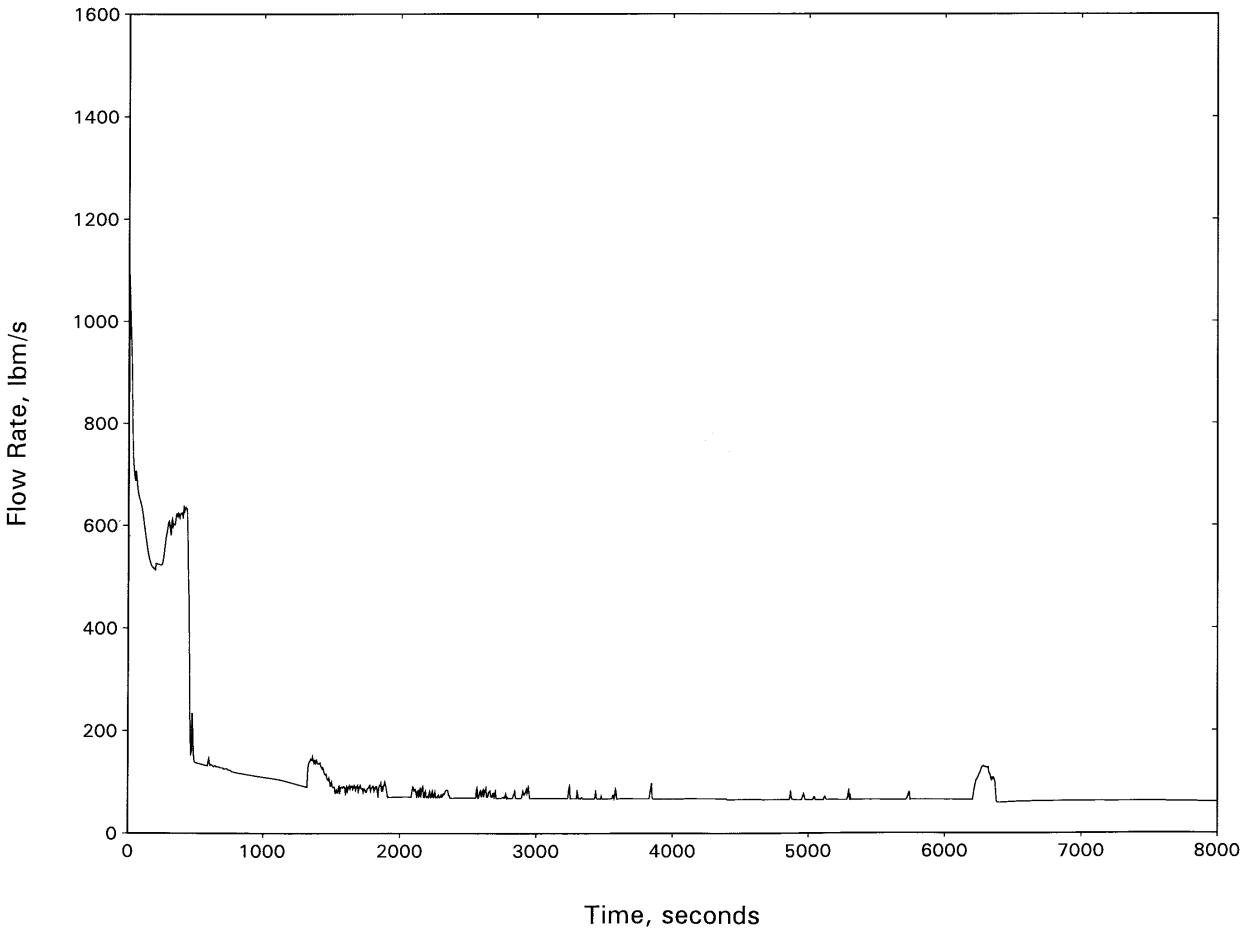

Figure 15.3-152
NORTH ANNA UNIT 2:
HOT CHANNEL MIXTURE LEVEL—3.0-INCH BREAK W/AFW FAILURE

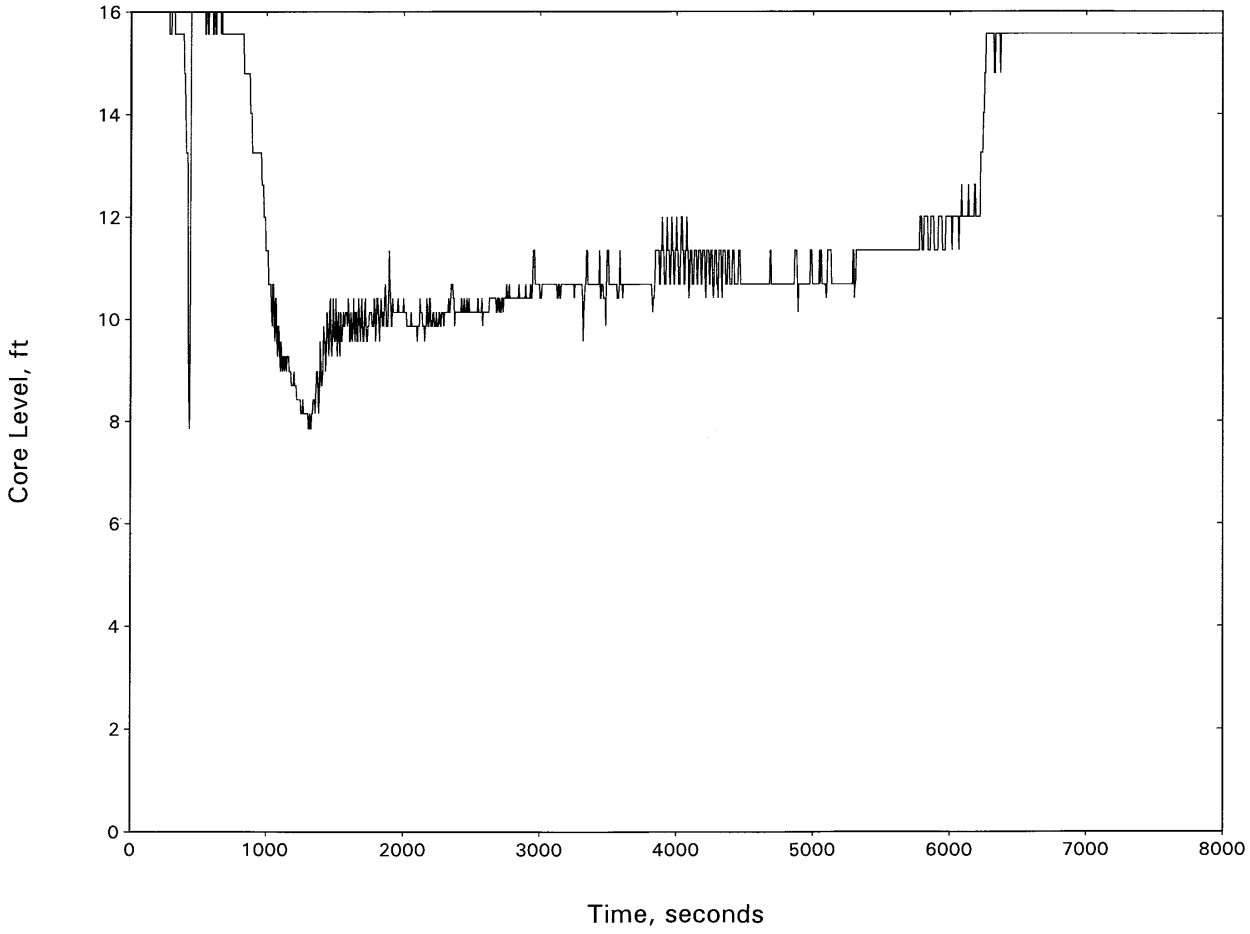

Figure 15.3-153
NORTH ANNA UNIT 2: HOT SPOT PCT—3.0-INCH BREAK W/AFW FAILURE

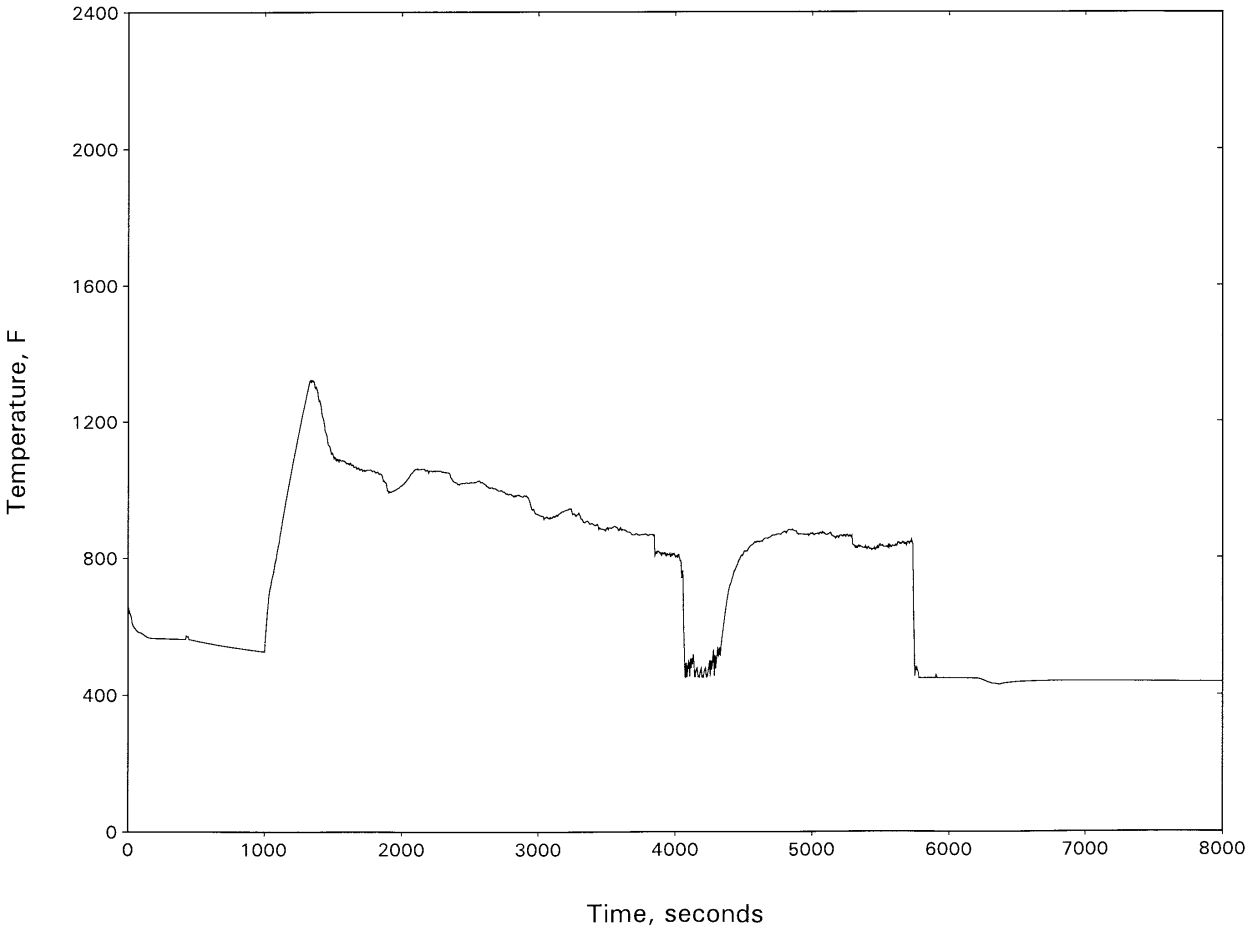

Figure 15.3-154
NORTH ANNA UNIT 2:
HOT CHANNEL OUTLET VAPOR TEMPERATURE—3.0-INCH BREAK W/AFW FAILURE

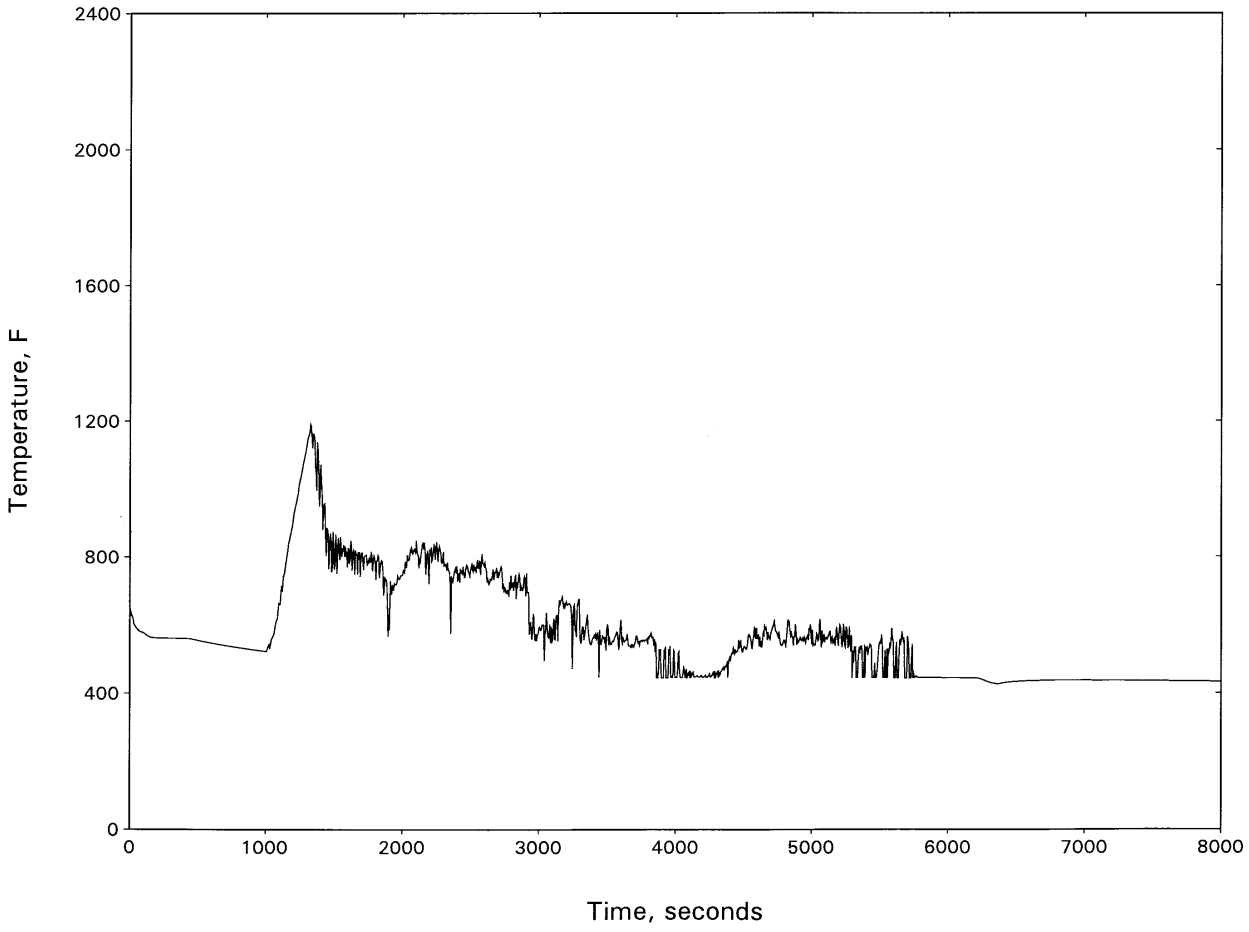

Figure 15.3-155
NORTH ANNA UNIT 2:
INTACT LOOP SEAL LEVEL—3.0-INCH BREAK W/AFW FAILURE

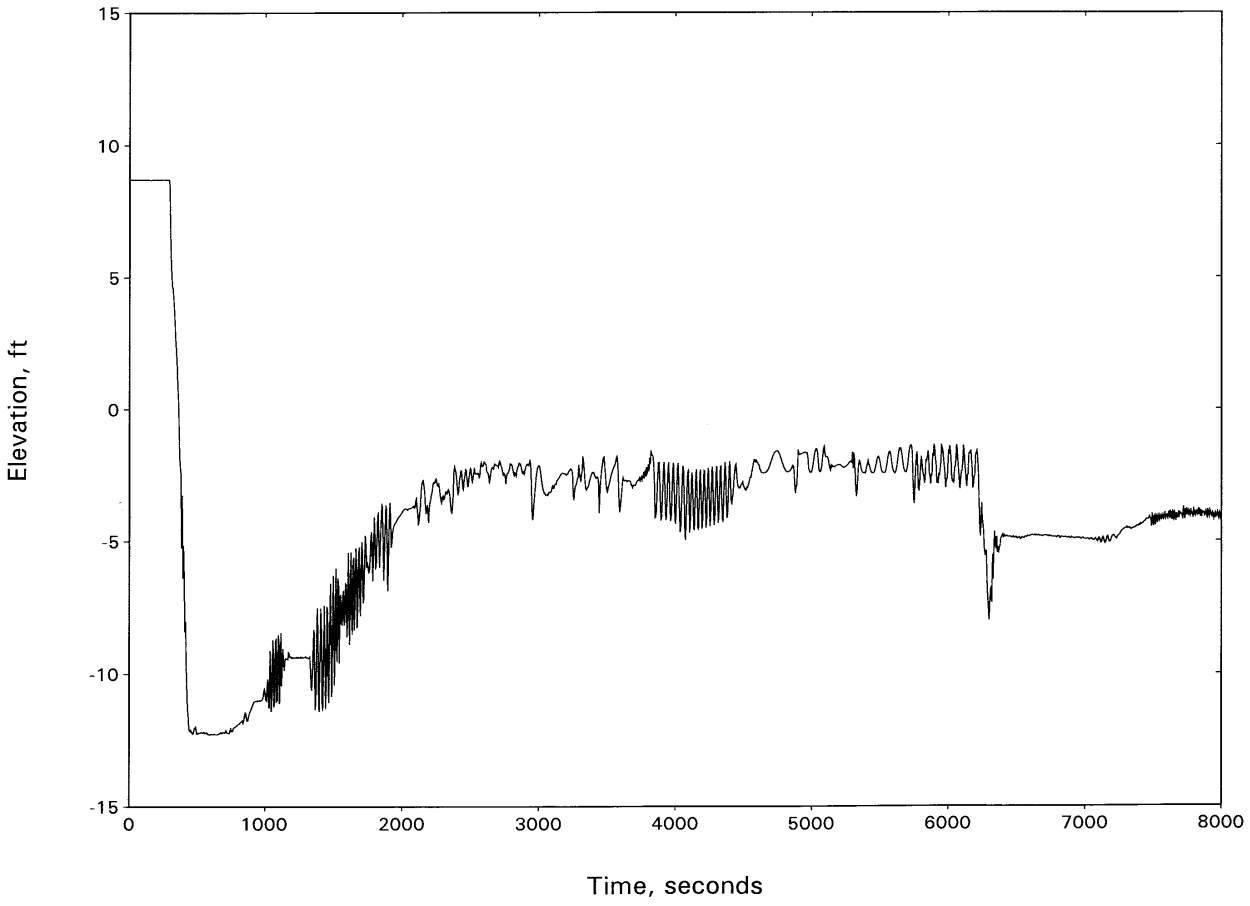

Figure 15.3-156
NORTH ANNA UNIT 2:
BROKEN LOOP SEAL LEVEL—3.0-INCH BREAK W/AFW FAILURE

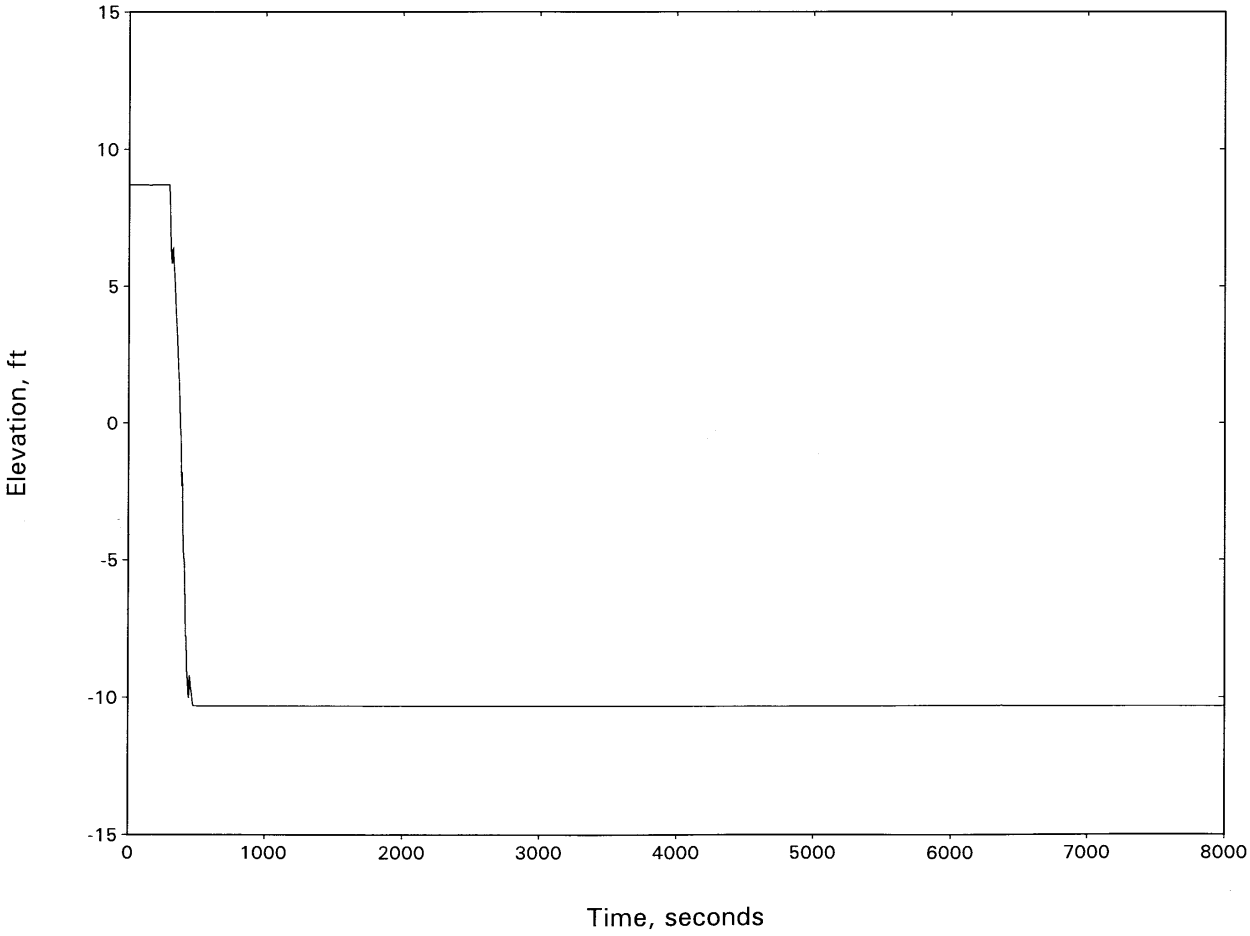

Figure 15.3-157
NORTH ANNA UNIT 2: RCS PRESSURE—3.0-INCH BREAK MIXED CORE

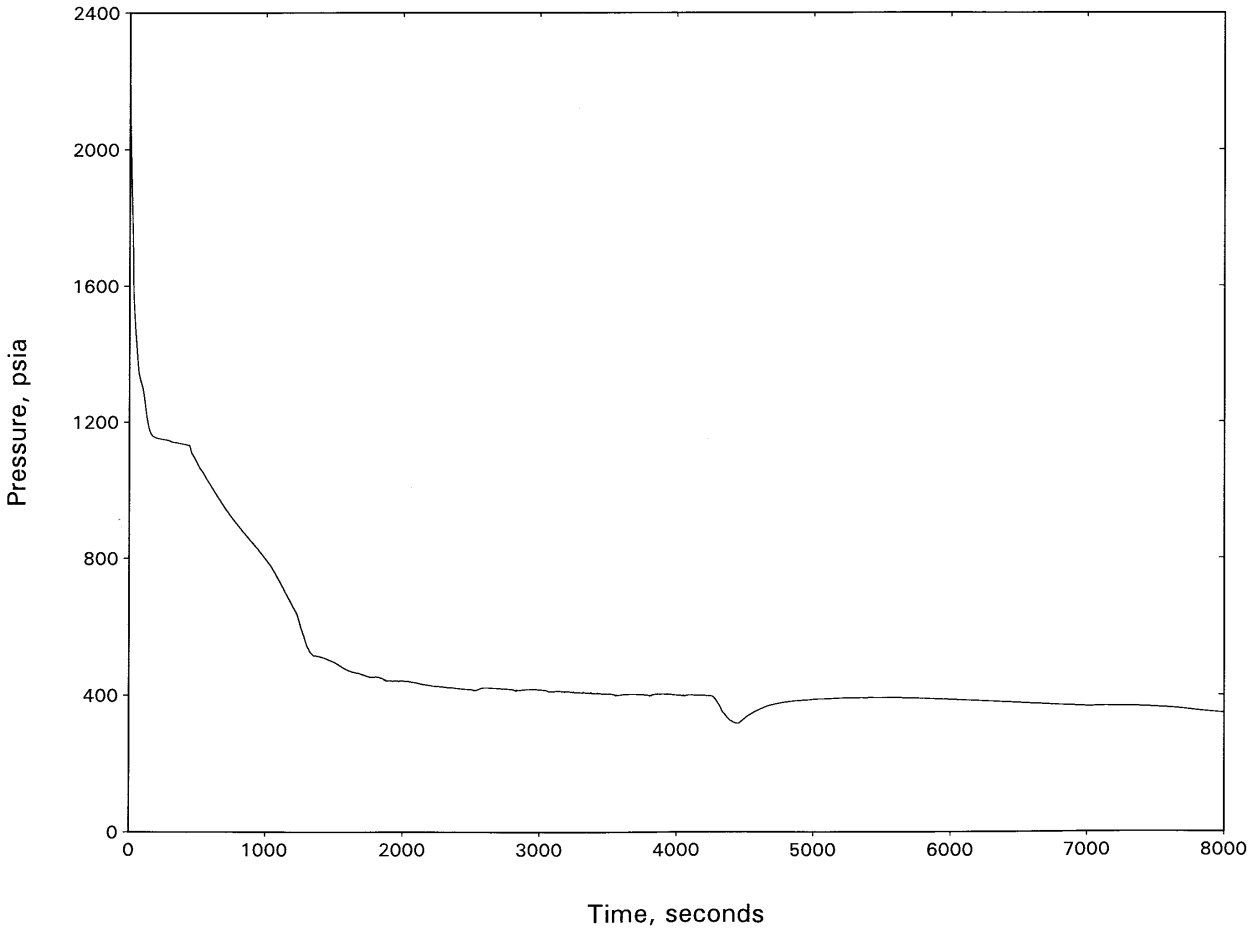

Figure 15.3-158
NORTH ANNA UNIT 2: BREAK FLOW—3.0-INCH BREAK MIXED CORE

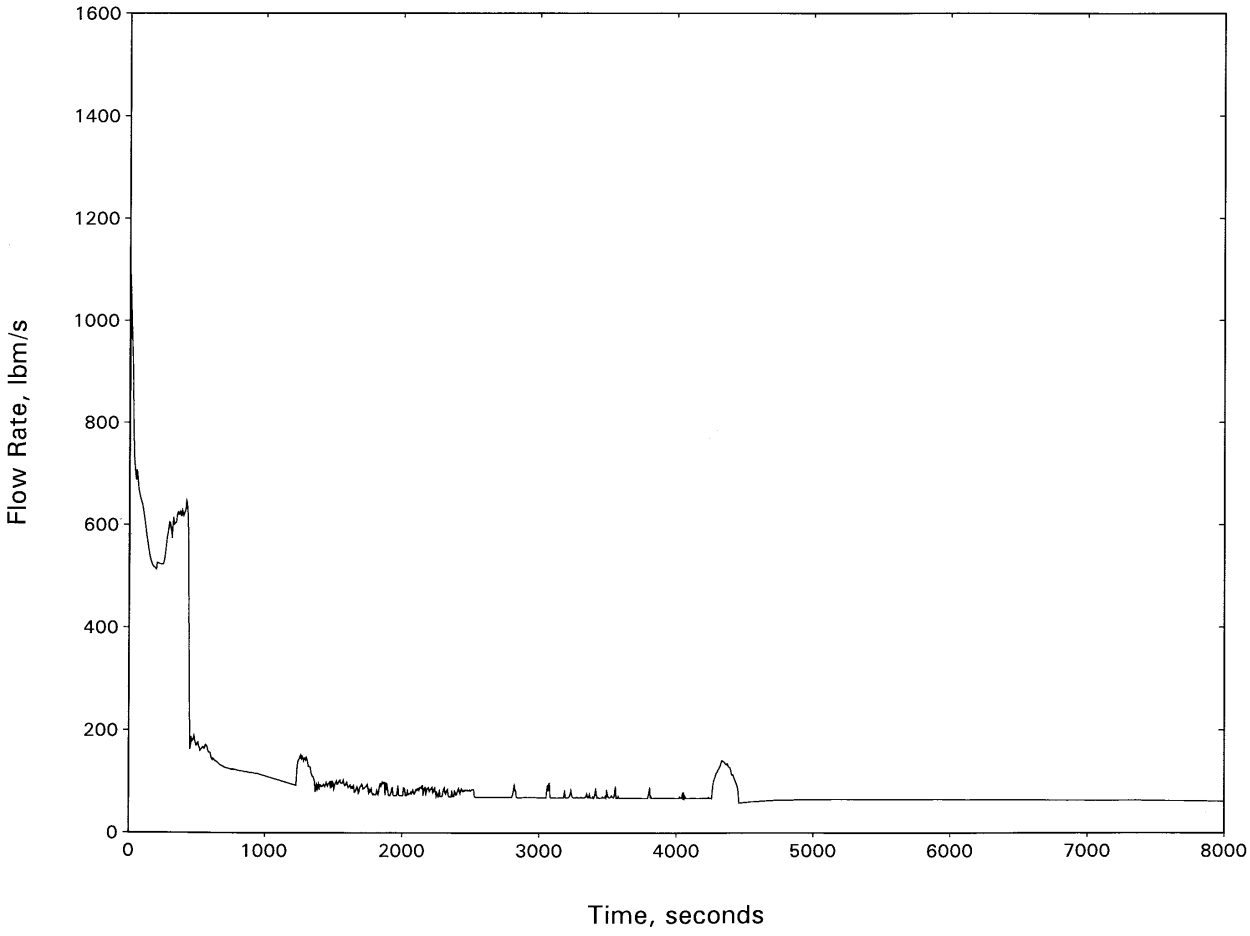

Figure 15.3-159
NORTH ANNA UNIT 2:
HOT CHANNEL MIXTURE LEVEL—3.0-INCH BREAK MIXED CORE

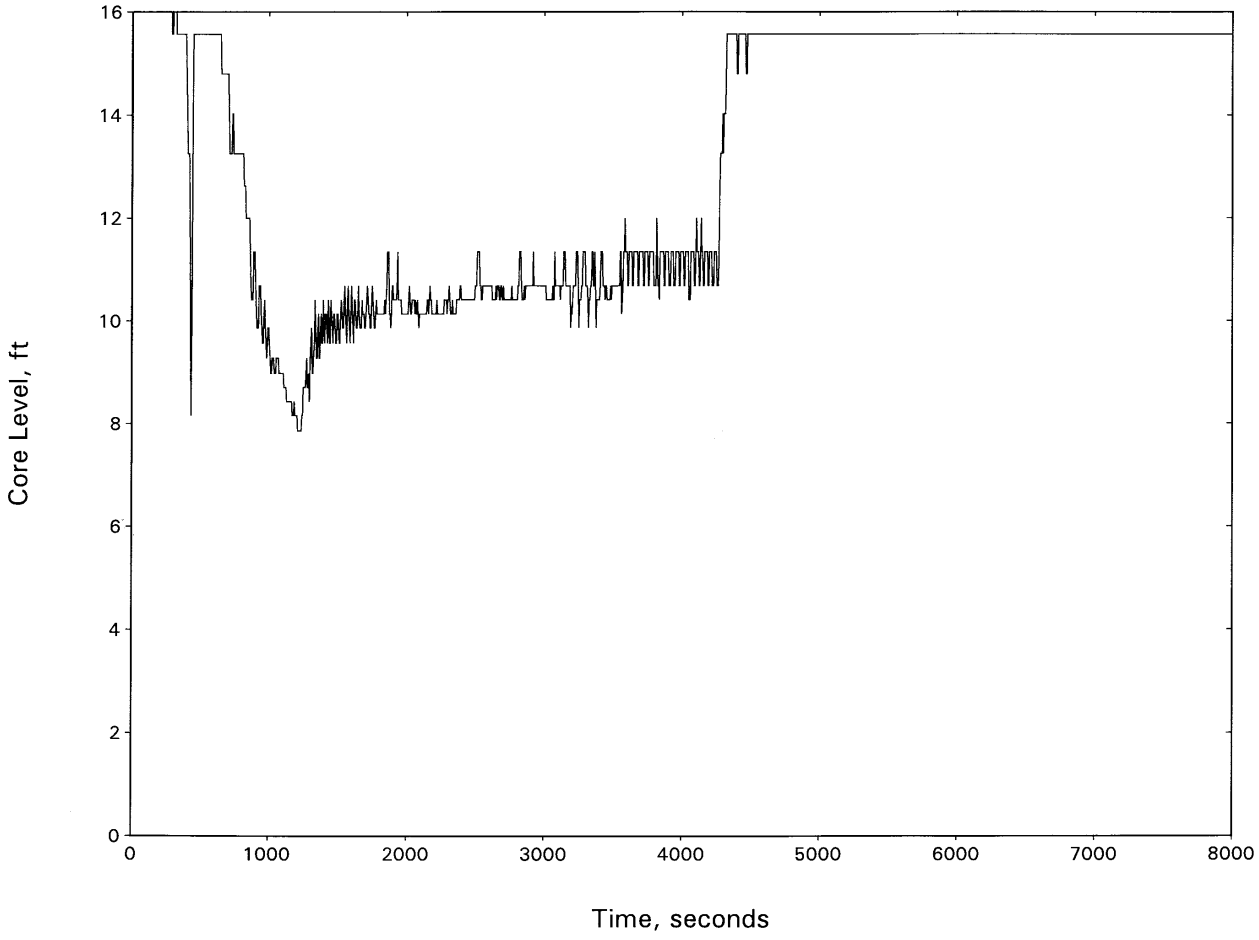

Figure 15.3-160
NORTH ANNA UNIT 2: HOT SPOT PCT—3.0-INCH BREAK MIXED CORE

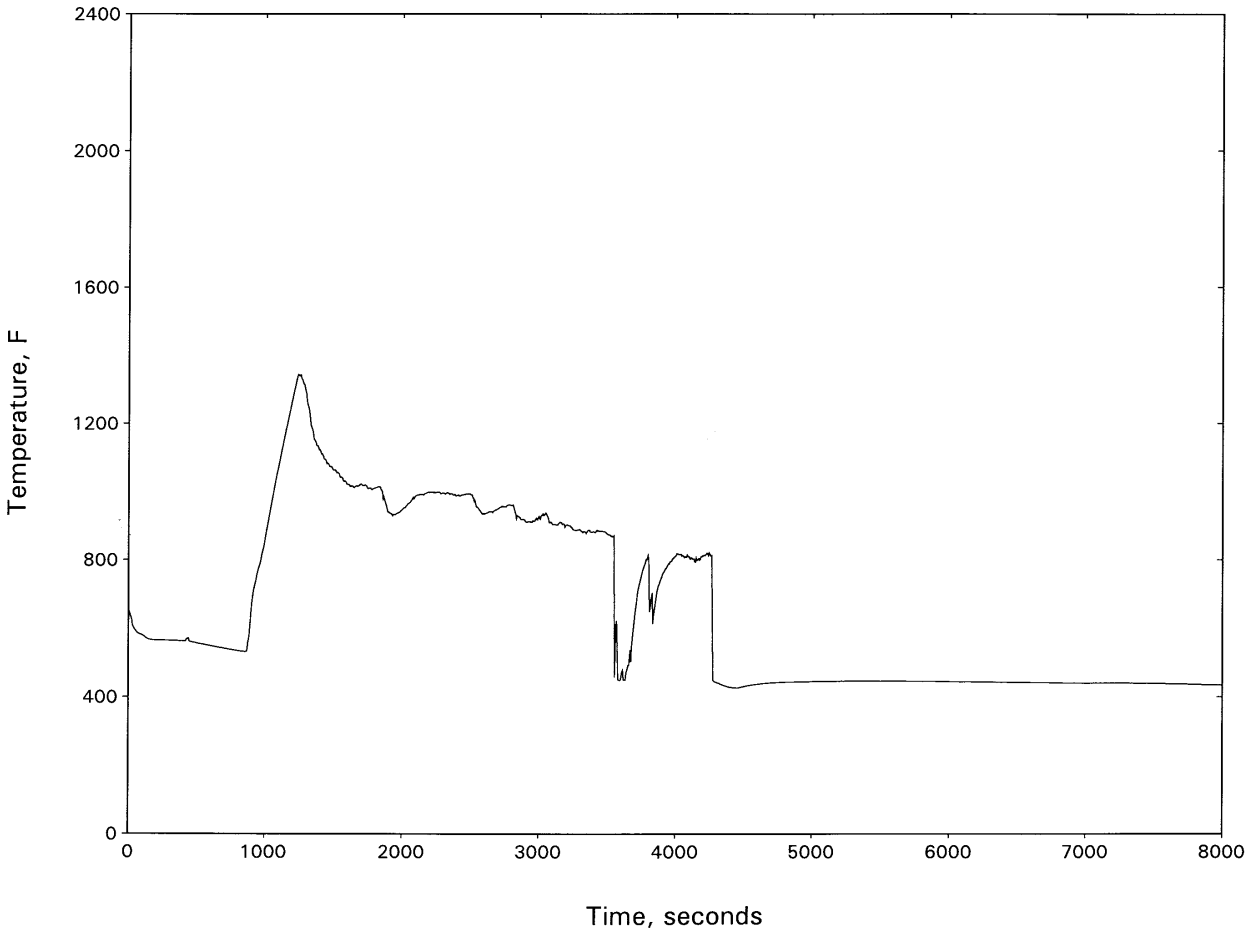

Figure 15.3-161
NORTH ANNA UNIT 2:
HOT CHANNEL OUTLET VAPOR TEMPERATURE—3.0-INCH BREAK MIXED CORE

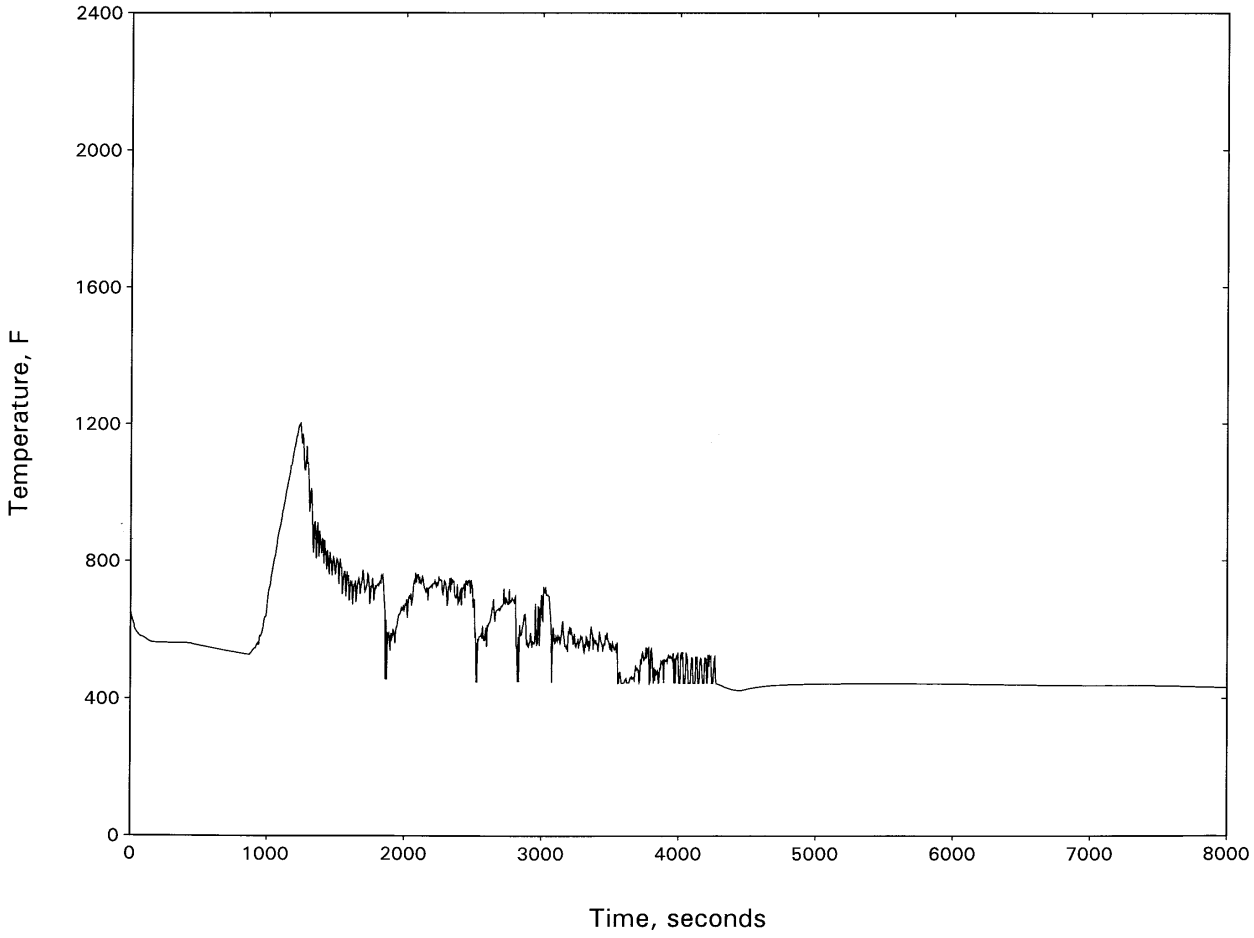

Figure 15.3-162
NORTH ANNA UNIT 2: INTACT LOOP SEAL LEVEL—3.0-INCH BREAK MIXED CORE

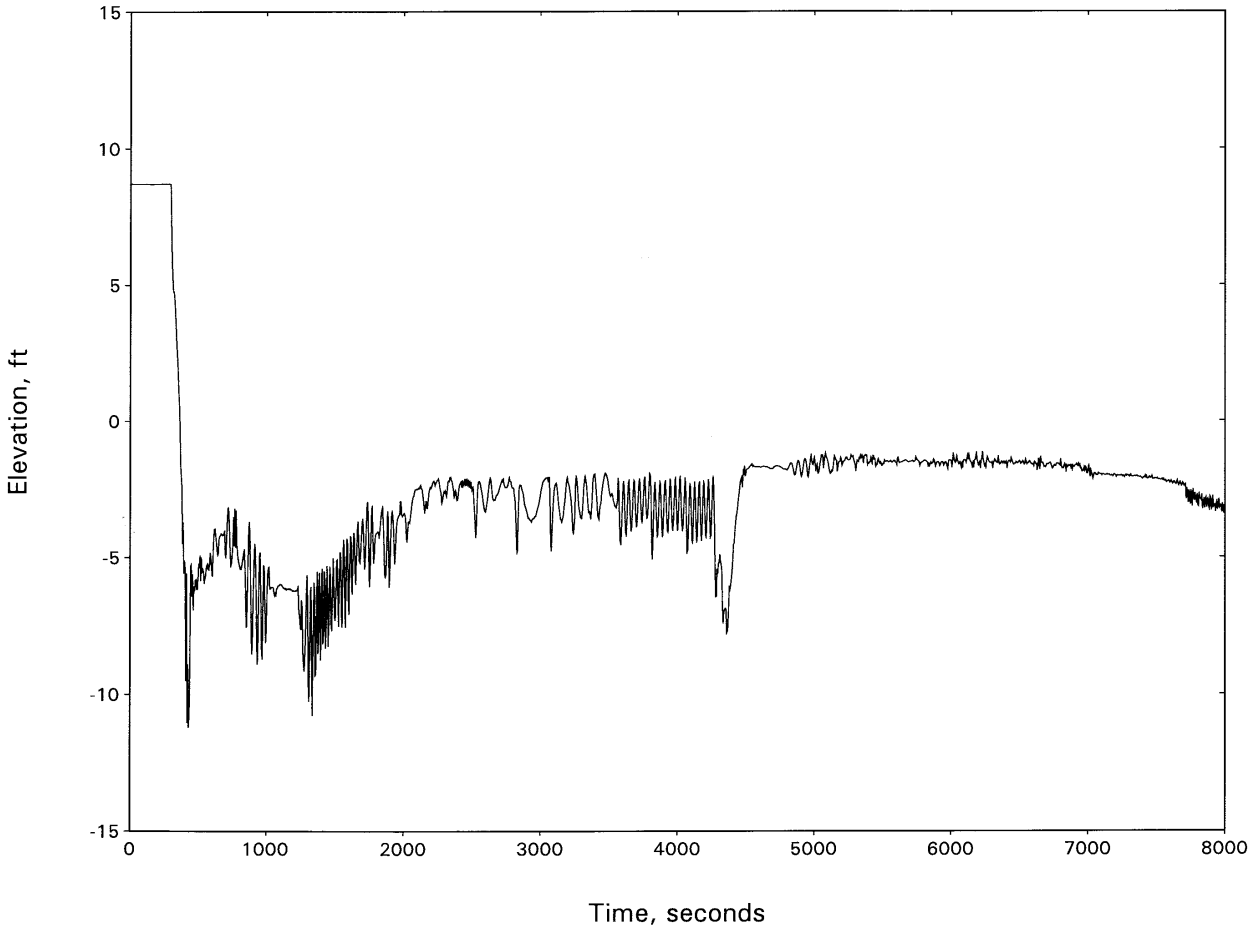

Figure 15.3-163
NORTH ANNA UNIT 2: BROKEN LOOP SEAL LEVEL—3.0-INCH BREAK MIXED CORE

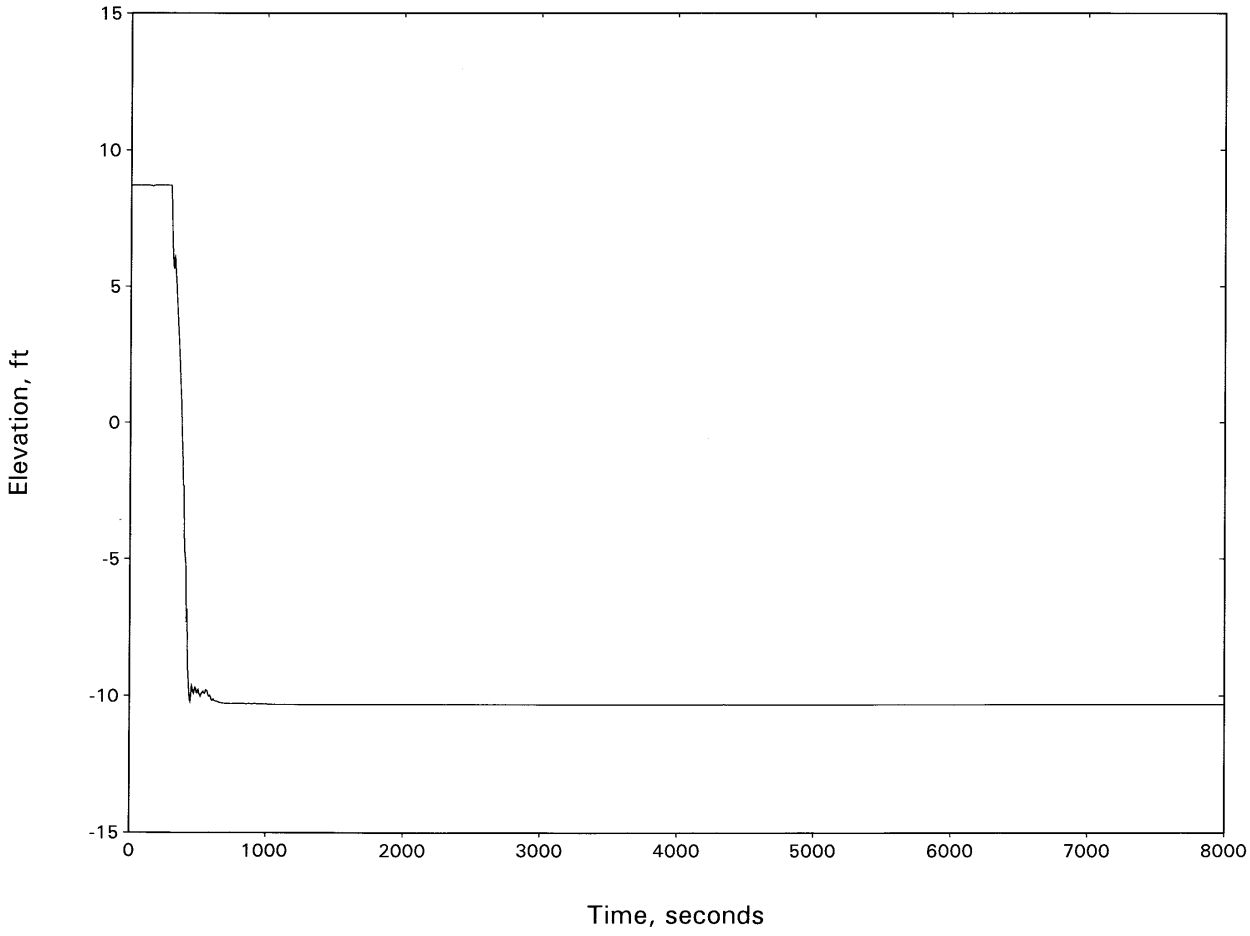

15.4 CONDITION IV - LIMITING FAULTS

Condition IV occurrences are faults that are not expected to take place, but are postulated because their consequences would include the potential for the release of significant amounts of radioactive material. They are the most drastic occurrences that must be designed against, and thus represent limiting design cases. Condition IV faults are not to cause a fission product release to the environment resulting in an undue risk to public health and safety and are within the limits provided in 10 CFR 50.67 or Regulatory Guide 1.183. A single Condition IV fault is not to cause a consequential loss of required functions of systems needed to cope with the fault, including those of the emergency core cooling system and the containment. For the purposes of this report, the following faults have been classified in this category:

1. Major rupture of pipes containing reactor coolant, up to and including double-ended rupture of the largest pipe in the reactor coolant system (loss-of-coolant accident) (Section 15.4.1).
2. Major secondary system pipe rupture, up to and including double-ended rupture (rupture of steam and feedwater lines) (Section 15.4.2).
3. Steam generator tube rupture (Section 15.4.3).
4. Single reactor coolant pump locked rotor (Section 15.4.4).
5. Fuel-handling accidents (Sections 15.4.5).
6. Rupture of a control rod mechanism housing (rod cluster control assembly ejection) (Section 15.4.6).

The analysis of Total Effective Dose Equivalent (TEDE) doses resulting from events leading to fission product release appear in succeeding sections of this chapter. Sections 6.1 and 6.2 also include the discussion of systems interdependency contributing to limiting fission product leakages from the containment following a Condition IV occurrence.

15.4.1 Loss of Reactor Coolant From Ruptured Pipes or From Cracks in Large Pipes Including Double Ended Rupture That Actuates the Emergency Core Cooling System (Large Break Loss of Coolant Accident)

The following sections present the results of the large break LOCA (LBLOCA) transient analyses, for fuel transition (Westinghouse NAIF to Framatome ANP Advanced Mark-BW), applicable to North Anna Units 1 and 2. The Westinghouse and Framatome ANP (FANP) LBLOCA analyses are presented below. The analyses for the Westinghouse NAIF fuel that are presented in Sections 15.4.1.1 through 15.4.1.8 remain valid for the NAIF in mixed cores with Advanced Mark-BW fuel. The FANP Advanced Mark-BW LBLOCA analyses are presented in Sections 15.4.1.9 through 15.4.1.18.

15.4.1.1 Introduction

This discussion presents the results of a revised large break LOCA analysis of record for Westinghouse fuel for North Anna Units 1 and 2. Analysis assumptions have been made which

reflect operation with the replacement steam generators, and upflow and downflow configurations in addition to changes in other key analysis inputs. Previous Westinghouse large break LOCA sensitivity studies for a three loop plant similar to North Anna have indicated that the downflow configuration has PCT results which bound that of the upflow design. However, since these results can be somewhat variable between different plants, the North Anna reanalysis is performed for both upflow and downflow configurations. Results and limitations associated with this analysis are applicable to the operation of North Anna Units 1 and 2.

The key input parameters and assumptions from the analysis are listed below. Each is described more fully in the following sections.

- Assumption of 7% uniform steam generator tube plugging
- Peak Heat Flux Hot Channel Factor, F_Q, of 2.19
- Peak Enthalpy Hot Channel Factor, $F_{\Delta h}$ of 1.55
- Hot Assembly Relative Power Factor of 1.45
- Containment Accumulator Water Temperature, of 100°F
- Improved Spacer Grid Heat Transfer Model (Reference 2)
- Upflow and downflow baffle/barrel designs
- Safety Injection, 1 HHSI + 1 LHSI, spilling to 10-psig containment pressure
- Assumed fuel temperature and rod internal pressure associated with core average burnup of 12,000 MWD/MTU
- North Anna Improved Fuel (NAIF) with ZIRLO^{TM} cladding and PERFORMANCE+ design features
- Incorporation of skewed axial power distribution evaluation methodology
- RCS total flow rate of 278,400 gpm

15.4.1.2 **General**

A reanalysis of the emergency core cooling system (ECCS) performance for the postulated large break loss of coolant accident (LOCA) has been performed in compliance with Appendix K to 10 CFR 50. The results of this reanalysis are presented here, and are in compliance with 10 CFR 50.46, *Acceptance Criteria for Emergency Core Cooling Systems for Light Water Reactors*. This analysis was performed with the NRC-approved version of the Westinghouse LOCA-ECCS evaluation model denoted as the 1981 model with BASH (Reference 35). The analytical techniques are in full compliance with 10 CFR 50, Appendix K.

As required by Appendix K to 10 CFR 50, certain conservative assumptions were made for the LOCA-ECCS analysis. The assumptions pertain to the conditions of the reactor and associated safety system equipment at the time that the LOCA is assumed to occur, and include such items as the core peaking factors, the containment pressure, and the performance of the emergency core cooling system. Selection of input parameters for Appendix K analysis is made to represent an appropriately conservative configuration of the plant initial conditions. This was accomplished by assuming bounding input values for key parameters such as core power, $F_{\Delta h}$, F_Q, steam generator tube plugging and RCS flow. The current analysis assumes nominal values for RCS temperatures and accumulator water volume, consistent with current approved Westinghouse LOCA analysis methods. Assuming delivery of nominal accumulator tank volume only, together with the minimum accumulator pressure assumption represents a condition which would be conservative for typical plant operating conditions.

Although LOCA analysis assumptions do not explicitly bound each plant parameter individually, analysis methods used ensure conservative results over the range of allowed Technical Specification and Core Operating Limits Report (COLR) parameter values. This is accomplished by selecting limiting values of parameters which have known impact upon results; for other parameters, nominal values are used. It can thus be concluded that, in the aggregate, the analysis is conservative and acceptable for all realistic plant operational configurations as currently defined.

15.4.1.3 **Identification and Causes and Accident Description**

A LOCA is the result of a rupture of the reactor coolant system (RCS) piping or of any line connected to the system. The system boundaries considered in the LOCA analysis are defined in Section 3.6 of the UFSAR. Sensitivity studies (Reference 4) have indicated that a double-ended cold-leg guillotine (DECLG) pipe break is limiting. Should a DECLG occur, rapid depressurization of the RCS occurs. The reactor trip signal subsequently occurs when the pressurizer low-pressure trip setpoint is reached. A safety injection system (SIS) signal is actuated when the appropriate setpoint is reached, activating the high-head safety injection pumps. The actuation and subsequent activation of the Emergency Core Cooling System, which occurs with the SIS signal, assumes the most limiting single-failure event. These countermeasures will limit the consequences of the accident in two ways:

1. Reactor trip and borated water injection complement void formation in causing rapid reduction of power to a residual level corresponding to fission product decay heat. No credit is taken in the analysis for the insertion of control rods to shut down the reactor.
2. Injection of borated water provides heat transfer from the core and limits the clad temperature increase.

Before the break occurs, the unit is in an equilibrium condition, i.e., the heat generated in the core is being removed via the secondary system. During blowdown, heat from fission product decay, hot internals and the vessel continue to be transferred to the reactor coolant system. At the

beginning of the blowdown phase, the entire reactor coolant system contains subcooled liquid that transfers heat from the core by forced convection with some fully developed nucleate boiling. After the break develops, the time to DNB is calculated, consistent with Appendix K of 10 CFR 50. Thereafter, the core heat transfer is based on local conditions, with transition boiling and forced convection to steam as the major heat transfer mechanisms.

During the refill period, it is assumed that rod-to-rod radiation is the only core heat transfer mechanism. The heat transfer between the reactor coolant system and the secondary system may be in either direction, depending on the relative temperatures. For the case of continued heat addition to the secondary side, secondary-side pressure increases and the main safety valves may actuate to reduce the pressure. Makeup to the secondary side is automatically provided by the auxiliary feedwater system. Coincident with the safety injection signal, normal feedwater flow is stopped by closing the main feedwater control valves and tripping the main feedwater pumps. Emergency feedwater flow is initiated by starting the auxiliary feedwater pumps. The secondary-side flow aids in the reduction of RCS pressure. When the reactor coolant system depressurizes to 600 psia, the accumulators begin to inject borated water into the reactor coolant loops. The conservative assumption is then made that injected accumulator water bypasses the core and goes out through the break until the termination of bypass. This conservatism is again consistent with Appendix K of 10 CFR 50. In addition, the reactor coolant pumps are assumed to be tripped at the initiation of the accident, and effects of pump coastdown are included in the blowdown analysis.

The water injected by the accumulators cools the core, and subsequent operation of the low-head safety injection pumps supplies water for long-term cooling. When the refueling water storage tank (RWST) is nearly empty, the long-term cooling of the core is accomplished by switching to the recirculation mode of core cooling, in which the spilled borated water is drawn from the containment sump by the low-head safety injection pumps and returned to the reactor vessel.

The containment spray system and the recirculation spray system operate to return the containment environment to subatmospheric pressure.

15.4.1.4 **Analysis Assumptions**

As required by Appendix K of 10 CFR 50, certain conservative assumptions were made for the Large Break LOCA-ECCS analysis. The assumptions pertain to the condition of the reactor and associated safety system equipment at the time that the LOCA is assumed to occur, and include such items as the core peaking factors, core decay heat and the performance of the Emergency Core Cooling System. Tables 15.4-1 and 15.4-2 present the values assumed for several key parameters in this analysis. Assumptions and initial operating conditions which reflect the requirements of Appendix K to 10 CFR 50 have been used in this analysis. These assumptions include:

1. The break is located in the cold leg between the pump discharge and the vessel inlet.

2. The safety injection flow spills to containment back pressure in the broken loop. Safety injection occurs only in the intact loops cold legs.
3. The accumulator in the broken loop also spills to containment.
4. 120 percent of 1971 ANS decay heat is assumed following reactor trip.
5. Initial power is 102% of the full core power, to account for the calorimetric uncertainty.

Several additional assumptions have been incorporated into the large break LOCA reanalysis described below. These changes are discussed here.

The analysis assumed that 7% of the tubes in each steam generator are plugged. This level of tube plugging is expected to bound that which is actually experienced with the replacement steam generators.

Consistent with current Westinghouse Evaluation Model input assumptions (Reference 43), the assumed initial accumulator water temperature is 100°F. The water temperature in each accumulator is assumed to equal the temperature in the surrounding containment compartment during full power operation. At North Anna Power Station, the accumulators are located on the containment floor. A review of temperature detector data at this location has confirmed that a temperature of 100°F is a conservative value for use in large break LOCA analysis.

The North Anna analysis uses a corrected version of the LOCBART code, which is part of the BASH Evaluation Model (EM). Westinghouse has corrected and improved the spacer grid heat transfer model used in the BART and BASH ECCS Evaluation Models (Reference 2). Since this model change is primarily a correction to the EM, it has been implemented in all versions of the BART and BASH EMs without prior NRC review. This process for addressing model changes is documented in WCAP-13451 (Reference 44).

The safety injection is assumed to spill to 10-psig containment pressure. This assumption has been confirmed to provide bounding safety injection flow for the LBLOCA analysis.

The analysis assumed a peak Heat Flux Hot Channel Factor, F_Q, value of 2.19 and a peak Nuclear Enthalpy Hot Channel Factor, $F\Delta h$, value of 1.55. As required by Technical Specification 5.6.5, the Core Operating Limits Report (COLR) documents the applicable limit values of key core-related parameters for each reload core. These values bound the limits in the current cycle specific COLRs. For future reload cycles, the COLR will specify the appropriate limits which account for all design considerations, particularly large and small break LOCA effects.

The analysis assumes a full core of North Anna Improved Fuel (NAIF) with ZIRLO^{TM} cladding and PERFORMANCE+ design features, which is similar and compatible to Westinghouse Vantage 5 Hybrid (V5H) fuel and the 17 x 17 Standard fuel. This modeling is applicable to full or mixed cores of either fuel product. The only mechanism available to cause a transition core to have a greater calculated large break LOCA PCT than a full core of either fuel

product is the possibility of flow redistribution due to fuel assembly hydraulic resistance mismatch. As stated in References 36 and 49, mixed core hydraulic resistance mismatches are not a significant factor for large break analyses and it is not necessary to apply a LOCA analysis transition core penalty.

Using these assumptions, it has been demonstrated that operation at the rated thermal power of 2893 MWt with SGTP up to 7% in any SG will comply with all of the acceptance criteria specified in 10 CFR 50.46.

15.4.1.5 **Analysis of Effects and Consequences**

15.4.1.5.1 Method of Analysis

The large break LOCA is divided, for analytical purposes, into three phases: blowdown, refill, and reflood. There are three distinct transients analyzed in each phase, including the thermal-hydraulic transient in the reactor coolant system, the pressure and temperature transient within the containment and the fuel clad temperature transient of the hottest fuel rod in the core. Based on these considerations, a system of interrelated computer codes has been developed for the analysis. These codes assess whether sufficient heat transfer geometry and core amenability to cooling are preserved during the time spans applicable to the blowdown, refill, and reflood phases of the LOCA.

The description of the various aspects of the LOCA analysis methodology is given in WCAP-8339 (Reference 5). This document describes the major phenomena modeled, the interfaces among the computer codes and the features of the codes that ensure compliance with 10 CFR 50, Appendix K. The Westinghouse LOCA-ECCS evaluation model denoted as the 1981 model with BASH (Reference 35) consists of a series of computer codes, SATAN-VI, COCO, WREFLOOD, BASH, and LOCBART, which are described in detail in WCAP-8306 (Reference 6), WCAP-8326 (Reference 7), WCAP-8171 (Reference 8), and WCAP-10266 (Reference 35), respectively. BASH and LOCBART are described together in Reference 35.

In the 1981 model with BASH, the SATAN-VI computer code analyzes the thermal-hydraulic transient of the reactor coolant system during blowdown, and the COCO computer code calculates the containment pressure transient during all three phases of the LOCA analysis. The WREFLOOD code performs the calculations of RCS response during refill and core reflood and is coupled with the COCO code to obtain a containment pressure history. The BASH code is an improved method for calculating the RCS response during the reflood phase for fuel rod analysis, but is not coupled with the COCO code. Instead, the containment transient pressure history from the WREFLOOD/COCO calculation is hand transferred as a boundary condition. Internal to the BASH code is the previously approved BART model, which is used to provide a mechanistic estimate of the heat transfer coefficient in the core during reflood.

An improvement to the BASH Evaluation Model codestream is described in Reference 50. The improved codestream provides for an interactive calculation between the BASH and COCO

codes. The containment pressure methodology during the blowdown phase of the transient has not been changed. The refill transient portion of the WREFLOOD code, which calculates the RCS behavior during vessel lower plenum refill following the end of blowdown, has been reprogrammed as a separate, but identical code (REFILL), which also runs interactively with the COCO code.

A further improvement in the BASH Evaluation Model codestream is described in Reference 51. With the improved codestream, the REFILL and LOCTA codes have been incorporated directly into the BASH code as subroutine modules. This eliminates all external transfer of data between these codes, and the need to perform two COCO calculations. In conjunction with this merging of codes, efforts were made to minimize any remaining code-to-code data transfer and to streamline and optimize some internal operations in the coding. The newly combined codes are configured as a single code which is identified as a new version of BASH.

The improved BASH codestream is described as follows:

SATAN-VI is used to determine the RCS pressure, enthalpy and density, as well as the mass and energy flow rates in the reactor coolant system and steam generator secondary, as a function of time during the blowdown phase of the LOCA. SATAN-VI also calculates the accumulator mass and pressure and the pipe break mass and energy flow rates that are assumed to be vented to the containment during blowdown. At the end of the blowdown, the mass and energy release rates during blowdown are transferred to the COCO code for use in the determination of the containment pressure response during this first phase of the LOCA. Additional SATAN-VI output data from the end of blowdown, including the core inlet flow rate and enthalpy, the core pressure and the core power decay transient are input to the LOCBART code.

With input from the SATAN-VI code at the end of blowdown, BASH is used to determine the vessel flooding rate, the coolant pressure and temperature and the quench of vessel metal mass during the refill phase of the LOCA (time period from end of blowdown to that time when flow enters the bottom of the core). BASH is also used to calculate the mass and energy flow rates assumed to be vented to the containment for the refill and reflood phases. Since the mass flow rate to the containment depends on core pressure, which is a function of the containment backpressure, the BASH and COCO codes are interactively linked.

The COCO code, which is used throughout all three phases of the LOCA analysis, calculates the containment pressure. Input to COCO is obtained from the mass and energy flow rates assumed to be vented to the containment, as calculated by the SATAN-VI and BASH codes. In addition, conservatively chosen initial containment conditions and an assumed mode of operation for the containment cooling system are input to COCO. These initial containment conditions and assumed modes of operation are provided in Table 15.4-2.

LOCBART is used throughout the analysis of the LOCA transient to calculate the fuel and clad temperature of the hottest rod in the core. Input to LOCBART consists of appropriate

thermal-hydraulic outputs from SATAN-VI and BASH, and conservatively selected initial RCS operating conditions. These initial conditions are summarized in Table 15.4-1. Using this information as boundary conditions, LOCBART computes the fluid conditions and heat transfer coefficient for the full length of the fuel rod by employing mechanistic models appropriate to the actual flow and heat transfer regimes.

With the improvements to the BASH codestream in References 50 and 51, no changes have been made to any of the approved physical models or basic techniques which form the basis of the methodology. However, these revisions to the BASH codestream can produce small changes to the results calculated by the improved codestream.

Large break LOCA analyses have been traditionally performed using a symmetric, chopped cosine, core axial power distribution. In Reference 52, Westinghouse informed the NRC of the withdrawal of the Westinghouse Power Shape Sensitivity Model (PSSM) topical (Reference 45) effective October 30, 1995. This power shape methodology had been employed to support Reload Safety Evaluations (RSEs). Westinghouse further indicated that future large break LOCA analysis with the 1981 model with BASH (Reference 35) would incorporate the explicit analysis approach to skewed power shapes as described in Reference 45. This analysis employs the Reference 45 explicit analysis methodology.

15.4.1.5.2 Results

Tables 15.4-1 and 15.4-2 and Figures 15.4-1 and 15.4-2 present the initial conditions and the modes of operation that were assumed in the analysis. Tables 15.4-3 and 15.4-4 tabulate the analysis results for the double ended guillotine break cases with the limiting downflow barrel/baffle configuration. These cases document a cosine axial power shape and a discharge coefficient (C_d) of 0.4 and 0.6, and the limiting skewed power shape with a C_d of 0.4. The double ended guillotine break has been determined to be the limiting break size and location based on the sensitivity studies reported in Reference 4. Prior Virginia Power and Westinghouse analyses employing approved large break LOCA evaluation models have demonstrated that limiting PCT is obtained for the $C_d = 0.4$ case. Results for other typical cases ($C_d = 0.6$, $C_d = 0.8$) are consistently bounded by 150–200°F in PCT. The limiting C_d determined using a cosine axial power shape sensitivity study provides the initial condition for the explicit skewed power shape analysis. The explicit skewed power shape analysis methodology described in Reference 45 determined that the limiting skewed power shape provided the bounding PCT results relative to the cosine axial power shape. This analysis resulted in a limiting peak clad temperature of 2010°F, a maximum local cladding oxidation of 4.03%, and a total core metal-water reaction of 0.39% for a cosine power shape and a discharge coefficient of 0.4. The results for a cosine power shape and a discharge coefficient of 0.6 were a limiting peak clad temperature of 1876°F, a maximum local cladding oxidation of 2.51%, and a total core metal-water reaction of less than 0.18%. The results for the limiting skewed power shape and a discharge coefficient of 0.4 were a limiting peak clad temperature of 2086°F, a maximum local cladding oxidation of 6.2%, and a total core metal-water

reaction of 0.54%. The detailed results of this LOCA analysis are provided in Tables 15.4-3 through 15.4-4 and Figures 15.4-1 through 15.4-56. The figures show the following:

1. Axial Power Shape–Figures 15.4-1 and 15.4-2 show the cosine power shape and the limiting skewed power shape used in this analysis. The limiting skewed power shape was found to bound the chopped-cosine power shape and the other potential skewed power shapes considered in the skewed axial power distribution evaluation methodology.
2. Core Mass Flow–Figures 15.4-3, 15.4-4, and 15.4-5 show the calculated core flow, both top and bottom.
3. Core Pressure–Figures 15.4-6, 15.4-7, and 15.4-8 show the calculated pressure in the core.
4. Accumulator Mass Flow–Figures 15.4-9, 15.4-10, and 15.4-11 show the calculated accumulator flow. The accumulator delivery during blowdown is discarded until the end of bypass is calculated. Accumulator flow, however, is established in the refill-reflood calculations. The accumulator flow assumed is the sum of that injected in the intact cold legs.
5. Core Pressure Drop–Figures 15.4-12, 15.4-13, and 15.4-14 show the calculated core pressure drop. The core pressure drop is interpreted as the pressure immediately before entering the core inlet to the pressure just outside the core outlet.
6. Break Mass Release–Figures 15.4-15, 15.4-16, and 15.4-17 show the calculated flowrate out of the break. The flowrate out of the break is plotted as the sum of flow at both the pressure vessel end and the reactor coolant pump end of the guillotine break.
7. Break Energy Release–Figures 15.4-18, 15.4-19, and 15.4-20 show the break energy released in the containment for the discharge coefficient used.
8. Core Power–Figures 15.4-21, 15.4-22, and 15.4-23 show the core power transient calculated by the SATAN-VI code.
9. Containment Wall Heat Transfer Coefficient–Figures 15.4-24, 15.4-25, and 15.4-26 show the containment wall heat transfer coefficient.
10. Containment Pressure–Figures 15.4-27, 15.4-28, and 15.4-29 show the calculated pressure transient. The analysis of this pressure transient is based on the containment data, reflood mass and energy release, and accumulator flow to containment.
11. Pumped ECCS Flow (Reflood)–Figures 15.4-30, 15.4-31, and 15.4-32 show the calculated flow of the emergency core cooling system.
12. Core and Downcomer Water Levels–Figures 15.4-33, 15.4-34, and 15.4-35 show the reactor vessel downcomer and core water levels.
13. Raw Flooding Rate Integral–Figures 15.4-36, 15.4-37, and 15.4-38 show the raw flooding rate integrals and smoothed line segment integrals used in the LOCBART calculations.

14. Core Flooding Rate–Figures 15.4-39, 15.4-40, and 15.4-41 show the resulting line segment integrals from previous figures.
15. Hot Rod Clad Average Temperature–Figures 15.4-42, 15.4-43, and 15.4-44 show the calculated hot-spot clad temperature transient and the clad temperature transient at the burst location.
16. Fluid and Vapor Temperature–Figures 15.4-45, 15.4-46, and 15.4-47 show the calculated fluid and vapor temperature for the hot spot location.
17. Hot Rod Heat Transfer Coefficient–Figures 15.4-48, 15.4-49, and 15.4-50 show the heat transfer coefficient at the hot spot location on the hottest rod.
18. Hot Rod Mass Flux–Figures 15.4-51, 15.4-52, and 15.4-53 show the mass velocity at the hot-spot location on the hottest fuel rod.
19. Hot Rod Fluid Quality–Figures 15.4-54, 15.4-55, and 15.4-56 show the fluid quality at the hot-spot location on the hottest fuel rod.

15.4.1.5.3 Post Analysis of Record Evaluations

In addition to the analyses presented in this section, evaluations and reanalyses may be performed as needed to address computer code errors, emergent issues, or to support plant changes. The issues or changes are evaluated, and the impact on the PCT is determined. The resultant increase or decrease in PCT is applied to the analysis of record PCT. The PCTs, including all penalties and benefits, are presented in Table 15.4-5 for the large break LOCA. The resultant PCT is demonstrated to be less than the 10 CFR 50.46(b) requirement of 2200°F.

15.4.1.5.4 Conclusions

This large break LOCA analysis was performed for a double ended rupture of a reactor coolant pipe with C_d= 0.4, at rated thermal power of 2893 MWt, assuming the operating conditions specified in Tables 15.4-1 and 15.4-2. Based upon these results, the emergency core cooling system will meet the acceptance criteria as presented in 10 CFR 50.46 as follows:

1. The calculated peak fuel rod clad temperature is below the requirement of 2200°F.
2. The amount of fuel element cladding that reacts chemically with water or steam does not exceed 1% of the total amount of Zircaloy in the reactor.
3. The clad temperature transient is terminated at a time when the core is still amenable to cooling. The localized cladding oxidation limits of 17% are not exceeded during or after quenching.
4. The core remains amenable to cooling during and after the break.
5. The core temperature is reduced and the long-term heat is removed for an extended period of time.

15.4.1.5.5 Impact of Fuel Reconstitution

The LOCA analysis of record assumes the use of fuel assemblies with 264 fuel rods. However, reconstituted fuel assemblies with a limited number of solid stainless steel or Zirconium alloy filler rods replacing fuel rods may also be used in reload cores. When solid metal filler rods are employed, a conservative peak clad temperature penalty is assessed to account for the possible steady state effects on the Large Break LOCA. The magnitude of this penalty is defined in Reference 47, and is proportional to the number of reconstituted rods in the fuel assembly. The potential increase in the linear heat rate (assuming no change to the total core power) is also incorporated into the Large Break LOCA analysis. The total PCT effect is determined by adding these contributions to the evaluations performed for the current plant configuration. The reconstitution penalty is tracked throughout the core residence of the affected assemblies, and is removed from the plant assessment against PCT margin when the reconstituted assemblies are removed from the core.

15.4.1.5.6 Impact of Steam Generator Flow Area on Large Break Loss-of-Coolant Accident

Each PWR is required to provide analytical and experimental evidence that steam generator tube integrity will be maintained for the combinations of the loads resulting from a LOCA with the loads from a safe shutdown earthquake (SSE). These loads are combined for added conservatism in the calculation of structural integrity.

Analyses performed by Westinghouse in support of the above requirement for various utilities, combined the most severe LOCA loads with the plant specific SSE. Generally, these analyses showed that while tube integrity was maintained, the combined loads led to some tube deformation. This deformation reduces the flow area through the steam generator. The reduced flow area increases the resistance through the steam generator to the flow of steam from the core during a LOCA, which potentially could increase the calculated PCT.

The ability of the steam generator to continue to perform its safety function was established by evaluating the effect of the resulting flow area reduction on the LOCA PCT. The postulated break examined was the steam generator outlet break, because this break was judged to result in the greatest loads on the steam generator, and thus the greatest flow area reduction. It was concluded that the steam generator would continue to meet its safety function because the degree of flow area reduction was small, and the postulated break at the steam generator outlet resulted in a low PCT.

In considering the effect of the combination of LOCA + SSE loadings on the steam generator, it was determined that the potential for flow area reduction due to the contribution of SSE loadings should be included in other LOCA analyses. With SSE loadings, flow area reduction may occur in all steam generators (not just the faulted loop). Therefore, it was concluded that the effects of flow area reduction during the most limiting primary pipe break affecting LOCA PCT, i.e., the reactor vessel inlet break (or cold leg break LOCA), had to be

evaluated to confirm that 10 CFR 50.46 limits continue to be met and that the affected steam generators will continue to perform their intended safety function.

Detailed analyses which provide an estimate of the degree of flow area reduction due to both seismic and LOCA forces are not available for the North Anna steam generators. The information that does exist indicates that the flow area reduction may range from 0 to 7.5 percent, depending on the magnitude of the postulated forces, and accounting for uncertainties. It is difficult to estimate the flow area reduction for a particular steam generator design, based on the results of a different design, due to the differences in the design and materials used for the tube support plates.

While a specific flow area reduction has not been determined for some earlier design steam generators, the risk associated with flow area reduction and tube leakage from a combined seismic and LOCA event has been shown to be exceedingly low. Based on this low risk, it is considered adequate to assume, for those plants that do not have a detailed analysis, that 5 percent of the tubes are susceptible to deformation.

The effect of potential steam generator flow area reduction on the cold leg break LOCA peak cladding temperature has been either analyzed or evaluated for each Westinghouse plant. Based on this generic analysis, a total steam generator tube reduction equivalent to 5% tube plugging was allocated as a permanent assessment for those plants that do not have a detailed analysis (Reference 3). The 5% steam generator tube plugging reduction is applied against the 7% tube plugging assumed in the large break LOCA analyses to account for the effects of a combined LOCA + SSE at North Anna.

15.4.1.6 **Containment Transient Analysis**

Sections 6.2.1 and 6.2.2 describe containment transients in detail after a design-basis accident (LOCA) with the minimum or with the normal engineered safety features for a hot-leg, a cold-leg, and a surge-line rupture under summer or winter conditions.

15.4.1.7 **Dose Consequences of Loss-of-Coolant Accident (LOCA)**

This discussion describes the methods employed and results obtained from the LOCA design basis radiological analysis. The analysis includes doses from several sources: the containment leakage, leakage from ECCS components, leakage from the RWST and shine from control room filter loading. The ECCS leakage, the RWST leakage and the control room filter loading shine contribute to the dose consequences throughout the assumed 30 day duration of the accident. The containment leakage is assumed to terminate after 6 hours. Doses were calculated at the exclusion area boundary (EAB), at the low population zone boundary (LPZ), and in the control room. This radiological analysis was based on the Alternate Source Term (AST) as defined in NUREG-1465 (Reference 77). The methodology used to evaluate the control room and offsite doses resulting from a LOCA was consistent with Regulatory Guide 1.183 (Reference 71).

The results have been compared with the acceptance criteria contained either in 10 CFR 50.67 or supplemental guidance in Reference 71.

Because the walls and ceiling of the control room envelope are concrete at least 18" thick, the containment shine and cloud shine doses to the control room were discounted. This was based on guidance in NUREG-0800, Section 6.4 (Reference 55).

NUREG-1465 (Reference 77) provides an explicit description of the key AST characteristics recommended for use in design basis radiological analyses. Reference 77 divides the releases from the core into two phases: (1) the fuel gap release phase during the first 30 minutes and (2) the early in-vessel release phase in the subsequent 1.3 hours. The later release phases documented in Reference 77 are not considered for design basis accidents, consistent with the guidance from Reference 71. The AST core fractions by chemical group and release phase from Reference 71 are:

Core Fractions by Release Phase

Group	Gap Release Phase	Early In-vessel Phase	Total
Noble Gases	5%	95%	100%
Halogens (Iodine)	5%	35%	40%
Alkali Metals (Cesium)	5%	25%	30%
Tellurium Metals	0%	5%	5%
Barium, Strontium	0%	2%	2%
Others	0%	0.02%–0.25%	0.02%–0.25%

The core radionuclide inventory was generated using the ORIGENS code. ORIGENS is part of the SCALE computer code system (Reference 80). The ORIGENS output was converted to Ci/MWt for input to the RADTRAD-NAI code (Reference 75). Reference 75 is a computer code for modeling radiological accidents and dose consequences from releases of radioactive material.

The MCR/ESGR envelope unfiltered inleakage was modeled at 250 cfm. The MCR/ESGR envelope filtered supply air flow was modeled at 900 cfm. No credit is taken for control room filtered recirculation or pressurization effects of the supply air systems. The occupancy factors, breathing rates and atmospheric dispersion factors shown in Tables 15.4-6 and 15.4-7 were used. The MCR/ESGR envelope volume was conservatively modeled at 7.910E+04 cubic feet, which is much lower than the actual MCR/ESGR envelope, since the extent of mixing between the different zones of the MCR/ESGR envelope was not known. All these values as well as the dose conversion factors and the Curies per megawatt for the 94 isotopes were input into the RADTRAD-NAI computer code that calculated doses in the control room and at the EAB and LPZ.

15.4.1.7.1 Atmospheric Dispersion Factors (χ/Q's)

The control room atmospheric dispersion factors were calculated using the ARCON96 code (Reference 78) and guidance from Regulatory Guide 1.194 (Reference 73). Site meteorological data taken over the years 1997-2001 were used in the calculations. χ/Qs were calculated for the LOCA for these source points: Unit 1 and Unit 2 Containment buildings, Auxiliary Building louvers, RWSTs, Equipment Hatches, Primary Ventilation Blowout Panels, and the Vent Stacks A and B. The receptor points modeled were the four emergency control room intakes as well as the normal control room air intake.

All the ARCON96 runs were considered ground level releases in accordance with the guidance of Reference 73. The Auxiliary Building louvers, the Equipment Hatches, the RWST vents, Vent Stacks A and B, and the Primary Ventilation Blowout Panels were modeled as point sources. The Containment Buildings were treated as diffuse sources. For all of the ARCON96 runs, the cross sectional above grade area of one of the Containment Buildings was used to model a wake effect since all of the receptor points modeled are expected to be in the wake of one of the Containment Buildings.

Table 15.4-7 shows the control room atmospheric dispersion factors used in the LOCA analysis.

The EAB and LPZ atmospheric dispersion factors were developed by Stone and Webster and are part of the existing design basis offsite dose calculations. These χ/Q values are included in Table 15.4-6.

15.4.1.7.2 Containment Spray Removal Coefficients

There are six spray headers belonging to two different systems (Quench Spray and Recirculation Spray) inside the North Anna containment. The Quench Spray system has two separate pump trains. Each Quench Spray pump train feeds one circular dome header near the top of the containment. The Recirculation Spray system has two trains consisting of two pumps and two heat exchangers and two 180-degree spray headers each. Two of the recirculation spray pumps on opposite trains are located inside containment and two of the recirculation spray pumps on opposite trains are located outside containment in the safeguards area. All four heat exchangers are inside containment. The two pumps located inside containment feed one 180-degree header each. The two pumps located outside containment also feed one 180-degree header each. Each train of the Quench Spray system and each train of the Recirculation Spray system is redundant. The flows used in the LOCA radiological analysis were based on only one train of the Quench Spray system and one train of the Recirculation Spray system.

The containment spray removal coefficients for aerosol fission products are calculated using the methodology of NUREG/CR-5966 (Reference 81), which presents removal equations at 10, 50, and 90 percentile levels. Only the 10 percentile (most conservative) equations were used. No credit was taken for iodine plateout.

For these calculations, QS start time is set at 73 seconds and termination is conservatively assumed at 1.5 hours. Both ORS and IRS are assumed to start at 40 minutes, which is conservative compared to LOCA containment depressurization analysis results that model RS pump start on RWST Level Low.

The QS flow rates used are lower than the flow rate values determined from the GOTHIC LOCA depressurization analyses in Section 6.2.

To simplify the modeling of the QS headers, both the upper and lower headers are modeled at the elevation of the lowest header or 391'-10" resulting in a drop height of 3048 cm. The 4 RS headers are modeled at the average elevation of the RS headers or 377'-4" resulting in a drop height of 2606 cm. This is appropriate since 1 train of IRS/ORS operating together supplies water to both elevations.

When QS and RS are operating together, a weighted average, based on flow rates, of the different elevations is used to calculate the drop height. A high QS flow rate is used for conservatism. The weighted drop height is set at 2701 cm during QS and RS operation.

NUREG/CR-5966 [Page 170] recommends that for a volume with continuing source, the removal constant associated with a mass fraction of 0.9 be used until the time-dependent source terminates. Hence, the mass fraction is assumed to remain at 0.9 from the start of the sprays until the end of the early in-vessel release phase at 1.8 hr. After this phase, the removal rate is adjusted stepwise by varying the mass fraction. The duration of time, t, required to change from a mass fraction m_{f0} to m_{f1} is determined using the following formula:

$$m_{f1} = m_{f0}e^{-\lambda t}$$
$$t = \ln(m_{f0}/m_{f1})/\lambda$$

Table 15.4-6 lists the aerosol removal coefficients for spray operation.

15.4.1.7.3 Dose Conversion Factors

The LOCA radiological analysis employed the TEDE calculational method, consistent with the radiation protection standards in 10 CFR Part 20 and as specified in Regulatory Guide 1.183 (Reference 71) for AST applications. The TEDE dose is defined as the sum of the deep dose equivalent, DDE, (from external exposure) and the committed effective dose equivalent, CEDE, (from internal exposure). In this manner, the TEDE dose assesses the impact of all relevant nuclides upon all body organs, in contrast with the previous single, critical organ (thyroid) concept for assessing internal exposure. The DDE is nominally equivalent to the effective dose equivalent (EDE) from external exposure if the whole body is irradiated uniformly. Since this is a reasonable assumption for submergence exposure situations, EDE is used in lieu of DDE in determining the contribution of external dose to the TEDE. EDE dose conversion factors were taken from Table III.1 of Federal Guidance Report 12 (Reference 74) per Section 4.1.4 of

Reference 71. The CEDE dose conversion factors were taken from Table 2.1 of Federal Guidance Report 11 (Reference 72) per Section 4.1.2 of Reference 71.

15.4.1.7.4 Containment Leakage

The following acceptance criteria were used to model the containment leakage. These acceptance criteria were only applicable to the LOCA radiological analysis.

- calculated peak pressure must be less than 45 psig
- containment must be depressurized to less than or equal to 2.0 psig within 1 hour, remain less than 2.0 psig from 1-6 hours and must be depressurized to subatmospheric pressure within 6 hours
- calculated pressure after 6 hours must be less than 0.0 psig

The LOCA radiological analysis assumed continued leakage during the 1-6 hour interval after the onset of the LOCA, but at a diminished rate corresponding to a containment pressure of 2.0 psig. Beyond 6 hours, the pressure was assumed to be less than 0.0 psig, terminating leakage from containment.

The containment was modeled with a volumetric leak rate of 0.1% per day for the first hour and 0.04% per day until leakage is terminated at the end of the sixth hour. The leak rate of 0.04% per day corresponded to the maximum allowable containment pressure of 2.0 psig for hours 1 through 6. The chemical form of the iodine is 4.85% inorganic, 0.15% organic and 95% aerosol.

As shown in Table 15.4-6, the total free volume of the containment was set at 1.916E+06 cubic feet. The mixing rate between the sprayed and unsprayed volumes of containment was modeled at 2 unsprayed volumes per hour as specified in Assumption 3.3 from Appendix A of Regulatory Guide 1.183 (Reference 71).

15.4.1.7.5 RWST Leakage

Following a design basis LOCA, valve realignment occurs to switch the suction water source for the low head safety injection (LHSI) and charging pumps from the RWST to the containment sump. This action is taken upon the level in the RWST reaching a defined setpoint and was modeled in the LOCA radiological analysis as occurring at 31.8 minutes following the initiation of the LOCA consistent with the GOTHIC analysis for LOCA containment depressurization. In this configuration, check valves in the normal suction line from the RWST provide isolation between this contaminated flowstream and the RWST. The ECCS fluid was assumed to leak through these valves back into the RWST with subsequent leakage of the evolved iodine through the gooseneck vent at the top of the North Anna RWST to the environment.

The RWST leakage was modeled at 480 cc/hr of ECCS fluid leaking through the recirculation lines from the discharge side of the LHSI pumps to the top of the RWST and 1920 cc/hr of ECCS fluid leaking back into the RWST through the 16" diameter LHSI suction

line. The evolution of iodine from the leakage was modeled with a decontamination factor (DF) of 40. The primary motive force moving air into or out of the RWST would be thermal expansion or contraction of the air and gases inside the RWST. Based on an estimated average daily thermal expansion and contraction, the flow of air from the tank was modeled at 3.7 cfm.

The isotopic inventory used to model the ECCS leakage into the RWST contained only the iodine isotopes. This is because the iodine isotopes are the only isotopes in the containment sump water which were modeled as coming out of solution and becoming airborne. Forty percent of the core inventory of iodine isotopes were modeled as being transported from the core to the containment sump in the release phase defined in Reference 71. This iodine was modeled as being 97% elemental iodine and 3% organic iodine in accordance with Regulatory Guide 1.183 (Reference 71). Dose calculations reduce GOTHIC reported sump volumes because a lower sump volume results in a higher dose due to less dilution volume. The reduced volumes are used in the RADTRAD-NAI (Reference 75) code. Table 15.4-36 lists the containment sump volume versus time used in the ECCS and RWST leakage analyses.

15.4.1.7.6 ECCS Leakage

The ECCS fluid consists of the contaminated water in the sump of the containment. This water was modeled as containing 40% of the core inventory of iodine isotopes in the release phase defined in Reference 71. During a LOCA the ECCS fluid is pumped from the containment sump to the recirculation spray headers and sprayed back into the containment sump. This is done to clean and cool the containment atmosphere after a LOCA. Since one set of recirculation spray pumps is located in the safeguards building there is a potential for ECCS fluid leakage in the safeguards building after a LOCA. Any iodine which evolves from the ECCS leakage in the safeguards building would be exhausted by ventilation fans out vent stack B on top of the service building next to the turbine building. Also, following a design basis LOCA, valve realignment occurs to switch the suction water source for the LHSI and charging pumps from the RWST to the containment sump. After this occurs, the high head charging pumps, located in the charging pump cubicles in the auxiliary building, would begin pumping ECCS fluid and would be another potential source of ECCS fluid leakage. Any iodine which evolves from the ECCS fluid leakage in the charging pump cubicles would be drawn by ventilation fans into the auxiliary building central exhaust flow and be exhausted out of vent stack A on top of the service building next to the turbine building. All ECCS leakage is assumed to start on early RS pump start at 14 minutes.

Dose calculations reduce GOTHIC reported sump volumes because a lower sump volume results in a higher dose due to less dilution volume. The reduced volumes are used in the RADTRAD-NAI (Reference 75) code. Table 15.4-36 lists the containment sump volume versus time used in the ECCS and RWST leakage analyses. The auxiliary building charcoal filters were conservatively modeled as not being available for filtering ECCS iodine gases for 60 minutes after the onset of the LOCA.

The isotopic inventory of the ECCS leakage contained only the iodine isotopes. This is because iodine is the only element in the containment sump water, which was modeled as coming out of solution and becoming airborne. Any other isotopes in the ECCS fluid were assumed to remain in solution or suspension in accordance with Regulatory Guide 1.183 (Reference 71). Ten percent of the iodine isotopes in the ECCS fluid were modeled as coming out of solution. This iodine was modeled as being 97% elemental iodine and 3% organic iodine in accordance with Reference 71.

Figure 15.4-110 is a graph of the allowable filtered and unfiltered ECCS leakage based on a total unfiltered inleakage rate of 250 cfm to the control room. During unit operations, the acceptability of the ECCS leakage will be assessed using this curve. If the combination of filtered and unfiltered ECCS leakage falls to the left and below the curve, leakage is acceptable because control room dose will be less than the values reported in Section 15.4.1.7.8. It should be noted the analyzed leak rate was twice the allowable leak rate per Assumption 5.2 in Appendix A of Reference 71. Reference 75 was used to calculate the data points on the curves in Figure 15.4-110.

15.4.1.7.7 Dose From Filter Loading

Within one hour following MCR/ESGR isolation at least one control room emergency fan is manually aligned to draw air from the environment into MCR/ESGR envelope to supply outside filtered air. This air passes through a set of HEPA and charcoal filters. The transition from bottled air to outside filtered air fan was modeled at one hour after the start of the LOCA. As a consequence of passing air containing radioactive contaminants through the filter, there will be a gradual buildup of radioactive material in the filter media.

The intake filter was modeled as being on the upper level of the control room envelope where the operators would be expected to reside for the 30 days following a LOCA. The isotopes inside the filter housing would emit gamma radiation that would create a shine dose to the operators.

To determine the isotopic loading on the intake filter as a result of the containment, ECCS, and RWST leakage, a time dependent analysis of the transport and capture of isotopes was performed. The intake filter efficiencies were modeled at 98% particulate, 95% elemental, and 95% organic. The contribution from noble gases was not credited since they are not normally held up in the filter media.

Once the loading of the intake filter was determined, the gamma spectrum was calculated using the ORIGENS code. Once the spectrum was determined, a conservative dose point was picked to maximize the shine dose the operator would get from the filter and the shine dose was calculated with the QADS code. QADS like ORIGENS is part of the SCALE computer code system (Reference 80).

15.4.1.7.8 Results

The design basis LOCA radiological dose results are less than the regulatory dose limits.

	Control Room (Rem TEDE)	Exclusion Area Boundary (Rem TEDE)	Low Population Zone (Rem TEDE)
Total Dose Consequences including contributions from containment, ECCS and RWST leakage	4.1	2.1	0.2
10 CFR 50.67 dose limits	5	25	25

Figure 15.4-110 will be used during unit operation to determine the acceptability of ECCS leakage. If the combination of filtered and unfiltered ECCS leakage is less than the curve described in Figure 15.4-110, the dose in the control room during a LOCA will be less than the values documented in this section. This curve is based on an inleakage rate of 250 cfm to the control room and assumed ECCS leakage values that are twice the allowable limits.

15.4.1.8 **Summary**

15.4.1.8.1 ECCS Evaluation

For breaks up to and including the double-ended rupture of a primary reactor coolant pipe, the minimum engineered safety features of the emergency core cooling system (Section 6.3) will ensure that the core will remain in place and substantially intact, with its essential heat transfer geometry preserved. The emergency core cooling system design meets the core cooling criteria with margin for all cases. This is confirmed by the results of the limiting cases for the small break and large break LOCA sensitivity analyses. The analyses demonstrate that the acceptance criteria are met throughout the range of break sizes with the high-head safety injection pumps mitigating the smaller breaks and the accumulators in conjunction with the pumped safety injection flow mitigating the larger breaks.

The design of the fuel assemblies and the core support structures is such that the pressure transients and flow oscillations resulting from any LOCA can be accommodated without changes in core geometry that would affect the capability of the safety injection system to perform its required function.

15.4.1.8.2 Containment Evaluation

The containment structure is capable of containing, without loss of integrity, any equipment failure in the reactor coolant system that could result in an undue hazard to the public (Section 6.2). The quench spray subsystem and the recirculation spray subsystem remove heat and airborne fission products from the containment atmosphere and will return the containment to a subatmospheric condition, thus terminating leakage to the environment. The recirculation spray subsystem transfers heat from the containment to the service water system, thereby removing

residual heat, and will maintain the containment in a subatmospheric pressure condition during the subsequent recovery period.

15.4.1.8.3 Dose Evaluation

The calculated dose at the EAB, LPZ and in the control room resulting from a design basis LOCA are within regulatory limits stated in 10 CFR 50.67(b)(2).

15.4.1.9 **Framatome ANP LBLOCA Analyses**

In accordance with 10 CFR 50.46, an evaluation of ECCS performance was performed for operation of FANP Advanced Mark-BW reload fuel, in the cores of North Anna Units 1 and 2. Separate analyses were performed for each unit to account for the difference in reactor vessel internals barrel-baffle configuration: Unit 1 (upflow) and Unit 2 (downflow). The analysis assumptions accommodate a mixed core configuration of NAIF and Advanced Mark-BW fuel designs, and other key parameter values as described more fully in the following sections.

The large break LOCA analyses employed the NRC-approved realistic large break LOCA evaluation model (EM) described in EMF-2103(P)(A), *Realistic Large Break LOCA Methodology,* (Reference 68). The realistic approach requires that a set of "sampled" cases be run. For each case, "key LOCA parameters" are randomly sampled over their uncertainty or operating limit ranges, and the cases are then run to steady state before transient initiation. Limiting PCT case set results are qualified at a 95/95 level.

The realistic large break loss-of-coolant accident (RLBLOCA) analyses supporting operation of the North Anna units with Advanced Mark-BW fuel use modeling that represents the initial core composition accounting for thermal and hydraulic influences of both NAIF and Advanced Mark-BW fuel assemblies in proportion to their count and distribution. Although the reactor core as constituted for this analysis is specific to the initial fuel reload cycle, the results bound the differing follow-on cycles as the transition to all FANP fuel is accomplished.

The non-parametric statistical methods inherent to the FANP RLBLOCA methodology provide for consideration of a full spectrum of break sizes, break configurations (guillotine or split breaks), axial shapes, and plant operational parameters. The analyses assume a conservative single-failure.

Beginning with Cycle 17 for Unit 2 and Cycle 18 for Unit 1, the Advanced Mark-BW fuel product was introduced in mixed cores with the LOPAR and NAIF assemblies.

15.4.1.10 **LBLOCA Event Description**

A LBLOCA is initiated by a postulated large break in the reactor coolant system (RCS) primary piping. The RLBLOCA EM identifies that the worst break location is in the cold leg piping between the reactor coolant pump and the reactor vessel for the RCS loop containing the pressurizer. The break initiates a rapid depressurization of the RCS. A reactor trip signal is

initiated when the low pressurizer pressure trip setpoint is reached; however, reactor trip is conservatively neglected in the analysis. The reactor is shut down by coolant voiding in the core.

The plant is assumed to be operating normally at full power prior to the accident. The large cold leg break is assumed to open instantaneously. For this break, a rapid depressurization occurs, along with a core flow stagnation and reversal. This causes the fuel rods to experience departure from nucleate boiling (DNB). Subsequently, the limiting fuel rods are cooled by film and transition boiling heat transfer. The coolant voiding creates a strong negative reactivity effect, and core fission ends. As heat transfer from the rods is reduced, the cladding temperature rises.

Coolant in all regions of the RCS begins to flash. At the break plane, the loss of subcooling in the coolant results in substantially reduced break flow. This reduces the depressurization rate and may lead to a period of positive core flow or reduced downflow as the reactor coolant pumps in the intact loops continue to provide flow to the vessel. Cladding temperatures may be reduced, and some portions of the core may rewet during this period.

This positive core flow or reduced downflow period ends as two-phase conditions occur in the reactor coolant pumps, reducing their effectiveness. Again, the core flow reverses as most of the vessel mass flows out through the broken cold leg.

Mitigation of the LBLOCA begins when the safety injection (SI) actuation signal occurs. This signal is initiated by either high containment pressure or low-low pressurizer pressure. Regulations require that the worst single failure be considered for ECCS safety analysis. This single failure has been determined to be the loss of one ECCS train of pumped injection, including one high-head safety injection (HHSI) pump and one low-head safety injection (LHSI) pump. The FANP RLBLOCA methodology assumes a conservatively early start and normal lineups of the containment spray to reduce containment pressure and increase break flow. Hence, the analysis assumes that one HHSI pump, one LHSI pump, and all containment spray pumps are operating (Reference 68).

When the RCS pressure falls below the accumulator pressure, fluid from the accumulators is injected into the cold legs. In the early delivery of accumulator water, high pressure and high break flow will cause some of this fluid to bypass the core. During this bypass period, core heat transfer is degraded, and fuel rod cladding temperatures increase. As RCS and containment pressures equilibrate, ECCS water begins to fill the lower plenum and eventually the lower portions of the core. As this occurs, core heat transfer improves, and cladding temperatures decrease.

Eventually, the relatively large volume of accumulator water is exhausted, and core recovery must rely on SI coolant delivery alone. As the accumulators empty, the nitrogen gas used to pressurize the accumulators exits through the break. This gas release may result in a short period of improved core heat transfer as the nitrogen gas displaces water in the downcomer. After the nitrogen gas has been expelled, the ECCS temporarily may not be able to sustain full core cooling because of the core decay heat and the higher steam temperatures created by quenching in

the lower portions of the core. Peak fuel rod cladding temperatures may increase for a short period until more energy is removed from the core by the safety injection than the decay heat produces. Steam generated from fuel rod rewet will entrain liquid as it passes through the core, vessel upper plenum, the hot legs, the steam generator, and the reactor coolant pump before it is vented out the break. The hydraulic resistance of this flow path to the steam flow is balanced by the driving force of water filling the downcomer. This resistance may act to retard the progression of the core reflood and postpone core-wide cooling. Eventually (within a few minutes of the accident), the core reflood will progress sufficiently to ensure core-wide cooling. Full core quench occurs within a few minutes after core-wide cooling. Long-term cooling is then sustained with the low-head safety injection.

15.4.1.11 **Large Break Evaluation Model**

The RLBLOCA methodology is documented in EMF-2103, *Realistic Large Break LOCA Methodology,* (Reference 68). The methodology follows the Code Scaling, Applicability, and Uncertainty (CSAU) evaluation methodology (Reference 69). This method outlines an approach for defining and qualifying a best-estimate thermal-hydraulic code and quantifying the uncertainties in a LOCA analysis.

The RLBLOCA methodology consists of two computer codes, S-RELAP5 and RODEX3A. The S-RELAP5 code calculates blowdown and refill/reflood system thermal-hydraulics, core power generation, and core thermal responses. The containment pressure response is also calculated by S-RELAP5. RODEX3A provides steady-state fuel inputs to S-RELAP5, consisting of initial fuel stored energy, fission gas release and fuel-cladding gap conductance.

S-RELAP5 uses a two-fluid (plus non-condensable) model with conservation equations for mass, energy, and momentum transfer. The reactor core is modeled in S-RELAP5 with heat generation rates determined from reactor kinetics equations (point kinetics) with reactivity feedback, and with actinide and decay heating.

The two-fluid formulation uses a separate set of conservation equations and constitutive relations for each phase. The effects of one phase on another are accounted for by interfacial friction, and heat and mass transfer interaction terms in the conservation equations. The conservation equations have the same form for each phase; only the constitutive relations and physical properties differ.

The modeling of plant components is performed by following guidelines developed to ensure accurate accounting for physical dimensions and the dominant phenomena expected during LBLOCA. The basic building blocks for modeling are the hydraulic volumes for fluid paths and the heat structures for heat transfer surfaces. In addition, special purpose components exist to represent specific components such as the pumps or the steam generator separators. Plant geometry is modeled at the resolution necessary to best resolve the flow field and the phenomena being modeled within practical computational limitations.

A typical calculation for each of the "sampled" cases using S-RELAP5 begins with the establishment of a steady-state initial condition with all loops intact. Following the establishment of an acceptable steady-state condition, the transient calculation is initiated by introducing a break into one of the loops. The evolution of the transient through blowdown, refill, and reflood is computed continuously using S-RELAP5.

The methods used in the application of S-RELAP5 to large break LOCA are described in Reference 68. A detailed assessment of this computer code was made through comparisons to experimental data. These assessments were used to develop quantitative estimates of the ability of the code to predict important physical phenomena in a PWR large break LOCA. The final step of the realistic LOCA methodology is to combine all the uncertainties related to the code and plant parameters and estimate the peak clad temperature (PCT) at a 95 percent probability level with 95 percent confidence. The steps taken to derive the PCT uncertainty estimate are summarized below:

1. Base Plant Input File Development

   First, base RODEX3A and S-RELAP5 input files for the plant (including the containment input file) are developed based on plant-specific, customer-supplied information. Code input development guidelines are applied to ensure that the model nodalization is consistent with the model nodalization used in the code validation.

2. Sampled Case Development

   The non-parametric statistical approach requires that many "sampled" cases be created and processed. For every set of input created, each "key LOCA parameter" is randomly sampled over a range established through code uncertainty assessment or expected operating limits (provided by the customer through plant Technical Specifications, data, etc.). Those parameters considered key LOCA parameters are listed in Table 15.4-17. This list includes both parameters related to LOCA phenomena (based on the PIRT provided in Reference 68) and to plant operating parameters.

3. Reported PCT & Oxidation Results

   The RLBLOCA methodology uses a non-parametric statistical approach to determine values of PCT, peak local oxidation, and total oxidation for comparison with the criteria set forth in 10 CFR 50.46(b). The PCT is determined at a 95 percent probability level with 95 percent confidence. The peak local oxidation and total oxidation are reported for the limiting PCT case.

15.4.1.12 **Mixed-Core Description**

The North Anna core model is representative of the number and placement of fuel assemblies that are anticipated for the first cycle of operation with Advanced Mark-BW fuel. The mixed-core configuration affects the hydraulic features of the core model in both the radial and axial directions. The RLBLOCA methodology simulates the core in four radial regions: (1) the

hot assembly, (2) the assemblies surrounding the hot assembly, (3) the average core, and (4) the core periphery. The hot assembly (and hot pin) is simulated by an Advanced Mark-BW fuel assembly. The core periphery is simulated by NAIF assemblies. The ring of fuel assemblies surrounding the hot fuel assembly and the average core are constructed to hydraulically simulate the axial and crossflow resistance of an approximate 50:50 mixture of NAIF and Advanced Mark-BW fuel assemblies. The axial modeling of the core accounts for the increased hydraulic resistance, due to the Advanced Mark-BW MSMGs, in radial regions where FANP fuel assemblies are located.

The core model bounds the results for subsequent cycles of operation, comprising progressively larger percentages of FANP fuel. Appendix B of Reference68 established that the analysis of fresh fuel bounds the analysis results for fuel in its second or third cycle of irradiation. The hydraulic characteristics of the NAIF and the Advanced Mark-BW assemblies create a preference for flow diversion toward the NAIF assemblies and away from the Advanced Mark-BW assemblies in the upper half of the core. The potential for this diversion is maximized during the first cycle of Advanced Mark-BW operation because of the small percentage of FANP fuel that is present in the core. As the percentage of FANP fuel increases in subsequent reload cycles, the potential for flow diversion is lowered. Because provision for this flow diversion is explicitly modeled in the North Anna mixed-core RLBLOCA calculations, the expected results for subsequent reload cycles would demonstrate lower PCTs and oxidation results. Together, the results of the Reference 68, Appendix B study and the increase in the number of Advanced Mark-BW fuel assemblies in the core lead to the conclusion that first cycle calculations bound subsequent cycles of operation with FANP fuel.

15.4.1.13 **Large Break Input Parameters and Initial Conditions**

Independent RLBLOCA plant analyses were performed for each of the two units at North Anna. The units are similar except that Unit 1 has an upflow barrel-baffle configuration while Unit 2 has a downflow configuration. The plants are Westinghouse-designed pressurized water reactors (PWRs) that have three loops, each with a hot leg, a U-tube steam generator, and a cold leg with a reactor coolant pump (RCP). The plants are bottom re-flooded. The RCS includes a pressurizer and pressurizer surgeline. The ECCS includes an accumulator path and a LHSI/HHSI path per RCS loop. The HHSI and LHSI feed into a common header that connects to each cold leg pipe downstream of the RCP discharge.

The S-RELAP5 model explicitly describes the RCS, reactor vessel, pressurizer, and passive ECCS back to the accumulators. The ECCS pumped injection is modeled as a table of flow versus backpressure. This model also describes the secondary-side steam generator that is instantaneously isolated (closed main steamline isolation valve (MSIV) and feedwater trip) at the time of the break. A symmetric steam generator tube plugging level of 12 percent per steam generator was modeled.

As described in the FANP RLBLOCA methodology, many parameters associated with LBLOCA phenomenological uncertainties and plant operation ranges (including appropriate Technical Specification allowed ranges) are sampled. A summary of those parameters sampled is given in Table 15.4-17. The LBLOCA phenomenological uncertainties are provided in Reference 68. Values for plant parameters are given in Table 15.4-18. The table provides values describing the physical plant, plant initial operating conditions, including operating ranges, and accident boundary conditions. Diesel start time is set consistent with the loss-of-offsite-power assumption for ECC pumped injection. Table 15.4-19 presents process parameters and statistical distributions used in the analyses. The distributions in the table include additional margin to accommodate parameter uncertainties.

15.4.1.14 **Realistic Large Break LOCA Results**

The analyses assume full-power operation at 2893 MWt (plus uncertainties), a steam generator tube plugging level of 12 percent in all generators, a total peaking factor (F_Q) of 2.32, and a nuclear enthalpy rise factor ($F_{\Delta h}$) of 1.65. These analyses accommodate operation within specified ranges for sampled parameters: pressurizer pressure and level, accumulator pressure, temperature (containment temperature) and level, RCS average temperature, core flow, and containment pressure and temperature.

A set of fifty-nine calculations was performed for each North Anna unit, sampling the parameters listed in Table 15.4-17. The remainder of this section provides results from those analyses.

15.4.1.14.1 North Anna Unit 1 Large Break LOCA Results

The limiting PCT case (1853°F) was number 28. It is characterized in Tables 15.4-20 and 15.4-21. The maximum oxidation (2.6%) and total oxidation (0.03%) results are also reported in Table 15.4-21. The fraction of total hydrogen generated was not directly calculated; however, it is conservatively bounded by the calculated total percent oxidation that is well below the 1 percent limit. A nominal 50/50 PCT case was identified as case 22. The nominal PCT is 1441°F. This result can be used to quantify the relative conservatism in the limiting PCT case result. In this analysis, it is 412°F.

The hot fuel rod results, event times and analysis plots for the limiting PCT case are shown in Table 15.4-21, Table 15.4-22, and in Figures 15.4-86 through 15.4-97, respectively. Figure 15.4-86 shows linear scatter plots of the important parameters sampled for the 59 calculations. Parameter labels appear to the left of each individual plot. These figures show the values of ranged parameters used in the analysis. Figure 15.4-87 shows a PCT scatter plot versus break size from the 59 calculations. Figures 15.4-88 through 15.4-97 show important parameters from the S-RELAP5 limiting calculation. Figure 15.4-88 is a plot of the fuel rod cladding surface temperature at the PCT elevation.

15.4.1.14.2 North Anna Unit 2 Large Break LOCA Results

The limiting PCT case (1789°F) was Case 8. It is characterized in Table 15.4-23 and Table 15.4-24. The maximum oxidation (1.8%) and total oxidation (0.04%) results are also reported in Table 15.4-24. The fraction of total hydrogen generated was not directly calculated; however, it is conservatively bounded by the calculated total percent oxidation that is well below the 1 percent limit. A nominal 50/50 PCT case was identified as Case 17. The nominal PCT is 1410°F. This result can be used to quantify the relative conservatism in the limiting PCT case result. In this analysis, it is 379°F.

The hot fuel rod results, event times and analysis plots for the limiting PCT case are shown in Table 15.4-24, Table 15.4-25, and in Figures 15.4-98 through 15.4-109, respectively. Figure 15.4-98 shows linear scatter plots of the important parameters sampled for the 59 calculations. Parameter labels appear to the left of each individual plot. These figures show the value of ranged parameters used in the analysis. Figure 15.4-99 shows a PCT scatter plot versus break size from the 59 calculations. Figures 15.4-100 through 15.4-109 show important parameters from the S-RELAP5 limiting calculation. Figure 15.4-100 is a plot of the fuel rod cladding surface temperature at the PCT elevation.

15.4.1.14.3 Departure from EMF-2103(P)(A) Methodology for Treatment of Forslund-Rohsenow Heat Transfer Correlation

During review of the North Anna 1 and 2 RLBLOCA application analyses, the NRC staff requested that Dominion justify the applicability of the Forslund-Rohsenow heat transfer modeling as defined in EMF-2103(P)(A). The NRC staff's concern was that peak cladding temperatures for the North Anna applications extended above 2000°F. The NRC staff indicated that the North Anna results exceeded the PCT values from certain sensitivities that formed part of the basis for approval of the Forslund-Rohsenow model as described in EMF-2103(P)(A), Reference 68.

In response to this concern (Reference 70), a penalty (currently 64°F) is added to the peak cladding temperature calculated with the methodology of EMF-2103(P)(A) for both North Anna Units 1 and 2. This PCT penalty was generated by running the limiting Unit 2 case and disabling the Forslund-Rohsenow correlation for rod-to-droplet heat transfer (on the hot rod) when $T_{wall} > T_{min}$. This approach represents an NRC-approved plant-specific departure from the methodology in the RLBLOCA topical report, EMF-2103(P)(A). This plant-specific requirement is addressed in the NRC Safety Evaluation Report for the use of Advanced Mark-BW fuel at North Anna (References 65 & 66). The peak cladding temperature and peak rod oxidation from this revised case increased by 64°F and 0.7%, respectively, as compared with the originally reported results. Table 15.4-26 includes the adjustment in reported PCT results that address this issue.

15.4.1.15 **Large Break LOCA Core Geometry**

Calculations performed for North Anna Units 1 and 2 indicate that deformation of the fuel pin lattice in some core periphery fuel assemblies occurs from the combined mechanical LOCA and seismic loads (Reference 63, Section 3.3.3). The predicted deformations have a maximum impact of reducing the sub-channel flow area of one row of pins by 32 percent.

Evaluations of the impact of this amount of flow area reduction on the LOCA performance of fuel pins in the peripheral assemblies were conducted with the following results: (1) The coolant flow within these assemblies is not substantially altered; and (2) The maximum cladding temperature during LOCA for the affected pins remain below 1800°F. This is less than the temperature at which significant metal-water reaction occurs. Hence, these grid deformations do not lead to conditions that interfere with core coolability; nor do they affect the reported PCT or metal-water oxidation results.

The consequences of thermal and mechanical deformation of the fuel assemblies in the core were assessed. The resultant deformed geometry maintains a coolable configuration. The conclusions rely on basic phenomena encountered during LOCA and are equally applicable to the Advanced Mark-BW fuel and the current resident NAIF. Therefore, the coolable geometry requirements of 10 CFR 50.46 are met, and the core remains amenable to cooling.

15.4.1.16 **Large Break LOCA Long-Term Cooling**

Successful initial operation of the ECCS is shown by demonstrating that the core is quenched, and the cladding temperature is returned to near saturation. Thereafter, long-term cooling is achieved by the pumped injection systems. These systems are redundant and provide a continuous flow of cooling water to the core fuel assemblies so long as the coolant channels in the core remain open. For a cold leg break, the concentration of boric acid within the core can induce a crystalline precipitation that may prevent coolant flow from reaching portions of the core. This section evaluates the initial operation of the ECCS, considers the long-term supply of water to the core, and discusses the procedures to mitigate the build-up of boric acid in the core.

15.4.1.16.1 Initial Cladding Cooldown

The RLBLOCA calculations provide a simulation of the hottest fuel pins through core quench. After quenching, core heat transfer is through pool nucleate boiling or forced convection to liquid, depending on the break location (cold leg breaks are in pool nucleate boiling and hot leg breaks are in forced convection to liquid). Either heat transfer mechanism is fully capable of maintaining the core within a few degrees of the coolant saturation temperature. Thus, within ten to fifteen minutes following a large break LOCA, the core is returned to an acceptably low temperature.

15.4.1.16.2 Extended Coolant Supply

Once the core is cooled to low temperature, maintaining that condition relies upon the systems that are designed to provide a continuous supply of coolant to the core. Detailed

descriptions of the plant systems and functions are provided elsewhere in the UFSAR. Long-term core cooling with the ECCS is independent of the fuel design. Thus, the current licensing basis remains valid for Advanced Mark-BW fuel assemblies.

15.4.1.16.3 Boric Acid Concentration

The long-term cooling mechanism for a hot leg break is forced convection to liquid. Once cooling is established, and a positive core flow is assured, boron precipitation is not an issue, and no further consideration is necessary. For cold leg breaks, there is no forced flow through the core. The liquid head balance between the core and the downcomer prevents ECCS water from entering the core at a rate faster than core boil-off. Extra injection simply flows out the break and spills to the containment floor. With no core flow, core boiling acts to concentrate boric acid adding to the potential for precipitation and core blockage. To eliminate boron precipitation and any accompanying core blockage, operator action is required to establish hot leg re-circulation (positive core flow).

In this mode, the ECCS is aligned to inject into the hot legs. In doing so, the hot leg injection provides a positive core flow capable of controlling the concentration of boric acid. The timing and effectiveness of the hot leg injection is established by demonstrating that the in-vessel concentration of boric acid is below solubility limits. There is no dependency on the fuel element design since concentrations depend on ECCS injection rate, RCS geometry, and core power level. Since the Framatome ANP fuel does not alter these factors, the current evaluation remains valid and is equally applicable to Advanced Mark-BW fuel. Emergency operating procedures provide guidance to address the boric acid precipitation issue and ensure that long-term cooling is maintained.

15.4.1.16.4 Adherence to Long-Term Cooling Criterion

Compliance with this criterion is independent of fuel design. The initial phase of core cooling results in low clad and fuel temperatures. A pumped injection system, capable of re-circulation, is available and operates to provide extended coolant injection. The core boric acid concentration is limited to acceptable levels through the timely implementation of hot leg injection. Hence, long-term cooling is established and compliance to 10 CFR 50.46 demonstrated.

15.4.1.17 **Post Analysis of Record Evaluations-Framatome Fuel**

In addition to the analyses presented in this section, evaluations and reanalyses may be performed as needed to address computer code errors, emergent issues, or to support plant changes. The issues or changes are evaluated, and the impact on the PCT is determined. The resultant increase or decrease in PCT is applied to the analysis of record PCT. The PCTs, including all penalties and benefits, are presented in Table 15.4-26 for the large break LOCA. The resultant PCT is demonstrated to be less than the 10 CFR 50.46(b) requirement of 2200°F.

15.4.1.18 **Large Break LOCA Conclusions**

The analyses support operation within the plant parameter values in Table 15.4-18. The RLBLOCA analyses verify the adequacy of the ECCS by demonstrating, with a high level of probability, that the following 10 CFR 50.46(b) criteria are met:

- The calculated maximum fuel element cladding temperature shall not exceed 2200°F.
- The calculated total oxidation of the cladding shall nowhere exceed 0.17 times the total cladding thickness before oxidation.
- The calculated total amount of hydrogen generated from the chemical reaction of the cladding with water or steam shall not exceed 0.01 times the hypothetical amount that would be generated if all of the metal in the cladding cylinders surrounding the fuel, excluding the cladding surrounding the plenum volume, were to react.
- The core remains amenable to cooling during and after the break.
- The core temperature is reduced and decay heat is removed for an extended period of time, as required by the long lived radioactivity remaining in the core.

The analyses reported herein support operations at a power level of 2893 MWt, a steam generator tube plugging level of 12 percent in each generator, a total peaking factor (F_Q) of 2.32 and a nuclear enthalpy rise factor ($F_{\Delta h}$) of 1.65. The analyses support peak rod average exposures of up to 62,000 MWd/mtU. The impact of NAIF co-resident fuel on FANP Advanced Mark-BW fuel is included within the analyses–the core model is representative of the initial core composition of both NAIF and Advanced Mark-BW fuel. The core model bounds the results for subsequent cycles of operation, with their increasing percentage of Advanced Mark-BW fuel. The analysis of the Westinghouse fuel remains valid. The co-resident FANP fuel, being 2.5 psi (based on rated flow) more resistive than NAIF, will promote favorable flow diversion to NAIF, thereby improving its LBLOCA performance. Hence, the NAIF will be positively (lower clad temperature and metal-water oxidation) affected by the co-resident FANP fuel. Results of the RLBLOCA analyses show that the PCT, maximum oxidation thickness and hydrogen generation for both units are well within regulatory requirements. The supplemental discussions above demonstrate compliance with the coolable geometry and long-term cooling criteria.

The LOCA analysis of record assumes the use of fuel assemblies with 264 fuel rods. However, reconstituted fuel assemblies with a limited number of solid stainless steel filler rods replacing failed fuel rods may also be used in reload cores. When solid metal filler rods are employed, the impact of the LOCA is evaluated on a cycle-specific basis. The effect on maximum linear heat rates is tracked throughout the core residence of the affected assemblies and is removed from the LOCA assessment once the reconstituted assemblies are removed from the core.

15.4.2 Major Secondary System Pipe Rupture

15.4.2.1 Rupture of a Main Steam Line

15.4.2.1.1 Identification of Causes and Accident Description

The steam release arising from a rupture of a main steam pipe would result in an initial increase in steam flow, which decreases as the steam pressure falls. The energy removal from the reactor coolant system causes a reduction of coolant temperature and pressure. In the presence of a negative moderator temperature coefficient, the cooldown results in a reduction of core shutdown margin. If the most reactive rod cluster control assembly is assumed stuck in its fully withdrawn position after reactor trip, there is an increased possibility that the core will become critical and return to power. A return to power following a steam pipe rupture is a potential problem mainly because of the high power peaking factors that exist, assuming the most reactive rod cluster control assembly to be stuck in its fully withdrawn position. The core is ultimately shut down by the boric acid injection delivered by the safety injection system.

The analysis of a main steam pipe rupture is performed to demonstrate that the following criteria are satisfied:

1. Assuming a stuck rod cluster control assembly, with or without offsite power, and assuming a single failure in the engineered safeguards, there is no consequential damage to the primary system, and the core remains in place and intact.
2. Energy release to containment from the worst steam pipe break does not cause failure of the containment structure.

Although departure from nucleate boiling and possible clad perforation following a steam pipe rupture are not necessarily unacceptable, the following analysis shows that no departure from nucleate boiling occurs for any rupture, assuming the most reactive assembly stuck in its fully withdrawn position.

The following functions provide the necessary protection against a steam pipe rupture:

1. Safety injection system actuation from any of the following:
   a. Two out of three low pressurizer pressure signals.
   b. High differential pressure signals between steam lines.
   c. High steam-line flow in two main steam lines (one out of two per line) in coincidence with either low-low reactor coolant system average temperature (two out of three) or low steam-line pressure in any two lines.
   d. Two out of three high containment pressure.
2. The overpower reactor trips (neutron flux and delta T) and the reactor trip occurring in conjunction with receipt of the safety injection signal.

3. Redundant isolation of the main feedwater lines. Sustained high feedwater flow would cause additional cooldown. Therefore, in addition to the normal control action that will close the main feedwater valves, a safety injection signal will rapidly close all feedwater control valves, trip the main feedwater pumps, and close the feedwater pump discharge valves.

4. Trip of the fast-acting main steam trip valves (designed to close in less than 5 seconds after receipt of the signal) on:

   a. High steam flow in two main steam lines (one-out-of-two per line) in coincidence with either low-low reactor coolant system average temperature or low steam line pressure in any two lines.

   b. Two out of three intermediate high-high containment pressure.

Each of the three main steam lines that connect the steam generators to the main steam header has a fast-acting trip valve with a downstream nonreturn valve. These valves prevent blowdown of more than one steam generator for any break in these main steam lines, even if one valve fails to close. For example, in the case of a break upstream of the trip valve in one line, closure of either the nonreturn valve in that line or the trip valves in the other lines will prevent blowdown of the other steam generators. Other branch lines off the main steam lines that are not isolated by the MSTVs, such as the decay heat release line, or the steam supply to the turbine-driven AFW pump, are bounded by the analysis discussed in Section 15.2.13.3.

Steam flow is measured by monitoring pressure difference between pressure taps in the steam drum and downstream of the steam line flow restrictor nozzles. These nozzles, which are of considerably smaller diameter than the main steam pipe, are located in the steam lines inside the containment near the steam generators to limit the maximum steam flow for any break further downstream. The Model 51F steam generators installed in the North Anna units have a steam dome flow outlet area identical to that of the steam line flow restrictor nozzle. Thus, after installing the Model 51F steam generators, the maximum possible steam line break size both inside and outside containment is the same size as the steam flow restrictor nozzle.

15.4.2.1.2 Analysis of Effects and Consequences

15.4.2.1.2.1 *Method of Analysis.* The analysis of the steam pipe rupture has been performed to determine

1. The core heat flux and reactor coolant system temperature and pressure resulting from the cooldown following the steam line break. The RETRAN (Reference 33) code has been used.

2. The thermal and hydraulic behavior of the core following a steam line break. A detailed thermal and hydraulic digital computer code, COBRA (Reference 34), has been used to determine if departure from nucleate boiling occurs for the core conditions computed in 1 above.

The following conditions were assumed to exist at the time of a main steam line break accident:

1. End-of-life shutdown margin at no-load, equilibrium xenon conditions, and the most reactive assembly stuck in its fully withdrawn position. Operation of the control rod banks during core burn-up is restricted so that addition of positive reactivity in a steam line break accident will not lead to a more adverse condition than the case analyzed.

2. The negative moderator coefficient corresponding to the end-of-life rodded core with the most reactive rod in the fully withdrawn position. The variation of the coefficient with temperature has been included. The Doppler reactivity feedback corresponds to a most negative hot zero power Doppler temperature coefficient. The effect of power generation in the core on overall reactivity is shown in Figure 15.4-57.

   The core properties associated with the core sector nearest the affected steam generator and those associated with the remaining portion of the core were conservatively combined to obtain average core properties for reactivity feedback calculations. This assumption of core power distribution uniformity causes an underprediction of the reactivity feedback in the high-power region near the stuck rod. To verify the conservatism of this method, the reactivity as well as the power distribution was checked for the statepoints shown on Table 15.4-8. These core analyses considered the Doppler reactivity from the high fuel temperature near the stuck rod cluster control assembly, moderator feedback from the high water enthalpy near the stuck rod cluster control assembly, power redistribution, and non-uniform core inlet temperature effects. For cases in which steam generation occurs in the high-flux regions of the core, the effect of void formation was also included. It was determined that the reactivity used in the kinetics analysis was always larger than the true value for all statepoints in Table 15.4-8, verifying conservatism; i.e., underprediction of negative reactivity feedback from power generation.

3. Minimum capability for injection of boric acid solution corresponding to the most restrictive single failure in the safety injection system.

   The most restrictive single failure corresponds to the flow delivered by one charging pump delivering its full flow to the cold leg header. The safety injection lines downstream of the refueling water storage tank isolation valves, the BIT itself, and the safety injection lines downstream of the BIT have a 0% boron concentration. Boron enters the safety injection system after the charging pump suction switches over from the volume control tank to the refueling water storage tank upon safety injection actuation.

The assumed single failure for the steam line break analysis is the failure of one safeguards train to function, thus resulting in the maximum delay time for boron to reach the core. Other failures that could affect the severity of the transient are as follows:

1. Main steam trip valve.

   The failure of any main steam trip valve would result in no more than one steam generator blowing down after steam line isolation and would not affect the severity of the transient.

2. Feedwater control valve.

   There is a backup feedline isolation valve in series with the feedwater control valve. The failure of either of these valves would not affect the severity of the transient.

3. Feedwater control valve bypass valve.

   Feedwater flow through the main feedwater control valve bypass line is regulated by the main feedwater control valve bypass valve. The design of the bypass line does not include a back-up isolation valve in this line. However, the automatic trip of the main feedwater pumps and closure of the feedwater pump isolation valves accomplishes the back-up feedwater isolation function. The reliance upon commercial grade isolation equipment as back-up feedwater isolation has been accepted as a generic industry position as documented in NUREG-0138. The failure of a feedwater control valve bypass valve to close upon a feedwater isolation signal has been evaluated and shown to be bounded by the assumptions in the limiting analysis described in this section.

4. Main steam safety valve, atmospheric dump valve, or steam dump valve.

   The failure of a main steam safety valve, atmospheric dump valve, or main steam dump valve would result in a small increase in steam flow that would be compensated for by full operation of the safety injection system, greatly reducing the delay of boron reaching the core.

5. Two base cases were considered to adequately bound the initial conditions found in the station design basis:

   a. Complete severance of a main steam line pipe, with the plant initially at no-load conditions, full reactor coolant flow with offsite power available.

   b. Case (a) above, with loss of offsite power simultaneous with the initiation of the steam line break. Loss of offsite power results in coolant pump coastdown.

6. Power peaking factors corresponding to one stuck rod cluster control assembly and non-uniform core inlet coolant temperatures are determined at end of core life. The coldest core inlet temperatures are assumed to occur in the sector with the stuck rod. The power peaking factors account for the effect of the local void in the region of the stuck control assembly during the return-to-power phase following the steam line break. This void, in conjunction with the large negative moderator coefficient, partially offsets the effect of the

stuck assembly. The power peaking factors depend upon the core power, temperature, pressure, and flow, and thus are different for each case studied.

A conservative thermal design flow rate for the steam line break analysis was assumed. This flow rate is lower than either the mechanical design flow rate or the measured flow rate. Using a high core flow rate may result in slightly higher peak heat fluxes and would also increase the minimum DNBR.

The statepoint values used for the analyzed steam line break accidents analyzed are shown on Table 15.4-8. The case assuming offsite power available contains four statepoints, while the case assuming loss of offsite power has five statepoints. The statepoints were selected on the basis of core parameters at specific points in the transient analysis that would most likely result in minimum DNBR in the hottest channel.

Both of the above cases assume hot zero power initial conditions at time zero, since this represents the bounding initial condition. Should the reactor be just critical or operating at power at the time of a steam line break, the reactor will be tripped by the normal overpower protection system when power level reaches the trip setpoint. Following a trip at power, the reactor coolant system contains more stored energy than at no-load, the average coolant temperature is higher than at no-load, and there is appreciable energy stored in the fuel. Thus, the additional stored energy is removed via the cooldown caused by the steam line break before the no-load conditions of reactor coolant system temperature and shutdown margin assumed in the analyses are reached. After the additional stored energy has been removed, the cooldown and reactivity insertions proceed in the same manner as in the analysis that assumes no-load condition at time zero.

However, since the initial steam generator water inventory is greatest at no-load, the magnitude and duration of the reactor coolant system cooldown are less for steam line breaks occurring at power.

7. In computing the steam flow during a steam-line break, the Moody Curve (Reference 16) for fL/D = 0 is used.

8. Perfect moisture separation in the steam generator is assumed. The assumption leads to conservative results since, realistically, considerable water would be discharged. Water carryover would reduce the magnitude of the RCS energy removal and system cooldown.

15.4.2.1.2.2 *Results.* The results presented are a conservative indication of the events that would occur assuming a steam line rupture, since it is postulated that all of the conditions described above occur simultaneously.

Core Power and Reactor Coolant System Transient

Figures 15.4-58 through 15.4-61 show the reactor coolant system transient and core heat flux following a main steam pipe rupture (complete severance of a pipe) at initial no-load conditions (Case a). The break assumed is the largest break that can occur, either upstream or

downstream of the trip valves. Offsite power is assumed available so that full reactor coolant flow exists. The transient shown assumes a steam release from only one steam generator after closure of the steam line trip valves. Should the core be critical at near zero power when the rupture occurs, the initiation of safety injection by high differential pressure between any steam line and the remaining steam lines, or by high steam flow signals in coincidence with either low-low reactor coolant system temperature or low steam line pressure, will trip the reactor. Steam release from more than one steam generator will be prevented by automatic trip of the fast-action trip valves in the steam lines by the high steam flow signals in coincidence with either low-low reactor coolant system temperature or low steamline pressure. The steam line trip valves are designed to be fully closed in less than 5 seconds after receipt of closure signal with no flow through them. With the high flow existing during a steam line rupture, the valves will close considerably faster.

As shown in Figures 15.4-58 through 15.4-61, the core attains criticality with the rod cluster control assemblies inserted (with the design shutdown assuming one stuck assembly) before boron solution enters the reactor coolant system from the safety injection system. The delay time consists of the time to receive and actuate the safety injection signal and the time to completely open or realign valve trains in the safety injection lines. The safety injection pumps are then ready to deliver flow. At this stage a further delay time is incurred before boron solution can be injected to the reactor coolant system due to 0% boron concentration water being swept from the boron injection tank and safety injection lines. This case attains a peak core power well below the nominal full-power value.

The calculation assumes that the boric acid is mixed with, and diluted by, the water flowing in the reactor coolant system prior to entering the reactor core. The concentration after mixing depends upon the relative flow rates in the reactor coolant system and in the safety injection system. The variation of mass flow rate in the reactor coolant system due to water density changes is included in the calculation, as is the variation of flow rate from the safety injection system due to changes in the reactor coolant system pressure. The safety injection system flow calculation includes the line losses in the system as well as the pump head curve. The integrated flow rate of borated water from the safety injection system for each of the cases analyzed is shown in Figures 15.4-66 and 15.4-67.

Figures 15.4-62 through 15.4-65 show the responses of the core parameters for Case b, which corresponds to the case discussed above with loss of offsite power at the time the main steam line break occurs. The safety injection system delay time includes 10 seconds to start the diesel and 10 seconds for the safety injection pump to reach full speed. Criticality is achieved later and the core power increase is slower than in the similar case with offsite power available. The ability of the emptying steam generator to extract heat from the reactor coolant system is reduced by the decreased flow in the reactor coolant system. The peak core power remains well below the nominal full-power value.

It should be noted that, following a steam line break, only one steam generator blows down completely. Thus, the remaining steam generators are still available for dissipation of decay heat

after the initial transient is over. In the case of loss of offsite power, this heat is removed to the atmosphere via the main steam safety valves, which have been sized to cover this condition.

A steam line break assuming an isolated loop is less severe than the case analyzed above. Although operation with an isolated loop results in a reduced primary coolant inventory, this condition is offset by the increased shutdown margin available due to the reduced power defect.

The sequence of events is shown in Table 15.4-9.

The steam line break analysis adequately (Reference 17) addresses the NRC's concerns expressed in IE Bulletin 80-04 (Reference 18).

Margin to Critical Heat Flux

Using the transients shown in Figures 15.4-58 through 15.4-65 the Westinghouse W-3 correlation was used in conjunction with the VEPCO version of the COBRA core thermal hydraulics code to determine the margin to DNB. Carefully chosen points from each transient were examined and the results showed that both cases have a minimum DNBR greater than the minimum DNBR limit. The power and flow conditions are shown together with pressure and core inlet temperatures in Table 15.4-8.

15.4.2.1.3 Dose Consequence of Main Steam Line Break (MSLB)

The radiological analysis of a MSLB accident includes doses associated with the releases of radioactive material initially present in primary liquid, secondary liquid, and secondary steam, plus releases from the fuel rods that fail before the transient. The methodology used to evaluate the control room and offsite doses resulting from the MSLB accident was consistent with Regulatory Guide 1.183 (Reference 71) in conjunction with TEDE radiological units and limits, ARCON96 (Reference 78) based onsite (control room) atmospheric dispersion factors, and Federal Guidance Reports No. 11 and 12 (References 72 & 74) dose conversion factors. Doses were calculated at the EAB, at the LPZ, and in the control room.

The MSLB accident begins with a break in one of the main steam lines leading from a steam generator (affected generator) to the turbine. In order to maximize control room dose, the break is assumed to occur in the turbine building. The affected steam generator releases steam for 30 minutes and is assumed to dry out, at which time it is isolated. Loss of off-site power is assumed. As a result, the condenser is lost and cool down of the primary system is through the release of steam from the unaffected generators. Releases from the unaffected generators continue for 8 hours through the Power Operated Relief Valves (PORVs). In accordance with Regulatory Guide 1.183, Appendix E, two cases of iodine spiking are evaluated. The first case assumes a pre-accident iodine spike up to the maximum value permitted by Technical Specifications. The second case assumes a concurrent iodine spike 500 times greater than the release rate corresponding to the iodine concentration at the equilibrium value specified in Technical Specifications.

15.4.2.1.3.1 *Source Term Definition.* The analysis of the MSLB accident indicates that no additional fuel rod failures occur as a result of the transient. Thus, radioactive material releases are determined by the radionuclide concentrations initially present in primary liquid, secondary liquid, and secondary steam, plus any releases from fuel rods that have failed before the transient.

The MSLB analysis uses the Steam Generator Tube Rupture (SGTR) analysis source term discussed in Section 15.4.3.4.1. The only exception is that the MSLB accident assumes a concurrent accident iodine spike 500 times the release rate corresponding to the Technical Specification limit for normal operation (1 μCi/gm DE I-131) for a period of 8 hours, consistent with Regulatory Guide 1.183. The concurrent iodine spike appearance rates used in the MSLB accident analysis are shown in Table 15.4-15.

15.4.2.1.3.2 *Release Transport.* The source term resulting from the radionuclides in the primary system coolant and from the iodine spiking in the primary system is transported to the secondary side of the steam generators assuming a leak-rate of 1 gpm. The maximum amount of primary to secondary leakage allowed by the Technical Specifications to any one steam generator is 150 gallon per day. Conservatively, 500 gpd was assigned to the affected generator and it is assumed to flash to steam and pass directly into the turbine building with no credit taken for scrubbing by the steam generator liquid. The remainder of the 1 gpm primary side to secondary side leakage (940 gpd) was assigned to the two unaffected generators (modeled as one generator). The radionuclides initially in the steam generator liquid and steam pass directly to the turbine building through the broken steam line. The release from the turbine building passes to the control room and to the environment. The transport model utilized for iodine and particulates was consistent with Appendix E of Regulatory Guide 1.183.

All radionuclides in the primary coolant leaking (940 gpd) into the unaffected generator are assumed to enter the steam generator liquid. Releases of radionuclides initially in the steam generator liquid and those entering the steam generator from the leakage flow are released as a result of secondary liquid boiling including an allowance for a partition factor of 100 for all non-noble gas isotopes. Thus 1% of the iodines and particulates are assumed to pass directly to the environment through the steam generator PORVs. No flow is assumed to pass from the liquid to the steam space to minimize holdup and decay. Radionuclides initially in the steam space are modeled to pass quickly to the environment through the PORVs. All noble gases that are released from the primary system to the unaffected generator are released to the environment through the PORVs without reduction or mitigation

15.4.2.1.3.3 *Atmospheric Dispersion Factors.* Table 15.4-16 contains the control room (CR) χ/Q atmospheric dispersion factors used in the MSLB dose consequence analysis. The control room χ/Q values are new values that were calculated using the ARCON96 code and guidance from Regulatory Guide 1.194. Control room χ/Q values are ground level χ/Q values calculated at the PORV release elevation with no credit for plume rise. The normal control room ventilation intake was used as the intake point for the control room since no credit was taken for control room isolation during the accident.

The EAB and LPZ χ/Q values used in the MSLB analysis are the same as those used in the LOCA analysis and are discussed in Section 15.4.1.7.

15.4.2.1.3.4 *Analysis Assumptions and Input Parameters.* The primary and secondary volumes along with the primary and secondary water and steam properties used in the MSLB analyses are the same as those used in the SGTR analyses. The limiting case for the control room dose assumes the control room does not isolate and unfiltered intake airflow is 3300 cfm, which includes 500 cfm of inleakage. Occupancy factor and breathing rate is given in Table 15.4-6. The RADTRAD-NAI code was used to analyze the pre-accident spike and concurrent iodine spike scenarios.

15.4.2.1.3.5 *MSLB Dose Analysis Results.* The MSLB dose analysis results of the RADTRAD-NAI cases for the Concurrent Spike and for the Pre-Accident Iodine Spike cases are presented in Table 15.4-27 along with the applicable dose limits. These results report the calculated dose for the worst 2-hour interval (EAB), and for the assumed 30 day duration of the event for the control room and the LPZ. The doses calculated with the TEDE methodology are compared with the applicable acceptance criteria specified in 10 CFR 50.67 and Regulatory Guide 1.183. As indicated in Table 15.4-27, each of the results meet the acceptance criteria.

15.4.2.2 **Major Rupture of a Main Feedwater Pipe**

15.4.2.2.1 Identification of Causes and Accident Description

A major feedwater line rupture is defined as a break in a feedwater pipe large enough to prevent the addition of sufficient feedwater to the steam generators to maintain shell-side fluid inventory in the steam generators. If the break is postulated in a feedline between the check valve and the steam generator, fluid from the steam generator may also be discharged through the break. Further, a break in this location could preclude the subsequent addition of auxiliary feedwater to the affected steam generator. (A break upstream of the feedline check valve would affect the nuclear steam supply system only as a loss of feedwater. This case is covered by the evaluation in Section 15.2.8.)

Depending upon the size of the break and the plant operating conditions at the time of the break, the break could cause either a reactor coolant system cooldown (by excessive energy discharge through the break) or a reactor coolant system heatup. Potential reactor coolant system cooldown resulting from a secondary pipe rupture is evaluated in Section 15.4.2.1. Therefore, only the reactor coolant system heatup effects are evaluated for a feedline rupture.

A feedline rupture reduces the ability to remove heat generated by the core from the reactor coolant system for the following reasons:

1. Feedwater to the steam generators is reduced. Since feedwater is subcooled, its loss may cause reactor coolant temperatures to increase prior to reactor trip.
2. Liquid in the steam generator may be discharged through the break, and would then not be available for decay heat removal after trip.

3. The break may be large enough to prevent the addition of any main feedwater after trip.

An auxiliary feedwater system is provided to ensure that adequate feedwater will be available to provide heat removal so that:

1. No substantial overpressurization of the reactor coolant system will occur.
2. Liquid in the reactor coolant system will be sufficient to cover the reactor core at all times.

The following provides the necessary protection against a main feedwater rupture:

1. A reactor trip on any of the following conditions:
   a. High pressurizer pressure.
   b. Overtemperature delta T.
   c. Low-low steam generator water level in any steam generator.
   d. Low steam generator level plus steam/feed flow mismatch in any steam generator.
   e. Safety injection signals from any of the following:
      1) Low steam-line pressure in coincidence with high steam flow.
      2) High containment pressure.
      3) High steam-line differential pressure.

   (Refer to Chapter 7 for a description of the actuation system.)
2. An auxiliary feedwater system to provide an assured source of feedwater to the steam generators for decay heat removal.

   (Refer to Chapter 10 for a description of the auxiliary feedwater system.)

15.4.2.2.2 Analysis of Effects and Consequences

15.4.2.2.2.1 *Method of Analysis.* A detailed analysis using the RETRAN (Reference 33) code is performed in order to determine the plant transient following a feedline rupture. The code describes the plant thermal kinetics, reactor coolant system including natural circulation, pressurizer, steam generators, and feedwater system, and computes pertinent variables including the pressurizer pressure, pressurizer water level, and reactor coolant average temperature. Assumptions are consistent with the methodology in Reference 30.

Major assumptions are:

a. The plant is initially operating at 102% of the uprated NSSS power level.
b. Initial reactor coolant average temperature is 4°F above the nominal value, and the initial pressurizer pressure is 30 psi above its nominal value.
c. No credit is taken for the pressurizer power-operated relief valves or pressurizer spray.

d. Initial steam generator water level is at the nominal value +5% in the faulted steam generator and at the nominal -5% in the intact steam generators.

e. No credit is taken for the high pressurizer pressure reactor trip. Note: This assumption is made for calculational convenience. Pressurizer power-operated relief valves and spray could act to delay the high pressure trip. Assumptions c and e permit evaluation of one hypothetical, limiting case rather than two possible cases: one with a high pressure trip and no pressure control; and one with pressure control but no high pressure trip. No pressure control is conservative. [Reference 62 noted that the low-low steam generator water level trip might not be effective for certain small feedline breaks (those resulting in reduced or zero flow added to the faulted steam generator). North Anna plant-specific studies showed that the high pressurizer pressure reactor trip, which is not credited in the full-size break analysis, provides effective protection for the range of small feedline breaks, for cases with and without pressure control available. Additionally, other diverse sources of protection were shown to function effectively. These include high pressurizer level, low RCS flow in the affected loop, overtemperature and overpower delta-T (for the case of no single protection channel failure), and safety injection/reactor trip on a high containment pressure.]

f. Main feed to all steam generators is assumed to stop at the time the break occurs (all main feedwater spills out through the break).

g. The break was conservatively modeled at the bottom of the steam generator.

h. The reactor trip was assumed to be actuated when the water level in the faulted steam generator decreases to the 0.0% of narrow range span.

i. A break area of 0.717 ft^2 is assumed. This corresponds to the total flow area of all of “J” tubes on the feedring.

j. No credit is taken for heat energy deposited in reactor coolant system metal during the reactor coolant system heatup.

k. No credit is taken for charging, or letdown.

l. Steam generator heat transfer area is assumed to decrease as the shellside liquid inventory decreases.

m. Conservative core residual heat generation is assumed based upon long term operation at the initial power level preceding the trip.

n. The auxiliary feedwater is assumed to be actuated by the low-low steam generator water level signals with the feed rate of 300 gpm, the capacity of one motor driven auxiliary feed pump. A 60-second delay was assumed following the low-low level signal to allow time for start-up of standby diesel generators and auxiliary feedwater pumps. Only one auxiliary feedwater pump is assumed to operate delivering auxiliary feedwater to one intact steam generator.

o. The auxiliary feedwater pump aligned with the faulted steam generator is shutdown by operator action 30 minutes after the trip. This ensures adequate emergency condensate storage tank head to provide heat removal for the duration of the analysis.

15.4.2.2.2.2 *Results.* Figures 15.4-68 through 15.4-73 show the calculated plant parameters following a feedline rupture. Results for the case with offsite power available are presented on Figures 15.4-68, 15.4-69, and 15.4-70. Results for the case where offsite power is lost are presented on Figures 15.4-71, 15.4-72, and 15.4-73. The reactor core remains covered with water throughout the transient, as water relief due to thermal expansion is limited by the heat removal capability of the AFW. The time sequence of events for both cases is shown on Table 15.4-10.

Westinghouse identified an issue relating to the pressure differential across the steam generator mid-deck plate that may cause the assumed initial steam generator mass for the feedline rupture accident analysis to be non-conservative (Reference 61). For the case with offsite power available, the effect of the decreased initial steam generator mass is offset by assuming a reduced emergency condensate storage tank temperature. For the cases with a loss of offsite power, the potential reduction in initial steam generator mass would not impact the steam generator's capacity to preclude bulk boiling in the RCS hot leg.

The durations associated with the sequence of events presented in Table 15.4-10 are marginally reduced when the impact of a reduced emergency condensate storage tank temperature and the reduced initial steam generator mass is considered. Additionally, the minor impact this would have on the plots presented for the limiting case with offsite power would be a slightly reduced pressurizer pressure, pressurizer water volume, and loop temperature. The RCS hot leg subcooling margin is insignificantly affected. Thus, the accident analysis acceptance criteria continue to be met after consideration of the previously unevaluated steam generator mid-deck plate pressure differential.

15.4.2.2.3 Conclusion

Results of the analysis show that for the postulated feedline rupture, the assumed auxiliary feedwater system capacity is adequate to remove decay heat, to prevent overpressurizing the reactor coolant system, and to prevent uncovering the reactor core.

15.4.3 Steam Generator Tube Rupture

15.4.3.1 Accident Description

The accident examined is the complete severance of a single steam generator tube. The accident is assumed to take place at power, with the reactor coolant contaminated with fission products corresponding to continuous operation with 1% of the fuel rods defective. The accident leads to an increase in contamination of the secondary system due to leakage of radioactive coolant from the reactor coolant system. In the event of a coincident loss of offsite power, or failure of the condenser dump system, discharge of activity to the atmosphere takes place via the steam generator safety and/or power-operated relief valves.

In view of the fact that the steam generator tube material is highly ductile, the assumption of a complete severance is somewhat conservative. The more probable mode of tube failure would be one or more minor leaks of undetermined origin. Activity in the steam generator blowdown is continuously monitored and an accumulation of minor leaks that exceeds the limits established in the Technical Specifications is not permitted during operation.

Throughout the discussion that follows, only an unplugged tube rupture will be addressed, as it is considered the worst case.

The operator is expected to determine that a steam generator tube rupture has occurred, and identify and isolate the faulty steam generator promptly, to minimize contamination of the secondary system and ensure termination of radioactive release to the atmosphere from the faulty unit. The recovery procedure can be carried out on a time scale that ensures that break flow to the secondary system is terminated before water level in the affected steam generator rises into the main steam pipe. Sufficient indications and controls are provided to enable the operator to carry out these functions satisfactorily.

Consideration of the indications provided at the control board, together with the magnitude of the break flow, leads to the conclusion that the isolation procedure can be completed within 30 minutes of accident initiation.

Assuming normal operation of the various plant control systems, the following sequence of events is initiated by a tube rupture:

1. Pressurizer low-pressure and low-level alarms are actuated, and charging pump flow increases in an attempt to maintain pressurizer level. On the secondary side, there is a steam flow/feedwater flow mismatch before trip as feedwater flow to the affected steam generator is reduced due to the additional break flow now being supplied to that unit.

2. Continued loss of reactor coolant inventory leads to a reactor trip signal generated by low pressurizer pressure. Resultant plant cooldown following reactor trip leads to rapid change of pressurizer level, and the safety injection signal, initiated by low-low pressurizer pressure, follows soon after the reactor trip. The safety injection signal automatically terminates normal feedwater supply and initiates auxiliary feedwater addition.

3. The steam generator blowdown liquid monitors (one each per steam generator and one on each units' high-capacity steam generator blowdown system effluent discharge line) and the condenser offgas radiation monitor will alarm, indicating a sharp increase in radioactivity in the secondary system. Additional monitors in the liquid waste system (Section 11.2) will terminate liquid discharge to the environment if preset radiation limits are exceeded. Steam generator blowdown can be manually terminated by the operator if required, or the high-capacity blowdown system will isolate automatically if the effluent line radiation monitor setpoint is exceeded.

4. The reactor trip automatically trips the turbine and, if offsite power is available, the steam dump valves open, permitting steam dump to the condenser. In the event of a coincident station blackout, the steam dump valves would automatically close to protect the condenser, and the steam generator pressure would rapidly increase, resulting in steam discharge to the atmosphere through the steam generator safety and/or power-operated relief valves.

5. Following reactor trip, the continued action of auxiliary feedwater supply and borated safety injection flow (supplied from the refueling water storage tank) provide a heat sink that absorbs some of the decay heat. Thus, steam bypass to the condenser, or, in the case of loss of offsite power, steam relief to atmosphere, is attenuated during the 30 minutes in which the recovery procedure leading to isolation is being carried out.

6. Safety injection flow results in increasing pressurizer water level. The time after trip at which the operator can clearly see returning level in the pressurizer is dependent upon the amount of operating auxiliary equipment.

15.4.3.2 **Analysis of Effects and Consequences**

15.4.3.2.1 Method of Analysis

The thermal hydraulic portion of the tube rupture analysis is performed using the RETRAN computer code (Reference 33). RETRAN predicts the break flow in the ruptured generator and the reactor coolant and main steam system responses. RETRAN also calculates the fraction of the break flow that flashes directly to steam, for use in the dose analysis, consistent with the methods of References 85 through 87, and steam releases from the ruptured and intact generators via the atmospheric steam dumps (PORVs) and safety valves.

In estimating the mass transfer from the reactor coolant system through the broken tube, the following assumptions are made:

1. Reactor trip occurs automatically as a result of overtemperature ΔT. The nominal overtemperature ΔT trip setpoint is used (no instrument uncertainty) in the analysis to cause an early reactor trip and turbine trip. This minimizes the time to open the steam generator PORVs which form part of the release path for radioisotopes.

2. Following the initiation of the safety injection signal, all high head safety injection pumps are actuated and continue to deliver flow for the period that the steam generator is unisolated.

3. After reactor trip, the break flow reaches equilibrium at the point when incoming safety injection flow is balanced by outgoing break flow, as shown in Figure 15.4-74. The resultant break flow is not reduced until the steam generator is isolated.

4. Cases with and without a loss of offsite power are considered. In both cases, the condenser steam dumps are conservatively assumed to be unavailable. After the reactor trip and turbine trip, steam releases from the steam generator PORVs and safety valves are modeled. The PORV on the ruptured generator is assumed to stick open on the first cycle, and to remain open until the operator locally isolates the valve at 30 minutes. This assumption represents a

limiting case for transport of radioiodine to the atmosphere, as shown by the generic studies of References 85 and 86.

5. The operator identifies the accident type and isolates the affected steam generator (terminating release to the atmosphere) within 30 minutes of accident initiation. The steam generator PORVs are equipped with manual isolation valves. The emergency procedures are structured to provide for early identification of a stuck PORV and direct local isolation. Evaluations have shown that this local isolation can be performed within the 30 minutes assumed in the analysis.

6. The dose analysis assumes that a release from the ruptured steam generator to the atmosphere exists for the first thirty minutes of the accident. After thirty minutes, it is assumed that the atmospheric relief and safety valves close and remain closed, and that ruptured steam generator water level is stabilized prior to water entering the steam lines.

15.4.3.2.2 Recovery Procedure

Immediately apparent symptoms of a tube-rupture accident, such as falling pressurizer pressure and level and increased charging pump flow, are also symptoms of small steam-line breaks and loss-of-coolant accidents. It is therefore important for the operator to determine that the accident is a rupture of a steam generator tube so that he may carry out the correct recovery procedure. The accident under discussion is uniquely identified by a condenser air ejector radiation alarm and/or a steam generator blowdown radiation alarm. In the event of a relatively large rupture, it will be clear soon after trip that the level in one steam generator is rising more rapidly than in the other. This too is a unique indication of a tube-rupture accident.

The operator carries out the procedures subsequent to reactor trip that lead to isolation of the ruptured steam generator and to unit cooldown. The major steps of these procedures are described generally below. The detailed instructions are contained in procedure 1-E-3 (Unit 1), *Steam Generator Tube Rupture*.

1. Stop the reactor coolant pumps if at least one safety injection pump is running and the minimum required RCS subcooling is not maintained.

2. If not already completed, identify the ruptured steam generator by rising water level or high radiation indication and isolate flow from this steam generator. Adjust auxiliary feedwater flow to maintain specified water levels in the ruptured and intact steam generators. Manual isolation of steam flow from the ruptured generator to the turbine-driven auxiliary feedwater pump is performed locally in the Main Steam Valve House. Also, the steam generator PORVs are verified available and their manual isolation valves are opened (if required) in preparation for subsequent steps.

3. Manually align condenser air ejector discharge to containment and open steam supply to air ejectors. This is necessary since the safety injection signal causes this path to be isolated.

4. Initiate RCS cooldown through the intact steam generators by dumping steam to the main condenser or through the steamline PORV (depending on the availability of offsite power).
5. Depressurize the RCS to minimize breakflow and refill the pressurizer using the pressurizer spray or PORV, if spray is unavailable. Maintain the pressurizer pressure within the pressure-temperature limit curve for the reactor coolant system.
6. Terminate safety injection flow, upon establishing minimum RCS subcooling, secondary heat sink and level in the pressurizer.
7. Establish letdown and charging functions and control RCS pressure to minimize primary-to-secondary leakage and begin post steam generator tube rupture cooldown.
8. Proceed to appropriate procedure for post-steam generator tube rupture cooldown.

There is ample time available to carry out the above recovery procedures so that isolation of the affected steam generator is established before water level rises into the main steam pipes. The available time scale is improved by the termination of auxiliary feedwater flow to the faulty steam generator and the regulation of pressurizer water level with only one charging pump operating. Normal operator vigilance therefore ensures that excessive water level will not be attained.

15.4.3.2.3 Results

Figure 15.4-74 illustrates the flow rate that would result through the ruptured steam generator tube. The total amount of reactor coolant transferred to the secondary side of the faulty steam generator as a result of a tube-rupture accident is approximately 115,000 lbm for the case with offsite power available, and approximately 113,000 lbm for the case with loss of offsite power.

15.4.3.3 **Conclusions**

A steam generator tube rupture will cause no subsequent damage to the reactor coolant system or the reactor core. An orderly recovery from the accident can be completed even assuming simultaneous loss of offsite power. Offsite dose consequences from this accident are presented in Section 15.4.3.4. The thermal/hydraulic results for the loss of offsite power (LOOP) case are summarized in Table 15.4-35.

15.4.3.4 **Dose Consequence of Steam Generator Tube Rupture (SGTR)**

The radiological analysis of a SGTR accident includes doses associated with the releases of radioactive material initially present in primary liquid, secondary liquid, and secondary steam, plus releases from the fuel rods that fail before the transient. The methodology used to evaluate the control room and offsite doses resulting from the SGTR accident was consistent with Regulatory Guide 1.183 (Reference 71) in conjunction with TEDE radiological units and limits, ARCON96 (Reference 78) based onsite (control room) atmospheric dispersion factors, and Federal Guidance Reports No. 11 and 12 (References 72 & 74) dose conversion factors. Doses were calculated at the EAB, at the LPZ, and in the control room.

A SGTR is a break in a tube carrying primary coolant through the steam generator. This postulated break allows primary liquid to leak to the secondary side of one of the steam generators (denoted as the affected generator) with an assumed release to the environment through the steam generator PORVs or the steam generator safety valves. The affected generator discharges steam to the environment for 30 minutes until the generator is isolated. The unaffected generator discharges steam for a period of 8 hours until the primary system has cooled sufficiently to allow a switchover to the residual heat removal system. Consistent with current licensing analysis basis, the SGTR analysis was performed assuming both a pre-accident iodine spike and a concurrent accident iodine spike. The analysis evaluated both loss-of-offsite power (LOOP) and no loss-of-offsite power (No LOOP).

15.4.3.4.1 Source Term Definition

Initial radionuclide concentrations in the primary and secondary systems for the SGTR accident must be determined. The analysis of the SGTR accident indicates that no additional fuel rod failures occur as a result of this transient. Thus, radioactive material releases are determined by the radionuclide concentrations initially present in primary liquid, secondary liquid, and secondary steam, plus any releases from fuel rods that have failed before the transient. The iodine appearance rate values have been conservatively calculated assuming letdown flow rates of 120 gpm, RCS leakage of 12 gpm, and letdown decontamination efficiency of 100%.

Radionuclide inventories and concentrations for the primary and secondary system liquid have previously been determined for 1% failed fuel and are documented in Tables 11.1-6 and 11.1-7, respectively. These initial values provided the starting point for determining the initial curie input for the RADTRAD-NAI code runs.

The released activities for the SGTR accident are maximized per the requirement of Regulatory Guide 1.183. The SGTR accident evaluates iodine spiking above the value allowed for normal operation based on a pre-accident and a concurrent iodine spike. The maximum iodine concentration allowed in iodine spike is 60 microcuries per gram dose equivalent I-131. The concurrent iodine spike has an accident initiated value 335 times the release rate corresponding to the Technical Specification limit for normal operation (1 μCi/gm DEI-131 RCS TS limit) for a period of 8 hours.

To limit the releases to the maximum allowed by the Technical Specifications, the quantity of each radionuclide in the primary system resulting from 1% failed fuel is converted to 1 μCi/gm dose equivalent I-131. The secondary steam noble gas inventory is found by multiplying the primary system noble gas inventory by the dilution ratio. This dilution ratio is the ratio of the primary to secondary leak rate divided by the steam flow rate. This assumes that all noble gases are carried through the steam generator with steam flow and pass out the PORVs or safety valves and do not build up in the secondary steam.

Table 15.4-28 lists the primary and secondary inventories used as a starting point for the concurrent and pre-accident iodine spike cases. The concurrent iodine spike appearance rates are

also listed in Table 15.4-28. The dose conversion factors used to calculate the TEDE doses for the SGTR accident are taken from Federal Guidance Report Nos. 11 and 12 for the isotopes required by Regulatory Guide 1.183.

15.4.3.4.2 Release Transport

The thermal hydraulic evaluation of the SGTR, which the release transport is based upon, is discussed in Section 15.4.3.2. The source term resulting from the radionuclides in the primary system coolant and from the iodine spiking in the primary system is transported to the affected steam generator by the break flow. A fraction of the break flow is assumed to flash to steam in the affected generator and to pass directly into the steam space of the affected generator with no credit taken for scrubbing by the steam generator liquid. The radionuclides initially in the steam space and those entering the steam space as the result of flashing, pass directly to the environment through the Steam Generator PORVs or safety valves. The remainder of the break flow enters the steam generator liquid. Releases of radionuclides initially in the steam generator liquid and those entering the steam generator from the break flow are released as a result of secondary liquid boiling, including an allowance for a partition factor of 100 for all non-noble gas isotopes. Thus 1% of the iodines and particulates are released from the steam generator liquid to the environment along with the steam flow (Moisture carryover is not actually modeled but is instead bounded by application of the partitioning factor). All noble gases are released from the primary system to the environment without reduction or mitigation. Releases were assumed to continue from the affected generator for 30 minutes until the affected generator was isolated. The transport model utilized for iodine and particulates is consistent with Appendix E of Regulatory Guide 1.183.

The source term resulting from the radionuclides in the primary system coolant and from the iodine spiking in the primary system is transported to the unaffected generators assuming a leak-rate of 1 gpm. All radionuclides in the primary coolant leaking into the unaffected generator are assumed to enter the steam generator liquid. Releases of radionuclides initially in the steam generator liquid and those entering the steam generator from the leakage flow are released as a result of secondary liquid boiling including an allowance for a partition factor of 100 for all non-noble gas isotopes. Thus 1% of the iodine and particulates are assumed to pass directly to the environment. No flow is assumed to pass from the liquid to the steam space to minimize holdup and decay. Radionuclides initially in the steam space are modeled to pass quickly to the environment. Again, all noble gases that are released from the primary system to the unaffected generator are released to the environment without reduction or mitigation. Releases were assumed to continue from the unaffected generator for a period of 8 hours until the primary system had cooled sufficiently to allow a switchover to the residual heat removal system.

15.4.3.4.3 Atmospheric Dispersion Factors

The control room (CR) χ/Q values are new values that were calculated by using the ARCON96 code and guidance from Regulatory Guide 1.194. The CR χ/Q values are ground level χ/Q values calculated at the PORV release elevation that have been reduced by a factor of 5 to credit plume rise. This reduction was taken after verifying that (1) the release point is uncapped

and vertically oriented, and (2) the time-dependent vertical velocity exceeds the 95th-percentile highest wind speed (at the release point height) by a factor of 5. The normal control room ventilation intake was used as the intake point for the control room since credit is not taken for control room isolation during the accident. The CR χ/Q values used in the SGTR analysis are listed in Table 15.4-29. The PORV release point bound the χ/Q values for releases from the steam generator safety valves.

The EAB and LPZ χ/Q values used in the SGTR analysis are the same as those used in the LOCA analysis and are discussed in Section 15.4.1.7.

15.4.3.4.4 Analysis Assumptions and Input Parameters

The primary and secondary volumes along with the primary and secondary water and steam properties used in the analyses are provided in Table 15.4-30. The limiting case for the control room dose assumes the control room is not isolated and an unfiltered intake airflow at 3300 cfm, which includes 500 cfm of inleakage. Occupancy factor and breathing rate is given in Table 15.4-6. The pre-accident iodine spike and concurrent iodine spike cases are modeled with the RADTRAD-NAI code assuming LOOP and No-LOOP.

15.4.3.4.5 SGTR Dose Analysis Results

The results of the SGTR dose analysis for the Concurrent and the Pre-Accident Iodine Spike cases are presented in Table 15.4-31 along with the applicable limits for both the LOOP and No LOOP scenarios. These results report the calculated dose for the worst 2-hour interval (EAB), and for the assumed 30 day duration of the event for the control room and the LPZ. The doses calculated with the TEDE methodology are compared with the applicable acceptance criteria specified in 10 CFR 50.67 and Regulatory Guide 1.183. As indicated in Table 15.4-32, all of the results meet the acceptance criteria.

15.4.4 Locked Reactor Coolant Pump Rotor

15.4.4.1 Identification of Causes and Accident Description

The Locked Rotor/Sheared Shaft events are characterized by the rapid loss of forced circulation in one Reactor Coolant System (RCS) loop. A Locked Rotor event is defined as the seizure of a Reactor Coolant Pump (RCP) motor due to a mechanical failure. The Sheared Shaft event is defined as the separation of the RCP impeller from the motor due to the severance of the impeller shaft. For both the Locked Rotor and the Sheared Shaft events, the postulated RCP failure causes the reactor coolant flow rate to decrease more rapidly than a normal RCP coastdown.

During power operation the reduction in RCS flow caused by a Locked Rotor or Sheared Shaft event results in degradation of the heat transfer between the fuel and the reactor coolant, and between the reactor coolant and the secondary coolant in the steam generator (SG). As a result of the reduced fluid velocity, the core differential (ΔT) and average temperatures (T_{avg}) increase. The reduced heat transfer to the secondary fluid also contributes to the reactor coolant temperature

increase. The expansion of the RCS fluid that accompanies the temperature increase causes an in-surge of coolant into the pressurizer, and thus an increase in the reactor coolant system pressure. The reduced fluid velocity and subsequent temperature rise also act to reduce the heat transfer from the fuel, causing the fuel temperature to increase. Fuel damage could then result if specified acceptable fuel damage limits are exceeded during the transient, i.e., if the fuel experiences a Departure from Nucleate Boiling (DNB). Due to the severe nature of these postulated failures, the likelihood that a limited number of fuel rods will experience DNB is significant. Thus, timely actuation of the Reactor Protection System (RPS) is required to help limit the number of potential fuel failures.

The immediate core power response during a Locked Rotor or Sheared Shaft event will change in accordance with the RCS temperature and pressure based on the magnitude and direction of the moderator reactivity feedback. As such, a Locked Rotor or Sheared Shaft event occurring in the presence of a positive Moderator Temperature Coefficient (MTC) will see an increase in core power as the RCS temperature increases. Conversely, the presence of a negative MTC will cause the core power to decrease as the RCS temperature increases. If the Rod Control System is in automatic, movement of the control rods will generally be in a direction such that a power reduction occurs.

The core power response is also influenced by the magnitude of the fuel Doppler coefficient. The reduced capability of the reactor coolant to remove energy from the reactor core causes the fuel temperature to increase. In the presence of a negative fuel Doppler coefficient, a fuel temperature increase contributes negative reactivity to the core, which acts to diminish the core power increase.

The potential for a Locked Rotor or Sheared Shaft event is present during all modes of operation where at least one RCP is functioning to provide forced circulation. However, the consequences of a Locked Rotor or Sheared Shaft event are reduced dramatically when the reactor is not at power. During subcritical or zero power operation, natural circulation is more than adequate to remove decay heat following the loss of forced circulation. Thus, the potential for exceeding the specified fuel design limits is nearly zero when the reactor is not at power.

Maintaining the fuel cladding integrity is a primary safety criterion for the Locked Rotor/Sheared Shaft event, although integrity may not be maintained for all fuel rods. Therefore, maintaining the RCS as a fission product barrier becomes more significant. Specifically, RCS integrity may be challenged as a result of the volumetric expansion of the fluid caused by the heating of the RCS fluid. Operation of the pressurizer sprays and PORVs can help limit the impact of the subsequent pressure increase, but cannot counteract the volumetric expansion of the RCS fluid. In general, the short duration of the locked rotor event acts in concert with the functioning of the pressurizer safety valves (PSVs), to prevent excessive RCS pressurization. Thus, timely actuation of the Reactor Protection System is also required to help limit the RCS pressure response.

Sensible and decay heat can be removed by steaming to the condenser through the steam bypass system, to the atmosphere through the main steam (MS) PORV or the main steam safety valves (MSSVs), or any combination of the three methods. However, the desirability of a given method is based on system availability and the extent to which the fission product barriers have been compromised. In all scenarios, feedwater remains available to the steam generators from either the main feedwater (MFW) system or the auxiliary feedwater (AFW) system to replenish the secondary coolant. Shortly after the reactor is shutdown, the energy removal capability of the SGs will exceed the RCS sensible and decay heat levels, and the reactor operators/automatic control systems will function to maintain the plant at the new equilibrium condition.

15.4.4.2 **Method of Analysis**

15.4.4.2.1 General

To cover all applicable phases of plant operation, Locked Rotor and Sheared Shaft events during Modes 1 through 5, as defined in the Technical Specifications, are considered. A transient analysis is only required for Locked Rotor and Sheared Shaft events at full power with manual rod control. The results of Locked Rotor or Sheared Shaft event analyses at any of the remaining operating conditions are bounded by those of the full power manual rod control cases.

The locked rotor/sheared shaft analysis considers the effects of a 1.7% power uprate by assuming a nominal initial core power level of 2893 × 1.017 MWt (2942.2 MWt). The transient analysis models the Westinghouse Standard and NAIF fuel products and the Framatome Advanced Mark-BW fuel product. The detailed core thermal/hydraulic analysis models the 17 x 17 Westinghouse Standard and NAIF fuels products using the Virginia Power Statistical DNBR Evaluation Methodology as described in Reference 53. As described in Reference 63, the detailed core thermal/hydraulic analysis for the Framatome Advanced Mark-BW fuel product is performed using the Framatome ANP Statistical Core Design Methodology with the Framatome ANP LYNXT thermal-hydraulic computer code and associated models, or the Dominion Statistical DNBR Evaluation Methodology with the VIPRE-D thermal-hydraulic computer code and associated models, as discussed in Section 4.5.

The analysis discussed below encompasses both the Westinghouse and Framatome fuel products. Beginning with Cycle 17 for Unit 2 and Cycle 18 for Unit 1, the Advanced Mark-BW fuel product was introduced in mixed cores with the LOPAR and NAIF assemblies.

Except where otherwise noted, the following assumptions are made in the Locked Rotor/Sheared Shaft transient analysis:

1. The DNB analysis employs a statistical treatment of key analysis uncertainties; the transient cases are assumed to initiate from nominal thermal/hydraulic conditions.
2. The main steam and RCS overpressurization analyses employ a deterministic treatment of key analysis uncertainties (102% of 2893 MW; nominal T_{avg} +4°F; nominal pressurizer pressure +30 psi; and RCS thermal design flow).

3. The DNB, RCS overpressurization, and main steam system overpressurization analyses consider full cores of North Anna Improved Fuel (NAIF), Westinghouse standard (STD) 17 x 17 fuel, and Framatome ANP Advanced mark-BW fuel.
4. Reactor protection is assumed to be provided by the low coolant loop flow rate reactor trip at 87% of the applicable analysis RCS flow rate.
5. Conservative integral and differential trip reactivity characteristics were assumed.
6. The analysis supports a +6.0 pcm/°F moderator temperature coefficient from 0% to 70% power, and 0.0 pcm/°F above 70% power.
7. The analysis assumes a conservative least negative Doppler Temperature Coefficient (DTC).
8. A minimum beginning-of-cycle delayed neutron fraction and a maximum prompt neutron lifetime were assumed in the DNB, main steam and RCS overpressurization analyses.
9. In the main steam and RCS overpressurization transient analyses, the steam dump system was conservatively assumed not to actuate.
10. No credit was taken for automatic rod control.
11. In the DNB transient analyses, the pressurizer sprays and PORVs are conservatively assumed to be operable. In the main steam and RCS overpressurization transient analyses, the pressurizer sprays and PORVs are conservatively assumed not to actuate.
12. In the main steam and RCS overpressurization analyses, the pressurizer heaters are conservatively assumed to be enabled.
13. Although there is no mechanism for early feedwater isolation during a locked rotor event, the main steam and RCS overpressurization analyses have conservatively assumed initiation of feedwater isolation upon reactor trip.
14. Conservative levels of steam generator tube plugging were assumed.
15. The main steam and RCS overpressurization analyses considered a water-filled loop seal with a 2% as-found lift setpoint tolerance. This modeling accommodates individual PSV lift setpoint deviations as high as 3%, provided the average PSV lift setpoint is deviated by less than 2%. For the main steam and RCS overpressurization analyses, it is conservative to assume a PSV lift setpoint at the high end of the allowable as-found lift setpoints, with a maximum loop seal purge time. PSV modeling does not affect the minimum DNBR, since the minimum DNBR occurs well before the safety valve is challenged.
16. The main steam and RCS overpressurization analysis assumes 50% bypass flow. The high degree of bypass flow in the overpressurization cases compensates for the uncertainty associated with the thermal/hydraulic behavior of the core due to coolant voiding during a locked rotor event.

17. The RPS setpoints assumed in the safety analysis (i.e., the low coolant loop flow rate reactor trip) are demonstrated to be conservative by the inclusion of appropriate uncertainties for process measurement and signal delay.

18. No mitigative operator actions, such as manual tripping of the reactor coolant pumps, are required to ensure that the acceptance criteria of the locked rotor event analysis are met. The locked rotor analysis conservatively assumes that the unaffected RCPs trip on low loop coolant flow two seconds following reactor trip. This assumption simulates the potential disruption of power supply to the unaffected RCP by the same mishap that caused the locked rotor event, or by the disassembly of the RCP following the locked rotor event.

15.4.4.2.2 Transient Analysis for DNB and Fuel Cladding Integrity

The transient analysis for DNB and fuel cladding integrity considerations utilizes the RETRAN transient analysis code (Reference 33) and the COBRA IIIC/MIT detailed core thermal/hydraulics code (Reference 34). Full cores of North Anna Improved Fuel (NAIF), Westinghouse standard (STD) 17 x 17 fuel, and Framatome ANP Advanced Mark-BW fuel are assumed. For the NAIF and STD fuel types, the WRB-1 critical heat flux correlation (Reference 53) is used in the analysis. DNB calculations for the Advanced Mark-BW fuel type were performed using the Framatome ANP Statistical Core Design Methodology with the Framatome ANP LYNXT thermal-hydraulic computer code and associated models, or the Dominion Statistical DNBR Evaluation Methodology with the VIPRE-D thermal-hydraulic computer code and associated models, as discussed in Section 4.5.

The transient analysis for DNB is performed to determine the number of fuel pins that experience DNB as a result of a Locked Rotor or Sheared Shaft event. A fuel pin is assumed to fail if the predicted MDNBR is less than the statistical DNBR (Reference 54) design limit. The Locked Rotor DNB event scenario is therefore designed to produce the most limiting DNB response. From an analytical perspective, this goal is achieved by choosing initial conditions and analysis assumptions that will maximize coolant temperature and the power-to-flow ratio, and minimize pressure during the event.

The analysis demonstrates that the fraction of fuel failure for this event is less than that which has been demonstrated to provide acceptable dose consequences.

15.4.4.2.3 Transient Analysis for RCS and Main Steam Overpressurization

The transient analysis for RCS and main steam overpressurization considerations utilizes the RETRAN transient analysis code (Reference 33). The transient analysis for overpressurization considerations verifies that the peak RCS pressure (intact cold leg pump exit pressure) and peak main steam pressure (intact loop steam generator pressure) remain below 110% of RCS and main steam design pressure (2750 psia and 1210 psia, respectively). The Locked Rotor overpressurization event scenario is designed to produce the most limiting overpressurization response. From an analytical perspective, this goal is achieved by choosing initial conditions and

analysis assumptions that will minimize RCS energy removal and minimize core coolant expansion during the transient.

Figures 15.4-75 through 15.4-81 present key analysis results from the limiting RCS and main steam overpressurization cases.

15.4.4.3 **Dose consequences of Locked Rotor Accident (LRA)**

The radiological analysis of a Locked Rotor design basis accident (LRA) includes doses associated with the failure of 13% of the fuel rods that are assumed to enter DNB during the accident. The methodology used to evaluate the control room and offsite doses resulting from the LRA accident was consistent with Regulatory Guide 1.183 (Reference 71) in conjunction with TEDE radiological units and limits, ARCON96 (Reference 78) based onsite (control room) atmospheric dispersion factors, and Federal Guidance Reports No. 11 and 12 (References 72 & 74) dose conversion factors. Doses were calculated at the EAB, at the LPZ, and in the control room.

The LRA begins with instantaneous seizure of the rotor or the break of the shaft of a reactor coolant pump. The sudden decrease in core coolant flow while the reactor is at power results in a degradation of core heat transfer, which could result in fuel damage. It is assumed in this analysis that the reactor is operating at 102% power level (2958 MWt). A turbine trip and coincident LOOP are incorporated into the analysis, resulting in a release of the accident source term through the steam generator PORVs and safety valves.

The release is modeled as starting immediately, at time t=0 seconds, and continuing for 8 hours, by which time the RCS temperature has reached 350°F. At this point the RHR system is activated, and the release to the atmosphere through the steam generator PORVs is terminated.

15.4.4.3.1 Source Term Definition

The core inventory was generated using the ORIGINS code as discussed in Section 15.4.1.7 and was converted to Curies/MWt to be used in the LRA analysis. These values were adjusted for use within RADTRAD-NAI to account for the assumed 102% core power (2958 MWt), the fraction of the fuel rods assumed to fail during the accident, and by the fractions of the core inventory assumed to be in the pellet to clad gap. In order to account for differences in power level across the core, a radial peaking factor was applied to the source term.

The LRA analysis is based on the assumption that 13% of the fuel in the core enters into DNB during the accident, and is therefore, assumed to fail. Currently, the analysis for the core DNBR response confirms that no (0%) fuel failures, defined as the minimum DNBR less than the limit, occur. However, the 13% failed fuel assumption has been retained for future core design changes that may result in a core DNBR response greater than 0% fuel failures.

For non-LOCA events (including the LRA) the fractions of the core inventory assumed to be in the pellet to clad gap for the various groups of isotopes are given in Table 15.4-32.

Regulatory Guide 1.183 indicates that a radial peaking factor from the COLR should be used to account for differences in the power level across the core. In order to accommodate future fuel transition to a different vendor and future design changes, a conservative radial peaking factor of 1.65 was used.

The chemical form of radioiodine released from the fuel was assumed to be 95% cesium iodide (CsI), 4.85 percent elemental iodine, and 0.15 percent organic iodide. Iodine releases from the steam generators to the environment were assumed to be 97% elemental and 3% organic.

15.4.4.3.2 Release Transport

The source term resulting from the fuel failures discussed above is transported by the primary coolant through the leaks in the steam generator into the secondary coolant and is released to the environment through the steam generator PORVs and safety valves. The primary to secondary leak rate is assumed to be 1 gpm. The leakage is assumed to continue until shutdown cooling is in operation and releases from the steam generators are terminated. The transport model utilized for iodine and particulates is consistent with Appendix E of Regulatory Guide 1.183. All noble gases released from the primary system are assumed released to the environment without reduction or mitigation.

15.4.4.3.3 Atmospheric Dispersion Factors

The CR χ/Q values are new values that were calculated by using the ARCON96 code and guidance from Regulatory Guide 1.194. The CR χ/Q values are ground level χ/Q values calculated at the PORV release elevation that have been reduced by a factor of 5 to credit plume rise. This reduction was taken after verifying that (1) the release point is uncapped and vertically oriented and (2) the time-dependent vertical velocity exceeds the 95th-percentile highest wind speed (at the release point height) by a factor of 5.

The EAB and LPZ χ/Q values used in the Locked Rotor analysis are the same as those used in the LOCA analysis and are discussed in Section 15.4.1.7.

15.4.4.3.4 Analysis Assumptions and Input Parameters

The LRA analysis assumes no control room isolation. It also does not credit the function of the main control room/ESGR Bottled Air System and Emergency Ventilation System. It assumes that throughout the duration of the LRA, air is supplied to the control room through the normal intake. The normal control room intake has a nominal flow rate of 2800 cfm, has no filters, and is closer to the PORV release point than the emergency ventilation intakes. The normal ventilation flow rate was varied from 1000 cfm to 4000 cfm to determine the control room dose calculation sensitivity to this parameter and to account for unfiltered inleakage. A value of 3500 cfm, which includes 500 cfm of unfiltered inleakage, is assumed in the analysis. Occupancy factor and breathing rate is given in Table 15.4-6.

Table 15.4-33 summarizes the analysis assumptions and key input parameter values that are used in the Locked Rotor analysis.

15.4.4.3.5 LRA Dose Analysis Results

The results of the design basis Locked Rotor analysis are presented in Table 15.4-34. These results report the calculated dose for the worst 2-hour interval (EAB), and for the assumed 30 day duration of the event for the control room and the LPZ. The doses calculated with the TEDE methodology are compared with the applicable acceptance criteria specified in 10 CFR 50.67 and Regulatory Guide 1.183. As indicated in Table 15.4-34, all of the results meet the acceptance criteria.

15.4.4.4 **Conclusions**

The following conclusions are applicable to the analyzed scenarios described in Section 15.4.4.2:

a. A coolable core geometry is maintained throughout the transient, since the Departure from Nucleate Boiling Ratio (DNBR) transient analysis demonstrates that limited fuel failure due to the onset of DNB is predicted to occur.

b. Acceptable offsite dose consequences are ensured, since the analysis demonstrates that the fraction of fuel rods predicted to experience Departure from Nucleate Boiling (DNB) is less than that which provides acceptable offsite dose analysis results.

c. Reactor Coolant System (RCS) integrity is maintained throughout the transient as demonstrated by analysis of transient RCS pressure. Specifically, the maximum RCS pressure, which occurred in the intact cold leg pump exit, remained below 2750 psia throughout the transient.

d. Main Steam System (MSS) integrity is maintained throughout the transient as demonstrated by analysis of transient MSS pressure. Specifically, the maximum main steam pressure, which occurred in the intact loop steam generator, remained below 1210 psia throughout the transient.

e. Containment integrity is maintained throughout the transient as demonstrated by engineering evaluation of the results of the RCS overpressurization analysis. Specifically, the RCS pressure boundary remains intact since it is not overpressurized, and mass and energy release to containment through the pressurizer safety valves and/or the pressurizer PORVs is bounded by that of the large break LOCA event.

15.4.5 Fuel Handling Accident (FHA)

The fuel handling accident (FHA) is defined as the dropping of a spent fuel assembly underwater such that the cladding of all the fuel rods in the fuel assembly rupture. The rods are assumed to instantaneously release their fission gas contents to the water surrounding the fuel assemblies. This accident can occur inside containment or in the fuel building. The radiological

analysis of the FHA was done as part of the change in the North Anna source term from TID-14844 (Reference 14) to the AST as defined in NUREG-1465 (Reference 77). The methodology used to evaluate the control room and offsite doses resulting from a FHA was consistent with Regulatory Guide 1.183 (Reference 71). The FHA radiological analysis employed the TEDE calculational method, consistent with the radiation protection standards in 10 CFR Part 20 and as specified in Regulatory Guide 1.183 (Reference 71) for AST applications. The results have been compared with the acceptance criteria contained either in 10 CFR 50.67(b)(2) or supplemental guidance in Regulatory Guide 1.183 (Reference 71). Dose calculations were performed at the EAB for the worst 2 hour period. All the radiological consequence calculations for the FHA were preformed with the RADTRAD-NAI computer code (Reference 75).

In accordance with regulatory position 3 of Regulatory Guide 1.183 (Reference 71), the FHA analysis core source was generated with the ORIGENS computer code at the End of Cycle (EOC) using a bounding cycle design (based on the Dominion fuel management scheme). ORIGENS is part of the SCALE computer code system (Reference 80) and was used to determine the decay of the isotopes at various times after shutdown. The design basis FHA is assumed to occur 100 hours after shutdown or the entrance into MODE 3. Table 15.4-11 contains the ORIGENS decay results at 100 hours after shutdown for the 14 Noble Gas and Iodine isotopes that have significant activity remaining, and would be gaseous and water insoluble, i.e., have the potential to become airborne and contribute to the dose consequences. The core inventory shown in Table 15.4-11 was used to calculate the gap activity of one fuel assembly, shown in Table 15.4-12.

15.4.5.1 Release and Transport of the Fuel Assembly Gap Activity

The limiting fuel assembly gap activity shown in Table 15.4-12 was modeled in RADTRAD-NAI (Reference 75) as being released instantaneously into the spent fuel pool or reactor cavity. Since the spent fuel pool or reactor cavity water is at least 23 feet above the top of the fuel, Regulatory Guide 1.183 indicates that an effective decontamination factor (DF) of 200 should be used to model iodine retention in the pool. In the RADTRAD-NAI model, the effective DF of 200 is modeled by dividing the gap activity of iodine from Table 15.4-12 by 200. The speciation of the iodine above the water is 57% elemental iodine and 43% organic iodine.

Nearly 100% (>99.9%) of the activity released into the containment or fuel building as a result of the FHA was assured to be released into the environment within 2 hours by assuming a flow rate of 80,000 cfm. This flow bounds the capacity of the fuel building and containment ventilation systems, maximizing the resulting doses.

The onsite atmospheric dispersion factors were calculated using the ARCON96 code (Reference 78) and guidance from Regulatory Guide 1.194 (Reference 73). Site meteorological data taken over the years 1997-2001 was used as ARCON96 input. Ground level χ/Q values were calculated with the control room normal and emergency intakes as receptors, using various release points. The control room dose consequences from the containment release were more limiting

than the dose consequences from the fuel building due to the larger χ/Qs. This is also why the equipment hatch release was bounded by the release from the containment via the personnel airlock. The control room χ/Qs used in the analysis are shown in Table 15.4-13. The EAB and LPZ atmospheric dispersion factors are the same as those used in the LOCA analysis and are discussed in Section 15.4.1.7 and are included in Table 15.4-13.

15.4.5.2 Control Room Configuration

The control room was modeled as isolated prior to the release reaching the normal control room intakes. The control room was assumed to have unfiltered inleakage of 400 cfm for the duration of the accident. The control room was modeled with 900 cfm of outside filtered air flow which is established 1 hour after isolation, with an elemental iodine filter efficiency of 95% and an organic iodine filter efficiency of 95% as shown in Table 15.4-13.

15.4.5.3 RADTRAN-NAI Model

The FHA analysis considered sufficient release pathways, MCR/ESGR envelope configurations, and ventilation system and release flow rates to determine the envelope and offsite doses. The analysis assumptions and key input parameter values used in the FHA analysis are summarized in Table 15.4-13.

15.4.5.4 FHA Analysis Results

The dose to the control room as a result of an FHA was analyzed to be 4.9 rem TEDE. The control room dose limit specified in 10 CFR 50.67 is 5.0 rem TEDE. The FHA analysis was based on a control room configuration that credits isolation and 900 cfm of outside filtered air flow established 1 hour after isolation.

The offsite dose was calculated to be 1.0 rem TEDE for the worst-case 2-hour EAB and 0.1 rem TEDE for the 30-day LPZ. These results are less than the offsite limit of 6.3 rem TEDE from Regulatory Guide 1.183 (Reference 71).

15.4.6 Rupture of a Control Rod Drive Mechanism Housing (Rod Cluster Control Assembly Ejection)

15.4.6.1 Identification of Causes and Accident Description

This accident is defined as the mechanical failure of a control rod mechanism pressure housing, resulting in the ejection of a rod cluster control assembly and drive shaft. The consequence of this mechanical failure is a rapid reactivity insertion together with an adverse core power distribution, possibly leading to localized fuel rod damage.

15.4.6.1.1 Design Precautions and Protection

Certain features in Westinghouse pressurized water reactors are intended to preclude the possibility of a rod-ejection accident, or to limit the consequences if the accident were to occur. These include a sound, conservative mechanical design of the rod housings, a thorough quality

control (testing) program during assembly, and a nuclear design that lessens the potential ejection worth of rod cluster control assemblies and minimizes the number of assemblies inserted at power.

15.4.6.1.1.1 *Mechanical Design.* The mechanical design is discussed in Section 4.2. Mechanical design and quality control procedures intended to preclude the possibility of a rod cluster control assembly (RCCA) drive mechanism housing failure sufficient to allow a rod cluster control assembly to be rapidly ejected from the core are listed below:

1. Each control rod drive mechanism housing is completely assembled and shop-tested at 4100 psi.
2. The mechanism housings are individually hydrotested as they are attached to the head adapters in the reactor vessel head, and checked during the hydrotest of the completed reactor coolant system.
3. Stress levels in the mechanism are not affected by anticipated system transients at power, or by the thermal movement of the coolant loops. Moments induced by the design-basis earthquake can be accepted within the allowable primary working stress range specified by the ASME Code, Section III, for Class I components.
4. The latch mechanism housing and rod travel housing are each a single length of forged type 304 stainless steel. This material exhibits excellent notch toughness at all temperatures that will be encountered.

A significant margin of strength in the elastic range, together with the large energy absorption capability in the plastic range, gives additional assurance that gross failure of the housing will not occur. The joints between the latch mechanism housing and head adapter, and between the latch mechanism housing and rod travel housing, are threaded joints reinforced by canopy-type rod welds. Administrative regulations require periodic inspections of these (and other) welds.

15.4.6.1.1.2 *Nuclear Design.* Even if a rupture of a RCCA drive mechanism housing is postulated, the operation of a plant using chemical shim is such that the severity of an ejected rod cluster control assembly is inherently limited. In general, the reactor is operated with the rod cluster control assemblies inserted only far enough to permit load follow. Reactivity changes caused by core depletion and xenon transients are compensated for by boron changes. Further, the location and grouping of control rod banks are selected during the nuclear design to lessen the severity of a RCCA-ejection accident. Therefore, should a rod cluster control assembly be ejected from its normal position during full-power operation, only a minor reactivity excursion, at worst, could be expected to occur.

However, it may occasionally be desirable to operate with larger than normal insertions. For this reason, a rod insertion limit is defined as a function of power level. Operation with the rod cluster control assemblies above this limit guarantees adequate shutdown capability and

acceptable power distribution. The position of all rod cluster control assemblies is continuously indicated in the control room. An alarm will occur if a bank of rod cluster control assemblies approaches its insertion limit or if one assembly deviates from its bank. There are low- and low-low-level insertion monitors with visual and audio signals.

15.4.6.1.1.3 *Reactor Protection.* The reactor protection in the event of a rod-ejection accident has been described in Reference 23. The protection for this accident is provided by high-neutron-flux trip (high and low setting) and high rate of neutron flux increase trip. These protection functions are described in detail in Section 7.2.

15.4.6.1.1.4 *Effects on Adjacent Housings.* Disregarding the remote possibility of the occurrence of a RCCA mechanism housing failure, investigations have shown that failure of a housing due to either longitudinal or circumferential cracking is not expected to cause damage to adjacent housings leading to increased severity of the initial accident.

15.4.6.1.2 Limiting Criteria

Due to the extremely low probability of a RCCA-ejection accident, limited fuel damage is considered an acceptable consequence.

Comprehensive studies of the threshold of fuel failure and of the threshold of significant conversion of the fuel thermal energy to mechanical energy have been carried out as part of the SPERT project by the Idaho Nuclear Corporation (Reference 24). Extensive tests of zirconium-clad UO_2 fuel rods representative of those in pressurized-water-reactor-type cores have demonstrated failure thresholds in the range of 240 to 257 cal/gm. However, other rods of a slightly different design have exhibited failures as low as 225 cal/gm. These results differ significantly from the TREAT (Reference 25) results, which indicated a failure threshold of 280 cal/gm. Limited results have indicated that this threshold decreases by about 10% with fuel burn-up. The clad failure mechanism appears to be melting for zero burn-up rods and brittle fracture for irradiated rods. Also important is the conversion ratio of thermal to mechanical energy. This ratio becomes marginally detectable above 300 cal/gm for unirradiated rods and 200 cal/gm for irradiated rods; catastrophic failure (large fuel dispersal, large pressure rise), even for irradiated rods, did not occur below 300 cal/gm.

In view of the above experimental results, conservative criteria are applied to ensure that there is little or no possibility of fuel dispersal in the coolant, gross lattice distortion, or severe shock waves. These criteria are:

1. Average fuel pellet enthalpy at the hot spot below 225 cal/gm for unirradiated fuel and 200 cal/gm for irradiated fuel.
2. Peak clad temperature at the hot spot below the temperature at which clad embrittlement may be expected (2700°F).
3. Peak reactor coolant pressure less than that which would cause stresses to exceed the faulted condition stress limits.

4. Fuel melting limited to less than 10% of the fuel volume at the hot spot even if the average fuel pellet enthalpy is below the limits of criterion 1 above.

Revised acceptance criteria have been developed for the response of light water reactor fuel under reactivity initiated accidents (Reference 67). Development of these revisions is part of an industry effort to extend burnup levels beyond currently licensed limits. The revised criteria are proposed for use in licensing burnup extensions or new fuel designs.

Reference 67 recommended more conservative acceptance criteria for average fuel pellet enthalpy at the hot spot assuming hot zero power initial conditions. The average fuel pellet enthalpy limits at the hot spot are 170 cal/gm for low burnup fuel (below 36 GWD/MTU) and 125 cal/gm for high burnup fuel (36 GWD/MTU or more). These limits were applied to the hot zero power cases considered in the analysis of record documented in this section.

15.4.6.2 **Analysis of Effects and Consequences**

15.4.6.2.1 Method of Analysis

Previous analyses of this event are documented in the original FSAR, and in References 31, 39 and 40. The original FSAR analysis was performed with the Westinghouse FACTRAN/TWINKLE methodology (Reference 26). Reference 39 updated the original analysis to accommodate higher ejected rod worths and peaking factors realized for Cycle 2 operation. The Reference 40 analysis was performed to reflect the positive (+6 pcm/°F) moderator temperature coefficient at beginning of cycle, and used Vepco methodology (Reference 41). Reference 31 updated the analyses for core power uprated conditions. The analysis of Reference 43 determined that the use of ZIRLO cladding results in a small reduction in both the fraction of fuel melting at the hot spot and the fuel peak stored energy when compared with the results for Zircaloy clad fuel (Reference 48). Therefore, this analysis is applicable for either clad material. The most recent analysis (Reference 63) is described in the detail below. The analysis of Reference 63 considered both a full core of Westinghouse fuel and a full core of Framatome Mark-Bw fuel in the rod ejection analysis of record. The analysis found that the results assuming a full core of Framatome fuel bound the results for a full core of Westinghouse fuel.

The analysis discussed below encompasses both the Westinghouse and Framatome fuel products. Beginning with Cycle 17 for Unit 2 and Cycle 18 for Unit 1, the Advanced Mark-BW fuel product was introduced in mixed cores with the LOPAR and NAIF assemblies.

The analysis of the RCCA-ejection accident is performed in two stages; first, an average core nuclear power transient calculation, and then a hot-spot heat transfer calculation. The average core power calculation is performed using point neutron kinetics methods to determine the average power generation with time, including the various total core feedback effects, i.e., Doppler reactivity and moderator reactivity. Enthalpy and temperature transients in the hot spot are then determined by multiplying the average core energy generation by the hot-channel factor

and performing a fuel rod transient heat transfer calculation. The power distribution calculated without feedback is pessimistically assumed to persist throughout the transient.

A detailed discussion of the method of analysis can be found in Reference 41.

15.4.6.2.1.1 *Average Core Analysis.* The point kinetics model of the RETRAN computer code (References 33 & 41) is used to perform the average core transient analysis. This code includes the simulation of prompt and delayed neutrons (using the six-group model), the thermal kinetics of the fuel and moderator and the balance of the NSS primary and secondary coolant system. Thermal feedback effects are modeled via temperature dependent reactivity coefficients with a detailed multiregion, transient fuel-clad-coolant heat transfer model. Reactivity insertion from the ejection of the control rod and the subsequent reactor trip are accounted for.

Since both the axial and radial dimensions are missing, it is necessary to use very conservative methods (described below) of calculating the ejected-rod worth and hot-channel factor.

15.4.6.2.1.2 *Hot-Spot Analysis.* The average core energy addition, calculated as described above, is multiplied by the appropriate hot-channel factors, and the hot-spot analysis is performed using the detailed fuel and clad transient heat transfer model of the RETRAN code termed the Hot Spot Model, (see Reference 41). This model calculates the transient temperature distribution in a cross section of a metal-clad UO_2 fuel rod, and the heat flux at the surface of the rod, using as input the nuclear power versus time and the local coolant conditions. The zirconium-water reaction is explicitly represented, and all material properties are represented as functions of temperature. A parabolic radial power generation is used within the fuel rod.

The RETRAN Hot Spot Model uses the Thom subcooled boiling correlation to determine the film heat transfer before departure from nucleate boiling, and the Bishop-Sandberg-Tong correlation (Reference 29) to determine the film-boiling coefficient after departure from nucleate boiling. The DNB heat flux is not calculated; instead, the code is forced into departure from nucleate boiling by specifying a conservative DNB heat flux. The gap heat transfer coefficient is adjusted to force the full-power steady-state temperature distribution to agree with that predicted by design fuel heat transfer codes.

For full-power cases, the design initial hot-channel factor (Fqt) is input to the code. The hot-channel factor during the transient is assumed to increase from the steady-state design value to the maximum transient value in 0.1 second, and remain at the maximum for the duration of the transient. This is conservative, since detailed spatial kinetics models show that the hot-channel factor decreases shortly after the nuclear power peak due to the power flattening caused by preferential feedback in the hot channel (Reference 26).

15.4.6.2.1.3 *System Overpressure Analysis.* Because safety limits for fuel damage specified earlier are not exceeded, there is little likelihood of fuel dispersal into the coolant. The pressure

surge may therefore be calculated on the basis of conventional heat transfer from the fuel and prompt heat generation in the coolant.

The pressure surge is calculated by first performing the fuel heat transfer calculation to determine the average and hot-spot heat flux versus time. Using these heat flux data, a THINC calculation is conducted to determine the volume surge. Finally, the volume surge is simulated in a plant transient computer code. This code calculates the pressure transient, taking into account fluid transport in the system, heat transfer to the steam generators, and the action of the pressurizer spray and pressure relief valves. No credit is taken for the possible pressure reduction caused by the assumed failure of the control rod pressure housing (Reference 41).

Due to the very conservative method of analysis, the peak surge rate is high enough to cause the reactor coolant pressure to exceed the pressurizer safety valve actuation pressure. However, this condition exists only for a few seconds; consequently, the pressurizer water volume does not change significantly (less than 150 ft^3). Therefore, the transient is not sensitive to the initial pressurizer level, and the programmed value is used.

15.4.6.2.2 Calculation of Basic Parameters

Input parameters for the analysis are conservatively selected on the basis of values calculated for this type of core. The more important parameters are discussed below. Table 15.4-14 presents the parameters used in this analysis.

15.4.6.2.2.1 *Ejected-Rod Worths and Hot-Channel Factors.* The values for ejected-rod worths and hot-channel factors are calculated using a synthesis of one-dimensional, two-dimensional and three-dimensional calculations. Standard nuclear design codes are used in the analysis. No credit is taken for the flux-flattening effects of reactivity feedback. The calculation is performed for the maximum allowed bank insertion at a given power level, as determined by the rod insertion limits. Adverse xenon distributions are considered in the calculation.

The total transient hot-channel factor, Fqt, is then obtained by combining the axial and radial factors.

Appropriate margins are added to the results to allow for calculational uncertainties, including an allowance for nuclear power peaking due to fuel densification.

15.4.6.2.2.2 *Reactivity Feedback Weighting Factors.* The largest temperature rises, and hence the largest reactivity feedbacks, occur in channels where the power is higher than average. Since the weight of a region is dependent on flux, these regions have high weights. This means that the reactivity feedback is larger than that indicated by a simple single-channel analysis. Physics calculations were carried out for a large number of radial temperature distributions. Reactivity changes are compared and effective weighting factors determined. These weighting factors take the form of multipliers that, when applied to single-channel feedbacks, correct them to effective whole-core feedbacks for the appropriate flux shape. In this analysis, although a point kinetics method is used, only a radial weighting factor is applied. In addition, no weighting is applied to

the moderator feedback. This very conservative radial weighting factor is applied to the Doppler reactivity feedback of the fuel as a function of the post-ejection radial power peaking factor to account for the missing spatial effect. This weighting factor has been shown to be conservative compared to three-dimensional analysis (see Reference 41).

15.4.6.2.2.3 *Moderator and Doppler Coefficient.* The critical boron concentrations at the BOC and EOC were adjusted in the nuclear code to obtain moderator density coefficient curves that are conservative compared to actual design conditions for the plant. As discussed above, no weighting factor is applied to this coefficient.

The Doppler reactivity coefficient is determined as a function of fuel temperature using a steady-state discrete ordinate transport computer code. The resulting curve is conservative compared to design predictions for this plant. The Doppler weighting factor will increase under accident conditions as discussed above. The transient weighting factor used in the analysis is presented in Table 15.4-14.

15.4.6.2.2.4 *Delayed Neutron Fraction, Beff.* Calculations of the effective delayed neutron fraction (Beff) typically yield values no less than 0.70% at BOC and 0.50% at EOC for the first cycle. The accident is sensitive to Beff if the ejected-rod worth is nearly equal to or greater than Beff, as in zero-power transients. To allow for future fuel cycles, conservative estimates of Beff of 0.52% at beginning of cycle and 0.43% at end of cycle were used in the analysis.

15.4.6.2.2.5 *Trip Reactivity Insertion.* The trip reactivity insertion is assumed to be 4% from hot full power and 1.77% from hot zero power, including the effect of one stuck rod (i.e., the ejected rod). The shutdown reactivity is simulated by a conservative curve of trip reactivity insertion versus time after trip. The start of the rod motion occurs 0.5 second after the high-neutron-flux point is reached. This delay is assumed to consist of 0.2 second for the instrument channel to produce a signal, 0.15 second for the trip breaker to open, and 0.15 second for the coil to release the rods. The analyses presented are applicable for a rod insertion time of 3.78 seconds. The choice of such a conservative insertion rate means that there is over 1 second after the trip point is reached before significant shutdown reactivity is inserted into the core. This is particularly significant conservatism for hot full-power accidents.

The rod insertion versus time is described in Section 15.1.5.

15.4.6.2.3 Results

The value of parameters used in the analysis, as well as the results of the analysis, are presented in Table 15.4-14 and discussed below.

15.4.6.2.3.1 *Beginning of Cycle, Full Power.* Control bank D was assumed to be inserted to its insertion limit. The worst ejected-rod worth and hot-channel factor were 0.18% delta k and 5.80, respectively. The peak hot-spot clad average temperature was 2585.1°F. The peak hot-spot fuel center temperature exceeded the assumed BOC melt temperature of 4900°F. However, melting was restricted to less than 10% of the pellet.

15.4.6.2.3.2 *Beginning of Cycle, Zero Power.* For this condition, control bank D was assumed to be fully inserted and control bank C was at its insertion limit. The worst ejected rod is located in control bank D and has a worth of 0.878 delta k and a hot-channel factor of 15.40. The peak hot-spot clad and fuel centerline temperatures reached 2636.5°F and 4193.2°F.

15.4.6.2.3.3 *End of Cycle, Full Power.* Control bank D was assumed to be inserted to its insertion limit. Conservative values of ejected-rod worth and hot-channel factor, 0.19% delta k and 5.70 respectively, were used. This resulted in a peak clad temperature of 2497.6°F. The peak hot-spot fuel temperature exceeded the assumed EOC melt temperature of 4800°F. However, melting was restricted to less than 10% of the pellet. The variation of melt temperature with burn-up is discussed in Section 4.4.1.

15.4.6.2.3.4 *End of Cycle, Zero Power.* The ejected-rod worth and hot-channel factor for this case were obtained assuming control bank D to be fully inserted and bank C at its insertion limit. Conservative values used in the analysis for this condition were 0.84% delta k and 16.0, respectively. The peak clad and fuel center temperatures reached 2213.6°F and 3626.1°F.

A summary of the cases presented above is given in Table 15.4-14. The nuclear power and hot-spot fuel and clad temperature transients for the worst cases (BOC full-power and EOC zero-power) are presented in Figures 15.4-82, 15.4-83, 15.4-84 and 15.4-85.

15.4.6.2.3.5 *Fission Product Release.* It is assumed that fission products are released from the gaps of all rods entering departure from nucleate boiling. In all cases considered, less than 10% of the rods entered departure from nucleate boiling, based on a detailed three-dimensional THINC analysis. Although limited fuel melting at the hot spot was predicted for the full-power cases, in practice, melting is not expected since the analysis conservatively assumed that the hot spots before and after ejection were coincident (Reference 41).

15.4.6.2.3.6 *Pressure Surge.* A detailed calculation of the pressure surge for an ejection worth of 1.5 dollars at BOC, HFP, indicates that the peak pressure does not exceed that which would cause stress to exceed the faulted condition stress limits (Reference 26). Since the severity of the present analysis does not exceed this worst-case analysis, the accident for this plant will not result in an excessive pressure rise or further damage to the reactor coolant system.

15.4.6.2.3.7 *Lattice Deformation.* A large temperature gradient will exist in the region of the hot spot. Since the fuel rods are free to move in the vertical direction, differential expansion between separate rods cannot produce distortion. However, the temperature gradients across individual rods may produce a force tending to bow the midpoint of the rods toward the hot spot. Physics calculations indicate that the net result of this would be a negative reactivity insertion. In practice, no significant bowing is anticipated, since the structural rigidity of the core is more than sufficient to withstand the forces produced. Boiling in the hot-spot region would produce a net flow away from the region. However, the heat from the fuel is released to the water relatively slowly, and it is considered inconceivable that cross flow will be sufficient to produce significant lattice forces. Even if massive and rapid boiling, sufficient to distort the lattice, is hypothetically postulated, the

large void fraction in the hot-spot region would produce a reduction in the total core moderator-to-fuel ratio, and a large reduction in this ratio at the hot spot. The net effect would therefore be a negative feedback. It can be concluded that no conceivable mechanism exists for a net positive feedback resulting from lattice deformation. In fact, a small negative feedback may result. The effect is conservatively ignored in the analyses.

15.4.6.3 **Conclusions**

Even on a pessimistic basis, the analyses indicate that the described fuel and clad limits are not exceeded. It is concluded that there is no danger of sudden fuel dispersal into the coolant. Since the peak pressure does not exceed that which would cause stresses to exceed the faulted condition stress limits, it is concluded that there is no danger of further consequential damage to the primary loop. The analyses have demonstrated that the upper limit in fission product release as a result of a number of fuel rods entering departure from nucleate boiling amounts to 10%.

15.4 REFERENCES

1. Letter from W. L. Stewart (VEPCO) to the USNRC, *Virginia Electric and Power Company, North Anna Power Station Unit 1, Proposed Technical Specification Change, Reduced Minimum RCS Flow Rate Limit to Support Increased Steam Generator Tube Plugging Level*, Serial No. 92-018, January 8, 1992.
2. Letter from Nick Liparulo (Westinghouse-Manager, Nuclear Safety & Regulatory Activities) to the USNRC, *Notification of Changes to the Westinghouse Large Break LOCA ECCS Evaluation Model*, ET-NRC-92-3787, December 22, 1992, transmittal of WCAP-10484, Addendum 1, *Spacer Grid Heat Transfer Effects During Reflood*.
3. Letter from W. L. Stewart to USNRC, *Virginia Electric and Power Company, Surry Power Station Units 1 and 2, North Anna Power Station Units 1 and 2, Report of ECCS Evaluation Model Changes Per Requirements of 10 CFR 50.46,* Serial No. 91-428, August 23, 1991.
4. T. L. Buterbaugh, W. J. Johnson, and S. D. Kopelic, *Westinghouse ECCS Plant Sensitivity Studies*, WCAP-8356, July 1974.
5. F. M. Bordelon, et al., *Westinghouse ECCS Evaluation Model - Summary*, WCAP-8339, July 1974.
6. F. M. Bordelon, et al., SATAN-VI Program: *Comprehensive Space-Time Dependent Analysis of Loss-of-Coolant*, WCAP-8306, June 1974.
7. F. M. Bordelon and E. T. Murphy, *Containment Pressure Analysis Code (COCO)*, WCAP-8326, June 1974.
8. R. D. Kelly, et al., *Calculational Model for Core Reflooding After a Loss-of-Coolant Accident (WREFLOOD Code*), WCAP-8171, June 1974.

9. F. M. Bordelon, et al., *LOCTA-IV Program: Loss-of-Coolant Transient Analysis*, WCAP-8305, June 1974.

10. Letter from C. M. Stallings, Vepco, to E. G. Case, NRC, Serial No. 092, dated February 17, 1978.

11. C. Eicheldinger, *Westinghouse ECCS Evaluation Model-1981 Version*, WCAP-9220-P-A, Revision 1 (Proprietary), WCAP-9221-A, Revision 1 (Non-proprietary), February 1982.

12. Letter from T. M. Anderson, Westinghouse, to J. F. Stolz, NRC, Serial No. NS-TMA-1981, dated November 1, 1978.

13. Letter from T. M. Anderson, Westinghouse, to R. Tedesco, NRC, Serial No. NS-TMA-2014, dated December 11, 1978.

14. J. J. DiNunno, F. D. Anderson, R. E. Baker, and R. L. Waterfield, *Calculation of Distance Factors for Power and Test Reactor Sites,* TID-14844, March 1962.

15. J. M. Geets, *MARVEL - A Digital Computer Code for Transient Analysis of a Multiloop PWR System*, WCAP-7909, June 1972.

16. F. S. Moody, *Transactions of the ASME*," *Journal of Heat Transfer*, February 1965, Figure 3, p. 134.

17. Letter from R. A. Clark, NRC, to R. H. Leasburg, Vepco, Subject: Main Steam Line Break with Continued Feedwater Addition, North Anna Power Station, Units 1 and 2, dated October 4, 1982.

18. U. S. Nuclear Regulatory Commission Office of Inspection and Enforcement, *Analysis of a PWR Main Steam Line Break with Continued Feedwater Additions*, *IE Bulletin 80-04*, February 8, 1980.

19. *Westinghouse Anticipated Transients Without Trip Analysis*, WCAP-8330, August 1974.

20. F. M. Bordelon, *Calculation of Flow Coastdown After Loss of Reactor Coolant Pump (PHOENIX Code)*, WCAP-7969, September 1972.

21. S. T. Maher, *LOFTRAN Code Description*, WCAP-7878, Revision 3, July 1981.

22. C. Hunin, *FACTRAN, A Fortran IV Code for Thermal Transients in a UO_2 Fuel Rod*, WCAP-7908, June 1972.

23. T. W. T. Burnett, *Reactor Protection System Diversity in Westinghouse Pressurized Water Reactor*, WCAP-7306, April 1969.

24. T. G. Taxelius, ed., *Annual Report - Spert Project, October 1968 and September 1969*, Idaho Nuclear Corporation IN-1370, June 1970.

25. R. C. Liimatainen and F. J. Testa, *Studies in TREAT of Zircaloy-2-Clad, UO_2-Core Simulated Fuel Elements*, ANL-7225, January - June 1966, p. 177, November 1966.

26. D. H. Risher, Jr., *An Evaluation of the Rod Ejection Accident in Westinghouse Pressurized Water Reactors Using Spatial Kinetics Methods*, WCAP-7588, Revision 1-A, January 1975.

27. D. H. Risher, Jr., and R. F. Barry, *TWINKLE - A Multi-Dimensional Neutron Kinetics Computer Code*, WCAP-7979, November 1972.

28. R. F. Barry, *LEOPARD - A Spectrum Dependent Non-Spatial Depletion Code for the IBM-7094*, WCAP 3269-26, September 1963.

29. A. A. Bishop, R. O. Sandberg, and L. S. Tong, *Forced Convection Heat Transfer at High Pressure After the Critical Heat Flux*, ASME 65-HT-31, August 1965.

30. G. E. Lang and J. P. Cunningham, *Report on the Consequences of a Postulated Main Feedline Rupture*, WCAP-9230, January 1978.

31. Letter from W. L. Stewart (Virginia Power) to Harold R. Denton (NRC), Amendment to Operating Licenses NPF-4 and NPF-7 for Rated Thermal Power of 2893 MWt, Serial No. 85-077, May 2, 1985.

32. Letter from L. B. Engle (NRC) to W. L. Stewart (Virginia Power), 2893 MWt Rated Thermal Power approval for North Anna Units 1 and 2, August 25, 1986.

33. N. A. Smith, *Vepco Reactor System Transient Analyses Using the RETRAN Computer Code*, VEP-FRD-41, Rev. 0.1-A, June 2004.

34. F. W. Sliz and K. L. Basehore, *Vepco Reactor Core Thermal-Hydraulic Analysis Using the COBRA IIIC/MIT Computer Code*, VEP-FRD-33-A, October 1983.

35. WCAP-10266-P-A, Rev. 2, *The 1981 Version of Westinghouse ECCS Evaluation Model Using the BASH Code*, March 1987.

36. WCAP-10444-P-A, Addendum 2, *Vantage 5H Fuel Assembly*, April 1988.

37. Letter from W. L. Stewart (Virginia Power) to Harold R. Denton (NRC), *North Anna Response to Request for Additional Information on Core Uprate*, Serial No. 85-772A, February 6, 1986.

38. Letter from W. L. Stewart (Virginia Power) to Harold R. Denton (NRC), *Transmitting Revised Results For CD=0.4 LOCA Analysis*, Serial No. 85-077A, August 20, 1986.

39. Letter from C. M. Stallings (Vepco) to H. R. Denton (NRC), Serial No. 867, November 2, 1979.

40. Letter from W. L. Stewart (Vepco) to H. R. Denton (NRC), Serial No. 666, *Amendment to Operating Licenses NPF-4 and NPF-7, North Anna Power Station Unit Nos. 1 and 2, Proposed Technical Specification Change*, February 7, 1985.

41. J. G. Miller and J. O. Erb, *Vepco Evaluation of the Control Rod Ejection Transient*, VEP-NFE-2-A, December 1984.

42. Letter from W. L. Stewart to NRC: *North Anna Power Station Units 1 and 2, Proposed Technical Specifications Change, North Anna Fuel Assembly Design Change*, Serial No. 89-795, dated January 15, 1990.

43. Letter from N. J. Liparulo (Westinghouse-Manager, Nuclear Safety & Regulatory Activities) to USNRC, *Results of Technical Evaluation of Containment Initial Temperature Assumptions for Large Break Loss of Coolant Accident Analysis*, ET-NRC-92-3699, June 1, 1992.

44. Letter from N. J. Liparulo (Westinghouse-Manager, Nuclear Safety & Regulatory Activities) to USNRC, *Westinghouse Methodology for Implementation of 10 CFR 50.46 Reporting*, ET-NRC-92-3755, October 30, 1992; transmittal of WCAP-13451, *Westinghouse Reporting Methodology for Implementation of 10 CFR 50.46 Reporting*.

45. *Westinghouse ECCS Evaluation Model: Revised Large Break LOCA Power Distribution Methodology,* WCAP-12909-P, June 1991.

46. Davidson, S. L. and Nuhfer, D. L. (Eds.), *VANTAGE+ Fuel Assembly Reference Core Report*, WCAP-12610-P-A (Proprietary), April 1995.

47. Slagle, W. H. (Editor), *Westinghouse Fuel Assembly Reconstitution Evaluation Methodology*, WCAP-13060-P-A (Proprietary), July 1993.

48. Letter from L. B. Engle to W. L. Stewart, *North Anna Unit 2 Issuance of Amendment Re: Reduction in Reactor Coolant System Flow Rate*, North Anna Unit 2 Amendment No. 152, dated August 30, 1993.

49. Brookmire, T. A., *Reload Transition Safety Report for Implementation of PERFORMANCE+ Debris Resistance Features at North Anna Units 1 and 2*, NE-0949, Revision 0, August 1993.

50. Letter from N. J. Liparulo (Westinghouse) to the USNRC, *Change in Methodology for Execution of BASH Evaluation Model*, NTD-NRC-94-4143, May 23, 1994.

51. Letter from N. J. Liparulo (Westinghouse) to the USNRC, *Change in Methodology for Execution of BASH Evaluation Model*, NTD-NRC-95-4540, August 29, 1995.

52. Letter from N. J. Liparulo (Westinghouse) to the USNRC, *Withdrawal of WCAP-12909-P on Power Shape Sensitivity Model (PSSM)*, NTD-NRC-95-4518, August 7, 1995.

53. R. C. Anderson, *Qualification of the WRB-1 CHF Correlation in the Virginia Power COBRA Code*, Topical Report VEP-NE-3, dated November 1986.

54. R. C. Anderson, *Statistical DNBR Evaluation Methodology*, Topical Report VEP-NE-2A, dated June 1987.

55. Standard Review Plan 6.4, *Control Room Habitability System,* 1981.

56. Standard Review Plan 15.6.5, *Loss-of-Coolant Accidents Resulting from Spectrum of Postulated Piping Breaks Within the Reactor Coolant Pressure Boundary,* 1981

57. U.S. Nuclear Regulatory Commission, Office of Standards Development, *Design, Testing, and Maintenance Criteria for Atmosphere Cleanup System Air Filtration and Adsorption Units of Light-Water-Cooled Nuclear Power Plants,* Regulatory Guide 1.52, June 1973.

58. K.G. Murphy and K.M. Campe, *Nuclear Power Plants Control Room Ventilation System Design for Meeting General Design Criterion 19,* 13th AEC Cleaning Conference, August 1974.

59. Letter from NRC to Virginia Power, Serial Number 90-116, *North Anna 1 and 2 - Issuance of Amendments Re: Limiting Dose to Control Room Operators,* February 28, 1990.

60. NUREG-0053, Safety Evaluation Report, *North Anna Power Station Units 1 and 2,* June 1, 1976.

61. Nuclear Safety Advisory Letter NSAL-02-5, Revision 1, *Steam Generator Water Level Control System Uncertainty Issue,* April 22, 2002.

62. WCAP-16115-P, *Steam Generator Level Uncertainties Program,* September 2003.

63. Letter from Leslie N. Hartz (Virginia Electric and Power Company) to USNRC, *Virginia Electric and Power Company North Anna Power Station Units 1 and 2, Proposed Technical Specifications Changes and Exemption Request Use of Framatome ANP Advanced Mark-BW Fuel,* Serial Number 02-167, March 28, 2002.

64. Letter from USNRC to D. A. Christian, *North Anna Power Station, Units 1 and 2, Issuance of Exemption from the Requirements of 10 CFR 50.44, 10 CFR 50.46, and 10 CFR Part 50, Appendix K, to Allow the Use of the M5 Alloy for Fuel Cladding Material (TAC Nos. MB4700 and MB4701),* September 23, 2003.

65. Letter from USNRC to D. A. Christian, *North Anna Power Station, Unit 2 - Issuance of Amendment Re: Use of Framatome ANP Advanced Mark-BW Fuel (TAC No. MB4715),* April 1, 2004.

66. Letter from USNRC to D. A. Christian, *North Anna Power Station, Unit 1 - Issuance of Amendments Re: Use of Framatome ANP Advanced Mark-BW Fuel (TAC No. MB4714 ,* August 20, 2004.

67. *Topical Report on Reactivity Initiated Accident: Bases for RIA Fuel and Coolability Criteria,* EPRI, Palo Alto, CA: 2002. 1002865.

68. EMF-2103(P)(A) Revision 0, Realistic Large Break LOCA Methodology, Framatome ANP, September 2003.

69. Technical Program Group, Quantifying Reactor Safety Margins, NUREG/CR-5249, EGG-2552, December 1989.

70. Letter from Leslie N. Hartz (Virginia Electric and Power Company) to USNRC, *Virginia Electric and Power Company North Anna Power Station Units 1 and 2, Proposed Technical Specifications Changes and Exemption Request Use of Framatome ANP Advanced Mark-BW Fuel, Supplemental Information for Realistic Large Break Loss of Coolant Accident (RLBLOCA) Analysis Results,* Serial Number 03-313G, November 10, 2003.

71. Regulatory Guide 1.183, *Alternative Radiological Source Terms for Evaluating Design Basis Accidents at Nuclear Power Reactors,* USNRC, Office of Nuclear Regulatory Research, July 2000.

72. Federal Guidance Report No. 11, *Limiting Values of Radionuclide Intake and Air Concentration and Dose Conversion Factors for Inhalation, Submersion, and Ingestion,* EPA 520/1-88-020, Environment Protection Agency, 1988.

73. Regulatory Guide 1.194, *Atmospheric Relative Concentrations for Control Room Radiological Habitability Assessments at Nuclear Power Plants,* U.S. Nuclear Regulatory Commission, Office of Nuclear Regulatory Research, June 2003.

74. Federal Guidance Report No. 12, *External Exposures to Radionuclides in Air, Water and Soil,* EPA 420-r-93-081, Environmental Protection Agency, 1993.

75. Computer Code RADTRAD-NAI, Version 1.0p3(QA), Numerical Applications, Inc., Richland, WA.

76. 10 CFR 50.67, Accident Source Term.

77. NUREG-1465, *Accident Source Terms for Light Water Nuclear Power Plants,* U.S. Nuclear Regulatory Commission, February 1995.

78. Computer Code ARCON96, *Atmospheric Relative Concentrations in Building Wakes,* NUREG/CR- 6331, PNNL-10521, Rev. 1, May 1997.

79. Letter SN 03-464, *North Anna Power Station Unit 1 and 2 - Proposed Technical Specification Changes Implementation of Alternate Source Term,* September 12, 2003.

80. Computer code Scale 4.4a, Version 1, Mod 0.

81. NUREG/CR-5966, *A Simplified Model of Aerosol Removal by Containment Sprays,* U.S. Nuclear Regulatory Commission, June 1993.

82. NUREG-0800, *Standard Review Plan,* Section 6.5.2, *Containment Spray as a Fission Product Cleanup System,* Rev. 2, U.S. Nuclear Regulatory Commission, December 1988.

83. Brookhaven National Laboratory Final Report, TTC-1010, Rev. 0, *Multi-Tracer Testing at Dominion's North Anna Station for Air In-Leakage Determination,* March 2004.

84. Letter SN 04-494A, *North Anna Power Station Unit 1 and 2 - Response to Request for Additional Information Proposed Technical Specification Changes Implementation of Alternate Source Term Revised Dose Analysis And Technical Specification Changes,* November 3, 2004.

85. WCAP-13132, *The Effect of Steam Generator Tube Uncovery on Radioiodine Release,* January 1992.

86. WCAP-13247, *Report on the Methodology for the Resolution of the Steam Generator Tube Uncovery Issue.*

87. Letter from R. C. Jones, USNRC, to L. A. Walsh, Westinghouse Owners Group, *Westinghouse Owners Group, Steam Generator Tube Uncovery Issue,* March 10, 1993.

88. BAW-2149-A, *Evaluation of Replacement Rods in BWFC Fuel Assemblies,* September 1993.

15.4 REFERENCE DRAWINGS

The list of Station Drawings below is provided for information only. The referenced drawings are not part of the UFSAR. This is not intended to be a complete listing of all Station Drawings referenced from this section of the UFSAR. The contents of Station Drawings are controlled by station procedure.

	Drawing Number	Description
1.	11715-FM-1E	Machine Location: Reactor Containment, Sections 1-1 & 5-5, Unit 1
2.	11715-FB-7A	Arrangement: Reactor Containment, Air Cooling and Purging System, Sheet 1
3.	11715-FB-7B	Arrangement: Reactor Containment, Air Cooling and Purging System, Sheet 2
4.	11715-FB-7C	Arrangement: Reactor Containment, Air Cooling and Purging System, Sheet 3
5.	11715-FB-7D	Arrangement: Reactor Containment, Air Cooling and Purging System, Sheet 4
6.	11715-FB-7E	Arrangement: Reactor Containment, Air Cooling and Purging System, Sheet 5
7.	11715-FK-9A	Instrument Piping, Radiation Monitoring, Sheet 1, Units 1 & 2
8.	11715-FK-9B	Instrument Piping, Radiation Monitoring, Sheet 2, Units 1 & 2

Table 15.4-1
INITIAL CORE CONDITIONS ASSUMED FOR THE
DOUBLE-ENDED COLD LEG GUILLOTINE BREAK (DECLG)

Calculational Input	
Core Power, 102% of	2893 MWt
Peak Linear Power, 102% of	12.43 kW/ft
Peak Heat Flux Hot Channel Factor	2.19 F_Q
Peak Nuclear Enthalpy Hot Channel Factor	1.55 $F\Delta h$
Accumulator Water Volume/accumulator	1025 ft^3
Reactor Vessel Upper Head Temperature	T_{hot}

Limiting Fuel Region and Cycle	Cycle	Region
Unit 1	All	All Regions
Unit 2	All	All Regions

Table 15.4-2
CONTAINMENT DATA

Net Free Volume	1.916×10^6 ft^3
Initial Conditions [a]	
Pressure	9.15 psia
Temperature	100.0°F
RWST Temperature	35.0°F
Outside Temperature	-10.0°F
Spray System [a]	
Number of Pumps Operating	2
Runout Flow Rate (per pump) [b]	2000 gpm
Time in Which Spray is Effective	53 sec

Structural Heat Sinks [a, c]

Thickness in.	Area (ft^2, with allowance for uncertainties)
6 concrete	8393
12 concrete	62,271
18 concrete	55,365
24 concrete	11,591
27 concrete	9404
36 concrete	3636
.375 steel, 54 concrete	22,039
.375 steel, 54 concrete	28,933
.500 steel, 30 concrete	25,673
26.4 concrete, 0.25 steel, 120 concrete	12,110
.407 stainless steel	10,527
.371 steel	160,328
.882 steel	9894
.059 steel	60,875

a. See UFSAR Section 6.3.3.12 for a detailed breakdown of the containment heat sinks and for justification of the other input parameters used to calculate containment pressure.
b. A bounding value was used for the runout pump flowrate.
c. For Advanced Mark-BW fuel only, a conservative metal surface area and mass were used to model the AECL containment sump strainer in the ECCS containment backpressure analysis.

Table 15.4-3
TIME SEQUENCE OF EVENTS

	Cosine, C_d=0.4	Cosine, C_d=0.6	Skewed, C_d=0.4
Start	0	0	0
Reactor Trip	0.54 sec	0.53 sec	0.54 sec
SI Signal Generated	2.8 sec	2.2 sec	2.8 sec
Accumulator Injection	17.0 sec	12.0 sec	17.0 sec
Pumped SI Starts	29.8 sec	29.2 sec	29.8 sec
End of Bypass/ End of Blowdown	33.8 sec	28.5 sec	33.8 sec
Bottom of Core Recovery	47.7 sec	42.0 sec	47.6 sec
Accumulator Empty	56.6 sec	51.3 sec	56.6 sec

Table 15.4-4
RESULTS FOR DECLG

	Cosine, C_d=0.4	Cosine, C_d=0.6	Skewed, C_d=0.4
Peak Clad Temperature	2009.7°F	1875.8°F	2086.0°F
Peak Clad Location	7.25 ft	7.25 ft	10.75 ft
Hot Rod Burst Data			
Location	5.25 ft	5.50 ft	8.25 ft
Time	47.68 sec	54.32 sec	54.20 sec
Zr/H_2O Results Data			
Local Maximum Reaction	4.03%	2.51%	6.19%
Location of Maximum	7.25 ft	9.00 ft	10.75 ft
Total Reaction	0.39%	0.18%	0.54%

Table 15.4-5

PEAK CLAD TEMPERATURE INCLUDING ALL PENALTIES AND BENEFITS
LARGE BREAK LOCA

Unit 1	
PCT for Analysis of Record	2086°F
PCT Assessments Allocated to AOR	
a. LOCBART Pellet Volumetric Heat Generation Rate	+45°F
LBLOCA PCT for Comparison to 10 CFR 50.46 Requirements	2131°F
Unit 2	
PCT for Analysis of Record	2086°F
PCT Assessments Allocated to AOR	
a. LOCBART Pellet Volumetric Heat Generation Rate	+45°F
LBLOCA PCT for Comparison to 10 CFR 50.46 Requirements	2131°F

Table 15.4-6
BASIC INPUTS AND ASSUMPTIONS USED IN
LOCA RADIOLOGICAL ANALYSIS

NSSS Parameters	
Core Power	2958 MWt [a]
Number of Fuel Assemblies	157
Containment Free Volume	1.916E+06 ft^3
Main Control Room (MCR) Parameters	
Effective Volume	7.910E+04 ft^3 [b]
Offsite Atmospheric Dispersion Factors	
Exclusion Area Boundary, EAB (0 – 2 hours)	3.10E-4 sec/m^3
Low Population Zone, LPZ	
0 – 8 hours	1.10E-5 sec/m^3
8 – 24 hours	7.30E-6 sec/m^3
24 – 96 hours	3.00E-6 sec/m^3
96 – 720 hours	8.20E-7 sec/m^3
Breathing Rates	
Control Room	3.5E-4 m^3/sec
Offsite (EAB & LPZ)	
0 – 8 hours	3.5E-4 m^3/sec
8 – 24 hours	1.8E-4 m^3/sec
24 – 720 hours	2.3E-4 m^3/sec
MCR/ESGR Envelope Occupancy Factors	
0 – 24 hours	1.0
24 – 96 hours	0.6
96 – 720 hours	0.4
MCR/ESGR Envelope Outside Supply Air Flow Rate	900 cfm
Filter Efficiencies	
EVS Filters	98% particulate iodine
	95% elemental iodine
	95% organic iodine
Auxiliary Building PREACS Filters	98% particulate iodine
	95% elemental iodine
	90% organic iodine

a. Rated thermal power for North Anna is 2893 MWt. Historically a value of 2958 MWt, which is slightly greater than 102% of rated thermal power, has been used in the dose analyses.

b. The nominal volume of the control room envelope is 230,000 ft^3. The value used was for the upper floor only and conservatively assumed no mixing between floors.

Table 15.4-6 (continued)
BASIC INPUTS AND ASSUMPTIONS USED IN
LOCA RADIOLOGICAL ANALYSIS

Time (hr)		Removal Coefficient (hr^{-1})
From	To	λ_{mf}
0.0203	0.556	5.83
0.556	0.667	6.17
0.667	0.833	12.34
0.833	1.11	12.45
1.11	1.39	12.45
1.39	1.50	12.34
1.50	1.80	11.87
1.80	1.88	7.57
1.88	1.97	5.29
1.97	2.35	2.82
2.35	3.82	1.53
3.82	5.46	1.37
5.46	7.13	1.35

Containment Sprayed Volume Versus Time

Time Period	Percent Sprayed	Volume Sprayed (ft^3)	Percent Unsprayed	Volume Unsprayed (ft^3)
73 seconds - 40 minutes	37.6%	7.204E+05	62.4%	1.196E+06
40 minutes - 1.5 hours	83.8%	1.606E+06	16.2%	3.104E+05
1.5 - 6 hours	73.1%	1.401E+06	26.9%	5.154E+05

Table 15.4-7
CONTROL ROOM ATMOSPHERIC DISPERSION FACTORS FOR THE LOCA

Source	Receptor Point	Atmospheric Dispersion Factor (sec/m^3)	
Containment Bldg	Normal Control Room Intake	2.61E-3	0-2 hr
		1.83E-3	2-8 hr
		7.72E-4	8-24 hr
		5.69E-4	24-96 hr
		4.35E-4	96-720 hr
Vent Stack	Emergency Control Room Intake	3.75E-3	0-2 hr
		2.65E-3	2-8 hr
		1.03E-3	8-24 hr
		7.77E-4	24-96 hr
		5.70E-4	96-720 hr
RWST Vent	Emergency Control Room Intake	2.18E-3	0-2 hr
		1.42E-3	2-8 hr
		4.89E-4	8-24 hr
		3.84E-4	24-96 hr
		2.72E-4	96-720 hr
Blowout Panel	Emergency Control Room Intake	2.12E-3	0-2 hr
		1.38E-3	2-8 hr
		5.29E-4	8-24 hr
		3.76E-4	24-96 hr
		2.93E-4	96-720 hr
Aux Bldg Louver	Emergency Control Room Intake	3.66E-3	0-2 hr
		2.46E-3	2-8 hr
		9.87E-4	8-24 hr
		6.80E-4	24-96 hr
		5.02E-4	96-720 hr
Equip Hatch	Emergency Control Room Intake	8.47E-4	0-2 hr
		6.41E-4	2-8 hr
		2.66E-4	8-24 hr
		1.84E-4	24-96 hr
		1.36E-4	96-720 hr
Contain Bldg	Emergency Control Room Intake	1.23E-3	0-2 hr
		9.02E-4	2-8 hr
		3.57E-4	8-24 hr
		2.55E-4	24-96 hr
		1.91E-4	96-720 hr

Table 15.4-8
CORE PARAMETERS USED IN STEAM BREAK DNB ANALYSIS

Parameter	State Points With Offsite Power Available				
	1	2	3	4	5
Loop A cold leg temperature, °F	403	401	401	401	
Loop B cold leg temperature, °F	472	470	468	468	
Loop C cold leg temperature, °F	473	470	468	468	
Pressurizer pressure, psia	834	873	902	909	
RCS volumetric flow,%	99.7	99.7	99.7	99.7	
Heat flux,%	18.80	20.26	21.14	20.62	
Time, sec.	84.0	182.4	244.4	262.0	
	State Points Without Offsite Power Available				
Loop A cold leg temperature, °F	339	321	306	289	273
Loop B cold leg temperature, °F	488	486	480	474	469
Loop C cold leg temperature, °F	498	493	487	481	474
Pressurizer pressure, psia	876	877	881	892	904
RCS volumetric flow,%	7.00	6.45	6.14	5.93	5.44
Heat flux,%	3.09	3.64	4.16	4.86	4.05
Time. sec	145.0	178.0	210.0	262.0	342.0

Table 15.4-9
TIME SEQUENCE OF EVENTS FOR MAJOR SECONDARY SYSTEM PIPE RUPTURE

Event	Time, sec
1.4 ft^2 Break with Offsite Power	
Steam Line Rupture	0.001
High ΔP	1.14
High Steam Flow	1.59
Pressurizer Empties	11.20
Low T_{avg}	12.81
Low Steam Line Pressure	16.53
Safety Injection	19.20
Main Feedline Isolation	19.30
Steam Line Isolation	19.56
Criticality	26.00
Boron Enters Core	243.2
Peak Heat Flux	244.4
1.4 ft^2 Break without Offsite Power	
Steam Line Rupture	0.001
RCP Trip	0.1
High ΔP	1.14
High Steam Flow	1.60
Low Steam Line Pressure	11.04
Pressurizer Empties	12.80
Low T_{avg}	15.27
Steam Line Isolation	16.04
Main Feedline Isolation	19.90
Safety Injection	24.04
Criticality	38.80
Boron Enters Core	250.0
Peak Heat Flux	262.8

Table 15.4-10
TIME SEQUENCE OF EVENTS FOR POSTULATED FEEDLINE RUPTURE

Accident	Event	Time (sec)
Feedwater System Pipe Break		
1. With offsite power available	Main feedline rupture occurs	0
	Low-low steam generator water level trip setpoint reached in faulted steam generator	6.8
	Rods begin to drop	8.8
	Steam generator safety valve setpoint reached in intact steam generators	16.4
	High steamline differential pressure SI setpoint reached	19.7
	One motor-driven auxiliary feedwater pump starts and supplies one intact steam generator	66.8
	Cold auxiliary feedwater is delivered to one intact steam generator	371
	Pressurizer safety valve setpoint reached	1850
	Core decay heat plus pump heat decreases to auxiliary feedwater heat removal capacity	≈7550
2. Without offsite power available	Main feedline rupture occurs	0
	Low-low steam generator water level trip setpoint reached in faulted steam generator	6.8
	Rods begin to drop	8.8
	Steam generator safety valve setpoint reached in intact steam generators	17.1
	High steamline differential pressure SI setpoint reached	19.7
	One motor-driven auxiliary feedwater pump starts and supplies one intact steam generator	66.8
	Cold auxiliary feedwater is delivered to one intact steam generator	371
	Pressurizer safety valve setpoint reached	1150
	Core decay heat decreases to auxiliary feedwater heat removal capacity	≈1800

Table 15.4-11
NOBLE GAS AND IODINE CORE INVENTORY AFTER 100 HOURS DECAY
(ORIGENS Output for 2981 MWt i.e., 103% core power)

Nuclide	Inventory (Ci)
Kr-83m	1.160E-05
Kr-85	7.932E+05
Kr-85m	3.821E+00
Kr-88	1.387E-03
I-130	6.148E+03
I-131	5.715E+07
I-132	4.854E+07
I-133	5.895E+06
I-135	4.095E+03
Xe-131m	9.959E+05
Xe-133	1.134E+08
Xe-133m	2.103E+06
Xe-135	2.158E+05
Xe-135m	6.688E+02

Table 15.4-12
NOBLE GAS AND IODINE GAP INVENTORY
FOR A FUEL ASSEMBLY AFTER 100 HOURS OF DECAY

(RADTRAD-NAI Input)

Isotope	Core Activity (Ci/MWt) [a] A	RG 1.183 Non-LOCA Gap Fraction B	Limiting FA Gap Activity @ 2958 MWt (Curies) [b] C
Kr-83m	3.891E-09	0.05	6.049E-09
Kr-85	2.661E+02	0.10	8.272E+02
Kr-85m	1.282E-03	0.05	1.992E-03
Kr-88	4.653E-07	0.05	7.232E-07
I-130	2.062E+00	0.05	3.206E+00
I-131	1.917E+04	0.08	4.768E+04
I-132	1.628E+04	0.05	2.531E+04
I-133	1.978E+03	0.05	3.074E+03
I-135	1.374E+00	0.05	2.135E+00
Xe-131m	3.341E+02	0.05	5.193E+02
Xe-133	3.804E+04	0.05	5.913E+04
Xe-133m	7.055E+02	0.05	1.097E+03
Xe-135	7.239E+01	0.05	1.125E+02
Xe-135m	2.244E-01	0.05	3.487E-01

a. Ci from Table 15.4-11 divided by 2981 MWt.
b. The Fuel Assembly Gap activity in Column C is determined by dividing the Core Activity by 157 assemblies and by multiplying by the core power (2958 MWt i.e., 102% core power), the non-LOCA gap fraction and the radial peaking factor of 1.65.

Table 15.4-13
ANALYSIS ASSUMPTIONS AND KEY PARAMETER VALUES
EMPLOYED IN FUEL HANDLING ACCIDENT ANALYSIS

Containment Parameters			
Release Flow Rate (0-720 hours)			80,000 cfm
Free Volume (for holdup; 50% of total)			920,000 ft^3
Core and Fuel Assembly Characteristics			
Number of Fuel Assemblies in Core			157
Maximum Fuel Assembly Radial Peaking Factor			1.65
Assumed Iodine Physical Form Above the Pool			57% elemental 43% organic
Control Room Atmospheric Dispersion Factors (sec/m^3)			
Source	Receptor		
Personnel Airlock	MCR Emergency Intake	0-2 hr	3.75E-03
		2-8 hr	2.60E-03
		8-24 hr	1.03E-03
		24-96 hr	7.03E-04
		96-720 hr	5.52E-04
Offsite Atmospheric Dispersion Factors (sec/m^3)			
	EAB		LPZ
0-720 hr	3.10E-04	0-8 hr	1.10E-05
		8-24 hr	7.30E-06
		24-96 hr	3.00E-06
		96-720 hr	8.20E-07
Control Room Filter Efficiencies			
Particulate	98%		
Elemental Iodine	95%		
Organic Iodine	95%		

Table 15.4-13 (continued)
ANALYSIS ASSUMPTIONS AND KEY PARAMETER VALUES
EMPLOYED IN FUEL HANDLING ACCIDENT ANALYSIS

Miscellaneous	
Effective Iodine Decontamination Factor	200
Minimum Depth of Water Over Fuel	23 feet
Fuel Building Release Flow Rate (0-720 hours)	80,000 cfm
Fuel Building Volume	160,000 ft^3
Control Room Volume (isolated)	77,000 ft^3
Unfiltered Environment Flow to the Control Room	400 cfm
Control Room Flow to the Environment	400, 1300 cfm [a]
Bottled Air Flow to the Control Room	None assumed
Filtered Outside Air Flow	900 cfm [a]
Breathing Rates	
Control Room	3.5E-4 m^3/sec
Offsite (EAB & LPZ)	
0-8 hours	3.5E-4 m^3/sec
8-24 hours	1.8E-4 m^3/sec
24-720 hours	2.3E-4 m^3/sec
Control Room Occupancy Factors	
0-24 hours	1.0
24-96 hours	0.6
96-720 hours	0.6 [b]

a. Filtered outside air flow of 900 cfm starts 1 hour after MCR isolation, which increases MCR flow to the environment from 400 cfm to 1300 cfm.
b. The North Anna Operations shift is based on a 12 hour workday plus turnover.

Table 15.4-14
PARAMETERS USED IN THE ANALYSIS OF THE
ROD CLUSTER CONTROL ASSEMBLY EJECTION ACCIDENT, FRAMATOME FUEL

Time in Life	Beginning	Beginning	End	End
Power level, %	102	0	102	0
Ejected-rod worth,% delta k	0.18	0.878	0.19	0.84
Delayed neutron fraction,%	0.52	0.52	0.43	0.43
Power weighting factor	1.46	3.13	1.44	3.23
Trip reactivity,% delta k	4.0	1.77	4.0	1.77
F_q before rod ejection	2.51	n/a	2.51	n/a
F_q after rod ejection	5.80	15.4	5.70	16.0
Number of operational RCPs	3	2	3	2
Maximum fuel pellet average temperature, °F	3969	3558	3866	3004
Maximum fuel center temperature, °F	4901	4193	4801	3626
Maximum clad temperature, °F	2585	2636	2498	2214
Maximum fuel stored energy, cal/gm	189	153	174	124

Table 15.4-15
APPEARANCE RATES MSLB CONCURRENT ACCIDENT SPIKE

Isotope	Appearance Rate Curries/hour
I-131	1.155E+04
I-132	1.231E+04
I-133	2.226E+04
I-134	1.583E+04
I-135	1.659E+04

Table 15.4-16
CONTROL ROOM ATMOSPHERIC DISPERSION FACTORS FOR MSLB

Control Room Atmospheric Dispersion Factors

Release Point	Receptor Point	Time Interval	Atmospheric Dispersion Factors (sec/m^3)
PORV	Normal CR Intake	0-2 hours	1.04E-02
		2-8 hours	8.20E-03
		8-24 hours	3.23E-03
		24-96 hours	2.25E-03
		96-720 hours	1.68E-03

Table 15.4-17
SAMPLED RLBLOCA PARAMETERS

Phenomenological
- Time in cycle (axial shape, rod properties, and burnup)
- Peaking factors
- Break type (guillotine versus split)
- Break size
- Critical flow discharge coefficients (break)
- Offsite power availability
- Decay heat
- Critical flow discharge coefficients (surgeline)
- Initial upper head temperature
- Film boiling heat transfer
- Dispersed film boiling heat transfer
- Critical heat flux
- T_{min} (intersection of film and transition boiling)
- Initial stored energy
- Downcomer hot wall effects
- Steam generator interfacial drag
- Condensation interphase heat transfer
- Metal-water reaction

Plant
- Core power
- Initial flow rate
- Initial operating temperature
- Pressurizer pressure
- Pressurizer level
- Containment volume
- Containment temperature
- Accumulator pressure
- Accumulator system volume

Table 15.4-18
PLANT PARAMETER VALUES SUPPORTED BY THE RLBLOCA ANALYSES

Parameter Description	Parameter Value
1.0 Plant Physical Description	
1.1 Fuel	
a. Cladding outside diameter	0.374 in
b. Cladding inside diameter	0.329 in
c. Cladding thickness	0.0225 in
d. Pellet outside diameter	0.3225 in
e. Pellet density	96% of theoretical
f. Active fuel length	144 in
g. Maximum rod average exposure	≤ 62,000 MWd/mtU
1.2 RCS	
a. Flow resistance	Analysis
b. Pressurizer location	Broken Loop
c. Hot assembly location	Anywhere in core
d. Hot assembly type	17 x 17
e. SG tube plugging	≤ 12%
2.0 Plant Initial Operating Conditions	
2.1 Reactor Power	
a. Core power	≤ 2893 MWt
b. Maximum core peaking (F_Q)	≤ 2.32[a] (normalized)
c. Maximum pin radial peaking (FDH)	≤ 1.65[b] (normalized)
d. Maximum assembly radial peaking	< 1.587[c] (normalized)
e. MTC	≤ 0 at HFP
f. HFP boron	Normal letdown
2.2 Fluid Conditions	
a. Loop flow	110.5 Mlbm/hr ≤ M ≤ 118.2 Mlbm/hr
b. RCS average temperature	580.8°F ≤ T ≤ 586.8°F
c. Upper head temperature	< Core Outlet Temperature
d. Pressurizer pressure	2220 psia ≤ P ≤ 2250 psia
e. Pressurizer level	64.5%[d] (nominal)

a. Includes 5% measurement uncertainty and 3% engineering uncertainty. Analyses applied no K(z) constraint; K(z) equals 1.0 for all core elevations.
b. Includes 4% measurement uncertainty.
c. Value equivalent to hot rod peaking factor without 4% uncertainty.
d. Value reflects nominal operating point maintained by the plant control system.

Table 15.4-18
PLANT PARAMETER VALUES SUPPORTED BY THE RLBLOCA ANALYSES

	Parameter Description	Parameter Value
2.0	Plant Initial Operating Conditions (continued)	
	f. Accumulator pressure	613.7 psia ≤ P ≤ 681.7 psia
	g. Accumulator system liquid volume	954.8 ft^3 ≤ V ≤ 978.5 ft^3
	h. Accumulator temperature	86°F ≤ T ≤ 120°F (coupled to containment temperature)
	i. Accumulator line resistance	As-built piping configuration
	j. Minimum ECCS boron	≥ 2200 ppm
3.0	Accident Boundary Conditions	
	a. Break location	Any RCS piping location
	b. Break type	Double-ended guillotine or split
	c. Break size per side (relative to cold leg pipe)	0.05 ≤ A ≤ 0.5 full pipe area (split) 0.5 ≤ A ≤ 1.0 full pipe area (guillotine)
	d. Worst single failure	Loss of one LHSI and one HHSI
	e. Offsite power	On or Off (sampled parameter)
	f. Low-head safety injection flow	Minimum flow of 1 pump delivered through 3 injection lines with no spillage
	g. High-head safety injection flow	Minimum flow of 1 pump delivered through 3 injection lines with no spillage
	h. RWST temperature	≤ 60°F
	i. Safety injection delay	≤ 13 seconds (with offsite power) ≤ 27 seconds (without offsite power)
	j. Containment pressure	Bounds TS Figure 3.6.4-1
	k. Containment temperature	86°F ≤ T ≤ 120°F
	l. Containment sprays	Minimum actuation time

Table 15.4-19
STATISTICAL DISTRIBUTIONS USED FOR PROCESS PARAMETERS

Parameter	Operational Uncertainty Distribution	Parameter Range	Standard Deviation, σ	Uncertainty Included in Parameter Range Endpoints
Core Power (%)	Gaussian	100	1.1%	N/A
Initial Flow Rate (Mlbm/hr)	Uniform	108.26–120.54	1.0%	2σ
Initial Average Operating Temperature (°F)	Uniform	576.8–590.8	2.0°F	2σ
Pressurizer Pressure (psia)	Uniform	2184–2286	18.0 psi	2σ
Pressurizer Level (%)	Uniform	54.5–74.5	5%	2σ
Containment Volume ($\times 10^6$ ft^3)	Uniform	1.825–2.087[a]	N/A	N/A
Containment Temperature (°F)	Uniform	84.5–121.5	0.75°F	2σ
Accumulator Pressure (psia)	Uniform	583.7–711.7	15.0 psi	2σ
Accumulator System Volume (ft^3)	Uniform	951.0–982.3	1.9 ft^3	2σ

a. Minimum value represents a lower bound, assuming minimum containment diameter, maximum installed equipment and provision for structural concrete; maximum value is gross volume of empty containment with nominal dimensions.

Table 15.4-20
SUMMARY OF MAJOR PARAMETERS
FOR LIMITING NORTH ANNA UNIT 1 TRANSIENT

Time (hrs)	4242
Burnup (MWd/mtU)	9100
Core Power (MWt)	2940
Core Peaking (F_Q)	2.144
Radial Peak ($F_{\Delta H}$)	1.65
Local Peaking (Fl)	1.068
Break Type	DEGB
Break Size per Side (ft^2)	3.26 (~79%)
Offsite Power Availability	No
Decay Heat Multiplier	0.9841

Table 15.4-21
SUMMARY OF RESULTS FOR THE NORTH ANNA UNIT 1 LIMITING PCT CASE

Case Number	28
PCT	
Temperature	1853°F
Time	87.4 seconds
Elevation	~8.4 ft
Metal-Water Reaction	
% Oxidation Maximum	2.6%
% Total Oxidation	0.03%
Total Hydrogen	0.50 lbm

Table 15.4-22
TIME SEQUENCE OF EVENTS FOR THE NORTH ANNA UNIT 1 LIMITING PCT CASE

Event	Time (sec)
Begin Analysis	0.0
Break Opens	0.0
RCP Trip	0.0
SI Actuation Signal Issued	0.7
Start of Broken Loop Accumulator Injection	7.0
Start of Intact Loop Accumulator Injection	10.5
Beginning of Core Recovery (Beginning of Reflood)	24.2
Start of HHSI	27.7
Start of LHSI	27.7
Broken Loop Accumulator Empties	34.3
Intact Loop Accumulators Empty	36.0, 36.1
PCT Occurs (1853°F)	87.4

Table 15.4-23
SUMMARY OF MAJOR PARAMETERS
FOR LIMITING NORTH ANNA UNIT 2 TRANSIENT

Time (hrs)	8114
Burnup (MWd/mtU)	18,000
Core Power (MWt)	2907
Core Peaking (F_Q)	2.295
Radial Peak ($F_{\Delta H}$)	1.65
Local Peaking (Fl)	1.05
Break Type	DEGB
Break Size per Side (ft^2)	2.59 (~63%)
Offsite Power Availability	No
Decay Heat Multiplier	1.0215

Table 15.4-24
SUMMARY OF RESULTS FOR THE NORTH ANNA UNIT 2 LIMITING PCT CASE

Case Number	8
PCT	
Temperature	1789°F
Time	86.9 seconds
Elevation	~9.9 ft
Metal-Water Reaction	
% Oxidation Maximum	1.8%
% Total Oxidation	0.04%
Total Hydrogen	0.67 lbm

Table 15.4-25
TIME SEQUENCE OF EVENTS FOR THE NORTH ANNA UNIT 2 LIMITING PCT CASE

Event	Time (sec)
Begin Analysis	0.0
Break Opens	0.0
RCP Trip	0.0
SI Actuation Signal Issued	1.0
Start of Broken Loop Accumulator Injection	10
Start of Intact Loop Accumulator Injection	13
Start of HHSI	28
Start of LHSI	28
Beginning of Core Recovery (Beginning of Reflood)	31
Broken Loop Accumulator Empties	36
Intact Loop Accumulators Empty	39,39
PCT Occurs (1789°F)	86.9

Table 15.4-26
PEAK CLAD TEMPERATURE INCLUDING ALL PENALTIES AND BENEFITS
- LARGE BREAK LOCA - ADVANCED MARK-BW FUEL

Unit 1	
PCT for Analysis of Record	1853°F
PCT Assessments Allocated to AOR	
A. Forslund-Rohsenow Correlation Modeling	+ 64°F
B. RWST Temperature Assumption	+ 8°F
C. LBLOCA/Seismic SG Tube Collapse	0°F
D. RLBLOCA Choked Flow Disposition	- 26°F
E. RBLOCA Changes in Uncertainty Parameters	+ 10°F
F. Advanced Mark-BW Top Nozzle Modification	+ 65°F
G. S-RELAP5 Code Mixture Model Limitation	- 29°F
H. RELAP5 Point Kinetics Programming Issue	- 20°F
LBLOCA PCT for Comparison to 10 CFR 50.46 Requirements	1925°F
Unit 2	
PCT for Analysis of Record	1789°F
PCT Assessments Allocated to AOR	
A. Forslund-Rohsenow Correlation Modeling	+ 64°F
B. RWST Temperature Assumption	+ 8°F
C. LBLOCA/Seismic SG Tube Collapse	0°F
D. RLBLOCA Choked Flow Disposition	+ 22°F
E. RBLOCA Changes in Uncertainty Parameters	+ 10°F
F. Advanced Mark-BW Top Nozzle Modification	+ 65°F
G. S-RELAP5 Code Mixture Model Limitation	- 19°F
H. RELAP5 Point Kinetics Programming Issue	- 20°F
LBLOCA PCT for Comparison to 10 CFR 50.46 Requirements	1919°F

Table 15.4-27
RADTRAD-NAI CODE MSLB RESULTS

MSLB Concurrent Iodine Spike

	EAB 2 hour TEDE (rem)	LPZ TEDE (rem)	Control Room TEDE (rem)
Concurrent Iodine Spike	3.00E-02	1.31E-03	3.33E+00
Dose Limits	2.05E+00	2.50E+00	5.00E+00

MSLB Pre-Accident Iodine Spike

	EAB 2 hour TEDE (rem)	LPZ TEDE (rem)	Control Room TEDE (rem)
Pre-Accident Iodine Spike	3.25E-02	1.21E-03	3.96E+00
Dose Limits	2.50E+01	2.50E+01	5.00E+00

Table 15.4-28
TECHNICAL SPECIFICATION WEIGHTED IODINE-EQUIVALENT
PRIMARY AND SECONDARY SIDE NUCLIDE INVENTORY
FOR USE IN THE CONCURRENT AND PRE-ACCIDENT IODINE SPIKE CASES

Isotope	Primary Coolant Activity Ci	Secondary Liquid Activity (All 3 SGs) Ci [a]	Secondary Steam Activity (All 3 SGs) Ci
Column A	Column B	Column C	Column D
Br-84	2.570E+00	9.102E-03	
Rb-88	2.238E+02	4.414E-01	
Rb-89	6.101E+00	1.007E-02	
I-131	1.495E+02 [b]	1.107E+01	7.754E-03
I-132	5.446E+01 [b]	1.613E+00	9.410E-04
I-133	2.416E+02 [b]	1.219E+01	1.043E-02
I-134	3.370E+01 [b]	1.928E-01	2.784E-04
I-135	1.301E+02 [b]	2.868E-02	4.018E-03
Cs-134	1.600E+01	1.254E+00	
Cs-136	8.888E+00	5.087E-01	
Cs-137	8.016E+01	6.284E+00	
Cs-138	5.648E+01	1.943E-01	
Kr-85	3.119E+02		7.771E-03
Kr-85m	1.285E+02		3.201E-03
Kr-87	7.434E+01		1.852E-03
Kr-88	2.246E+02		5.597E-03
Xe-133	1.721E+04		4.288E-01
Xe-133m	1.907E+02		4.751E-03
Xe-135	3.733E+02		9.302E-03
Xe-135m	1.155E+01		2.879E-04
Xe-138	4.105E+01		1.023E-03

a. Value for the affected generator is 1/3 of this value and value for the unaffected generator is 2/3 of this value.
b. Iodine values must be multiplied by a value of 60 for the Pre-Accident Iodine Spike Case.

Table 15.4-28 (continued)
TECHNICAL SPECIFICATION WEIGHTED IODINE-EQUIVALENT
PRIMARY AND SECONDARY SIDE NUCLIDE INVENTORY
FOR USE IN THE CONCURRENT AND PRE-ACCIDENT IODINE SPIKE CASES

Concurrent Spike Iodine Appearance Rates (Ci/hr) are:

I-131	7.7385E+03
I-132	8.2477E+03
I-133	1.4914E+04
I-134	1.0606E+04
I-135	1.1100E+04

Appearance rates are based on a 120 gpm letdown flowrate and maximum Technical Specification allowable primary-to-secondary leakage.

Table 15.4-29
CONTROL ROOM ATMOSPHERIC DISPERSION FACTORS FOR SGTR

Release Point	Receptor Point	Time Interval	Atmospheric Dispersion Factors (sec/m^3)
PORV	Normal CR Intake	0–2 hours	2.08E-03
		2–8 hours	1.64E-03
		8–24 hours	6.46E-04
		24–96 hours	4.50E-04
		96–720 hours	3.36E-04
PORV	Emergency CR Intake	0–2 hours	6.28E-04
		2–8 hours	4.36E-04
		8–24 hours	1.67E-04
		24–96 hours	1.18E-04
		96–720 hours	8.72E-05

Table 15.4-30
ANALYSIS ASSUMPTIONS AND KEY PARAMETER VALUES
EMPLOYED IN THE SGTR ANALYSIS

Primary and Secondary Side Parameters	Value
Primary system volume (cubic feet)	9786
SG Steam volume (cubic feet/SG)	3838
SG Liquid volume (cubic feet/SG)	2054
SG liquid mass (gm/SG)	4.43E+07
Control room volume (cubic feet)	2.30E+05
Primary System Mass (lb or gm)	4.37845E+05 lb or 1.986E+08 gm
Secondary Steam Mass (lb or gm per generator)	7200 lb/sg or 3.266E+06 gm/sg
Steam Mass Dilution	2.81E+05

Full Power Properties	Steam Generator	RCS Coolant Liquid
Temperature (°F)	525.24	580.6
Pressure (psia)	850	2250
Density (gm/cc)	0.76096	0.7166

Table 15.4-31
RADTRAD-NAI CODE SGTR RESULTS

SGTR Concurrent Iodine Spike

	EAB 2 hour TEDE (rem)	LPZ TEDE (rem)	Control Room TEDE (rem)
No-LOOP	1.05E-01	3.96E-03	6.16E-01
LOOP	1.71E-01	6.31E-03	1.02E+00
Dose Limit	2.50E+00	2.50E+00	5.00E+00

SGTR Pre-accident Iodine Spike

	EAB 2 hour TEDE (rem)	LPZ TEDE (rem)	Control Room TEDE (rem)
No-LOOP	4.90E-01	1.75E-02	3.06E+00
LOOP	6.67E-01	2.38E-02	4.19E+00
Dose Limit	2.50E+01	2.50E+01	5.00E+00

Table 15.4-32
NON-LOCA FRACTION OF FISSION PRODUCT INVENTORY IN GAP FOR LRA

Group	Fraction
I-131	0.08
Kr-85	0.10
Other Noble Gases	0.05
Other Halogens	0.05
Alkali Metals	0.12

Table 15.4-33
ANALYSIS ASSUMPTIONS AND KEY PARAMETER VALUES
EMPLOYED IN THE LOCKED ROTOR ANALYSIS

NSSS Parameters	
Core Power	2958 MWt
Number of Fuel Assemblies	157
Primary System (RCS) Volume	9786 ft^3
Steam Generator Liquid Volume	6162 ft^3
Steam Generator Steam Volume	11 514 ft^3
Radial Peaking Factor	1.65
Fuel Failure During Event	13%
Main Control Room (MCR) Parameters	
Free Volume	2.30E5 ft^3
Normal Intake Flow Rate	3500 cfm
No Isolation of the Control Room	
Onsite Atmospheric Dispersion Factors	
Main Control Room Normal Intake	
0–2 hours	2.08E-3 sec/m^3
2–8 hours	1.64E-3 sec/m^3
8–24 hours	6.46E-4 sec/m^3
24–96 hours	4.50E-4 sec/m^3
96–720 hours	3.36E-4 sec/m^3

Table 15.4-34
LOCKED ROTOR ANALYSIS RESULTS

	Control Room Dose (rem TEDE)	EAB Dose (rem TEDE)	LPZ Dose (rem TEDE)
Total Dose	2.33	0.24	0.03
Dose Limits	5.0	2.5	2.5

Table 15.4-35
SEQUENCE OF EVENTS AND THERMAL/HYDRAULIC RESULTS
STEAM GENERATOR TUBE RUPTURE ACCIDENT
[CASE WITH LOSS OF OFFSITE POWER]

Event	Time (sec)	Notes
Tube Rupture	0.0	
Reactor trip on OTΔT	99.42	Nominal Protection setpoint used; results in earlier reactor trip and PORV opening time
Turbine trip	99.92	
PORV on ruptured steam generator opens	103.0	Integral of break flow, 0-103.0 sec = 7880.84 lbm
		Integral of flashed break flow, 0-103.0 sec = 894.50 lbm
Safety injection actuated by low pressurizer pressure	231.70	Integral of break flow, 103-232 sec = 7701.2 lbm
		Integral of flashed break flow, 103-232 sec = 333.8 lbm
Main feedwater isolated	231.80	
Auxiliary feedwater initiated	291.70	
End of transient simulation/ruptured generator assumed isolated	1800.0	Integral of break flow, 0-1800 sec = 113374 lbm
		Integral of flashed break flow, 0-1800 sec = 6907.6 lbm
Integrated steam release from stuck PORV, lbm	103-1800	170016
Integrated steam release from intact SG PORVs	103-1800	153049
Total integrated flow from main steam safety valves, lbm		
SG A (faulted)	187-233	3488
SG B+C (intact)	188-204	6179
Steam release from intact SGs during post-accident cooldown, lbm	30 min to 2 hours	230,000
	2 hours to 8 hours	662,000

Table 15.4-36
CONTAINMENT SUMP VOLUME VS. TIME FOR LOCA RADIOLOGICAL ANALYSIS

Time (seconds)	Sump Volume (ft^3)
840	16,800
1500	25,700
1900	31,400
2500	39,900
3000	46,800
4000	60,000
5000	68,800
6000	73,200
8000	76,000

Figure 15.4-1
PEAKING FACTOR VERSUS CORE HEIGHT
COSINE AXIAL POWER SHAPE

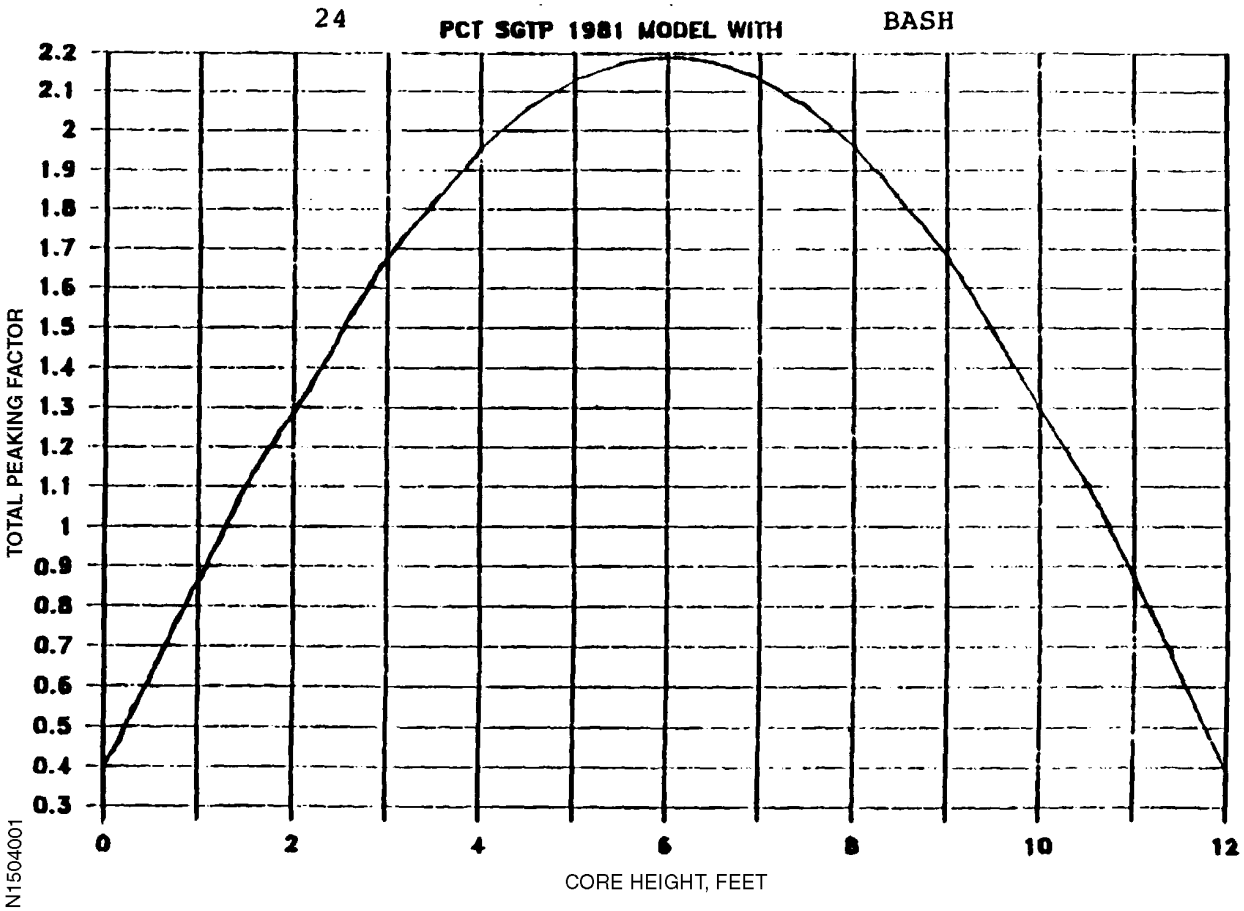

Figure 15.4-2
PEAKING FACTOR VERSUS CORE HEIGHT,
LIMITING SKEWED AXIAL POWER SHAPE

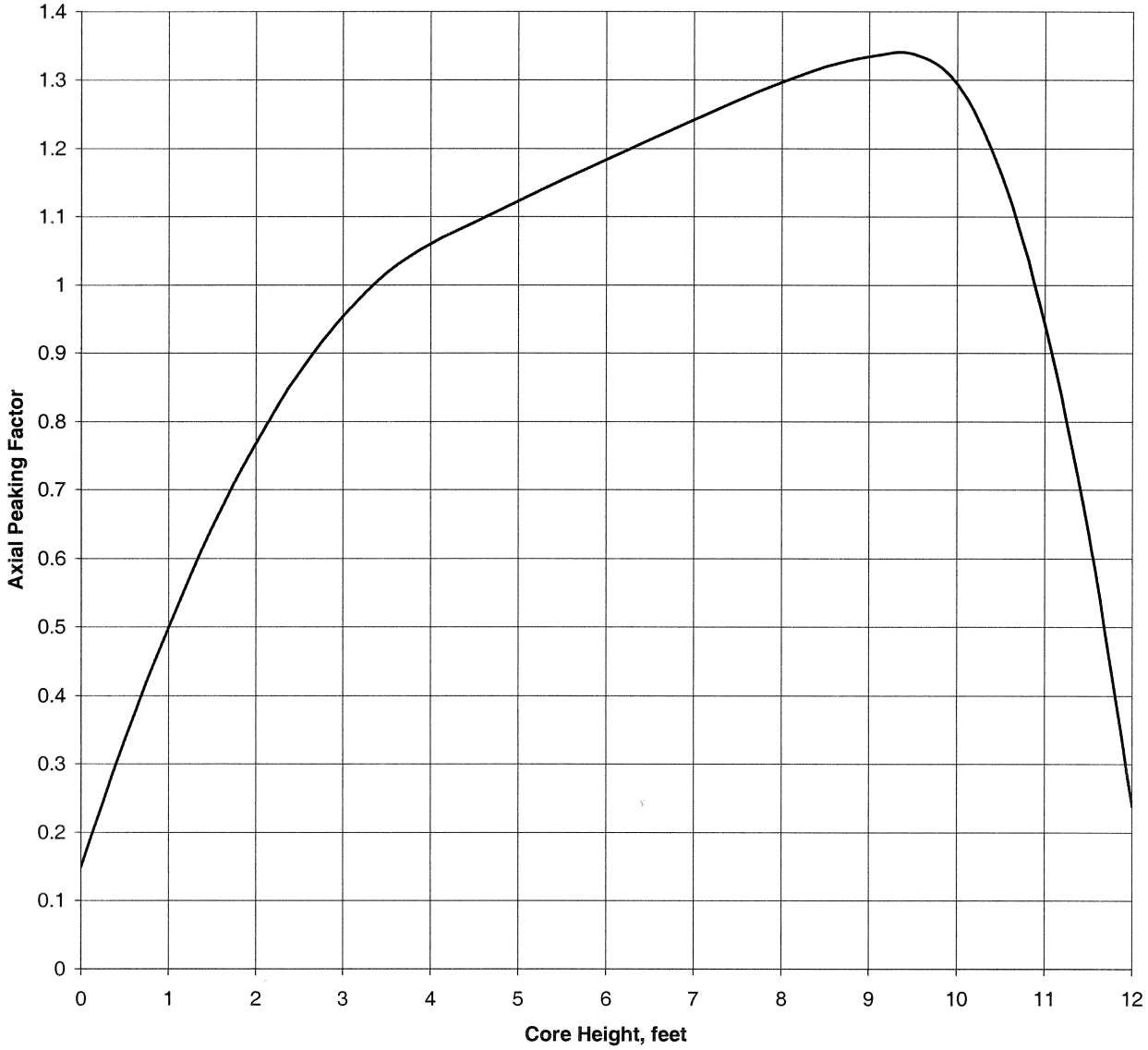

Figure 15.4-3
CORE MASS FLOW
(DECLG, COSINE SHAPE, C_d=0.4)

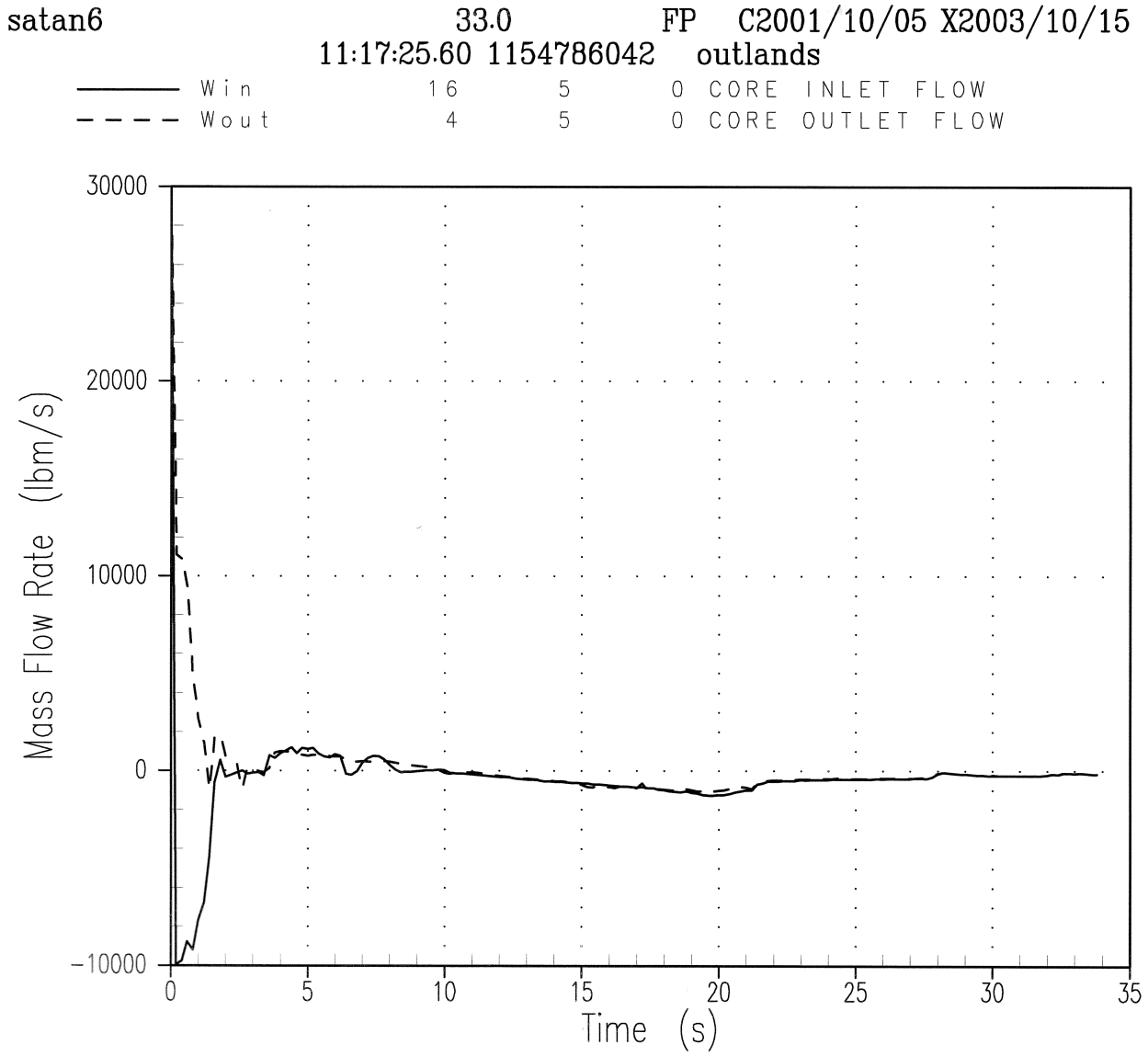

Figure 15.4-4
CORE MASS FLOW
(DECLG, COSINE SHAPE, C_d=0.6)

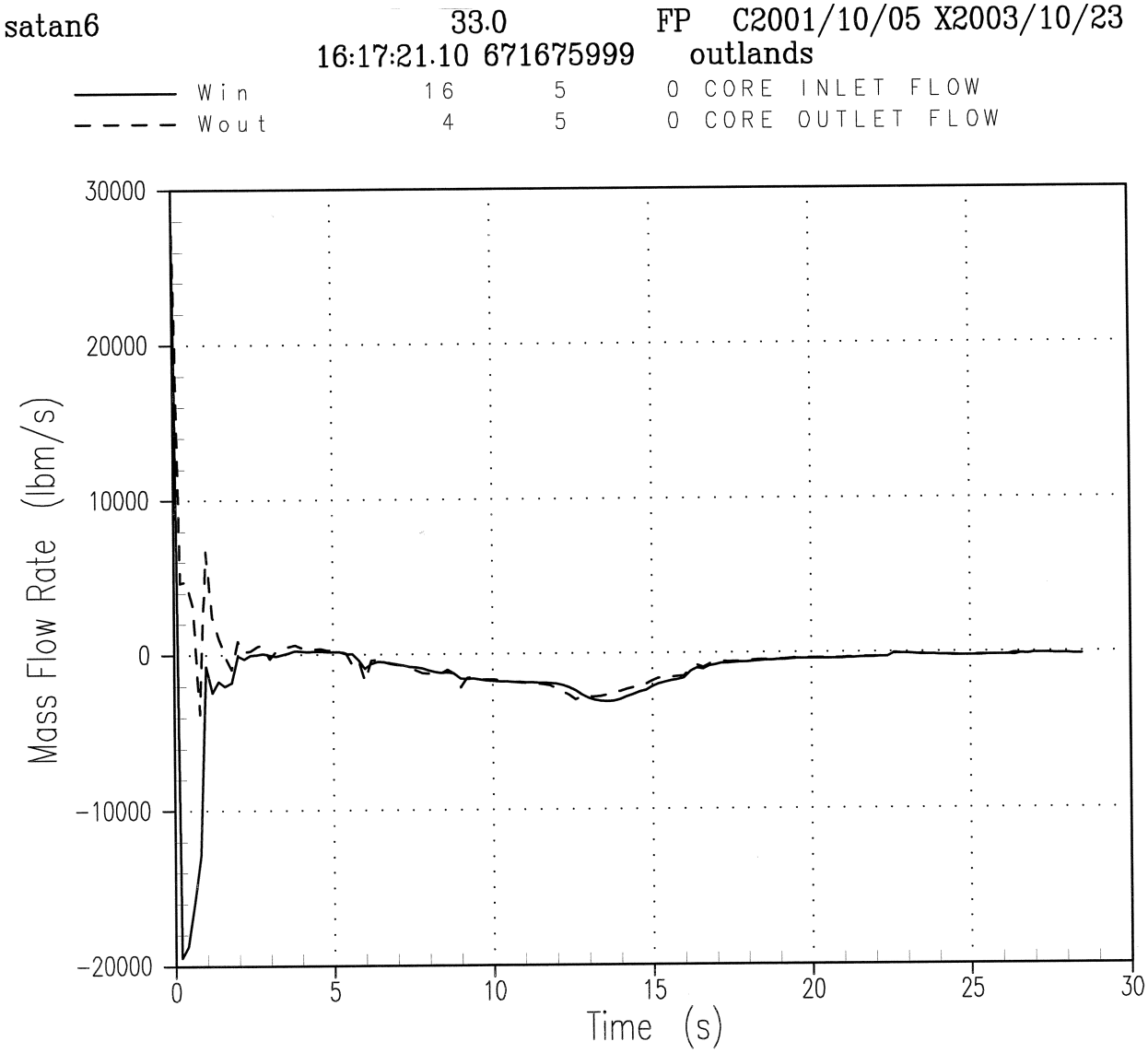

Figure 15.4-5
CORE MASS FLOW
(DECLG, LIMITING SKEWED SHAPE, C_d=0.4)

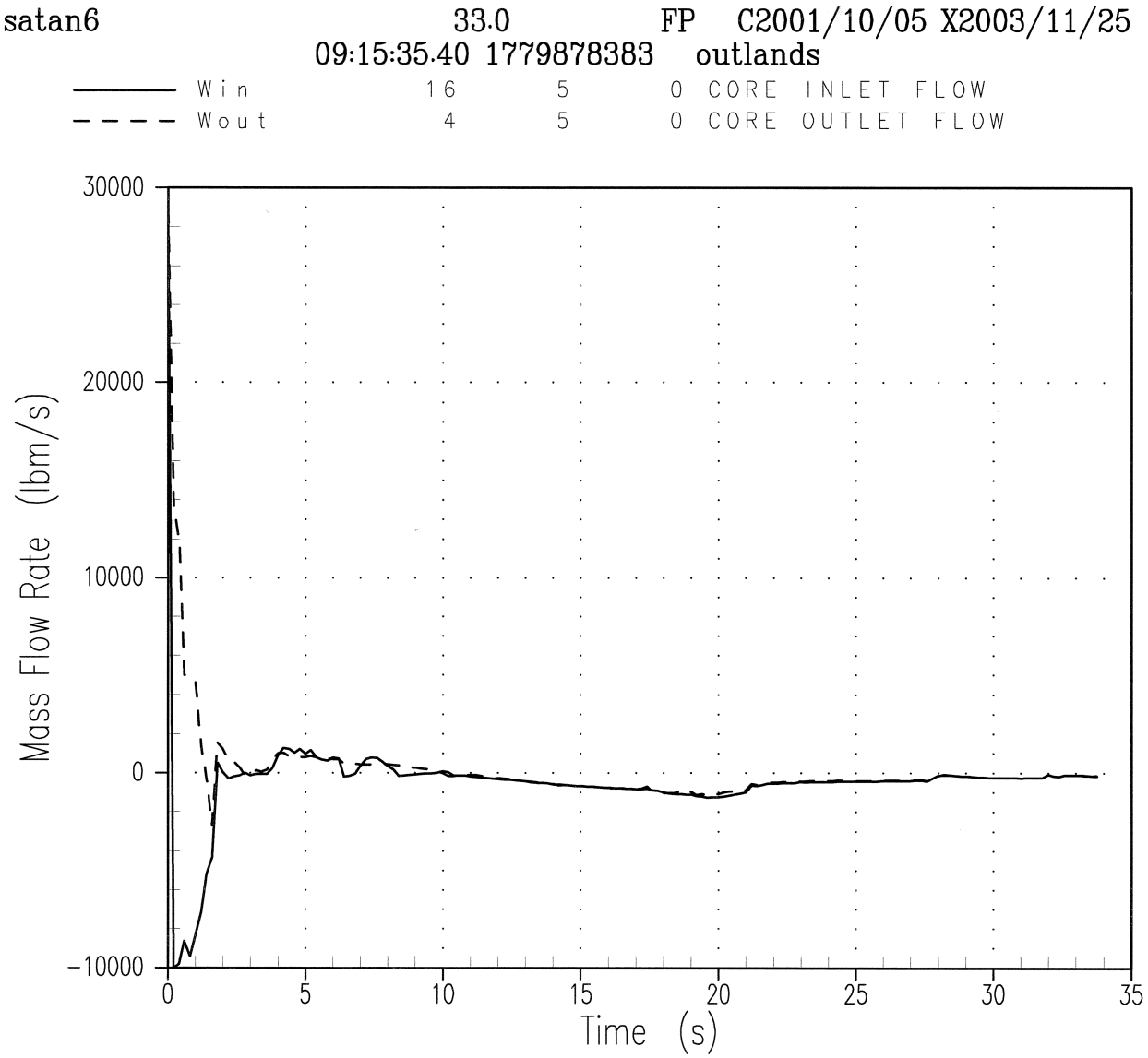

Figure 15.4-6
CORE PRESSURE
(DECLG, COSINE SHAPE, C_d=0.4)

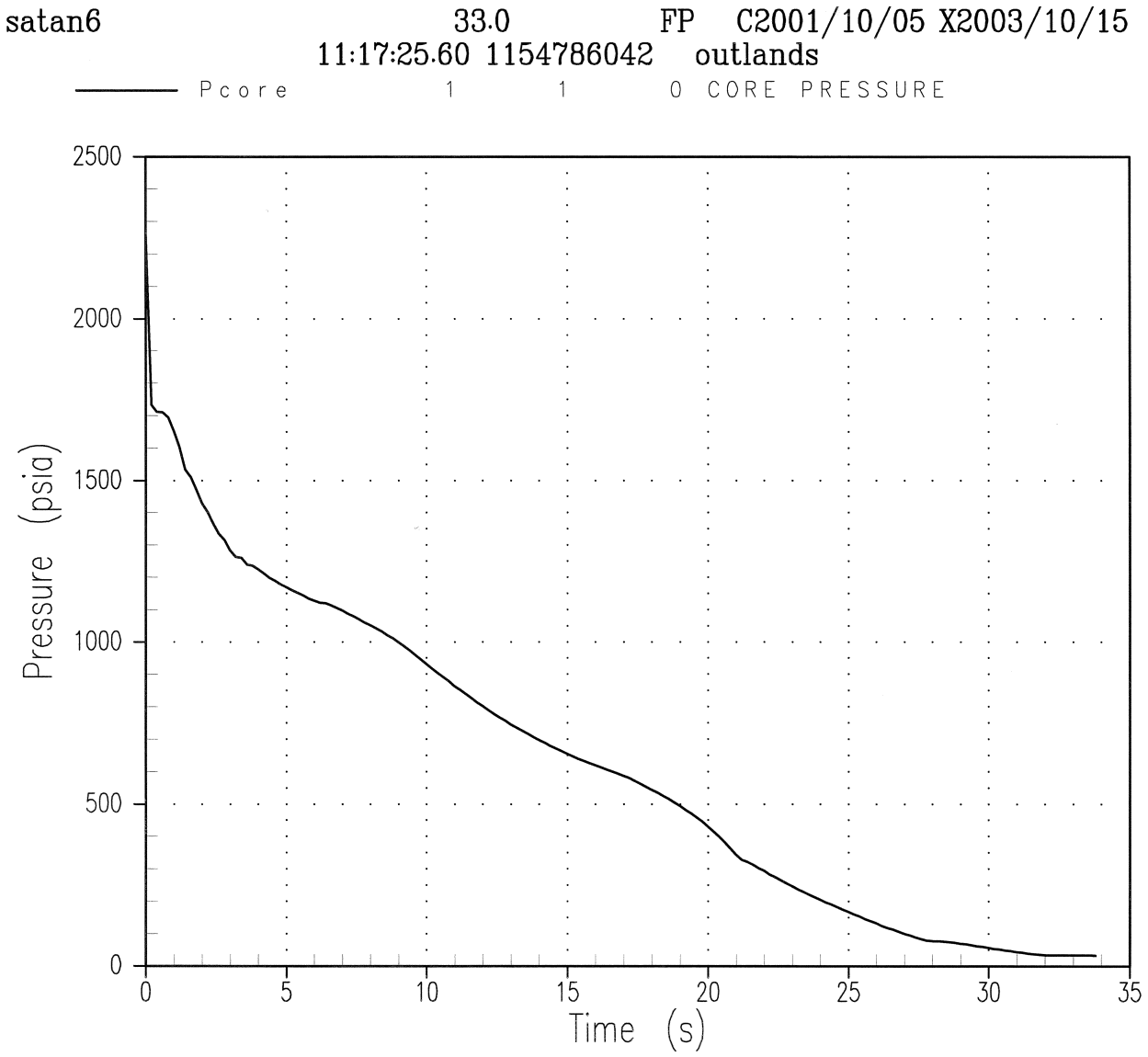

Figure 15.4-7
CORE PRESSURE
(DECLG, COSINE SHAPE, C_d=0.6)

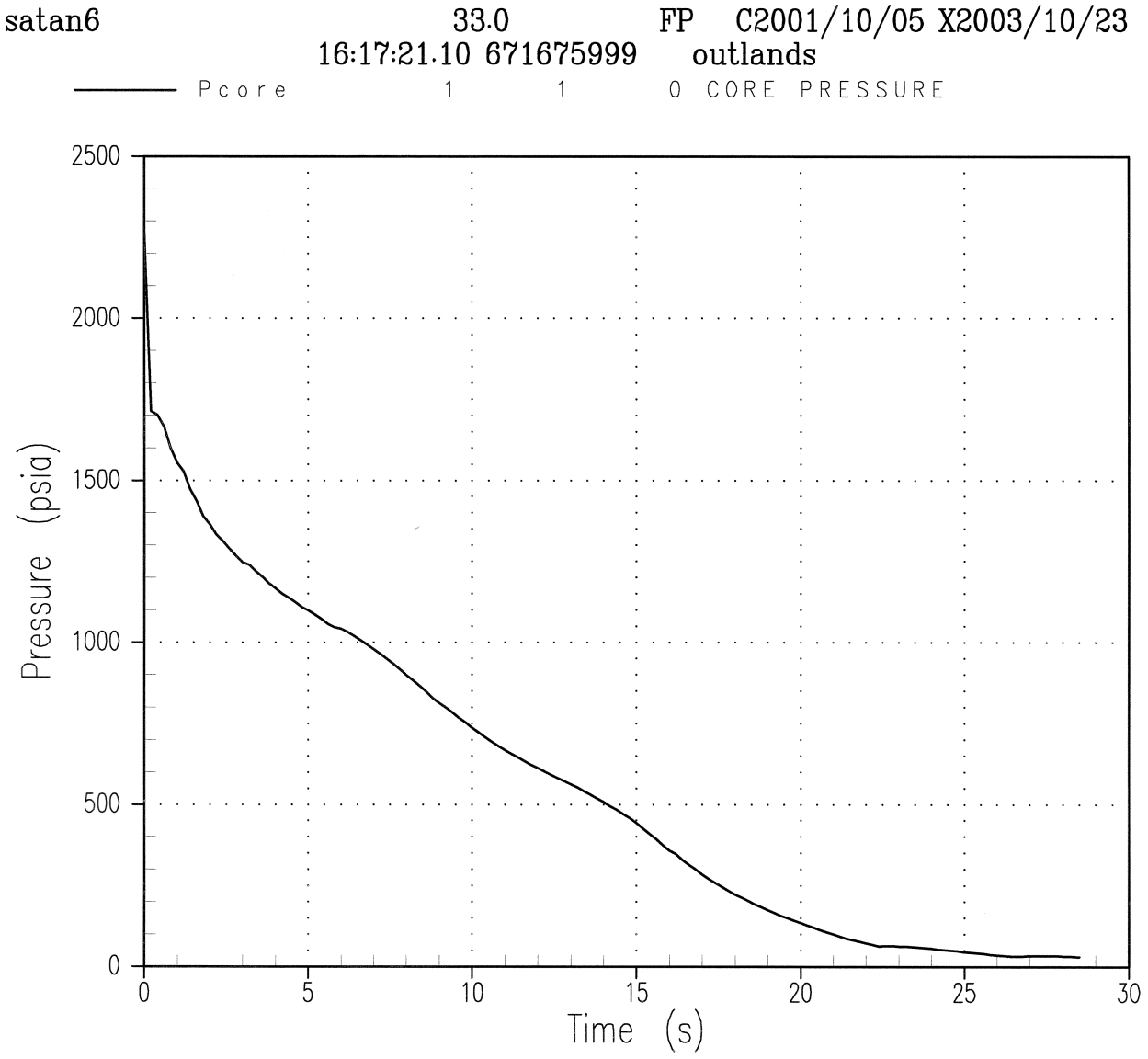

Figure 15.4-8
CORE PRESSURE
(DECLG, LIMITING SKEWED SHAPE, C_d=0.4)

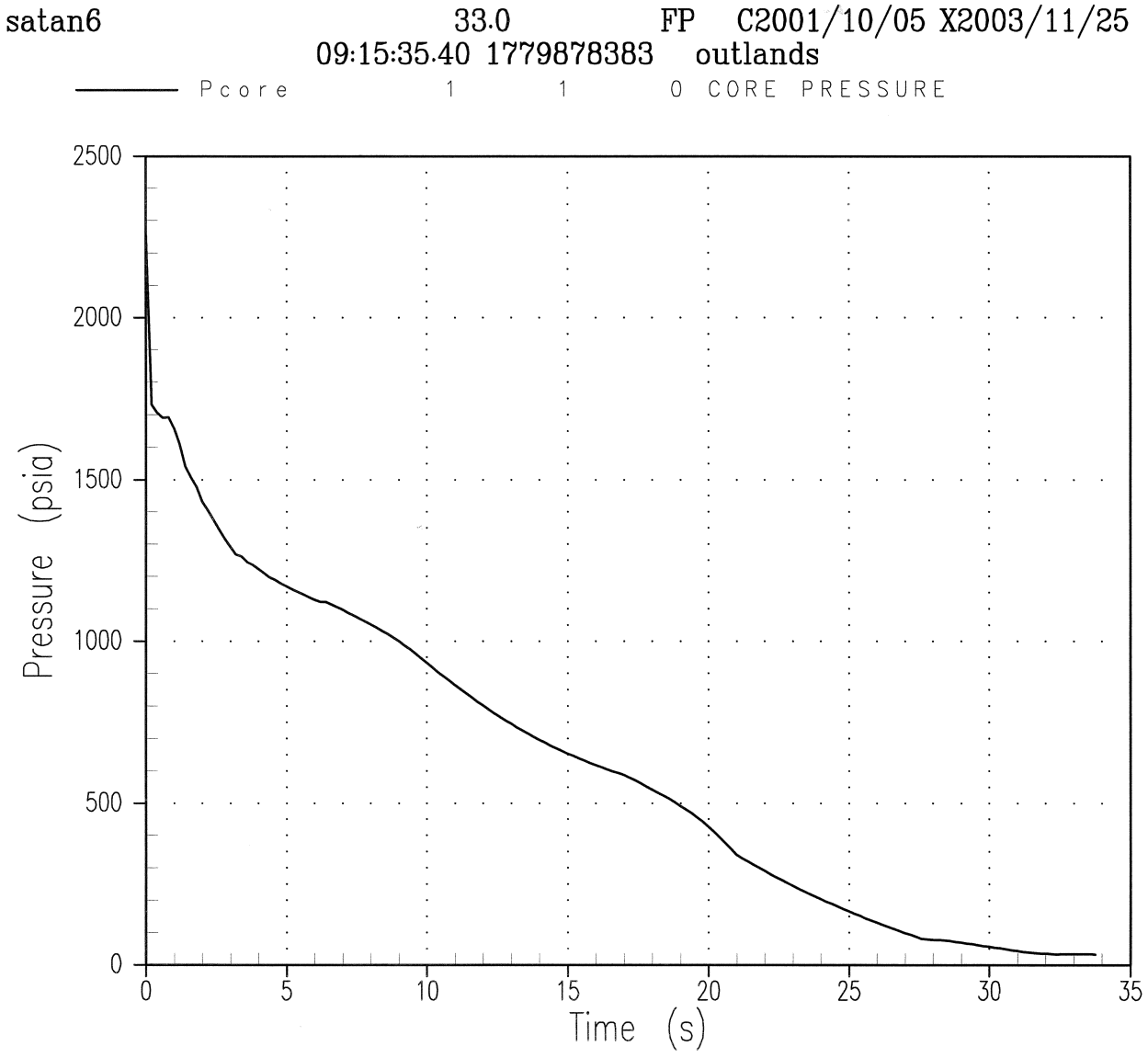

Figure 15.4-9
ACCUMULATOR MASS FLOW
(DECLG, COSINE SHAPE, C_d=0.4)

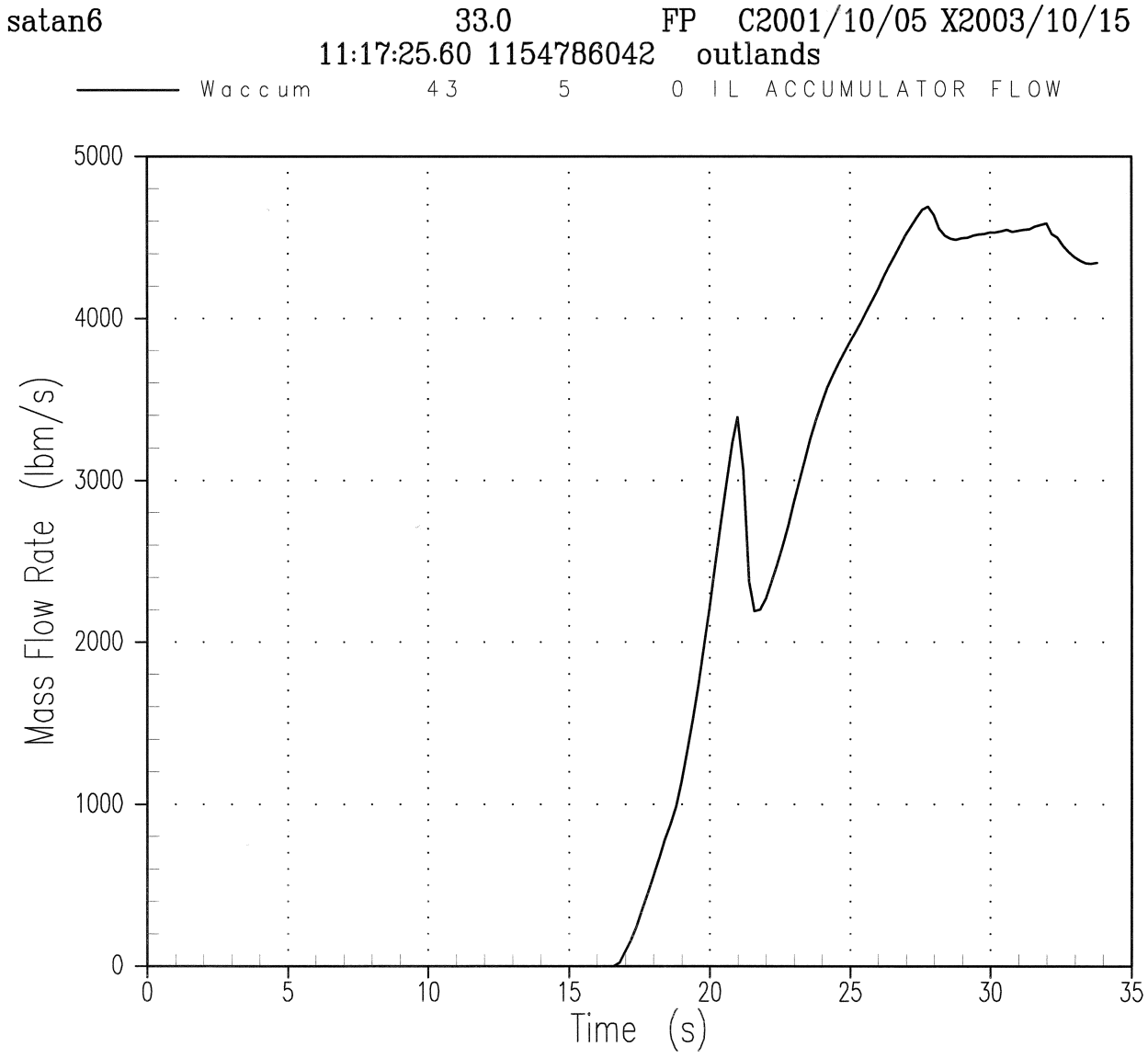

Figure 15.4-10
ACCUMULATOR MASS FLOW
(DECLG, COSINE SHAPE, C_d=0.6)

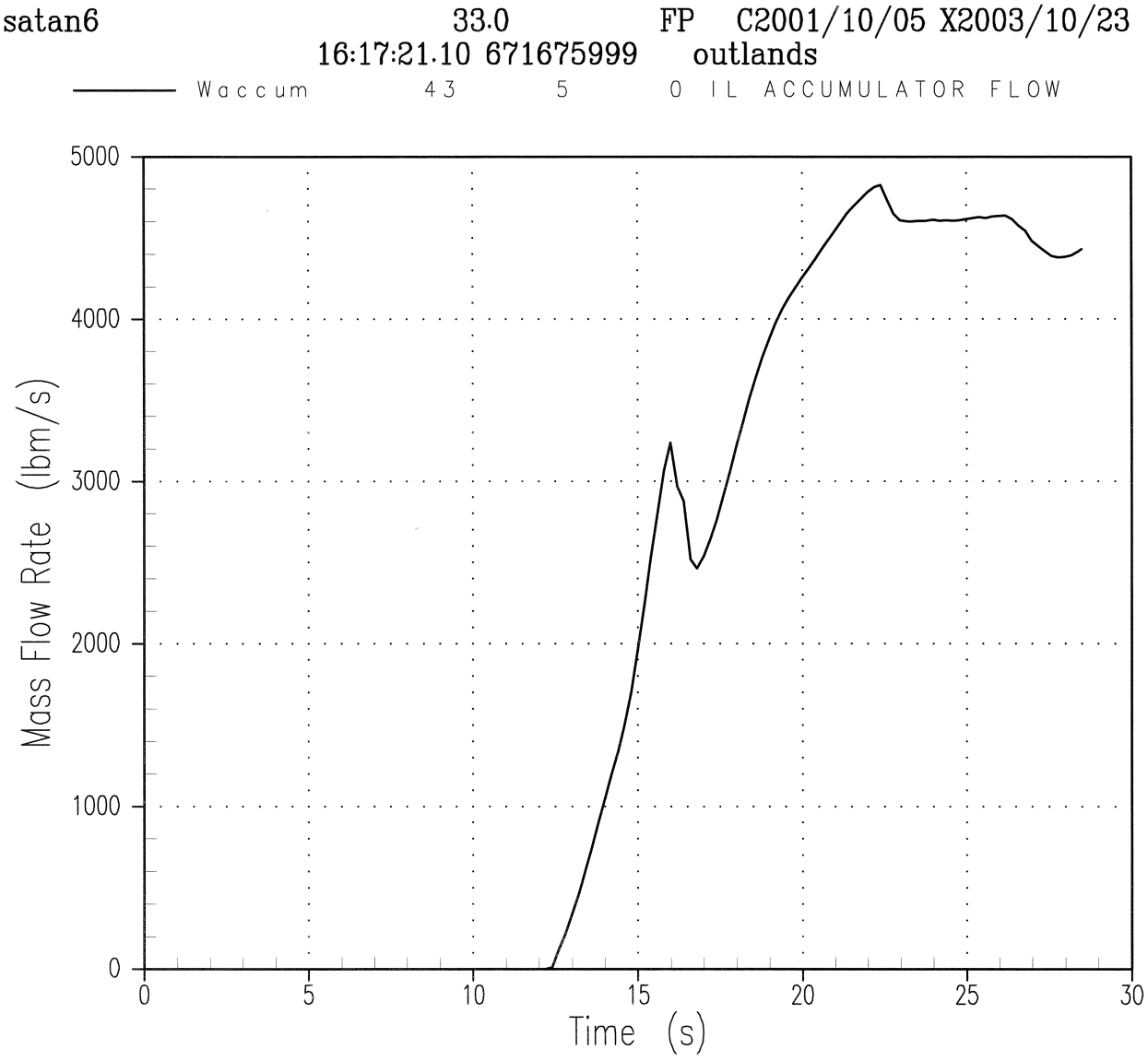

Figure 15.4-11
ACCUMULATOR MASS FLOW
(DECLG, LIMITING SKEWED SHAPE, C_d=0.4)

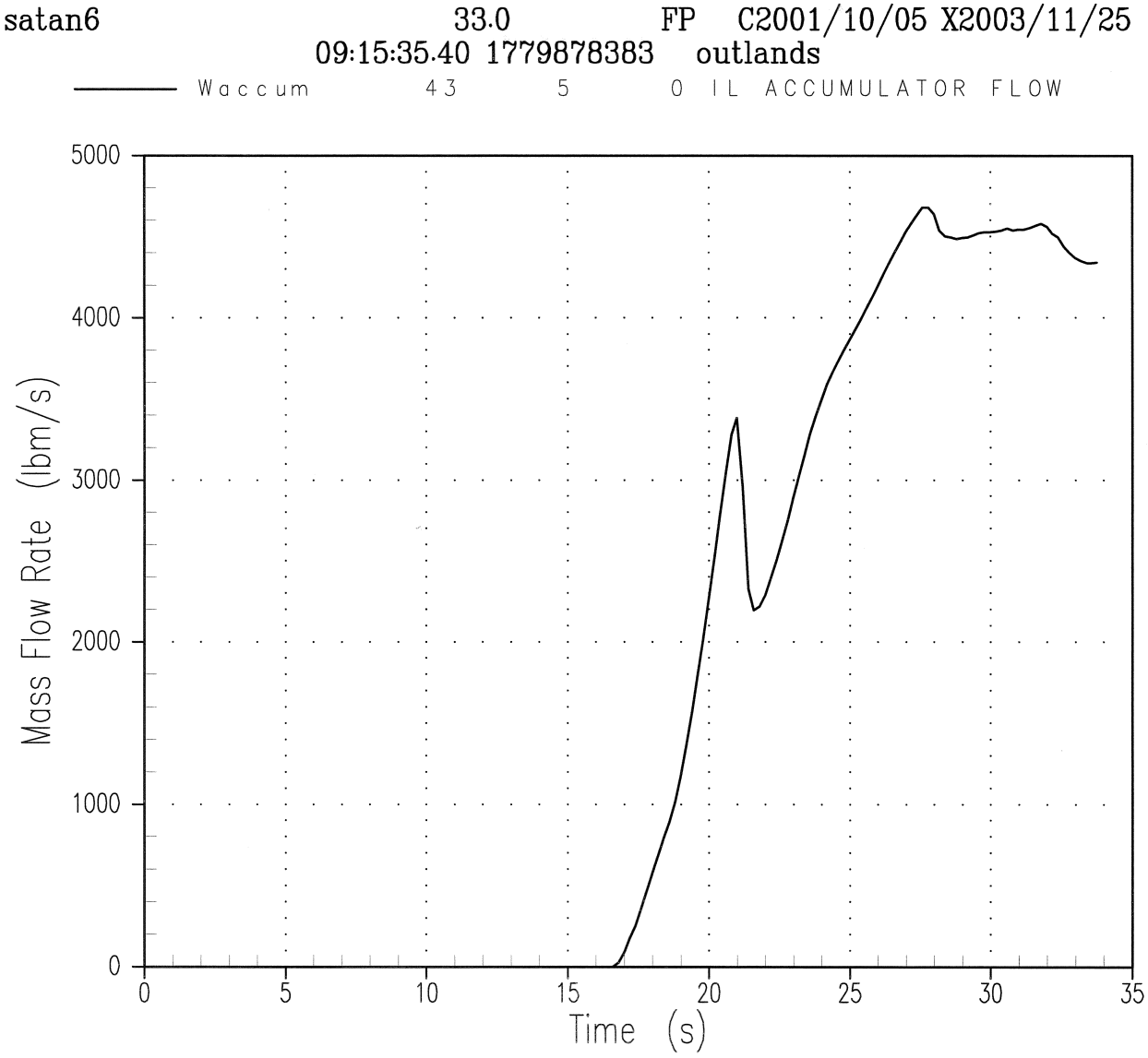

Figure 15.4-12
CORE PRESSURE DROP
(DECLG, COSINE SHAPE, C_d=0.4)

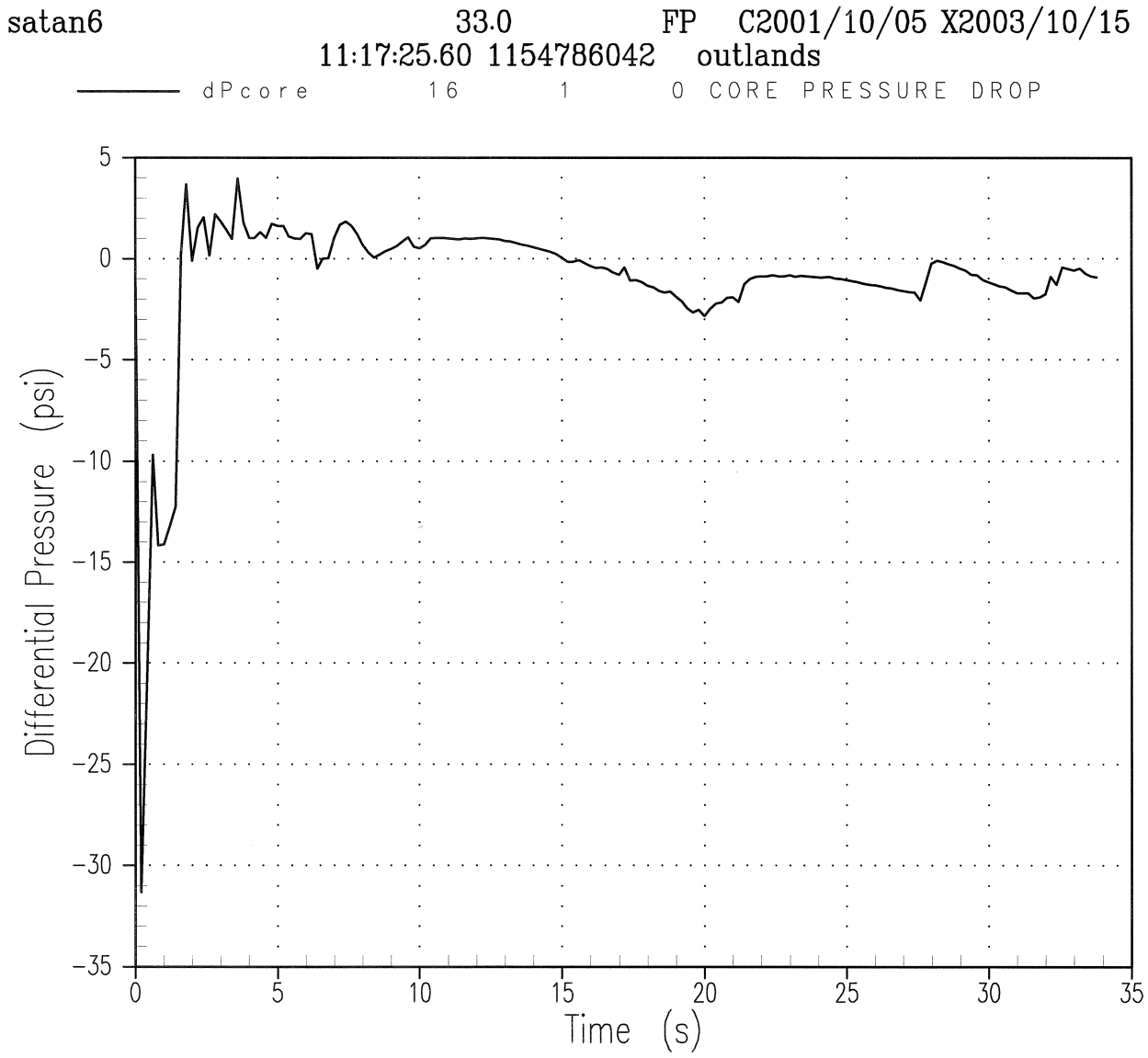

Figure 15.4-13
CORE PRESSURE DROP
(DECLG, COSINE SHAPE, C_d=0.6)

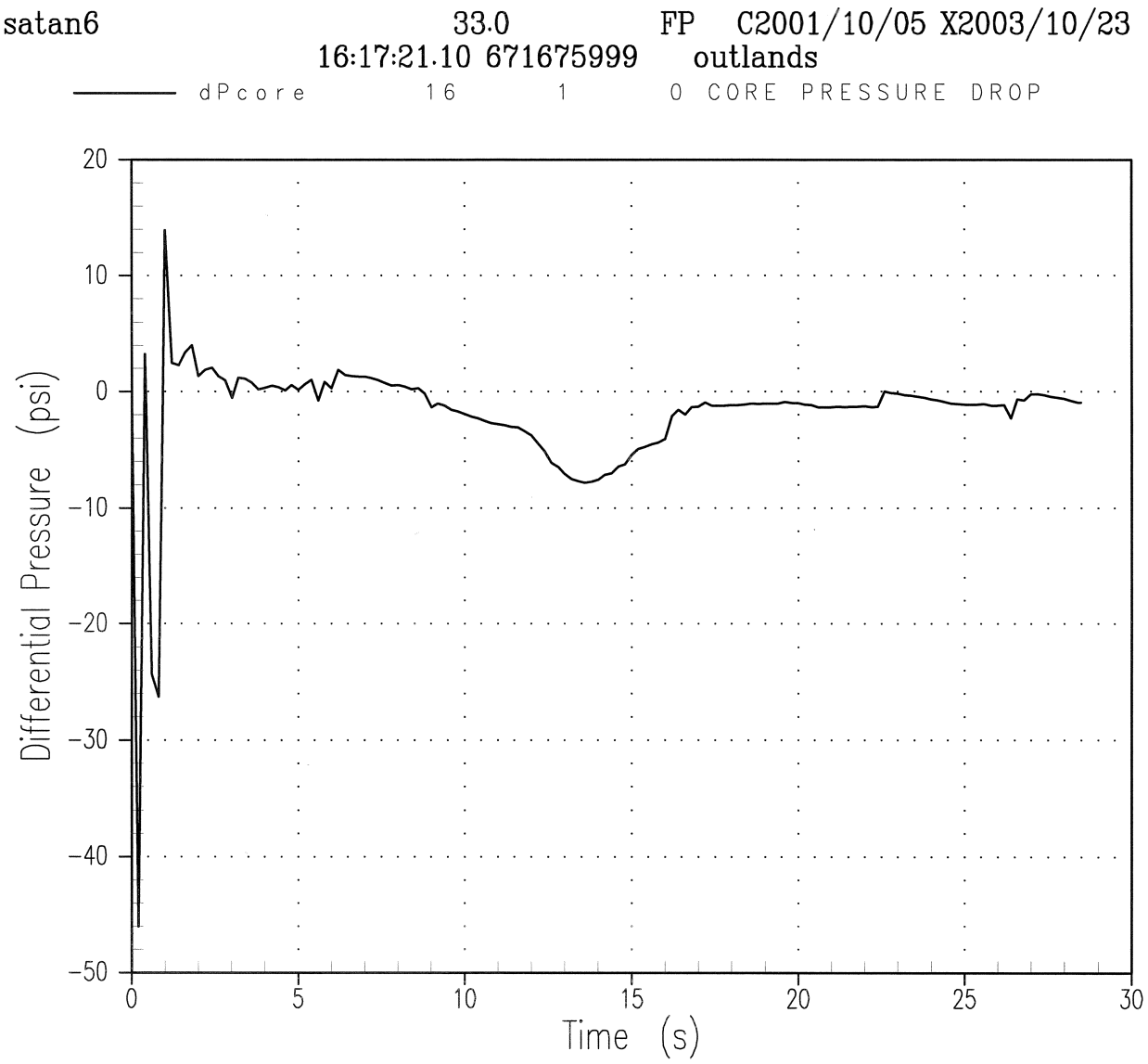

Figure 15.4-14
CORE PRESSURE DROP
(DECLG, LIMITING SKEWED SHAPE, C_d=0.4)

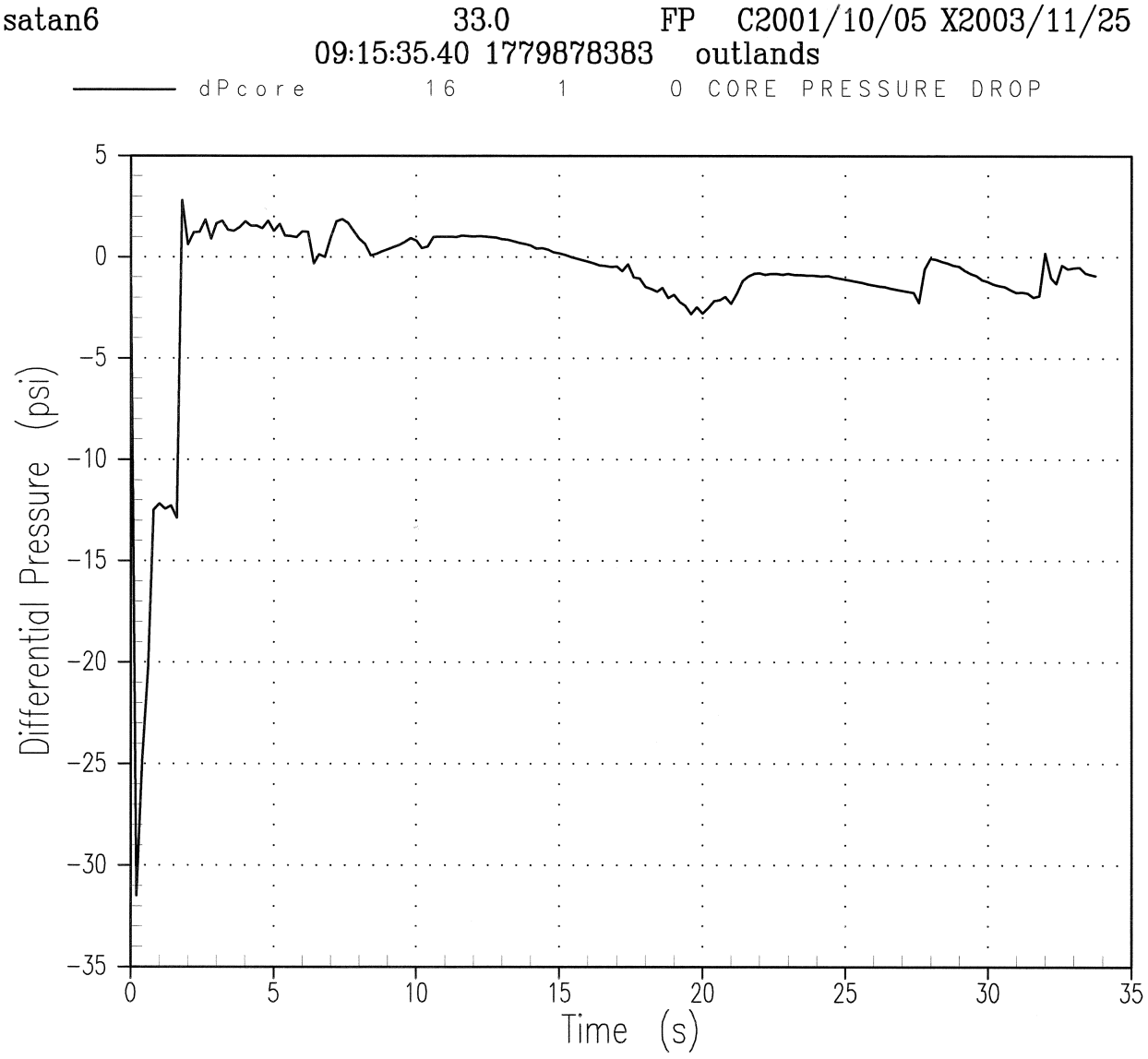

Figure 15.4-15
BREAK MASS RELEASE
(DECLG, COSINE SHAPE, C_d=0.4)

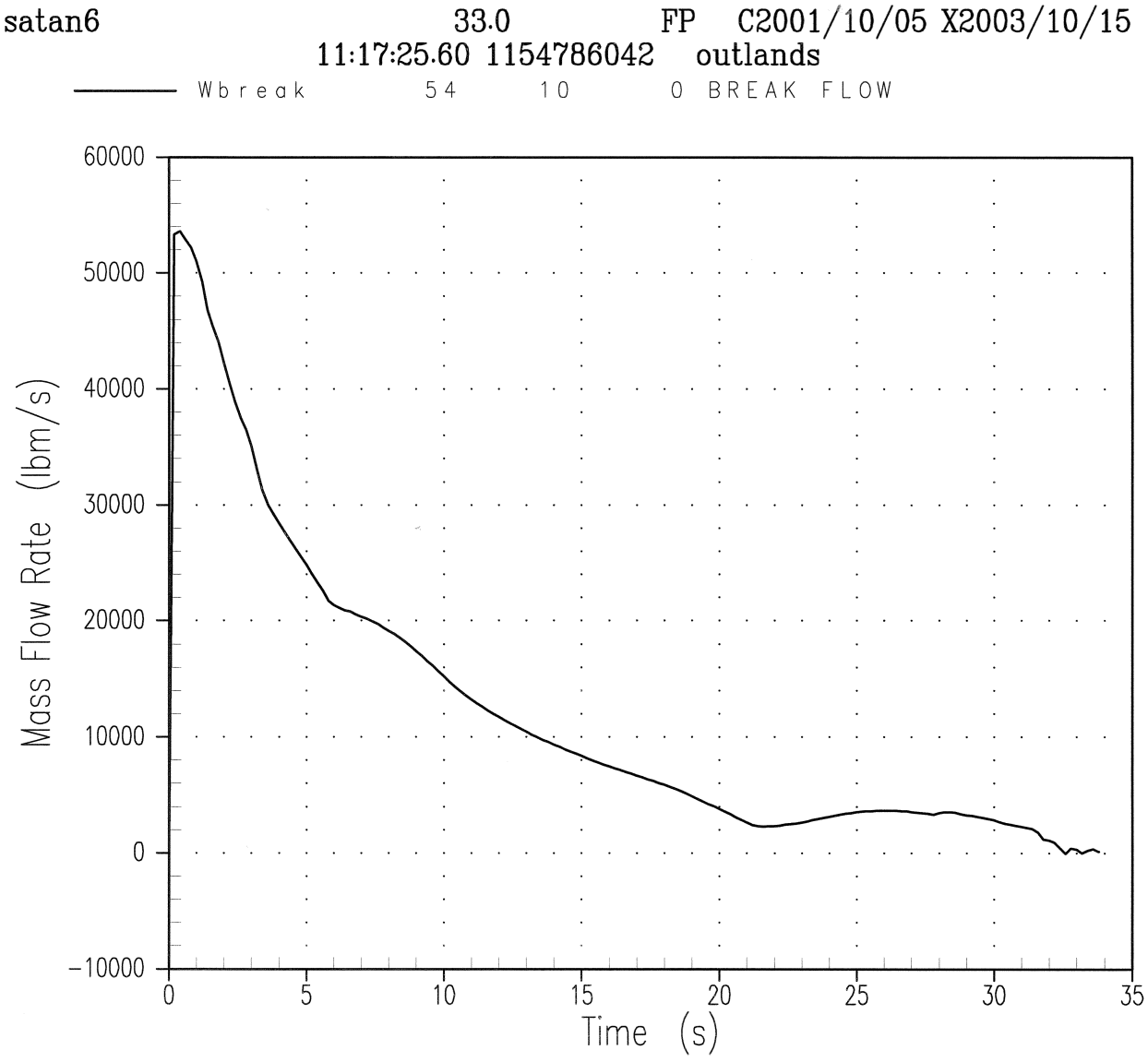

Figure 15.4-16
BREAK MASS RELEASE
(DECLG, COSINE SHAPE, C_d=0.6)

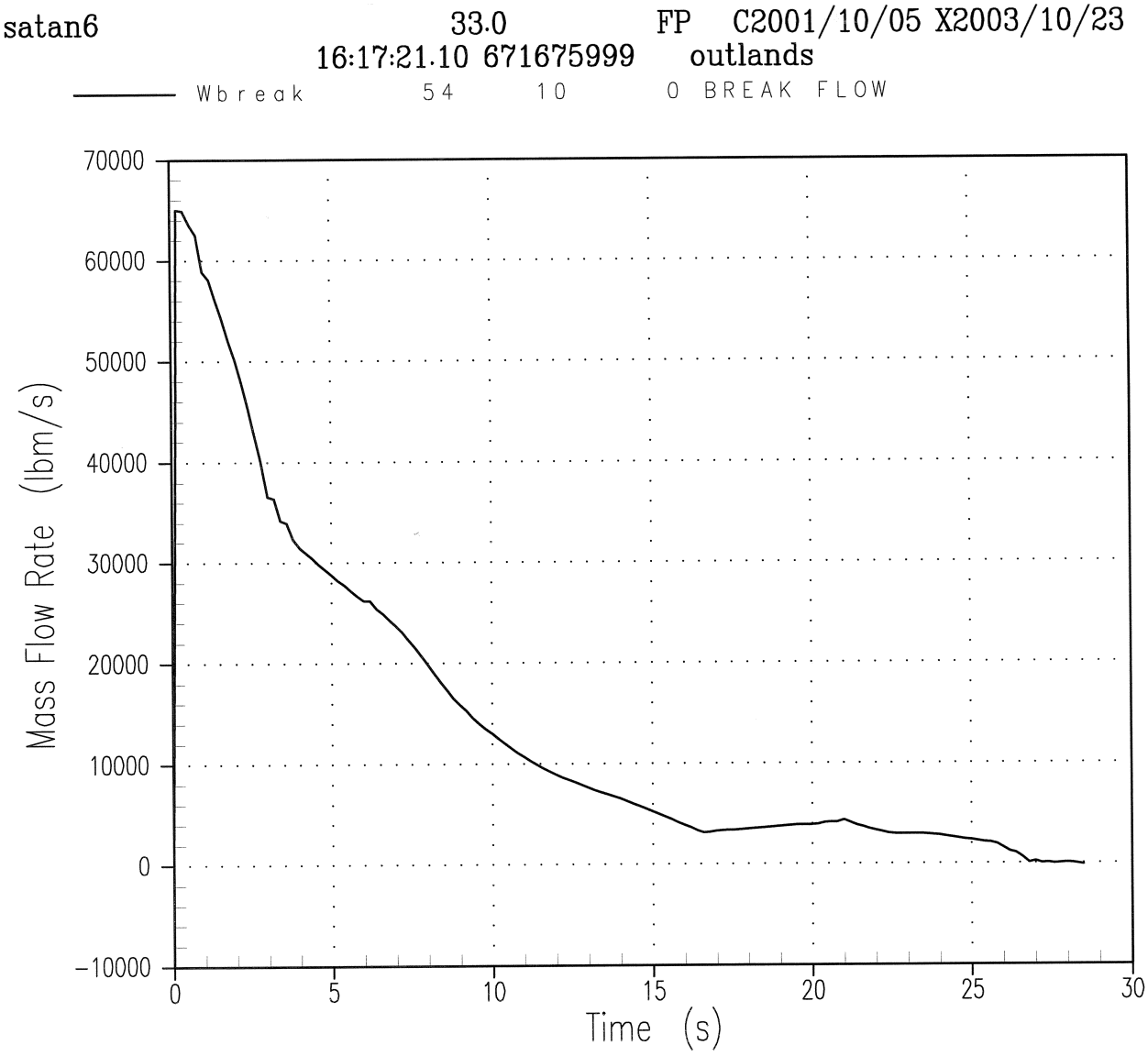

Figure 15.4-17
BREAK MASS RELEASE
(DECLG, LIMITING SKEWED SHAPE, C_d=0.4)

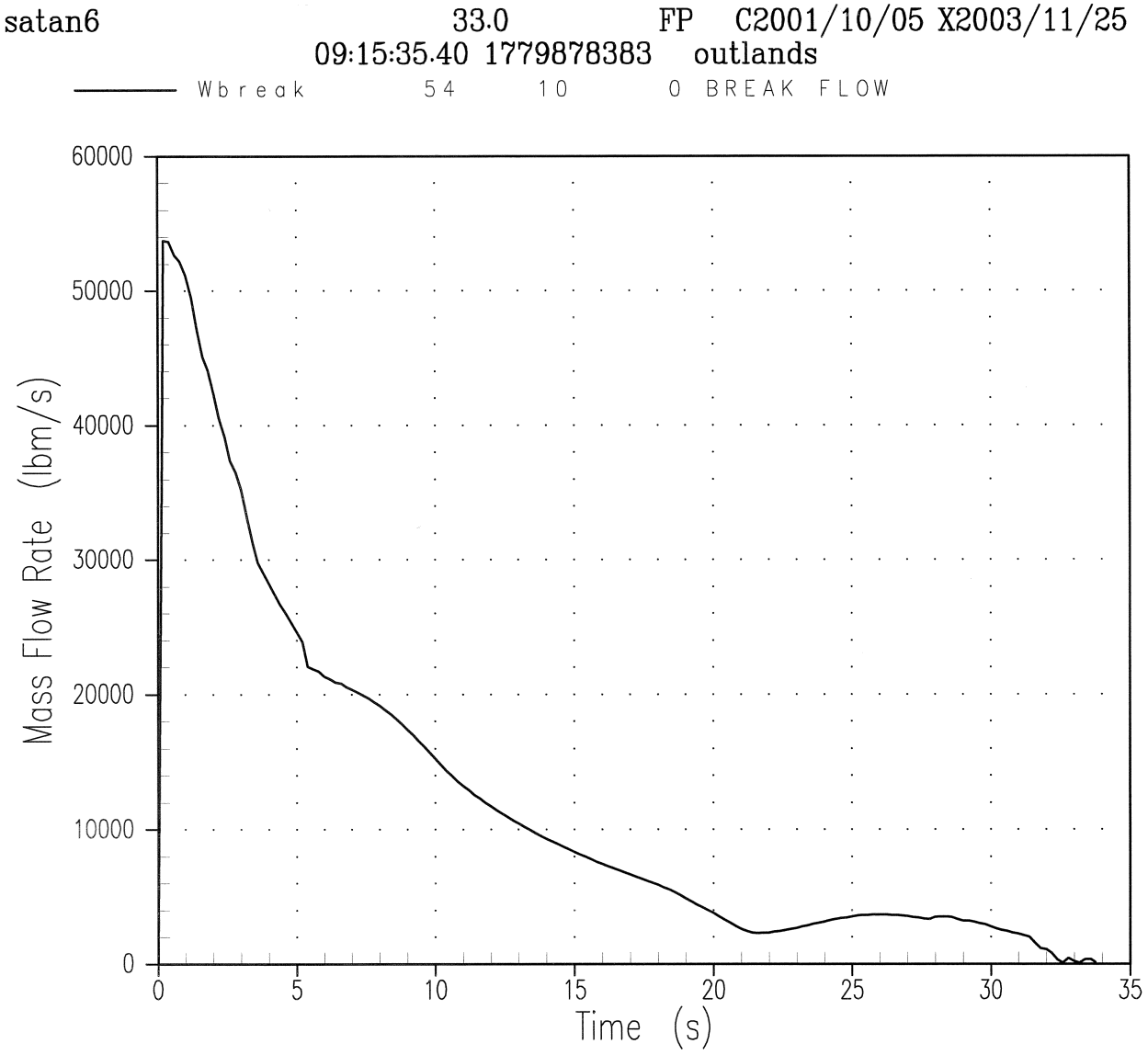

Figure 15.4-18
BREAK ENERGY RELEASE
(DECLG, COSINE SHAPE, C_d=0.4)

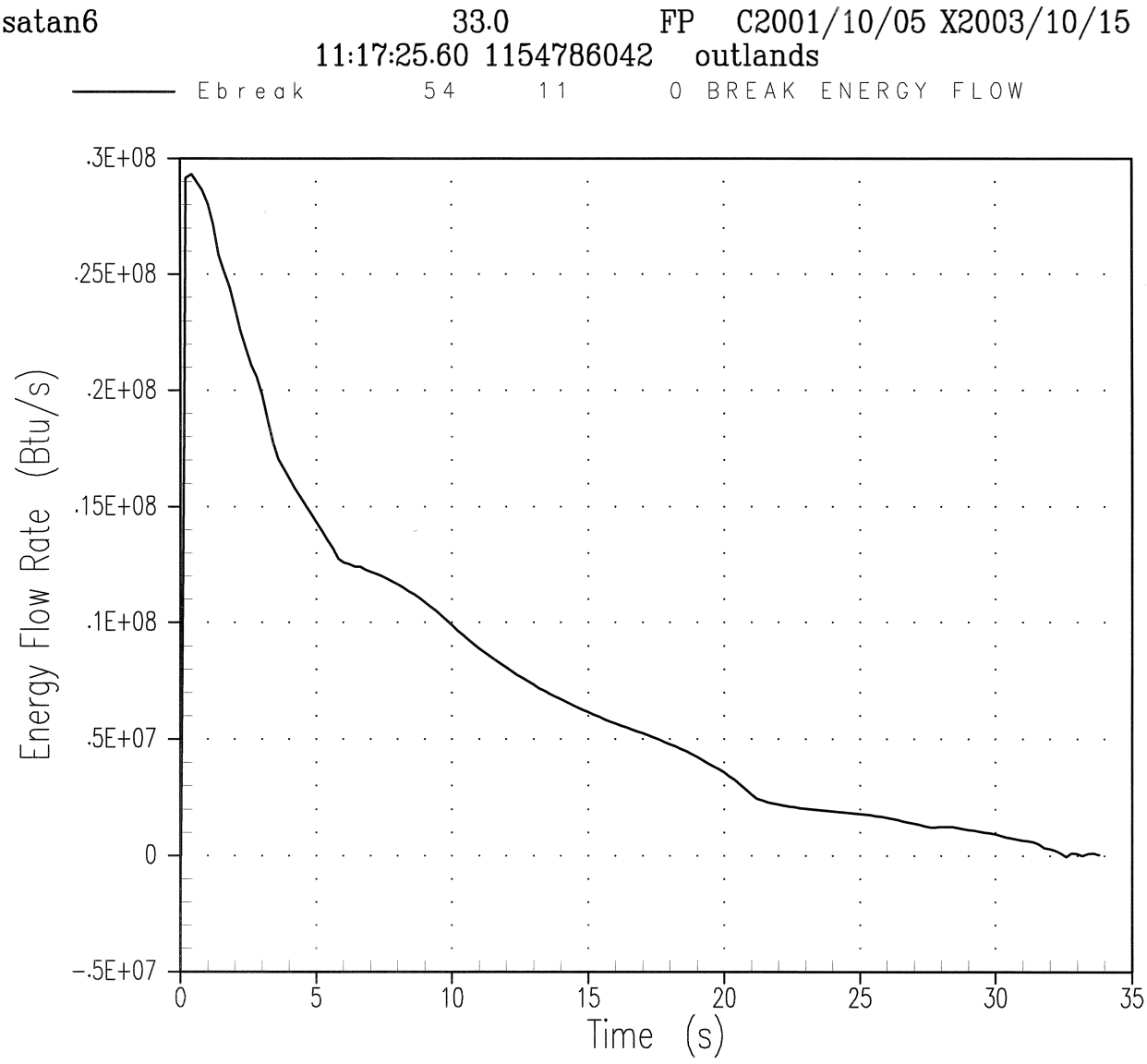

Figure 15.4-19
BREAK ENERGY RELEASE
(DECLG, COSINE SHAPE, C_d=0.6)

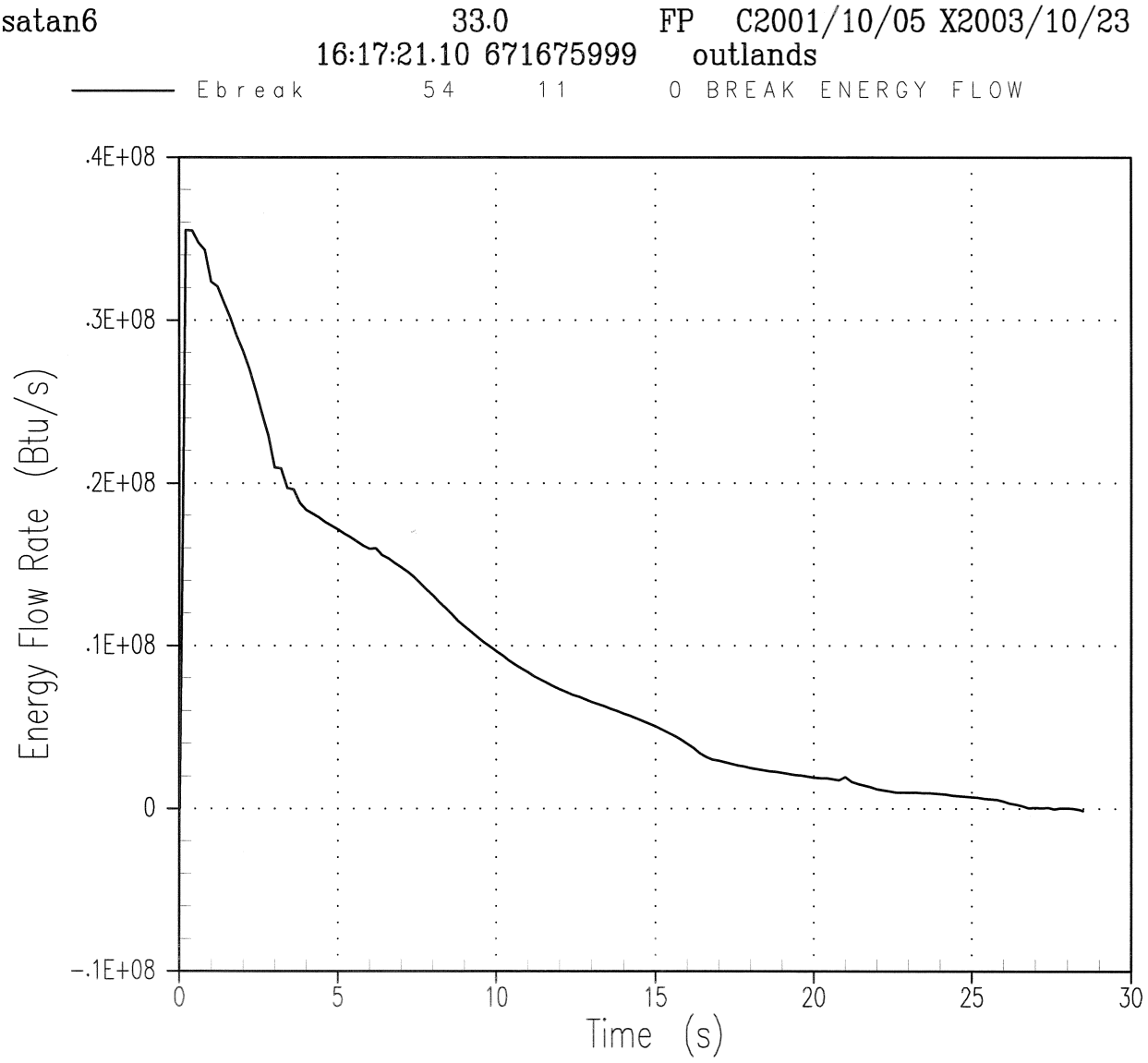

Figure 15.4-20
BREAK ENERGY RELEASE
(DECLG, LIMITING SKEWED SHAPE, C_d=0.4)

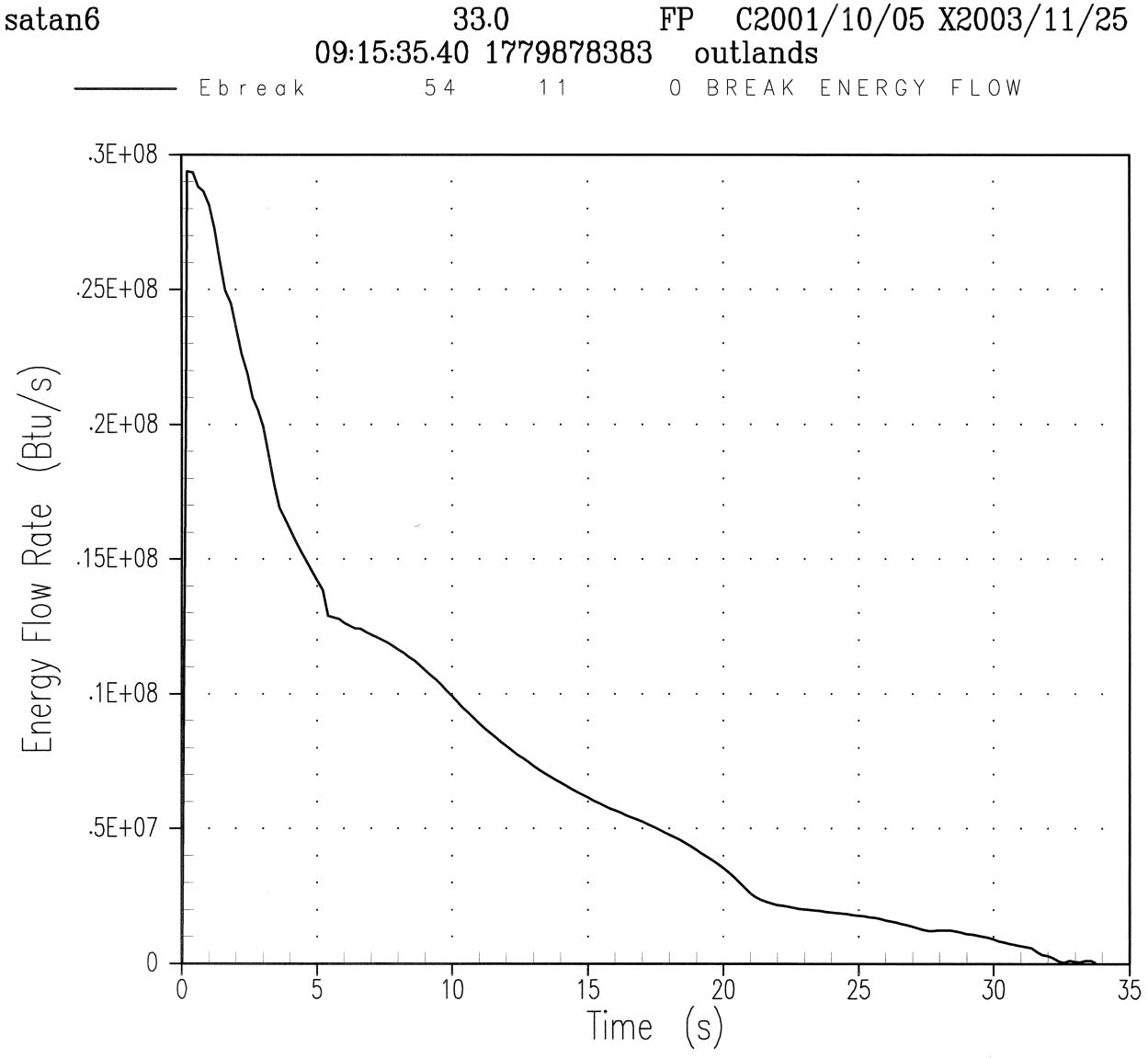

Figure 15.4-21
CORE POWER
(DECLG, COSINE SHAPE, C_d=0.4)

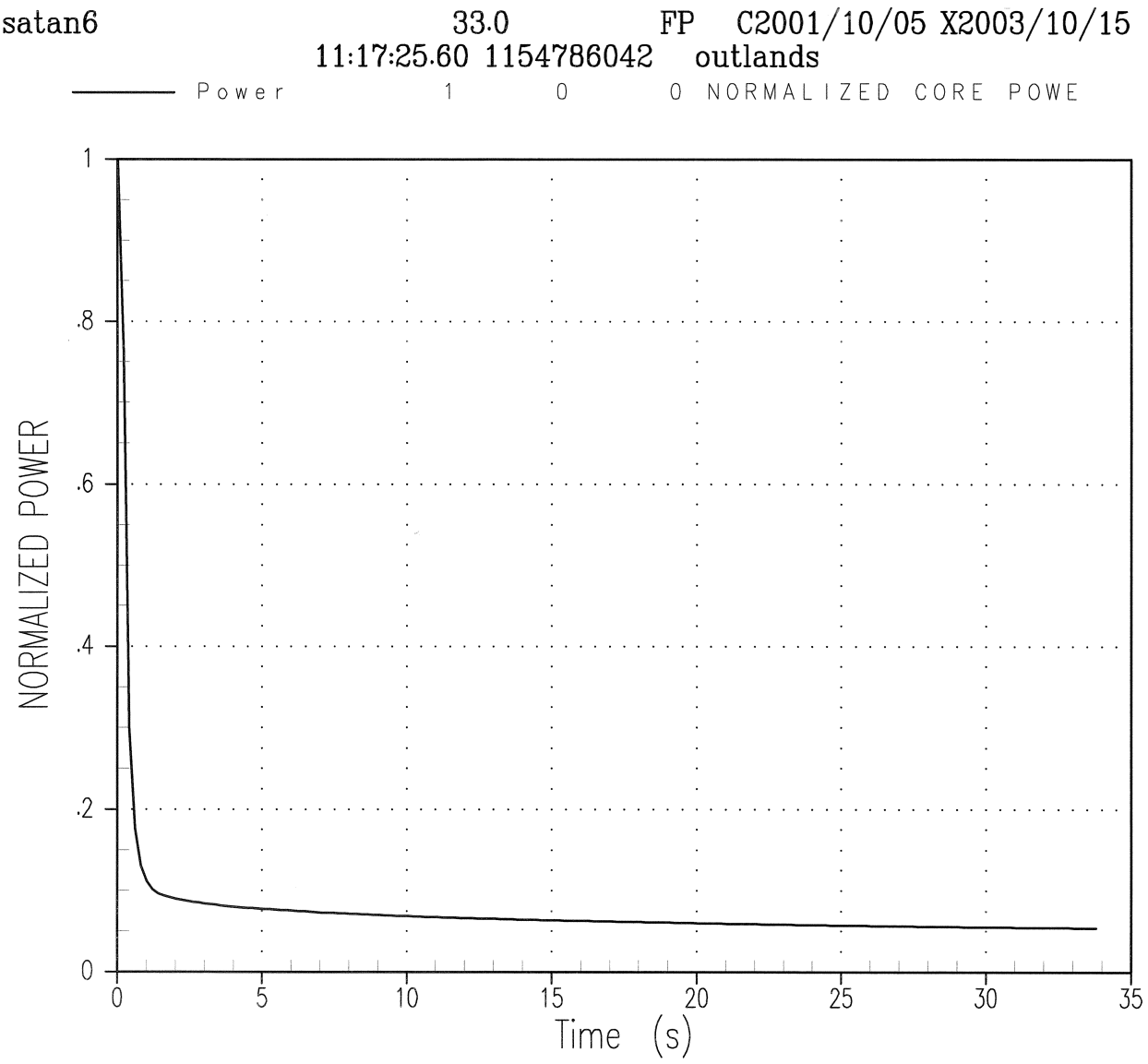

Figure 15.4-22
CORE POWER
(DECLG, COSINE SHAPE, C_d=0.6)

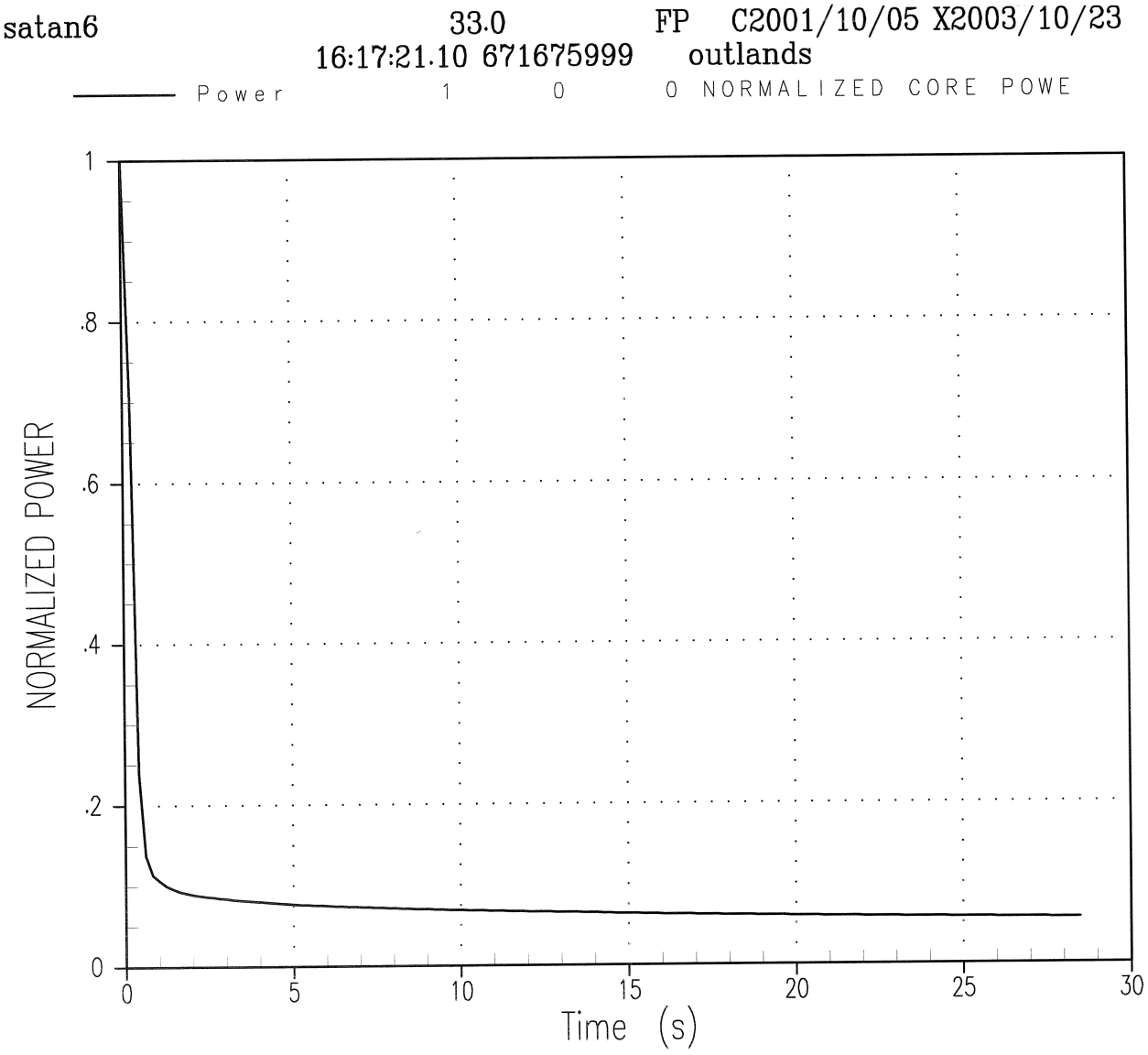

Figure 15.4-23
CORE POWER
(DECLG, LIMITING SKEWED SHAPE, C_d=0.4)

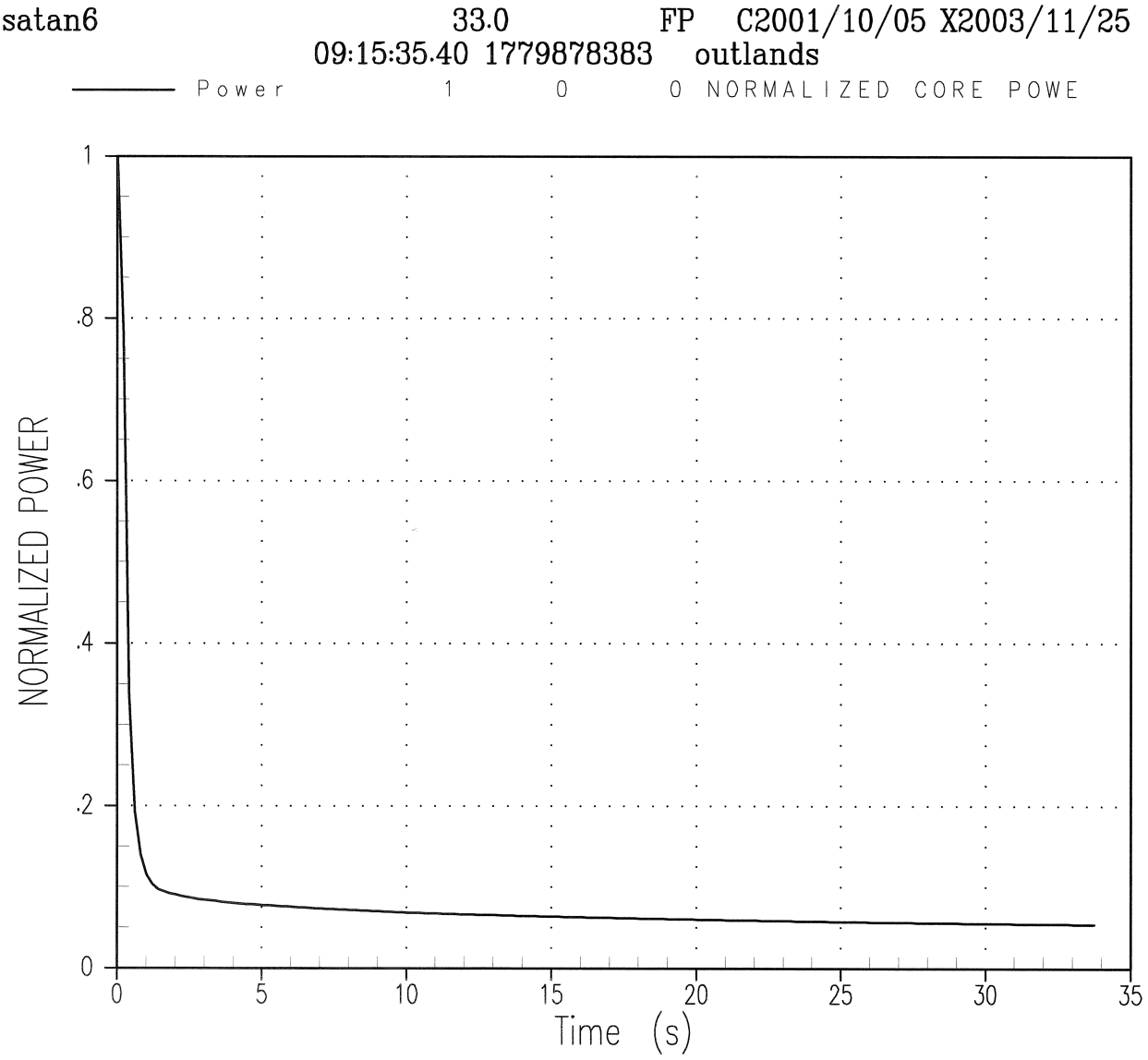

Figure 15.4-24
CONTAINMENT WALL HEAT TRANSFER COEFFICIENT (DECLG, COSINE SHAPE, C_d=0.4)

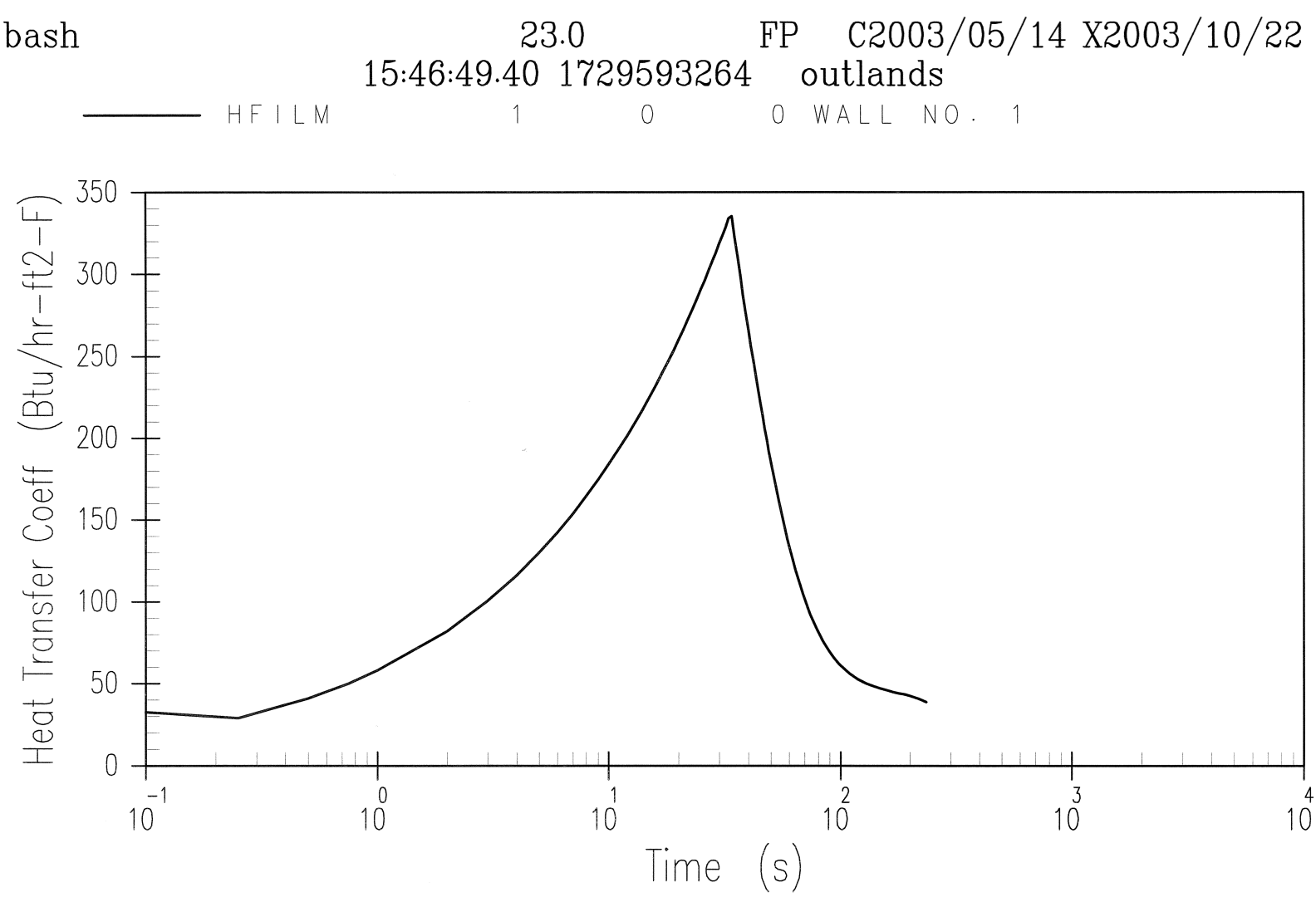

Figure 15.4-25
CONTAINMENT WALL HEAT TRANSFER COEFFICIENT (DECLG, COSINE SHAPE, C_d=0.6)

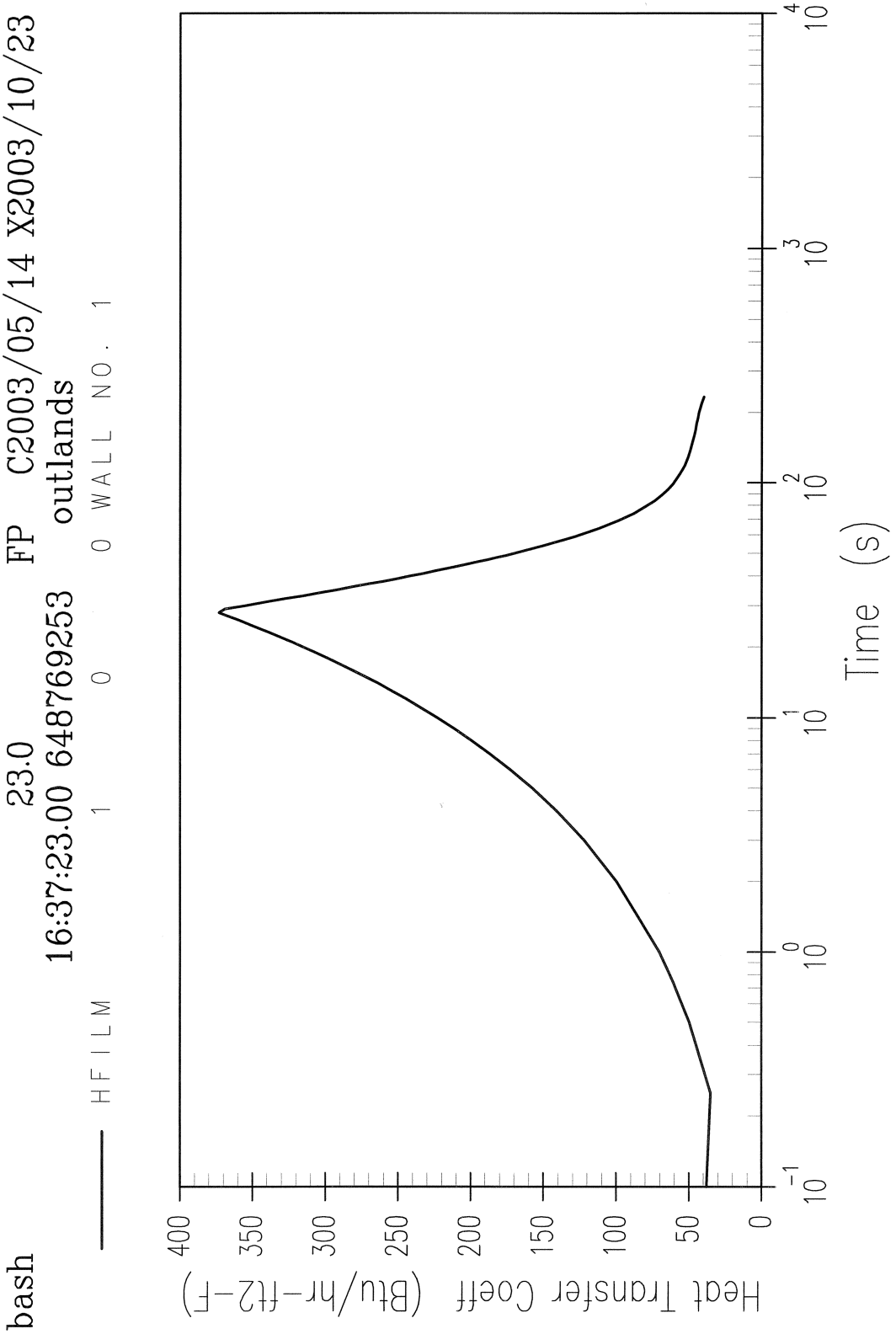

Figure 15.4-26
CONTAINMENT WALL HEAT TRANSFER COEFFICIENT (DECLG, LIMITING SKEWED SHAPE, C_d=0.4)

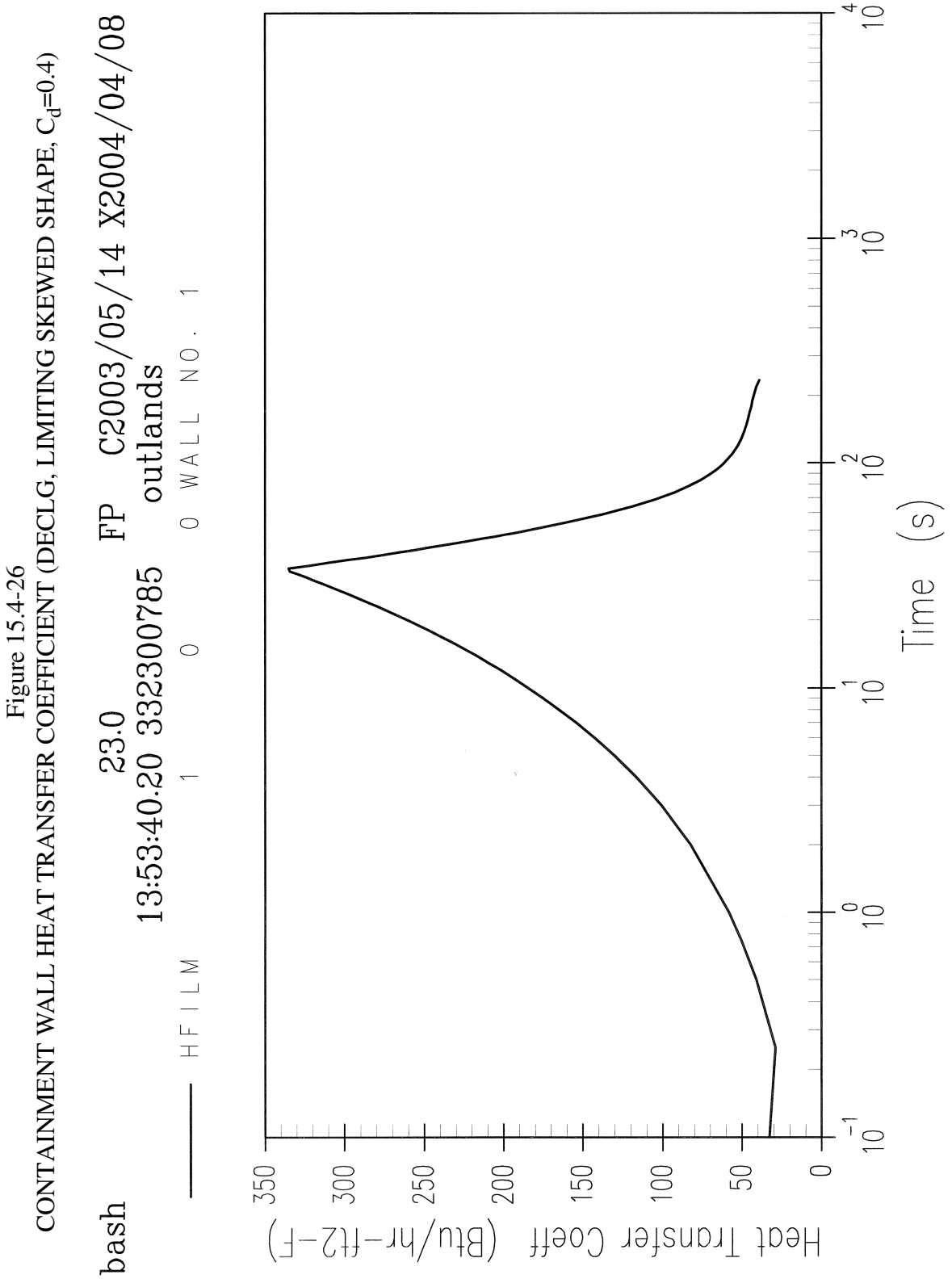

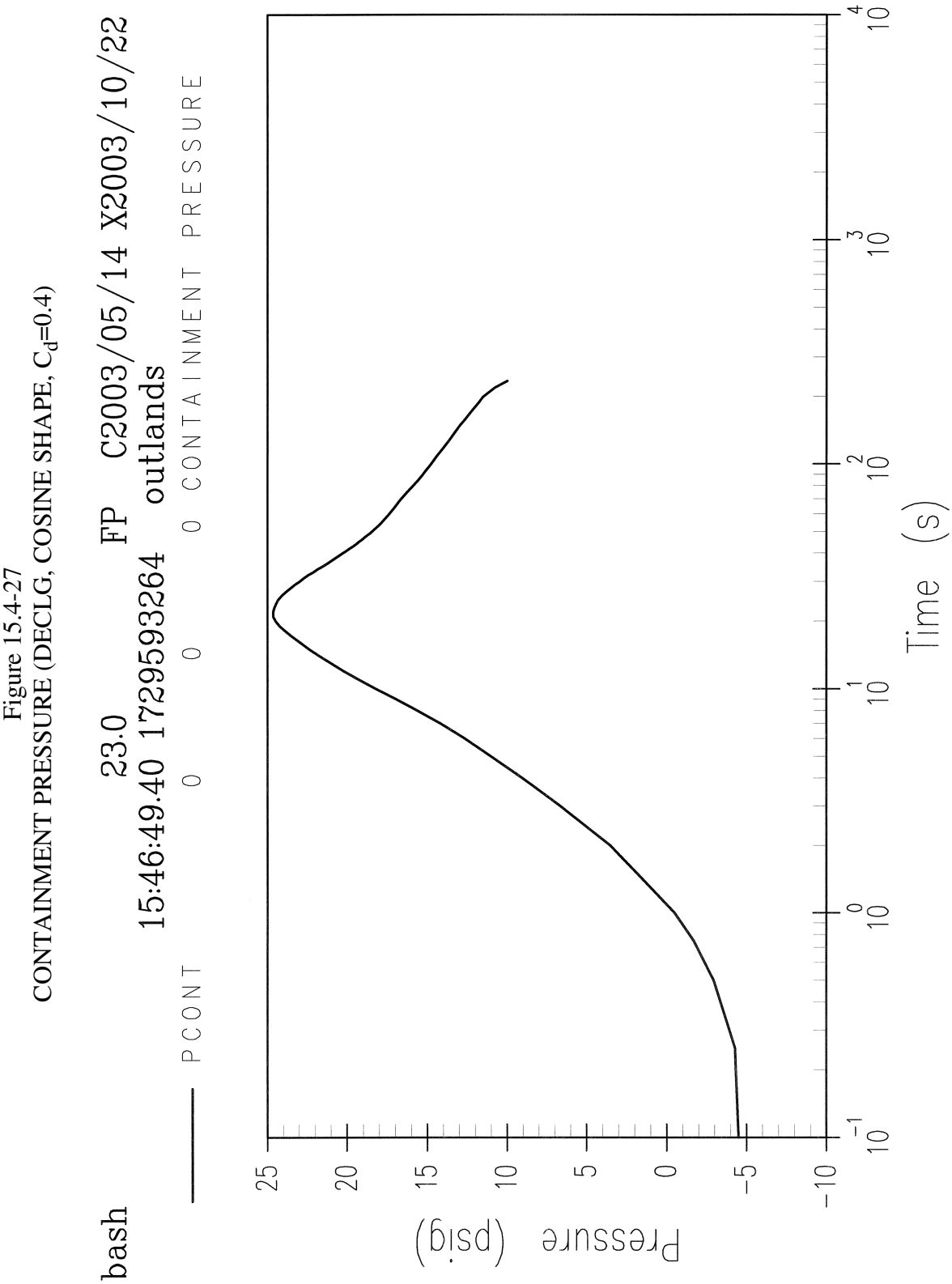

Figure 15.4-27
CONTAINMENT PRESSURE (DECLG, COSINE SHAPE, C_d=0.4)

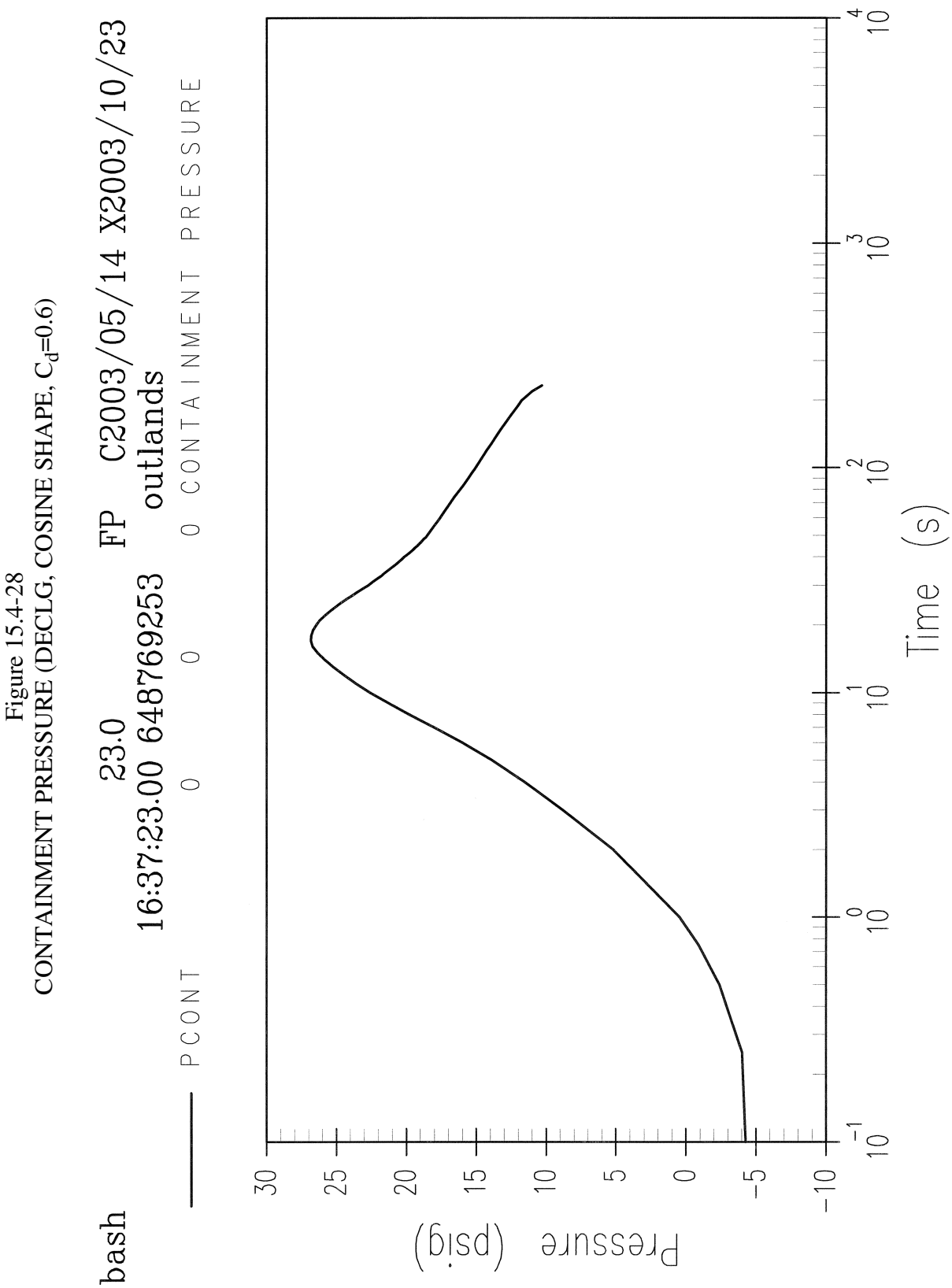

Figure 15.4-28
CONTAINMENT PRESSURE (DECLG, COSINE SHAPE, C_d=0.6)

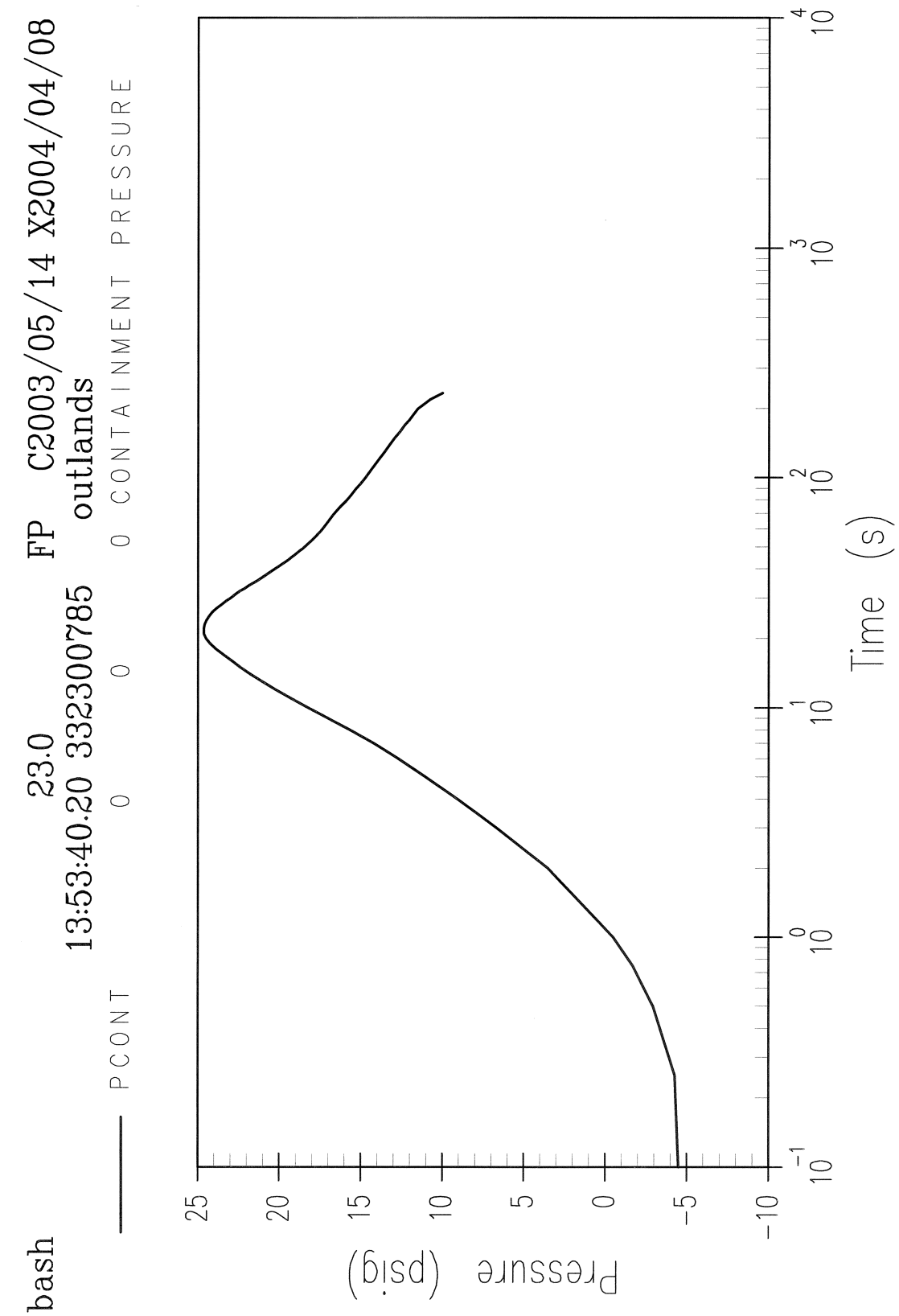

Figure 15.4-29
CONTAINMENT PRESSURE (DECLG, LIMITING SKEWED SHAPE, C_d=0.4)

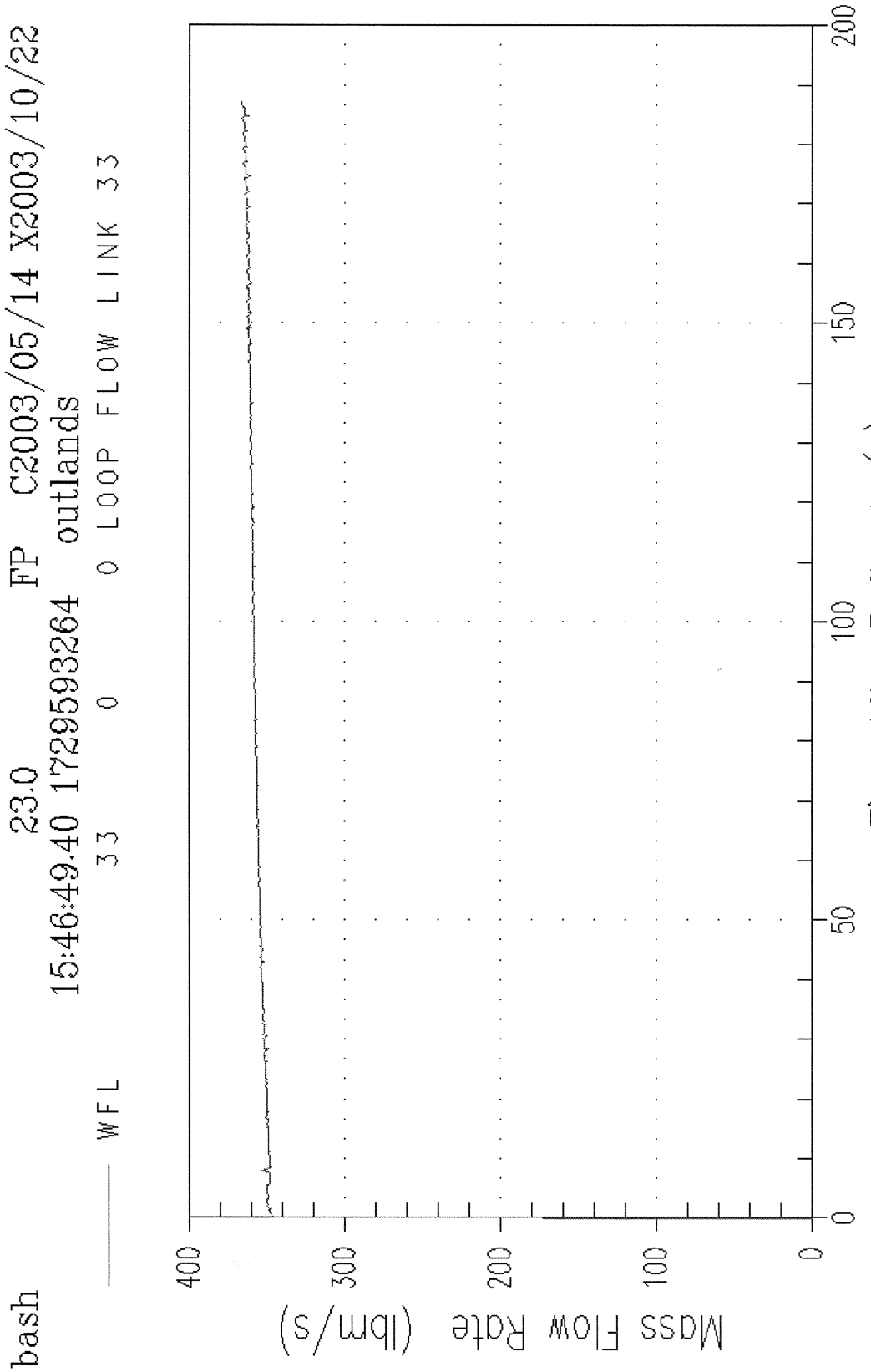

Figure 15.4-30
PUMPED ECCS FLOW (DECLG, COSINE SHAPE, C_d=0.4)

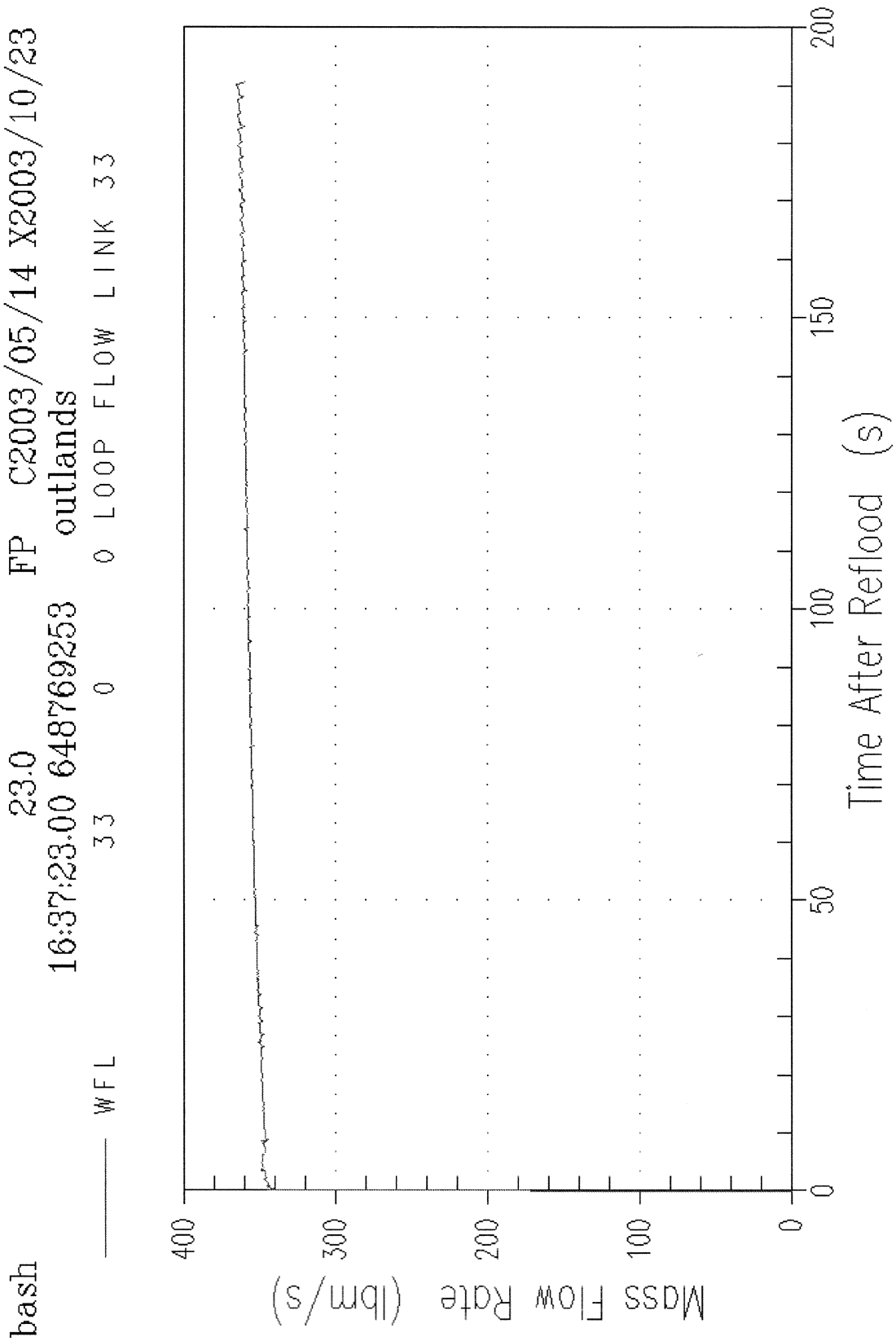

Figure 15.4-31
PUMPED ECCS FLOW (DECLG, COSINE SHAPE, C_d=0.6)

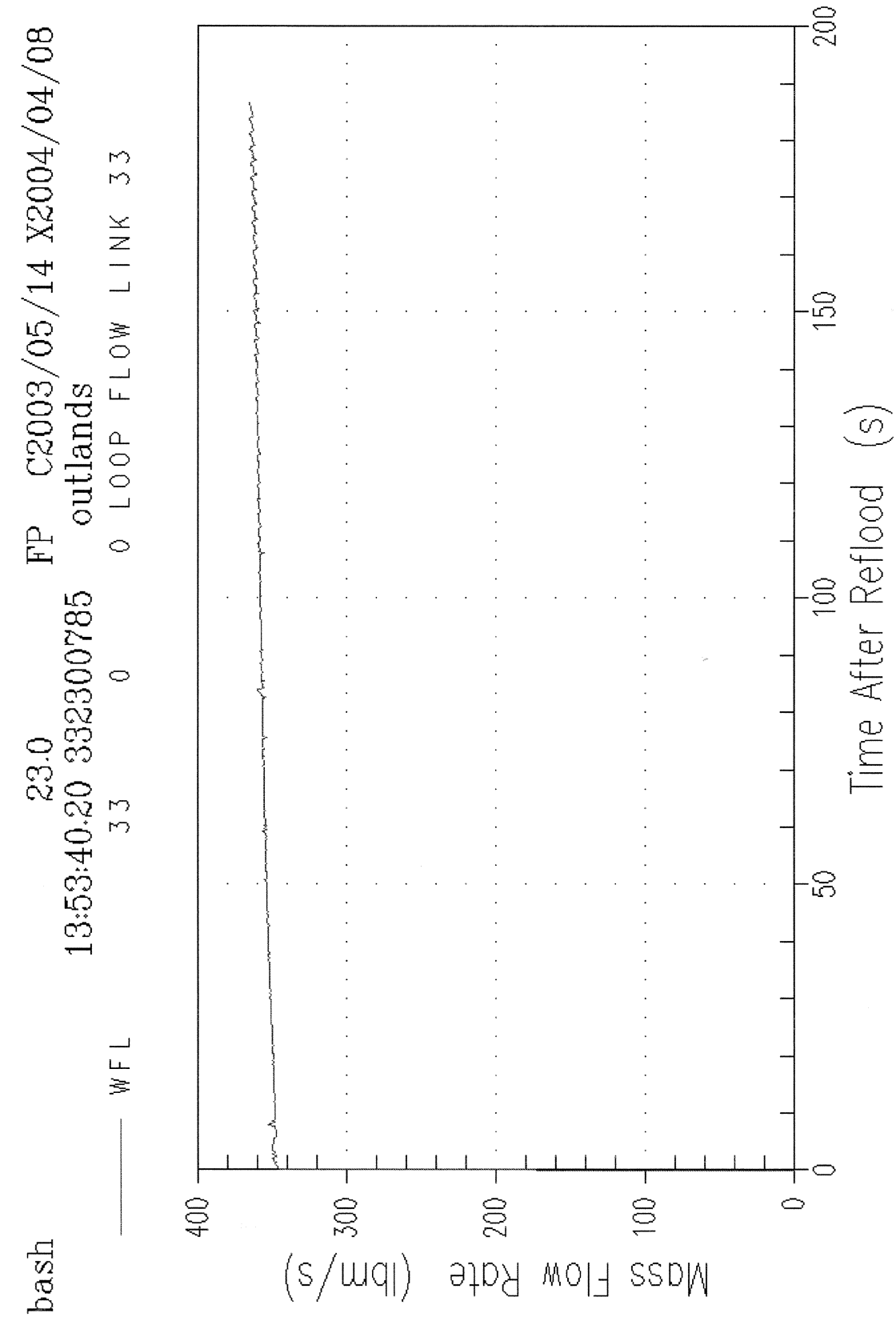

Figure 15.4-32
PUMPED ECCS FLOW (DECLG, LIMITING SKEWED SHAPE, C_d=0.4)

Figure 15.4-33
CORE AND DOWNCOMER WATER LEVELS (DECLG, COSINE SHAPE, C_d=0.4)

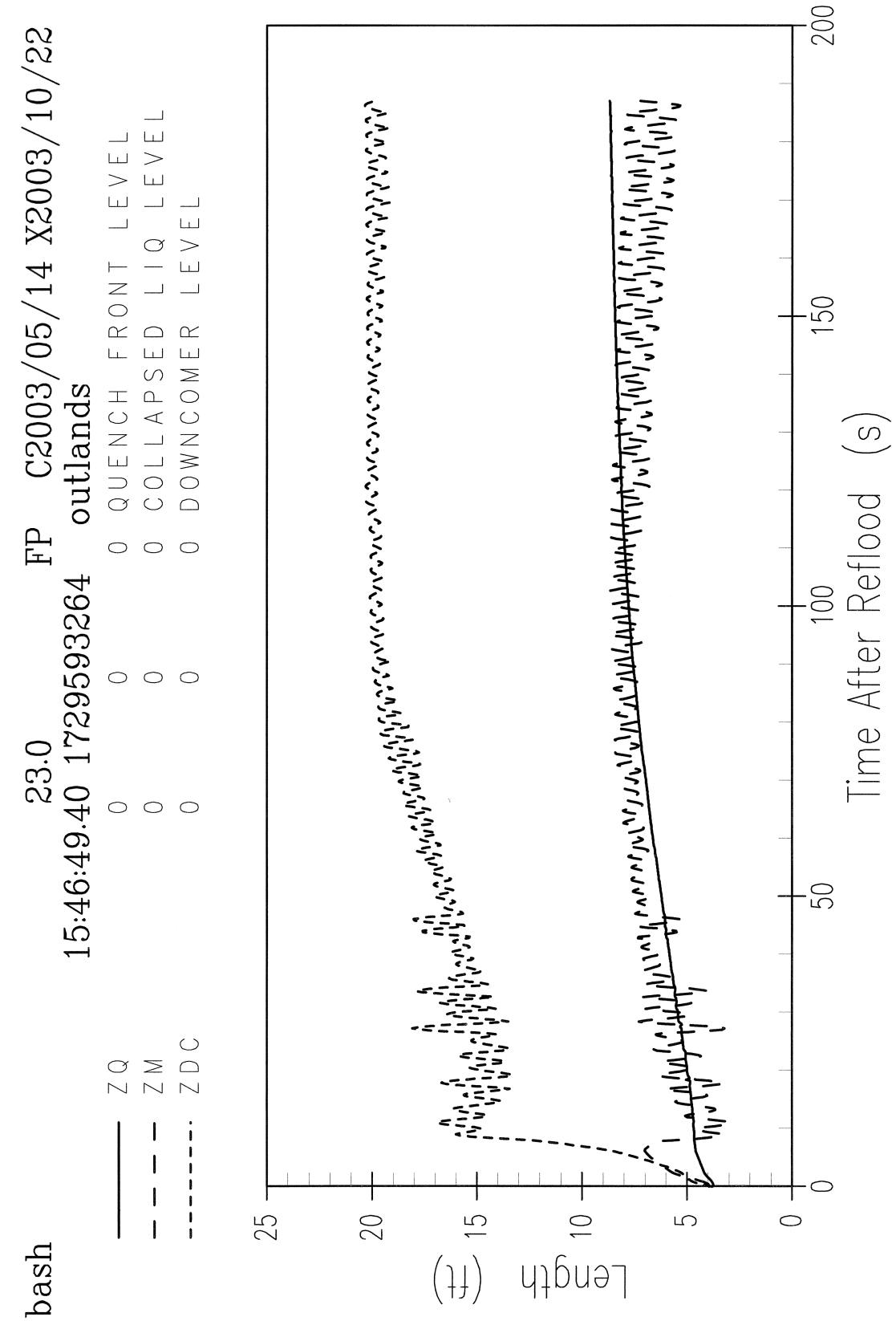

Figure 15.4-34
CORE AND DOWNCOMER WATER LEVELS (DECLG, COSINE SHAPE, C_d=0.6)

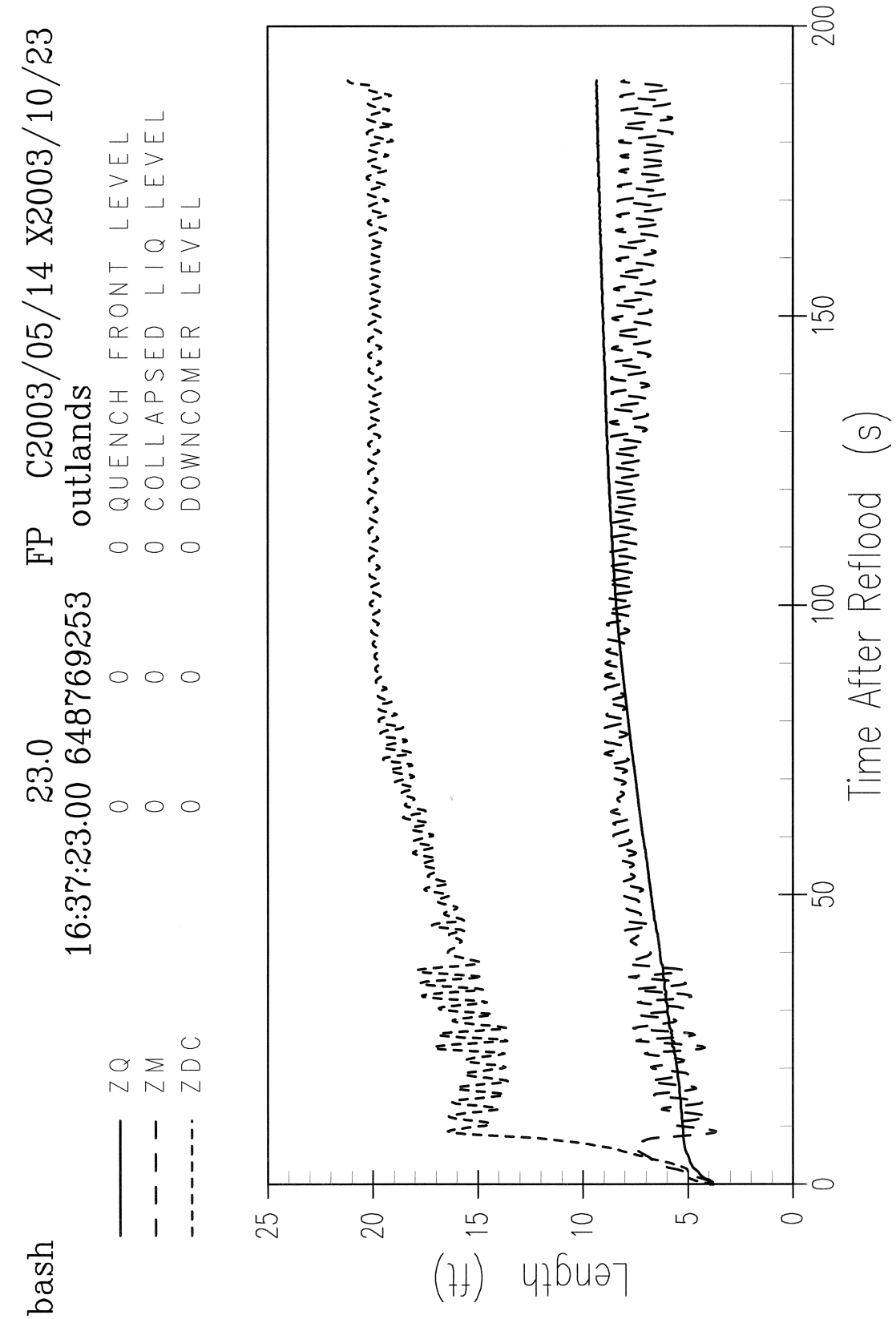

Figure 15.4-35
CORE AND DOWNCOMER WATER LEVELS (DECLG, LIMITING SKEWED SHAPE, C_d=0.4)

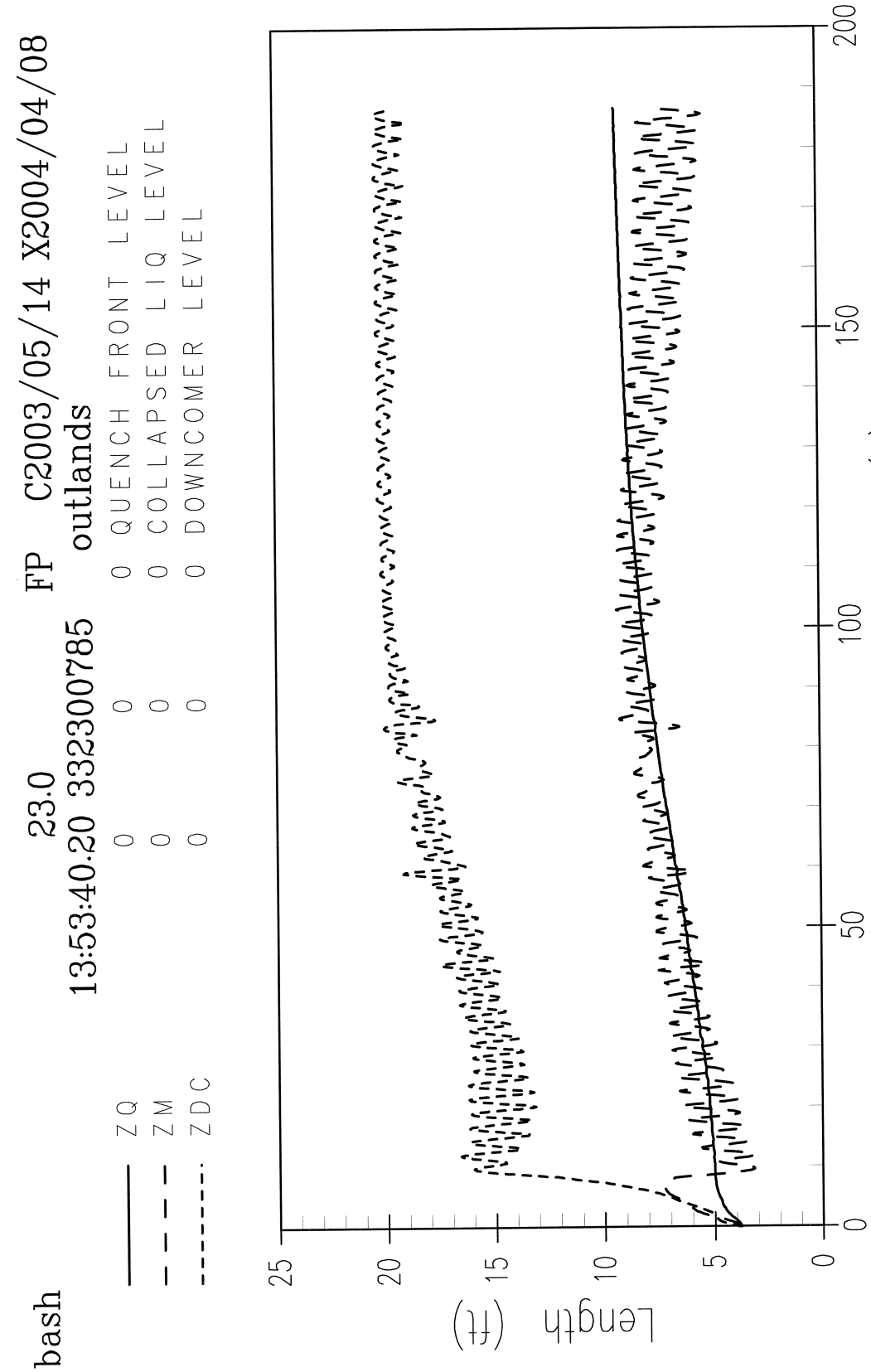

Figure 15.4-36
RAW FLOODING RATE INTEGRAL AND LINE SEGMENT INTEGRAL (DECLG, COSINE SHAPE, C_d=0.4)

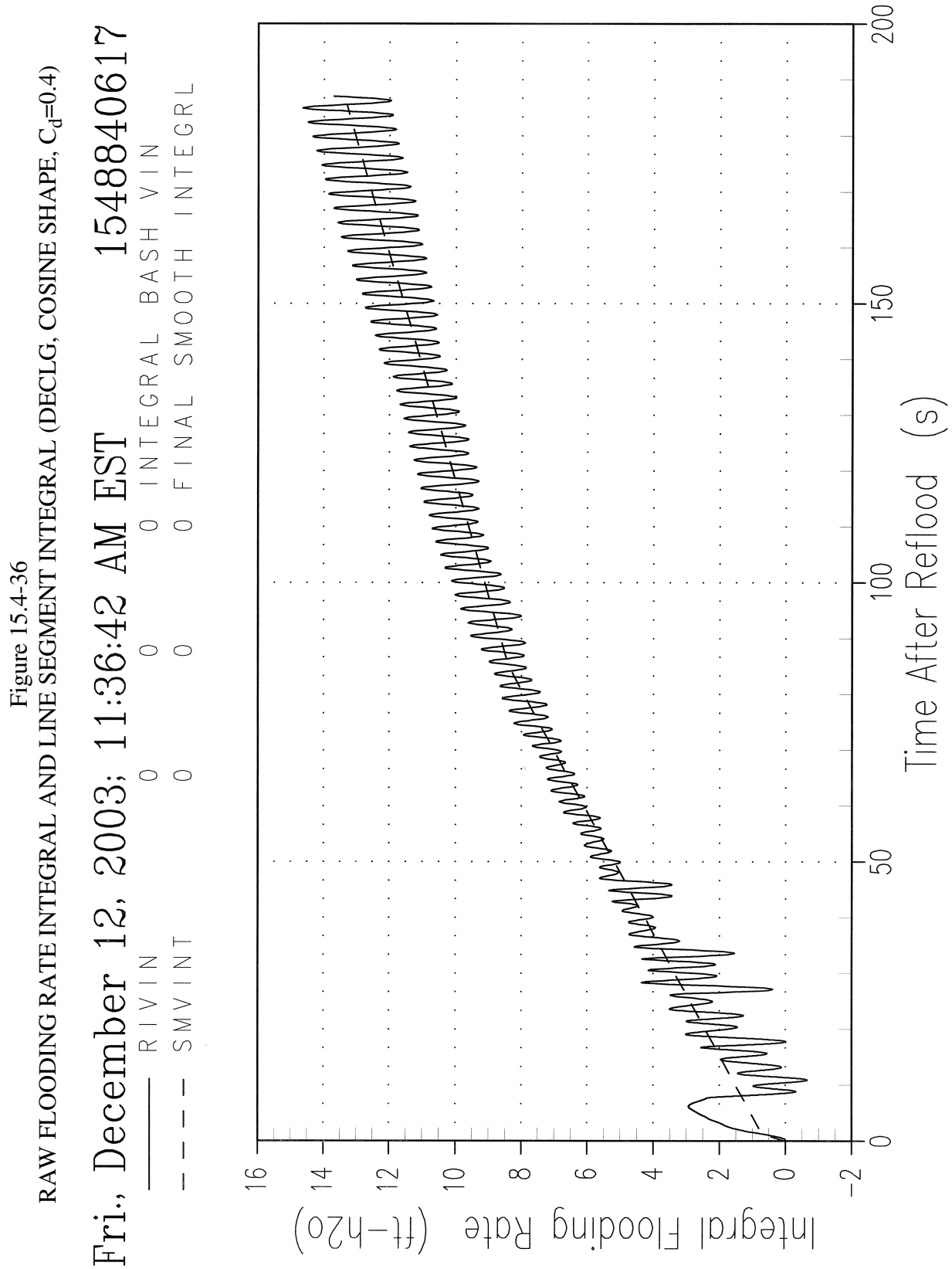

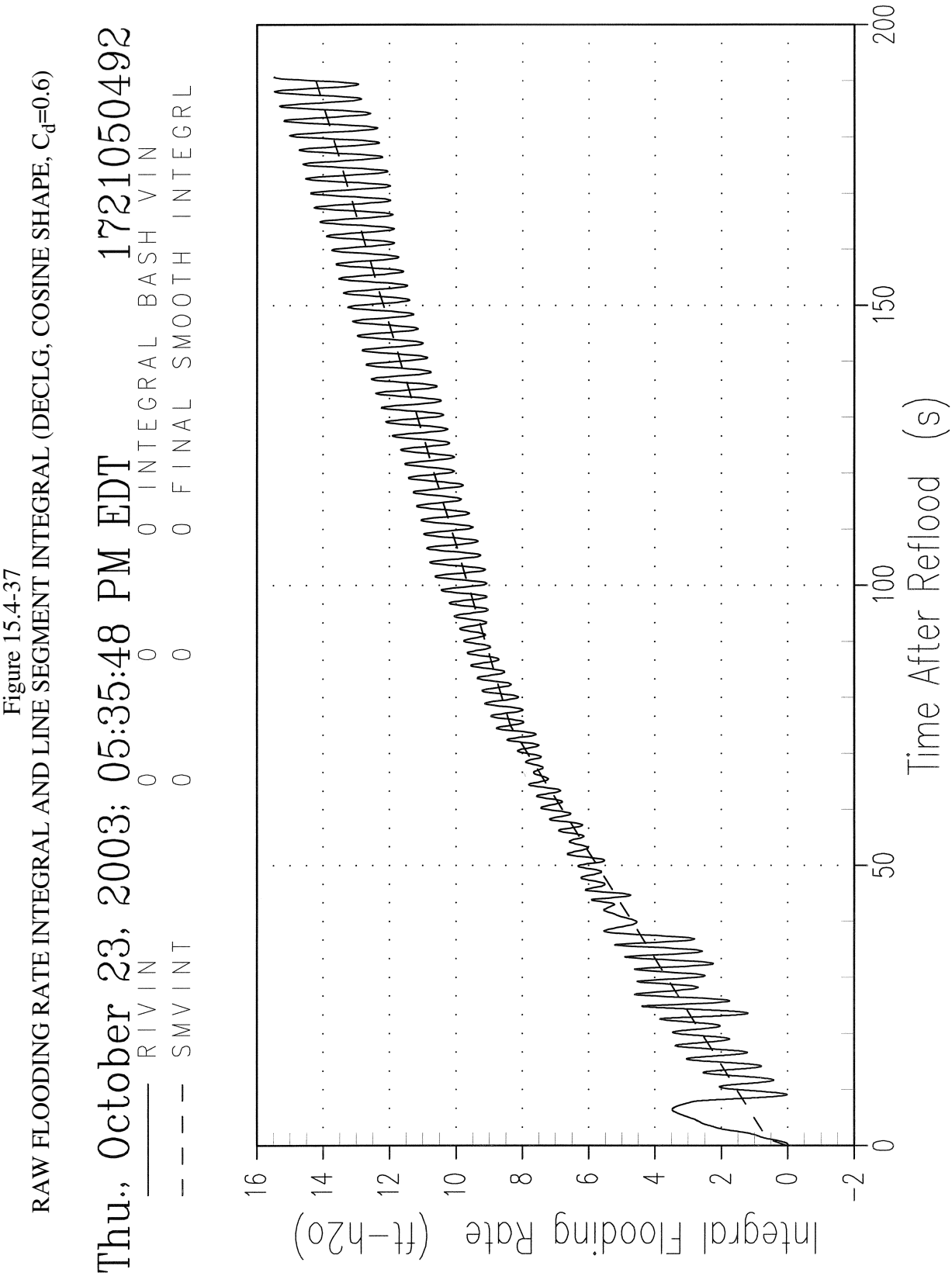

Figure 15.4-37
RAW FLOODING RATE INTEGRAL AND LINE SEGMENT INTEGRAL (DECLG, COSINE SHAPE, C_d=0.6)

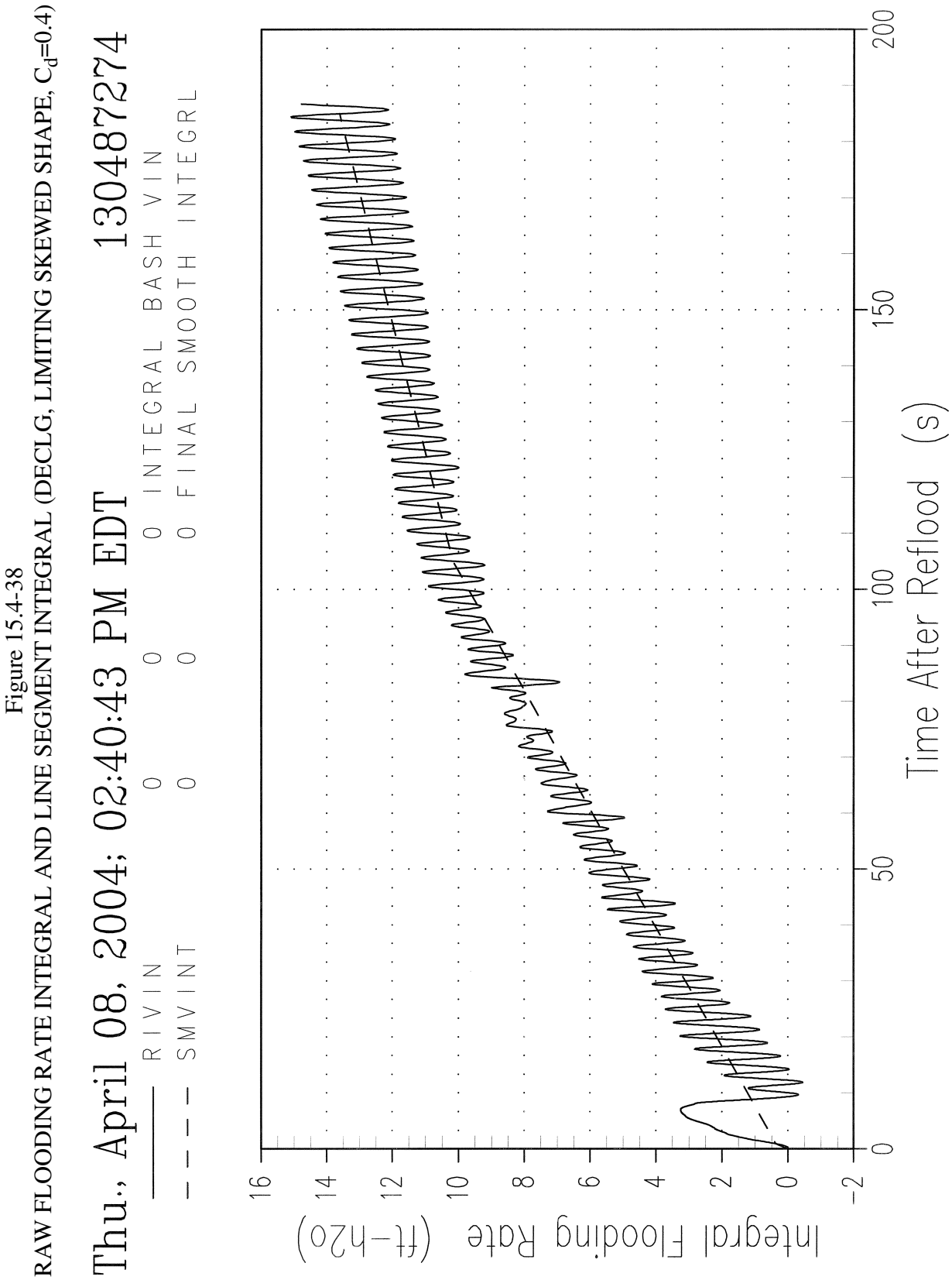

Figure 15.4-38
RAW FLOODING RATE INTEGRAL AND LINE SEGMENT INTEGRAL (DECLG, LIMITING SKEWED SHAPE, C_d=0.4)

Figure 15.4-39
RESULTING LINE SEGMENT FLOODING RATE (DECLG, COSINE SHAPE, C_d=0.4)

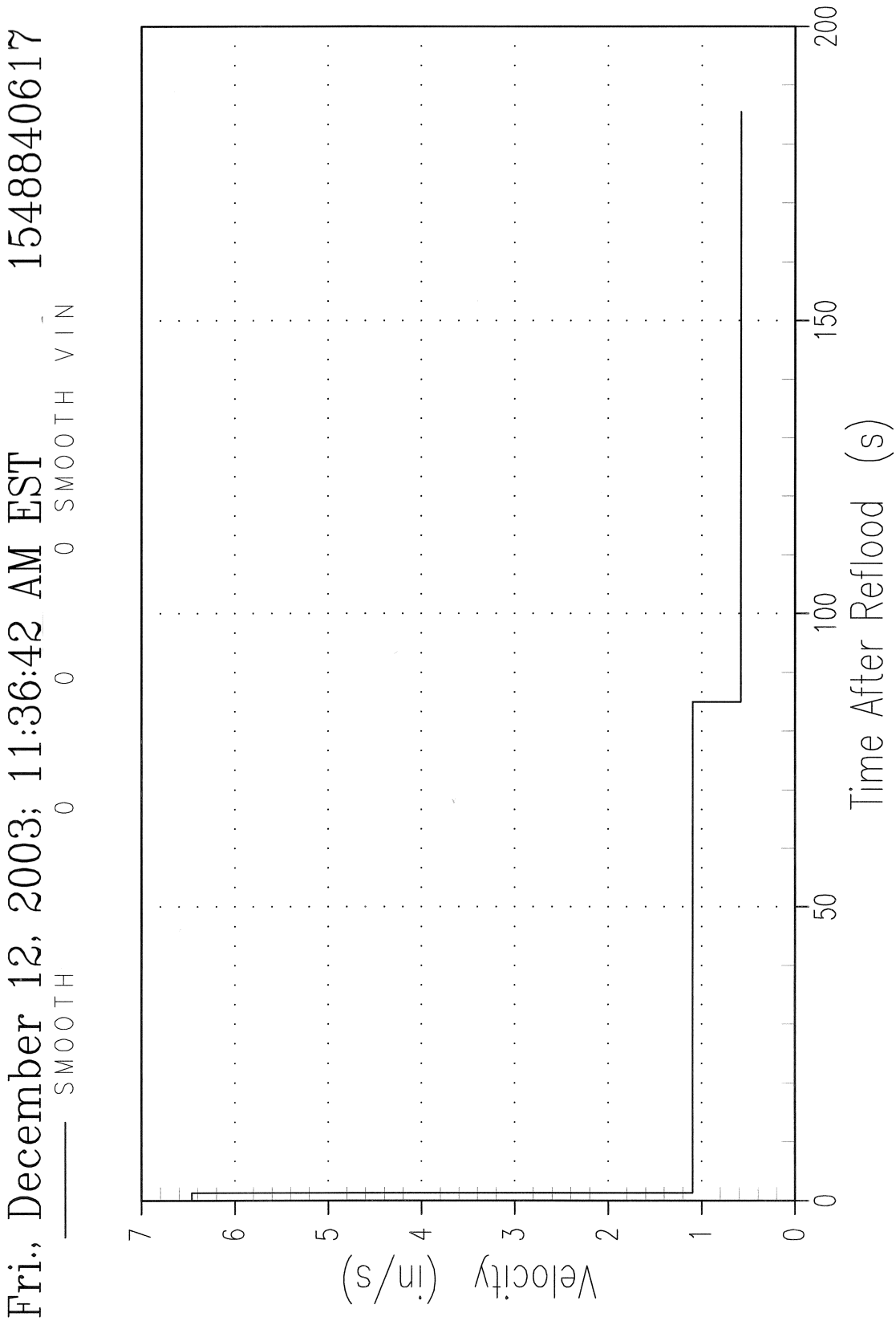

Figure 15.4-40
RESULTING LINE SEGMENT FLOODING RATE (DECLG, COSINE SHAPE, C_d=0.6)

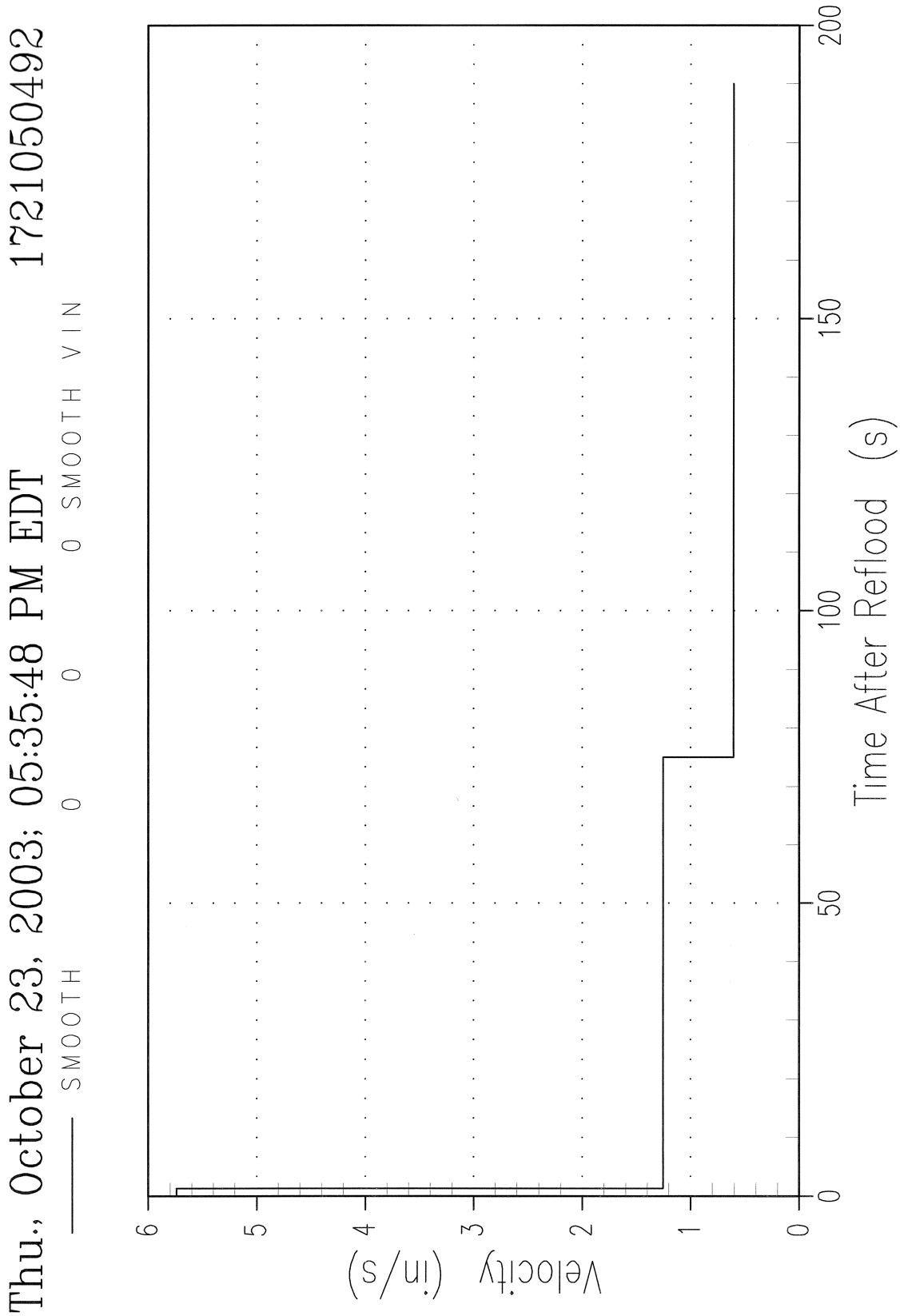

Figure 15.4-41
RESULTING LINE SEGMENT FLOODING RATE (DECLG, LIMITING SKEWED SHAPE, C_d=0.4)

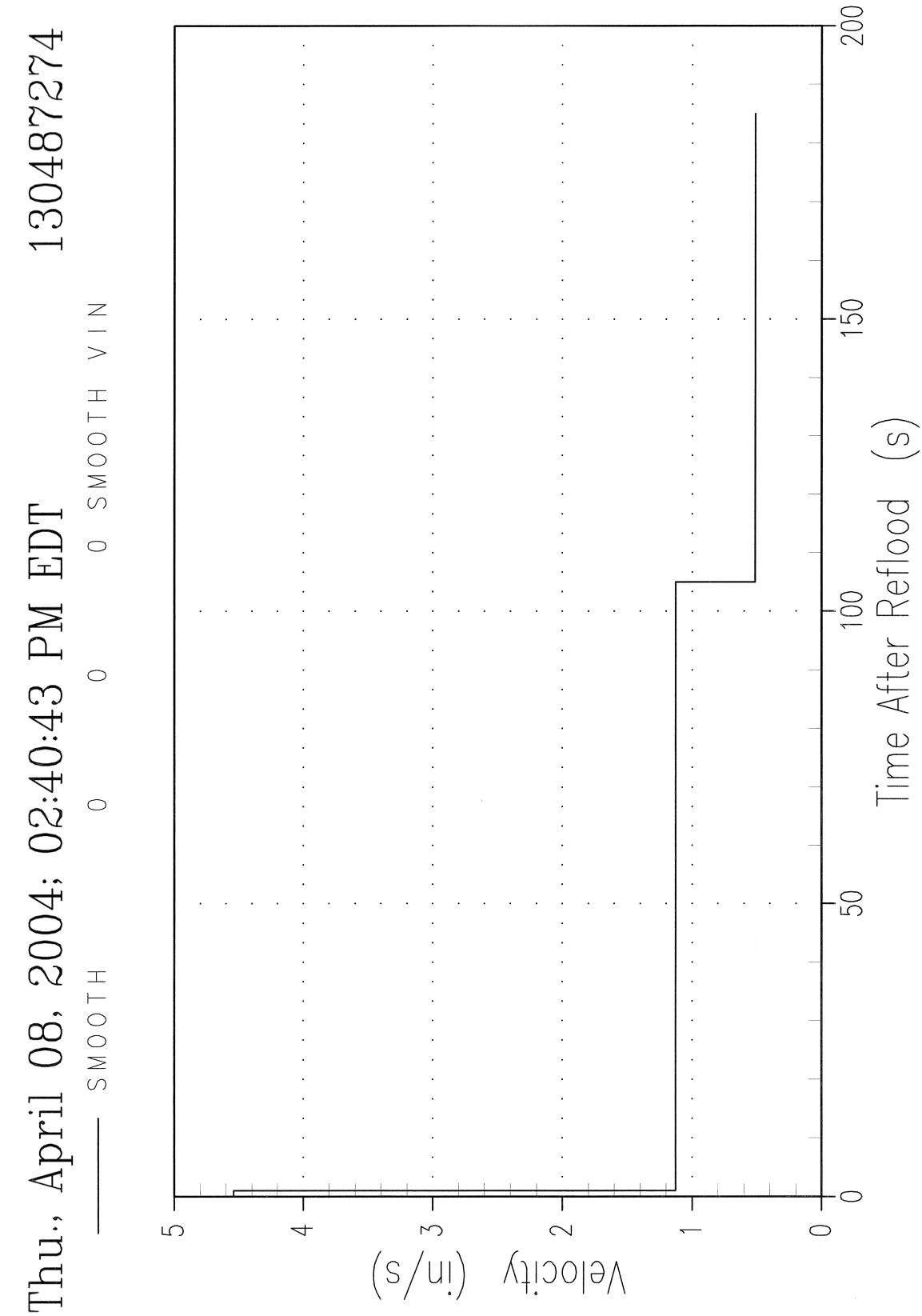

Figure 15.4-42
HOT ROD CLAD AVERAGE TEMPERATURE (DECLG, COSINE SHAPE, C_d=0.4)

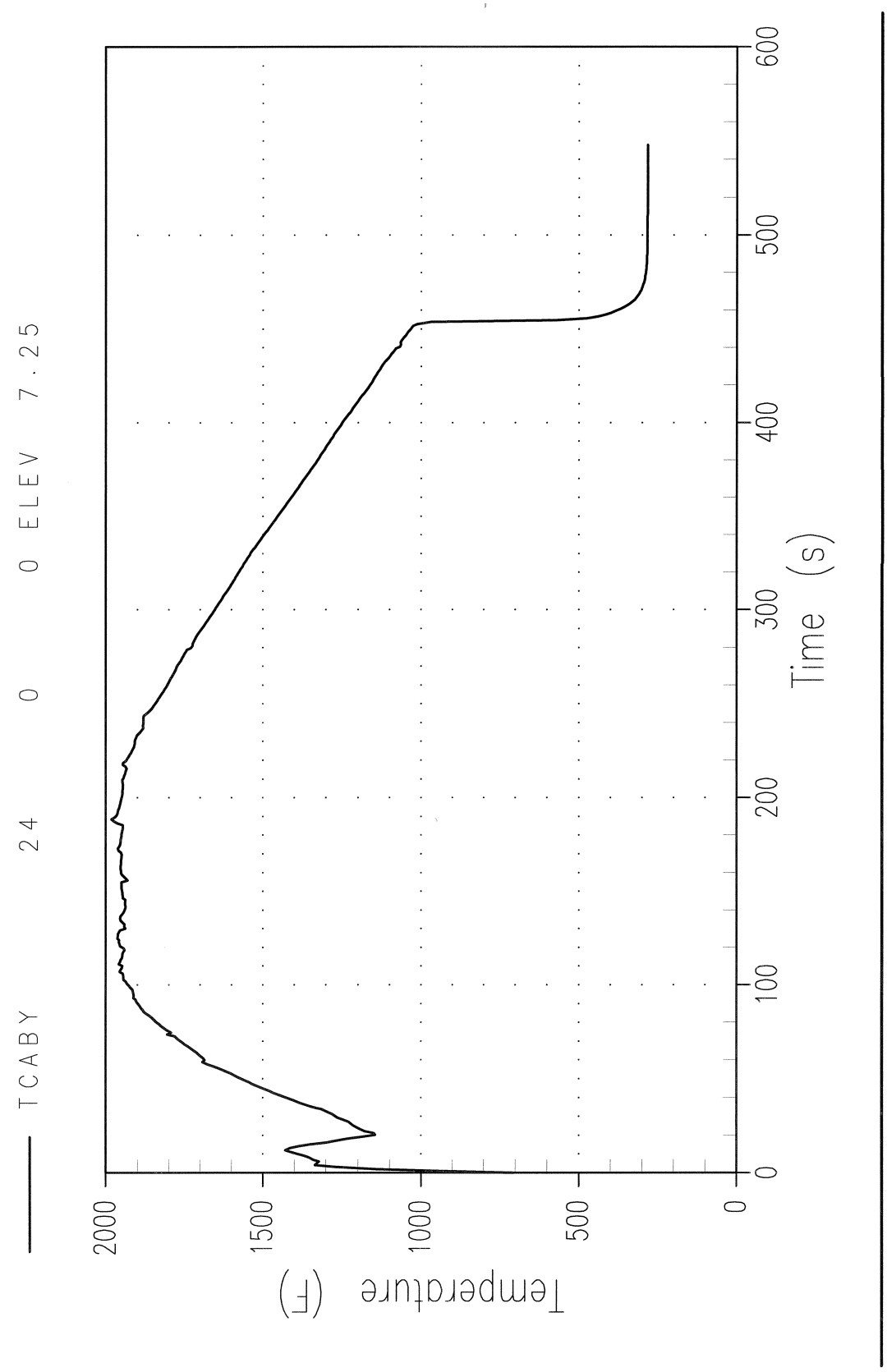

Figure 15.4-43
HOT ROD CLAD AVERAGE TEMPERATURE (DECLG, COSINE SHAPE, C_d=0.6)

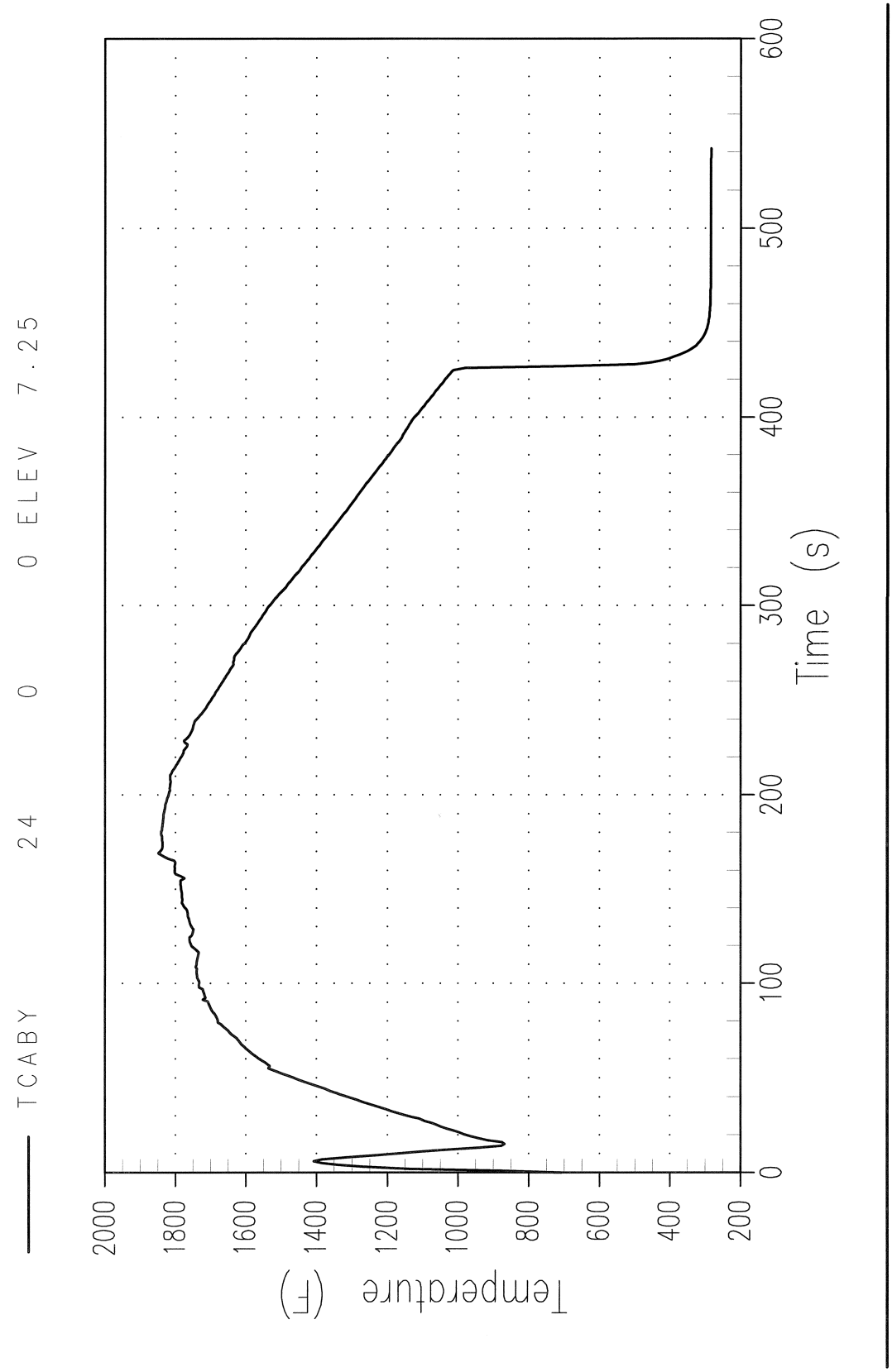

Figure 15.4-44
HOT ROD CLAD AVERAGE TEMPERATURE (DECLG, LIMITING SKEWED SHAPE, C_d=0.4)

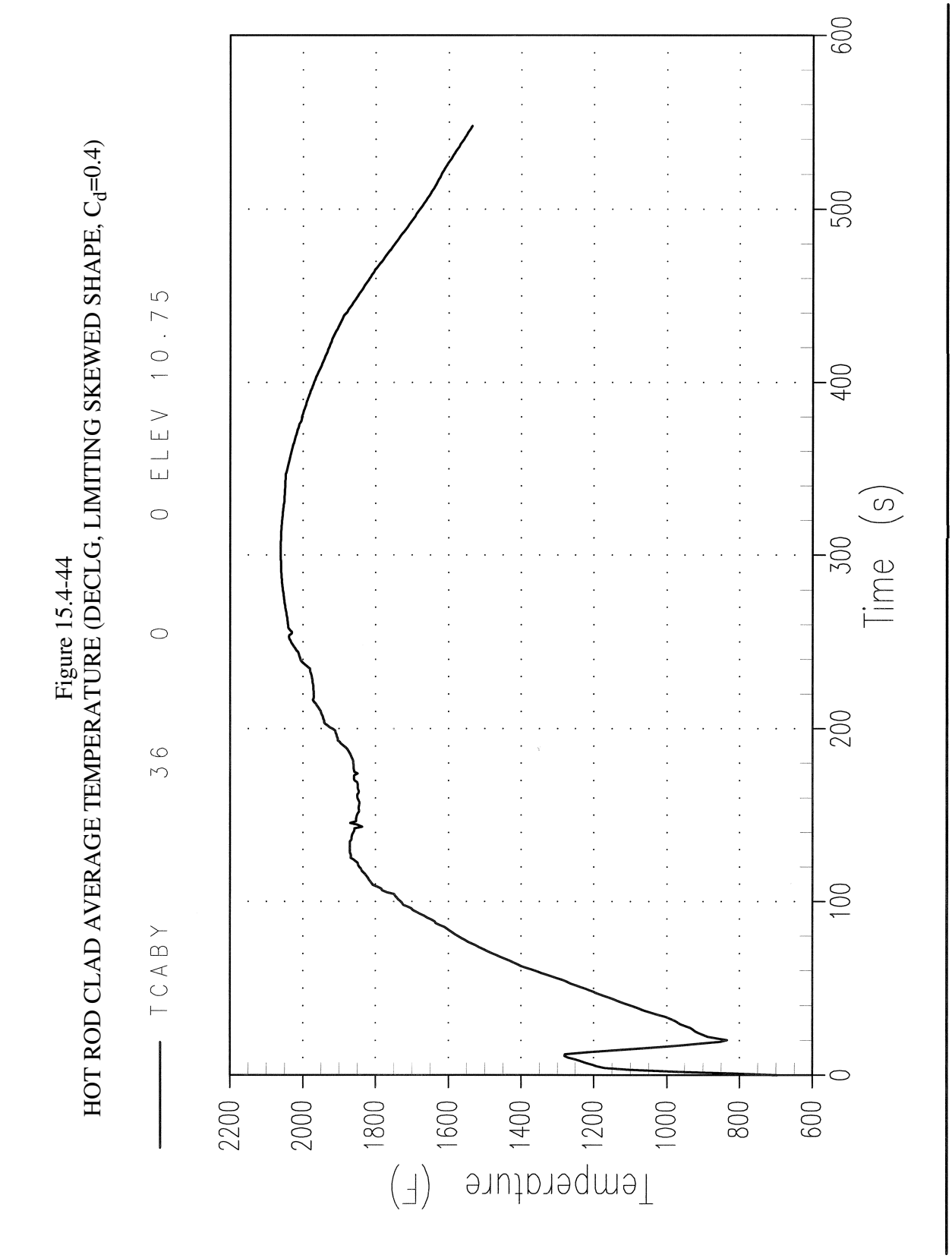

Figure 15.4-45
FLUID AND VAPOR TEMPERATURE (DECLG, COSINE SHAPE, C_d=0.4)

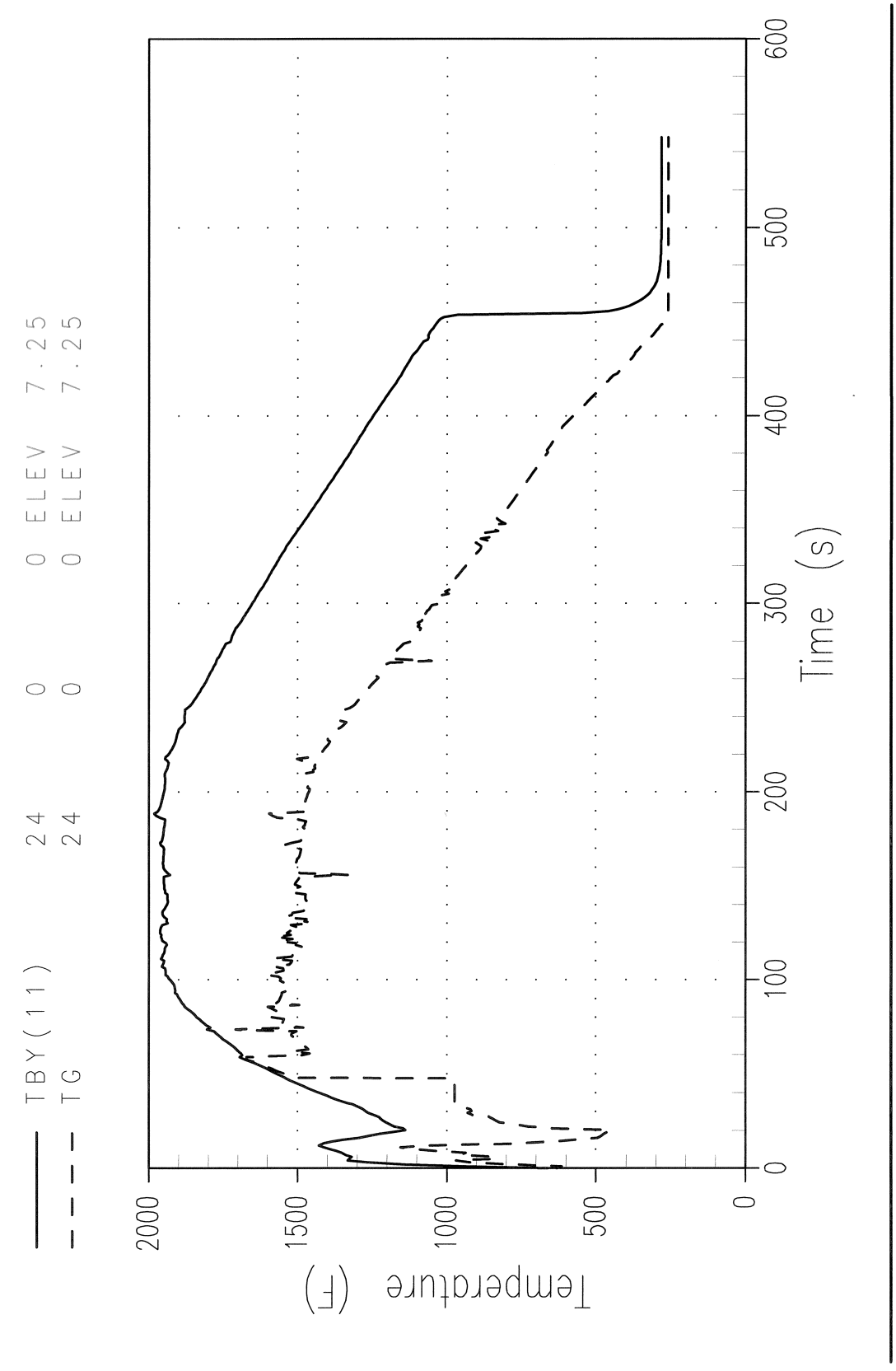

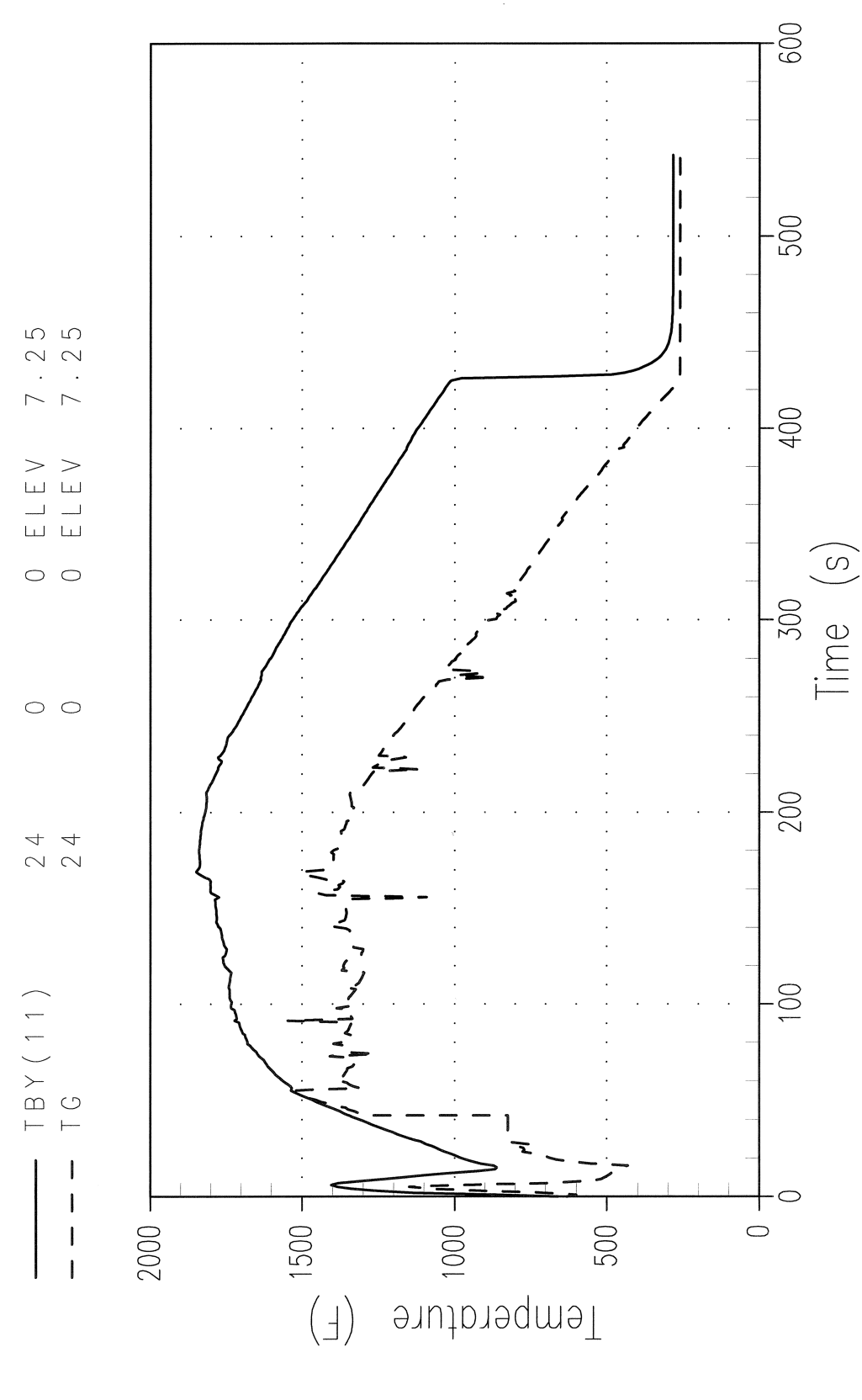

Figure 15.4-46
FLUID AND VAPOR TEMPERATURE (DECLG, COSINE SHAPE, C_d=0.6)

Figure 15.4-47
FLUID AND VAPOR TEMPERATURE (DECLG, LIMITING SKEWED SHAPE, C_d=0.4)

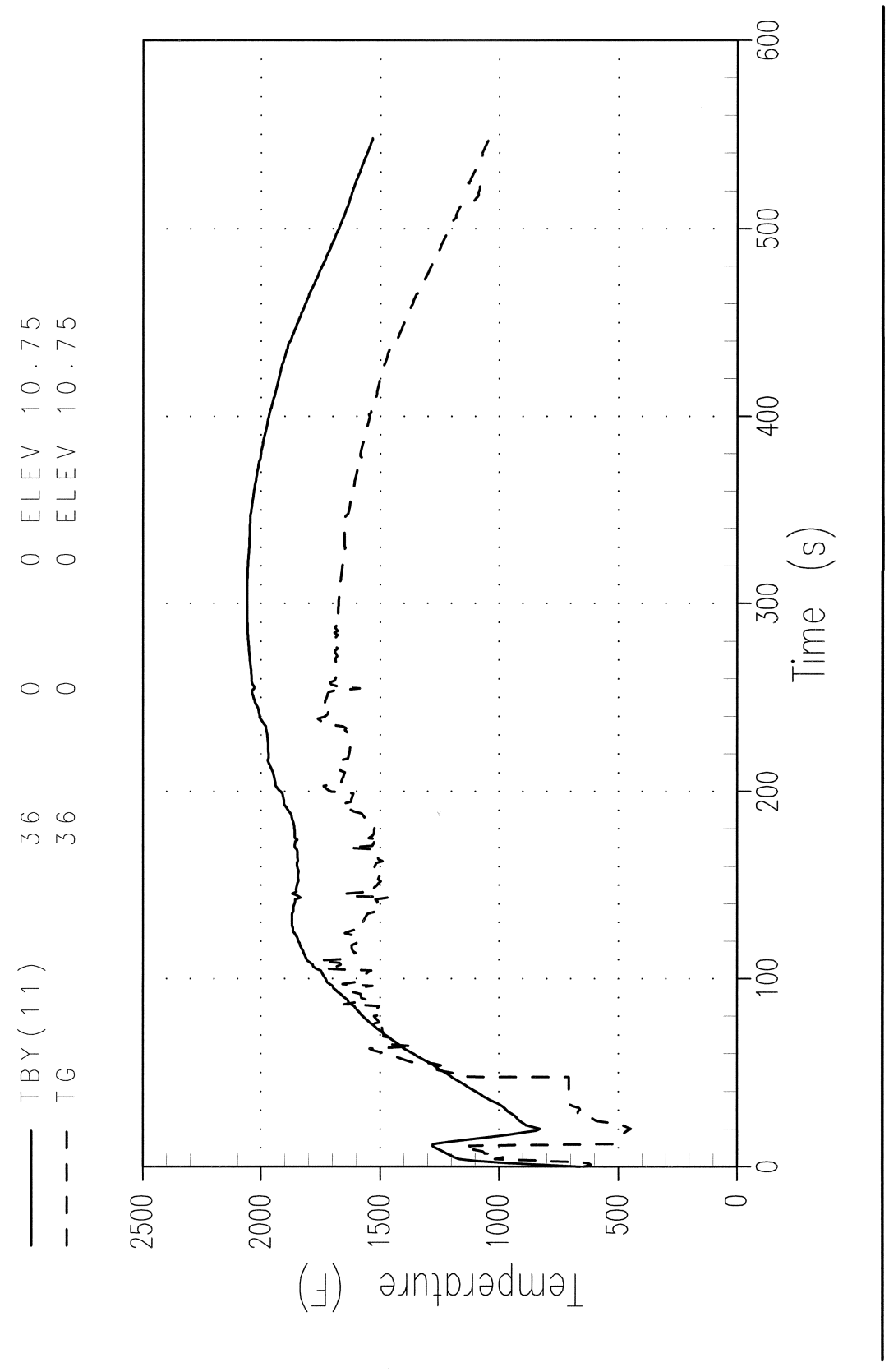

Figure 15.4-48
HOT ROD HEAT TRANSFER COEFFICIENT (DECLG, COSINE SHAPE, C_d=0.4)

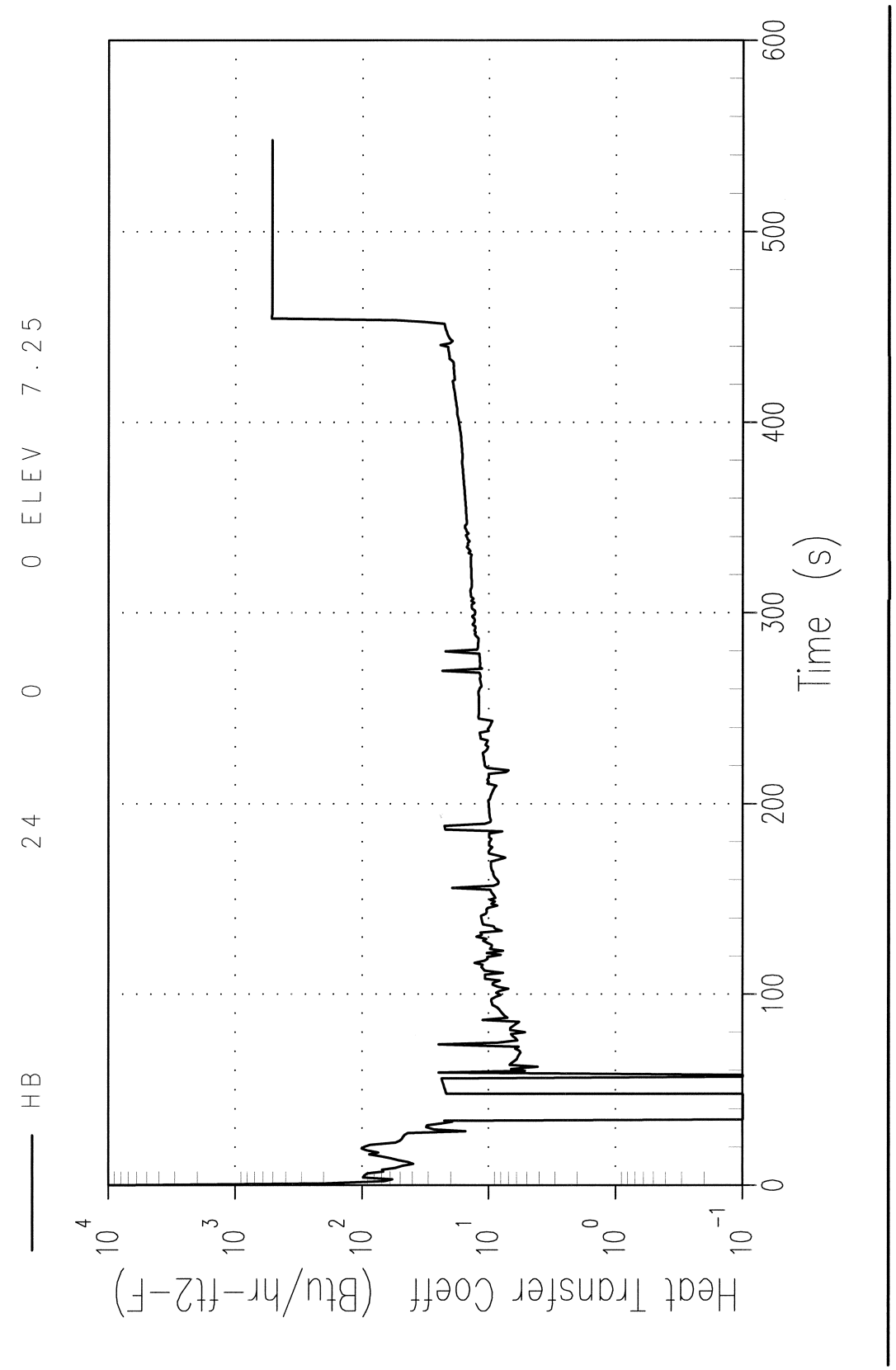

Figure 15.4-49
HOT ROD HEAT TRANSFER COEFFICIENT (DECLG, COSINE SHAPE, C_d=0.6)

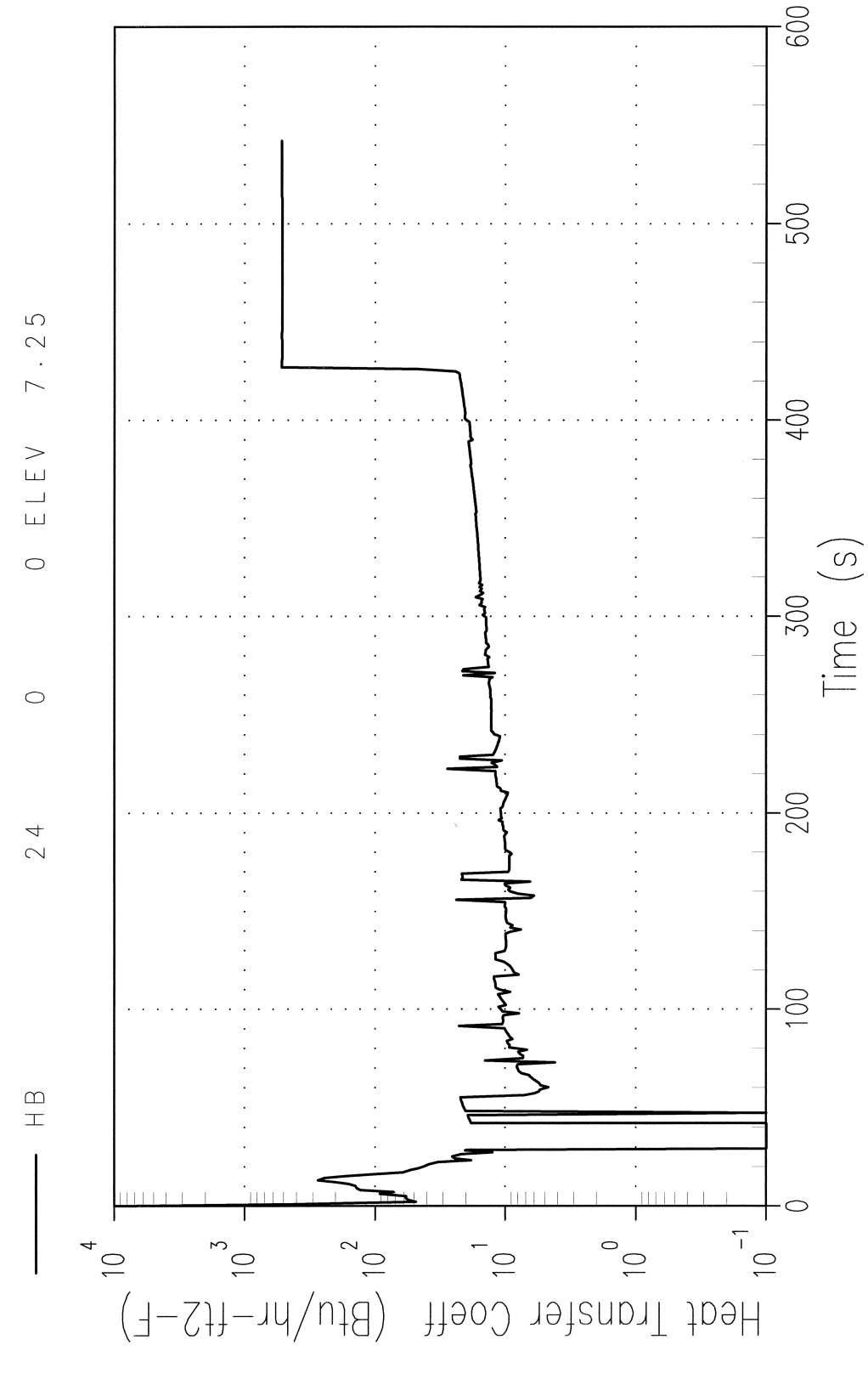

Figure 15.4-50
HOT ROD HEAT TRANSFER COEFFICIENT (DECLG, LIMITING SKEWED SHAPE, C_d=0.4)

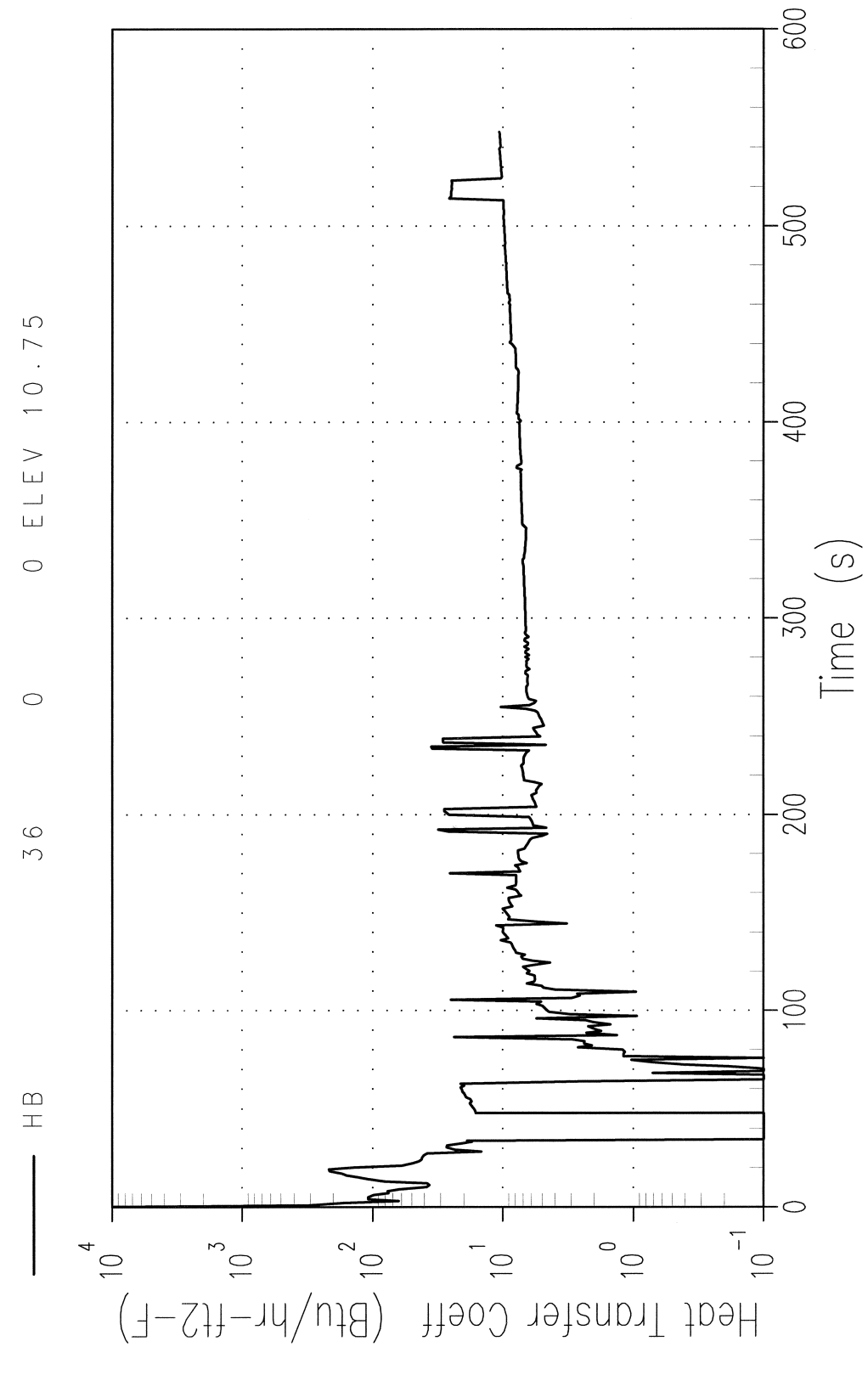

Figure 15.4-51
HOT ROD MASS FLUX (DECLG, COSINE SHAPE, C_d=0.4)

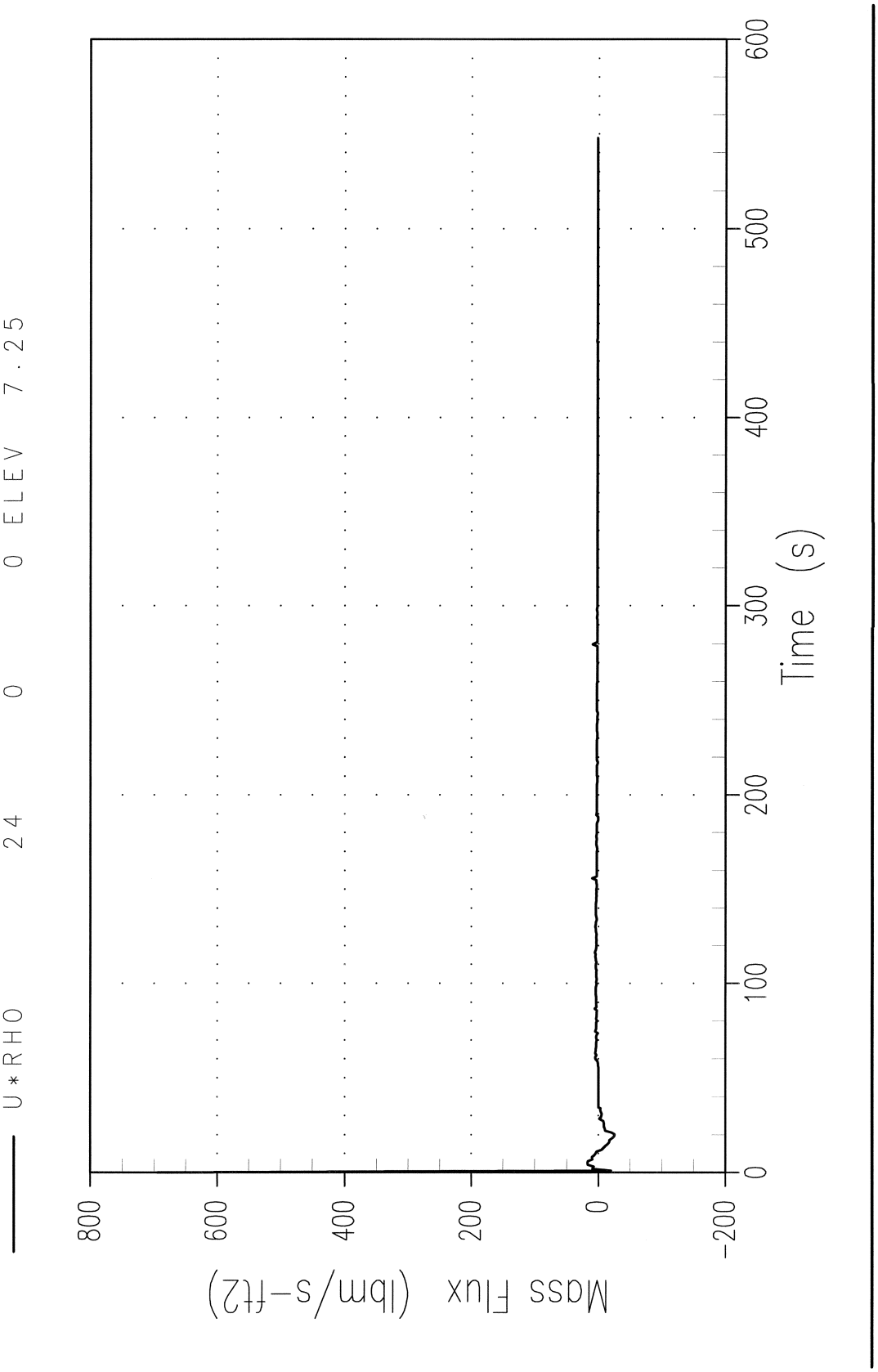

Figure 15.4-52
HOT ROD MASS FLUX (DECLG, COSINE SHAPE, C_d=0.6)

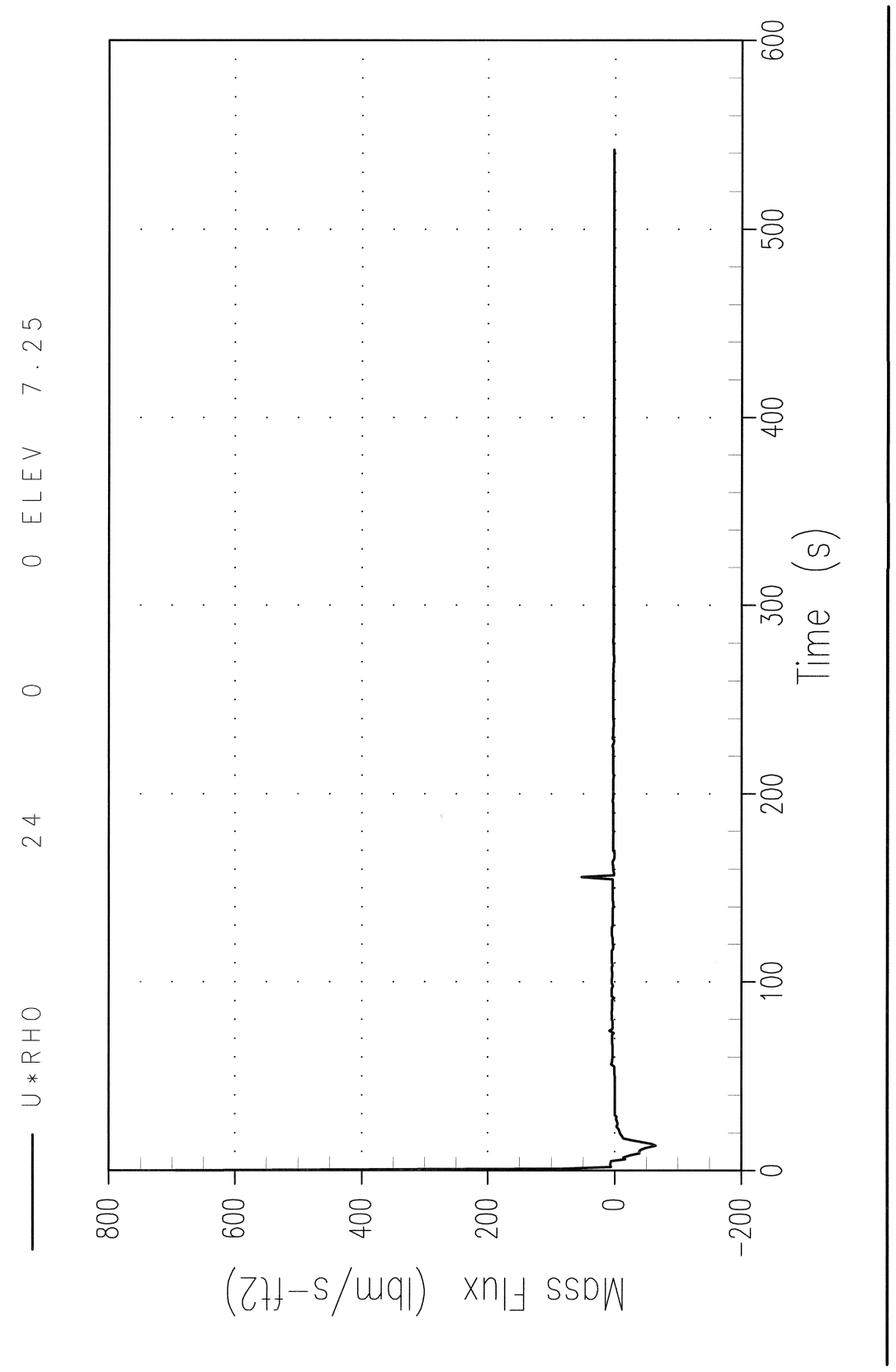

Figure 15.4-53
HOT ROD MASS FLUX (DECLG, LIMITING SKEWED SHAPE, C_d=0.4)

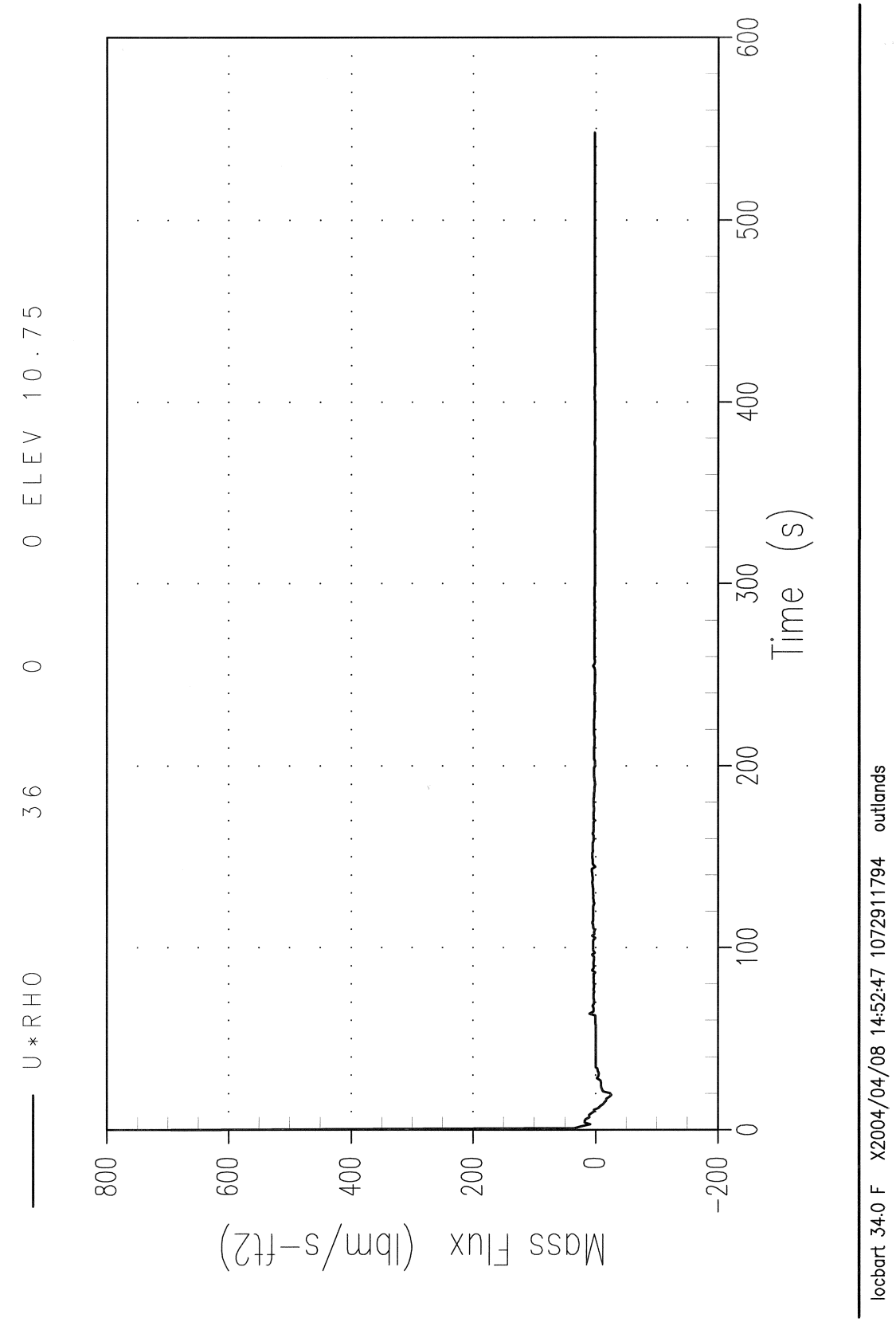

Figure 15.4-54
FLUID QUALITY (DECLG, COSINE SHAPE, C_d=0.4)

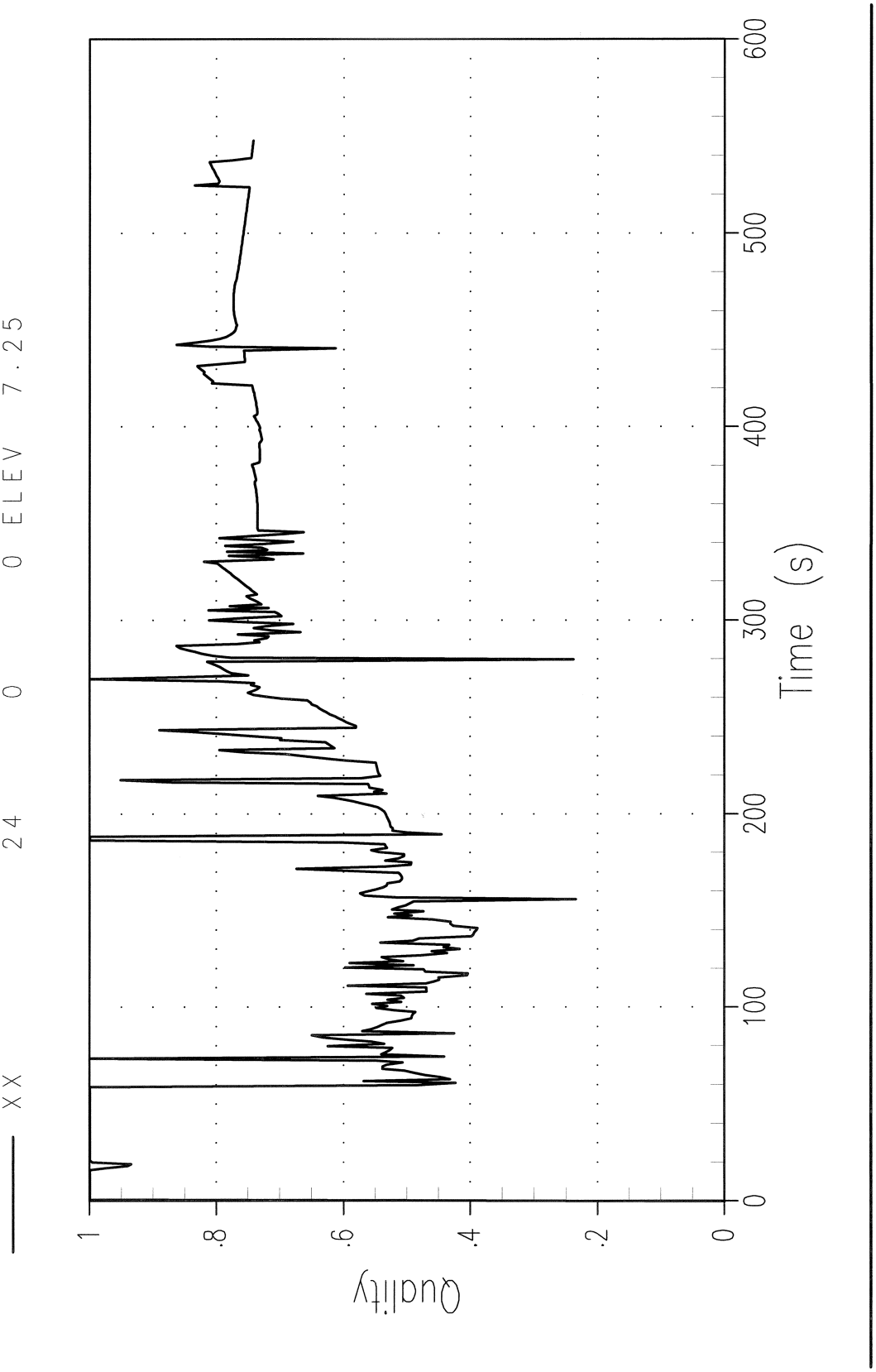

Figure 15.4-55
FLUID QUALITY (DECLG, COSINE SHAPE, C_d=0.6)

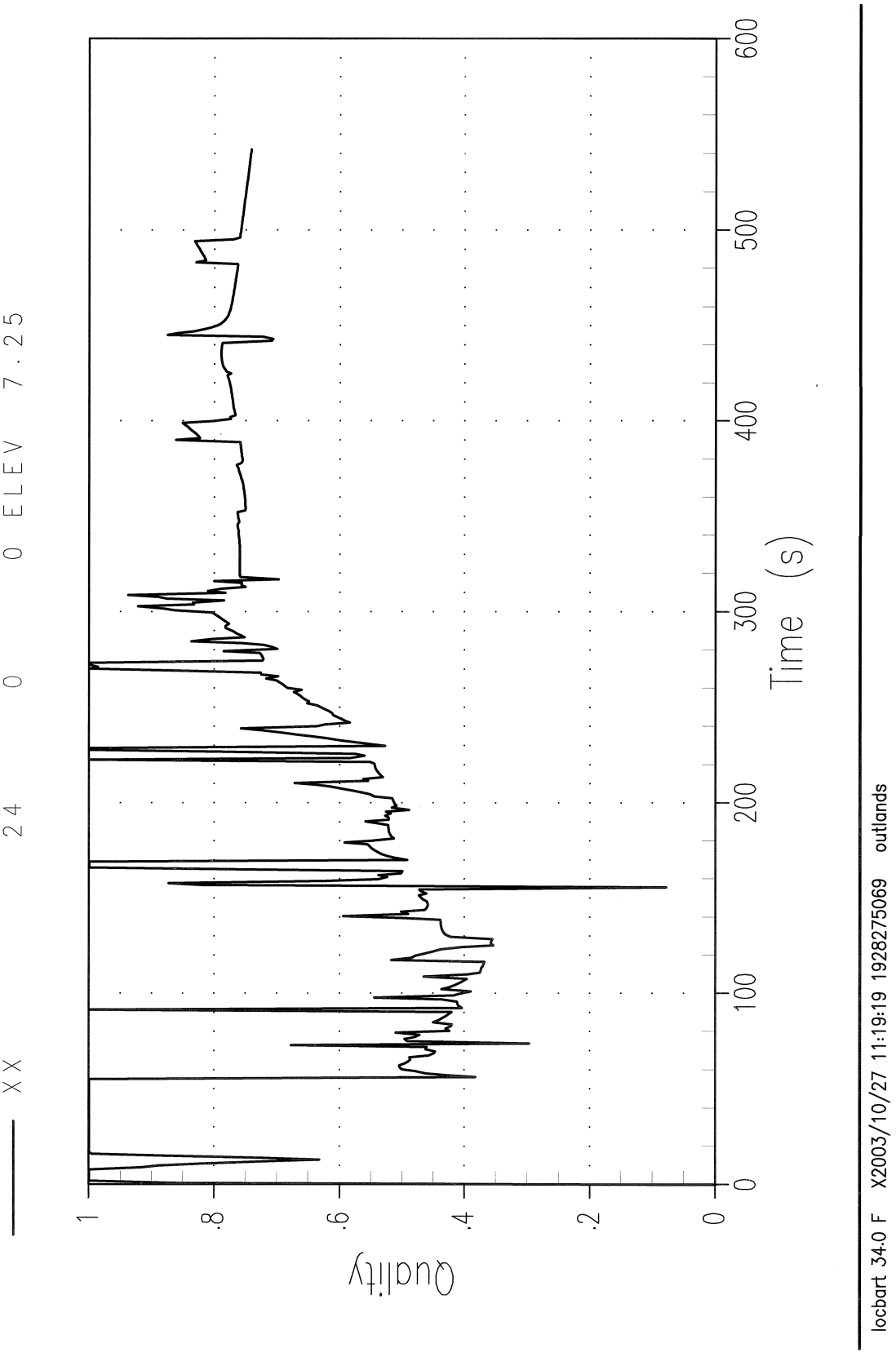

Figure 15.4-56
FLUID QUALITY (DECLG, LIMITING SKEWED SHAPE, C_d=0.4)

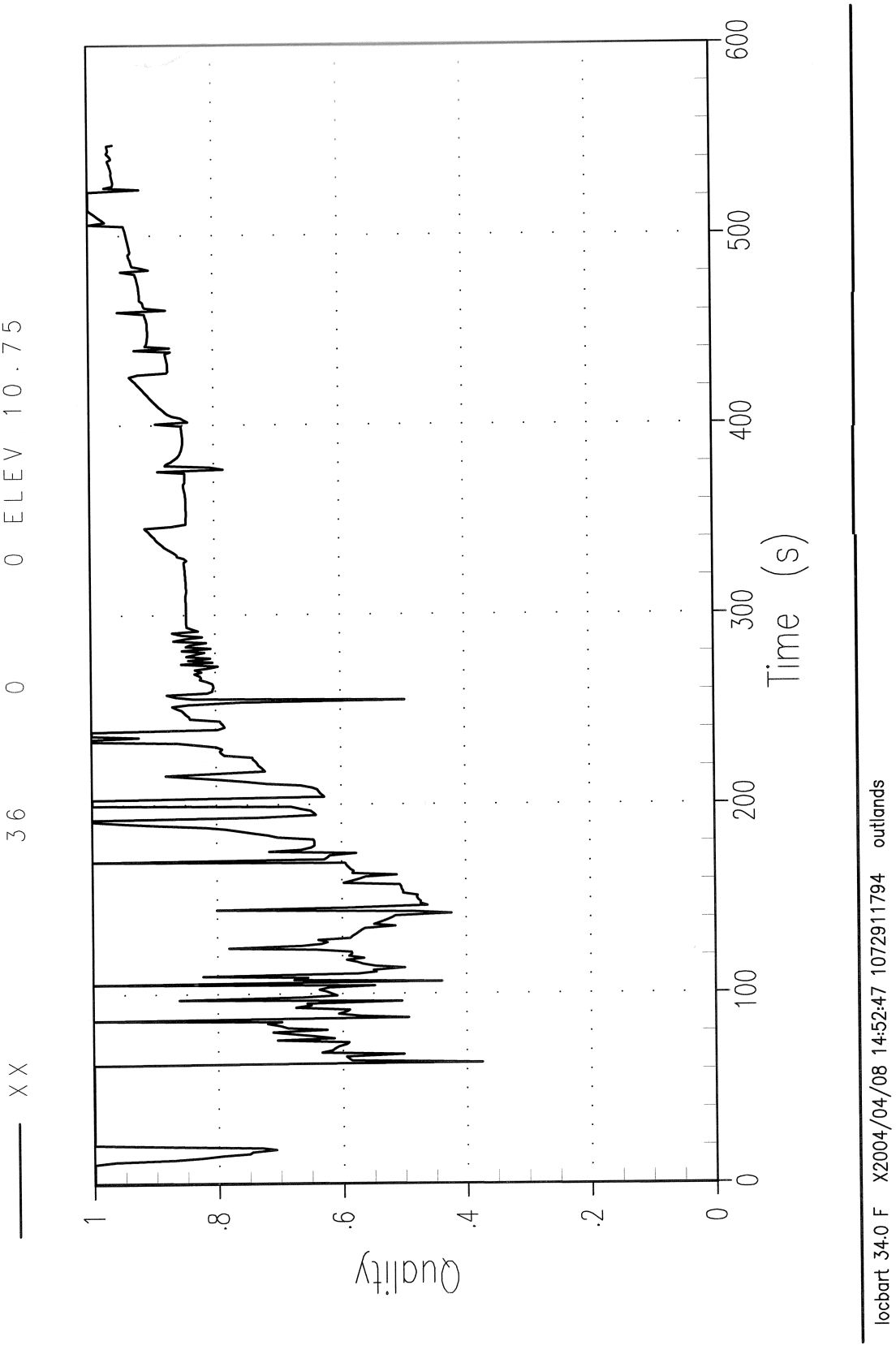

Figure 15.4-57
VARIATION OF REACTIVITY WITH POWER

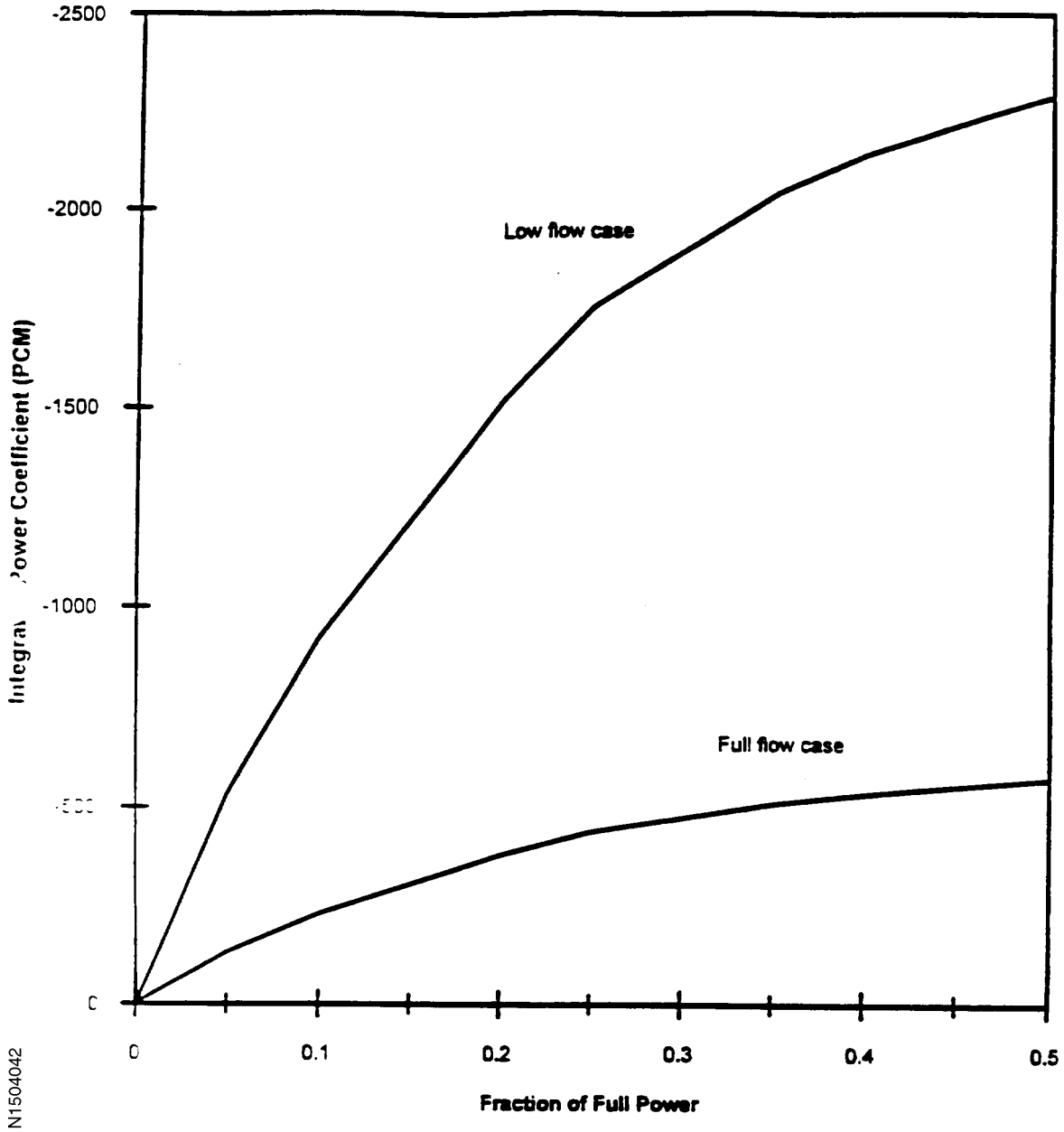

Figure 15.4-58
MAIN STEAM LINE BREAK ANALYSIS
1.4 FT^2 BREAK, 0% BIT, OFFSITE POWER AVAILABLE
PRESSURIZER PRESSURE

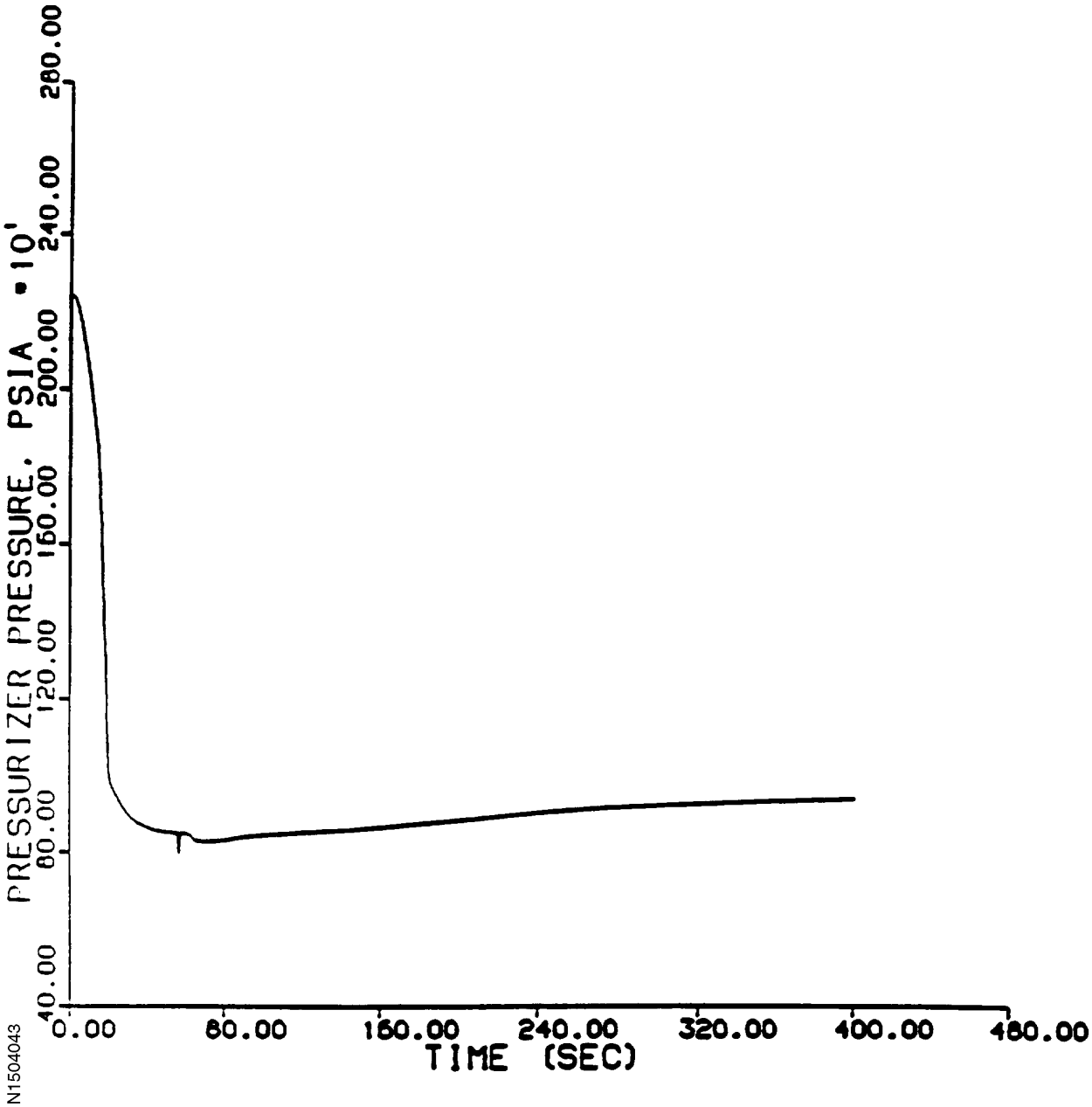

Figure 15.4-59
MAIN STEAM LINE BREAK ANALYSIS
1.4 FT^2 BREAK, 0% BIT, OFFSITE POWER AVAILABLE
ACTUAL LOOP AVERAGE TEMPERATURES

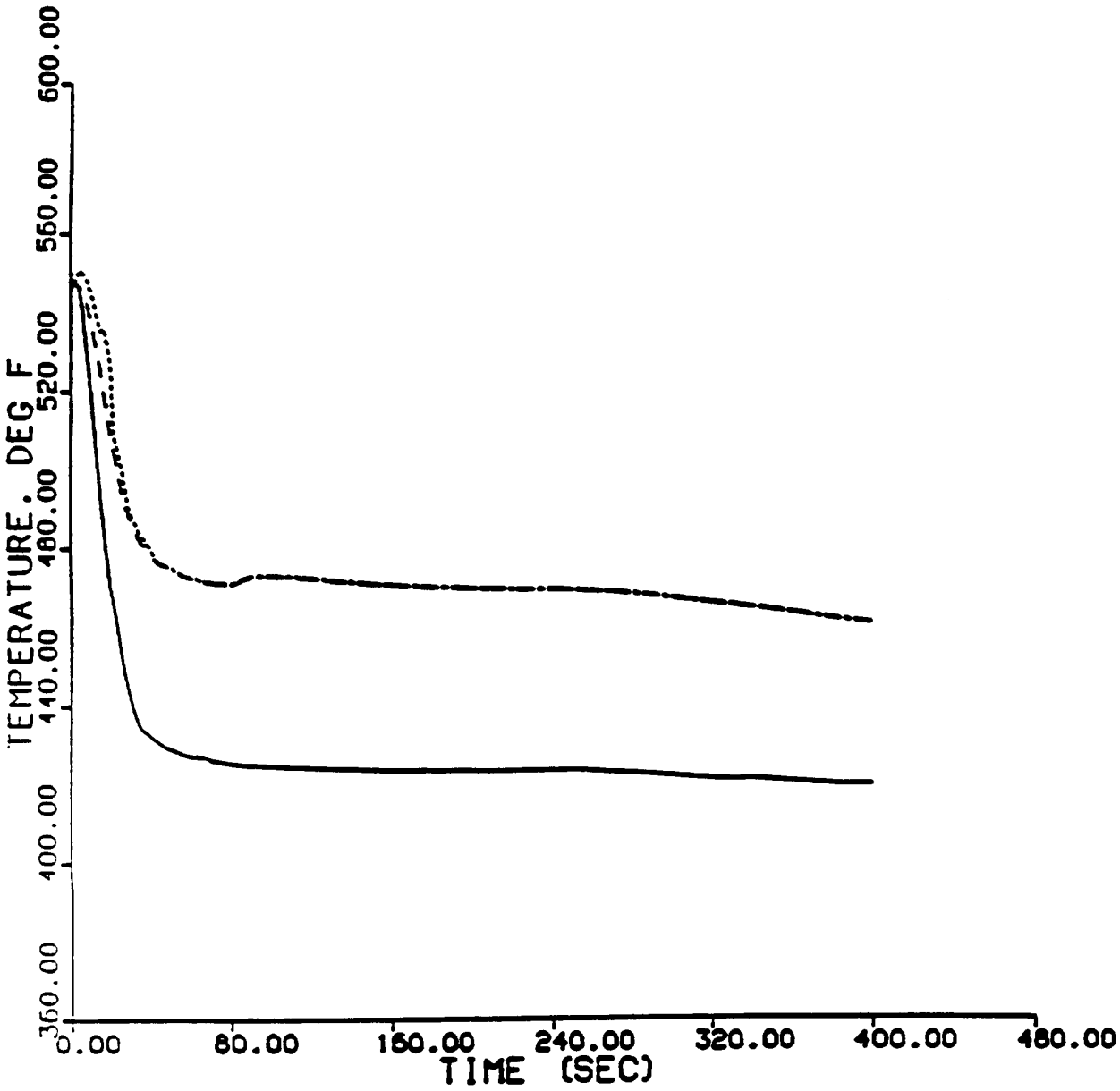

Figure 15.4-60
MAIN STEAM LINE BREAK ANALYSIS
1.4 FT^2 BREAK, 0% BIT, OFFSITE POWER AVAILABLE
NORMALIZED CORE HEAT FLUX

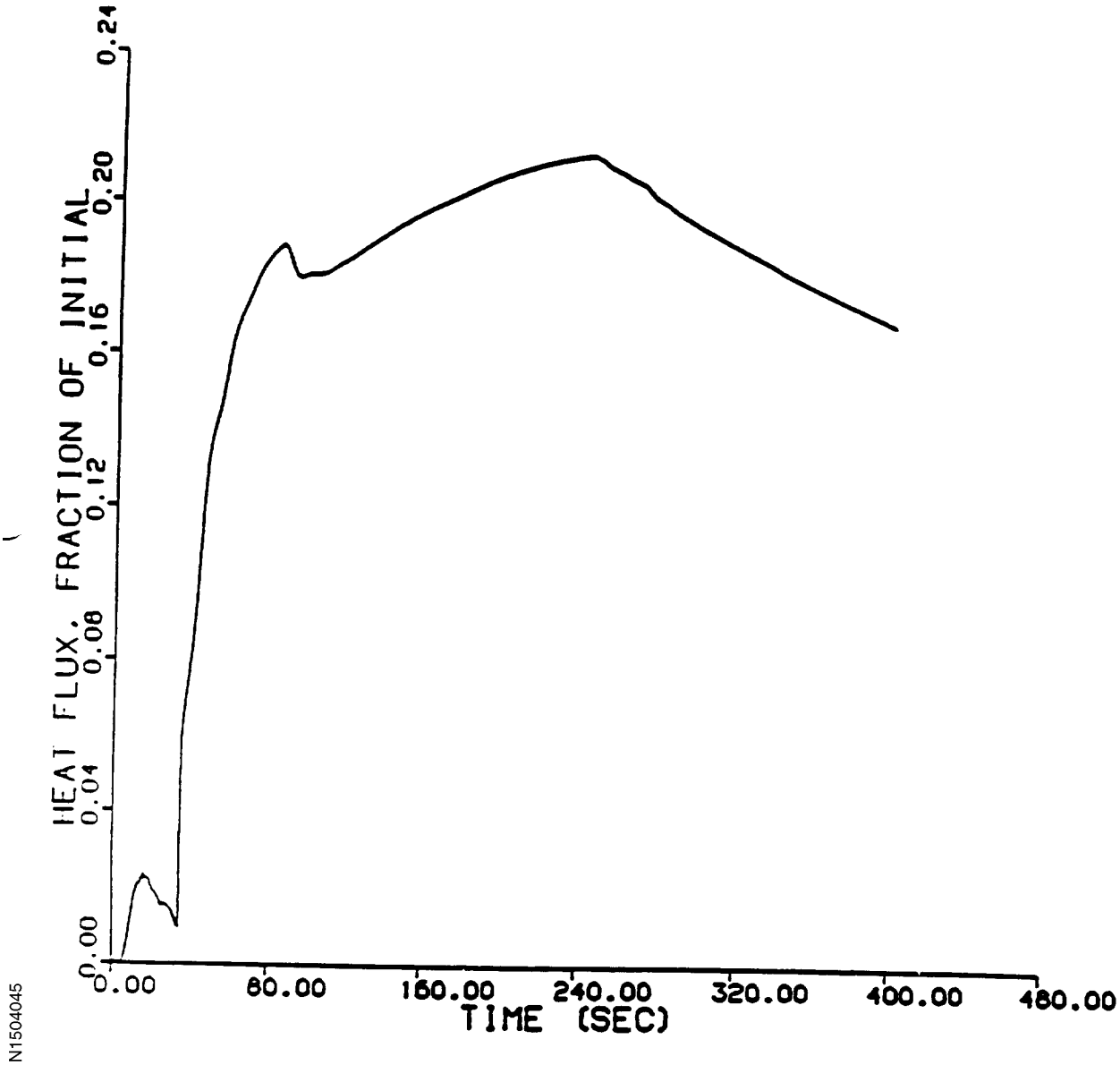

Figure 15.4-61
MAIN STEAM LINE BREAK ANALYSIS
1.4 FT^2 BREAK, 0% BIT, OFFSITE POWER AVAILABLE
CORE REACTIVITY,%ΔK/K

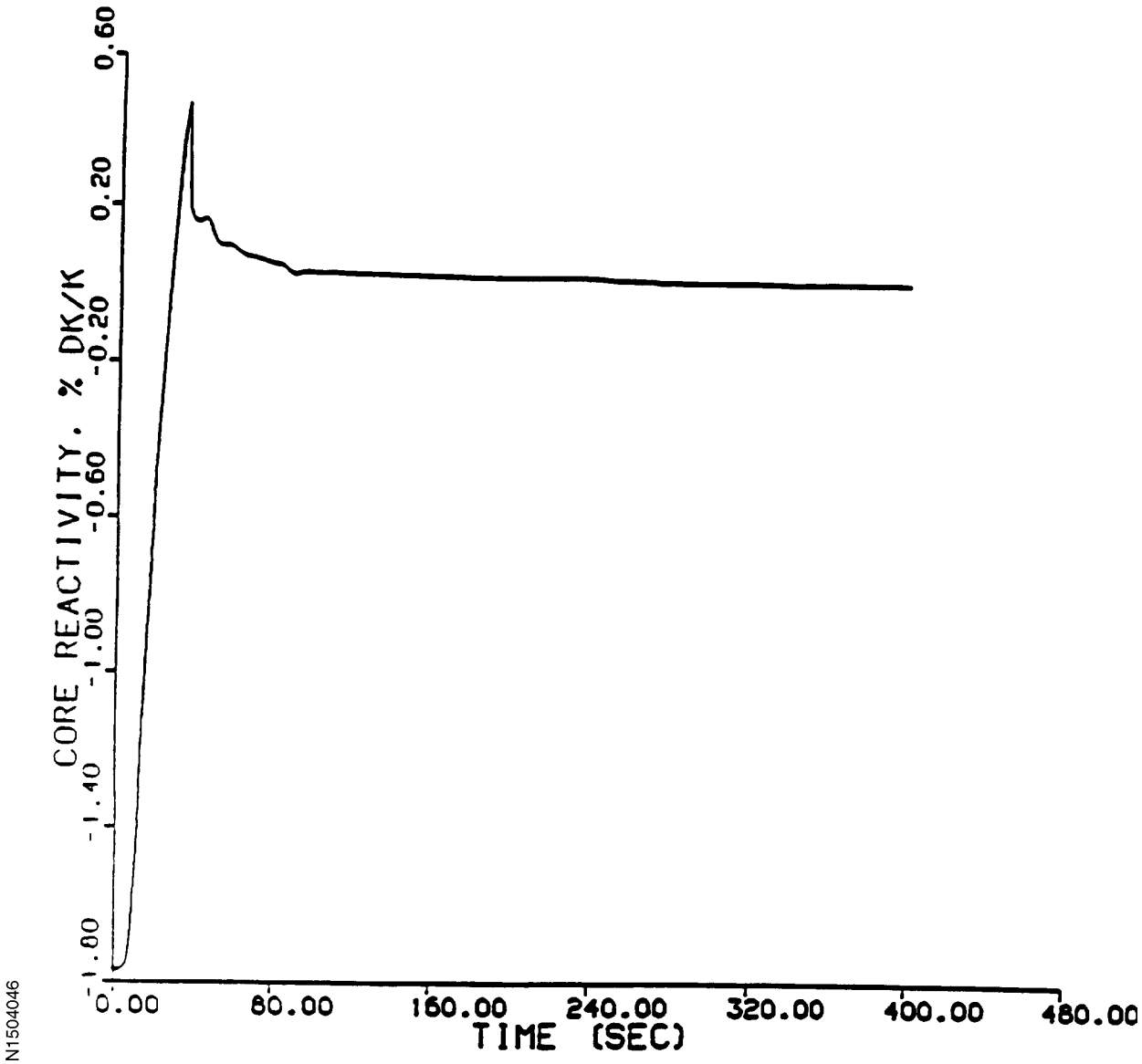

Figure 15.4-62
MAIN STEAM LINE BREAK ANALYSIS
1.4 FT^2 BREAK, 0% BIT, WITHOUT OFFSITE POWER AVAILABLE
PRESSURIZER PRESSURE

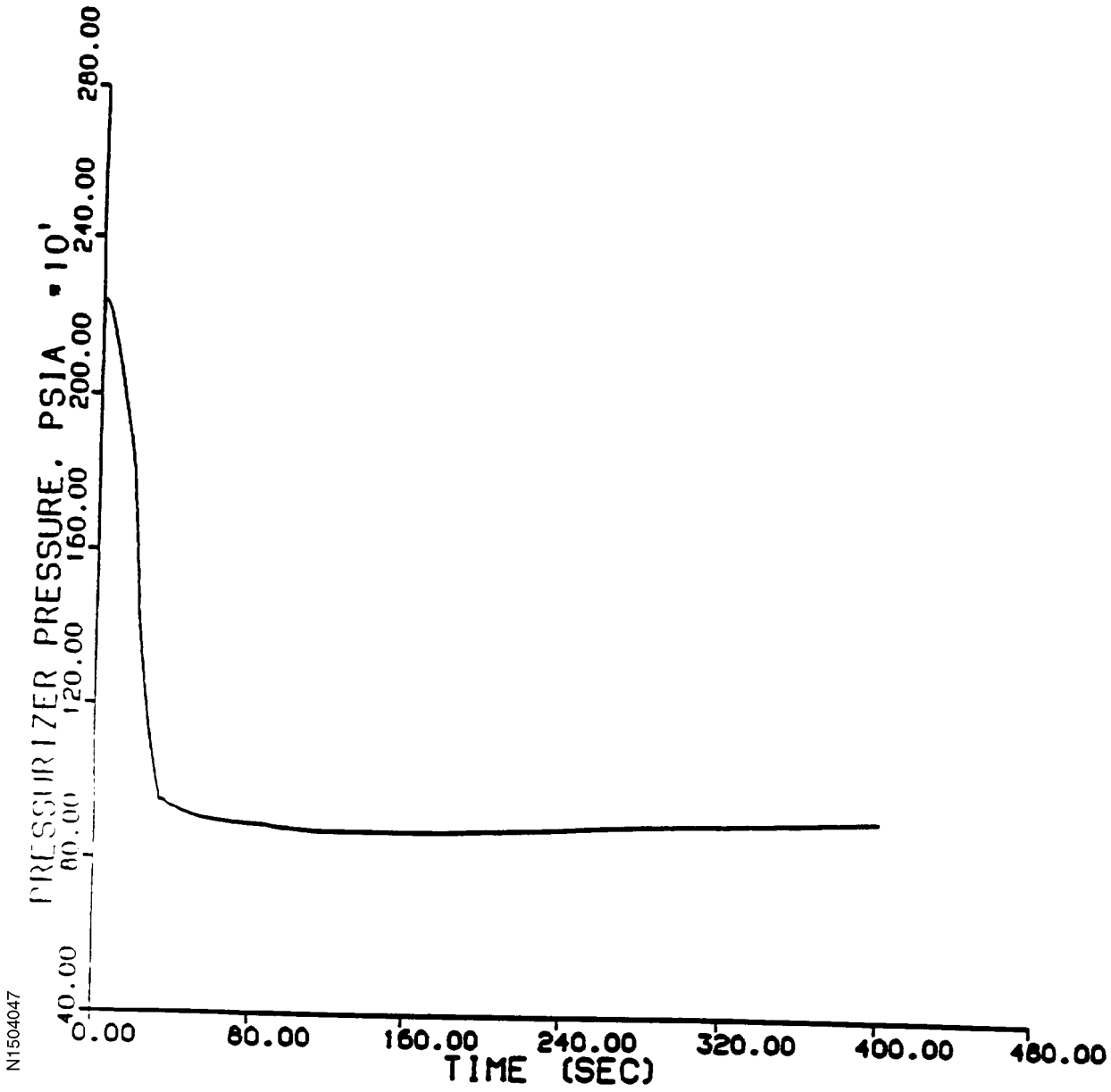

Figure 15.4-63
MAIN STEAM LINE BREAK ANALYSIS
1.4 FT^2 BREAK, 0% BIT, WITHOUT OFFSITE POWER AVAILABLE
ACTUAL LOOP AVERAGE TEMPERATURES

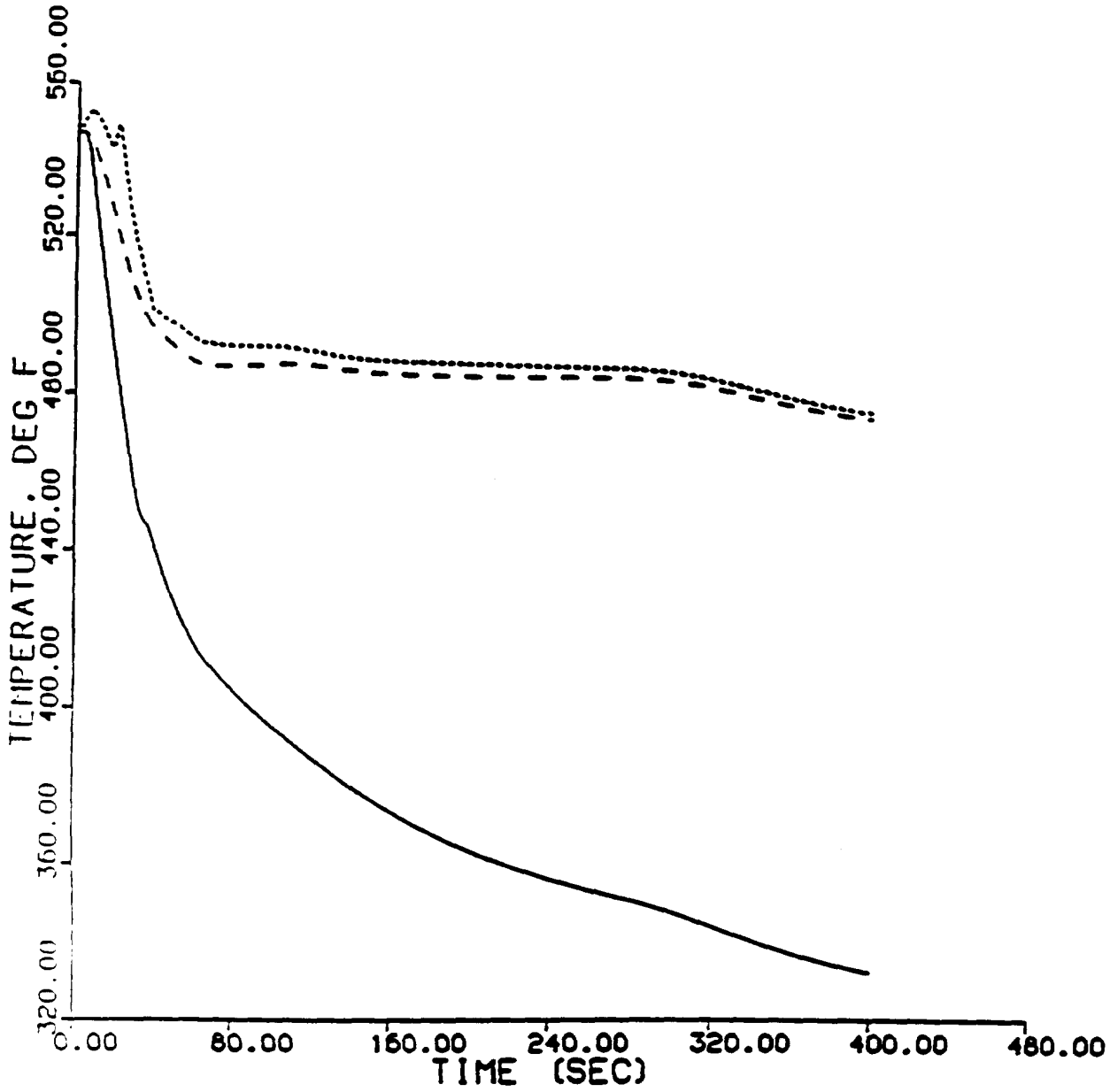

Figure 15.4-64
MAIN STEAM LINE BREAK ANALYSIS
1.4 FT^2 BREAK, 0% BIT, WITHOUT OFFSITE POWER AVAILABLE
NORMALIZED CORE HEAT FLUX

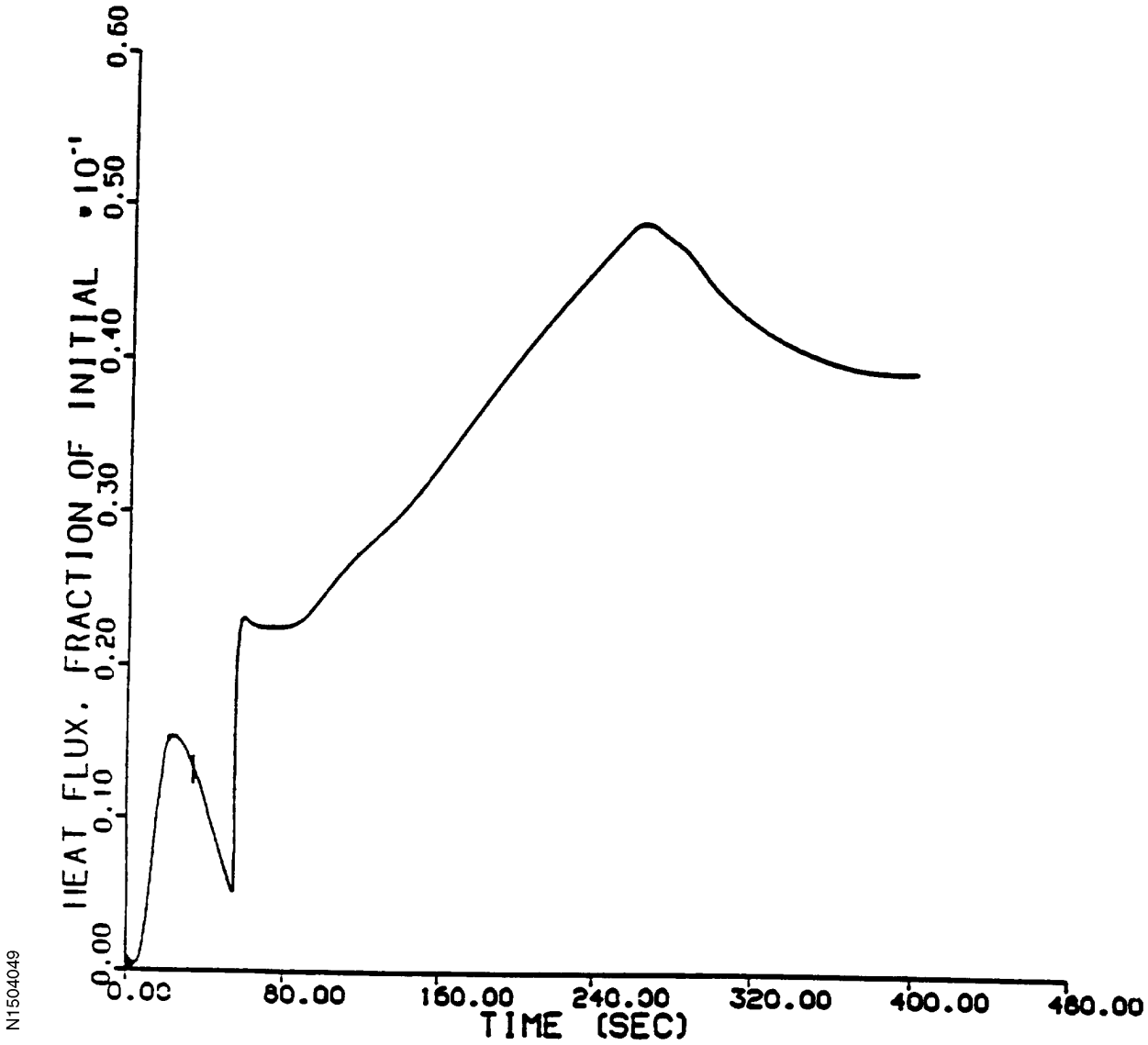

Figure 15.4-65
MAIN STEAM LINE BREAK ANALYSIS
1.4 FT^2 BREAK, 0% BIT, WITHOUT OFFSITE POWER AVAILABLE
CORE REACTIVITY,%ΔK/K

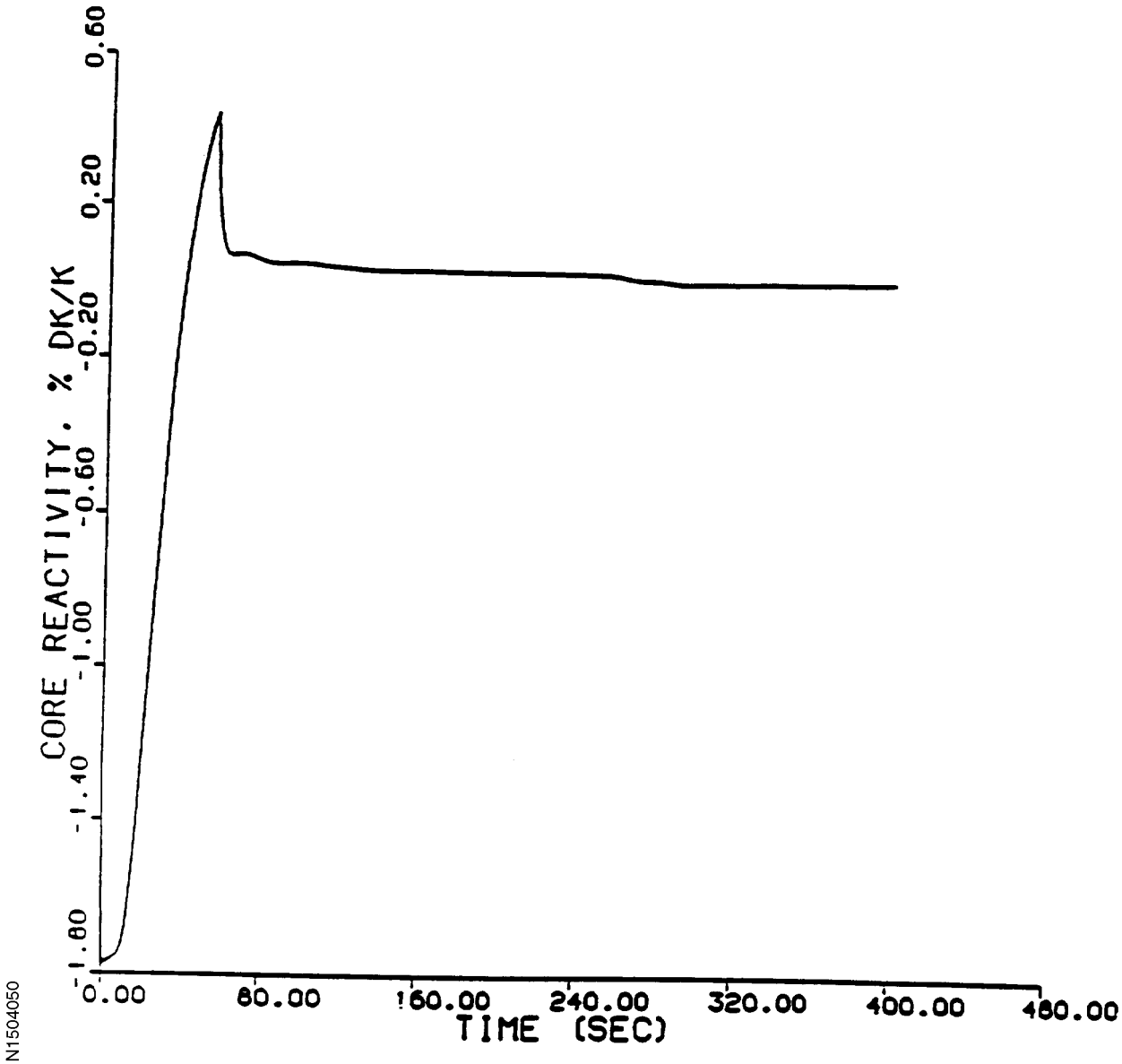

Figure 15.4-66
MAIN STEAM LINE BREAK ANALYSIS
1.4 FT^2 BREAK, 0% BIT, OFFSITE POWER AVAILABLE
INTEGRATED FLOW RATE OF BORATED WATER

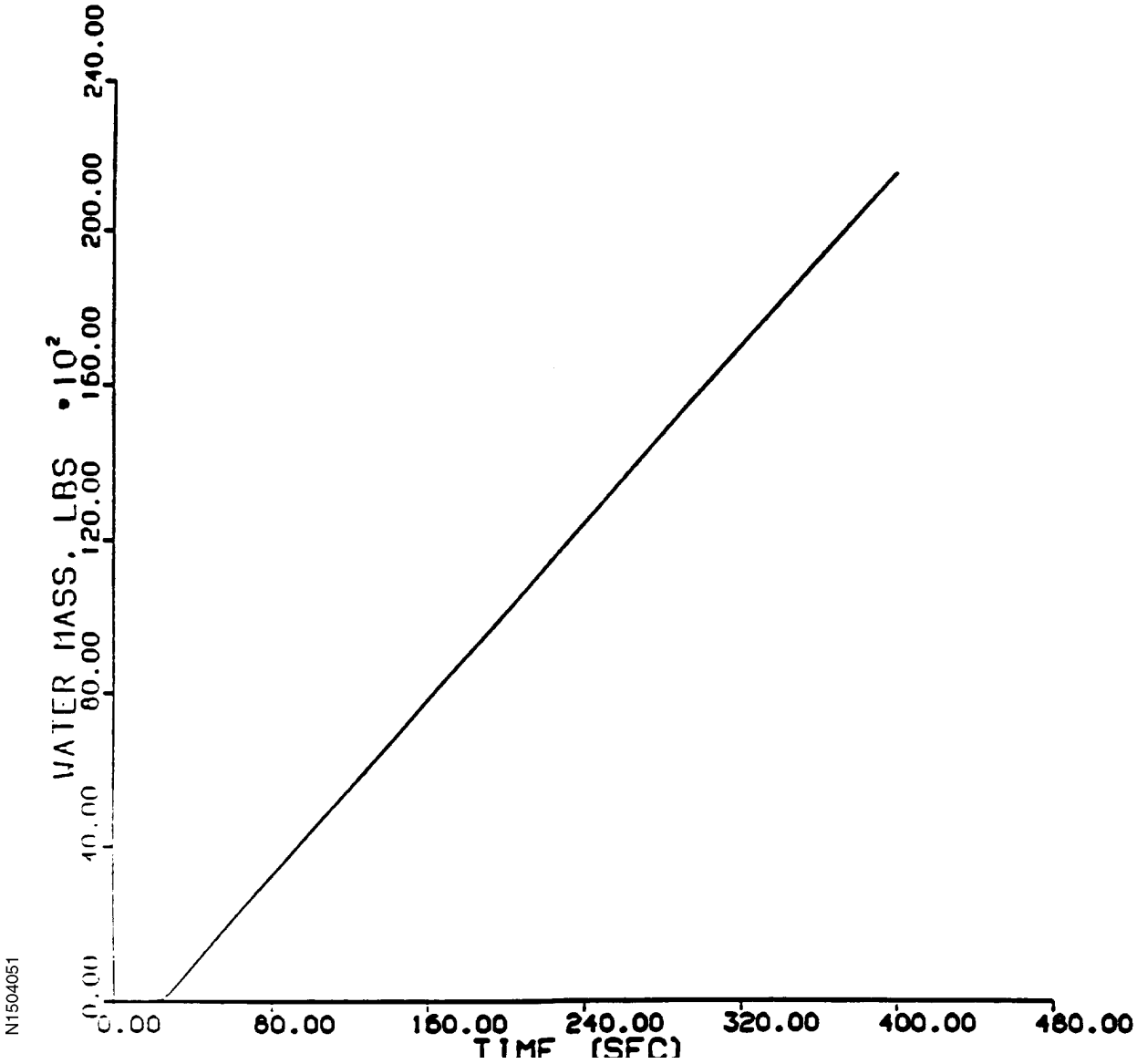

Figure 15.4-67
MAIN STEAM LINE BREAK ANALYSIS
1.4 FT^2 BREAK, 0% BIT, WITHOUT OFFSITE POWER AVAILABLE
INTEGRATED FLOW RATE OF BORATED WATER

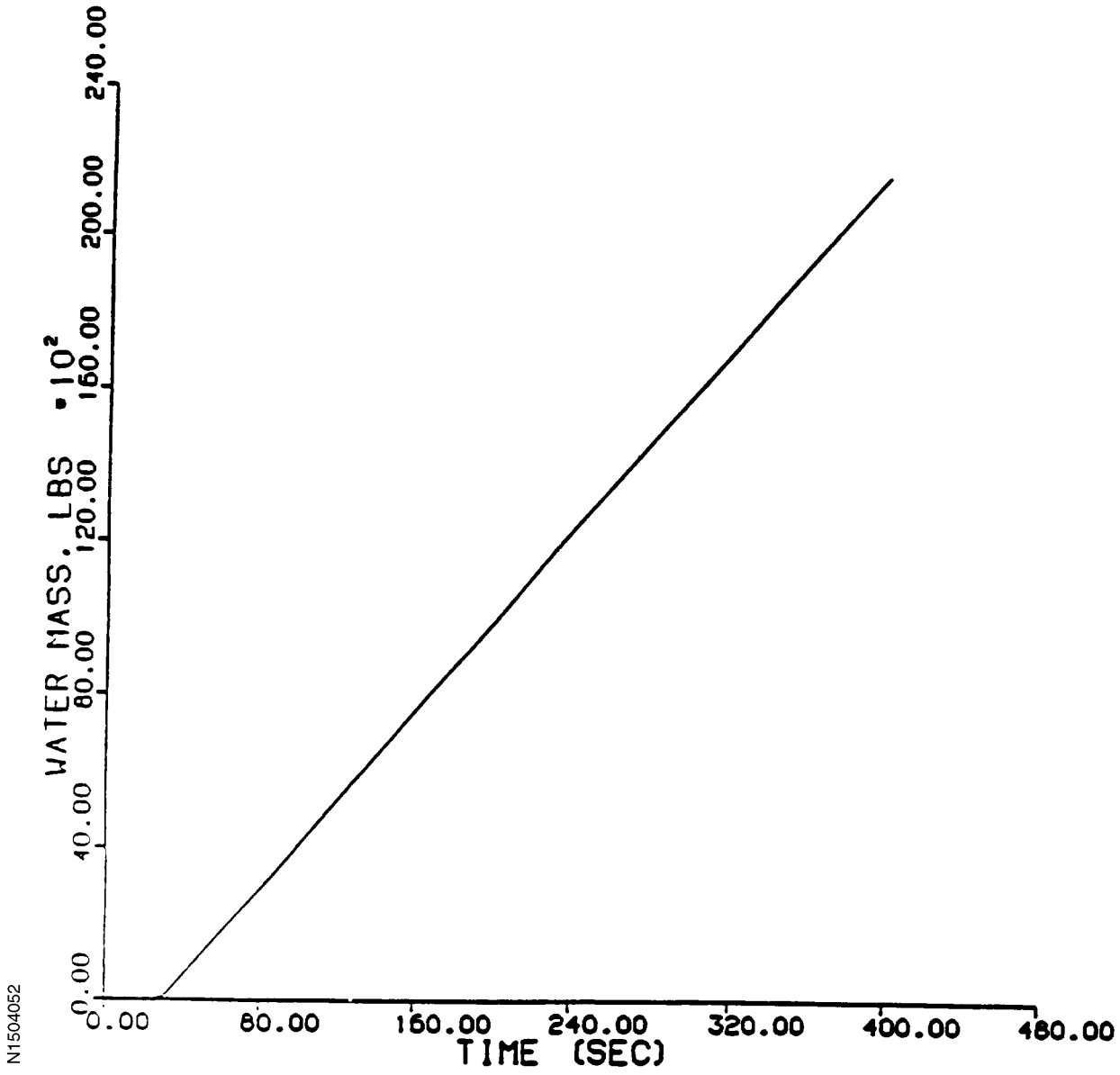

Figure 15.4-68
MAIN FEEDLINE RUPTURE ACCIDENT
PRESSURIZER PRESSURE AS A FUNCTION OF TIME
WITH OFFSITE POWER

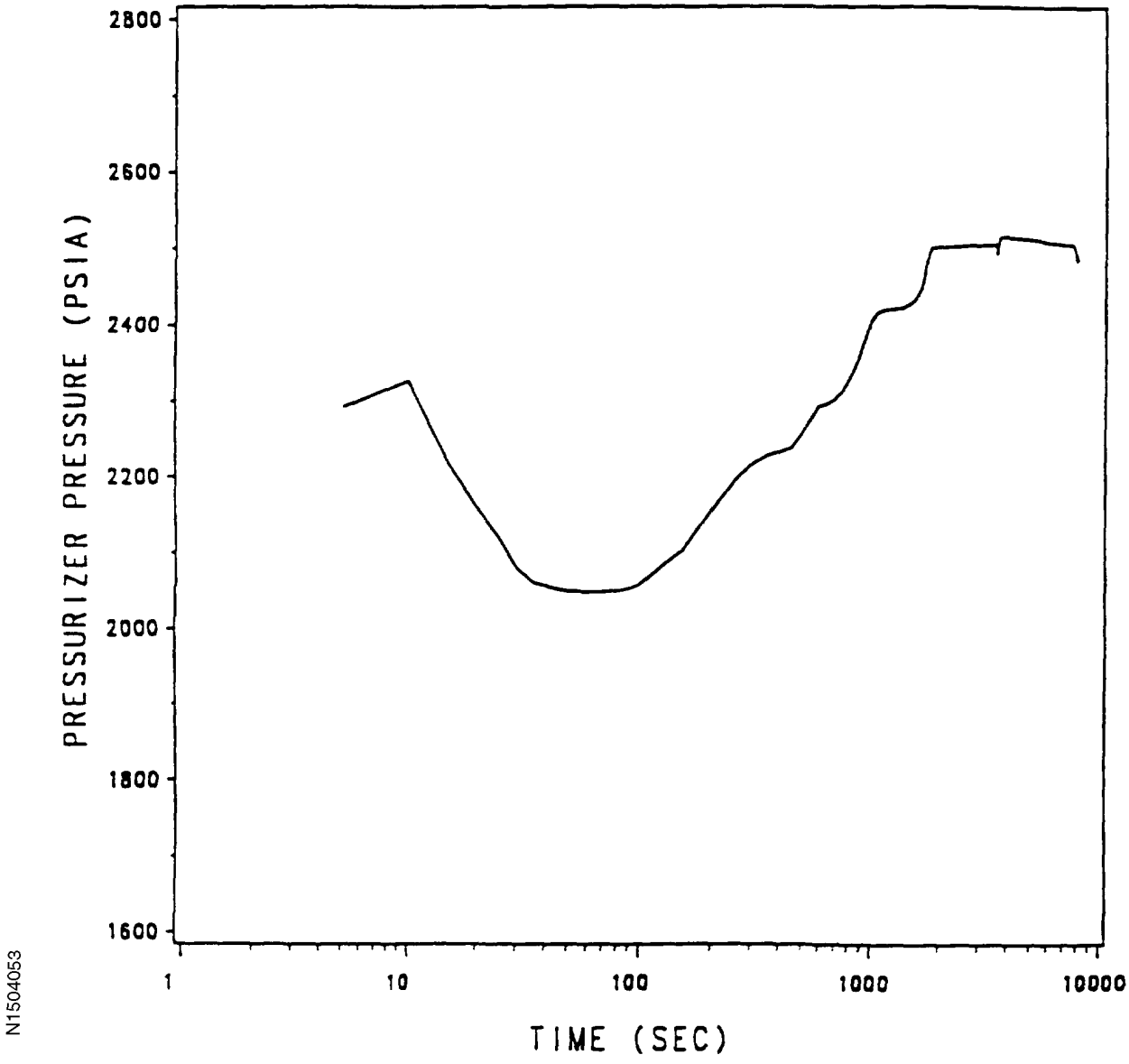

Figure 15.4-69
MAIN FEEDLINE RUPTURE ACCIDENT
PRESSURIZER WATER VOLUME AS A FUNCTION OF TIME
WITH OFFSITE POWER

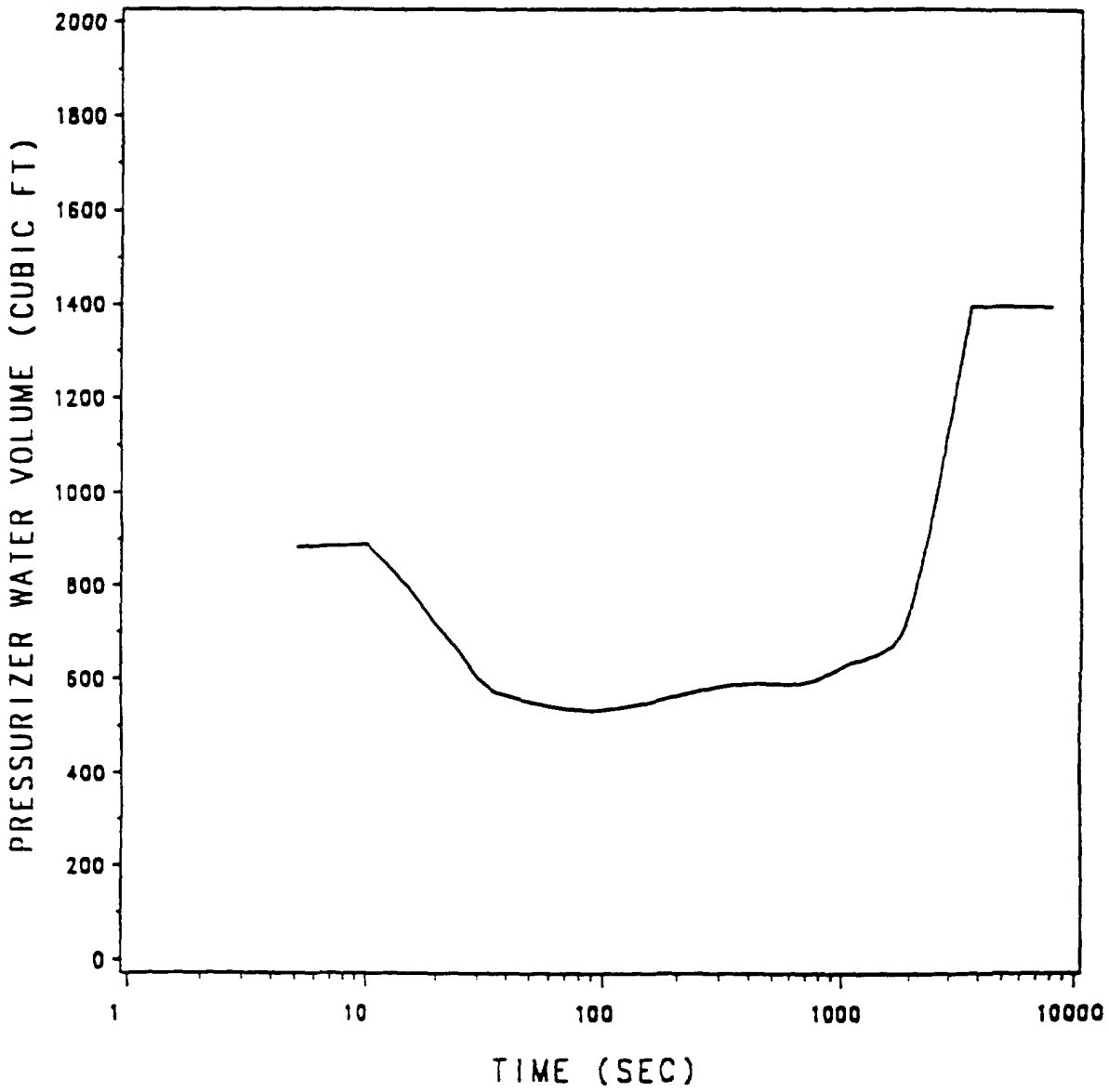

N1504054

Figure 15.4-70
MAIN FEEDLINE RUPTURE ACCIDENT
REACTOR COOLANT TEMPERATURE AS A FUNCTION OF TIME
WITH OFFSITE POWER

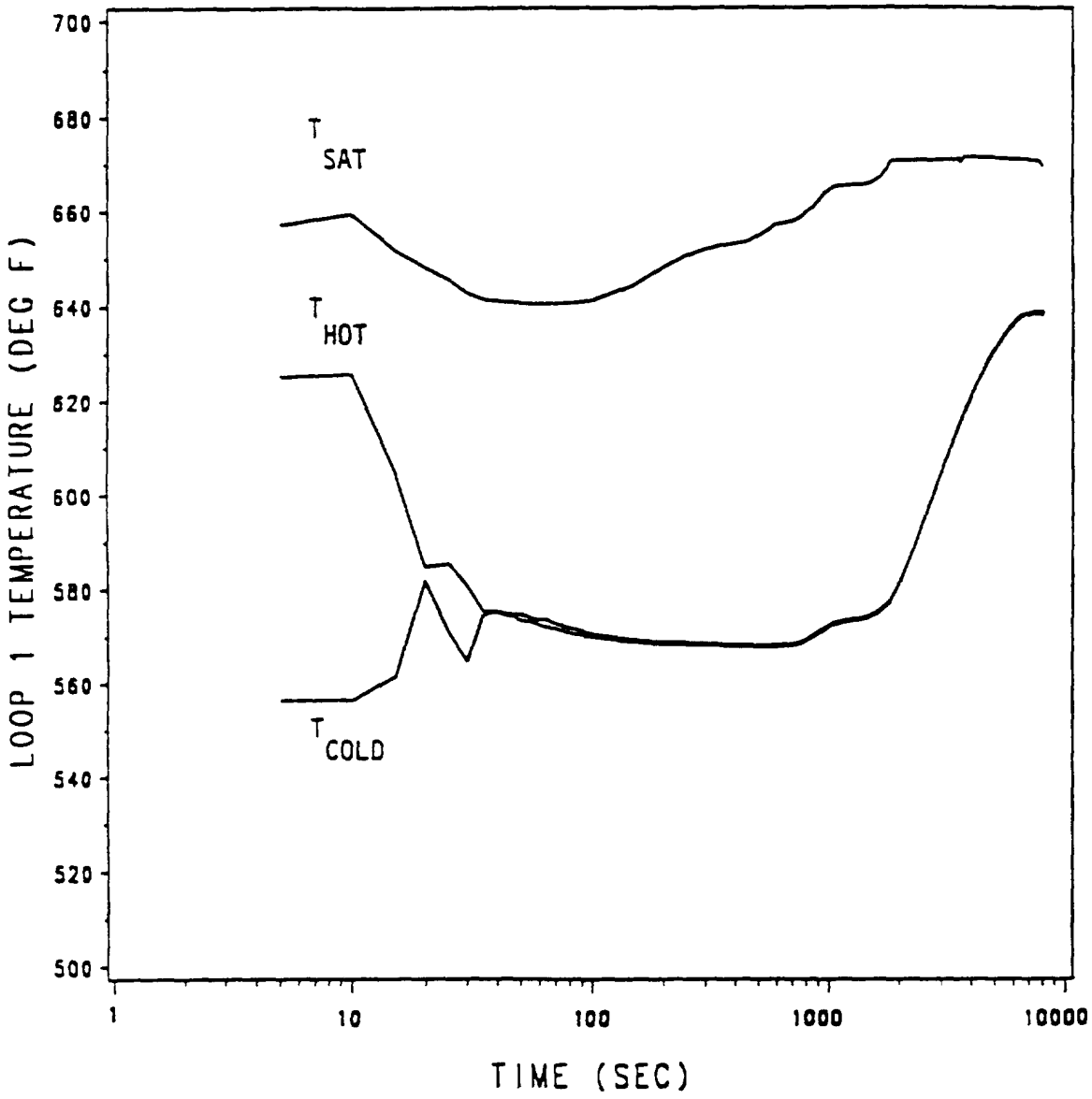

N1504055

Figure 15.4-71
MAIN FEEDLINE RUPTURE ACCIDENT
PRESSURIZER PRESSURE AS A FUNCTION OF TIME
WITHOUT OFFSITE POWER

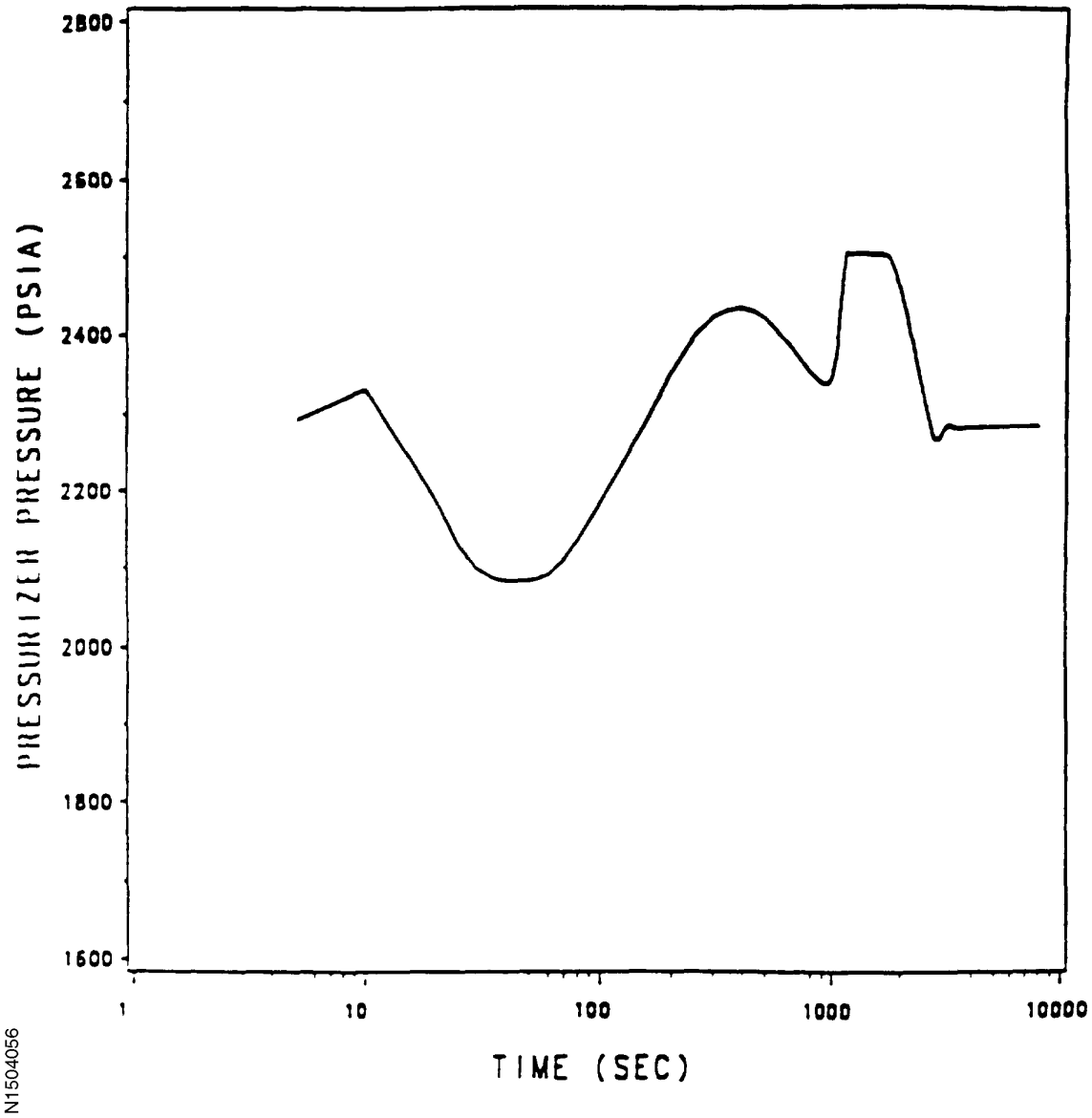

Figure 15.4-72
MAIN FEEDLINE RUPTURE ACCIDENT
PRESSURIZER WATER VOLUME AS A FUNCTION OF TIME
WITHOUT OFFSITE POWER

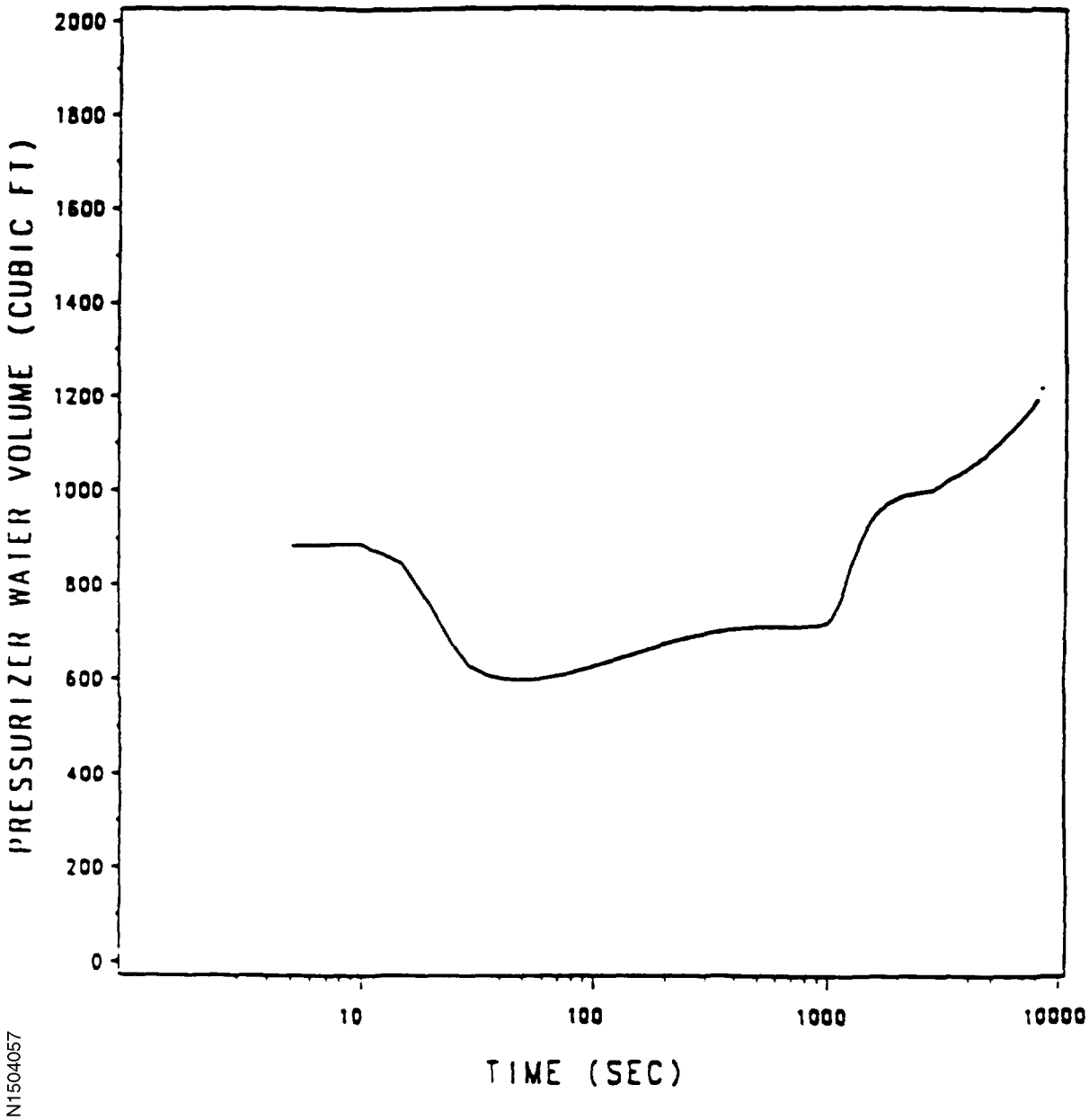

Figure 15.4-73
MAIN FEEDLINE RUPTURE ACCIDENT
REACTOR COOLANT TEMPERATURE AS A FUNCTION OF TIME
WITH OFFSITE POWER

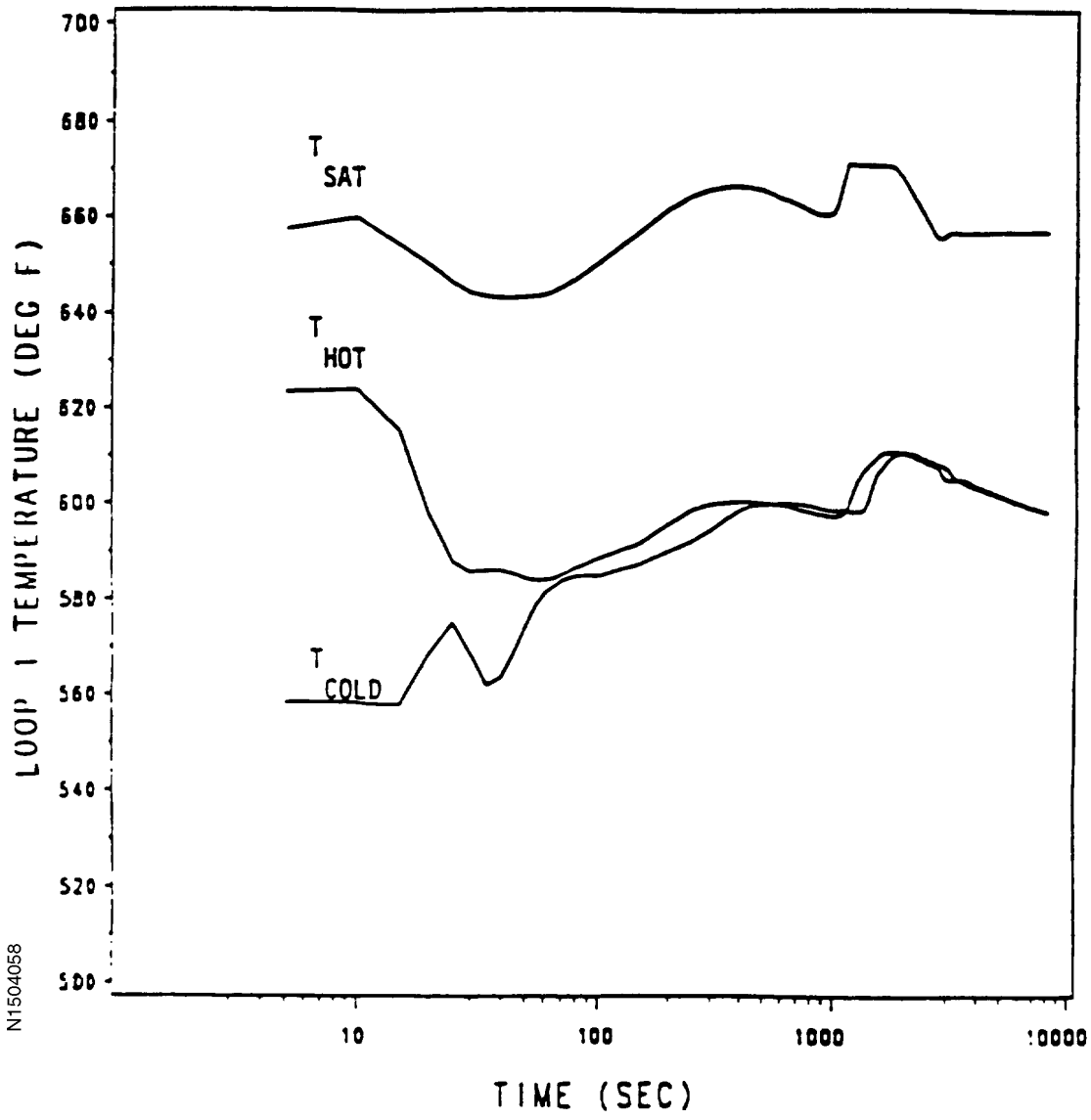

Figure 15.4-74
NORTH ANNA STEAM GENERATOR TUBE RUPTURE INTEGRATED BREAK FLOW
(OFFSITE POWER AVAILABLE CASE)

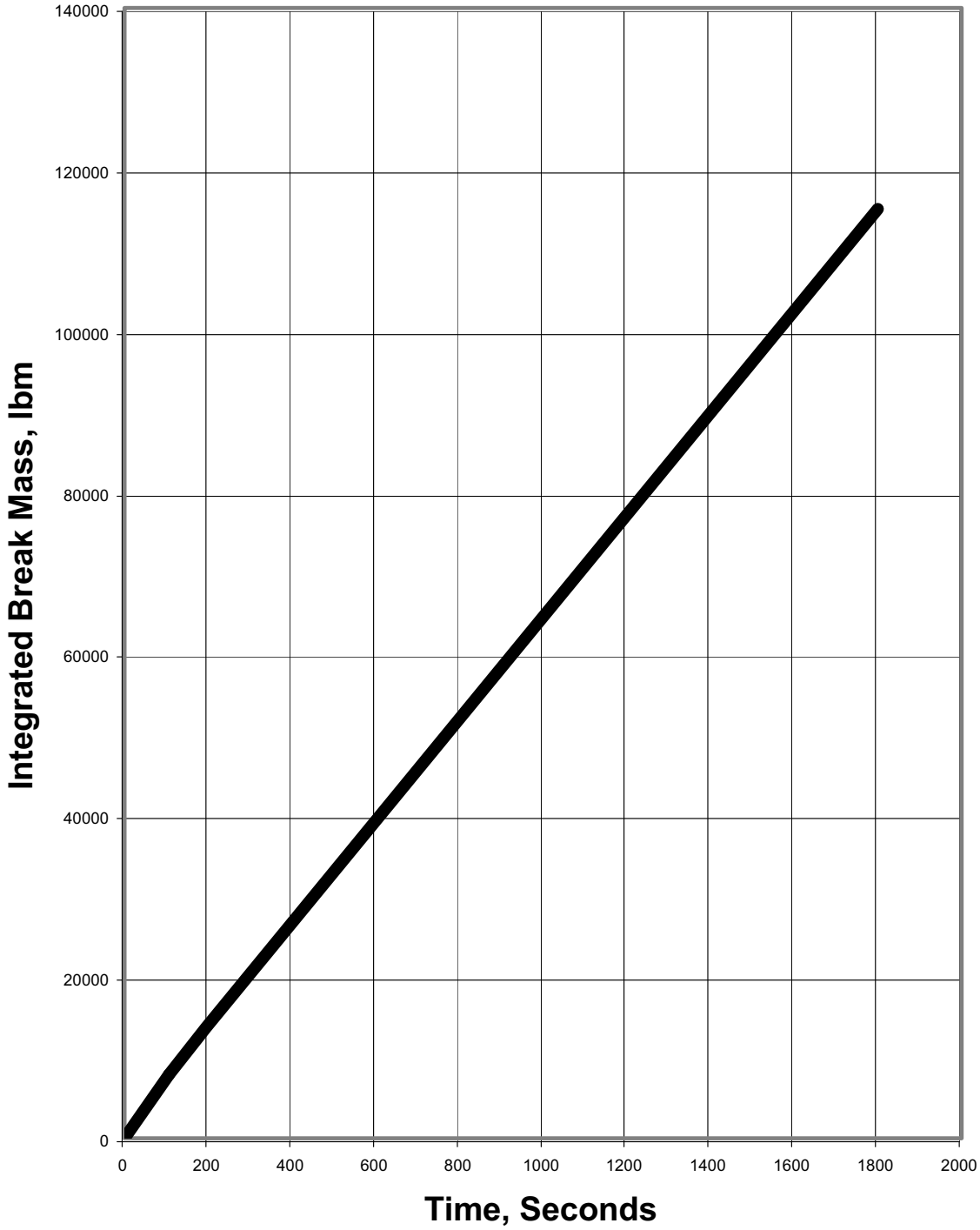

Figure 15.4-75
LOCKED ROTOR OVERPRESSURE CASE
0 PCM/F MTC/2% PSV TOL RCS PRESSURES

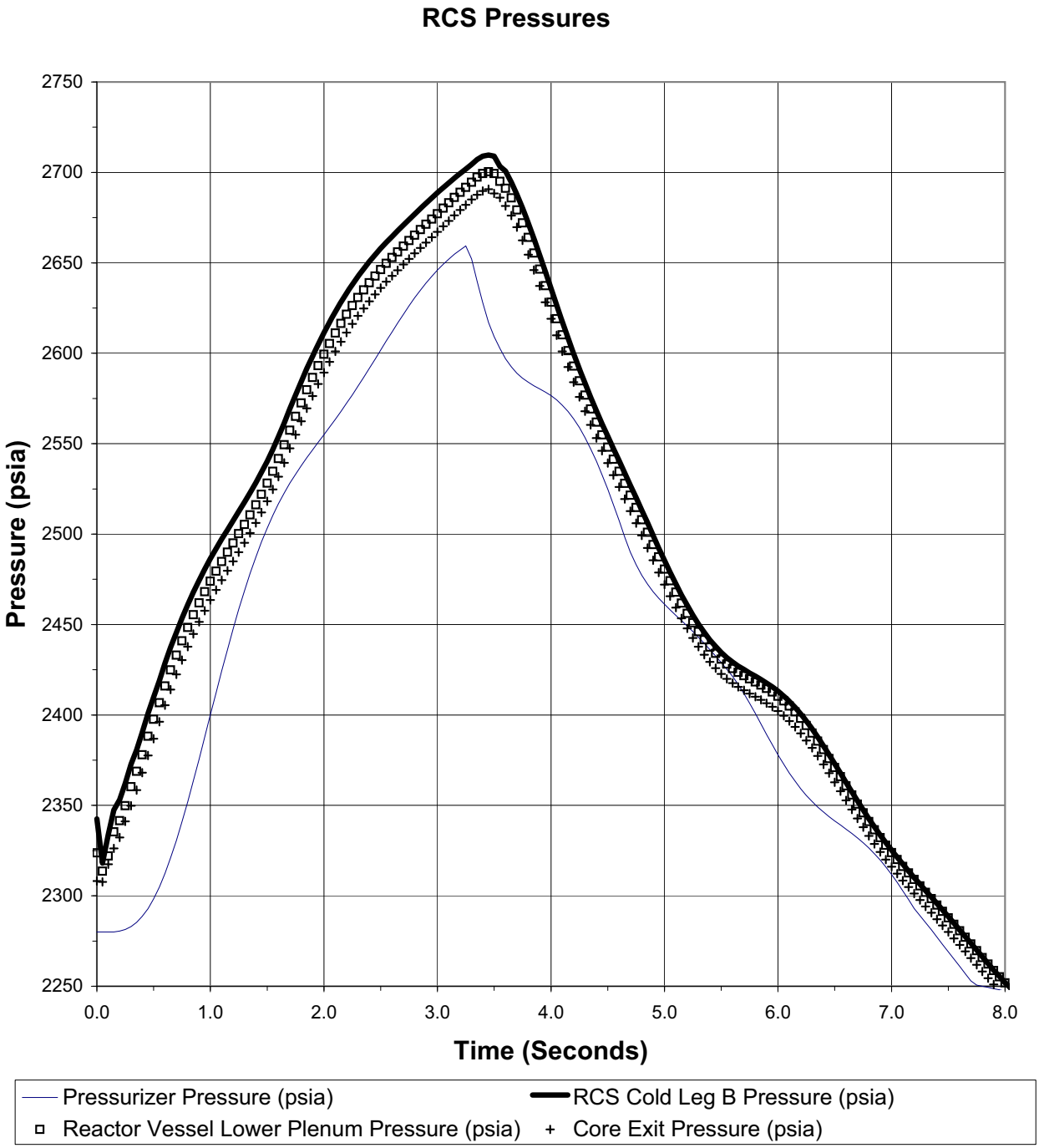

Figure 15.4-76
LOCKED ROTOR OVERPRESSURE CASE
0 PCM/F MTC/2% PSV TOL CORE INLET TEMPERATURE

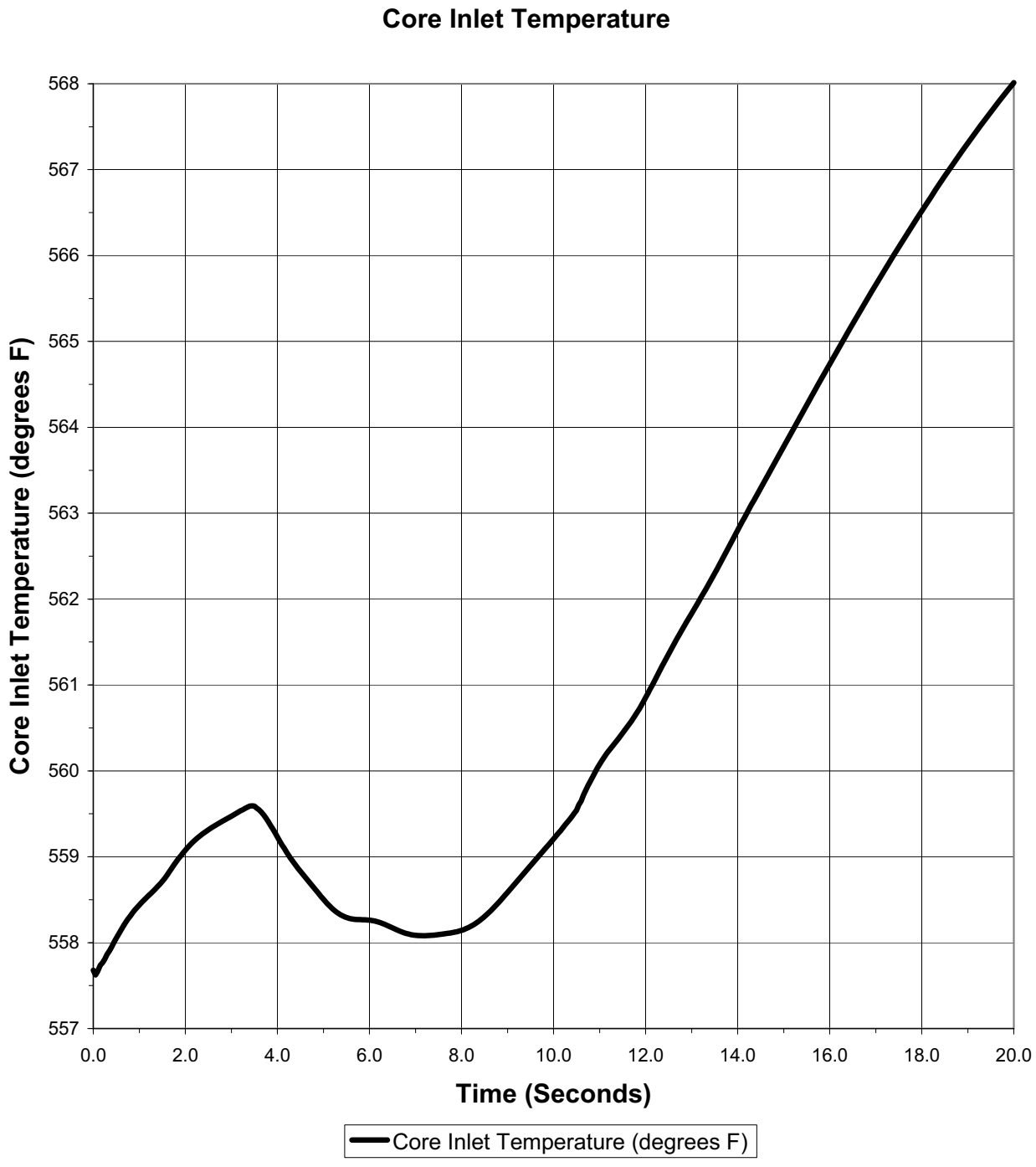

Figure 15.4-77
LOCKED ROTOR RCS OVERPRESSURE CASE
0 PCM/F MTC/2% PSV TOL CORE INLET MASS FLOW RATE

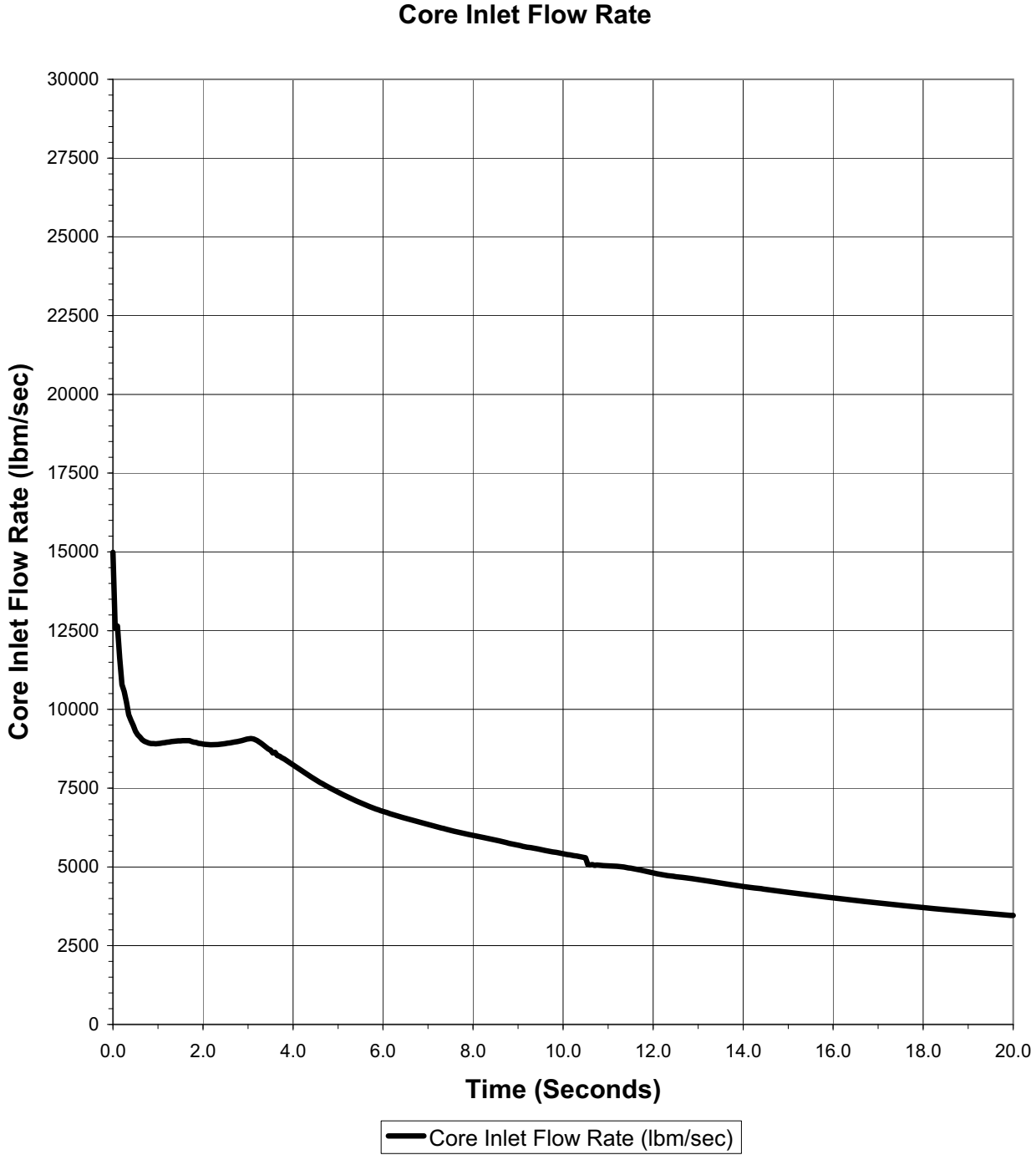

Figure 15.4-78
LOCKED ROTOR RCS OVERPRESSURE CASE
0 PCM/F MTC/2% PSV TOL CORE AVERAGE HEAT FLUX

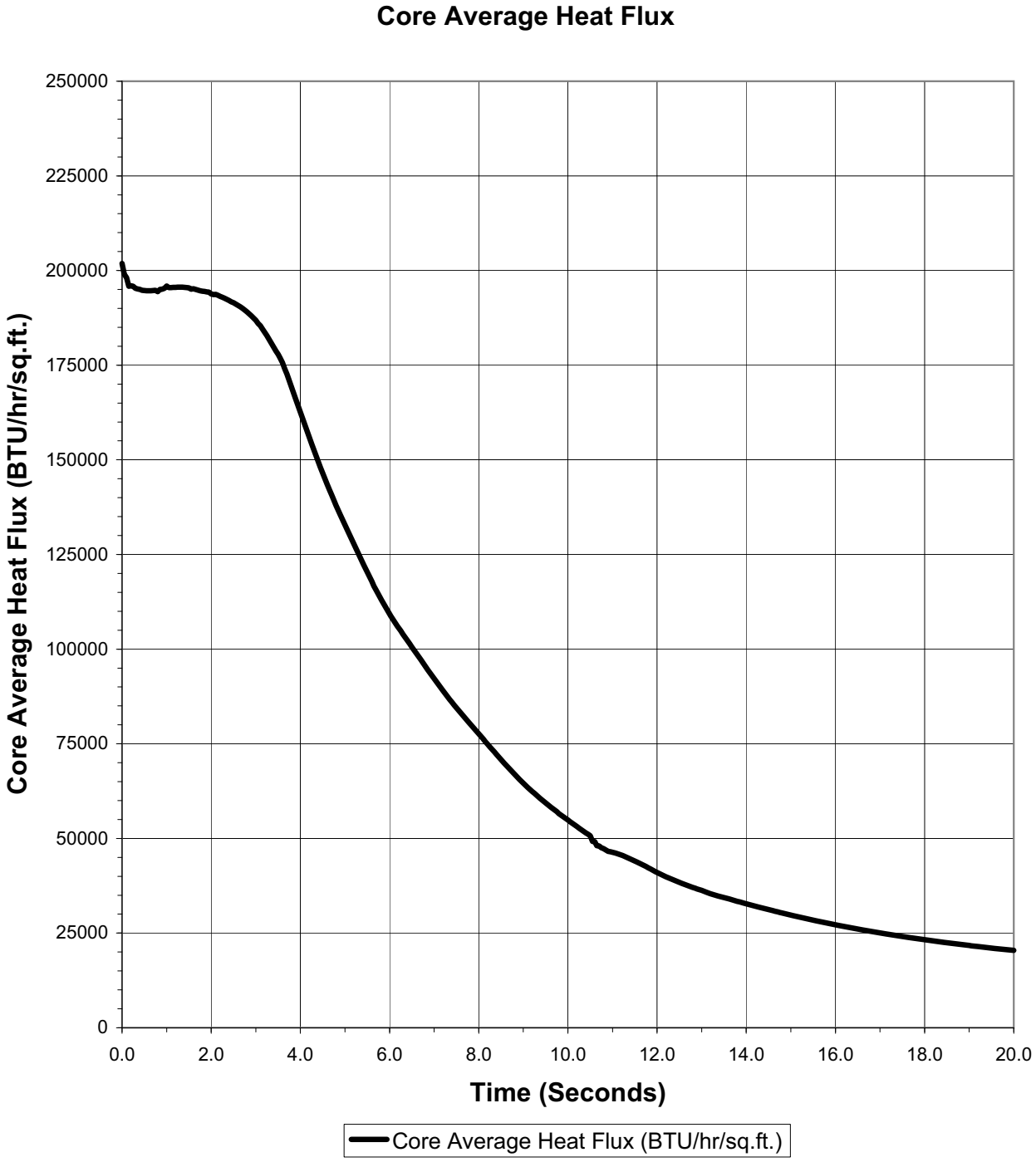

Figure 15.4-79
LOCKED ROTOR RCS OVERPRESSURE CASE
0 PCM/F MTC/2% PSV TOL NUCLEAR POWER

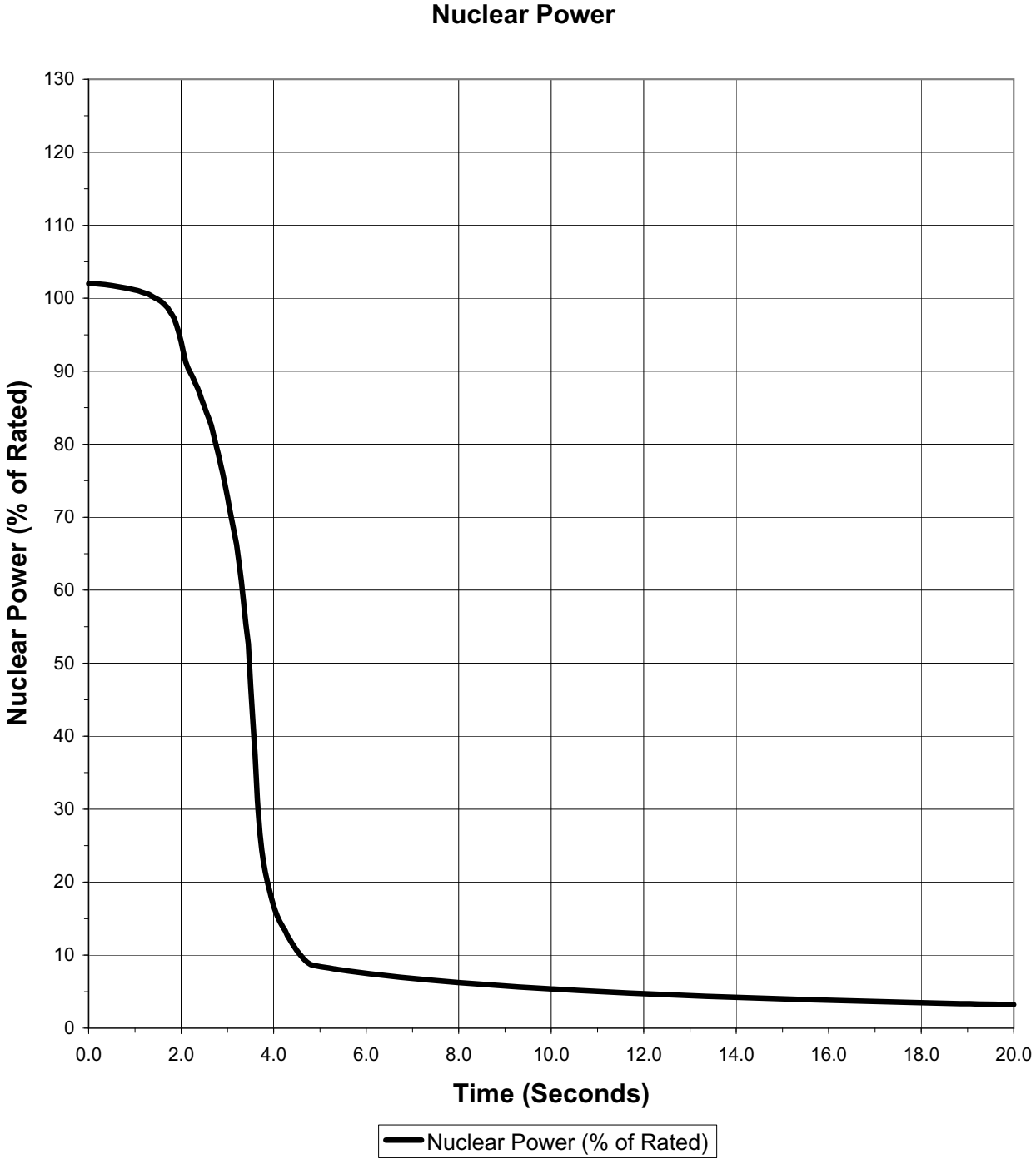

Figure 15.4-80
LOCKED ROTOR MAIN STEAM OVERPRESSURE CASE
STEAM GENERATOR PRESSURE (UNAFFECTED LOOP)

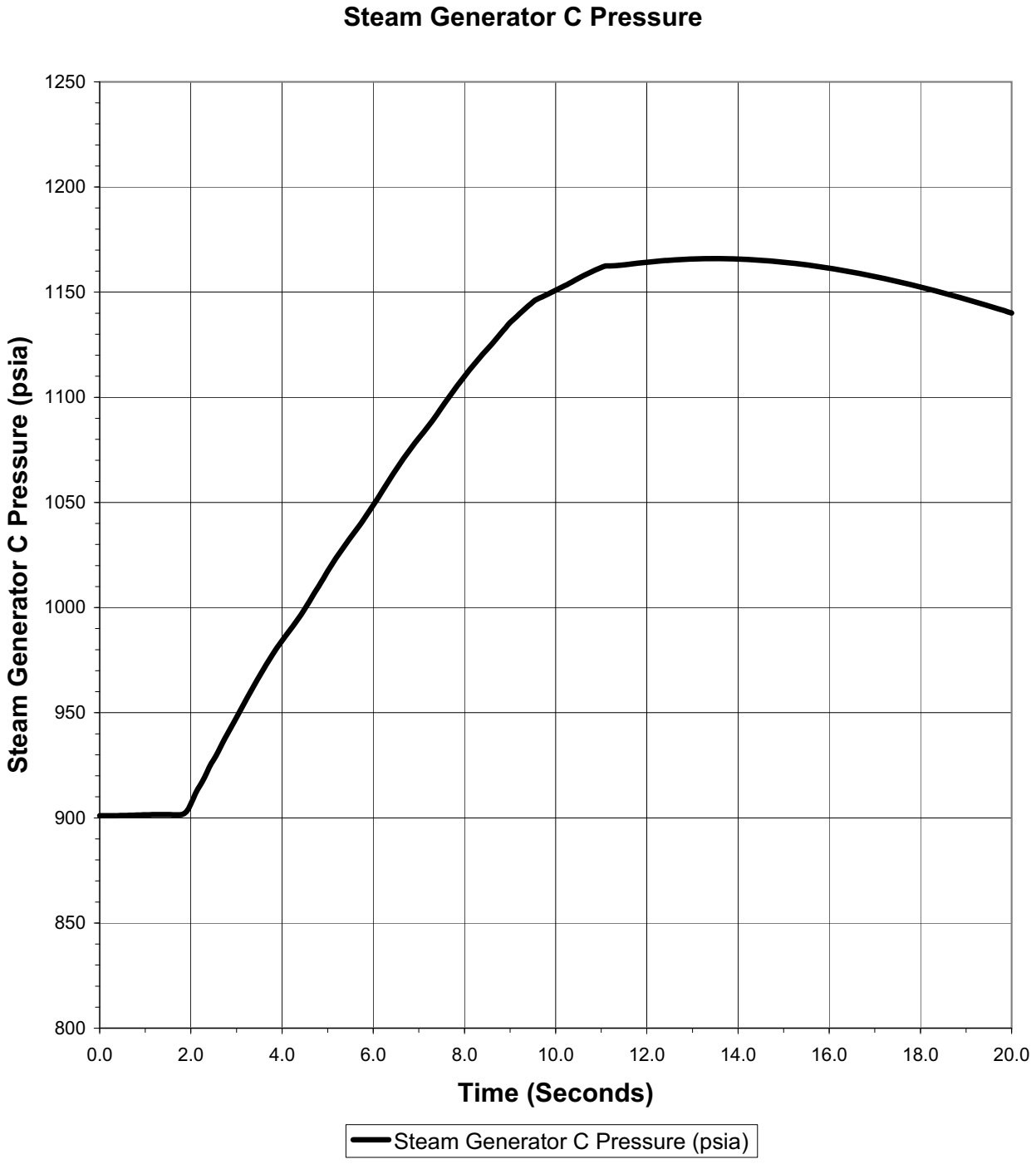

Figure 15.4-81
LOCKED ROTOR RCS OVERPRESSURE CASE
0 PCM/F MTC/2% PSV TOL
PRESSURIZER SAFETY VALVE FLOW RATE (TOTAL OF 3 PSVs)

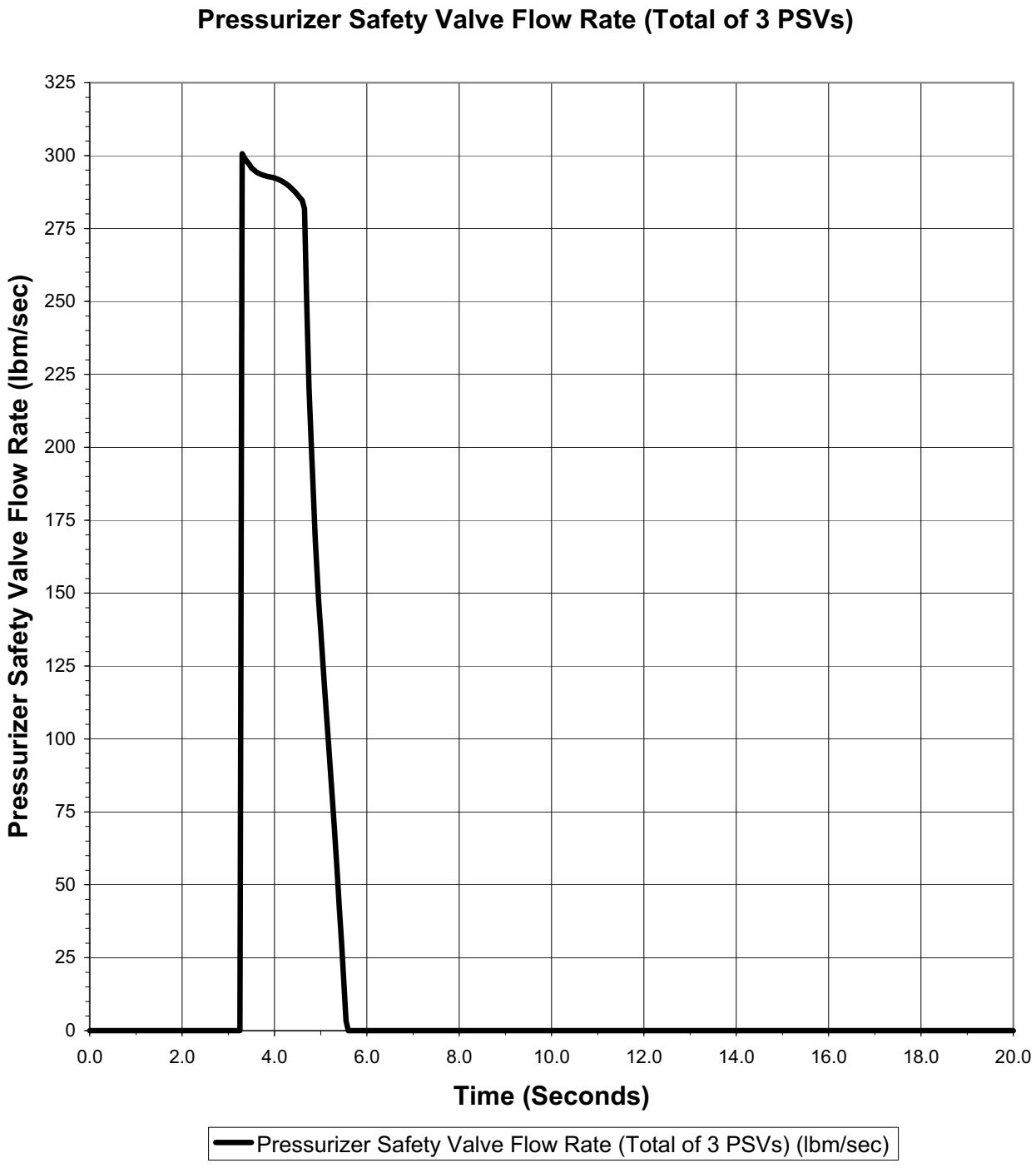

Figure 15.4-82
NUCLEAR POWER TRANSIENT
BOL HFP ROD EJECTION ACCIDENT

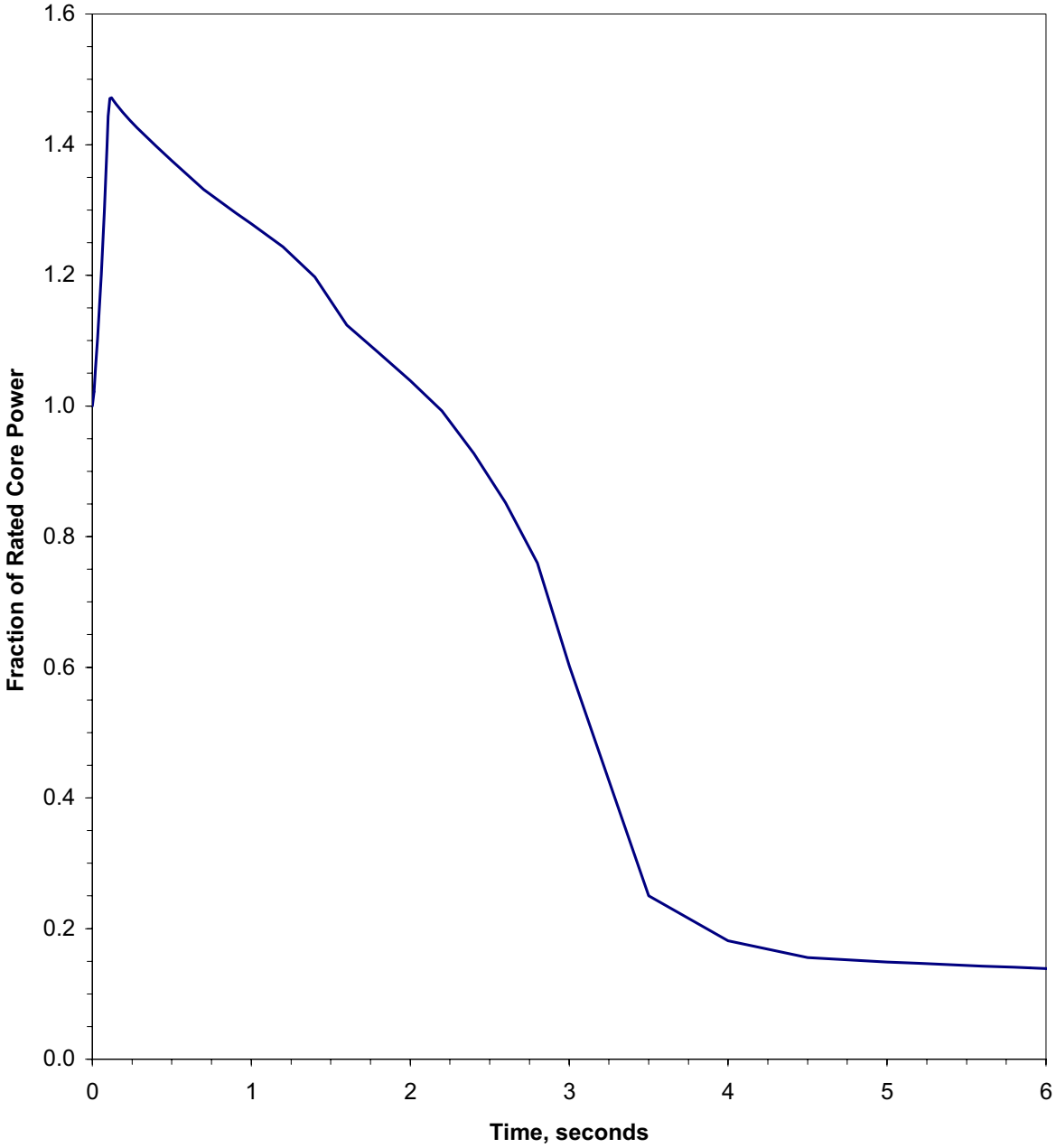

Figure 15.4-83
HOT SPOT FUEL AND CLAD TEMPERATURE VERSUS TIME
BOL HFP ROD EJECTION ACCIDENT

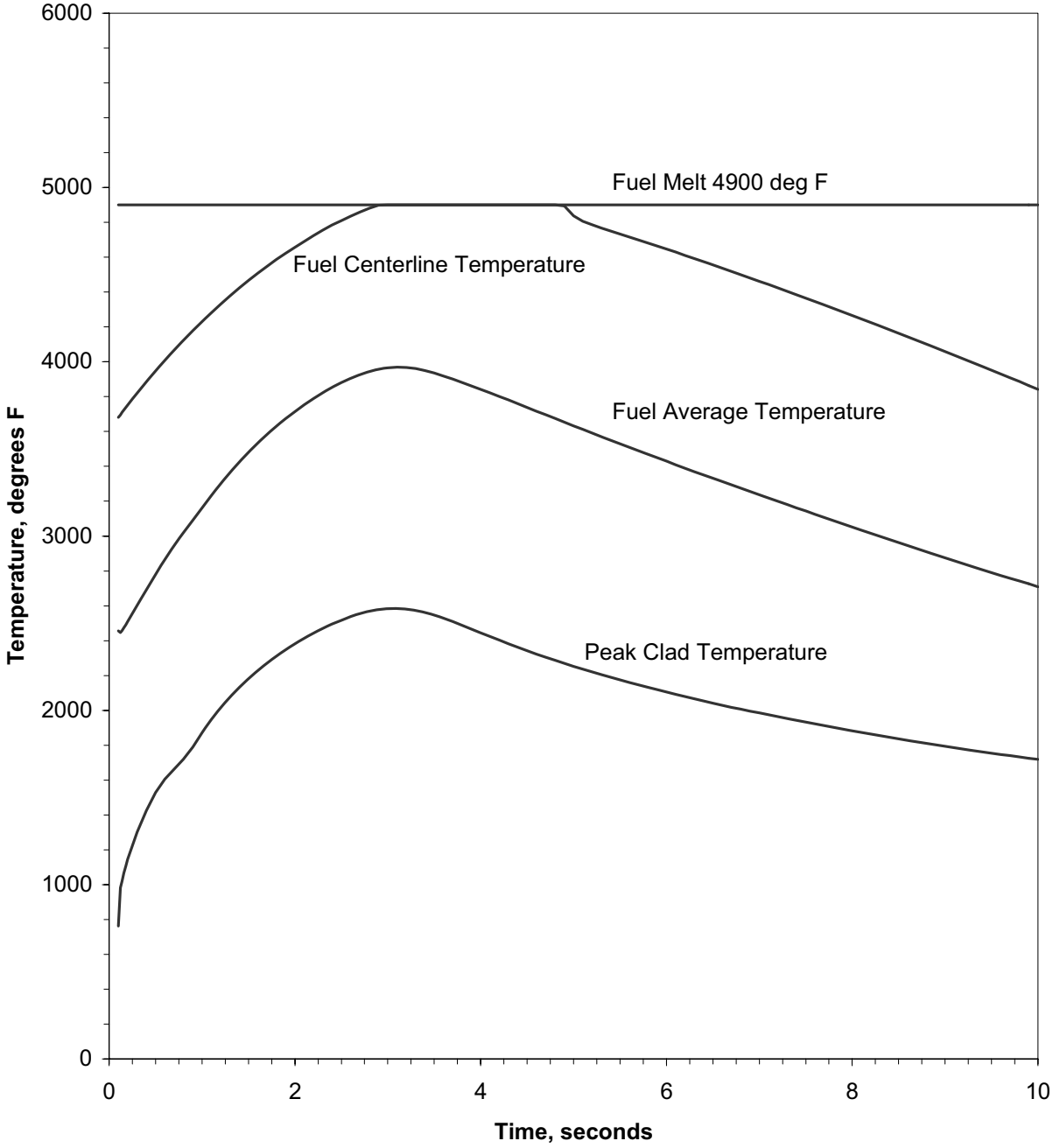

Figure 15.4-84
NUCLEAR POWER TRANSIENT
EOL HZP ROD EJECTION ACCIDENT

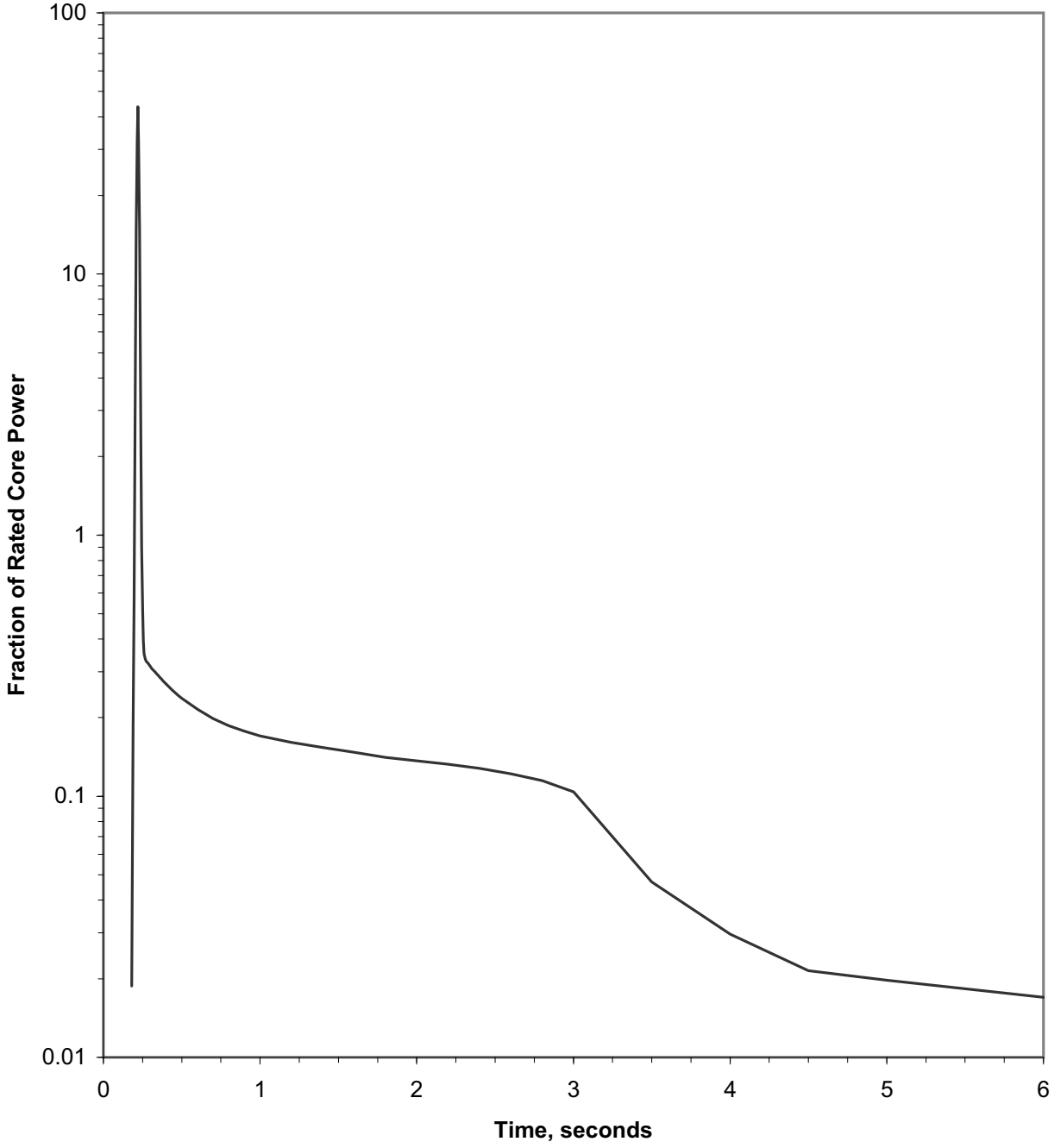

Figure 15.4-85
HOT SPOT FUEL AND CLAD TEMPERATURE VERSUS TIME
EOL HZP ROD EJECTION ACCIDENT

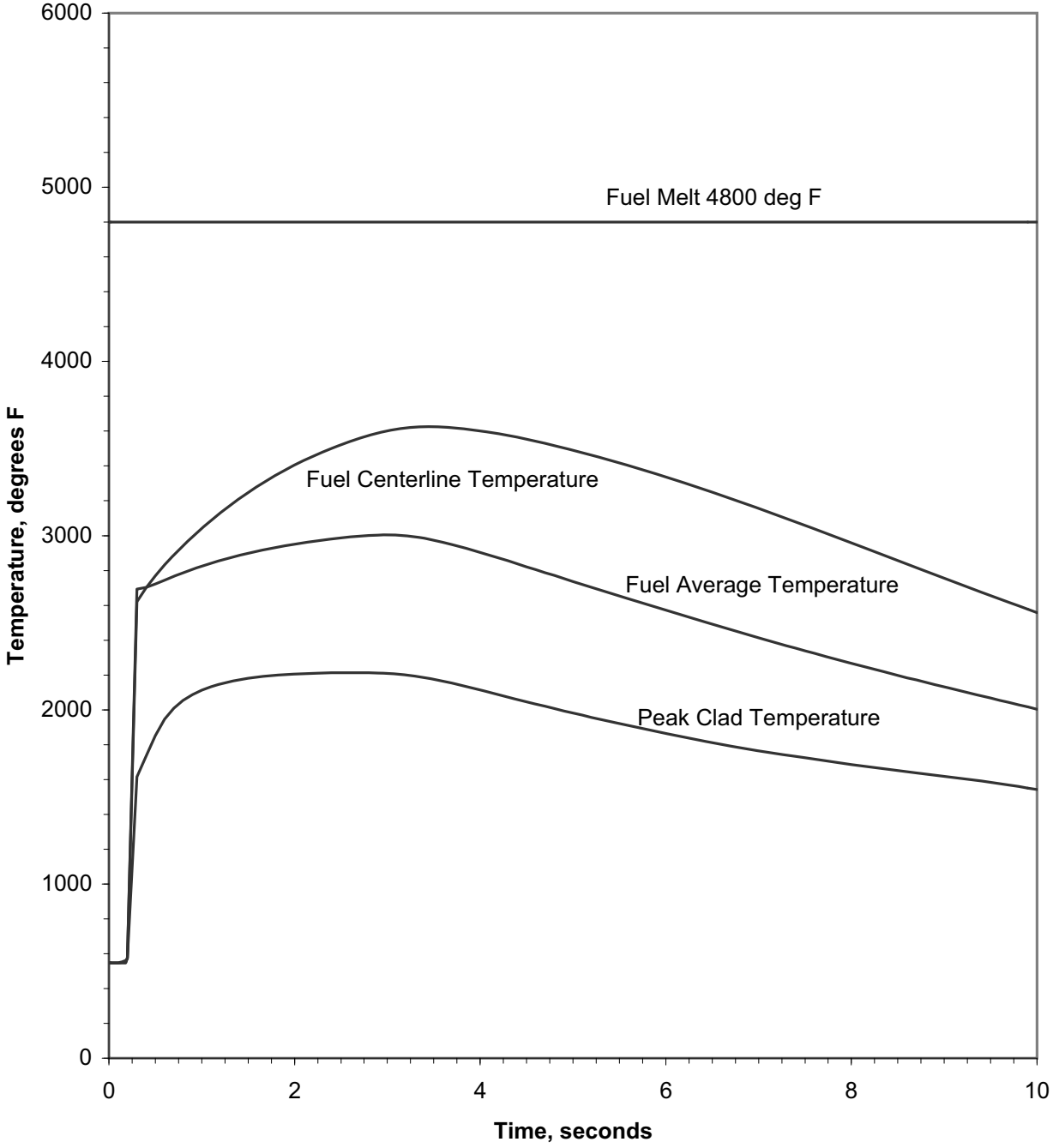

Figure 15.4-86
NORTH ANNA UNIT 1 SCATTER PLOTS OF OPERATIONAL PARAMETERS

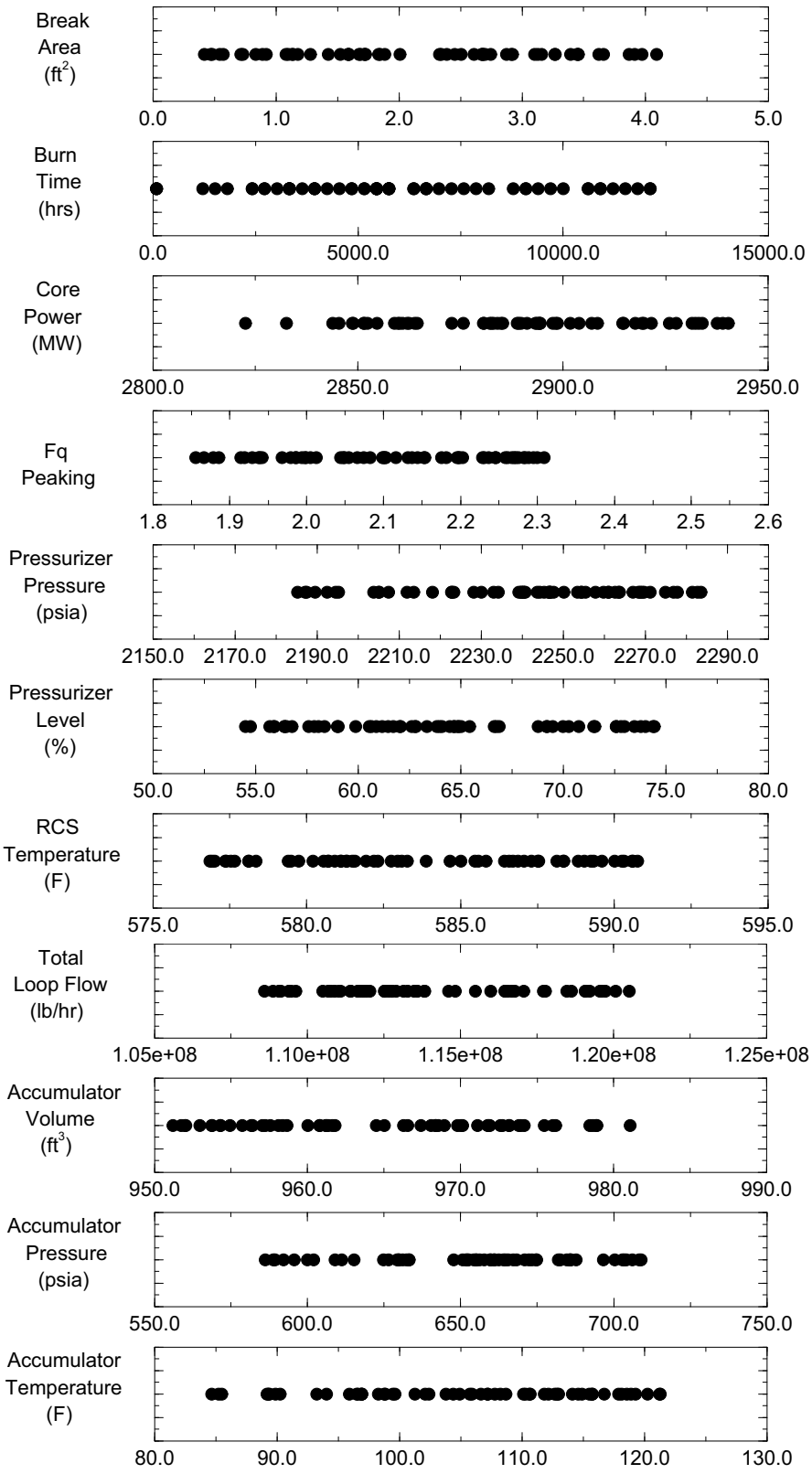

Figure 15.4-87
NORTH ANNA UNIT 1 PCT VERSUS BREAK SIZE PER SIDE SCATTER PLOT

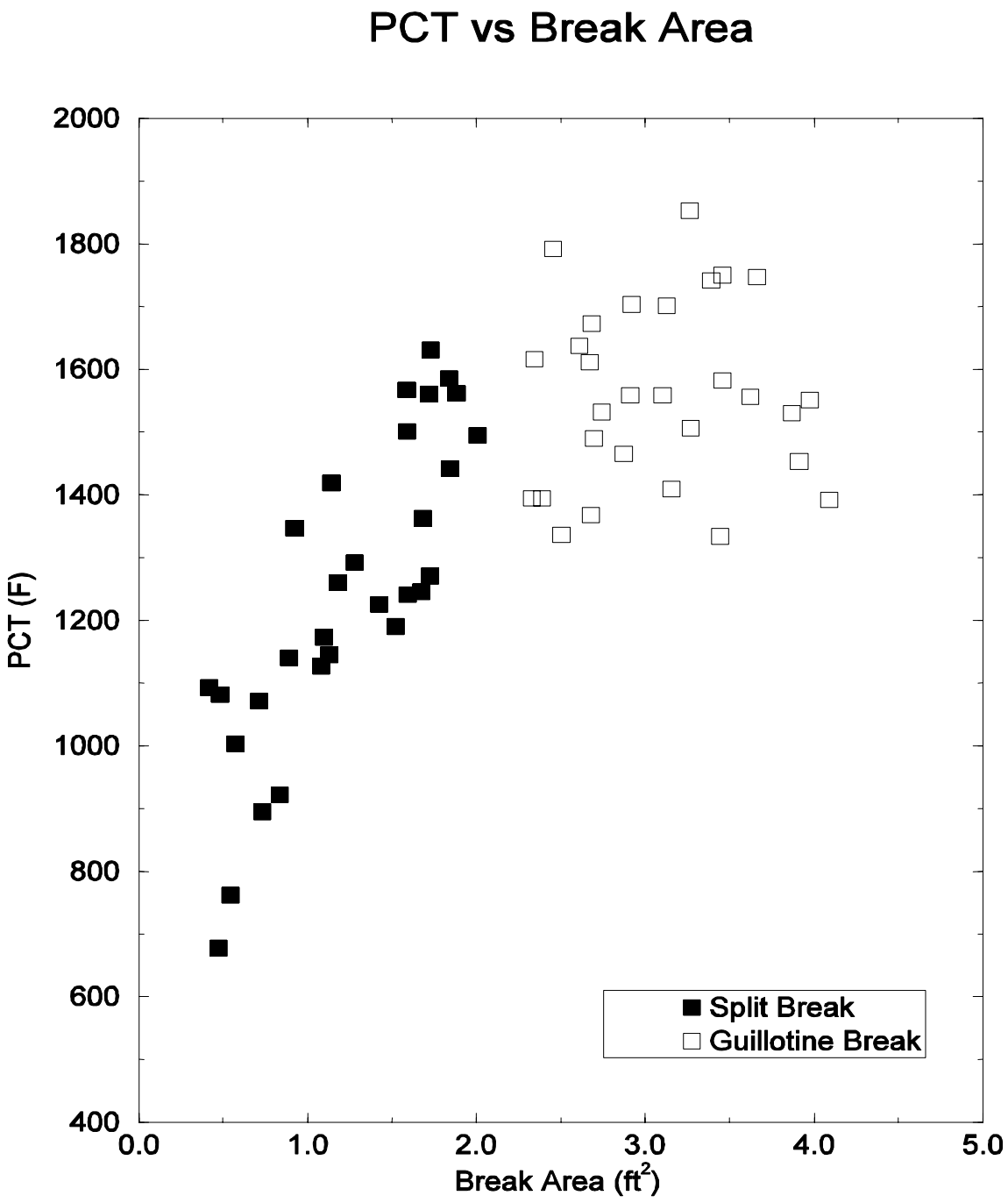

Figure 15.4-88
NORTH ANNA UNIT 1 PEAK CLADDING TEMPERATURE FOR THE LIMITING BREAK

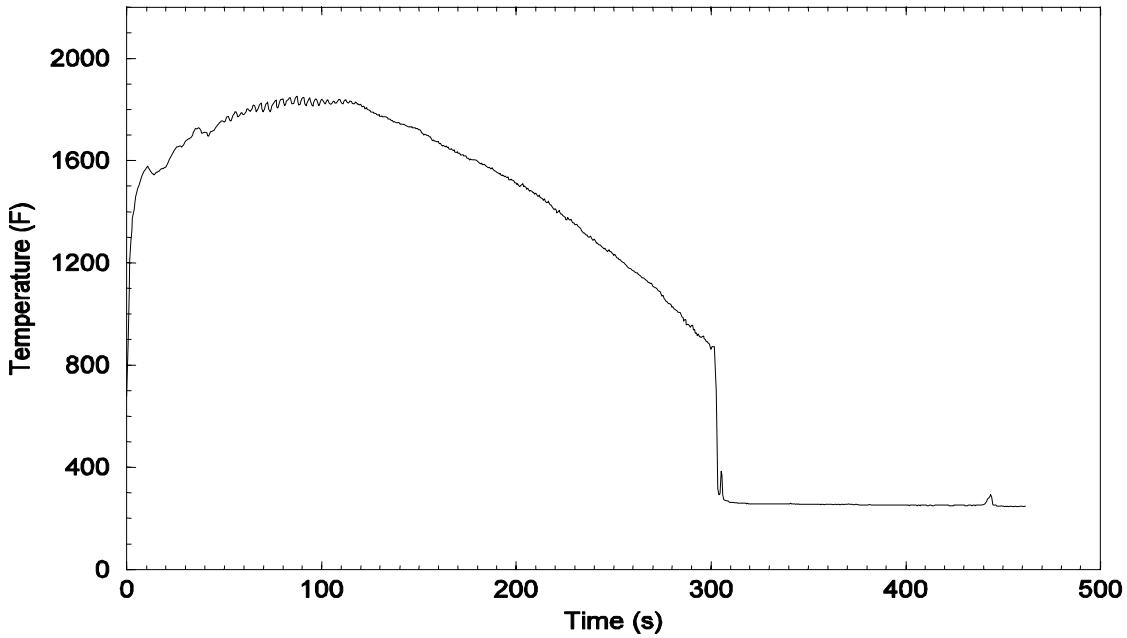

Figure 15.4-89
NORTH ANNA UNIT 1 SYSTEM (UPPER PLENUM) PRESSURE
FOR THE LIMITING BREAK

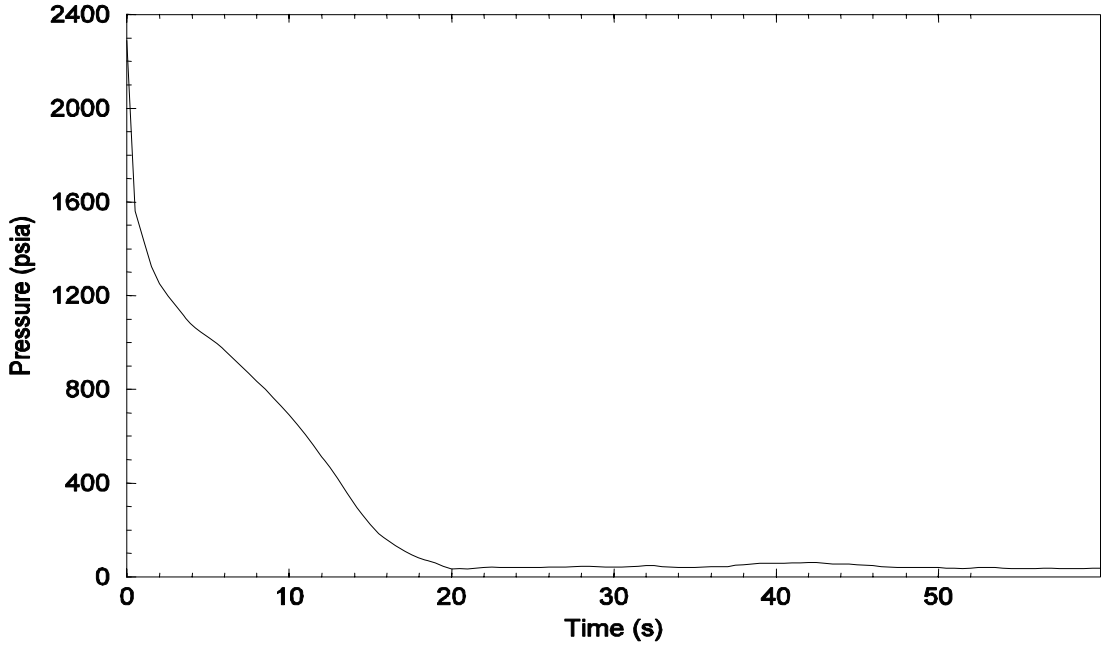

Figure 15.4-90
NORTH ANNA UNIT 1 CONTAINMENT PRESSURE FOR THE LIMITING BREAK

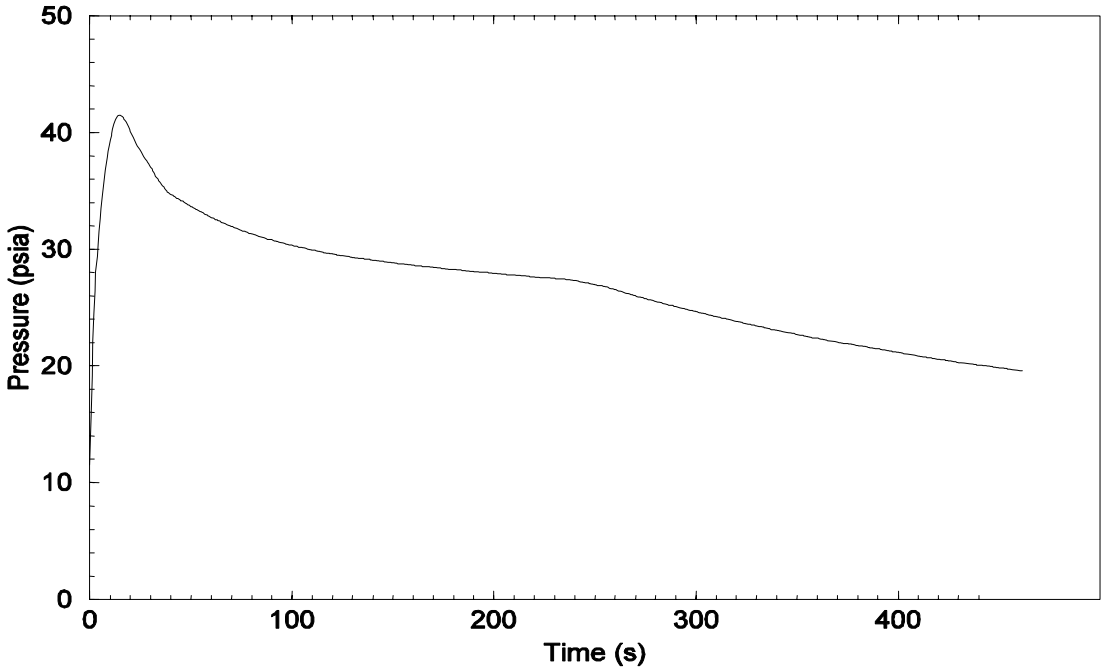

Figure 15.4-91
NORTH ANNA UNIT 1 HOT ASSEMBLY INLET AND OUTLET MASS FLOW RATES
FOR THE LIMITING BREAK

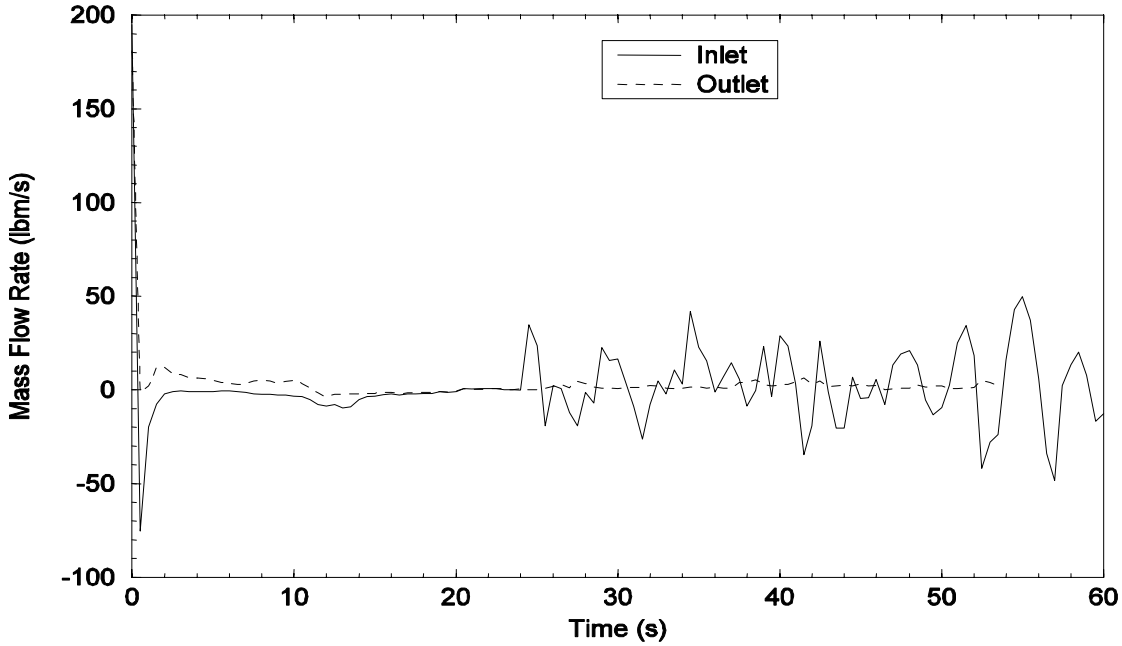

Figure 15.4-92
NORTH ANNA UNIT 1 HOT ASSEMBLY MASS FLOW RATE AT THE PCT LOCATION
FOR THE LIMITING BREAK

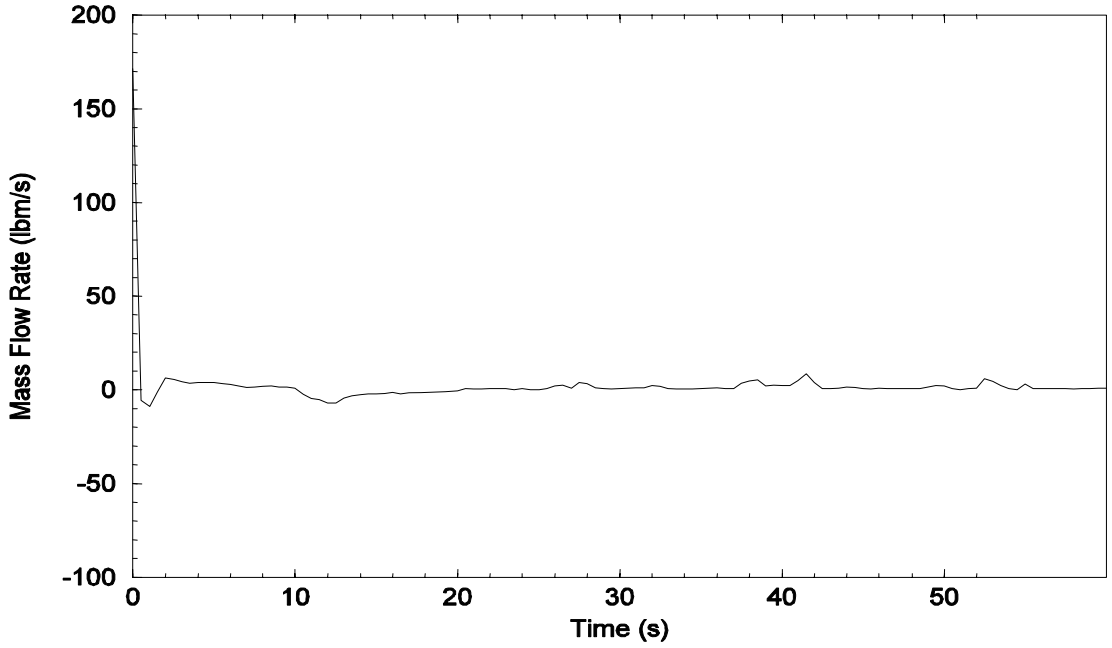

Figure 15.4-93
NORTH ANNA UNIT 1 ACCUMULATOR DISCHARGE FLOW RATES
FOR THE LIMITING BREAK

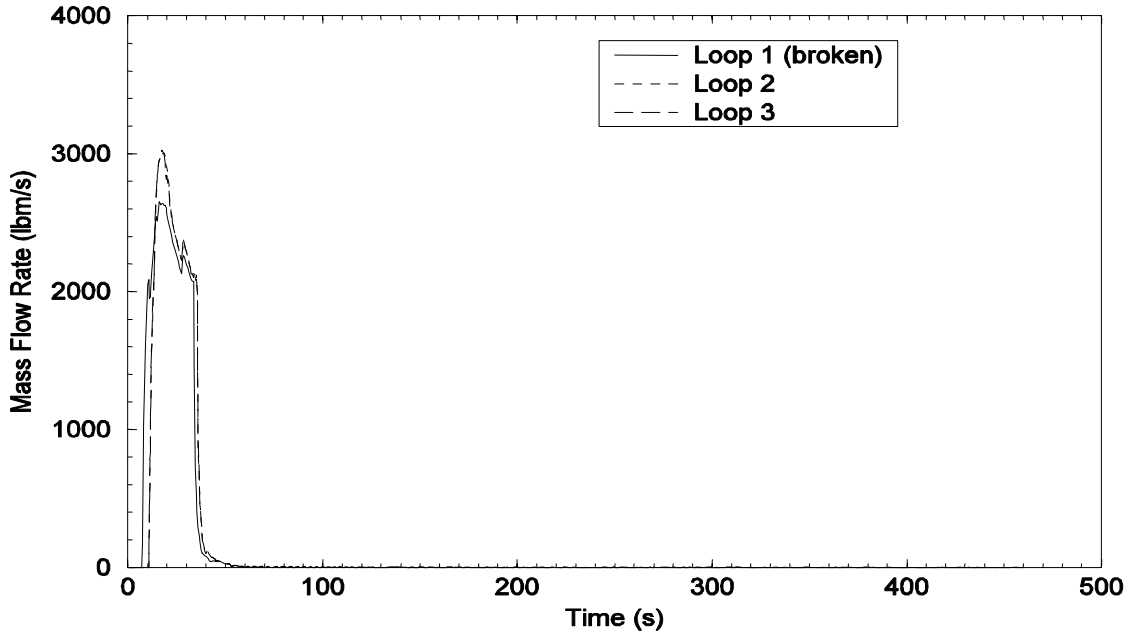

Figure 15.4-94
NORTH ANNA UNIT 1 PUMPED ECC INJECTION FLOW RATES
FOR THE LIMITING BREAK

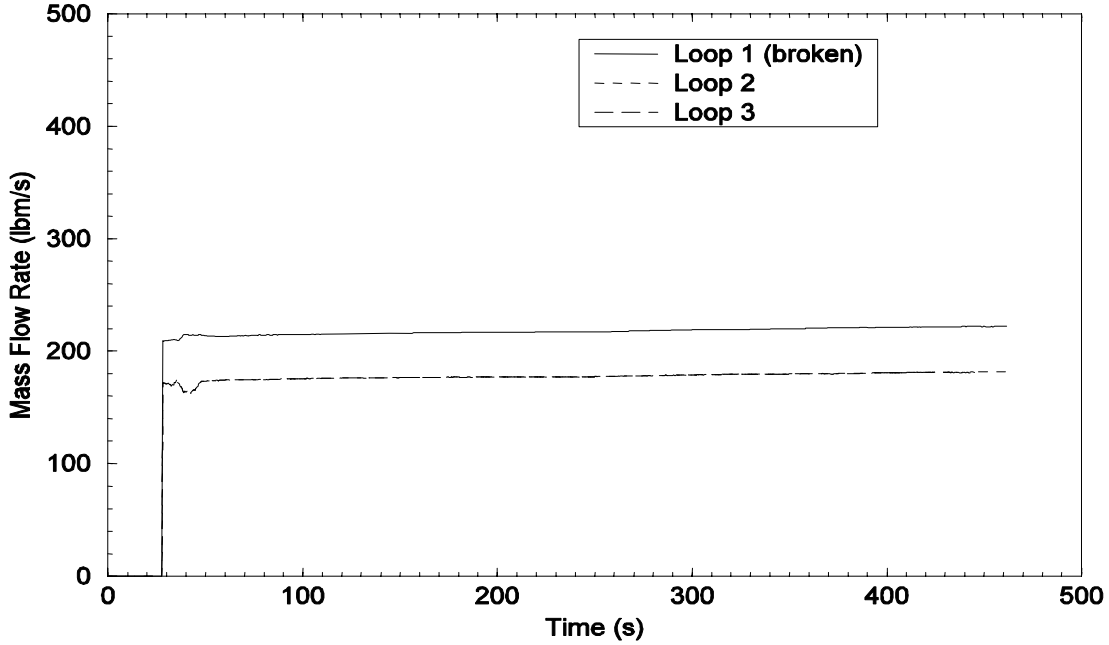

Figure 15.4-95
NORTH ANNA UNIT 1 COLLAPSED LIQUID LEVEL IN THE DOWNCOMER
FOR THE LIMITING BREAK

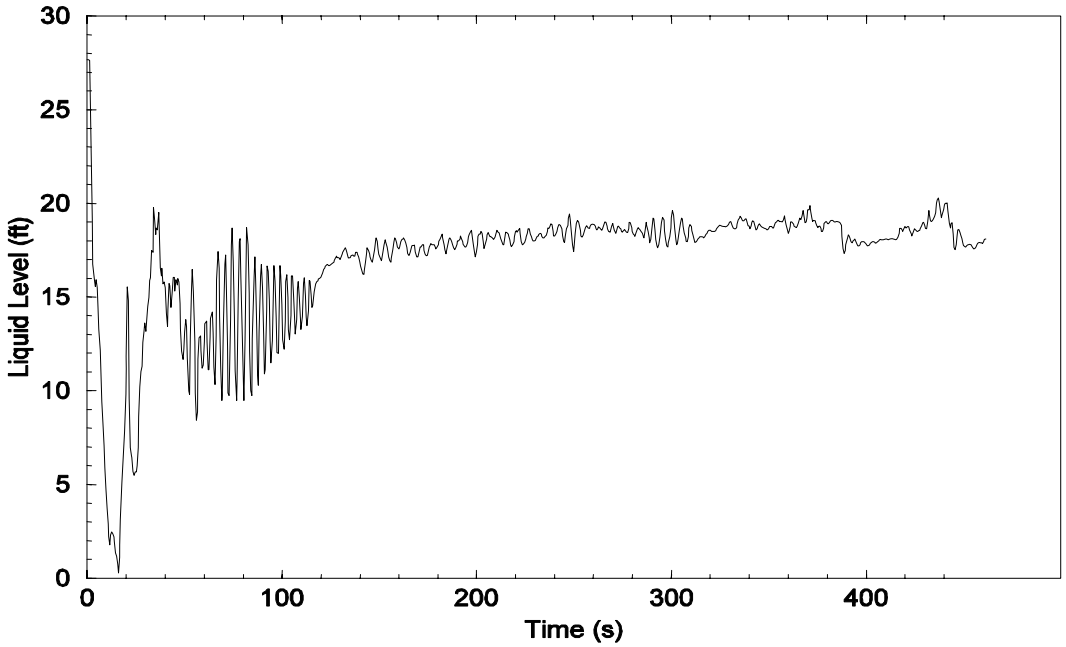

Figure 15.4-96
NORTH ANNA UNIT 1 COLLAPSED LIQUID LEVEL IN THE LOWER VESSEL
FOR THE LIMITING BREAK

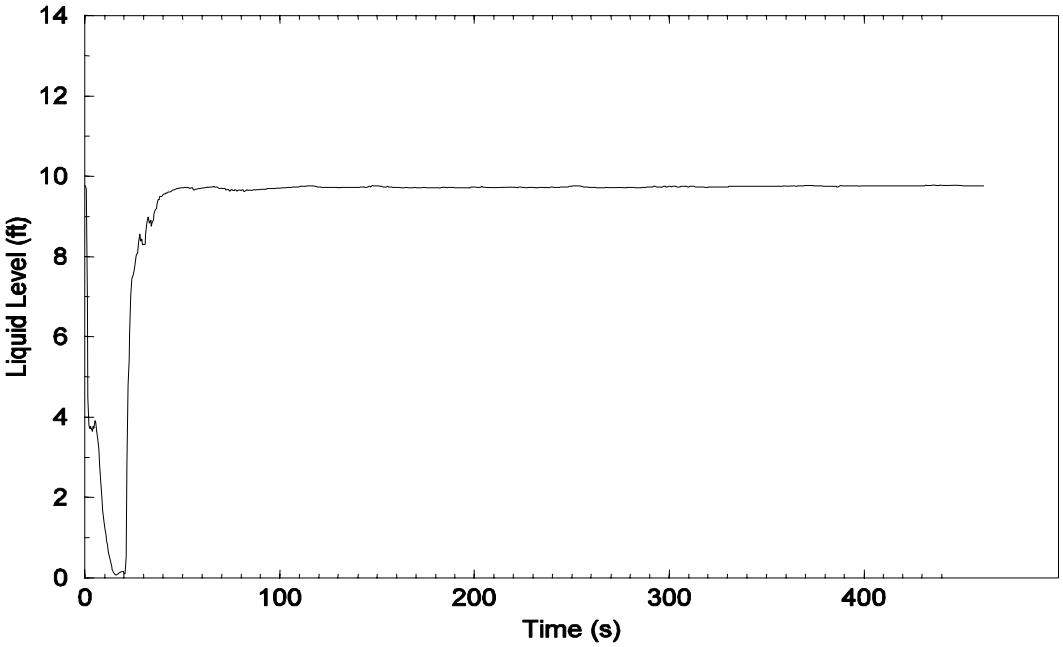

Figure 15.4-97
NORTH ANNA UNIT 1 COLLAPSED LIQUID LEVEL IN THE HOT ASSEMBLY
FOR THE LIMITING BREAK

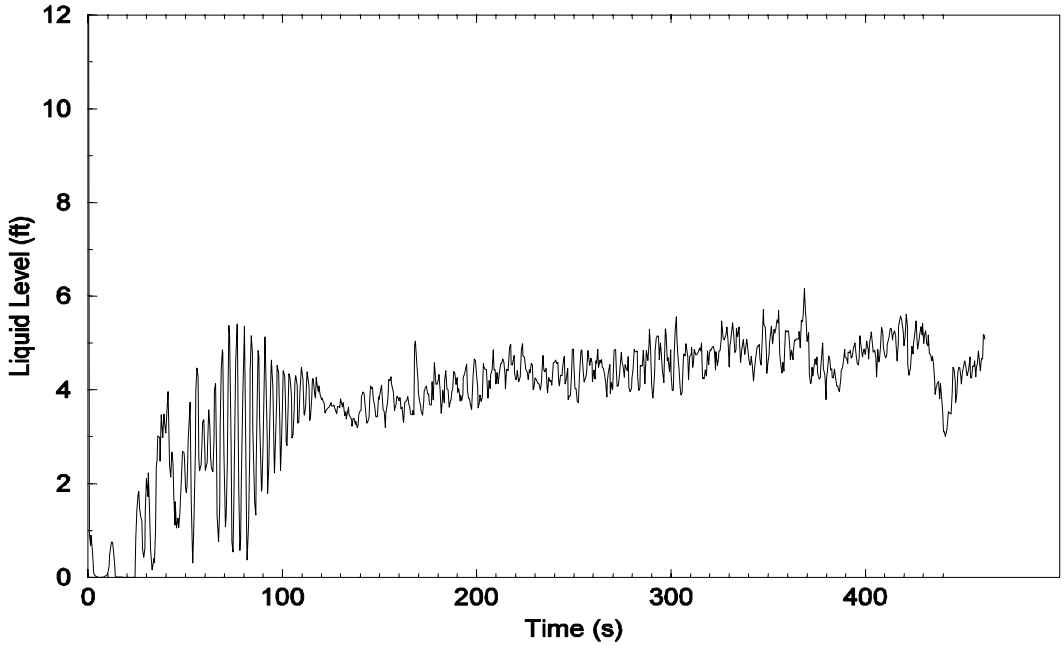

Figure 15.4-98
NORTH ANNA UNIT 2 SCATTER PLOTS OF OPERATIONAL PARAMETERS

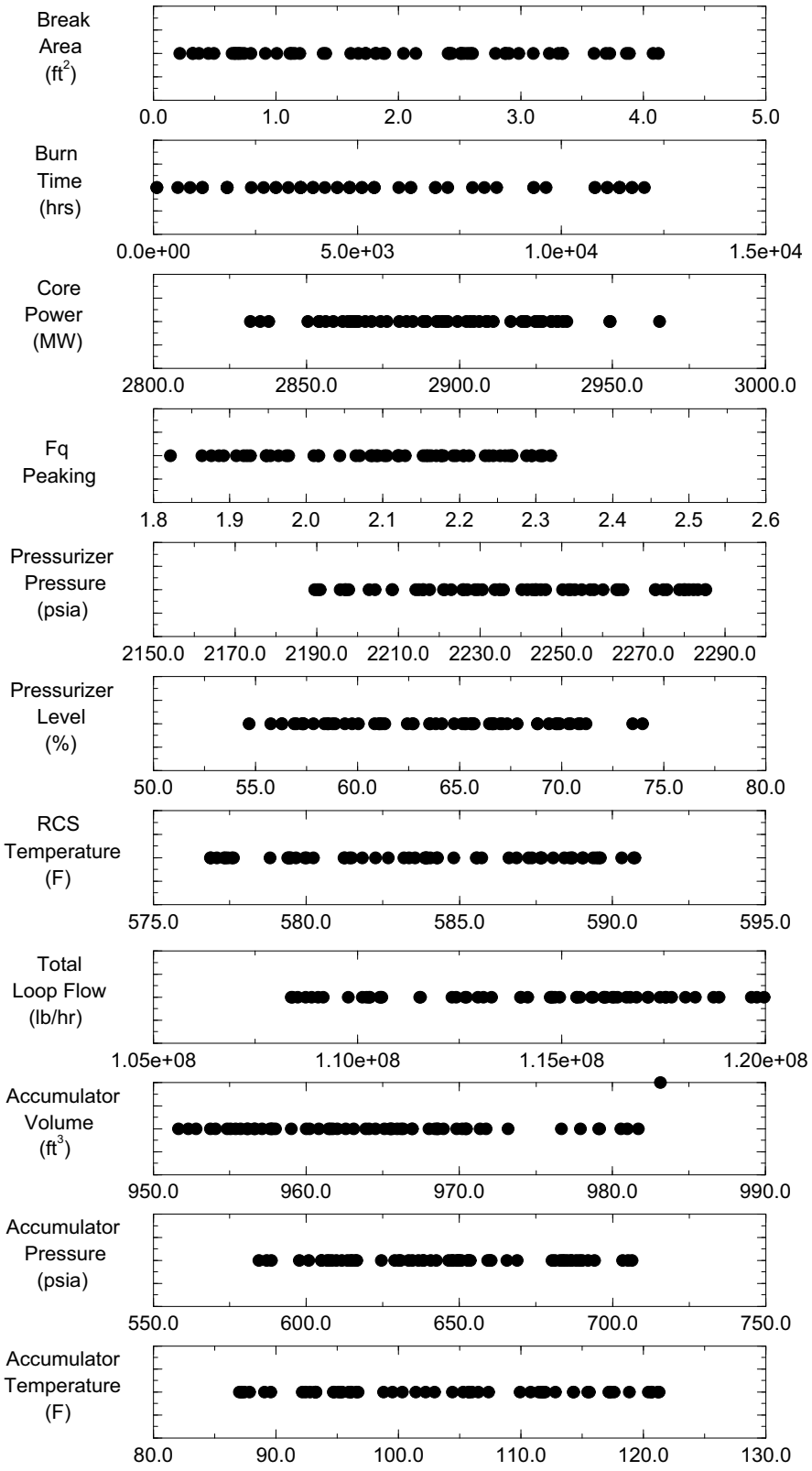

Figure 15.4-99
NORTH ANNA UNIT 2 PCT VERSUS BREAK SIZE PER SIDE SCATTER PLOT

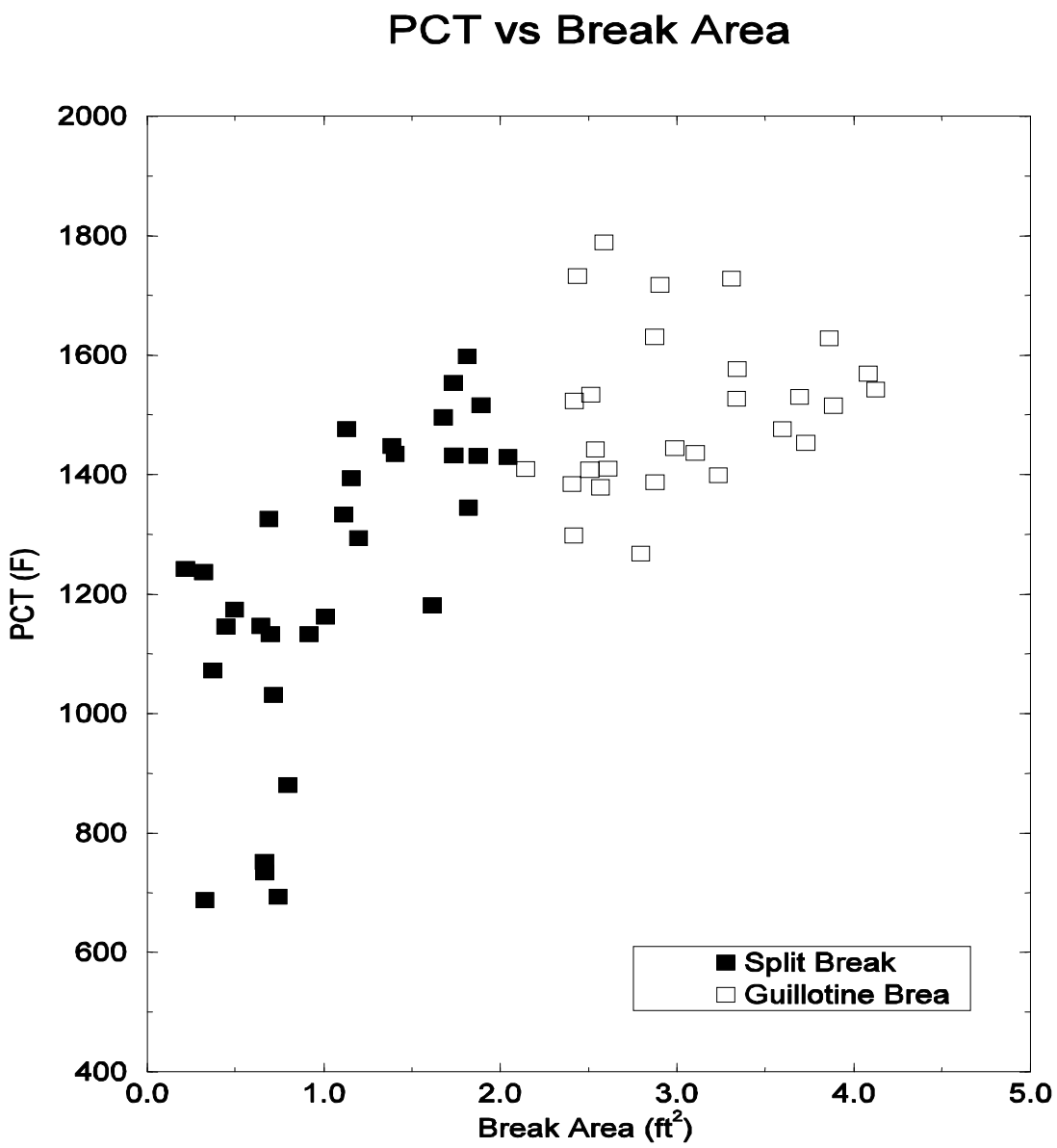

Figure 15.4-100
NORTH ANNA UNIT 2 PEAK CLADDING TEMPERATURE FOR THE LIMITING BREAK

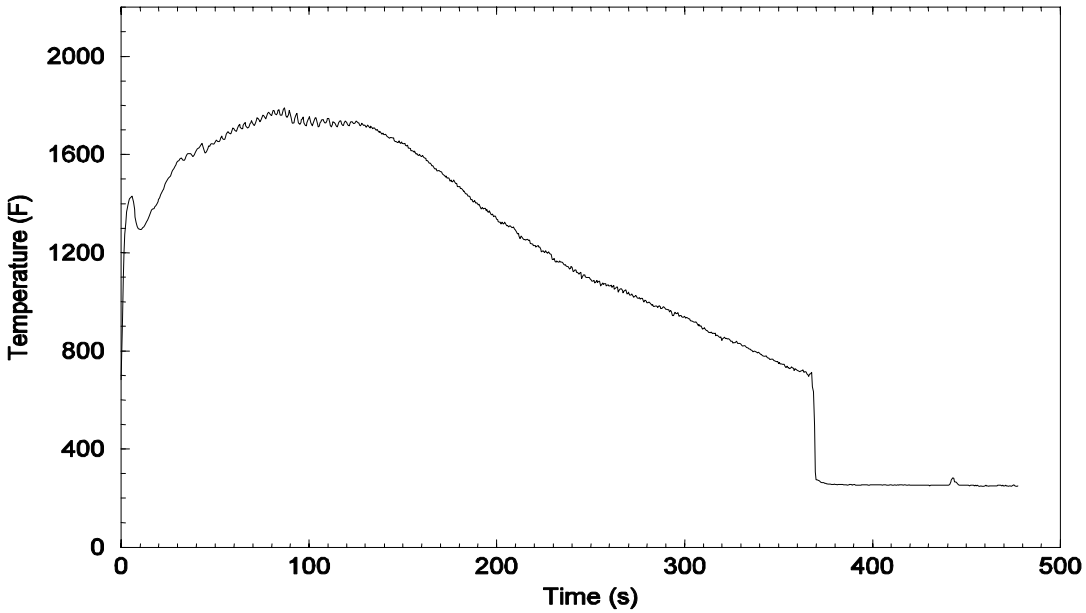

Figure 15.4-101
NORTH ANNA UNIT 2 SYSTEM (UPPER PLENUM) PRESSURE
FOR THE LIMITING BREAK

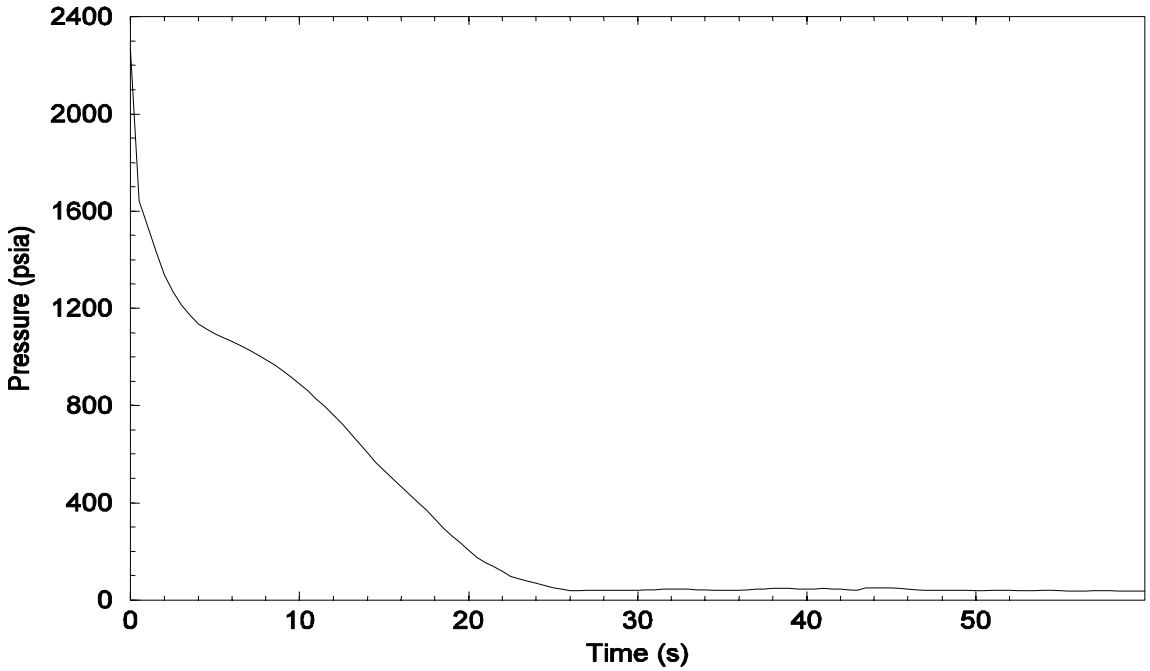

Figure 15.4-102
NORTH ANNA UNIT 2 CONTAINMENT PRESSURE FOR THE LIMITING BREAK

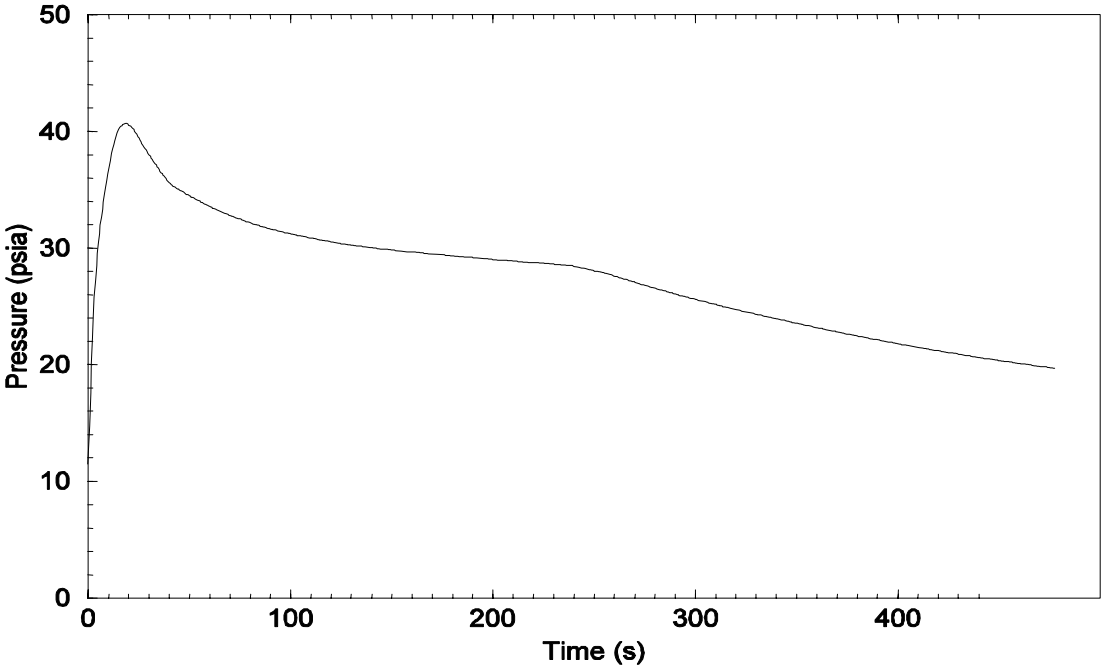

Figure 15.4-103
NORTH ANNA UNIT 2 HOT ASSEMBLY INLET AND OUTLET MASS FLOW RATES
FOR THE LIMITING BREAK

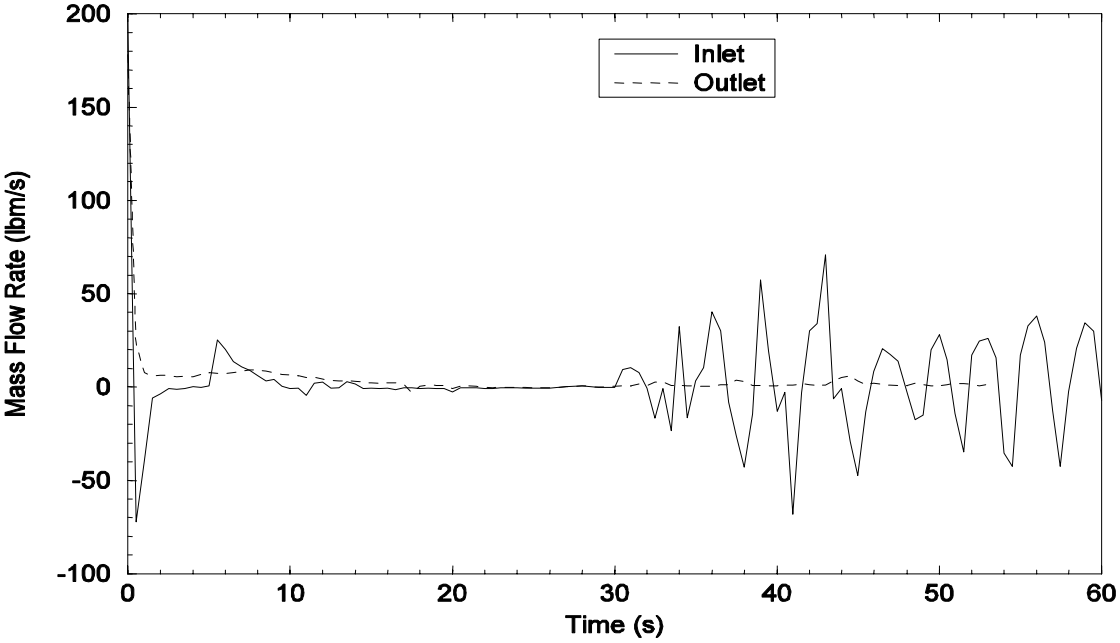

Figure 15.4-104
NORTH ANNA UNIT 2 HOT ASSEMBLY MASS FLOW RATE AT THE PCT LOCATION
FOR THE LIMITING BREAK

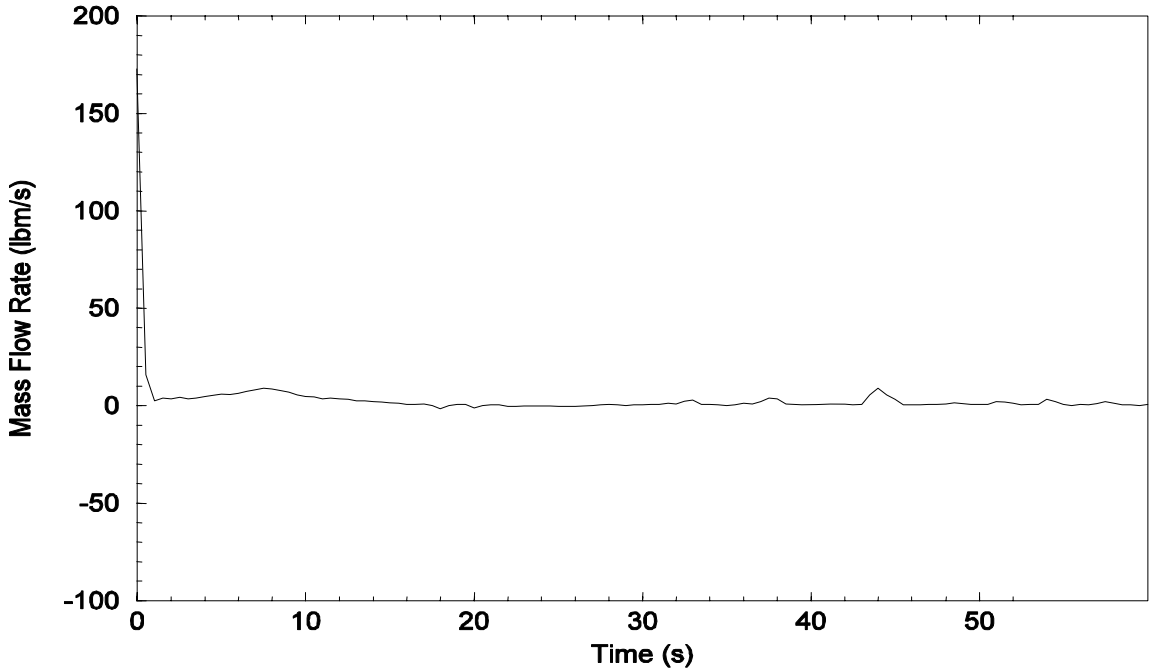

Figure 15.4-105
NORTH ANNA UNIT 2 ACCUMULATOR DISCHARGE FLOW RATE
FOR THE LIMITING BREAK

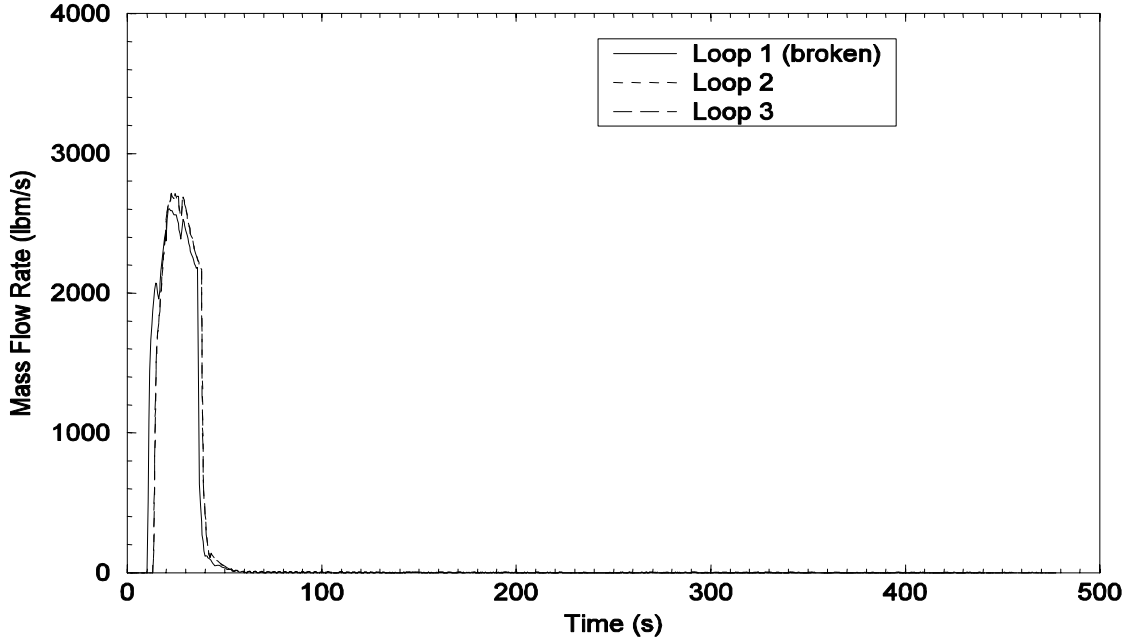

Figure 15.4-106
NORTH ANNA UNIT 2 PUMPED ECC INJECTION FLOW RATE
FOR THE LIMITING BREAK

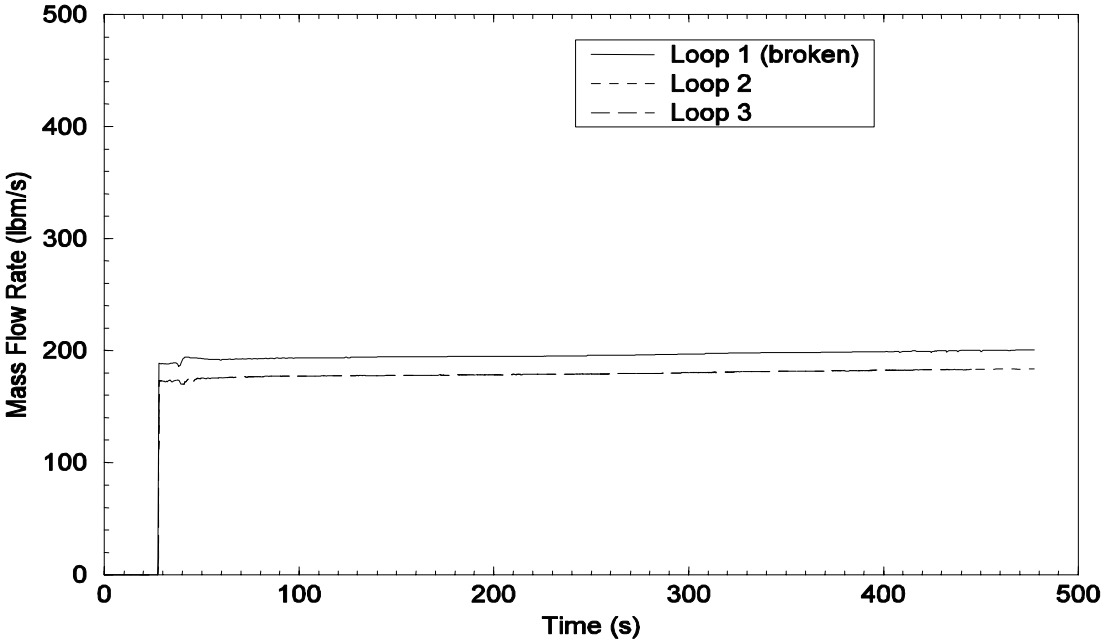

Figure 15.4-107
NORTH ANNA UNIT 2 COLLAPSED LIQUID LEVEL IN THE DOWNCOMER
FOR THE LIMITING BREAK

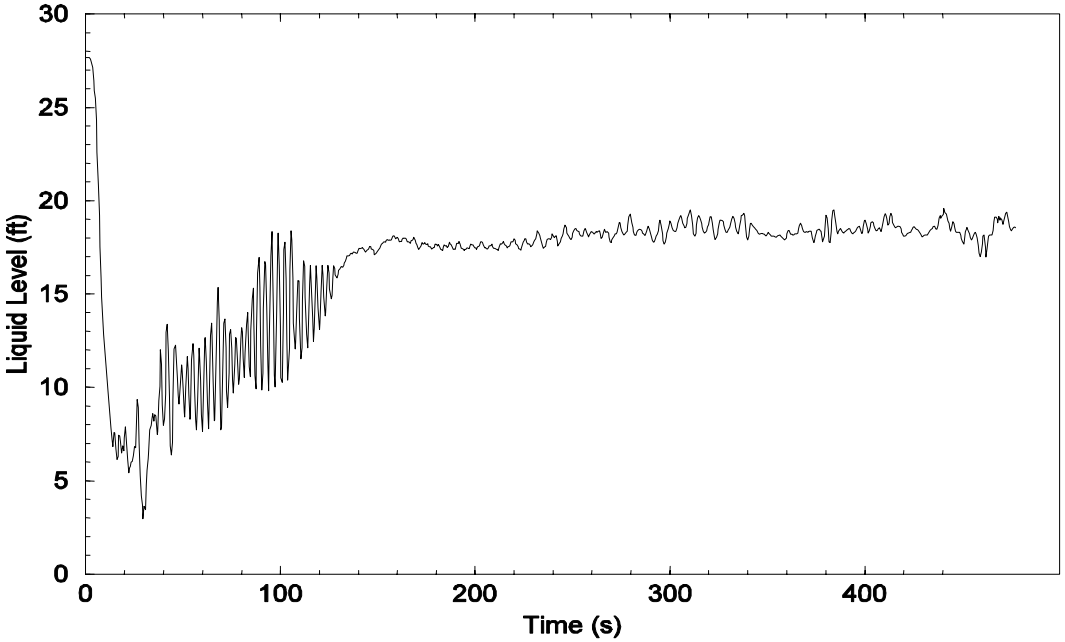

Figure 15.4-108
NORTH ANNA UNIT 2 COLLAPSED LIQUID LEVEL IN THE LOWER VESSEL
FOR THE LIMITING BREAK

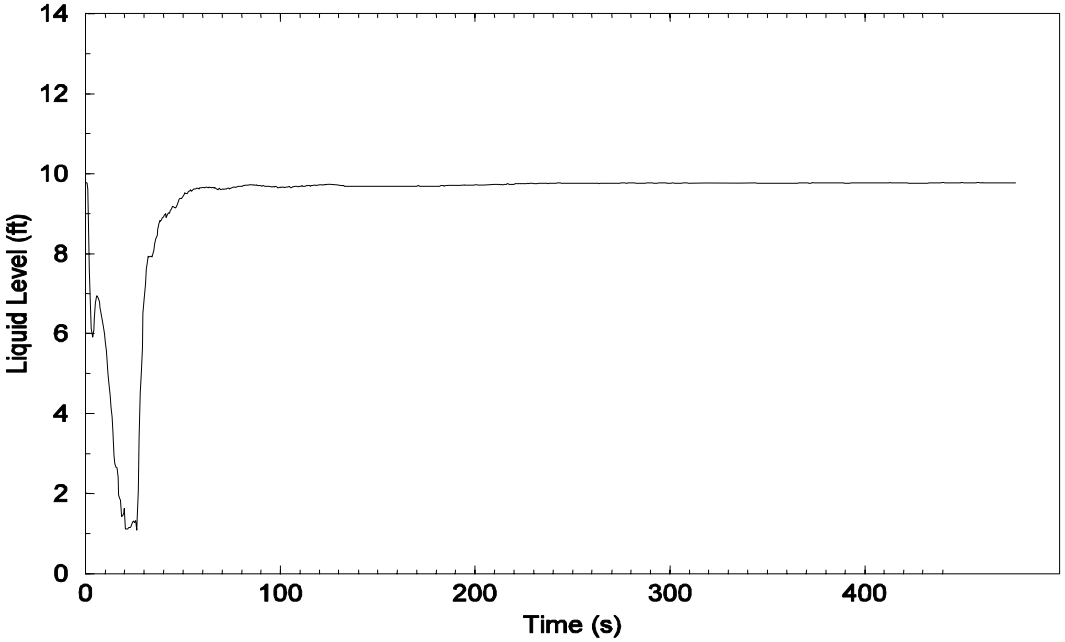

Figure 15.4-109
NORTH ANNA UNIT 2 COLLAPSED LIQUID LEVEL IN THE HOT ASSEMBLY
FOR THE LIMITING BREAK

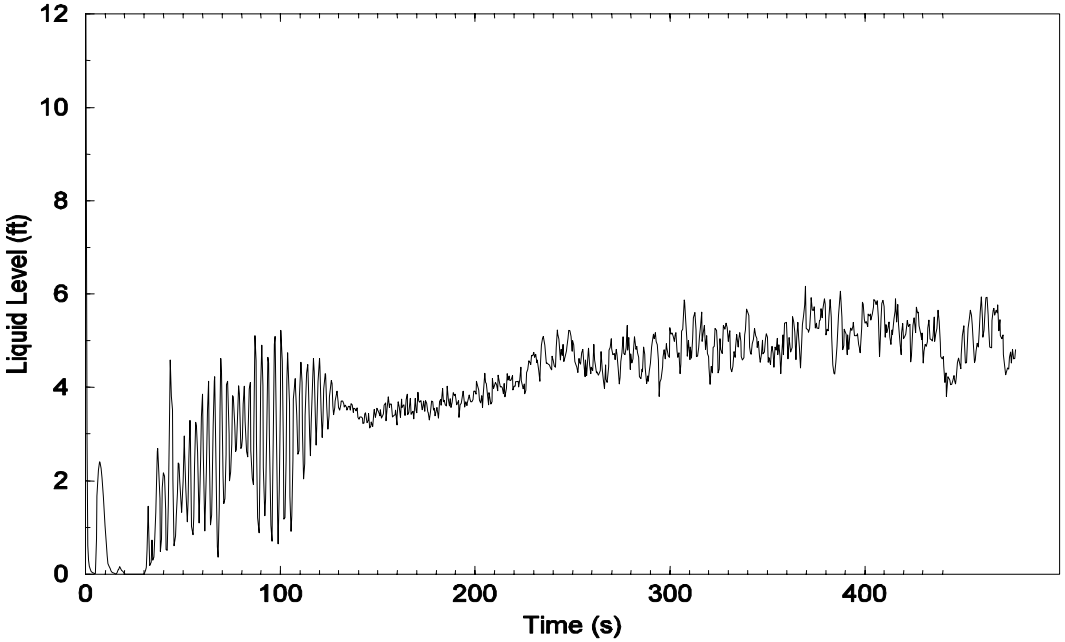

Figure 15.4-110
ACCEPTABLE ECCS LEAKAGE, COMBINED FILTERED AND UNFILTERED FLOWS, FOR CONTROL ROOM INLEAKAGE OF 250 CFM

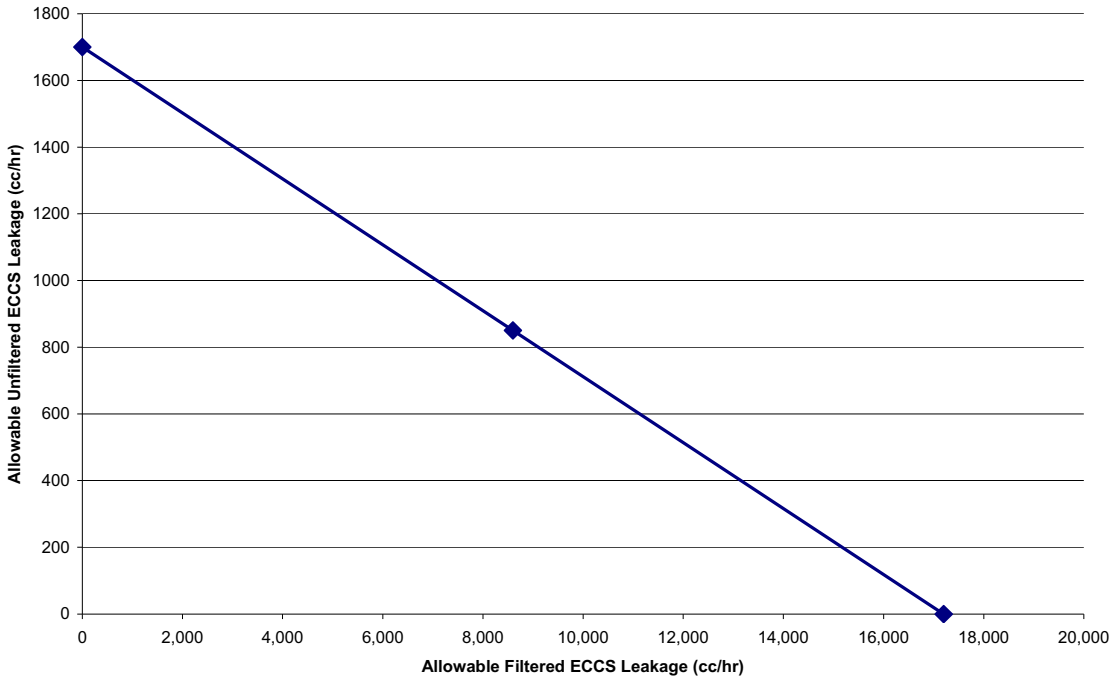

Curve Data

Unfiltered Control Room Inleakage	Filtered ECCS Leakage (cc/hr)	Unfiltered ECCS Leakage (cc/hr)
250 cfm	17,200	0
	8600	850
	0	1700

Appendix 15A[1]
Spent Fuel Cask Drop Analysis

1. Appendix 15A was submitted as Appendix 9B in the original FSAR.

Intentionally Blank

Intentionally Blank

Appendix 15A
SPENT FUEL CASK DROP ANALYSIS

15A.1 INTRODUCTION

This appendix contains the results of a spent fuel cask drop analysis conducted for North Anna Power Station Units 1 and 2. Although spent fuel is not scheduled to be shipped from North Anna for several years, it was necessary to perform the analysis at this time to confirm that the spent fuel handling system would be adequate to handle shipments of spent fuel.

During the course of the analysis, it was determined that a separation wall should be installed to prevent an accidentally dropped cask from coming in contact with the spent fuel.

A meeting was held with the NRC Staff on May 10, 1976, to discuss the separation wall concept and associated accident analyses. Vepco's letter of May 20, 1976, informed the NRC that Vepco was initiating procurement and construction activities.

When a cask is selected for use at some time in the future, this analysis will be re-evaluated to ensure that the cask used would not cause an accident more severe than that described in this report.

A subsequent safety evaluation concluded that the consequences from the drop of either an NLI 1/2 or an NLI 10/24 cask are bounding for a TN-32 storage cask and are bounding for a NUHOMS OS-187H transfer cask. The TN-32 cask is described in the North Anna ISFSI Safety Analysis Report and the TN-32 Topical Safety Analysis Report. The NUHOMS OS-187H transfer cask is described in the NUHOMS-HD Final Safety Analysis Report. A 32-inch high pedestal has been placed in the deep end of the cask loading area to allow the fuel assemblies in the spent fuel cask to be at approximately the same elevation as the assemblies in the spent fuel racks. An evaluation of this pedestal shows that the original TN-32 drop and tip analyses remain bounding.

15A.2 ARRANGEMENT OF SPENT FUEL CASK HANDLING SYSTEM

The following items should be noted with respect to the general arrangement of the spent fuel cask handling system:

1. The spent fuel cask crane is on a fixed runway. Movement of the crane can only occur in the north-south direction. No movement of the cask over the spent fuel is possible.
2. The maximum elevation of the NLI 1/2 and NLI 10/24 casks while over the cask loading area will be limited to 1 foot above floor elevation 291 ft. 10 in. The maximum elevation of the TN-32 and the NUHOMS OS-187H casks while over the cask loading area will be limited to 1.5 feet above the handrail around the spent fuel pool or 5 feet above floor elevation 291 ft.

10 in. For defense-in-depth conservatism, the cask loading area gate will be installed while a cask is either being lowered into or lifted out of the cask loading area. Use of the cask loading area gate will prevent the loss of water from the spent fuel pool through the cask loading area. These restrictions will be included in cask loading and unloading procedures. There are no other cask lift height restrictions involving the use of the 125-ton cask crane.

3. There is no safety-related equipment under the path of the spent fuel cask outside the pool area that could be damaged as the result of a cask drop.
4. The arrangement of the separation wall will ensure that the spent fuel cask will remain in the cask loading area and cannot come in contact with the spent fuel, as confirmed by appropriate accident analysis presented in Spent-Fuel Cask Drop Analysis for North Anna Power Station Units 1 & 2 Attachment 1 of this report.

15A.3 CASK DROP ANALYSIS

15A.3.1 Dose Resulting From Cask Drop

Site boundary doses for postulated cask drop accidents are tabulated below and are less than the exclusion area boundary dose for the fuel handling accident (FHA) as described in Section 15.4.5.

	Cask Drop Dose Consequences
TN-32 cask	< 1 rem TEDE
OS-187H	< 1 rem TEDE

The NLI 10/24 cask drop dose consequences are < 1 rem Whole Body and < 1 rem TEDE. These results are considered historical. The TN-32 storage cask and the NUHOMS OS-187H transfer cask are the only cask types in use at North Anna and there is no plan to use the NLI 10/24 cask. The values for the NLI 10/24 cask are based on ten 15 x 15 fuel assemblies with the source term provided in Table 11.1-1, but decayed for 150 days since shutdown. Fuel gap activity for 15 x 15 fuel assemblies, as stated in Section 11.1, is used with all activity being released from the fuel and from the cask. A χ/Q value of 3.1×10^{-4} sec/m^3 is assumed, as stated in Section 15.4.

The values for the TN-32 cask are based on 32 17 x 17 fuel assemblies decayed for seven years with the source term as stated in the North Anna ISFSI Safety Analysis Report, Table 8.2-1. Fuel gap activity is released from the fuel and from the cask, and a portion of the cobalt activity present on the fuel cladding is also released. A χ/Q value of 3.1×10^{-4} sec/m^3 is assumed to be consistent with the χ/Q value used above.

The values for the OS-187H transfer cask are based on 32 17 x 17 fuel assemblies with the source term based on fuel that has decayed seven years, initial enrichment of 4.0 weight percent

U235 and burnup of 60,000 MWD/MTU. Fuel gap activity is released from the fuel and from the cask, and a portion of the cobalt activity present on the fuel cladding is also released. A χ/Q value of 3.1×10^{-4} sec/m^3 is assumed to be consistent with the χ/Q value used above.

15A.3.2 Cask Drop in Cask Loading Area

Nuclear Energy Services, Inc., performed a cask drop analysis to evaluate the potential structural damage to the cask loading area of the spent fuel pool due to a number of postulated cask drop accidents. Spent-Fuel Cask Drop Analysis for North Anna Power Station Units 1 & 2 Attachment 1 hereto is a copy of their report.

The cask drop analysis was performed using a multi-element cask and a single-element cask. For each of the postulated cask drop accidents, missile impact effects on structures were evaluated for local damage (penetration, perforation, and spalling) as well as overall structural response and potential consequences. The results of the analysis indicated that the cask drop events could cause minor structural damage to the walls and moderate structural damage to the floor of the cask loading area. There would be some local penetration and cracking of the cask loading area floor and wall. However, the arrangement of the new separating wall ensures that the spent fuel will remain covered with water for all of the postulated accident scenarios.

15A.3.3 Design of Fuel Pool Separation Wall

During the course of Nuclear Energy Services' analysis, it was determined that a separation wall should be installed to prevent an accidentally dropped cask from coming in contact with spent fuel. Stone & Webster Engineering Corporation was then asked to design a separation wall that could be installed between the cask-loading area and the spent-fuel storage area. The design and arrangement of the separation wall ensure that the spent-fuel cask will remain in the cask-loading area. The wall was designed to absorb plastically, in flexure, the kinetic energy of the cask at impact, in conjunction with concurrent seismic, hydrostatic, and dead load. See Appendix 9B for a more detailed discussion and analysis.

Intentionally Blank

Appendix 15A[1]
Attachment 1

Spent-Fuel Cask Drop Analysis
for
North Anna Power Station Units 1 & 2

1. Attachment 1 to Appendix 15A was submitted as Appendix M in the original FSAR.

Intentionally Blank

NES 81A0478

SPENT FUEL CASK DROP ANALYSIS

FOR

NORTH ANNA POWER STATION UNITS 1 & 2

Prepared Under NES Project 5111 for

VIRGINIA ELECTRIC AND POWER COMPANY

NUCLEAR ENERGY SERVICES, INC.
Danbury, Connecticut 06810

Prepared by: I. Husain

Approved by: Iqbal Husain
Project Engineer

A. H. Yale
V. P. Engineering

Date: 8/23/76

TABLE OF CONTENTS

LIST OF FIGURES

LIST OF TABLES

1. SUMMARY

This report, prepared for Virginia Electric and Power Company, presents the results of the spent fuel shipping cask drop analysis for North Anna Power Station Units 1 and 2. Nuclear Energy Services, Inc. has performed the cask drop analysis to evaluate the potential structural damage to the fuel cask loading area of the spent fuel pool due to a number of postulated cask drop accidents. The cask drop analysis has been performed for two different types of spent fuel shipping casks; a multi-element cask and a single-element cask. For each of the postulated cask drop accident events, the maximum velocity and kinetic energy of impact, local damage as well as overall structural response and potential consequences have been evaluated. The cask drop analysis have been performed using empirical equations and energy/momentum balance methods given in BC-TOP-9A (Revision 2), Topical Report; Design of Structures for Missile Impact, Bechtel Power Corporation. Based upon the results of the analysis, the cask drop events could cause minor structural damage to the walls and moderate structural damage to the floor of the cask loading area. There will be some local penetration and cracking of the cask loading area floor and walls. However, the arrangement of the proposed separating wall will insure that the spent fuel will remain covered with water for all of the postulated accident scenarios.

2. INTRODUCTION

Virginia Electric and Power Company (VEPCO) requested Nuclear Energy Services, Inc. (NES) to evaluate the potential local damage and overall structural effects to the fuel cask loading area of the spent fuel pool due to the following postulated spent fuel shipping cask drop accident scenarios.

Cask Drop Accident Scenario 1:

As the cask is raised over the decontamination building and moved into the fuel storage building, the cask drops on the edge of the spent fuel pool wall. Potential consequences of this event include damage to the railways and pool wall.

Cask Drop Accident Scenario 2:

While the cask is placed on the ledge in the cask set-down area and the yoke is being replaced with a longer yoke, the cask falls off the set-down area ledge. During this cask drop event, the cask will tip over and either hit the south wall of the pool or fall toward the fuel storage racks and hit the proposed separating wall.

Cask Drop Accident Scenario 3:

After the cask is loaded with spent fuel and is raised to its highest elevation over the spent fuel pool, the loaded cask drops straight down and strikes the pool floor of the cask loading area.

The cask drop accident scenarios have been analyzed for two different types of shipping cask, a multi-element spent fuel shipping cask (10/24 Cask) and a single element spent fuel shipping cask (1/2 Cask). In addition, two cask drop

attitudes have been considered for each cask type: the cask dropping in the upright position with its axis vertical and the cask dropping on its edge at an angle that would cause maximum damage.

For each of the cask drop accident cases, the maximum velocity and kinetic energy at the instant of impact, local effects and the overall structural response have been determined. Local effects consists of: (1) missile penetration into the target, (2) missile perforation through the target, and (3) spalling of the target. Empirical equations presented in References 3, 4, and 5 have been used in evaluating local effects. The overall structural response have been evaluated using energy balance methods given in References 3, 5, and 12.

Section 3 of this report presents detail descriptions of the cask loading area of the spent fuel pool and both shipping casks. Applicable codes, standards and various load cases considered in the analyses are given in Sections 4 and 5 respectively. The analytical procedures and structural acceptance criteria are summarized in Sections 6 and 7. The results and conclusions of the analysis are presented in Section 8 and 9 of the report.

3. DESCRIPTION OF SPENT FUEL POOL AND SHIPPING CASKS

3.1 Spent Fuel Pool

The spent fuel pool is a Category I structure, its primary functions are to load, unload, transfer and store used fuel assemblies. A schematic plan of the North Anna Power Station Units 1 and 2, spent fuel pool is shown in Figure 3.2-1, Figures 3.2-2 and 3.2-3 shows the elevation of the cask loading area of the spent fuel pool.

The spent fuel pool is a 72'-6" long, 29'-3" wide and 42'-6" deep reinforced concrete well resting on rock foundation. The floor and walls of the pool are 6 feet thick concrete structure reinforced with #11 bars at 12 inches, each way, each face. The pool is lined with 1/4-inch thick stainless steel liner plate. The spent fuel shipping cask loading area (21'-4" x 12'-0") is located on the west end of the pool. As indicated in Figures 3.2-1 and 9B.3.2-2, the cask loading area consists of a 9'-4" x 12'-0" set-down area ledge with its top at elevation 269'-0" and a 12'-0" x 12'-0" area with its floor at elevation 246'-10". The floor of the cask loading area is 2'-6" lower than the pool floor (elevation 249'-4"). Drawings of Reference 1 shows the mechanical and structural details of the spent fuel pool.

The shipping cask is brought in by the overhead crane and first placed on the set-down area ledge. The yoke is then replaced with a longer yoke, and the cask is picked up and lowered by the overhead crane and set on the cask loading area floor. This procedure is essentially reversed for the removal of the shipping cask from the spent fuel pool.

3.2 Multi-Element Spent Fuel Shipping Cask 10/24

As shown in Figure 3.2-4 the Multi-Element Spent Fuel Shipping Cask 10/24 of National Lead Company is 82 inches in diameter by 204 inches long. It is fabricated from stainless steel lined with a 6 inch layer of lead. For the purpose of the cask drop analysis, it is assumed that the shipping cask weighs 221 kips when loaded with spent fuel and including the weights of the yoke, upper/lower crane hoist block, hook and rope. The effective diameter of the cask impact area is taken as 70.89 inches. Drawings of Reference 2 gives various details of the 10/24 cask.

3.3 Single-Element Spent Fuel Shipping Cask 1/2

As shown in Figure 3.2-5, the Single-Element Spent Fuel Shipping Cask 1/2 of National Lead Company is 36.5 inches in diameter and 193 inches long. It is fabricated from stainless steel and is lined with 2-1/8 inch layer of lead. For the purpose of the cask drop analysis, it is assumed that the shipping cask weighs 58 kips when loaded with spent fuel including the weight of the yoke, upper and lower crane hoist block, hook and rope. The effective diameter of the cask impact area for vertical drop is taken as 33.5 inches. Drawings of Reference 2 gives the various details of 1/2 cask.

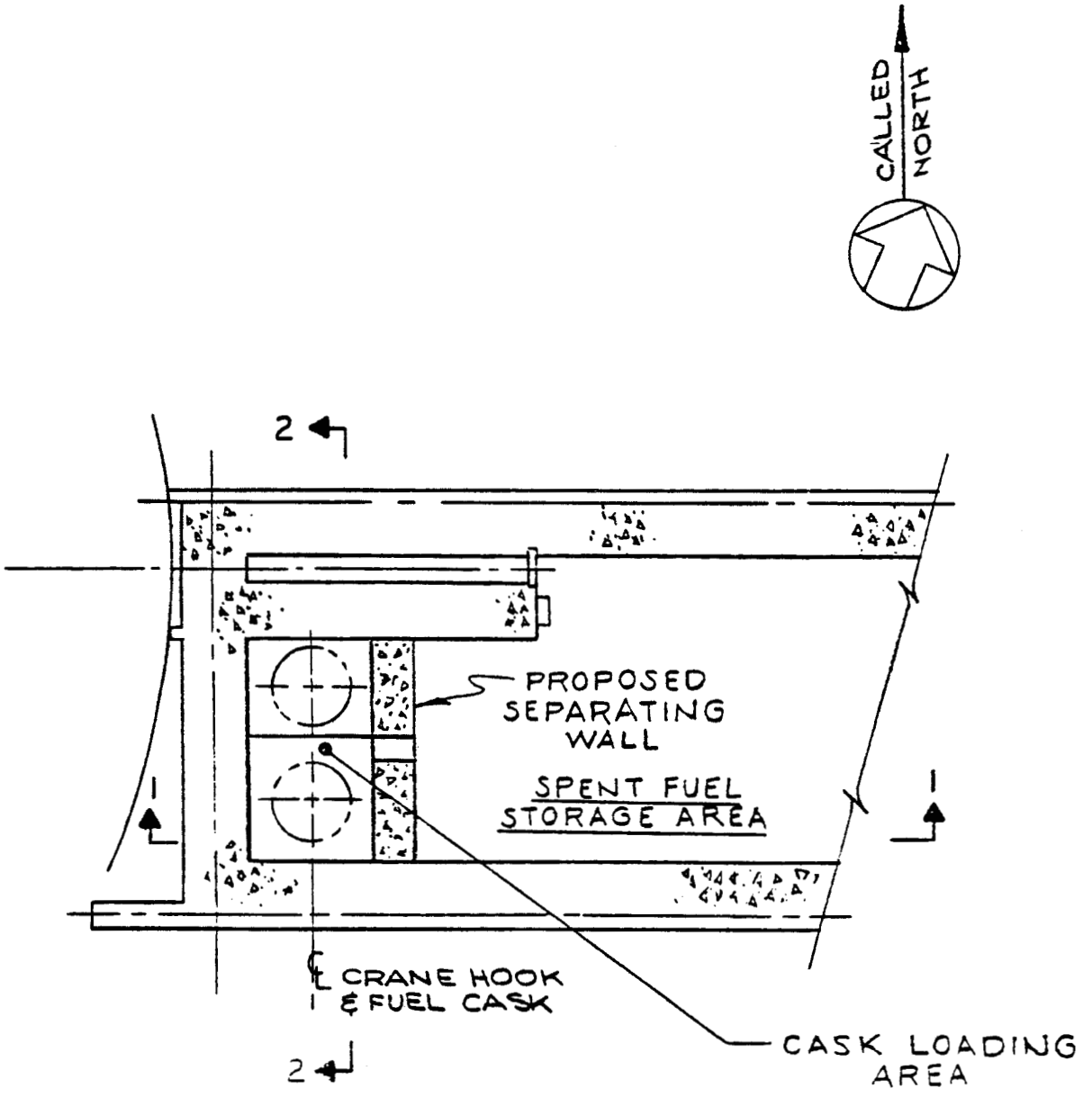

PLAN EL 272'-0"

FIGURE 3.2-1

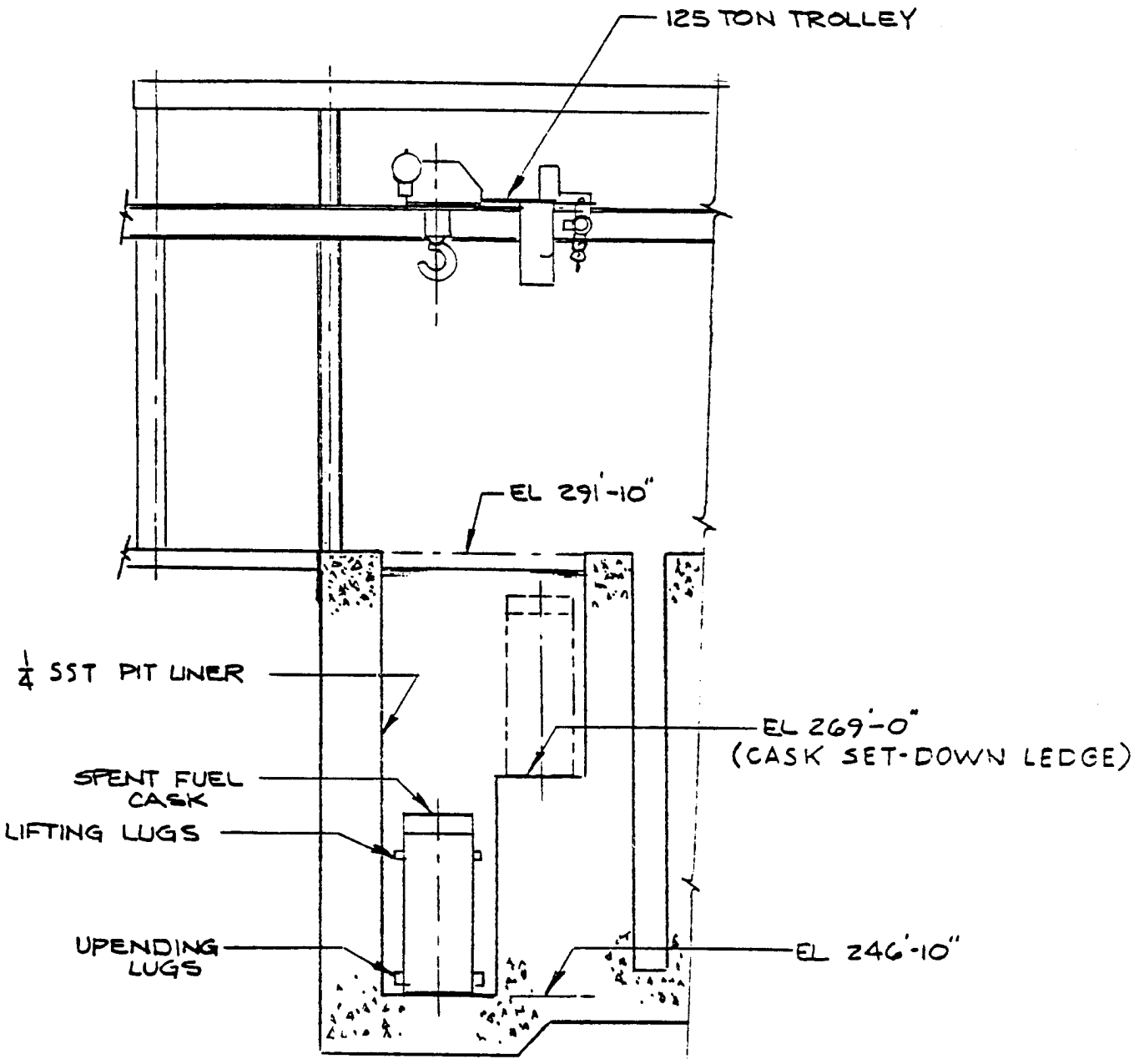

CASK LOADING AREA

ELEV 2-2

FIGURE 3.2-2

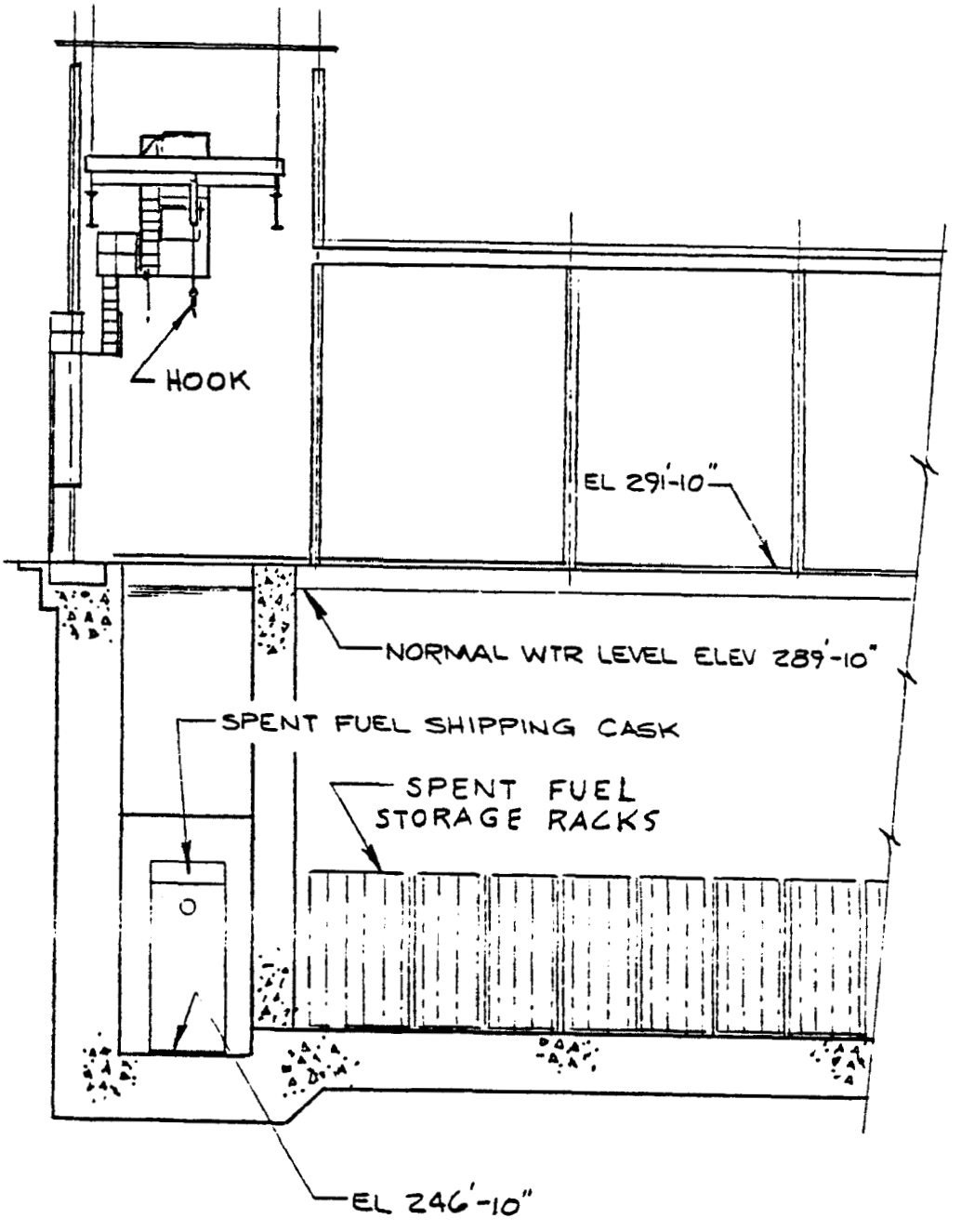

ELEV 1-1

FIGURE 3.2-3

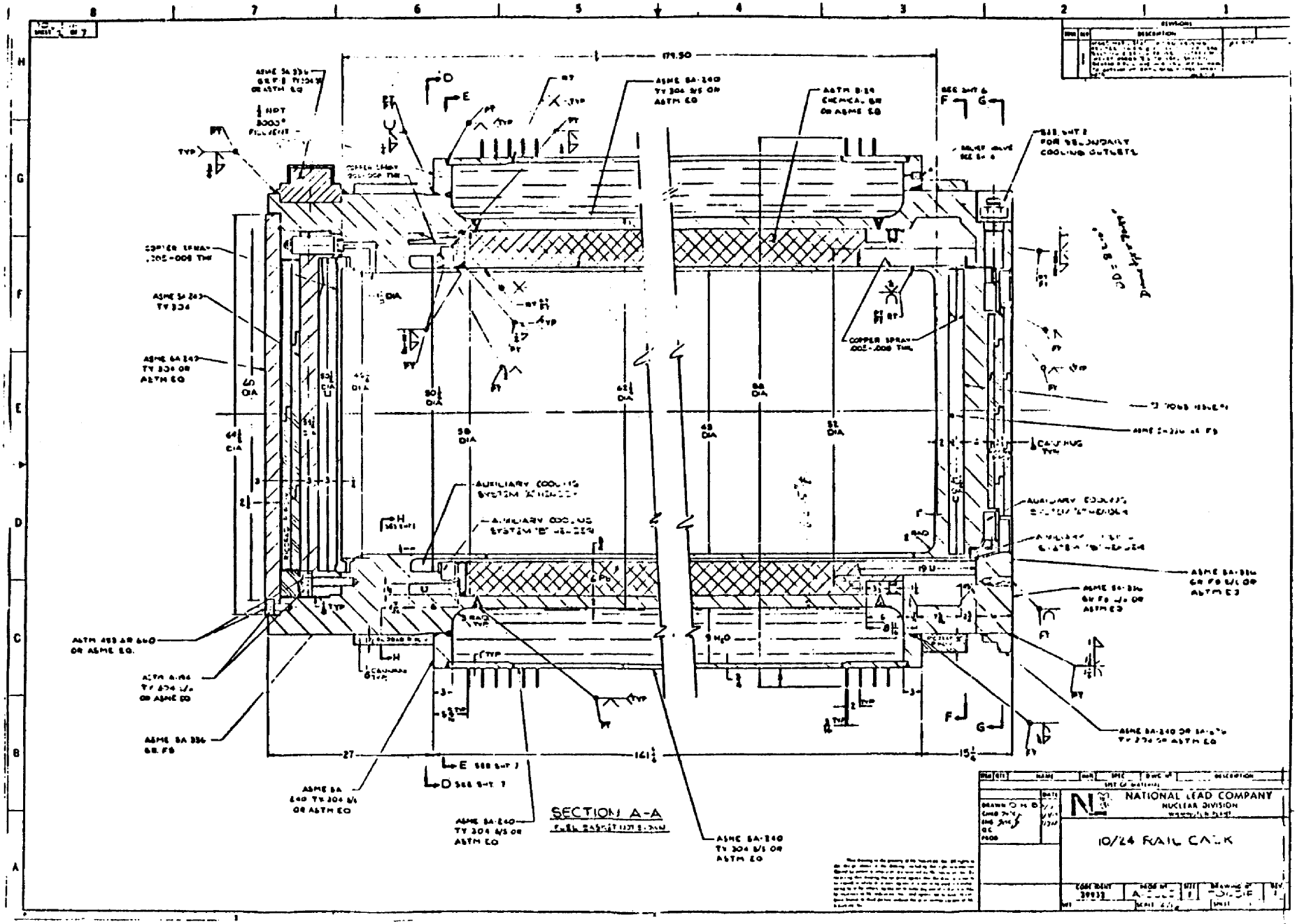
SECTION A-A
NATIONAL LEAD COMPANY
NUCLEAR DIVISION
10/24 RAIL CASK

FIGURE 3.2-4

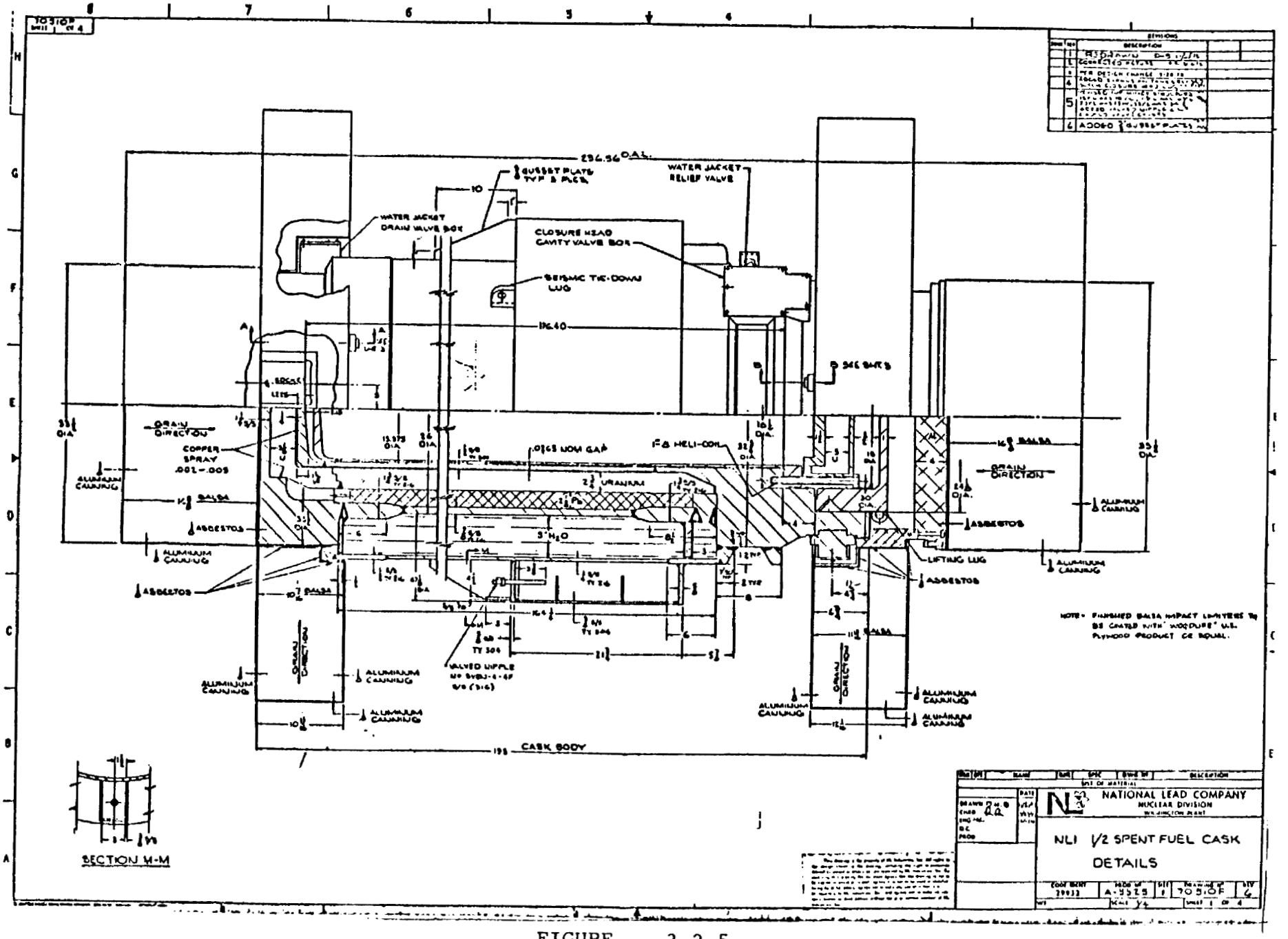
296.56 O.A.L.
GUSSET PLATE TYP 8 PLCS
WATER JACKET RELIEF VALVE
WATER JACKET DRAIN VALVE BOX
CLOSURE HEAD CAVITY VALVE BOX
SEISMIC TIE-DOWN LUG
196.40
SEE BASE
GRAIN DIRECTION
COPPER SPRAY .001-.005
0 GAS NOM GAP
F.S. HELI-COIL
URANIUM
3" H2O
BALSA
ASBESTOS
ALUMINUM CANNING
LIFTING LUG
VALVED NIPPLE
CASK BODY
SECTION M-M
NOTE: FINISHED BALSA IMPACT LIMITERS TO BE CLAD WITH "WOODFLEX" U.S. PLYWOOD PRODUCT OR EQUAL.
NATIONAL LEAD COMPANY
NUCLEAR DIVISION
NLI 1/2 SPENT FUEL CASK
DETAILS

FIGURE 3.2-5

4. APPLICABLE CODES, STANDARDS AND SPECIFICATIONS

The following codes of practice, regulatory guides and references have been used in the subject cask drop analysis.

1. ACI 318-71 - "Building Code Requirements for Reinforced Concrete" American Concrete Institute.

2. AISC "Specifications for the Design, Fabrication and Erection of Structural Steel for Building" Feb. 12, 1969.

3. USNRC Regulatory Standard Review Plan, Section 3.8.3 and Section 3.8.4; Directorate of Licensing U.S. Atomic Energy Commission.

4. BC-TOP-9A (Revision 2) - "Design of Structures for Missile Impact", Bechtel Power Corporation, San Francisco, California September, 1974.

5. TM 5-1300 "Structures to Resist the Effects of Accidental Explosions (with Addenda)", Department of the Army, Washington, DC, June 1969.

6. Ammann and Whitney - "Primary Fragment Characteristics and Impact Effects in Protective Design," Ammann and Whitney, Consulting Engineers, New York, NY.

7. Structural Analysis and Design of Nuclear Plant Facilities; American Society of Civil Engineers, 1976.

8. ORNL-NSIC-22 - "Missile Generation and Protection in Light-Water-Cooled Power Reactor Plants".

9. George Winter, et al - "Design of Concrete Structures", McGraw Hill Book Company, 1964.

10. R.H. Wood - "Plastic and Elastic Design of Slabs and Plates", The Ronald Press Company, 1961.

5. LOADS AND LOADING COMBINATIONS

Three postulated cask drop accident scenarios as described in Section 2 have been considered in the cask drop analysis.

5.1 Cask Drop Accident Scenario 1

The spent fuel cask arrives at the station by truck or rail car and is positioned under the spent fuel trolley hook. The cask is raised over the decontamination building and into the fuel storage building. As the cask is moved over the edge of the spent fuel pool, the cask drops. The following four accident cases have been considered for this postulated cask drop scenario.

Cask Drop Accident Case 1 (a):

The 10/24 cask drops on its edge from a height of 1.0 feet above floor elevation 291'-10" on top of the spent fuel pool wall as shown in Figure 3.2-6(a).

Cask Drop Accident Case 1 (b):

The 10/24 cask drops upright from a height of 1.0 feet above floor elevation 291'-10" on the rail located at the top of the spent fuel pool wall as shown in Figure 3.2-6(b).

Cask Drop Accident Case 1 (c):

The 1/2 cask drops on its edge from a height of 1.0 feet above floor elevation 291'-10" on top of the spent fuel pool wall as shown in Figure 3.2-6(c).

Cask Drop Accident Case 1 (d):

The 1/2 cask drops upright from a height of 1.0 feet above floor elevation 291'-10" on the rail located at the top of the spent fuel pool wall as shown in Figure 3.2-6(d).

5.2 Cask Drop Accident Scenario 2

While the cask is placed on the ledge in the cask loading area and the yoke is being replaced with a longer yoke, the cask tips over and falls off the set-down area ledge and either hits the south wall of the spent fuel pool or falls toward the fuel storage racks and hits the proposed separating wall. Four accident cases as described below have been considered for this postulated cask drop scenario.

Cask Drop Accident Case 2 (a):

The 10/24 cask tips over and falls off the set-down area ledge from a position as shown in Figure 3.2-7(a) and hits the south wall of the pool.

Cask Drop Accident Case 2 (b):

The 10/24 cask tips over and falls off the set-down area ledge from a position as shown in Figure 3.2-7(b) and hits the south wall of the pool.

Cask Drop Accident Case 2 (c):

The 1/2 cask tips over and falls off the set-down area ledge from a position shown in Figure 3.2-7(c) and hits the south wall of the pool.

Cask Drop Accident Case 2 (d):

The 1/2 cask tips over and falls off the set-down area ledge from a position indicated in Figure 3.2-7(d) and hits the south wall of the pool.

Because the clearance between either shipping cask and the proposed separating wall is small, the velocity and kinetic energy of impact of the cask as it tips over and hits the separating wall would be much smaller than those resulting from the above load cases. Therefore no analyses have been performed for the separating wall in the subject study.

5.3 Cask Drop Accident Scenario 3

After the cask is loaded with spent fuel and is raised to its highest elevation over the cask loading area, the cask drops and strikes the pool floor in the cask loading area. The following four accident cases have been considered for this postulated cask drop scenario.

Cask Drop Accident Case 3 (a):

The 10/24 cask drops upright from a height of 1.0 feet above floor elevation 291'-10" and strikes the pool floor in the upright position with its axis vertical as shown in Figure 3.2-8(a).

Cask Drop Accident Case 3 (b):

The 10/24 cask drops from a height of 1.0 feet above floor elevation 291'-10" and strikes the pool floor at an angle which would cause the maximum structural damage to the pool floor as shown in Figure 3.2-8(b).

Cask Drop Accident Case 3 (c):

The 1/2 cask drops upright from a height of 1.0 feet above floor elevation 291'-10" and strikes the pool floor in the upright position with its axis vertical as shown in Figure 3.2-8(c).

Cask Drop Accident Case 3 (d):

The 1/2 cask drops from a height of 1.0 feet above floor elevation 291'-10" and strikes the pool floor at an angle which would cause maximum structural damage to the pool floor as shown in Figure 3.2-8(d).

The dead, live and seismic loadings are considerable smaller than the cask drop reaction loads. Specifically, the effects of the dead and seismic loadings are quite small on the localized area of the reinforced concrete floor and walls where the cask drop accident would cause minor damage. Therefore, the effects of dead and seismic loadings have not been included in the subject analysis.

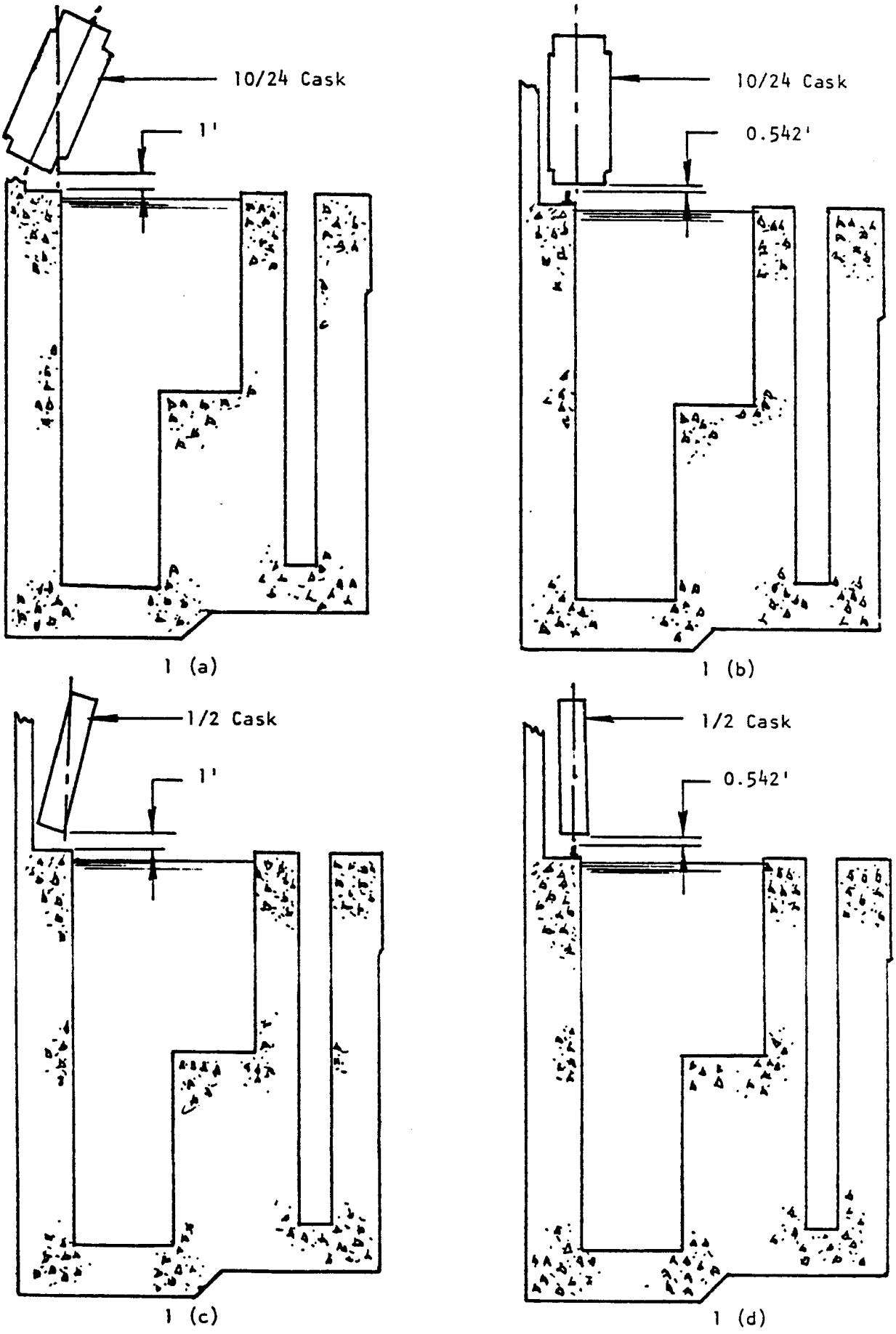

FIGURE 3.2-6 - CASK DROP ACCIDENT SCENARIO 1 ELEV. 2-2

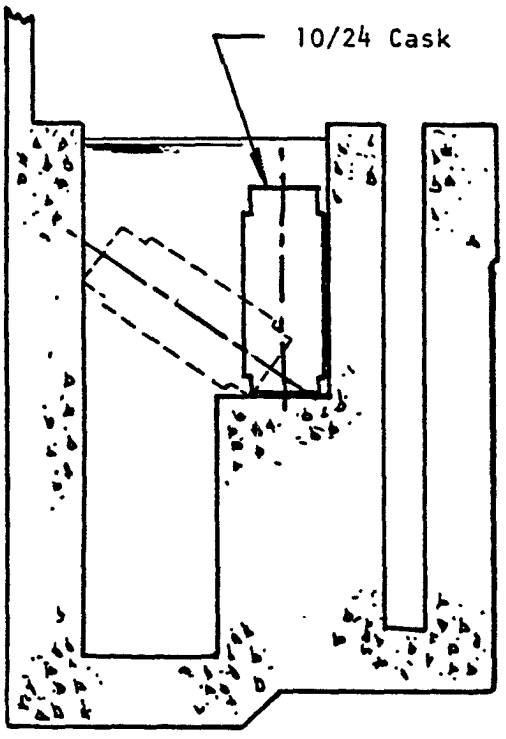

2 (a)

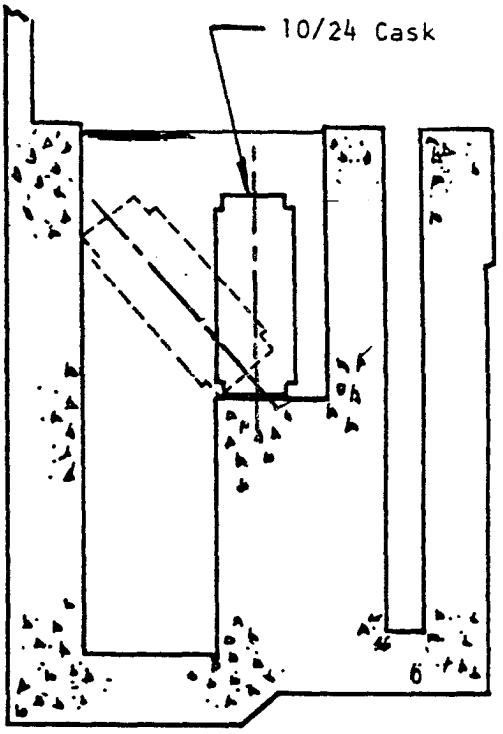

2 (b)

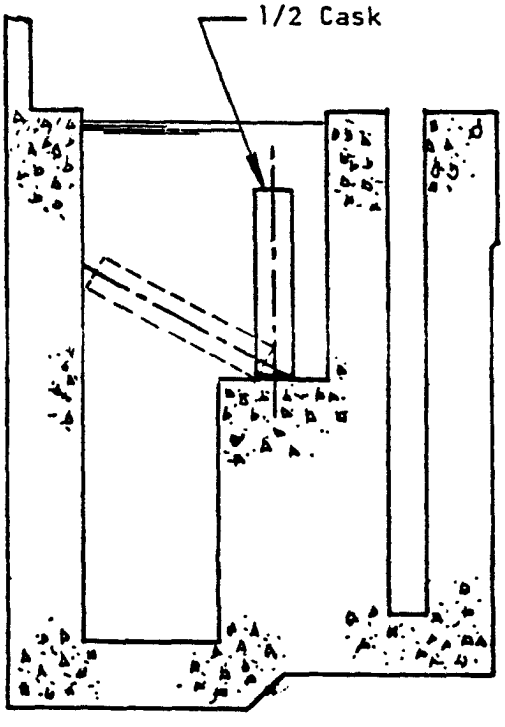

2 (c)

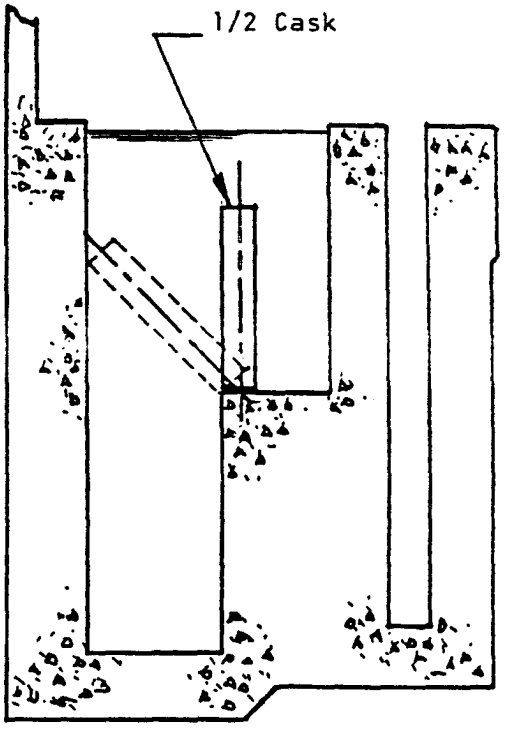

2 (d)

FIGURE 3.2-7 - CASK DROP ACCIDENT SCENARIO 2 ELEV. 2-2

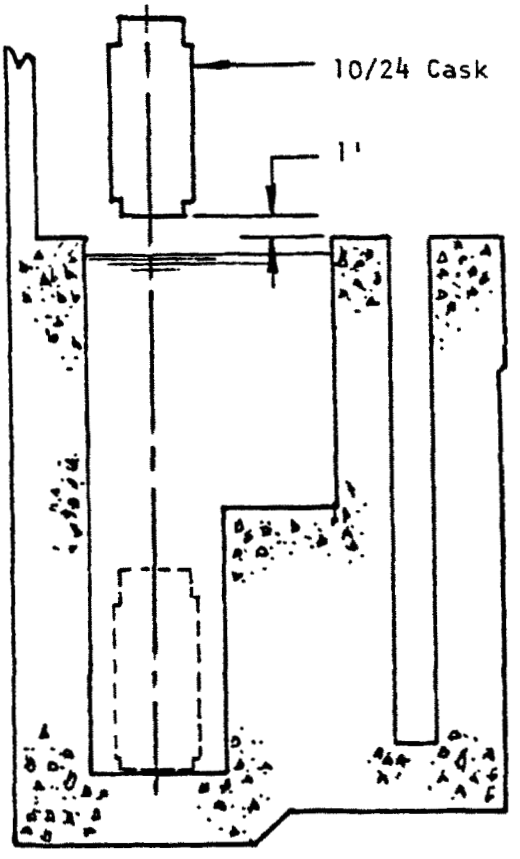

3 (a)

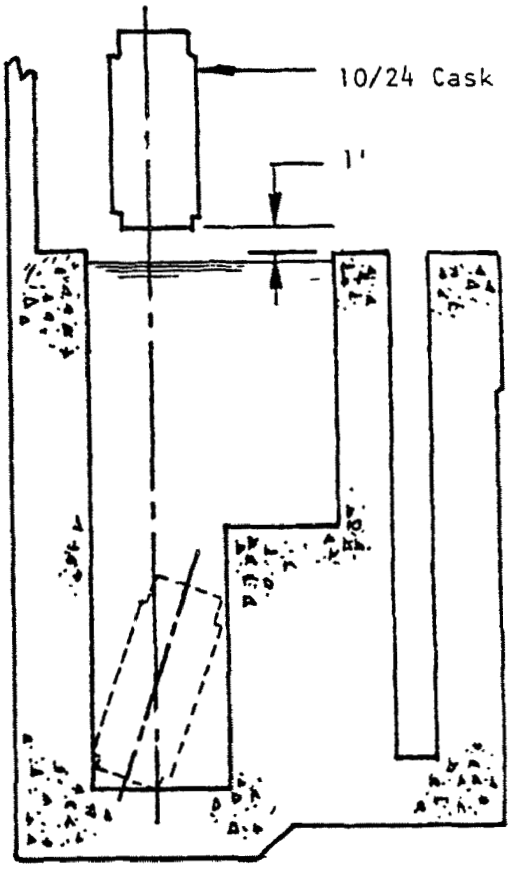

3 (b)

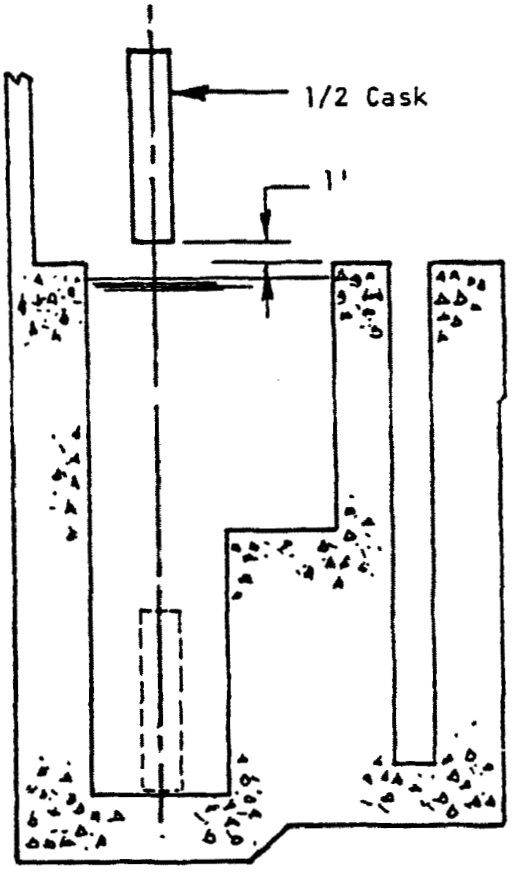

3 (c)

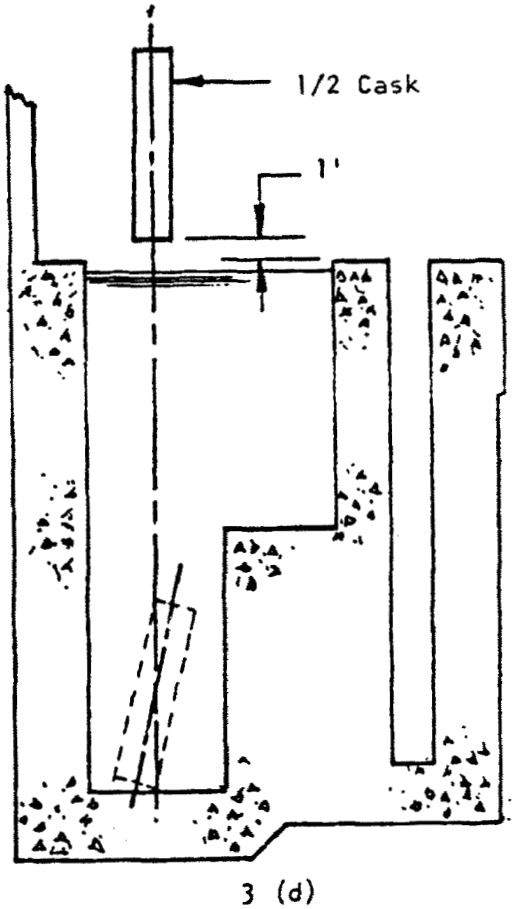

3 (d)

FIGURE 3.2-8 - CASK DROP ACCIDENT SCENARIO 3 ELEV. 2-2

6. ANALYTICAL PROCEDURES

6.1 Velocity and Kinetic Energy of Impact:

For cask drop accident cases 1(a) through 1(d) and 2(a) through 2(d), the maximum velocity and kinetic energy at the instant of impact have been calculated by equating the change in potential energy to the maximum kinetic energy at the instant of impact. For load cases 2(a) through 2(d) the effects of resistance offered by the hydrodynamic forces (drag forces) have been conservatively neglected. For cask drop accident cases 3(a) through 3(d), the maximum velocity and kinetic energy of impact have been calculated considering the effects of the bouyancy and drag forces using the procedure given in detail in Reference 3 and as summarized below.

Assuming that the cask drops vertically and conservatively neglecting the loss of velocity during compression phase of liquid entry and assuming constant drag co-effecient, the equation of motion of the cask is given by:

$$\frac{W}{g}\ddot{x} = W - F_b - F_d \qquad (1)$$

where:

W = weight of missile (lbs.)

g = gravitational acceleration (ft/sec^2)

x = depth of missile c.g. below the initial c.g. (ft)

t = time after initial contact of missile with liquid (sec)

F_b = bouyant force = $W\gamma/\gamma_m$, (lb)

F_d = drag force = $\gamma A_m C_D v^2/2g$ (lb)

γ = weight density of liquid (lb/ft^3)

γ_m = weight density of cask = $\frac{W}{A_o L}$ (lb/ft^3)

A_o = horizontal cross-sectional area (ft^2)

L = vertical length of the missile (ft)

C_D = drag coefficient

A_m = maximum horizontal cross-sectional area of missile (ft^2)

$v = \dot{x}$ = velocity of missile at depth x (ft/sec)

Substituting and rearranging equation (1)

$$\ddot{x} + a\dot{x}^2 + g\gamma/\gamma_m - g = 0 \qquad (2)$$

where:

$$a = \gamma A_m C_D / 2W$$

Solving equation (2) and using initial conditions yields

$$v = \left[V_2^2 + e^{-2ax} \left[bA_0 \left(e^{2aL} (1 - 2aL) - 1 \right) / 2a^2 + V_0^2 + g \left(e^{2aL} \gamma/\gamma_m - 1 \right) / a \right] \right]^{1/2} \qquad (3)$$

where:

V_0 = initial velocity of the missile at x = 0

V = striking velocity of the missile at x = H

V_2 = terminal velocity = $\left[g(1 - \gamma/\gamma_m)/a \right]^{1/2}$

Maximum kinetic energy of impact E is given by:

$$E = \frac{1}{2} \frac{W}{g} V^2 \qquad (4)$$

6.2 Local Damage:

The local damage to the impacted area (target) are largely independent of the dynamic characteristics of the structure. Local effects consist-of: (1) missile penetration into the target, (2) missile perforation through the target, and (3) spalling of the target. The following defines the local effects terminology and the various symbols used in their evaluation.

Terminology:

Penetration: Penetration is the displacement of the missile into the target. It is a measure of the depth of the crater formed at the zone of impact.

Perforation: Perforation is "full penetration" or where the missile passes through the target with or without exit velocity (of missile).

Spalling: Spalling is the peeling of the back face of the target opposite to the face of impact. Spalling is defined as scabbing in Reference 5.

Symbols:

W = weight of missile (lb.)

V_o, V_s = striking velocity of missile (ft/sec.)

d, D = diameter of missile (in.)

A_p = $\frac{\text{Missile Weight}}{\text{Projected frontal area of missile}}$ (psf)

X = Depth of penetration into slab of infinite thick concrete (in.)

t = thickness of the slab (in.)

f'_c = compressive strength of concrete (psi)

K_p = experimentally obtained material coefficient for penetration (see Reference 3).

N = Nose Factor = $0.72 + 0.25\ (n - 0.25)^{1/2}$

n = $\frac{\text{radius of nose section}}{\text{diameter of missile}}$

k = concrete penetrability factor $K = \frac{180}{\sqrt{f'_c}}$

N' = projectile shape factor

T, e = perforation thickness (in.). The maximum thickness of a target which a missile with a given impact velocity will completely penetrate.

Ts, s = spalling thickness (in.). The thickness of target to be just spalled.

Local damage depends on missile characteristics, target material properties and structural response. Because of the complex phenomena associated with missile impact, empirical methods as given in Reference 3, 4 and 5, have been used in estimating the local damage. These equations are summarized in Section 6.2.1, 6.2.2 and 6.2.3.

6.2.1 Depth of Penetration

The depth to which a rigid missile will penetrate a reinforced concrete target of infinite thickness can be estimated by the following formulas:

Modified Petry: (References 3, 5, 9)

$$X = 12K_p A_p \log_{10}\left(1 + \frac{V_s^2}{215{,}000}\right) \qquad (5)$$

Army Corps of Engineers and National Defense Research Committee:

(References 3, 5, 9)

$$X = \frac{282}{\sqrt{f'_c}} \frac{W D^{0.215}}{D^2} \left(\frac{V_s}{1000}\right)^{1.5} + 0.5D \qquad (6)$$

Ammann and Whitney 1: (References 3, 5, 7)

$$X = \frac{282}{\sqrt{f'_c}} \frac{N W D^{0.2}}{D^2} \left(\frac{V_s}{1000}\right)^{1.8} \qquad (7)$$

Ammann and Whitney 11: (Reference 4)

$$X = \left[\frac{826}{\sqrt{f'_c}} \frac{N W D^{0.2}}{D} \left(\frac{V_s}{1000}\right)^{1.8}\right]^{0.5} \qquad (8)$$

Modified National Defense Research Committee: (Reference 5)

$$X = \sqrt{4KN'Wd \left(\frac{v_o}{1000d}\right)^{1.80}} \quad \text{for } \frac{x}{d} \leq 2.0 \qquad (9)$$

Refer to the references indicated above regarding various assumptions, restrictions etc. in the use of these formulas.

6.2.2 Concrete Thickness to Be Just Perforated

The thickness of a concrete element that will be just perforated by a missile can be estimated by the following empirical formulas.

Modified Petry: (References 3, 5, 9)

$$T = 2X \qquad (10)$$

X is obtained from Equation 5

Ballistic Research Laboratories: (Modified) References 3, 5, 9)

$$T = 7.8 \frac{W}{D^{1.8}} \left(\frac{V_s}{1000}\right)^{1.33} \quad (11)$$

Army Corps of Engineers: (References 3, 9)

$$T = 1.35D + 1.24X \quad (12)$$

X is obtained from Equation (6)

National Defense Research Committee: (References 3, 13)

$$T = 1.23D + 1.07X \quad (13)$$

X is obtained from Equation 6

Ammann and Whitney 11: (Reference 4)

$$T = 1.13 \times D^{0.1} + 1.31 D \quad (14)$$

Modified National Defense Research Committee: (Reference 5)

$$\frac{e}{d} = 3.19 \left(\frac{x}{d}\right) - 0.178 \left(\frac{x}{d}\right)^2 \text{ for } \frac{x}{d} \leq 1.35 \quad (15)$$

6.2.3 Concrete Thickness to be Just Spalled:

The thickness of a concrete element that will just start spalling (spalling of concrete from the side opposite the contact surface) can be estimated by the following empirical formulas:

Modified Ballistic Research Laboratory: (References 3, 5, 9)

$$T_s = 2T \quad (16)$$

Army Corps of Engineers (References 3, 9)

$$T_s = 2.2D + 1.35X \quad (17)$$

X is obtained from Equation 6

National Defense Research Committee (References 3, 13)

$$T_s = 2.28D + 1.13X \quad (18)$$

X is obtained from Equation 6

Ammann and Whitney 11: (Reference 4)

$$T_s = 1.22 \times D^{0.1} + 2.12D \quad (19)$$

Modified National Defense Research Committee: (Reference 5)

$$\frac{s}{d} = 7.91 \frac{x}{d} - 5.06\left(\frac{x}{d}\right)^2 \quad \text{for } \frac{x}{d} \leq 0.65 \quad (20)$$

6.3 Overall Structural Effects

The overall structural effects resulting from cask drop accident events have been evaluated by assuming a hard missile impacting on a soft target. Due to significant local deformations of the concrete structure during a cask drop event, this assumption is valid. The forcing function applied to the structure by the missile has been calculated, based on application of the equation of motion during deceleration of the missile.

It is assumed that the velocity varies linearly to zero as a function of time as the missile penetrates the structure. The characteristic of the rectangular impulse loading applied to the structure can be calculated by equating the work done by the missile as it penetrates the structure to the initial kinetic energy of the missile. Thus:

$$F_1 X = \frac{1}{2} \frac{W v_o^2}{g}$$

or

$$F_1 = \frac{W v_o^2}{2gX}$$

$$t_d = \frac{2X}{v_o}$$

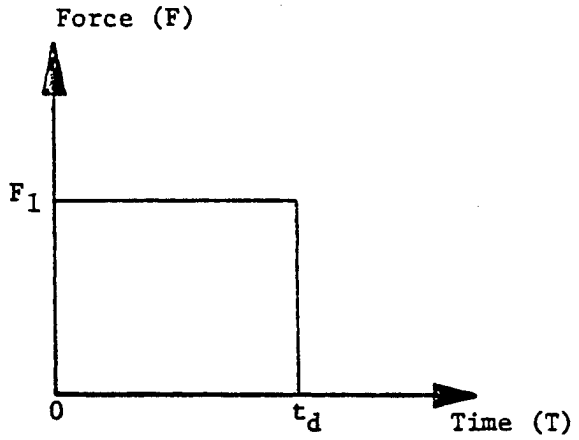

where:

F_1 = force of impact

g = acceleration of gravity

W = weight of missile

v_o = initial velocity of missile

X = penetration

t_d = duration of pulse

The maximum response of the structure subjected to the rectangular pulse load can be obtained using linear and non-linear methods of dynamic analysis. Parametric curves for simplified linear and non-linear dynamic analysis are given in Reference 5. Based upon the recommendations given in Reference 5, penetration depth X as calculated by the Modified National Defense Research Committee formula has been used in the calculations of overall structure effects.

The maximum bearing, shearing and compressive stresses in the concrete members are then calculated using ultimate strength design methods of the ACI 318-71

Code (Reference 8). The limit load (collapse load) carrying capacity of the spent fuel pool floor and walls are calculated using the "yield line method" of analysis described in Reference 3, 5, 10 and 12.

7. STRUCTURAL ACCEPTANCE CRITERIA

The acceptable maximum stresses in the reinforced concrete floor and walls of the spent fuel pool are established based on the guidelines given in USNRC Standard Review Plan, Sections 3.8.3 and 3.8.4 and various design codes and standards (References 5, 6, 8 and 11). Loadings associated with cask drop events are classified as extreme environmental loads. Acceptance criteria applicable to the factored load conditions are used in evaluation of structural effects. These structural acceptance criteria are summarized below.

A. Degree of Damage - None

Compressive Stress = $1.25 \times 0.85\Phi f'_c$ = 2709 psi

Shearing Stress = $4\Phi \sqrt{f'_c}$ = 186 psi

Bearing Stress = $1.25 \times 0.85\Phi' f'_c$ = 2331 psi

Yield Stress for reinforcing steel = 1.2×40000.0 = 48000.0 psi

Where f'_c = Compressive Strength of concrete at 28 days = 3000 psi

Φ = Strength reduction coefficient = 0.85

Φ' = Strength reduction coefficient = 0.70

Factors 1.25 and 1.2 are to account for increase in stress values for short term impact loadings (Reference 5)

B. Degree of Damage - Minor, Hairline Cracks; Structural Integrity maintained.

Compressive Stress = $1.25 \times 3.3 \times 0.45 \times f'_c$ = 5569 psi (Ref. 11)

Shearing Stress = $2.5 \times 2\sqrt{f'_c}$ = 274 psi (Ref. 11)

Bearing Stress = $1.25 \times 2.5 \times 0.375\ f'_c$ = 3516 psi (Ref. 11)

C. Degree of Damage - Moderate-can see through cracks, structural integrity of section maintained, loss of liquids at a moderate rate.

Compressive Stress = $1.25 \times 10 \times 0.45\ f'_c = 16875$ psi (Ref. 11)

Shearing Stress = $7.5 \times 2\sqrt{f'_c} = 822$ psi (Ref. 11)

Bearing Stress = $1.25 \times 7.5 \times 0.375\ f'_c = 10547$ psi (Ref. 11)

8. SUMMARY OF RESULTS

The detailed calculations for the cask drop analysis are given in Appendix A. The results of the analysis are summarized in Table 3.2-1 through 3.2-3.

8.1 Cask Drop Accident Scenario 1

From Table 3.2-1, it can be seen that for cask drop accident cases 1(a), 1(b), 1(c) and 1(d), the depth of penetration, concrete thickness to be just perforated and spalled are nominal. The maximum impact load, ductility ratio, maximum bearing and compressive stresses for the reinforced concrete walls of the spent fuel pool are lower than the allowable stress values permitted by the ACI code for ultimate strength design methods. Therefore, it has been concluded for cask drop accident scenario 1 that there will be local penetration and cracking; however, the structural integrity of the spent fuel pool and its leak-tightness will be maintained.

8.2 Cask Drop Accident Scenario 2

From Table 3.2-2 it can be seen that for 10/24 cask drop accident cases 2(a) and 2(b), maximum average depth of penetration is of the order of 7.99 inches and concrete thicknesses to be just perforated are lower than the thickness of the spent fuel pool wall. From Table 3.2-2, it can be seen that the average concrete thickness to be just spalled is slightly greater than the allowable value for cask drop accident case 2(a) due to very conservative estimate of concrete thickness to be just spalled given by Ballistic Research Laboratory formula. For cask drop accident case 2(b)

the concrete thickness to be just spalled is lower than the allowable value. For both the cask drop accident cases 2(a) and 2(b), the maximum impact load, ductility ratio, and maximum punching shear stresses are lower than the allowable values. The maximum bearing and compressive stresses are greater than the allowable stress values for no damage and lower than the allowable values for minor damage. Therefore, it has been concluded for cask drop accident cases 2(a) and 2(b) that there will be local penetration and minor cracking of the south wall of the spent fuel pool; however the overall structural integrity of the spent fuel pool will be maintained. Due to the limited depth of these hair-line cracks as compared with the thickness of the wall, there should not be any significant loss of water.

For cask drop accident cases 2(c) and 2(d), Table 3.2-2 shows that the depth of penetration is nominal, the concrete thickness to be just perforated and spalled are lower than the thickness of the spent fuel pool wall. From Table 3.2-2 it can be seen that the maximum impact load, ductility ratio and maximum punching shear stresses are lower than the allowable values. The maximum compressive and bearing stresses for accident Case 2(c) and the maximum compressive stress for accident case 2(d) are greater than the allowable stress values for no damage and lower than the allowable values for minor damage. The maximum bearing stress for accident case 2(d) is slightly greater than the stress value for minor damage and substantially lower than the stress value for moderate damage. Since it is unlikely that the 1/2 cask will ever be placed at the edge of the ledge, the probability of accident case 2(d) occurring is very small. Therefore, it has been concluded that due to the

tipping of 1/2 cask towards to south wall, there will be local penetrations and minor cracking of the south wall of the spent fuel pool; however, its overall structural integrity will be maintained. Due to the limited depth of these hair-line cracks as compared with the thickness of the wall, there should not be any significant loss of water.

8.3 Cask Drop Accident Scenario 3

From Table 3.2-3 it can be seen that for 10/24 cask drop accident cases 3(a) and 3(b), the maximum average depth of penetration is of the order of 15.91 inches (about 22 percent of the total thickness of the concrete floor). Average concrete thickness to be perforated is slightly greater than the floor thickness for accident case 3(a) and slightly smaller than the floor thickness for accident case 3(b). The maximum impact load, ductility ratio and compressive stresses are about equal to the allowable values. The maximum bearing stress for load case 3(a) is greater than the stress value for no damage and less than the stress value for minor damage. The maximum punching shear stresses for accident cases 3(a) and 3(b) are greater than the allowable stress values for minor damage and smaller than the allowable stress values for moderate damage. The maximum foundation pressures is lower than the allowable value. Therefore, it has been concluded that the 10/24 cask drop event in the cask loading area will cause fair amount of local and overall damage to the spent fuel pool floor. However, due to the presence of the rock foundation, there will not be any gross structural failure. The loss rate of pool water through the cracked concrete pool floor resting on a rock foundation is difficult to estimate but the arrangement of the proposed separating wall will insure that the spent fuel will remain covered with water for the postulated accidents.

From Table 3.2-3 it can be seen that for 1/2 cask drop accident cases 3(c) and 3(d), the average depth of penetration are of the order of 9.27 and 7.02 inches respectively. Average concrete thicknesses to be perforated are smaller than the fuel pool floor thickness. The maximum impact load, ductility ratio, maximum bearing, compressive and punching stresses are significantly greater than the allowable values. The maximum foundation pressure is lower than the allowable value. Therefore, it has been concluded that 1/2 cask drop event in the cask loading area will cause a fair amount of local and overall damage to the spent fuel pool floor. However, due to the presence of rock foundation underneath the spent fuel pool floor, there will not be any catastrophic structural failure of the fuel pool floor.

TABLE 3.2-1 CASK DROP ACCIDENT SCENARIO 1 (a)

(10/24 Cask Drop on Wall)

	CALCULATED	ALLOWABLE
Maximum Velocity at Instant of Impact (ft/sec)	8.021	
Maximum Kinetic Energy at Instant of Impact (in-kip)	2652.0	
Striking Angle with Vertical (degree)	19.162	
Depth of Penetration		
Modified Petry (in)	1.362	
Army Corps of Engineers and National Defense Research Committee (in)	5.25	
Ammann and Whitney I (in)	3.08	
Ammann and Whitney II (in)	6.87	
Modified National Defense Research Committee (in)	6.86	
Average Depth of Penetration (in)	4.68	
Concrete Thickness to be Just Perforated		
Modified Petry (in)	2.72	
Ballistic Research Laboratories (in)	56.39	
Army Corps of Engineers (in)	29.34	
National Defense Research Committee (in)	26.42	
Ammann and Whitney II (in)	39.61	
Modified National Defense Research Committee (in)	37.68	
Average Concrete Thickness to be Just Perforated (in)	32.03	540.0
Concrete Thickness to be Just Spalled		
Modified Ballistic Research Laboratory (in)	90.22	
Army Corps of Engineers (in)	44.30	
National Defense Research Committee (in)	44.50	
Ammann and Whitney II (in)	58.40	
Modified National Defense Research Committee (in)	56.19	
Average Concrete Thickness to be Just Spalled (in)	58.72	540.0
Maximum Impact Load (K)	773.78	1030.96
Ductility Ratio	1.0	1.3
Maximum Bearing Stress in Concrete (ksi)	2.015	2.231
Maximum Compressive Stress in Concrete (ksi)	2.015	2.709

TABLE 3.2-1 CASK DROP ACCIDENT SCENARIO 1 (b)

(10/24 Cask Drop on Rail)

	CALCULATED	ALLOWABLE
Maximum Velocity at Instant of Impact (ft/sec)	5.905	
Maximum Kinetic Energy at Instant of Impact (in-kip)	1437.24	
Striking Angle with Vertical (degree)	0.0	
Depth of Penetration		
Modified Petry (in)	0.19	
Army Corps of Engineers and National Defense Research Committee (in)	14.16	
Ammann and Whitney I (in)	0.29	
Ammann and Whitney II (in)	4.57	
Modified National Defense Research Committee (in)	4.95	
Average Depth of Penetration (in)	4.83	
Concrete Thickness to be Just Perforated		
Modified Petry (in)	0.38	
Ballistic Research Laboratories (in)	5.70	
Army Corps of Engineers (in)	51.32	
National Defense Research Committee (in)	45.41	
Ammann and Whitney II (in)	39.89	
Modified National Defense Research Committee (in)	39.16	
Average Concrete Thickness to be Just Perforated (in)	30.39	540.0
Concrete Thickness to be Just Spalled		
Modified Ballistic Research Laboratory (in)	11.39	
Army Corps of Engineers (in)	74.14	
National Defense Research Committee (in)	73.02	
Ammann and Whitney II (in)	60.71	
Modified National Defense Research Committee (in)	59.76	
Average Concrete Thickness to be Just Spalled (in)	55.80	540.0
Maximum Impact Load (K)	580.4	1319.3
Ductility Ratio	1.0	1.3
Maximum Bearing Stress in Concrete (ksi)	1.182	2.231
Maximum Compressive Stress in Concrete (ksi)	1.182	2.709

TABLE 3.2-1 CASK DROP ACCIDENT SCENARIO 1 (c)

(1/2 Cask Drop on Wall)

	CALCULATED	ALLOWABLE
Maximum Velocity at Instant of Impact (ft/sec)	8.021	
Maximum Kinetic Energy at Instant of Impact (in-kip)	696.0	
Striking Angle with Vertical (degree)	9.847	
Depth of Penetration		
Modified Petry (in)	0.67	
Army Corps of Engineers and National Defense Research Committee (in)	2.20	
Ammann and Whitney I (in)	1.29	
Ammann and Whitney II (in)	3.58	
Modified National Defense Research Committee (in)	3.57	
Average Depth of Penetration (in)	2.26	
Concrete Thickness to be Just Perforated		
Modified Petry (in)	1.34	
Ballistic Research Laboratories (in)	18.89	
Army Corps of Engineers (in)	20.31	
National Defense Research Committee (in)	18.37	
Ammann and Whitney II (in)	33.32	
Modified National Defense Research Committee (in)	32.41	
Average Concrete Thickness to be Just Perforated (in)	20.77	540.0
Concrete Thickness to be Just Spalled		
Modified Ballistic Research Laboratory (in)	37.79	
Army Corps of Engineers (in)	31.62	
National Defense Research Committee (in)	32.18	
Ammann and Whitney II (in)	50.97	
Modified National Defense Research Committee (in)	49.79	
Average Concrete Thickness to be Just Spalled (in)	40.47	540.0
Maximum Impact Load (K)	389.82	947.33
Ductility Ratio	1.0	1.3
Maximum Bearing Stress in Concrete (ksi)	1.105	2.231
Maximum Compressive Stress in Concrete (ksi)	1.105	2.709

TABLE 3.2-1 CASK DROP ACCIDENT SCENARIO 1 (d)

(1/2 Cask Drop on Rail)

	CALCULATED	ALLOWABLE
Maximum Velocity at Instant of Impact (ft/sec)	5.905	
Maximum Kinetic Energy at Instant of Impact (in-kip)	377.20	
Striking Angle with Vertical (degree)	0.0	
Depth of Penetration		
Modified Petry (in)	0.09	
Army Corps of Engineers and National Defense Research Committee (in)	9.97	
Ammann and Whitney I (in)	0.13	
Ammann and Whitney II (in)	2.64	
Modified National Defense Research Committee (in)	2.87	
Average Depth of Penetration (in)	3.14	
Concrete Thickness to be Just Perforated		
Modified Petry (in)	0.18	
Ballistic Research Laboratories (in)	2.59	
Army Corps of Engineers (in)	37.25	
National Defense Research Committee (in)	33.34	
Ammann and Whitney II (in)	28.15	
Modified National Defense Research Committee (in)	27.89	
Average Concrete Thickness to be Just Perforated (in)	21.57	540.0
Concrete Thickness to be Just Spalled		
Modified Ballistic Research Laboratory (in)	5.18	
Army Corps of Engineers (in)	54.02	
National Defense Research Committee (in)	53.30	
Ammann and Whitney II (in)	43.40	
Modified National Defense Research Committee (in)	42.99	
Average Concrete Thickness to be Just Spalled (in)	39.78	540.0
Maximum Impact Load (K)	263.24	716.95
Ductility Ratio	1.0	1.3
Maximum Bearing Stress in Concrete (ksi)	0.986	2.231
Maximum Compressive Stress in Concrete (ksi)	0.986	2.709

TABLE 3.2-2 CASK DROP ACCIDENT SCENARIO 2 (a)

(10/24 Cask Drop off of Ledge)

	CALCULATED	ALLOWABLE
Maximum Velocity at Instant of Impact (ft/sec)	13.81	
Maximum Kinetic Energy at Instant of Impact (in-kip)	2621.28	
Striking Angle with Vertical (degree)	52.57	
Depth of Penetration		
Modified Petry (in)	2.73	
Army Corps of Engineers and National Defense Research Committee (in)	9.33	
Ammann and Whitney I (in)	5.81	
Ammann and Whitney II (in)	11.06	
Modified National Defense Research Committee (in)	11.04	
Average Depth of Penetration (in)	7.99	
Concrete Thickness to be Just Perforated		
Modified Petry (in)	5.47	
Ballistic Research Laboratories (in)	65.78	
Army Corps of Engineers (in)	37.68	
National Defense Research Committee (in)	33.78	
Ammann and Whitney II (in)	47.10	
Modified National Defense Research Committee (in)	31.38	
Average Concrete Thickness to be Just Perforated (in)	36.37	72.0
Concrete Thickness to be Just Spalled		
Modified Ballistic Research Laboratory (in)	131.56	
Army Corps of Engineers (in)	55.15	
National Defense Research Committee (in)	54.64	
Ammann and Whitney II (in)	67.01	
Modified National Defense Research Committee (in)	60.34	
Average Concrete Thickness to be Just Spalled (in)	73.74	72.0
Maximum Impact Load (K)	1424.8	4744.64
Ductility Ratio	1.0	1.15
Maximum Bearing Stress in Concrete (ksi)	3.470	3.516*
Maximum Compressive Stress in Concrete (ksi)	3.470	5.569*
Maximum Punching Shear Stress in Concrete (ksi)	0.099	0.186

*Indicate Allowable Values for Minor Damage

TABLE 3.2-2 CASK DROP ACCIDENT SCENARIO 2 (b)

(10/24 Cask Drop Off of Ledge)

	CALCULATED	ALLOWABLE
Maximum Velocity at Instant of Impact (ft/sec)	6.83	
Maximum Kinetic Energy at Instant of Impact (in-kip)	641.34	
Striking Angle with Vertical (degree)	42.568	
Depth of Penetration		
Modified Petry (in)	1.63	
Army Corps of Engineers and National Defense Research Committee (in)	6.52	
Ammann and Whitney I (in)	3.77	
Ammann and Whitney II (in)	7.10	
Modified National Defense Research Committee (in)	7.08	
Average Depth of Penetration (in)	5.22	
Concrete Thickness to be Just Perforated		
Modified Petry (in)	3.26	
Ballistic Research Laboratories (in)	59.49	
Army Corps of Engineers (in)	25.77	
National Defense Research Committee (in)	23.09	
Ammann and Whitney II (in)	29.11	
Modified National Defense Research Committee (in)	27.53	
Average Concrete Thickness to be Just Perforated (in)	28.04	72.0
Concrete Thickness to be Just Spalled		
Modified Ballistic Research Laboratory (in)	118.98	
Army Corps of Engineers (in)	37.62	
National Defense Research Committee (in)	37.24	
Ammann and Whitney II (in)	41.48	
Modified National Defense Research Committee (in)	39.75	
Average Concrete Thickness to be Just Spalled (in)	55.01	72.0
Maximum Impact Load (K)	542.76	4744.64
Ductility Ratio	1.0	1.15
Maximum Bearing Stress in Concrete (ksi)	3.417	3.516*
Maximum Compressive Stress in Concrete (ksi)	3.417	3.568*
Maximum Punching Shear Stress in Concrete (ksi)	0.038	0.186

* Indicate Allowable Values for Minor Damage

TABLE 3.2-3 CASK DROP ACCIDENT SCENARIO 2 (c)

(1/2 Cask Drop off of Ledge)

	CALCULATED	ALLOWABLE
Maximum Velocity at Instant of Impact (ft/sec)	24.51	
Maximum Kinetic Energy at Instant of Impact (in-kip)	2166.88	
Striking Angle with Vertical (degree)	62.70	
Depth of Penetration		
Modified Petry (in)	2.67	
Army Corps of Engineers and National Defense Research Committee (in)	7.06	
Ammann and Whitney I (in)	4.67	
Ammann and Whitney II (in)	9.45	
Modified National Defense Research Committee (in)	9.45	
Average Depth of Penetration (in)	6.66	
Concrete Thickness to be Just Perforated		
Modified Petry (in)	5.33	
Ballistic Research Laboratories (in)	40.40	
Army Corps of Engineers (in)	32.14	
National Defense Research Committee (in)	28.86	
Ammann and Whitney II (in)	44.98	
Modified National Defense Research Committee (in)	27.32	
Average Concrete Thickness to be Just Perforated (in)	29.84	72.0
Concrete Thickness to be Just Spalled		
Modified Ballistic Research Laboratory (in)	80.80	
Army Corps of Engineers (in)	47.64	
National Defense Research Committee (in)	47.47	
Ammann and Whitney II (in)	64.92	
Modified National Defense Research Committee (in)	55.15	
Average Concrete Thickness to be Just Spalled (in)	59.20	72.0
Maximum Impact Load (K)	1378.40	4744.64
Ductility Ratio	1.0	1.15
Maximum Bearing Stress in Concrete (ksi)	2.921	3.516*
Maximum Compressive Stress in Concrete (ksi)	2.921	3.569*
Maximum Punching Shear Stress in Concrete (ksi)	0.089	0.186

* Indicate Allowable Values for Minor Damage

TABLE 3.2-2 CASK DROP ACCIDENT SCENARIO 2 (d)

(1/2 Cask Drop Off of Ledge)

	CALCULATED	ALLOWABLE
Maximum Velocity at Instant of Impact (ft/sec)	16.57	
Maximum Kinetic Energy at Instant of Impact (in-kip)	989.60	
Striking Angle with Vertical (degree)	45.647	
Depth of Penetration		
Modified Petry (in)	2.24	
Army Corps of Engineers and National Defense Research Committee (in)	6.51	
Ammann and Whitney I (in)	4.14	
Ammann and Whitney II (in)	7.79	
Modified National Defense Research Committee (in)	7.77	
Average Depth of Penetration (in)	5.69	
Concrete Thickness to be Just Perforated		
Modified Petry (in)	4.47	
Ballistic Research Laboratories (in)	43.09	
Army Corps of Engineers (in)	25.67	
National Defense Research Committee (in)	22.99	
Ammann and Whitney II (in)	31.99	
Modified National Defense Research Committee (in)	30.15	
Average Concrete Thickness to be Just Perforated (in)	26.39	72.0
Concrete Thickness to be Just Spalled		
Modified Ballistic Research Laboratory (in)	86.18	
Army Corps of Engineers (in)	37.46	
National Defense Research Committee (in)	37.07	
Ammann and Whitney II (in)	45.53	
Modified National Defense Research Committee (in)	43.51	
Average Concrete Thickness to be Just Spalled (in)	49.95	72.0
Maximum Impact Load (K)	765.29	4744.64
Ductility Ratio	1.0	1.15
Maximum Bearing Stress in Concrete (ksi)	4.040	3.516* (10.547)**
Maximum Compressive Stress in Concrete (ksi)	4.040	5.569*
Maximum Punching Shear Stress in Concrete (ksi)	0.053	0.186

* Indicate Allowable Values for Minor Damage

** Indicate Allowable Values for Moderate Damage

TABLE 3.2-3 CASK DROP ACCIDENT SCENARIO 3 (a)

(10/24 Cask Drop In Cask Fill Area - Vertical Drop)

	CALCULATED	ALLOWABLE
Maximum Velocity at Instant of Impact (ft/sec)	45.79	
Maximum Kinetic Energy at Instant of Impact (in-kip)	86423.88	
Striking Angle with Vertical (degree)	0	
Depth of Penetration		
Modified Petry (in)	1.42	
Army Corps of Engineers and National Defense Research Committee (in)	40.99	
Ammann and Whitney I (in)	1.74	
Ammann and Whitney II (in)	19.03	
Modified National Defense Research Committee (in)	16.39	
Average Depth of Penetration (in)	15.91	
Concrete Thickness to be Just Perforated		
Modified Petry (in)	2.84	
Ballistic Research Laboratories (in)	13.31	
Army Corps of Engineers (in)	146.53	
National Defense Research Committee (in)	131.06	
Ammann and Whitney II (in)	125.79	
Modified National Defense Research Committee (in)	49.58	
Average Concrete Thickness to be Just Perforated (in)	78.19	72.0
Maximum Impact Load (K)	10547.02	10064.6
Ductility Ratio	1.05	1.3
Maximum Bearing Stress in Concrete (ksi)	2.672	3.516*
Maximum Compressive Stress in Concrete (ksi)	2.672	2.709
Maximum Punching Shear Stress in Concrete (ksi)	0.527	0.822**
Maximum Foundation Pressure (ksf)	63.43	100***

* Indicate Allowable Values for Minor Damage
** Indicate Allowable Values for Moderate Damage
*** FSAR, Table 2.5-2

TABLE 3-2-3 CASK DROP ACCIDENT SCENARIO 3 (b)

(10/24 Cask Drop in Cask Fill Area - Angular Drop)

	CALCULATED	ALLOWABLE
Maximum Velocity at Instant of Impact (ft/sec)	45.79	
Maximum Kinetic Energy at Instant of Impact (in-kip)	86423.88	
Striking Angle with Vertical (degree)	19.162	
Depth of Penetration		
Modified Petry (in)	5.57	
Army Corps of Engineers and National Defense Research Committee (in)	13.41	
Ammann and Whitney I (in)	9.44	
Ammann and Whitney II (in)	21.05	
Modified National Defense Research Committee (in)	21.01	
Average Depth of Penetration (in)	14.10	
Concrete Thickness to be Just Perforated		
Modified Petry (in)	11.14	
Ballistic Research Laboratories (in)	60.94	
Army Corps of Engineers (in)	74.98	
National Defense Research Committee (in)	67.25	
Ammann and Whitney II (in)	125.23	
Modified National Defense Research Committee (in)	62.33	
Average Concrete Thickness to be Just Perforated (in)	66.98	72.0
Maximum Impact Load (K)	8229.34	9192.55
Ductility Ratio	1.0	1.3
Maximum Bearing Stress in Concrete (ksi)	2.283	2.231
Maximum Compressive Stress in Concrete (ksi)	2.283	2.709
Maximum Punching Shear Stress in Concrete (ksi)	0.482	0.822**
Maximum Foundation Pressure (ksf)	57.32	100***

** Indicate Allowable Values for Moderate Damage

*** FSAR, Table 2.5-2

TABLE 3.2-3 CASK DROP ACCIDENT SCENARIO 3 (c)

(1/2 Cask Drop in Cask Fill Area - Vertical Drop)

	CALCULATED	ALLOWABLE
Maximum Velocity at Instant of Impact (ft/sec)	47.48	
Maximum Kinetic Energy at Instant of Impact (in-kip)	24386.51	
Striking Angle with Vertical (degree)	0.0	
Depth of Penetration		
Modified Petry (in)	1.79	
Army Corps of Engineers and National Defense Research Committee (in)	22.61	
Ammann and Whitney I (in)	1.88	
Ammann and Whitney II (in)	13.59	
Modified National Defense Research Committee (in)	6.46	
Average Depth of Penetration (in)	9.47	
Concrete Thickness to be Just Perforated		
Modified Petry (in)	3.59	
Ballistic Research Laboratories (in)	14.13	
Army Corps of Engineers (in)	73.26	
National Defense Research Committee (in)	65.39	
Ammann and Whitney II (in)	65.70	
Modified National Defense Research Committee (in)	19.71	
Average Concrete Thickness to be Just Perforated (in)	40.30	72.0
Maximum Impact Load (K)	7550.78	2247.6
Ductility Ratio	>1.3	1.3
Maximum Bearing Stress in Concrete (ksi)	8.567	10.547**
Maximum Compressive Stress in Concrete (ksi)	8.567	16.875**
Maximum Punching Shear Stress in Concrete (ksi)	0.408	0.822**
Maximum Foundation Pressure (ksf)	56.11	100***

** Indicate Allowable Values for Moderate Damage
*** FSAR, Table 2.5-2

TABLE 3.2-3 CASK DROP ACCIDENT SCENARIO 3 (d)

(1/2 Cask Drop in Cask Fill Area - Angular Drop)

	CALCULATED	ALLOWABLE
Maximum Velocity at Instant of Impact (ft/sec)	47.48	
Maximum Kinetic Energy at Instant of Impact (in-kip)	24386.51	
Striking Angle with Vertical (degree)	9.847	
Depth of Penetration		
Modified Petry (in)	2.90	
Army Corps of Engineers and National Defense Research Committee (in)	5.72	
Ammann and Whitney I (in)	4.05	
Ammann and Whitney II (in)	11.23	
Modified National Defense Research Committee (in)	11.20	
Average Depth of Penetration (in)	7.02	
Concrete Thickness to be Just Perforated		
Modified Petry (in)	5.79	
Ballistic Research Laboratories (in)	25.70	
Army Corps of Engineers (in)	52.92	
National Defense Research Committee (in)	47.88	
Ammann and Whitney II (in)	106.62	
Modified National Defense Research Committee (in)	34.38	
Average Concrete Thickness to be Just Perforated (in)	45.55	72.0
Maximum Impact Load (K)	4354.5	2749.2
Ductility Ratio	2.5	1.3
Maximum Bearing Stress in Concrete (ksi)	4.039	10.547**
Maximum Compressive Stress in Concrete (ksi)	4.039	5.569*
Maximum Punching Shear Stress in Concrete (ksi)	0.258	0.274*
Maximum Foundation Pressure (ksf)	34.95	100***

● Indicate Allowable Value for Minor Damage
** Indicate Allowable Value for Moderate Damage
*** FSAR, Table 2.5-2

9. CONCLUSION

1. The results of the cask drop analysis indicate that for cask drop accident cases 1(a) through 2(d), there will be local penetration and minor cracking of the south wall of the spent fuel pool; however, the overall structural integrity of the spent fuel pool will be maintained. Due to the limited depth of these hair-line cracks as compared with the thickness of the wall, there will not be any significant loss of water.

2. For cask drop accident events 3(a) through 3(d), the analysis indicates that there will be a moderate amount of local and overall damage to the spent fuel pool floor; however, there will not be any gross structural failure of the pool floor. Furthermore, the arrangement of the proposed separating wall will insure that the spent fuel will remain covered with water for all of the postulated accident scenarios.

3. The following conservatisms in the subject cask drop analysis should be noted:

    a. The effects of the 1/4" stainless steel liner plate are conservatively neglected in the analysis. The ductile stainless steel liner plate will act as an energy absorbing cushion between the floor/wall of the spent fuel pool and the impacting cask.

    b. The casks are conservatively assumed as non-deformable bodies with the spent fuel pool structure absorbing the entire impact energy. Local deformations of the ductile stainless steel cask will, in effect, reduce the kinetic energy transmitted to the wall and floor of the spent fuel pool.

c. The empirical equations and analytical procedures used in subject analysis represent the present "state of the art" in the field of design of structures and components against missile impact. Although some of these empirical equations, generally apply to low mass, small diameter, high velocity missiles, their use in the design of the nuclear power plant structures for large mass, large diameter, small velocity missiles is judged conservative (Reference 3).

d. Due to the limitations of the empirical equations, it is conservatively assumed for all angular cask drop accident cases, that the diameter of the cask remains constant during impact. In effect, as the cask penetrates deeper into the concrete wall/floor, its contact area and the resulting effective diameter will keep increasing.

Intentionally Blank